Applied Ecology and Environmental Research

International Scientific Journal

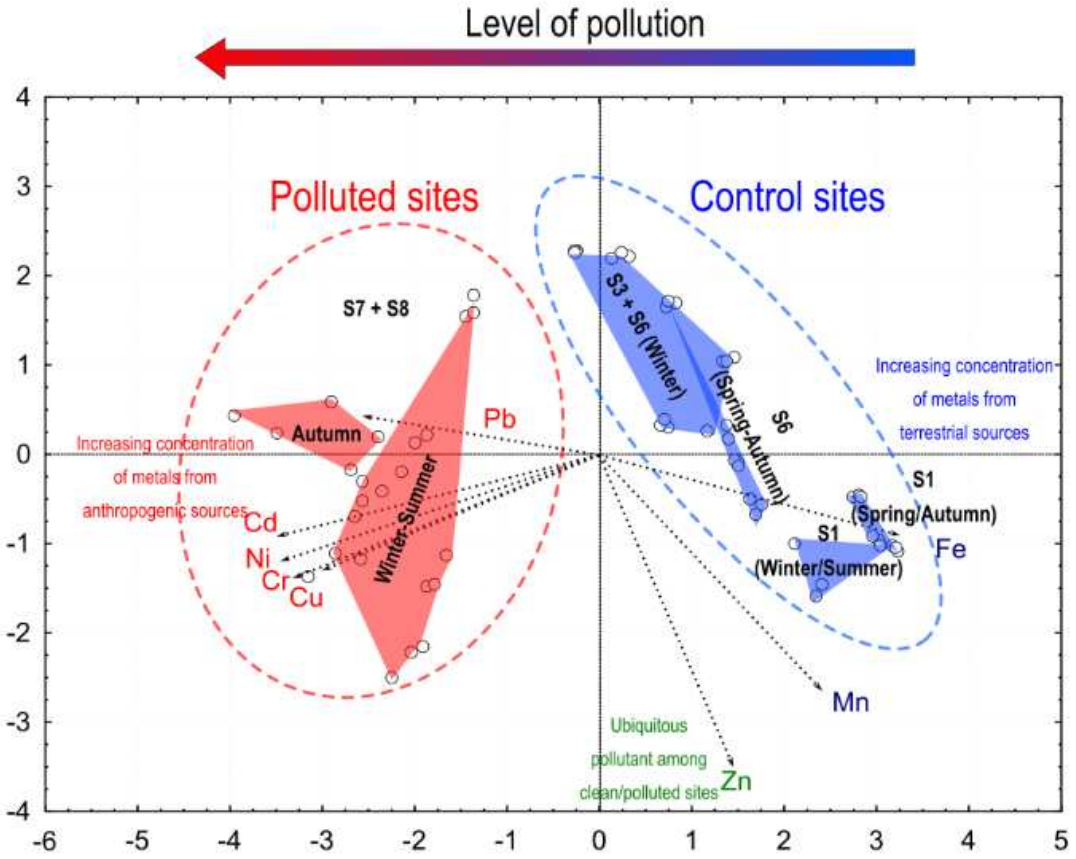

VOLUME 20 * NUMBER 1 * 2022

Published: January 31, 2022
http://www.aloki.hu
ISSN 1589 1623 / ISSN 1785 0037
DOI: http://dx.doi.org/10.15666/aeer

FLORISTIC DIVERSITY IN NORTH-EASTERN BAKHTIARI PROVINCE ON THE CENTRAL ZAGROS MT RANGE OF IRAN

MOUSAVI, S. – SHARIFI-TEHRANI, M.* – SHAHROKHI, A.

Department of Biology, University of Shahrekord, Rahbar st., Shahrekord, Iran

**Corresponding author*
e-mail: msht.ir@gmail.com; phone: +98-913-311-2733; fax: +98-38-3232-4419

(Received 30th Jun 2021; accepted 28th Oct 2021)

Abstract. The present study dealt with the plant species diversity of north-eastern Bakhtiari province located in central Zagros Mt. chain of Iran; one of the diversity-rich areas in the middle east. Three nesting datasets were compiled in this study, corresponding to one, eight and twenty-two local floras across the region. Results showed that a total of 1512 species of flowering plants are distributed in 22 local floras (dataset 3), belonging to 517 genera and 96 families. Dataset 2 corresponding to flora of north-eastern Bakhtiari province, comprised of 714 species belonging to 323 genera and 60 families, of which 60 species were exclusively identified from Babazaki mountain area. Babazaki flora (dataset 1) was characterized by 84 medicinal and 59 endemic plants (to Iran) and sixty percent of the species native to Irano-Turanian phytochorion. Floristic characteristics and relations between the local floras of dataset 2 are presented. Multivariate analysis of 22 local floras in dataset 3 based on occurrence data resulted in four coherent groups. Floristic specifications of groups are presented. This study represents a considerable update on the previous knowledge and a contribution to the diversity and distribution of taxa in the central Zagros Mt chain of Iran.
Keywords: *Babazaki, Middle-East, multivariate analysis, occurrence data, plant*

Introduction

The basic information used in conservation biology for identifying and monitoring the distribution of species, is provided through ecological and taxonomic works. Species near extinction and areas with high diversity, that should be considered for conservation are indicated in such studies. Heywood (2004) stated that Taxonomists should ask themselves just how they reacted to the alarming situation regarding the continuing loss of biodiversity which was widely reported. It requires the inventory of plant diversity and floristic studies to be continued (Heywood, 2004). Documenting the distribution of plant species at regional scale is needed for predicting ongoing changes in contemporary ecosystems. However, diversity inventories do not show how complete the local floras or plant communities are (Pärtel et al., 2013). Compilation of local floras and groups of them into nested datasets may provide clearer view of diversity and distribution of species at different scales. This may also help reveal the dark diversity (Pärtel et al., 2011; Lewis et al., 2016), which is used for calculating the community completeness indices (Pärtel et al., 2013).

Multivariate analyses could be used for grouping of species distributed over areas and/or environmental variables. The rationale behind this type of analysis is that they may exploit relations between the species that are present in the data. These techniques could be used to construct a "species map" in which species that frequently co-occur are grouped close together; species that hardly co-occur are depicted far apart (Van Der Maaten et al., 2012). Clustering of species distributions could also be used for identifying floristic elements in regional floras (Finnie et al., 2007). Those analyses put biological species as objects of the analysis rather than variables. Data reduction methods could also

http://www.aloki.hu ● ISSN 1589 1623 (Print) ● ISSN 1785 0037 (Online)
DOI: http://dx.doi.org/10.15666/aeer/2001_001019

be used for grouping of areas, sites, and communities, etc., as objects, considering species as variables. The rational is that, species are identifiable independent biological identities, that could serve as independent variables of an analysis, providing reliable occurrence data. The local flora method is based on the concept that detailed information from a limited number of sites could provide more reliable knowledge of regional flora, compared to occasional irregular samplings (Tolmatchev, 1931). Study of local floras could provide opportunities to study gradients of floristic variables, such as, differences in taxonomical features of local floras (Khitun et al., 2016). This approach which has been used in a limited number of diversity-oriented studies (Talbot et al., 2007; Khitun et al., 2016; Veiskarami and Sharifi-Tehrani, 2017), is followed in this study on the central Zagros region of Iran.

Central Zagros region, is a diversity-rich area in the middle east (Heywood, 2004), located in Zagros mountain chain stretched from northwest to southwest of Iran (Djamali et al., 2009). Western slopes are faced to and affected from the Mediterranean climate, and the Eastern slopes boarder Iran's inland dry deserts, mainly comprised of Irano-Turanian vegetations. Northern Zagros neighboring Caucasus and consisting of Euro-Siberian vegetations, and Southern parts, neighboring Sahara-Sindian vegetations, also prevalent in Northern Arabian Peninsula. Although a relatively large proportion of species in Central parts of the Zagros are endemics of Irano-Turanian floristic region, due to diverse geological, geographical, topological and climatic conditions, the regional flora of Central Zagros is complex in terms of species composition and distribution. Plant species diversity and distribution of species across local flora has been studies in this region, through several investigations, yet flora of the region is not fully acknowledged. Contemporary flora of this region is evolving rapidly due to the changing climate and intense human activities, especially grazing and agricultural activities. To date, a number of local floras in the Bakhtiari Province at the heart of Central Zagros range, have been investigated (*Tables 1, 2*) and many areas remain to be studied. This study is concerned with the diversity of plant species in north-eastern Bakhriari province. Some local floras of this region are investigated by the authors in recent years. In this study, flora of Babazaki mountain area characterized by its relatively rich flora with high percentage of medicinal and endemic species, located near the Tang-e-Sayad National Park in Bakhtiari province, is being added to our previous datasets. This study was also aimed to compile a floristic checklist of local floras, to assess similarities and differences between sites, and to analyze the floristic structure of north-eastern part of the Bakhtiari province in the central Zagros region of Iran, which is shaped and altered throughout time by changing climate and topography.

Materials and Methods

Three nested floristic datasets comprising one, eight, and twenty-two local floras, are compiled in this study. The first dataset, consists of a checklist of the Babazaki mountain and the lands towards southern parts of the Saman region, acquired through our recent field survey. Babazaki local flora is located between 50.878 and 51.064 eastern longitudes and 32.431 and 32.287 northern latitudes, in north-east of Bakhtiari province of Iran (*Fig. 1*). It covers an area of 12052 ha. Altitude ranges from 2120 to 2810 m a.s.l. (average: 2350 m). Mean temperature ranges from -0.4 °C (minimum in Jan) to 25.74 °C (maximum in July) with an annual average of 12.98 °C, according to meteorological data acquired from Iranian meteorological organization. The average sum of annual

http://www.aloki.hu ● ISSN 1589 1623 (Print) ● ISSN 1785 0037 (Online)
DOI: http://dx.doi.org/10.15666/aeer/2001_001019

precipitation is 218.51 mm (data from three meteorological stations adjacent to the study area). Climate type of the study area for dataset 1 was 'semi-arid' based on Amberger (*Eq.1*), and Thornth-Waite's (*Eq.2*) coefficients, separately calculated for three adjacent synoptic stations: Saman (Q_2= 32.43, IPE= 32.8), Shahrekord (Q_2= 27.77, IPE= 38), and Farrokhshahr (Q_2=23.58, IPE= 20.4). Ombrothermic charts (*Fig. 2*) show that drought period span between May and October.

$$Q_2 = 2000\ P / (M^2 - m^2) \quad \text{(Eq.1)}$$

$$IPE = 10\sum ((0.1645\ P) / (T + 12.2))^{10/9} \quad \text{(Eq.2)}$$

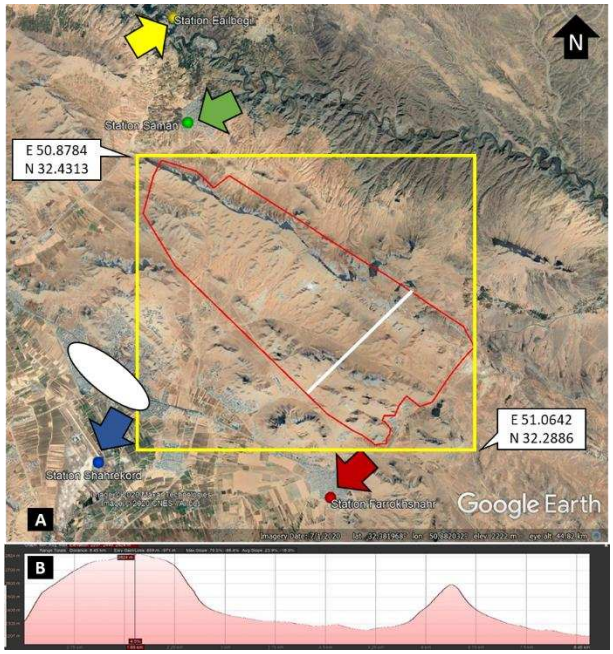

Figure 1. *Map showing study area of the first dataset (Babazaki flora). A: white boxes: Coordinates of circumferential rectangle, white elliptic: city of Shahrekord, black arrow: north direction, colored arrows: four meteorological stations (green: Saman station, blue: Shahrekord-airport station, red: Farrokhshahr station, yellow: newly stablished Eilbegi station), red line: circumferential polygon around the study area, B: altitudinal profile along the white line in Fig. 1A*

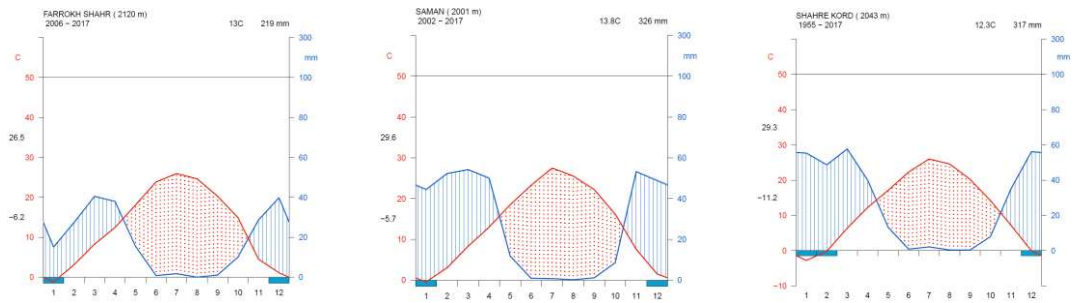

Figure 2. *Ombrothermic charts drawn based on meteorological data of three adjacent synoptic stations to the Dataset 1 study area. Left: Station Farrokhshahr, Mid: Station Saman, Right: Station Shahrekord. Meteorological data obtained from Iranian national meteorological organization (www.irimo.ir)*

http://www.aloki.hu ● ISSN 1589 1623 (Print) ● ISSN 1785 0037 (Online)
DOI: http://dx.doi.org/10.15666/aeer/2001_001019

Species occurring in Babazaki flora (dataset 1) were recorded by collecting specimens during grow seasons of 2018-2019, using random sampling method. Taxonomic determinations performed using available literature i.e. Flora Iranica (Rechinger, 1963-2012), Flora of Iran (Assadi, 1989-2016), Flora of Turkey (Davis, 1965-1985), and Flora Europaea (Tutin et al., 1968-1980). Vouchers are deposited in the Herbarium of the Shahrekord University (SKU). For dataset 2, comprising eight local floras (including dataset 1), checklists of two local floras (Jahanbin and Sheet Mt areas) were prepared by the author through field surveys during 2015-2016, and checklists of five remaining local floras are compiled from literature (*Table 1*). Eight local floras (*Table 1*, *Fig. 3*) adjacent to (and including) Babazaki flora in north-eastern Bakhtiari province were compiled into dataset 2 and used for comparing between adjacent local flora to elucidate dark diversity. The third dataset in which datasets 1 and 2 were nested, comprised of twenty-two local floras in the central Zagros region (*Table 2*, *Fig. 3*); it was compiled for determining floristic structure of the region through multivariate analysis.

Table 1. *Local floras compiled into the second dataset*

ID	Coordinates	Alt. (m)	Area (ha)	Prec (mm)	Alpha		1	2	3	4	5	6	7
211	N 32.05 E 50.983	2720	27000	304	235	**1**							
213	N 32.281 E 50.831	2045	2045	-	55	**2**	224						
228	N 32.375 E 50.873	2120-2660	1070	349	211	**3**	272	214					
229	N 32.575 E 50.656	2100-3165	22164	435	314	**4**	273	301	319				
232	N 32.174 E 50.755	2150-3300	12187	324	271	**5**	318	254	266	339			
264	N 32.265 E 50.994	2142-2890	6402	-	95	**6**	172	112	218	279	266		
380	N 32.433 E 50.583	2100-2900	3151	441	158	**7**	223	161	221	260	269	147	
534	N 32.35 E 50.95	2125-2824	12052	276	257	**8**	284	266	262	363	328	260	261

ID: identification number of the local flora in floristic database, Alt.: Altitude of the site from sea level, Prec = Sum of annual precipitation, Alpha= alpha diversity (=species richness), numbers 1-8: local floras; components of the second dataset. Seven right-most columns of the table showing beta diversity measures

Dataset 2 encompasses an area between 50.583 and 50.994 eastern longitudes and 32.050 and 32.575 northern latitudes (*Fig. 3, up*), covering an area of 132800 ha. Altitude of local floras within dataset 2 ranges from 2045 to 3300 m a.s.l. Mean temperature ranges from -0.8 °C to 25.74 °C and the average sum of annual precipitation ranges from 218 to 441 mm. Dataset 3 encompasses an area between 50.083 and 51.188 eastern longitudes and 31.472 and 32.994 northern latitudes (*Fig. 3, down*), covering an area of 1261920 ha. Altitude of local floras within dataset 3 ranges from 834 to 4135 m a.s.l. Mean temperature ranges from -19 °C to 39.8 °C and the average sum of annual precipitation ranges from 188 to 505.9 mm.

http://www.aloki.hu ● ISSN 1589 1623 (Print) ● ISSN 1785 0037 (Online)
DOI: http://dx.doi.org/10.15666/aeer/2001_001019

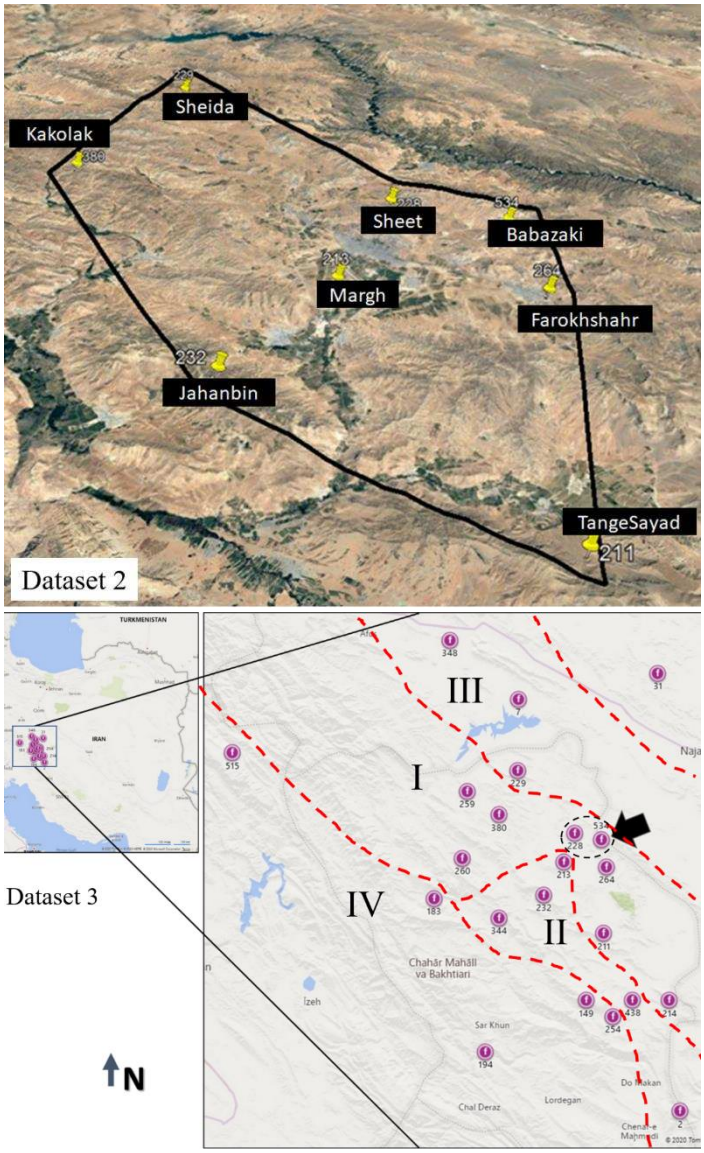

Figure 3. *Up: Map showing location of seven local floras (dataset 2) adjacent to Babazaki. Down: map showing location of 22 local flora (the third dataset), selected for multivariate analysis. Marked areas correspond to four groups (K=4) resulted in multivariate analysis (see text and Fig. 6)*

Datasets were prepared using a developing floristic database (Sharifi-Tehrani and Rahiminejad-Ranjbar, 2013), in which occurrence data considered at the species level (Van Der Maaten et al., 2012).

Species names were checked using International Plant Names Index (IPNI) and The Plant List (TPL) online taxonomic databases through the CheckName program (Sharifi-Tehrani, 2014) which uses software API codes to connect to online databases. Geographical distribution, endemism and conservation status of species were determined according to Red Data Book of Iran (Jalili and Jamzad, 1999), and available relevant literature (Rechinger, 1963-2012; Zohary, 1973). Life forms determined based on direct observation of specimens (for three surveyed local floras), according to Raunkiaer's classification (1934).

http://www.aloki.hu ● ISSN 1589 1623 (Print) ● ISSN 1785 0037 (Online)
DOI: http://dx.doi.org/10.15666/aeer/2001_001019

Table 2. *Twenty-two local floras; checklists of them compiled into the third dataset and used for multivariate analysis*

	ID	Publ.	Area (ha)	Alpha	Flora (Abbreviation used in Fig. 6)
1	534	this paper	12052	257	Babazaki Flora (4MB_bbzk)
2	214	Tahmasebi, 2014b	Na	79	Ghorogh Boroujen (4MB_Brojen)
3	260	Kafash-Saei et al., 2014a	6905	69	Darreh Sir (4MB_DarrehSir)
4	264	Kafash-Saei et al., 2014b	6402	95	Farrokhshahr (4MB_Farrokh)
5	183	Shirmardi et al., 2014a	9816	487	Gheysari (4MB_Gheisar)
6	194	Shirmardi et al., 2014b	40231	392	Helen (4MB_HelenPA)
7	232	Jalali et al., 2016	12187	271	Jahanbin (4MB_Jhnbn)
8	380	Naghipoor-Borj, 2016	3151.5	158	Kakolak (4MB_Kakolak)
9	149	Shahrokhi, 2005	50800	514	Kallar (4MB_Kallar)
10	259	Pairanj et al., 2011	576	276	Karsanak (4MB_Karsnk3)
11	213	Tahmasebi, 2014a	Na	55	Margh Shahrekord (4MB_Margh)
12	228	Dehghani et al., 2015	1070	211	Sheet Mt. (4MB_MtSheet)
13	515	Gholami et al., 2018	213300	343	RobatKouh Bazoft (4MB_RobatKuh)
14	254	Assadi et al., 2009	54010	433	SabzKouh (4MB_Sabzkouh)
15	344	Hasanzadeh et al., 2017	13943	267	Saldaran (4MB_Saldrn)
16	229	Vahabi et al., 2018	22164	314	Sheida (4MB_Sheida)
17	211	Heydari-Ghahfarrokhi et al., 2012	27000	235	TangeSayad PA (4MB_TangSayad)
18	438	Iranmanesh et al., 2017	2870	137	Bakhtiari Wetlands (4MB_Wetlands)
19	7	Yousofi et al., 2011	10000	339	Chadegan (Isf_Chadegan)
20	348	unpublished	97645	364	Fereydan/Daran (Isf_Daran)
21	31	Yousofi, 2006	50000	143	Ghameshloo (Isf_Ghameshloo)
22	2	Parishani, 2005	40000	614	Vanak-Semirom (Isf_Vanak)

ID: identification number of the local flora in floristic database. Publ.: Publication. Alpha: Alpha diversity (= species richness). Most of the checklists are published in native language. Na: not available

Presence (1) or absence (0) of each species were entered into a data matrix comprising 22 rows and 1512 columns (species). Data matrix was used for calculating alpha, beta, and gamma diversity measures, for comparing local floras, and for multivariate floristic analyses. Required data matrices were prepared and formatted by using the "Alamut floristic database" (Sharifi-Tehrani and Rahiminejad-Ranjbar, 2013). Data was analyzed using Dice (*Eq.3*) and SMC (*Eq.4*) coefficients for qualitative data, in which a= co-occurrence of species, b= species present in one flora, c= species present in another flora, m= number of matches, and n= number of non-matches.

$$SDice = 2a / (2a + b + c) \quad \text{(Eq.3)}$$

$$SM = m / n \quad \text{(Eq.4)}$$

PCO and clustering analyses were conducted using NTSYSpc (Rohlf, 2000) and SplitTree (Huson and Bryant, 2006) software packages. Best fit for number of clusters in the multivariate analyses was inferred by exploratory data analysis in CLUTO software package (Karypis, 2003) which computes the maximum internal similarities inside each group by minimizing the similarity between groups.

http://www.aloki.hu ● ISSN 1589 1623 (Print) ● ISSN 1785 0037 (Online)
DOI: http://dx.doi.org/10.15666/aeer/2001_001019

Results

Results of this study are based on three nesting datasets. The first dataset which is presented for the first time in this study (*Table 3*), comprises of species checklist of Babazaki flora. There are 257 plant species growing in this local flora belonging to 177 genera and 45 families. Species to family, genera to family and species to genus ratios are 5.71, 3.93, and 1.45, respectively. Checklist of plant species in this area was interesting as it revealed that a high percentage (82%; 212 spp) of plant species growing in this site are not previously evaluated for conservation status (NE category). Sixteen percent (40 species) are in LR (lower risk) category and three species (*Astragalus cyclophyllon* Beck, *Astragalus griseus* Boiss., and *Ziziphora clinopodioides* Lam.) are vulnerable species (VU). Babazaki flora consists of 84 medicinal, 59 endemics (to Iran), and 47 range species growing in relatively scarce water conditions. Climate type (semi-arid) of this area prefers for hemicryptophyte (48%) and therophyte (32%) life forms (*Fig. 4*). Sixty percent of the plant species growing in this site, are native elements of Irano-Turanian chorotype (*Fig. 4*). Checklist of the plant species growing in this site along with their properties (being medicinal, range, or endemic), life forms and chorotypes are presented in *Table 3*. The largest families of the region in terms of species richness are Asteraceae (17%), Brassicaceae (11%), and Apiaceae and Lamiaceae (7% each). The sequence of large families in terms of generic richness is: Asteraceae (16%), Lamiaceae (11%) and Brassicaceae (10%). The largest species-rich genera in this flora are *Astragalus* (14 spp), *Nepeta* (6 spp), and *Allium*, *Centaurea* and *Salvia* (5 spp each). Most of the genera in this flora are represented with few species, which could also be inferred from species to genera ratio (sp/gen=1.45). There are sixty species growing in Babazaki flora, which are not reported from adjacent local floras in dataset 2.

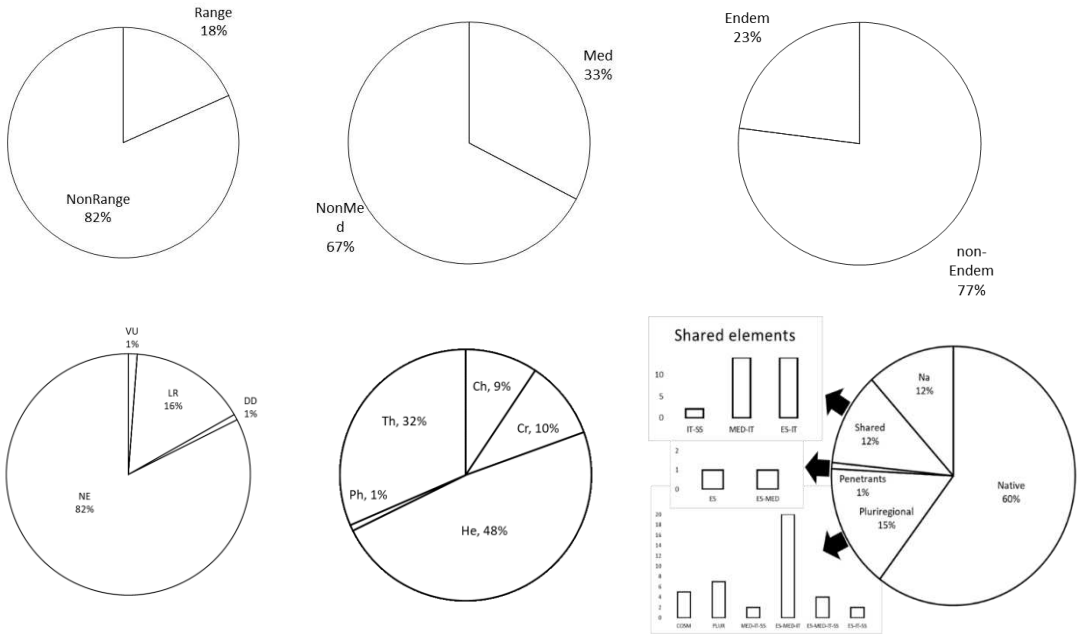

Figure 4. *Percentage of range (upper left), medicinal (up middle), and endemic species (upper right), and each IUCN category (lower left), life forms (low mid), and percentage of plant species belonging to each chorotype, in Flora of Babazaki. He: hemicriptophyte, Cr: cryptophyte, Ch: chamaeophyte, Th: therophyte, Ph: phanerophyte, Vu: vulnerable, LR: lower risk, DD: data deficient, NE: not evaluated*

http://www.aloki.hu ● ISSN 1589 1623 (Print) ● ISSN 1785 0037 (Online)
DOI: http://dx.doi.org/10.15666/aeer/2001_001019

Table 3. *Checklist of 257 plant species growing in Babazaki flora (dataset 1, id: 534), consisting 59 endemic and 84 medicinal species. Plant families are listed according to LAPGIII and modifications by APGIV. Species names are listed alphabetically*

Group & Family	Scientific Name	Characteristics
Monocots		
Liliales		
Colchicaceae	*Colchicum wendelboi* K.Perss.	LEM [IT] [Cr]
Liliaceae	*Fritillaria gibbosa* Boiss.	[IT] [Cr]
Liliaceae	*Fritillaria pinardii* Boiss.	[IT] [Cr]
Liliaceae	*Gagea reticulata* Schult.f.	[Plur] [Th]
Liliaceae	*Ornithogalum orthophyllum* Ten.	M [IT] [Cr]
Liliaceae	*Tulipa biflora* Pall.	[ES, IT] [Cr]
Liliaceae	*Tulipa systola* Stapf	[IT] [Cr]
Asparagales		
Ixioliriaceae	*Ixiolirion tataricum* (Pall.) Herb. & Traub	M [ES, Med, IT] [Th]
Iridaceae	*Iris barnumiae* Baker & Foster	LE [IT] [Cr]
Iridaceae	*Iris songarica* Schrenk	M [IT] [Th]
Iridaceae	*Iris* sp.	[Cr]
Asphodelaceae	*Eremurus* sp.	[Cr]
Amaryllidaceae	*Allium akaka* S.G.Gmel. ex Schult. & Schult.f.	EM [IT] [Cr]
Amaryllidaceae	*Allium ampeloprasum* L.	M [Med, IT] [Cr]
Amaryllidaceae	*Allium scabriscapum* Boiss.	M [IT] [Cr]
Amaryllidaceae	*Allium* sp.	[Cr]
Amaryllidaceae	*Allium tripedale* Trautv.	[IT] [Cr]
Asparagaceae	*Bellevalia glauca* (Lindl.) Kunth	M [IT] [Cr]
Asparagaceae	*Muscari neglectum* Guss. ex Ten.	M [ES, Med, IT] [Th]
Asparagaceae	*Pseudomuscari inconstrictum* (Rech.f.) Garbari	[ES, Med, IT] [Cr]
Poales		
Juncaceae	*Juncus inflexus* L.	[Plur] [Th]
Poaceae	*Boissiera squarrosa* (Sol.) Nevski	[IT] [Th]
Poaceae	*Bromus danthoniae* Trin. ex C.A.Mey.	[IT] [Th]
Poaceae	*Bromus gracillimus* Bunge	[IT] [Th]
Poaceae	*Bromus tectorum* L.	[Plur] [Th]
Poaceae	*Bromus tomentellus* Boiss.	[ES, IT] [He]
Poaceae	*Eremopoa persica* (Trin.) Roshev.	[Med, IT] [Th]
Poaceae	*Heteranthelium piliferum* Hochst. ex Jaub. & Spach	[Med, IT] [Th]
Poaceae	*Hordeum murinum* L.	[Med, IT] [Th]
Poaceae	*Melica persica* Kunth	[IT] [He]
Poaceae	*Piptatherum holciforme* Roem. & Schult.	[IT] [He]
Poaceae	*Poa bulbosa* L.	[ES, IT] [Cr]
Poaceae	*Psathyrostachys fragilis* (Boiss.) Nevski	[IT] [He]
Poaceae	*Stipa arabica* Trin. & Rupr.	[IT] [He]
Poaceae	*Taeniatherum caput-medusae* (L.) Nevski	[Med, IT] [Th]
Basal Eudicots		
Ranunculales		
Papaveraceae	*Corydalis* sp.	[Cr]
Papaveraceae	*Corydalis verticillaris* DC.	LEM [IT] [Cr]
Papaveraceae	*Fumaria asepala* Boiss.	M [Med, IT] [Th]
Papaveraceae	*Glaucium corniculatum* Curtis	M [Med, IT] [Th]
Papaveraceae	*Glaucium oxylobum* Boiss. & Buhse	M [IT] [He]
Papaveraceae	*Hypecoum pendulum* L.	M [ES, IT] [Th]
Papaveraceae	*Papaver dubium* L.	M [Plur] [Th]
Papaveraceae	*Roemeria hybrida* (L.) DC.	M [Med, IT, SS] [Th]
Papaveraceae	*Roemeria refracta* DC.	M [ES, IT] [Th]
Berberidaceae	*Bongardia chrysogonum* Boiss.	M [IT] [Th]
Berberidaceae	*Leontice armeniaca* Boiv.	[IT] [Cr]
Ranunculaceae	*Adonis aestivalis* L.	M [IT] [Th]

http://www.aloki.hu ● ISSN 1589 1623 (Print) ● ISSN 1785 0037 (Online)
DOI: http://dx.doi.org/10.15666/aeer/2001_001019

Ranunculaceae	*Anemone biflora* DC.	M [IT] [Th]
Ranunculaceae	*Ceratocephala falcata* (L.) Pers.	M [ES, Med, IT] [Th]
Ranunculaceae	*Consolida orientalis* (J. Gay) Schrodinger	M [ES, Med, IT] [Th]
Ranunculaceae	*Delphinium pallidiflorum* Freyn	[IT] [Cr]
Ranunculaceae	*Ranunculus kotschyi* Boiss.	LEM [IT] [He]
Ranunculaceae	*Ranunculus* sp.	[Th]
Ranunculaceae	*Thalictrum isopyroides* C.A. Mey.	M [IT] [He]
Super Rosids		
Saxifragales		
Crassulaceae	*Pseudosedum multicaule* (Boiss. & Buhse) Boriss.	[IT] [He]
Crassulaceae	*Rosularia elymaitica* A.Berger	LE [IT] [He]
Crassulaceae	*Rosularia sempervivum* (M. Bieb.) A. Berger	[IT] [He]
Rosids		
Fabales		
Fabaceae	*Alhagi maurorum* Medik.	M [IT] [He]
Fabaceae	*Astragalus babakhanloui* Maassoumi & Podlech	LE [IT] [He]
Fabaceae	*Astragalus campylanthus* Boiss.	LE [IT] [Ch]
Fabaceae	*Astragalus campylorhynchus* Fisch. & C.A.Mey.	[IT] [Th]
Fabaceae	*Astragalus cephalanthus* DC.	LEM [IT] [Ch]
Fabaceae	*Astragalus chahartaghensis* Maassoumi & Podlech	LE [IT] [He]
Fabaceae	*Astragalus cyclophyllon* Beck	VEM [IT] [He]
Fabaceae	*Astragalus fragiferus* Bunge	LE [IT] [Ch]
Fabaceae	*Astragalus grammecalyx* Boiss. & Hohen.	[IT] [He]
Fabaceae	*Astragalus griseus* Boiss.	VE [IT] [He]
Fabaceae	*Astragalus holopsilus* Bunge	LE [IT] [He]
Fabaceae	*Astragalus macropelmatus* Bunge	[IT] [Th]
Fabaceae	*Astragalus ovinus* Boiss.	M [IT] [He]
Fabaceae	*Astragalus rhodosemius* Boiss. & Hausskn.	E [IT] [Ch]
Fabaceae	*Astragalus* sp.	[Ch]
Fabaceae	*Hedysarum grandiflorum* Pall.	[ES, IT] [He]
Fabaceae	*Vicia* sp.	[Th]
Rosales		
Rosaceae	*Amygdalus lycioides* Spach	LEM [IT] [Ph]
Rhamnaceae	*Rhamnus persica* Boiss.	LEM [IT] [Ph]
Urticaceae	*Parietaria judaica* L.	M [ES, Med, IT] [He]
Malpighiales		
Euphorbiaceae	*Euphorbia bungei* Boiss.	[IT] [He]
Euphorbiaceae	*Euphorbia* sp.	[He]
Linaceae	*Linum album* Kotschy ex Boiss.	LEM [IT] [He]
Linaceae	*Linum austriacum* L.	[ES, IT] [He]
Geraniales		
Geraniaceae	*Erodium cicutarium* (L.) L'Hér.	M [ES, Med, IT] [Th]
Geraniaceae	*Geranium lucidum* L.	M [ES, Med] [Th]
Geraniaceae	*Geranium tuberosum* L.	M [ES, Med, IT] [Cr]
Sapindales		
Biebersteiniaceae	*Biebersteinia multifida* DC.	M [Med, IT] [Th]
Nitrariaceae	*Peganum harmala* L.	M [ES, Med, IT] [He]
Rutaceae	*Haplophyllum acutifolium* (DC.) G. Don	[IT] [He]
Rutaceae	*Haplophyllum rechingeri* C.C.Towns.	EM [IT] [He]
Malvales		
Malvaceae	*Alcea koelzii* I.Riedl	EM [IT] [He]
Malvaceae	*Malva neglecta* Wallr	M [Plur] [He]
Brassicales		
Resedaceae	*Reseda lutea* L.	M [ES, Med, IT] [He]
Cleomaceae	*Cleome coluteoides* Boiss.	M [IT] [He]
Brassicaceae	*Aethionema carneum* B.Fedtsch.	M [IT] [Th]
Brassicaceae	*Aethionema virgatum* (Boiss.) Hedge	[IT] [Th]
Brassicaceae	*Alyssum linifolium* Stephan ex Willd.	M [Med, IT] [Th]

http://www.aloki.hu ● ISSN 1589 1623 (Print) ● ISSN 1785 0037 (Online)
DOI: http://dx.doi.org/10.15666/aeer/2001_001019

Brassicaceae	*Arabis caucasica* Willd.	[ES, Med, IT] [He]
Brassicaceae	*Arabis nova* Vill.	[ES, Med, IT] [Th]
Brassicaceae	*Aubrieta parviflora* Boiss.	[IT] [Ch]
Brassicaceae	*Capsella bursa-pastoris* (L.) Medik.	M [Cosm] [Th]
Brassicaceae	*Cardamine* sp.	[Th]
Brassicaceae	*Conringia clavata* Boiss.	[IT] [Th]
Brassicaceae	*Descurainia sophia* (L.) Webb ex Prantl	M [ES, Med, IT] [Th]
Brassicaceae	*Draba rosularis* Chodat & Wilczek	[IT] [He]
Brassicaceae	*Eruca vesicaria* (L.) Cav.	[ES, Med, IT] [Th]
Brassicaceae	*Erysimum repandum* L.	M [IT] [He]
Brassicaceae	*Fibigia suffruticosa* (Vent.) Sweet	M [IT] [He]
Brassicaceae	*Fibigia umbellata* (Boiss.) Boiss.	EM [IT] [He]
Brassicaceae	*Hesperis persica* Boiss.	[IT] [He]
Brassicaceae	*Isatis cappadocica* Desv.	M [IT] [He]
Brassicaceae	*Isatis* sp.	[He]
Brassicaceae	*Lepidium draba* L.	M [Cosm] [Th]
Brassicaceae	*Malcolmia* sp.	[Th]
Brassicaceae	*Matthiola farinosa* Bunge ex Boiss.	[IT] [He]
Brassicaceae	*Matthiola ovatifolia* Boiss.	LEM [IT] [He]
Brassicaceae	*Pseudocamelina glaucophylla* N.Busch	LE [IT] [He]
Brassicaceae	*Sameraria elegans* Boiss.	LE [IT] [Th]
Brassicaceae	*Sameraria* sp.	[Th]
Super Asterids		
Santalales		
Santalaceae	*Thesium kotschyanum* Boiss.	[IT] [Cr]
Caryophyllales		
Plumbaginaceae	*Acantholimon senganense* Bunge	E [IT] [Ch]
Polygonaceae	*Atraphaxis spinosa* L.	M [ES, IT] [Ch]
Polygonaceae	*Polygonum aridum* Boiss. & Hausskn. ex Boiss.	LEM [IT] [Ch]
Polygonaceae	*Polygonum aviculare* L.	M [Cosm] [Th]
Polygonaceae	*Rheum ribes* L.	M [IT] [Th]
Polygonaceae	*Rumex* sp.	[IT] [Cr]
Caryophyllaceae	*Acanthophyllum crassifolium* Boiss.	LEM [IT] [Ch]
Caryophyllaceae	*Acanthophyllum mucronatum* C.A.Mey.	M [IT] [Ch]
Caryophyllaceae	*Acanthophyllum* sp.	[Ch]
Caryophyllaceae	*Bufonia* sp.	[He]
Caryophyllaceae	*Cerastium dichotomum* L.	[ES, Med, IT, SS] [Th]
Caryophyllaceae	*Dianthus macranthoides* Hausskn. ex Bornm.	LEM [IT] [Ch]
Caryophyllaceae	*Dianthus orientalis* Adams	ERM [IT] [He]
Caryophyllaceae	*Gypsophila* sp.	[He]
Caryophyllaceae	*Mesostemma kotschyanum* (Fenzl ex Boiss.) Vved.	[IT] [He]
Caryophyllaceae	*Paronychia caespitosa* Stapf	LE [IT] [He]
Caryophyllaceae	*Silene longipetala* Vent.	[IT] [He]
Caryophyllaceae	*Silene* sp.	[He]
Caryophyllaceae	*Stellaria media* (L.) Vill.	M [ES, Med, IT, SS] [Th]
Caryophyllaceae	*Vaccaria* sp.	[Th]
Amaranthaceae	*Camphorosma monspeliaca* L.	M [ES, IT] [Ch]
Asterids		
Ericales		
Primulaceae	*Androsace maxima* L.	[ES, Med, IT, SS] [Th]
Gentianales		
Rubiaceae	*Asperula glomerata* (M.Bieb.) Griseb.	M [IT] [He]
Rubiaceae	*Asperula* sp.	[He]
Rubiaceae	*Callipeltis cucullaris* (L.) DC.	[Th]
Rubiaceae	*Galium* sp.	[Th]

http://www.aloki.hu ● ISSN 1589 1623 (Print) ● ISSN 1785 0037 (Online)
DOI: http://dx.doi.org/10.15666/aeer/2001_001019

Boraginales		
Boraginaceae	*Alkanna frigida* Boiss.	E [IT] [He]
Boraginaceae	*Anchusa strigosa* Banks & Sol.	M [IT] [He]
Boraginaceae	*Asperugo procumbens* L.	M [Plur] [Th]
Boraginaceae	*Buglossoides arvensis* (L.) I.M.Johnst.	M [ES, Med, IT, SS] [Th]
Boraginaceae	*Lappula microcarpa* Gürke	[ES, IT] [Th]
Boraginaceae	*Nonea caspica* G.Don	M [ES, IT] [Th]
Boraginaceae	*Onosma elivendica* Wettst. ex Stapf	E [IT] [He]
Boraginaceae	*Onosma microcarpa* DC.	M [IT] [He]
Boraginaceae	*Onosma* sp.	[He]
Boraginaceae	*Rindera lanata* Bunge	[IT] [He]
Boraginaceae	*Solenanthus bakhtiaricus* Khat.	E [IT] [He]
Boraginaceae	*Solenanthus circinatus* Ledeb.	M [IT] [He]
Boraginaceae	*Trichodesma aucheri* DC.	LE [IT] [He]
Solanales		
Convolvolaceae	*Convolvulus arvensis* L.	M [Cosm] [Th]
Convolvolaceae	*Convolvulus commutatus* Boiss.	M [IT] [He]
Solanaceae	*Hyoscyamus reticulatus* L.	M [IT] [He]
Lamiales		
Plantaginaceae	*Linaria michauxii* Chav.	EM [IT] [He]
Plantaginaceae	*Veronica hederifolia* L.	[ES] [Th]
Plantaginaceae	*Veronica* sp.	[He]
Scrophulariaceae	*Verbascum nudicaule* (Wydler) Takht.	[IT] [He]
Lamiaceae	*Ajuga chamaecistus* Ging. ex Benth.	LEM [IT] [Ch]
Lamiaceae	*Clinopodium graveolens* (M.Bieb.) Kuntze	M [ES, Med, IT] [Th]
Lamiaceae	*Eremostachys molucelloides* Bunge	[IT] [He]
Lamiaceae	*Hymenocrater bituminosus* Fisch. & C.A.Mey.	[IT] [Ch]
Lamiaceae	*Lagochilus aucheri* Boiss.	LE [IT] [Ch]
Lamiaceae	*Marrubium cuneatum* Banks & Sol.	M [IT] [He]
Lamiaceae	*Nepeta ispahanica* Boiss.	M [IT] [Th]
Lamiaceae	*Nepeta pungens* (Bunge) Benth.	M [IT] [Th]
Lamiaceae	*Nepeta saccharata* Bunge	M [IT] [Th]
Lamiaceae	*Nepeta* sp.	[Th]
Lamiaceae	*Nepeta straussii* Hausskn. & Bornm.	LEM [IT] [Th]
Lamiaceae	*Nepeta supina* Steven	[IT] [He]
Lamiaceae	*Phlomis olivieri* Benth.	EM [IT] [He]
Lamiaceae	*Phlomis persica* Boiss.	LEM [ES, IT, SS] [He]
Lamiaceae	*Salvia aristata* Aucher ex Benth.	LEM [IT] [He]
Lamiaceae	*Salvia atropatana* Bunge	M [IT] [He]
Lamiaceae	*Salvia hydrangea* DC. ex Benth.	M [IT] [He]
Lamiaceae	*Salvia multicaulis* Vahl	M [IT] [He]
Lamiaceae	*Salvia reuteriana* Boiss.	EM [IT] [He]
Lamiaceae	*Scutellaria multicaulis* Boiss.	LEM [IT] [Ch]
Lamiaceae	*Scutellaria tomentosa* Bertol.	[IT] [He]
Lamiaceae	*Stachys aucheri* Benth.	LE [IT] [Ch]
Lamiaceae	*Stachys inflata* Benth.	M [ES, IT] [He]
Lamiaceae	*Stachys lavandulifolia* Vahl	M [IT] [He]
Lamiaceae	*Stachys pilifera* Benth.	LEM [IT] [Ch]
Lamiaceae	*Teucrium orientale* L.	M [IT] [He]
Lamiaceae	*Teucrium polium* L.	M [Med, IT] [Ch]
Lamiaceae	*Ziziphora clinopodioides* Lam.	VM [IT] [Ch]
Lamiaceae	*Ziziphora tenuior* L.	M [IT] [Th]
Orobanchaceae	*Orobanche oxyloba* (Reut.) Beck	[ES, IT] [Cr]
Asterales		
Campanulaceae	*Campanula incanescens* Boiss.	M [IT] [He]
Campanulaceae	*Michauxia laevigata* Vent.	[IT] [He]

http://www.aloki.hu ● ISSN 1589 1623 (Print) ● ISSN 1785 0037 (Online)
DOI: http://dx.doi.org/10.15666/aeer/2001_001019

Asteraceae	*Achillea santolinoides* Lag.	M [IT] [He]
Asteraceae	*Anthemis odontostephana* Boiss.	M [IT] [Th]
Asteraceae	*Carduus pycnocephalus* L.	M [Med, IT] [Th]
Asteraceae	*Carthamus oxyacantha* M.Bieb.	M [IT] [Th]
Asteraceae	*Centaurea aucheri* (DC.) Wagenitz	LEM [IT] [He]
Asteraceae	*Centaurea gaubae* (Bornm.) Wagenitz	LE [IT] [He]
Asteraceae	*Centaurea ispahanica* Boiss.	LEM [IT] [He]
Asteraceae	*Centaurea virgata* Lam.	M [ES, Med, IT] [He]
Asteraceae	*Centaurea xeranthemoides* Rech.f.	E [IT] [He]
Asteraceae	*Chardinia orientalis* (L.) Kuntze	M [IT] [Th]
Asteraceae	*Cichorium intybus* L.	M [Plur] [He]
Asteraceae	*Cirsium bracteosum* DC.	LEM [IT] [He]
Asteraceae	*Cirsium sorocephalum* Fisch. & C.A.Mey.	[Med, IT] [He]
Asteraceae	*Cirsium* sp.	[He]
Asteraceae	*Cirsium spectabile* DC.	LE [IT] [He]
Asteraceae	*Cousinia calcitrapa* Boiss.	LE [IT] [He]
Asteraceae	*Cousinia* sp.	[He]
Asteraceae	*Cousinia tenuiramula* Rech.f.	ER [IT] [He]
Asteraceae	*Crepis sancta* (L.) Babc.	M [Med, IT, SS] [Th]
Asteraceae	*Crupina crupinastrum* Vis.	M [Med, IT] [Th]
Asteraceae	*Cyanus depressus* (M.Bieb.) Soják	M [IT] [Th]
Asteraceae	*Echinops leiopolyceras* Bornm.	[IT] [He]
Asteraceae	*Gundelia tournefortii* L.	M [Med, IT] [He]
Asteraceae	*Helichrysum oligocephalum* DC.	LEM [IT] [Ch]
Asteraceae	*Hertia angustifolia* Kuntze	LEM [IT] [Ch]
Asteraceae	*Jurinea berardioides* (Boiss.) O.Hoffm.	[IT] [He]
Asteraceae	*Jurinea carduiformis* Boiss.	[IT] [He]
Asteraceae	*Lactuca microcephala* DC.	[IT] [He]
Asteraceae	*Lactuca orientalis* Boiss.	[IT] [He]
Asteraceae	*Lactuca persica* Boiss.	[IT] [Th]
Asteraceae	*Launaea acanthodes* (Boiss.) Kuntze	EM [IT] [He]
Asteraceae	*Onopordum leptolepis* DC.	M [IT, SS] [He]
Asteraceae	*Phagnalon nitidum* Fresen.	[IT] [He]
Asteraceae	*Picris strigosa* M.Bieb.	E [IT] [He]
Asteraceae	*Rhaponticum repens* (L.) Hidalgo	M [IT] [He]
Asteraceae	*Scorzonera laciniata* Jacq.	M [ES, Med, IT] [He]
Asteraceae	*Serratula latifolia* Boiss.	M [IT] [He]
Asteraceae	*Siebera nana* (DC.) Bornm.	[IT] [Th]
Asteraceae	*Sonchus oleraceus* L.	M [Cosm] [Th]
Asteraceae	*Stizolophus balsamita* (Lam.) Cass. ex Takht.	[IT] [Th]
Asteraceae	*Tanacetum polycephalum* Sch.Bip.	LEM [IT] [He]
Asteraceae	*Tragopogon porrifolius* L.	[ES, Med, IT] [He]
Dipsacales		
Caprifoliaceae	*Lomelosia olivieri* (Coulter) Greuter & Burdet	[IT] [Th]
Caprifoliaceae	*Pterocephalus canus* Coult. ex DC.	[IT] [He]
Caprifoliaceae	*Valeriana sisymbriifolia* Vahl	M [IT] [He]
Caprifoliaceae	*Valerianella oxyrhyncha* Fisch. & C.A.Mey.	M [IT] [Th]
Caprifoliaceae	*Valerianella* sp.	[Th]
Apiales		
Apiaceae	*Bunium* sp.	[Cr]
Apiaceae	*Chaerophyllum macrospermum* (Willd. ex Schult.) Fisch. & C.A.Mey.	[IT] [He]
Apiaceae	*Ducrosia anethifolia* Boiss.	M [IT, SS] [He]
Apiaceae	*Echinophora platyloba* DC.	LEM [IT] [He]
Apiaceae	*Eryngium billardierei* Heldr. ex Boiss.	M [ES, Med, IT] [He]
Apiaceae	*Ferula ovina* Boiss.	M [IT] [He]
Apiaceae	*Ferula* sp.	[He]
Apiaceae	*Ferulago* sp.	[He]

http://www.aloki.hu ● ISSN 1589 1623 (Print) ● ISSN 1785 0037 (Online)
DOI: http://dx.doi.org/10.15666/aeer/2001_001019

Apiaceae	*Prangos ferulacea* Lindl.	M [ES, IT] [He]
Apiaceae	*Scandix stellata* Banks & Sol.	M [ES, IT, SS] [Th]
Apiaceae	*Smyrniopsis* sp.	[He]
Apiaceae	*Smyrnium cordifolium* Boiss.	M [IT] [He]
Apiaceae	*Turgenia latifolia* Hoffm.	M [ES, Med, IT] [Th]
Apiaceae	*Zosima absinthifolia* absinthifolia	M [IT] [He]

Right column: L: Lower risk, E: Endemic (to Iran), M: Medicinal, V: Vulnerable. First Backet: Chorotypes; IT: Irano-Turanian, ES: Euro-Siberian, Med: Mediterranean, SS: Saharo-Sindian. Second Backet: Life Form: Ph: Phanerophyte, Ch: Chamaephyte, He: Hemicryptophyte, Cr: Cryptophyte, Th: Therophyte

The second dataset which was compiled to compare among local floras in north-eastern Bakhtiari province (*Table 2*, map in *Fig. 3*), consisted of a matrix of species occurrence data in 8 adjacent floras (Heydari-Ghahfarrokhi et al., 2012; Tahmasebi, 2014a; Kafash-Saei et al., 2014b; Jalali et al., 2016; Dehghani et al., 2016; Naghipoor-Borj et al., 2016; Vahabi et al., 2018). This dataset comprises of 714 species (9.5% of the total species in Iran), belonging to 323 genera and 60 families. Species to family, genera to family and species to genus ratios are 11.9, 5.38, and 2.21, respectively. This compiled dataset consists of 16 rare, 133 endemics (to Iran), and 258 medicinal plant species. The largest families in dataset 2 in terms of species richness are Asteraceae (15.4%), Fabaceae (11.2%), and Brassicaceae (8.4%). The largest families in terms of generic richness are Asteraceae (14%), Brassicaceae (11%) and Poaceae (10%). The most-rich genera are *Astragalus* (35 spp), *Euphorbia* (18 spp), and *Salvia* (12 spp). 244 genera (out of of 323) are represented in this area by only one or two species, resulting in sp/gen ratio as low as 2.21. Although components (local floras) of dataset 2 encompass an area of only 146000 ha; i.e. they are not much far apart, beta diversity (variation between sites) was significant. *Table 1* presents names, geographical coordinates, alpha and beta diversity measures of each local flora in the second dataset. Flora of Sheida protected area (id: 229) was the most species-rich site in this area (alpha diversity = 314). Beta diversity (variation between sites) ranged from 112 to 363. Flora Farrokhshahr (id: 264, alpha= 95) and Margh (id: 213, alpha= 55) were the most similar local floras, and flora Sheida (id: 229, alpha= 314) and Babazaki (dataset 1, id: 534, alpha= 257) were the most dissimilar local floras (*Table 1*). Gamma diversity (net count of species in the second dataset) was 714. Beta diversity between Babazaki and its adjacent floras range from 260 to 363, indicating a relatively high variation between sites.

Comparison between dataset 1 (Babazaki flora) and the set of its adjacent local floras in dataset 2 is summarized in *Fig. 5*. Babazaki flora (set A) shares 178 species with its adjacent local floras (set B). There are 457 species growing in local floras of set B, which are not observed in Babazaki (set A). Babazaki flora, on the other hand, comprises of 79 species not reported from set B floras. Results demonstrated that diversity of plant species in Babazaki flora is significantly different from its adjacent sites.

http://www.aloki.hu ● ISSN 1589 1623 (Print) ● ISSN 1785 0037 (Online)
DOI: http://dx.doi.org/10.15666/aeer/2001_001019

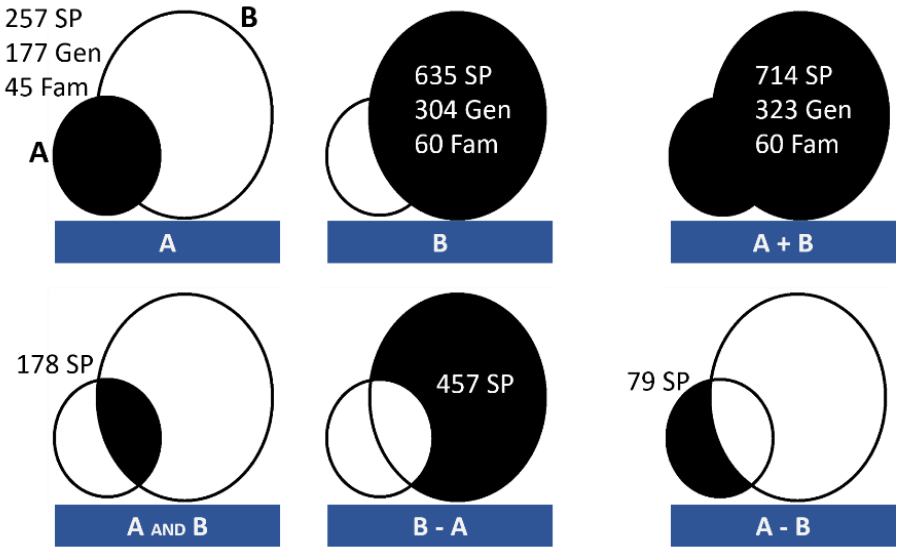

Figure 5. *A brief comparison of Babazaki flora (set A) with a compilation of seven adjacent local floras (set B). See text for more details*

The third dataset in this study, comprises of twenty-two local floras (*Table 2*) in a broader area consisting various sites in two provinces Bakhtiari and Esfahan (Parishani, 2005; Shahrokhi, 2005; Yousofi, 2006; Assadi et al., 2009; Yousofi et al., 2011; Pairanj et al., 2011; Heidari et al., 2012; Kafash-Saei et al., 2014a,b; Shirmardi et al., 2014a,b; Tahmasebi, 2014a,b; Dehghani et al., 2016; Jalali et al., 2016; Naghipoor-Borj et al., 2016; Hasanzadeh et al., 2017; Iranmanesh et al., 2017; Gholami et al., 2018; Vahabi et al., 2018). The map in *Fig. 3* shows geographical distribution of the local floras in the third dataset, in which the location of Babazaki is shown with a black arrow. This dataset comprises of 1512 species (20.1% of the Iranian flora), belonging to 517 genera and 96 families. Species to family, genera to family and species to genus ratios were 15.75, 5.38, and 2.92, respectively. Checklist of the third dataset consists of 60 rare, 318 endemics (to Iran), and 510 medicinal plant species. There are 4 endangered, 22 vulnerable and 202 lower-risk category species present in this dataset.

Discussion

Results of multivariate analysis of the third dataset (22 sites × 1439 spp), using different K values, showed that the 22 local floras (objects) could be separated into four well-defined groups. Flora of Babazaki and Sheet mountain area, along with six more adjacent local floras: Kakolak (id 380), Karsanak (id 259), Tang-e-Sayad (id 211), Farrokh-Shahr (id 264), Darreh_Sir (id 260) and Broujen (id 214) made the first group. This group consists of 624 species, 299 genera and 60 families. There are 74 descriptive species in local floras of group 1 which are not found in other three groups of local floras in the third dataset. Local floras of group 1, are characterized also by 115 endemics (to Iran), 13 rare, 222 medicinal and 100 range species. One endangered species (*Ferula assa-foetida*), five vulnerable (*Astragalus cyclophyllon*, *A. griseus*, *A. pinetorum*, *Isatis campylocarpa*, *Ziziphora clinopodioides*) and 84 species in lower risk category, are growing in this group of local floras.

http://www.aloki.hu ● ISSN 1589 1623 (Print) ● ISSN 1785 0037 (Online)
DOI: http://dx.doi.org/10.15666/aeer/2001_001019

Second group in *Fig. 6* consists of five local floras including flora Jahanbin mountain area (id 232), Saldaran protected area (id 344) and Vanak (id 2), and also two small floras Margh (id 213), and wetlands of the province (id 438). This group consists of 852 species, 386 genera and 86 families. There are 271 descriptive species in local floras of group 2, not found in other groups. Local floras of group 2, consist of 154 endemics (to Iran), 31 rare, 292 medicinal and 152 range species. One endangered species (*Ferula persica*), ten vulnerable and 105 species in lower risk category, are growing in local floras of this group.

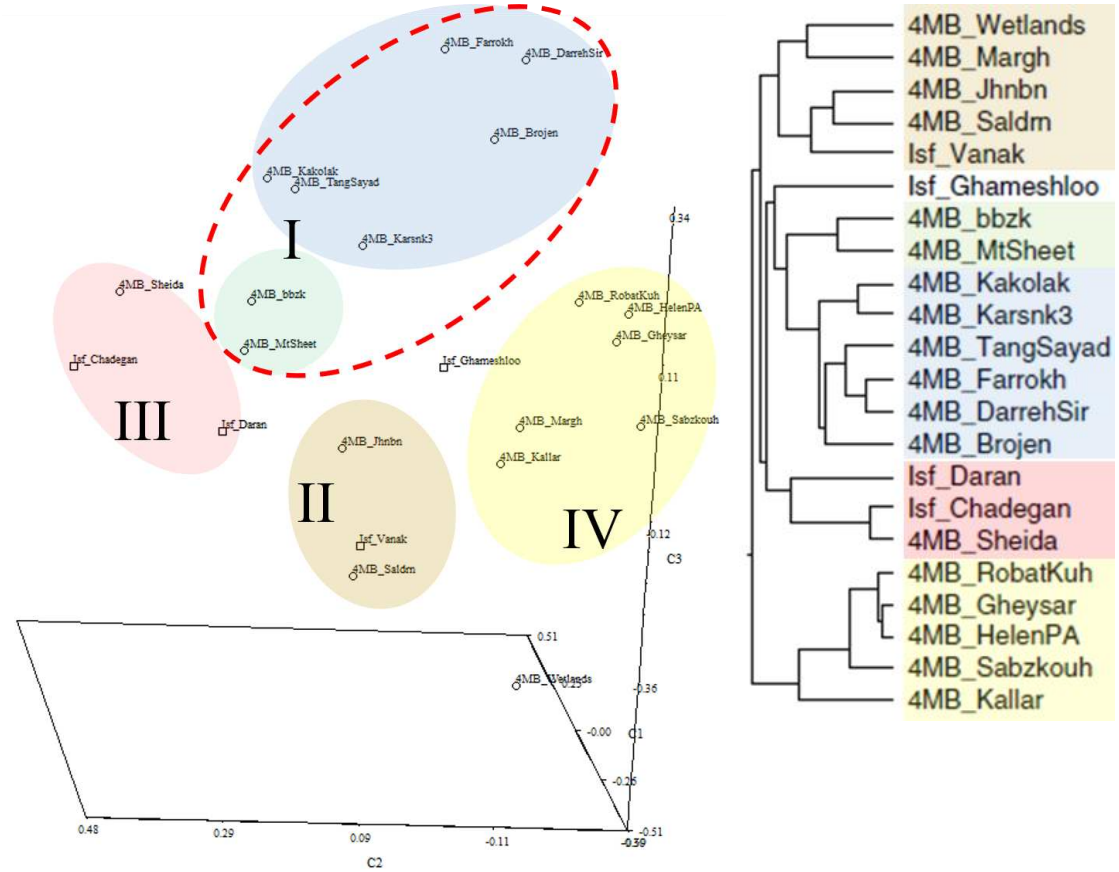

Figure 6. *Left: Ordination plot of third dataset (data matrix of presence/absence data of 22 local floras). Right: Clustering diagram demonstrating four coherent groups (K=4). Floras Babazaki and Sheet mountain areas are a subgroup of the group 1 (colored with pale blue); see text for more details*

Three closely related floras Daran (id 348), Chadegan (id 7) and Sheida (id 229) constitute the third group in *Fig. 6*. Group 3 consists of 601 species, 309 genera and 71 families. There are 139 descriptive species in group 3 which are not found in other three groups. Group 3 local floras, consist of 119 endemics (to Iran), 21 rare, 322 medicinal and 93 range species. Two endangered species (*Ferula assa-foetida* and *Dracocephalum kotschyi*), four vulnerable (*Tribulus terrestris*, *Astragalus cyclophyllon*, *Ziziphora clinopodioides* and *Scabiosa persica*) and 78 species in lower risk category, are growing in local floras of this group.

http://www.aloki.hu ● ISSN 1589 1623 (Print) ● ISSN 1785 0037 (Online)
DOI: http://dx.doi.org/10.15666/aeer/2001_001019

Forth group on the dendrogram consists of five local floras: Robat-Kouh (id 515), Gheysari protected area (id 183), Helen protected area (id 194), Sabzkouh protected area (id 254) and Kallar mountain area (id 149). This group consists of 828 species, 402 genera and 86 families, and there are 216 descriptive species in local floras of group 4, not found in other three groups. Group 4 *local* floras, consist of 178 endemics (to Iran), 26 rare, 308 medicinal and 114 range species. Two endangered species (*Ferula assa-foetida* and *Astragalus phlomoides*), 13 vulnerable and 111 lower risk category species are growing in this group.

Flora of Ghameshloo (id 31) which is poorly studied, appeared as an outlier of the groups described above. Of 78 species (61 genera and 22 fams), identified from this site, 26 species were exclusive relative to other 21 members of the third dataset. The majority of taxa in the three datasets in this study are hemicryptophytes; a life form adopted by plants of this region to cope with the relatively scarce water, and cold temperature in the high-*altitude* region of central Zagros. Most of the species in family Asteraceae, prevalent in this region, showed this life form. The checklist of northeastern Bakhtiari Province of Iran (dataset 2) counts 714 species of flowering plants belonging to 60 families, with 65% of the species belonging to the 6 largest families, i.e. Asteraceae (110 spp), Fabaceae (80 spp), Brassicaceae (60 spp), Lamiaceae (54 spp), Poaceae (52 spp), and Apiaceae (42 spp).

Conclusion

Sixty species growing in Babazaki flora, which were not reported from adjacent local floras in dataset 2 could be regarded as an indication of significant variation among nearby local floras in this study. Understanding the biodiversity and distribution of taxa in this region is difficult, because datasets are usually incomplete, not easily accessible or inconsistent. Compilation of datasets and comparisons between them could easily become unreliable due to ongoing taxonomic revisions. Floristic databases such as Alamut (is developing and used by the author in this study), are necessary tools for converting scientific names to consistent data. Diversity, endemism and IUCN conservation categories in the central Zagros have been underestimated in previously reports (Vajari et al., 2014). Results of this study may provide a considerable update on the available information on the floristic diversity and distribution of taxa in the studied local floras. Conservation of biodiversity in central Zagros could be challenging for more reasons, including: incomplete knowledge, unassessed dark diversity, land-use histories, gradual climate change, and the increasing encroachment of habitats by humans. Resulting checklist in this study would help botanical research and nature conservation planning in the region. Datasets compiled in this study are deposited in the Alamut floristic database, which is intended to grow in size, to be the core base for future investigations. Further sampling in gap location may elucidate the dark diversity although it is also expected that certain missing taxa could simply have not habituated in some sites.

Acknowledgements. This study was supported by the Deputy of Research at the Shahrekord University (grants 99GRN31M873 and 98GRD30M873). Iranian National Science Foundation; INSF supported the software and floristic database system development (Grant no. 91003358).

REFERENCES

http://www.aloki.hu ● ISSN 1589 1623 (Print) ● ISSN 1785 0037 (Online)
DOI: http://dx.doi.org/10.15666/aeer/2001_001019

[1] Assadi, E., Ebrahimi, A., Shahrokhi, A., Shirmardi, H. A. (2009): Introducing plant vegetation and collecting specimens of sabz-e kouh region. – Scientific Report, Environmental organization of Chaharmahal and Bakhtiari, Iran.
[2] Assadi, M. (1989-2016): Flora of iran. – Research Institute of Forests and Rangelands, Tehran, Iran. (in Persian).
[3] Davis, P. H. (1965-1985): Flora of Turkey and the East Aegean Island. – Edinburgh: Edinburgh University Press.
[4] Dehghani, R., Sharifi-Tehrani, M., Shirmardi, H. A. (2016): Floristic study of sheet mountain in Chaharmahal and Bakhtiari province, Iran. – Taxonomy and Biosystematics Journal 8(26): 61-76.
[5] Djamali, M., De Beaulieu, J. L., Miller, N. F., Andrieu-Ponel, V., Ponel, P., Lak, R., Sadeddin, N., Akhani, H., Fazeli, H. (2009): Vegetation history of the se section of the Zagros mountains during the last five millennia; a pollen record from the Maharlou lake, Fars province, Iran. – Vegetation History and Archaeobotany 18(2): 123-136.
[6] Finnie, T. J., Preston, C. D., Hill, M. O., Uotila, P., Crawley, M. J. (2007): Floristic elements in European vascular plants: An analysis based on atlas florae Europaeae. – J Biogeogr 34(11): 1848-1872.
[7] Gholami, P., Shirmardi, H. A., Lashkari-Sanami, N. (2018): Investigation of flora, biological form and geographical distribution of plants in Robat Kouh area, Bazoft county, Chaharmahal and Bakhtiari province, Iran. – Taxonomy and Biosystematics 37: 87-114.
[8] Hasanzadeh, F., Kharazian, N., Parishani, M. R. (2017): Floristic, life form, and chorological studies of Saldaran protected region, Chaharmahal and Bakhtiari province, Iran. – Journal of Genetic Resources 3(2): 113-129.
[9] Heydari-Ghahfarrokhi, Z., Tavakoli, M., Tahmasebi, P. (2012): Floristic study of Tang-e-sayad portected area of Shahrekord. – Paper presented at: Proceedings of First national conference on environmental protection and planning, 3 Esfand 1391, Hamedan, Iran.
[10] Heywood, V. H. (2004): Modern approaches to floristics and their impact on the region of sw Asia. – Turkish Journal of Botany 28(1-2): 7-16.
[11] Huson, D. H., Bryant, D. (2006): Application of phylogenetic networks in evolutionary studies. – Molecular Biololgy Evolution 23(2): 254-267.
[12] Iranmanesh, Y., Jalili, A., Shirmardi, H. A., Jahanbazi-Goujani, H. (2017): Flora, life form and chorology of plants in the important wetlands of Chaharmahal and Bakhtiari province. – Taxonomy and Biosystematics 9(30): 83-104.
[13] Jalali, M., Sharifi-Tehrani, M., Shirmardi, H. A. (2016): Flora of Jahanbin mountain area: A contribution to flora of the central Zagros region of Iran. – Journal of Genetic Resources 2(1): 26-40.
[14] Jalili, A., Jamzad, Z. (1999): Red data book of Iran: A preliminary survey of endemic, rare and endangered plant species in Iran. – Research Institute of Forests and Rangelands, Tehran.
[15] Kafash-Saei, E., Ghaderi, N., Moradi, M. (2014a): Floristic evaluation of Darreh-sir basin in Bakhtiari province. – Paper presented at: First National Conference on Sustainable Agriculture and Natural Resources, Tehran, Iran.
[16] Kafash-Saei, E., Ghaderi, N., Moradi, M. (2014b): Floristic study of downstream of Farrokhshahr basin in Chaharmahal and Bakhtiari province. – Paper presented at: First National Conference on Sustainable Agriculture and Natural Resources, Tehran, Iran. (in Persian).
[17] Karypis, G. (2003): Cluto: A clustering toolkit, release 2.1.1. – Minneapolis, MN: University of Minnesota, Department of Computer Science.
[18] Khitun, O. V., Koroleva, T. M., Chinenko, S. V., Petrovsky, V. V., Pospelova, E. B., Pospelov, I. N., Zverev, A. (2016): Applications of local floras for floristic subdivision and monitoring vascular plant diversity in the Russian arctic. – Arctic Science 2(3): 103-126.

http://www.aloki.hu ● ISSN 1589 1623 (Print) ● ISSN 1785 0037 (Online)
DOI: http://dx.doi.org/10.15666/aeer/2001_001019

[19] Lewis, R. J., Szava-Kovats, R., Pärtel, M. (2016): Estimating dark diversity and species pools: An empirical assessment of two methods. – Methods in Ecology and Evolution 7(1): 104-113.
[20] Naghipoor-Borj, A. A., Ghasareh-Ardestani, E., Raeisi, M., Noroozi, S., Taheri, F. (2016): Flora, life forms and phytogeography of vegetations in Kakolak region in Bakhtiari province. – Paper presented at: First Symposium of Natural resources in C. Zagos, Shahrekord, Iran.
[21] Pairanj, J., Ebrahimi, A., Tarnain, F., Hassanzadeh, M. (2011): Investigation on the geographical distribution and life form of plant species in sub alpine zone Karsanak region, Shahrekord. – Taxonomy and Biosystematics 3(7): 1-10.
[22] Parishani, M. R. (2005): Flora of Vanak region of Semirom (Isfahan province). – Pajouhesh-va-Sazandegi 68: 84-103.
[23] Pärtel, M., Szava-Kovats, R., Zobel, M. (2011): Dark diversity: Shedding light on absent species. – Trends in Ecology and Evolution 26(3): 124-128.
[24] Pärtel, M., Szava-Kovats, R., Zobel, M. (2013): Community completeness: Linking local and dark diversity within the species pool concept. – Folia Geobotanica 48(3): 307-317.
[25] Raunkiaer, C. (1934): The life forms of plants. – Oxford: Oxford University Press.
[26] Rechinger, K. H. (1963-2012): Flora Iranica. – Wien: Naturhistorisches Museum: Graz: Akademische Druck-und Verlasanstalt.
[27] Rohlf, F. J. (2000): Ntsys-pc: Numerical taxonomy and multivariate analysis system, version 2.1. – Setauket, NY: Exeter Software.
[28] Shahrokhi, A. (2005): Study of Kallar mountain in Charmahal and Bakhtiari province. – MSc Thesis, University of Urmia, Urmia, Iran.
[29] Sharifi-Tehrani, M. (2014): Introduction of the new program "checkname" with applications in integration and increased precision and certitude of floristic inventories. – Taxonomy and Biosystematics 6(20): 111-121.
[30] Sharifi-Tehrani, M., Rahiminejad-Ranjbar, M. R. (2013): Compilation of floristic and herbarium specimen data in iran: Proposal to data structure. – Taxonomy and Biosystematics 5(15): 94-75.
[31] Shirmardi, H. A., Heydari, G., Gholami, P., Mozaffarian, V., Tahmassebi, P. (2014a): A study of flora in rangelands of Gheissari Koohrang region in Chaharmahal and Bakhtiari province. – Taxonomy and Biosystematics 6(18): 85-104.
[32] Shirmardi, H. A., Mozaffarian, V., Gholami, P., Heidari, G., Safaei, M. (2014b): Introduction of the flora, life form and chorology of Helen protected area in Chaharmahal and Bakhtiari province. – Journal of Plant Biology 6(20): 75-96.
[33] Tahmasebi, P. (2014a): Flora of Margh area, in Shahrekord, Iran. – University of Shahrekord (unpublished data).
[34] Tahmasebi, P. (2014b): Floristic study of Broojen hunting prohibited region. – Shahrekord University (unpublished data).
[35] Talbot, S. S., LeBlanc, M. C., Aiken, S. G. (2007): Floristic Subregions of the Canadian Arctic Archipelago. – In: Conservation of Arctic Flora and Fauna (CAFF) Flora Group Workshop, Faroe Islands, May 2007.
[36] Tolmatchev, A. I. (1931): About the methods of comparative floristics' investigations. 1. Flora concept in comparative floristics. – Zhurnal Russkogo botanicheskogo obschestva 16(1): 111-124.
[37] Tutin, T. G., Heywood, V. H., Burges, N. A., Moore, D. M., Valentine, D. H., Walters, S. M., Webb, D. A. (1968-1980): Flora Europaea. – Cambridge University Press, Cambridge.
[38] Vahabi, M. R., Tarkesh-Isfahani, M., Farhang, H. R., Salehi, A. (2018): The investigation of the flora, life forms and chorotypes of the plants in the Sheida protected area Chaharmahal and Bakhtiari province, Iran. – Journal of Plant Research (Iranian Journal of Biology) 31(2): 335-345. (in Persian).

http://www.aloki.hu ● ISSN 1589 1623 (Print) ● ISSN 1785 0037 (Online)
DOI: http://dx.doi.org/10.15666/aeer/2001_001019

[39] Vajari, K. A., Veiskarami, G., Attar, F. (2014): Recognition of endemic plants in Zagros region (case study: Lorestan province, Iran). – Ecologia Balkanica 6(1): 95-101.
[40] Van Der Maaten, L., Schmidtlein, S., Mahecha, M. D. (2012): Analyzing floristic inventories with multiple maps. – Ecological Informatics 9: 1-10.
[41] Veiskarami, G., Sharifi-Tehrani, M. (2017): Plant species diversity in the central Zagros region of Iran. – Phytologia Balcanica: International Journal of Balkan Flora and Vegetation 23(1): 101-118.
[42] Yousofi, M. (2006): An introductory survey of the vegetation units of Ghameshloo wildlife refuge. – Iranian Journal of Biology 3(19): 355-362.
[43] Yousofi, M., Safari, R., Nowroozi, M. (2011): An investigation of the flora of the Chadegan region in Isfahan province. – Journal of Plant Biology 9: 75-96.
[44] Zohary, M. (1973): Geobotanical foundations of the middle east. – Stuttgart: Fischer.

http://www.aloki.hu ● ISSN 1589 1623 (Print) ● ISSN 1785 0037 (Online)
DOI: http://dx.doi.org/10.15666/aeer/2001_001019

BIOMONITORING OF HEAVY METAL POLLUTION USING THE BROWN SEAWEED *ERICARIA SELAGINOIDES* ALONG THE ATLANTIC COAST OF MOROCCO

BOUNDIR, Y.[1,2,3*] – HAROUN, R.[2] – SÁNCHEZ DE PEDRO, R.[4] – HASNI, M.[5] – OUAZZANI, N.[1,3] – MANDI, L.[1,3] – RAFIQ, F.[6] – WEINBERGER, F.[7] – CHERIFI, O.[1,3]

[1]*Lab. Water, Biodiversity and Climate Changes, Fac. Sciences Semlalia, Cadi Ayyad University, Bd. Prince My Abdellah, PO Box 2390, 40000 Marrakesh, Morocco*

[2]*Biodiversity & Conservation Research Group, IU-ECOAQUA, Univ. Las Palmas de Gran Canaria, Crta. Taliarte s/n, 35214 Telde, Canary Islands, Spain*

[3]*National Center for Studies and Research on Water and Energy (CNEREE), Cadi Ayyad University. Avenue Abdelkrim Khattabi, PO Box 511, 40000 Marrakesh, Morocco*

[4]*Universidad de Málaga, Andalucía Tech, Departamento de Botánica y Fisiología Vegetal, Campus de Teatinos, 29010 Málaga, Spain*

[5]*Fac. Sciences, Ibn Zohr University, PO Box 8106, 80000 Agadir, Morocco*

[6]*Environment and Health Team, Polydisciplinary Fac. Cadi Ayyad University. Route Sidi Bouzid PO Box 4162 Avenue Mohamed Belkhadir, 46000 Safi, Morocco*

[7]*GEOMAR Helmholtz-Center for Ocean Research, Düsternbrooker Weg 20, 24105 Kiel, Germany*

[*]*Corresponding author*
e-mail: younes.boundir@ced.uca.ma; phone: +212-638-846-052; fax: +212-0543-3170

(Received 24th Jun 2021; accepted 1st Oct 2021)

Abstract. Increased pollution in the coastal areas may cause changes in the biodiversity of marine organisms depending upon their physiological capacity and resilience to thrive under stressing environmental conditions. The present research evaluates the heavy metals pollution degree of coastal waters using the macroalgae *Ericaria selaginoides* as bioindicator along the Atlantic coast of Morocco. Eight stations were chosen: two located near Eljadida city, three nearby Safi city and three around the city of Essaouira. Results showed that the heavy metal content in the thalli of *E. selaginoides*, in seawater and sediment varied seasonally. At the same time, it was negatively correlated with algal biodiversity onsite. However, the Chemical Oxygen Demand was significantly higher at the polluted station S5 than at other stations, while Dissolved Oxygen and Biological Oxygen Demand were lower. *E. selaginoides* accumulated metals in the following order Fe > Zn > Mn > Cu > Ni > Pb > Cr > Cd. In conclusion, *E. selaginoides* is overall more resilient to heavy metal pollution than other marine organisms in the Atlantic coast of Morocco, as indicated by substantially elevated concentrations of heavy metals in some sites. Our results support that *E. selaginoides* would be a suitable bioindicator for monitoring of heavy metals in polluted coastal areas.
Keywords: *bioindicator, ecotoxicology, marine water quality, monitoring, seaweed resilience*

Introduction

Due to anthropogenic pressure resulting mainly from high population densities and the concentration of diverse anthropogenic activities along shorelines many coastal areas are among the most severely degraded ecosystems worldwide (Lotze et al., 2001; Halpern et

http://www.aloki.hu ● ISSN 1589 1623 (Print) ● ISSN 1785 0037 (Online)
DOI: http://dx.doi.org/10.15666/aeer/2001_021041

al., 2008). Correspondingly, littoral and sublittoral communities are particularly sensitive to such pressures since they are exposed to a wide range of extreme environmental conditions at the edge of marine, as well as terrestrial realms (Crowe et al., 2000; Martínez et al., 2012).

Heavy metal contamination is an environmental issue of increasing importance in many coastal areas, especially when those metals are found at concentrations higher than natural loads (Islam and Tanaka, 2004; Akcali and Kucuksezgin, 2011; Scherner et al., 2013; Thibaut et al., 2015). In aquatic ecosystems, metals are naturally found at low concentrations, and are distributed among the different compartments of the aquatic ecosystem, such as organisms, water, or sediments (Squadrone et al., 2018; Haghshenas et al., 2020). Brown algae have been reported to be often severely affected by heavy metal pollution (Alahverdi and Savabieasfahani, 2012).

Macroalgae play a fundamental role in structuring benthic ecosystems and maintaining their ecological balance (Umanzor et al., 2019; Wernberg and Filbee-Dexter, 2019). Apart from their valuable ecosystemic services (Cheminée et al., 2013; Cuadros et al., 2013), they are part of the blue economy due to their industrial and biotechnological interest (Radmer, 1996; Bowles, 2007; Mazarrasa et al., 2013). Seaweeds have been widely used in environmental status assessments for more than 50 years (Bryan et al., 1980, 1985; Rainbow and Phillips, 1993). On one hand, macroalgal biodiversity and abundance have been used as general indicators of the health status of coastal areas, due to their tolerance or sensitivity to marine pollutants (Levine, 1984; Norton et al., 1996; Vasquez and Guerra, 1996; de Caralt et al., 2019). On the other hand, seaweeds can be good indicators of micropollution (Gopinath et al., 2011; Sekabira et al., 2011), and have been used to obtain information on the concentrations or availability of heavy metals in their surrounding environment (Melville and Pulkownik, 2006; Akcali and Kucuksezgin, 2011). There is an extensive scientific literature concerning macroalgae as marine organisms that may bioaccumulate metals and micropollutants up to levels many times higher than those found in the surrounding waters (i.e. Jones, 1922; Black and Mitchell, 1952; Farías et al., 2002; Varma et al., 2011; Gubelit et al., 2016). As one of the main primary producers in coastal systems, seaweeds may facilitate the entry of pollutants into aquatic food chains via a biomagnification process, which increases their relevance as bioindicators of the ecological status of aquatic ecosystems (Conti et al., 2007; Conti and Finoia, 2010).

In recent years, Morocco has experienced a tremendous population growth, concomitantly with a significant acceleration in urbanization and land use for industrial and agricultural purposes. All these human-derived processes have led to a huge increase in the discharge of a wide range of pollutants into coastal waters, causing deleterious effects on the various components of the aquatic environment, including macroalgae (Kaimoussi et al., 2001; Mouradi et al., 2014). The present study aims to characterize the heavy metal content and biomonitoring potential of *Ericaria selaginoides* (Linnaeus) Novoa and Guiry (2020) (Ochrophyta; synonym: *Cystoseira tamariscifolia*), a warm temperate brown seaweed widely distributed in the Eastern Atlantic and the Mediterranean Sea (Guiry and Guiry, 2020). Diverse species included in the basal genus *Cystoseira* (Orellana et al., 2019) meet with the pre-requisites proposed by Phillips (1980) for marine bioindicator organisms and are among the most used seaweeds in biomonitoring. Heavy metal pollution occasionally caused disappearance of these species from habitats (Sales et al., 2011; Thibaut et al., 2015; Celis-Plá et al., 2018). A previous study conducted by Boundir et al. (2019) in the same Moroccan coastal section

http://www.aloki.hu ● ISSN 1589 1623 (Print) ● ISSN 1785 0037 (Online)
DOI: http://dx.doi.org/10.15666/aeer/2001_021041

investigated in the present work demonstrated that while populations of *E. selaginoides* exist in the less polluted areas; their physiology seems to be significantly affected by pollution. Moreover, in the highly polluted areas this brown seaweed tends to disappear (Boundir et al., 2019). Based upon these observations we hypothesized that individuals of *E. selaginoides* will present higher heavy metal content in polluted than less polluted or unpolluted areas. In the present contribution, we aim to test this hypothesis and we present heavy metal concentrations and variation of abiotic parameters in *E. selaginoides* collected across a pollution gradient in three different cities in the Atlantic coast of Morocco. Thus, our study also aimed to test the value of this brown seaweed as a bioindicator of coastal pollution.

Materials and Methods

Target species

The brown seaweed *Ericaria selaginoides* (Linnaeus) (Novoa and Guiry, 2020); Synonyms: *Cystoseira tamariscifolia* (Papenfuss, 1950) and *Carpodesmia tamariscifolia*, Orellana et al. (2019), is the main subject of this study, with extant populations in most of the sampling sites. According to Guiry and Guiry (2020), the geographic distribution of *E. selaginoides* includes the coasts of the Eastern Atlantic from Mauritania to The Netherlands, Ireland and the archipelagos of Azores, Canaries and Cabo Verde, as well as the coast of the Mediterranean Sea.

Sampling sites

The coastline in the study area is characterized by a succession of rocky outcrops and sandy beaches. The coordinates of the sampling sites along the Atlantic coast of Morocco are described in *Table 1*. The eight sampling stations are located near to or within the perimeter of three cities. They were selected as control sites or polluted sites as described in the following paragraph and as indicated in (*Table 1 and Fig. 1*):

- In Eljadida city two stations were designated: Sidi Bouzid beach was selected as a control area (S1) and Jorf Lasfar (S2) as a polluted one. Sidi Bouzid beach was selected as a control site as it has been awarded the eco-label "Blue Flag" starting from 2006 (site ID 7167) by The Mohammed VI Foundation for the Protection of the Environment (F.M.6, 2018), this distinction is renovated each year to beaches that fit the international standard norms of cleanliness. In contrast, the Jorf Lasfar area is characterized by the presence of multiple industrial units, including a phosphate production complex and a thermal power plant (Kaimoussi et al., 2001; Essedaoui and Sif, 2001; Ferssiwi et al., 2004).
- In Safi city three stations were designated: Beddouza (S3) was selected as a less polluted control site, as it is located 34 km North from the industrial city of Safi (Goumri et al., 2018). In contrast, Industrial Area (S4) and Phosphate Area (S5), were selected as polluted sites.
- Finally, in (3) Essaouira city three stations were selected: Moulay Bouzerktoun (S6) is located approximately 15 km north from the enclosure of the city and was selected as a control site since it is the less affected by anthropogenic impact, with just some tourism activities during the summer, than the other two sites. These were Bab Doukala (S7) and the Port (S8), which both receive domestic and some industrial wastewater.

http://www.aloki.hu ● ISSN 1589 1623 (Print) ● ISSN 1785 0037 (Online)
DOI: http://dx.doi.org/10.15666/aeer/2001_021041

Table 1. *Nearest cities and GPS coordinates of the sampling sites of E. selaginoides along the Atlantic coast of Morocco. Type indicates control (C) or polluted (P) stations*

City	ID	Type	Station	Coordinates
Eljadida	S1	C	Sidi Bouzid	33°13’52"N-8°33’17.89"W
	S2	P	Jorf Lasfar	33°08’15"N -8°36’57.28"W
Safi	S3	C	Beddouza	32°32’23.06"N-9°17’2.44"W
	S4	P	Industrial Area	32°17’8.29"N-9°14’50.09"W
	S5	P	Phosphate Area	32°09’53.18"N-9°16’20.83"W
Essaouira	S6	C	Moulay Bouzerktoun	31°38’3.49"N-9°40’31.99"W
	S7	P	Bad Doukala	31°30’56.22"N-9°46’10.89W
	S8	P	The Port	31°30’33.3"N-9°46’30.38W

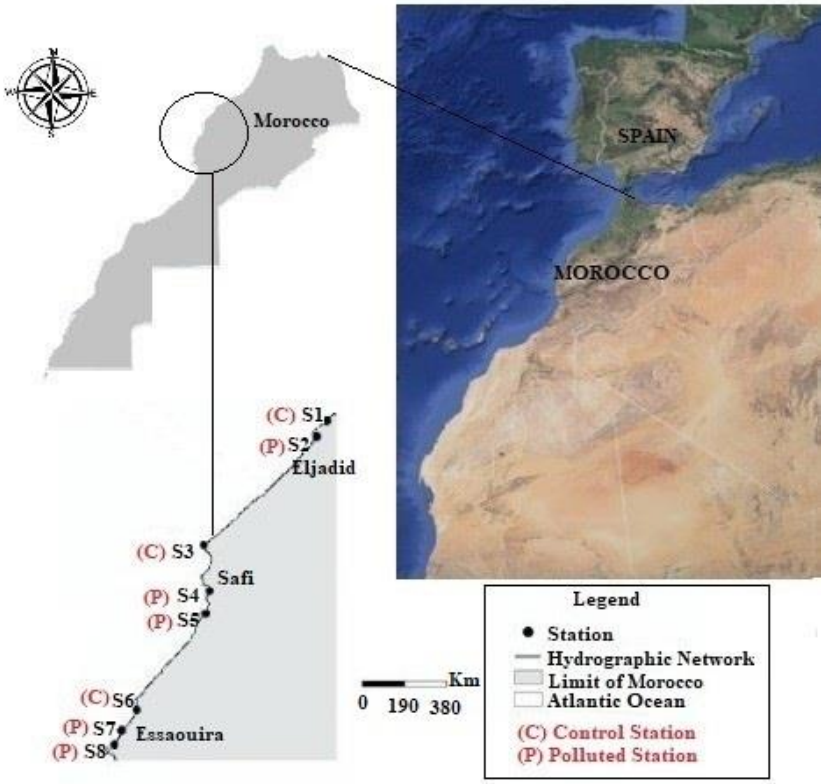

Figure 1. *Study area of E. selaginoides at the Atlantic coast of Morocco with sampling sites located near three cities*

Algal collection, seawater and sediment samples

10 whole individuals of *Ericaria selaginoides* were collected between autumn 2018 and summer 2019, four times at the beginning of each season at eight stations (*Fig. 1*) from hard substrata in the sublittoral zone between 0-5 m below Lowest Astronomical Tide, either by walking from the shoreline at low tide or with mask and fins. The collected specimens were washed in seawater, put in plastic bags and transported in a cooler to the laboratory for later metal analysis.

http://www.aloki.hu ● ISSN 1589 1623 (Print) ● ISSN 1785 0037 (Online)
DOI: http://dx.doi.org/10.15666/aeer/2001_021041

Hydrographical parameters measurements

The seawater abiotic parameters, Temperature (T), pH, Electrical Conductivity (EC), Dissolved Oxygen (DO), Salinity and Total Dissolved Solids (TDS), were measured seasonally in situ at each station, using a multi-parameter probe: Horiba, Model U-5000, Kyoto, Japan. Seawater samples for Chemical Oxygen Demand (COD) and Biological Oxygen Demand (BOD_5) analysis were sampled with algae and measured according to AFNOR, 2001 (French Association of Normalization), NF T90-103 for BOD_5 and NF T90-101 for COD, while the Oxidizable Matter (OM) was calculated according to the following equation:

$$OM = \frac{(BOD5 \times 2) + COD}{3} \quad \text{(Eq.1)}$$

Heavy metals determination in E. selaginoides, seawater and sediment

All samples were analyzed using a SHIMADZU AA-6300 Atomic Absorption Spectrophotometer (Shimadzu Scientific Instruments, Inc., Kyoto, Japan). Triplicates of dried samples of *E. selaginoides* were digested with concentrated HNO_3. Eight metal elements namely Iron, Zinc, Manganese, Nickel, Copper, Lead, Chromium and Cadmium were determined following the methodology of Conti et al. (2010); atomization was carried out with flame (air/acetylene) as described in the mentioned protocol, heavy metal concentration was expressed as µg of metal per gram of algal dry weight ($\mu g.g^{-1}$ DW). Samples of seawater were collected in glass bottles with stabilizing agent (0.5 ml HNO_3) according to the protocol of Rodier (2009) and heavy metal concentration was expressed as $mg.L^{-1}$. Moreover, heavy metal concentrations in sediment samples were determined following the protocol of Tahiri et al. (2005) and concentration are expressed in $mg.g^{-1}$. To prevent contamination, all bottles were drown in the acid.

Statistical analysis

To determine the potential relationships between the heavy metals studied and the abiotic parameters at the different stations, Pearson correlation was applied, using SPSS version 25 (IBM, USA). One-way ANOVA, Principal Component Analysis (PCA) and Cluster Analysis were performed using Statistica 7 (StatSoft Inc., USA) to identify data clusters among the stations, seasons and heavy metals to visualize the distribution of heavy metals and the hydrographical parameters at the eight studied stations. The broken-stick criterion (Jackson, 1993) was followed to identify the number of significant components in the PCA analysis and was obtained with the software PAST (Hammer et al., 2001).

Results

Ericaria selaginoides distribution in the Eljadida-Essaouira section

Ericaria selaginoides was not regularly found at the different sampling stations along the study area during the 4 seasons of 2018/2019; moreover, it was entirely absent during the overall research period from the industrialized areas at Jorf Lasfar coast (S2) and at Safi coast (S4 and S5) as presented in *Fig. 2*.

http://www.aloki.hu ● ISSN 1589 1623 (Print) ● ISSN 1785 0037 (Online)
DOI: http://dx.doi.org/10.15666/aeer/2001_021041

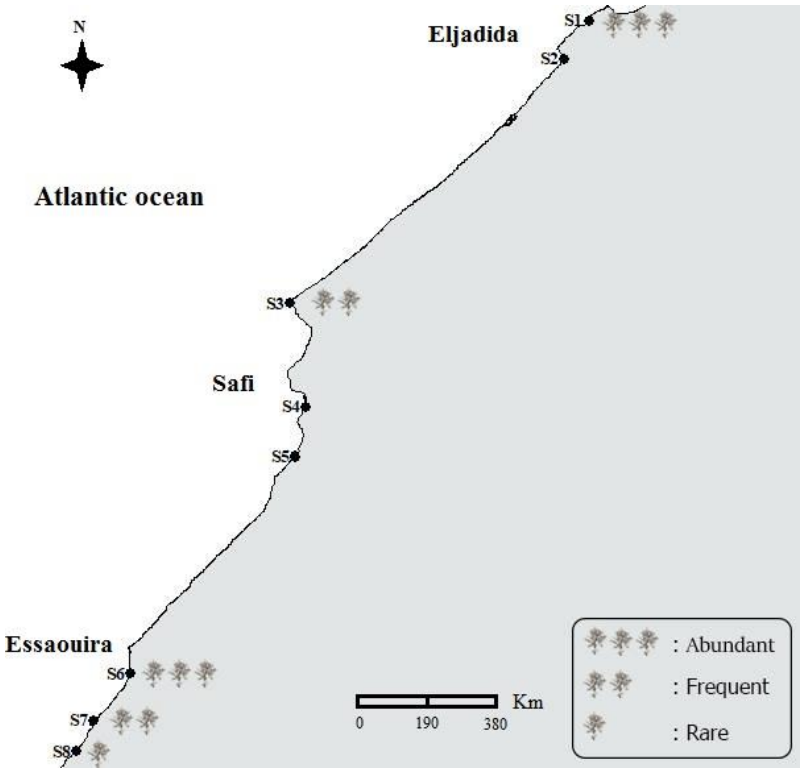

Figure 2. *Overall distribution and abundance of Ericaria selaginoides distribution from Eljadida-Essaouira section during 2019. At S2, S4 and S5 E. selaginoides is absent*

Hydrographical parameters

Temperature (T), pH, electrical conductivity (EC), dissolved oxygen (DO), salinity (Sal) and total dissolved solids (TDS)

The results of the hydrographical parameters, Temperature (T), pH, Electrical Conductivity (EC), Dissolved Oxygen (DO), Salinity (Sal) and Total Dissolved Solids (TDS) of seawater measured in situ during the study period are presented in *Table 2*. Temperature values varied between 14.30 °C during winter at S4 and 25.58 °C during summer at S5. pH values ranged between 6.38 at S3 and 9.00 at S1, and both minimum and maximum were reached during summer. The EC, DO, Sal and TDS values reached maxima of 58 $mS.cm^{-1}$, 9.40 $mg.L^{-1}$, 27.50 σt and 28.00 $g.L^{-1}$ at the same station S1 during summer, and in the case of TDS only during autumn. The minimum of EC was 23.30 $mS.cm^{-1}$ at S4 during autumn and the minimum of DO 4.20 $mg.L^{-1}$ at S5 during winter. Minima of Sal and TDS were around 15.00 σt and 13.90 $g.L^{-1}$, respectively, and both minima were reached during autumn at the same station S4 of Safi city (*Table 2*).

Biological oxygen demand (BOD_5), chemical oxygen demand (COD) and oxydable matter (OM)

The maximum value of BOD_5 was recorded at S3 in summer with 417.34 $mg.L^{-1}$, while the minimum was reached at S5 with only 3.00 $mg.L^{-1}$ during the same summer season. Furthermore, values of COD ranged from 806.40 $mg.L^{-1}$ at S5 in summer to 135.00 $mg.L^{-1}$ at S1 in winter. OM results reached a maximum of 474.18 $mg.L^{-1}$ at S3 in summer and a minimum of 70.00 $mg.L^{-1}$ at S7 in autumn (*Table 3*).

http://www.aloki.hu ● ISSN 1589 1623 (Print) ● ISSN 1785 0037 (Online)
DOI: http://dx.doi.org/10.15666/aeer/2001_021041

Table 2. *Spatial variation of abiotic parameters in situ at the different stations during 2019. EC: Electrical conductivity, DO: Dissolved Oxygen, Sal: Salinity, TDS: Total Dissolved solids*

Station	Season	T (°C)	pH	EC (mS.cm^{-1})	DO mg/L	Sal (σt)	TDS (g.L^{-1})
S1	Autumn	19.80±2.96	8.40±0.35	55.00±3.01	7.15±0.80	26.00±1.62	28.00±1.25
	Winter	16.20±3.08	8.10±0.57	54.30±4.89	8.20±1.12	25.60±3.04	27.80±4.02
	Spring	19.40±3.28	8.20±0.69	49.60±4.69	8.44±1.65	23.00±2.87	25.40±3.39
	Summer	24.50±3.29	9.00±0.74	58.00±5.43	9.40±1.71	27.50±3.38	25.40±3.26
S2	Autumn	18.10±1.75	7.40±0.11	45.00±3.77	6.30±0.60	19.40±2.54	17.20±2.54
	Winter	15.50±1.86	7.30±0.61	52.00±3.36	5.24±0.99	23.10±2.28	21.40±2.06
	Spring	18.60±1.16	7.20±0.63	45.00±3.56	5.22±1.05	19.20±2.38	17.90±2.13
	Summer	20.40±1.36	7.10±0.58	53.00±0.25	6.53±0.63	25.20±0.45	23.40±0.45
S3	Autumn	19.60±1.70	8.60±0.88	53.10±0.47	7.60±0.49	24.20±0.38	22.30±0.63
	Winter	17.30±1.72	8.10±0.78	53.50±13.23	7.88±1.08	24.50±4.13	22.50±3.93
	Spring	20.80±2.90	8.40±0.78	53.60±13.79	8.22±1.75	24.00±4.15	22.30±4.15
	Summer	21.87±2.74	6.38±0.67	54.40±11.52	8.90±1.70	25.00±3.91	23.80±4.06
S4	Autumn	19.30±2.74	7.90±0.49	23.30±7.32	6.00±0.56	15.00±2.84	13.90±2.67
	Winter	14.30±2.84	8.10±0.48	30.50±8.52	4.50±0.35	18.00±3.38	16.00±3.37
	Spring	19.20±2.53	7.70±0.41	35.40±7.46	5.00±0.47	16.00±3.74	14.00±3.68
	Summer	21.86±2.50	6.82±0.46	43.40±4.23	5.50±0.48	22.40±1.27	20.50±1.15
S5	Autumn	16.50±3.17	7.80±0.49	53.00±0.86	5.00±0.33	24.50±0.63	22.40±0.50
	Winter	15.30±2.95	7.80±0.50	53.40±2.55	4.20±1.34	25.70±1.80	23.50±1.48
	Spring	18.80±2.74	8.00±0.46	53.10±3.55	4.63±1.38	25.30±2.31	23.10±2.32
	Summer	23.58±2.80	6.74±0.69	51.20±3.14	5.00±1.16	24.10±1.97	22.30±2.09
S6	Autumn	18.60±1.44	7.20±0.53	47.00±1.42	7.64±0.19	21.10±1.18	19.70±1.33
	Winter	16.00±1.46	7.50±0.43	44.00±0.89	7.50±0.44	19.50±2.36	17.20±2.38
	Spring	17.9±1.05	8.60±0.45	43.20±1.77	7.85±0.47	19.10±2.13	17.30±2.10
	Summer	20.00±1.01	8.00±0.39	45.00±1.77	8.00±0.43	22.00±1.19	20.10±1.12
S7	Autumn	18.80±2.04	7.60±0.40	45.50±2.05	6.85±0.23	25.00±1.79	23.00±1.84
	Winter	17.20±2.09	8.70±0.33	41.00±4.09	7.21±0.36	23.00±2.31	21.50±2.51
	Spring	18.20±2.55	8.10±0.20	43.10±3.96	7.10±0.51	24.50±2.23	22.60±2.38
	Summer	22.60±2.53	7.90±0.28	40.20±3.31	7.50±0.69	20.40±1.40	18.30±1.54
S8	Autumn	18.20±2.86	7.90±0.25	32.30±2.71	6.50±0.44	18.50±1.25	16.30±1.19
	Winter	15.50±3.26	8.40±0.05	39.00±2.78	6.20±0.49	19.90±1.42	17.50±1.35
	Spring	18.80±2.33	8.50±0.04	34.00±0.75	5.60±0.60	16.80±0.10	14.20±0.70
	Summer	23.45±2.00	8.50±0.06	32.50±0.33	6.80±0.45	17.00±0.25	15.60±0.61

Heavy metals

Heavy metals in E. selaginoides

The mean concentrations of heavy metals in *E. selaginoides* showed a decrease in the following order: Fe > Zn > Mn > Cu > Ni > Pb > Cr > Cd (*Table 4*). The highest concentrations of Fe, Zn and Mn were recorded at the Sidi Bouzid station (S1) of Eljadida city, while Cu, Ni, Pb, Cr and Cd peaked at the Port station of Essaouira city (S8) (*Table 4*). According to the Kruskal-Wallis H test (non-parametric one-way ANOVA) for internal heavy metal concentration in *E. selaginoides* differed significantly ($p < 0.05$) among the groups for all metals analyzed (*Appendix Table 8*).

http://www.aloki.hu ● ISSN 1589 1623 (Print) ● ISSN 1785 0037 (Online)
DOI: http://dx.doi.org/10.15666/aeer/2001_021041

Table 3. *Spatial variation of Biological Oxygen Demand (BOD_5) and Chemical Oxygen Demand (COD) mean concentrations in seawater along the studied stations in the Moroccan Atlantic coast during 2018/2019*

Station	Season	BOD_5 ($mg \cdot L^{-1}$)	COD ($mg \cdot L^{-1}$)	OM ($mg \cdot L^{-1}$)
S1	Autumn	144.00±33.59	265.00±73.26	184.33±45.37
	Winter	165.00±36.65	135.00±74.70	155.00±44.12
	Spring	186.00±38.01	265.00±66.28	212.33±36.49
	Summer	294.94±39.55	487.87±56.32	359.25±37.68
S2	Autumn	123.00±42.92	362.00±78.97	202.66±53.64
	Winter	147.00±36.17	564.00±89.33	286.00±49.90
	Spring	232.00±27.77	623.00±117.20	362.33±53.62
	Summer	311.34±41.06	739.56±107.78	454.08±54.96
S3	Autumn	176.00±55.24	316.00±72.47	222.66±58.95
	Winter	243.00±80.23	256.00±76.67	247.33±58.64
	Spring	365.00±88.79	412.00±41.53	380.66±60.09
	Summer	417.34±83.38	587.87±27.62	474.18±60.94
S4	Autumn	56.00±31.84	562.00±72.98	224.66±42.54
	Winter	123.00±37.09	461.00±92.38	235.66±54.46
	Spring	86.00±42.90	522.00±90.38	231.33±57.76
	Summer	203.32±44.61	794.88±90.10	400.50±58.19
S5	Autumn	26.00±6.47	364.00±92.67	138.66±27.96
	Winter	17.00±36.60	497.00±130.90	177.00±23.68
	Spring	33.00±35.24	562.00±142.33	209.33±25.73
	Summer	3.00±49.48	806.40±137.97	270.80±35.66
S6	Autumn	162.00±28.80	171.00±54.22	165.00±32.78
	Winter	95.00±48.03	289.00±51.87	159.66±49.26
	Spring	235.63±51.24	422.35±53.71	297.87±48.92
	Summer	173.00±34.41	364.00±65.51	236.66±35.80
S7	Autumn	14.00±14.82	182.00±79.06	70.00±35.59
	Winter	56.00±16.42	388.00±38.01	166.66±14.19
	Spring	52.00±19.01	498.00±20.82	200.66±15.20
	Summer	86.32±19.40	533.23±44.25	235.29±22.83
S8	Autumn	6.64±1.89	561.48±61.01	191.58±20.87
	Winter	9.23±1.96	465.79±82.62	161.41±28.66
	Spring	10.47±2.59	362.41±141.42	127.78±48.87
	Summer	15.66±1.89	645.25±61.01	225.52±20.87

Heavy metals in sediment and seawater

All mean concentrations of heavy metals in sediment revealed significantly higher values at sites S4 and S5, the polluted stations of the industrial and phosphate zones at Safi city, than at other sites. The average concentrations of Zn, Cu, Pb and Cr do not exceed the standards of the French norm for sediments (FNHMIS, 2000) in all the studied stations. However, the Cd concentration at S5 exceeded the norm threshold value ($3.97>2.4$ $mg.g^{-1}$) (*Table 5*). However, all mean concentrations of heavy metals in seawater were under the Moroccan Norm (FAO 2006). Concentrations of Cu, Pb, Cr and

http://www.aloki.hu ● ISSN 1589 1623 (Print) ● ISSN 1785 0037 (Online)
DOI: http://dx.doi.org/10.15666/aeer/2001_021041

Cd in seawater were the highest concentrations of toxic metals recorded in the two polluted stations near to Safi coast S4 and S5. At the industrial discharges S4 with 1.18±0.09 $\mu g.L^{-1}$ for Cd, 3.26±0.83 $\mu g.L^{-1}$ for Pb, 0.25±0.04 $\mu g.L^{-1}$ for Cu and 1.12±0.15 $\mu g.L^{-1}$ for Cr. The phosphate discharge area S5 with a concentration of 1.10±0.08 $\mu g.L^{-1}$ for Cd, 1.63±0.22 $\mu g.L^{-1}$ for Pb, 0.75±0.13 $\mu g.L^{-1}$ for Cu and 0.92±0.05 $\mu g.L^{-1}$ for Cr (*Table 6*). Furthermore, Fe, Mn and Ni were not detectable in seawater using the spectrophotometer.

Table 4. *Mean concentration (Mean ± SD) in ($\mu g.g^{-1}$ DW) of Fe, Zn, Mn, Ni, Cu, Pb, Cr and Cd in E. selaginoides collected from the Atlantic coast of Morocco during 2018/2019*

Station	Season	Fe	Zn	Mn	Ni	Cu	Pb	Cr	Cd
S1	Autumn	1668.67±2.31	46.65±0.38	20.58±0.64	1.33±0.04	0.22±0.15	2.30±0.08	0.12±0.03	0.10±0.02
	Winter	1201.67±77.36	36.43±1.95	**25.82±2.99**	2.45±0.39	3.77±0.27	1.23±0.02	0.32±0.06	0.23±0.02
	Spring	**1718.67±24.85**	37.82±1.47	16.74±0.67	1.60±0.04	0.38±0.04	1.36±0.12	0.39±0.08	0.35±0.05
	Summer	1056.67±5.13	**49.16±0.32**	20.47±0.34	1.24±0.03	0.16±0.05	0.49±0.03	0.15±0.02	0.11±0.03
S3	Autumn	446.33±30.99	11.46±0.61	6.20±0.17	1.42±0.27	4.04±0.19	2.48±0.03	0.12±0.03	0.20±0.02
	Winter	504.67±16.65	26.88±0.36	16.10±0.42	3.01±0.32	2.60±0.68	2.12±0.06	0.24±0.04	0.43±0.05
	Spring	449.67±10.50	19.50±0.47	15.08±0.12	2.35±0.20	0.44±0.05	1.26±0.04	0.25±0.06	0.13±0.02
	Summer	445.67±5.13	27.67±1.61	17.38±0.09	2.60±0.30	1.83±0.05	1.24±0.07	0.32±0.06	0.22±0.06
S6	Autumn	751.67±27.61	12.83±1.34	7.14±0.62	2.56±0.25	2.55±0.39	1.12±0.09	0.23±0.02	0.48±0.06
	Winter	457.67±15.50	9.15±0.08	3.50±0.08	1.53±0.08	4.54±0.34	2.18±0.07	0.61±0.08	0.60±0.03
	Spring	675.00±6.24	46.47±1.38	14.21±0.25	1.52±0.27	4.09±0.02	1.11±0.03	0.25±0.06	0.23±0.06
	Summer	878.67±10.50	36.44±0.85	12.37±0.23	1.64±0.07	6.10±0.00	1.09±0.06	0.14±0.06	0.10±0.02
S7	Autumn	164.00±24.25	19.15±1.22	11.96±1.19	4.74±0.34	4.87±0.48	3.10±0.15	**2.88±0.91**	1.22±0.04
	Winter	243.33±11.37	7.96±0.37	3.60±0.46	4.37±0.34	5.68±0.44	1.30±0.20	0.85±0.23	1.24±0.08
	Spring	256.67±11.68	35.85±0.75	4.74±0.55	5.61±0.43	7.55±0.38	2.20±0.07	1.94±0.61	1.82±0.13
	Summer	263.00±8.54	37.08±0.74	14.81±0.56	4.74±0.20	8.13±0.32	2.20±0.02	1.83±0.69	1.74±0.28
S8	Autumn	181.67±2.52	18.28±2.92	7.09±0.52	4.61±0.15	4.99±0.56	**4.09±0.09**	2.73±0.64	2.45±0.36
	Winter	244.00±38.00	19.22±0.22	11.54±1.88	**5.44±0.42**	5.32±0.99	1.92±0.56	1.30±0.17	**2.75±0.44**
	Spring	248.00±9.54	31.53±1.21	11.22±0.23	4.54±0.14	**11.14±0.87**	2.20±0.08	2.22±0.19	2.55±0.37
	Summer	275.00±24.25	47.15±1.89	14.01±0.88	5.43±0.42	10.19±0.23	1.64±0.28	2.60±0.34	1.49±0.33

NB: At S2, S4 and S5 E. Selaginoides is absent

Table 5. *Mean concentrations of heavy metals in sediment (Mean ± SD) of Fe, Zn, Mn, Ni, Cu, Pb, Cr and Cd expressed in $mg{\cdot}g^{-1}$ during 2018/2019*

Station	Fe	Zn	Mn	Ni	Cu	Pb	Cr	Cd
S1	2965±23.30	123±0.32	51±1.65	-	9.12±0.53	-	-	2.15±0.05
S2	1695±23.00	56±32	23±2.03	-	10.75±0.65	-	-	2.22±0.22
S3	3231±15.32	-	16±0.26	-	8.19±0.25	-	-	2.18±0.05
S4	2563±12.03	173.62±2.35	62±0.45	-	29.10±0.58	49.5±0.33	14.22±0.55	3.77±0.04
S5	2361±6.32	148.1±1.22	21±0.32	-	15.06±0.62	21.27±0.51	12.32±0.87	3.97±0.02
S6	1563±3.26	64±0.32	45±1.38	-	10.25±0.56	-	-	1.55±0.23
S7	1233±5.32	146±1.31	22±0.56	-	13.45±0.75	-	-	2.32±0.55
S8	865±3.12	166±0.22	36±0.55	-	14.24±0.65	-	-	1.66±0.65
French Norm (FNHMIS, 2000)	-	552	-	74	90	200	180	2.4

http://www.aloki.hu ● ISSN 1589 1623 (Print) ● ISSN 1785 0037 (Online)
DOI: http://dx.doi.org/10.15666/aeer/2001_021041

Table 6. *Mean concentrations of heavy metals in seawater (Mean ± SD) of Fe, Zn, Mn, Ni, Cu, Pb, Cr and Cd expressed in µg.L^{-1} during 2018-2019*

Station	Fe	Zn	Mn	Ni	Cu	Pb	Cr	Cd
S1	-	1.90±0.56	-	-	-	-	-	-
S2	-	2.55±0.96	-	-	0.17±0.14	0.88±0.41	0.11±0.08	0.14±0.02
S3	-	-	-	-	0.15±0.12	-	-	0.10±0.01
S4	-	1.82±0.33	-	-	0.25±0.04	3.26±0.83	1.12±0.15	1.18±0.09
S5	-	1.93±0.18	-	-	0.75±0.13	1.63±0.22	0.92±0.05	1.10±0.08
S6	-	1.70±0.44	-	-	-	1.17±0.38	-	-
S7	-	0.88±0.23	-	-	0.19±0.05	0.68±0.23	0.08±0.01	0.12±0.07
S8	-	0.56±0.22	-	-	-	0.57±0.15	0.06±0.01	0.11±0.03
Moroccan Norm. (FAO, 2006)		500		500	500	500	2000	200

Statistical sampling sites grouping

Pearson correlation results (*Fig. 3*) were supported by the PCA ordination (*Figs. 4, 5*) and the dendrogram (*Fig. 6*). Indeed, the Principal Component Analysis (PCA) performed on the eight heavy metals (Cd, Pb, Zn, Cu, Fe, Ni, Cr and Mn) and the physico-chemical parameters (T, pH, EC, DO, Salinity, TDS, BOD, COD and OM) under study showed two principal components that have been extracted by covering 60% of the cumulative variance (*Appendix Tables 9, 10*).

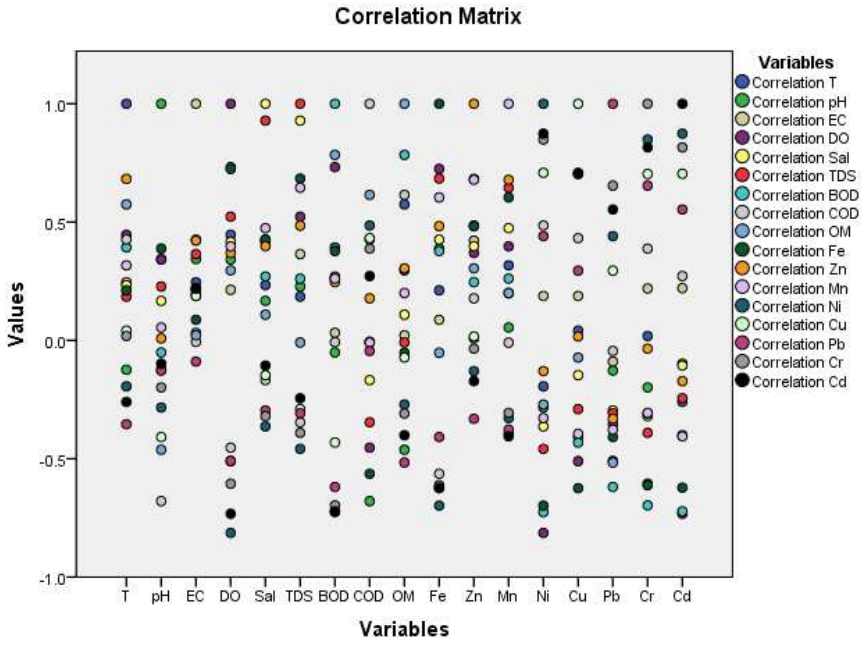

Figure 3. *Pearson correlation for all the studied hydrographical parameters and heavy metals in E. selaginoides*

http://www.aloki.hu ● ISSN 1589 1623 (Print) ● ISSN 1785 0037 (Online)
DOI: http://dx.doi.org/10.15666/aeer/2001_021041

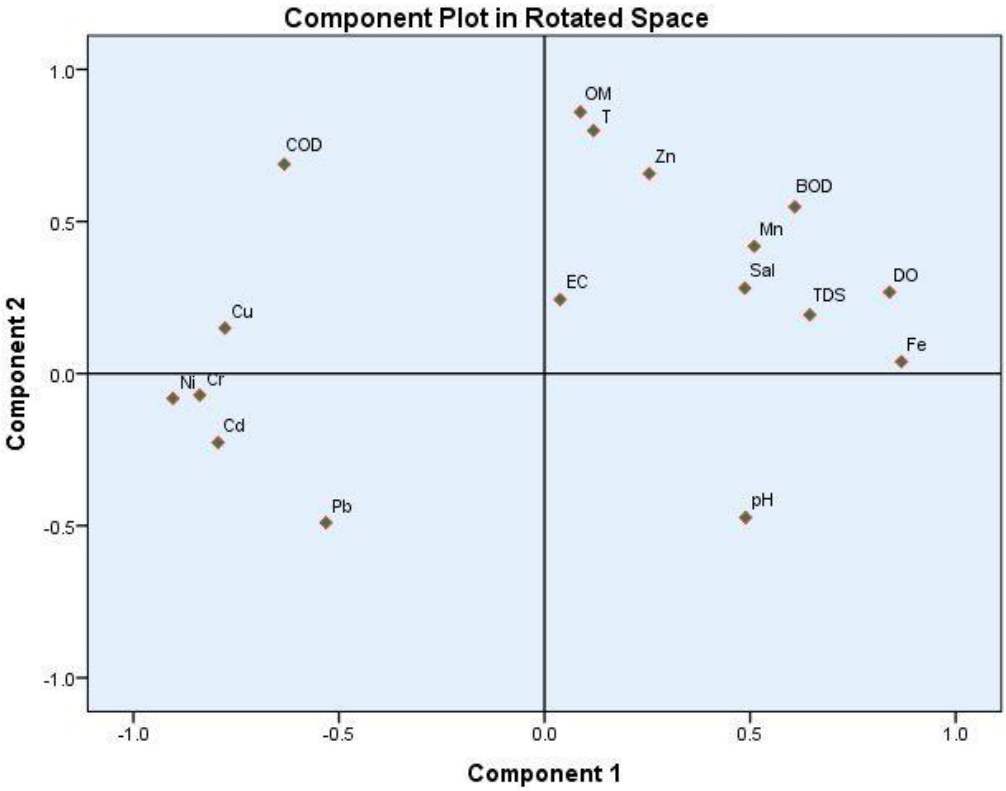

Figure 4. *PCA Analysis regrouping all the studied hydrographical parameters and heavy metals in E. selaginoides*

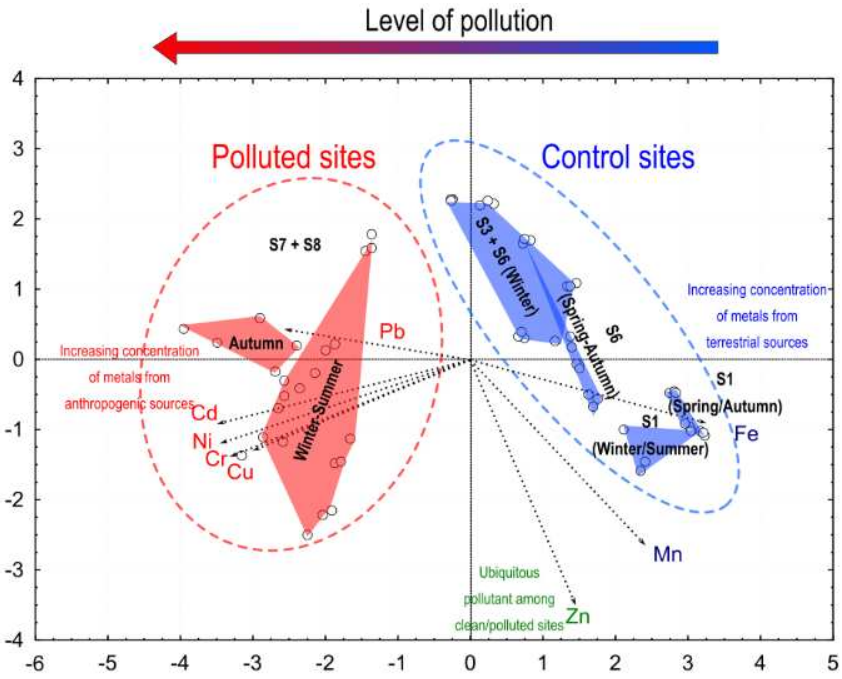

Figure 5. *Component plot representing PC1 and PC2 in rotated space for the eight studied heavy metals in E. selaginoides from the Atlantic coast of Morocco*

http://www.aloki.hu ● ISSN 1589 1623 (Print) ● ISSN 1785 0037 (Online)
DOI: http://dx.doi.org/10.15666/aeer/2001_021041

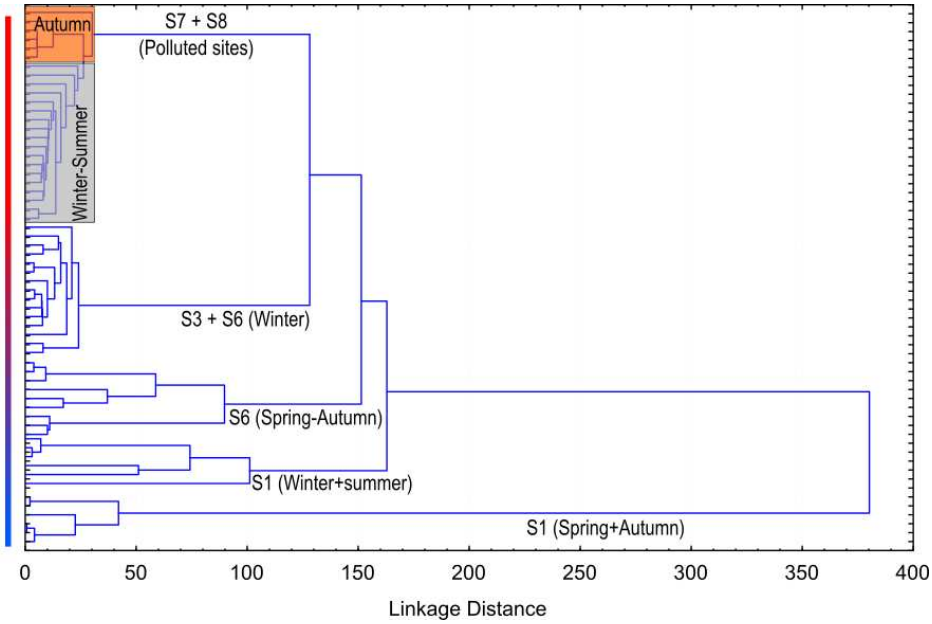

Figure 6. *Dendrogram using average linkage (between groups) obtained by hierarchical clustering analysis for the eight heavy metals studied in E. selaginoides from the Atlantic coast of Morocco*

Eigenvalue percentages of PC1 and PC2 were above broken-stick random forest model analysis, which confirmed that both principal components were suitable for interpretation (*Appendix Fig. 7*). Based on PCA results, PC1 explained a lower percentage of total variance than PC2 (38.286% and 59.208%, respectively). Fe and Mn were the dominant metals increasing along PC1, component 1 with values of 0.868 and 0.510, respectively, while Ni, Cu, Pb, Cr and Cd were the dominant metals decreasing along this component with values around -0.904, -0.777, -0.532, -0.839 and -0.794 respectively. However, Zn was the only dominant metal increasing along PC2, component 2 with a value of 0.657. These metals were the most informative heavy metals to identify the environmental quality of a site based on the bioindicator role of *E. selaginoides*, given their higher weight on the first component (*Appendix Table 9*). In contrast, the hydrographical parameters of DO, TDS, BOD were the dominant ones increasing along PC1 with 0.839, 0.645 and 0.609, respectively; while COD was the only decreasing one with -0.633. Moreover, T, COD and OM were the dominant parameters increasing along PC2, represented with values around 0.799, 0.689 and 0.860, respectively.

Clustering analysis allowed us to represent data clusters in the PCA plot by means of convex hulls (*Fig. 5*). The statistical significance among groups was confirmed by K-W ANOVA from the metals with higher factor loadings in each case (*Appendix Table 8*). The metals PCA and clustering analysis also allowed to group sampling stations along PC1, which represented a pollution gradient (*Figs. 5, 6*). Polluted sites (S7, S8) were located towards negative values of PC1, due to the presence of higher concentrations of Cd, Pb, Cu, Ni and Cr. On the other hand, control sites were placed at positive PC1 values, given their lower concentrations of heavy metals from polluted sites and their higher content in Fe and Mn (*Figs. 5, 6*). For this second analysis, only PC1 was suitable for interpretation, as the eigenvalue percentage of PC2 was below the values generated by the broken-stick random forest model (*Appendix Fig. 7*).

http://www.aloki.hu ● ISSN 1589 1623 (Print) ● ISSN 1785 0037 (Online)
DOI: http://dx.doi.org/10.15666/aeer/2001_021041

Discussion

The comparison of the present heavy metals results with those previously studied by other authors revealed that iron predominates at all sites (Caliceti et al., 2002; Akcali and Kucuksezgin, 2011) (*Tables 4, 5*). The concentrations of Cadmium (2.75 $\mu g.g^{-1}$ DW) were lowest among the 8 heavy metals analyzed in *E. selaginoides*, but that value was higher than that reported by Akcali and Kucuksezgin (2011) from the Aegean Sea, Turkey (0.18 $\mu g.g^{-1}$); Schintu et al. (2010) from Sardinia, Italy (1.72 $\mu g.g^{-1}$); Calisti et al. (2002) from Venice lagoon, Italy (0.2 $\mu g.g^{-1}$); Al-Masri et al. (2003) from the Syrian Coast (0.1-0.5 $\mu g.g^{-1}$) and Conti et al. (2010) from Linosa island (1.07 $\mu g.g^{-1}$). In the case of Chromium concentrations, Calisti et al. (2002) and Conti et al. (2010) detected lower values in Venice lagoon and Linosa island (Italy) (1.5 and 0.32 $\mu g.g^{-1}$ DW, respectively) than that recorded in the present study (2.9 $\mu g.g^{-1}$ DW). The same result was found for nickel concentrations by Calisti et al. (2002) (2.7 µg g-1 DW) which is lower than that found in this study (5.24 $\mu g.g^{-1}$ DW). With respect to lead concentration, the values found in the present study (4.43 $\mu g.g^{-1}$ DW) were higher than those found by Akcali and Kucuksezgin (2011) from the Aegean Sea, Turkey (0.003 $\mu g.g^{-1}$ DW) and Al-Masri et al. (2003) from the Syrian Coast (1.31 $\mu g.g^{-1}$ DW), and lower than those found by Conti et al. (2010) and Schintu et al. (2010) from Italian coastlines (4.78 and 10.3 $\mu g.g^{-1}$, respectively) (*Table 7*).

Table 7. *Comparison of heavy metals concentrations ($\mu g.g^{-1}$ DW) in diverse species of the genus Cystoseira complex from other coastal locations*

Location	References	Fe	Zn	Mn	Ni	Cu	Pb	Cr	Cd
Bulgarian black sea coast	Jordanova et al., 1999	-	-	10-100	-	-	-	-	-
Venice lagoon, Italy	Caliceti et al., 2002	609	88	-	2.7	21	5.6	1.5	0.2
Syrian Coast	Al-Masri et al., 2003	-	14.37	-	-	7.21	1.31	-	0.1-0.5
Linosa Island, Sicily	Conti et al., 2010	-	26.2	-	-	6.78	4.78	0.32	1.07
Sardinia, Italy	Schintu et al., 2010	-	52.4	-	-	1.80	10.3	-	1.72
Aegean Sea, Turkey	Akcali and Kucuksezgin., 2011	271.42	51.25	-	-	6.00	0.003	-	0.18
Atlantic coast of Morocco	Present study. 2019	1718.67	49.16	25.82	5.61	11.14	4.09	2.88	2.75

The PCA ordination method allowed us to identify a first group represented by Fe, Zn and Mn, being the elements with the highest abundance in *E. selaginoides*, and a second group including the rest of them at lower concentrations (*Table 2, Fig. 2*). The classification obtained in our study strongly agreed with the sources for each element: Fe and Mn are commonly related to terrestrial inputs whereas Pb, Cu, Zn and Cd gave evidence of anthropogenic contamination (Harris et al., 1998). In general, brown algae are one of the frequently and firmly affected algae among the algal source (Kaviarasan et al., 2018). We found that elements from the first group were more abundant in the most pristine site (S1, Eljadida control station), and they come from terrestrial runoff in the case of Fe and Mn. However, the presence of high concentrations of Zn at that control site suggest potential inputs from some industrial activities inland that contribute to its presence (FAO, 2019).

Seasonality had a significant effect in the Fe content of *E. selaginoides* in S1 (Spring> Autumn> Winter> Summer), being consistent with the clustering and the PCA results,

http://www.aloki.hu ● ISSN 1589 1623 (Print) ● ISSN 1785 0037 (Online)
DOI: http://dx.doi.org/10.15666/aeer/2001_021041

demonstrating that seasonal differences were also significant at a lower clustering level. Furthermore, in S3, Fe concentrations were similar throughout the year, whereas in S6 there was a significant increase towards summer (S6 spring to autumn as shown in the PCA and the dendrogram) and minimum values in winter (*Figs. 5, 6*), which were similar to that of S3, which explain why S6-winter was in same cluster than S3. Irrespective of the season, Fe concentrations were always significantly higher in S1 than in the rest of sites, followed by S6, S3 and then the polluted sites. In the case of Mn, such differences were more progressive and there was more overlapping among the groups. Concentrations of Ni, Cr and Cd were significantly greater at the polluted sites. Nevertheless, S3 at some seasons presented some similar concentrations than in polluted areas, which in the PCA was represented by its location closer to zero values in the first component (*Fig. 5*). This would indicate that S3 could be considered as the "less clean" from the control sites. Therefore, it is possible to say that a "pollution gradient" may also be found among the three control sites. Besides, the increase in Pb in autumn would explain why polluted sites in that season lie in a different cluster than the rest of the year. That is because it was the only element for which that value was significantly higher than in spring-winter. For the other heavy metals, seasonal differences were not marked and neither the differences between stations S7 and S8.

E. selaginoides seemed to take up higher concentrations of these heavy metals, which are used inside physiological processes like Na, Ca, Mg and Fe, whereas lower concentrations of those which do not participate in these processes, for example Cd and Pb (Malea, 1994). Copper is essential for organisms' life and its toxicity is connected with the concentrations of other essential elements. The main sources of pollution in this area in the Atlantic coast of Morocco are the two-phosphate chemical complex (OCP) of Jorf lasfar (20 km south of El Jadida) and the cannery fish factory at Safi city (5 km south of Safi) (Boundir et al., 2019). The concentrations of the eight (8) heavy metals in the tissue of *E. selaginoides* were variable depending on the sampled stations and seasons. Given the toxicity of heavy metals, it is important to know the source and what happens to them in the environment.

For a long time in Morocco, seaweeds have remained absent from the debate on the impact and effects of anthropogenic activities in the marine biodiversity. Heavy metals in the Moroccan waters have been studied more recently than other chemical parameters. Research focused on water and sediment compartments, as well as some coastal marine areas (FAO, 2019). Worldwide, the use of algae (including brown seaweeds such as *Cystoseira* complex) in biomonitoring has been well established. Metal content and accumulation in seaweed is recognized as a suitable bioindicator for assessing the degree of contamination in marine ecosystems (Alahverdi Savabieasfahani, 2012). Nevertheless, until now there were no studies focusing on the bioaccumulation of these heavy metals in macroalgae, especially *Cystoseira* complex species from the Atlantic coast of Morocco.

In general, studies on the levels and distribution of contaminants, including heavy metals, in Morocco have focused on urban and industrial areas. As a result, the actual ground levels of water, sediment and biota, may not be exactly known, which can also distort the interpretation of the data. Heavy metals entering the aquatic environment come from natural and anthropogenic sources (Ghorab, 2018). Their entry can be the result of either direct discharges into marine ecosystems and fresh waters or indirect pathways such as dry and wet dumps and agricultural runoff. In addition, the mining activities are responsible for significant contributions of heavy metals to the Moroccan coastlines. For most heavy metals, anthropogenic emissions are equal to or greater than natural

http://www.aloki.hu ● ISSN 1589 1623 (Print) ● ISSN 1785 0037 (Online)
DOI: http://dx.doi.org/10.15666/aeer/2001_021041

emissions. The combustion of leaded gasoline in cars, for example, is responsible for the wide spread of lead around the world (FAO, 2019).

In the next future, seaweeds will have to adapt to the new environmental conditions in the projected scenarios derived from global change and the increase of local stressors (Viejo et al., 2011; Bellard et al., 2012) or, conversely, to suffer local extinction, as it has been documented with increasing frequency in the scientific literature (e.g. Lima et al., 2007; Wernberg et al., 2011; Scherner et al., 2013; Thibaut et al., 2015; Mineur et al., 2015; Valdazo et al., 2017). The ecosystem services provided by brown macroalgal forests, such in the case of *Cystoseira* sensu lato, seems to be affected by diverse environmental and anthropogenic factors (Mineur et al., 2015). As demonstrated by Cheminée et al. (2013) the nursery value of *Cystoseira* complex forest changes not only as function of the depth gradient, but more importantly by the height of the plant canopy; comparatively, *E. selaginoides* forest hosted richer and three-fold more abundant juvenile fish assemblages. Therefore, the loss of *E. selaginoides* biomass and/or its complete extinction in some of the studied localities along the Atlantic Moroccan coasts are probably affecting negatively the richness and abundance of the local juvenile fish populations.

Conclusion

The reduction in biomass and eventually the extinction of *E. selaginoides* populations from the studied sites along the Atlantic coasts of Morocco seems to be related to the increasing pressure of anthropogenic activities, mainly leading towards high levels of heavy metal pollution. *E. selaginoides* accumulate heavy metals differently in the different localities studied and hence, can be used to monitor heavy metals levels in seawaters. Moreover, we suggest using it as a model for coastal pollution studies in Morocco and worldwide. The highest concentrations of Fe, Zn and Mn were recorded at Sidi Bouzid station (S1) of Eljadida city, while those of Cu, Ni, Pb, Cr and Cd were detected at the Port station of Essaouira city (S8). The concentrations of Chemical Oxygen Demand were significantly higher at the polluted station S5, while Dissolved Oxygen and Biological Oxygen Demand were lower. To rationally manage and control marine pollution in the Atlantic coast of Morocco, it is necessary to study everything related to the inputs, distribution and destiny of contaminants, including land-based heavy metals that flow into aquatic ecosystems. It is essential to address their effects on seaweed biodiversity, especially in Safi city where the growth of phosphate industry is accelerating. In conclusion, the loss of brown seaweed populations in the studied locations seems to be affecting the biodiversity richness and abundance of marine life; this biological effect needs further studies in the future. Moreover, the analysis of heavy metals in *E. selaginoides* gives a reasonable indication of water environmental quality at discrete points along the study area in the Atlantic coast of Morocco, providing a comparative methodology for monitoring purposes in subsequent years or with other coastal areas that could be implemented through the implementation of coastal biomonitoring programs.

Acknowledgements. The first author would like to thank the Lab. Water, Biodiversity and Climate Changes, the National center for studies and research on water and Energy (CNEREE) of Cadi Ayyad University and the Biodiversity & Conservation Research Group (IU-ECOAQUA) of Las Palmas University for supplying the research materials (facilities, equipments, etc.). Thanks also to Mr. Rezzoum

http://www.aloki.hu ● ISSN 1589 1623 (Print) ● ISSN 1785 0037 (Online)
DOI: http://dx.doi.org/10.15666/aeer/2001_021041

N. from the National Institute of Fisheries in Casablanca, Morocco (INRH) who has been relevant for the development of the benthic/macroalgal research in the Atlantic coast of Morocco and the good strategy to harvest algal samples from the Moroccan coastlines.

REFERENCES

[1] AFNOR (2001): NF T90-103 for BOD5 and NF T90-101 for COD.
[2] Akcali, I., Kucuksezgin, F. (2011): A biomonitoring study: Heavy metals in macroalgae from eastern Aegean coastal areas. – Marine Pollution Bulletin 62(3): 637-645.
[3] Alahverdi, M., Savabieasfahani, M. (2012): Metal pollution in seaweed and related sediment of the Persian Gulf, Iran. – Bulletin of Environmental Contamination and Toxicology 88(6): 939-945.
[4] Al-Masri, M. S., Mamish, S., Budier, Y. (2003): Radionuclides and trace metals in eastern Mediterranean Sea algae. – Journal of Environmental Radioactivity 67: 157-168.
[5] Bellard, C., Bertelsmeier, C., Leadley, P., Thuiller, W., Courchamp, F. (2012): Impacts of climate change on the future of biodiversity. – Ecology Letters 15: 365-377.
[6] Black, W. A. P., Mitchell, R. L. (1952): Trace elements in the common brown algae and in sea water. – Journal of the Marine Biological Association of the United Kingdom 30: 575-579.
[7] Boundir, Y., Hasni, M., Rafik, F., Sabri, H., Bahammou, N., Cheggour, M., Achtak, H., Cherifi, O. (2019): First study of the ecological status in the atlantic coast of morocco using the brown seaweed Cystoseira tamariscifolia. – Applied Ecology and Environmental Research 17(6): 14315-14331.
[8] Bowles, D. J. (2007): Micro- and macro-algae: utility for industrial applications: outputs from the EPOBIO project. – CPL Press, 82p.
[9] Bryan, G. W., Langston, W. J., Hummerstone, L. G. (1980): The use of biological indicators of heavy metal contamination in estuaries: with special reference to an assessment of the biological availability of metals in estuarine sediments from south-west Britain. – Occasional Publications of the Marine Biological Association of the United Kingdom 1: 1-73.
[10] Bryan, G. W., Langston, W. J., Hummerstone, L. G., Burt, G. R. (1985): A guide to the assessment of heavy metal contamination in estuaries using biological indicators. – Occasional Publications of the Marine Biological Association of the United Kingdom 4: 1-92.
[11] Caliceti, M., Argese, E., Sfriso, A., Pavoni, B. (2002): Heavy metal contamination in the seaweeds of the Venice lagoon. – Chemosphere 47(4): 443-454.
[12] Celis-Plá, P. S. M., Brown, M. T., Santillán-Sarmiento, A., Korbee, N., Sáez, C. A., Figueroa, F. L. (2018): Ecophysiological and metabolic responses to interactive exposure to nutrients and copper excess in the brown macroalga Cystoseira tamariscifolia. – Marine Pollution Bulletin 128: 214-222.
[13] Cheminée, A., Sala, E., Pastor, J., Bodilis, P., Thiriet, P., Mangialajo, L., Cottalorda, J. M., Francour, P. (2013): Nursery value of Cystoseira forests for Mediterranean rocky reef fishes. – Journal of Experimental Marine Biology and Ecology 442: 70-79.
[14] Conti, M. E., Iacobucci, M., Cecchetti, G. (2007): A biomonitoring study: Trace metals in seagrass, algae and molluscs in a marine reference ecosystem (Southern Tyrrhenian Sea). – International Journal of Environment and Pollution 29(1-3): 308-332.
[15] Conti, M. E., Finoia, M. G. (2010): Metals in molluscs and algae: A north-south Tyrrhenian Sea baseline. – Journal of Hazardous Materials 181(1-3): 388-392.
[16] Conti, M. E., Bocca, B., Iacobucci, M., Finoia, M. G., Mecozzi, M., Pino, A., Alimonti, A. (2010): Baseline trace metals in seagrass, algae, and mollusks in a southern tyrrhenian ecosystem (Linosa Island, Sicily). – Archives of Environmental Contamination and Toxicology 58(1): 79-95.

http://www.aloki.hu ● ISSN 1589 1623 (Print) ● ISSN 1785 0037 (Online)
DOI: http://dx.doi.org/10.15666/aeer/2001_021041

[17] Crowe, T. P., Thompson, R. C., Bray, S., Hawkins, S. J. (2000): Impacts of anthropogenic stress on rocky intertidal communities. – Journal of Aquatic Ecosystem Stress and Recovery 7: 273-297.
[18] Cuadros, A., Cheminée, A., Vidal, E., Thiriet, P., Bianchimani, O., Basthard-Bogain, S., Francour, P., Moranta, J. (2013): The Identification, Conservation, and Management of Estuarine and Marine Nurseries for Fish and Invertebrates. – Journal of Experimental Marine Biology and Ecology 51.
[19] de Caralt, S., Verdura, J., Vergés, A., Ballesteros, E., Cebrián, E. (2019): Effects of pollution on populations of Cystoseira crinita. – European Journal of Phycology. Keynote and Oral Papers 54(Sup1): 31-117.
[20] Essedaoui, A., Sif, J. (2001): Bioaccumulation des métaux lourds et induction des métallo-protéines au niveau de la glande digestive de Mytilus galloprovincialis. – Revue Marocaine des Sciences Agronomiques et Vétérinaires 21: 17-25.
[21] F.M.6. (2018): The Mohammed VI foundation for the protection of environment. – https://www.fm6e.org/en.html.
[22] FAO. (2006): Projet de gestion des ressources en eau: Elaboration des dossiers techniques relatifs aux valeurs limites des rejets industriels dans le Domaine Public Hydraulique. Elaboration des fiches techniques des valeurs limites des rejets industriels. – Conventio.
[23] FAO. (2019): Food and Agriculture Organization of the United Nations. – http://www.fao.org.
[24] Farías, S., Arisnabarreta, S. P., Vodopivez, C., Smichowski, P. (2002): Levels of essential and potentially toxic trace metals in Antarctic macro algae. – Spectrochimica Acta, Part B Atomic Spectroscopy 57(12): 2133-2140.
[25] Ferssiwi, A., Sif, J., El Hamri, H., Rouhi, A., Amiard, J. C. (2004): Contamination par le cadmium de l'Annélide Polychète Hediste diversicolor dans la région d'El Jadida (Maroc) implication des protéines type métallothionéines. – Journal de Recherche Océanographique 29: 59-64.
[26] FNHMIS. (2000): Arrêté du 14/06/2000 relatif aux niveaux de référence à prendre en compte lors d'une analyse de sédiments marins ou estuariens présents en milieu naturel ou portuaire. – AIDA, https://aida.ineris.fr/consultation_document/5479.
[27] Ghorab, M. A. (2018): Environmental Pollution by Heavy Metals in the Aquatic Ecosystems of Egypt. – Open Access Journal of Toxicology 3(1).
[28] Gopinath, A., Muraleedharan, N. S., Chandramohanakumar, N., Jayalakshmi, K. V. (2011): Statistical significance of biomonitoring of marine algae for trace metal levels in a coral environment. – Environmental Forensics 12(1): 98-105.
[29] Goumri, M., Cheggour, M., Maarouf, A., Mouabad, A. (2018): Preliminary data on the composition and spatial distribution patterns of echinoderms along Safi rocky shores (NW Morocco). – AACL Bioflux 11: 1193-1202.
[30] Gubelit, Y., Polyak, Y., Dembska, G., Pazikowska-Sapota, G., Zegarowski, L., Kochura, D., Krivorotov, D., Podgornaya, E., Burova, O., Maazouzi, C. (2016): Nutrient and metal pollution of the eastern Gulf of Finland coastline: Sediments, macroalgae, microbiota. – Science of the Total Environment 550: 806-819.
[31] Guiry, M., Guiry, G. M. (2020): AlgaeBase. World-wide electronic publication. – National University of Ireland, Galway. https://www.algaebase.org/.
[32] Haghshenas, V., Kafaei, R., Tahmasebi, R., Dobaradaran, S., Hashemi, S., Sahebi, S., Sorial, G. A., Ramavandi, B. (2020): Potential of green/brown algae for monitoring of metal(loid)s pollution in the coastal seawater and sediments of the Persian Gulf: ecological and health risk assessment. – Environmental Science and Pollution Research 27(7): 7463–7475.
[33] Halpern, B. S., Walbridge, S., Selkoe, K. A., Kappel, C. V., Micheli, F., D'Agrosa, C., Bruno, J. F., Casey, K. S., Ebert, C., Fox, H. E., Fujita, R., Heinemann, D., Lenihan, H. S., Madin, E. M. P., Perry, M. T., Selig, E. R., Spalding, M., Steneck, R., Watson, R. (2008): A global map of human impact on marine ecosystems. – Science 319(5865): 948-952.

http://www.aloki.hu ● ISSN 1589 1623 (Print) ● ISSN 1785 0037 (Online)
DOI: http://dx.doi.org/10.15666/aeer/2001_021041

[34] Hammer, Ø., Harper, D. A. T., Ryan, P. D. (2001): Past: Paleontological Statistics Software Package for Education and Data Analysis. – Palaeontologia Electronica 4(1).
[35] Harris, P. A., Fichez, R., Fernandez, J. M., Badie, C. (1998): Heavy metals profiles in dated sediments from the lagoon of Papeete (Tahiti, French Polynesia): influence of mixing phenomena. – IAEA.
[36] Islam, M. S., Tanaka, M. (2004): Impacts of pollution on coastal and marine ecosystems including coastal and marine fisheries and approach for management: A review and synthesis. – Marine Pollution Bulletin 48(7-8): 624-649.
[37] Jackson, D. A. (1993): Stopping rules in principal components analysis: A comparison of heuristical and statistical approaches. – Ecology 74(8): 2204-2214.
[38] Jones, A. J. (1922): The arsenic content of some of the marine algae. – The Pharmaceutical Journal 109: 86-91.
[39] Kaimoussi, A., Chafik, A., Mouzdahir, A., Bakkas, S. (2001): The impact of industrial pollution on the Jorf Lasfar coastal zone (Morocco, Atlantic Ocean): the mussel as an indicator of metal contamination. – Comptes Rendus de l'Académie Des Sciences - Series IIA - Earth and Planetary Science 333: 337-341.
[40] Kaviarasan, T., Gokul, M. S., Henciya, S., Muthukumar, K., Dahms, H. U., James, R. A. (2018): Trace Metal Inference on Seaweeds in Wandoor Area, Southern Andaman Island. – Bulletin of Environmental Contamination and Toxicology 100(5): 614-619.
[41] Levine, H. G. (1984): Use of seaweeds for monitoring coastal waters. – In: Schubert, E. (ed.) Algae as ecological indicators. Academic Press, pp. 189-210.
[42] Lima, F. P., Ribeiro, P. A., Queiroz, N., Hawkins, S. J., Santos, A. M. (2007): Do distributional shifts of northern and southern species of algae match the warming pattern? – Global Change Biology 13: 2592-2604.
[43] Lotze, H. K., Worm, B., Sommer, U. (2001): Strong bottom-up and top-down control of early life stages of macroalgae. – Limnology and Oceanography 46: 749-757.
[44] Malea, P. (1994): Seasonal variation and local distribution of metals in the seagrass Halophila stipulacea (Forsk.) Aschers. in the Antikyra Gulf, Greece. – Environmental Pollution 85(1): 77-85.
[45] Martínez, B., Arenas, F., Rubal, M., Burgués, S., Esteban, R., García-Plazaola, I., Figueroa, F. L., Pereira, R., Saldaña, L., Sousa-Pinto, I., Trilla, A., Viejo, R. M. (2012): Physical factors driving intertidal macroalgae distribution: Physiological stress of a dominant fucoid at its southern limit. – Oecologia 170: 341-353.
[46] Mazarrasa, I., Olsen, Y. S., Mayol, E., Marba, N., Duarte, C. M. (2013): Rapid growth of seaweed biotechnology provides opportunities for developing nations. – Nature Biotechnology 31(7): 591.
[47] Melville, F., Pulkownik, A. (2006): Investigation of mangrove macroalgae as bioindicators of estuarine contamination. – Marine Pollution Bulletin 52(10): 1260-1269.
[48] Mineur, F., Arenas, F., Assis, J., Davies, A. J., Engelen, A. H., Fernandes, F., Malta, E., Thibaut, T., Van Nguyen, T., Vaz-Pinto, F., Vranken, S., Serrão, E. A., De Clerck, O. (2015): European seaweeds under pressure: Consequences for communities and ecosystem functioning. – Journal of Sea Research 98: 91-108.
[49] Mouradi, A., Bennasser, L., Gloaguen, V., Mouradi, A., Zidane, H. (2014): Accumulation of heavy metals by macroalgae along the Atlantic coast of Morocco between El Jadida and Essaouira. – World Journal of Biological Research 6: 1-9.
[50] Norton, T. A., Melkonian, M., Andersen, R. A. (1996): Algal biodiversity. – Phycologia 35(4): 308-326.
[51] Novoa, E. A. M., Guiry, M. D. (2020): Reinstatement of the genera Gongolaria Boehmer and Ericaria Stackhouse (Sargassaceae, Phaeophyceae): AlgaeBase. – World-wide electronic publication, National University of Ireland. https://img.algaebase.org/pdf/AC1F2AC91dd6c1D68BNM6EDA199A/65399.pdf.
[52] Orellana, S., Hernández, M., Sansón, M. (2019): Diversity of Cystoseira sensu lato (Fucales, Phaeophyceae) in the eastern Atlantic and Mediterranean based on morphological

http://www.aloki.hu ● ISSN 1589 1623 (Print) ● ISSN 1785 0037 (Online)
DOI: http://dx.doi.org/10.15666/aeer/2001_021041

and DNA evidence, including Carpodesmia gen. emend. and Treptacantha gen. emend. – European Journal of Phycology 54(3): 447-465.
[53] Papenfuss, G. F. (1950): Review of the genera of algae described by Stackhouse. – Hydrobiologia 2: 181-208.
[54] Phillips, D. J. H. (1980): Quantitative aquatic biological indicators: their use to monitor trace metal and organochlorine pollution. – Applied Science Publishers, London.
[55] Radmer, R. J. (1996): Algal Diversity and Commercial Algal Products. – BioScience 46: 263-270.
[56] Rainbow, P. S., Phillips, D. J. H. (1993): Cosmopolitan biomonitors of trace metals. – Marine Pollution Bulletin 26(11): 593-601.
[57] Rodier, J. (2009): L'analyse de l'eau. 9ème édition. – Dunod, Paris.
[58] Sales, M., Cebrian, E., Tomas, F., Ballesteros, E. (2011): Pollution impacts and recovery potential in three species of the genus Cystoseira (Fucales, Heterokontophyta). – Estuarine, Coastal and Shelf Science 92(3): 347-357.
[59] Scherner, F., Horta, P. A., De Oliveira, E. C., Simonassi, J. C., Hall-Spencer, J. M., Chow, F., Nunes, J. M. C., Pereira, S. M. B. (2013): Coastal urbanization leads to remarkable seaweed species loss and community shifts along the SW Atlantic. – Marine Pollution Bulletin 76(1-2): 106-115.
[60] Schintu, M., Marras, B., Durante, L., Meloni, P., Contu, A. (2010): Macroalgae and DGT as indicators of available trace metals in marine coastal waters near a lead-zinc smelter. – Environmental Monitoring and Assessment 167: 653-661.
[61] Sekabira, K., Origa, H. O., Basamba, T. A., Mutumba, G., Kakudidi, E. (2011): Application of algae in biomonitoring and phytoextraction of heavy metals contamination in urban stream water. – International Journal of Environmental Science and Technology 8(1): 115-128.
[62] Squadrone, S., Brizio, P., Battuello, M., Nurra, N., Sartor, R. M., Riva, A., Staiti, M., Benedetto, A., Pessani, D., Abete, M. C. (2018): Trace metal occurrence in Mediterranean seaweeds. – Environmental Science and Pollution Research 25(10): 9708-9721.
[63] Tahiri, L., Bennasser, L., Idrissi, L., Fekhaoui, M., El Abidi, A., Mouradi, A. (2005): Metal Contamination of Mytilus galloprovincialis and Sediments in the Bouregreg Estuary (Morocco). – Water Quality Research Journal of Canada 40(1): 111-119.
[64] Thibaut, T., Blanfune, A., Boudouresque, C. F., Verlaque, M. (2015): Decline and local extinction of Fucales in French Riviera: the harbinger of future extinctions? – Mediterranean Marine Science 16(1): 206-224.
[65] Umanzor, S., Ladah, L., Calderon-Aguilera, L. E., Zertuche-González, J. A. (2019): Testing the relative importance of intertidal seaweeds as ecosystem engineers across tidal heights. – Journal of Experimental Marine Biology and Ecology 511: 100-107.
[66] Valdazo, J., Viera-Rodríguez, M. A., Espino, F., Haroun, R., Tuya, F. (2017): Massive decline of Cystoseira abies-marina forests in Gran Canaria Island (Canary Islands, eastern Atlantic). – Scientia Marina 81(4): 499-507.
[67] Varma, R., Turner, A., Brown, M. T. (2011): Bioaccumulation of metals by Fucus ceranoides in estuaries of South West England. – Marine Pollution Bulletin 62(11): 2557-2562.
[68] Vasquez, J. A., Guerra, N. (1996): The use of seaweeds as bioindicators of natural and anthropogenic contaminants in northern Chile. – Hydrobiologia 326/327: 327-333.
[69] Viejo, R. M., Martínez, B., Arrontes, J., Astudillo, C., Hernández, L. (2011): Reproductive patterns in central and marginal populations of a large brown seaweed: Drastic changes at the southern range limit. – Ecography 34(1): 75-84.
[70] Wernberg, T., Russell, B. D., Thomsen, M. S., Gurgel, C. F. D., Bradshaw, C. J. A., Poloczanska, E. S., Connell, S. D. (2011): Seaweed communities in retreat from ocean warming. – Current Biology 21(21): 1828-1832.
[71] Wernberg, T., Filbee-Dexter, K. (2019): Missing the marine forest for the trees. – Marine Ecology Progress Series 612: 209-215.

http://www.aloki.hu ● ISSN 1589 1623 (Print) ● ISSN 1785 0037 (Online)
DOI: http://dx.doi.org/10.15666/aeer/2001_021041

APPENDIX

Table 8. *Kruskal-Wallis H test (non-parametric one-way ANOVA) for internal heavy metal concentration in E. selaginoides. Combination of sites and seasons was used as categorical grouping variable in the analysis*

	Fe	Zn	Mn	Cu	Ni	Pb	Cr	Cd
Total N	60	60	60	60	60	60	60	60
H	57.41	57.52	58.05	57.77	56.1	55.11	56.07	57.76
df	19	19	19	19	19	19	19	19
P	<0.0001	<0.0001	<0.0001	<0.0001	<0.0001	<0.0001	<0.0001	<0.0001

Table 9. *Factor loadings of the variables analysed in the PCA. Rotated Component Matrix, Extraction Method: Principal Component Analysis. Rotation Method: Varimax with Kaiser Normalization. Rotation converged in three iterations*

Parameter	Component	
	1	2
T	0.119	0.799
pH	0.489	-0.473
EC	0.038	0.243
DO	0.839	0.268
Sal	0.487	0.281
TDS	0.645	0.193
BOD	0.609	0.548
COD	-0.633	0.689
OM	0.087	0.860
Fe	0.868	0.039
Zn	0.255	0.657
Mn	0.510	0.418
Ni	-0.904	-0.082
Cu	-0.777	0.149
Pb	-0.532	-0.490
Cr	-0.839	-0.071
Cd	-0.794	-0.227

Table 10. *Percentage of total variance explained by the first two components of the PCA analysis*

Component	Initial Eigenvalues			Extraction Sums of Squared Loadings			Rotation Sums of Squared Loadings		
	Total	% of Variance	Cumulative %	Total	% of Variance	Cumulative %	Total	% of Variance	Cumulative %
1	6.937	40.807	40.807	6.937	40.807	40.807	6.509	38.286	38.286
2	3.128	18.401	59.208	3.128	18.401	59.208	3.557	20.922	59.208

Extraction Method: Principal Component Analysis.

http://www.aloki.hu ● ISSN 1589 1623 (Print) ● ISSN 1785 0037 (Online)
DOI: http://dx.doi.org/10.15666/aeer/2001_021041

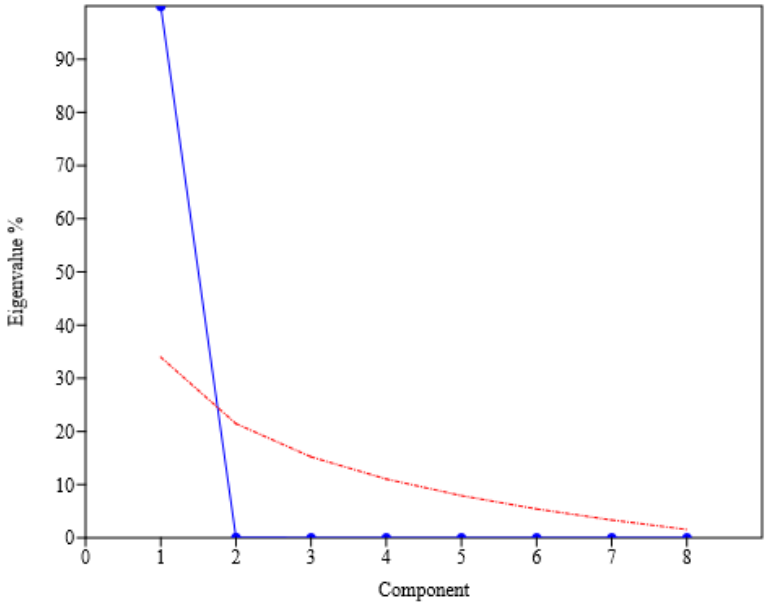

Figure 7. *Scree plot of PCA analysis of heavy metals in E. selaginoides, representing ordination eigenvalues for each component (blue line) and broken-stick random-forest model (red dashed line)*

http://www.aloki.hu ● ISSN 1589 1623 (Print) ● ISSN 1785 0037 (Online)
DOI: http://dx.doi.org/10.15666/aeer/2001_021041

ARBUSCULAR MYCORRHIZAL FUNGI USED TO SUPPORT IRANIAN BARLEY CULTIVATED ON CADMIUM CONTAMINATED SOILS (*Hordeum vulgare* L.)

KESHAVARZ, H.[1*] – HOSSEINI, S. J.[1] – SEDIBE, M. M.[2*] – ACHILONU, M. C.[3]

[1]*Tarbiat Modares University, Department of Agronomy, Faculty of Agriculture, Tehran, Iran*

[2]*Central University of Technology, Free State Department of Agriculture, Private Bag x20539, Bloemfontein, South Africa*
(phone: +27 51-507-4054)

[3]*Mangosuthu University of Technology, Technology Station in Chemical, P.O. Box 12363 Durban, Jacobs 4026, Durban, South Africa*

[*]*Corresponding authors*
e-mail: msedibe@cut.ac.za; H.Keshavarz@modares.ac.ir

(Received 12th Jul 2021; accepted 28th Oct 2021)

Abstract. To study the effect of arbuscular mycorrhizal fungi (AMF) on the agronomic, physiological, and biochemical parameters of barley (*Hordeum vulgare* L.) grown on Cd contaminated soils of Iran, an experiment was carried out in Tehran, Iran for two seasons. The results showed that soil Cd caused a significant decrease in leaf area index (LAI), chlorophyll content, 1000 seed weight, and total dry mass per plant, whereas increased proline content, superoxide dismutase, and catalase enzyme activity were elevated by soil Cd. Mycorrhizal fungi significantly reduced the adverse effects of Cd and increased yield of barley. Decreased proline content, leaf antioxidant activity was also observed where mycorrhizal fungi were used. The use of mycorrhizal fungi had a positive mitigating effect on plant height, 1000 seed weight, chlorophyll contents, proline, LAI, root AMF colonization, foliar cadmium, catalase, peroxidase, and superoxide dismutase. Therefore, AMF have a potential to mitigate the effects of Cd pollution on soil. These results obtained formed a basis for future studies under open field condition before its application can be recommended to barley production under similar condition.
Keywords: *antioxidant activity, chlorophyll, yield component, heavy metals, PCA, proline*

Introduction

Cadmium (Cd) is a toxic heavy metal that occurs in nature in minute quantities in association with other natural heavy metal deposits, including Zn, Pb, Cu and others and produced as a byproduct of the mining of major metals. Mining activities are known to generate huge numbers of harmful metals including Cd, which are carried as fugitive dust or by waterways and contaminate the biota and food chain through assimilation and bioaccumulation processes (Ebenebe et al., 2017). Generally, heavy metals present in waterbodies above peamisible limits, not only endanger the lives of aquatic organisms in the waters, but they also make the water courses unsafe for domestic and agricultural uses as well (Tohidi-Moghadam, 2017; Ebenebe et al., 2017). Cadmium is known to be very toxic even at low concentration (Galas-Gorcher, 1991). Studies have shown that human ingestation or exposure to Cd up to the toxic dose of about 10 µg/dL, can cause irritation of the stomach, cramps, nausea, vomiting, diarrhea, headache, brown urine, hypertension, renal failure, flu‑like symptoms, kidney and liver damage, swelling of the throat and tingling of hands (Bano and Ashfaq, 2013; Ebenebe et al., 2017).

http://www.aloki.hu ● ISSN 1589 1623 (Print) ● ISSN 1785 0037 (Online)
DOI: http://dx.doi.org/10.15666/aeer/2001_043053

Hence, there are various government legislation to control the amount of the toxic metal allowed into the environment to avert unintended poisoning of the biota. The critical limit of Cd metal in light, medium, and heavy textured soils is 5.33, 6.33 and 9.29 mg kg^{-1}, respectively (Keshavarz, 2020). Through food products, Europe and North America allow daily intake of about 15-25 Cd µg, while in Japan the average allowed intake is between 40 and 50 Cd µg (WHO, 2000). The intake of Cd is found to be higher in Cd polluted areas. World average Cd obtained via food products is about 1 µg/day (Bano and Ashfaq, 2013).

The absorption and accumulation of Cd on plants is influenced by the soil conditions and the interaction between Cd and other minerals (Wang et al., 2016). Mycorrhizal fungi ameliorates plant yield by increasing water and nutrient uptake (Pharudi, 2010). According to Azcon-Aguilar and Barea (1997), the efficiency and activity of soil microbes are affected by rhizosphere conditions, including the level of salinity, moisture content and fertility. Extensive extra-radical hyphae network enhances efficiency in the absorption of nutrients and in close association with plant root hair playing an important symbiotic role in the uptake and transfer of water and nutrients by the root system. In exchange, the plant supplies the fungal organism with carbon compound (Gadd, 2004). These fungi reduce the concentration of heavy metals in the cell wall by binding the heavy metal to chitin and secreting glomalin and reduce the accumulation of heavy metals by coexisting with plants (Gadd, 2004).

The upper limit of cadmium allowed in root, tuber and leafy vegetables in Australia is 0.1 mg of cadmium per kg of produce and in Iran, there is no policy regulating Cd levels on food stuff and soil (Tavakkoli and Khanjani. 2016). Cadmium in soils is generally low but once it has been added to the soil through pollution, it can take between 100 and 1000 years for the levels to drop by 50%. When Cd is present in soil, it is more available to plants if the soil is sandy, acidic or low in organic matter (Tavakkoli and Khanjani, 2016).

Plants accumulates harmful metal over time, that eventually affect the plants' activities such as nutrient absorption and photosynthesis. The hampering of the plants ability to absorb nutrients results to leaf decoloration, growth inhibition, poor yields, and eventual death of the plant (Ebenebe et al., 2017). However, the symbioses of some soil microbes and plants, help to restore soils that have been impoverished by toxic heavy metals (Qiu et al., 2018). Studies have established that AMF is effective, not only in restoration/bioremediation of soils polluted by heavy metals such as Cd, but the microbes also improve availability of nutrients, activities of enzymes and fertility of the soil (Qiu et al., 2018; Keshavarz, 2020). Due to the vital role of cereals in human diet, it is essential to find ways that can be used to reduce Cd uptake by cultivated plants (Shi et al., 2019). Therefore, the effect of AMF *Rhizophagus intraradices* (also known as *Glomus intraradices*) species on Cd contaminated soil of Iran was evaluated on agronomic, physiological, and biochemical parameters of barley.

Material and methods

Research site

This experiment was conducted in a greenhouse of Tarbiat Modares University farm located in Tehran, Iran. The latitude of the research farm is 35.325241, and the longitude is 51.647198 category with the GPS coordinates of 35° 19' 30.8676" N and 51° 38' 49.9128" E. The study was conducted in 2020 using a 2×4 factorial design where, two levels of AMF (applied at zero and 20 mg $plant^{-1}$) and 4 levels of cadmium applied zero

http://www.aloki.hu ● ISSN 1589 1623 (Print) ● ISSN 1785 0037 (Online)
DOI: http://dx.doi.org/10.15666/aeer/2001_043053

mg kg^{-1} soil (control), 40 mg kg^{-1} soil, 80 mg kg^{-1} of soil, and 120 mg kg^{-1} of soil. This experiment had three replications and *Rhizophagus intraradices* was the only AMF used. The greenhouse was equipped with cool white fluorescent lamps and had a day and night temperature 22 and 20 ºC, respectively, containing 16/8 hr light/dark photoperiod. The potting sandy loam soil had 0.02%-N, 556.4-K mg kg^{-1}, 8.7-P mg kg^{-1}, 3.98-Fe mg kg^{-1}, 7.01-Mn mg kg^{-1}, 2.2-Cu mg kg^{-1} and 0.52-Zn mg kg^{-1}, 7.1-pH and 0.47 dS/m- EC.

Parameters

Five plants per treatments were used to measure plant height, number of grains per panicle, 1000 seed weight, total dry mass, chlorophyll contents, proline concentration, leaf area index (LAI), leaf cadmium and phosphorus content, colonization percentage, peroxidase activity (POX), malondialdehyde (MDA) and superoxide dismutase activity (SOD). Chlorophyll content was measured on young and fully developed leaves using the method described by Arnon (1949). LAI was measured using a Delta-T Devices leaf area meter (Delta-T Devices Ltd., Cambridge, UK).

Leaves of barley were freeze-dried using liquid nitrogen (-80ºC) thereafter, 0.3 g were milled using 5 mL of 50 mM phosphate buffer (pH 7.0). SOD, CAT and POX activity were determined using a method of Giannopolitis and Ries (1977), Cakmak and Horst (1991) and Ghanati et al. (2002), respectively. The content of MDA of the extracts was calculated using De Vos et al. (1991) method. Proline content was determined using Bates et al. (1973) method.

Analysis of variance was performed using SAS and Excel, and the means were compared using LSD test at $P < 0.05$. All analysis was performed by using the SAS (SAS release 9.0 2002) software. Principal Component Analysis (PCA) based on biplot (SAS 9.1) and coefficient of correlation were applied to consider the visualization of similarities or differences and interrelationships by acute and obtuse angles among all parameters.

Results and discussion

As shown in *Table 1*, plant height ($p<0.0001$), number of grains per panicle ($p<0.0001$), 1000 seed weight ($p<0.0001$), total dry mass ($p<0.001$) and chlorophyll contents ($p<0.0001$) were affected by the concentration of Cd in the soil. Plant height, number of grains per panicle, 1000 seed weight, chlorophyll contents and LAI were reduced by 14.68%, 26.85%, 12.24%, 36.31%, 20.85% and 7.28%, respectively. Despite this decline, the use of AMF increased plant height ($p<0.05$), number of grains per panicle ($p<0.0001$), 1000 seed weight ($p<0.0001$), chlorophyll contents ($p<0.0001$) and LAI ($p<0.001$). Unexpectedly, no significant effect of AMF was found on the number of grains per panicle, and total dry mass of barley. Dhir et al. (2009) reported that reduction of leaf chlorophyll is attributed to Fe content reduction and the decrease of enzyme efficiency involved in chlorophyll biosynthesis. Pandey and Sharma (2002) further reported that increased Ni, and Co concentration in the soil led to a significant reduction in chlorophyll "a" and "b" contents measured in cabbage (*Brassica oleracea* L). Increased chlorophyll content in mycorrhizae inoculated plants is attributed to improved P and N uptake. In contrast, leaf P was not increased by mycorrhizal fungi (*Table 1*). However, application of AMF improved chlorophyll contents by 4.54%, these results were in agreement with Pereira et al. (2012), who reported increased chlorophyll a and b by 23% and 38% respectively in chestnut (*Castanea alnifolia*). In addition, AMF reduce active uptake of heavy metals through the roots while maintaining active uptake of other elements such as

http://www.aloki.hu ● ISSN 1589 1623 (Print) ● ISSN 1785 0037 (Online)
DOI: http://dx.doi.org/10.15666/aeer/2001_043053

N and phosphorus (Neumann and George, 2005). Heavy metals affect homeostasis processes such as water uptake, transport, transpiration, and metabolism of nutrients and uptake of N, P, K, Ca, and magnesium (Tripathi et al., 2014).

Table 1. *Effect of soil Cd and mycorrhizal fungi on agronomic physiological parameters of barley*

Treatment	Plant height (cm)	Number of seed panicle^{-1}	1000 seed weight (g plant^{-1})	Dry mass (g plant^{-1})	Chlorophyll (mg g^{-1} FW)	Proline (mg g^{-1} FW)	Leaf area index
Cadmium (mg kg^{-1})							
0	72.28±2.22^{a}	41.03±2.72^{a}	41.90±0.80^{a}	30.43±2.88^{a}	1.87±0.03^{a}	1.15±0.15^{d}	6.86±0.06^{a}
40	68.65±2.09^{b}	37.85±4.45^{ab}	40.20±1.10^{b}	26.54±3.89^{ab}	1.81±0.06^{b}	2.45±0.45^{c}	6.51±0.05^{b}
80	64.93±2.15^{c}	33.72±3.94^{bc}	38.16±1.38^{c}	23.94±3.82^{bc}	1.71±0.05^{c}	3.16±0.39^{b}	6.36±0.08^{c}
120	61.66±2.19^{d}	30.01±4.86^{c}	36.7±1.99^{d}	19.38±3.62^{c}	1.48±0.05^{d}	3.81±0.33^{a}	6.76±0.07^{d}
$LSD_{0.05}$	2.47***	5.64***	1.35***	4.6**	0.047***	0.27***	0.067***
Mycorrhizae							
-Myco	65.67±4.61^{b}	34.55±5.99^{a}	38.37±2.61^{b}	23.57±5.52^{a}	1.68±0.16^{b}	2.89±1.13^{a}	6.40±0.31^{b}
+Myco	68.09±4.30^{a}	36.74±5.44^{a}	40.10±1.88^{a}	26.58±4.79^{a}	1.76±0.15^{a}	2.40±0.97^{b}	6.50±0.28^{a}
$LSD_{0.05}$	1.74*	3.98^{ns}	0.96**	3.20^{ns}	0.03**	0.19***	0.05**
Cadmium × Mycorrhizae							
$LSD_{0.05}$	3.49^{ns}	7.97^{ns}	1.92^{ns}	6.58^{ns}	0.07^{ns}	0.38^{ns}	0.09^{ns}
	Cadmium (mg kg^{-1} DW)	**Colonization (%)**	**CAT (Δ Abs mg protein min^{-1})**	**Leaf-P content (mg kg^{-1} DW)**	**POX (Δ Abs mg protein min^{-1})**	**MAD (µmol g^{-1} FW)**	**SOD (Δ Abs mg protein min^{-1})**
Cadmium (mg kg^{-1})							
0	0.82±0.13^{d}	42.59±32.45^{a}	52.23±4.80^{d}	3.65±0.29^{a}	2.32±0.14^{d}	8.37±1.96^{c}	111.16±14.60^{d}
40	3.73±0.66^{c}	40.65±29.34^{a}	121.74±14.70^{c}	3.85±0.31^{a}	8.18±0.63^{c}	9.14±1.88^{bc}	322.46±293.85^{c}
80	5.01±0.54^{b}	38.84±25.4^{a}	146.33±18.67^{b}	2.39±0.32^{b}	11.09±0.75^{b}	10.91±1.92^{ab}	451.6±32.42^{b}
120	6.26±5.28^{a}	36.91±25.46^{a}	165.12±19.49^{a}	2.67±0.36^{b}	13.39±0.89^{a}	13.11±1.52^{a}	492.1±22.49^{a}
$LSD_{0.05}$	0.20***	4.16^{ns}	9.92***	0.431***	0.27***	2.35**	20.7***
Mycorrhizae (20 mL plant^{-1})							
-Myco	4.361±2.27^{a}	14.17±3.08^{b}	133.07±50.29^{a}	3.02±0.68^{a}	9.27±4.60^{a}	11.20±2.52^{a}	363.34±160.01^{a}
+Myco	3.55±1.95^{b}	65.32±5.64^{a}	109.61±40.02^{b}	3.26±0.74^{a}	8.22±4.05^{b}	9.57±2.35^{a}	325.33±151.41^{b}
$LSD_{T\ 0.05}$	0.14***	2.94***	7.01***	0.31^{ns}	0.19***	1.66^{ns}	14.64***
Cadmium × Mycorrhizae							
$LSD_{0.05}$	0.28**	5.88*	14.03^{ns}	0.61^{ns}	0.38**	3.327^{ns}	29.28^{ns}

Statistical significance was at 0.05 p value. *** = p<0.0001, ** p < 0.001, * p <0.05, ns = not significant at p<0.05, ± standard deviation, LSD = Least significant difference at 5% level of significance. Means with the same letter used as superscripts within a column are not significantly different (p<0.05), -Myco= zero mycorrhizae, +Myco= mycorrhizae applied at 20 mL plant^{-1}

Table 1 shows foliar Cd and P contents were reduced by Cd toxicity. Foliar Cd content was reduced by 278%, 17.68%, and 5.8% in soils that had 40, 80, and 120 mg Cd kg^{-1} (*Table 1*, *Fig. 1*). These results are supported by work done on *Lactuca sativa* (L.) where leaf Cd was lowered by AMF at the same time plant growth was increased (Cozzolino et al., 2010). At a higher level, Cd, competes with P in the cytoplasm affecting the physiological processes of the plant cell, which reduces phosphorus uptake, due to the similarity of Cd and mineral phosphate (Zhao et al., 2010). A negative relationship

http://www.aloki.hu ● ISSN 1589 1623 (Print) ● ISSN 1785 0037 (Online)
DOI: http://dx.doi.org/10.15666/aeer/2001_043053

occurred between P and Cd in shoots in both zero AMF (r = -0.62**) and AMF use (r = -0.70**) treatments (*Table 2*). As an indication of stress, the proline levels were increased with increasing levels of Cd. This is an indication that barley production can be improved on Cd polluted soil using AMF; thus, the observed proline increase was to protect plants against the stress caused by soil Cd toxicity (Ullah, 2016). Proline protects the cell membranes and proteins from the oxidative stress of hydroxyl ions and superoxide ions through chemical and physical processes (Keshavarz et al., 2016).

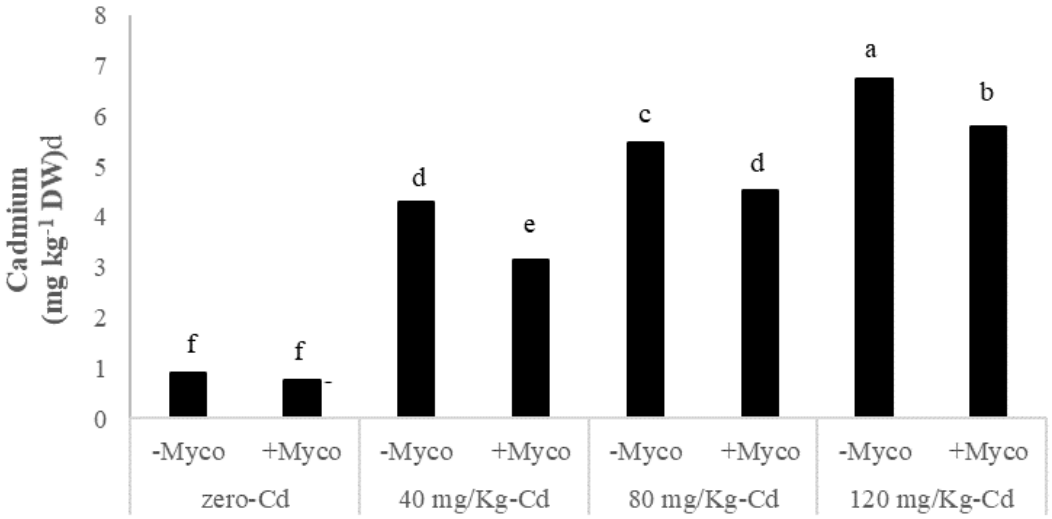

Figure 1. *Foliar Cd of barley grown on Cd polluted soil amended with mycorrhizal fungi (-Myco= zero mycorrhizae, +Myco= mycorrhizae applied at 20 mL plant^{-1})*

AMF colonization of the root was affected significantly ($p<0.05$) by the interaction between Cd and mycorrhizal fungi as depicted in *Fig. 2*. Fungal colonization was increased where AMF was used. Javaid (2009) study showed a contrary effect to our study of Cd polluted soil on mycorrhizal fungi. On the other hand, Garg et al. (2015) and Al-Agely et al. (2005) reported an increase in root colonization by AMF under Cd toxicity. These differences in plant response to inoculation is attributed to the type of host plant, environmental conditions and the amount of energy provided by the host.

Table 1 shows that CAT ($p<0.0001$), SOD ($p<0.0001$), and MDA were significantly increased by increasing levels of Cd contamination, however the activity of SOD and CAT were decreased where mycorrhizal fungi was used. Superoxide dismutase is a key enzyme for protecting cells against oxidative stress, it accelerates the conversion of O_2^- to H_2O_2 and O_2. Research by Parlak (2016) showed that increasing Ni concentration increased the activity of superoxide dismutase in barley seedlings. In this study, the use of mycorrhizae in different levels of Cd reduced the enzymatic activity, which can be attributed to the development of root volume and increased water availability (Neumann and George, 2005). Therefore, as the stress level decreases, the production of oxygen free radicals decreases, and the activity of the leaf superoxide dismutase enzyme decreases (Ullah, 2016).

http://www.aloki.hu ● ISSN 1589 1623 (Print) ● ISSN 1785 0037 (Online)
DOI: http://dx.doi.org/10.15666/aeer/2001_043053

Table 2. *Pearson correlation coefficients between measured parameters of barley cultivated on Cd contaminated soils*

	Parameters	Root colonization	LAI	Chlorophyll	MDA	Proline	Cadmium	Phosphorous	Catalase	Peroxidase	SOD	100 seed weight	Dry mass
Zero mycorrhizal inoculation	Root colonization	1											
	LAI	-0.18 ^{ns}	1										
	Chlorophyll	-0.13 ^{ns}	0.95 **	1									
	Malondialdehyde	0.37 ^{ns}	-0.70 **	-0.70 **	1								
	Proline	0.26 ^{ns}	-0.95 **	-0.87 **	0.59 *	1							
	Cadmium	0.17 ^{ns}	-0.96 **	-0.86 **	0.61 *	0.97 **	1						
	Phosphorous	-0.09 ^{ns}	0.62 *	0.63 *	0.43 ^{ns}	-0.64 *	-0.62 *	1					
	Catalase	0.21 ^{ns}	-0.94 **	-0.83 **	0.60 *	0.96 **	0.99 **	-0.68 *	1				
	Peroxidase	0.26 ^{ns}	-0.95 **	-0.84 **	0.67 *	0.97 **	0.98 **	-0.61 *	0.97 **	1			
	SOD	0.20 ^{ns}	-0.97 **	-0.88 **	0.65 *	0.93 **	0.99 **	-0.66 *	0.98 **	0.99 **	1		
	1000 seed weight	-0.16 ^{ns}	0.89 **	0.83 **	0.74 **	-0.87 **	-0.89 **	0.65 *	-0.89 **	0.88 **	-0.91 **	1	
	Dry mass	0.20 ^{ns}	0.77 **	0.77 **	-0.16 ^{ns}	-0.77 **	-0.77 **	0.63 *	-0.75 **	-0.68 *	-0.77 **	0.67 *	1
20 ml mycorrhizal inoculation	Root colonization	1											
	LAI	0.85 **	1										
	Chlorophyll	0.74 **	0.90 **	1									
	Malondialdehyde	-0.63 *	-0.86 **	-0.87 **	1								
	Proline	-0.84 **	-0.95 **	-0.86 **	0.83 **	1							
	Cadmium	-0.88 **	-0.97 **	-0.85 **	0.81 **	0.97 **	1						
	Phosphorous	0.72 **	0.63 *	0.61 *	-0.64 *	-0.70 **	-0.70 **	1					
	Catalase	-0.88 **	-0.95 **	-0.77 **	0.77 **	0.95 **	0.99 **	-0.72 **	1				
	Peroxidase	-0.89 **	-0.95 **	-0.76 **	0.80 **	0.92 **	0.96 **	-0.64 *	0.97 **	1			
	SOD	-0.85 **	-0.96 **	-0.81 **	0.78 **	0.97 **	0.99 **	-0.69 *	0.99 **	0.97 **	1		
	100 seed weight weight	0.64 *	0.83 **	0.72 **	-0.85 **	-0.87 **	-0.86 **	0.73 **	-0.86 **	-0.84 **	-0.88 **	1	
	Dry mass	0.77 **	0.74*	0.70 *	-0.38 ^{ns}	-0.77 **	-0.79 **	0.50 ^{ns}	-0.76 **	-0.69 *	-0.79 **	0.56 ^{ns}	1

Statistical significance was at 0.05 p value. *** = p<0.0001, ** p < 0.001, * p <0.05, ns = not significant at p<0.05

http://www.aloki.hu ● ISSN 1589 1623 (Print) ● ISSN 1785 0037 (Online)
DOI: http://dx.doi.org/10.15666/aeer/2001_043053

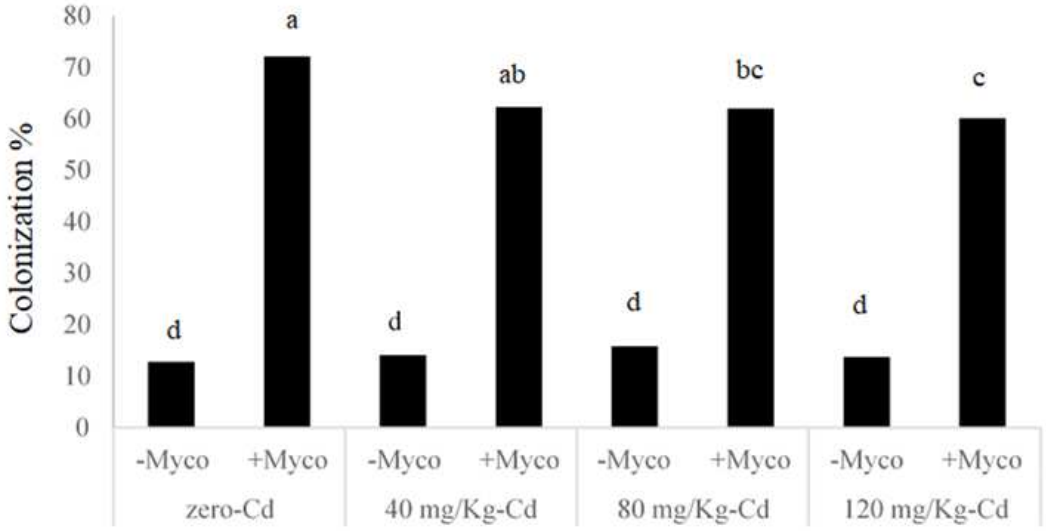

Figure 2. *Mycorrhizal root colonisation of barley grown on Cd polluted soil amended with mycorrhizal fungi (-Myco= zero mycorrhizae, +Myco= mycorrhizae applied at 20 mL plant^{-1})*

Table 1 and *Fig.* 3 shows a significant interaction, that is the activity of POX was significantly increased by soil Cd, its activity was increased by 31.63% at the same time it was decreased by AMF inoculum. The levels of CAT and POX were increased with increasing levels of soil Cd and were both decreased by the use of mycorrhizal fungi. Previously an increased activity of the antioxidant enzymes catalase and peroxidase under the Cd, Hg, Ni, and Pb stress was reported (Azcon-Aguilar et al., 1997). Increased activity of catalase can be due to the fact that these enzymes are involved in the antioxidant defense system of plants under oxidative stress caused by heavy metals (Tohidi-Moghaddam, 2017). CAT and POX are other important enzymes that are activated under stress. These enzymes are able to digest and remove hydrogen peroxide (H_2O_2) (Khatun et al., 2008). Thus, hydrogen peroxide (H_2O_2), which is a toxic product of SOD function, is used by these enzymes (Keshavarz et al., 2016). Arbuscular mycorrhizal fungi help the host plant to absorb nutrients, but also improve the tolerance of the plant to non-environmental environmental factors (Jahromi et al., 2008). These fungi reduce the concentration of heavy metal in the cell wall by binding heavy metal to chitin (Hildebrandt et al., 2007) and glomalin secretion (González-Chávez et al., 2004; Wang et al., 2016). Therefore, it seems that AMF reduce the activity of CAT and POX by reducing the absorption of heavy metals and thus reducing the oxidative stress caused by the absorption of heavy metals. Plants grown in the presence of heavy metals showed a decrease in water uptake, photosynthesis, nutrient uptake, and 1000 seed weight. The use of mycorrhizae can cause the development of longitudinal meristems of the roots and reduce the activity of catalase and peroxidase of leaves.

Table 3 shows the PCA used to reduce the redundancy interaction between Cd and mycorrhizal data, and the eigenvalue of correlation matrix. *Table 3* and *Fig. 4* show the interaction between Cd and AMF treatment, out of fourteen principal components (PC) used, the first two (PC1 and PC2) accounted for most of the variability, with a cumulative variability >77.01%. PC1 accounted for 77.02%, while PC2 accounted for 7.12% of the total variance. *Table 3* and *Fig. 4* show that plant height, number of grains, 1000 seed weight, total dry mass, chlorophyll, proline, SOD, CAT, P, POX, LAI, MDA, leaf Cd

http://www.aloki.hu ● ISSN 1589 1623 (Print) ● ISSN 1785 0037 (Online)
DOI: http://dx.doi.org/10.15666/aeer/2001_043053

content, were loaded positively on PC1, however only colonization was loaded on PC2. This is an indication that mycorrhizal can be used to mitigate against Cd pollution in the soil.

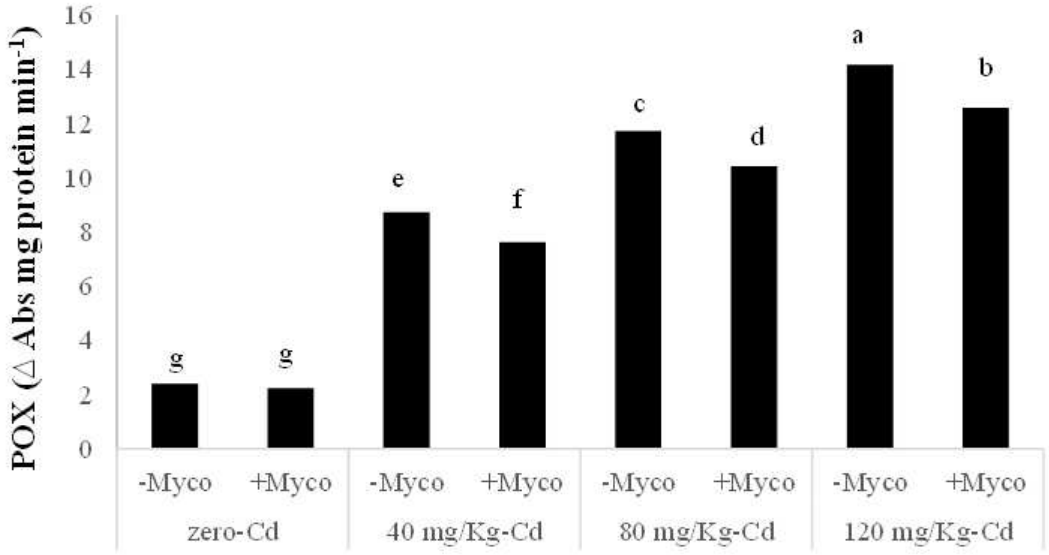

Figure 3. *Peroxidae activity of barley grown on Cd polluted soil inoculated with mycorrhizal fungi (-Myco= zero mycorrhizae, +Myco= mycorrhizae applied at 20 mL plant^{-1})*

Table 3. *Eigenvalues and principal component factor loading of parameters affected by the interaction between Cd and mycorrhizal fungi*

Principal component	PC1	PC2
Eigenvalues:	10.782	0.996
Variability (%)	77.017	7.117
Cumulative %	77.017	84.133
Factor loading		
Height	**0.881**	0.002
Number of grain	**0.629**	0.003
1000 seed weight	**0.832**	0.019
DM	**0.624**	0.006
Chlorophyll	**0.853**	0.000
Proline	**0.949**	0.004
SOD	**0.927**	0.027
CAT	**0.931**	0.003
P	**0.540**	0.001
POX	**0.947**	0.029
LAI	**0.956**	0.015
MDA	**0.632**	0.023
Cadmium	**0.962**	0.011
Colonization	0.119	**0.854**

http://www.aloki.hu ● ISSN 1589 1623 (Print) ● ISSN 1785 0037 (Online)
DOI: http://dx.doi.org/10.15666/aeer/2001_043053

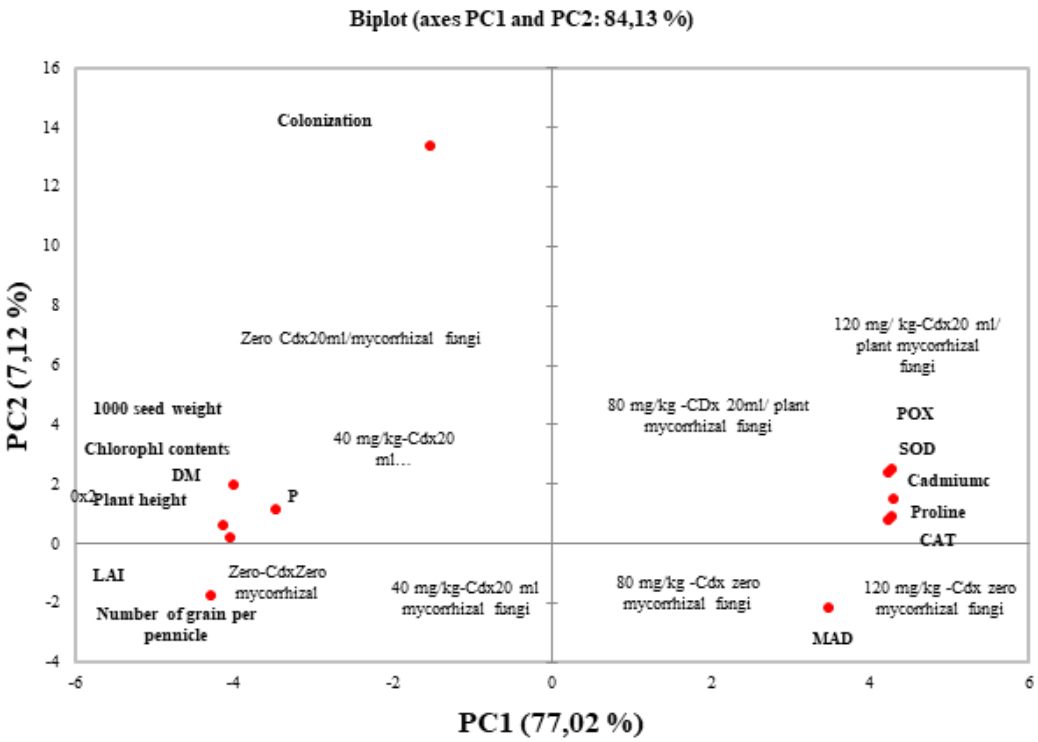

Figure 4. *Rotated principal component loadings of agronomic and physiological attributes of barley affected by the interaction between Cd and mycorrhizal fungi*

Conclusion

Leaf area index, 1000 seed weight, and dry mass of barley were affected by Cd. At the same time chlorophyll and leaf P were decreased and with a subsequent increase was observed in proline, superoxide dismutase, catalase, and peroxidase activity in leaves. The use of mycorrhizae under cadmium contaminated conditions improved yield attributes of barley. Therefore, future studies must focus on testing this effect under field conditions before the use of AMF on Cd contaminated soils can be recommended.

REFERENCES

[1] Al-Agely, A., Sylvia, D. M., Ma, L. Q. (2005): Mycorrhizae increase arsenic uptake by the hyperaccumulator Chinese brake fern (*Pteris vittata* L.). – J Environ Qual 34(6): 2181-2186. doi: 10.2134/jeq2004.0411.

[2] Arnon, D. I. (1949): Copper enzymes in isolated chloroplasts. Polyphenoloxidase in *Beta vulgaris*. – Plant Physiology 24: 1-15. http://dx.doi.org/10.1104/pp.24.1.1.

[3] Azcon-Aguilar, C., Cantos, M., Troncoso, A., Barea, J. M. (1997): Beneficial effect of arbuscular mycorrhizas on acclimatization of micropropagated plantlets. – Scientia Horticulturae 72: 63-71. http://dx.doi.org/10.1016/S0304-4238(97)00120-9.

[4] Bano, S. A., Ashfaq, D. (2013): Role of mycorrhiza to reduce heavy metal stress. – Natural Science 5(12): 16-20. DOI: 10.4236/ns.2013.512A003.

[5] Bates, L. S., Waldern, R. P., Teave, I. D. (1973): Rapid determination of free proline for water stress studies. – Plant and Soil 39: 205-207. http://dx.doi.org/10.1007/BF00018060.

http://www.aloki.hu ● ISSN 1589 1623 (Print) ● ISSN 1785 0037 (Online)
DOI: http://dx.doi.org/10.15666/aeer/2001_043053

[6] Cakmak, I., Horst, W. (1991): Effect of aluminum on lipid peroxidation, superoxide dismutase, catalase and peroxidase activities in root tip of soybean (*Glycine max* L.). – Plant Physiology 83: 463-468. https://doi.org/10.1111/j.1399-3054.1991.tb00121.x.
[7] Cozzolino, V., Pigna, M., Di Meo, V., Caporale, A. G., Violante, A. (2010): Effects of arbuscular mycorrhizal inoculation and phosphorus supply on the growth of *Lactuca sativa* L. and arsenic and phosphorus availability in an arsenic polluted soil under non-sterile conditions. – App. Soil Eco. 45: 262-268. https://doi.org/10.1016/j.apsoil.2010.05.001.
[8] De Vos, C., Schat, H., De Waal, M., Vooijs, R., Ernst, W. (1991): Increased to copper-induced damage of the root plasma membrane in copper tolerant *Silene cucubalus*. – Plant Physiol. 82: 523-528. doi:abs/10.1111/j.1399-3054.1991.tb02942.x.
[9] Dhir, B., Sharmila, P., Saradhi, P. P., Nasim, S. A. (2009): Physiological and antioxidantresponses of *Salvinia natans* exposed to chromium-rich wastewater. – Ecotoxicology and Environmental Safety 72(6): 1790-1797. doi:10.1016/j.ecoenv. 2009.03.015.
[10] Ebenebe, P. C., Shale, K., Sedibe, M. M., Tikilili, P., Achilonu, M. C. (2017): South African mine effluents: Heavy metal pollution and impact on the ecosystem. – Int. J. Chem. Sci. 15: 198-208.
[11] Gadd, G. M. (2004): Microbial onfluence on metal mobility and application for bioremediation. – Geoderma 122: 109-119. doi:10.1016/j.geoderma.2004.01.002.
[12] Galas-Gorcher, H. (1991): Dietary intake of pesticide residues: Cadmium, mercury and lead. – J Food add Contam. 8: 79-80.
[13] Garg, N., Singla, P., Bhandari, P. (2015): Metal uptake, oxidative metabolism, and mycorrhization in pigeonpea and pea under arsenic and cadmium stress. – Turk. J. Agri. Forest. 39: 234-250. https://doi.org/10.3906/tar-1406-121.
[14] Ghanati, F., Morita, A., Yokota, H. (2002): Induction of suberin and increase of liginin content by exess boron in tobacco cell. Soil Science. – Plant Nutri. 48: 357-364. doi: 10.1104/pp.59.2.309.
[15] Giannopolitis, C., Ries, S. (1977): Superoxide dismutases. I. Occurence in higher plant. – Plant Physiol. 59: 309-314.
[16] González-Chávez, M. C., Carrillo-González, R., Wright, S. F., Nichols, K. A. (2004): The role of glomalin, a protein produced by arbuscular mycorrhizal fungi, in sequestering potentially toxic elements. – Environmental Pollution 130: 17-323. https://doi.org/10.1016/j.envpol.2004.01.004.
[17] Hildebrandt, U., Regvar, M., Bothe, H. (2007): Arbuscular mycorrhiza and heavy metal tolerance. – Phytochemistry 68: 139-146. 10.1016/j.phytochem.2006.09.023.
[18] Jahromi, F., Aroca, R., Porcel, R., Ruiz-Lozano, J. M. (2008): Influence of salinity on the in vitro development of *Glomus intraradices* and on the in vivo physiological and molecular responses of mycorrhizal lettuce plants. – Microbial Eco. 55: 45-53. https://doi.org/10.1007/s00248-007-9249-7.
[19] Javaid, A. (2009): Arbuscular mycorrhizal mediated nutrition in plants. – Journal of Plant Nutrition 32: 1595-1618. http://dx.doi.org/10.1080/01904160903150875.
[20] Keshavarz, H., Modarres-Sanavy, S. A. M., Sadegh Gol-Moghadam, R. (2016): Impact of foliar application with Salicylic Acid on Biochemical Characters of Canola Plants under Cold Stress Condition. – Not. Sci. Biol. 8(1): 98-105. https://doi.org/10.15835/nsb.8.1.9766.
[21] Keshavarz, H. (2020): Study of water deficit conditions and beneficial microbes on the oil quality and agronomic traits of canola (*Brassica napus* L.). – Grasas Y Aceites. 71(3): e373. https://doi.org/10.3989/gya.0572191.
[22] Khatun, S., Ali, M. B., Hahn, E. J., Paek, K. Y. (2008): Cooper toxicity in *Withania somnifera*: Growth and antioxidant enzymes responses of in vitro grown plants. – Environ. Exp. Bot. 64: 279-285. http://dx.doi.org/10.1016/j.envexpbot.2008.02.004.
[23] Neumann, E., George, E. (2005): Does the presence of arbuscular mycorrhizal fungi influence growth and nutrient uptake of a wild-type tomato cultivar and a mycorrhiza-

http://www.aloki.hu ● ISSN 1589 1623 (Print) ● ISSN 1785 0037 (Online)
DOI: http://dx.doi.org/10.15666/aeer/2001_043053

defective mutant, cultivated with roots sharing the same soil volume? – New Phytol. 166(2): 601-609. https://doi.org/10.1111/j.1469-8137.2005.01351.x.

[24] Pandey, N., Sharma, C. P. (2002): Effect of heavy metals CO_2^+, Ni^{2+} and Cd^{2+} on growth and metabolism of cabbage. – Plant Sci. 163: 753-758. doi:10.1016/S0168-9452(02)00210-8.

[25] Parlak, K. U. (2016): Effect of nickel on growth and biochemical characteristicsof wheat (*Triticum aestivum* L.) seedlings. – NJAS - Wageningen J. Life Sci. 76: 1-5. https://doi.org/10.1016/j.njas.2012.07.001.

[26] Pereira, E., Coelho, V., Tavares, R. M., Lino-Neto, T., Baptista, P. (2012): Effect of competitive interactions between ectomycorrhizal and saprotrophic fungi on *Castanea sativa* performance. – Mycorrhiza 22: 41-49. doi:10.1007/s00572-011-0379-x.

[27] Pharudi, J. A. (2010): Effect of mycorrhizal inoculation and phosphorus levels on growth and yield of wheat and maize crops grown on a phosphorus deficient sandy soil. – MSc, Agric (Agronomy) dissertation, University of Stellenbosch, South Africa.

[28] Qiu, L., Bi, Y., Jiang, B., Wang, Z., Zhang, Y., Zhakypbek, Y. (2018): Arbuscular mycorrhizal fungi ameliorate the chemical properties and enzyme activities of rhizosphere soil in reclaimed mining subsidence in northwestern China. – J. Arid Land 11: 135-147. https://doi.org/10.1007/s40333-018-0019-9.

[29] Shi, G., Ma, H., Chen, Y., Liu, H., Song, G., Cai, Q., Lou, L., Rengel, Z. (2019): Low arsenate influx rate and high phosphorus concentration in wheat (*Triticum aestivum* L.): a mechanism for arsenate tolerance in wheat plants. – Chemosphere 214: 94-102. 10.1016/j.chemosphere.2018.09.090.

[30] Tavakkoli, L., Khanjani, N. (2016): Environmental and occupational exposure to cadmium in Iran: A systematic review. – Rev. Environ. Health 31(4): 457-463. doi: 10.1515/reveh-2016-0042. PMID: 27902453.

[31] Tohidi-Moghadam, H. R. (2017): Super absorbent polymer mitigates deleterious effects of arsenic in wheat. – Rhizosphere 3: 40-43. 10.1016/j.rhisph.2016.12.003.

[32] Tripathi, R. D., Tripathi, P., Dwivedi, S., Kumar, A., Mishra, A., Chauhan, P. S., Norton, G. J., Nautiyal, C. S. (2014): Roles for root iron plaque in sequestration and uptake of heavy metals and metalloids in aquatic and wetland plants. – Metallomics 6: 1789-1800. https://doi.org/10.1039/C4MT00111G.

[33] Ullah, H. A. (2016): Alleviating effect of exogenousm application of ascorbic acid on growth and mineral nutrients in cadmium stressed barley (*Hordeum vulgare*) seedlings. – Int. J. Agri. Biol. Faisalabad 18: 73-79.

[34] Wang, H. Y., Wen, S. L., Chen, P., Zhang, L., Cen, K., Sun, G. X. (2016): Mitigation of cadmium and cadmium in rice grain by applying different silicon fertilizers in contaminated fields. – Environ. Sci. Pollution Res. 23: 3781-3788. doi:10.1007/s11356-015-5638-5.

[35] WHO. (2000): Cadmium. – Air Quality Guidelines - Second Edition. Chapter 6.3. WHO Regional Office for Europe, Copenhagen, Denmark.

[36] Zhao, F. J., McGrath, S. P., Meharg, A. A. (2010): Arsenic as a food chain contaminant: mechanisms of plant uptake and metabolism and mitigation strategies. – Annu. Rev. Plant Biol. 61: 535-559. https://doi.org/10.1146/annurev-arplant-042809-112152.

http://www.aloki.hu ● ISSN 1589 1623 (Print) ● ISSN 1785 0037 (Online)
DOI: http://dx.doi.org/10.15666/aeer/2001_043053

EVALUATION OF THE POTENTIAL TOXICITY OF TAU-FLUVALINATE ON ADULT HONEYBEES *APIS MELLIFERA*, UNDER LABORATORY CONDITIONS

ALJEDANI, D. M.

Department of Biological Sciences, College of Science, University of Jeddah, Jeddah, Saudi Arabia
(e-mail: dmaljedani@uj.edu.sa)

(Received 10th Sep 2021; accepted 28th Oct 2021)

Abstract. In this study, honeybees have been exposed to tau-fluvalinate to assess survival and determine the concentration at which the highest mortality occurred, and the extent to which this pesticide affects the internal organs of the digestive system. Four different concentrations of tau-fluvalinate were used (3.6, 6.25, 12.5, 25.5 mg/L) on the forager honeybee worker. The adult workers were under continuous observation and assessed after 12, 24, 48, 72, and 96 h following the treatment by LC_{50} of tau-fluvalinate to determine adult workers' longevity. According to the results of this study, a 13.700 mg/L concentration of tau-fluvalinate kills half of the individuals. Also, there is a direct relationship between the time of exposure to the pesticide and its effect on the survival of adult workers. Also, the midgut was found to be torn and incoherent and showed signs of shrinking. The colour of the ileum became transparent also after the treatment, its walls shrunk, and thin lines appeared. Also, it was found that the rectum, after the treatment had very thin walls that were almost lacerated. This provides a useful indicator of the possible effect of tau-fluvalinate, which was found to have negative effects on worker body parameters and bee anatomy.
Keywords: *Acaricide, Apis mellifera jemenatica, concentrations, digestive system, longevity, mortality*

Introduction

The social insect honeybee (*Apis mellifera*) is the most critical pollinator on the globe, the health of *Apis mellifera* colonies has been a major concern in recent years (VanEngelsdorp et al., 2017). Many factors, both biotic and abiotic, affect honeybee colonies. Varroa mites (Varroa destructor) are one of the biotic causes that have a heavy adverse effect on honeybees all over the world. As described by Rangel and Tarpy (2016) these mites were thought to be one of the causes of colony collapse disorder (CCD). For decades, the ectoparasitic mite *Varroa destructor* has become the most serious issue in beekeeping around the world. The Varroa mite's destructive effect on *Apis mellifera* has become especially evident in recent years, with a substantial increase in controlled colony mortality and global honeybee population declines (Potts et al., 2010).

Varroa control has been developed and tested using a variety of natural, mechanical, and chemical methods (Allam et al., 2021). Beekeepers usually rely on a reduced set of acaricides to manage the parasite, the pyrethroids tau-fluvalinate or flumethrin, the organophosphate coumaphos, and the formamidine amitraz. However, the evolution of resistance in the mite populations is leading to an unsustainable scenario with almost no alternatives to reach an adequate control of the mite (Sara et al., 2021). Chemical materials (i.e. acaricides) are, however, almost always the most efficient method. But the problem with using acaricides is the high residue level in bee products; additionally, acaricides used in beehives affect Varroa mites and honeybees. Unfortunately, acaricides' long-term effects on honeybees have yet to be identified (Semkiw et al., 2013).

http://www.aloki.hu ● ISSN 1589 1623 (Print) ● ISSN 1785 0037 (Online)
DOI: http://dx.doi.org/10.15666/aeer/2001_055067

Contaminants can alter organism behavior and, as a result, their ability to survive. The active ingredient in a pesticide widely used in North America to control *Varroa destructor* mites in honeybee (*Apis mellifera*) colonies is tau-fluvalinate, the effects of fluvalinate on honeybees are unknown to now (Frost et al., 2013). The effects of tau-fluvalinate, which is the active ingredient of Apistan®, were investigated by Davies et al. (2007) they found the sensitivity of honeybees to stimuli and the mortality of honeybees of fluvalinate, which is a form of neurotoxin that acts as an agonist for voltage-gated sodium channels to prolong membrane depolarization.

Honeybees nurse larvae inside the hive, while worker bees forage on pollen and nectar from flowers outside the hive as they grow older (Vojvodic et al., 2013). The adult gut is divided into four main organs (crop, midgut, ileum, and rectum), each of which serves a different role in catabolism and absorption (Kakamand et al., 2008). Furthermore, many pathogens begin to be diagnosed through the internal tissues and structures (Gisder and Genersch, 2020). Moreover, honeybee Pharmacology examines the effects of different drugs and chemical substances experienced by the honeybee while foraging for nectar, pollen, propolis, and water, as well as the effects of drug treatments applied to the colony deliberately and is discussed in a comparative manner using the individual honeybee as a model for extrapolation of these principles to the superorganism (Davidson, 2021).

A variety of chemicals, including tau-fluvalinate, are available for the management of Varroa mites in honeybee colonies. The optimal dose of these chemicals should provide the best Varroa control with the least amount of harm to honeybees. Honeybees are likely to be harmed as a result of the high doses (Allam et al., 2021). Fluvalinate residues detected in both honey and wax collected from colonies treated with the strips method exceeded the maximum residue limits (0.05 ppm for both honey and wax) according to the EU pesticides database (Abd El-Wahab et al., 2021). So, further research has been needed to do on the impact of these chemicals on honeybees. As a result, assessing the possible effects of acaricides on honeybees is important. So, this study aimed into the effects of sub-lethal concentrations of a common acaricide (tau-fluvalinate) on the survival parameters of honeybee workers who were exposed to it and the extent to which this pesticide affects the internal organs of the gastrointestinal tract.

Materials and methods

Honeybees and insect cells

The present study was carried out in the apiary and a lab in March 2021 on adult worker honeybees (*Apis mellifera jemenatica*) (Hymenoptera: Apidae), which were collected from an apiary at the Faculty of Environmental Sciences research station in Saudi Arabia. It has been preserved in a pesticide-free environment and handled according to traditional beekeeping practices. The colonies had not undergone any chemical therapies for at least six months. Visual observation was used to monitor the colonies' health weekly until research. It was then moved to the University of Jeddah's Laboratory of Entomology.

Bee rearing and feeding

Emerging brood frames were collected from colonies and placed in an incubator at 35 °C and 50% relative humidity. Groups of 450 newly emerged workers were gathered

http://www.aloki.hu ● ISSN 1589 1623 (Print) ● ISSN 1785 0037 (Online)
DOI: http://dx.doi.org/10.15666/aeer/2001_055067

and placed in 15 x 15 x 15 cm wood cages with wire mesh and were followed until they reached the age of foraging honeybee workers. For breeding, wooden boxes were used, with one side of the wooden box covered in metal wire mesh and the other with glass. The workers were fed. On the top side of the cage, two plastic medical syringes (50 ml) were inserted, one with water and the other with a 50% w/v sugar solution, added to it different concentrations of the pesticide(Aljedani, 2017). Also, in the control group sugar solution was introduced only, without any insecticide. In addition, they were given pollen. In three cages per treatment (Ardalani et al., 2021), and the chronic oral toxicity test on adult worker honeybees under laboratory conditions over an exposure period of 10 days was based on the OECD Acute Oral Toxicity Test, described by OECD (2017).

Tau-fluvalinate

The tau-fluvalinate pyrethroid, a subset of fluvalinate isomers, was the first synthetic varroacide approved for use in honeybee colonies in the United States (Johnson et al., 2010). The tau-fluvalinate has been commonly used to control Varroa mites. Four different concentrations (3.6, 6.25, 12.5, 25.5 mg/L) of tau-fluvalinate (Qi et al., 2020) were used.

Tau-fluvalinate is the ISO common name for (RS)- α -cyano-3-phenoxybenzyl N-(2-chloro-α, α, α -trifluoro-p-tolyl)-$_D$-valinate (IUPAC). Tau-fluvalinate represents a 1:1 mixture of two isomers (R- α -cyano and S- α -cyano isomers) whereby fluvalinate consists of four isomers (Brancato et al., 2018).
Product name: tau-Fluvalinate, Pestanal ^{TM}, analytical standard (96.9% purity).
Brand: Sigma-Aldrich, Product of Switzerland.
Formula: C_{26} H_{22} ClF_3 N_2 O_3
For structural formula, see *Figure 1*.

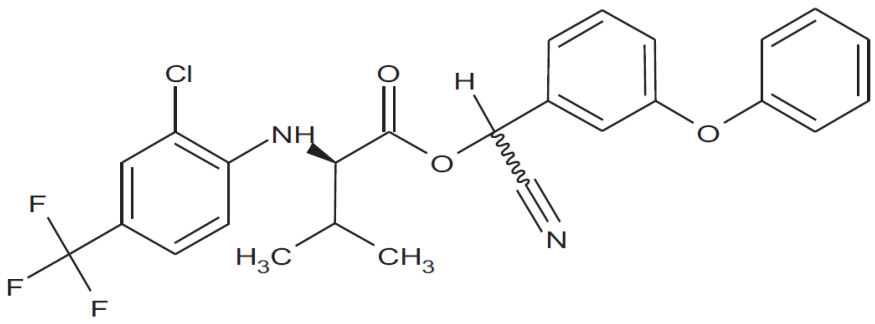

Figure 1. *Structural formula of tau-fluvalinate*

Procedures for conducting research

In this analysis, forager honeybee workers *Apis mellifera jemenatica* were exposed to different concentrations of tau-fluvalinate, and the benchmark for dose was prepared by diluting them in 95% ethanol LD_{50} (2.0 mg/ml) on the day of treatments. The aim was to see how long they survived after being exposed to it and the extent to which the internal organs of the gastrointestinal tract are affected by this pesticide.

http://www.aloki.hu ● ISSN 1589 1623 (Print) ● ISSN 1785 0037 (Online)
DOI: http://dx.doi.org/10.15666/aeer/2001_055067

The mortality

After incubation and feeding on sucrose adult honeybees were orally exposed to four different concentrations (3.6, 6.25, 12.5, 25.5 mg/L) of tau-fluvalinate. The mortality was assessed, and the lethal concentration (LC_{50}) was determined. The survival data on caged bees under exposure to tau-fluvalinate had in addition to a control group (0.00 mg/L). If the adults could not move after being prodded with a fine hairbrush, they were considered dead.

Longevity

The adult honeybee workers were followed up and assessed after 12, 24, 48, 72, and 96 h, after treatment by LC_{50} of tau-fluvalinate, in addition to a control group (0.00 mg/L) to determine adult workers' longevity.

The anatomical structure

Internal anatomy in the alimentary canal of adult workers

A group of the forager honeybee workers was exposed to concentration LC_{50} for four days, where honeybee workers were fed for 4 days with concentration LC_{50}, and then surviving workers were frozen and then stored at −4 ℃ until dissection, in addition to a control group (0.00 mg/L).

For all insects, preserving as much tissue as possible without degradation is crucial, so freezing and converting the cadavers to 70% ethanol allows for short-term storage and later dissection.

A good understanding of bee internal anatomy is needed to conduct these dissections; the anatomy of *Apis mellifera* is well described by Baker et al. (1982) Dissection techniques are defined, and the methods are described by Carreck et al. (2013).

Sections of the alimentary canals (midgut (Mig), ileum (IL), Rectum (Rect)) in honeybee workers were dissected, in preparation for examination and imaging was carried out with an anatomy microscope connected to a digital camera (Light microscope with Digital camera (Canon power shot S80 DC150).

Statistical analysis

After determining the correction rate of death using Abbott's formula (Abbott, 1925) the findings were evaluated using the toxicity value, Chi-Square test, and values of LC_{50} were calculated and drawing mortality regression lines Ldp line by a computer program (Ldp Line). Besides, results were obtained as mean ± Standard deviation (std) using SPSS software (version 22.0) according to variance (ANOVA). Statistical significance was tested using Student's t-test between two groups and one-way ANOVA for more than two groups and was compared at the 0.05 level by a program SPSS. Statistical differences between each treatment and control were determined separately at each experimental time point to determine adult workers' longevity after treatment by (LC_{50}) of tau-fluvalinate.

Results

When foraging honeybee workers *Apis mellifera jemenatica* were exposed to different concentrations of tau-fluvalinate, the long-term survival of honeybees was

http://www.aloki.hu ● ISSN 1589 1623 (Print) ● ISSN 1785 0037 (Online)
DOI: http://dx.doi.org/10.15666/aeer/2001_055067

tested. The present result of this study showed the extent to which anatomical structure of the internal organs of the gastrointestinal tract is affected by this pesticide after treatment by (LC_{50}) of tau-fluvalinate.

The mortality

In this study, laboratory toxicity was evaluated for tau-fluvalinate of this pesticide 96 h after the treatment of the forager honeybee workers by tau-fluvalinate. By analyzing the toxicological results of tau-fluvalinate it was found that there was a direct proportion between the tested concentrations and the mortality percentages of the treated adult workers with these concentrations. The results also showed that the effective concentrations of the tau-fluvalinate were at (3.6, 6.25, 12.5, 25.5 mg/L). Death rates for treated adult workers ranged from 28%, the lowest concentration to 65% the highest concentration as presented in *Table 1*. On the other hand, the laboratory toxicological lines of the tau-fluvalinate and the statistical constants derived from them showed the difference of the lethal concentration values for half of the number of tested adult workers 50%, 90% and for 99%, which is known as LC_{50}, LC_{90} and LC_{99}, in the treatment with the tau-fluvalinate pesticide 13.700, 175.628, 1404.975 mg/L, respectively. The confidence intervals ranged from the minimum to the upper limit corresponding to these concentrations from (10.615, 19.541 mg/L), (80.282, 856.068 mg/L), and (380.443, 20474.99 mg/L) respectively, at a 95% confidence (*Table 2*). The concentration of tau-fluvalinate that caused 50 percent of forager honeybee workers to die after being exposed to it (LC_{50} = 13.700 mg/L), (*Fig. 2*).

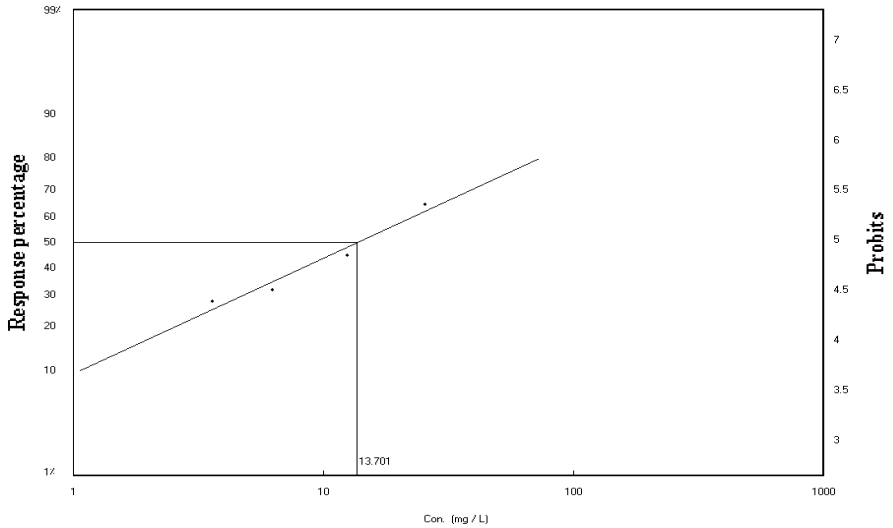

Figure 2. *Lethal concentration (LC_{50}) values after 96 h of exposure of forager honeybee workers to different concentrations of tau-fluvalinate*

The longevity

In the current study, which evaluated the toxicity of the effects of tau-fluvalinate on adult honeybee workers after being affected by lethal half concentration (LC_{50} = 13.700 mg/L), after the 12, 24, 48, 72, and 96 hours of treatment, to determine the long-term effects of tau-fluvalinate on adult honeybee workers. The group that was not treated with any type of insecticide (control group (0.000 mg/L) and were fed naturally did show some type of

http://www.aloki.hu ● ISSN 1589 1623 (Print) ● ISSN 1785 0037 (Online)
DOI: http://dx.doi.org/10.15666/aeer/2001_055067

changes and death, but these were within normal limits continued to the end of the experiment. Also, it was evident from the results of the current study that there is a direct relationship between the time of exposure to the pesticide and its effect on the survival of adult workers. The greater the duration of exposure to this pesticide was, the fewer the number of adult workers and the lower their chance of survival was. The death rate after 12 h in the control group was 1 while 9 in the pesticide-treated group. On the other hand, after 96 h, the number of dead individuals in the control group reached 11 and rose to 43 in the pesticide-treated group (*Fig. 3*).

Table 1. *Relation between different concentrations of tau-fluvalinate and mortality of the forage honeybee workers death after 96 h of treatment*

Con. (mg/L)	Log (Con. * 10)	Observed response %	Linear response%	Linear probit
0.00	0.000	0.000	0.000	0.000
3.6	0.556	28	25.097	4.328
6.25	0.795	32	34.669	4.605
12.5	1.096	45	48.163	4.953
25.5	1.406	65	62.248	5.312

Table 2. *LC_{50}, LC_{90}, and LC_{99} values, slope values for tau-fluvalinate toxicity line, and maximum and minimum values*

Slope	Chi	r	LC_{50}	LC_{90}	LC_{99}
1.1568	1.490	0.977	13.7005	175.628	1404.975
+ /- 0.205	Tabulated 6	Tabulated 0.95			
Lower limit (mg/L)			10.615	80.282	380.443
Upper limit (mg/L)			19.541	856.068	20474.99

Chi-Square (Chiinv) (Chi), probability (p), correlation coefficients (r)

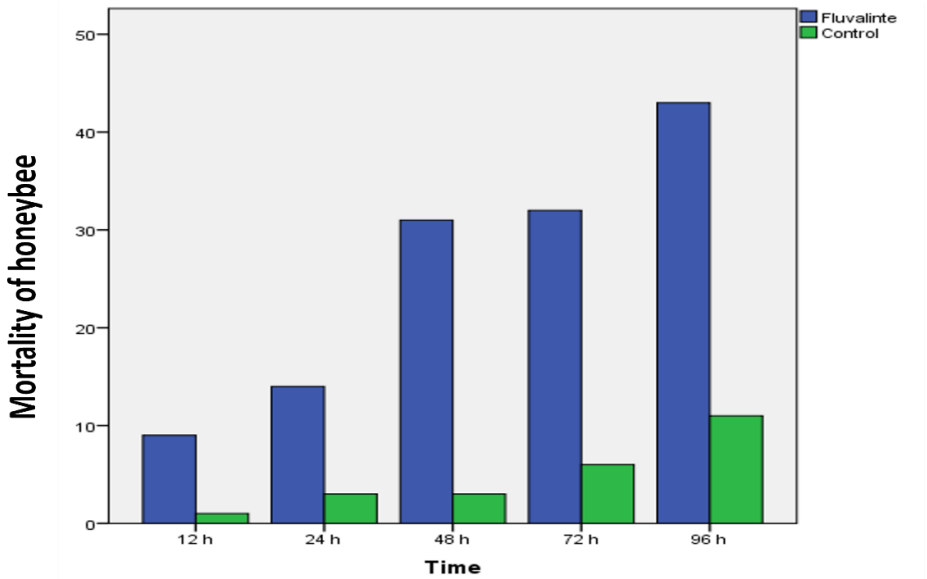

Figure 3. *Comparison of the effect of tau-fluvalinate against forager honeybee worker using the mortality of LC_{50} = 13.7005 mg/L at different times (h)*

http://www.aloki.hu ● ISSN 1589 1623 (Print) ● ISSN 1785 0037 (Online)
DOI: http://dx.doi.org/10.15666/aeer/2001_055067

Furthermore, a group of adult honeybee workers exposed to tau-fluvalinate had a clear impact on its survival. In the control group, the significance (p-value) value reached 0.05 high significance at $P<0.05$. While the group treated with tau-fluvalinate reached 0.01. On the other hand, the value of (Mean ± SD), in the control group reached (4.800 ± 3.898). While the group treated with tau-fluvalinate reached (25.800 ± 13.989) (*Table 3*).

Table 3. *Value of longevity of foragers honeybee workers at 96 h after treatment by tau-fluvalinate at 95% confidence interval of the difference*

Treatment	Sig. (2 tailed)	t	Mean	SD	SE	Minimum	Maximum
Control	0.051	2.753	4.800	3.898	1.743	1.000	11.000
Fluvalinate	0.015	4.124	25.800	13.989	6.256	9.000	43.000

Std. deviation (SD), Std. error mean (SE), Sig. at $P < 0.05$

The anatomical structure

Internal anatomy in the alimentary canal of the adult workers

External anatomical structure of the forager honeybee workers was described and compared between a group of forager honeybee workers exposed to concentration (LC_{50}) for four days, and a control group (0.00 mg/L).

In the first set (the control group) of results were obtained by the anatomical study conducted on the gastrointestinal tract of honeybee workers, that the midgut, which is an organ that follows the gut, and folds into the body cavity in the form of a U-shape, and occupies a large area of the abdominal cavity of the honeybee worker. Among the results of the autopsy on honeybee workers, the following was noted: the midgut is firm and has a homogeneous mass so that the folds almost disappear and are yellow.

Overall, these results of the anatomical study of honeybee workers indicate that the hindgut region is distinguished into two regions; one, the anterior segment, known as the ileum, is a fine, small, and convoluted segment (small intestine), which gets rid of body remnants and wastes and absorbs water, and food residues are stored in the rectum until the bee gets rid of them outside the cell from the anus, and from the autopsy results, the forager honeybee workers are yellow. As a result of emptying, its walls are slightly shrunken and have fine lines.

Secondly, the back part, known as the rectum, is enlarged, and elongated, opening into the cavity of the stinging machine, from the results of the anatomical study that was conducted, it was found that the rectum connects from the front to the back of the small intestine (ileum), which is a cylindrical part, and from the backside, it is in the form of a tube that leads to the anus. The rectum is known to contain a large number of waste products before it is discharged into the outside of the cell, this was evident in *Figure 4* showing (A) midgut (Mig), (B) ileum (IL), (C) Rectum (Rect) in the control group.

In the second set (the group treated with (LC_{50} = 13.700 mg/L) of tau-fluvalinate) of results of the anatomical study that was conducted, it was found that the midgut after treatment appears to be torn and incoherent, and it appears to be shrinking. At the same time the ileum after treatment with the insecticide became transparent, its walls shrunk, and thin lines appeared. From the results of this anatomical study, it was found that the rectum, after treatment with tau-fluvalinate, had very thin walls that were almost

http://www.aloki.hu ● ISSN 1589 1623 (Print) ● ISSN 1785 0037 (Online)
DOI: http://dx.doi.org/10.15666/aeer/2001_055067

lacerated, this was evident in *Figure 4* showing (D) midgut (Mig), (E) ileum (IL), (F) Rectum (Rect) in the group treated with tau-fluvalinate.

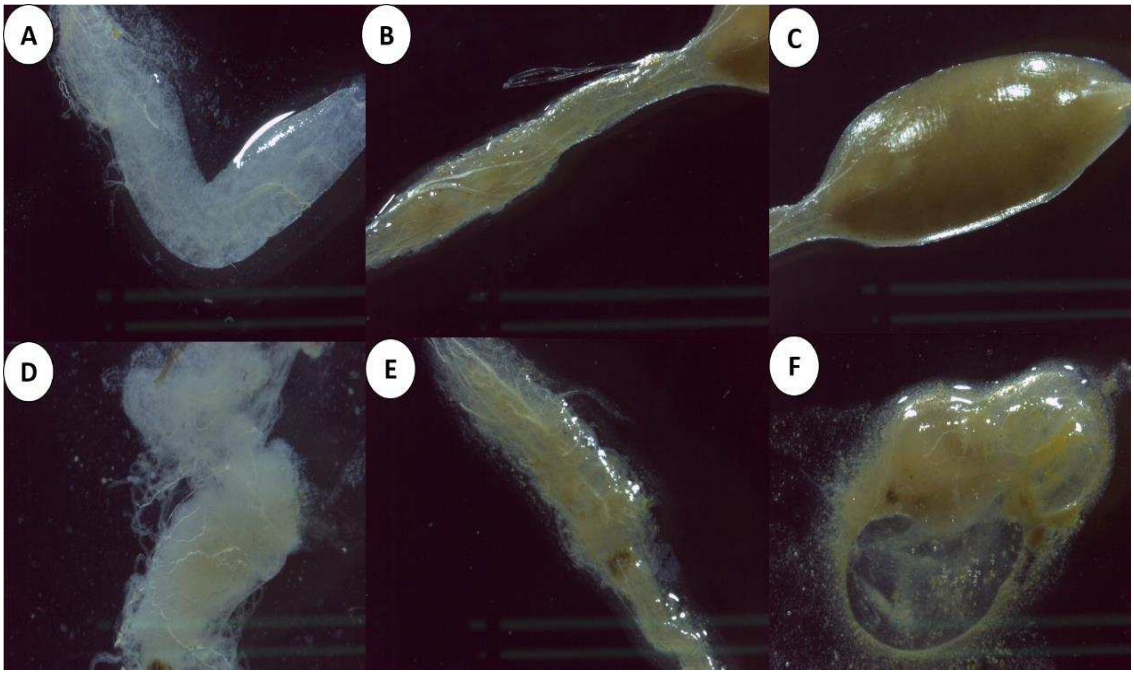

Figure 4. *The anatomical structure of the forager honeybee workers, (A) midgut (Mig), (B) ileum (IL), (C) Rectum (Rect) in the Control group. (D) midgut (Mig), (E) ileum (IL), (F) Rectum (Rect) in the group treated with tau-fluvalinate (x-40)*

Discussion

Recently, the widespread distribution of pesticides found in the hive has posed serious concerns regarding pesticide exposure on honeybees (*Apis mellifera* L.), a honeybee rearing system was adapted to determine the chronic oral toxicity of certain pesticides on honeybees (*Apis mellifera* L.) (Zhu et al., 2014). Tau-fluvalinate, a popular pyrethroid pesticide, is commonly used as an acaricide in honeybee hives to combat the devastating Varroa mite (Wu et al., 2020). And it was discovered to be extremely persistent in the hive, with a half-life of around 5 years in beeswax (Bogdanov, 2006). Fluvalinate's long-term use as an apicultural tool, combined with its absorption by wax in the hive, has resulted in a high level of fluvalinate residue in bee colonies all over the world (Johnson et al., 2010).

Our findings indicate that feeding on common pesticide ingredients, including the miticide fluvalinate, has statistically significant effects on honeybee survival, after 96 h of feeding, and a significant increase in adult worker mortality was observed after treatment. On the other hand, the laboratory toxicological lines of the tau-fluvalinate and the statistical constants derived from them showed the difference of the lethal concentration values for half of the number of tested adult workers 50%, 90% and also for 99%, which is known as LC_{50}, LC_{90}, and LC_{99}, and treatment with the tau-fluvalinate pesticide at 13.700, 175.628, 1404.975 mg/L concentrations, respectively. In a study by Ardalani et al. (2021) Bees were split into two classes and fed either a quercetin-sucrose paste or just sucrose for 72 h to see if dietary quercetin affected the contents of tau-fluvalinate. After that, touch-exposed to 0.9 mg/bee tau-fluvalinate, no

http://www.aloki.hu ● ISSN 1589 1623 (Print) ● ISSN 1785 0037 (Online)
DOI: http://dx.doi.org/10.15666/aeer/2001_055067

significant effect on tau-fluvalinate concentration was observed in bees fed quercetin after 1 h of oral exposure or 24 h of contact exposure. In their hives, honeybees are frequently exposed to tau-fluvalinate. Because of its low acute toxicity to honeybees, acute tau-fluvalinate poisoning is uncommon. The toxicity of tau-fluvalinate and tebuconazole to honeybees is low (LD_{50} ¼ 12 mg/bee and > 200 mg/bee, respectively), but research into the mechanisms that contribute to acaricide and fungicide metabolization is necessary to establish synergistic and antagonistic interactions with natural xenobiotics (European Food Safety Authority, 2010). During an 8-week procedure, up to 10% of the tau-fluvalinate in a single strip can diffuse from the plastic strip formulation into the hive matrices (Bogdanov et al., 1998).

From our results, we conclude that confidence intervals ranged from the minimum to the upper limit corresponding to these concentrations from (10.615, 19.541 mg/L), (80.282, 856.068 mg/L), and (380.443, 20474.99 mg/L) respectively, at a 95% confidence level. On the other hand, our results are not consistent with a study by Johnson et al. (2009) who discovered that tau-fluvalinate is safe for bees under normal circumstance since certain subfamilies of honeybees can efficiently metabolize fluvalinate (Mao et al., 2011). There have been several studies that indicate that high oral fluvalinate treatments have the most negative effects on sucrose responsiveness, whereas control dermal treatments have the least negative effect. Oral procedures seemed to decrease responsiveness in general, which may be due to an antifeedant effect that is more pronounced when honeybees ingest compounds directly (Frost et al., 2013). Furthermore, only oral fluvalinate treatments induced distinct probosci extension behaviors, implying that the high fluvalinate dose (a 10-fold improvement over the low-oral dose) has distinct behavioral effects (e.g. hyperexcitability of muscles). Physiologically, pharmacological activity can disrupt normal feeding (Frost et al., 2013). Fluvalinate mortality rates have been reported to be variable (LD50 of 0.97 μg per honeybee; Santiago, et al., 2000). In general, there have been several studies that indicate fluvalinate mortality rates rise with dosage and that fluvalinate is more lethal when applied orally rather than topically (Frost et al., 2013), this was consistent with our study.

It is evident from the results of the current study that there is a direct relationship between the time of exposure to the pesticide and its effect on the survival of adult workers. The greater the duration of exposure to this pesticide was, the fewer number of the adult workers and the lower their chance of survival was. It is possible that honeybee detoxification processes are not triggered by long-term exposure to low concentrations of active substances, but that honeybee susceptibilities are influenced by higher, more acute concentrations. Also, due to the time required for pesticide bioaccumulation, bee mortality would be latent, which would be preferred by more lipophilic pesticides like fluvalinate as described in the report (Johnson et al., 2013). On the same side, workers who received honey/pollen paste and were exposed to nestmates fared better than all other groups in terms of survival, led by workers who received lactalbumin and were exposed to nestmates, who lived substantially longer than all other groups (Retschnig et al., 2021). When compared to longer-lived workers who ate pollen, negative impact of the antibiotic treatment could be greater in pollen-deprived and therefore short-lived workers (Ricigliano and Simone-Finstrom, 2020). The results by Moro et al. (2021) suggest a shift in host resistance mechanisms within three years. Although the mechanistic explanations of how mites and bees are adapting to each other are currently lacking and call for a holistic view of this particular host-parasite system,

http://www.aloki.hu ● ISSN 1589 1623 (Print) ● ISSN 1785 0037 (Online)
DOI: http://dx.doi.org/10.15666/aeer/2001_055067

including investigations of mite and bee traits in the very same populations over time. Such an approach is required to finally enable a more complete mechanistic understanding of the ability of *Apis mellifera* colonies to survive infestations by *Varroa destructor* through natural selection. This may also offer an avenue towards more sustainable beekeeping with *Apis mellifera* globally.

Therefore, adult workers may be exposed to many factors, whether inside or outside the hive. These study findings found the forager honeybee workers when they were exposed to concentration (LC_{50}) for four days, the midgut was appearing to be torn and incoherent, and it appears to be shrinking. while the ileum after treatment with the tau-fluvalinate, became transparent and its walls shrunk, and thin lines appeared. On the other hand, in the rectum, it was found that the rectum, after treatment with tau-fluvalinate had very thin walls that were almost lacerated. That is consistent with other studies when they found adult honeybee health more affected by pesticides. In a study by Wu et al. (2020), we found that antibiotic treatment significantly attenuated the expression of certain key detox honeybee cytochrome P450s (P450s) in the midgut, and that co-treatment of antibiotics with thiacloprid and fluvalinate led to reduced survivorship and increased pesticide residues within the honeybee, suggesting that dysbiosis resulting from antibiotic exposure affects honeybee detoxification capability and honeybee health.

As well, in the anatomical study that was shown the ileum which gets rid of body remnants and wastes and absorbs water, food residues are stored in the rectum until the bee gets rid of them outside the cell from the anus, and the autopsy results showed that the forager honeybee workers are yellow. As a result of emptying, its walls are slightly shrunken and have fine lines. That is consistent with other studies the *Apis mellifera* ileum is a relatively small organ between the midgut and the rectum that has deep infoldings that provide surface area for the absorption of nutrients not collected in the midgut (Mutinelli, 2021).

The study by van Engelsdorp (2009) forward methods using dissections with dissecting microscopes to find pathologies and describe these pathologies both for adult bees of different ages in healthy colonies and also for adult bees from collapsing colonies and bees in apiaries with CCD. Colonies near collapsing colonies are at a high risk of dying, according to previous studies. Many references and manuals have been written about how to diagnose diseases and pests that might be present in the colony. Thymol powder has the highest efficacy against Varroa mites, with 73.72% mite mortality, followed by formic acid with 72.23%, and fluvalinate strips with 69.21% mite mortality (Ahmad, et al., 2013). Besides, a study by Shoukry et al. (2013) discovered formic acid 60% had a lower effect on honeybee drone mating potential than oxalic acid, fluvalinate, thymol, and amitraz. Most of the research focused on the comparison of essential oils and chemical materials.

Conclusion

Laboratory monitoring of acute effects on the honeybee, *Apis mellifera*, is usually the first step in assessing chemical hazards for bees. The ability to extrapolate acute effects observed in one of the most important agricultural pollinators the honeybee, and longer exposure times, are critical for a thorough risk assessment. Furthermore, the findings of our research have revealed some adverse effects of tau-fluvalinate on forager honeybees *Apis mellifera jemenatica*, at least in preliminary testing and under laboratory

http://www.aloki.hu ● ISSN 1589 1623 (Print) ● ISSN 1785 0037 (Online)
DOI: http://dx.doi.org/10.15666/aeer/2001_055067

conditions. Further research into the effects of sub-lethal doses of tau-fluvalinate on honeybees is urgently needed, particularly because honeybees are frequently exposed to sub-lethal doses of it.

Conflict of interests. The author declares no conflict of interests.

REFERENCES

[1] Abbott, W. S. (1925): A method of computing the effectiveness of an insecticide. – Journal of Economic Entomology 18: 265-267. DOI: https://doi.org/10.1093/jee/18.2.265a.

[2] Abd El-Wahab, T. E., Shalaby, S. E. M., Al-Kahtani, S. N., et al. (2021): Mode of application of acaricides against the ectoparasitic mite (*Varroa destructor*) infesting honeybee colonies, determines their efficiencies and residues in honey and beeswax. – Journal of King Saud University - Science 33: 101236. DOI: 10.1016/j.jksus.2020.101236.

[3] Ahmad, K. J., Razzaq, A., Abbasi, K. H., Shafiq, M., Saleem, M. Arshadullah, M. (2013): Thymol as control agent of mites (*Varroa destructor*) on honeybees (*Apis mellifera*). – Pakistan J Agri Res 26: 316-320.

[4] Aljedani, D. M. (2017): Detection of toxicity and effects of some insecticides to local honey bee race (*Apis mellifera jemenatica*). – Journal of American Science 13: 19-31. DOI: 10.7537/marsjas130317.04.

[5] Allam, S. F. M., Hassan, M. F., Hassan, A. S., Abada, M. K. A. (2021): Simple approaches for environmental and mechanical management of the Varroa mite, *Varroa destructor Anderson and Trueman* (Parasitiformes: Varroidae), on the honey bee, *Apis mellifera* L. (Hymenoptera: Apidae) in Egypt. – Egyptian Journal of Biological Pest Control 31. DOI: 10.1186/s41938-021-00368-8.

[6] Ardalani, H., Vidkjær, N. H., Laursen, B. B., et al. (2021): Dietary quercetin impacts the concentration of pesticides in honey bees. – Chemosphere 262: 127848. DOI: 10.1016/j.chemosphere.2020.127848.

[7] Baker, N. T., Richards, A. G., Cook, E. F. (1982): Reexamination of the exoskeletal and muscular anatomy of the honey bee, *Apis mellifera*, L and a polarized light microscopy technique for morphological studies. – Annals of the Entomological Society of America 75: 494-497. DOI: 10.1093/aesa/75.5.494.

[8] Bogdanov, S., Kilchenmann, V., Imdorf, A. (1998): Acaricide residues in some bee products. – Journal of Apicultural Research 37: 57-67. DOI: 10.1080/00218839.1998.11100956.

[9] Bogdanov, S. B. (2006): Contaminants of bee products. – Apidologie 37: 1-18.

[10] Brancato, A., Brocca, D., Carrasco Cabrera, L., et al. (2018): Review of the existing maximum residue levels for tau-fluvalinate according to Article 12 of Regulation (EC) No 396/2005. – EFSA Journal 16. DOI: 10.2903/j.efsa.2018.5475.

[11] Carreck, N. L., Andree, M., Brent, C. S., et al. (2013): Standard methods for *Apis mellifera* anatomy and dissection. – Journal of Apicultural Research 52. DOI: 10.3896/IBRA.1.52.4.03.

[12] Davidson, G. (2021): Honey Bee Pharmacology. – In: Kane, T. R., Faux, C. M. (eds.) Honey Bee Medicine for the Veterinary Practitioner. Wiley & Sons, Inc., Hoboken, NJ, pp 135-148.

[13] Davies, T. G. E., Field, L. M., Usherwood, P. N. R., Williamson, M. S. (2007): DDT, pyrethrins, pyrethroids and insect sodium channels. – IUBMB Life 59: 151-162. DOI: 10.1080/15216540701352042.

http://www.aloki.hu ● ISSN 1589 1623 (Print) ● ISSN 1785 0037 (Online)
DOI: http://dx.doi.org/10.15666/aeer/2001_055067

[14] European Food Safety Authority (2010): Conclusion on the peer review of the pesticide risk assessment of the active substance bromadiolone. – EFSA Journal 8: 1-102. DOI: 10.2903/j.efsa.2010.1783.
[15] Frost, E. H., Shutler, D., Hillier, N. K. (2013): Effects of fluvalinate on honey bee learning, memory, responsiveness to sucrose, and survival. – Journal of Experimental Biology 216: 2931-2938. DOI: 10.1242/jeb.086538.
[16] Gisder, S., Genersch, E. (2020): Direct evidence for infection of Varroa destructor mites with the bee-pathogenic deformed wing virus variant B, but not variant A, via fluorescence in situ hybridization analysis. – Journal of Virology 95: 1-15. DOI: 10.1128/jvi.01786-20.
[17] Johnson, R. M., Wen, Z., Schuler, M. A., Berenbaum, M. R. (2009): Mediation of pyrethroid insecticide toxicity to honey bees (Hymenoptera: Apidae) by cytochrome P450 monooxygenases. – Journal of Economic Entomology 99: 1046-1050. DOI: 10.1603/0022-0493-99.4.1046.
[18] Johnson, R. M., Ellis, M. D., Mullin, C. A., Frazier, M. (2010): Pesticides and honey bee toxicity - USA. – Apidologie 41: 312-331. DOI: 10.1051/apido/2010018.
[19] Johnson, R. M., Dahlgren, L., Siegfried, B. D., Ellis, M. D. (2013): Acaricide, fungicide and drug interactions in honey bees (*Apis mellifera*). – PLoS ONE 8. DOI: 10.1371/journal.pone.0054092.
[20] Kakamand, F., Mahmoud, T., Amin, A. (2008): The role of three insecticides in disturbance the midgut tissue in honey bee *Apis mellifera* L. workers. – Journal of Dohuk University, Iraq 11: 144-151.
[21] Mao, W., Schuler, M. A., Berenbaum, M. R. (2011): CYP9Q-mediated detoxification of acaricides in the honey bee (*Apis mellifera*). – Proceedings of the National Academy of Sciences of the United States of America 108: 12657-12662. DOI: 10.1073/pnas.1109535108.
[22] Moro, A., Blacquière, T., Panziera, D., et al. (2021): Host-parasite co-evolution in real-time: changes in honey bee resistance mechanisms and mite reproductive strategies. – Insects 12: 1-13. DOI: 10.3390/insects12020120.
[23] Mutinelli, F. (2021): Euthanasia and welfare of managed honey bee colonies. – Journal of Apicultural Research 0: 1-9. DOI: 10.1080/00218839.2021.1895569.
[24] OECD (2017): OECD GD 245: Honeybees (*Apis mellifera*, L.), chronic oral toxicity test (10-day feeding). – OECD Guidelines for the Testing of Chemicals 1-7.
[25] Potts, S. G., Roberts, S. P. M., Dean, R., et al. (2010): Declines of managed honey bees and beekeepers in Europe. – Journal of Apicultural Research 49: 15-22. DOI: 10.3896/IBRA.1.49.1.02.
[26] Qi, S., Niu, X., Wang, D. H., et al. (2020): Flumethrin at sublethal concentrations induces stresses in adult honey bees (*Apis mellifera* L.). – Science of the Total Environment 700: 134500. DOI: 10.1016/j.scitotenv.2019.134500.
[27] Rangel, J. R., Tarpy, D. (2016): In-hive miticides and their effect on queen supersedure and colony growth in the honey bee (*Apis mellifera*). – Journal of Environmental & Analytical Toxicology 06: DOI: 10.4172/2161-0525.1000377.
[28] Retschnig, G., Rich, J., Crailsheim, K., et al. (2021): You are what you eat: relative importance of diet, gut microbiota and nestmates for honey bee, *Apis mellifera*, worker health. – Apidologie. DOI: 10.1007/s13592-021-00851-z.
[29] Ricigliano, V. A., Simone-Finstrom, M. (2020): Nutritional and prebiotic efficacy of the microalga Arthrospira platensis (spirulina) in honey bees. – Apidologie 51: 898-910. DOI: 10.1007/s13592-020-00770-5.
[30] Santiago, G. P., Otero-Colina, G., Sánchez, D. M., Guzmán, M. E. R., Vandame, R. (2000): Comparing effects of three acaricides on Varroa jacobsoni (Acari: Varroidae) and *Apis mellifera* (Hymenoptera: Apidae) using two application techniques. – Fla Entomol 83: 468-476. DOI: doi.org/10.2307/3496722.

http://www.aloki.hu ● ISSN 1589 1623 (Print) ● ISSN 1785 0037 (Online)
DOI: http://dx.doi.org/10.15666/aeer/2001_055067

[31] Sara, C., Mar, Ó., Calatayud, F., et al. (2021): Large-scale monitoring of resistance to coumaphos, amitraz, and pyrethroids in Varroa destructor. – Insects 12: 27. DOI: https://doi.org/10.3390/insects12010027.
[32] Semkiw, P., Skubida, P., Pohorecka, K. (2013): Skuteczność zwalczania roztoczy Varroa Destructor paskami z amitrazem po wieloletnim stosowaniu tej substancji w pasiekach. – Journal of Apicultural Science 57: 107-121. DOI: 10.2478/jas-2013-0012.
[33] Shoukry, R. S., Khattaby, A. M., El-Sheakh, A. A., et al. (2013): Effect of some materials for controlling varroa mite on the honeybee drones (*Apis mellifera* L.). – Egyptian Journal of Agricultural Research 91: 825-834.
[34] VanEngelsdorp, D., Evans, J. D., Saegerman, C., et al. (2009): Colony collapse disorder: a descriptive study. – PLoS ONE 4. DOI: 10.1371/journal.pone.0006481.
[35] VanEngelsdorp, D., Traynor, K. S., Andree, M., et al. (2017): Colony Collapse Disorder (CCD) and bee age impact honey bee pathophysiology. – PLoS ONE 12: 1-23. DOI: 10.1371/journal.pone.0179535.
[36] Vojvodic, S., Rehan, S. M., Anderson, K. E. (2013): Microbial gut diversity of Africanized and European honey bee larval instars. – PLoS ONE 8. DOI: 10.1371/journal.pone.0072106.
[37] Wu, Y., Zheng, Y., Chen, Y., et al. (2020): Honey bee (*Apis mellifera*) gut microbiota promotes host endogenous detoxification capability via regulation of P450 gene expression in the digestive tract. – Microbial Biotechnology 13: 1201-1212. DOI: 10.1111/1751-7915.13579.
[38] Zhu, W., Schmehl, D. R., Mullin, C. A., Frazier, J. L. (2014): Four common pesticides, their mixtures and a formulation solvent in the hive environment have high oral toxicity to honey bee larvae. – PLoS ONE 9. DOI: 10.1371/journal.pone.0077547.

http://www.aloki.hu ● ISSN 1589 1623 (Print) ● ISSN 1785 0037 (Online)
DOI: http://dx.doi.org/10.15666/aeer/2001_055067

TOXICITY OF 3-METHYLPHENANTHRENE ON JAPANESE SPIKY SEA CUCUMBER (*APOSTICHOPUS JAPONICUS*)

LIU, S.[1,2,3] – CHE, J.[4] – ZHAO, Y. M.[1,2,3] – WEI, H. F.[1,2,3*] – LIU, C. F.[1,2,3]

[1]*Liaoning Key Laboratory of Coastal Marine Environmental Science and Technology, Dalian 116023, China*

[2]*College of Marine Science, Technology and Environment, Dalian Ocean University, Dalian 116023, China*

[3]*North Key Laboratory of Marine Aquaculture, Ministry of Agriculture and Rural Affairs, Dalian Ocean University, Dalian 116023, China*

[4]*Dalian Xinyulong Marine Biological Seed Technology Co., Ltd., Dalian 116222, China*

[*]*Corresponding author*
e-mail: weihaifeng@dlou.edu.cn

(Received 4th Mar 2021; accepted 10th Jun 2021)

Abstract. In the Marine environment, 3-methylphenanthrene mainly comes from Marine oil spill accidents and the waste water discharge from the coastal petrochemical enterprises. In order to reveal the ecotoxicological effects of 3-methylphenanthrene pollutants on *A. japonicus*, it was exposed to different concentrations of the substance. The results showed, the survival rate of *A. japonicus* gastrula decreasing gradually with the extension of exposure time and the increase of exposure concentration; The bioaccumulation of 3-methylphenanthrene in *A. japonicus* increased significantly with the extension of exposure time and the increase of exposure concentration; Compared to the control group, the expression of *CYP450* and *p53* genes of *A. japonicus* was significantly inhibited in each treatment group. The above results provide the basic data for the evaluation of the biological toxicity of 3-methylphenanthrene towards *A. japonicus*.
Keywords: *pollutants, ecotoxicological effects, survival rate, bioaccumulation, gene expression*

Introduction

Petroleum hydrocarbon pollution is one of the significant factors that may harm the safety of marine ecological environment in global (Li et al., 2019). The toxicity of it is mainly caused by PAH components, which are highly toxic and commonly found in aquatic systems (Guo et al., 2017). 3-methylphenanthrene is the most representative tricyclic PAHs with high content in petroleum, but its toxicity has been reported less in the international scope (Guan et al., 2016; Liu et al., 2020). The physiological activities and metabolism of organisms living in marine environments containing 3-methylphenanthrene were altered (Xu et al., 2018).

Apostichopus japonicus covered with meat spines, which feed on algae and plankton and are widely distributed in the world's oceans. It is an important mariculture economic species in China, with functions of improving memory, delaying aging, preventing atherosclerosis and anti-tumor (Bo, 2017; Zhao et al., 2020). At present, most scholars have studied the toxic effects of microplastic fibre (Mohsen et al., 2020, 2021), heavy metals (Wang et al., 2016; Zhang et al., 2016), and organic pollutants (Luo et al., 2015; Li et al., 2016a; Khazaali et al., 2016) on their larvae and adults and the accumulation of residual pollutants in their bodies, but there has been no report on the toxicity of

http://www.aloki.hu ● ISSN 1589 1623 (Print) ● ISSN1785 0037 (Online)
DOI: http://dx.doi.org/10.15666/aeer/2001_069077

3-methylphenanthrene on *A. japonicus.* Therefore, it is of great significance to study the toxicity of 3-methylphenanthrene to *A. japonicus* in China, so as to improve the quality of *A. japonicus* and strengthen the utilization and protection of marine resources.

Marine oil spill and industrial wastewater discharge cause PAHs to invade the Marine environment and destroy the balance of Marine ecosystem. 3-methylphenanthrene is widely found in marine water environment (Honda and Suzuki, 2020). It participates in the normal physiological process of marine organisms and is closely related to its life process. This article explores the different concentration of 3-methylphenanthrene on *A. japonicus* gastrula survival rate, bioaccumulation of 3-methylphenanthrene at different concentrations in *A. japonicus* and effects of different concentrations of 3-methylphenanthrene on the expression of *CYP450* and *p53* genes in *A. japonicus*, to provide basic data and theoretical basis for risk assessment of marine environment and aquatic organisms.

Materials and methods

Experimental materials

The seawater for the experiment was taken from the sand-filtered seawater of Dalian Heishi jiao. *A. japonicus* was purchased from Dalian Pacific Marine treasure co. LTD. The body length was (2±0.3) cm. After 2 weeks of clean sea water domestication, healthy young *A. japonicus* was selected for experiment.

Experimental methods

Effects of 3-methylphenanthrene on early development of A. japonicus

The experiment was carried out in a 10 ml test tube, with the gastrula density of 2 ~ 3 a·mL^{-1} in each test tube. The experiment used continuous micro-aeration method which was used to ensure that the dissolved oxygen in the experimental water was greater than 6 mg·L^{-1}. The experimental method was semi-static. During the experiment, the water was replaced every 24 hours, and the water was controlled at the temperature of 20 ~ 21℃, the salinity of 30 ~ 31, and the pH of 8.1 ~ 8.2. According to the preliminary experiment, set four treatment groups with 3-methylphenanthrene concentrations of 10, 50, 100 and 200 μg·L^{-1}, a blank control group and a 1‰ acetone solvent control group, each group set up three parallel experiments, and the number of survivors was observed at 24, 48, 72 and 96 h, and the survival rate was calculated.

Bioaccumulation of 3-methylphenanthrene in A. japonicus

The medial lethal concentration (LC_{50}) of 3-methylphenanthrene was 264.3 μg·L^{-1} by 96 h acute toxicity test. Based on this, the concentration of 3-methylphenanthrene was set as 5, 10 and 100 μg·L^{-1}. During the experiment, the dissolved oxygen was controlled above 6 mg·L^{-1}, and the water temperature was 20 ~ 21℃. Algal powder of *Sargassum thunbergii* was fed regularly once a day, and the feeding amount was 1.5% of the body weight. Samples were taken at the 3 d, 7 d and 14 d of the experiment and stored in a refrigerator at -80℃ for measurement. The freeze-dried biological samples were fully weighed and added with anhydrous sodium sulfate and deuterium, followed by a mixture of 100 mL n-hexane and acetone (1:1, *v*: *v*) for accelerated solvent extraction. The sample extraction solution passed minicolumns of anhydrous sodium sulfate, and added

http://www.aloki.hu ● ISSN 1589 1623 (Print) ● ISSN1785 0037 (Online)
DOI: http://dx.doi.org/10.15666/aeer/2001_069077

desulphuration of copper powder which treated with hydrochloric acid. Concentrate the extract to about 2.0 mL, after purification, pre-leaching and eluent taking, concentrate the eluent to constant volume, then add 1μl internal standard. The sample gas-phase separated by DB-5ms capillary column, and mass spectrometric detection was performed by EI ionization method.

Effects of 3-methylphenanthrene on expression of CYP450 and p53 genes in A. japonicus

Filled 1 L glass beaker with seawater, and added reserve solution of a certain concentration of 3-methylphenanthrene. The concentration of 3-methylphenanthrene was set as 5, 10, and 100 $\mu g \cdot L^{-1}$, each group placed 10 young *A. japonicus*. Test conditions: water temperature (15±2) ℃, salinity (30±1), pH (8.0±0.5), intermittent oxygenation, ensure that the dissolved oxygen is greater than 4.5 $mg \cdot L^{-1}$, avoid light. After 3, 7 and 14 days of treatment with 3-methylphenanthrene, taking one young *A. japonicus* of each treatment group was placed on the ice, and *A. japonicus* body fluid was extracted by pipet-gun, then quickly put into the prepared liquid nitrogen in the tube and stored at -80 ℃. Trizol method was used to extract the total RNA of the above samples, DNase I was used for DNA digestion, the concentration and purity of total RNA were detected by micronucleic acid protein analyzer, and the RNA integrity was detected by Agilent 2100 biological analyzer. The total RNA of the above samples were retranscribed by Prime-Script™ RT reagent Kit(TaKaRa). Mx3005p™ real-time fluorescence quantitative PCR instrument and SYBR Prime-Script™ RT-PCR Kit II were used for real-time quantitative PCR.

Data statistics and processing

The test data were expressed as mean±S.D. , SPSS 22.0 statistical software was used for statistical analysis of the data, and One-Way ANOVA and Duncan's new multiple range method were used to analyze the difference of the data. Set $P<0.05$, the difference was significant.

Results

The effect of 3-methylphenanthrene on the early development of A. japonicus

The changes of survival rate of *A. japonicus* gastrula under different concentration of 3-methylphenanthrene were shown in *Figure 1*. Compared with the control group, the stress of 3-methylphenanthrene significantly inhibited the growth of *A. japonicus* gastrula, and its survival rate significantly decreased with the increase of stress time ($P<0.05$). Under the stress of 3-methylphenanthrene for 24 h, the survival rate of *A. japonicus* gastrula decreased gradually with the gradually increasing exposure concentration, and the survival rate of *A. japonicus* gastrula reached the minimum value of 79% when the stress concentration reached 200 $\mu g \cdot L^{-1}$. Under 3-methylanthracene stress for 48 h, the survival rate of *A. japonicus* gastrula was significantly different from the control group ($P<0.05$), and with the gradual increase of exposure concentration, the survival rate of *A. japonicus* gastrula decreased gradually. When the stress concentration reached 200 $\mu g \cdot L^{-1}$, the survival rate of *A. japonicus* gastrula reached the minimum value of 66%. Under 3-methylanthracene stress for 72 h, the survival rate of *A. japonicus* gastrula was similar to result of 3-methylanthracene stress for 48 h, and the survival rate of *A. japonicus* gastrula was 0% at 200 $\mu g \cdot L^{-1}$. Under the stress of 3-methylanthracene

http://www.aloki.hu ● ISSN 1589 1623 (Print) ● ISSN1785 0037 (Online)
DOI: http://dx.doi.org/10.15666/aeer/2001_069077

for 96 h, the survival rate of *A. japonicus* gastrula reached the lowest value as a whole, and the survival rate of *A. japonicus* gastrula reached 0% at 100 μg·L^{-1} and 200 μg·L^{-1}.

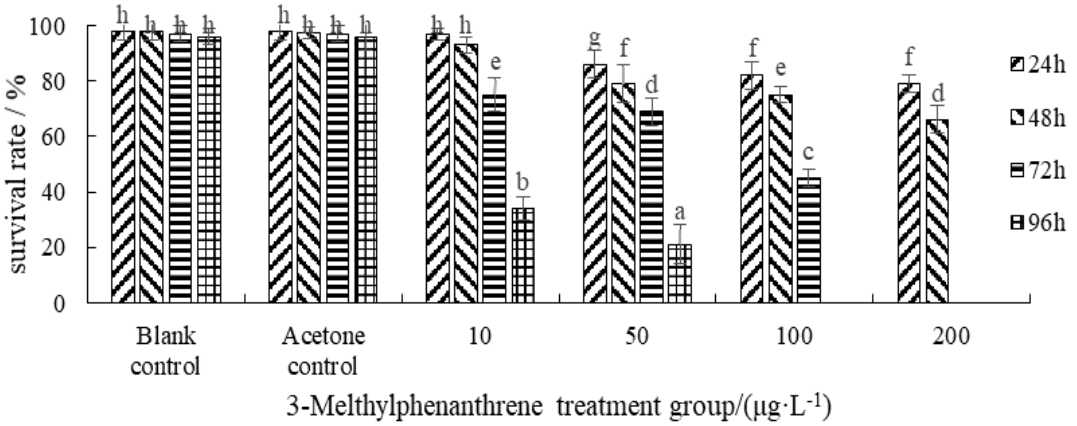

Figure 1. *Results of acute toxicity test of 3-Melthylphenanthrene on early development of A. japonicus. Note: The means with different letters significant differences at the 0.05 probability level, and the means with the same letters not significant differences. The error line in the figure is expressed by standard deviation, which is the mean of the distance of each data from the mean*

Results of 3-methylanthracene bioaccumulation in A. japonicus

Figure 2 shows that under 5 μg·L^{-1} and 10 μg·L^{-1} concentrations, the bioaccumulation process of *A. japonicus* does not conform to the two-box dynamic model, and the bioaccumulation equilibrium is not reached within 14 d. Under concentration of 100 μg·L^{-1}, the bioaccumulation of 3-methylanthracene in *A. japonicus* increased with time, and the two - box dynamic model was used to fit, $K_1 = 24.94$, $K_2 = 0.210$, $R_2 = 0.923$ (95% confidence interval). At low concentrations, the bioaccumulation of 3-methylanthracene in *A. japonicus* did not obviously increase with time; In the case of high concentration of 10 μg·L^{-1}, the bioaccumulation of 3-methylanthracene in *A. japonicus* increased rapidly with the extension of exposure time, and even the enrichment coefficient BCF reached 154.6. At the same time, there was exponential correlation between the concentration of 3-methylphenanthrene and the bioaccumulation of 3-methylphenanthrene in *A. japonicus*, the correlation equations are $y_{3d} = 6.492e^{1.2398x}$ ($R^2_{3d} = 0.9448$), $y_{7d} = 5.4134e^{1.331x}$ ($R^2_{7d} = 0.8876$) and $y_{14d} = 5.5551e^{1.4745x}$ ($R^2_{14d} = 0.9446$). Under the conditions of three concentrations, the content of 3-methylphenanthrene in *A. japonicus* increased rapidly, indicating that the bioaccumulation rate of *A. japonicus* was much higher than the metabolic rate.

Effects of 3-methylphenanthrene on expression of CYP450 and p53 genes in A. japonicus

The effect of 3-methylphenanthrene on expression of *CYP450* gene in *A. japonicus* is shown in *Figure 3*. The results showed that, compared with the control group, 3-methylphenanthrene (c≥5 μg·L^{-1}) showed significant inhibitory effect on the expression of *CYP450* gene of *A. japonicus* under certain concentration stress (P<0.05). Compared with the control group, the overall relative expression of *CYP450* gene in the treatment group was lower than that in the control group, and the relative expression of *CYP450*

http://www.aloki.hu ● ISSN 1589 1623 (Print) ● ISSN1785 0037 (Online)
DOI: http://dx.doi.org/10.15666/aeer/2001_069077

gene gradually increased with the increase of the concentration. The maximum expression of *CYP450* gene in the 100 μg·L^{-1} treatment group reached 0.56 at 14 d, and the inhibition rate was 44% compared with the control group.

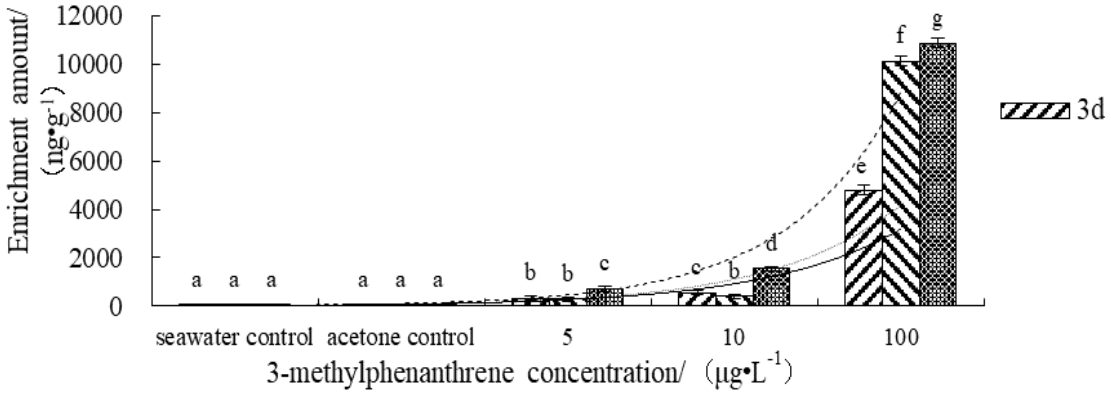

Figure 2. *Bioaccumulation of dimethylanthracene by A. japonicus*

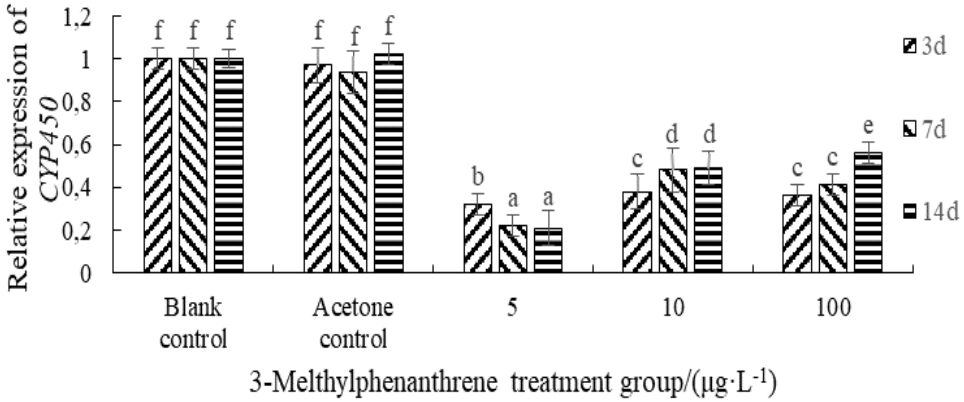

Figure 3. *The effects of 3-methylphenanthrene on the CYP450 of A. japonicus*

The effect of 3-methylphenanthrene on expression of *p53* gene in *A. japonicus* is shown in *Figure 4*. At the early stress of 3-methylphenanthrene (3 d), all the 3-methylphenanthrene treatment groups showed significant inhibitory effect on the expression of *p53* gene (P<0.05), and the inhibition effect decreased with the increase of stress concentration. At the middle stress of 3-methylphenanthrene (7 d), with the increase of stress concentration, the relative expression of *p53* gene in *A. japonicus* showed a rule of increasing first and then decreasing, and it was at the lowest value of 0.137 when the stress concentration was 5 μg·L^{-1}, which the inhibition rate was 86.3% compared with the control group. At the later stress of 3-methylphenanthrene (14 d), with the increase of stress concentration, the relative expression of *p53* gene in *A. japonicus* showed a gradually decreasing pattern, and reached the minimum value of 0.31 when the stress concentration was 100 μg·L^{-1}, which the inhibition rate was 69% compared with the control group.

http://www.aloki.hu ● ISSN 1589 1623 (Print) ● ISSN1785 0037 (Online)
DOI: http://dx.doi.org/10.15666/aeer/2001_069077

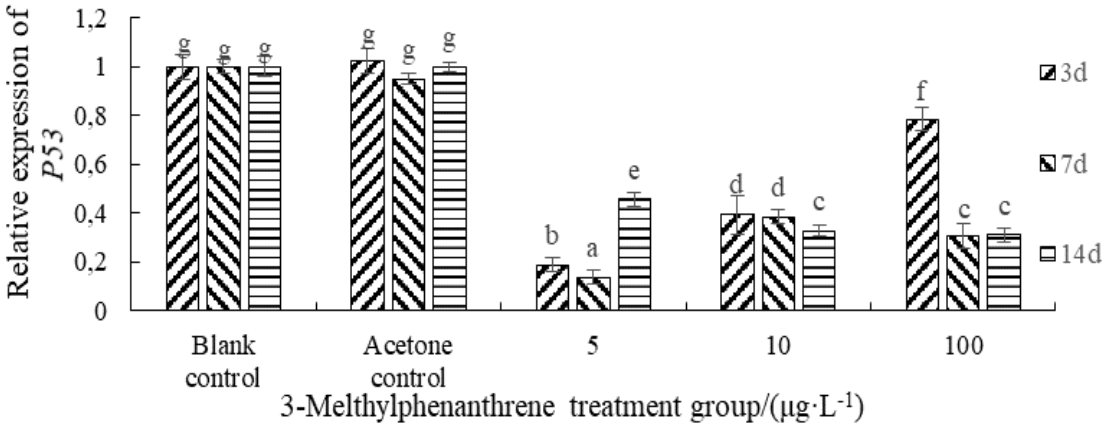

Figure 4. *The effects of 3-methylphenanthrene on the p53 of A. japonicus*

Discussion

3-methylphenanthrene can accelerate the accumulation of PAHs in Marine organisms, which is related to the high 1-octyl alcohol/water partition coefficient of PAHs (Hodson, 2017). Studies had found that PAHs can quickly dissolve in fat through respiration and surface penetration into aquatic organisms, thus causing harm to organisms (Li et al., 2016a). In addition to shellfish, other invertebrates have a certain role in the metabolism of PAHs (Yu et al., 2018; Mana et al., 2021). Therefore, the high concentration of 3-methylphenanthrene in the water environment can be degraded and absorbed by marine biodegradation, and eventually digested through the intestinal tract, which binds to the adipose tissue (Hodson, 2017). The results showed that the bioaccumulation amount and bioaccumulation rate of 3-methylphenanthrene increased with the increase of exposure concentration, and the bioaccumulation rate in high concentration increased rapidly with the increase of pollutant concentration. In addition, BCF decreases with the increase of pollutant concentration, which may be due to the combination of fat and organic pollutants is easier to reach the saturation state (Simning et al., 2019; Li et al., 2021).

The experimental results showed that with the extension of exposure time and the increase of exposure concentration, the survival rate of *A. japonicus* gastrula decreased gradually, and no individuals survived when the exposure concentrations were 100 $\mu g \cdot L^{-1}$ (96 h) and 200 $\mu g \cdot L^{-1}$ (72 h and 96 h). Simning et al. (2019) reported that the cumulative mortality of embryo exposure of *Cyprinodon variegatus* significantly increased with the increase of HEWAF concentration (6.25%-50%) under low salt conditions, and the results of the study were similar to the rule in this paper. Through exploratory analysis, PAHs have different effects on marine gastrulas and larvae (Simning et al., 2019): four kinds of PAHs can damage the tissues of *A. japonicus*, resulting in the death of the organism (Luo et al., 2015); Xylene reduces the hatching rate of *Brachydanio rerio* gastrula, leading to the death of gastrula or abnormal movement of developmental malformed larvae (Zhang et al., 2016). Therefore, it can be speculated that 3-methylphenanthrene is related to the toxic damage of *A. japonicus* gastrulas.

The expression of *CYP450* and *p53* genes showed an overall inhibitory effect under the stress of 3-methylphenanthrene, which was related to the different main functions and mechanisms of *CYP450* and *p53* genes in organisms. Different exogenous chemicals can cause oxidative stress, genotoxic stress and protein toxic stress after entering the

http://www.aloki.hu ● ISSN 1589 1623 (Print) ● ISSN1785 0037 (Online)
DOI: http://dx.doi.org/10.15666/aeer/2001_069077

organism, thereby activating the biological cellular detoxification metabolic system to maintain the relative stability of the environment inside organism (Duan et al., 2018). Marine invertebrates produce a large number of by-products -- reactive oxygen in the phase I metabolism of organic pollutants, and excessive reactive oxygen will lead to oxidative damage of organisms (Li et al., 2016b; Lister et al., 2017; Danielli et al., 2017; Duan et al., 2018). The *CYP450* enzyme system can provide the basis for the second stage of glutathione transferase (GST) to transform the exogenous (Tang, 2019). In this study, the expression of *CYP450* gene in *A. japonicus* was significantly inhibited under 3-methylphenanthrene stress compared with the control group ($P<0.05$) and the relative expression of *CYP450* gene gradually increased with the increase of concentration, which showed a similar pattern to the effect of benzo[a]pyrene on gill tissue GSH activity of *Mytilus coruscus* (Tang, 2019). Therefore, it was speculated that the expression of *CYP17A1* gene in *A. japonicus* was significantly increased after long treatment, because of it induces the detoxification and metabolism of cytochrome *P450* related system, and causes the production of excessive oxidative free radical ROS in the cell body.

P53 gene is the main attack site of chemical mutagenesis. After *p53* gene mutation, it loses its regulatory effect on cell growth, apoptosis and DNA repair. And the complex network of regulation of cellular stress and cellular response is composed of its various regulatory factors and related genes (Li et al., 2019). In this study, the expression of *p53* gene in *A. japonicus* was significantly inhibited under 3-methylphenanthrene compared with the control group ($P<0.05$). However, in the same time period (3 d and 7 d), the relative expression level of *p53* gene increased with the increase of the concentration, which was due to the system in *A. japonicus* did not respond in time at the beginning and so as to inhibit the expression of *p53* gene in *A. japonicus*. When the stress concentration increased, the detoxification and metabolism process of cytochrome related system was induced, and oxidative stress occurred, and the expression level of *p53* increased significantly (Liu et al., 2015). It has been reported that nano-silica coated with manganese oxide can induce the increase of *p53* gene expression in He La cells and L929 cells (Yu et al., 2015). Therefore, it is speculated that 3-methylphenanthrene has no strong toxic effect on *A. japonicus* under low concentration ($c\leq100$ $\mu g \cdot L^{-1}$) and short time ($t\leq14$ d) stress.

Conclusion

In this study, high concentration of 3-methylphenanthrene inhibited the survival of *A. japonicus* gastrula and inhibited the metabolism of 3-methylphenanthrene in *A. japonicus*, resulting in the bioaccumulation of 3-methylphenanthrene. The expression of *CYP450* and *p53* genes in *A. japonicus* gastrula was significantly inhibited by 3-methylphenanthophane, thus inhibiting the metabolic effect of pollutants and losing the regulatory effect on cell growth, apoptosis and DNA repair. Changes in the metabolic mechanism and regulatory mechanism of marine organisms may lead to the death of marine organisms. Therefore, the relevant marine departments should prohibit the discharge of industrial wastewater into the sea and timely deal with marine oil spills, strengthen the monitoring of PAHs in the marine environment and the management of the total amount of marine pollutants discharged, which will provide a good living environment and solve the major problems of aquaculture.

http://www.aloki.hu ● ISSN 1589 1623 (Print) ● ISSN1785 0037 (Online)
DOI: http://dx.doi.org/10.15666/aeer/2001_069077

Acknowledgments. We acknowledge the Key Projects of the National Science and Technology Pillar Program (No:201305002), Open Fund of the Key Laboratory of Marine Oil Spil Identification and Damage Assessment Technology, State Oceanic Administration (No.201309, 201809), the Key Laboratory of Coastal Ecological Environment, State Oceanic Administration (No.201013), Local Projects of the Department of Education of Liaoning Province (DL201804) and The Major and Special Program on Science and Technology Projects in Dalian City (2020ZD23SN009) for supporting this research and Dalian Ocean University for providing facilities.

REFERENCES

[1] Bo, K. (2017): Identification and purchasing techniques of sea cucumber. – China Anti-counterfeiting Report 6: 124-125.

[2] Danielli, N. M., Trevisan, R., Mello, D. F., Fischer, K., Deconto, V. S., Daiane, D. S. A., Bianchini, A., Bainy, A. C. D., Dafre, A. L. (2017): Upregulating Nrf2-dependent antioxidant defenses in pacific oysters, *Crassostrea gigas*: Investigating the Nrf2/Keap1 pathway in bivalves. – Comparative Biochemistry & Physiology Part C Toxicology & Pharmacology 195: 16-26.

[3] Duan, M., Xiong, D., Bai, X., Gao, Y., Xiong, Y., Gao, X., Ding, G. H. (2018): Transgenerational effects of heavy fuel oil on the sea urchin *Strongylocentrotus intermedius* considering oxidative stress biomarkers. – Marine Environmental Research 141: 138-147.

[4] Guan, X. Y., Wang, B., Dong, Y., Li, S. Q., Gao, S., Liu, W. D., Zhou, Z. C. (2016): Effects of Xylene, Anthracene, and Benzo[a]pyrene on Enzymatic Activities of SOD and CAT in the Japanese Scallop (*Mizuhopecten yessoensis*) Serums. – Journal of Ecotoxicology 11(1): 289-294.

[5] Guo, R. M., Pan, L. Q., Lin, P. F., Zheng, L. (2017): The detoxification responses, damage effects and bioaccumulation in the scallop *Chlamys farreri* exposed to single and mixtures of benzo[a]pyrene and chrysene. – Comparative Biochemistry and Physiology Part C 191: 36-51.

[6] Hodson, P. V. (2017): The Toxicity to Fish Embryos of PAH in Crude and Refined Oils. – Archives of Environmental Contamination and Toxicology 73(1): 12-18.

[7] Honda, M., Suzuki, N. (2020): Toxicities of Polycyclic Aromatic Hydrocarbons for Aquatic Animals. – International Journal of Environmental Research and Public Health 17(4): 1-23.

[8] Khazaali, A., Kunzmann, A., Bastami, K. D., Baniamam, M. (2016): Baseline of polycyclic aromatic hydrocarbons in the surface sediment and sea cucumbers (*Holothuria leucospilota* and *Stichopus hermanni*) in the northern parts of Persian Gulf. – Marine Pollution Bulletin 110(1): 539-545.

[9] Li, C., Zhou, S., Ren, Y. C., Jiang, S. H., Xia, B., Dong, X. Y. (2016a): Toxic effects in juvenile sea cucumber *Apostichopus japonicas* (Selenka) exposure to benzo[a]pyrene. – Fish and Shellfish Immunology 59: 375-381.

[10] Li, L., Jiang, M., Shen, X. (2016b): Variability in antioxidant/detoxification enzymes of *Sinonovacula constricta* exposed to benzo[a]pyrene and phenanthrene. – Marine Pollution Bulletin 109(1): 507-511.

[11] Li, X., Wei, H. F., Liu, C. F., Song, X., Zhao, X. Y., Zhao, Y. M., Xia, N., Huo, Y. J. (2019): Effects of 2 Kinds of alkyl-PAHs on the Expression of *CYP450* and *P53* Genes of *Apostichopus japonicus*. – Journal of Ecotoxicology 14(1): 83-89.

[12] Li, X. S., Wang, C. Y., Li, N., Gao, Y. L., Ju, Z. L., Liao, G. X., Xiong, D. Q. (2021): Combined Effects of Elevated Temperature and Crude Oil Pollution on Oxidative Stress and Apoptosis in Sea Cucumber (*Apostichopus japonicus*, Selenka). – International Journal of Environmental Research and Public Health 18(2): 801-801.

http://www.aloki.hu ● ISSN 1589 1623 (Print) ● ISSN1785 0037 (Online)
DOI: http://dx.doi.org/10.15666/aeer/2001_069077

[13] Lister, K. N., Lamare, M. D., Burritt, D. J. (2017): Maternal antioxidant provisioning mitigates pollutant-induced oxidative damage in embryos of the temperate sea urchin evechinus chloroticus. – Scientific Reports 7(1): 1954.
[14] Liu, L., Zhao, Q. F., Zhu, S. Q., Xu, F. (2015): Oxidative damage of zinc oxide nanoparticles to zebrafish intestine. – Acta Aquatica Sinica 39(11): 1702-1711.
[15] Liu, S., Su, T. T., Liu, C. F., Wei, H. F., Zhao, X. Y., Song, X. (2020): Effects of 3 Kinds of PAHs on the Expression of *CYP17A1* Genes of *Strongylocentrotus intermedius*. – Journal of Ecotoxicology 15(5): 345-351.
[16] Luo, Y. M., Xu, W. D., Li, D. H., Chen, D. F., Wang, X. Y. (2015): Acute Toxicity of Propylene Oxide, Acrylic Acid and Isoprene to Juvenile Sea Cucumber *Apostichopus japonicus*. – Fisheries Science 34(7): 444-447.
[17] Mana, I., Jun, S., Takeshi, H., Tohru, M., Katsutoshi, I. (2021): Immune toxicity of phenanthrene and its combined effects of white spot syndrome virus on the survival of kuruma shrimp (*Penaeus Japonicus*). – Ecotoxicology and Environmental Safety 208.
[18] Mohsen, M., Zhang, L. B., Sun, L. N., Lin, C. G., Wang, Q., Yang, H. S. (2020): Microplastic fibers transfer from the water to the internal fluid of the sea cucumber *Apostichopus japonicus*. – Environmental Pollution 257: 113606.
[19] Mohsen, M., Zhang, L. B., Sun, L. N., Lin, C. G., Wang, Q., Liu, S. L., Sun, J. C., Yang, H. S. (2021): Effect of chronic exposure to microplastic fibre ingestion in the sea cucumber *Apostichopus japonicus*. – Ecotoxicology and Environmental Safety 209: 111794.
[20] Simning, D., Sepulveda, M., De, G. S., Bosker, T., Griffitt, R. J. (2019): The combined effects of salinity, hypoxia, and oil exposure on survival and gene expression in developing sheepshead minnows, *Cyprinodon variegatus*. – Aquatic Toxicology (Amsterdam, Netherlands) 214: 105234.
[21] Tang, Z. R. (2019): Study on antioxidant reaction and Nrf2 gene expression of mussel with single and mixed cadmium and benzo[a]pyrene exposure. – Zhejiang Ocean University.
[22] Wang, J., Ren, T. J., Wang, F. Q., Han, Y. Z., Liao, M. L., Jiang, Z. Q., Liu, H. Y. (2016): Effects of dietary cadmium on growth, antioxidants and bioaccumulation of sea cucumber (*Apostichopus japonicus*) and influence of dietary vitamin C supplementation. – Ecotoxicology and Environmental Safety 129: 145-153.
[23] Xu, Y. Q., Zhong, Y. W., Han, J. H., Qin, Z. B., Li, W. F., Ding, Z. K. (2018): Effect and mechanism of phenanthrene on the reproduction, development, and growth of aquatic animal. – Feed Industry 39(16): 61-64.
[24] Yu, C., Zhou, Z., Wang, J., Sun, J., Liu, W., Sun, Y. N., Kong, B., Yang, H., Yang, S. P. (2015): In depth analysis of apoptosis induced by silica coated manganese oxide nanoparticles in vitro. – Journal of Hazardous Materials 283: 519-528.
[25] Yu, N., Ding, Q. Q., Li, E. C., Qin, J. G., Chen, L. Q., Wang, X. D. (2018): Growth, energy metabolism and transcriptomic responses in Chinese mitten crab (*Eriocheir sinensis*) to benzo[a]pyrene (BaP) toxicity. – Aquatic Toxicology 203: 150-158.
[26] Zhang, P., Xing, X. L., Sun, J. X., Zhao, W. (2016): Research progress on the pollution and toxicity of heavy metals on sea cucumber. – Marine Environmental Science 35(1): 149-154.
[27] Zhao, G. H., Zhao, W. F., Han, L. S., Ding, J., Chang, Y. Q. (2020): Metabolomics analysis of sea cucumber (*Apostichopus japonicus*) in different geographical origins using UPLC–Q-TOF/MS. – Food Chemistry 333: 127453.

http://www.aloki.hu ● ISSN 1589 1623 (Print) ● ISSN1785 0037 (Online)
DOI: http://dx.doi.org/10.15666/aeer/2001_069077

ISOLATION AND CHARACTERIZATION OF INDIGENOUS BIOSURFACTANT PRODUCING *BACILLUS* AND *STAPHYLOCOCCUS* SPP. DURING MOTOR OIL DEGRADATION

JAVED, S.[1] – FAISAL, M.[1*] – RAZA, Z. A.[2*] – REHMAN, A.[1] – SHAHID, M.[3]

[1] *Institute of Microbiology and Molecular Genetics, Faculty of Life Sciences, University of the Punjab, Lahore-54590, Pakistan*

[2] *Department of Applied Science, School of Science, National Textile University, Faisalabad-37610, Pakistan*

[3] *Department of Bioinformatics and Biotechnology, Government College University, Faisalabad 38000, Pakistan*

[*] *Corresponding authors*
e-mail: faisal.mmg@pu.edu.pk (Dr. M. Faisal), zarazapk@yahoo.com (Dr. Z. A. Raza)

(Received 1st Jun 2021; accepted 28th Oct 2021)

Abstract. The present study dealt with the isolation and characterization of some biosurfactant-producing bacterial strains obtained from motor oil contaminated soil samples collected from the local auto-workshops of Lahore. Thereby, four bacterial species were selected based on CTAB/methylene blue-agar, emulsification index, and drop-collapse assays, and then, biochemically identified as *Staphylococcus hominis*, *Staphylococcus* sp., *Bacillus flexus,* and *Bacillus oceanisediminis,* and confirmed through 16S rRNA gene sequencing. Fourier transform infrared spectroscopic analysis was done to track the surface chemistry of the isolated bacterial surfaces. The isolated bacterial strains were then employed at different concentrations (1-3%, w/v) of motor oil, and various temperatures, pH values, incubation intervals, and in the absence or presence of certain inhibitors like sodium dodecyl sulfate and the Cr(VI) ions. There observed a maximum of 81.8% (w/w) oil degradation at 1% (w/v) oil concentration with *Staphylococcus* sp. at 37°C, pH 7, and 96 h of incubation, whereas in the presence of Cr(VI) ions under the same physiological conditions, the oil degradation was suppressed to 6.0% (w/w). The results demonstrate that the identified bacterial strains could effectively be used to bioremediate the motor oil-contaminated soil at drilling sites as well as in the aquifers.
Keywords: *biodegradation, bioremediation, crude oil, emulsion, surfactant*

Introduction

Surfactants, whether derived from chemical or biological origins, possess both hydrophilic and hydrophobic moieties which not only support emulsification but also decrease the surface and interfacial tensions (Raza et al., 2009; Sakamoto et al., 2017; Pinazo et al., 2019), and those of biological origin are called biosurfactants (Singh et al., 2020). They can modify the surface characteristics of certain substrates like surface adsorption, surface energy, and wettability. They can also enhance the bioavailability of hydrophobic substrates for their prompt degradation and biotransformation under certain fermentation conditions (Raza et al., 2007; Henkel and Hausmann, 2019). The biosurfactants represent an assorted class of surface-active molecules and are synthesized by diverse microbes under suitable culture conditions. They are valuable biological molecules with widespread attributes like biocompatibility, biodegradability, specific activity, activity in extreme environments, and so on. This makes them versatile green chemicals for a wide range of industrial and environmental applications (Khubaib et al.,

http://www.aloki.hu ● ISSN 1589 1623 (Print) ● ISSN1785 0037 (Online)
DOI: http://dx.doi.org/10.15666/aeer/2001_079102

2021). The biosurfactants can effectively be employed in medical and industrial applications for emulsification, de-emulsification, encapsulation, enhanced recovery, and ore floatation processes (Gregorich et al., 2015; Naik et al., 2018). Thereby, glycolipids, lipopeptides or lipoproteins, phospholipids, biopolymeric surfactants, and fatty acids are the major varieties of structurally diverse biological surfactants produced by certain bacteria, yeast, and fungi (da Silva et al., 2020).

The rapid and careless use of synthetic chemical reagents has resulted in serious environmental concerns (Karlapudi et al., 2018). It has been well recognized that petroleum-based hydrocarbons and their derivatives like diesel, motor oil, mineral oil, engine oil, and their residues deteriorate the environment. Motor oil being a mixture of certain aromatics, cyclic alkanes, additives, and anticorrosive compounds, is difficult to degrade under ambient conditions (Sharma et al., 2019). Moreover, the used motor oil carries in it a rather enhanced proportion of heavy metals, carcinogenic compounds, toxic metals, and polycyclic aromatic hydrocarbons that cause serious threats not only to human beings but also to vegetation (Bhattacharya et al., 2019).

Different chemo-physical and biological techniques had been used for the degradation of hydrocarbons containing water and soil systems. One way is the emulsify the hydrocarbon oils using synthetic surfactants, but being toxic thus may also cause secondary environmental issues. Thereby, researchers are trying to explore alternative surfactants that may not only be nontoxic and biodegradable but also effective under both mild and severe conditions (Paniagua-Michel and Rosales, 2015). The biosurfactants, employed during bioremediation, would emulsify the hydrophobic substances (like motor oil) in the aqueous systems making them more available as the carbon source for the oil-degrading microbes (Vijayakumar and Saravanan, 2015; Duan et al., 2015; Trellu et al., 2016). The microbes detoxify the hydrocarbon pollutants through different modes including polymerization, transformation, or mineralization. Although sole bacterial strain may be enough to remediate the hydrocarbons yet at times bacterial consortia are used for more effective bioremediation. Mostly, Pseudomonads had been reported as exceptional biosurfactant producing species, nevertheless, they exhibit opportunistic human pathogenicity (Khubaib et al., 2021). In that way, it is inevitable to introduce some non-Pseudomonad especially, non-pathogenic bacterial species as a source for biosurfactant-producing strains to remediate the crude oil contaminated systems. For instance, *Bacillus* species had been reported as lipopeptide producers (Rita de Cássia et al., 2021) whereas *Staphylococcus* species being a lipopeptide producer with double bonds in its fatty acid chains (Varadavenkatesan and Murty, 2013).

The present study is aimed to isolate and identify some novel non-Pseudomonad – non-pathogenic biosurfactant producing bacterial species from the local oil-contaminated soil specimens and use them for the biodegradation of motor oil in the aqueous media under certain physiological and environmental conditions.

Material and methods

Materials

Luria Bertani (LB) agar and agar were purchased from Hi-Media (Mumbai, India), cetyltrimethylammonium bromide (CTAB), and methylene from Merck (NJ, USA), ammonium nitrate (NH_4NO_3), potassium dihydrogen phosphate (KH_2PO_4), dipotassium hydrogen phosphate (K_2HPO_4), calcium chloride ($CaCl_2$), magnesium sulfate ($MgSO_4$), ferric chloride ($FeCl_3$), sodium dodecyl sulfate (SDS), potassium chromate (K_2CrO_4), 2,6

http://www.aloki.hu ● ISSN 1589 1623 (Print) ● ISSN1785 0037 (Online)
DOI: http://dx.doi.org/10.15666/aeer/2001_079102

dichlorophenol indophenol (DCPIP) and heavy metal salts of lead sulfate ($PbSO_4$), zinc sulfate ($ZnSO_4$), cobalt chloride ($CoCl_2$), manganese sulfate ($MnSO_4$) and nickel sulfate ($NiSO_4$) from Sigma (Missouri, USA) and petrol (Premium Unleaded) from the local market. The antibiotic discs of Ampicillin, Streptomycin, Tetracycline, Erythromycin, and Kanamycine were purchased from Biolab Pharma, Islamabad, Pakistan.

Specimens' collection

Motor oil-contaminated soil specimens (as 10-100 g) were collected from the three different points of three local auto workshops of Lahore, Pakistan. The specimens were noted for temperature and pH values and transferred to the laboratory under sterile conditions for working.

Isolation of test bacterial strains

A desirable amount of soil sample was dispersed in sterilized normal saline serial diluted up to 10^{-6} spread on LB agar plate prepared in triplicate and placed in an incubator at 37℃ overnight. The next day, 20 different bacterial strains were indicated, four out of which were shortlisted based on different screening tests (CTAB/methylene blue-agar, drop collapse, and emulsification assays) as described in the following text.

CTAB/methylene blue-agar assay

The blue agar plates were prepared as (g/l): 15, 0.2, and 0.005 for agar, CTAB, and methylene blue, in distilled water. The plates were engraved with tiny, cavities and filled with the separate cell cultures of the selected strains and incubated at 37℃ for 24 h to identify any production of extracellular glycolipid. The presence of blue halos around the bacterial colonies indicated the production of biosurfactants (Siegmund and Wagner, 1991).

Drop collapse assay

This technique was employed to screen the biosurfactant-producing strains out of the bacterial strains in hand (Batista et al., 2006). The test bacterial culture was inoculated into LB broth media and further incubated at 37℃ overnight. Later the centrifugation was performed at 4℃ and 14,000 rpm for 5 min to get the supernatant. A 10 µl of supernatant was put on a Petri plate and a drop of motor oil was placed over it followed by a few minutes of equilibration. If the drop is collapsed, it indicates that the bacterial strain has secreted some surface-active molecules in the culture media. The procedure was repeated with distilled water as a control.

Emulsification index

In this test, an aliquot of 2 ml of petrol and an equal amount of supernatant was added in screw-capped test tubes and vortexed vigorously for 2 min. The emulsion hence produced was allowed to settle at 25℃ for 24 h. Then the height of the emulsification column was measured and put into *Eq. (1)* to find out the emulsification index (E_{24}) (Cooper and Goldenberg, 1987).

$$E_{24} = \frac{\text{Height of emulsion formed}}{\text{Total height of liquids column}} \times 100 \qquad \text{(Eq.1)}$$

http://www.aloki.hu ● ISSN 1589 1623 (Print) ● ISSN1785 0037 (Online)
DOI: http://dx.doi.org/10.15666/aeer/2001_079102

Surface tension measurement

The surface tension changes of the cell-free culture broth were measured using a digital tensiometer (Krüss K10T) calibrated against distilled water (~72 mN/m).

Identification of the bacterial strains

Once selected, the bacterial strains were undergone biochemical assays using QTS 24 kit following the standard protocols. The resultant biosurfactant-producing bacterial strains (coded as F1, F9, SJ20, and SJ32) were then analyzed for 16S rRNA gene sequencing.

FTIR analysis

Fourier transform infrared (FTIR) spectroscopy is widely employed for rapid identification of surface chemistry of bacterial strains and their metabolites containing any lipids, proteins, glycopeptides, polyphosphates, polysaccharides, teichoic acid contents, and so on (Nandiyanto et al., 2019). In the present study, we used the FTIR-attenuated total reflection (ATR) technique for the surface characterization of bacterial cell biomass and a representative isolated biosurfactant.

Fermentation setups

The biosurfactant producing strains were separately inoculated in Bushnell-Hass media containing the components (g L^{-1}) as reported elsewhere (Vandenbergh and Gonzalez, 1984): KH_2PO_4 (1.0), K_2HPO_4 (1.0), $CaCl_2$ (0.02), NH_4NO_3 (1.0), $MgSO_4$ (0.2), and $FeCl_3$ (0.05). The pH of the minimal media was set (at 6, 7, or 8) and autoclaved, accordingly. Then the desirable amount of autoclaved motor oil (as 1, 1.5, 2, 2.5, or 3%, w/v) was added as the sole carbon source into the minimal media and incubated on an orbital shaker at a desirable temperature (of 32, 37, or 42℃) and 200 rpm for a desirable period (as 24, 48, 72 or 96 h) in the absence or presence of certain inhibitors including SDS and Cr(VI) ions. All the experiments and analyses were performed in triplicates and their respective analyses were done thrice for concordant data sets. The results are reported as averages on all respective values with standard deviation (SD).

Motor oil biodegradation assay

The motor oil degradation behavior of the test biosurfactant-producing strains was investigated by adding 2,6 dichlorophenolindophenol (DCPIP: as 1% w/v, 10 µl) as a redox indicator in the respective culture media on the orbital shaker at 200 rpm, 37℃ for 120 h and after the incubation period, the culture was centrifuged at 1,000 rpm and 4℃ for 15 min. Any changes in the color of DCPIP were observed by measuring its optical density on a UV-visible spectrophotometer at 750 nm. The oil degradation was indicated by a change in color of the cell-free culture broth.

Heavy metal resistance profile

A modified version of the method reported elsewhere was used for determining the heavy metal resistance profile of the test bacterial strains (Miranda and Castillo, 1998). The bacterial tolerances to 5 heavy metals, i.e., lead (Pb^{2+} as $PbSO_4$), zinc (Zn^{2+} as $ZnSO_4$), cobalt (Co^{2+} as $CoCl_2$), manganese (Mn^{2+} as $MnSO_4$), and nickel (Ni^{2+} as $NiSO_4$) were measured on the LB agar plates provided with heavy metal ions (100 to

http://www.aloki.hu ● ISSN 1589 1623 (Print) ● ISSN1785 0037 (Online)
DOI: http://dx.doi.org/10.15666/aeer/2001_079102

40,000 μg mL^{-1}). Then, overnight bacterial cultures were streaked onto the prepared LB agar plates and incubated for 24 h at 37℃. The bacteria exhibiting resistance above 500 μg mL^{-1} were tested against higher concentrations to achieve maximum resistance against the above-mentioned metals.

Antibiotic resistance profile

The test bacterial strains were investigated for antibiotic resistance against some model drugs (at 20 μg ml^{-1}) including Ampicillin, Streptomycin, Tetracycline, Erythromycin, and Kanamycine on the LB agar media. Fresh bacterial strains were spread on LB agar plates and the above-mentioned antibiotic discs were placed on media with the help of sterilized forceps. The above-mentioned antibiotics discs were placed on the LB agar plates and incubated at 37℃ for 24 h. Then the zone of inhibition was observed for determining the antibiotic resistance of selected bacterial strains. The width of the clear zone was determined using the *Eq. (2)*:

$$\text{Width of clear zone, mm} = \left[\frac{\text{Dia. of test specimen plus clear zone, mm}}{\text{Dia. of the specimen, mm}}\right] \div 2 \quad \text{(Eq.2)}$$

Statistical analysis

Analysis of variance (ANOVA) was used for statistical analysis of the experimental data. The *p*-value usually indicates if a factor were either significant (<0.05) or insignificant (>0.05). The F-value indicates if the ratio of variances of two data sets were significantly different.

Extraction and quantification of biosurfactants

The biosurfactants were extracted from the CFCB of the culture media using the solvent extraction method. Briefly, an aliquot of 200 ml of CFCB mixed with twice equal volumes of ethyl acetate in a separating funnel. The aqueous layer was discarded whereas the organic layer was removed on a rotary evaporator till a brownish residue was obtained which was redissolved in methanol and filtered. The filtrate was recondensed on the rotary evaporator to collect the product (Carrillo et al., 1996).

Results and discussion

The contaminated soil in the vicinity of workshops contains a high proportion of used or spilled off motor oil where the oil-degrading bacteria naturally reach. The oil and water phases being immiscible need a dispersant for making them miscible at the oil-water interface. Herein, it might be some bacterial secretions behaving as surface-active agents (biosurfactants) which disperse the oily phase into the aqueous media thus making it accessible for bacterial uptake and degradation (Zhao et al., 2015; Gao, 2018). The biosurfactants find extensive applications in various fields of science and technology due to their surface-active and emulsification properties even under extreme conditions (Dhote et al., 2018).

Isolation and characterization of strains

There observed 20 distinct bacterial strains from the oil-contaminated soil samples (*Table S1*). The isolates were undergone for emulsification indices and morphological

http://www.aloki.hu ● ISSN 1589 1623 (Print) ● ISSN1785 0037 (Online)
DOI: http://dx.doi.org/10.15666/aeer/2001_079102

and biochemical analyses. The CTAB/methylene blue agar assay was done, being a semi-quantitative assay for the identification of anionic surfactants and any extracellular glycolipids in the vicinity of secreting microbes. The appearance of dark blue halos indicated the secretion of glycolipid biosurfactants (*Fig. 1a*). The separate cell-free supernatants of the selected strains were undergone a drop collapse assay on a glass surface (*Fig. 1b*). The supernatants containing any surface-active inclusions collapsed the droplet of motor oil whereas the motor oil droplet remained intact in beaded shapes when it was placed over the control sample or a supernatant not containing any surface-active secretions. Based on the above results, four distinct bacterial strains (designated as F1, F9, SJ20, and SJ32) were indicated as biosurfactants producers which were used for the ongoing study.

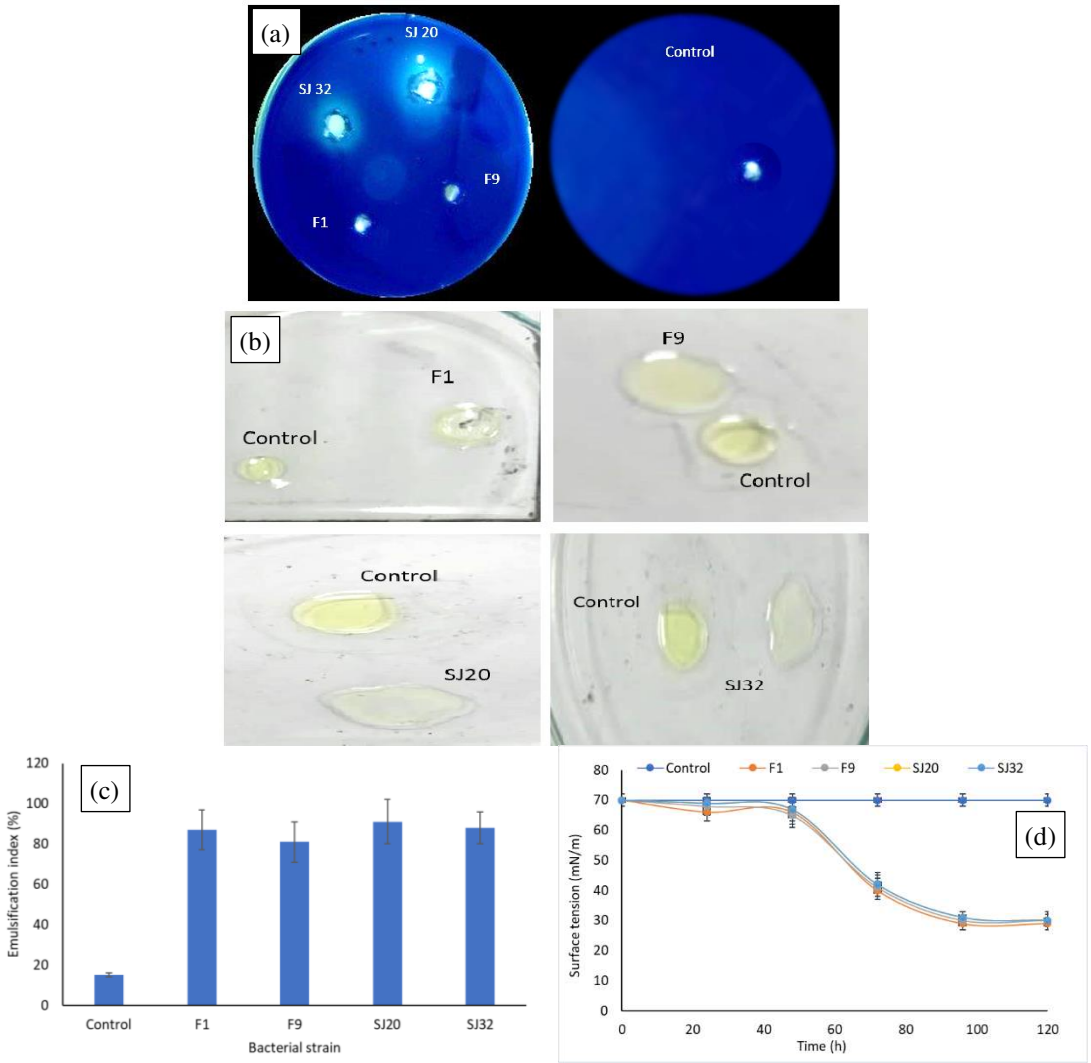

Figure 1. *(a) CTAB/methylene blue-agar assay of selected bacterial strains and the control, (b) drop collapse test results selected of bacterial strains and the control, (c) emulsification index of cell-free culture broth of selected bacterial strains and the control against petrol, and (d) surface tension profiles of respective cell-free culture broths; bar = SD*

http://www.aloki.hu ● ISSN 1589 1623 (Print) ● ISSN1785 0037 (Online)
DOI: http://dx.doi.org/10.15666/aeer/2001_079102

The selected bacterial strains of F1, F9, SJ20, and SJ32 exhibited the emulsification indices of 87±10, 81±10, 91±11, and 88±8%, respectively against petrol (*Fig. 1c*). The results indicated that the selected bacterial strains exhibited the ability to extracellularly secrete some surface-active metabolites (may be biosurfactants) into the culture media. The results were further confirmed by measuring surface tension changes of the cell-free culture broths of the respective bacterial strains. The biosurfactants due to extracellular secretions reduced the surface tension of minimal media from ~70±2 mN/m to below 30±1 mN/m (*Fig. 1d*).

The selected extracellular surface-active metabolites producing strains then undergone biochemical characterization (*Table S1*). The strains F1 and F9 showed positive results against catalase, mannitol salt agar, methyl red, and motility tests while negative results against other mentioned biochemical tests. However, the strains SJ20 and SJ32 exhibited positive results against catalase, oxidase, and mobility tests. Eventually, the results demonstrated that the bacterial strains of F1and F9 were Gram-positive cocci whereas the SJ20 and SJ32 strains as the Gram +ve bacilli.

The phylogenetic analysis of four selected bacterial strains was carried out and the resultant 16S rRNA sequences were sent to the GenBank for assigning the accession numbers as MT107124, MT107125, MT103051, and MT103052 for the selected isolates of F1, F9, SJ20, and SJ32, respectively (*Fig. S1*). The BLAST analysis indicated that F1 and F9 isolates expressed 99% homology to the genera *Staphylococcus,* whereas SJ20 and SJ32 isolates showed homology with the genera *Bacillus* (*Fig. S2*). Hence, the selected isolates of F1, F9, SJ20, and SJ32 were identified as *Staphylococcus hominis*, *Staphylococcus* sp., *Bacillus flexus,* and *Bacillus oceanisediminus*, respectively, being of non-Pseudomonad origin. The results reported in this study have been supported by the literature (Kumar et al., 2018).

FTIR analysis of bacterial surfaces

The FTIR analysis of cell surface of *Staphylococcus hominis* F1 expressed a sharp peak at 3301 cm^{-1} for C-H and H-N stretching vibrations, the latter indicated the presence of amino group (*Fig. 2a*). The peaks at 2919 and 2874 cm^{-1} indicated the presence of -CH_2-and -CH_3 moieties, respectively. There observed a peak at 1637 cm^{-1} designated for the CO-N stretching. The peaks at 1457, 1244, and 1111 cm^{-1} expressed C-H, C-O-C (ester), and C-O stretching vibrations, respectively. The FTIR spectrum of the cell surface of *Staphylococcus sp* F9 (*Fig. 2b*) indicated a peak at 3243 cm^{-1} for N-H bond, and two more peaks at 2966 and 2863 cm^{-1} for asymmetric stretching of -CH_3 and -CH_2- moieties, respectively. Two peaks at 1747 and 1686 cm^{-1} indicated C=O stretching vibrations. The peaks at 1652, 1557, and 1264 cm^{-1} corresponded to the presence of peptide bond, N-H deformation, and C-N stretching, respectively. The FTIR spectrum of the cell surface of *Bacillus flexus* (SJ20) (*Fig. 2c*) expressed a sharp peak at 3413 cm^{-1} corresponded to the N-H stretching vibration of the amino group. A peak at 1650 cm^{-1} indicated -CO-N stretching vibration which might be due to some lipopeptide secretions on the cell surface (Kanmani et al., 2017). The peaks at 2924 and 2880 cm^{-1} indicated symmetric and asymmetric stretching of C-H, respectively. A peak at 1101 cm^{-1} could be due to the C-O-C stretching vibration belonging to the ester moieties. The FTIR spectrum of *Bacillus oceanisediminis* (SJ32) (*Fig. 2d*) expressed peaks at 2860 and 2960 cm^{-1} indicating the presence of -CH_2- and -CH_3 bonds while that in the range 2800-3400 cm^{-1} indicated the presence of OH stretching. The sharp peak at 1735 cm^{-1} showed the presence of ester linkage. The peaks at 1456 cm^{-1} and 1348 cm^{-1} indicated bending vibrations of -CH_2- and

http://www.aloki.hu ● ISSN 1589 1623 (Print) ● ISSN1785 0037 (Online)
DOI: http://dx.doi.org/10.15666/aeer/2001_079102

-CH_3 moieties while that at 3381 cm^{-1} indicated the presence of N-H/C-H bonds. A peak at 1559 cm^{-1} indicated the presence of N-H bending vibration.

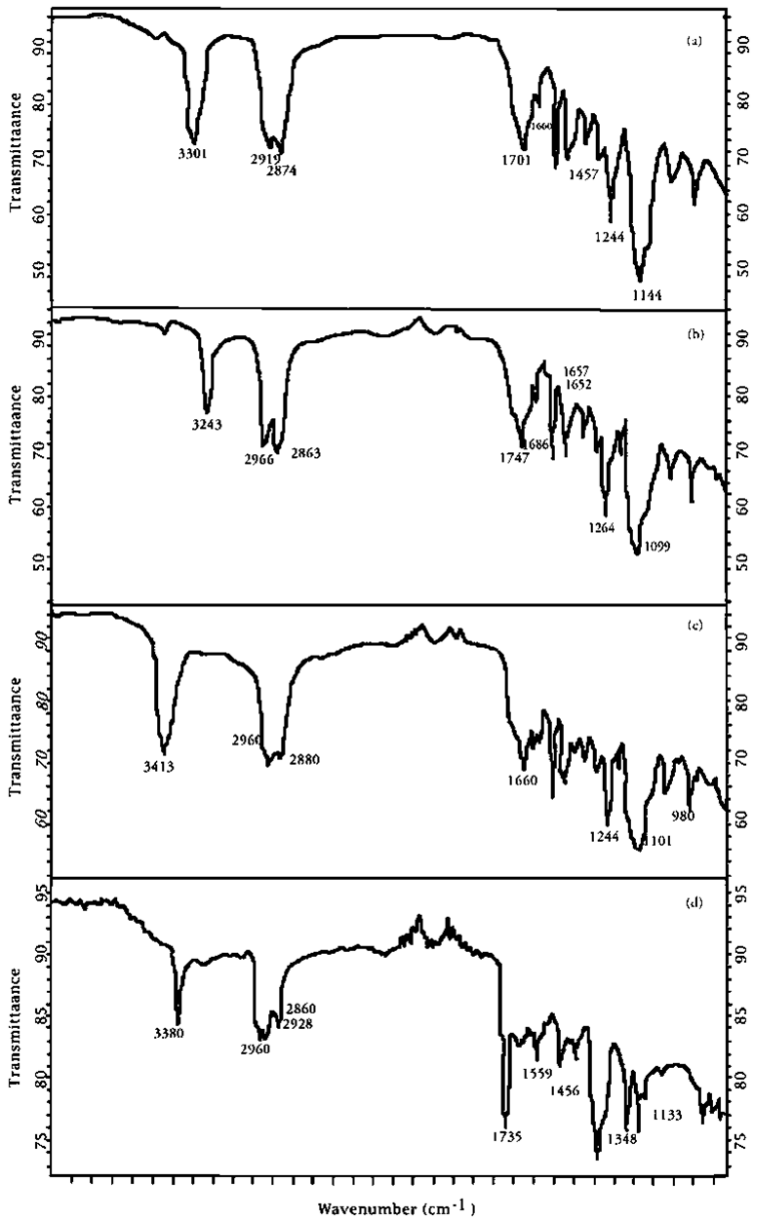

Figure 2. *FTIR spectra of cell surfaces of (a) Staphylococcus hominis F1, (b) Staphylococcus sp. F9, (c) Bacillus flexus SJ20, and (d) Bacillus oceanisediminis SJ32. (The transmittance has been reported in percent)*

Antibiotic resistance profile

The biosurfactant producing bacterial isolates were also tested for resistance against different commonly used antibiotics (as 20 µg mL^{-1}) as shown in *Fig. 3* and the respective data is expressed in *Table S2*. The selected bacterial isolates were found to be resistant against Ampicillin, Streptomycin, Tetracycline, Erythromycin, and Kanamycine, while one isolate i.e., *Bacillus oceanisediminis* expressed sensitivity towards Kanamycin.

http://www.aloki.hu ● ISSN 1589 1623 (Print) ● ISSN1785 0037 (Online)
DOI: http://dx.doi.org/10.15666/aeer/2001_079102

Metal resistance test

The results demonstrated that most of the selected biosurfactant-producing strains showed resistance against the heavy metals of lead (Pb) and manganese (Mn). The least resistance was observed against Zn^{+2} followed by Co^{+2}, and Ni^{+2} ions with all bacterial isolates (*Table S2*). In general, the heavy metal resistance profile of all the biosurfactant-producing strains was as follows: $Pb^{+2}>Mn^{+2}>Ni^{+2}>Co^{+2}>Zn^{+2}$. Heavy metals are regarded as one of the influential parameters that play a significant role not only in bacterial growth but also in their degradation behavior. For determining the potential of bacterial strains to resist heavy metals, the cross-metal resistance of bacterial strains was determined. This is helpful especially concerning heavy metals bioremediation because bacteria can behave more effectively if they can grow in the presence of toxic heavy metals.

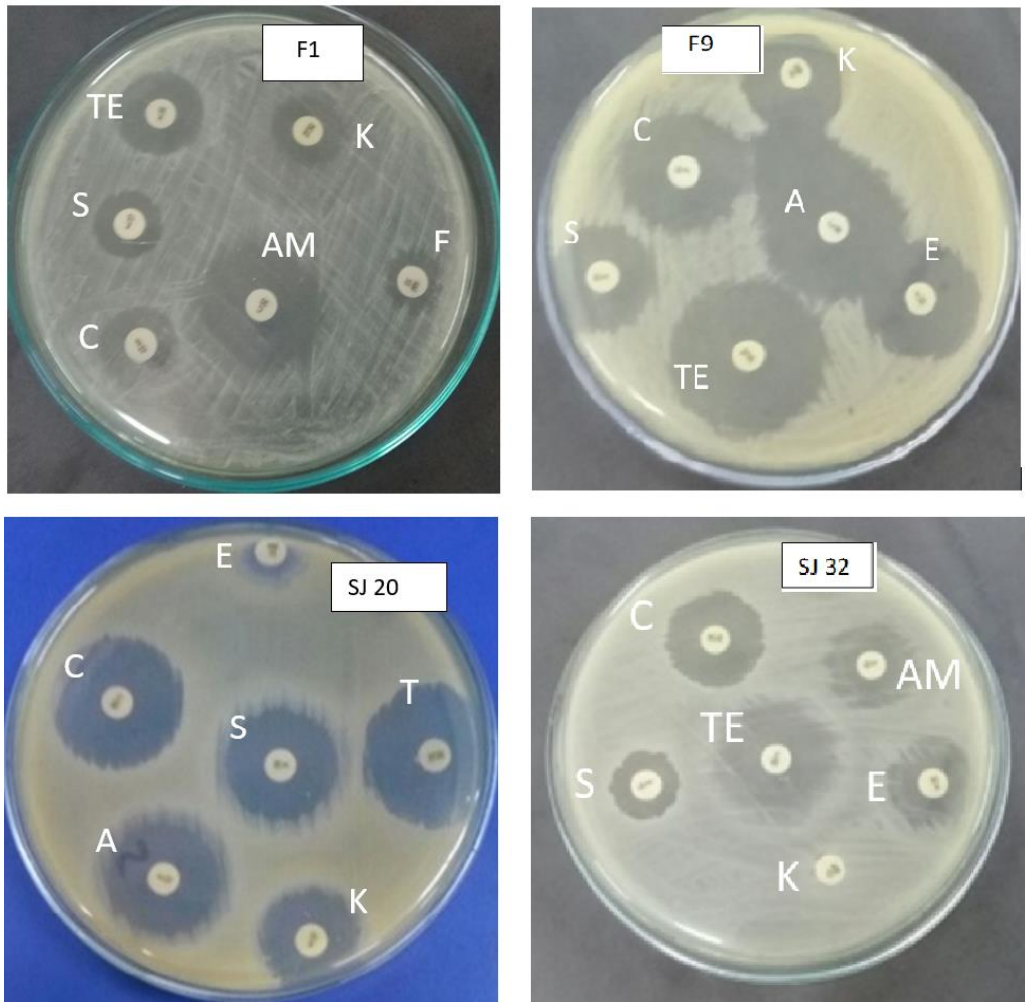

Figure 3. *Antibiotic resistance profile of selected bacterial strains (as per labeled F1(Staphylococcus hominis), F9 (Staphylococcus sp.), SJ20 (Bacillus flexus), and SJ32 (Bacillus oceanisediminis) against the drugs (as 20 µg/mL) of streptomycin (S), ampicillin (AM), tetracycline (T), kanamycin (K), erythromycin (E), and chloramphenicol (C)*

http://www.aloki.hu ● ISSN 1589 1623 (Print) ● ISSN1785 0037 (Online)
DOI: http://dx.doi.org/10.15666/aeer/2001_079102

Motor oil biodegradation study

Effect of initial motor oil concentration

The effect of different concentrations of motor oil (1-3%, w/v) on the degradation behavior in the minimal media has been investigated using the DCPIP assay. The bacterial degradation of the motor oil was observed as the reduced color intensity of 2,6 DCPIP in comparison to the control. The DCPIP, being an electron acceptor, ensures the capability of the test bacterial strain in utilizing the hydrocarbon substrate; as on biodegradation, the change of DCPIP color from blue to colorless shows the change from oxidized state to the reduced state. Thereby, all the selected bacterial strains possessed the capability to use motor oil as the sole carbon source, though to different extents, under certain fermentative conditions (*Fig. 4*). The trend of percent removal of motor oil decreased on increasing the respective initial concentration of motor oil. On increasing the carbon source of the minimal media, a decrease in percent carbon source utilization had also been reported in the literature (El-Sayed et al., 1995; Bayat et al., 2015). This might be due to excessive carbon contents in the minimal media which might imbalance the C/N ratio, in that case. The highest percent removal of motor oil could be observed with the *Staphylococcus* sp. at 1% (w/w) motor oil at 37°C, pH 7, 200 rpm after 96 h of incubation. In general, the lowest percent motor oil removal was observed at 3% (w/w) initial oil concentration. This might be due to the excess availability of carbon contents in the culture media which might form a miscible layer on the aqueous minimal media, particularly in the early days of incubation. However, after a certain time interval, enough biosurfactant contents could be secreted into the culture media thus enabling both phases to miscible into each other which facilitates the motor oil degradation. In an earlier study, the maximum hydrocarbon utilization of up to 73.97% (w/w) was achieved by the bacterial cultures with 1% (v/v) *n*-hexadecane as the sole carbon source. On increasing the *n*-hexadecane concentration to 2 and then to 3% (v/v), the oil degradation was limited to 61.90 and 47.33% (w/w), respectively (Cameotra and Singh, 2009). The carbon source contents above a certain limit also hider the bacterial growth hence the oil degradation too (Abid et al., 2016).

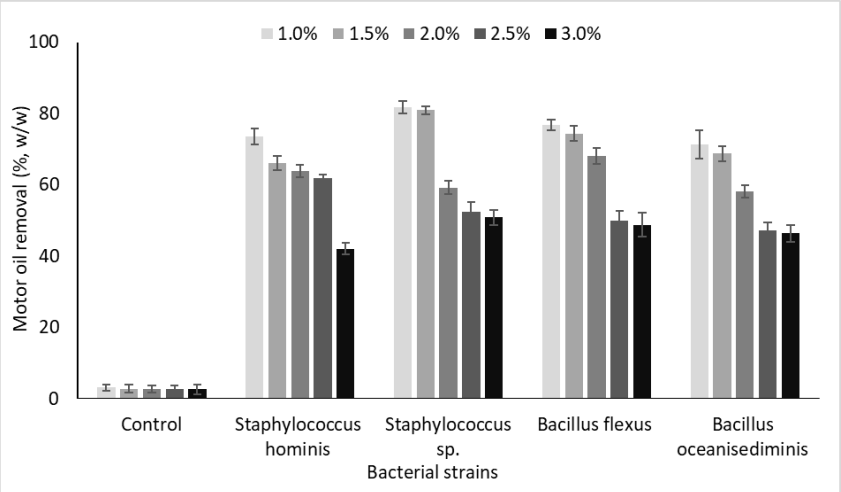

Figure 4. *Effect of motor oil concentration on biodegradation behavior with the selected bacterial strains at 37°C, pH at 7, 200 rpm after 96 h of incubation; control = in media without any bacterial strain, bar = SD*

http://www.aloki.hu ● ISSN 1589 1623 (Print) ● ISSN1785 0037 (Online)
DOI: http://dx.doi.org/10.15666/aeer/2001_079102

The combined effect of pH and motor oil concentration

The pH value of the culture media is also an important factor that affects the oil degradation behavior of bacterial strains. Since the extracellular metabolites might fluctuate the pH of the media so the fermentation was conducted in the phosphate buffer saline at the desirable pH values (6-8) with the desirable initial motor oil concentrations (being 1-3%, w/v) (*Fig. 5*). In general, at either motor oil consideration or with any selected bacterial strain, the highest percent oil removal was observed at pH 7 of the culture media. The highest percent oil removal was observed at 81.8 % (w/w) with 1% (w/v) motor oil at pH 7 by the bacterial strain of S*taphylococcus* sp. after 96 h of incubation at 37℃ and 200 rpm (*Fig. 5a*). The acidic pH, in general, was least favorable for bacterial growth which was reflected by the lowest respective motor oil degradation results. The lowest oil degradation being 9-5% (w/w) was observed at 3% (w/w) initial oil concentration in the presence of *S. hominies* (*Fig. 5e*). These results are consistent with the findings of other researchers who found that different bacterial strains showed maximum oil biodegradation at pH 7 (Palanisamy et al., 2014; Sivagamasundari, 2017; Behera et al., 2021).

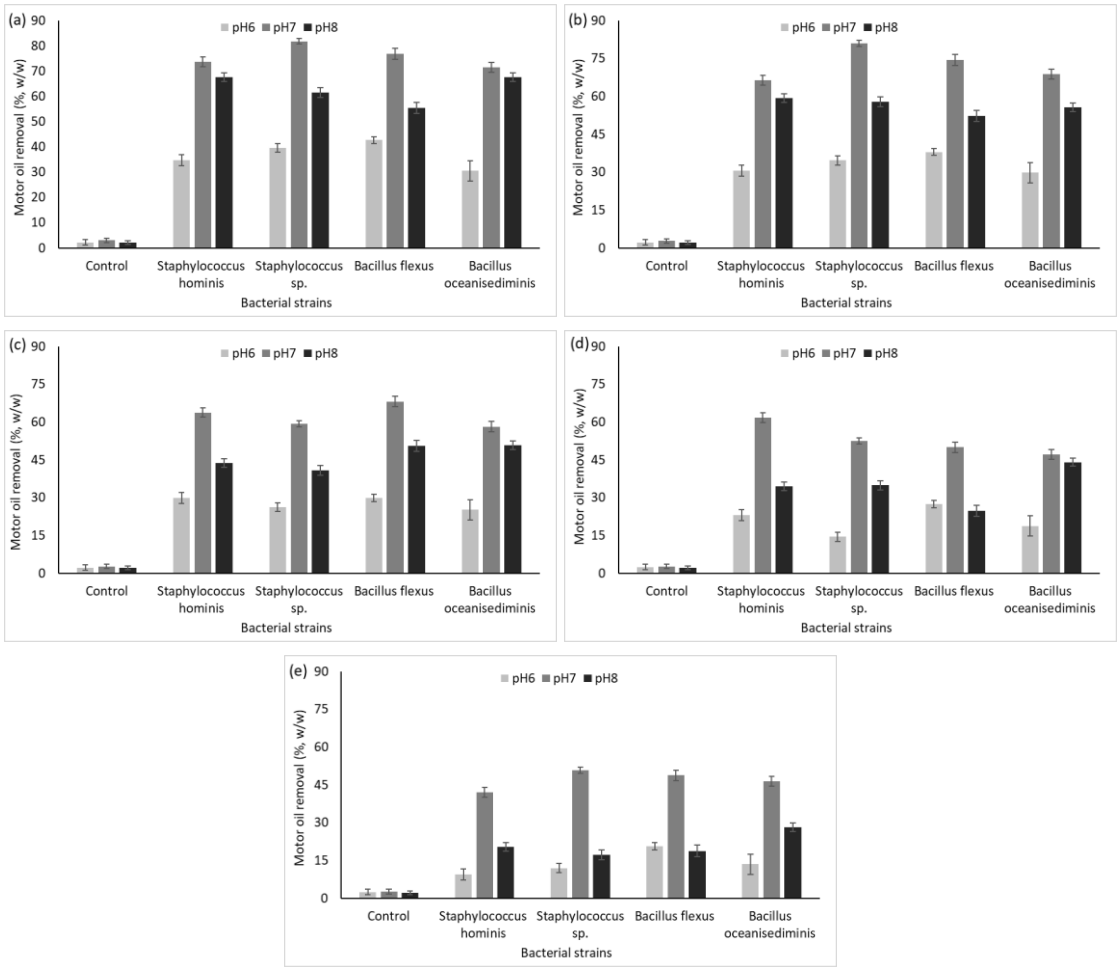

Figure 5. *Effect of bacterial strains at different levels of pH (6,7 and 8) and motor oil concentrations (1.0 (a), 1.5 (b), 2.0 (c), 2.5 (d) and 3 % (w/v) (e)) on degradation profiles at 37℃ and 200 rpm after 96 h of incubation (2, 6 Dichlorophenol indophenol assay at 750 nm); control = in media without any bacterial strain, bar = SD*

http://www.aloki.hu ● ISSN 1589 1623 (Print) ● ISSN1785 0037 (Online)
DOI: http://dx.doi.org/10.15666/aeer/2001_079102

The combined effect of incubation temperature and motor oil concentration

Once the pH of the media was optimized to be 7, the culture media were investigated at various incubation temperatures for all the selected bacterial strains at various initial oil contents (*Fig. 6*). Any changes in temperature from the optimum value may affect the physicochemical and biogenic attributes of the motor oil as the sole carbon source. The experiments were conducted at 32, 37, or 42℃. In general, the optimum incubation temperature was observed to be 37℃ at either initial oil contents with either selected bacterial strain. The highest percent oil removal (81.8%, w/w) was observed at 37℃ and 1% (w/w) initial oil concentration with the bacterial strain of *Staphylococcus* sp. The incubation temperatures of 32 and 42℃ were observed to be unfavorable for bacterial growth at either oil concentration. The bacterial strain of *Staphylococcus* sp. was observed to remove just 1.6% (w/w) oil contents at 42℃ after 96 h of incubation. These findings coincide with the results of Kao et al. (2005) who reported that the biodegradation rate was the highest at the optimum growth temperature of the mesophilic bacteria that ranged between 25-30℃ (Bossert and Bartha, 1984; Rahman et al., 2002; Ren et al., 2021).

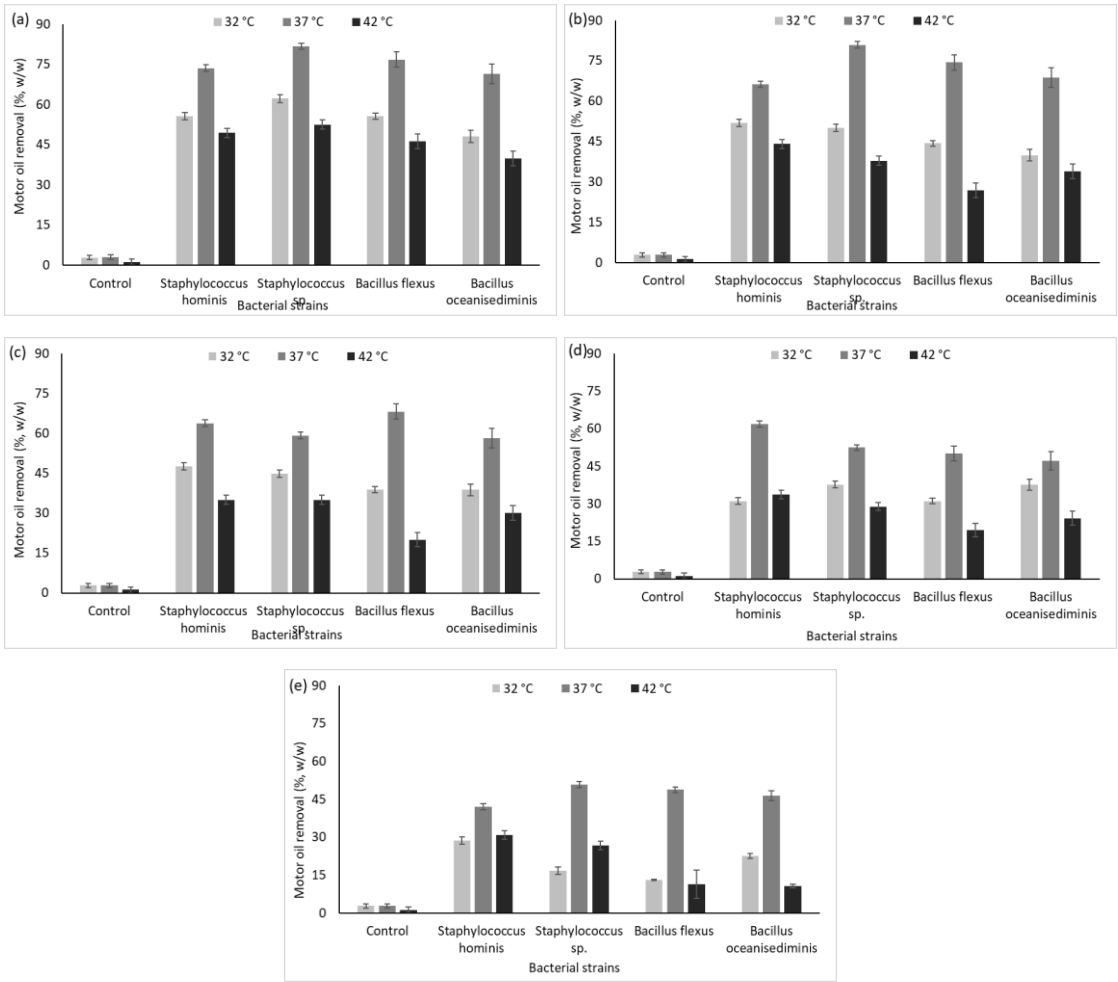

Figure 6. *Effect of bacterial strains at different temperatures (32, 37 and 42℃) and motor oil concentrations (1.0 (a), 1.5 (b), 2.0 (c), 2.5 (d) and 3 % (w/w) (e)) on degradation profiles at pH 7 and 200 rpm after 96 h of incubation (2, 6 Dichlorophenol indophenol assay at 750 nm); control = in media without any bacterial strain, bar = SD*

http://www.aloki.hu ● ISSN 1589 1623 (Print) ● ISSN1785 0037 (Online)
DOI: http://dx.doi.org/10.15666/aeer/2001_079102

The combined effect of incubation time on motor oil concentration

For determining the impact of incubation time on motor oil biodegradation behavior of selected bacterial strains different incubation times (24, 48, 72, and 96 h) were selected. It can be seen from *Figure 7* that as the incubation time was increased the selected bacterial strains showed higher biodegradation of motor oil. It was found that incubation time is directly proportional to the motor oil biodegradation activity of microorganisms (Javed et al., 2015). At 1% (w/v) motor oil concentration, when the incubation time was increased from 24 to 96 h, the biodegradation rate also increased from 40.0 to 81.8% (w/w). Similar behavior of motor oil biodegradation was observed with other motor oil concentrations and it was found that motor oil biodegradation was increased with an increase in incubation time. Although with an increase of incubation time, the biodegradation activity was increased, however, it was found that biodegradation activity was slowed time with the increase of incubation time. The previous literature also shows that higher incubation time favors oil biodegradation (John et al., 2021).

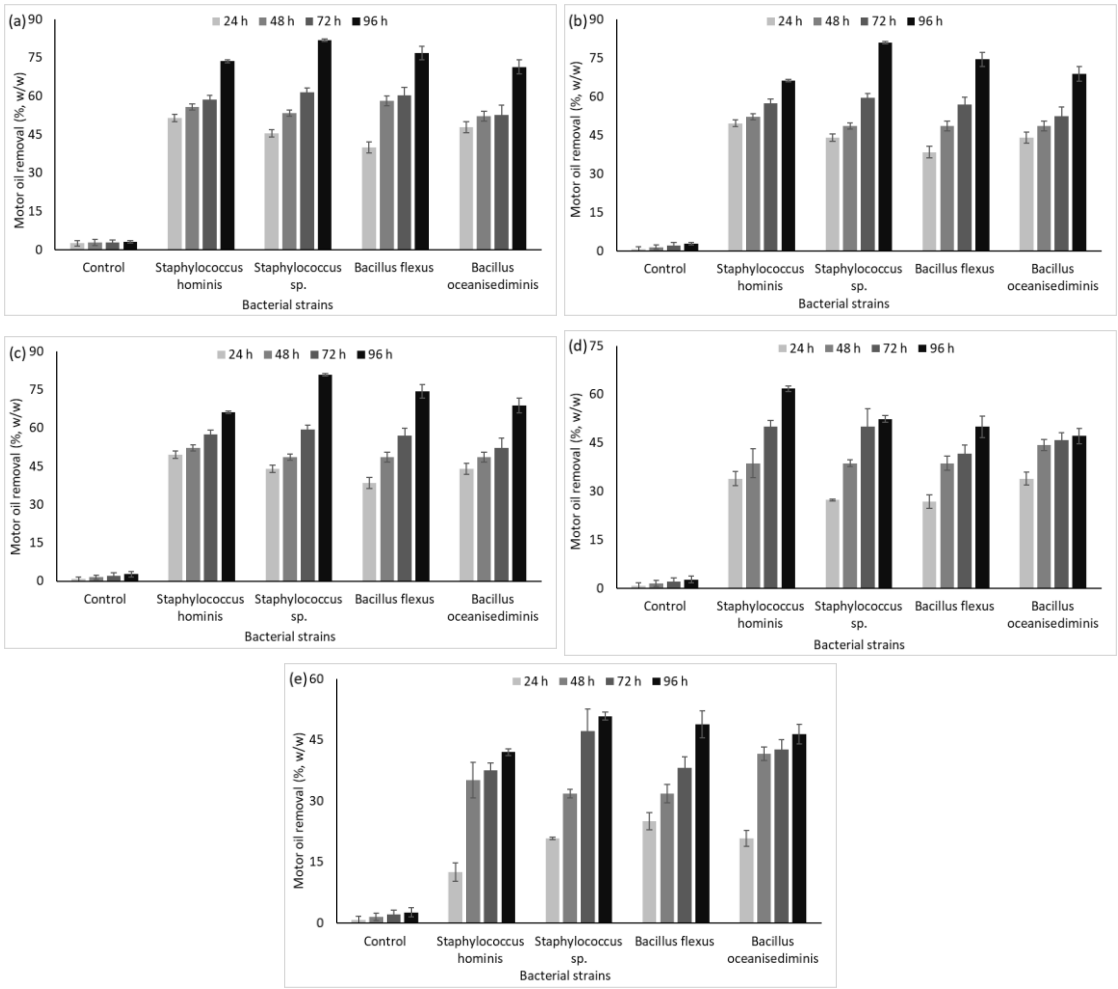

Figure 7. *Effect of bacterial strains at different incubation time (24, 48, 72 and 96 h) and motor oil concentrations (1.0 (a), 1.5 (b), 2.0 (c), 2.5 (d) and 3 % (w/v) (e)) on degradation profiles at 37 °C, pH at 7 and 200 rpm after 96 h of incubation (2, 6 Dichlorophenol indophenol assay at 750 nm); control = in media without any bacterial strain, bar = SD*

http://www.aloki.hu ● ISSN 1589 1623 (Print) ● ISSN1785 0037 (Online)
DOI: http://dx.doi.org/10.15666/aeer/2001_079102

Effect of inhibitors

The SDS was tested if it could inhibit the growth of biosurfactant-producing bacteria. Two concentrations of SDS (as 1 and 2%, w/v) were tested at different concentrations of motor oil (*Fig. 8a,b*). At SDS 1% (w/v), maximum inhibition of 3 to 11% was observed with 1 and 2% (w/v) motor oil concentrations, respectively. On increasing the SDS content to 2% (w/v), the inhibition of 0.8% was observed at 3% (w/v) oil concentration, while other test concentrations of motor oil did not exhibit significant inhibition. Heavy metals are also present in the environment in a small proportion; however, their proportion is increasing due to the increase in industrial activities. Heavy metals can either inhibit or increase the biodegradation process. In this study, Cr(VI) ions were selected for studying the inhibitory effect of heavy metals on the biodegradation process. When 1,000 µg/ml concentration of Cr(VI) ions was used the maximum inhibition of biodegradation was shown by bacterial strain *Staph. hominis* at 1% (w/v) oil concentration. At a higher concentration of heavy metals, the micro-organisms showed higher inhibition as they instantaneously stop their activities (Javed et al., 2015).

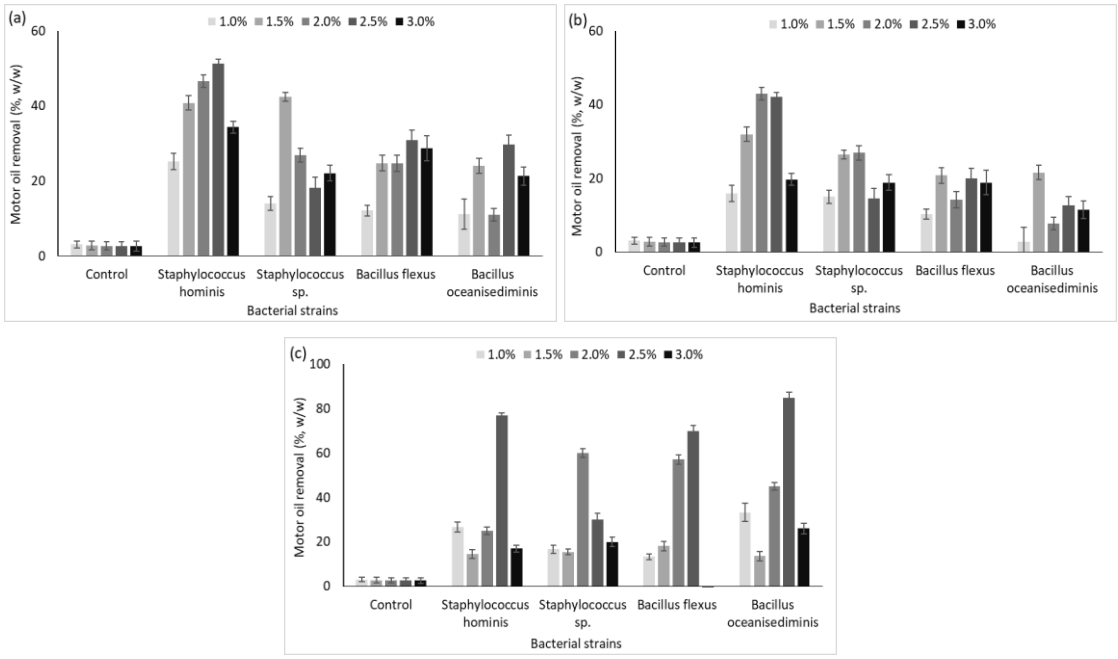

Figure 8. *Effect of inhibitors: SDS at 1% (a) and 2% (w/v) (b) w/v and chromium (1,000 µg/ml) (c) on the motor oil degradation behavior at different concentrations (1.0, 1.5, 2.0, 2.5 and 3 %, w/v) by using selected bacterial at 37℃ and 200 rpm (2, 6 Dichlorophenol indophenol assay at 750 nm); control = in media without any bacterial strain, bar = SD*

The statistical analysis indicated that the initial oil concentration, pH value of the culture media, incubation time, and SDS and Cr(IV) ions concentrations were significant factors at either fermentation setup whereas the bacterial strain type was observed to be an insignificant parameter in either case except on changing the SDS concentration in the culture media (*Table 1*). Since the selected bacterial strains were all capable to degrade the motor oil so the choice of the bacterial strains becomes insignificant in the comparison. However, the prior presence of surfactant (i.e., SDS) in the culture media supports the motor oil degradation in the culture media due to its emulsification behavior.

http://www.aloki.hu ● ISSN 1589 1623 (Print) ● ISSN1785 0037 (Online)
DOI: http://dx.doi.org/10.15666/aeer/2001_079102

Table 1. *Effect of multiple factors on the motor oil degradation (%) under various fermentation setups*

Setup	Constants	Factors	Hypothesis	F-value	P-value	Remarks
I	pH = 7 Incubation time = 96 h Temp. 37°C	Bacterial strains	H_o: $\mu_1=\mu_2=\mu_3=\mu_4$ H_1: at least two means are unequal	1.73	0.214	Insignificant
		Int. oil conc.	H_o: $\mu_5=\mu_6=\mu_7=\mu_8=\mu_9$ H_1: at least two means are unequal	25.25	0.00	Significant
II	Incubation time = 96 h Temp. 37°C	Bacterial strains	H_o: $\mu_1=\mu_2=\mu_3=\mu_4$ H_1: at least two means are unequal	0.34	0.80	Insignificant
		Int. oil conc.	H_o: $\mu_5=\mu_6=\mu_7=\mu_8=\mu_9$ H_1: at least two means are unequal	5.01	0.002	Significant
		pH	H_o: $\mu_{10}=\mu_{11}=\mu_{12}$ H_1: at least two means are unequal	20.4	0.00	Significant
III	pH = 7 Incubation time = 96 h	Bacterial strains	H_o: $\mu_1=\mu_2=\mu_3=\mu_4$ H_1: at least two means are unequal	0.63	0.59	Insignificant
		Int. oil conc.	H_o: $\mu_5=\mu_6=\mu_7=\mu_8=\mu_9$ H_1: at least two means are unequal	7.73	0.00	Significant
		Temperature	H_o: $\mu_{13}=\mu_{14}=\mu_{15}$ H_1: at least two means are unequal	32.57	0.00	Significant
IV	pH = 7 Temp. = 37°C	Bacterial strains	H_o: $\mu_1=\mu_2=\mu_3=\mu_4$ H_1: at least two means are unequal	0.16	0.92	Insignificant
		Oil conc.	H_o: $\mu_5=\mu_6=\mu_7=\mu_8=\mu_9$ H_1: at least two means are unequal	12.60	0.00	Significant
		Incubation time	H_o: $\mu_{16}=\mu_{17}=\mu_{18}=\mu_{19}$ H_1: at least two means are unequal	25.12	0.00	Significant
V	pH = 7 Incubation time = 96 h Temp. 37°C	Bacterial strains	H_o: $\mu_1=\mu_2=\mu_3=\mu_4$ H_1: at least two means are unequal	2.84	0.039	Significant
		Int. oil conc.	H_o: $\mu_5=\mu_6=\mu_7=\mu_8=\mu_9$ H_1: at least two means are unequal	8.45	0.00	Significant
		SDS	H_o: $\mu_{20}=\mu_{21}$ H_1: Two means are unequal	4.40	0043	Significant

http://www.aloki.hu ● ISSN 1589 1623 (Print) ● ISSN1785 0037 (Online)
DOI: http://dx.doi.org/10.15666/aeer/2001_079102

Setup	Constants	Factors	Hypothesis	F-value	P-value	Remarks
VI	pH = 7 Incubation time = 96 h Temp. 37℃ Cr(IV) = 1000 µg/ml	Bacterial strains	H_o: $\mu_1=\mu_2=\mu_3=\mu_4$ H_1: at least two means are unequal	0.66	0.594	Insignificant
		Oil concentration	H_o: $\mu_5=\mu_6=\mu_7=\mu_8=\mu_9$ H_1: at least two means are unequal	8.83	0.001	Significant

Designate: H_o = Null hypothesis (All means are equal), H_1 = Alternate hypothesis (At least two means are unequal), μ_1, μ_2, μ_3 and μ_3= Population mean of bacterial strains, μ_5, μ_6, μ_7, μ_8, μ_9 = Population mean of initial motor oil concentration, $\mu_{10}=\mu_{11}=\mu_{12}$ = Population mean of different pH, $\mu_{13}=\mu_{14}=\mu_{15}$ = Population mean of different temperatures, $\mu_{16}=\mu_{17}=\mu_{18}=\mu_{19}$ = Population mean of different incubation time, $\mu_{20}=\mu_{21}$ = Population mean of SDS concentrations

http://www.aloki.hu ● ISSN 1589 1623 (Print) ● ISSN1785 0037 (Online)
DOI: http://dx.doi.org/10.15666/aeer/2001_079102

Extraction and characterization of biosurfactants

The test bacterial strains were investigated for possible biosurfactant secretions in its culture media up to 96 h of incubation. After solvent extraction, we obtained the crude biosurfactant yields of 0.9, 1.8, 1.6, 1.7g L^{-1}, respectively, with *Staphylococcus hominis*, *Staphylococcus sp.*, *Bacillus flexus,* and *Bacillus oceanisediminus* strains. Previously, a bacterial strain of *Bacillus licheniformis* resulted in 1.28 g L^{-1} of biosurfactant (Kumar et al., 2016). Likewise, *Bacillus subtilus* had been reported to produce 3.24 g L^{-1} of biosurfactant (Nayarisseri et al., 2018). The bacterial strain of *Staphylococcus* sp. had been reported to produce 2.1 g L^{-1} biosurfactant (Eddouaouda et al., 2012). The biosurfactant produced from *Staphylococcus* sp., being the highest motor oil degrader and biosurfactant producer, was investigated using the FTIR analysis. The FTIR spectrum of biosurfactant collected from the *Staphylococcus* sp. is shown in *Fig. 9*. A sharp absorbance peak at 3292 cm^{-1} confirmed the existence of -NH and -OH functional groups in the biosurfactant, which indicated the presence of amino groups in the product. Other peaks at 2956, 2925, and 2854 cm^{-1} confirmed the existence of -C-CH_3 vibrations. The presence of a peak at 1664 cm^{-1} indicated the CO-N stretching vibrations which are similar to the lactone ring present in the lipopeptides. The presence of peaks at 1456 and 1406 cm^{-1} corresponded to -C-CH_2 and -C-CH_3 vibrations of aliphatic chains, respectively. The peak at 1194 cm^{-1} indicated the probable existence of C-O-C vibration of the ester linkage. The results demonstrate that the biosurfactant produced from the bacterial strain of *Staphylococcus* sp. was a lipopeptide.

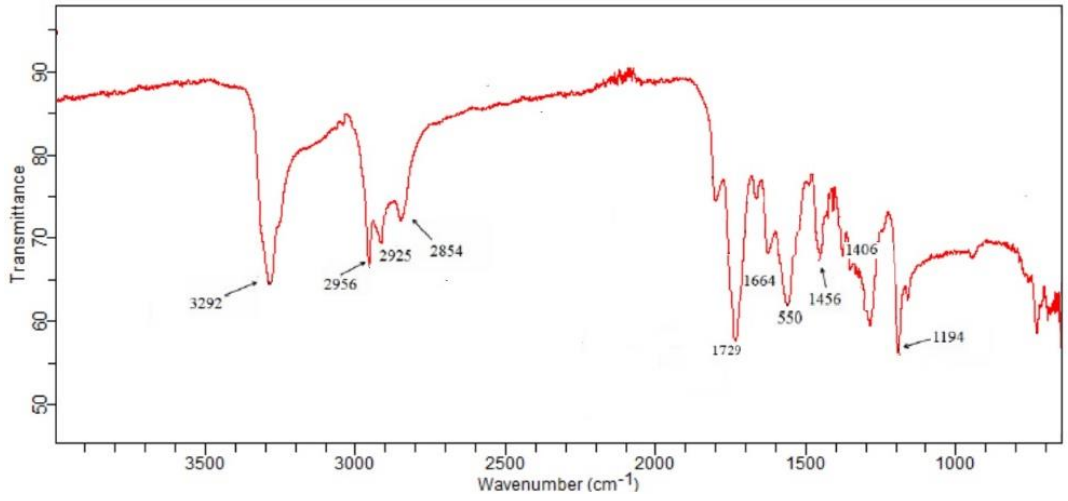

Figure 9. *Representative FTIR spectrum of the biosurfactant isolated from Staphylococcus sp.*

Conclusion

The isolated and identified non-Pseudomonads at different motor oil concentrations, pH, temperatures, incubation time, and parameters showed different levels of biodegradation. The trend of higher biodegradation was observed at low motor oil concentrations while a higher concentration of motor oil declined the bacterial growth. The biosurfactants behaved more effectively in the neutral medium as compared to in the acidic or alkaline media. The SDS and Cr(VI) ions inhibited the process of motor oil biodegradation in the presence of microbial isolates. It was concluded that the identified

http://www.aloki.hu ● ISSN 1589 1623 (Print) ● ISSN1785 0037 (Online)
DOI: http://dx.doi.org/10.15666/aeer/2001_079102

non-Pseudomonads isolated from soil of auto workshops could effectively be employed for successful biodegradation of motor oil and its biotransformation into biosurfactants. The future developments in this area might be to further tune the biosurfactant-producing strains for enhanced yields and to obtain particular congeners using the advanced techniques of synthetic and molecular biology. The bacterial consortia may also be investigated for enhanced remediation of crude oils contaminated soils.

Acknowledgment. The authors acknowledge the financial support of the Higher Education Commission, Islamabad for pursuing this study.

Conflict of interests. The authors declared that they have no conflict of interests.

Ethical statement. This article does not contain any studies with human participants or animals performed by any of the authors.

REFERENCES

[1] Abid, S., Raza, Z. A., Hussain, T. (2016): Production kinetics of polyhydroxyalkanoates by using *Pseudomonas aeruginosa* gamma ray mutant strain EBN-8 cultured on soybean oil. – 3 Biotech 6(2): 1-10.
[2] Batista, S., Mounteer, A., Amorim, F., Totola, M. (2006): Isolation and characterization of biosurfactant/bioemulsifier-producing bacteria from petroleum contaminated sites. – Bioresource technology 97(6): 868-875.
[3] Bayat, Z., Hassanshahian, M., Hesni, M. A. (2015): Enrichment and isolation of crude oil degrading bacteria from some mussels collected from the Persian Gulf. – Marine pollution bulletin 101(1): 85-91.
[4] Behera, I. D., Nayak, M., Biswas, S., Meikap, B. C., Sen, R. (2021): Enhanced biodegradation of total petroleum hydrocarbons by implementing a novel two-step bioaugmentation strategy using indigenous bacterial consortium. – Journal of Environmental Management 292: 112746.
[5] Bhattacharya, M., Guchhait, S., Biswas, D., Singh, R. (2019): Evaluation of a microbial consortium for crude oil spill bioremediation and its potential uses in enhanced oil recovery. – Biocatalysis and agricultural biotechnology 18: 101034.
[6] Bossert, I., Bartha, R. (1984): The fate of petroleum in soil ecosystems. – New York (USA), Macmillan.
[7] Cameotra, S. S., Singh, P. (2009): Synthesis of rhamnolipid biosurfactant and mode of hexadecane uptake by *Pseudomonas* species. – Microbial cell factories 8(1): 1-7.
[8] Carrillo, P., Mardaraz, C., Pitta-Alvarez, S., Giulietti, A. (1996): Isolation and selection of biosurfactant-producing bacteria. – World Journal of Microbiology and Biotechnology 12(1): 82-84.
[9] Cooper, D. G., Goldenberg, B. G. (1987): Surface-active agents from two Bacillus species. – Applied and environmental microbiology 53(2): 224-229.
[10] da Silva, I. A., Bezerrac, K. G. O., Batista, I. J. (2020): Evaluation of the emulsifying and antioxidant capacity of the biosurfactant produced by *Candida bombicola* URM 3718. – Chemical Engineering 79(1): 67-72.
[11] Dhote, M., Kumar, A., Juwarkar, A. (2018): Petroleum contaminated oil sludge degradation by defined consortium: Influence of biosurfactant production. – Proceedings of the National Academy of Sciences, India Section B: Biological Sciences 88(2): 517-523.
[12] Duan, L., Naidu, R., Thavamani, P., Meaklim, J., Megharaj, M. (2015): Managing long-term polycyclic aromatic hydrocarbon contaminated soils: a risk-based approach. – Environmental Science and Pollution Research 22(12): 8927-8941.

http://www.aloki.hu ● ISSN 1589 1623 (Print) ● ISSN1785 0037 (Online)
DOI: http://dx.doi.org/10.15666/aeer/2001_079102

[13] Eddouaouda, K., Mnif, S., Badis, A., Younes, S. B., Cherif, S., Ferhat, S., Mhiri, N., Chamkha, M., Sayadi, S. (2012): Characterization of a novel biosurfactant produced by *Staphylococcus* strain 1E with potential application on hydrocarbon bioremediation. – Journal of Basic Microbiology 52(4): 408-418.
[14] El-Sayed, A., Shebl, A., Ramadan, M. (1995): Laboratory study of microbial cleaning of oil spills under Saudi environmental conditions. – Middle East Oil Show, 1995. Society of Petroleum Engineers.
[15] Gao, C. (2018): Experiences of microbial enhanced oil recovery in Chinese oil fields. – Journal of Petroleum Science and Engineering 166: 55-62.
[16] Gregorich, E., Gillespie, A., Beare, M., Curtin, D., Sanei, H., Yanni, S. (2015): Evaluating biodegradability of soil organic matter by its thermal stability and chemical composition. – Soil Biology and Biochemistry 91: 182-191.
[17] Henkel, M., Hausmann, R. (2019): Diversity and classification of microbial surfactants. – Biobased surfactants, Chapter 2, Elsevier, pp. 41-63.
[18] Javed, S., Sarwar, A., Tassawar, M., Faisal, M. (2015): Conversion of selenite to elemental selenium by indigenous bacteria isolated from polluted areas. – Chemical Speciation & Bioavailability 27(4): 162-168.
[19] John, W. C., Ogbonna, I. O., Gberikon, G. M., Iheukwumere, C. C. (2021): Evaluation of biosurfactant production potential of *Lysinibacillus fusiformis* MK559526 isolated from automobile-mechanic-workshop soil. – Brazilian Journal of Microbiology 52(2): 663-674.
[20] Kanmani, P., DivyaSri, E., Rajakarvizhi, R., Senthamil, O., Sivasankari, V., Aravind, J. (2017): Optimization of biosurfactant production and crude oil emulsification by *Bacillus* sp. isolated from hydrocarbon contaminated soil sample. – In: Bioremediation and Sustainable Technologies for Cleaner Environment, Springer, pp. 305-317.
[21] Kao, C., Liu, J., Chen, Y., Chai, C., Chen, S. (2005): Factors affecting the biodegradation of PCP by *Pseudomonas mendocina* NSYSU. – Journal of hazardous materials 124(1-3): 68-73.
[22] Karlapudi, A. P., Venkateswarulu, T., Tammineedi, J., Kanumuri, L., Ravuru, B. K., Ramu Dirisala, V., Kodali, V. P. (2018): Role of biosurfactants in bioremediation of oil pollution-a review. – Petroleum 4(3): 241-249.
[23] Khubaib, M. A., Raza, Z. A., Abid, S., Nazir, A., Tariq, M. R. (2021): Cell-Free Culture Broth of *Pseudomonas aeruginosa* - an alternative source of biodispersant to synthetic surfactants for dyeing the polyester fabric. – Journal of Surfactants and Detergents 24(2): 343-355.
[24] Kumar, A. P., Janardhan, A., Viswanath, B., Monika, K., Jung, J.-Y., Narasimha, G. (2016): Evaluation of orange peel for biosurfactant production by *Bacillus licheniformis* and their ability to degrade naphthalene and crude oil. – 3 Biotech 6(1): 43-53.
[25] Kumar, S., Stecher, G., Li, M., Knyaz, C., Tamura, K. (2018): MEGA X: molecular evolutionary genetics analysis across computing platforms. – Molecular Biology and Evolution 35(6): 1547-1549.
[26] Miranda, C., Castillo, G. (1998): Resistance to antibiotic and heavy metals of motile aeromonads from Chilean freshwater. – Science of the Total Environment 224(1-3): 167-176.
[27] Naik, S. N., Saxena, D. K., Dole, B. R., Khare, S. K. (2018): Potential and perspective of castor biorefinery. – Waste Biorefinery, Chapter 21, Elsevier, pp. 623-656.
[28] Nandiyanto, A. B. D., Oktiani, R., Ragadhita, R. (2019): How to read and interpret FTIR spectroscope of organic material. – Indonesian Journal of Science and Technology 4(1): 97-118.
[29] Nayarisseri, A., Singh, P., Singh, S. K. (2018): Screening, isolation and characterization of biosurfactant producing *Bacillus subtilis* strain ANSKLAB03. – Bioinformation 14(6): 304-314.

http://www.aloki.hu ● ISSN 1589 1623 (Print) ● ISSN1785 0037 (Online)
DOI: http://dx.doi.org/10.15666/aeer/2001_079102

[30] Palanisamy, N., Ramya, J., Kumar, S., Vasanthi, N., Chandran, P., Khan, S. (2014): Diesel biodegradation capacities of indigenous bacterial species isolated from diesel contaminated soil. – Journal of Environmental Health science and Engineering 12(1): 1-8.
[31] Paniagua-Michel, J., Rosales, A. (2015): Marine bioremediation - a sustainable biotechnology of petroleum hydrocarbons biodegradation in coastal and marine environments. – Journal of Bioremediation & Biodegredation 6(2): 1-6.
[32] Pinazo, A., Pérez, L., del Carmen Morán, M., Pons, R. (2019): Arginine - based surfactants: synthesis, aggregation properties, and applications. – Biobased Surfactants, Chapter 13, Elsevier, pp. 413-445.
[33] Rahman, K., Rahman, T. J., McClean, S., Marchant, R., Banat, I. M. (2002): Rhamnolipid biosurfactant production by strains of Pseudomonas aeruginosa using low-cost raw materials. – Biotechnology Progress 18(6): 1277-1281.
[34] Raza, Z. A., Khan, M. S., Khalid, Z. M. (2007): Evaluation of distant carbon sources in biosurfactant production by a gamma ray-induced *Pseudomonas putida* mutant. – Process Biochemistry 42(4): 686-692.
[35] Raza, Z. A., Khalid, Z. M., Banat, I. M. (2009): Characterization of rhamnolipids produced by a *Pseudomonas aeruginosa* mutant strain grown on waste oils. – Journal of Environmental Science and Health, Part A, 44(13): 1367-1373.
[36] Ren, J., Fan, B., Niu, D., Gu, Y., Li, C. (2021): Biodegradation of waste cooking oils by *Klebsiella quasivariicola* IUMR-B53 and characteristics of its oil-degrading enzyme. – Waste and Biomass Valorization 12: 1243-1252.
[37] Rita de Cássia, F., Luna, J. M., Rufino, R. D., Sarubbo, L. A. (2021): Ecotoxicity of the formulated biosurfactant from *Pseudomonas cepacia* CCT 6659 and application in the bioremediation of terrestrial and aquatic environments impacted by oil spills. – Process Safety and Environmental Protection 154: 338-347.
[38] Sakamoto, K., Lochhead, R., Maibach, H., Yamashita, Y. (2017): Cosmetic Science and Technology: theoretical Principles and Applications. – Elsevier.
[39] Sharma, S., Verma, R., Pandey, L. M. (2019): Crude oil degradation and biosurfactant production abilities of isolated *Agrobacterium fabrum* SLAJ731. – Biocatalysis and Agricultural Biotechnology 21(1): 101322-101331.
[40] Siegmund, I., Wagner, F. (1991): New method for detecting rhamnolipids excreted by *Pseudomonas* species during growth on mineral agar. – Biotechnology Techniques 5(4): 265-268.
[41] Singh, S., Kumar, V., Singh, S., Dhanjal, D. S., Datta, S., Sharma, D., Singh, N. K., Singh, J. (2020): Biosurfactant-based bioremediation. – Bioremediation of Pollutants, Chapter 16, Elsevier, pp. 333-358.
[42] Sivagamasundari, T. (2017): Optimization of Diesel oil degrading Bacterial strains at various culture parameters. – International Journal of Research and Development in Pharmacy & Life Sciences 6(6): 2840-2844.
[43] Trellu, C., Mousset, E., Pechaud, Y., Huguenot, D., Van Hullebusch, E. D., Esposito, G., Oturan, M. A. (2016): Removal of hydrophobic organic pollutants from soil washing/flushing solutions: a critical review. – Journal of Hazardous Materials 306: 149-174.
[44] Vandenbergh, P. A., Gonzalez, C. F. (1984): Method for protecting the growth of plants employing mutant siderophore producing strains of *Pseudomonas putida*. – Google Patents, PubChem.
[45] Varadavenkatesan, T., Murty, V. R. (2013): Production of a lipopeptide biosurfactant by a novel *Bacillus* sp. and its applicability to enhanced oil recovery. – International Scholarly Research Notices, Article ID: 621519.
[46] Vijayakumar, S., Saravanan, V. (2015): Biosurfactants-types, sources and applications. – Research Journal of Microbiology 10(5): 181-192.
[47] Zhao, F., Shi, R., Zhao, J., Li, G., Bai, X., Han, S., Zhang, Y. (2015): Heterologous production of *Pseudomonas aeruginosa* rhamnolipid under anaerobic conditions for microbial enhanced oil recovery. – Journal of Applied Microbiology 118(2): 379-389.

http://www.aloki.hu ● ISSN 1589 1623 (Print) ● ISSN1785 0037 (Online)
DOI: http://dx.doi.org/10.15666/aeer/2001_079102

APPENDIX

Table S1. *Emulsification index (E_{24}) vs. petrol at 25 ℃, and the morphological and biochemical characterization of indigenous bacterial isolates*

Isolate	E_{24} (%)	Morphological characterization					Biochemical characterization					
		Gram stain	Spore stain	Cell shape	Catalase test	Oxidase test	Motility test	Methyl red test	Indole test	Mannitol salt agar test	Triple sugar iron test	
											slant	butt
F1	87±10	+	-ve	Cocci	+ve	-ve	+ve	+ve	-ve	+ve	Y	Y
F9	81±10	+	-ve	Cocci	+ve	-ve	+ve	+ve	-ve	+ve	Y	Y
F19	40±6	+	-ve	Cocci	+ve	-ve	+ve	+ve	-ve	+ve	Y	Y
S6	42±5	+	+	Rods	+ve	-ve	-ve	+ve	-ve	-ve	Y	R
SJ1	49±12	+	+	Rods	+ve	-ve	-ve	-ve	-ve	-ve	Y	R
SJ4	41±10	+	+ve	Rods	+ve	-ve	+ve	+ve	-ve	-ve	Y	Y
SJ10	43±8	+	+	Rods	+ve	+ve	-ve	-ve	-ve	-ve	Y	Y
SJ12	31±16	+	-ve	Cocci	-ve	+ve	+ve	-ve	-ve	-ve	Y	R
SJ15	48±14	+	+	Rods	+ve	-ve	-ve	-ve	-ve	-ve	Y	R
SJ17	40±7	+	+	Rods	+ve	-ve	-ve	-ve	-ve	-ve	Y	R
SJ19	46±9	+	+	Rods	+ve	-ve	-ve	-ve	-ve	-ve	Y	R
SJ20	91±11	+	+	Rods	+ve	-ve	+ve	-ve	-ve	-ve	Y	R
SJ32	88±8	+	+	Rods	+ve	-ve	+ve	-ve	-ve	-ve	Y	R
SJ36	42±6	+	+	Rods	+ve	-ve	+ve	-ve	-ve	-ve	Y	R
SJ37	41±8	+	-ve	Rods	+ve	-ve	-ve	+ve	-ve	-ve	Y	Y
SJ39	47±12	+	-ve	Cocci	+ve	-ve	+ve	+ve	-ve	+ve	Y	Y
SJ40	46±13	+	+	Rods	+ve	-ve	+ve	+ve	-ve	-ve	Y	Y
SJ41	38±7	+	+	Rods	+ve	+ve	+ve	-ve	-ve	-ve	Y	R
SU2	40±9	+	-ve	Rods	+ve	+ve	-ve	-ve	-ve	-ve	R	Y
U8	45±9	+	+	Rods	+ve	-ve	-ve	-ve	-ve	-ve	Y	R

http://www.aloki.hu ● ISSN 1589 1623 (Print) ● ISSN1785 0037 (Online)
DOI: http://dx.doi.org/10.15666/aeer/2001_079102

Table S2. *Antibiotic (at 20 µg/mL) resistance and heavy metal resistant profiles of the selected strains*

Code	Strain	Antibiotic resistance (Inhibition zones, mm)					Heavy metal resistance (µg/ml)					Order of metal resistance
		S	AM	TE	K	E	Zn^{+2}	Pb^{+2}	Co^{+2}	Mn^{+2}	Ni^{+2}	
F1	*Staphylococcus hominis*	17±1	30±2	27±2	18±2	11±2	1,000	40,000	1,000	10,000	5,000	Pb^{+2}>Mn^{+2}>Ni^{+2}> Co^{+2}, Zn^{+2}
F9	*Staphylococcus sp.*	15±2	25±2	27±4	14±2	19±2	700	20,000	800	8,000	1,000	Pb^{+2}>Mn^{+2}>Ni^{+2}>Co^{+2}>Zn^{+2}
SJ20	*Bacillus flexus*	23±2	27±4	32±3	20±3	7±5	500	15,000	500	5,000	2,000	Pb^{+2}>Mn^{+2}>Ni^{+2}>Co^{+2}, Zn^{+2}
SJ32	*Bacillus Oceanisediminis*	11±3	11±4	24±4	0	15±4	700	30,000	700	9,000	4,000	Pb^{+2}>Mn^{+2}>Ni^{+2}>Co^{+2}, Zn^{+2}

Note: S = streptomycin, AM = ampicillin, T = tetracycline, K = kanamycin, E = erythromycin, and C = chloramphenicol

http://www.aloki.hu ● ISSN 1589 1623 (Print) ● ISSN1785 0037 (Online)
DOI: http://dx.doi.org/10.15666/aeer/2001_079102

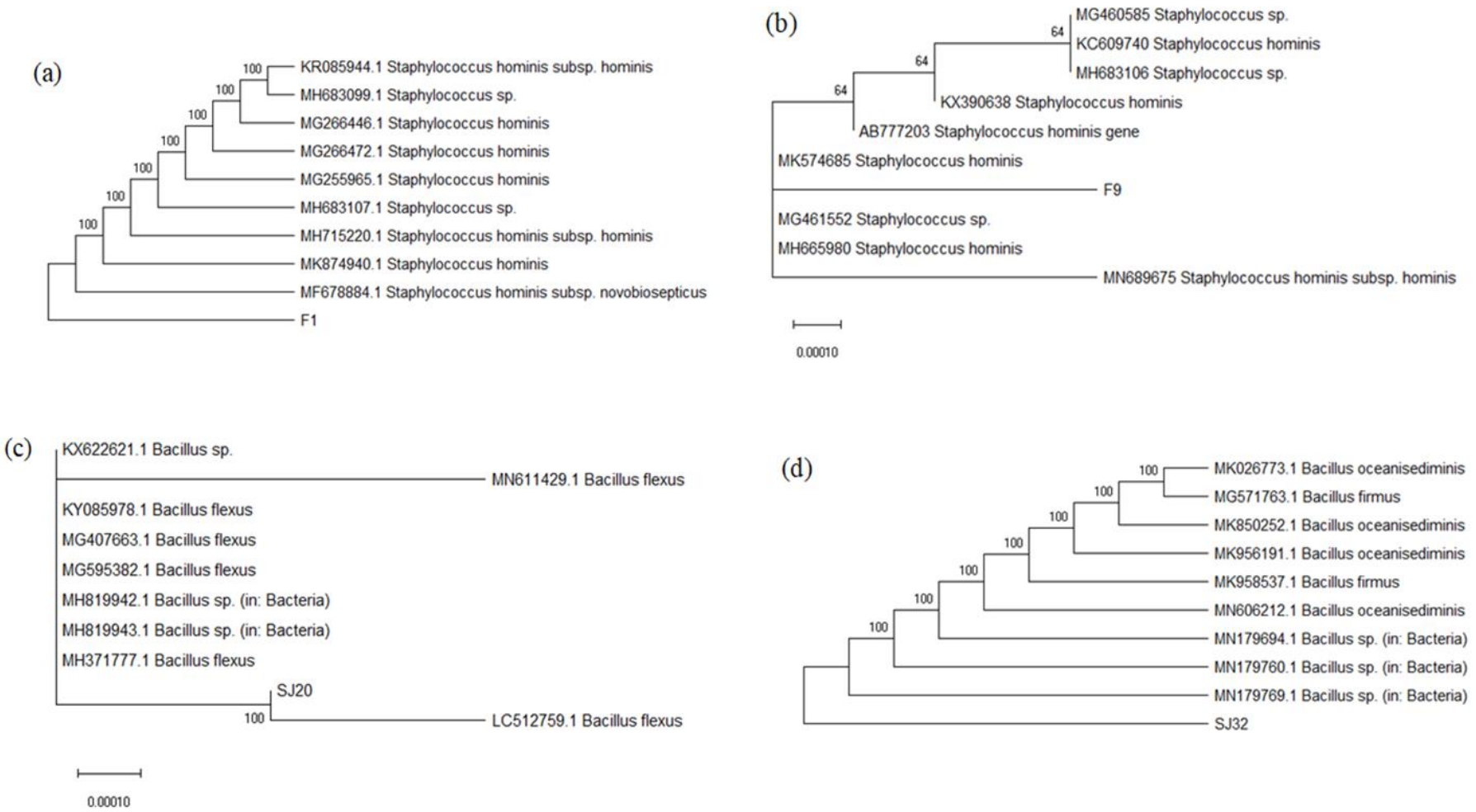

Figure S1. *Phylogenetic trees of selected bacterial strains of (a) F1, (b) F9, (c) SJ20, and (d) SJ32*

http://www.aloki.hu ● ISSN 1589 1623 (Print) ● ISSN1785 0037 (Online)
DOI: http://dx.doi.org/10.15666/aeer/2001_079102

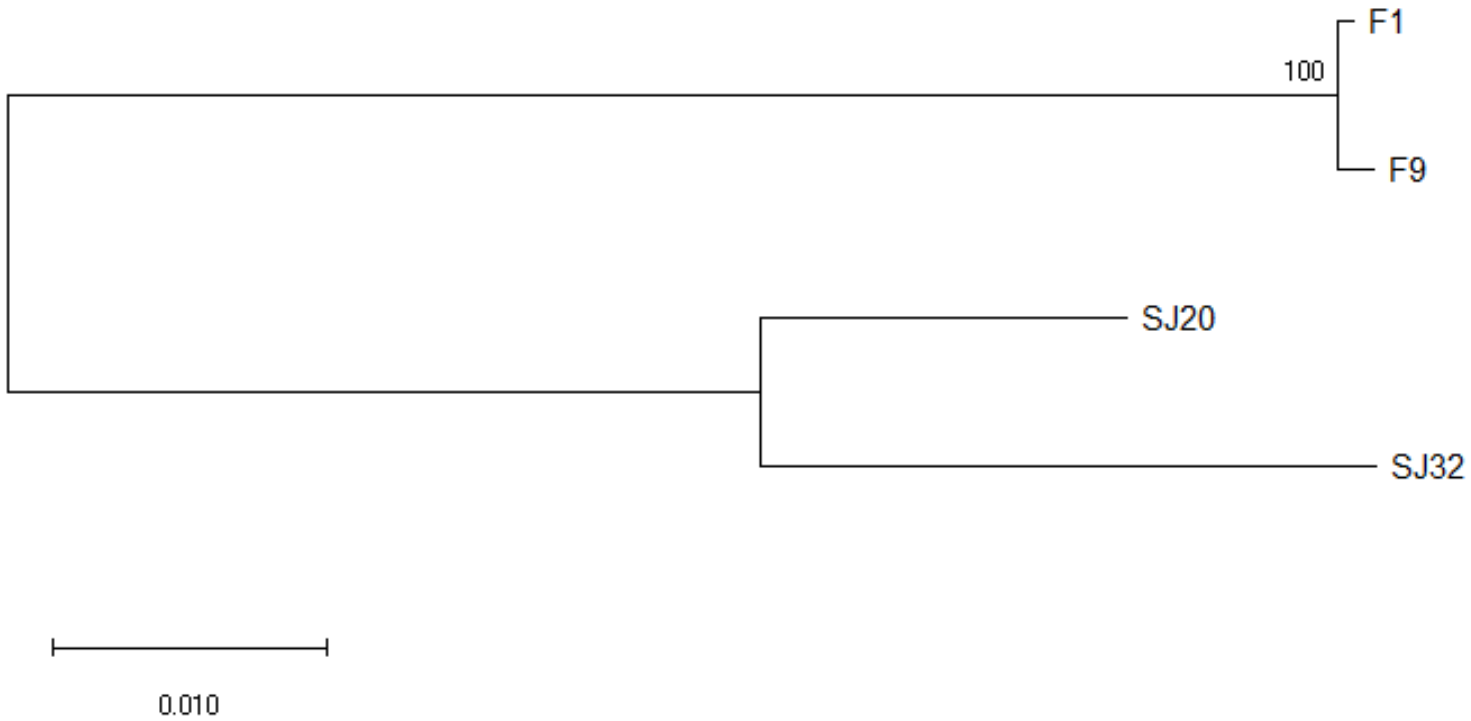

Figure S2. *16 Sr RNA sequencing of the selected strains*

http://www.aloki.hu ● ISSN 1589 1623 (Print) ● ISSN1785 0037 (Online)
DOI: http://dx.doi.org/10.15666/aeer/2001_079102

ENERGY BALANCE AND EVAPOTRANSPIRATION CHARACTERISTICS OF RUBBER TREE (*HEVEA BRASILIENSIS*) PLANTATIONS IN XISHUANGBANNA, SOUTHWEST OF CHINA

LING, Z.[1,2,3] – SHI, Z. T.[2*] – GU, S. X.[3,4] – PENG, H. Y.[5] – FENG, G. J.[1] – HUO, H.[1]

[1]*Kunming University, Kunming, 650214 Yunnan, China*

[2]*College of Tourism and Geographic Sciences, Yunnan Normal University, Kunming, 650500 Yunnan, China*

[3]*State Key Laboratory of Water Resources and Hydropower Engineering Science, Wuhan University, Wuhan, 430072 Hubei, China*

[4]*Yunnan Institute of Water & Hydropower Engineering Investigation, Design and Research, Kunming, 650021 Yunnan, China*

[5]*Institute of Land & Resources and Sustainable Development of Yunnan University of Finance and Economics, Kunming, 650221 Yunnan, China*

**Corresponding author*
e-mail: shizhengtao@163.com

(Received 17th May 2021; accepted 28th Oct 2021)

Abstract. Rubber tree (*Hevea brasiliensis*) is important economic agroforestry with high water demand during its growth. Evapotranspiration as the main component of water and energy balance in forest ecosystem which is a vital link between its ecological and hydrological processes. Therefore, it is of extreme significance to study the energy balance and evapotranspiration of rubber plantations for in-depth study of the regional water vapor cycle, scientific and efficient management of water resources. Based on the meteorological and energy data measured by the Bowen ratio system in 2016 at Xishuangbanna, the energy balance and evapotranspiration characteristics of rubber plantations were analyzed by Bowen ratio-energy balance. The result showed that: (1) The daily variations of net radiation (R_n), latent heat flux (LE), sensible heat flux (H) and soil heat flux (G) in rubber plantation were high value in rainy season and low in dry season; (2) The annual ET of the rubber plantation was 1035.91 mm, the average daily ET was 2.83 mm/d in 2016. The ET was about 114%-140% of precipitation in the dry season which indicated that ET of rubber plantation was mainly dependent on the volumetric soil water content (VWC); (3) The dominant environmental factors were R_n, vapour pressure deficit (VPD) and VWC which affect ET of rubber plantation.
Keywords: *tropical deciduous trees, Bowen ratio, Montane Southeast Asia, humid tropics, land-cover change, evapotranspiration*

Instruction

Evapotranspiration (ET) is a complex process involving soil, vegetation and atmosphere. It is one of the most important elements in the water cycle and energy balance of ecosystem and a key factor in the regional water balance as well. The ET of rubber plantation is also related to the water cycle and energy balance of its ecosystem.

In the past few decades, over 200,000 ha of rubber plantations have been established in Xishuangbanna (Ziegler et al., 2009; Mann, 2009). With the rising natural rubber prices, growing population and land management policies, the monoculture rubber plantations gradually replace natural forests and expand into "unsuitable areas" where

http://www.aloki.hu ● ISSN 1589 1623 (Print) ● ISSN 1785 0037 (Online)
DOI: http://dx.doi.org/10.15666/aeer/2001_103117

high altitudes in the mountain. Numerous potential negative ecological and environmental consequences of converting primary and secondary forests into rubber plantations have been suggested: reduce in biodiversity (Ling et al., 2020; Monkai et al., 2018; Ahrends et al., 2015); decrease of total biomass carbon; acceleration of erosion (Guillaume et al., 2016; Liu et al., 2015; Zhang et al., 2006) and excessive water consumption (Ma et al., 2019; Liu et al., 2013; Zou et al., 2020; Martius et al., 2004; Qiu, 2009; Xu et al., 2014; Liu et al., 2015). The local population seriously begins to face rare water shortages during the dry season (Li, 2016; Zhou et al., 2011; Qiu, 2009). The research on the ET characteristics of rubber plantation was attracted increasing attention (Tan et al., 2011; Giambelluca et al., 2016; Lin et al., 2018).

Our research is motivated by the concern that if rubber does maintain high annual ET rates as found by Tan et al. (2011) and as suggested by Guardiola-Claramonte et al. (2010). The replacement of native and other non-rubber vegetation by rubber in Xishuangbanna may have significant negative consequences for water resources in the region.

To enhance the understanding of the energy cycle and ET processes of rubber plantation in Xishuangbanna, we used the Bowen ratio-energy method to study the ET of the rubber plantation ecosystem based on field monitoring data. The objectives of this study were to:(1) analyzed the characteristics of the fluxes of the rubber plantation ecosystem at different time scales; (2) determined annual ET of rubber plantations at representative sites in Xishuangbannna, in order to compare ET of rubber plantations with natural forests which dominated land covers to assess whether rubber is exceptional in its water use traits; (3) discussed the roles of phenological and environmental controls on the annual cycle of ET and elucidate the mechanisms promoting high annual ET.

Materials and methods

Site description

Our study site was located in Bubeng Village (21°34′10″N, 101°35′24″E), Mengla County, Xishuangbanna, Southwest of China, as shown in *Figure 1*. The climate included dry season (November - April the next year) and wet season (May - October) which is strongly seasonal. While dry season can be divided into cool-dry season (November - February the next year) and hot-dry season (February - May) (Zhang, 1963). The multi-year (1970-2017) mean annual precipitation was 1599.5 mm, and approximately 85% of the rainfall occurs during the rainy season. The annual average sunshine hours 1853.4 h. The annual average temperature was 21.5 °C and the monthly values range from 18 to 22 °C. The main soil type of study area is mainly brick red loam.

The characteristics of the rubber plantation were shown in *Table 1*. The rubber plantation study site was transformed from the original tropical monsoon forest with a slope length of about 300 m. Rubber trees were planted 2-3 m in rows of mixed spacing between 4 - 6 m. Understory with a small amount of shrubs and weeds.

Table 1. *Characteristics of the plant structure and the study site*

Planting year	Location	Altitude (m)	Slope (°)	Plot area (m × m)	Diameter at breast height (cm)	Tree height (m)	Planting density (trees/ha)
1992	21°34′10″N 101°35′24″E	726	22	200×200	20 ± 2	11.58 ± 2.3	300 ± 50

http://www.aloki.hu ● ISSN 1589 1623 (Print) ● ISSN 1785 0037 (Online)
DOI: http://dx.doi.org/10.15666/aeer/2001_103117

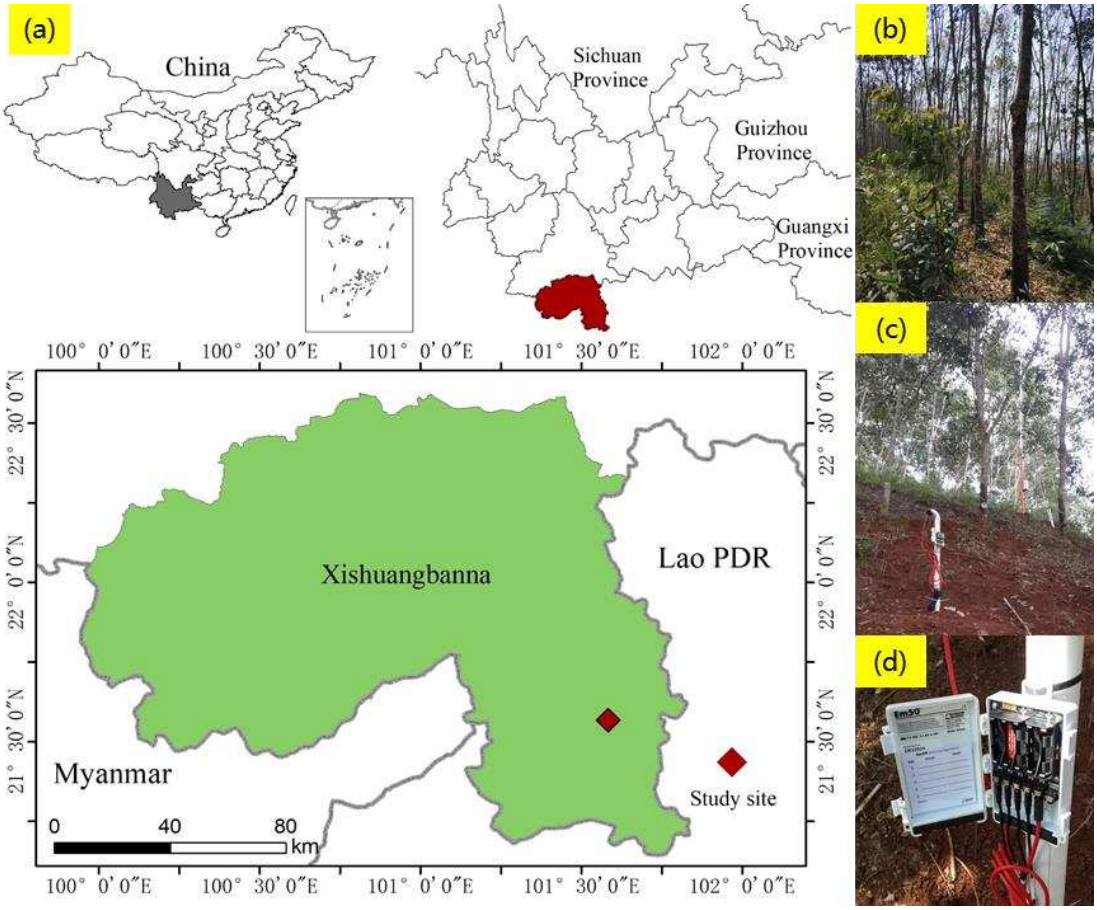

Figure 1. *The study site of Rubber Plantation (indicated by a solid square; 21°55'39"N; 101°15'55"E) in Xishuangbanna, Yunnan Province, Southwest China. (a) Location of area; (b) observed rubber plantation; (c) Bowenby system; (d) EM50 monitor sensor*

Methods

Meteorological measurements

Environmental variables including precipitation (Pe, mm), air temperature (Ta, °C) and net radiation (R_n, $MW \cdot m^{-2}$) were measured by sensors mounted on a 15-m-tall automatic weather station system sensor (WS-BR06, USA) that was established in Bubeng in 2016. The water vapour pressure deficit (VPD, hPa) was calculated from Ta and relative humidity (RH, %), which were monitored by air humidity sensor (SKH2060, Vaisala, Finland). Volumetric soil water content (VWC, %) was measured by a depth profile at each site using time domain reflectometers (ECH2O 5TE, Pullman, Washington, USA) at a depth of -10 cm, -20 cm, -30 cm, -40 cm. All meteorological data were collected using a data logger (CR1000, Campbell Sci., USA) every 30 min, as shown in *Table 2*.

Energy flux measurements

The canopy tower was 20 m tall were constructed at Bubeng village for micrometeorological and energy flux measurements. The latent heat flux (LE) and sensible heat flux (H) were measured using the Bowen ratio system. Wind speeds was

http://www.aloki.hu ● ISSN 1589 1623 (Print) ● ISSN 1785 0037 (Online)
DOI: http://dx.doi.org/10.15666/aeer/2001_103117

all sampled and stored at 10 Hz on a data logger. All variances and covariances required for the Bowen ratio flux estimates were computed over a 30-min averaging interval.

The ratio of mean annual LE + H to mean annual available energy (A), which was estimated as R_n - G, was 0.71 for the whole observation period. Whereas, LE + H accounted for only 58% and 65% in the wet and cool-dry seasons in Xishuangbanna influenced by fog drops. We used "Bowenby ratio closure" method for closing the canopy surface energy balance for each 30-min interval (Wilson., 2002; Twine et al., 2000).

In this study, the meteorological data and energy flux data were processed by coordinate correction, wild point rejection, data interpolation and data quality analysis to eliminate abnormal value of rubber plantation due to uncontrollable factors (Falge et al., 2001; Baldocchi et al., 2001; Liu et al., 2014).

Table 2. *Sensor parameters and installation of WS-BR06 automatic weather station system*

Sensor	Model	Installation height (m)	Unit	Observation interval/min
Data logger	CR1000	0.5		30
Wind speed and direction sensor	05103L	15	m/s	30
Heat flux plate	HFP01	15		30
Global radiation	Long wave radiation sensor	14.5	U mol/(sm^{-2})	30
Net solar radiation	CNR4	14.5	W m^{-2}	30
Tipping-bucket rain recorder	TE525MM	15	Mm	30
Air temperature sensor	SKH2060	14.5	℃	30
Air humidity sensor		14.5	%	30
Canopy temperature sensor		11	℃	30

Leaf area index measurements

The Leaf area index (LAI) was measured using plant canopy analyzer (LI-COR, Lincorn, USA) at irregular time intervals over the course of the study at an interval of 6 to 5 m at study site, along transects oriented diagonally with respect to tree rows.

Calculation of energy-balance

According to the principle of energy conservation (Tang et al.,1996; Maruyama et al., 2019; Li et al., 2021):

$$R_n = \lambda ET + H + G \quad \text{(Eq.1)}$$

where R_n is the net radiation, $W \cdot m^{-2}$; λET is the latent heat flux, $W \cdot m^{-2}$; λ is the latent heat of vaporization, J/kg, generally taken as 2.45 MJ/kg; ET is the evapotranspiration; H is the sensible heat flux, $W \cdot m^{-2}$; G is the soil heat flux, $W \cdot m^{-2}$.

According to the boundary diffusion theory, the diffusion of water vapor and heat on the evaporation surface can be described by the following equation:

$$\lambda ET = -\lambda_\rho K_w \left(\frac{0.622}{P} \right) \frac{\partial e}{\partial z} \quad \text{(Eq.2)}$$

http://www.aloki.hu ● ISSN 1589 1623 (Print) ● ISSN 1785 0037 (Online)
DOI: http://dx.doi.org/10.15666/aeer/2001_103117

$$H = -\rho C_p K_h \frac{\partial T}{\partial z} \quad \text{(Eq.3)}$$

where ρ is the air density, kg/m^3; P is the atmospheric pressure, kPa; C_p is the specific heat of air at constant pressure, J·kg^{-1} K^{-1}; K_w and K_h are the turbulent exchange coefficients for λ ET and H transport, respectively, m^2/s; $\partial e/\partial z$ is the water vapor pressure gradient, k Pa/m; and $\partial T/\partial z$ is the temperature gradient, °C /m.

If $K_w = K_h$ and quote the Bowen ratio β is the ratio of H to λET, we obtain:

$$\beta = \frac{H}{\lambda ET} = \frac{PC_p K_h}{0.622\lambda K_w} \bullet \frac{\Delta T}{\Delta e} = \gamma \frac{\Delta T}{\Delta e} \quad \text{(Eq.4)}$$

where ΔT is the temperature difference between the two heights (upper layer temperature - lower layer temperature), °C; Δe is the water vapor pressure difference between the two heights (upper layer humidity - lower layer humidity), k Pa; γ is the humidity counting coefficient, k Pa/°C, for:

$$\gamma = \frac{PC_p}{0.622\lambda} \quad \text{(Eq.5)}$$

Then, λET and H can be written as:

$$\lambda ET = \frac{R_n - G}{1+\beta} \quad \text{(Eq.6)}$$

$$H = \frac{\beta(R_n - G)}{1+\beta} \quad \text{(Eq.7)}$$

Results and discussion

Characteristics of dynamic variation of meteorological factors in rubber plantation

Xishuangbanna is influenced by the southwest monsoon where with more sunny weather and high temperature in March and April (the late hot-dry season) but with more cloudy rainy days in June. As shown in *Figure 2,* the annual rainfall was 1565.5 mm including 1241.5 mm in the rainy season in 2016. The average temperature of 22.1 °C. The VPD reached maximum value in April which about 1.48 kPa and minimum value about 0.36 kPa in December.

The monthly average R_n increased to the maximum value in April and May was 98.6 W·m^{-2}, and then started to decrease to minimum was 49.3 W·m^{-2} in December. The VWC of each soil layer remained high values were 0.37 to 0.22 cm^3/cm^3 in the rainy season and reduced with the depth of the soil layer increased. In dry season, the VWC decreased to the lowest value when it was consumed by rubber tree. The T_{asoil} was 17.3 °C which was lowest in January and February, and high from June to September average value up to 25.2 °C. The T_{asoil} in the 0-20 cm layer of the rubber plantation was more sensitive by environmental changes. The periodic defoliation of the

http://www.aloki.hu ● ISSN 1589 1623 (Print) ● ISSN 1785 0037 (Online)
DOI: http://dx.doi.org/10.15666/aeer/2001_103117

rubber plantation led to large fluctuations in LAI within the year. The LAI was 0.75 ± 0.072 m^2/m^2 in the dormant defoliation period from January to February up to 2.87 ± 0.11 m^2/m^2 in the first canopy leaf period. Then the mean LAI reached a maximum value was 4.26 ± 0.45 m^2/m^2 in the second canopy leaf period. The monthly average value of meteorological factors in rubber plantation as shown in *Table 3*.

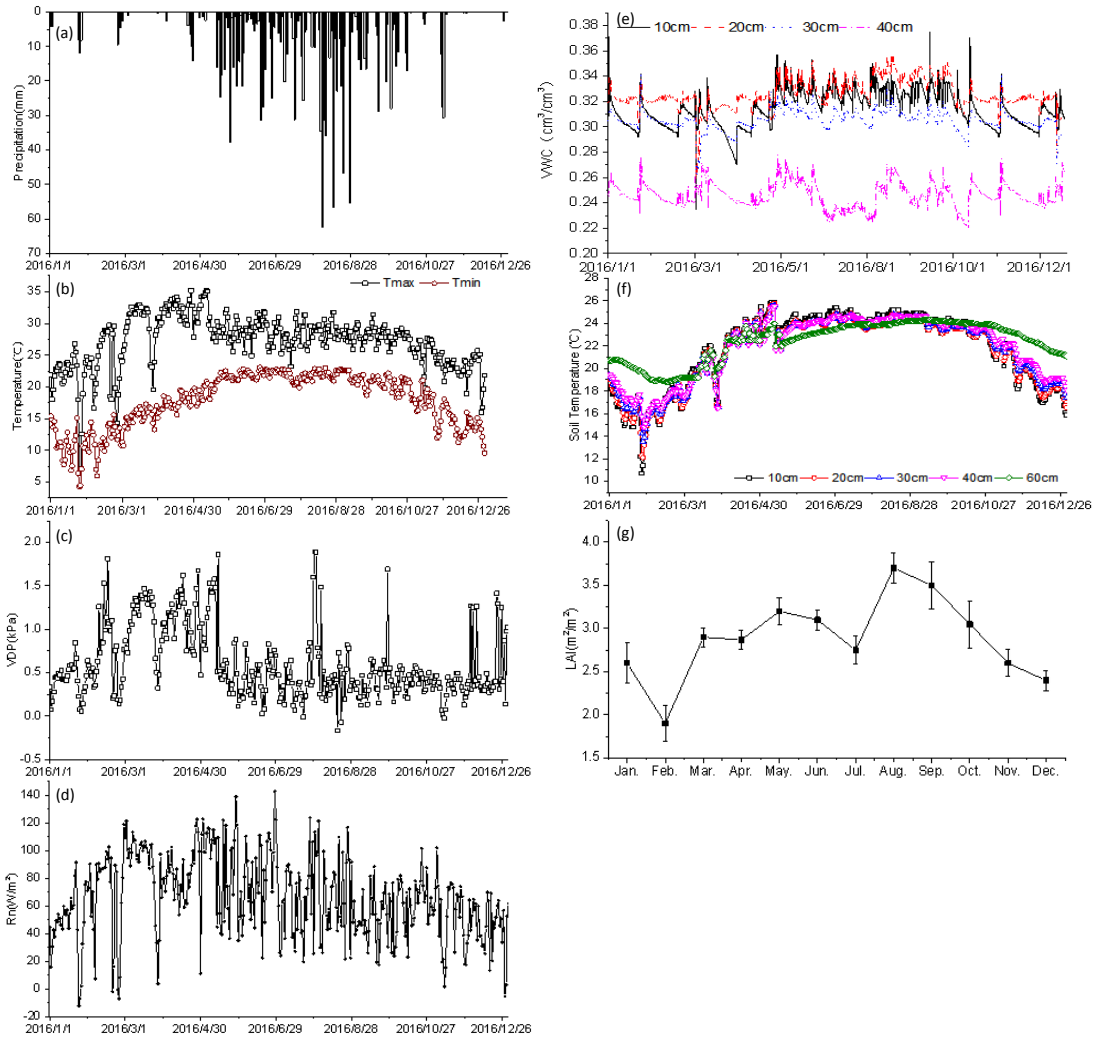

Figure 2. *Variation characteristics of meteorological factors in rubber plantation. (a) Rainfall outside the plantation; (b) the temperature; (c) saturated vapor pressure difference; (d) net radiation; (e) soil moisture content; (f) soil temperature; (g) leaf area index*

Table 3. *Monthly average value of meteorological factors in rubber plantation*

	Jan.	**Feb.**	**Mar.**	**Apr.**	**May**	**Jun.**	**Jul.**	**Aug.**	**Sep.**	**Oct.**	**Nov.**	**Dec.**
Pe (mm)	77.7	34.5	35.4	58.9	186.3	188.7	193.3	431.0	172.6	69.6	92.0	25.5
Tmax (℃)	21.1	23.5	29.6	32.1	30.6	29.1	27.9	28.9	28.3	27.8	24.9	22.7
Tmin (℃)	10.5	11.6	15.2	17.5	20.2	21.9	21.8	21.9	21.3	20.4	17.1	13.5
VDP (kPa)	0.41	0.70	1.09	1.14	0.81	0.45	0.48	0.44	0.44	0.41	0.32	0.59
Rn ($W \cdot m^{-2}$)	47.70	67.24	89.29	81.77	89.59	82.45	63.79	66.38	52.26	61.39	52.25	44.81
VWC (cm^3/cm^3)	0.297	0.293	0.289	0.290	0.301	0.305	0.300	0.308	0.306	0.296	0.295	0.292
Tsoil (℃)	17.34	17.39	19.60	22.78	23.64	24.03	24.21	24.39	24.12	23.62	21.63	19.26
LAI (m^2/m^2)	2.6±0.23	1.9±0.21	2.9±0.11	2.87±0.11	3.2±0.16	3.1±0.12	2.75±0.16	3.7±0.18	3.5±0.27	3.05±0.27	2.6±0.16	2.4±0.12

http://www.aloki.hu ● ISSN 1589 1623 (Print) ● ISSN 1785 0037 (Online)
DOI: http://dx.doi.org/10.15666/aeer/2001_103117

Rubber plantation energy flux distribution

Diurnal variation of evapotranspiration in rubber plantations

According to *Equation 1,* the daily variation in R_n, G, H and LE in the rubber plantation were all showing a 'single-peaked' curve. R_n is the driving factor of ET in forest ecosystem. The daily average changes of R_n in rubber plantation were shown in *Figure 3a*. The change of H (*Fig. 3b*) was most similar to R_n, but lagged behind R_n.

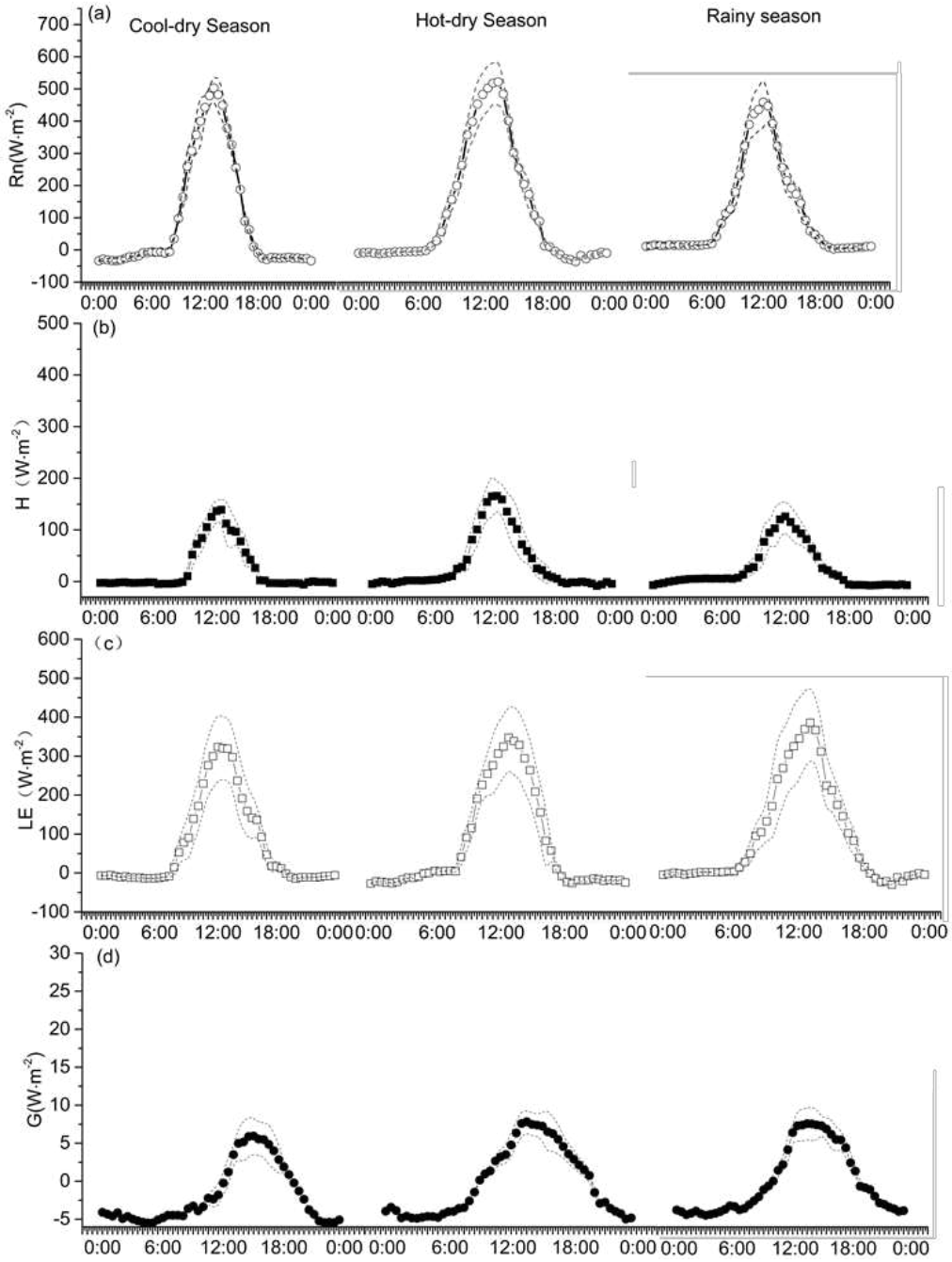

Figure 3. *Diurnal variations of ecosystem ET (represented by latent heat flux), sensible heat flux (H), net radiation (R_n), soil heat flux (G) in the cool-dry season, hot-dry season and rainy season. Solid circles are the means of all available 30-min data in each of the three seasons. Dash lines represent the standard deviation of the 30-minute data*

http://www.aloki.hu ● ISSN 1589 1623 (Print) ● ISSN 1785 0037 (Online)
DOI: http://dx.doi.org/10.15666/aeer/2001_103117

The intermittent of LE makes its changes rough but almost synchronous with the R_n. The LE appeared that in the rainy season was larger than the hot-dry and the cool-dry season which indicated the rubber plantation use much more energy for water vapor transport in the rainy season than in the dry season.

During the cool-dry season, LE of the rubber plantation reached a maximum value of 320.25 ± 80.04 $W \cdot m^{-2}$ (*Fig. 3c*) lagging about 1 h behind the R_n. The VPD (*Fig. 2c*) and Ta (*Fig. 2b*) increased faster in the hot-dry season because of clear weather. Substantially, the evapotranspiration increased while the rubber trees inter to leaf flushing period at this time. Then the LE rose up to 347.33 ± 80.79 $W \cdot m^{-2}$ (*Fig. 3c*).

The daily distribution of LE during the rainy season roughly increased with the R_n and H (*Fig. 3 a, c*). The maximum value of LE in the rainy season was 385.45 ± 93.32 $W \cdot m^{-2}$ which was much higher than the maximum value of H (*Fig. 3b*). There were large variations of LE (*Fig, 3c*) and R_n (*Fig. 3a*) (large standard deviations) which was reflected that the ET of the rubber plantation was affected by the variable weather conditions in the rainy season. Although the VPD (*Fig. 2c*) and Ta (*Fig. 2b*) increased rapidly and the ET also rose substantially in the hot-dry season, the maximum value of LE in rubber plantation was still lower than that in the rainy season (*Fig. 3c*). It was due to the reduced soil water moisture and the rose VPD of rubber plantation which produced some limitation on ET of rubber plantation in the dry season (Li, 2010).

G was little seasonal variation in the year. The change of G was similar to R_n but lag behind R_n. G showed less variation in the rainy season than dry season in rubber plantation. It means there were more energy for ET in the rainy season than dry season.

As shown in *Figure 4,* The Bowen ratio ranges from 0.48 to 0.63 in the rainy season (May to October) that the LE of rubber plantation was higher than H; The Bowen ratio ranged from 0.52 to 1.38 in all the dry season but its average was still less than 1. The high values of Bowen ratio appear in January and February that were 1.38 and 1.16, respectively. Because January and February in Xishuangbanna were dry period that the water vapor exchange between the rubber plantation and the atmosphere was reduced. The ET was minimized because of deficit soil moisture and rubber plantation defoliation.

Seasonal variation and annual total evapotranspiration of rubber plantation

We used Bowen ratio-energy balance to estimate the ET of rubber plantation at representative sites in Xishuangbannna. The annual ET was 1035.91 mm and the average daily ET was 2.83 mm/d. The ET of rubber plantation was maximum in rainy season and minimum in cool-dry season, as shown in *Figure 5*.

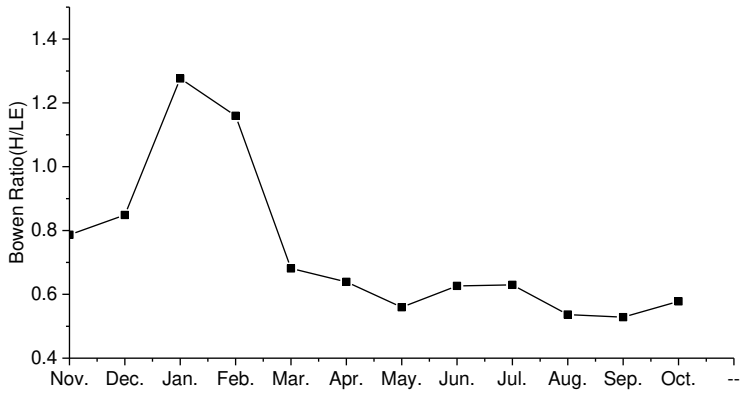

Figure 4. *Trend of monthly mean Bowen ratio of rubber forest ecosystem*

http://www.aloki.hu ● ISSN 1589 1623 (Print) ● ISSN 1785 0037 (Online)
DOI: http://dx.doi.org/10.15666/aeer/2001_103117

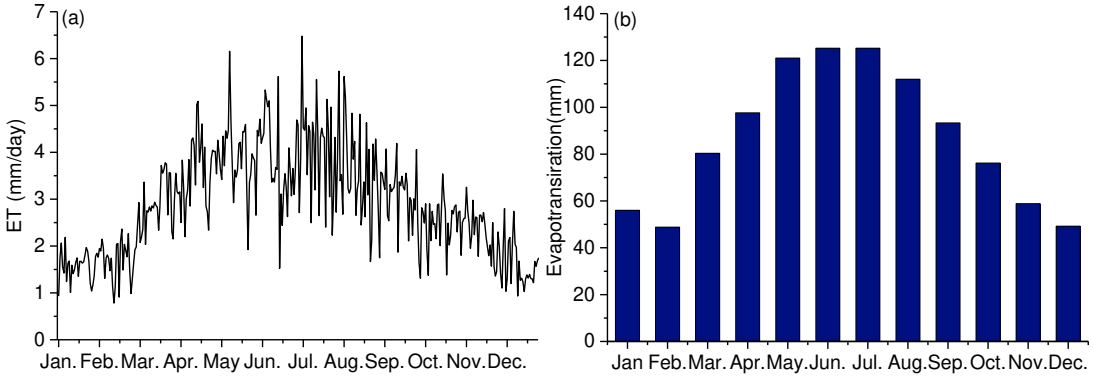

Figure 5. *The trend of daily mean (a) and monthly mean (b) of evapotranspiration ET in rubber plantation*

The ET of the rubber plantation decreased from November to January (early and middle of the cool-dry season) due to the reduced Ta; The Ta reached its minimum value of about 10 °C at the end of December and the beginning of February (*Fig. 2b*). Also, the VPD was very low during this period (*Fig. 2c*). The minimum ET value of rubber trees at the end of the cool-dry season in February when it started to drop leaves.

The Ta and the VPD increased at the begin of the hot-dry season in March which lead to the ET of rubber plantation rise; however, the surface soil water moisture decreased rapidly during this period. So the deeper soil water incontestable supported the increasing ET during the hot-dry season.

The LE has high values accompanied by large fluctuations (large standard deviation, as in *Fig. 3c*) which were mainly related to the extremely variable weather conditions during the rainy season from May to October. In our study, the maximum value of daily ET in rubber plantation was already over 6 mm day^{-1} in the rainy season.

As shown in *Table 4,* the ET was 630.19 mm in the rainy season, 211.67 mm in the cool-dry season, and 194.05 mm in the hot-dry season, accounting for 51%, 114%, and 140% of the seasonal rainfall, respectively.

Table 4. *Annual and seasonal amounts of rainfall and evapotranspiration in rubber plantation*

Year	**Cool-dry (Nov.- Feb.)**			**Hot-dry (Mar.-Apr.)**		
2016	P	ET	ET/P	P	ET	ET/P
	185.75	211.67	1.14	138.30	194.05	1.40
Year	**Rainy (May - Oct.)**			**Year**		
2016	P	ET	ET/P	P	ET	ET/P
	1241.55	630.19	0.51	1565.60	1035.91	0.66

The amount of fog drops entered the rubber plantation ecosystem can account for about 13% and 2.3% of the rainfall during the cool-dry and hot-dry seasons. The ET in cool-dry and hot-dry seasons would decreased significantly to 100.85% and 137.15%, if we added the retention of fog drops by the rubber plantation canopy in the rainfall water. It shown that fog precipitation plays a very important role in the ET of rubber

http://www.aloki.hu ● ISSN 1589 1623 (Print) ● ISSN 1785 0037 (Online)
DOI: http://dx.doi.org/10.15666/aeer/2001_103117

plantation in the dry season. However, the ET of rubber plantation in Xishuangbanna was still higher than the total precipitation (rainfall + fog precipitation). It can be seen that the recharge of subsurface soil water was another important supplement to the ET water in rubber plantations during the dry season when precipitation was insufficient (e.g., *Fig. 2e*) and the soil water content substantial and continuous decreased during the dry season.

From the changes of soil water content in rubber plantation (*Fig. 2e*), it can be seen that the large consumption of soil water by rubber plantation in the late dry season was one of the reason for the high annual ET. The rubber plantation in Xishuangbanna fell their leaves in February. While the LAI and ET increased rapidly until the beginning of the rainy season in May (*Fig. 2g*). As we known, the average ET of rubber plantation in April can reach about 85% of it was the rainy season (May to October). Although the dry season soil water content was the lowest, the rubber plantation still maintain a high ET in the late dry season. The rubber trees were able to access water which reserved in the deep soil (Kumagai et al., 2015). Therefore, soil water in Xishuangbanna played a very important role in the ET of rubber plantation in the dry season.

In all, the self-regulatory function of the rubber plantation ecosystem for water use was an important reason for its able to survive and develop well in Xishuangbanna where was less precipitation than its original area.

Effects of environmental factors on evapotranspiration in rubber plantation ecosystem

A linear regression of ET and environmental factors for each season in the year was conducted to analyze the key environmental factors affecting seasonal ET in rubber plantation. The equation was:

$$ET = -18.956 + 0.029R_n + 0.082T_{air} - 0.139VPD + 15.233VWC + 0.028T_{soil} + 0.086LAI \quad \text{(Eq.8)}$$

where ET is evapotranspiration, mm day^{-1}; R_n is net radiation, $W \cdot m^{-2}$; T_{air} is air temperature, °C; VPD is saturated water vapor pressure difference, kPa; VWC is soil water content, m^3/m^3; T_{soil} is soil temperature (20 cm), °C; LAI is leaf area index, m^2/m^2. $R^2 = 0.781$.

According to *Equation 8* the results showed that ET of rubber plantations in Xishuangbanna was mainly affected by R_n ($r = 0.697$, $p < 0.01$), VPD ($r = 0.664$, $p < 0.01$), VWC ($r = 0.616$, $p < 0.01$), T_{air} ($r = 0.549$, $p < 0.01$), T_{air} ($r = 0.549$, $p < 0.01$), LAI ($r = 0.534$, $p < 0.01$) and 20 cm soil temperature T_{soil} ($r = 0.388$, $p < 0.01$).

The results were consistent with Zhang (2016) and Giambelluca et al. (2016) that R_n, VPD and VWC were the dominant environmental factors which affect ET of rubber plantation in each season of year, as shown in *Table 5*. The R was not obvious in the cool-dry season because of the low ET of the rubber plantation and the influence of environmental factors on ET was greatly reduced.

Discussion

The daily change of R_n, G, H, and LE in rubber plantation were similar but with large differences between seasonal change. Energy was used for ET in the rainy season.

http://www.aloki.hu ● ISSN 1589 1623 (Print) ● ISSN 1785 0037 (Online)
DOI: http://dx.doi.org/10.15666/aeer/2001_103117

While the little difference between H and LE consumed in the dry season. There were consistent with the energy flux changes in Hainan rubber plantation studied by Zhang (2016) and similar to the energy flux changes in Xishuangbanna monsoon rainforest studied by Li (2010).

Table 5. *Stepwise regression analysis results of ET and different influencing factors in different seasons*

Season	Factors	R	Regression equation
Cool-dry season	Rn, VPD, VWC, T_{soil}	0.596	$ET=3.769+0.013R_n+0.18VPD-3.15VWC+0.056T_{soil}$
Hot-dry season	Rn, VPD, VWC, T_{soil}, LAI	0.644	$ET=-3.428+0.017R_n+0.4VPD+2.477VWC+0.009T_{soil}+0.62LAI$
Rainy season	Rn, Ta, VPD, VWC	0.743	$ET=-6.506+0.046R_n+0.231Ta+0.516VPD+0.007VWC$
Year	Rn, Ta, VPD, VWC, T_{soil}, LAI	0.781	$ET=-18.956+0.029R_n+0.082Ta-0.139VPD+15.233VWC+0.028T_{soil}+0.086LAI$

Compared with the ET of rubber plantations in Southeast Asia, as shown in *Table 6*. The annual of ET from rubber plantation in our study was 1035.91 mm monitored by Bowenby ratio system which with an average daily ET of 2.83 mm/d. There was little lower which compared to other study regions in Southeast Asia that because it mainly influenced by some factors such as precipitation and age of rubber trees (Lin et al., 2016, 2019). Nobuhiro et al. (2007) studied the ET of rubber plantation in Cambodia was similarly higher than that of evergreen forest by 28%. It indicated that ET of rubber plantation was generally higher than that of natural forest, as shown in *Table 6*.

Table 6. *Comparative study on evapotranspiration between rubber plantations and natural forests in different regions*

	Study area	Location	Annual precipitation (mm)	Annual net radiation (w/m^2)	ET (mm)	ET/P	
Rubber plantation	Xiushuangbanna, China	21°34′10″N, 101°35′24″E	1565.6	125.13	1108.7	0.71	Our study
	Xiushuangbanna, China	21°55′39″, 101°15′55″	1504	123.3	1125	0.75	Tan et al. (2011)
	Som Sanuk, Thailand	18°12'N, 103°25'E	2145	129.5	1211	0.56	Giambelluca et al. (2016)
	CRRI, Cambodia	11°57'N, 105°34'E	1439	151.0	1459	1.01	Giambelluca et al. (2016)
Tropical seasonal forest	Xishuangbanna, China	21°55′39″, 101°15′55″	1534	119.2	927	0.60	Tan et al. (2011)
	Kampong Thom, Cambodia	12°44′ N, 105°28′ E	1600	161.3	1140	0.71	Nobuhiro et al. (2007)
	Chiang Mai, Thailand	19.55 N, 99.5 E	1573	115.7	812	0.52	Tanaka et al. (2003), Igarashi et al. (2015b)
	Kog-Ma, Thailand	18.48 N, 98.54 E	1768		812	0.46	Tanaka et al. (2008)

As *Figure 2e,* the large consumption of soil water in the late hot-dry season was the important reason for the high annual ET of rubber plantation. The rubber plantation fell their leaves in February then quickly entered leaf flushing period in Xishuangbanna. The ET increased with the increasing LAI. Normally, the average ET of rubber

http://www.aloki.hu ● ISSN 1589 1623 (Print) ● ISSN 1785 0037 (Online)
DOI: http://dx.doi.org/10.15666/aeer/2001_103117

plantation in April can reach more than 85% of it was in the rainy season (May-October). Although the soil water content was near the minimum value in dry season, the ET of rubber plantation was high in the late dry season because it can access the water in the deep soil layer.

Guardiola-Claramonte et al. (2008) showed that the use of deep soil water increased after the rubber planation surface soil layer dried out in Xishuangbanna. Gonkhamdee et al. (2010) found that there were amount of fine roots of rubber plantations in deep soil (below 300 cm) in Baan Sila were active only during the dry season. Giambelluca et al. (2016) also suggested that rubber tree extracted more than half of the water from the deeper soil layers by the end of the dry season. In order to maintain a high ET, the distribution of rubber roots respond to the changing of soil water when the surface layer was dry in the late dry season.

Conclusion

The main reasons for the high annual total evapotranspiration of the rubber plantations were not only that it still used a large amount of water to make strong evapotranspiration during the whole rainy season, but also that the rubber plantations rapidly grew leaves and reached a higher LAI in the late cool-dry season after concentrated defoliation; secondly, the rubber plantations had developed roots to utilize the deep soil water reserve to maintain a high evapotranspiration even affected by the soil water content limitation in the late hot-dry season.

With the expansion of the area used to grow rubber plantations in the region, the relatively high ET rates of rubber should use deep soil moisture during the dry season to maintain physiological activity may result in reduced river flow and drier catchments throughout the region. In that case, rubber plantations are rapidly becoming the main emerging land cover in Xishuangbanna has affected or intensified the seasonal drought in the region. It could have impacts on water security.

In summary, we accurately estimate the ET of rubber plantation at typical site using Bowen ratio-energy method. We also analyzed the main environmental factors which affected the ET of rubber plantation at each season. The results provide important data support subsequent studies on ET of rubber plantations.

Acknowledgements. We thank researchers in State key laboratory of Water Resources and Hydropower Engineering Science, Wuhan University who provide suggestions on revision for us. The study financial supported by the Special Basic Cooperative Research Programs of Yunnan Provincial Undergraduate Universities Association (grant NO. 202001BA070001-243, 202001BA070001-130, 2018FH001-050, 2018FH001-104), Basic Research Project of Yunnan Province 202101AT070144 and YJL18018. And we would like to thank the editors for their constructive suggestions and comments.

REFERENCES

[1] Ahrends, A., Hollingsworth, P. M., Ziegler, A. D., Fox, J. M., Chen, H. F., Su, Y. F., Xu, J. C. (2015): Current trends of rubber plantation expansion may threaten biodiversity and livelihoods. – Global Environmental Change 34: 48-58. DOI: 10.1016/j.gloenvcha.2015.06.002.

[2] Baldocchi, D., Falge, E., Gu, L. H., Olson, R., Hollinger, D., Running, S., Anthoni, P., Bernhofer, C., Davis, K., Evans, R., Fuentes, J., Goldstein, A., Katul, G., Law, B., Lee,

http://www.aloki.hu ● ISSN 1589 1623 (Print) ● ISSN 1785 0037 (Online)
DOI: http://dx.doi.org/10.15666/aeer/2001_103117

X. H., Malhi, Y., Meyers, T., Munger, W., Oechel, W., Paw, K. T., Pilegaard, K., Schmid, H. P., Valentini, R., Verma, S., Vesala, T., Wilson, K., Wofsy, S. (2001): FLUXNET: a new tool to study the temporal and spatial variability of ecosystem–scale carbon dioxide, water vapor, and energy flux densities. – Bulletin of the American Meteorological Society 82(11): 2415-2434. DOI: 10.1175/1520-0477(2001)082.

[3] Falge, E., Baldocchi, D. D., Olson, R., Anthoni, Peter., Aubinet, M., Bernhofer, C., Burba, G., Ceulemans. R., Clement, R., Dolman, H., Granier, A., Gross, P., Grünwald, T., Hollinger, D., Jensen, N. O., Katul, G., Keronen, P., Kowalski, A., Lai, C., Ta., Law, B. E., Meyers, T., Moncrieff, J., Moors, Eddy., Munger, J. W., Pilegaard, K., Rannik, Ü., Rebmann, C., Suyker, A., Tenhunen, J., Tu, K., Verma, S., Vesala, T., Wilson, K., Wof, S. (2001): Gap filling strategies for defensible annual sums of net ecosystem exchange. – Agricultural & Forest Meteorology 107: 43-69. DOI: 10.1016/S0168-1923(00)00225-2.

[4] Giambelluca, T. W., Mudd, R. G., Liu, W., Ziegler, A. D., Kobayashi, N., Kumagai, T., Miyazawa, Y., Lim, T. K., Huang, M. Y., Fox, J., Yin, S., Mak, S. V., Kasemsap, P. (2016): Evapotranspiration of rubber (Hevea brasiliensis) cultivated at two plantation sites in Southeast Asia. – Water Resour. Res. 52: 1-20. DOI: 10.1002/2015WR017755.

[5] Gonkhamdee, S., Pierret, A., Maeght, J. L., Serra, V., Pannengpetch, K., Doussan, C., Pages, L. (2010): Effects of corn (Zea mays L.) on the local and overall root development of young rubber tree (Hevea brasiliensis Muel. Arg). – Plant and Soil 334(1-2): 335-351.

[6] Guardiola-Claramonte, M., Troch, P. A., Ziegler, A. D., Giambelluca, T. W., Vogler, J. B., Nullet, M. A. (2008): Local hydrologic effects of introducing non-native vegetation in a tropical catchment. – Ecohydrology 1: 13-22. DOI: 10.1002/eco.3.

[7] Guillaume, T., Holtkamp, A. M., Damris, M., Brummer, B., Kuzyakov, Y. (2016): Soil degradation in oil palm and rubber plantations under land resource scarcity. – Agriculture Ecosystems & Environment 232: 110-118. DOI: 10.1016/j.agee.2016.07.002.

[8] Igarashi, Y., Katul, G. G., Kumagai, T., Yoshifuji, N., Sato, T., Tanaka, N., Tanaka, K., Fujinami, H., Suzuki, M., Tantasirin, C. (2015): Separating physical and biological controls on long-term evapotranspiration fluctuations in a tropical deciduous forest subjected to monsoonal rainfall. – Journal of Geophysical Research: Biogeosciences 120(7): 1262-1278. DOI: 10.1002/2014JG002767.

[9] Kumagai, T., Mudd, R. G., Giambelluca, T. W., Kobayashi, N., Miyazawa, Y., Lim, T. K., Liu, W., Huang, M. Y., Fox, J. M., Ziegler, A. D., Yin, S., Mak, S. V., Kasemsap, P. (2015): How do rubber (Hevea brasiliensis) plantations behave under seasonal water stress in northeastern Thailand and central Cambodia. – Agric. For. Meteorol. 213: 10-22. DOI: 10.1016/j.agrformet.2015.06.011.

[10] Li, Z. H. (2010): Evapotranspiration and Its Simulation in a Tropical Seasonal Rain Forest in Xishuangbanna, Southwest China. – Xishuangbanna Tropical Botanic Garden, Xishuangbanna.

[11] Li, Y., Lan, G., Xia, Y. (2016): Rubber trees demonstrate a clear retranslocation under seasonal drought and cold stresses. – Frontiers in Plant Science 7: 1907-1910.

[12] Li, C. J., Hu, S. J., Zheng, B. W. (2021): Energy balance and evapotranspiration characteristics of pokeweed (Haloxylon ammodendron) communities in the southern margin of Gurbantunggut Desert. – Journal of Ecology 41(1).

[13] Lin, Y. X., Grace, J., Zhao, W., Dong, Y. X., Zhang, X., Zhou, L. G., Fei, X. H., Jin, Y. Q., Li, J., Nizami, S. M., Balasubramanian, D., Zhou, W. J., Liu, Y. T., Song, Q. H., Sha, L. Q., Zhang, Y. P. (2018): Water-use efficiency and its relationship with environmental and biological factors in a rubber plantation. – Journal of Hydrology 563: 273-282. DOI: 10.1016/j.jhydrol.2018.05.026.

[14] Lin, Y. X., Zhang, Y. P., Fei, X. H., Song, H. Q., Xu, K., Deng, Y., Liu, W. W., Chen, A. G., Li, P. G., Huang, H., Jin, Y. Q., Li, Jing. (2019): A comparative study of evapotranspiration characteristics of different forest ecosystems in Yunnan. – Journal of Yunnan University (Natural Science Edition) 41(01): 205-218.

http://www.aloki.hu ● ISSN 1589 1623 (Print) ● ISSN 1785 0037 (Online)
DOI: http://dx.doi.org/10.15666/aeer/2001_103117

[15] Ling, Z., Shi, Z. T., Dong, M. H., Yang, F., Su, B. (2020): Soil microbial community change during natural forest conversion to rubber plantations. – Applied Ecology and Environmental Research 18(3): 4371-4382. DOI: 10.15666/aeer/1803_43714382.
[16] Liu, X. N., Feng, Z. M., Jiang, L. G., Li, P., Liao, C. H., Yang, Y. Z., You, Z. (2013): Rubber plantation and its relationship with topographical factors in the border region of China, Laos and Myanmar. – Journal of Geographical Sciences 23(6): 1019-1040.
[17] Liu, Y. L., Jiang, H., Zhou, G. M., Chen, Y. F., Sun, C., Yang, S. (2014): Characteristics of water vapor flux changes in Anji moso bamboo forest and its relationship with environmental factors. – Journal of Ecology 34(17): 4900-4909.
[18] Liu, W. J., Luo, Q. P., Li, J. T., Wang, P. Y., Lu, H. J., Liu, W. Y., Li, H. M. (2015): The effects of conversion of tropical rainforest to rubber plantation on splash erosion in Xishuangbanna, SW China. – Hydrology Research 46(1): 168-174. DOI: 10.2166/nh.2013.109.
[19] Ma, X., Lacombe, G., Harrison, R., Xu, J. C., van Noordwijk, M. (2019): Expanding rubber plantations in southern China: evidence for hydrological impacts. – Water 11(4): 651. DOI: 10.3390/w11040651.
[20] Mann, C. C. (2009): Addicted to rubber. – Science 325(5940): 564-566. DOI: 10.1126/science.325_564.
[21] Martius, C., Höfer, H., Garcia, M. V. B., Römbke, J., Förster, B., Hanagarth, W. (2004): Microclimate in agroforestry systems in Central Amazonia: does canopy closure matter to soil organisms? – Agroforestry Systems 60(3): 291-304.
[22] Maruyama, T., Ito, K., Takimoto, H. (2019): Abnormal data rejection range in the Bowen ratio and inverse analysis methods for estimating evapotranspiration. – Agricultural and Forest Meteorology 269-270: 323-334. DOI: 10.1016/j.agrformet.2018.12.013.
[23] Monkai, J., Goldberg, S. D., Hyde, K. D., Harrison, R. D., Mortimer, P. E., Xu, J. C. (2018): Natural forests maintain a greater soil microbial diversity than that in rubber plantations in Southwest China. – Agriculture Ecosystems & Environment 265: 190-197. DOI: 10.1016/j.agee.2018.06.009.
[24] Nobuhiro, T., Shimizu, A., Kabeya, N., Tsuboyama, Y., Kubota, T., Abe, T., Araki, M., Tamai, K., Chann, S., Keth, N. (2007): Year-Round Observation of Evapotranspiration in an Evergreen Broadleaf Forest in Cambodia. – In: Sawada, H. et al. (eds.) Forest Environments in the Mekong River Basin. Springer, Tokyo. DOI: 10.1007/978-4-431-46503-4_7.
[25] Qiu, J. (2009): Where the rubber meets the garden. – Nature 457(7227): 246-247. DOI: 10.1038/457246a.
[26] Tan, Z. H., Zhang, Y. P., Song, Q. H., Liu, W. J., Deng, X. B., Tang, J. W., Deng, Y., Zhou, W. J., Yang, L. Y., Yu, G. R., Sun, X. M., Liang, N. S. (2011): Rubber plantations act as water pumps in tropical China. – Geophysical Research Letters 38(24): L24406. DOI: 10.1029/2011GL050006.
[27] Tanaka, K., Takizawa, H., Tanaka, N., Kosaka, I., Yoshifuji, N., Tantasirin, C., Piman, S., Suzuki, M., Tangtham, N. (2003): Transpiration peak over a hill evergreen forest in northern Thailand in the late dry season: assessing the seasonal changes in evapotranspiration using model. – Journal of Geophysical Research 108(D17): 4533. DOI: 10.1029/2002JD003028.
[28] Tanaka, N., Kume, T., Yoshifuji, N., Tanaka, K., Takizawa, H., Shiraki, K., Tantasirin, C., Tangtham, N., Suzuki, M. (2008): A review of evapotranspiration estimates from tropical forests in Thailand and adjacent regions. – Agricultural & Forest Meteorology 148(5): 807-819. DOI: 10.1016/j.agrformet.2008.01.011.
[29] Tang, S. Z., Cai, H. J. (1996): Agricultural Water Management. – China Agricultural Press, Beijing.
[30] Twine, T. E., Kustas, W. P., Norman, J. M. (2000): Correcting eddy-covariance flux underestimates over a grassland. – Agricultural and Forest Meteorology 103(3): 279-300.

http://www.aloki.hu ● ISSN 1589 1623 (Print) ● ISSN 1785 0037 (Online)
DOI: http://dx.doi.org/10.15666/aeer/2001_103117

[31] Wilson, K., Goldstein, A., Falge, E., Aubinet, M., Baldocchi, D., Berbigier, P., Bernhofer, C., Ceulemans, R., Dolman, H., Field, C., Grelle, A., Ibrom, A., Law, B. E., Kowalski, A., Meyers, T., Moncrieff, J., Monson, R., Oechel, W., Tenhunen, J., Valentini, R., Verma, S. (2002): Energy balance closure at FLUXNET sites. – Agricultural and Forest Meteorology 113(1-4): 223-243. DOI: 10.1016/S0168-1923(02)00109-0.

[32] Xu, J., Grumbine, R. E., Beckschaefer, P. (2014): Landscape transformation through the use of ecological and socioeconomic indicators in Xishuangbanna, Southwest China, Mekong Region. – Ecological Indicators 36: 749-756.

[33] Zhang, X. J. (2016): Study on the Evapotranspiration Characteristics of Rubber Forest Ecosystem in Western Hainan Island. – Hainan University, Haikou.

[34] Zhang, Y. P., He, Y. L., Yang, G. C. (2006): Mitigation effects of tropical seasonal rainforests and rubber forests on rainfall erosion forces in southern Yunnan. – Journal of Ecology (7): 731-737.

[35] Zhou, W., He, C. C., Wu, Z. L., Lu, C. (2011): Rubber cultivation and drinking water shortage: the case of Goniu village in Xishuangbanna. – Journal of Ecology 30(07): 1570-1574.

[36] Ziegler, A. D., Fox, J. M., Xu, J. (2009): The rubber juggernaut. – Science 324(5930): 1024-1025. DOI: 10.1126/science.1173833.

[37] Zou, X., Chen, C. F., Liu, W. J. (2020): Effects of rubber cultivation on soil aggregates and physicochemical properties in Xishuangbanna. – Soil Bulletin 51(03): 597-605.

http://www.aloki.hu ● ISSN 1589 1623 (Print) ● ISSN 1785 0037 (Online)
DOI: http://dx.doi.org/10.15666/aeer/2001_103117

ALLEVIATING THE DELETERIOUS EFFECTS OF SALT STRESS ON WHEAT (*TRITICUM AESTIVUM* L.) BY FOLIAR APPLICATION OF GIBBERELLIC ACID AND SALICYLIC ACID

IQBAL, M. S.[1*] – ZAHOOR, M.[1] – AKBAR, M.[1] – AHMAD, K. S.[2] – HUSSAIN, S. A.[1] – MUNIR, S.[1] – ALI, M. A.[1] – ARSHAD, N.[1] – MASOOD, H.[1] – ZAFAR, S.[1] – AHMAD, T.[1] – SHAHEEN, N.[1] – MASHOOQ, R.[1] – SAJJAD, H.[1] – SHAHBAZ, K.[1] – ARSHAD, H.[1] – FATIMA, N.[1] – ANSAR, B.[1] – ISLAM, M.[3]

[1]*Biodiversity Informatics, Genomics and Post-Harvest Biology Lab, Department of Botany, University of Gujrat, Gujrat, Pakistan*

[2]*Department of Botany, University of Poonch, Rawalakot, 12350 Azad Jammu and Kashmir, Pakistan*

[3]*Department of Biotechnology and Genetic Engineering, Hazara University, Mansehra, Pakistan*

[*]*Corresponding author*
e-mail: drsajjad.iqbal@uog.edu.pk; ORCID: https://orcid.org/0000-0002-7728-7922

(Received 31st May 2021; accepted 4th Sep 2021)

Abstract. Plant growth regulators gibberellic acid (GA_3) and salicylic acid (SA) were applied in the form of foliar spray to two varieties of wheat viz., Anaj-2017 and Ujala-2016 to alleviate the deleterious effects of soil salinity. Salt was applied at the concentration of 150mM after 2 weeks of seed germination. Ten treatments including control were used; T0 (control), T1 (150 mM NaCl), T2 (0.5 mM SA), T3 (1.0 mM SA), T4 (100 mg/L GA_3), T5 (150 mg/L GA_3), T6 (150 mM NaCl+0.5 mM SA), T7 (150 mM NaCl+1.0 mM SA), T8 (150 mM NaCl+100 mg/L GA_3), T9 (150 mM NaCl+150 mg/L GA_3). GA_3 and SA were applied after one week of salinity stress and repeated thrice. Morphophysiological, biochemical, and yield parameters were recorded. Findings revealed that both growth regulators promote the growth of plants treated with salt stress. Anthocyanin was promoted by 0.0035% at 100 mg/L GA_3 while glycine betaine was also enhanced by 0.26% in Ujala-2016 at 150 mg/L. It was noted that 1.0 mM salicylic acid and 150 mg/L gibberellic acid enhanced significantly various growth parameters. In conclusion, concentration of 0.1 mM SA and 150 mg/L GA_3 along variety Ujala-2016 recommended for the alleviation of salt stress with better growth and yield for future cultivation.
Keywords: *wheat, salinity, plant growth regulators, physiological, biochemical attributes*

Introduction

Wheat is an annual cereal crop cultivated throughout the world in temperate regions. It belongs to family Poaceae while 40% of the world population consumed it as staple food (Salim and Raza, 2020). It is the major source of calories (21%) and proteins due to it 4.5 billion people depend on it (Nawaz et al., 2013; Saddiq et al., 2021). It is predicted that production increase up to 2% annually till 2050 would be required to meet demands of rapidly growing population (Braun et al., 2010). Further, wheat is the major part of diet consumed regularly that have an impact nutritionally for public health. It has an ability to produce high yield and to tolerate a wide range of conditions. The most prominent factor is the ability of gluten protein of wheat to form viscoelastic dough, which is required particularly to bake leavened bread (Braun et al., 2010).

http://www.aloki.hu ● ISSN 1589 1623 (Print) ● ISSN1785 0037 (Online)
DOI: http://dx.doi.org/10.15666/aeer/2001_119134

Salinity stress is the major deleterious factor that limits crop germination, ultimately productivity. Most of the crop plants are vulnerable to salinity because of presence of higher quantity of salts in the soil (Dadshani et al., 2019). One-third of food production of the world is produced by approximately 20% of irrigated land that is under salt stress (Shrivastava and Kumar, 2015). The reactive oxygen species (ROS) under these stress conditions accumulated in leaves, resulted in oxidation of components of cells i.e. proteins, lipids, and chlorophyll. It can cause severe damages to plants, these undesirable ROS reacts with organic molecules triggering the peroxidation of membrane lipid, oxidation of proteins, inhibition of enzymes, RNA and DNA damage (Ahmad, 2010).

Plant growth regulators are organic substances which can hamper alternation in the cellular metabolism of plants. Environmental factors can badly affect the synthesis of plant growth regulators, in return disturbance in plant physiological processes, consequently, inhibit their growth potential. Use of such growth hormones in low concentration can control the growth and development of plants, either by inhibition or by promotion, and allow the physiological processes to take place at their usual rate. Usually these growth regulators or growth substances play their respective role in the control of plant growth and development, growing under stress or normal conditions (Hadia et al., 2020). Gibberellic acid (GA_3) is a growth regulator of plants; regulates various physiological responses that are most beneficial for better germination, photosynthetic activity, and growth of the plant (Sudharmaidevi et al., 2017; Rout et al., 2017). GA_3 stimulates the effective ion uptake in plants resulting in growth enhancement and maintaining the plant metabolism under both normal and stress conditions. The application of auxin also stimulates gibberellin synthesis. Further, GA_3 involved in mineral nutrition and nitrogen metabolism directly (Iqbal and Ashraf, 2013). Similarly, salicylic acid (SA) is the phenolic compound and an important endogenous growth hormone of plants. It plays great role in controlling different biochemical and physiological processes i.e. nitrogen metabolism, growth, flowering, and production of ethylene (Hayat et al., 2010). It has been found that salicylic acid is the main endogenous signal involved in defense responses of plants against environmental stresses including low temperature, pathogen infection, salinity, and ozone (Sawada et al., 2008). Moreover, treatment of SA is supplemented by a temporary increase in water level (Wahid et al., 2007). Considering this, an experiment was performed to find the efficacy of GA_3 and SA for better growth and yield by evaluating various morphophysiological, biochemical attributes, and antioxidant activities to suggest the most suitable variety for future cultivation under salinity hit areas.

Materials and methods

Experimental setup

A pot experiment was conducted at the experimental site of the Department of Botany, University of Gujrat, Gujrat, Pakistan during 2019-2020. During summer the climate of the area is hot and humid and cold in winter. Hottest months include May, June and July. Temperature may range during winter as drop to -2°C and maximum ranged from 40 to 50°C. basically the area is agriculture with plain and fertile land. Mild to warm weather can be observed with occasionally heavy rainfall occurs during winter from mid-November to March. The average annual rainfall is 1000 mm (Iqbal et al., 2021).

Two known wheat cultivars viz., Anaj-2017 and Ujala-2016 were selected but there was no report available against salinity tolerance. Seeds were purchased from Punjab

http://www.aloki.hu ● ISSN 1589 1623 (Print) ● ISSN1785 0037 (Online)
DOI: http://dx.doi.org/10.15666/aeer/2001_119134

Seed Corporation distribution shop from Gujrat city. The earthen pots were of 12-inch width ×11 inch tall. The experiment was arranged in a completely randomized design (CRD) with three replicates. Ten treatments were applied through foliar spray after 14 days of germination (*Table 1*). Data were recorded after 21 days of treatments for morphological and biochemical parameters like shoot length, root length, number of leaves, leaf area, chlorophyll contents, antioxidant activities, carbohydrates, and protein contents.

Table 1. *Detail of the treatments applied on two wheat cultivars with various combinations*

No.	Treatment composition
T0	Control
T1	150mM Sodium chloride (NaCl)
T2	0.5mM Salicylic acid (SA)
T3	1.0mM Salicylic acid (SA)
T4	100mg/L Gibberellic acid (GA3)
T5	150mg/L Gibberellic acid (GA3)
T6	150mM Sodium chloride+ 0.5mM Salicylic acid
T7	150mM Sodium chloride (NaCl) + 1.0mM Salicylic acid (SA)
T8	150mM Sodium chloride (NaCl) + 100mg/L Gibberellic acid (GA3)
T9	150mM sodium chloride (NaCl) +150mg/L Gibberellic acid (GA3)

Pots were filled with sand and then salt treatment was provided. Later, ten seeds were sown in every pot. Plants were covered with plastic sheets to prevent environmental impact and to maintain conditions uniform. Hoagland solution was applied to plants after the one-week interval to fulfill their nutritional needs. The concentration of 500ml Hoagland solution was applied to each pot.

Germination percentage, determination of growth and biomass

After one week of seed germination, the germination percentage was recorded by counting the number of seeds germinated in each pot. Five randomly healthy plants were selected for recording of the data. Roots and shoots were washed with water to clean the sand and weighted in grams (g) by using electric balance (Shimadzu Koyoto, Japan. Model: ELB600). Dry root and shoot biomass were recorded after oven drying at 65°C for three days. Likewise, fresh root and shoot length were recorded in centimeters (cm). The number of leaves and plant flag leaves were measured manually at vegetative stage (*Fig. 1*). Leaf area was measured by following formula; Length × Breadth × 0.75, where 0.75 was the correction factor.

Gas exchange parameters

Gas exchange parameters such as the rate of photosynthesis, CO_2 concentration in the cell, rate of transpiration, degree of stomatal opening, and water use efficiency were measured by using an infrared gas analyzer (IRGA) (Serial No: 32641, Model: LCi Console (ADC) Bioscientific Ltd was used). The estimation was carried out during the time 9:00-11:00 A.M under conditions of saturating light intensity, air relative humidity, leaf temperature, and CO_2 concentration.

http://www.aloki.hu ● ISSN 1589 1623 (Print) ● ISSN1785 0037 (Online)
DOI: http://dx.doi.org/10.15666/aeer/2001_119134

Anaj-2017 **Ujala-2016**

Figure 1. *Pot evaluation of both wheat varieties Anaj-2017 and Ujala-2016*

Estimation of photosynthetic pigments

Photosynthetic pigments were measured by following the method of Arnon (1949). Fresh leaves were collected from various treatments. Leaf sample (0.5 g) obtained from one replication was crushed in 4 ml of 80 % acetone. The samples were then filtered and the final volume rose to 10 ml by adding acetone. The supernatant was recovered by vortex and then the absorbance was taken by using Hitachi Spectrophotometer (Hitachi, Model U2001, Tokyo, Japan). Absorbance was measured at 3 wavelengths for chlorophyll a, b, c and carotenoids by the following formula:

Chlorophyll 'a' (mg/g fwt) = [12.7(OD 663) – 2.69 (OD 645)] × V/ 1000 × W

Chlorophyll 'b' (mg/g fwt) = [22.9 (OD645 – 4.68(OD 663) × V/1000 × W

Carotenoids (mg/g fwt) = [7.6(OD 480) – 1.49(OD 510)] × V/1000 × W

W = Fresh leaves weight in grams (g), V = Volume of extract of leaves in milliliter (ml)

Determination of glycine betaine and malondialdehyde (MDA)

Glycine betaine concentration was estimated in flag leaves (Grieve and Grattan, 1983). Leaves (0.5 g) were grinded in 5 ml water toluene solution. After that, the extract was transferred to a test tube and shakes for 24 hours at room temperature through shaker. Sample solution was then filtered. Potassium iodide 0.1 ml and 1 ml of the HCl solution were added into 0.5 ml filtrate and shake for 90 minutes in an ice bath. Followed by addition of super cool H_2O (2 ml). 1, 2-dichloromethane in the quantity of 10 ml was added and kept at room temperature for 2 hrs. Two prominent layers were established. The top layer was removed and discarded and the lower layer was used to measure the absorbance at 360 nm by using a spectrophotometer (PG Instruments LTD, UK. Model: T80 UV/VIS Spectrophotometer UV3000).

Malondialdehyde contents were measured by following Cakmak and Horst (1991). One gram of fresh leaves was crushed in 1% trichloroacetic acid (TCA) at 4 °C. The mixture obtained was then centrifuged at 2000 rpm for 15 minutes. Supernatant was

http://www.aloki.hu ● ISSN 1589 1623 (Print) ● ISSN1785 0037 (Online)
DOI: http://dx.doi.org/10.15666/aeer/2001_119134

recovered and TCA and TBA in the quantity of 3 mL were then added (0.5 by 20%). To prevent the reaction, the samples were kept in a water bath for about 90 minutes at 95 °C. Sample absorbance was measured at 532 nm and 600 nm by using the following formula;

Malondialdehyde (MDA) level = (A532 nm – A 600nm) / 1.56 × 105

Antioxidant enzyme assay

For determining the antioxidant potential, 0.5 g fresh leaves representing each treatment were grinded by the addition of 5ml phosphate buffer (cooled) and placed in an ice bath. Samples were centrifuged at 15000 rpm for 20 minutes at 4 °C. The supernatant was removed and used to study catalase and peroxidase dismutase activity (Chance and Meahly, 1995). For measuring the activity of CAT, solution was prepared with the final volume of 3 ml. In the reaction mixture, 50 mM phosphate buffer solution at neutral pH was added, 5.9 mM H_2O_2, and prepared enzyme extract in the quantity of 0.1 ml. The reaction started with the addition of enzyme extract. For measuring CAT activity, spectrophotometer was set on 240 nm and the change in absorbance was noted after every 20 seconds. For measuring of one-unit CAT activity change in absorbance 0.01 units/mint was considered.

To determine the POD activity, 3 ml solution was prepared that contained final volume. The solution was consisted of 50 mM phosphate buffer, 40 mM water, and 20 mM guaiacol. Enzyme extract of 0.1 mL was added to the solution simultaneously. POD was measured by spectrophotometer at the wavelength of 470 nm wavelength, absorbance change was observed after every 20 sec. Absorbance change 0.01 units/mint was observed to calculate the 1 unit of POD activity.

The superoxide dismutase activity was measured by following Giannopolitis and Ries (1977). Plant leaves (0.5 g) were crushed with 5 ml of phosphate buffer. An extraction sample in the quantity of 3 ml was transferred to the falcon tube. Then 50 µm of Nitro blue tetra-zolium (NBT) was added. Additionally, 13 µm of riboflavin, extract 20-50 ml of enzyme extract, 75 mM EDTA, 13 mM methionine, and phosphate buffer (pH 7.8) were added to the sample. After that, the samples were kept under the fluorescent lamp for about 15 minutes. Absorbance was measured using the spectrophotometer at 560 nm.

Estimation of protein and carbohydrates

To estimate the protein content 0.5 gram fresh leaves were crushed by adding 10 ml of 50 mM potassium phosphate buffer with 7.8 pH. Samples were then centrifuged at 10,000 rpm for 15 min at 4 °C (Bradford, 1996). Supernatant 0.1 ml was mixed with 2 ml of Bradford reagent. Protein content was determined at 590 nm absorbance by using a spectrophotometer.

For the preparation of plant extract (0.5 g), fresh leaves were crushed with 80% ethanol. After that, 10 ml water was added to the sample. For different sample concentrations, the final volume raised to 1 ml. Then H_2SO_4 (90% concentrated) was added in the quantity of 5 ml. Mixture shaking and incubation performed at a temperature of 30 °C for 40 mints. After incubation 1 ml of 5% solution of phenol was added to each test tube. Absorbance was measured at 490 nm by using a spectrophotometer.

Determination of anthocyanin and electrolyte leakage

Leaves 0.2 g was crushed with methanol and HCl at 99:1 ratio (methanol 9 ml: HCl 1 ml). This extract was then centrifuged at 18,000 rpm for 30 minutes at 4 °C. The

http://www.aloki.hu ● ISSN 1589 1623 (Print) ● ISSN1785 0037 (Online)
DOI: http://dx.doi.org/10.15666/aeer/2001_119134

supernatant was then separated and incubated at 4 °C for 24 hours in dark. Readings at two wavelengths viz., 530 nm and OD 657nm were recorded. The following formula was used to calculate the anthocyanin content (Krizek et al., 1993);

Content of Anthocyanin = [OD530-0.25 OD657] ×TV / [dry wt. ×1000]

OD = represents the optical density, TV = total extract volume (ml), Dry wt. = weight of the dry leave tissue.

For the determination of electrolyte leakage, the method of Lutts et al. (1995) was followed. Fresh flag leaves were taken from the plants. Leaves were washed with water and divided into different pieces through a blade or scissor. In Falcon tubes 50 ml double distilled water was added and leaves were dipped in the water. Then, tubes were incubated for 24 hours. After 24 hours EC was measured with the help of an electrolyte leakage meter. The value was named EC_1. Now the sample was autoclaved for 20 minutes at 121 °C and again electrolyte leakage was measured. This value was named EC_2. The final value was calculated with the help of the following formula; Electrolyte Leakage $=EC_1/EC_2 \times 100$.

Yield parameter determination

At physiological maturity following yield parameters were recorded on per plant basis (number of spikes, number of grains, spikelets per plant, and 100 grain weight).

Statistical analysis

Statistical analysis was performed by using Minitab software for determining significant and non-significant values through analysis of variance (ANOVA). For comparing mean values Tuckey's HSD (honestly significant difference) test was used along P values < 0.05 to differentiate one parameter from another by applying different alphabets. Different alphabets showed that this treatment is more significant than other treatment/s as compared to same alphabets on the other treatments.

Results

Germination percentage, growth and biomass of plants

The effect of the plant growth regulators on the germination percentage of wheat was found highly significant ($P \leq 0.001$) (*Fig. 2 A-J*), which showed the exogenous application of 1.0 mM of salicylic acid (SA) and 150 mg/L of gibberellic acid (GA_3) positively influenced the 90% germination percentage in Ujala-2016. Highly significant effects of GA_3 were found on root and shoot length, as well as fresh and dry weight of root and shoot. The fresh and dry weight of root and shoot decreased significantly at 150 mM NaCl stress and increased by the application of GA_3 and SA. The length of the root increased 22 cm by the application of 1.0 mM (SA). The fresh weight of plant root was also increased by 4.53 g in Ujala-2016 by the treatment of 150 mg/L GA_3 while dry root weight was increased 2 g in Ujala-2016 with the application of (150 mM NaCl + 150 mg/L GA_3). The highest number of leaves (30%) and leaf area were observed at a concentration of 150 mg/L GA_3 and 1. 0 mM SA (*Fig. 2 A-J*).

http://www.aloki.hu ● ISSN 1589 1623 (Print) ● ISSN1785 0037 (Online)
DOI: http://dx.doi.org/10.15666/aeer/2001_119134

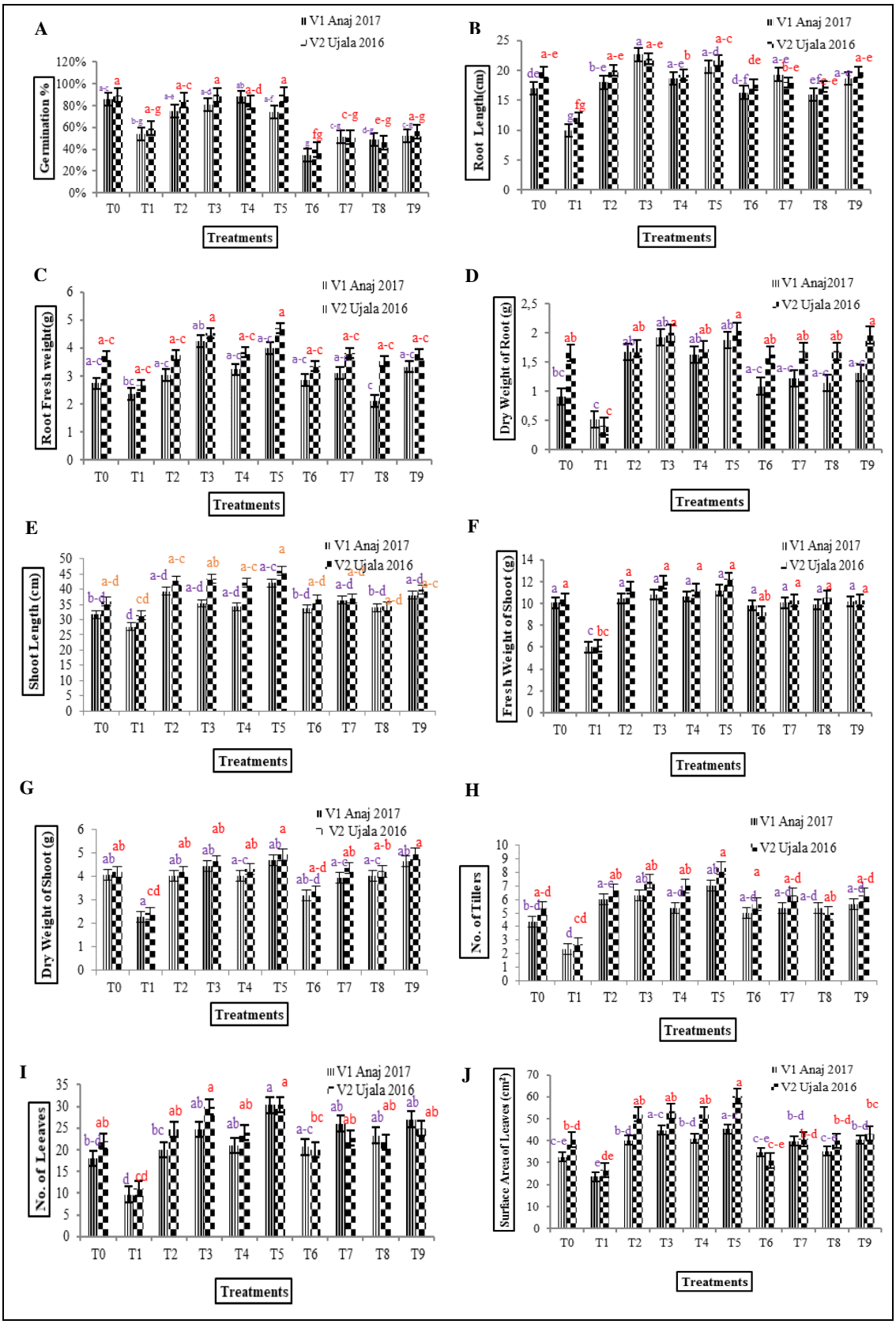

Figure 2. *(A-J): Effect of GA_3 and SA on germination, growth, and biomass production of wheat (Triticum aestivum L.) under NaCl stress (at 150 mM NaCl) and without stress. Values are the means of three replicates*

http://www.aloki.hu ● ISSN 1589 1623 (Print) ● ISSN1785 0037 (Online)
DOI: http://dx.doi.org/10.15666/aeer/2001_119134

Gas exchange attributes

Photosynthesis is a significant character of the plant that is reduced considerably under NaCl stress. *Fig. 3 K-O* indicates a substantial decline in the photosynthetic rate of wheat that was 15.9 (µmol CO_2 $m^{-2}s^{-1}$); however, a prominent increase was noticed after the treatment of GA_3 and SA. The photosynthetic rate of wheat was increased by 30.4 (µmol CO_2 $m^{-2}s^{-1}$) by the application of (150 mM NaCl + 150mg/L GA_3) in Ujala-2016. The response of variety was non-significant. The response of varieties on the rate of transpiration of plants was significant, as well as the hormonal response was highly significant ($P \leq 0.001$). Foliar application of gibberellic acid and salicylic acid increases the transpiration rate 1.5 (mmol H_2O m^{-2} s^{-1}) and intercellular CO_2 concentration 206 (µmol CO_2 mol^{-1}) after the treatment of 100 mg/L GA_3 concentration in Ujala-2016. The varieties and hormonal response on the conductance of stomata were non-significant. Results indicate that the stomatal conductance was highest 0.2 (mol H_2O m^{-2} s^{-1}) at 150 mg/L GA_3 in Ujala-2016. The hormonal response was highly significant on the water use efficiency of wheat while the response of variety was non-significant. Water use efficiency was highest at concentration of 150 mM NaCl+ 100mg/L GA_3.

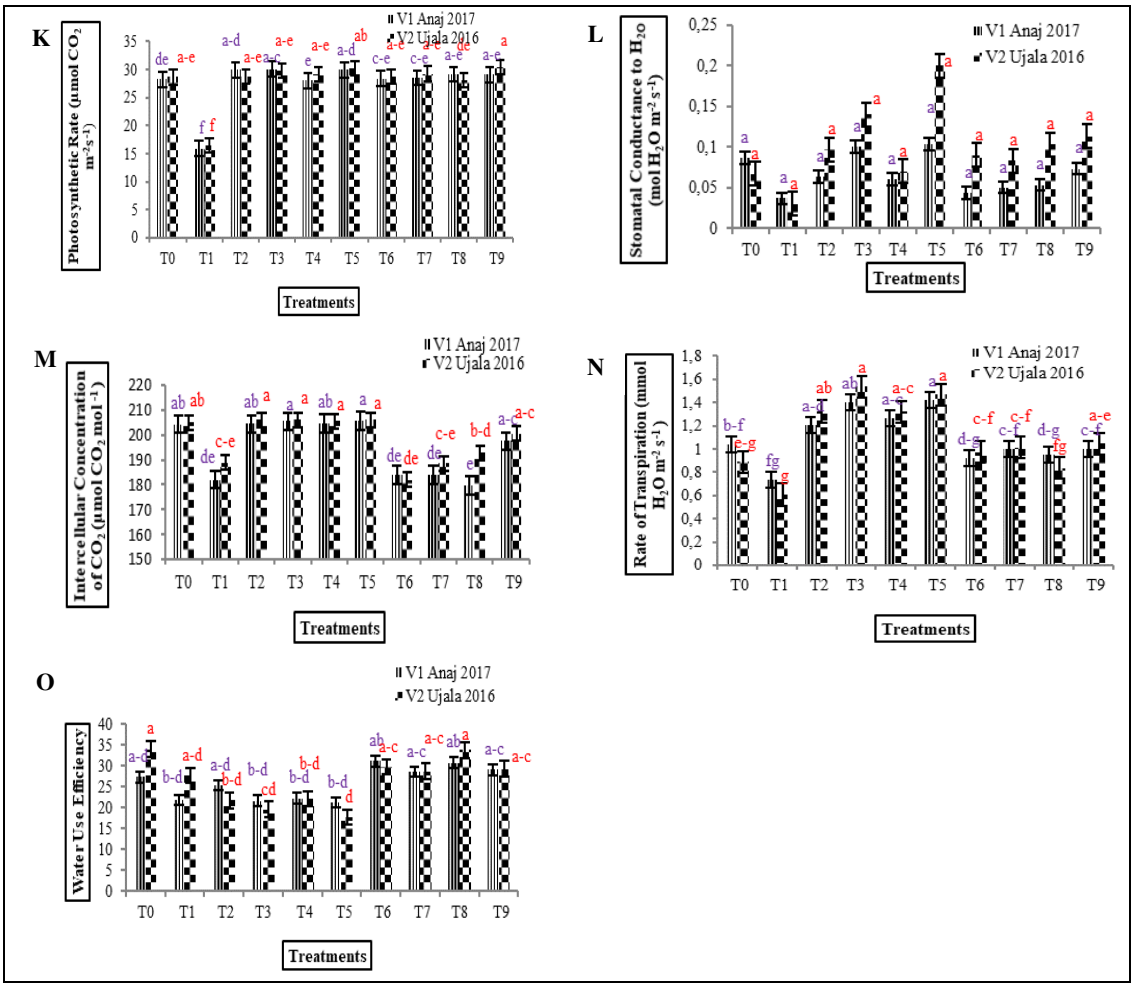

Figure 3. *(K-O): Effect of GA_3 and SA on gas exchange parameters (photosynthetic rate, stomatal conductance, transpiration rate, intercellular CO_2 concentration and water use efficiency) of wheat (Triticum aestivum L.) under NaCl stress (at 150mM NaCl) and without stress. Values are the means of three replicates ± standard error (SE)*

http://www.aloki.hu ● ISSN 1589 1623 (Print) ● ISSN1785 0037 (Online)
DOI: http://dx.doi.org/10.15666/aeer/2001_119134

Photosynthetic pigments

All photosynthetic pigments including; chlorophyll a, b, total chlorophyll, and carotenoids content were enhanced through the application of SA and GA_3. Highly significant ($P \leq 0.001$) effect of GA_3 and SA was noted on chlorophyll a. Content of chlorophyll b was highest 0.058 (mg/g fwt) at 1.0 mM SA concentration (*Fig. 4 P-R*).

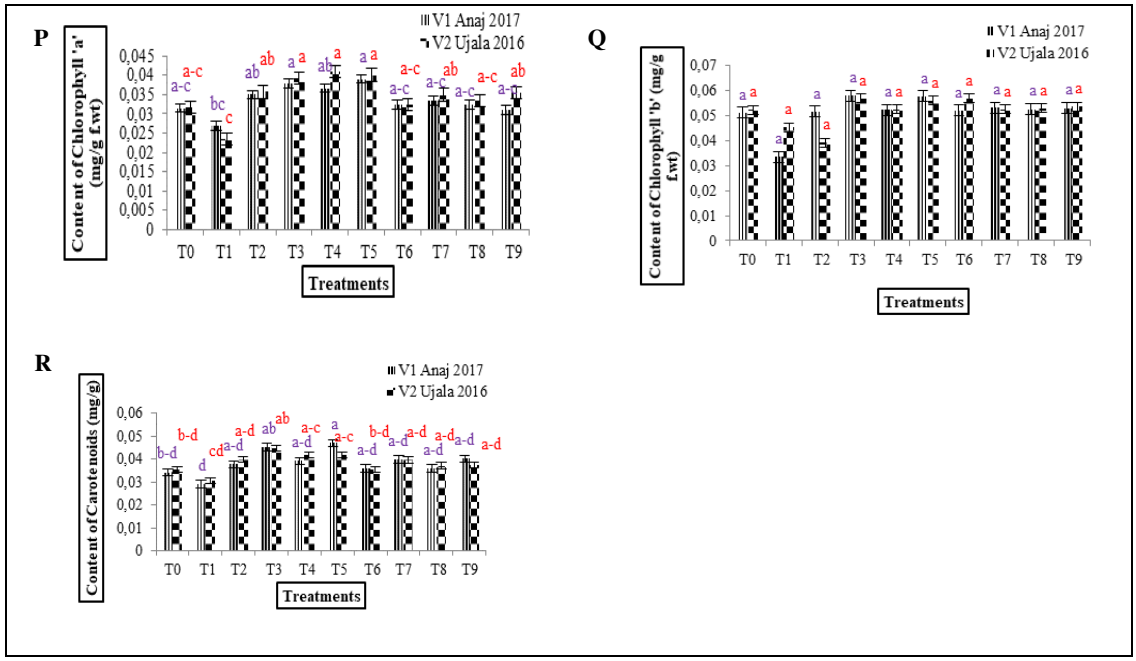

Figure 4. *(P-R): Effect of gibberellic acid GA_3 and SA on photosynthetic pigments (Chlorophyll a, chlorophyll b, and carotenoids) of wheat (Triticum aestivum L.) under NaCl stress (at 150 mM NaCl) and without stress. Values represent the means of three replicates ± standard error (SE)*

Glycine betaine, MDA, carbohydrates, protein, and electrolyte leakage

Highly significant ($P \leq 0.001$) response of SA and GA_3 was observed on all these parameters (*Fig. 5 S-X*). Glycine betaine content was highest 0.3 (µmol/g dry wt.) at 100 mg/L GA_3 and 150 mg/L GA_3 concentration among all treatments. By accumulation of NaCl into plant roots the value of MDA content become higher. On the basis of comparison in both varieties, content of Malondialdehyde was greater in Ujala-2016 than Anaj-2017 due to the accumulation of salt stress. Whereas use of both GA_3 and SA by foliar means demonstrated the positive outcome and reduced the level of Malondialdehyde content. The effect of both GA_3 and SA MDA content was highly significant. Likewise, carbohydrate content was also found highly significant. Plant growth and development is dependent on carbohydrates but under salinity stress it becomes hampered. Although both of the varieties showed reduction in carbohydrate content but Ujala-2016 suffered more as compared to Anaj-2017.

Normal healthy plants have large amount of proteins but under abiotic stress this quantity may suffer and reduction of soluble proteins occur. It was evident from current experiment that NaCl stress was the major cause of depletion of soluble proteins within wheat varieties. The interaction between hormones and varieties were non-significant. On

http://www.aloki.hu ● ISSN 1589 1623 (Print) ● ISSN1785 0037 (Online)
DOI: http://dx.doi.org/10.15666/aeer/2001_119134

the other hand, application of SA and GA_3 proved beneficial in order to enhance the content of total soluble protein in both NaCl affected and non-affected plants.

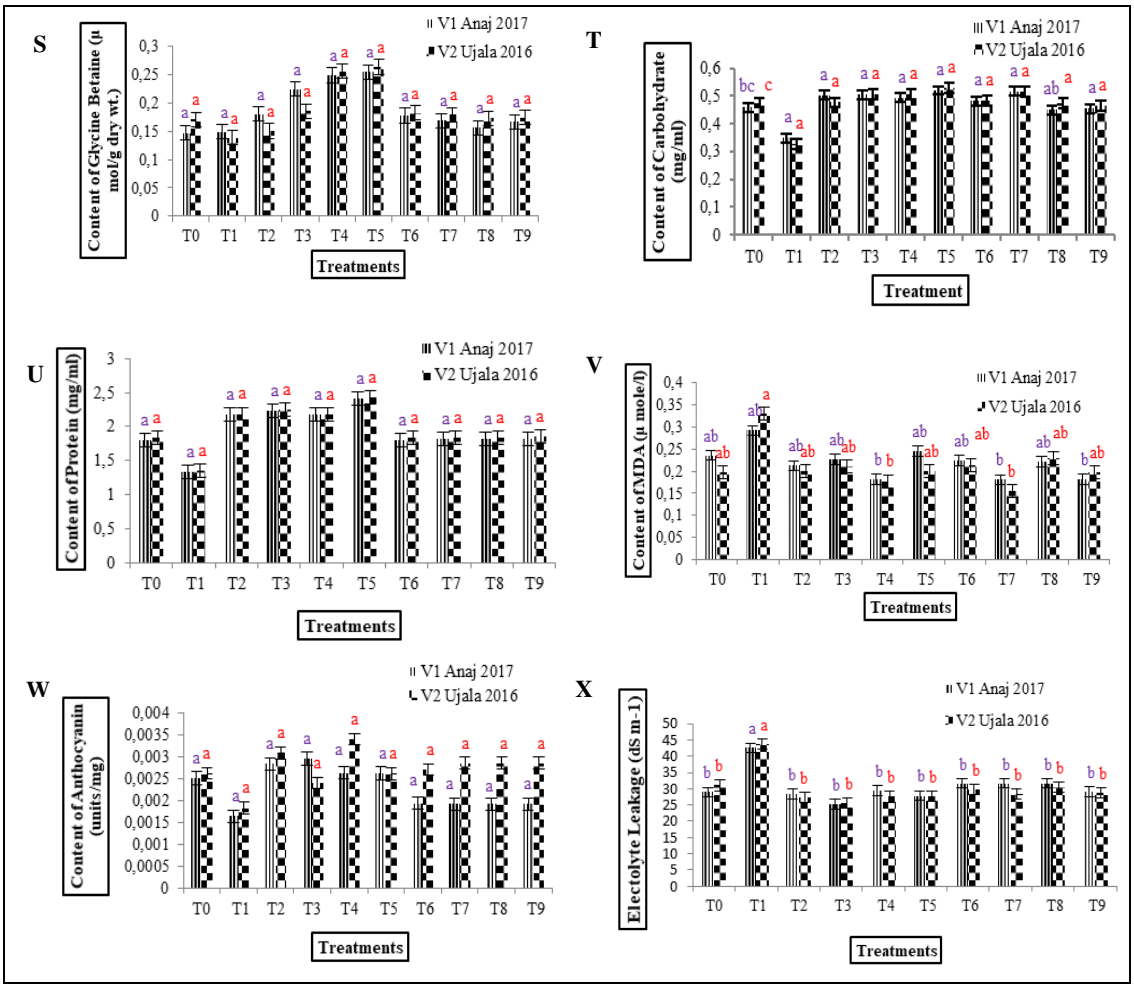

Figure 5. *(S-X): Effect of GA_3 and SA on different biochemical parameters (glycine betaine, carbohydrates, protein, MDA, anthocyanin and electrolyte leakage) of wheat (Triticum aestivum L.) under NaCl stress (at 150 mM NaCl) and without stress. Values represent the means of three replicates ± standard error (SE)*

When plants were subjected to salinity stress then higher level of electrolyte leakage was observed within plant leaves. Ujala-2016 showed higher level of electrolyte leakage than Anaj-2017. The influence of both GA_3 and SA on electrolyte leakage was found highly significant. But by treating NaCl affected plants through GA_3 and SA spray it was noted that the level of electrolyte leakage decreased and reached nearly to control conditions.

Antioxidant activities of enzymes

It was observed that NaCl enhanced antioxidant activities of enzymes including SOD and POD while CAT activity was reduced. The highest SOD activity 0.42 (units/mg protein) was observed at 150 mM NaCl in Ujala-2016 (V_2) when the concentration of NaCl was increased. The activity of POD was also enhanced at the highest concentration

http://www.aloki.hu ● ISSN 1589 1623 (Print) ● ISSN1785 0037 (Online)
DOI: http://dx.doi.org/10.15666/aeer/2001_119134

of NaCl (150 mM NaCl), while minimum POD activity was observed at 0.5 mM concentration of SA. On the other hand, CAT activity was highest 0.3 (units/mg protein) at 150 mg/L GA_3 and is reduced with the rise in the concentration of NaCl as indicated. The hormonal response was significant but the response of varieties was non-significant (*Fig. 6 A1-C1*).

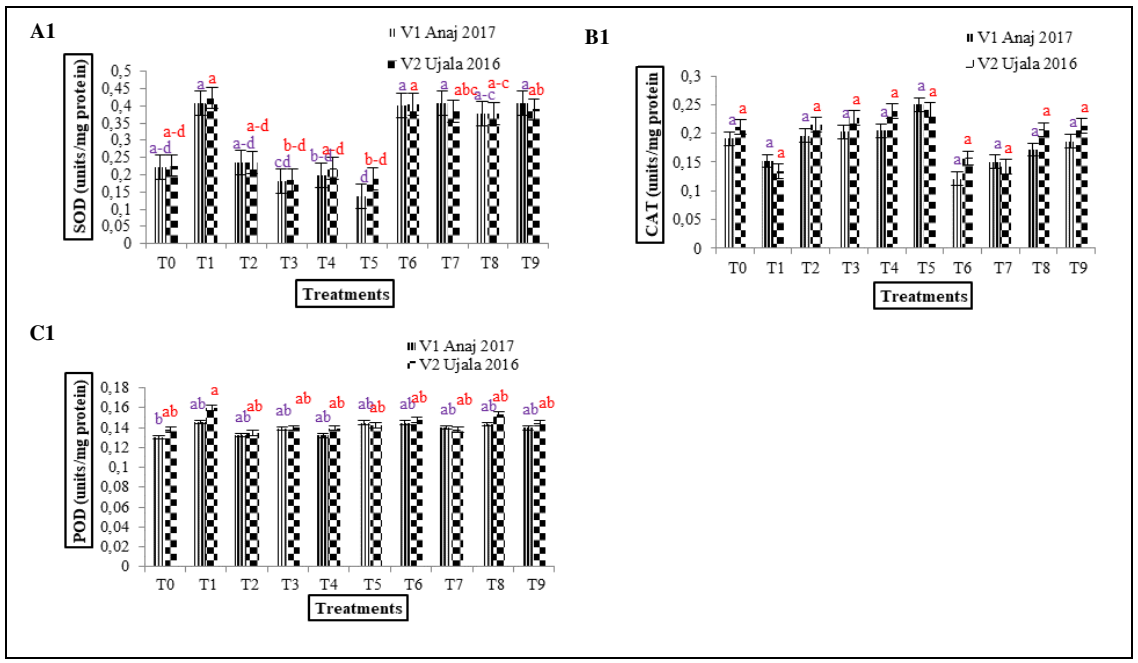

Figure 6. *(A1-C1): Effect of GA_3 and SA on activity of antioxidant enzymes (SOD, POD and CAT) of wheat (Triticum aestivum L.) under NaCl stress (at 150 mM NaCl) and without stress. Values represent the means of three replicates ± standard error (SE)*

Yield parameters

Salt stress substantially reduced the weight of seeds in 100 g value among both varieties of wheat. Plants that were affected with salinity stress showed that seeds were observed with smaller in size. It was noted that the weight of seeds in variety Ujala-2016 was lower than that of Anaj-2017 due to the effect of salt stress. Highest 100 g seed weight 3.2 g was observed in V_2 (Ujala-2016) at a concentration of 1.0 mM SA. The positive impact of both GA_3 and salicylic acid on seed weight were highly significant but between hormones and varieties was non-significant. Use of Gibberellic acid and Salicylic acid by foliar means proved beneficial for increasing the weight of the seeds. Both plant growth stimulators showed highly significant impact on number of spikes/plant but within varieties that was non-significant. It was observed that NaCl is the major cause of reduction in the number of spikes per plant of wheat. The highest number of spikes/plant was recorded at 150 mg GA_3/L. The hormonal response of all yield parameters was highly significant (*Fig. 7 A2-D2*). Both varieties of wheat showed the equal reduction rate of spikes. It was observed that the grain yield was also declined by the addition of salt in plant roots. While it was observed that plants treated by Gibberellic acid and Salicylic acid hormones manifested the positive results and improved the grain yield in plants.

http://www.aloki.hu ● ISSN 1589 1623 (Print) ● ISSN1785 0037 (Online)
DOI: http://dx.doi.org/10.15666/aeer/2001_119134

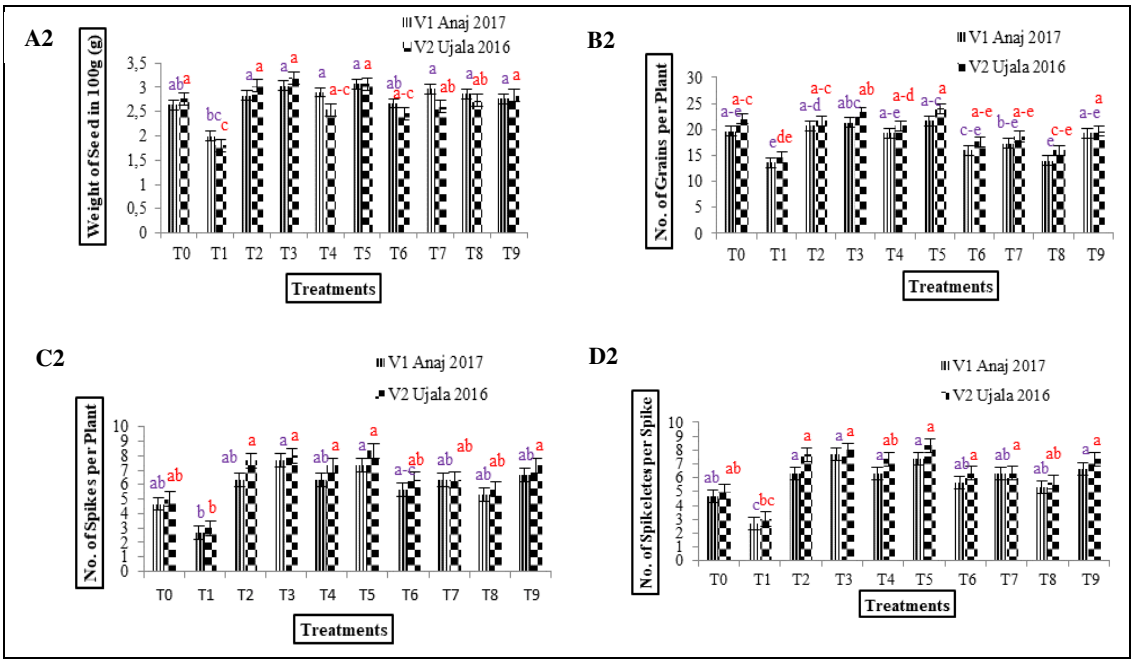

Figure 7. *(A2-D2): Effect of GA_3 and SA on activity of antioxidant enzymes (SOD, POD and CAT) of wheat (Triticum aestivum L.) under NaCl stress (at 150 mM NaCl) and without stress. Values represent the means of three replicates ± standard error (SE)*

Discussion

Published reports showed that the yield of many crops decreased under salt stress but after foliar use of phytohormones such as GA_3 and SA the effect of NaCl can be mitigated and ultimately showed positive effects on plants. Germination of seed is the most important and initial stage for plant growth. The germination of the seeds was affected by the addition of salt in the soil (Mena et al., 2015). In the beginning, plant roots are affected by NaCl because it has direct contact with the soil where NaCl is present. In another study, Ehtaiwesh (2016) reported that mean effect of salinity was significant on plant height, spikelet number, dry weight, grain number, and gain yield etc. further, findings suggested seedling length and dry weight to be considered a selection criterion for salt tolerance. Likewise, Ibrahim et al. (2019) stated that low rate of seed production and quality is threat toward agriculture and industry. GA3 has ability to reduce the rate of transpiration and it also increased the seed weight by maintaining all physiological parameters of the plant. These findings are in agreement with current studies. It is evident that plant photosynthetic mechanism greatly affected by saline environment, resultantly it also reduces the surface area of the leaf and the number of leaves per plant. In the same context, it was observed through the results of the current experiment that the area of leaf in wheat plants decreased when they were subjected to a 150 mM concentration of NaCl. It was evident that salinity stress becomes suppressed in both varieties. The impact of salt stress was also visible on photosynthetic pigments viz., chlorophyll "a", chlorophyll "b", and carotenoids (Zeng et al., 2013). Moreover, Saddiq et al. (2021) advocated that salt stress adversely impacted photosynthesis by damaging chlorophyll pigments and limiting PSII activity while conducting an experiment on winter and spring wheat. In further elaboration it was confirmed that stomatal closing ultimately disturbs the photosynthesis under salt stress.

http://www.aloki.hu ● ISSN 1589 1623 (Print) ● ISSN1785 0037 (Online)
DOI: http://dx.doi.org/10.15666/aeer/2001_119134

Further, the conductance of stomata (GS), Intercellular concentration of carbon dioxide (CI), and the total photosynthetic rate (A) were decreased due to NaCl accumulation. Current results were also supported by the findings of Wasaya et al. (2021) who determined that the water stress and salt had harmful effects upon the rate of transpiration, rate of photosynthesis, and conductance of stomata within wheat genotypes. Anthocyanins (flavonoids) are pigments that are soluble in water and are present within the tissues of all plants. Anthocyanins have a vital role in higher plants because they provide the color of fruits and flowers. Moreover, these pigments also played an important role in the antioxidant activities of plants. Current findings also emphasized that the reduction of anthocyanin pigment was occurred by salinity stress. According to Mbarki et al. (2018) higher dry matter production can be maintained in pigmented wheat genotypes under salt stress. Additionally, salt stress showed a deleterious effect on the biochemical parameters of many plants. It was observed that the amount of carbohydrates within the leaves of the wheat plant was depleted by salinization (Hasanuzzaman et al., 2017). Reduction in carbohydrates decreased through the incorporation of sodium chloride in wheat was recorded in the past. NaCl impact on protein contents was also destructive but the exogenous applications of SA and GA_3 have improved the content of protein within salinity-affected plants. Datir et al. (2020) also reported a similar type of results that the treatment of salt stress lowered the quantity of protein in wheat and foliar applied GA_3 raised the amount of proteins among salinity affected plants. Under salt stress, generation of ROS due to Na+ toxicity, which damage biomolecules (e.g., lipids, proteins, and nucleic acids) on the cellular level and alters redox homeostasis is a common phenomenon (Kundu et al., 2018; Sabagh et al., 2021).

Antioxidant activity was also hampered by the application of salt stress but alleviated through the addition of phytohormones in both varieties. It was noted that the catalase enzyme activity was decreased through the addition of salt within the soil but inversely its level was improved after the treatment of Gibberellic acid and Salicylic acid. Current findings were similar to Datir et al. (2020) that stated the activity of catalase enzyme was declined in wheat. Results showed that the level of SOD and POD was enhanced when the concentration of NaCl was greater within the soil. It showed that the highest level of SOD and POD is the indication of stress for plants. While the foliar use of GA_3 and SA proved beneficial for the reduction of SOD and POD levels. The result is in opinion with the findings of Wang et al. (2014) who noticed that the activity of SOD and POD were elevated by the treatment of salt and it can reduce after the application of hormones. Electrolyte leakage of plant leaves between both varieties of wheat showed an elevated level of NaCl stress. Similarly, Mandhania et al. (2006) and Hasanuzzaman et al. (2017) reported that the concentration of electrolyte leakage in the roots and the leaves of wheat were enhanced by raising the amount of salt. The amount of Malondialdehyde was increased due to the accumulation of NaCl within the wheat plant. Our findings are in agreement with the outcomes of Mandhania et al. (2006), who reported that the content of MDA was increased by the application of sodium chloride (NaCl) within the apical portion of leaf in wheat while the application of GA_3 and Salicylic acid decreased the content of Malondialdehyde (MDA).

In the same context, yield parameters also showed adverse effects of salt stress. Results proved that yield parameters such as number of spikes, number of spikelets, seed weight, and number of grains were reduced due to salt concentration. Datir et al. (2020) reported similar results according to their findings all yield parameters like the grain yield, height of spike, weight of spike, the number of seed, the weight of seed, and the number of

http://www.aloki.hu ● ISSN 1589 1623 (Print) ● ISSN1785 0037 (Online)
DOI: http://dx.doi.org/10.15666/aeer/2001_119134

spikelet were declined by the harmful impacts of salinity stress in wheat whereas, the spray of Salicylic acid proved beneficial to ameliorate the harmful effects of salinity stress.

Conclusion

In conclusion both salicylic acid and gibberellic acid promotes growth like root length (22.6 cm), shoot length (42 cm) and shoot fresh weight (11.4 g), physiological characters such as photosynthetic rate (30.1%) and yield of 100 g seed weight (3.7%). The nutritional constituents including protein, carbohydrates were also enhanced by 0.53 mg/mL. Anthocyanin pigment was increased by 0.0035% at 100mg/L GA_3 in Ujala-2016 while glycine betaine by 0.26% at 150 mg/L. Consequently, the concentration of 0.1 mM SA and 150 mg/L GA_3 along variety Ujala-2016 recommended for the alleviation of salt stress with better growth and yield for future cultivation.

Acknowledgements. We are grateful to the staff of botanical garden, University of Gujrat, Gujrat, Pakistan for provision of experimental facilities.

Disclosure statement. The authors declare no conflict of interests.

REFERENCES

[1] Ahmad, M., Ghafoor, A., Asif, M., Farid, H. U. (2010): Effect of irrigation techniques on wheat production and water saving in soils. – Soil and Environment 29: 69-72.
[2] Arnon, D. I. (1949): Copper enzymes in isolated chloroplasts. Polyphenoloxidase in *Beta vulgaris*. – Plant Physiology 24(1): 1-15.
[3] Bradford, M. M. (1996): A rapid and sensitive method for the quantitation of microgram quantities of protein utilizing the principle of protein-dye binding. – Analytical Biochemistry 72: 248-254.
[4] Braun, H. J., Atlin, G., Payne, T. (2010): Multi-location testing as a tool to identify plant response to global climate change. – Climate Change 1: 115-138.
[5] Cakmak, I., Horst, W. J. (1991): Effect of aluminium on lipid peroxidation, superoxide dismutase, catalase, and peroxidase activities in root tips of soybean (*Glycine max*). – Plant Physiology 83: 463-468. https://doi.org/10.1111/j.1399-3054.1991.tb00121.x.
[6] Chance, B., Meahly, A. C. (1995): Assay of catalase and peroxidase. – Methods Enzymology 2: 764-775.
[7] Dadshani, S., Sharma, R. C., Baum, M., Ogbonnaya, F. C., Léon, J., Ballvora, A. (2019): Multidimensional evaluation of response to salt stress in wheat. – PLoS One 14(9): e0222659. https://doi.org/10.1371/journal.pone.0222659.
[8] Datir, S., Singh, N., Joshi, I. (2020): Effect of NaCl-induced salinity stress on growth, osmolytes and enzyme activities in wheat genotypes. – Bulletin of Environmental Contamination and Toxicology 104: 351-357.
[9] Ehtaiwesh, A. F. A. (2016): Effects of salinity and high temperature stress on winter wheat genotypes. – PhD Dissertation, Kansas State University, USA, 322p.
[10] Giannopolitis, C. N., Ries, S. K. (1977): Superoxide dismutase occurrence in higher plants. – Plant Physiology 59: 309-314.
[11] Grieve, C. M., Grattan, S. R. (1983): Rapid assay for determination of water soluble quaternary ammonium compounds. – Plant and Soil 70: 303-307.
[12] Hadia, E. H., Slama, A., Romdhane, L., M'hamed, H. C., Abodoma, A. H., Fahej, M. A. S., Radhouane, L. (2020): Morphophysiological and molecular responses of two Libyan

http://www.aloki.hu ● ISSN 1589 1623 (Print) ● ISSN1785 0037 (Online)
DOI: http://dx.doi.org/10.15666/aeer/2001_119134

bread wheat cultivars to plant growth regulators under salt stress. – Italian Journal of Agronomy 15(1633): 246-252. https://doi.org/10.4081/ija.2020.1633.

[13] Hasanuzzaman, M., Nahar, K., Rahman, A., Anee, T. I., Alam, M. U., Bhuiyan, T. F., Oku, H., Fujita, M. (2017): Approaches to enhance salt stress tolerance in wheat. – Wheat improvement, management and utilization. Intech Open Science/Open Minds, pp. 151-187.

[14] Hayat, Q., Hayat, S., Irfan, M., Ahmad, A. (2010): Effect of exogenous salicylic acid under changing environment: a review. – Environmental and Experimental Botany 68: 14-25.

[15] Ibrahim, M. E. H., Zhu, X., Zhou, G., Ali, A. Y. A., Elsiddig, A. M. I., Farah, G. A. (2019): Response of Some wheat varieties to gibberellic acid under saline conditions. – Agrosystems, Geosciences and Environment 2(1): 1-7.

[16] Iqbal, M., Ashraf, M. (2013): Gibberellic acid mediated induction of salt tolerance in wheat plants: growth, ionic partitioning, photosynthesis, yield and hormonal homeostasis. – Environmental and Experimental Botany 86: 76-85.

[17] Iqbal, M. S., Ahmad, K. S., Ali, M. A., Akbar, M., Mehmood, A., Nawaz, F., Hussain, S. A., Arshad, N., Munir, S., Arshad, H., Shahbaz, K., Bussmann, R. W. (2021): An ethnobotanical study of wetland flora of Head Maralla Punjab Pakistan. – Plos One 16(10): e0258167.

[18] Krizek, D. T., Kramer, G. F., Upadhyaya, A., Mirecki, R. M. (1993): UV-B response of cucumber seedlings grown under metal halide and high pressure sodium/deluxe lamps. – Journal of Plant Physiology 88: 350-358.

[19] Kundu, P., Gill, R., Ahlawat, S., Anjum, N. A., Sharma, K. K., Ansari, A. A., Hasanuzzaman, M., Akula, R., Chauhan, N., Tuteja, N., Gill, S. S. (2018): Targeting the redox regulatory mechanisms for abiotic stress tolerance in crops. – In: Wani, S. H. (ed.) Biochemical, Physiological and Molecular Avenues for Combating Abiotic Stress Tolerance in Plants. Elsevier Academic Press, pp. 151-220. doi: 10.1016/B978-0-12-813066-7.00010-3.

[20] Lutts, S., Kinet, J. M., Bouharmont, J. (1995): NaCl-induced senescence in leaves of rice (*Oryza sativa* L.) cultivars differing in salinity resistance. – Annals of Botany 78: 389-398.

[21] Mandhania, S., Madan, S., Sawhney, V. (2006): Antioxidant defense mechanism under salt stress in wheat seedlings. – Biologia Plantarum 50: 227-231.

[22] Mbarki, S., Sytar, O., Zivcak, M., Abdelly, C., Cerda, A., Brestic, M. (2018): Anthocyanins of coloured wheat genotypes in specific response to salt stress. – Molecules 23: 1518. doi: 10.3390/molecules23071518.

[23] Mena, E., Leiva-Mora, M., Jayawardana, E. K. D., Garcia, L., Veitía, N., Bermudez-Caraballoso, I., Ortiz, R. C. (2015): Effect of salt stress on seed germination and seedlings growth of *Phaseolus vulgaris* L. – Cultivos Tropicales 36: 71-74.

[24] Nawaz, R., Inamullah, Ahmad, H., Din, S. U., Iqbal, M. S. (2013): Agromorphological studies of local wheat varieties for variability and their association with yield related traits. – Pakistan Journal of Botany 45(5): 1701-1706.

[25] Rout, S., Beura, S., Khare, N., Patra, S. S., Nayak, S. (2017): Effect of seed pre-treatment with different concentrations of gibberellic acid (GA_3) on seed germination and seedling growth of *Cassia fistula* L. – Journal of Plant Sciences 5: 135-138.

[26] Sabagh, A. E., Islam, M. S., Skalicky, M., Raza, M. A., Singh, K., Hossain, M. A., Hossain, A., Mahboob, W., Iqbal, M. A., Ratnasekera, D., Singhal, R. K., Ahmed, S., Kumari, A., Wasaya, A., Sytar, O., Brestic, M., Çig, F., Erman, M., Rahman, M. H. U., Ullah, N., Arshad, A. (2021): Salinity stress in wheat (*Triticum aestivum* L.) in the changing climate: adaptation and management strategies. – Frontiers of Agronomy 3: 661932. doi: 10.3389/fagro.2021.661932.

[27] Saddiq, M. S., Iqbal, S., Hafeez, M. B., Ibrahim, A. M. H., Raza, A., Fatima, E. M., Baloch, H., Jahanzaib, Woodrow, P., Ciarmiello, L. F. (2021): Effect of salinity stress on physiological changes in winter and spring wheat. – Agronomy 11: 1193. https://doi.org/10.3390/agronomy11061193.

http://www.aloki.hu ● ISSN 1589 1623 (Print) ● ISSN1785 0037 (Online)
DOI: http://dx.doi.org/10.15666/aeer/2001_119134

[28] Salim, N., Raza, A. (2020): Nutrient use efficiency (NUE) for sustainable wheat production: A review. – Journal of Plant Nutrition 43: 297-315.
[29] Sawada, H., Shim, I. S., Usui, K., Kobayashi, K., Fujihara, S. (2008): Effect of salicylic acid on salt sensitivity. – Journal of Plant Sciences 174: 583-589.
[30] Shrivastava, P., Kumar, R. (2015): Soil salinity: a serious environmental issue and plant growth promoting bacteria as one of the tools for its alleviation. – Saudi Journal of Biological Sciences 22: 123-131.
[31] Sudharmaidevi, C. R., Thampatti, K. C. M., Saifudeen, N. (2017): Rapid production of organic fertilizer from degradable waste by thermochemical processing. – International Journal of Recycling of Organic Waste in Agriculture 6: 1-11.
[32] Wahid, A., Perveen, M., Gelani, S., Basra, S. M. (2007): Pretreatment of seed with H_2O_2 improves salt tolerance of wheat seedlings by alleviation of oxidative damage and expression of stress proteins. – Journal of Plant Physiology 164: 283-294.
[33] Wang, H. M., Xiao, X. R., Yang, M. Y., Gao, Z. L., Zang, J., Fu, X. M., Chen, Y. H. (2014): Effects of salt stress on antioxidant defense system in the root of *Kandelia candel*. – Botanical Studies 55: 57.
[34] Wasaya, A., Manzoor, S., Yasir, T. A., Sarwar, N., Mubeen, K., Ismail, I. A., Raza, A., Rehman, A., Hossain, A., El Sabagh, A. (2021): Evaluation of fourteen bread wheat (*Triticum aestivum* L.) genotypes by observing gas exchange parameters, relative water and chlorophyll content, and yield attributes under drought stress. – Sustainability 13: 4799.
[35] Zeng, J., Chen, A., Li, D., Yi, B., Wu, W. (2013): Effects of salt stress on the growth, physiological responses, and glycoside contents of *Stevia rebaudiana* Bertoni. – Journal of Agricultural and Food Chemistry 61: 5720-5726.

http://www.aloki.hu ● ISSN 1589 1623 (Print) ● ISSN1785 0037 (Online)
DOI: http://dx.doi.org/10.15666/aeer/2001_119134

USING FACE MASKS IN THE CLASSROOM: THE EFFECT ON THE INDOOR ENVIRONMENT PARAMETERS AND FACE THERMOPHYSIOLOGICAL REACTIONS

ANGELOVA, R. A.* – VELICHKOVA, R.

Centre for Research and Design in Human Comfort, Energy and Environment (CERDECEN), Technical University of Sofia, 8 Kliment Ochridski blv., 1000 Sofia, Bulgaria

**Corresponding author*
e-mail: joy_angels@abv.bg, radost@tu-sofia.bg

(Received 7th Jun 2021; accepted 28th Oct 2021)

Abstract. Masks have been recommended as a protective tool for effectively combating the COVID-19 pandemic. In many countries, masks are required indoors, but the obligation temporarily and sporadically extends to all public places indoors and outdoors in some regions. Our study investigated the effect of wearing face masks in the classroom on the indoor environmental parameters and the human body experimentally. The study was performed at the Technical University of Sofia with 14 volunteers during regular lecture classes. Two stages were considered: with and without face masks. Measurement of the indoor environment parameters, oxygen (O_2) and carbon dioxide (CO_2) concentration was continuously performed. Thermal image analysis was used to obtain the face thermograms of the participants. The results clearly showed the retention effect of the face masks on the exhaled air, leading to lower CO_2 concentration in the classroom and higher O_2 concentration and humidity. It was also found that the continuous wear of a face mask for 40-45 min provoked an increment of the facial skin temperature under the mask to 37 °CC and even more. The rise of the temperature of the inner cantus of the eye showed that the face mask triggered the body's thermoregulation, causing thermophysiological reactions.
Keywords: *COVID-19, infrared thermography, carbon dioxide concentration, thermophysiological comfort, university classroom*

Introduction

The SARS-CoV2 (COVID-19) pandemic has led to people being required to wear protective face masks. In many countries, the requirement is limited to wearing masks indoors – in buildings and vehicles, but in some regions, the obligation temporarily and sporadically extends to all public places indoors and outdoors. Masks have been recommended as a protective tool for massively combating the COVID-19 pandemic in China (Wang et al., 2020), although their use varies by time and province (Feng et al., 2020).

Health organisations, politicians and societies are seeking sufficient evidence of the benefits of restrictive measures (one of which is wearing masks) as a tool in the fight against COVID-19 in the light of the existing context: a complex environment for making solutions, difficult to foresee spread of the pandemic, fast development of new research, and continuous increase in the number of people infected and deaths in many countries.

Though there is no a deficit anymore of N95 respirators (classified by the National Institute of Occupational Safety in the United States) or FFP2 respirators (certified by the European Union and filtering over 94% of airborne particles), masks for hospital use (Smith et al., 2020) and ordinary textile masks are primarily in use. The American and European Centers for Disease Control (Howard et al., 2021) recommended this practical public-use approach. The use of face masks and their effectiveness can be considered

http://www.aloki.hu ● ISSN 1589 1623 (Print) ● ISSN 1785 0037 (Online)
DOI: http://dx.doi.org/10.15666/aeer/2001_135151

from different points of view: medical (e.g., to what extent they are effective against viral particles of cell size), social (e.g., how they protect risk groups), psychological (e.g., to what extent they limit facial expression, as an essential part of communication). At the same time, contradictory data exist on the effect of face masks as a tool in the fight against SARS-CoV2 (Rieger, 2020).

During the COVID-19 pandemic in Hong Kong, a telephone study found increased adherence to wearing masks in public places; with no mandatory requirements, the number of people wearing masks outside the home increased from 74.5% to 97.5% in just three weeks (Cowling et al., 2020). Similar studies were reported during the SARS pandemic in 2003: 79% of people reported wearing masks outside the home voluntarily (Leung et al., 2004). These facts suggest that society raises its awareness of risk and is more inclined to adhere to prevention strategies. Simultaneously, the widespread use of masks is a visual reminder of the need for physical distancing, which is among the safest strategies to prevent SARS-CoV2 transmission. Third, the wearing of masks by all avoids public stigmatisation of virus carriers or patients, as described in other diseases, e.g., tuberculosis (Buregyeya et al., 2012).

Several research papers dealing with the use of textile and surgical masks focused mainly on the effectiveness of filtration against aerosols (liquid or dry) with a particle size from 0.01 μm to 10 μm (Van der Sande et al., 2008; Rengasamy et al., 2010; Chughtai et al., 2013; Davies et al., 2013; Shakya et al., 2017; Konda et al., 2020). The study of Aydin et al. (2020) also proposed a method for assessing the retention capacity of textile masks to larger droplets released when coughing, sneezing or talking. However, a few studies have been conducted with the start of the COVID-19 pandemic to evaluate the effectiveness of wearing a mask over time and assess the individual's comfort and possible side effects. Among the first exceptions was the editorial letter of Lazzarino et al. (2020). Perhaps, the reason for this was that for the first time, the policymakers put on the agenda the need for long-term wearing of masks by various segments of the population outside the medical institutions. Some of these segments involve children or adults with side effects of the respiratory tract (asthma, respiratory allergies).

The side effects of the widespread, long-term and continuous use of masks can be summarised as follows (Desai et al., 2020; Kyung et al., 2020; Lazzarino et al., 2020; Liu et al., 2020a; World Health Organization, 2020).

- Psychological:
  - They create a false sense of proper measures taken against the infection and neglect other measures (handwashing, distance) (World Health Organization, 2020).
  - They are associated with religious behaviour patterns (covering the face), which is unacceptable for some Western societies (Liu et al., 2020a).
- Behavioral:
  - Touching the masks with hands (due to the mask's displacement on the face) increases the risk of infection (Desai et al., 2020; World Health Organization, 2020).
  - Shortening the distance to the interlocutor: due to the inability to follow the lips, some people do not understand speech well and unconsciously approach the interlocutor.
  - More frequent eye touch since part of the exhaled air is directed to the eyes increases the risk of infection.

http://www.aloki.hu ● ISSN 1589 1623 (Print) ● ISSN 1785 0037 (Online)
DOI: http://dx.doi.org/10.15666/aeer/2001_135151

- With an effect on the health and comfort:
  - Change in respiration rate, blood oxygen saturation and exhaled CO_2 levels before and after using the N95 mask (Kyung et al., 2020).
  - Creation of a humid environment favourable for the spread of the virus (Lazzarino et al., 2020).

A recent study (Liu et al., 2020b) reported measurements of the face temperature when using both N95 and surgical masks, finding that N95 masks provoked more significant thermal discomfort and higher facial skin temperature. Another study (Scarano et al., 2020) evaluated the influence of different face masks on human comfort indoors, aiming to facilitate selecting different masks from the rational and scientific point of view.

The aim of our study was to evaluate the effect of wearing face masks on people's comfort in a university classroom and on the parameters of the indoor environment. The idea was provoked by the episodic requirement that students in schools and universities, together with their teachers, stay in the classrooms with masks. Our hypotheses were that wearing face masks could provoke local thermal discomfort and inhibit the transition of exhaled air to the environment. The thermal comfort was evaluated based on infrared thermal imaging and consequent processing of the thermograms. Sensors for measuring the air temperature, relative humidity, pressure, oxygen (O_2) concentration and carbon dioxide (CO_2) concentration were used together with software to monitor the parameters change directly.

Materials and methods

Participants and environmental conditions

The study was performed in October 2020 at the Technical University of Sofia (Sofia, Bulgaria) in a classroom at Building 2 (*Fig. 1*) with installed heating, ventilation and air conditioning (HVAC) system. The classroom volume was 204 m^3 (11.8 m length, 5.4 m width, and 3.2 m height).

(**a**) (**b**)

Figure 1. *The university classroom with an HVAC system: (a) View to the front zone; (b) view to the back zone*

The measurements were done during regular lectures, with twelve volunteers, students (age 21-28 years). Two teachers (age 40 and 51) also participated in the

http://www.aloki.hu ● ISSN 1589 1623 (Print) ● ISSN 1785 0037 (Online)
DOI: http://dx.doi.org/10.15666/aeer/2001_135151

experiment: one lecturing and one dealing with the infrared measurements. The participants declared that they had no symptoms of COVID-19 or influenza. They gave permission for the use of their thermograms' data.

The field study was performed following the current governmental and university prescriptions (as of October 2020). In that period, the students and teachers were not obliged to use face masks in the classrooms, whilst the distance between the working places and occupants were large enough. The particular classroom could accommodate 24 people, and in this case, only 50% of its seats were occupied.

The room air temperature was set to 22 °C, recirculation mode of the HVAC system. All windows and the door were closed to avoid entering of outside air.

The outdoor temperature was 11 °C at the beginning of the measurements and 11.8 °C at the end. The relative humidity was 65%.

Face masks

Surgical face masks of a disposal type with loops (Etropal JSC, Etropole, Bulgaria) were given to all participants in the experiment (*Fig. 2*). The masks correspond to ISO 13485 (2016), and EN 14683 + AC (2019).

Figure 2. *The used face masks*

Three non-woven layers, whose microscopic views are presented in *Figure 3,* form the mask. The outer one (*Fig. 3a*) protects from droplets, the middle one (*Fig. 3*b) filters viruses (over 95%), particles (over 98%) and bacteria (over 98%) (ISO 13485, 2016; EN 14683 + AC, 2019).

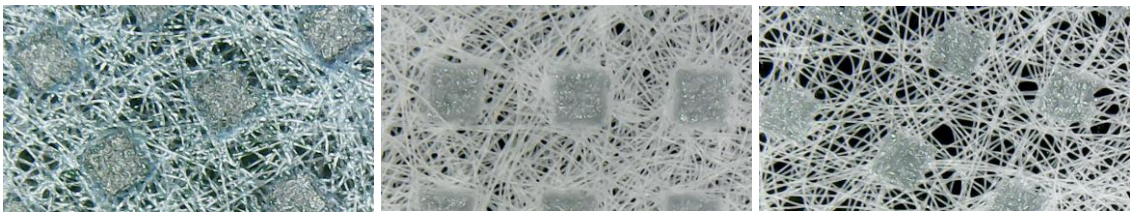

(**a**) (**b**) (c)

Figure 3. *Microscopic view of the mask layers: (a) Outer layer (blue); (b) middle layer (invisible); (c) inner layer (white)*

http://www.aloki.hu ● ISSN 1589 1623 (Print) ● ISSN 1785 0037 (Online)
DOI: http://dx.doi.org/10.15666/aeer/2001_135151

According to ISO 13485 (2016) and EN 14683+AC (2019) the inner one (*Fig. 3c*) assures the comfort of the skin face. The average thickness of a mask (from 10 measurements) was 0.92 mm.

Measurements

During the experiment, the air temperature, relative humidity and pressure were continuously recorded with a time step of 5 s. The change in the oxygen (O_2) and carbon dioxide (CO_2) concentration in the room was also monitored continuously with a time step of 5 s. As the CO_2 concentration was of primary interest, two CO_2 sensors (K30 FR Fast Response 10000 ppm CO_2 sensor of CO2Meter, USA) were used – in the front and the back zone of the classroom (*Fig. 1*). A sensor for joint monitoring of the O_2 concentration, air temperature, relative humidity and pressure (CM-4X of CO2Meter, USA) was placed in the middle of the classroom. The results were red using the GasLab specialised software (CO2Meter, USA).

The remote recording of the face temperature (with and without face masks) was done with FLIR E6 infrared thermal camera (FLIR Systems Inc., Wilsonville, OR, US) with the following parameters: thermal sensitivity < 0.06 °C; -20 °C to 250 °C temperature range; IR 19200 (160 × 120) pixels resolution; Imaging resolution 320 × 240; 0.1 to 1 adjustment of the radiation; 3 measurement modes. The recording was done at 0.5 m away from the face of the person.

Experimental protocol

The study involved two stages (Stage 1 and Stage 2) with the same protocol. The HVAC system was set in a recirculation mode with 22 °C air temperature. All windows and the door were closed to avoid entering fresh air.

After entering the classroom, the participants were asked to sit evenly distributed among the workplaces: 1 person per a table (*Fig. 4*). They were also requested not to change their clothing ensemble during the experiment.

Figure 4. *During the measurements, Stage 1*

In Stage 1, the participants wore surgical masks. The duration of the lecture class was 45 min, which resulted in a 2600 s measurement period (seconds at the beginning of the lecture were omitted to equalize the recordings from all sensors). The participants

http://www.aloki.hu ● ISSN 1589 1623 (Print) ● ISSN 1785 0037 (Online)
DOI: http://dx.doi.org/10.15666/aeer/2001_135151

were sitting, listening to the lecture and taking notes. Five thermograms were taken of each person: after the acclimatization (a reference thermogram) at the beginning of the class; 20 min after the first measurement; and at the end of the class – a thermogram with the mask and a thermogram of the face immediately after the mask was taken off.

Stage 2 took place after a 30 min break. All windows were open during the break. The students took the same seats in the classroom as during Stage 1. They did not wear masks. *Figure 5* illustrates the experimental protocol in Stage 1.

Figure 5. *The experimental protocol*

Statistical analysis

All data were statistically analysed using Excel Data Analysis ToolPack. The experimental results are presented as the average value ± standard deviation. The Student test (t-test) was performed to evaluate the existence of a statistically proven difference between the average values in each group. The significance level α was set to 0.05.

Results

Indoor environmental parameters

Stage 1 (with masks)

Figure 6 presents the change in the room air temperature, relative humidity and pressure during Stage 1 when the participants wear face masks. Though the temperature maintained by the HVAC system was set to 22 °C, the average value of the temperature in the room was 23.66 ± 0.35 °C. The increment was due to the radiation heat from the inhabitants, their breath and the radiation heat from the windows (facing to the East) on that sunny day.

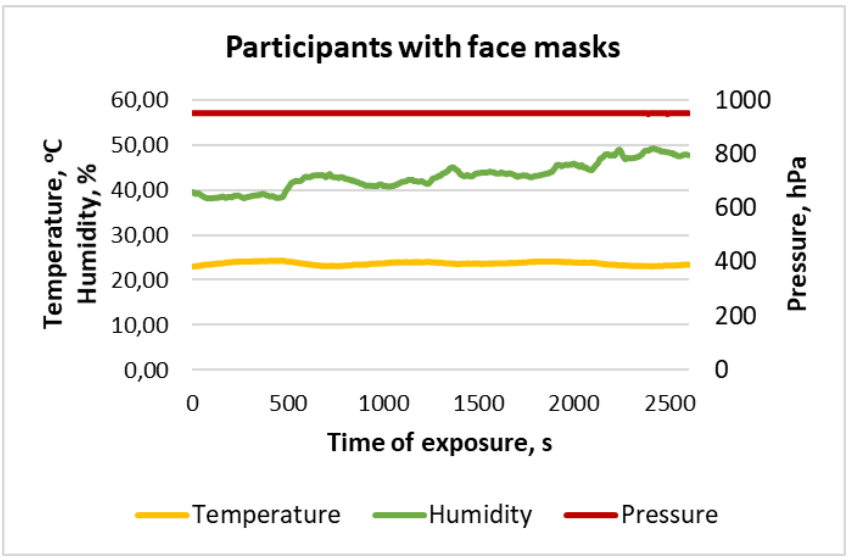

Figure 6. *Indoor environmental parameters, Stage 1*

http://www.aloki.hu ● ISSN 1589 1623 (Print) ● ISSN 1785 0037 (Online)
DOI: http://dx.doi.org/10.15666/aeer/2001_135151

The air pressure remained constant, 950 ± 0.06 hPa.

The air humidity increased with the time from 38% to 49.2% due to the exhalation of the inhabitants. The recirculation mode of the ventilation system did not allow the entrance of outside air. The average air humidity during Stage 1 was 43.07 ± 3.07%.

Figure 7 presents the results for the CO_2 concentration, summarising the data from the sensors in the front and back zone of the room. The back zone sensor measured higher CO_2 concentration in the classroom than the front one. The statistical analysis of the data proved the difference between the readings of the two sensors ($t_{stat} = 130$, $t_{crit} = 1.96$, $\alpha = 0.05$). The Pearson correlation (0.98) showed that a linear dependence exists between the two sets of data.

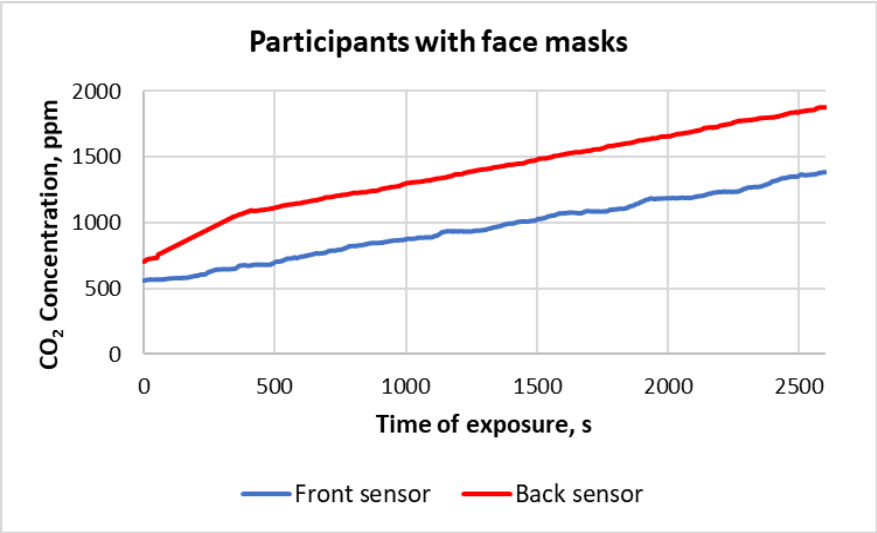

Figure 7. *Carbon dioxide concentration, Stage 1*

Stage 2 (no masks)

Figure 8 summarises the results for the room air temperature, relative humidity and pressure in Stage 2 when the participants did not wear face masks. The temperature in the room was 23.81 ± 0.28 °C, again higher than the set temperature of 22 °C. The air pressure remained constant, 949 ± 0.33 hPa.

The air humidity increased during the lecture from 41.1% to 50.2%. The average air humidity during Stage 2 was 44.29 ± 1.93%.

Figure 9 visualizes the results for the CO_2 concentration, measured by the front and back sensors in the classroom. Similar to *Figure 7,* the CO_2 concentration in the back zone of the classroom was higher than in the front zone. The statistical analysis showed a proven difference between the readings of the two sensors ($t_{stat} = 182.72$, $t_{crit} = 1.96$, statistical level $\alpha = 0.05$). The Pearson correlation (0.998) showed that a linear dependence exists between the two sets of data.

Comparison between Stage 1 and Stage 2

In Stage 1, the average air temperature in the classroom was 23.66 ± 0.34 °C and in Stage 2 was 23.81 ± 0.28 °C. Though the average values were similar, the statistical comparison showed a proven difference between the two sets of data: $t_{stat} = 8.97$, $t_{crit} = 1.96$, $\alpha = 0.05$.

http://www.aloki.hu ● ISSN 1589 1623 (Print) ● ISSN 1785 0037 (Online)
DOI: http://dx.doi.org/10.15666/aeer/2001_135151

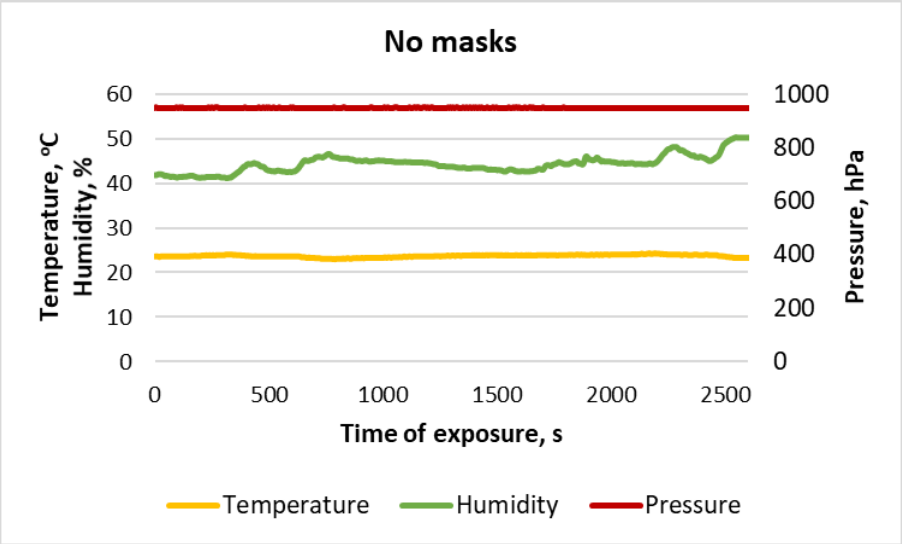

Figure 8. *Indoor environmental parameters, Stage 2*

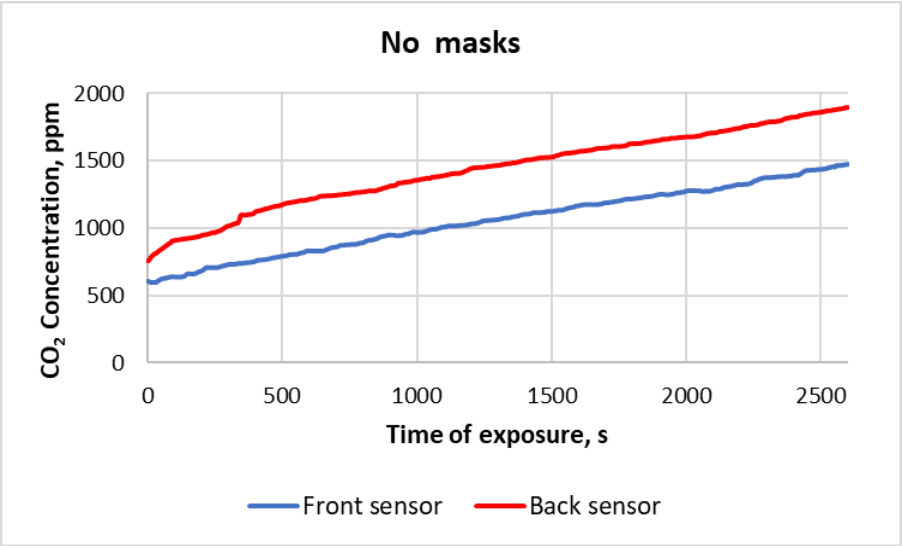

Figure 9. *Carbon dioxide concentration, Stage 1*

The average humidity in Stage 1 was 43.07 ± 3.07%, while in Stage 2, it was 44.29 ± 1.93%. The statistical analysis allowed us to conclude that there was a proven effect of wearing face masks on the air humidity in the classroom: $t_{stat} = 12.5$, $t_{crit} = 1.96$, $\alpha = 0.05$.

The results for the oxygen (O_2) concentration in the two stages are compared in *Figure 10*. The tendency is towards slight decrement due to the recirculation mode and the breathing of the inhabitants. However, it is visible that much more fluctuations in the O_2 concentration were present in Stage 2, while in Stage 1, the decrement line was smoother. The average value of the O_2 concentration in Stage 1 was 202924.8 ± 306.1 ppm. In Stage 2, the average value of the O_2 concentration was quite similar: 203041.6 ± 392.1 ppm. The statistical analysis showed that the two data sets were statistically different: $t_{stat} = 13.468$, $t_{crit} = 1.96$, $\alpha = 0.05$.

http://www.aloki.hu ● ISSN 1589 1623 (Print) ● ISSN 1785 0037 (Online)
DOI: http://dx.doi.org/10.15666/aeer/2001_135151

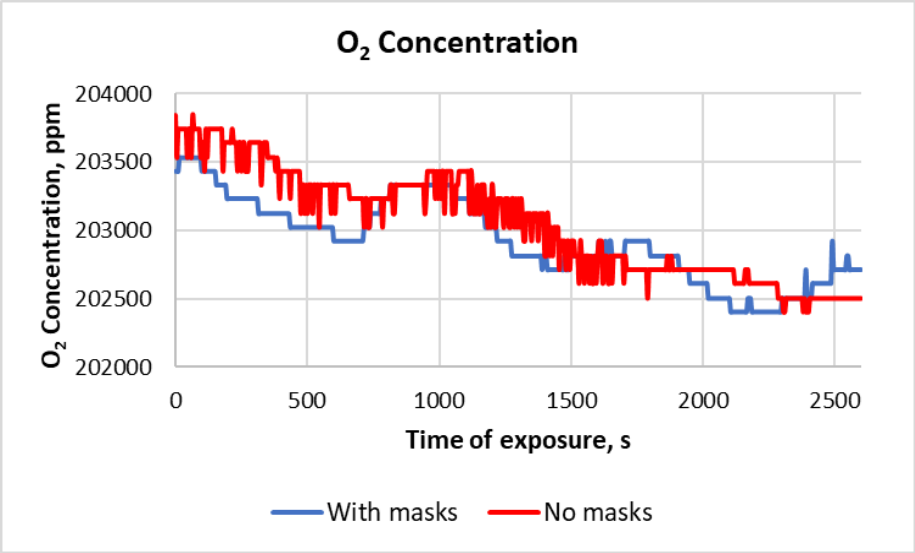

Figure 10. *Oxygen concentration during Stage 1 and Stage 2*

Figure 11 illustrates the comparison between the CO_2 concentration, measured in the fronts zone of the classroom in Stage 1 and Stage 2. When the participants wore face masks, the CO_2 concentration was 962 ± 238 ppm. When the participants were without masks, the CO_2 concentration was 1051 ± 244 ppm. It is noteworthy that the average value of CO_2 concentration in Stage 2 was higher by 90 ppm, but the standard deviation in both measurements was almost the same. The statistical check showed a proven difference between the two data groups, i.e. the presence of masks affected the CO_2 concentration: $t_{stat} = 125.247$, $t_{crit} = 1.96$, $\alpha = 0.05$.

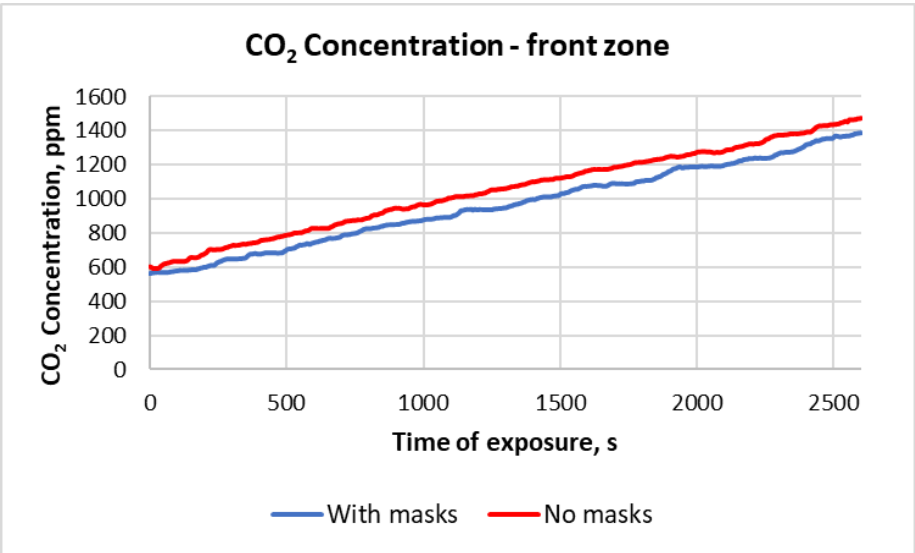

Figure 11. *Carbon dioxide concentration in the front zone of the classroom during Stage 1 and Stage 2*

Figure 12 compares the results for the CO_2 concentration, measured in the back zone of the classroom in Stage 1 and Stage 2. When the participants were with face masks,

http://www.aloki.hu ● ISSN 1589 1623 (Print) ● ISSN 1785 0037 (Online)
DOI: http://dx.doi.org/10.15666/aeer/2001_135151

the CO_2 concentration was 1389 ± 302 ppm. When the participants were without masks, the CO_2 concentration was 1434 ± 287 ppm. The statistical analysis showed a proven difference between the two data sets, i.e. the use of masks affected the CO_2 concentration: $t_{stat} = 42.246$, $t_{crit} = 1.96$, $\alpha = 0.05$.

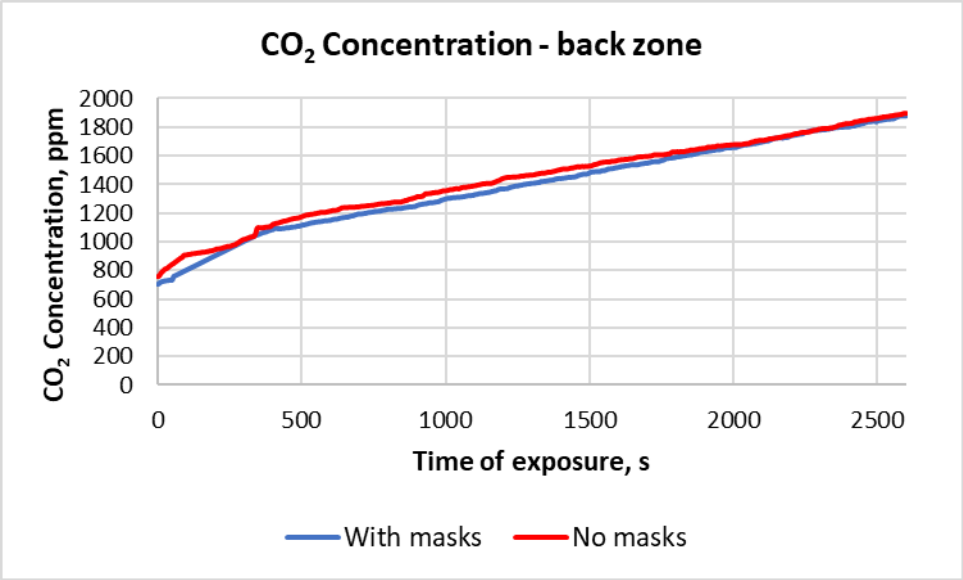

Figure 12. *Carbon dioxide concentration in the back zone of the classroom during Stage 1 and Stage 2*

Thermal infrared imaging

Figure 13 shows the changes in the surface temperature of the face mask in Stage 1. For all participants (except Participant #4), the surface temperature of the mask was lowest at the beginning of the stage. The heat exchange "face – mask" led afterwards to an increment of the temperature of the mask surface. The increment was more significant in the first 20 min than in the second half of Stage 1. The average temperature of the mask surface was 30.04 ± 0.68 °C at the start of Stage 1, 31 ± 0.74 °C in the middle of the stage and 31.18 ± 0.7 °C at the end.

The analysis proved the statistical difference between the mask temperature at the beginning and in the middle of Stage 1 ($t_{stat} = 3.52$, $t_{crit} = 2.16$, $\alpha = 0.05$). However, the difference between the mask temperature in the middle and at the end of Stage 1 was not proven statistically ($t_{stat} = 0.94$, $t_{crit} = 2.16$, $\alpha = 0.05$).

The results for the change of the skin face temperature at the beginning of Stage 1 (after the acclimatisation) and at the end of the stage (immediately after the mask was taken off) are summarised in *Figure 14*. The face skin temperature at the beginning of Stage 1 was 35.34 ± 0.92 °C. The face skin temperature at the end of Stage 1 was 36.84 ± 0.50 °C. The statistical analysis showed that the difference between the two data sets was statistically proven: $t_{stat} = 6.16$, $t_{crit} = 2.16$, $\alpha = 0.05$. Hence, the changed factor – the presence of a mask on the face, influenced the skin temperature of the face.

The registered temperature of the skin face above 37 °C led to additional analysis of the thermograms. The thermograms were processed to show in red areas the skin temperature above a certain limit. This limit was set to 36.7 °C for the reference thermograms (after the acclimatisation in Stage 1) and the thermograms of the face

http://www.aloki.hu ● ISSN 1589 1623 (Print) ● ISSN 1785 0037 (Online)
DOI: http://dx.doi.org/10.15666/aeer/2001_135151

immediately after the removal of the masks. An additional limit was set for the thermograms at the end of Stage 1: 37 °C. Obviously, the coloured in red area was smaller compared to the thermograms with a temperature limit above 36.7 °C. *Figure 15* summarises the thermal infrared (IR) images of all participants in Stage 1.

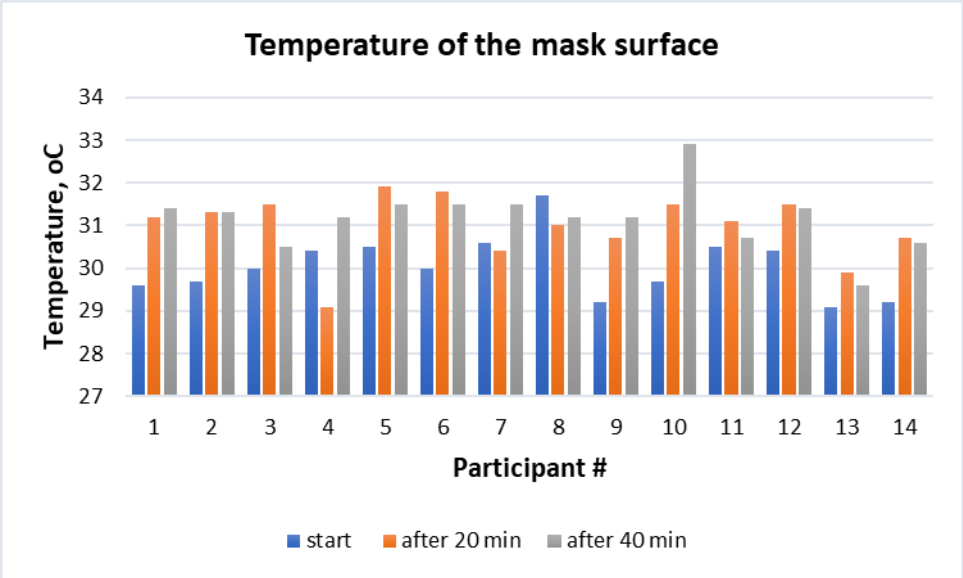

Figure 13. *The temperature on the mask surface at the beginning of Stage 1 (start), in the middle (after 20 min) and at the end of the stage (after 40 min)*

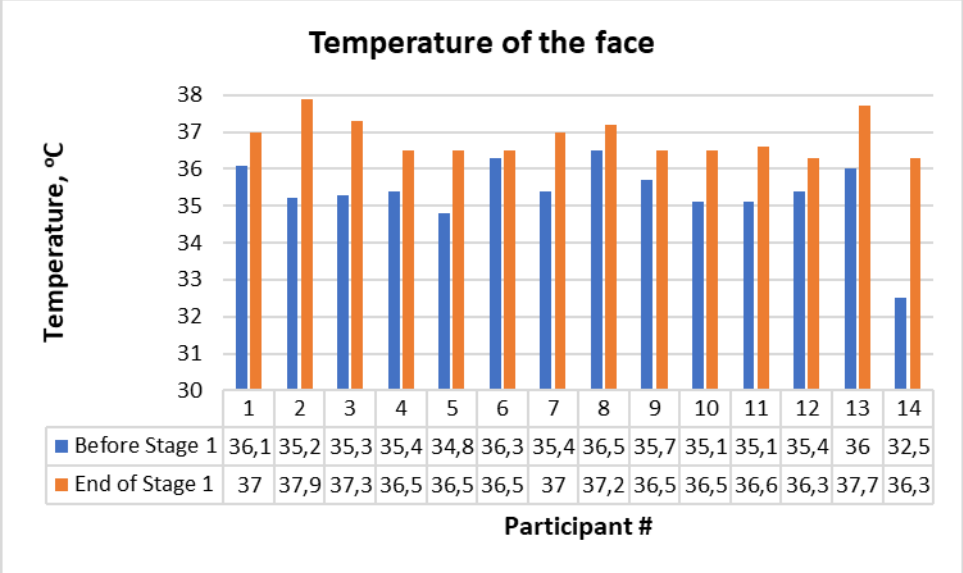

	1	2	3	4	5	6	7	8	9	10	11	12	13	14
Before Stage 1	36,1	35,2	35,3	35,4	34,8	36,3	35,4	36,5	35,7	35,1	35,1	35,4	36	32,5
End of Stage 1	37	37,9	37,3	36,5	36,5	36,5	37	37,2	36,5	36,5	36,6	36,3	37,7	36,3

Figure 14. *The temperature of the face before Stage 1 (after the acclimatisation) and after the mask taking off at the end of Stage 1*

Figure 16 shows the results of determining the temperature of the inner canthus of the eye (the place where the upper and lower eyelids meet). Twelve measurements were considered, as two of the participants wore glasses when the thermograms were taken.

http://www.aloki.hu ● ISSN 1589 1623 (Print) ● ISSN 1785 0037 (Online)
DOI: http://dx.doi.org/10.15666/aeer/2001_135151

The average temperature of the inner cantus before Stage 1 was 36.35 ± 0.7 °C, and after wearing the masks, the temperature increased to 37.08 ± 0.22 °C. The statistical analysis proved the existence between the two sets of measurements: $t_{stat} = 3.9$, $t_{crit} = 2.2$, $\alpha = 0.05$.

The average temperature of the inner cantus of the eye before Stage 1 was 36.35 ± 0.7 °C, and after wearing the masks, the average temperature increased to 37.08 ± 0.22 °C. The statistical analysis proved the difference between the two sets of measurements:

$$t_{stat} = 3.9, t_{crit} = 2.2, \alpha = 0.05.$$

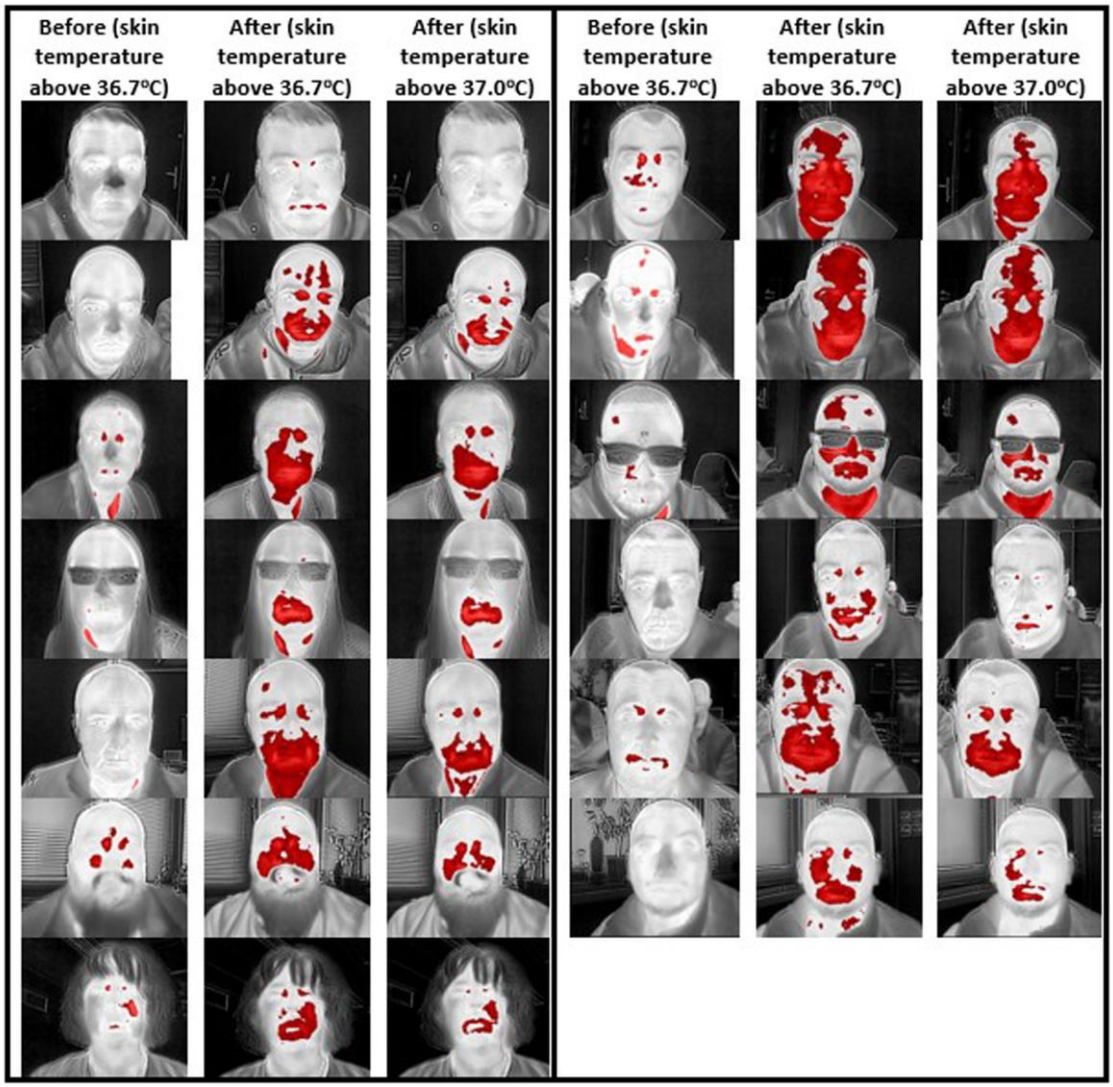

Figure 15. *Thermograms of the participants*

Discussion

The study's main result is that the continuous use of face masks in the classroom for 40-45 min leads to statistically proven changes in both the indoor environment and thermophysiological reactions of the participants. The effect on the indoor environment

http://www.aloki.hu ● ISSN 1589 1623 (Print) ● ISSN 1785 0037 (Online)
DOI: http://dx.doi.org/10.15666/aeer/2001_135151

is due to the presence of the mask and the formation of a stagnation microzone between the face and the mask, which affects the inhaled and exhaled air.

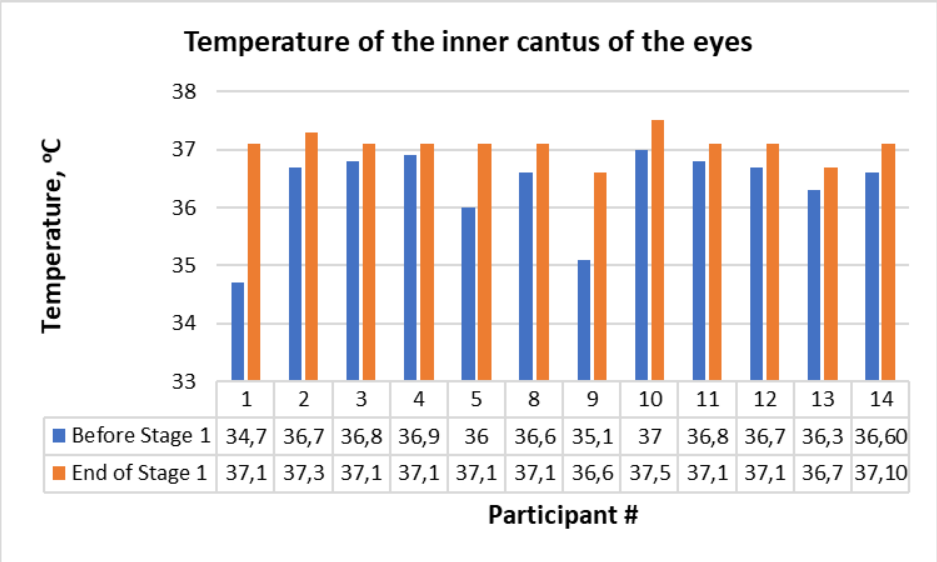

	1	2	3	4	5	8	9	10	11	12	13	14
Before Stage 1	34,7	36,7	36,8	36,9	36	36,6	35,1	37	36,8	36,7	36,3	36,60
End of Stage 1	37,1	37,3	37,1	37,1	37,1	37,1	36,6	37,5	37,1	37,1	36,7	37,10

Figure 16. *The temperature of the inner cantus of the eye before Stage 1 (after the acclimatisation) and after the mask taking off at the end of Stage 1*

To check this hypothesis, additional measurements were performed with the same type of masks and three of the participants. The CO2 concentration sensor was firmly fixed on a person's face under a face mask near the mouth. As the zone under the mask was of primary interest, it was considered that the day of the measurement and the classroom indoor environment conditions would not be significant. The idea was only to measure the CO_2 concentration under the face mask with a step of 5 s. The measurements were performed 6 times with three volunteers (two measurements for a person).

Figure 17 shows a typical result from the measurements. At the beginning of the measurement, the person is with the face mask under the chin. The CO_2 concentration measured is 1165 ppm, which is higher than the CO_2 concentration of the air in the room (840 ppm). This could be due to the human breathing influencing the sensor on the face. After lifting the mask on the face, covering both the mouth and nose, the sensor was left on the face. In 15 s, the CO_2 concentration reached 10000 ppm, which was the top of the sensor sensitivity (designed for indoor environment measurements).

When the face was uncovered again, the CO_2 concentration decreased but much slower. The new covering of the face with the mask resulted in a new fast increase (approx. 15 s) of the CO_2 concentration under the mask (the second pick in *Fig. 17*). Indeed, this preliminary result is only a sign of the process under the face mask and need further investigation with a CO_2 concentration sensor with a higher measurement range. Using a special device (Sofronova et al., 2021), this would be a point of further research within the project.

The comparison between the indoor environmental parameters when the participants were with and without face masks showed a significant, statistically proven change in the CO_2 concentration in the classroom. The use of face masks led to lower CO_2 concentration in the air. An explanation could be the retention of some of the exhaled CO_2 in the microzone under the mask.

http://www.aloki.hu ● ISSN 1589 1623 (Print) ● ISSN 1785 0037 (Online)
DOI: http://dx.doi.org/10.15666/aeer/2001_135151

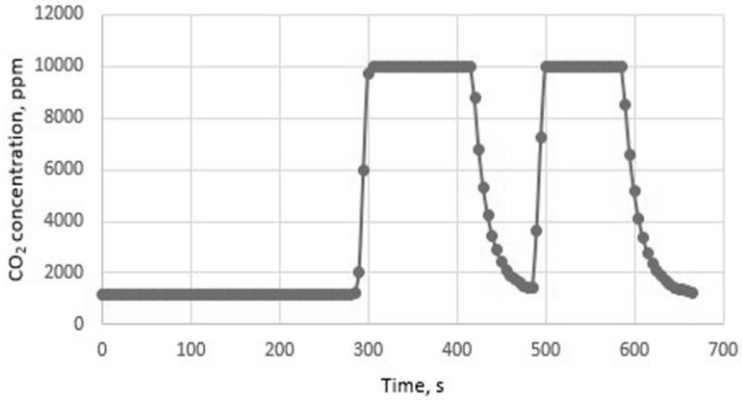

Figure 17. *CO_2 concentration in the stagnation zone under the mask*

The study showed a difference in the measurement of CO_2 concentration from the sensor in the front and back zone of the classroom. The reason is the configuration of the workplaces in the room: there were more occupants in the back zone. Of course, the effect of the ventilation system should be considered as well: it can provide a different mixing effect in the distinct areas of the classroom. The essential result is that both sensors registered a lower CO_2 concentration in the air when participants were with masks.

The oxygen concentration also changed: the O_2 in the air was depleted faster when participants wore masks. It may be related to the rapid breathing observed when wearing a mask (Roberge et al., 2012). Inhalations are also deeper, which is associated with both the high CO_2 concentration of air from the microzone under the mask and the greater effort required to inhale through the pores of the mask. Fluctuations in the O_2 concentration when breathing without a mask and the absence of such when participants are wearing masks also showed an altered breathing pattern.

The air temperature and relative humidity in the classroom at Sate 1 and Stage 2 also differ. However, it is difficult to determine that the presence of masks affected the temperature. The reason is that the radiant heat through the windows changed (increased) with the rising of the sun and the progress of the day. The effect of occupancy should also not be overlooked: before Stage 1, the room was empty, while Stage 2 followed Stage 1, in which the HVAC system warmed the room.

Nevertheless, the effect of wearing masks on the humidity in the room needs comments. Humidity was higher in Stage 2 due to the missing mask and the free passage of water vapour through the exhaled air from the lungs to the environment. The study in (Mansour et al., 2020) has shown that the relative humidity of the exhaled air is between 41.9-91.0%. In the presence of a mask, the passage of water vapour from the exhaled air to the room is retained by the mask. This is why the accumulation of moisture in the microzone under the mask was also a subject of complaints by the participants. How the retained moisture under the mask affects comfort and its quantity is a matter of future evaluation.

The thermal image analysis clearly shows the increase in the temperature of the face under the mask over time. The heat transfer between the face and the mask is evidence of an increase in the temperature of the skin under the mask. From the thermograms of the masked persons it is clear that there is a proven difference between the surface temperatures of the mask at the beginning and middle of the wearing period, but not

http://www.aloki.hu ● ISSN 1589 1623 (Print) ● ISSN 1785 0037 (Online)
DOI: http://dx.doi.org/10.15666/aeer/2001_135151

between the middle and the end of Stage 1. It is logical to conclude that heat transfer is very more intense at the beginning of wearing the mask, then slows down and probably follows the slow rate of rise in facial skin temperature under the mask.

The rise in facial skin temperature under the mask is unquestionable. Facial thermograms immediately after removing the masks clearly show elevated temperature areas compared to the reference thermograms before Stage 1. These are the areas around the mouth and nose. Thirteen of the 14 participants had a skin surface temperature above 37 °C. In 9 thermograms, there was a temperature rise above 36.7 °C in the neck area. In 5 participants, an increase in temperature was found in the upper part of the forehead and scalp. These results for the skin temperature are higher than the reported in (Mansour et al., 2020).

The temperature of the inner canthus of the eye is considered to be a reliable source of information about the core body temperature (Childs et al., 2012), although in (Teunissen et al., 2011), it was found that it differs by 1.80 ± 0.89 °C from the temperature of the oesophagus, considered the "gold standard" in terms of core body temperature. The increase of the inner cantus of the eye's temperature is a sign of the thermophysiological reactions that occur in the body due to wearing the mask. Similar was the conclusions in (Yip et al., 2005), where an increment of the intraoral temperature of persons wearing masks, with 37.5 °C and more, was found.

The change in the temperature of the inner cantus of the eye indicates that the presence of a mask affects the local rise of the facial temperature and triggers the body's thermoregulation system. Probably these reactions are related to the participants' complaints of discomfort and deteriorating thermal comfort during Stage 1. Future research is required to determine this effect in prolonged continuous standing with a face mask.

Conclusions

Our study used a combination of indoor environmental measurements and thermal imaging testing to study the effect of wearing surgical face masks on the comfort of the wearers and the indoor environment parameters. It was found that:

- The continuous wear of a face mask for 40-45 min in the classroom forms a stagnation microzone between the face and the mask. The microzone changes the breathing pattern, and the restricted flow motion affects the CO_2 and O_2 concentration in the classroom and the air relative humidity. The parameters of the microzone need further investigation.
- The continuous wear of a face mask for 40-45 min leads to an increment of the facial skin temperature, which could reach more than 37 °C under the mask. The increment of the temperature of the inner cantus of the eye confirms that the face mask triggers the body's thermoregulation, causing thermophysiological reactions. Future research is required to determine this effect in prolonged continuous standing with a face mask.

Our future research will be dedicated to the effect of wearing different types of masks indoors (textile, N95, FFP2), using the same protocol. Another field of research will be measuring the CO_2 concentration in the air, detained under different types of face masks, using a sensor that can measure very high concentration (30000 ppm or

http://www.aloki.hu ● ISSN 1589 1623 (Print) ● ISSN 1785 0037 (Online)
DOI: http://dx.doi.org/10.15666/aeer/2001_135151

higher). The effect of the prolonged wearing of face masks (over 60 min) on the thermophysiological comfort of the person indoors would also be considered.

Acknowledgements. This research and publication were supported by the Bulgarian Science Fund of the Ministry of Education and Science, Project No. КП-06-Н47/3.

REFERENCES

[1] Aydin, O., Emon, B., Cheng, S., Hong, L., Chamorro, L. P., Saif, M. T. A. (2020): Performance of fabrics for home-made masks against the spread of COVID-19 through droplets: a quantitative mechanistic study. – Extreme Mechanics Letters 40: 100924.

[2] Buregyeya, E., Mitchell, E. M., Rutebemberwa, E., Colebunders, R., Criel, B., Kiguli, J., Nuwaha, F. (2012): Acceptability of masking and patient separation to control nosocomial tuberculosis in Uganda: a qualitative study. – Journal of Public Health 20(6): 599-606.

[3] Childs, C., Zu, M. M., Wai, A. P., Tsai, Y. T., Wu, S., Li, W. (2012): Infra-red thermal imaging of the inner canthus: correlates with the temperature of the injured human brain. Rapid determination of sexually transmitted infections by real-time polymerase chain reaction using microchip analyzer. – Engineering 5: 53-6.

[4] Chughtai, A. A., Seale, H., MacIntyre, C. R. (2013): Use of cloth masks in the practice of infection control—evidence and policy gaps. – Int J Infect Control 9(3): 1-12.

[5] Cowling, B. J., Ali, S. T., Ng, T. W., Tsang, T. K., Li, J. C., Fong, M. W., ... Leung, G. M. (2020): Impact assessment of non-pharmaceutical interventions against coronavirus disease 2019 and influenza in Hong Kong: an observational study. – The Lancet Public Health 5(5): e279-e288.

[6] Davies, A., Thompson, K. A., Giri, K., Kafatos, G., Walker, J., Bennett, A. (2013): Testing the efficacy of homemade masks: would they protect in an influenza pandemic? – Disaster Medicine and Public Health Preparedness 7(4): 413-418.

[7] Desai, A. N., Aronoff, D. M. (2020): Masks and coronavirus disease 2019 (COVID-19). – JAMA 323(20): 2103-2103.

[8] EN 14683+AC (2019): Medical Face Masks - Requirements and Test Methods. – European Committee for Standardization, Belgium.

[9] Feng, S., Shen, C., Xia, N., Song, W., Fan, M., Cowling, B. J. (2020): Rational use of face masks in the COVID-19 pandemic. – The Lancet Respiratory Medicine 8(5): 434-436.

[10] Howard, J., Huang, A., Li, Z., Tufekci, Z., Zdimal, V., van der Westhuizen, H. M., ... & Rimoin, A. W. (2021): An evidence review of face masks against COVID-19. – Proceedings of the National Academy of Sciences 118(4).

[11] ISO 13485 (2016): Medical devices—Quality Management Systems—Requirements for Regulatory Purposes. – International Organization for Standardization, Switzerland.

[12] Konda, A., Prakash, A., Moss, G. A., Schmoldt, M., Grant, G. D., Guha, S. (2020): Aerosol filtration efficiency of common fabrics used in respiratory cloth masks. – ACS nano 14(5): 6339-6347.

[13] Kyung, S. Y., Kim, Y., Hwang, H., Park, J. W., Jeong, S. H. (2020): Risks of N95 face mask use in subjects with COPD. – Respiratory Care 65(5): 658-664.

[14] Lazzarino, A. I., Steptoe, A., Hamer, M., Michie, S. (2020): Covid-19: important potential side effects of wearing face masks that we should bear in mind. – The BMJ 369.

[15] Leung, G. M., Quah, S., Ho, L. M., Ho, S. Y., Hedley, A. J., Lee, H. P., Lam, T. H. (2004): A tale of two cities: community psychobehavioral surveillance and related impact on outbreak control in Hong Kong and Singapore during the severe acute respiratory syndrome epidemic. – Infection Control and Hospital Epidemiology 25(12): 1033-1041.

http://www.aloki.hu ● ISSN 1589 1623 (Print) ● ISSN 1785 0037 (Online)
DOI: http://dx.doi.org/10.15666/aeer/2001_135151

[16] Liu, C., Diab, R., Naveed, H., Leung, V. (2020a): Universal public mask wear during COVID-19 pandemic: rationale, design and acceptability. – Respirology (Carlton, Vic.): 25(8): 895.
[17] Liu, C., Li, G., He, Y., Zhang, Z., Ding, Y. (2020b): Effects of wearing masks on human health and comfort during the COVID-19 pandemic. – IOP Conference Series: Earth and Environmental Science 531(1): 012034).
[18] Mansour, E., Vishinkin, R., Rihet, S., Saliba, W., Fish, F., Sarfati, P., Haick, H. (2020): Measurement of temperature and relative humidity in exhaled breath. – Sensors and Actuators B: Chemical 304: 127371.
[19] Rengasamy, S., Eimer, B., Shaffer, R. E. (2010): Simple respiratory protection—evaluation of the filtration performance of cloth masks and common fabric materials against 20–1000 nm size particles. – Annals of Occupational Hygiene 54(7): 789-798.
[20] Rieger, M. O. (2020): To wear or not to wear? Factors influencing wearing face masks in Germany during the COVID-19 pandemic. – Social Health and Behavior 3(2): 50.
[21] Roberge, R. J., Kim, J. H., Benson, S. M. (2012): Absence of consequential changes in physiological, thermal and subjective responses from wearing a surgical mask. – Respiratory Physiology & Neurobiology 181(1): 29-35.
[22] Scarano, A., Inchingolo, F., Lorusso, F. (2020): Facial skin temperature and discomfort when wearing protective face masks: thermal infrared imaging evaluation and hands moving the mask. – International Journal of Environmental Research and Public Health 17(13): 4624.
[23] Shakya, K. M., Noyes, A., Kallin, R., Peltier, R. E. (2017): Evaluating the efficacy of cloth facemasks in reducing particulate matter exposure. – Journal of Exposure Science & Environmental Epidemiology 27(3): 352-357.
[24] Smith, P. B., Agostini, G., Mitchell, J. C. (2020): A scoping review of surgical masks and N95 filtering facepiece respirators: learning from the past to guide the future of dentistry. – Safety Science 131: 104920.
[25] Sofronova, D., Sofronov, Y., Angelova, R. A. (2021): Design of a Device for Measuring the Parameters of the Microenvironment under Protective Face Masks. – 2021 6th International Symposium on Environment-Friendly Energies and Applications (EFEA), Technical University of Sofia, Bulgaria, 24-26 March 2021, pp. 1-4.
[26] Teunissen, L. P. J., Daanen, H. A. M. (2011): Infrared thermal imaging of the inner canthus of the eye as an estimator of body core temperature. – Journal of Medical Engineering & Technology 35(3-4): 134-138.
[27] Van der Sande, M., Teunis, P., Sabel, R. (2008): Professional and home-made face masks reduce exposure to respiratory infections among the general population. – PloS One 3(7): e2618.
[28] Wang, M. W., Cheng, Y. R., Ye, L., Zhou, M. Y., Chen, J., Feng, Z. H. (2020): The COVID-19 outbreak: the issue of face masks. – Infection Control & Hospital Epidemiology 41(8): 974-975.
[29] World Health Organization (2020): Advice on the use of masks in the community, during home care and in healthcare settings in the context of the novel coronavirus (2019-nCoV) outbreak: interim guidance, 29 January 2020 (No. WHO/nCov/IPC_Masks/2020.1). – WHO, Geneva.
[30] Yip, W. L., Leung, L. P., Lau, P. F., Tong, H. K. (2005): The effect of wearing a face mask on body temperature. – Hong Kong Journal of Emergency Medicine 12(1): 23-27.

http://www.aloki.hu ● ISSN 1589 1623 (Print) ● ISSN 1785 0037 (Online)
DOI: http://dx.doi.org/10.15666/aeer/2001_135151

THE EFFECT OF ENVIRONMENTAL AND HUMAN FACTORS ON THE DISTRIBUTION OF BROWN BEAR (*URSUS ARCTOS ISABELLINUS)* IN IRAN

HOSSEINI, S. P.[1*] – AMIRI, M.[2] – SENN, J.[3]

[1]*Range and Watershed Management Department, Natural Resources Faculty, Isfahan University of Technology, Isfahan, Iran*
(e-mail: seyedpouyahosseini@gmail.com; phone: +98-918-999-6289)

[2]*Natural Resources Department, University of Applied Science and Technology (UAST), Branch of Mazandaran, Wood and Paper Industries, Sari, Iran*
(e-mail: mohaddesehamiri@yahoo.com; phone: +98-936-731-1969)

[3]*Swiss Federal Institute for Forest, Snow and Landscape Research, WSL, Zurich, Switzerland*
(e-mail: Josef.senn@wsl.ch; phone: +41-447-392-381)

[*]*Corresponding author*
e-mail: seyedpouyahosseini@gmail.com; phone: +98-918-999-6289

(Received 15th Jun 2021; accepted 28th Oct 2021)

Abstract. Brown bear (*Ursus arctos isabellinus*) in Kurdistan Province of Iran is considered as a regionally threatened species. Therefore, understanding spatial distribution of brown bear and influencing factors is fundamental to their conservation. In this study, occurrence records of brown bear coupled with environmental and habitat data were compiled, and suitable habitats of this species was predicted through five species distribution models (SDMs) including Random Forest (RF), Classification Tree Analysis (CTA), Artificial Neural Network (ANN), Generalized Linear Model (GLM), Maximum Entropy (MaxEnt), as well as an ensemble approach. To evaluate each model's predictive performance, area under the curve (AUC) and true skill statistic (TSS) were measured. All models showed AUC values higher than 0.9 under scenario I, indicating excellent overall prediction accuracy. The accuracy statistics derived by the ensemble maps were higher than those derived by single SDMs. Among the single models, GLM and MaxEnt scored the highest partial AUC values under both scenarios. Temperature seasonality, isothermality, precipitation of the driest month, and distance to village were recognized as the most effective variables in predicting suitable habitats for brown bear. Our findings demonstrated the usefulness of the ensemble approach and the high accuracy of GLM and MaxEnt in the species distribution modelling.
Keywords: *bioclimatic variables, habitat suitability modelling, human-bear conflict, ensemble, conservation, Zagros Forests*

Introduction

Large carnivores like brown bears (*Ursus arctos isabellinus*, Linnaeus 1758) are highly susceptible to habitat loss and fragmentation caused by human activities (Zanin et al., 2015), climate change (Rodriguez et al., 2007), and are in priority for conservation, as assuring the needs of these umbrella species also helps in protecting other species (Beier et al., 2008). Brown bear as the biggest carnivore in Iran is an important species and is found in the north, west, and north-west of the country and across the Alborz and Zagros mountain ranges. During the last decades and due to the deforestation and heavy harvesting of non-timber products in the Zagros Forests, brown bear has become highly endangered (Gutleb and Ziaie, 1999); and this species is officially placed in the list of threatened species in many regions (McLellan et al., 2016). The presence of brown bear may also be used as an indicator for healthy ecosystems supporting natural ecological

http://www.aloki.hu ● ISSN 1589 1623 (Print) ● ISSN 1785 0037 (Online)
DOI: http://dx.doi.org/10.15666/aeer/2001_153170

processes and species interaction little affected by human presence and intervention (Yousefi, 2016). Predicting potential habitat beyond the present range is an essential step towards proactive management strategies minimizing human-wildlife conflict, thereby promoting large carnivore population viability in the future (Treves et al., 2004).

Species distribution models (SDMs) are an important tool for studying basic questions regarding the potentially suitable habitat for species and their environmental determinants and are used for many purposes in biogeography, conservation and ecology (Elith and Leathwick, 2009). Over the last decades, several algorithms have been developed to model species distributions (Thuiller et al., 2009). Some studies have suggested that the accuracy of species distribution predictions could be substantially improved by applying consensus methods (Thuiller et al., 2009; Araújo et al., 2011).

The Zagros Forests cover an area of about six million hectares and account for around 45% of Iran's forests. The Zagros Forests provide home for approximately 10% of Iran's human population (Department of Environment, 2014). These forests are recognized as pastoral ecosystems, which for thousands of years have been exposed to grazing by livestock influencing the structure and function of the forest (Hoekstra and Shachak, 1999). The Zagros Forests are made up of northern and southern main divisions. In the northern division due to the special economic and social situations, people are dependent on the forests in many aspects, including non-timber product harvesting and cultivation of crops under the forest canopy resulting in forest degradation. Further, local communities traditionally coppice trees for fodder for livestock in winter (Ghazanfari, 2003; Henareh-Khalyani et al., 2014). Additionally, the Zagros Forests have lately been influenced by intensive drought (Arsalani et al., 2015); and fungal pathogen outbreaks, leading to a gradual dieback of the oak forests (Mirabolfathy et al., 2011). Habitat degradation especially due to agricultural expansion and intensification leads to conflicts between brown bear and humans (Can et al., 2014).

There are three central objectives of this study: 1) identifying brown bear habitat and propose priority regions for conservation programs and areas for the protection of the species in Kurdistan Province, 2) identifying anthropogenic and environmental parameters affecting habitat suitability and distribution, and 3) evaluating and comparing the performance of the modelling algorithms and the ensemble approach in species distribution modelling.

Materials and methods

In the present study, occurrence data was collected and together with additional bioclimatic data and ecological parameters distribution of the species was projected. In continue study area, our approach for collecting data in the field, as well as the approaches used for modelling of the species distribution will be described.

Study area and species

This study was carried out in Kurdistan Province in the north-west of Iran and along the border with Iraq. Kurdistan is a mountainous province covering an area of about 29048 km^2 and includes the Zagros oak-dominated forests. These forests are home to many mammals including brown bear (Ziaie, 2008); and plants like *Quercus spp.* (oaks), *Pistacia mutica* (wild pistachio), *Crategus spp.* and *Pyrus spp.* (Jazirehi and Rostaghi, 2003). The northern part of the Zagros Forests is an exclusive habitat for *Q. infectoria* associated with *Q. libani* or *Q. brantii* or both of them, while, the southern part of the

http://www.aloki.hu ● ISSN 1589 1623 (Print) ● ISSN 1785 0037 (Online)
DOI: http://dx.doi.org/10.15666/aeer/2001_153170

forests is dominated by *Q. brantii* (Sagheb-Talebi et al., 2003). The Zagros Mountain Range thanks to their height and longitude receive precipitation from air masses coming from the Persian Gulf and the Mediterranean Sea in the west. The western part of the Iranian plateau in the mid-Zagros range experiences a pronounced seasonal change in precipitation and temperature (Sharifi et al., 2009). The northern part of the Zagros Forests is wetter and cooler than the southern part (Sagheb-Talebi et al., 2003). The average precipitation of Kurdistan Province accounts for 517 mm with maximum precipitation of 990 mm in the west of the province and the average temperature varies from 7 to 14 °C (Hanafi and Hatammi, 2013). In the study area (*Fig. 1*), the altitude ranges from 740 meters to 3161 meters above sea level. In the western part of the Zagros Mountain Range many seasonal and perennial rivers are fed by the snow accumulated in winter at the higher altitudes (Sharifi et al., 2009). The main stream is Sirwan River running through Shaho-Kosalan and flowing into Daryan Dam in the south-west of the study area.

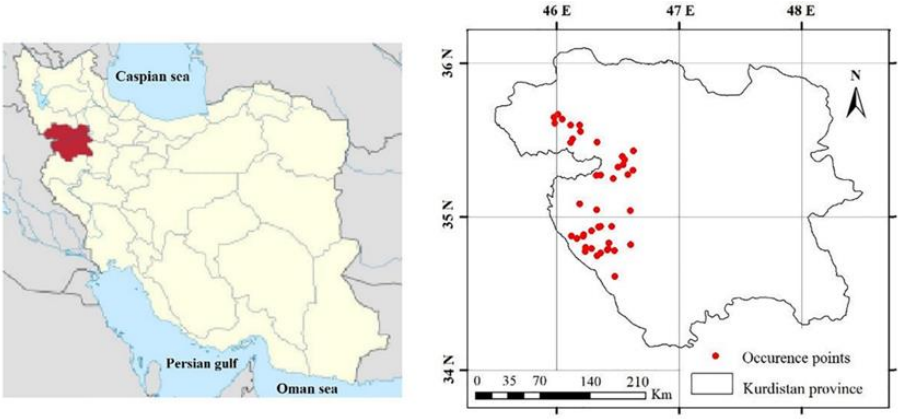

Figure 1. *Map of Iran and Kurdistan Province (left) and the brown bear's occurrence points in Kurdistan Province (right)*

Brown bears are opportunistic omnivores that rapidly learn to use new food sources once they become available. Food availability is a determining factor in the distribution and home range of bears (Hwang et al., 2010). Gutleb et al. (2002) estimated population of this species in the Zagros Forests fewer than one hundred and found these forests as relatively poor habitats for the species. Brown bears prefer densely forested areas (Kobler and Adamic, 2000); and feed on a wide range of foods including green vegetation, such as graminoids, forbs, and fruits in springs and early summer depending on the availability. In autumn and winter, brown bears forage on tree masts like acorns (*Quercus*) and chestnuts (*Castanea sativa*) (Swenson et al., 2000). Brown bear is an important disperser of seeds as it may swallow large amounts of fruits and seeds (Welch et al., 1997); and usually travels over long ranges, spreading seeds far away from the origin. There is evidence that seed passage through the species digestive tracts may improve germination rates to some degree in a number of plant species (Willson and Gende, 2004); making bears an effective agent for the conservation of certain plant species.

Availability of high energy foods in late summer and autumn is essential for the species hibernation. Brown bears need large continuous areas of habitat and occur in low population densities. They may be active during the day and at night, and their activity

http://www.aloki.hu ● ISSN 1589 1623 (Print) ● ISSN 1785 0037 (Online)
DOI: http://dx.doi.org/10.15666/aeer/2001_153170

depends on food, environmental conditions, and human activity (Swenson et al., 2000). Brown bears are considered dangerous to humans and their livestock resulting in conflicts with local human communities, including attacks on humans, damage to human properties and agricultural products, and preying on livestock and domestic animals (Can et al., 2014).

Species occurrence and environmental data

In this work, a database of brown bear occurrences within Kurdistan Province was used that consists of geo-referenced localities where the species has been observed directly, or recorded damage to livestock, beehives, and crops caused by the species. Additional records from the existing scientific literature and researchers were included, too. Finally, a total of 40 independent records with a minimum distance of one km between the records were obtained.

Environmental data include multiple remote sensing and other spatial layers such as bioclimatic, physiographic, Normalized Difference Vegetation Index (NDVI), and anthropogenic variables. Climatic variables and variations in precipitation and temperature have a profound effect on species distribution range (Moraitis et al., 2019; Wang et al., 2019). Bioclimatic variables including eleven temperature and eight precipitation factors were collected from the WorldClim database. WorldClim version two has average monthly climate data for minimum, mean, and maximum temperature and for precipitation for 1970-2000 (http://www.worldclim.org). Autocorrelation between input variables could lead to collinearity, overfitting, and misinterpretation of results. In order to detect and exclude highly correlated variables, Pearson's correlation coefficient between each pair of predictors was calculated. In case two variables had a significant correlation coefficient ($-0.7 < r < 0$), one of them that was ecologically more important was selected to be involved in the modelling (Yi et al., 2016) (*Table 1*).

Table 1. *Environmental predictor variables employed for modelling the brown bear distribution and the sources data were derived*

Predictor variables	Description	Source/Reference
Climatic	Bio3 = Isothermality ($Bio2/Bio7$) (× 100)	WorldClim
	Bio4 = Temperature Seasonality (standard deviation × 100)	WorldClim
	Bio8 = Mean Temperature of Wettest Quarter (°C)	WorldClim
	Bio14 = Precipitation of Driest Month (mm)	WorldClim
Physiographic	Elevation (m)	SRTM DEM data
	Slope	SRTM DEM data
	Aspect	SRTM DEM data
	Distance to river (m)	1/25000 Topographic map
NDVI	NDVI	USGS
Anthropogenic	Distance to road (m)	1/25000 Topographic map
	Distance to village (m)	1/25000 Topographic map

Physiographic data involves aspect, elevation, slope, and distance to river, and anthropogenic includes distance to village and distance to roads. Using the 90-meter spatial resolution digital elevation model (DEM) from the shuttle radar topography

http://www.aloki.hu ● ISSN 1589 1623 (Print) ● ISSN 1785 0037 (Online)
DOI: http://dx.doi.org/10.15666/aeer/2001_153170

mission (SRTM) three topographic explanatory variables including slope, elevation, and aspect were compiled. A topographic map (scale 1:25000) of the study area was employed for the calculation of distance to village, distance to road, and distance to river. NDVI was another variable used in the modelling as an index for greenness, which permitted discrimination of vegetated areas.

Among the vegetation indices that permit discrimination of vegetated areas, NDVI is widely used. NDVI is the difference between the red and near-infrared band combination, divided by the sum of the red and near-infrared band combination (*Equation 1*). In this study, MODIS-derived NDVI with 1 km spatial resolution obtained from USGS (United States Geological Survey, 2020) was selected as a remote sensing predictor for mapping distributions. NDVI is calculated as follows:

$$NDVI = \frac{(\rho NIR - \rho Red)}{(\rho NIR + \rho Red)} \quad \text{(Eq.1)}$$

where ρNIR and ρRed represent the surface reflectance values of the near-infrared and the red wavelengths, respectively. The layers finally were resampled to 30-arc second resolution to be utilized in the modelling process.

Modelling approaches

Locating suitable habitats as well as determining the most important factors for species distribution are among the most common applications of SDMs (Phillips et al., 2006). Modelling was implemented in the Biomod2 package where it was developed for the R 4.0.3 statistical-programing software. Ten modelling algorithms are available in this package, of which we used five to evaluate and compare the model's predictability and to develop an ensemble forecasting map for brown bear in the study area and finally to investigate the effects of anthropogenic and environmental variables on the distribution of the species. Modelling algorithms used in this study are briefly introduced in continue.

Generalized Linear Models (GLMs) are a set of parametric methods (McCullagh and Nelder, 1989); allowing more flexible relationships to be specified in terms of many link functions between the response and predictor variables as compared to linear regression models. When response data is binary, the appropriate GLM is a logistic model using a logit link to depict the relationship between the response and the linear sum of the predictor variables (Hosmer and Lemeshow, 2000).

Artificial Neural Network (ANN) techniques are one of the robust rule-based approaches that used in bioclimatic envelope modelling (Berry et al., 2002; Thuiller et al., 2003). Such model is based on the function of the human brain and has been developed to build mathematical models that mimic the computing power of the human brain and has great benefits in different applications (Tripathi, 2015). ANN is composed of primary computational units called neurons combined based on different architectures. For instance, they can be ordered in layers (multi-layer network), or they may have a connection topology. According to *Figure 2*, layered networks include, 1) input layer, consist of n neurons, 2) hidden layer, made of one or several hidden (intermediate) layer consisting of m neurons, 3) output layer, consisting of p neurons, 4) the feedback and feedforward architecture (feedback architecture has connections between neurons of the same or previous layer, but feedforward architecture does not have any feedback connections) (Gallo, 2015).

http://www.aloki.hu ● ISSN 1589 1623 (Print) ● ISSN 1785 0037 (Online)
DOI: http://dx.doi.org/10.15666/aeer/2001_153170

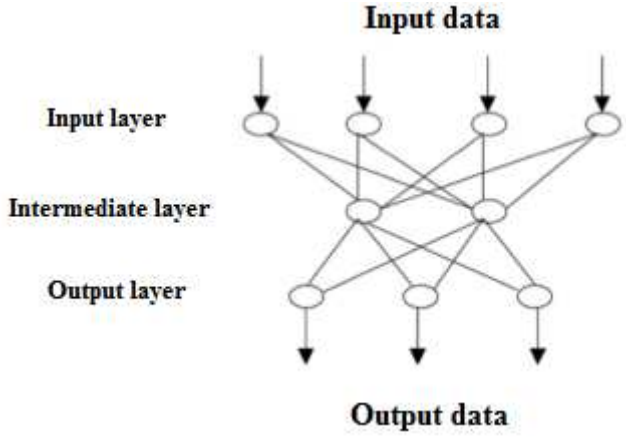

Figure 2. *A simple structure of an artificial neural network (ANN) with input, hidden (intermediate) and output layers*

Random Forest (RF) in performance is one of the most accurate classificatory regression tree-based models. In RF, bootstrap aggregation is used to select many subsamples from the data, generated through a bagging algorithm, a large number of de-correlated regression trees. RF tree predictors are combined in a way that each is dependent on the values of independently sampled random vectors, assuming similar distribution for each tree in the forest (Breiman, 2001).

Classification Tree Analysis (CTA) is a supervised non-parametric statistical classification approach based on binary recursive partitioning techniques. In CTA, a binary decision (True or False) is made by considering only one of the environmental parameters at each node of the tree. Then the node divides a class into two different subclasses whose purity level increases (Breiman et al., 1984; De'Ath, 2007).

Maximum Entropy (MaxEnt) is a machine learning program based on maximum entropy that estimates the probability distribution for species occurrence based on environmental constraints. It requires species presence data only (not absence) and environmental variable (continuous or categorical) layers for the study area (Phillips et al., 2006). MaxEnt is known as one of the most accurate methods used most extensively for predicting the geographical distribution of animal and plant species (Phillips et al., 2006, 2009).

The ensemble map represents the averaging of the projections made by different models (Marmion et al., 2009). The ensemble approach decreases the uncertainty of each model predictions by simultaneous assessment of the results obtained by the different models (Araújo and New, 2007; Amiri et al., 2020). The ensemble maps were achieved by combining the binary habitat maps from the five individual models into a single map. In this case, *Se* which is called 'consensus suitability' in BiodiversityR is calculated as the weighted mean of suitabilities obtained from single models (*Si*) (*Equation 2*). This allows obtaining more robust predictions and estimating the variability across techniques (Buisson et al., 2010).

$$S_e = \frac{\sum_i^n W_i S_i}{\sum_i^n W_i} \qquad \text{(Eq.2)}$$

http://www.aloki.hu ● ISSN 1589 1623 (Print) ● ISSN 1785 0037 (Online)
DOI: http://dx.doi.org/10.15666/aeer/2001_153170

where *Si* is the probability surface generated by a single model (*i*); and *Wi* is the weight assigned to a single model (*i*) that was calculated as a ratio of the AUC value of a single model divided by the total AUC values of the five single models (Kindt, 2018).

The employed models required simulated pseudo-absence data on locations where the brown bear is absent. Thus, we randomly generated a collection of pseudo-absence points using the Create Random Point tool in ArcGIS 10.3. In order to create pseudo-absence points not within or near the presence points, a random sampling plan was applied that excluded the buffer zone of 2.5 km around the presence points.

In the predictive phase of modelling, each of the modelling methods generates an estimate of probability of the species presence ranging from 0 to 1 where 0 stands for the lowest probability and 1 stands for the highest probability corresponding to the probability that a pixel is a favorable habitat for the species. Ranges were then classified into four probability classes using an equal interval classification scheme as follows: low suitability (0 - 0.25), moderate suitability (0.25 - 0.5), good suitability (0.5 - 0.75), and high suitability (0.75 - 1) to interpret easily.

Modelling evaluation

Statistical evaluations of SDM predictions have generally been performed through the true skill statistic (TSS) and the area under the receiver operating characteristic (ROC) curve (AUC). AUC plots the accuracy of the predicted presence (sensitivity) against the accuracy of predicted absence (1 − specificity) (Allouche et al., 2006). Sensitivity (*Equation 3*) is the probability that a model correctly classifies the presence data (positive rate in the positive results) and specificity (*Equation 4*) represents the probability of classifying correctly the absence data points (negative rate in the negative results) (Ray et al., 2016).

$$Sensitivity = \frac{a}{(a+b)} \quad \text{(Eq.3)}$$

where *a* is the number of cells where the models predict presence correctly (true positive) and *b* is the number of cells in which the species was not found although presence was predicted by the model (false positive; commission error).

$$Specificity = \frac{d}{(d+c)} \quad \text{(Eq.4)}$$

where *d* is the number of cells where the models predict absence correctly (true negative) and *c* denotes the number of cells in which the species was found although absence was predicted by the model (false negative; omission error).

TSS considers both omission and commission errors and varies from −1 to +1 in which +1 exhibits the total agreement and 0 or less denote that the model's predictability is random. TSS values are categorized as follows: 0 - 0.4 = failing, 0.4 - 0.55 = poor, 0.55 - 0.7 = fair, 0.7 - 0.85 = good, 0.85 - 1 = excellent (Allouche et al., 2006) (*Equation 5*):

$$TSS = ad - \frac{bc}{(a+c)+(b+d)} = Sensitivity + Specificity \quad \text{(Eq.5)}$$

AUC value ranges between 0.5 - 1 in which values around 0.5 show that the model's performance is random and 1 represent a perfect performance. Evaluation criteria for

http://www.aloki.hu ● ISSN 1589 1623 (Print) ● ISSN 1785 0037 (Online)
DOI: http://dx.doi.org/10.15666/aeer/2001_153170

AUC are as follows: 0.5 - 0.6 = poor, 0.6 - 0.7 = fair, 0.7 - 0.8 = good, 0.8 - 0.9 = very good, 0.9 - 1.0 = excellent (Swets, 1988).

Variable selection is one of the most biological-based decisions in SDM which helps us to bring the more informative variables into the modelling. Unsuitable variable selection may lead to misleading model projections (Velez-Liendo et al., 2013). Two scenarios, that represent two common approaches to variable selection, were run for the species using different sets of predictor variables and to obtain a potential distribution map with the highest accuracy. In the first scenario bioclimatic variables which are identified as the most widely employed set of variables in SDM (Porfirio et al., 2014) as well as NDVI, and in the second scenario all twenty-six variables including bioclimatic variables, physiographic variables, NDVI, and anthropogenic factors were used.

Species response curve

After evaluating the models and finding the model with the highest efficiency, response curves of the species to the environmental variables were drawn, and relationships between the habitat suitability and the input variables were assessed. Response curve is an essential part of SDM and plots species presence data in relation to environmental variations. The range between the upper and lower boundaries of ecological conditions in the species' response curve is identified as the species ecological niche (Jongman et al., 1995; Gégout and Krizova, 2003).

Results

Models accuracy assessment

Table 2 compares the performance of the modelling under the scenarios. It is apparent from the table that achieved accuracy of the models were good to excellent. Among the employed modelling approaches under both scenarios, the ensemble modelling performed best with AUC values of 0.99. Among the individual models, GLM and MaxEnt had the best predictability based on accuracy statistics. However, CTA algorithm ranked the lowest with AUCs of 0.92 and 0.88 under scenarios I and II, respectively (*Table 2*).

Table 2. *Accuracy statistics used to evaluate applied model's performance. Values are averages over 10 replicate runs*

	Scenario I				**Scenario II**			
	TSS	**AUC**	**Sensitivity**	**Specificity**	**TSS**	**AUC**	**Sensitivity**	**Specificity**
GLM	0.94	0.97	100	93.64	0.92	0.97	98	94.32
ANN	0.92	0.96	100	92.48	0.83	0.92	93	90.08
RF	0.88	0.95	99	89.54	0.91	0.96	100	90.96
CTA	0.83	0.92	90	93.5	0.76	0.88	84	92.58
MaxEnt	0.94	0.97	100	93.64	0.93	0.97	100	92.62
Ensemble	0.96	0.99	100	96.35	0.98	0.99	100	98.05

According to *Table 2* mean accuracy under scenario I was higher when compared to under scenario II. These higher mean AUC ratios highlight the effectiveness of climatic variables for the prediction of species habitat. Analysis of the relative importance of environmental variables showed that under scenario I, Bio-04, Bio-03, Bio-08, Bio-14,

http://www.aloki.hu ● ISSN 1589 1623 (Print) ● ISSN 1785 0037 (Online)
DOI: http://dx.doi.org/10.15666/aeer/2001_153170

and NDVI contributed most to the performance of our models with 31.58, 27.35, 21.97, 17.15, and 1.95 percent contribution, respectively (*Table 3*).

Table 3. *Percent contribution of predictors under scenario I. Values shown are averages over 10 replicate runs*

	GLM	ANN	RF	CTA	MaxEnt	Ensemble
Bio14	20.98	17.15	3.96	21.18	22.49	17.15
Bio3	30.07	35.96	16.63	24.36	29.72	27.35
Bio4	32.81	29	33.98	32.94	29.15	31.58
Bio8	16.1	17.7	36.95	21.06	18.06	21.97
NDVI	0.04	0.19	8.48	0.46	0.58	1.95

Under scenario II, Bio4 was the most impacting factor for species distribution with 22.43% contribution rate. The other four environmental factors affecting species distribution include distance to village (17.05%), Bio3 (15.16%), and Bio14 (10.6%) (*Table 4*).

Table 4. *Percent contribution of predictors under scenario II. Values shown are averages over 10 replicate runs*

	GLM	ANN	RF	CTA	MaxEnt	Ensemble
Elevation	2.28	12.82	14.88	0	3.4	6.67
Aspect	2.69	8.26	6.33	1.42	6.28	5
Bio14	10.13	13.93	0.45	14.16	14.32	10.6
Bio3	16.96	15.11	7.25	12.28	24.2	15.16
Bio4	17.78	10.6	23.15	39.87	20.75	22.43
Bio8	4.3	13.43	7.45	0	4.41	5.92
NDVI	1.47	0.13	9.11	0	1.08	2.36
Distance to road	8.34	7.73	6.59	6.49	1.56	6.14
Slope	1.08	2.8	6.58	0	2.64	2.62
Distance to village	20.68	8.64	13.09	25.78	17.08	17.05
Distance to river	14.29	6.55	5.12	0	4.28	6.05

Species distribution by different scenarios

The habitat suitability map indicated that a vast region within the study area has low suitability for brown bear. The species suitable habitats were distributed along the Zagros oak-dominated forests where because of higher altitude weather is characterized by a higher precipitation than the whole region's mean values. Spatial distribution of brown bear projected by the models and under scenarios I and II are displayed in *Figure 3* and *Figure 4*, respectively. It is apparent from *Figure 2* that different models even with nearly equal AUC value projects the habitat suitability and potential habitats differently.

Among the climatic factors, under both scenarios Bio-04, Bio-03, and Bio-14 variables were recognized as the most influential parameters in the modelling process. The species' response curves to the most important predictors are shown in *Figure 4*.

Bio3 (Isothermality) quantifies how extensively the day-to-night temperatures oscillate relative to the summer-to-winter (annual) oscillations.

http://www.aloki.hu ● ISSN 1589 1623 (Print) ● ISSN 1785 0037 (Online)
DOI: http://dx.doi.org/10.15666/aeer/2001_153170

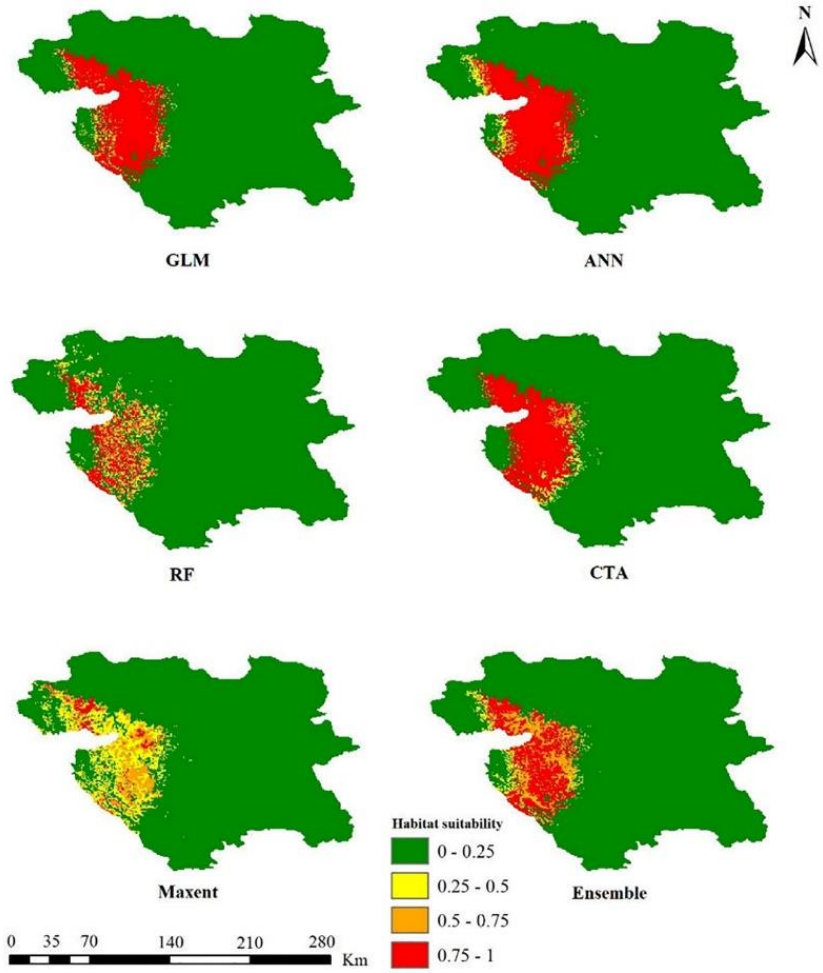

Figure 3. *Potential distribution maps for brown bear modelled using GLM, ANN, RF, CTA, MaxEnt, and Ensemble under scenario I. Values range from 0 to 1 where 0 represent sites with the lowest suitability and 1 represent sites with the highest suitability*

According to the related response curve, brown bear shows a preference for regions with isothermality of less than 34 and habitat suitability was lowest when it is higher than 37. In other words, the species prefers smaller level of temperature variability within an average month relative to the year.

Bio4 is defined as the amount of temperature variation over a given year (or averaged years) based on the standard deviation (variation) of monthly temperature averages. According to the species response curve to this variable, maximum habitat suitability was observed when temperature seasonality is higher than 9500. Further, a positive relationship was observed between occurrence records and the variable so that the probability of brown bear presence increases as the temperature seasonality increases.

Bio14 is defined as the total precipitation in the driest month. As the curve shows this variable is negatively correlated with distribution of the species. The maximum presence of the species occurs in regions where precipitation of the driest month is lower than 0.5 mm and habitat suitability drastically decreases and then stabilizes as the precipitation of driest month rises. Response curve of brown bear to distance to villages indicates that a high probability of occurrence of this species is in proximity to villages (*Fig. 5*).

http://www.aloki.hu ● ISSN 1589 1623 (Print) ● ISSN 1785 0037 (Online)
DOI: http://dx.doi.org/10.15666/aeer/2001_153170

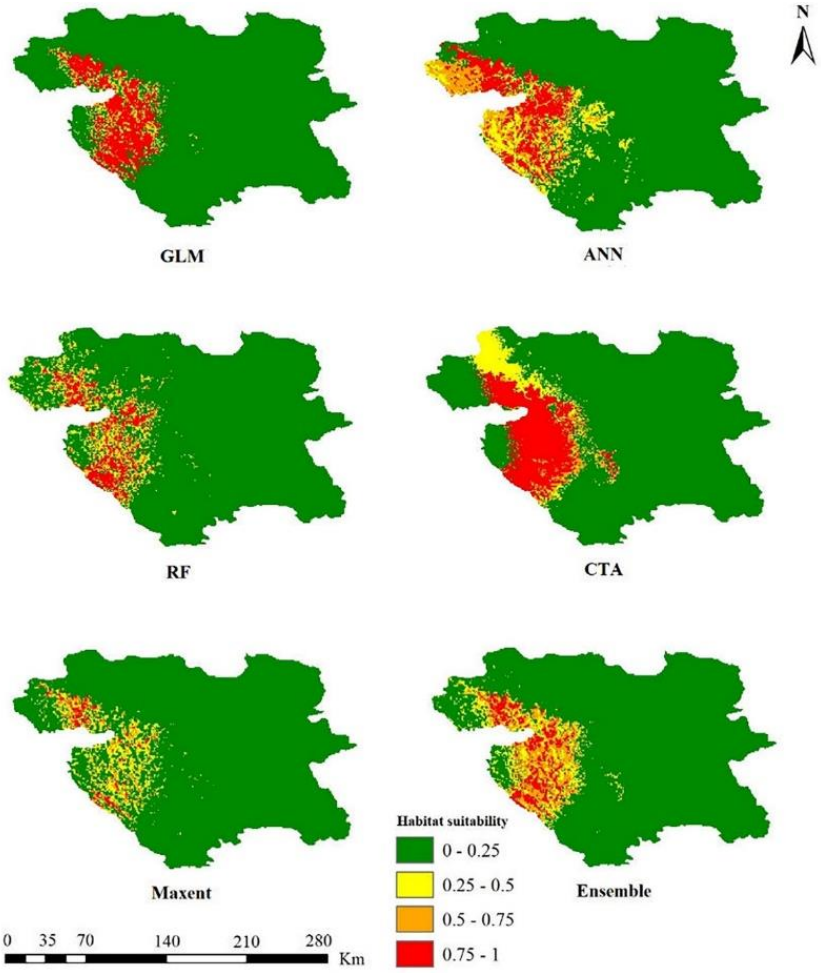

Figure 4. *Potential distribution maps for brown bear modelled using GLM, ANN, RF, CTA, MaxEnt, and Ensemble under scenario II. Values range from 0 to 1 where 0 represents the sites with the lowest suitability and 1 represents the sites with the highest suitability*

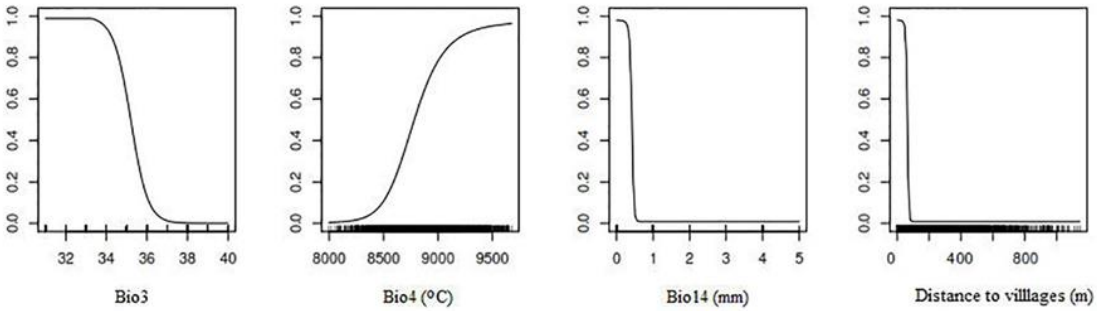

Figure 5. *Relationships between environmental predictor variables and the probability of presence of brown bear in Kurdistan, Iran. Vertical axis exhibits the projected values of habitat suitability, and horizontal axis exhibits the value of environmental factor*

http://www.aloki.hu ● ISSN 1589 1623 (Print) ● ISSN 1785 0037 (Online)
DOI: http://dx.doi.org/10.15666/aeer/2001_153170

Discussion

In this study modelling potential sites for brown bear in Kurdistan Province was performed using five different algorithms and performance of the algorithms was compared with each other. This kind of comparison enables us to find and take advantage of the most efficient methods that can provide more accurate and credible results. We found that different algorithms despite of having the same AUC value projected the potential habitat differently. Amiri et al. (2020) also have confirmed the point of view that the accuracy of projections could be fundamentally different among SDMs. In this matter, the ensemble approach revealed the lowest error to delineate suitable habitat of the species in the regions which is in line with results of Shabani et al. (2016). After the ensemble approach, GLM and MaxEnt had the most accurate performance. A study conducted by Shabani et al. (2016) showed similarly that GLM and MaxEnt among five modelling algorithms had the most accurate performance. The reason could be explained by the fact that MaxEnt works based on presence-background data instead of presence-absence data and most importantly, does not presume that background data precludes the probability of occurrence (Evangelista et al., 2008). CTA was recognized as the model with the weakest predictability, which is in line with the result of Marmion et al. (2009).

Response curves of the species to the variables as well as the relationship between predictor variables and habitat suitability were obtained based on observations in the study area. In our study bioclimatic variables found to be more important in the species distribution when compared to physiographic parameters. Hemami et al. (2015), also introduced climatic parameters as the most effective determinants in distribution of brown bear. We found that isothermality, temperature seasonality, and precipitation of driest month variables may challenge the distribution of brown bear by potential effects. These effects are predicted to trigger shifts in the species distribution and threatening its viability due to habitat loss (Parmesan, 2006).

It could be understood from the response curve of the species to precipitation of driest month that brown bear could be observed more frequently during the dry period. Precipitation and availability of water are essential for brown bear as low precipitation leads to changes in plant community and biomass in the following months. One reason may be that brown bear become more visible during the driest month first because of less vegetation and the fact that they have to move around to find higher quality habitats (Su et al., 2018). Another reason could be that the dry period leads to a concentration in the brown bear population in response to lack of water. Doan-Crider et al. (2017) stated that in dry periods occurrence frequency of black bear (*Ursus americanus*) and the concentration of this species around water sources increases.

We also investigated the effect of anthropogenic disturbance on habitat suitability by employing distance to village variable in the modelling. Kouchali et al. (2019) modelled spatial distribution of brown bear in Alborz Forests and concluded that suitability of habitat decreases with increasing distance to village that is in line with results of present study. However, Almasieh et al. (2019) modelled habitat suitability for brown bear in the northern Zagros Forests along the Iran-Iraq border and found that there is a direct relationship between the probability of presence and distance from village which is against results of present study. The reason could be because of employing higher number of the occurrence records in or around the villages in the current study due to higher sampling density closer to villages. This emphasizes the importance of even sampling effort across the study area. Previous studies provided many reasons for higher bear presence in proximity to humans such as (1) naive behavior or lack of experience in young

http://www.aloki.hu ● ISSN 1589 1623 (Print) ● ISSN 1785 0037 (Online)
DOI: http://dx.doi.org/10.15666/aeer/2001_153170

brown bears with people (Kaczensky et al., 2006), (2) high mobility of the species in combination with its nocturnal activity peaks (Mueller et al., 2004), and, (3) because of the high-quality and high-calorie foods that are provided by humans. Despite wildland foods being available, bears may prefer garbage, fruit trees in orchards, honey, and field crops as high-quality and high-calorie food sources available in and around villages (Fahimi et al., 2018).

Originally brown bears avoid humans (Støen et al., 2015); but due to forest degradation, climate and land cover change and consequently habitat loss, natural food sources for brown bear may become insufficient and lead to incidence of this species moving to anthropogenic areas in search of foods like garbage, fruit trees, livestock, and bee yards (Rodriguez et al., 2007; Yousefi, 2016). Any loss of habitat especially within protected areas may result in brown bears moving out of the protected habitat or illegal hunting area and encounter with human. So it is vital to upgrade distribution of protected habitats to enhance species conservation under climate change (Hannah et al., 2007). Large scale forest and habitat degradation in the Zagros Forests during the last decades is shown in different studies as following. Henareh-Khalyani et al. (2014) found that because of unemployment and poverty in a part of the northern Zagros Forests in Kurdistan Province people overexploited the forests which led to a decrease in area of productive and arable lands. Other studies also showed that forest area in Kurdistan Province decreased recently mainly because of agricultural and residential expansion (Yousefi et al., 2011), and habitats of other species like Persian squirrel (*Sciurus anomalus*) have been lost (Sadeghi, 2014). Anthropogenic pressure in human-modified landscapes may intensify negative impacts of climate change (Maiorano et al., 2011). Henareh-Khalyani et al. (2013) revealed that climate change and population growth in urbans are main causes of the Zagros Forests degradation. Aryal (2011) showed that food availability did affect the home range of Asiatic black bears (*Ursus thibetanus*). This has resulted in increasing human-bear coexistence and finally a higher probability of human-bear conflicts and bear mortalities. Gutleb and Ziaie (1999) emphasized on the importance of management plans to mitigate such conflicts in the Zagros Forests. Several studies conducted on black bear in the south of Iran showed that in response to habitat degradation and scarcity of natural foods human-bear conflicts have increased and black bears have been frequently killed by locals (Gutleb and Ziaie, 1999; Ghadirian et al., 2017). A similar increase in human-bear conflict has been reported in North America after the reduction of white bark pine (*Pinus albicaulis*) forests on which grizzly bear relied particularly after mast seed production (Schrag et al., 2008). Degradation and destruction of forests makes them a less secure habitat and thus leaves brown bears more exposed to hunters.

Conclusion

The Zagros Forests are currently considered as rapidly changing and being degraded forests. Oak trees are slow growing plants and take decades to mature making oak forests susceptible to destruction. In the study area, local people are strongly depending on forests and recently anthropogenic disturbances have adversely affected habitat suitability for low-density brown bear making environmental studies necessary for the conservation of this species. In the present study, we found that brown bear distribution is attributed to bioclimatic variables representing impact of future meteorological conditions on this species habitat. Distance to village variable proved to be a key anthropogenic parameter

http://www.aloki.hu ● ISSN 1589 1623 (Print) ● ISSN 1785 0037 (Online)
DOI: http://dx.doi.org/10.15666/aeer/2001_153170

in the distribution of the species and indicated that a major portion of brown bear populations overlap with residential areas resulting in human-bear conflicts. Further land use change and forest destruction especially due to the development of gardens, agricultural lands, and residential areas, as well as climate change would increase this conflict in the future. This conflict raises conservation concerns and magnifies the importance of habitat conservation programs and also human-bear conflict management plans. These plans should include helping local communities to reduce or compensate economic losses caused by brown bear as well as enhancing people's awareness. Eventually, large-scale conservation efforts and further studies in the Zagros region should be performed to ensure the long-term viability of brown bear and to protect habitats that can support a whole range of species, of which some may be threatened but less in focus of conservation actions.

REFERENCES

[1] Allouche, O., Tsoar, A., Kadmon, R. (2006): Assessing the accuracy of species distribution models: prevalence, kappa, and the true skill statistics (TSS). – Journal of Applied Ecology 43: 1223-1232.

[2] Almasieh, K., Rouhi, H., Kaboodvandpour, S. (2019): Habitat suitability and connectivity for the brown bear (*Ursus arctos*) along the Iran-Iraq border. – European Journal of Wildlife Research 65(4).

[3] Amiri, M., Tarkesh Esfahani, M., Jafari, R., Jetschke, G. (2020): Bioclimatic variables from precipitation and temperature records vs. remote sensing-based bioclimatic variables: which side can perform better in species distribution modeling? – Ecological informatics 57: 101060.

[4] Araújo, M. B., New, M. (2007): Ensemble forecasting of species distributions. – Trends in Ecology and Evolution 22: 42-46.

[5] Araújo, M. B., Alagador, D., Cabeza, M., Nogués-Bravo, D., Thuiller, W. (2011): Climate change threatens European conservation areas. – Ecology Letters 14: 484-492.

[6] Arsalani, M., Azizi, G., Bräuning, A. (2015): Dendroclimatic reconstruction of May-June maximum temperatures in the central Zagros Mountains, western Iran. – International Journal of Climatology 35(3): 408-416.

[7] Aryal, A. (2011): Cultural and Religious Beliefs Pose Challenges for Bear Conservation in Nepal. – International Bear News 20(1): 12-14.

[8] Beier, P., Majka, D., Spencer, W. D. (2008): Forks in the road: choices in procedures for designing wildland linkages. – Conservation Biology 22(4): 836-851.

[9] Berry, P. M., Dawson, T. P., Harrison, P. A., Pearson, R. G. (2002): Modelling potential impacts of climate change on the bioclimatic envelope of species in Britain and Ireland. – Global Ecology and Biogeography 11: 453-462.

[10] Breiman, L. (2001): Random forests. – Machine Learning 45: 5-32.

[11] Breiman, L., Friedman, J., Stone, C. J., Olshen, R. A. (1984): Classification and regression trees. – Chapman and Hall/CRC press, London.

[12] Buisson, L., Thuiller, W., Casajus, N., Lek, S., Grenouillet, G. (2010): Uncertainty in ensemble forecasting of species distribution. – Global Change Biology 16: 1145-1157.

[13] Can, Ö. E., Cruze, N. D., Garshelis, D. L., Beecham, J. J., Macdonald, D. W. (2014): Resolving human–bear conflict: a global survey of countries, experts and key factors. – Conservation Letters 7: 501-513.

[14] De'Ath, G. (2007): Boosted trees for ecological modeling and prediction. – Ecology Letters 88: 243-251.

[15] Department of Environment (2014): Conservation of biodiversity in the central Zagros landscape conservation zone. Zagros project office. – Zagros project office. Tehran, Iran.

http://www.aloki.hu ● ISSN 1589 1623 (Print) ● ISSN 1785 0037 (Online)
DOI: http://dx.doi.org/10.15666/aeer/2001_153170

[16] Doan-Crider, D. L., Tri, A. N., Hewitt, D. G. (2017): Woody cover and proximity to water increase American black bear depredation on cattle in Coahuila, Mexico. – Ursus 28(2): 208-217.
[17] Elith, J., Leathwick, J. R. (2009): Species distribution models: ecological explanation and prediction across space and time. – Annual Review of Ecology, Evolution, and Systematics 40: 677-697.
[18] Evangelista, P. H., Kumar, S., Stohlgren, T. J., Jarnevich, C. S., Crall, A. W., Norman, J. B., Barnet, D. T. (2008): Modelling invasion for a habitat generalist and a specialist plant species. – Diversity and Distributions 14(5): 808-817.
[19] Fahimi, H., Qashqaei, A. T., Chalani, M., Asadi, Z., Broomand, S., Ahmadi, N., Yusefi, G. H. (2018): Evidence of seed germination in scats of the Asiatic Black Bear (*Ursus thibetanus*) in Iran (Mammalia: Carnivora). – Zoology in the Middle East 64(2): 182-184.
[20] Gallo, C. (2015): Artificial neural networks tutorial. – Encyclopedia of information science and technology: third edition, pp. 179-189.
[21] Gégout, J.-C., Krizova, E. (2003): Comparison of indicator values of forest understory plant species in Western Carpathians (Slovakia) and Vosges Mountains (France). – Forest Ecology and Management 182: 1-11.
[22] Ghadirian, T., Qashqaei, A. T., Soofi, M., Abolghasemi, H., Ghoddousi, A. (2017): Diet of Asiatic black bear in its westernmost distribution range, southern Iran. – Ursus 28: 15-19.
[23] Ghazanfari, H. (2003): Evaluation of growth and changes in diameter distribution of *Quercus libani* and *Quercus infectoria* stands to present forest adjustment pattern in Baneh region (Case study: Hawarakhol). – PhD Thesis. University of Tehran, Iran. (In Persian).
[24] Gutleb, B., Ziaie, H. (1999): On the distribution of the Brown Bear, (*Ursus arctos*), & the Asiatic Black Bear, (*Ursus thibetanus*), in Iran. – Zoology in the Middle East 18(1): 5-8.
[25] Gutleb, B., Ghaemi, R. A., Kusak, J. (2002): Brown bear in Iran. – International bear news 11-20.
[26] Hanafi, A., Hatammi, I. (2013): Producing climate map for Kurdistan Province using information technology system. – Scientific-research quarterly of geographical data (SEPEHR) 22(87): 24-28. (In Persian).
[27] Hannah, L., Midgley, G., Andelman, S., Araujo, M., Hughes, G., Martinez-Meyer, E., Pearson, R., Williams, P. (2007): Protected area needs in a changing climate. – Frontiers in Ecology and the Environment 5: 131-138.
[28] Hemami, M. R., Esmaeili, S., Soffianian, A. R. (2015): Predicting the Distribution of Asiatic Cheetah, Persian Leopard and Brown Bear in Response to Environmental Factors in Isfahan Province. – Iranian Journal of Applied Ecology 4(13): 51-64.
[29] Henareh Kalyani, A., Mayer, A. L., Falkowski, M. J., Muralidharan, D. (2013): Deforestation and landscape structure changes related to socioeconomic dynamics and climate change in Zagros forests. – Journal of Land Use Science 8: 321-340.
[30] Henareh Khalyani, J., Namiranian, M., Heshmatol Vaezin, S. M., Feghhi, J. (2014): Development and evaluation of local communities incentive programs for improving the traditional forest management: A case study of Northern Zagros forests, Iran. – Journal of Forestry Research 25: 205-210.
[31] Hoekstra, T. W., Shachak, M. (1999): Arid Lands Management: Toward Ecological Sustainability. – Urbana University of Illinois Press.
[32] Hosmer, D. W., Lemeshow, S. (2000): Applied Logistic Regression. – Wiley, New York.
[33] Hwang, M. H., Garshelis, D. L., Wu, Y. H., Wang, Y. (2010): Home ranges of Asiatic black bears in the Central Mountains of Taiwan: Gauging whether a reserve is big enough. – Ursus 21(1): 81-96.
[34] Jazirehi, M. H., Rostaghi, E. M. (2003): Silviculture in Zagros. – University of Tehran Press, Tehran.
[35] Jongman, R. H. G., Ter Break, C. J. F., Van Tongeren, O. F. R. (1995): Data analysis in community and landscape ecology (2th edition). – Cambridge University Press, Cambridge.

http://www.aloki.hu ● ISSN 1589 1623 (Print) ● ISSN 1785 0037 (Online)
DOI: http://dx.doi.org/10.15666/aeer/2001_153170

[36] Kaczensky, P., Huber, D., Knauer, F., Roth, H., Wagner, A., Kusak, J. (2006): Activity patterns of brown bears (*Ursus arctos*) in Slovenia and Croatia. – Journal of Zoology 269(4): 474-485.
[37] Kindt, R. (2018): Ensemble species distribution modelling with transformed suitability values. – Environmental Modelling and Software 100: 136-145.
[38] Kobler, A., Adamic, M. (2000): Identifying brown bear habitat by a combined GIS and machine learning method. – Ecological Modelling 135: 291-300.
[39] Kouchali, F., Nezami, B., Goshtasb, H., Rayegani, B., Ramezani, J. (2019): Brown Bear (*Ursus arctos*) habitat suitability modelling in the Alborz Mountains. – Internaional Journal of Environmenal Science and Bioengineering 12: 45-54.
[40] Maiorano, L., Falcucci, A., Zimmermann, N. E., Psomas, A., Pottier, J., Baisero, D., Rondinini, C., Guisan, A., Boitani, L. (2011): The future of terrestrial mammals in the mediterranean basin under climate change. – Philosophical Transactions of the Royal Society B: Biological Sciences 366: 2681-2692.
[41] Marmion, M., Luoto, M., Heikkinen, R. K., Thuiller, W. (2009): The performance of state-of-the-art modelling techniques depends on geographical distribution of species. – Ecological Modeling 220: 3512-3520.
[42] McCullagh, P., Nelder, J. A. (1989): Generalized Linear Models. – Chapman and Hall, London.
[43] McLellan, B. N., Proctor, M. F., Huber, D., Michel, S. (IUCN SSC Bear Specialist Group). (2016): Brown bear (*Ursus arctos*) isolated populations (supplementary material to *Ursus arctos* redlisting account). – The IUCN red list of threatened species.
[44] Mirabolfathy, M., Groenewald, J. Z., Crous, P. W. (2011): The occurrence of characoal disease caused by Biscogniauxia mediterranea on chestnut-leaved oak (*Quercus castaneifolia*) in the Golestan Forests of Iran. – Plant Disease 95: 876.
[45] Moraitis, M. L., Valavanis, V. D., Karakassis, I. (2019): Modelling the effects of climate change on the distribution of benthic indicator species in the Eastern Mediterranean Sea. – Science of the Total Environment 667: 16-24.
[46] Mueller, C., Herrero, S., Gibeau, M. L. (2004): Distribution of subadult grizzly bears in relation to human development in the Bow River Watershed, Alberta. – Ursus 15: 35-47.
[47] Parmesan, C. (2006): Ecological and evolutionary responses to recent climate change. – Annual Review of Ecology, Evolution, and Systematics 37: 637-669.
[48] Phillips, S. J., Anderson, R. P., Schapire, R. E. (2006): Maximum entropy modeling of species geographic distributions. – Ecological Modeling 190: 231-259.
[49] Phillips, S. J., Dudík, M., Elith, J., Graham, C. H., Lehmann, A., Leathwick, J., Ferrier, S. (2009): Sample selection bias and presence-only distribution models: Implications for background and pseudo-absence data. – Ecological Applications 19: 181-197.
[50] Porfirio, L. L., Harris, R. M. B., Leofroy, E. C., Hugh, S., Gould, S. F., Lee, G., Bindoff, N. L., Mackey, B. (2014): Improving the use of species distribution models in conservation planning and management under climate change. – PLoS ONE 9(11): e113749.
[51] Ray, D., Behera, M. D., Jacob, J. (2016): Predicting the distribution of rubber trees (*Hevea brasiliensis*) through ecological niche modeling with climate, soil, topography and socioeconomic factors. – Ecological Research 31: 75-91.
[52] Rodriguez, C., Naves, J., Fernandez-Gil, A., Obeso, J. R., Delibes, M. (2007): Long-term trends in food habitats of a relict brown bear population in northern Spain: The influence of climate and local factors. – Environmental Conservation 34: 36-44.
[53] Sadeghi, M. (2014): Habitat change detection of Persian squirrel (*Sciurus anomalus*) in Kurdistan province. – MSc Thesis. Isfahan University of Technology, Iran. (In Persian).
[54] Sagheb-Talebi, Kh., Sajedi, T., Yazdian, F. (2003): Forests of Iran, Tehran. – Research Institute of Forests and Rangelands of Iran: 56. (In Persian).
[55] Schrag, A. M., Bunn, A. G., Graumlich, L. J. (2008): Influence of bioclimatic variables on tree-line conifer distribution in the Greater Yellowstone Ecosystem: Implications for species of conservation concern. – Journal of Biogeography 35: 698-710.

http://www.aloki.hu ● ISSN 1589 1623 (Print) ● ISSN 1785 0037 (Online)
DOI: http://dx.doi.org/10.15666/aeer/2001_153170

[56] Shabani, F., Kumar, L., Ahmadi, M. (2016): A comparison of absolute performance of different correlative and mechanistic species distribution models in an independent area. – Ecology and Evolution 6(16): 5973-5986.
[57] Sharifi, M., Hadidi, M., Vessali, E., Mosstafakhani, P., Taheri, K., Shahoie, S., Khodamoradpour, M. (2009): Integrating multi-criteria decision analysis for a GIS-based hazardous waste landfill sitting in Kurdistan Province, western Iran. – Waste Management 29: 2740-2758.
[58] Støen, O. G., Ordiz, A., Evans, A. L., Laske, T. G., Kindberg, J., Fröbert, O., Swenson, J. E., Arnemo, J. M. (2015): Physiological evidence for a human-induced landscape of fear in brown bears (*Ursus arctos*). – Physiology and Behavior 152: 244-248.
[59] Su, J., Aryal, A., Hegab, I. M., Shrestha, U. B., Coogan, S. C. P., Sathyakumar, S., Dalannast, M., Dou, Z., Suo, Y., Dabu, X., Fu, H., Wu, L., Ji, W. (2018): Decreasing brown bear (Ursus arctos) habitat due to climate change in Central Asia and the Asian Highlands. – Ecology and Evolution 8(23): 11887-11899.
[60] Swenson, J. E., Dahle, B., Gerstl, N., Zedrosser, A. (2000): Action Plan for the conservation of the Brown Bear (*Ursus arctos*) in Europe, Conventiononthe Conservation of European Wildlife and Natural Habitats (Bern Convention). – Nature and Environment 114. Council of Europe Publishing, Strasbourgh, France.
[61] Swets, J. (1988): Measuring the accuracy of diagnostic systems. – Science 240: 1285-1293.
[62] Thuiller, W., Araújo, M. B., Lavorel, S. (2003): Generalized models vs classification tree analysis: predicting spatial distributions of plant species at different scales. – Journal of Vegetation Science 14: 669-680.
[63] Thuiller, W., Lafourcade, B., Engler, R., Araújo, M. B. (2009): BIOMOD - A platform for ensemble forecasting of species distributions. – Ecography 32: 369-373.
[64] Treves, A., Naughton-treves, L., Mladenoff, D. J., Harper, E. K., Mladenoff, D. J., Rose, R. A., Sickley, T. A., Wydeven, A. P. (2004): Predicting human carnivore conflict: a spatial model derived from 25 years of data on wolf predation on livestock. – Conservation Biology 18: 114-125.
[65] Tripathi, B. K. (2015): High Dimensional Neurocomputing - Growth, Appraisal and Applications. – Springer, Germany.
[66] United States Geological Survey (2020): Earthexplorer. – Available at: http://www.earthexplorer.usgs.gov (accessed: 28 November 2020).
[67] Velez-Liendo, X., Strubbe, D., Matthysen, E. (2013): Effects of variable selection on modelling habitat and potential distribution of the Andean bear in Bolivia. – Ursus 24(2): 127-138.
[68] Wang, B., Deverson, E. D., Waters, C., Spessa, A., Lawton, D., Feng, P. Y., Liu, D. L. (2019): Future climate change likely to reduce the Australian plague locust (*Chortoicetes terminifera*) seasonal outbreaks. – Science of the Total Environment 668: 947-957.
[69] Welch, C. A., Keay, J., Kendall, K. C., Robbins, C. T. (1997): Constraints on frugivory by bears. – Ecology 78: 1105-1119.
[70] Willson, M., Gende, S. (2004): Seed Dispersal by Brown Bears, (*Ursus arctos*), in Southeastern Alaska. – The Canadian Field-Naturalist 118(4): 499-503.
[71] Worldclim (2019): Global Climate Data, Version 2 (Free climate data for ecological modeling and GIS). – http://worldclim.org/version2 (accessed 08.02.2020).
[72] Yi, Y. J., Cheng, X., Yang, Z. F., Zhang, S. H. (2016): Maxent modelling for predicting the potential distribution of endangered medicinal plant (H. riparia Lour) in Yunnan, China. – Ecological Engineering 92: 260-269.
[73] Yousefi, G. (2016): Strategic plan for brown bear (*Ursos arctos*) conservation in Iran. – Department of Environment, Iran, Tehran. (In Persian).
[74] Yousefi, S., Moradi, H. R., Hosseini, S. H., Mirzaee, S. (2011): Land use change detection using Landsat TM and ETM+ satellite images over Marivan. – Journal of applied RS and GIS for natural resources 2(3): 97-105.

http://www.aloki.hu ● ISSN 1589 1623 (Print) ● ISSN 1785 0037 (Online)
DOI: http://dx.doi.org/10.15666/aeer/2001_153170

[75] Zanin, M., Palomares, F., Brito, D. (2015): What we (don't) know about the effects of habitat loss and fragmentation on felids. – Oryx 49: 96-106.
[76] Ziaie, H. (2008): A field Guide to the Mammals of Iran. – Iranian wildlife center, Tehran, Iran. (In Persian).

http://www.aloki.hu ● ISSN 1589 1623 (Print) ● ISSN 1785 0037 (Online)
DOI: http://dx.doi.org/10.15666/aeer/2001_153170

INFLUENCE OF FOLIAR NUTRITION ON YIELD AND YIELD COMPONENTS OF DURUM WHEAT (*TRITICUM DURUM* DESF.) GROWN IN SYSTEM OF ORGANIC PRODUCTION

ZEČEVIĆ, V.[1*] – MILENKOVIĆ, S.[2] – BOŠKOVIĆ, J.[3] – ROLJEVIĆ NIKOLIĆ, S.[4] – LUKOVIĆ, K.[5] – ĐORĐEVIĆ, R.[1] – KNEŽEVIĆ, D.[6]

[1]*Institute for Vegetable Crops, Karadjordjeva 71, 11420 Smederevska Palanka, Serbia*

[2]*Faculty of Ecological Agriculture, Educons University, Vojvode Putnika 85-87, 21208 Sremska Kamenica, Serbia*

[3]*Faculty of Economy and Engineering Management, University Business Academy, Cvećarska 2, Novi Sad, Serbia*

[4]*Institute of Agricultural Economics, Volgina 15, 11050 Belgrade, Serbia*

[5]*Centre for Small Grains, Save Kovačevića 31, 34000 Kragujevac, Serbia*

[6]*Faculty of Agriculture, University of Pristina, Kosovska Mitrovica-Lešak, Kopaonička bb Lešak, Kosovo and Metohia, Serbia*

**Corresponding author*
e-mail: vzecevic@institut-palanka.rs

(Received 1st Jul 2021; accepted 28th Oct 2021)

Abstract. This paper examines the effect of foliar nitrogen nutrition on seven durum wheat genotypes produced according to the principles of organic production. The experiments were performed during two growing seasons on organic farm in Čačak, Serbia. Three different N fertilization strategies have been compared: T1- control without N application after the stem elongation stage; T2- foliar N fertilization at the beginning of heading, one spray with 0.3% organic fertilizer Trainer (5% N and 31% amino acids); T3- foliar N fertilization in both stages, heading and anthesis with 0.3% organic fertilizer Trainer (5% N) each. Analysis of grain yield and yield components (number of spikes m^{-2}, number of grains per spike and thousand grain weight (TGW) was performed. The number of spikes per square meter, number of grains $spike^{-1}$, TGW, and grain yield significantly increased ($P \leq 0.01$) with different levels of fertilizers. Foliar fertilization had a significant effect on yield in both growing seasons. Grain yield, on average for all genotypes and years after spraying were 22% (one N treatment), and 54% (two N treatments) higher than in the control. Grain yield was about 26% higher in two N treatments than in one N treatment. Grain yield was positively correlated with other traits (TGW, number of spikes m^{-2} and number of grains/spike).
Keywords: *durum wheat, organic management, N treatment, grain yield, correlations*

Abbreviations: ANOVA, analysis of variance; G, genotype; LSD, least significant difference; T, N treatment; T1, control without N application after the stem elongation stage; T2, foliar liquid N fertilization at the beginning of heading; T3, foliar liquid N fertilization in both stages, heading and anthesis; TGW, thousand grain weight; Y, year.

Introduction

Durum wheat (*Triticum durum* Desf.) is a plant species represented on only 8 to 10% of all wheat growing areas. Despite of its small area, durum wheat is economically important species because of its unique characteristics and end products. Durum wheat grain is characterized by high protein and gluten content which makes it suitable for the

http://www.aloki.hu ● ISSN 1589 1623 (Print) ● ISSN 1785 0037 (Online)
DOI: http://dx.doi.org/10.15666/aeer/2001_171187

production of a variety of food products, such as pasta, couscous, bread, etc. (Rao et al., 2010). Compared to the ordinary wheat, durum has a larger grain of higher absolute mass, a much higher content of yellow pigment, and relatively higher protein inelastic gluten contents which reduces the elasticity of the dough (Li et al., 2013). Pasta is the most common end product of durum wheat consumed in Europe, North America and the former USSR (Mohammadi et al., 2011). Durum wheat is one of the most widespread plant species in arid conditions and Mediterranean environments, where high temperatures limit the productivity of genotypes (Araus et al., 2002), although this condition provides the ability to produce high quality durum.

Creating durum wheat genotypes with increased productivity in arid conditions has been an important aspect of many breeding programs. Durum wheat corresponds to the warmer regions, where annual rainfall of 350-450 mm is concentrated in the vegetative phase, high temperatures after fertilization, less humidity (improves grain quality), occasional showers and prolonged sunny and warm weather in the grain filling phase.

In an organic production system, it is desirable that the varieties possess the following characteristics: efficiency of absorption and use of nutrients from the soil, good competitiveness with weeds, tolerance to climatic and environmental stresses, stability of yield and good quality of products (Lammerts van Bueren et al., 2002; Bošković et al., 2016; Branković et al., 2018). Organic durum wheat production is topical due to the increasing demands of consumers and the food industry for organic products.

Wheat grain yield is influenced by various factors, primarily the genotype characteristics, the soil fertility and the applied agro-technical measures. Studies have shown that nitrogen, in interaction with other elements of the mineral nutrition, is the main carrier of wheat grain yield and quality (Matković et al., 2015). The effect of nitrogen on wheat yield depends on the time of nitrogen application. The application of nitrogen with watering generally increases the yield beyond the degree of tillering, which is the number of spikes and grains per unit area (Langer, 1979). The application of nitrogen between stem elongation and flowering phase increases yield through increasing the percentage of productive tillering and number of grains in the spike. The application of nitrogen in the later stages of development increases yield by increasing grain mass and often by increasing the number of grains per spike (Kostić and Đokić, 1975). Tedone et al. (2014) found that N application efficiency and N recovery efficiency in wheat crops increased when N fertilizer is applied at the stem elongation phase, whereas high amounts of N at sowing time and tillering resulted in poor efficiency.

The application of balanced fertilizers is one of the most important factors for increasing crop yields. In wheat cultivation, the farmers are paying great attention only to N fertilisation but very often P and K application are partially or completely ignored (Arshadullah et al., 2015). Optimal doses of nitrogen for wheat yield change depending on climatic factors, soil fertility, crop rotation, fertilization in the previous period, etc. Favorable climatic performance in the filling phase of the kernels can favor both the accumulation of amidaceous and protein substances so the availability of nitrogen in the soil at this time is critical to the qualitative improvement of the grain (Branković et al., 2015a, 2016; Tedone et al., 2017).

The aim of this paper is investigation of influence of foliar nutrition on yield value and yield components variability in durum wheat grown in system of organic farming production.

http://www.aloki.hu ● ISSN 1589 1623 (Print) ● ISSN 1785 0037 (Online)
DOI: http://dx.doi.org/10.15666/aeer/2001_171187

Materials and methods

Plant material

Seven genotypes were used in the experiment. Three varieties of winter durum wheat Windur (Germany), Žitka, KG Olimpik (Serbia), and four breeding lines KG-28-6, KG-3405-03, KG-43-33-1, and KG-44-3-1 (Serbia) were grown during two growing seasons (2012/2013 and 2013/2014) at certified organic trial parcel which is located in Mršinci, in the Municipality of Čačak, Serbia (20°30' E, 43°48' N, 220 m a.s.l.). Origin of cultivar Windur is Germany, Žitka is the property of the Center for Agricultural and Technological Research, Zaječar (Serbia), and other investigated genotypes were selected in Small Grains Research Centre in Kragujevac (Serbia).

Field trials and methods

The field experiment was conducted in a randomized block design with three replications on plot of 5 m² on the soil which belongs to the clay loam soil type. Experiment was carried out by the organic technology of scientific farming production of wheat. Potato was preceding crop in the first growing season (2012/2013), while bean was preceding in the second year (2013/2014). In autumn, starter fertilization was done with two tons of organic fertilizer *Italpollina* (4:4:4) – 80 kg ha^{-1} of pure nitrogen (N). The soil is cultivated only with rototiller. Sowing was done on November 6, 2012, and in October 25, 2013 with 600 seeds per square meter. The treatment of the crops during the growing seasons respected the principles of the organic farming.

At the tillering stage (in February 2013), crop was fertilized with 500 kg h^{-1} organic fertilizer *Dix 10* (10:3:3) - 50 kg ha^{-1} of pure N. The fertilizers applied are produced at Hello Nature, former Italpollina (Italy). Three different strategies of N application in different phase of plant development have been compared: T1- control without N application after the stem elongation stage; T2- foliar liquid N fertilization at the beginning of heading (Z 52 according to Zadox, 1974), 10 April 2013 and 14 April 2014, one spray with 0.3% organic fertilizer Trainer (5% N and 31% amino acids); T3- foliar liquid N fertilization in both stages heading (Z 52) and anthesis- Z 60 (8 May 2013 and 12 May 2014), two sprays with 0.3% organic fertilizer Trainer according to the commercial recommended rate.

In full maturity stage of wheat, samples were taken from m^{-2} in three replications to determine the yield and yield components in both years. All spikes from m^{-2} were threshed on the Wintersteiger Hege 16 laboratory thresher in Laboratory of Small Grains Research Centre of Kragujevac. Grain yield, number of spikes per square meter, number of grains per spike and thousand grain weight (TGW) were determined. The number of grains per spike was determined from 30 random spikes, which were threshed manually.

Soil analysis

The topsoil samples were taken from the depth 0-30 cm. This depth was chosen as a zone of the most active root systems of observed crops. The samples were taken using a soil drill agrochemical probes. One composite sample represented 20-25 subsamples from random points in each sampling site. The soil samples were air-dried (room temperature), milled and sieved to a particle size of < 2 mm, in accordance with ISO 11464: 2006.

http://www.aloki.hu ● ISSN 1589 1623 (Print) ● ISSN 1785 0037 (Online)
DOI: http://dx.doi.org/10.15666/aeer/2001_171187

Laboratory analysis

All laboratory analyses were performed at the Laboratory for Soil and Agroecology of the Institute of Field and Vegetable Crops, Novi Sad, Serbia, accredited according to the standard ISO/IEC 17025: 2017 (*Fig. 1*). The pH value in 1:2.5 (v/v) suspension of soil in 1 M KCl and H_2O was determined using a glass electrode, in accordance with the ISO method 10390:2005. The hydrolytic acidity values were determined according to Kappen (1929) in calcium acetate solution by titration method. The carbonate content as free $CaCO_3$ was determined by the volumetric method ISO 10693:1995. The organic matter content (OM) was measured by the sulfochromic oxidation method ISO 14235:1998. The total N and S were determined by elemental analysis on the CHNS analyser VARIO El III according to AOAC 972.43 (2000) method. Readily available phosphorus (P_2O_5) and available potassium (K_2O) were extracted by ammonium lactate extraction (AL method), and measured by the means of spectrophotometry and flame photometry respectively (Egner and Riehm, 1955). Particle size distribution in the <2 mm soil fraction was determined by the pipette method (Van Reeuwijk, 2002) and soil texture determined according to International Union of Soil Sciences (IUSS) system of classification of soil particles.

(a) (b) (c) (d)

Figure 1. *Equipment of soil analysis. (a) CHNS elemental analyser for soil total N and S determination. (b) Flame photometer for determination of available potassium in soil. (c) Soil particle size determination by pipet method. (d) Determination of carbonate content in soil by Scheibler's calcimeter, volumetric method*

Based on the analysis of the potential hydrolytic acidity, it was established that the soil on which the experiments were performed belongs to acidic soil. The plots are characterized by a carbonless soil type. The low pH value and low content of free $CaCO_3$ indicate the possibility of calcium deficiency, which at some stages of plant development may cause reduced availability of magnesium, molybdenum and phosphorus. The soil is medium provided with organic matter and belongs to the class of poorly humus soils. This soil is medium supplied with readily available phosphorus and potassium. The tested soil samples have loam, as well as clay texture and belong to clay loam soil class (*Table 1*). According to the Ordinance on Control and Certification in Organic Production in Serbia, a maximum intake of 170 kg N ha^{-1} per year is foreseen for organic agriculture in order to prevent leaching of nitrogen, introduction of heavy metals and harmful organic substances, spread of weeds, pollution of soil by harmful organisms, etc.

Climate data for the tested period

The production of cultivated plants is highly dependent on climatic factors, primarily rainfall and air temperature, which significantly affect the availability and utilization of

http://www.aloki.hu ● ISSN 1589 1623 (Print) ● ISSN 1785 0037 (Online)
DOI: http://dx.doi.org/10.15666/aeer/2001_171187

fertilizers by the plants, and thus the growth and development of the cultivated plants and weeds. We analyzed weather condition (temperature and precipitation) during two year of experiment and during long term period (1992-2010 year) and compared average values of those factors. According to our results, temperature in March and April 2014 (13.5 °C, 16.3 °C, respectively) was significantly higher than in 2013 (6.6 °C, 13.2 °C) and long term period (7.1 °C, 12.0 °C). Other temperatures for growing seasons were similar (*Figs. 2* and *3*). The meteorological parameters were monitored and registered in the Meteorological station located in Fruit Research Institute, Čačak.

Table 1. *Physicochemical analysis of the soil at organic farm*

Parameters	Soil under bean	Soil under potato	Average
pH in KCL	4.30	4.77	4.53
pH in H_2O	5.95	5.84	5.89
Hydrolytic acidity – H (meq/100 g)	11.18	9.73	10.46
$CaCO_3$ (%)	0.00	0.00	0.00
Humus (%)	2.91	2.50	2.70
Content of macronutrients			
Total N (%)*	0.720	0.798	0.76
Available phosphorus P_2O_5 (mg/100 g)	10.0	26.7	18.35
Available potassium K_2O (mg/100 g)	18.6	24.5	21.55
Total S (%)*	1.05	1.24	1.14
Organic matter (%)			
Coarse sand (2-0.2 mm)	9.57	11.31	10.44
Fine sand (0.2-0.02 mm)	40.67	37.89	39.28
Powder (0.02-0.002 mm)	26.56	27.52	27.04
Clay (<0.002 mm)	23.20	23.28	23.24
Texture class	Clay loam	Clay loam	Clay loam

*Determined by elementary analysis after dry combustion

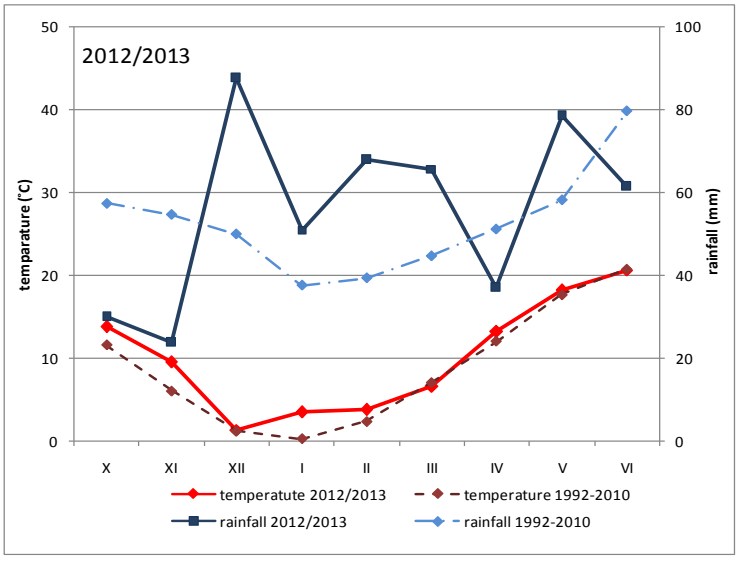

Figure 2. *Average temperatures and total rainfall for each month during 2012/2013 growing season and a long-term period (1992-2010)*

http://www.aloki.hu ● ISSN 1589 1623 (Print) ● ISSN 1785 0037 (Online)
DOI: http://dx.doi.org/10.15666/aeer/2001_171187

Precipitation in January 2014 was only 0.8 mm, which was significantly lower than in 2013 (51 mm) and long term period (37.6 mm). The two growing seasons differed mainly as far as the total rainfall. The total rainfall also differed between two investigated years and long term period. Total precipitation in 2013 was 503 mm, 414 mm in 2014 and for long term period it was 473 mm. In 2012/2013 rainfall was 30 mm higher than long term period and 89 mm higher than 2013. Compared to the multi-year period, in 2013/2014 there was 50 mm less rain. In the period from October to March 2012/2013, there was 326 mm rainfall while in the same period of 2013/2014 there was only 95 mm of rainfall. The 2013/2014 wheat growing season was characterized by high rainfall in May (167.8 mm) and June (149.8 mm), which negatively affected plant health and crop maturity. In March 2014 was no precipitation, which has slowed the growth of wheat plants (*Fig. 3*).

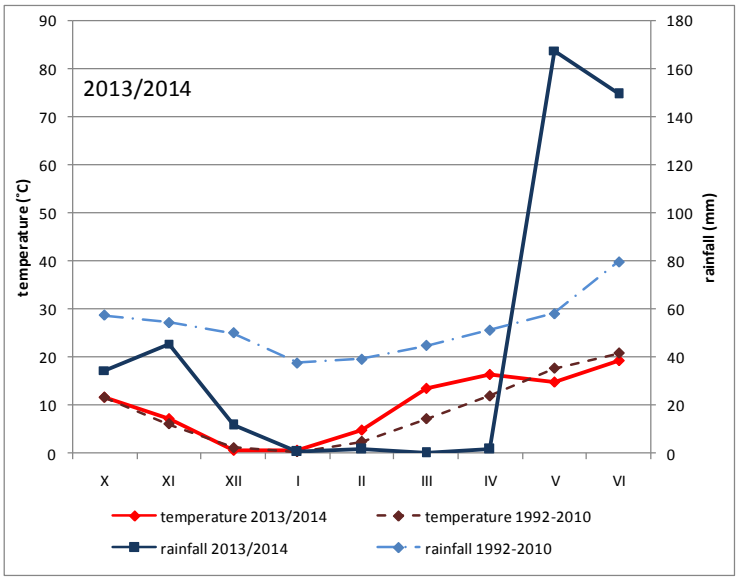

Figure 3. *Average temperatures and total rainfall for each month during 2013/2014 growing season and a long-term period (1992-2010)*

Statistical data processing

All the recorded parameters were compared by means of an analysis of variance (ANOVA) according to a random block system with three factors using the MSTAT-C program (Michigan State University, 1990). The significant differences between the average values were estimated by least significant difference test (LSD). Simple correlations between investigated traits were also calculated using MSTAT-C program.

Results

Mean values for number of spikes m^{-2} of durum wheat are presented in *Table 2*. Cultivar Olimpik had the highest average number of spikes per square meter (341.3). Significant lower number of spikes had cultivar Windur (244.9) and genotype KG-44-3/1 (294.7). The highest values for this component were found with two N foliar treatments in both investigated year (307.67, 323.86, respectively). In 2014, cultivar Olimpik showed the highest value for number of spikes m^{-2} in variant with two N

http://www.aloki.hu ● ISSN 1589 1623 (Print) ● ISSN 1785 0037 (Online)
DOI: http://dx.doi.org/10.15666/aeer/2001_171187

treatments (428.0). Nitrogen had a positive effect on the number of spikes m^{-2}. The number of spikes m^{-2}, average for all genotypes and years, on variant with one N treatment was lower about 3% than in the control, while on variant with two N treatments it was higher 14% than in the control (*Table 2*).

High significant differences were established between genotypes (G), years (Y) and its interaction (G×Y). Applied N treatment (T) also had high significant influence to number of spikes, interaction between year and applied N treatment (Y×T) was highly significant ($P \leq 0.01$). Other interactions (G×T and G×Y×T) were significant ($P \leq 0.05$) (*Table 2*).

Table 2. *Mean values and analysis of variance for number of spikes m^{-2} of durum wheat*

Genotype	Foliar fertilization						Average
	T1		T2		T3		
	2013	2014	2013	2014	2013	2014	
Olimpik	411.7^{ab}	255.7^{f-m}	346.3^{a-e}	247.0^{i-m}	359.0^{a-d}	428.0^{a}	341.3
Windur	320.7^{c-j}	236.0^{klm}	263.0^{f-l}	175.0^{m}	235.3^{lm}	239.7^{j-m}	244.9
Žitka	297.0^{c-l}	265.0^{e-l}	260.3^{f-l}	247.3^{i-m}	373.7^{abc}	251.7^{h-m}	282.5
KG-28-6	330.3^{b-h}	262.7^{f-l}	323.0^{c-i}	278.7^{d-l}	300.7^{c-l}	338.0^{b-f}	305.6
KG-44-3/1	253.0^{h-m}	242.7^{i-m}	318.3^{c-k}	311.3^{c-l}	306.3^{c-l}	336.3^{b-g}	294.7
KG-43-33/1	258.3^{f-l}	248.3^{h-m}	256.7^{f-m}	262.0^{f-l}	284.7^{d-l}	349.3^{a-d}	276.6
KG-3405-03	253.7^{h-m}	255.7^{f-m}	242.3^{i-m}	254.0^{g-m}	294.0^{c-l}	324.0^{c-i}	270.6
Average	303.53	252.30	287.13	253.61	307.67	323.86	288.02
LSD	G	Y	G × Y	T	G × T	Y × T	G × Y × T
0.05	37.87	-	53.54	43.59	58.40	61.65	82.60
0.01	57.38	-	81.14	100.6	81.88	142.2	115.8

Analysis of variance

	G	Y	G×Y	T	G×T	Y×T	G×Y×T	Error	Total
df	6	1	6	2	12	2	12	82	125
MS	16525.6	16457.1	5772.8	24844.4	4189.9	12830.9	1443.3	2155.7	-
F	7.666**	7.634**	2.678**	11.525**	1.944*	5.952**	1.922*	-	-

Means followed by different letter(s) within the columns differ significantly at 5% level of significance
*Significant differences per $P \leq 0.05$. **Significant differences per $P \leq 0.01$

The number of grains $spike^{-1}$ is presented in *Table 3*. On average for all years and N treatments, genotype KG-3405-03 had the highest value of number of grains $spike^{-1}$ (48.6). Similar results were shown by cultivar KG-28-6 (48.2). The lowest, significantly different average number of grains $spike^{-1}$ had genotype Olimpik (39.1). On average for all genotypes, in control and both N foliar treatments, higher number of grains $spike^{-1}$ was established in the second year of investigation. The highest value of this trait, on average, was 2014 in variant with two N treatments (50.47), and the lowest was 2013 in the control variant (36.71). The number of grains $spike^{-1}$, on average for all genotypes and years, after spraying were increased about 16% (variant with one N treatment), and 28% (variant with two N treatments) higher than in the control.

High significant differences ($P \leq 0.01$) were established between genotypes (G), years (Y), applied N treatment (T) and its interactions, except interactions Y×T which was not significant (*Table 3*). In this investigation, genotypes had different response to foliar nutrition in both year of investigation. All the treatments resulted in a significantly more grains $spike^{-1}$ than the check plots did.

http://www.aloki.hu ● ISSN 1589 1623 (Print) ● ISSN 1785 0037 (Online)
DOI: http://dx.doi.org/10.15666/aeer/2001_171187

Table 3. *Mean values and analysis of variance for number of grains per spike*

Genotype	Foliar fertilization						Average
	T1		T2		T3		
	2013	2014	2013	2014	2013	2014	
Olimpik	31.33^{uv}	39.33^{qrs}	35.0^{t}	41.0^{opq}	44.33^{jkl}	43.33^{klm}	39.1
Windur	40.0^{pqr}	38.0^{s}	45.0^{jk}	43.0^{lmn}	48.0^{gh}	47.0^{hi}	43.5
Žitka	40.0^{pqr}	39.33^{qrs}	41.0^{opq}	45.0^{jk}	46.0^{ij}	47.67^{ghi}	43.2
KG-28-6	40.33^{o-r}	43.0^{lmn}	47.33^{hi}	49.33^{fg}	53.0^{cd}	56.0^{b}	48.2
KG-44-3/1	29.67^{v}	44.67^{jkl}	39.0^{rs}	51.0^{ef}	42.0^{mno}	54.33^{bc}	43.4
KG-43-33/1	31.67^{u}	39.0^{rs}	41.33^{nop}	44.33^{jkl}	46.0^{ij}	53.33^{cd}	42.6
KG-3405-03	44.0^{kl}	37.67^{s}	56.0^{b}	44.0^{kl}	58.33^{a}	51.67^{de}	48.6
Average	36.71	40.14	43.52	45.38	48.24	50.47	44.01
LSD	G	Y	G×Y	T	G×T	Y×T	G×Y×T
0.05	1.736	-	2.456	1.999	2.074	NS	1.753
0.01	2.631	-	3.721	4.611	2.908	NS	2.458

Analysis of variance

	G	Y	G×Y	T	G×T	Y×T	G×Y×T	Error	Total
df	6	1	6	2	12	2	12	82	125
MS	198.63	198.13	197.15	1256.44	16.55	7.06	10.68	4.53	-
F	43.824^{**}	43.714^{*}	43.498^{**}	277.658^{**}	3.651^{**}	1.557^{ns}	2.358^{**}	-	-

Means followed by different letter(s) within the columns differ significantly at 5% level of significance
*Significant differences per $P \leq 0.05$. **Significant differences per $P \leq 0.01$. ^{ns}Non significant

Genotype KG-3405-03, on average, had the highest value of TGW (40.36 g), while Olimpik genotype had the lowest (35.44 g). On average for all genotypes, the highest TGW was in 2013 on variant with two N treatments (45.24 g), and the lowest was in 2014 on control variant (32.72 g) (*Table 4*).

On average for all variants and genotypes, higher TGW was established in the first investigated year compared to the second year. TGW, on average for all genotypes and years, after spraying were up 7% (variant with one N treatment), and 13% (variant with two N treatments) higher than in the control. Thousand grains weight highly depended of genotype, year, N treatment and interactions G×Y and Y×T. Interactions G×T and G×Y×T were not significant for TGW. Year had the highest influence on TGW (*Table 4*).

The tested durum genotypes on average did not significantly differ in regards to grain yield (*Table 5*). Cultivar Olimpik, on average for all treatments, had the highest grain yield (178.4 g m^{-2}), and KG-28-6 had the lowest yield (159.8 g m^{-2}). On average for all N variants and genotypes, it was established that grain yield in the first year of experiment was higher than in the second year. The highest average value of grain yield of all genotypes was established in the variant with two N treatments in 2013 year (221.5 g m^{-2}). The lowest grain yield (128.6 g m^{-2}) was found on the control variant in 2014. Grain yield, on average for all genotypes and years after spraying, was increased for 22% (one N treatment), and 54% (two N treatments) were higher than in the control. Also, the grain yield on average for all genotypes and years on variant with two N treatments was higher for about 26% than on variant with one N treatment.

http://www.aloki.hu ● ISSN 1589 1623 (Print) ● ISSN 1785 0037 (Online)
DOI: http://dx.doi.org/10.15666/aeer/2001_171187

Table 4. *Mean values and analysis of variance for TGW of durum wheat (g)*

Genotype	Foliar fertilization						Average
	T1		T2		T3		
	2013	2014	2013	2014	2013	2014	
Olimpik	34.13^{h-k}	33.27^{ijk}	35.20^{f-j}	33.47^{ijk}	40.83^{b-h}	35.73^{f-j}	35.44
Windur	42.93^{a-e}	34.93^{f-j}	43.00^{a-e}	36.07^{e-j}	48.43^{a}	33.57^{ijk}	39.82
Žitka	39.43^{c-i}	27.40^{k}	40.90^{b-h}	32.83^{ijk}	43.70^{a-d}	32.80^{ijk}	36.18
KG-28-6	37.80^{d-j}	33.47^{ijk}	41.40^{a-g}	33.60^{ijk}	48.43^{a}	35.60^{f-j}	38.38
KG-44-3/1	35.27^{f-j}	34.40^{g-k}	38.73^{d-j}	35.40^{f-j}	41.83^{a-f}	36.80^{d-j}	37.07
KG-43-33/1	37.20^{d-j}	32.23^{jk}	43.30^{a-d}	34.60^{g-j}	47.07^{ab}	34.70^{g-j}	38.18
KG-3405-03	40.97^{b-h}	33.33^{ijk}	45.90^{abc}	37.53^{d-j}	46.43^{abc}	38.00^{d-j}	40.36
Average	38.25	32.72	41.20	34.78	45.24	35.31	37.92
LSD	G	Y	G×Y	T	G×T	Y×T	G×Y×T
0.05	3.238	-	4.580	3.728	NS	5.272	NS
0.01	4.906	-	6.939	8.599	NS	12.160	NS

Analysis of variance

	G	Y	G×Y	T	G×T	Y×T	G×Y×T	Error	Total
df	6	1	6	2	12	2	12	82	125
MS	59.31	1675.72	45.02	241.86	6.73	56.95	6.57	15.72	-
F	3.772**	106.574**	2.863*	15.382**	0.428^{ns}	3.622*	0.418^{ns}	-	-

Means followed by different letter(s) within the columns differ significantly at 5% level of significance
*Significant differences per $P \leq 0.05$. **Significant differences per $P \leq 0.01$; ^{ns}Not significant

Table 5. *Mean values and analysis of variance for grain yield of durum wheat (g m^{-2})*

Genotype	Foliar fertilization						Average
	T1		T2		T3		
	2013	2014	2013	2014	2013	2014	
Olimpik	133.8^{l-o}	116.3^{o}	190.3^{c-h}	147.00^{i-o}	253.0^{a}	229.8^{abc}	178.4
Windur	153.1^{q-o}	136.7^{l-o}	156.0^{f-o}	149.3^{h-o}	219.3^{a-d}	198.7^{b-e}	168.8
Žitka	140.0^{k-o}	130.0^{mno}	174.7^{e-l}	151.5^{g-o}	187.9^{d-i}	182.7^{d-j}	161.1
KG-28-6	139.8^{k-o}	127.3^{n-o}	170.2^{e-m}	143.5^{j-o}	192.1^{c-g}	186.0^{d-i}	159.8
KG-44-3/1	131.2^{mno}	130.7^{mno}	192.3^{c-g}	150.2^{h-o}	259.7^{a}	190.4^{c-h}	175.7
KG-43-33/1	135.6^{l-o}	129.7^{mno}	196.0^{b-f}	140.9^{k-o}	236.0^{ab}	180.5^{d-k}	169.8
KG-3405-03	137.1^{l-o}	129.7^{mno}	173.2^{e-l}	155.0^{f-o}	202.4^{b-e}	167.0^{e-n}	160.7
Average	138.7	128.6	179.0	148.2	221.5	190.7	167.78
LSD	G	Y	G × Y	T	G × T	Y × T	G × Y × T
0.05	NS	-	NS	21.90	29.34	NS	NS
0.01	NS	-	NS	50.52	41.13	NS	NS

Analysis of variance

	G	Y	G×Y	T	G×T	Y×T	G×Y×T	Error	Total
df	6	1	6	2	12	2	12	82	125
MS	1013.65	17935.80	539.95	55687.88	1133.80	1503.86	410.49	544.05	-
F	1.863^{ns}	32.967**	0.992^{ns}	102.357**	2.084*	2.764^{ns}	0.754^{ns}	-	-

Means followed by different letter(s) within the columns differ significantly at 5% level of significance
*Significant differences per $P \leq 0.05$. **Significant differences per $P \leq 0.01$. ^{ns}Non significant

http://www.aloki.hu ● ISSN 1589 1623 (Print) ● ISSN 1785 0037 (Online)
DOI: http://dx.doi.org/10.15666/aeer/2001_171187

Significant differences were found between tested years, N treatments and G×T interaction for grain yield. The differences between genotypes and other interactions (G×Y, Y×T and G×Y×T) were not statistically significant (*Table 5*). Treatment and year had the highest influence to grain yield (F = 102.357**; 32.967**, respectively).

The correlations between the studied yield components and grain yield of durum wheat were analyzed (*Table 6*). Grain yield positively correlated to the other traits (TGW, number of spikes m^{-2} and number of grains spike^{-1}), which were statistically highly significant. The highest correlation was between yield and TGW (0.501**). The correlation between number of grains spike^{-1} and TGW (0.288**), were also positive and statistically highly significant.

Table 6. *Correlations between yield and other investigated parameters of durum wheat*

Components	TGW	Number of spikes m^{-2}	Number of grains spike^{-1}
Yield	0.501**	0.339**	0.333**
TGW		0.039^{ns}	0.288**
Number of spikes m^{-2}			0.055^{ns}
Number of grains spike^{-1}			-

**Significant differences per $P \leq 0.01$. ^{ns}Not significant

Discussion

Agricultural land is, as a rule, scarce in nitrogen. This is the reason that it is necessary to add fertilizer with the appropriate nitrogen content, which is an important mineral element in growing crops and achieving higher yields and quality. The effect of nitrogen nutrition on increasing wheat grain yield depends on the dose of nitrogen and the time and manner of its application (Tedone et al., 2017; Dolijanović et al., 2019). The application of nitrogen fertilizer must be appropriate for each genotype, which differ in their capacity for N absorption, translocation and reutilization. Excessive addition of nitrogen causes the lodging of plants, which creates favorable conditions for the development of diseases, weeds, less capacity and competition of lodged plants for the use of mineral nutrients, water, light (Mascianica and Valden, 1986; Bruckner and Morey, 1988; Zhang et al., 2017).

Generally, according to our results, the nitrogen foliar application had a positive effect on the number of spikes m^{-2}, number of grains spikes^{-1}, TGW and grain yield, which is in line with other studies (Arif et al., 2006; Khan et al., 2009; Tedone et al., 2014; Arshadullah et al., 2015), who also found a positive effect of nitrogen on these properties. Blandino et al. (2015) have established a significant effect of N fertilization at the time of late stage of plant development on grain yield in durum wheat, as well as in common wheat (Khan et al., 2009). Galieni et al. (2016) also established that N fertilization had a significant effect on yield in durum wheat. In our results, it was established that grain yield of genotypes is significantly affected by the N rate, year and its interactions, which was similar to another research in durum wheat (Ayadi et al., 2014).

Our investigation found that the two growing seasons greatly differed in the amount and distribution of rainfall. Climatic conditions during 2012/2013 were characterized by even distribution of precipitation during the vegetative and generative development of the examined genotypes. In 2013/2014 a significant lack of precipitation was recorded

http://www.aloki.hu ● ISSN 1589 1623 (Print) ● ISSN 1785 0037 (Online)
DOI: http://dx.doi.org/10.15666/aeer/2001_171187

(December - April) during the vegetative development of the examined genotypes. On the other hand, large amounts of rainfall were recorded at the time of heading, grain filling and maturation (Maj - June), favored the development of fungal diseases of spikes and grains, which affected yield components and formation of yield. Overall, the mean values of grain yield, number of spikes m^{-2} and TGW of wheat genotypes were higher in the more favorable 2013/2014 than in the unfavorable 2013/2014 growing season.

Observed by years and applied treatments, a specific reaction of genotypes was recorded in the examined traits. For the number of spikes m^{-2}, the application of different treatments of foliar application of nitrogen in the cultivar Windur did not affect the increase of the average values of the observed trait. In the variety Žitka, an increased number of spikes m^{-2} was determined only during 2012/2013, considering the favorable climatic conditions in the phase of vegetative development. The variety Olimpik and breeding lines selected at the Small Grains Research Centre in Kragujevac expressed wide adaptability and stability and thus the predominant influence of genotype in the formation of the examined trait, regardless of climatic conditions in the years of testing. Similarly, the high adaptability and stability of bread wheat genotypes selected at the Center from Kragujevac were found in research by Luković et al. (2020) in years with unfavorable climatic conditions.

For the number of grains per spike, all tested genotypes responded positively to foliar application of nitrogen, especially in T3 treatment. It can be concluded that the application of nitrogen and amino acids in the heading and anthesis phase had a positive effect on reducing stress in the examined genotypes due to excessive rainfall. However, the number of grains per spike was on average higher in the 2013/2014 growing season, but due to unfavorable conditions during the stage of grain filling the grains were underdeveloped and small, which had a negative impact on yield. Drought in the early stages of development can seriously affect the number of plants per square meter, and in the tillering phase affects the number of shoots per plant, while drought during stem elongation influenced decreasing of plant height. Later, drought in the phases of flowering, fertilization and grain formation significantly affects the number of grains per area. In the stage of forming grains, drought significantly affects the process of translocation of assimilates to the grain, which had impact on reducing of weight of grains (Sarto et al., 2017).

In contrast to the previously examined traits, a more significant impact of the year was recorded for TGW, which is reflected in lower average values during 2013/2014 for all applied treatments compared to 2012/2013.

Excessive precipitation recorded during heading and anthesis in 2013/2014 influenced that examined genotypes achieved lower average grain yields for all observed treatments compared to 2012/2013. The lower average values of TGW in the tested genotypes, determined during 2013/2014 vegetation season that characterized with excessive amount of precipitation. In this season there was a high degree of correlation between TGW and grain yield. The results of the research indicate that climatic conditions during the year of testing have a decisive influence on the efficiency of foliar application of N in the phases of heading and anthesis and the formation of the final grain yield in durum wheat genotypes.

Previous research (Hirzel et al., 2010) has shown that splitting the application of nitrogen into three periods (sowing, tillering, stem elongation), appears more efficient than just one application, producing an increase of 15%, or twice, where the increase is

http://www.aloki.hu ● ISSN 1589 1623 (Print) ● ISSN 1785 0037 (Online)
DOI: http://dx.doi.org/10.15666/aeer/2001_171187

7% (Tedone et al., 2014). This strategy appears to be effective in reducing the loss of soil nitrates, which is more dangerous during the winter period, as reported from several authors, due to the rainfall (López-Bellido, 2005). Foliar fertilization is necessary and recommended as a measure that can reduce plant stress due to adverse climatic conditions: high or low air temperature, drought, short or long-term water shortages, etc. (Doflerus, 2014; Trnka et al., 2014; Knežević et al., 2019). In conventional production, where the nutrition of plants is balanced based on the quality of the soil, foliar fertilization achieves a smaller effect. In organic production, plants are more exposed to stressful conditions, because the application of mineral fertilizers and plant protection products is restricted or prohibited, foliar application of nutrients gives better results. The yield of durum wheat with organic cropping system was 21% lower than in conventional based on the findings of the researchers Fagnano et al. (2012).

Some authors, with foliar fertilizer applications have found increases in grain yield in some years, but on average of five years, foliar fertilizers did not increase grain yield (Staugaitis et al., 2017). Zečević et al. (2004) reported increasing of grain yield and quality under N applications in flowering and milky stages. Woolfolk et al. (2002) suggested that foliar N applications before or immediately after flowering may significantly increase grain protein in winter wheat. Managing N fertilizer is difficult because it depends on many terms such as fertilizer source, quantity, mode of application, application time, variety response and climatic conditions. In this respect, the grain filling period is crucial for the quality of the durum wheat (Orcen et al., 2013; Branković et al., 2015b).

The application of fertilizers in system of organic production has the function of increasing the fertility and biological activity of the soil and at the same time providing the nutrients necessary for the growth and development of the plants. In organic system of production, the basic principles are increasing of organic matter in soil and production of healthy food. In order to allow efficient use of nitrogen by plants, when determining the required quantities of organic matter and right time of introduction into the soil, it is necessary to consider all factors that affect the dynamics and balance of nitrogen in the soil, and thus the availability of nitrogen for plants. The results obtained in our investigation were compared with those in the earlier reports (Gopinath et al., 2008), which found that grain yields increased in response to increasing application rates of organic amendments. Dolijanović et al. (2017) found a significant effect of organic and microbiological fertilizers on grain yield in durum, spelt and bread wheat varieties growing in system of organic productions.

Đokić (1988) points out that when wheat is forming grain yield, it is possible to compensate N deficiency through certain components of the yield. Therefore, if the improved nitrogen nutrition did not sufficiently reflect on tillering, the N deficiency would be compensated by increasing the number of grains per spike. In case the grain number does not increase, the grain mass will be increased.

According to our study, the grain yield was positively correlated with other traits (TGW, number of spike m^{-2} and number of grains $spike^{-1}$), which were statistically highly significant. These results are in agreement with studies of Khan et al. (2013), Matković et al. (2018) and Nofouzi (2018) who also established positive correlations between yield and yield components in durum wheat. García del Moral et al. (2003) have also found that number of spikes per square meter, TGW and number of kernels/spike were positively related with grain yield. Lupini et al. (2021) have found high positive correlation (0.97) between grain yield and nitrogen use efficiency of

http://www.aloki.hu ● ISSN 1589 1623 (Print) ● ISSN 1785 0037 (Online)
DOI: http://dx.doi.org/10.15666/aeer/2001_171187

durum wheat. Investigation by Mariem et al. (2020) had shown that nitrogen fertilization applied from anthesis to maturity had small effects on durum wheat grain yield but had a major impact on grain quality.

Conclusion

Nitrogen nutrition is one of the main factors that leads to increased productivity and improved quality of wheat grain. In this study, foliar application of nitrogen in heading and anthesis caused an increase in grain yield and the yield components tested.

Number of spikes per square meter, number of grains m^{-2}, thousand grain weight, and wheat yield were significantly increased ($P \leq 0.01$) by different levels of fertilizers. The foliar fertilization had a significant effect on yield in both growing seasons. Grain yield, on average for all genotypes and years, after spraying were 22% (one N treatment), and 54% (two N treatments) higher than in the control. Grain yield was higher for about 26% in variant with two N treatments than in variant with one N treatment.

Grain yield was positively correlated with other traits (TGW, number of spike m^{-2} and number of grains $spike^{-1}$), which were statistically highly significant. The difference in grain yield was found between the investigated genotypes of durum wheat by individual years, but on average for both years, the genotypes responded similarly to the applied foliar nitrogen nutrition. The tested genotypes showed significantly lower yields compared to their genetic potential because durum wheat has low frost-tolerance and during the winter period some of the plants die and the potential for grain yield decreases.

The conducted research indicates that the foliar application of nitrogen and amino acids in the most important stages of plant development (heading and anthesis) is economically justified, especially in years with optimal conditions, considering the established statistical significance of the examined traits.

The significant impact in achievement of potential yield of wheat genotype as well as other cultivated plants, have soil biological and phisico-chemical properties, which can change and modified under scientific farming measures practices: tillage, fertilizing, land reclamation to enhance soil fertility, creation and maintenance of optimal water-air regime of the soil, in order to provide favorable conditions for the growth and development of wheat cultivation and to achieve stable yields. The further investigation is necessary to be done to establish the optimum fertilizer combination to improved crop production, as well as application of nitrogen and amino acids in the grain feeling phenophase on the final yield and technological grain quality of durum wheat.

Acknowledgements. This study was supported by the Ministry of Education, Science and Technological Development of the Republic of Serbia (Grant No. 451-03-9/2021-14/200216).

REFERENCES

[1] AOAC 972.43 (2000): Method 972.43. Micro-chemical Determination of Carbon, Hydrogen, and Nitrogen, Automated Method. Official Methods of Analysis of AOAC International. 17th Ed. – AOAC International, Arlington, VA.

[2] Araus, J. L., Slafer, M. P., Reynolds, M. P., Royo, C. (2002): Plant breeding and drought in C3 cereals: what should we breed for? – Annals of Botany 89(7): 925-940. DOI: 10.1093/aob/mcf049.

http://www.aloki.hu ● ISSN 1589 1623 (Print) ● ISSN 1785 0037 (Online)
DOI: http://dx.doi.org/10.15666/aeer/2001_171187

[3] Arif, M., Chohan, M. A., Ali, S., Gul, R., Khan, S. (2006): Response of wheat to foliar application of nutrients. – Journal of Agricultural and Biological Science 1(4): 30-34.
[4] Arshadullah, M., Ali, A., Hyder, S. I., Mahmood, I. A., Zaman, B. (2015): Effect of K_2SO_4 and KNO_3 foliar application on wheat growth. – Pakistan Journal of Science and Industrial Researsh Series B: Biological Science 58(1): 19-22.
[5] Ayadi, S., Karmous, C., Hammami, Z., Trifa, Y., Rezgui, S. (2014): Variation of durum wheat yield and nitrogen use efficiency under Mediterranean rainfed environment. – International Journal of Agriculture and Crop Sciences 7(10): 693-699.
[6] Blandino, M., Vaccino, P., Reyneri, A. (2015): Late-season nitrogen increases improver common and durum wheat quality. – Agronomy Journal 107: 680-690. DOI: 10.2134/agronj14.0405.
[7] Bošković, J., Hojka, Z., Zečević, V., Prodanović, R., Vukić, M. (2016): Significant resources of sustainable agriculture and organic food production system in Serbia. – Acta Agriculturae Serbica 21(41): 65-85.
[8] Branković, G., Dragičević, V., Dodig, D., Zorić, M., Knežević, D., Žilić, S., Denčić, S., Šurlan, G. (2015a): Genotype × Environment interaction for antioxidants and phytic acid contents in bread and durum wheat as influenced by climate. – Chilean Journal of Agricultural Research 75(2): 139-146.
[9] Branković, G., Dragičević, V., Dodig, D., Knežević, D., Kobiljski, B., Šurlan-Momirović, G. (2015b): Albumin content in bread wheat (*Triticum aestivum* L.) and durum wheat (*Triticum durum* Desf.) as affected by environment. – Scientific Journal Zemdirbyste - Agriculture 102(3): 281-288.
[10] Branković, G., Dragičević, V., Žilić, S., Knežević, D., Đurić, N., Dodig, D. (2016): Expected genetic advance and stability of phytic acid and antioxidants content in bread and durum wheat. – Genetika 48(3): 867-880.
[11] Branković, G., Dodig, D., Pajić, V., Kandić, V., Knežević, D., Đurić, N., Živanović, T (2018): Genetic parameters of *Triticum aestivum* and *Triticum durum* for technological quality properties in Serbia. – Zemdirbyste - Agriculture 105(1): 39-48.
[12] Bruckner, P. L., Morey, D. D. (1988): Nitrogen effects on soft red winter wheat yield. Agronomic characteristics and quality. – Crop Science 28: 152-157.
[13] Doflerus, R. (2014): To grow or not to grow: a stressful decision for plants. – Plant Science 229: 247-261. https://doi.org/10.1016/j.plantsci.2014.10.002.
[14] Dolijanović, Ž., Kovačević, D., Oljača, S., Roljević Nikolić, S., Šeremešić, S. (2017): Effect of fertilizers on the yield of alternative small grains. – Contemporary Agriculture 66(3-4): 15-21. DOI: 10.1515/contagri-2017-0014.
[15] Dolijanović, Ž., Roljević Nikolić, S., Kovačević, D., Djurdjić, S., Miodragović, R., Jovanović Todorović, M., Popović Djordjević, J. (2019): Mineral profile of the winter wheat grain: effects of soil tillage systems and nitrogen fertilization. – Applied Ecology and Environmental Research 17(5): 11757-11771. DOI: http://dx.doi.org/10.15666/aeer/1705_1175711771.
[16] Đokić, D. (1988): The role of nitrogen in the increase of wheat yield and quality improvement. – Agrohemija, Belgrade 5-6: 321-332 (in Serbian).
[17] Egner, H., Riehm, H. (1955): Die Untersuchung von Böden. – In: Thun, R., Herrmann, R., Knickmann, E. (eds.) Methodenbuch Band I. Neumann Verlag, Radebeul/Berlin, pp. 110-125.
[18] Fagnano, M., Fiorentino, N., D'Egidio, M. G., Quaranta, F., Ritieni, A., Ferracane, R., Giampaolo Raimondi, G. (2012): Durum wheat in conventional and organic farming: yield amount and pasta quality in Southern Italy. – The Scientific World Journal 973058. DOI: 10.1100/2012/973058.
[19] Galieni, A., Stagnari, F., Visioli, G., Marmiroli, N., Speca, S., Angelozzi, G., D'Egidio, S., Pisante, M. (2016): Nitrogen fertilisation of durum wheat: a case study in Mediterranean area during transition to conservation agriculture. – Italian Journal of Agronomy 11: 12-23. DOI: 10.4081/ija.2016.662.

http://www.aloki.hu ● ISSN 1589 1623 (Print) ● ISSN 1785 0037 (Online)
DOI: http://dx.doi.org/10.15666/aeer/2001_171187

[20] García del Moral, L. F., Rharrabti, Y., Villegas, D., Royo, C. (2003): Evaluation of grain yield and its components in durum wheat under Mediterranean conditions: an ontogenic approach. – Agronomy Journal 95: 266-274.
[21] Gopinath, K. A., Saha, S., Mina, B. L., Pande, H., Kundu, S., Gupta, H. S. (2008): Influence of organic amendments on growth, yield and quality of wheat and on soil properties during transition to organic production. – Nutr. Cycling in Agroecosystems 82: 51-60. DOI 10.1007/s10705-008-9168-0.
[22] Hirzel, J., Matus, I., Madariaga, R. (2010): Effect of split nitrogen applications on durum wheat cultivars in volcanic soil. – Chilean Journal of Agricultural Research 70(4): 590-595.
[23] ISO 10693 (1995): Soil Quality—Determination of Carbonate Content—Volumetric Method. – International Organization for Standardization, Genève.
[24] ISO 14235 (1998): Soil Quality—Determination of Organic Carbon by Sulfochromic Oxidation. – International Organization for Standardization, Genève.
[25] ISO 11464 (2006): Soil Quality—Pretreatment of Samples for Physico-chemical Analysis. – International Organization for Standardization, Genève.
[26] ISO 10390 (2010): Soil Quality—Determination of pH. – International Organization for Standardization, Genève.
[27] ISO/IEC 17025 (2017): General Requirements for the Competence of Testing and Calibration Laboratories. – International Organization for Standardization, Genève.
[28] Kappen, H. (1929): Bodenazidität. – Springer Verlag, Berlin.
[29] Khan, P., Memon, M. Y., Imtiaz, M., Aslam, M. (2009): Response of wheat to foliar and soil application of urea at different growth stages. – Pakistan Journal of Botany 41(3): 1197-1204.
[30] Khan, A. A., Alam, M. A., Alam, M. K., Alam, M. J., Sarker, Z. I. (2013): Correlation and path analysis of durum wheat *(Triticum turgidum* L. var. *Durum)*. – Bangladesh Journal of Agricultural Research 38(3): 515-521.
[31] Knežević, D., Paunović, A., Kondić, D., Radosavac, A., Laze, A., Kovačević, V., Mićanović, D. (2019): Variability in seed germination of barley cultivars (*Hordeum vulgare* L.) grown under different nitrogen application rates. – Acta Agriculturae Serbica 24(47): 61-69. 1. DOI: 10.5937/AASer1947061K.
[32] Kostić, M., Đokić, D. (1975): Influence of nitrogen given in the flowering stage of wheat on vegetation length and grain yield and quality. – Journal for Scientific Agricultural Research, Belgrade 101: 153-159 (in Serbian).
[33] Lammerts van Bueren, E., Struik, P., Jacobsen, E. (2002): Ecological aspects in organic farming and its consequences for an organic crop ideotype. – Netherlands Journal of Agricultural Science 50: 1-26.
[34] Langer, R. H. M. (1979): The dynamics of wheat yield. – New Zealand Wheat Review 14: 32-40.
[35] Li, Y. F., Wu, Y., Hernandez-Espinosa, N., Pena, R. J. (2013): Heat and drought stress on durum wheat: responses of genotypes, yield, and quality parameters. – Journal of Cereal Science 57: 398-404.
[36] López-Bellido, L., López-Bellido, R. J., Redondo, R. (2005): Nitrogen efficiency in wheat under rainfed Mediterranean conditions as affected by split nitrogen application. – Field Crops Research 94: 86-97.
[37] Luković, K., Prodanović, S., Perišić, V., Milovanović, M., Perišić, V., Rajičić, V., Zečević, V. (2020): Multivariate analysis of morphological traits and the most important productive traits of wheat in extreme wet conditions. – Applied Ecology and Environmental Research 18(4): 5857-5871. DOI: http://dx.doi.org/10.15666/aeer/1804_58575871,
[38] Lupini, A., Preiti, G., Badagliacca, G., Abenavoli, M. R., Sunseri, F., Monti, M., Bacchi, M. (2021): Nitrogen use efficiency in durum wheat under different nitrogen and water

http://www.aloki.hu ● ISSN 1589 1623 (Print) ● ISSN 1785 0037 (Online)
DOI: http://dx.doi.org/10.15666/aeer/2001_171187

regimes in the Mediterranean Basin. – Frontiers in Plant Science 11: 607226. DOI: 10.3389/fpls.2020.607226.

[39] Mariem, S. B., González-Torralba, J., Collar, C., Aranjuelo, I., Morales, Fermín (2020): Durum wheat grain yield and quality under low and high nitrogen conditions: insights into natural variation in low- and high-yielding genotypes. – Plants (Basel) 9(2) 1636. DOI: 10.3390/plants9121636.

[40] Mascianica, M. P., Valden, R. F. (1986): Performans of winter wheat under conventional and intensive N management. – Journal of Applied Agricultural Research 1: 32-36.

[41] Matković, M., Bošković, J., Zečević, V., Knežević, D., Đurić, N. (2015): Influence of genotype on yield and quality components of durum wheat in organic production. – Proceedings. Fifth International Symposium on Natural Resources Management. May 23rd, Faculty of Management, Zaječar, Republic of Serbia, pp. 17-22.

[42] Matković Stojšin, M., Zečevć, V., Petrović, S., Dimitrijević, M., Mićanović, D., Banjac, B., Knežević, D. (2018): Variability, correlation, path analysis and stepwise regression for yield components of different wheat genotypes. – Genetika 50(3): 817-828.

[43] Michigan State University (1990): User's Guide to MSTAT-C. – Michigan State University, Michigan.

[44] Mohammadi, M., Karimizadeh, R., Mohammad Kazem Shefazadeh, M. K., Sadeghzadeh, B. (2011): Statistical analysis of durum wheat yield under semi-warm dryland condition. – Australian Journal of Crop Science 5(10): 1292-1297.

[45] Nofouzi, F. (2018): Evaluation of seed yield of durum wheat (*Triticum durum*) under drought stress and determining correlation among some yield components using path coefficient analysis. – UNED Research Journal 10(1): 179-183. https://www.scielo.sa.cr/pdf/cinn/v10n1/1659-4266-cinn-10-01-179.pdf.

[46] Orcen, N., Tosun, M., Irget, E. (2013): Effect of nitrogen fertilizer timing and source on some yield and quality parameters of durum wheat (*Triticum durum*). – Journal of Food Agriculture and Environment 11: 943-948.

[47] Rao, B. N., Pozniak, C. J., Hucl, P. J., Briggs, C. (2010): Baking quality of emmer-derived durum wheat breeding lines. – Journal of Cereal Science 51: 299-304.

[48] Sarto, M. V. M., Sarto, J. R. W., Rampim, L., Rosset, J. S., Bassegio, D., Costa, P. F., Inagaki, A. M. (2017): Wheat phenology and yield under drought: a review. – Australian Journal of Crop Science 11(08): 941-946. DOI: 10.21475/ajcs.17.11.08.pne351.

[49] Staugaitis, G., Aleknavičienė, L., Brazienė, Z., Marcinkevičius, A., Paltanavičius, V. (2017): The influence of foliar fertilization with nitrogen, sulphur, amino acids and microelements on spring wheat. – Zemdirbyste-Agriculture 104(2): 123-130. DOI: 10.13080/z-a.2017.104.016.

[50] Tedone, L., Verdini, L., Grassano, N., Tarraf, W., De Mastro, G. (2014): Optimising nitrogen in order to improve the efficiency, eco-physiology, yield and quality on one cultivar of durum wheat. – Italian Journal of Agronomy 9: 49-54. DOI: 10.4081/ija.2014.536.

[51] Tedone, L., Ali, S. A., De Mastro, G. (2017): Optimization of Nitrogen in Durum Wheat in the Mediterranean Climate: The Agronomical Aspect and Mediterranean Climate: The Agronomical Aspect and Greenhouse Gas (GHG) Emissions. – In: Amanullah, Fahad, S. (eds.) Nitrogen in Agriculture. IntechOpen, London, pp. 131-162. http://dx.doi.org/10.5772/intechopen.70195.

[52] Trnka, M., Reimund, P., Rötter, R. P., Ruiz-Ramos, M., Kersebaum, K. C., Olesen, J. E., Žalud, Z., Semenov, M. A. (2014): Adverse weather conditions for European wheat production will become more frequent with climate change. – Nature Climate Change 4: 637-643. https://doi.org/10.1038/nclimate2242.

[53] Van Reeuwijk, L. P. (ed) (2002): Procedures for Soil Analysis. Sixth Ed. – ISRIC FAO Technical Paper Vol. 9. International Soil Reference and Information Centre, Wageningen, pp 12-16.

http://www.aloki.hu ● ISSN 1589 1623 (Print) ● ISSN 1785 0037 (Online)
DOI: http://dx.doi.org/10.15666/aeer/2001_171187

[54] Woolfolk, C. W., Raun, W. R., Johnson, G. V., Thomason, W. E., Mullen, R. W., Wynn, K. J., Freeman, K. W. (2002): Influence of late-season foliar nitrogen applications on yield and grain nitrogen in winter wheat. – Agronomy Journal 94(3): 429-434. https://doi.org/10.2134/agronj2002.4290.

[55] Zadoks, J. C., Chang, T. T., Konzak, C. F. (1974): A decimal code for the growth stages of cereals. – Weed Research 14: 415-421.

[56] Zečević, V., Đokić, D., Knežević, D., Mićanović, D. (2004): The influence of nitrogen foliar applications on yield and bread making quality parameters of wheat. – Kragujevac Journal of Science 26: 89-90.

[57] Zhang, M., Wang, H., Yi, Y., Ding, J., Zhu, M., Li, C., Guo, W., Feng, C., Zhu, X. (2017): Effect of nitrogen levels and nitrogen ratios on lodging resistance and yield potential of winter wheat (*Triticum aestivum* L.). – PLoS ONE 12(11): e0187543. https://doi.org/10.1371/journal.pone.0187543.

http://www.aloki.hu ● ISSN 1589 1623 (Print) ● ISSN 1785 0037 (Online)
DOI: http://dx.doi.org/10.15666/aeer/2001_171187

DISTRIBUTION PATTERN OF MACROINVERTEBRATE FUNCTIONAL FEEDING GROUPS IN THE STEELPOORT RIVER, SOUTH AFRICA

MAKGOALE, M. M.[1] – ADDO-BEDIAKO, A.[1*] – AYISI, K. K.[2]

[1]*Department of Biodiversity, University of Limpopo*
Private Bag X1106, Sovenga 0727, South Africa

[2]*Risk and Vulnerability Science Centre, University of Limpopo*
Private Bag X1106, Sovenga 0727, South Africa

**Corresponding author*
e-mail: abe.addo-bediako@ul.ac.za; phone: +27-15-268-3145; ORCID: 0000-0002-5055-8315

(Received 12th Jul 2021; accepted 20th Sep 2021)

Abstract. The various human activities along the Steelpoort River in South Africa are causing changes in water quality and affecting the distribution of macroinvertebrate functional feeding groups (FFG). The objectives of this study were to assess the spatial and temporal distribution of FFG of macroinvertebrates and to determine if the community structure corresponds to the River Continuum Concept (RCC). The distribution of the FFG varied significantly among sites and the variation was related to the different characteristics of the sites. The collector-gatherers were the most abundant functional feeding group at Site 1, collector-filterers were the most dominant group at Site 4 and Site 5, predators were the most dominant group at Site 2, Site 3 and Site 6. Shredders were least represented at all sites of the river. Seasonally, the collector-gatherers were dominant in winter, collector-filterers were dominant in spring and predators were the dominant group in autumn and summer. The study showed that the distribution of FFG was not in conformity to the RCC. The results suggest that land use changes in the catchment is affecting the FFG distribution pattern. It is therefore important that policies governing land use changes should take into account the impact on the macroinvertebrate community.
Keywords: *bioindicators, functional feeding groups, land use changes, riparian disturbance, water quality*

Introduction

Freshwater systems are under constant pressure due to anthropogenic activities, such as agriculture, urbanization, industries and mining (Li et al., 2018; Chen et al., 2019; Addo-Bediako, 2020). Land-use activities in river catchments have been linked to water quality deterioration, which can affect the composition and diversity of aquatic biota including benthic macroinvertebrates (Munyika et al., 2014).

Aquatic macroinvertebrates constitute an important component of secondary production within freshwater ecosystems and are integrated into the structure and function of their habitats (Li et al., 2010). They are therefore expected to vary consistently in relation to the intensity of disturbance in an ecosystem (Dalu et al., 2017). They are good bioindicators because they continuously dwell in water and they respond to every change they encounter in their environment, such as pollution (Santhosh and Ashadevi, 2017). Different taxa of macroinvertebrates respond differently to environmental stressors and are therefore considered as good bioindicators (Rasifudi et al., 2018). Information on macroinvertebrates is important for a long-term analysis of changes in water quality and may reflect historical processes such as stream

http://www.aloki.hu ● ISSN 1589 1623 (Print) ● ISSN 1785 0037 (Online)
DOI: http://dx.doi.org/10.15666/aeer/2001_189206

degradation, pollution, discharge variations and silting (Wright and Ryan, 2016; Castro et al., 2018).

Benthic macroinvertebrates as bioindicators in habitat monitoring programs use basic metrics such as abundance, taxa richness and diversity, however, many biomonitoring programs are also considering a functional approach based on Functional Feeding Groups (FFGs) (Fu et al., 2016; Jun et al., 2016; Kim et al., 2016; Fierro et al., 2017). The FFG classification is based on the food consumed and also considers the morphological and behavioural characteristics used in the food acquisition (Ramirez and Gutiérrez-Fonseca, 2014). The functional feeding groups reflect the four most important food resources found in streams: periphyton, coarse particulate organic matter (CPOM), fine particulate organic matter (FPOM) and animal prey. Shredders feed on coarse particulate organic matter, scrapers consume algae and microbes attached to the coarse particulate organic matter, collector-filterers and collector-gatherers filter the fine particulate organic matter from the water column and directly from the substrate, and predators consume animals or some of their parts (Merritt et al., 2017; Cummins, 2018).

The River Continuum Concept (RCC) is widely used to explain the functioning of lotic ecosystems and predicts how relative FFG abundance changes along a river gradient (Vannote et al., 1980). The RCC proposes that community structure should shift from an allochthonous in the headwater to an autochthonous in the downstream of the river, as the river widens and algal production increases (Allan and Castillo, 2007). Functional composition is therefore necessary for management actions to enhance ecosystem functioning (Ferreira et al., 2012; Meira et al., 2021). This approach is seen to provide more accurate assessment of water quality and ecological integrity of rivers, which indeed could be used for conservation and restoration strategies in managing river ecosystems (Príncipe et al., 2010).

The Steelpoort River, like many South African rivers suffers from water loss, degradation, and poor water quality due to various human activities such as agriculture, mining, industries and informal settlements in the catchment (Dallas, 2007). These have resulted in a wide range of disturbances in the river and its riparian vegetation which can affect the distribution and diversity of aquatic biota, such as macroinvertebrates. The Steelpoort River was selected for this study because of the rapid increase in mining activities and human population in the area, which are putting a lot of pressure on the local natural resources, such as the Steelpoort River (Ashton and Dabrowski, 2011). The objectives of the study were to assess the effects of land use changes on spatio-temporal distribution of the functional groups of benthic macroinvertebrate communities and to determine if FFG conform to the River Continuum Concept (RCC). It is envisaged that the results of the study would be used to design proper conservation tool in the river system. The hypothesis tested was that due to land use changes affecting the river, the macroinvertebrate functional feeding groups would not fully conform to the river continuum concept (RCC).

Materials and methods

Study area

The Steelpoort River sub-catchment is one of the four sub-catchments of the Olifants River Catchment in South Africa and covers an area of about 7,139 km^2 (Stimie et al., 2001). Summers are usually warm with mean daytime temperatures vary between 19 and 22 °C and mean winter temperatures are between 13 and 19 °C (Stemie et al.,

http://www.aloki.hu ● ISSN 1589 1623 (Print) ● ISSN 1785 0037 (Online)
DOI: http://dx.doi.org/10.15666/aeer/2001_189206

2001). The mean annual rainfall of the area is between 630 and 1000 mm. Rainfall occurs predominantly in summer months (December to February). According to DWAF (1995), the water quality of the middle Steelpoort sub-catchment in both surface and ground water is being threatened by an increasing level of contaminations from mining, industrial, agricultural and residential sources. The Steelpoort River basin is characterized mainly by mining and agricultural activities (Van Veelen and Dhemba, 2011). The mining and industrial activities include chrome, coal, granite, magnesite, alluvial gold, platinum and vanadium mines concentrated in the upper sub-catchment (Stimie et al., 2001).

This study was conducted in summer (February), autumn (April), winter (July) and spring (October) of 2019. Samples were collected at six selected sites potentially receiving different forms of pollution along the river. Site 1 was located upstream with little human activities, though the riparian vegetation is disturbed, Site 2, near a human settlement, Sites 3, near farming and human settlement, Site 4, near mines and smelter, Site 5, domestic and industrial activities, and Site 6, settlement and cattle grazing area (*Fig. 1*). The co-ordinates of the sites are given in *Table 1*.

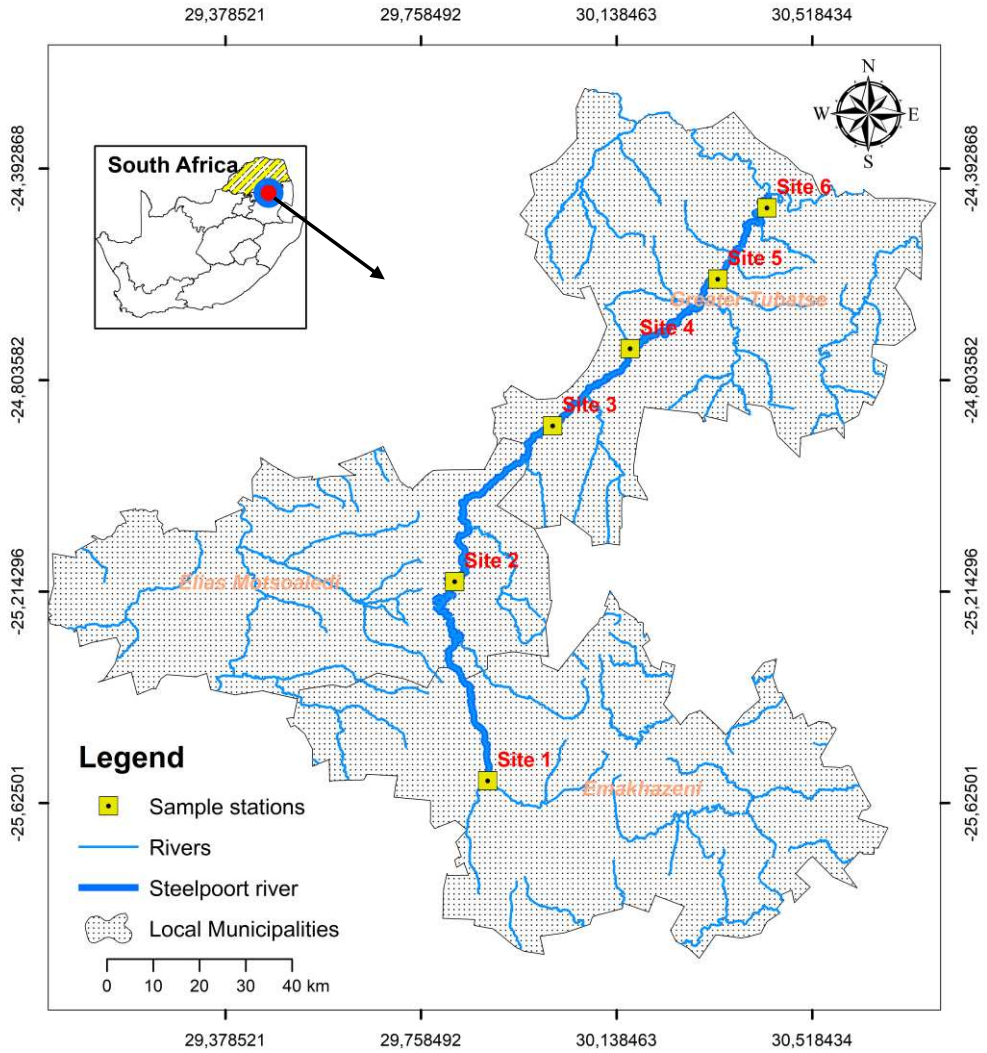

Figure 1. *Map of the study area, showing the locations of the sampling sites of the Steelpoort River*

http://www.aloki.hu ● ISSN 1589 1623 (Print) ● ISSN 1785 0037 (Online)
DOI: http://dx.doi.org/10.15666/aeer/2001_189206

Table 1. *Geographical positions of the sampling sites of the Steelpoort River*

Sites	Geographical positions
Site 1	25.1010S, 29.84705E
Site 2	24.8939S, 30.01717E
Site 3	24.83048S, 30.07906E
Site 4	24.71797S, 30.20094E
Site 5	24.65910S, 30.30202E
Site 6	24.64331S, 30.30793E

Water physicochemical variables

Water samples were collected in 500 ml 10% nitric acid pre-treated plastic containers. Collected water samples were kept on ice and sent to the laboratory. The samples were kept at 4 °C prior to chemical analysis. Nutrient (nitrite, nitrate and phosphate) concentrations and turbidity in the water samples were analysed using spectrophotometer (Merk Pharo 100 Spectroquant™) with Merck cell test kits at the University of Limpopo, Biodiversity Laboratory. Conductivity, pH, salinity, total dissolved solids (TDS), water temperature and dissolved oxygen were measured in situ using a YSI Model 554 portable multi-parameter probe (YSI Inc. Yellow Springs, OH, USA). Flow velocity was measured using a Flo-mate portable flowmeter Model 2000 (Marsh McBirney, Maryland, US). Channel width and water depth were measured using a measuring tape and graduated measuring rod, respectively.

Macroinvertebrate sampling

Benthic macroinvertebrates were collected using a 30 cm by 30 cm sampling net with a 500 µm mesh size. The substrate was disturbed by kicking to free macroinvertebrates from the substrate. At each sampling site aquatic habitats (i.e. riffles, pools and vegetated margins) were sampled for approximately 6 min. The samples were preserved in 70% ethanol in 1 L polypropylene buckets and transported to the laboratory for identification. The macroinvertebrates were identified to family level except in the case of Oligochaeta and Hirudinea which were identified to class level, using keys by Gerber and Gabriel (2002). The samples were identified with the aid of a stereomicroscope (Leica EZ4) and magnifying glass.

Family level identification was also used to determine the functional feeding group (FFG) in the river except Oligochaeta and Hirudinea (Merritt and Cummins 1996; Cummins et al., 2005). The macroinvertebrates were classified into the following functional feeding groups: Shredders (SH), Gathering Collectors (GC), Filtering Collectors (FC), Scrapers (SC) and Predators (P).

Data analysis

Analysis of variance (ANOVA) was used to compare water variables among river sites and seasons, after testing for homogeneity of variances (Levene's test, $p > 0.05$) and normality of distribution (Shapiro-Wilk test, $p > 0.05$). The same tests were used to assess for differences in macroinvertebrate abundance among sites and seasons. In order to assess whether functional feeding group abundances were different among sites, an analysis of variance was performed, followed by Tukey HSD test. The

http://www.aloki.hu ● ISSN 1589 1623 (Print) ● ISSN 1785 0037 (Online)
DOI: http://dx.doi.org/10.15666/aeer/2001_189206

analysis was carried out using Statistica version 10.0 (2007). The macroinvertebrate assemblage composition was determined for each sampling site and seasons using number of taxa (S), total number of individuals and abundance of each taxon. The Shannon–Wiener diversity index (H′), was used to assess diversity as follows:

$$H' = \Sigma[(n/N) \times \ln(n/N)]$$

To assess compositional differences among sites, the percentage of intolerant taxa, Ephemeroptera + Plecoptera + Trichoptera (EPT), which is widely used as an indicator of disturbance to stream communities was also calculated. The South African Scoring System version 5 (SASS5) score, which is the sum of all macroinvertebrates pre-determined taxa tolerance values to pollution within a sample, and the Average Score Per Taxon (ASPT), calculated by dividing the SASS5 score by the sample number of taxa (Dickens and Graham, 2002), were further used to assess the river quality. Cluster analysis and non-metric multi-dimensional scaling (MDS) were used to identify grouping of sampling sites with similar macroinvertebrate assemblages using Euclidean distances (Kruskal, 1964). The percentage contribution of each FFG to the different communities was determined to find out the relative contribution of each group. The influence of physicochemical variables on macroinvertebrate communities and functional feeding groups were determined by canonical correspondence analysis (CCA) using CANOCO version 5.1 software (Ter Braak and Smilauer, 2002).

Results

Physiochemical variables

The pH values observed at the sites varied between 7.1 at Site 5 to 8.9 at Site 3 (*Table 2*). The mean temperature ranged from 18.3 °C at Site 6 to 20.6 °C at Site 3. The mean oxygen content ranged from 7.4 mg/l at Site 4 to 8.5 mg/l at Site 6. The highest mean conductivity and TDS were recorded at Site 5 and the lowest conductivity and TDS were recorded at Site 1 and Site 2 respectively. Temperature, pH, DO, conductivity, TDS, salinity and turbidity did not differ significantly among the sites (ANOVA, $P > 0.05$). However, temperature and turbidity differed significantly among the seasons (ANOVA, $P < 0.05$) (*Table 3*). Mean nitrate concentrations were generally higher at Sites 5 and Site 6, while phosphate concentration was below detection level at all sites. There was a significant seasonal variation in nitrate concentration among the seasons ($p < 0.002$). There were significant differences in channel width, water depth and velocity among the different sites and seasons.

Macroinvertebrate community structure

A total of 7,624 individual macroinvertebrates belonging to 39 families, 9 orders and two classes of Annelida (Oligochaeta and Hirudinea) were collected in the Steelpoort River. The dominant taxa were Baetidae (1757), Hydropsychidae (1140), followed by Simuliidae (611). Site 6 had the highest number of individuals of 1708 (22.4%), followed by Site 3 with 1451 (19.03%), Site 2 with 1243 (16.30%), Site 5 with 1230 (16.30%), Site 1 with 1020 (13.4%) and Site 4 had the lowest with 972 individuals (12.74%) (*Table 4*). Taxa richness ranged from 25 at Site 4 and Site 5 to 36 at Site 3.

http://www.aloki.hu ● ISSN 1589 1623 (Print) ● ISSN 1785 0037 (Online)
DOI: http://dx.doi.org/10.15666/aeer/2001_189206

The EPT index ranged from 5 at Site 5 to 12 at Site 3. Seasonally, the highest abundance was recorded during winter (2660), followed by autumn (2496), spring (1748) and then summer (720). Taxa richness differed among seasons, with the highest taxa richness recorded in Autumn (32) followed by summer (31), Spring (30) and the lowest in winter (29). Hierarchical cluster analysis used to evaluate the faunal similarities among the study sites showed three groups (*Fig. 2*). Cluster I was composed of Site 1 and Site 3), cluster II, was composed of Site 2 and Site 6, and cluster III, Site 4 and Site 5.

Table 2. *Mean water physical variables (±standard deviation) recorded across six sites of the river (range values are in the brackets)*

Variables	Site 1	Site 2	Site 3	Site 4	Site 5	Site 6
	Mean ± SD	Mean ± SD	Mean ± SD	Mean ± SD	Mean ± SD	Mean ± SD
Depth (m)	0.31 ± 0.31 (0.14-0.54)	0.41 ± 0.17 (0.31-0.61)	0.48 ± 0.05 (0.42-0.52)	0.54 ± 0.25 (0.29-0.87)	0.5 ± 0.07 (0.43-0.59)	0.44 ± 0.11 (0.31-0.54)
Width (m)	13 ± 3.26 (9.70-17.5)	11.6 ± 1.9 (9.8-13.6)	12.11 ± 1.92 (10.4-13.8)	13.02 ± 3.0 (9.4-16.7)	11.35 ± 1.18 (10.0-12.7)	18.12 ± 3.9 (10.5-30.0)
Velocity (m/s)	0.31 ± 0.21 (0.10-0.56)	0.57 ± 0.21 (0.44-0.70)	0.37 ± 0.12 (0.21-0.5)	0.63 ± 0.39 (0.28-1.15)	0.69 ± 0.16 (0.56-0.93)	0.54 ± 0.32 (0.19-0.90)
pH	8.6-8.7	7.7-8.2	7.5-8.9	7.5-8.7	7.1-8.7	7.7-8.7
Temperature (°C)	19.6 ± 3.9 (16.3-24.7)	20.17 ± 2.9 (17.3-23.3)	20.6 ± 2.4 (17.8-23.2)	19.8 ± 3.3 (16.2-22-6)	18.8 ± 2.7 (15.9-21.9)	18.3 ± 3.8 (13.8-21.7)
DO (mg/l)	7.9 ± 1.63 (6.5-10.2)	7.5 ± 0.46 (7.1-7.9)	8.2 ± 1.94 (6.8-11.0)	7.4 ± 0.64 (6.6-8.0)	8.3 ± 1.42 (6.7-10.0)	8.5 ± 1.75 (6.9-11.0)
EC (mS/cm)	227.7 ± 44.9 (188.0-275.2)	267.7 ± 21.3 (245-294.3)	280.3 ± 30.5 (248-319.9)	311.6 ± 40.1 (285.6-376)	324.9 ± 37.6 (285.6-376)	317.3 ± 22.9 (283.6-334.7)
TDS (mg/l)	214.8 ± 66.5 (148.1-305.5)	212.9 ± 55.0 (174.0-294.3)	221.1 ± 66.6 (180.7-319.9)	253.7 ± 76.0 (204-366.4)	264.7 ± 75.9 (214.5-376.0)	259.6 ± 26.9 (224-283.6)
Salinity (‰)	0.14 ± 0.05 (0.09-0.22)	0.15 ± (0.13-0.17)	0.15 ± 0.01 (0.13-0.16)	0.15 ± 0.02 (0.13-0.17)	0.17 ± 0.02 (0.16-0.19)	0.18 ± (0.15-0.21)
Turbidity (NTU)	3.57 ± 1.80 (1.6-5.8)	1.78 ± 0.82 (0.6-2.5)	7.0 ± 2.65 (0.7-7.0)	4.52 ± 3.58 (0.7-8.4)	6.17 ± 3.45 (2.8-9.2)	6.75 ± 1.60 (4.4-8.0)
Nitrate (mg/l)	0.035	0.021	0.165	0.191	0.97	1.315
Ortho-phosphate-P (mg/l)	< 0.01	< 0.01	< 0.01	< 0.01	< 0.01	< 0.01

Table 3. *One–way analysis of variance (ANOVA) based on the differences of physicochemical variables among sites and seasons (Bold values indicate $p < 0.05$)*

Variable	Site			Season		
	MS	F	p-value	MS	F	p-value
pH	0.243	0.971	0.46	0.470	2.184	0.12
Temperature	2.952	0.286	0.91	56.469	36.069	< 0.0001
Conductivity	1982	0.337	0.88	7345	1.566	0.22
TDS	1695	1.376	0.27	1169	0.862	0.48
DO	0.710	0.710	0.90	1.178	1.573	0.23
Salinity	0.01	1.150	0.37	0.001	1.447	0.26
Turbidity	3525	0.61	0.70	22830	8.642	< 0.001

http://www.aloki.hu ● ISSN 1589 1623 (Print) ● ISSN 1785 0037 (Online)
DOI: http://dx.doi.org/10.15666/aeer/2001_189206

Table 4. *Families and the FFGs of macroinvertebrates from the Steelpoort River*

Order/Class	Family	Site 1	Site 2	Site 3	Site 4	Site 5	Site 6	Total	FFG
Annelida	Oligochaeta	4	12	4	3	3	4	30	CG
	Hirudinea	0	6	53	3	3	1	66	P
Plecoptera	Perlidae	2	0	1	0	0	0	3	P
Ephemeroptera	Baetidae	376	281	462	73	218	537	1947	CG
	Caenidae	3	2	1	0	0	1	7	CG
	Heptageniidae	1	3	1	1	0	0	6	CG
	Leptophlebiidae	165	4	17	7	0	0	193	CG
	Teloganodidae	3	0	8	3	3	0	17	CG
	Tricorythidae	5	2	2	0	6	1	16	CG
Odonata	Synlestidae	0	0	0	0	0	6	6	P
	Coenagrionidae	57	41	308	7	12	29	454	P
	Aeshnidae	0	11	0	68	21	48	148	P
	Gomphidae	41	184	83	85	53	77	523	P
	Libellulidae	3	66	52	81	104	208	514	P
Hemiptera	Belostomatidae	3	20	34	2	2	3	64	P
	Gerridae	1	0	0	2	1	1	5	P
	Hydrometridae	0	0	3	0	1	0	4	P
	Naucoridae	13	3	1	8	2	10	37	P
	Veliidae	67	6	2	3	1	257	336	P
Trichoptera	Ecnomidae	1	7	4	36	40	19	107	P/CG
	Hydropsychidae	155	44	113	239	402	187	1140	CF
	Philopolamidae	0	0	4	0	0	0	4	CF
	Psychomyiidae	6	2	4	0	0	2	14	P
	Hydroptilidae	0	5	4	0	0	1	10	Sc/P
Coleoptera	Dytiscidae	3	3	6	1	1	26	40	P
	Elmidae	9	7	21	71	32	26	166	CG/Sc/Sh
	Gyrinidae	1	5	3	2	6	3	20	P
	Helodidae	1	1	5	0	0	0	7	Sh
	Hydrophilidae	0	0	4	0	0	3	7	P
Diptera	Athericidae	0	0	2	1	0	0	3	P
	Chironomidae	9	1	3	63	45	62	183	CG
	Muscidae	2	1	0	4	3	5	15	P
	Psychodidae	0	0	1	0	0	3	4	CG
	Simuliidae	22	208	25	103	208	45	611	CF
	Tabanidae	16	30	17	41	10	20	134	P
	Tipulidae	1	0	3	0	0	0	4	Sh/CG/P
Gastropoda	Lymnaeididae	0	2	7	0	1	4	14	Sc
	Physidae	0	1	22	0	0	16	39	Sc
	Planorbinae	0	1	5	0	0	3	9	Sc
	Thiaridae	0	223	66	15	0	0	304	Sc
Lepidoptera	Pyralidae	0	1	0	0	2	0	3	Sh
Total		970	1183	1351	922	1180	1608	7214	

Relationship between macroinvertebrates and physicochemical variables

Based on CCA carried out for individual variables, pH, EC, TDS, DO, temperature, salinity and turbidity were found to have a significant effect on macroinvertebrate community structure (*Fig. 3*). Site 1 was characterized by high temperature and pH and the macroinvertebrates that were associated with this site included Baetidae, Leptophlebiidae and Perlidae, which are sensitive to pollution. Sites 5 and 6 were characterized by conductivity, TDS, nitrate and salinity and associated with both

http://www.aloki.hu ● ISSN 1589 1623 (Print) ● ISSN 1785 0037 (Online)
DOI: http://dx.doi.org/10.15666/aeer/2001_189206

sensitive and tolerant taxon, such as Aeshnidae, Ecnomidae and Chironomidae. The first and second axes of the CCA analysis accounted for 35.5% and 58.8% variance (*Table 5*).

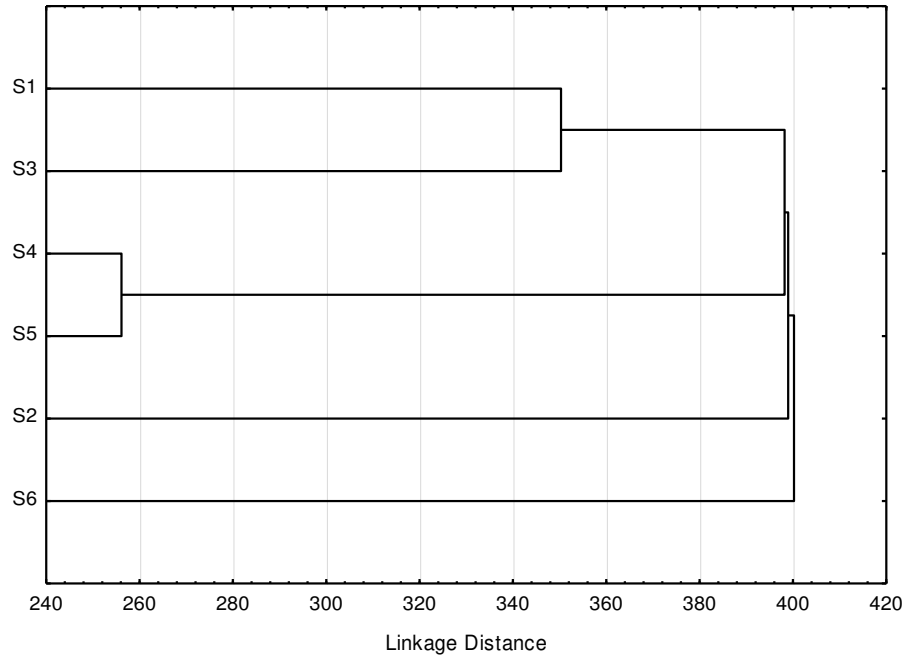

Figure 2. *Dendrogram showing the hierarchical cluster analysis of aquatic macroinvertebrate assemblages among the sampling site, with the following groupings; S1 and S3, S4 and S5, S2 and S6)*

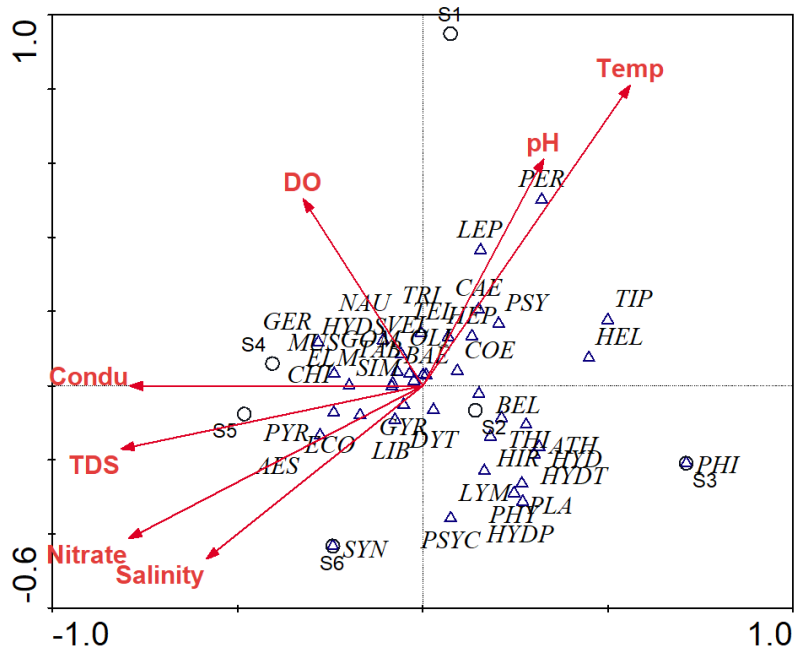

Figure 3. *CCA plots showing the relationship between measured environmental variables with macroinvertebrate families and sampling sites (abbreviations for macroinvertebrate families are in Table 2)*

http://www.aloki.hu ● ISSN 1589 1623 (Print) ● ISSN 1785 0037 (Online)
DOI: http://dx.doi.org/10.15666/aeer/2001_189206

Table 5. *The canonical correspondence analysis (CCA) between functional feeding groups and environmental variables for Dwars and Spekboom rivers*

Eigenvalues:	0.131	0.087	0.081	0.044	0.370
Taxa-environment correlations:	1.000	1.000	1.000	1.000	
% cumulative variance:	35.5	58.8	80.7	92.5	
of taxa-environment:	35.5	58.8	80.7	92.5	
Sum of all eigenvalues					0.370

Functional feeding groups

The collector-gatherers were the most abundant functional feeding group at Site 1, collector-filterers were the most dominant group at Site 4 and Site 5, predators were the most dominant group at Site 2, Site 3 and Site 6 (*Fig. 4*). Shredders were least represented at all sites of the river. The collector-gatherers made up of 34.82%, followed by predators (33.96%), collector-filterers (24.33%), scrapers (5.89%), and then shredders (1.00%). The abundance of collector-gatherers and predators increased at Site 6 (*Table 6*). There was less variation in abundance of predators among the sites as compared to the other groups. Seasonally, the collector-gatherers were dominant in winter, collector-filterers were dominant in spring and predators were the dominant group in autumn and summer (*Table 7*). The highest seasonal composition was in winter (34.79%), followed by autumn (32.80%), spring (2312%) and then summer (9.29%) (*Fig. 5*). The abundance of collector-gatherers increased in winter, collector-filterers and shredders in spring, predators and scrapers increased in autumn. However, there were no significant variations in terms of distribution of the FFGs among seasons ($p > 0.05$).

Table 6. *Relative abundance of functional feeding groups of macro invertebrates at the various sites in the Steelpoort River. The functional feeding groups (FFG)—Filterers (Ft), collector–gatherers (CG), predators (Pr), scrappers (Sc) and shredders (Sh)*

Site	CF	CG	P	Sc	Sh	Total	Relative abundance (%)
1	177	570	215	3	5	920	13.45
2	252	311	383	232	5	1183	16.40
3	142	509	578	109	13	1351	18.72
4	342	191	326	38	25	922	12.78
5	610	305	240	11	14	1180	16.36
6	232	626	708	32	10	1608	22.29
Total	1755	2512	2450	425	72	7214	100
Relative abundance (%)	24.33	34.82	33.96	5.89	1.00	100	

Table 7. *Functional feeding groups of macroinvertebrates collected during different seasons in the Steelpoort River. The functional feeding groups (FFG)—Filterers (Ft), collector–gatherers (CG), predators (Pr), scrappers (Sc) and shredders (Sh)*

FFG	Summer	Autumn	Winter	Spring	Total
CF	71	558	398	728	1755
CG	144	799	1252	317	2512
P	310	842	774	525	2451
Sc	129	151	78	68	426
Sh	16	16	8	30	70
Total	670	2366	2510	1668	7214

http://www.aloki.hu ● ISSN 1589 1623 (Print) ● ISSN 1785 0037 (Online)
DOI: http://dx.doi.org/10.15666/aeer/2001_189206

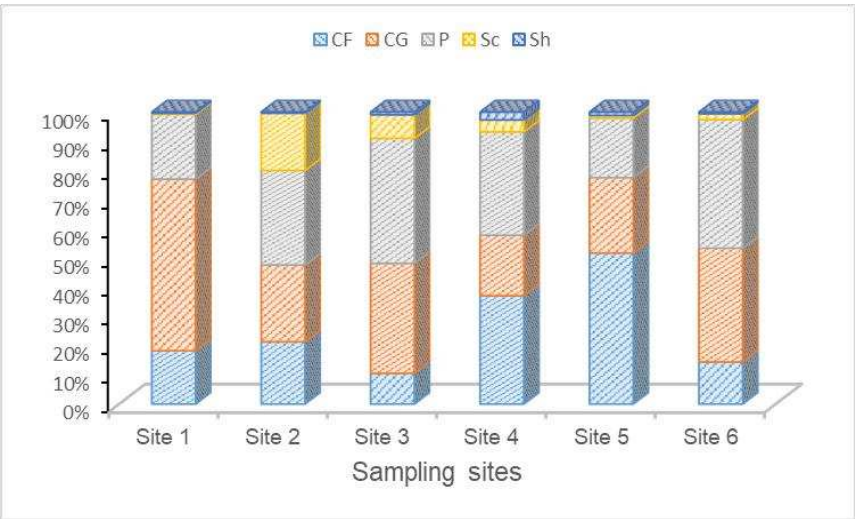

Figure 4. *Composition of the functional feeding groups of aquatic macroinvertebrates in the Steelpoort River*

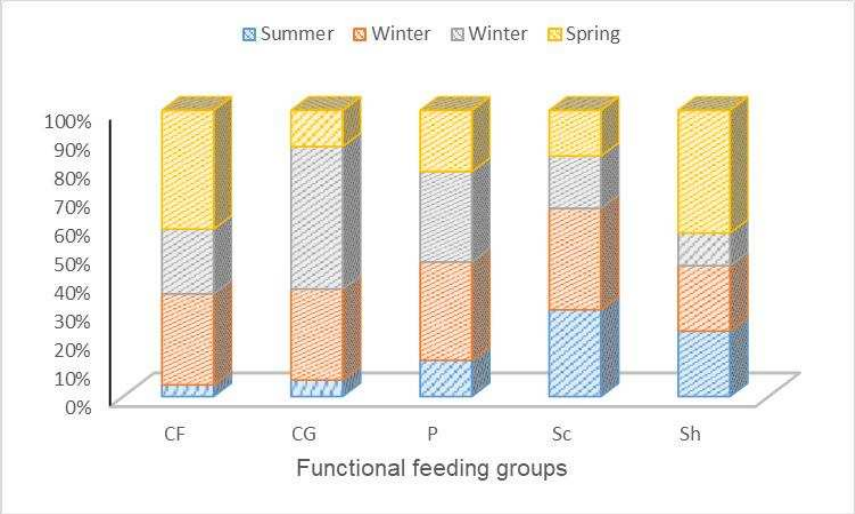

Figure 5. *Seasonal composition of the FFGs of aquatic macroinvertebrates in the Steelpoort River*

The CCA tri-plot of the selected water quality variables (physicochemical parameters and nutrients) showed that collector-gatherers and collector-filterers were associated with turbidity, ammonium, salinity, TDS and conductivity, predators with nitrite, phosphate and velocity and scrapers were associated with depth, and shredders were associated with temperature (*Fig. 6*).

Discussion

Physicochemical variables

Most of the physicochemical variable changed relatively little across sites with more variables changing across seasons. The mean value of water temperature was found

http://www.aloki.hu ● ISSN 1589 1623 (Print) ● ISSN 1785 0037 (Online)
DOI: http://dx.doi.org/10.15666/aeer/2001_189206

within the permissible limits, which was between 25 and 30 °C (DWAF, 1996). The highest mean DO was recorded at Site 6 which had the lowest mean temperature, as solubility of oxygen increases with decreasing temperature. The high DO could also be from photosynthesis due to high exposure to sunlight and high stream velocity (Connollym et al., 2004). Site 6 had less canopy cover that could have facilitated more sunlight reaching the water for photosynthesis. Significant increase in conductivity, TDS, salinity, turbidity and nitrate at the downstream sites, Sites 5 and 6, could be attributed to increase flow discharge and flooding from other parts of the river. High TDS levels are known to occur in streams draining mining sites after large volumes of rock are exposed to weathering elements such as air and water, causing rapid dissolution of rocks and minerals into waters draining the site (Bernhardt et al., 2012).

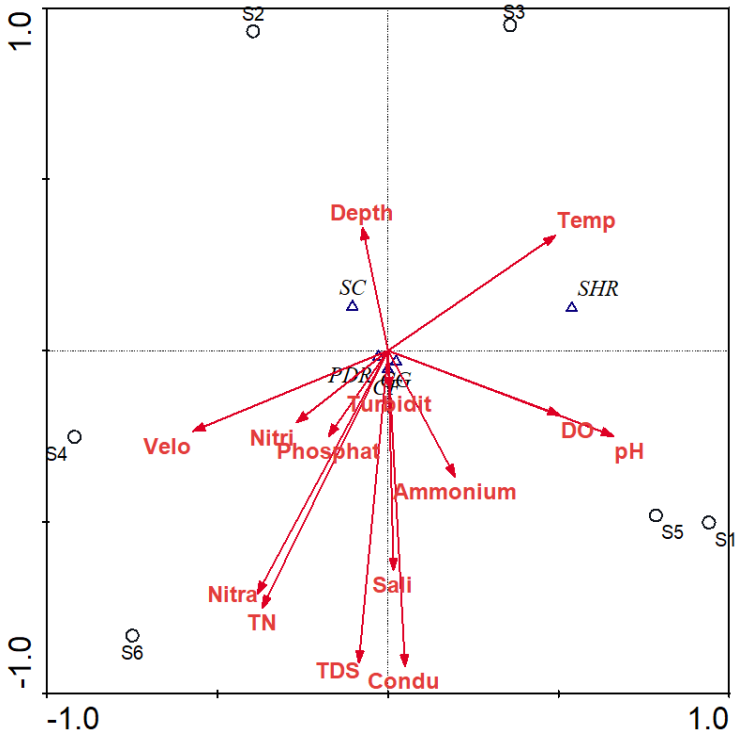

Figure 6. *CCA tri-plot shows the relationship between FFG and physicochemical parameters at the Steelpoort River*

In areas of human settlement, such as Site 5 and Site 6, TDS is increased by pollution from sewage, urban runoff and industrial wastewater. Water with TDS less than 400 mg/l as observed in this study is generally considered to be good water (WHO, 2004). However, the downstream of the river needs to be monitored as it has potential for disturbing the ecosystem integrity if it continues to increase. For nitrate, the high concentration at Site 5 and Site 6 could be due to sewage (and industrial effluents) and storm water runoff. Several studies have shown that urban streams worldwide are often polluted by runoff and combined sewer outflows (Bere and Nyamupingidza, 2014).

Macroinvertebrates

There was spatial variation of macroinvertebrate assemblages. The sites with strong anthropogenic pressures had lower abundances than less impacted sites. The variation

http://www.aloki.hu ● ISSN 1589 1623 (Print) ● ISSN 1785 0037 (Online)
DOI: http://dx.doi.org/10.15666/aeer/2001_189206

among the sites in macroinvertebrate abundance could be due to the variation in the physicochemical factors which favours their survival and perhaps due to the presence of high organic matter within the site (Sharma et al., 2013). The high abundance of macroinvertebrates at Site 2 and Site 6 could be due to the relatively good water quality the Steelpoort River receives from the Dwars and Spekboom rivers respectively. This shows the importance of tributaries in restoring main stream ecosystem. However, the high abundance at Site 3 could be due to the presence of different biotopes. The family with the highest abundance at all the sites except Site 4 and Site 5 was Baetidae. Baetidae has a cosmopolitan distribution and represents a quarter of the Ephemeroptera diversity worldwide both at generic and specific levels (Gattolliat and Nieto, 2009; Sartori and Brittain, 2015).

Hierarchical cluster analysis showed three groups. Cluster I was composed of Site 1 and Site 3, this could be due to agricultural activities near both sites, cluster II, was composed of Site 2 and Site 6, both sites receive water of relatively good quality from Dwars and Spekboom respectively, and cluster III, Site 4 and Site 5 were more affected by mining and municipal waste waters. Thus, the human activities in the catchment affected the water quality and hence the distribution of the macroinvertebrates. The CCA analysis revealed a correlation between the aquatic macroinvertebrate taxa and water quality. Cumulative percentage variance of taxa-environmental variable relations for axis 1 and 2 was 58.8%. This is an indication that no single environmental variable fully explained taxon composition and distribution pattern across the sites (Niba and Sakwe, 2018).

Seasonally, the highest abundance of macroinvertebrates was in winter (dry season). This confirms the assertion that temperature is a dominant factor in the seasonal structuring of the macroinvertebrate community (Beltrán et al., 2011; Hudu and Rawi, 2019). Thus, in dry seasons, macroinvertebrates have greater possibilities of colonising the river area, since the habitat becomes homogenised and their densities and specific richness can increase (Reynaga and Dos Santos, 2013). In summer (rainy season), with high precipitation and flooding, some of the macroinvertebrates' habitats could have been destroyed and some drifted to downstream. Studies by Gualdoni and Oberto (2012) found that in rainy seasons, when the water flow increases due to the high level of precipitation, macroinvertebrates are drifted downstream.

Functional feeding groups

The collector-gatherers were the most dominant functional feeding group. The predominance of collector-gatherers is attributed to their ecological plasticity and capacity for the occupation of rapid water environments (Brasil et al., 2014) and their ability to occupy in a broad variety of habitats (Castro et al., 2016). The collector-filterers and collector-gatherers together made up of more than 50% of the total macroinvertebrates recorded. Collectors are commonly abundant in streams and typically increase in abundance with stream size (Vannote et al., 1980). The predators were well distributed along the whole river and could be due to availability of food and less competition (Ono et al., 2020). Predators normally have a similar proportion throughout the length of a stream channel, according to the river continuum concept or, alternatively, their abundance may depend on prey availability (Vannote et al., 1980). Similar to other studies, the predator distribution was almost similar at all sites. Scraper abundance can be related to algal primary production, which is in turn affected by available nutrients and light.

http://www.aloki.hu ● ISSN 1589 1623 (Print) ● ISSN 1785 0037 (Online)
DOI: http://dx.doi.org/10.15666/aeer/2001_189206

The low numbers of shredders in the river could be due to the fact that effective microbial activities replace shredder activity at high temperatures (Kaboré et al., 2016; Madomguia et al., 2016). The highest abundance of scrapers at S2 could be due to the open canopy causing more sunlight to reach the water for photosynthesis. This also explains the scarcity of shredders at S1 and S2 due to less riparian canopy to provide enough leaf litter as an energy source. Human activities have contributed to the loss of riparian vegetation along the river. Similar results have been reported that shredders are intimately related to the riparian vegetation, because of their reliance on allochthonous feeding resources (Brasil et al., 2014; Masese et al., 2014). The low numbers of shredders and scrapers could also be due to the fact that these two groups are more sensitive to disturbances, while collector-gatherers and collector-filterers are more tolerant to pollution that might alter the availability of certain food (Barbour et al., 1996). It has even been found that some taxa can shift their feeding in response to changes in land use and riparian conditions (Benstead and Pringle, 2004; Li and Dudgeon, 2008). Thus, the functional groups can potentially be used to assess aquatic ecosystem health (Bhawsar et al., 2015; Fu et al., 2016).

Seasonally, the highest taxon abundance was in winter. Winter is the drier season of the year in the study area hence, the river receives less runoff draining from the catchment. In general, factors driving macroinvertebrate seasonal variation include precipitation/discharge, temperature, and photoperiod, and each of these factors can influence disturbance regimes in streams (Bêche et al., 2006). Seasonal variation of macroinvertebrate distribution can also be caused by changes in current velocity, substrate type and organic matter.

According to the continuum river concept, low order rivers such as the Steelpoort River should contain mainly collector-gatherers and shredder organisms (Vannote et al., 1980). However, in this study the predominant group was the predators and collector-gatherers, and the least predominant group was the shredders. The RCC states that the shredders should dominate among the functional feeding groups when the source of the river is within a shaded area (Vannote et al*.,* 1980). The riparian zone of this particular river has been disturbed due to anthropogenic activities. Shredders are intimately related with the riparian vegetation, given their dependence on allochthonous feeding resources (Allan and Castillo, 2007). The high diversity and non-compliance of many tropical rivers to the Vannote's RCC model have also been observed by other studies (e.g. Masese et al., 2014; Brasil et al., 2014; Doong et al., 2021). Removal of indigenous vegetation is known to deplete the allochthonous resources of a river and therefore reduces shredder abundance (Minaya et al., 2013). The most noticeable impact observed during this study was pipeline construction which has resulted in the removal of riparian vegetation and causing erosion of stream banks along the river. This has contributed to the sediment loads entering the river and therefore reduction in microhabitats for the macroinvertebrates. Substrate heterogeneity positively affects the richness and functional diversity of macroinvertebrate communities (Milesi et al., 2016). In many parts of the world, land use change, particularly loss of riparian vegetation, has resulted in loss of diversity and major shifts in the structural and functional organization of macroinvertebrates in streams (Jinggut et al., 2012; Silva-Araújo et al., 2020; Addo-Bediako, 2021).

http://www.aloki.hu ● ISSN 1589 1623 (Print) ● ISSN 1785 0037 (Online)
DOI: http://dx.doi.org/10.15666/aeer/2001_189206

Conclusion

The variations of macroinvertebrate community structure observed could be attributed to land-use changes that affected water quality of the river. There was no trend of distribution of macroinvertebrates which emphasized that localized disturbance had an influence on their distribution. Predators, collector-gatherers and collector-filterers dominated throughout the river. This finding partially agrees with the RCC prediction that midstream should be co-dominated by collectors (collector-gatherers and collector-filterers) and scrapers. The downstream site (Site 6) was also dominated by the collectors, which agree with the prediction of the RCC. The low number of shredders in the river especially at the upstream sites is an indication of degradation in the catchment especially loss of riparian vegetation. The highest abundance of FFG in winter indicates seasonal variation in water quality. The study shows that ecosystem function can be altered by changes in environmental factors and FFG composition could also be used as an indicator of ecosystem change. Thus, the human activities in the catchment of the Steelpoort River is affecting the river and the aquatic biota, such as the macroinvertebrate communities. There is a need therefore to develop an effective and sustainable water quality monitoring programme for the river. Future studies should include broader consequence of land use changes and climate change on ecosystem functioning and functional mechanism of macroinvertebrates.

Acknowledgements. We are grateful to South Africa National Research Foundation (NRF) for providing financial support for study.

Conflict of interests. The authors declare that they have no conflicts of interests.

REFERENCES

[1] Addo-Bediako, A. (2020): Assessment of heavy metal pollution in the Blyde and Steelpoort Rivers of the Olifants River System, South Africa. – Polish Journal of Environmental Studies 29(5): 3023-3039.

[2] Addo-Bediako, A. (2021): Spatial distribution patterns of benthic macroinvertebrate functional feeding groups in two rivers of the Olifants River System, South Africa. – Journal of Freshwater Ecology 36(1): 97-109.

[3] Allan, J. D., Castillo, M. M. (2007): Stream Ecology: Structure and Function of Running Waters. – Springer, Dordrecht.

[4] Ashton, P. J., Dabrowski, J. M. (2011): An overview of water quality and the causes of poor water quality in the Olifants River Catchment. – WRC Project No. K8/887. Water Research Commission, Pretoria.

[5] Barbour, M., Gerritsen, J., Griffith, G., Frydenborg, R., Mccarron, E., White, J., Bastian, M. (1996): A framework for biological criteria for Florida streams using benthic macroinvertebrates. – Journal of the North American Benthological Society 15(2): 185211.

[6] Bêche, L. A., Mcelravy, E. P., Resh, V. H. (2006): Long-term seasonal variation in the biological traits of benthic-macroinvertebrates in two Mediterranean climate streams in California, U.S.A. – Freshwater Biology 51: 56-75.

[7] Beltrán, L., Miserendino, M. L., Pessacq, P. (2011): Life history, seasonal variation and production of Andesiops torrens (Lugo-Ortiz & McCafferty) and Andesiops peruvianus (Ulmer) (Ephemeroptera: Baetidae) in a headwater Patagonian stream. – Limnologica 41: 57-62.

http://www.aloki.hu ● ISSN 1589 1623 (Print) ● ISSN 1785 0037 (Online)
DOI: http://dx.doi.org/10.15666/aeer/2001_189206

[8] Benstead, J. P., Pringle, C. M. (2004): Deforestation alters the resource base and biomass of endemic stream insects in eastern Madagascar. – Freshwater Biology 49: 490-501.
[9] Bere, T., Nyamupingidza, B. (2014): Use of biological monitoring tools beyond their country of origin: a case study of the South African Scoring System Version 5 (SASS5). – Hydrobiologia 722: 223-232.
[10] Bernhardt, E. S., Lutz, B. D., King, R. S., Fay, J. P., Carter, C. E., Helton, A. M., Campagna, D., Amos, J. (2012): How many mountains can we mine? Assessing the regional degradation of Central Appalachian rivers by surface coal mining. – Environmental Science and Technology 46: 8115-8122.
[11] Bhawsar, A., Bhat, M. A., Vyas, V. (2015): Distribution and composition of macroinvertebrates functional feeding groups with reference to catchment area in Barna Sub-Basin of Narmada River Basin. – International Journal of Scientific Research and Engineering Studies 3(11): 385-393.
[12] Brasil, S., Juen, L., Batista, J. D., Pavan, M. G., Cabette, H. S. R. (2014): Longitudinal distribution of the functional feeding groups of aquatic insects in streams of the Brazilian Cerrado Savanna. – Neotropical Entomology 43: 421-428.
[13] Castro, D. M. P., Carvalho, D. R., Pompeu, P. S., Moreira, M. Z., Nardoto, G. B., Callisto, M. (2016): Land use influences niche size and the assimilation of resources by benthic macroinvertebrates in tropical headwater streams. – PLoS One 11: 1-19.
[14] Castro, D. M. P., Dolédec, S., Callisto, M. (2018): Land cover disturbance homogenizes aquatic insect functional structure in neotropical savanna streams. – Ecological Indicators 84: 573-582.
[15] Chen, N., Chen, L., Ma, Y., Chen, A. (2019): Regional disaster risk assessment of China based on self-organizing map: clustering, visualization and ranking. – International Journal of Disaster Risk Reduction 33: 196-206.
[16] Connollym, N. M., Crossland, R., Pearson, R. G. (2004): Effect of low dissolved oxygen on survival, emergence, and drift of tropical stream macroinvertebrates. – Journal of the North American Benthological Society 23(2): 251-270.
[17] Cummins, K. W. (2018): Functional Analysis of Stream Macroinvertebrates. – In: Gokce, D. (ed.) Limnology. IntechOpen, London. DOI: 10.5772/intechopen.79913.
[18] Cummins, K. W., Merritt, R. W., Andrade, P. C. N. (2005): The use of macroinvertebrate functional groups to characterize ecosystem attributes in selected streams and rivers in south Brazil. – Studies on Neotropical Fauna Environment 40(1): 69-89.
[19] Dallas, H. F. (2007): The influence of biotope availability on macroinvertebrate assemblages in South African Rivers: implications for aquatic bioassessment. – Freshwater Biology 52: 370-380.
[20] Dalu, T., Wasserman, R. J., Tonkin, J. D., Mwedzi, T., Magoro, M. L., Weyl, O. L. F. (2017): Water or sediment? Partitioning the role of water column and sediment chemistry as drivers of macroinvertebrate communities in an austral South African stream. – Science of the Total Environment 607-608: 317-325.
[21] Department of Water Affairs and Forestry (DWAF) (1995): Middle Steelpoort Catchment, Groundwater Management Plan. – DWAF, Pretoria.
[22] Department of Water Affairs and Forestry (DWAF) (1996): South African Water Quality Guidelines. Volume 7: Aquatic Ecosystems. Second Ed. – DWAF, Pretoria.
[23] Doong, M. K. T., Anticamara, J. A., Magbanua, F. S. (2021): Spatial variations in the distribution of benthic macroinvertebrate functional feeding groups in tropical rivers. – Indonesian Journal of Limnology 2(1): 35-52.
[24] Ferreira, V., Encalada, A. C., Graça, M. A. S. (2012): Effects of litter diversity on decomposition and biological colonization of submerged litter in temperate and tropical streams. – Freshwater Science 31: 945-962.
[25] Fierro, P., Bertrán, C., Tapia, J., Hauenstein, E., Peña-Cortés, F., Vergara, V., Cerna, C., Vargas-Chacoff, L. (2017): Effects of local land-use on riparian vegetation, water quality,

http://www.aloki.hu ● ISSN 1589 1623 (Print) ● ISSN 1785 0037 (Online)
DOI: http://dx.doi.org/10.15666/aeer/2001_189206

and the functional organization of macroinvertebrate assemblages. – Science of the Total Environment 609: 724-734.

[26] Fu, L., Jiang, Y., Ding, J., Liu, Q., Peng, Q. Z., Kang, M. Y. (2016): Impacts of land use and environmental factors on macroinvertebrate functional feeding groups in the Dongjiang River basin, southeast China. – Journal of Freshwater Ecology 31(1): 21-35.

[27] Gattolliat, J. L., Nieto, C. (2009): The family Baetidae (Insecta: Ephemeroptera): synthesis and future challenges. – Aquatic Insects 31: 41-62.

[28] Gerber, A., Gabriel, M. J. M. (2002): Aquatic Invertebrates of South African Rivers: Field Guide. – Resource Quality Services, Department of Water Affairs and Forestry, Pretoria.

[29] Gualdoni, C. M., Oberto, A. M. (2012): Estructura de la comunidad de macroinvertebrados del arroyo Achiras (Córdoba, Argentina): análisis previo a la construcción de una presa. – Iheringia Serie Zoologia 102: 177-186.

[30] Hudu, A. N., Rawi, C. S. M. (2019): Functional Feeding Group (FFG) of Aquatic Macroinvertebrate in Middle Reach of Kerian River Basin of North Malaysia Peninsula. – Tropical Life Sciences Research 30(2): 1-12.

[31] Jinggut, T., Yule, C. M., Boyero, L. (2012): Stream ecosystem integrity is impaired by logging and shifting agriculture in a global megadiversity center (Sarawak, Borneo). – Science of the Total Environment 437: 83-90.

[32] Jun, Y-C., Kim, N-Y., Kim, S-H., Park, Y-S., Kong, D-S., Hwang, S-J. (2016): Spatial distribution of benthic macroinvertebrate assemblages in relation to environmental variables in Korean Nationwide streams. – Water 8(1): 27.

[33] Kaboré, I., Moog, O., Alp, M., Guenda, W., Koblinger, T., Mano, K., Ouéda, A., Ouédraogo, R., Trauner, D. and Melcher, A. H. (2016): Using macroinvertebrates for ecosystem health assessment in semi-arid streams of Burkina Faso. – Hydrobiologia 766: 57-74.

[34] Kim, D-H., Chon, T-S., Kwak, G-S., Lee, S-B., Park, Y-S. (2016): Effects of land use types on community structure patterns of benthic macroinvertebrates in streams of urban areas in the South of the Korea Peninsula. – Water 8(5): 187.

[35] Kruskal, J. B. (1964): Multidimensional scaling by optimising goodness of fit to a nonmetric hypothesis. – Psychometrica 29: 1-27.

[36] Li, A. O. Y., Dudgeon, D. (2008): Food resources of shredders and other benthic macroinvertebrates across a range of shading conditions in tropical Hong Kong streams. – Freshwater Biology 53: 2011-2025.

[37] Li, L., Zheng, B., Liu, L. (2010): Biomonitoring and bioindicators used for river ecosystems: definitions, approaches and trends. – Procedia Environmental Sciences 2: 1510-1524.

[38] Li, H., You, S., Zhang, H., Zheng, W., Zou, L. (2018): Investigating the environmental quality deterioration and human health hazard caused by heating emissions. – Science of the Total Environment 628: 1209-1222.

[39] Madomguia, D., Zebaze, T. S. H. and Fomena, A. (2016): Macro invertebrates functional feeding groups, Hilsenhoff biotic index, percentage of tolerant taxa and intolerant taxa as major indices of biological assessment in ephemeral stream in Sudano-Sahelian zone (Far-North, Cameroon). – International Journal of Current Microbiology and Applied Sciences 5: 792-806.

[40] Masese, F. O., Kitaka, N., Kipkemboi, J., Gettel, G. M., Irvine, K., McClain, M. E. (2014): Macroinvertebrate functional feeding groups in Kenyan highland streams: evidence for a diverse shredder guild. – Freshwater Science 33: 435-450.

[41] Meira, B. R., Progênio, M., Leite, E. C., Lansac-Tôha, F. M., Durán, C. L. G., Jati, S., Rodrigues, L. C., Lansac-Tôha, F. A., Velho, L. F. M. (2021): Functional feeding groups of Protist Ciliates (Protist: Ciliophora) on a neotropical flood plain. – Annales de Limnologie International Journal of Limnology 57: 13.

http://www.aloki.hu ● ISSN 1589 1623 (Print) ● ISSN 1785 0037 (Online)
DOI: http://dx.doi.org/10.15666/aeer/2001_189206

[42] Merritt, R. W., Cummins, K. W., Berg, M. B. (2017): Trophic Relationships of Macroinvertebrates. Chap. 20. – In: Hauer, F. R., Lamberti, G. A. (eds.) Methods in Stream Ecology. Academic Press (Elsevier), London, pp. 413-433.
[43] Milesi, S. V., Dolédec, S., Melo, A. S. (2016): Substrate heterogeneity infuences the trait composition of stream insect communities: an experimental in situ study. – Freshwater Science 35: 1321-1329.
[44] Minaya, V., McClain, M. E., Moog, O., Omengo, F., Singer, G. A. (2013): Scale-dependent effects of rural activities on benthic macroinvertebrates and physico-chemical characteristics in headwater streams of the Mara River, Kenya. – Ecological Indicators 32: 116-122.
[45] Munyika, S., Kongo, V., Kimwaga, R. (2014): River health assessment using macro-invertebrates and water quality parameters: a case of the Orange River Namibia. – Physics and Chemistry of the Earth 76: 140-148.
[46] Niba, A., Sakwe, S. (2018): Turnover of benthic macroinvertebrates along the Mthatha River, Eastern Cape, South Africa: implications for water quality bio-monitoring using indicator species. – Journal of Freshwater Ecology 33: 157-171.
[47] Ono, E. R., Manoel, P. S., Melo, A. L. U., Uieda, V. S. (2020): Effects of riparian vegetation removal on the functional feeding group structure of benthic macroinvertebrate assemblages. – Community Ecology 21: 145-157.
[48] Príncipe, R., Gualdoni, C., Oberto, A., Raffaini, G., Corigliano, M. (2010): Spatial-temporal patterns of functional feeding groups in mountain streams of Córdoba, Argentina. – Ecologia Austral 20: 257−268.
[49] Ramirez, A., Gutiérrez-Fonseca, P. E. (2014): Functional feeding groups of aquatic insect families in Latin America: a critical analysis and review of existing literature. – Revista de Biologia Tropical 62: 155-167.
[50] Rasifudi, L., Addo-Bediako, A., Swemmer, A., Bal, K. (2018): Distribution and diversity of benthic macroinvertebrates in the Selati River of Olifants River System, South Africa. – African Entomology 26: 398-406.
[51] Reynaga, M. C., Dos Santos, D. A. (2013): Contrasting taxonomical and functional responses of stream invertebrates across space and time in a Neotropical basin. – Fundamental and Applied Limnology 183: 121-133.
[52] Santhosh, S. K., Ashadevi, R. (2017): Biomonitoring as a strategy for ecosystem health—a case study at the upper reaches of Vamanapuram River, Kerala. – International Journal of Science and Research 6: 750-754.
[53] Sartori, M., Brittain, J. E. (2015): Order Ephemeroptera. – In: Thorp, J. H., Rogers, D. C. (eds.) Thorp and Covich's Freshwater Invertebrates. 4th Ed. Vol. I. Ecology and General Biology. Academic Press, Cambridge, MA.
[54] Sharma, K. K., Antal, N., Kour, S., Devi, A., Sharma, V. (2013): Biodiversity and Abundance of benthic macroinvertebrates communities of Datta-Da-Talab Pond, Birpur, India. – International Multidisciplinary Research Journal 3: 13-17.
[55] Silva-Araújo, M., Silva-Junior, E. F., Neres-Lima, V., Feijó-Lima, R., Tromboni, F., Lourenco-Amorim, C., Thomas, S. A., Moulton, T. P., Zandonà, E. (2020): Effects of riparian deforestation on benthic invertebrate community and leaf processing in Atlantic forest streams. – Perspectives in Ecology and Conservation 18: 277-282.
[56] Stimie, C., Richters, E., Thompson, H., Perret, S., Matete, M., Abdallah, K., Kau, J., Mulibana, E. (2001): Hydro-Institutional Mapping in the Steelpoort River Basin, South Africa. – Working Paper 17 (South Africa Working Paper No. 6). International Water Management Institute. Colombo.
[57] Ter Braak, C. J. F. and Smilauer, P. (2002): CANOCO Reference Manual and CanoDraw for Windows User's Guide: Software for Canonical Community Ordination (version 4.5). – Biometris, Wageningen.

http://www.aloki.hu ● ISSN 1589 1623 (Print) ● ISSN 1785 0037 (Online)
DOI: http://dx.doi.org/10.15666/aeer/2001_189206

[58] Vannote, R. L., Minshall, G. W., Cummins, K. W., Sedell, J. R., Cushing, C. E. (1980): The river continuum concept. – Canadian Journal of Fisheries and Aquatic Sciences 37: 130-137.
[59] Van Veelen, M., Dhemba, N. (2011): Development of reconciliation strategy for the Olifants River water supply. – Water Quality Report No. PWMA04/B50/00/8310/7, South Africa. P76.
[60] WHO (World Health Organization Standard for Drinking Water) (2004): Guidelines for Drinking Water Quality Vol. 1 Recommendation. – France.
[61] Wright, I., Ryan, M. (2016): Impact of mining and industrial pollution on stream macroinvertebrates: importance of taxonomic resolution, water geochemistry and EPT indices for impact detection. – Hydrobiologia 772: 103-115.

http://www.aloki.hu ● ISSN 1589 1623 (Print) ● ISSN 1785 0037 (Online)
DOI: http://dx.doi.org/10.15666/aeer/2001_189206

STRAW RETURN WITH BIOCHAR INCREASED SOIL MACRO-AGGREGATES AND IMPROVED FLUE-CURED TOBACCO (*Nicotiana tabacum* L.) YIELD AND QUALITY

JIANG, C.[1] – ZU, C.[1] – WANG, H.[2] – YAN, Y.[1] – LIU, Y.[3] – SHEN, J.[1*]

[1]*Tobacco Research Institute, Anhui Academy of Agricultural Sciences, Hefei 230031, China (e-mail: chaoqjiang@163.com (Jiang, C.); lcz2468@sina.com (Zu, C.); feng9686@163.com (Yan, Y.))*

[2]*Institute of Soil Science, Chinese Academy of Sciences, Nanjing 210008, PR China (e-mail: 656490434@qq.com (Wang, H.))*

[3]*Anhui provincial tobacco company, Hefei 230031, China (e-mail: clonelin@163.com (Liu, Y.))*

[*]*Corresponding author*
e-mail: shenjia0000@126.com; phone: +86-551-6514-8987; fax: +86-551-6514-8991

(Received 15th Jul 2021; accepted 28th Oct 2021)

Abstract. Straw return and biochar are often applied to improve soil fertility and increase crop yield. However, the effects of these practices on soil aggregates and tobacco leaf yield and quality are still unclear. Five treatments: no straw (CK), application of rice straw (RS), tobacco straw biochar (TSB), RS plus TSB (RS+TSB), and RS plus pig manure (RS+PM) were conducted to evaluate the effects of straw return and biochar on soil aggregates, tobacco leaf yield and quality in Southern Anhui, China. Results showed that TSB significantly increased soil pH by 0.38. The RS+TSB and RS+PM significantly increased the contents of soil organic matter, available nitrogen (N) and potassium (K). Biochar and straw return increased >5 mm aggregates fraction in topsoil (0-20 cm) with an order of RS+PM > RS+TSB > TSB > RS. The RS+TSB and RS+PM significantly increased the yield, appearance and sensory quality of tobacco leaf. The leaf yield and quality were positively correlated with >5 mm aggregates fraction, but negatively correlated with <0.25 mm aggregates. These results indicated that straw return with pig manure (375 kg ha^{-1}) or biochar (1050 kg ha^{-1}) increased the yield and quality of tobacco leaf, likely due to their effect on large soil aggregate and the available of macronutrients in soil.
Keywords: *tobacco-planting soil, soil quality, sensory quality of tobacco leaf, aggregate fractions, pig manure*

Introduction

Flue-cured tobacco (*Nicotiana tabacum* L.) is an essential economic crop in China, and the yield and quality of tobacco leaves are closely related to the soil structure and fertility (Zheng et al., 2019; Jiang et al., 2020). However, soil hardening and nutrient imbalance are prevalent in tobacco growing areas in China due to the long-term excessive application of chemical fertilizer and less input of organic fertilizer, which significantly affect the growth and development of tobacco plants, leading to the decline of tobacco leaf yield and quality (Mu et al., 2017; Jia et al., 2020). Therefore, it is urgent to improve the soil structure and quality of tobacco fields. At present, studies on soil improvement were mainly focuses on straw return, organic manure application, biochar application and green manure planting and so on (Lehmann, 2007; Jia et al., 2020). As a common organic material, reasonable application of straw return can improve the soil physical and chemical properties. It was reported that straw return significantly improved soil

http://www.aloki.hu ● ISSN 1589 1623 (Print) ● ISSN 1785 0037 (Online)
DOI: http://dx.doi.org/10.15666/aeer/2001_207219

structure, physical and chemical properties, and increased the percentage of macro-aggregates (Sun et al., 2012; Wang et al., 2010; Jia et al., 2020). Sun et al. (2012) found that straw return not only significantly increased the percentage of macro-aggregates, but also increased their organic carbon content. Bo et al. (2014) also reported that soil organic matter content increased with the increasing of amount of straw return. In addition, straw return combined with chemical fertilizer effectively reduced soil bulk density and improved soil physical condition (Lu et al., 2019). Therefore, straw return plays an important role in increasing soil organic matter, improving soil structure and fertility.

Biochar application is also commonly used in soil melioration. Biochar could increase soil organic carbon and cation exchange capacity (CEC), reduce nutrient loss, and therefore increase crop yield and quality (Lehmann, 2007; Laird et al., 2010; Sagrilo et al., 2015). Biochar also improves soil structure, enhances soil aeration and water retention, and enhances soil aggregate composition and stability (Wu et al., 2012; Zong et al., 2016). However, laboratory culture experiments showed that biochar application did not increase the content of large aggregates and even reduce the stability of soil aggregates (Busscher et al., 2010; Hou et al., 2015). Therefore, the effects of biochar on soil aggregates are unclear. More experiments are needed to clarify the effects of biochar on soil aggregates in both field and laboratory condition.

Tobacco growing area in southern Anhui is a typical tobacco-rice rotation region in China. In recent years, due to the increase of multiple cropping and the extensive application of chemical fertilizer, soil quality has declined significantly, such as soil acidification, soil hardening, and nutrient imbalance, which significantly decreased the yield and quality of tobacco leaves, and also reduced the income of tobacco planting and farmers (Zheng et al., 2019; Wang et al., 2020). Therefore, it is imperative to improve the soil quality of tobacco field in Southern Anhui, China. In tobacco-rice rotation region, a large amount of straw resources is produced after rice harvest, but most of them did not been utilized efficiently due to lack of reasonable straw returning method (Zheng et al., 2019). Therefore, in this study, we explored the effects of straw return and biochar application on the soil aggregates characteristics, and the yield and quality of tobacco leaf in Southern Anhui, China. The results of this study will provide guidance for the efficient utilization of straw, soil conservation and tobacco leaf quality improvement in tobacco-rice rotation region.

Materials and methods

Field experimental site

The field experiments were conducted from 2018 to 2019 (two growing seasons) in Yangliu Town (118°37'56", 30°49'35"), Xuancheng City, Anhui Province, China, which is a typical a tobacco-rice rotation area. The experimental site is a low hilly area with subtropical humid monsoon climate, with an average annual air temperature of 15.9℃ and 1294 mm annual precipitation. The rainfall was 528.4 mm and 467.9 mm during March and July (the tobacco growing period) in 2018 and 2019, respectively. The average air temperature was from 12.7℃ to 29.4℃, and from 11.9℃ to 28.2℃ during March and July in 2018 and 2019, respectively. The soil type of the experiment field is paddy soil, with an initial pH of 5.52, 16.8 g kg^{-1} organic matter, 86.2 mg kg^{-1} alkali-hydrolyzed N, 21.3 mg kg^{-1} available phosphorus (P) and 126.7 mg kg^{-1} available K in the 0-20 cm soil layer.

http://www.aloki.hu ● ISSN 1589 1623 (Print) ● ISSN 1785 0037 (Online)
DOI: http://dx.doi.org/10.15666/aeer/2001_207219

Experimental design

Five treatments were established in the study: no straw (CK), an application of 2700 kg ha^{-1} rice straw (RS), an application of 2250 kg ha^{-1} tobacco straw biochar (TSB), an application of 1350 kg ha^{-1} rice straw and 1050 kg ha^{-1} tobacco straw biochar (RS+TSB), 2400 kg ha^{-1} rice straw and 375 kg ha^{-1} pig manure (RS+PM). The amount of rice straw, tobacco straw biochar and pig manure used in the treatments was designed based on an equal carbon (1000 kg ha^{-1}) input to the field. The amount of rice straw, tobacco straw biochar was calculated by dry matter, and the water content of pig manure was 40%. RS, TSB and PM had average total carbon content of 372.3, 453.8, 256.6 g kg^{-1} and total nitrogen content of 12.6, 11.8, 315.7 g kg^{-1} on a dry matter basis, respectively. The rice straw, tobacco straw biochar and pig manure were evenly spread on the soil surface of the plot, and mixed fully with soil a rotary tiller, and then fertilized and ridged. All the fertilizers were applied in a band way before ridging. Fertilizers application rate was 115 kg N ha^{-1}, 157.5 kg P_2O_5 ha^{-1} and 315 kg K_2O ha^{-1}. All the treatments were replicated three times in the randomized complete block design. The plot area was 36 m^2 (7.5 m long and 4.8 m wide), with four rows of plants in each plot. Tobacco seedlings were planted in rows, 120 cm between rows and 50 cm between plants at a depth of 15 cm. The variety of flue-cured tobacco planted was "Yunyan 97". After the harvest of tobacco leaves, all plots were planted rice, and the fertilization and field management were identical in all treatments. The fertilizers were 75 kg ha^{-1} urea (N 46%) and 150 kg ha^{-1} compound fertilizer ($N:P_2O_5:K_2O$ = 15:15:15) during rice planting. The field experiment was repeated in 2019, and all the treatments and operations were exactly the same as in 2018. Tobacco seedlings were transplanted on March 22, 2018 and March 26, 2019. Tobacco leaves were harvested from June 10, 2018 and June 12, 2019, and the leaves were harvested four times by hand at 7- or 8-day intervals, by removing three to four leaves each time. Other cultivation measures including plant protection were carried out according to the technical guidelines recommended by Tobacco Research Institute, Anhui Academy of Agricultural Sciences. Photos of the experimental culture were shown in *Fig. 1*.

Figure 1. *Photos of fertilization and ridging stage of the experiment (left) and 75 days after transplanting (right) in 2018*

http://www.aloki.hu ● ISSN 1589 1623 (Print) ● ISSN 1785 0037 (Online)
DOI: http://dx.doi.org/10.15666/aeer/2001_207219

Sampling and measurements

Before the experiment started, soil samples of surface layer (0-20 cm) were collected to determine the basic fertility. After tobacco harvesting, soil samples were collected on July 15, 2019. S-type sampling method was used to collect soil samples (0-20 cm) in the middle of two plants on a row of each plot. At the same time, the undisturbed soil was collect and put into a plastic box with a volume of 10 cm×8 cm×5 cm, and minimized the damage to the undisturbed soil in the process of collection. Physicochemical properties of the topsoil soil (0–20 cm) were determined according to the method of Bao (2007). Soil aggregates were determined according to the method of Zhou et al. (2007), and divided into five aggregate size fractions: >5 mm, 2-5 mm, 1-2 mm, 0.25-1 mm, <0.25 mm.

The mature tobacco leaves were harvested separately in each plot, and cured immediately in a flue-curing barn. The cured leaves were classified according to the grading standards of flue-cured tobacco, and the trade yield and output value were calculated. About 1.0 kg of the cured central tobacco leaves were randomly selected from each treatment for evaluating the appearance and sensory quality according to the methods of Karaivazoglou et al. (2007). Appearance quality and sensory quality was evaluated by three experts from China Tobacco Anhui Industrial Co. LTD, according to the Standard of the People's Republic of China (GB2635-1992, 1992; GB5606.4-2005, 2005). There were seven indices for appearance quality: color, maturity, identity, leaf structure, oil content, and color intensity. Ten indices for sensory quality: odor quality, odor amount, offensive odor, smoke content, vigour, exquisite degree, irritation, dry sensation, remaining taste and sweetness. At the same time, about 1.0 kg of the cured central leaves were randomly selected for chemical analysis. Samples were dried to constant dry weight at 70°C, and milled into powder. The content of total nitrogen, nicotine, total sugar, reducing sugar, potassium and chlorine in tobacco leaves was determined by Continuous Flow Analysis according to the method of Wang (2003).

Statistical analyses

Data analysis was conducted using one-way ANOVA with SPSS 19.0 (SPSS Inc., Chicago, IL, USA). Least significance difference (LSD) test was performed for the comparisons of the means at $P < 0.05$. Pearson correlations were used to analyse the relationships between leaf yield, output value, appearance quality, sensory quality, >5 mm aggregates, 5-2 mm aggregates, 2-1 mm aggregates, 1-0.25 mm aggregates and 1-0.25 mm aggregates parameters.

Results

Tobacco leaf yield and output value

As shown *Fig. 2*, the RS+TSB and RS+PM significantly increased the leaf yield by 7.9% and 6.7% compared with the CK, respectively, while there was no significant difference in the leaf yield among the RS, TSB, and CK. Similarly, RS+TSB significantly increased the output value of tobacco leaf by 9.3% compared with the CK. However, there was no significant difference of the output value of tobacco leaf in the other treatments. Short-term straw return did not increase the yield and output value of tobacco leaf, but straw return combined with biochar (RS+TSB) significantly increased the yield and output value of tobacco, and the RS+PM also increased the tobacco leaf yield.

http://www.aloki.hu ● ISSN 1589 1623 (Print) ● ISSN 1785 0037 (Online)
DOI: http://dx.doi.org/10.15666/aeer/2001_207219

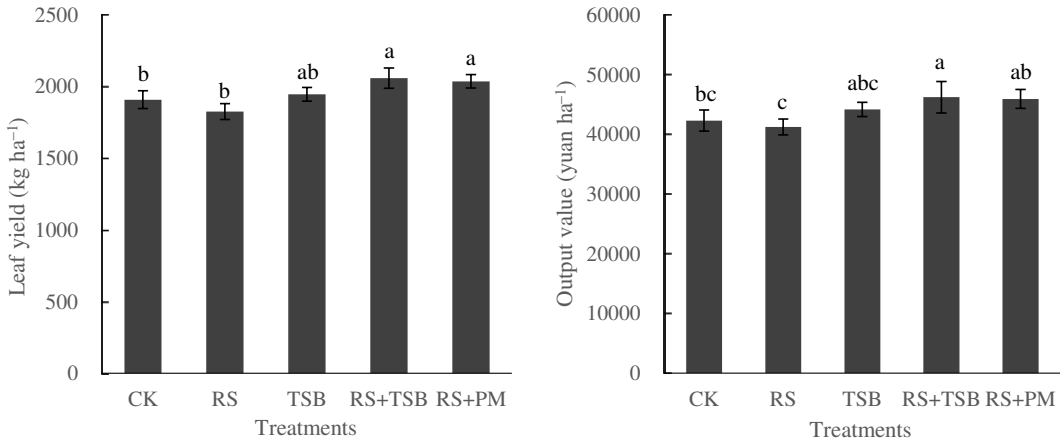

Figure 2. *Effects of different treatment on yield and output value of tobacco leaf. Vertical bars indicate standard error of mean (n = 3). Columns with different lowercase letters indicate significant differences (P < 0.05)*

Tobacco leaf appearance and sensory quality

No significant difference was found in the appearance and sensory quality of cured leaves between the CK and RS (*Fig. 3*). However, the TSB, RS+TSB and RS+PM significantly increased the appearance quality of cured leaves by 11.2%, 10.3% and 9.6% compared with CK, respectively. Similarly, the TSB, RS+TSB and RS+PM significantly enhanced the sensory quality of cured leaves by 4.7%, 4.5% and 6.6%, respectively. There was no significant difference in the appearance quality and sensory quality of cured leaves among TSB, RS+TSB and RS+PM.

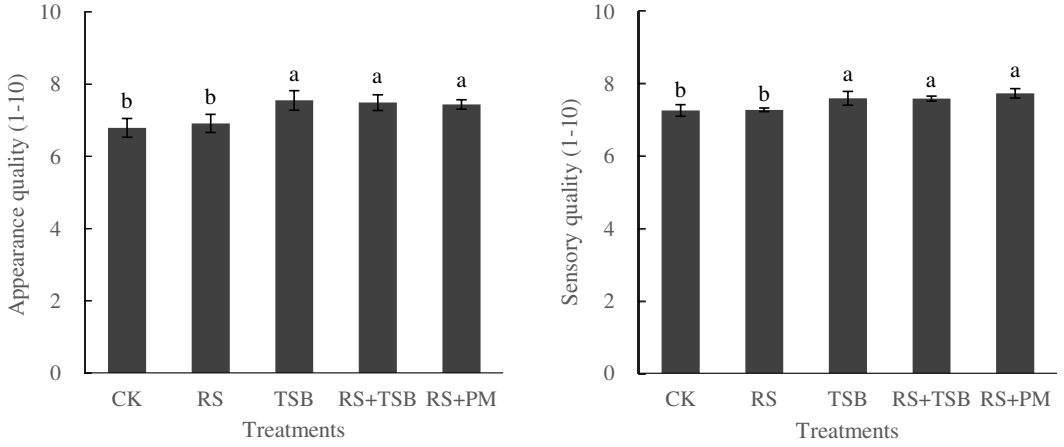

Figure 3. *Effects of different treatment on appearance and sensory quality of tobacco leaves. Vertical bars indicate standard error of mean (n = 3). Columns with different lowercase letters indicate significant differences (P < 0.05)*

Tobacco leaf chemical composition

As shown in *Table 1*, the CK had the lowest contents of total N and nicotine content in cured leaves, while RS+PM significantly increased the total N and nicotine content in

http://www.aloki.hu ● ISSN 1589 1623 (Print) ● ISSN 1785 0037 (Online)
DOI: http://dx.doi.org/10.15666/aeer/2001_207219

cured leaves by 11.7% and 12.9%, respectively, compared with the CK. In addition, the K content of the cured leaves in the RS+PM (2.2%) was significantly increased by 13.9% compared with the CK. There was no significant difference in the contents of total sugar, reducing sugar and chlorine in cured leaves in all treatments.

Table 1. *Effect of different treatment on chemical components content of cured leaves*

Treatment	Total N content (%)	Nicotine content (%)	Total sugars (%)	Reducing sugars (%)	K content (%)	Cl content (%)
CK	1.80 b	1.86 b	26.07 a	22.18 a	1.93 b	0.18 a
RS	1.99 ab	2.05 a	25.49 a	21.05 a	2.16 ab	0.21 a
TSB	1.94 ab	1.97 ab	26.88 a	22.76 a	1.98 ab	0.19 a
RS+TSB	1.96 ab	2.00 ab	26.60 a	22.91 a	2.07 ab	0.19 a
RS+PM	2.01 a	2.10 a	27.25 a	22.51 a	2.20 a	0.16 a

Means followed by different lowercase letters within a column indicate a significant difference ($P < 0.05$)

Soil physicochemical properties of the topsoil soil

As shown in *Table 2*, the TSB and RS+TSB significantly increased the soil pH by 0.40 and 0.38, respectively, compared with CK, while there was no significant difference in pH among the CK, RS and RS+PM. The RS, RS+TSB and RS +PM significantly increased the soil organic matter content. Moreover, the RS+TSB and RS +PM also significantly increased the soil CEC. The RS and RS +PM significantly enhanced the soil DOC. Therefore, straw return increased the soil organic matter and DOC, while the biochar application increased the soil pH.

Table 2. *Effects of different treatments on soil pH, organic matter, CEC and DOC*

Treatment	pH	Organic matter (g kg^{-1})	CEC (cmol kg^{-1})	DOC (mg kg^{-1})
CK	5.56 b	14.69 b	7.36 b	134.94 b
RS	5.64 b	15.83 a	7.62 ab	162.28 a
TSB	5.96 a	14.78 b	7.87 ab	144.68 ab
RS+TSB	5.94 a	15.62 a	8.13 a	155.03 ab
RS+PM	5.59 b	16.02 a	7.97 a	162.09 a

Means followed by different lowercase letters within a column indicate a significant difference ($P < 0.05$)

The RS, RS+TSB and RS+PM significantly increased the soil total N and total K compared with the CK (*Table 3*). There was no significant difference in soil total P among all treatments. The TSB, RS, RS+TSB and RS+PM significantly increased soil available N by 12.4%, 10.9%, 11.5% and 13.6%, and increased soil available N by 24.6%, 17.5%, 19.0% and 24.4%, respectively. Moreover, RS, RS+PM and RS+TSB also significantly increased soil available K by 25.6%, 15.3% and 26.3%, respectively. Therefore, straw return could increase the soil available N, P and K content.

http://www.aloki.hu ● ISSN 1589 1623 (Print) ● ISSN 1785 0037 (Online)
DOI: http://dx.doi.org/10.15666/aeer/2001_207219

Table 3. *Effects of different treatments on soil N, P and K concentration*

Treatment	Total N (g kg^{-1})	Total P (g kg^{-1})	Total K (g kg^{-1})	Available N (mg kg^{-1})	Available P (mg kg^{-1})	Available K (mg kg^{-1})
CK	0.99 b	0.43 a	10.66 b	90.78 b	22.57 b	133.16 c
RS	1.07 a	0.40 a	11.42 a	102.05 a	28.12 a	167.12 a
TSB	0.99 b	0.46 a	11.09 ab	100.66 a	26.52 a	147.21 bc
RS+TSB	1.08 a	0.43 a	11.20 a	101.26 a	26.86 a	153.60 ab
RS+PM	1.09 a	0.46 a	11.44 a	103.15 a	28.08 a	168.16 a

Means followed by different lowercase letters within a column indicate a significant difference ($P < 0.05$)

Soil aggregate composition

As shown in *Fig. 4*, straw return and biochar application significantly increased >5 mm size fraction aggregates compared with the CK. The proportion of >5 mm size fraction was highest in RS+PM, which was 9.0% more than that in CK. There was no significant difference in 5-2 mm size fraction in all treatments. However, the TSB, RS+TSB and RS+PM significantly increased the content of <0.25 mm size fraction compared with the CK. Therefore, straw returning combined with pig manure (RS+PM) or biochar (RS+TSB) significantly increased the proportion of >5 mm size fraction, while reduced <0.25 mm size fraction.

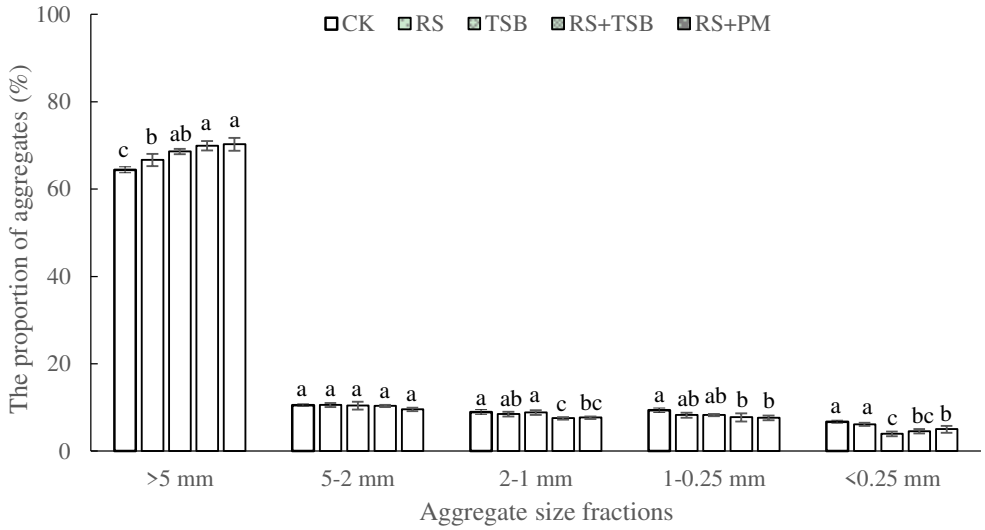

Figure 4. *Effects of different treatments on soil aggregate composition. Vertical bars indicate standard error of mean (n = 3). Columns with different lowercase letters within the same aggregate fractions indicate significant differences ($P < 0.05$)*

Relationship between tobacco yield and soil aggregate composition

As shown in *Table 4*, both the yield and output value of cured leaves were significantly positively correlated with the proportion of >5 mm aggregates, while the output value of cured leaves was negatively correlated with 1-0.25 mm and <0.25 mm aggregates. The appearance and sensory quality of cured leaves were positively correlated with the

http://www.aloki.hu ● ISSN 1589 1623 (Print) ● ISSN 1785 0037 (Online)
DOI: http://dx.doi.org/10.15666/aeer/2001_207219

proportion of >5 mm aggregates, but negatively correlated with <0.25 mm aggregates. Thus, the yield and quality of tobacco cured leaves were significantly positively correlated with the proportion of >5 mm aggregates, but negatively correlated with <0.25 mm aggregates.

Table 4. *Relationship between tobacco yield and soil aggregate composition*

	Leaf yield	**Output value**	**Appearance quality**	**Sensory quality**	**>5 mm aggregates**	**5-2 mm aggregates**	**2-1 mm aggregates**	**1-0.25 mm aggregates**	**1-0.25 mm aggregates**
Leaf yield	1								
Output value	0.876**	1							
Appearance quality	0.613*	0.667**	1						
Sensory quality	0.598*	0.681**	0.732**	1					
>5 mm aggregates	0.575*	0.631*	0.675**	0.724**	1				
5-2 mm aggregates	-0.299	-0.145	-0.342	-0.274	-0.528*	1			
2-1 mm aggregates	-0.437	-0.385	-0.415	-0.546*	-0.754**	0.537*	1		
1-0.25 mm aggregates	-0.437	-0.589*	-0.359	-0.553*	-0.820**	0.191	0.563*	1	
1-0.25 mm aggregates	-0.476	-0.599*	-0.734**	-0.652**	-0.784**	0.137	0.286	0.566*	1

* indicate significance at the level of 0.05, ** indicates significance at the level of 0.01

Discussion

Effects of straw return and biochar on yield and quality of tobacco leaf

Previous studies had proved that both straw return and biochar application could significantly increase the growth and yield of many crops. In this study, tobacco straw biochar, especially tobacco straw biochar with rice straw return significantly improved the growth of tobacco plant, increased the yield and output value of flue-cured tobacco leaves (*Fig. 2*). Similarly, biochar have been proved to improve the growth and yield of corn (Oguntunde et al., 2008), rice (Lehmann et al., 2003), wheat (Van Zwieten et al., 2010) and so on. Studies have also found that straw return could improve the yield and quality of tobacco leaves (Zheng et al., 2019; Lu et al., 2019). Straw return significantly reduced the soil bulk density of topsoil, improved the soil hydrothermal conditions and nutrient supply, and thus promoted the plant growth and development, and increased crop yield (Lu et al., 2019). Tan et al. (2018) found that the application of 1500 kg ha^{-1} tobacco straw biochar significantly promoted the growth of flue-cured tobacco and increased the yield of tobacco leaves. The promotion effect of biochar application on promoting crop growth was mainly due to the improvement in soil physical and chemical properties, the increase on soil nutrient availability, and the improvement in soil microbial abundance and community structure (Van Zwieten et al., 2010). Tan et al. (2018) found that the returning of tobacco straw biochar to the field significantly promoted the reproduction of bacteria and actinomycetes, while reduced the number of soil fungi in the in the continuous cropping tobacco soil, which had a remarkable effect on decreasing tobacco bacterial wilt. In this study, the incidence of tobacco bacterial wilt in all treatments was

http://www.aloki.hu ● ISSN 1589 1623 (Print) ● ISSN 1785 0037 (Online)
DOI: http://dx.doi.org/10.15666/aeer/2001_207219

relatively low, and there was no significant difference between treatments (data not shown), which may be due to the fact that the soil in the tobacco-rice rotation areas underwent crop rotation through flood and drought, therefore, the tobacco bacterial wilt was relatively low (Kong et al., 2007).

Effects of straw return and biochar on soil physicochemical properties

Many studies showed that biochar application could increase soil pH (Van Zwieten et al., 2010; Yuan and Xu, 2010). In this study, it was found that the application of tobacco straw biochar significantly increased the soil pH. Previous research results showed that the application of biochar with fertilizer increased the soil pH by 0.19 and 0.27 in yellow brown soil and red soil, respectively (Yuan and Xu, 2010). The effect of biochar on increasing soil pH increased with the increase of its application amount (Van Zwieten et al., 2010). Due to the biochar contains base ions such as Ca^{2+}, K^{+} and Mg^{2+}, some of these cations are released to exchange H^{+} and Al^{3+} in the soil when it was applied to the soil, and thus reducing the acidity of the soil, increasing the base saturation and pH of the soil (Topoliantz et al., 2005; Van Zwieten et al., 2010). The soil of continuous tobacco cropping system is seriously acidified and has a low pH (Jiang et al., 2020). Therefore, the biochar can be used to neutralize the acid and increase the pH of the tobacco-growing soil.

Biochar contains a lot of soluble mineral nutrients, which can improve the level of available nutrients in soil after its application. In this study, tobacco straw biochar significantly increase the contents of available N, P and K in tobacco planting soil (*Table 3*). The increase in soil fertility by biochar application is most likely due to its ability to absorb cations (Atkinson et al., 2010). It was reported that, after the applied of biochar to the soil, its surface could be oxidized to form a carbonyl, phenolic and quinone groups, and the adsorption capacity of soil cations can be increased in the oxidized biochar (Atkinson et al., 2010). Glaser et al. (1998) found that adding bamboo charcoal could significantly increase the exchangeable base ions in the soil. This present study was consistent with the results of Glaser et al. (1998), we found that the application of tobacco straw biochar in the tobacco field significantly increased the soil CEC.

The present study show that straw return significantly increased the soil organic matter content (*Table 2*), which is consistent with the research results of Bo et al. (2014). It was reported that the soil organic matter content of tobacco field increased to varying degrees with the increasing of the amount of corn and wheat straw returned to the field (Bo et al., 2014). As most of the straw is organic composition, among them, the cellulose, hemicellulose and protein complex are difficult to be decomposed by microorganisms, which will be remain in the soil to form organic matter. On the other hand, straw return to the field could enhance the activity and aromatization degree of soil humus, maintain the balance of soil organic matter (Bo et al., 2014). In addition, the straw contains a large number of nutrient elements, which plays an important role in soil fertilization. The results of this study showed that straw return increased the soil available N, P and K to varying degrees, which is similar to the results of Wang et al. (2010) and Zheng et al. (2019).

Effects of straw return and biochar on soil aggregates

As a basic unit of soil structure, the content and stability of soil aggregates have an important role in soil water and fertilizer conservation ability (Yin et al., 2015). In this study, the application of biochar with straw significantly increased the proportion of

http://www.aloki.hu ● ISSN 1589 1623 (Print) ● ISSN 1785 0037 (Online)
DOI: http://dx.doi.org/10.15666/aeer/2001_207219

>5 mm aggregates in surface soil (0-20 cm), and it was in the roder: RS+PM > RS+TSB > TSB > RS > CK, while significantly decreased the content of <0.25 mm aggregates. This is consistent with previous studies (Qiao et al., 2018; Jia et al., 2020). Jia et al. (2020) also found that biochar and straw application significantly increased the proportion of 0.5-1.0 mm aggregates in the 0-20 cm soil layer, and significantly reduced the proportion of <0.25 mm aggregates. On the one hand, the biochar can promote the formation of macro-aggregates due to its porous structure and large specific surface area (Brodowski et al., 2006). On the other hand, the application of biochar increased the content of soil organic carbon, which as a good soil cementing agent, also promoted the formation of macro-aggregates (Puget et al., 2000; Abiven et al., 2009; Jia et al., 2020). After applied in the soil, the straw served as the core for the formation of large aggregates (Wang et al., 2015), and after the straw decomposition, the content of carbohydrate, aromatic and aliphatic carboesters, ester compounds and amino compounds in the soil will be increased. Carbohydrates are the important binders for soil aggregates, which play an important role in the formation and stability improvement of soil aggregates (Yousefi et al., 2008; Wang et al., 2018). In this study, RS+PM and RS+TSB treatments had the best effect on increasing the proportion of >5 mm aggregates, which may be the result of the complementary effect of biochar and straw, as well as the effect of pig manure on straw decomposition.

It was reported that the application of exogenous carbon can promote the formation of >0.25 mm aggregates in soil, particularly for increasing the proportion of 1-2 mm grain size aggregates (Puttaso et al., 2013). Bo et al. (2014) conducted field experiments on brown soil in Shandong for four consecutive years and found that continuous return of corn straw to the field promoted the formation of soil aggregates and improved its stability. In this study, the RS and TSB had less significant effect on soil aggregates improvement than that of RS+PM (*Fig. 3*). This result also suggested that although straw return is beneficial to the formation of aggregates, it needs to be applied for a long time to have good effects (Abiven et al., 2009; Bo et al., 2014). In addition, because flue-cured tobacco is a dry season crop, the soil in the tobacco field did not cover all the rice straw completely to form an anaerobic and high-humidity environment, leading to slow decomposition of the wax layer outside the straws (Zhu et al., 2018), therefore, rice straw return alone could not improve soil aggregates effectively in a short time. However, rice straw combined with pig manure or biochar can effectively improve the soil aggregates.

In this study, it was found that the yield and quality of tobacco leaf were significantly positively correlated with the proportion of >5 mm aggregates, but negatively correlated with <0.25 mm aggregates. Both the application of biochar and straw significantly increased the proportion of >5 mm aggregates in surface soil (0-20 cm). This study suggested that the application of tobacco straw biochar, especially the application of biochar combined with straw promoted the growth of tobacco plant and increased the yield and output value of tobacco leaf. Therefore, straw return with pig manure or biochar could be used to improve soil aggregate structure, increase soil nutrient, and enhance the yield and quality of tobacco leaf. However, more experiments need to be carried out to explore the effects of long-term straw return on the yield and quality of tobacco leaf and soil conservation.

http://www.aloki.hu ● ISSN 1589 1623 (Print) ● ISSN 1785 0037 (Online)
DOI: http://dx.doi.org/10.15666/aeer/2001_207219

Conclusion

The present study concluded that the application TSB significantly increased pH by 0.38 in the tobacco field soil, and more studies are needed to elucidate the mechanism of tobacco straw biochar on soil acidity. Biochar and straw return increased the proportion of >5 mm aggregates in topsoil (0-20 cm) with an order of RS+PM > RS+TSB > TSB > RS. The RS+TSB and RS+PM significantly increased the yield, appearance and sensory quality of tobacco leaf. The yield and quality of tobacco leaf significantly positively correlated with the proportion of > 5 mm aggregates, but negatively correlated with <0.25 mm aggregates. Therefore, straw return with pig manure (375 kg ha^{-1}) or biochar (1050 kg ha^{-1}) could be used to improve soil aggregate structure, increase soil nutrient, and enhance the yield and quality of tobacco leaf.

Acknowledgements. This study was supported by the Discipline Construction Project of Anhui Academy of Agricultural Sciences (No. 2021YL082), the Science and Technology Project of Anhui Province Tobacco Company (No. 20180551009).

REFERENCES

[1] Abiven, S., Menasseri, S., Chenu, C. (2009): The effects of organic inputs over time on soil aggregate stability - a literature analysis. – Soil Biology and Biochemistry 41: 1-12.
[2] Atkinson, C. J., Fitzgerald, J. D., Hipps, N. A. (2010): Potential mechanisms for achieving agricultural benefits from biochar application to temperate soils: a review. – Plant and Soil 337: 1-18.
[3] Bao, S. D. (2007): Soil agro-chemistrical analysis. – 3rd ed. Beijing: China Agriculture Press, pp. 268-270, 389-391.
[4] Bo, G. D., Zhang, J. G., Shen, G. M., Yu, H. Y., Gao, L., Sun, Y. Y., Wang, Y., Zhou, X. S., Zhang, Y., Liu., M. (2014): Effects of straw returning on soil organic matter and characteristics of soil aggregates in tobacco planting field. – Chinese Tobacco Science 35(3): 12-16.
[5] Brodowski, S., John, B., Flessa, H., Amelung, W. (2006): Aggregate-occluded black carbon in soil. – European Journal of Soil Science 57: 539-546.
[6] Busscher, W. J., Novak, J. M., Evans, D. E., Watts, D. W., Niandou, M. A. S., Ahmedna, M. (2010): Influence of pecan biochar on physical properties of a Norfolk loamy sand. – Soil Science 175(1): 10-14.
[7] Glaser, B., Haumaier, L., Guggenberger, G., Zech, W. (1998): Black carbon in soils: The use of benzene carboxylic acids as specific markers. – Organic Geochemistry 29(4): 811-819.
[8] Hou, X., Li, H., Zhu, L., Han, Y., Tang, Z., Li, Z., Tan, J., Zhang, S. (2015): Effects of biochar and straw additions on lime concretion black soil aggregate composition and organic carbon distribution. – Scientia Agricultura Sinica 48(4): 705-712.
[9] Jia, H., Zhao, Y. P., Fu, Y. P., He, T. T., Fu, X. Y., Yun, F., Liu, J. J., Nie, Q. K. (2020): Effects of biochar and straw on stability and organic carbon distribution of tobacco-planting soil aggregates. – Tobacco Science & Technology 53(4): 11-19.
[10] Jiang, C., Shen, J., Cui, Q., Yan, Y., Liu, Y., Zu, C. (2020): Optimal lime application rates for ameliorating acidic soils, improving the yield and quality of tobacco leaves. – Applied Ecology and Environmental Research 18(4): 5411-5423.
[11] Karaivazoglou, N. A., Tsotsolis, N. C., Tsadilas, C. D. (2007): Influence of liming and form of nitrogen fertilizer on nutrient uptake, growth, yield, and quality of Virginia (flue-cured) tobacco. – Field Crops Research 100(1): 52-60.

http://www.aloki.hu ● ISSN 1589 1623 (Print) ● ISSN 1785 0037 (Online)
DOI: http://dx.doi.org/10.15666/aeer/2001_207219

[12] Kong, F. W., Liu, X. S., Zhang, M. W., Liu, Z. F., Yuan, F. P. (2007): Integrated control of main diseases and insect pests of flue-cured tobacco in tobacco-rice rotation area. – Acta Agriculturae Jiangxi 19(8): 56-58.
[13] Laird, D. A., Fleming, P., Davis, D. D., Horton, R., Wang, B. Q., Karlen, D. L. (2010): Impact of biochar amendment on the quality of a typical Midwestern agricultural soil. – Geoderma 158(3-4): 443-449.
[14] Lehmann, J., da Silva, J. P., Steiner, C., Nehls, T., Zech, W., Glaser, B. (2003): Nutrient availability and leaching in an archaeological anthrosol and a ferralsol of the central amazon basin: Fertilizer, manure and charcoal amencents. – Plant and Soil 249(2): 343-357.
[15] Lehmann, J. (2007): Bio-energy in the black. – Frontiers in Ecology and the Environment 5(7): 381-387.
[16] Lu, W. L., Dong, J. X., Song, W. J., Liu, K. L., Zhang, Q. M., Zhang, H. W., Su, P. F., Zhang, J. Q., Liang, H. B. (2019): Effects of deep soil tillage and straw returning on soil physical properties and yield and quality of tobacco leaves. – Chinese Tobacco Science 40(1): 25-32.
[17] Mu, J. L., Tan, J., Liu, G. S., Ding, S. S., Wen, X. Y. (2017): Effects of humic acid and nitrogen levels and their interaction on tobacco planting soil quality. – Soils 49(1): 27-32.
[18] Oguntunde, P. G., Abiodun, B. J., Ajayi, A. E., van de Giesen, N. (2008): Effects of charcoal production on soil physical properties in Ghana. – Journal of Plant Nutrition and Soil Science 171(4): 591-596.
[19] Puget, P., Chenu, C., Balesdent, J. (2000): Dynamics of soil organic matter associated with particle-size fractions of water-stable aggregates. – European Journal of Soil Science 51(4): 595-605.
[20] Puttaso, A., Vityakon, P., Rasche, F., Saenjan, P., Treloges, V., Cadisch., G. (2013): Does organic residue quality influence carbon retention in a tropical sandy soil. – Soil Science Society of America Journal 77: 1001-1011.
[21] Qiao, D. D., Wu, M. Y., Zhang, Q., Han, Y. L., Zhang, Y. B., Li, P. P., Li, H. (2018): Effect of biochar and straw with chemical fertilizers on soil aggregate distribution and organic carbon content in yellow cinnamon soil. – Soils and Fertilizers Sciences in China 3: 92-99.
[22] Sagrilo, E., Jeffery, S., Hoffland, E., Kuyper, T. W. (2015): Emission of CO_2 from biochar-amended soils and implications for soil organic carbon. – Global Change Biology Bioenergy 7(6): 1294-1304.
[23] Standard of the People's Republic of China (1992): GB 2635-1992 Flue-Cured Tobacco. – Beijing, China: China Standard Press.
[24] Standard of the People's Republic of China (2005): GB 5606.4-2005 Cigarettes Part 4: Technical Requirements for Sense Evaluation. – Beijing, China: China Standard Press.
[25] Sun, H. Y., Ji, Q., Wang, Y., Wang, X. D. (2012): The distribution of water-stable aggregate-associated organic carbon and its oxidation stability under different straw returning modes. – Journal of Agro-Environment Science 31(2): 369-376.
[26] Tan, H., Peng, W. X., Xiang, B. K., Yin, Z. C., Su, Y. X., Shi, H. L. (2018): Influence of carbonized tobacco stem on physiochemical properties of continuous tobacco-cropping soil and growth of flue-cured tobacco. – Soils 50(4): 726-731.
[27] Topoliantz, S., Ponge, J. F., Ballof, S. (2005): Manioc peel and charcoal: a potential organic amendment for sustainable soil fertility in the tropics. – Biology and Fertility of Soils 41(1): 15-21.
[28] Van Zwieten, L., Kimber, S., Morris, S., Chan, K. Y., Downie, A., Rust, J., Joseph, S., Cowie, A. (2010): Effects of biochar from slow pyrolysis of paper mill waste on agronomic performance and soil fertility. – Plant and Soil 327(1/2): 235-246.
[29] Wang, R. X. (2003): Tobacco chemistry. – Beijing: China Agricultural Press, pp. 244-275.
[30] Wang, J., Wang, D. J., Zhang, G., Wang, C. (2010): Effect of different nitrogen fertilizer rate with continuous full amount of straw incorporated on paddy soil nutrients. – Journal of Soil Water Conservation 24(5): 40-44, 62.

http://www.aloki.hu ● ISSN 1589 1623 (Print) ● ISSN 1785 0037 (Online)
DOI: http://dx.doi.org/10.15666/aeer/2001_207219

[31] Wang, B. S., Cai, D. X., Wu, X. P., Li, J., Liang, G. P., Yu, W. S., Wang, X. L., Yang, Y. Y., Wang, X. B. (2015): Effects of long-term conservation tillage on soil organic carbon, maize yield and water utilization. – Plant Nutrition and Fertilizer Science 21(6): 1455-1464.
[32] Wang, X. J., Xie, Z. J., Dong, H., Zhao, Y., Liu, H. Y., Lou, C. (2018): Effects of straw returning on yield and soil aggregates composition and organic carbon distribution. – Journal of Maize Sciences 26(1): 108-115.
[33] Wang, H. T., Jiang, C. Q., Jiang, Y. J., Chen, L. J., Zu, C. L., Sun, B. (2020): Relationship between soil aggregate composition with yield and quality of flue-cured tobacco under different rice-tobacco rotation years in Yangtse Plain South Anhui. – Soils 52(5): 1057-1067.
[34] Wu, P. B., Xie, Y., Qi, Z. P., Wu, W. D. (2012): Effects of biochar on stability and total carbon distribution of aggregates in granitic laterite. – Acta Agrestia Sinica 20(4): 643-648.
[35] Yin, Y., Liang, C. H., Pei, Z. J. (2015): Effect of greenhouse soil management on soil aggregation and organic matter in northeast China. – Catena 133: 412-419.
[36] Yousefi, M., Hajabbasi, M., Shariatmadari, H. (2008): Cropping system effects on carbohydrate content and water-stable aggregates in a calcareous soil of central Iran. – Soil and Tillage Research 101(1/2): 57-61.
[37] Yuan, J. H., Xu, R. K. (2010): Effects of rice-hull-based biochar regulating acidity of red soil and yellow brown soil. – Journal of Ecology and Rural Environment 26(5): 472-476.
[38] Zheng, M. Y., Liu, Y. T., Zhang, Z. F., Cheng, S., Cai, X. J., Zhu, Q. F., Xue, L., Xu, Q., Lin, W., Zhang, J. G. (2019): Effect of straw returning on soil aggregate characteristics and tobacco yield and quality. – Chinese Tobacco Science 40(6): 11-18.
[39] Zhou, H., Lv, Y. Z., Yang, Z. C., Li, B. G. (2007): Effects of conservation tillage on the soil aggregates characteristics in Huabei Plain, China. – Scientia Agricultura Sinica 40(9): 1973-1979.
[40] Zhu, J. W., Zhang, Y. G., Li, Z. H., Ran, C. X., Zhang, H., Liu, Q. L., Li, X. H., Shi, J. X. (2018): Effects of different soil amendments on soil aggregate composition from a renovated tobacco field. – Journal of Nanjing Agricultural University 41(2): 341-348.
[41] Zong, Y., Xiao, Q., Lu, S. (2016): Acidity, water retention, and mechanical physical quality of a strongly acidic ultisol amended with biochars derived from different feedstocks. – Journal of Soils and Sediments 16(1): 177-190.

http://www.aloki.hu ● ISSN 1589 1623 (Print) ● ISSN 1785 0037 (Online)
DOI: http://dx.doi.org/10.15666/aeer/2001_207219

IDENTIFICATION AND CHARACTERIZATION OF *PSWRKY1* INVOLVED IN THE ABIOTIC STRESS RESPONSES OF *POLYGONATUM SIBIRICUM* (SOLOMON'S SEAL)

YU, S. H. – YE, J. F.* – FAN, J. G.* – MA, D. J. – ZHENG, Y. – BU, P. T.

Forestry Biotechnology and Analysis Test Center, Liaoning Academy of Forestry Sciences, Shenyang 110032, China

**Corresponding authors*
e-mail: yejingfeng527@163.com (Ye, J. F.); fanjungang178@163.com (Fan, J. G.)

(Received 16th Jul 2021; accepted 28th Oct 2021)

Abstract. WRKY protein is an important transcription factor in response to abiotic stress in plants. However, a systematic identification and characterization of WRKY genes has not been carried out for the medicinal plant *Polygonatum sibiricum* that has a strong ability to resist various abiotic stresses. In this study, we isolated a novel WRKY gene from *P. sibiricum* and compared its sequence structure with other plants. *PsWRKY1* possesses two typical WRKY domains and two C_2H_2 zinc-finger motifs. Evolutionary analysis indicated that *PsWRKY1* is most closely related to the WRKY protein from *Eucalyptus grandis.* Expression analysis showed that expression levels of *PsWRKY1* were induced by cold and drought stresses but not salt stress. Overexpression of *PsWRKY1* in *Arabidopsis* improved the seed germination and growth conditions of transgenic plants under drought and cold stresses. Furthermore, SOD activity and proline content in transgenic plants were higher than those in WT under cold and drought stresses, whereas MDA levels and relative electrolyte leakage in transgenic plants were lower than those in WT under same stresses. These results indicated that *PsWRKY1* improved the tolerance to cold and drought stresses. This study is significant for understanding the molecular mechanism behind *P. sibiricum* cold and drought stresses tolerance.
Keywords: *WRKY transcription factors, medicinal plant, cold stress, drought stress, overexpression*

Abbreviations: TF, Transcription factor; H_2O_2, hydrogen peroxide; TCM, Traditional Chinese Medicine; ABA, Abscisic acid; SOD, Super oxide dismutase; MDA, Malondialdehyde; NJ, Neighbor-joining; PCR, Polymerase chain reaction; qRT-PCR, Quantitative real time polymerase chain reaction; NBT, Nitro blue tetrazolium; WT, Wild type; NLS, Nuclear localization signal; POD, Peroxidase; CAT, Catalase; ROS, Reactive oxygen species; *POD*, Peroxidase; TBA, thiobarbituric acid

Introduction

Plants are easily exposed to a great variety of abiotic and biotic stresses, including extreme changes of temperature, light, drought, and pathogens etc. The main limiting environmental factors influencing plant cultivation worldwide are abiotic stresses, especially low temperature and drought stress. To endure these stresses, plants have evolved comprehensive reprogramming of the cellular metabolism (Rushton et al., 2012). A key step in the responses to all kinds of stresses is transcription factor (TF), which regulates transcriptional regulation of many downstream target genes (Mitsuda and Ohme-Takagi, 2009). WRKY protein is an important family of transcription factors, which are named after highly conserved WRKYGQK motifs. WRKY members include three groups (I, II and III) and various subgroups (e.g. IIa, IIb, etc.) based on the number of WRKY domains and the type of zinc finger motifs. WRKY TFs play an essential role in resistance of biotic or abiotic stresses in plants (Jiang et al., 2017; Eulgem et al., 2000). Many WRKY genes have been isolated in various plant species. For example, 72 WRKY genes have been identified in Arabidopsis, 55 in cucumber, 104 in poplar, 109 in rice, 83 in tomato,79 in potato, 46 in

http://www.aloki.hu ● ISSN 1589 1623 (Print) ● ISSN1785 0037 (Online)
DOI: http://dx.doi.org/10.15666/aeer/2001_221233

rapeseed, and 119 in corn (Eulgem et al., 2000; Amorim et al., 2017; Ng et al., 2018; Liu et al., 2019).

Some WRKY TFs are closely related to tolerance of abiotic stresses for plant such as cold, salt, drought, and heat etc. Four banana fruit WRKY TFs are involved in ABA (abscisic acid)-induced cold tolerance by increasing ABA levels (Luo et al., 2017). *FcWRKY70* is a WRKY gene from *Fortunella crassifolia*, which confers drought tolerance by modulating putrescine synthesis (Gong et al., 2015). MuWRKY3 from *Arachis hypogaea* can enhance drought resistance by accumulating less malondialdehyde and hydrogen peroxide (H_2O_2) (Kiranmai et al., 2018). PbrWRKY53 plays a positive role in drought resistance by promoting production of vitamin C via regulating *PbrNCED1* expression in *Pyrus betulaefolia*. GsWRKY20 from soybean improves drought stress resistance in transgenic soybean (Luo et al., 2013). VaWRKY12 and VaWRKY33 from grapevine both improve the cold tolerance of transgenic Arabidopsis and grapevine calli (Zhang et al., 2019; Sun et al., 2019). CsWRKY46 from cucumber enhances cold tolerance in transgenic plants and positively regulates the ABA-dependent cold signaling pathway (Zhang et al., 2016). Although some WRKY genes have been studied in many plants, the functions of most of WRKY genes are still poorly understood, especially in many non-model plants.

Polygonatum species which belong to the family Asparagaceae are widely distributed throughout the temperate Northern Hemisphere with 71 species. Due to their positive effect on human health, these plants have been used in Traditional Chinese Medicine (TCM). *P. sibiricum* is known as 'Huangjing' (Solomon's seal), which distributes in the northern hemisphere, mainly from southwest China to Japan (Pan et al., 2020). Huangjing can treat some disease such as lung disorders, osteoporosis, fatigue, and feebleness. More particularly, Huangjing has stronger tonic effect than other *Polygonatum* species, tonifying the spleens and kidneys (Jo et al., 2017; Zhao et al., 2018). Because *P. sibiricum* distributes mostly in thickets, woodlands or hillsides, it can resist various abiotic stresses such as drought, cold, and water etc. (Liu et al., 2009; Qu et al., 2010; Zhao et al., 2018). Although *P. sibiricum* has a strong ability to resist abiotic stresses, the genes related to abiotic stresses resistance from *P. sibiricum* are still poorly identified.

In this study, we cloned a novel WRKY gene *PsWRKY1* in *P. sibiricum* and analyzed its sequence structure and evolution relationship. Expression analysis indicated expressing pattern of *PsWRKY1* under drought, cold, and salt stress. Overexpression of *PsWRKY1* was generated to evaluate its function during drought, cold, and salt stresses. The growth conditions of transgenic Arabidopsis under drought, cold, and salt stresses were identified. SOD activity, proline content, relative electrolyte leakage, and MDA levels were analyzed in transgenic *Arabidopsis* to evaluate function of *PsWRKY1* for resisting abiotic stresses.

Materials and methods

Plant materials and treatments

Seedlings of *P. sibiricum*, which were originally collected from Qingyuan county in Fushun city (Liaoning Province, China), were transplanted in plastic boxes filled with soil substrates and placed in a controlled growth chamber with the temperature set at 25 ℃, a 16 h light/8 h dark photoperiod, and a humidity of 45%. Three-week-old plantlets with three well developed leaves were used for different treatments. For the cold treatments, whole plantlets grown in conical flasks were placed at 4°C in an illuminated incubation chamber (16 h light/8 h dark, 8000 Lux), and fresh leaves were harvested at 0, 2, 6, ,12, 24, 48 h, and 72 h time points. For dehydration treatment, seedlings were treated with 20%PEG 6000 for

http://www.aloki.hu ● ISSN 1589 1623 (Print) ● ISSN1785 0037 (Online)
DOI: http://dx.doi.org/10.15666/aeer/2001_221233

0, 2, 6,12, 24, 48 h, and 72 h. For salt stress, the seedlings were treated with 200 mM NaCl solution for 0, 1, 3, 6, 12 and 24 h. For each treatment, at least 15 seedlings were used and the leaves, stems and roots were sampled from three randomly collected seedlings at designated time point and frozen immediately in liquid nitrogen and stored at - 80 °C until use. Three biological replicates were collected for each sample.

RNA extraction, gene isolation and bioinformatic analysis

Total RNA of from the collected samples was extracted by TaKaRa MiniBEST Plant RNA Extraction Kit (TaKaRa, Japan) according to the manufacturer's instruction. First strand cDNA synthesis was performed using PrimeScriptTM RT reagent Kit with gDNA Eraser (Takara), and stored at - 20 °C until use. To isolate WRKY gene from *P. sibiricum*, homologous sequences from other species in the Genbank were aligned. A set of primers for gene amplification were designed by Primer 5 software (http://www.Premierbiosoft.com) (*Table S1*). The conserved fragment of WRKY gene was amplified from cDNA and several clones were sequenced. To obtain the whole sequence of WRKY gene, 5'-RACE and 3'-RACE experiments were performed using a Full RACE Kit (TaKaRa) after the acquisition of the conserved sequence. To validate the whole coding sequence of WRKY genes, primers were designed on the basis of the assembled results, and several clones were sequenced to correct errors introduced during PCR. Multiple sequence alignments were done using DNAMAN 8 (http://www.lynnon.com) and MEGA 5.10 (http://www.megasoftware.net/mega.php). Conserved motifs were identified using MEME Suite 4.10.1 (http://meme-suite.org/) and WebLogo 3.4 (http://weblogo.threeplusone.com/). To compare evolutionary relationship of WRKY genes in plants, the phylogenetic trees were constructed by MEGA 5.10 (http://www.megasoftware.net/mega.php) based on the neighbor-joining (NJ) method and bootstrap analysis (1,000 replicates). Highly similar homologous genes were downloaded from NCBI (http://www.ncbi.nlm.nih.gov/) and presented in *Table S2*.

Vector constructs and plant transformation for overexpression

The PCR products of WRKY, carried by vector pMD-18-T, were cloned into vector pCAMBIA 1301. In this vector, the enhanced CaMV 35S promoter drives the constitutive expression of transgenes. The expression vectors were transformed into *Agrobacterium tumefaciens* EHA105 by the freeze-thaw method (Zhang et al., 2016). The foreign genes were then transfected into wild-type *Arabidopsis thaliana* using leaf disc transformation (Kiranmai et al., 2018). The resulting seeds were screened on 1/2 MS medium containing 50 $mg \cdot L^{-1}$ hygromycin (HPT), and the presence of the transgene in T0 and T1 plants was confirmed by PCR amplification of the HPT gene on genomic DNA and by analyzing the expression of *WRKY* from cDNA T3 transgenic plants were subjected to screening. Initially, PCR was carried out to identify the presence of the target transgenes in the transgenic plants.

Expression analysis of WRKY genes

To detect the expression of WRKY gene under abiotic stress, qRT-PCR was performed using 10 μL of FastStart Universal SYBR Green Master (Aidlab, Beijing) on a StepOne Plus real-time PCR instrument (Aidlab, Beijing). Each sample was prepared with three biological and three technical replicates, and the relative expression was calculated using the relative quantification method ($2^{-\Delta\Delta CT}$). *β-actin* (GenBank accession no. EC969944) was used as a reference gene for *P. sibiricum* samples.

http://www.aloki.hu ● ISSN 1589 1623 (Print) ● ISSN1785 0037 (Online)
DOI: http://dx.doi.org/10.15666/aeer/2001_221233

Relative electrolyte leakage test

After treatment of 4℃ cold stress, 200 mM NaCl, 20%PEG for 12 h, respectively, three T3 transgenic plants for WRKY and WT plants were immediately sampled, and 10 leaf discs of each sample were obtained to determine relative electrolyte leakage. Leaf discs were immersed in deionized water for 10h at ambient temperature. The initial electrical conductivity (S_1) was measured using a DDS-IIA detector (Shanghai, China), and then the final electrical conductivity (S_2) was measured after boiling for 10 min. Relative electrolyte leakage (L) was calculated as:

$$L(\%) = S_1 \div S_2 \times 100 \quad \text{(Eq.1)}$$

Nine replications were used for all treatments.

Estimation of malondialdehyde (MDA) contents

MDA contents were analyzed using the thiobarbituric acid method (Del-Rio et al., 2005). Briefly, after treatment mentioned above, three T3 transgenic plants for WRKY and WT plants were accurately weighed with the leaves (0.5 g) to be tested, and was added with pre-cooled phosphate buffer (1 ml), then grinded, diluted with buffer solution to 5 ml. After centrifuging the solution at 1000 r/min for 20 min, the supernatant solution (2 ml) was added and mixed with TBA (2 ml). The reaction mixture was boiled for 30 min and then cooled down to room temperature. Lastly, the absorbance was noted at 532 and 600 nm. MDA concentration was calculated using the extinction coefficient of 155 m M^{-1} cm^{-1} and expressed as l μmol g^{-1} dry weight. Nine replications were used for all treatments.

Superoxide dismutase (SOD) activity assay

SOD activity was assayed by monitoring the inhibition of photochemical reduction of nitro blue tetrazolium (NBT). After treatment mentioned above, the 3 ml reaction mixture contained 2.4 ml of 50 mM buffered phosphate solution (pH 7.8), 0.2 ml of 195 mM methionine, 0.1 ml of 3 μM EDTA, 0.2 ml of 1.125 mM NBT, 0.1 ml of 60 μM riboflavin, and 40 μl enzyme extract. The reaction mixtures were illuminated for 20 min at a light intensity of 300 $\mu mol \cdot m^{-2} \cdot s^{-1}$. One unit of SOD activity was defined as the amount of enzyme required to cause 50% inhibition of the reduction of NBT as monitored at 560 nm.

Determination of proline content

After treatment mentioned above, leaf materials of T3 transgenic plants and WT plants (0.5 g) were homogenized in 3% (w/v) sulfosalicyclic acid and homogenate filtered through filter paper. After addition of acid ninhydrin and glacial acetic acid, the resulting mixture was heated at 100°C for 1 h in a water bath. The reaction was then stopped by using an ice bath. The mixture was extracted with toluene, and the absorbance of the fraction with toluene extracted from the liquid phase was read at 520 nm.

Statistical analysis

All data that needed statistical analysis are shown as mean values ± *standard errors* of *the* mean. SPSS Statistics (www.ibm.com/products/spss-statistics) software was used for statistical analysis via Student's *t*-test. Significant differences were considered significant with a probability level of $p < 0.05$.

http://www.aloki.hu ● ISSN 1589 1623 (Print) ● ISSN1785 0037 (Online)
DOI: http://dx.doi.org/10.15666/aeer/2001_221233

Results

Sequence analysis of WRKY gene and evolutionary relationship analysis

According to sequences of conserved domains in typical WRKY genes, a fragment with 512 bp was amplified by RT-PCR. Using 5'- and 3'-RACE technology, a 751 bp fragment and another 803 bp fragment were obtained, respectively. The mRNA full-length of a WRKY gene was obtained by sequence assembly and re-amplification. This gene is 1,833 bp in length, including an open reading frame (ORF) of 1533 bp that encodes 510 amino acids. This gene was named as *PsWRKY1* with an accession No. MK256764 in Genbank. It was showed that PsWRKY1 has the similar typical primary structures to those known WRKY proteins from other plants by comparison of amino acid sequences. All WRKY amino acid sequences all contain two typical WRKY domains that includes the highly conserved amino acid sequence 'WRKYGQK'. Two C_2H_2 zinc-finger motifs were adjacent to each WRKY domains, respectively. A conserved nuclear localization signal (NLS) with amino acid sequence KKKV was found at 227–230 amino acid region of PsWRKY1 protein. In addition, we found some differences from each other by some insertions, substitutions and deletions of some amino acid residues in all WRKY proteins (*Fig. 1*).

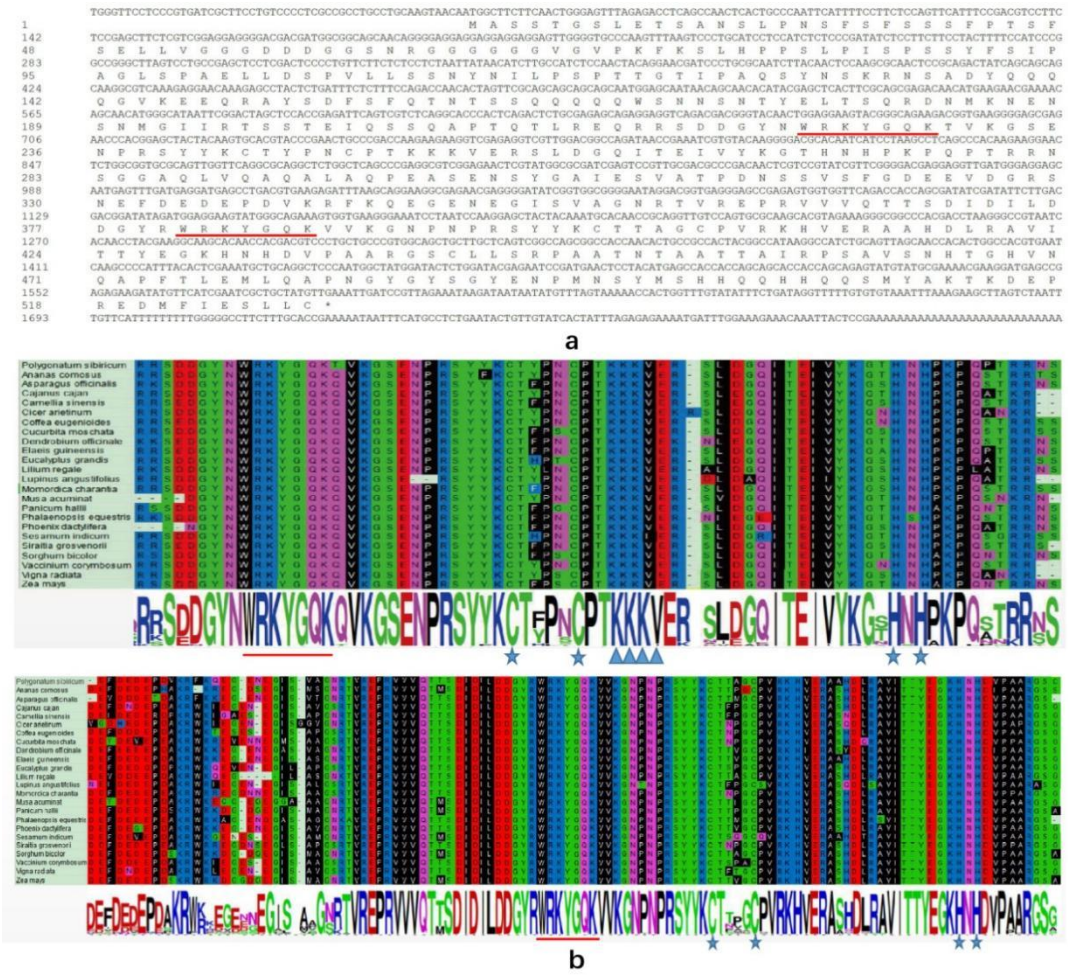

Figure 1. *Nucleotide and deduced amino-acid sequences of PsWRKY1 (a) and sequence alignment of PsWRKY1 with several typical WRKY proteins (b). The conserved WRKY domains are marked by red lines. C and H residues in the zinc-finger motifs are marked by asterisks. The conserved nuclear localization signal (NLS) is marked by triangles. GenBank accession number is MK256764*

http://www.aloki.hu ● ISSN 1589 1623 (Print) ● ISSN1785 0037 (Online)
DOI: http://dx.doi.org/10.15666/aeer/2001_221233

To understand evolutionary relationship of WRKY proteins, we constructed a phylogenetic tree using the PsWRKY1 and 23 WRKY proteins from other plants. It was showed that all WRKY TFs could be classified into six major groups, and PsWRKY1 was clustered into a monophyletic group with five TFs from *Eucalyptus grandis, Sesamum indicum, Ananas comosu*, *Panicum hallii*, and *Sorghum bicolor* in Group I. PsWRKY1 is most closely related to WRKY protein from *Eucalyptus grandiss* (*Fig. 2*).

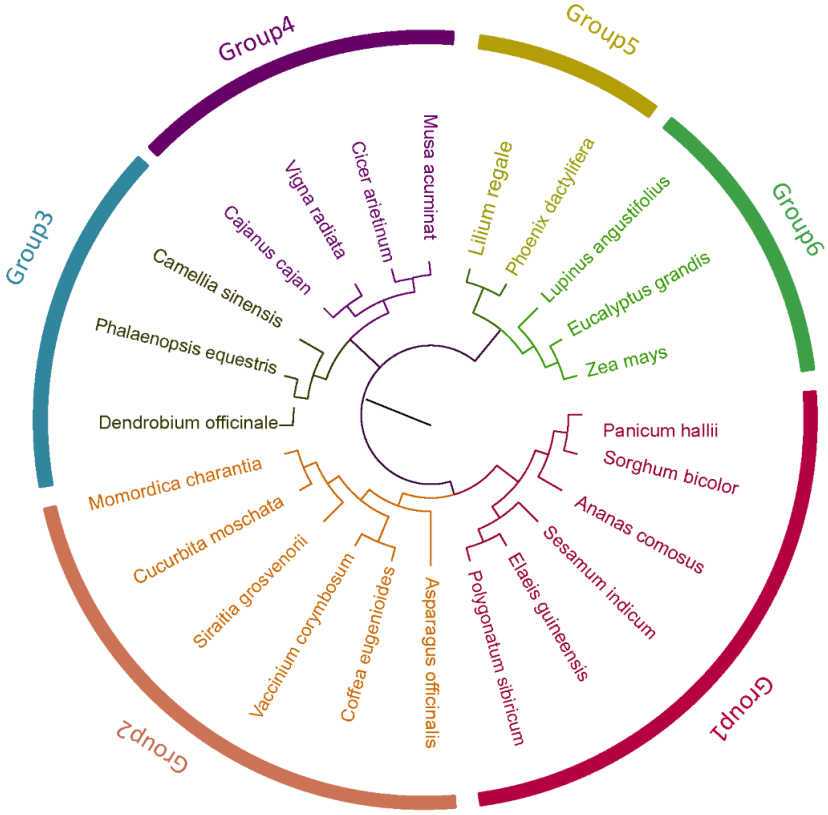

Figure 2. *Phylogenetic relationship of PsWRKY1 protein and other stress-related WRKY TFs. The trees were constructed via the neighbor-joining method with a poisson correction model and 1000 bootstrap replicates*

Expression of PsWRKY1 during abiotic stresses

To identify the expression patterns of *PsWRKY1* under abiotic stresses, the transcript levels of *PsWRKY1* in stems, leaves, and roots were detected during cold, drought, and salt stresses by qRT-PCR. After cold stress, *PsWRKY1* was expressed in leaves and stems of *P. sibiricum,* but not in roots. The expression levels of *PsWRKY1* in leaves and stems both increased gradually with the increase of time for cold stress, reaching a peak at 12 h, at approximately 10.70-fold and 8.23-fold of the control (0 h), respectively. The expression level of *PsWRKY1* in leaves is higher than that in stems. For dehydration stress, *PsWRKY1* was expressed in all detected tissues. The expression levels of *PsWRKY1* increased gradually with the increase of treatment time, reaching a peak at 2 days (*Fig. 3*). Compared to leaves and stems, the expression level of *PsWRKY1* in roots is highest, at approximately 14-fold of the control (0 d). However, the expression of *PsWRKY1* is not significantly changed under salt stress (data not shown).

http://www.aloki.hu ● ISSN 1589 1623 (Print) ● ISSN1785 0037 (Online)
DOI: http://dx.doi.org/10.15666/aeer/2001_221233

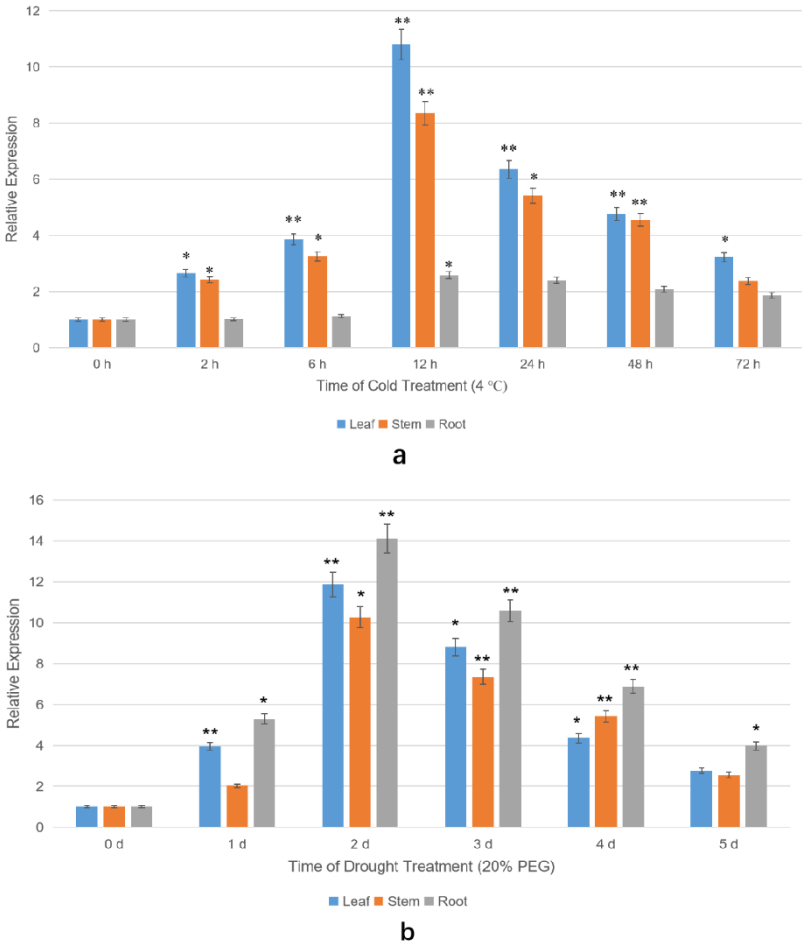

Figure 3. *Expression of PsWRKY1 gene under cold stress (a) and drought stress (b). Error bars indicate the standard error; the experiments were repeated three times along with at least three independent repetitions of the biological experiments. Asterisks indicate a significant difference by Student's t-test (**P<0.01 and *P<0.05)*

Seed germination and seedling growth conditions in transgenic plants under abiotic stresses

To investigate the main role of PsWRKY1 TFs, an expression construct pCAMBIA 1301-PsWRKY1 was transformed into *Arabidopsis thaliana*. A homozygous transgenic line was confirmed by qRT-PCR (*Fig. S1*). Seed germination and growth conditions of wild type (WT) and transgenic plants were tested to evaluate the role of PsWRKY1 under drought and cold stresses, respectively. The germination rate of transgenic plants was higher than that of WT during drought stress, while the growth conditions of transgenic plants were better than those of WT under cold stress (*Fig. 4*). These results showed that PsWRKY1 might improve the resistance to cold and drought stress in transgenic plants.

Physiological indicators of PsWRKY1 overexpression plants

To further identify the role of PsWRKY1, SOD activity, proline content, relative electrolyte leakage, and MDA were tested under cold, drought, and salt stress, respectively. The results indicated that SOD activity and proline content in transgenic plants were all higher than those in WT plants under cold stress and dehydration treatment,

http://www.aloki.hu ● ISSN 1589 1623 (Print) ● ISSN1785 0037 (Online)
DOI: http://dx.doi.org/10.15666/aeer/2001_221233

while MDA levels and relative electrolyte leakage were lower than those in WT plants. However, there are no significant differences in all physiological indicators between the transgenic plants and the WT control under salt stress conditions (*Fig. 5*). These results showed that PsWRKY1 enhanced the cold and drought tolerances by increasing the SOD activity and proline content, and reducing the relative electrolyte leakage and MDA content in *P. sibiricum*.

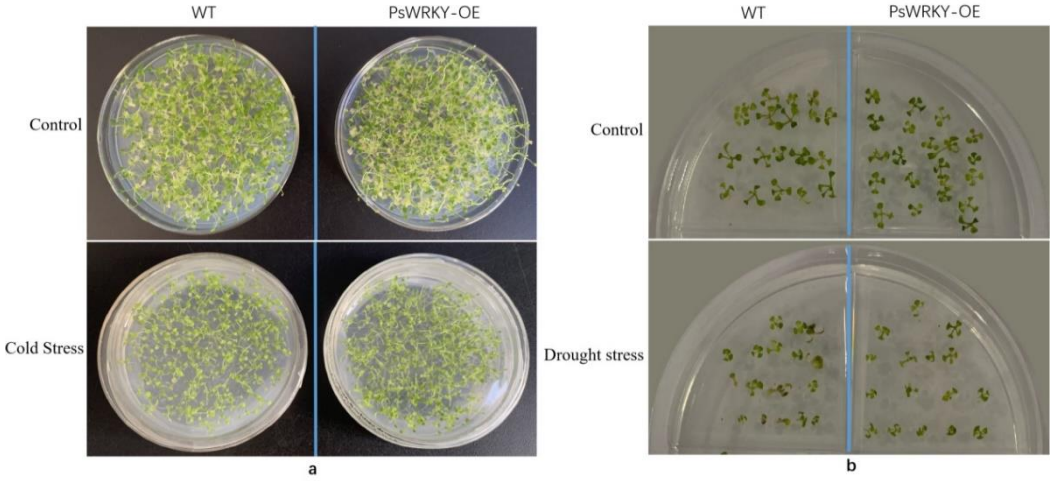

Figure 4. *The growth conditions of WT and PsWRKY1 overexpression plants (OE) on MS medium under abiotic stresses. (a) The phenotypes of the three-week-old seedlings on MS medium after cold treatment (4 °C) for 7 days and recovery under normal growth conditions for 7 days. (b) Germination conditions of WT and PsWRKY1 OE plants on MS medium under drought stress with 20% PEG 6000. WT and OE seeds were vernalized for 3 days and grown on MS medium with 20% PEG 6000 for 7 days*

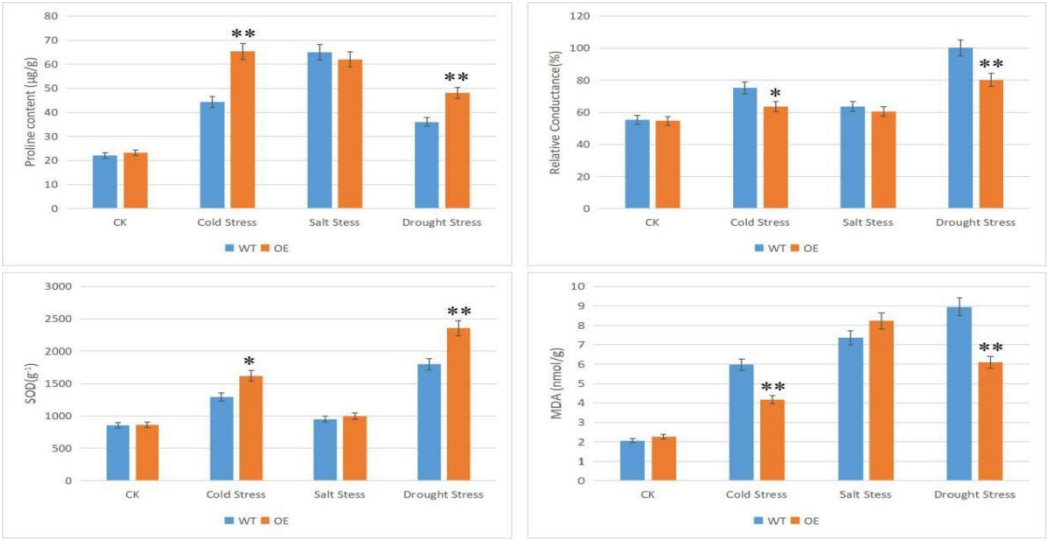

Figure 5. *Physiological indexes of PsWRKY1 overexpression plants (OE) under abiotic stresses, including the SOD activity, proline content, relative electrolyte leakage, and MDA content under cold stress, salt stress, and drought stress. Error bars represent standard deviations (SDs). All the data represent the means ± SDs of three independent biological replicates. Asterisks indicate a significant difference compared to WT by Student's t-test (**P<0.01 and *P<0.05)*

http://www.aloki.hu ● ISSN 1589 1623 (Print) ● ISSN1785 0037 (Online)
DOI: http://dx.doi.org/10.15666/aeer/2001_221233

Discussion

Previous studies indicated WRKY transcription factors play vital roles in medicating the responses to abiotic and biotic stresses. Abiotic stresses including salinity stress, drought stress, cold and heat stress, and oxidative stress etc. adversely affect the development processes in plants (Rushton et al., 2012). Expression of many WRKY genes is induced under various abiotic stresses, improving the tolerance to abiotic stresses in plants. *P. sibiricum*, a kind of medicinal plant, is often used to treat some diseases and tonify the spleens and kidneys. Due to the medicinal value of *P. sibiricum*, its studies mainly focus on active ingredient and pharmacodynamics. Because of growth habit of *P. sibiricum,* it grows mostly in worse conditions. The special growth condition gives *P. sibiricum* strong ability to resist some abiotic stresses (Jo et al., 2017; Zhao et al., 2018; Pan et al., 2020). To date, however, studies on molecular basis of resistance to abiotic stresses in *P. sibiricum* are extremely rare. In this study, a novel WRKY TF gene from *P. sibiricum* was isolated and identified for the first time. Due to numbers of conserved WRKY domain, the WRKY proteins in plants are mainly classified into three groups with I, II, and III groups. Members of group I include two WRKY domains and one or two C_2H_2 zinc-finger sequences, while Group II contains a WRKY-domain along with a zinc-finger (C_2H_2) sequence (Eulgem et al., 2000). Furthemore, the WRKY domain also presents in group III but contained a C_2HC type zinc-finger sequence. In this study, it is showed that PsWRKY1 belongs to group I because of two WRKY domains and two C_2H_2 zinc-finger sequence.

It has been indicated that the WRKY TFs are involved in some abiotic stress responses. However, they probably have different function in various plants even in same plant. For example, OsWRKY74 from rice is involved in tolerance to cold stress (Nuruzzaman et al., 2014), but *OsWRKY30 can* enhance resistance to drought stress. *VpWRKY1, VpWRKY2*, and *VpWRKY3* from *V. pseudoreticulata* all are involved in salt stress, while *VpWRKY2* can enhance resistance to cold stress (Srivastava et al., 2018). *TaWRKY2* from wheat can enhance tolerance to drought and salt stresses, while *TaWRKY19* not only improves resistance to salt and drought, but also enhances cold tolerance. Similarly, *GmWRKY27* from soybean can improve resistance to cold stress, but not resistance to drought or salt stresses, whereas *GmWRKY54* exhibit more tolerance to drought and salt stresses (Song et al., 2016). In this study, the transcriptional levels of *PsWRKY1* gene are induced by low temperature and drought stresses but not by salt stress, which showed that *PsWRKY1* might enhance tolerance to low temperature and drought stresses.

It is well known that abiotic stress in plants are related to a complicated antioxidant defense system for ROS scavenging. Many ROS-scavenging enzymes such as POD, CAT, SOD, and non-enzymatic antioxidants can impact various physiological and biochemical processes (Banerjee et al., 2015). Previous studies showed that the antioxidant-related genes are closely related to WRKY TFs. *CaWRKY40* in pepper can increase the expression of *NtAPX, NtSOD1, NtGST1*, and *NtCAT1*, enhancing high temperature tolerance in tobacco (Zhang et al., 2019). Some *GhWRKY* genes from cotton can improve the resistance to salt stress by reducing the MDA content and increasing antioxidant activities. *GmWRKY27* from soybeans can improve resistance to the salt and drought stresses by modulating peroxidase genes (Song et al., 2016). *ZmWRKY106* from *Zea may* can reduce ROS content and increase the activities of SOD, POD and CAT under drought treatment (Zhang et al., 2019). *OsWRKY76* in rice increases the expression of antioxidant enzymes related genes, such as peroxidases and GST (*OsGSTU5*), thereby enhancing resistance to cold stress (Yokotani et al., 2013). *WRKY44* in wheat also enhances drought

http://www.aloki.hu ● ISSN 1589 1623 (Print) ● ISSN1785 0037 (Online)
DOI: http://dx.doi.org/10.15666/aeer/2001_221233

and salt tolerance by increasing soluble sugar and proline contents and SOD, CAT, and POD activities (Satapathy et al., 2018). According to what mentioned above, when SOD activity and proline content increase but MDA levels and relative electrolyte leakage reduce, the abiotic stress resistance of plants improves more. Here, it was showed that SOD activity and proline content all increased under cold and drought stresses in overexpression *Arabidopsis*, whereas MDA levels and relative electrolyte leakage reduced under same stresses.

Conclusion

P. sibiricum has very strong ability of abiotic resistance because of the special growth conditions. We identified a novel WRKY gene *PsWRKY1* in *P. sibiricum* for the first time. Sequence and evolutionary analysis showed that PsWRKY1 has the typical domains of WRKY protein, which is most closely related to the WRKY protein from *E. grandis.* Gene expression analysis indicated that expression of *PsWRKY1* was induced by drought and cold stresses. Characterization of *PsWRKY1* in transgenic *Arabidopsis* indicated that *PsWRKY1* enhanced the drought and cold resistance. These results indicated the functions of *PsWRKY1* in response to cold and drought stresses in *P. sibiricum*, which could be utilized in *Polygonatum* plants improvement program to develop cold and drought tolerance variety for getting high yields. The cold and drought tolerances in plants are the complex quantitative trait. It is not enough to assess the cold and drought tolerance ability of *P. sibiricum* only based on identification of *PsWRKY1* in *Arabidopsis.* The specific regulatory relationship among *PsWRKY1* and other impact factors in *P. sibiricum* still requires further investigation.

Acknowledgments. We express our gratitude to the anonymous reviewers for helpful comments to improve the manuscript. This work was supported by the Promotion and Demonstration Project of Forestry Science and Technology from Central Finance (2022TG16), Liaoning Revitalization Talents Program (XLYC1902081) and Project of Task for Discipline Construction in Liaoning Academy of Agricultural Sciences (2019DD217032).

REFERENCES

[1] Amorim, L. L. B., da Fonseca, R., Neto, J. P. B., Guida-Santos, M., Crovella, S., Benko-Iseppon, A. M. (2017): Transcription Factors Involved in Plant Resistance to Pathogens. – Curr. Protein Pept. Sci. 18(4): 335-351.

[2] Banerjee, A., Roychoudhury, A. (2015): WRKY proteins: Signaling and regulation of expression during abiotic stress responses. – World J. Sci. 2015: 807560.

[3] Del-Rio, D., Stewart, A. J., Pellegrini, N. (2005): A review of recent studies on malondialdehyde as toxic molecule and biological marker of oxidative stress. – Nutr. Metab Cardiovasc Dis. Sci. 15(4): 316-28.

[4] Eulgem, T., Rushton, P. J., Robatzek, S., Somssich, I. E. (2000): The WRKY superfamily of plant transcription factors. – Trends. Plant Sci. 5: 199-206.

[5] Gong, X., Zhang, J., Hu, J., Wang, W., Wu, H., Zhang, Q., Liu, J. (2015): FcWRKY70, a WRKY protein of *Fortunella crassifolia*, functions in drought tolerance and modulates putrescine synthesis by regulating arginine decarboxylase gene. – Plant Cell Environ. Sci. 38(11): 2248-2262.

[6] Jiang, J., Ma, S., Ye, N., Jiang, M., Cao, J., Zhang, J. (2017): WRKY transcription factors in plant responses to stresses. – J. Integr Plant Biol. Sci. 59(2): 86-101.

http://www.aloki.hu ● ISSN 1589 1623 (Print) ● ISSN1785 0037 (Online)
DOI: http://dx.doi.org/10.15666/aeer/2001_221233

[7] Jo, K., Jeon, S., Ahn, C. W., Han, S. H., Suh, H. J. (2017): Changes in Drosophila melanogaster Sleep-Wake Behavior Due to Lotus (Nelumbo nucifera) Seed and Hwang Jeong (*Polygonatum sibiricum*) Extracts. – Prev. Nutr. Food Sci. 22(4): 293-299.

[8] Kiranmai, K., Lokanadha, R. G., Pandurangaiah, M., Nareshkumar, A., Reddy, V., Lokesh, U., Venkatesh, B., Johnson, A., Sudhakar, C. (2018): A Novel WRKY Transcription Factor, MuWRKY3 (*Macrotyloma uniflorum* Lam. Verdc.) Enhances Drought Stress Tolerance in Transgenic Groundnut (*Arachis hypogaea* L.). – Plants. Front. Plant Sci. 9: 346.

[9] Liu, G. J., Liu, M. K., Xu, Z. R., Yan, X. F., Wei, Z. G., Yang, C. P. (2009): Construction and analysis of a forward and reverse subtractive cDNA library from leaves and stem of *Polygonum sibiricum* Laxm. under salt stress. – Yi Chuan Sci. 31(4): 426-33.

[10] Liu, Y., Yang, T., Lin, Z., Gu, B., Xing, C., Zhao, L., Dong, H., Gao, J., Xie, Z., Zhang, S., Huang, X. (2019): A WRKY transcription factor PbrWRKY53 from *Pyrus betulaefolia* is involved in drought tolerance and AsA accumulation. – Plant. Biotechnol. J. Sci. 17(9): 1770-1787.

[11] Luo, X., Bai, X., Sun, X., Zhu, D., Liu, B., Ji, W., Cai, H., Cao, L., Wu, J., Hu, M., Liu, X., Tang, L., Zhu, Y. (2013): Expression of wild soybean WRKY20 in Arabidopsis enhances drought tolerance and regulates ABA signalling. – J. Exp Bot. Sci. 64(8): 2155-21691.

[12] Luo, D. L., Ba, L. J., Shan, W., Kuang, J. F., Lu, W. J., Chen, J. Y. (2017): Involvement of WRKY Transcription Factors in Abscisic-Acid-Induced Cold Tolerance of Banana Fruit. – J. Agric Food Chem. Sci. 65(18): 3627-3635.

[13] Mitsuda, N., Ohme-Takagi, M. (2009): Functional analysis of transcription factors in Arabidopsis. – Plant Cell Physiol. Sci. 50: 1232-1248.

[14] Ng, D. W., Abeysinghe, J. K., Kamali, M. (2018): Regulating the Regulators: The Control of Transcription Factors in Plant Defense Signaling. – Int. J Mol. Sci. 19(12): 3737.

[15] Nuruzzaman, M., Sharoni, A. M., Satoh, K., Kumar, A., Leung, H., Kikuchi, S. (2014): Comparative transcriptome profiles of the WRKY gene family under control, hormone-treated, and drought conditions in near-isogenic rice lines reveal differential, tissue specific gene activation. – J. Plant Physiol. Sci. 171(1): 2-13.

[16] Pan, J., Lu, W., Chen, S., Cao, T., Chi, L., He, F. (2020): Characterization of the complete chloroplast genome of *Polygonatum sibiricum* (*Liliaceae*), a well-known herb to China. – Mitochondrial. DNA B Resour. Sci. 5(1): 528-529.

[17] Qu, C. P., Xu, Z. R., Liu, G. J., Liu, C., Li, Y., Wei, Z. G., Liu, G. F. (2010): Differential expression of copper-zinc superoxide dismutase gene of *Polygonum sibiricum* leaves, stems and underground stems, subjected to high-salt stress. – Int. J. Mol. Sci. 11(12): 5234-45.

[18] Rushton, D. L., Tripathi, P., Rabara, R. C., Lin, J., Ringler, P., Boken, A. K., Langum, T. J., Smidt, L., Boomsma, D. D., Emme, N. J., Chen, X., Finer, J. J., Shen, Q. J., Rushton, P. J. (2012): WRKY transcription factors: Key components in abscisic acid signalling. – Plant Biotechnol. J. Sci. 10: 2-11.

[19] Satapathy, L., Kumar, D., Kumar, M., Mukhopadhyay, K. (2018): Functional and DNA-protein binding studies of WRKY transcription factors and their expression analysis in response to biotic and abiotic stress in wheat (*Triticum aestivum* L.). – 3 Biotech. Sci. 8(1): 40.

[20] Song, H., Wang, P., Hou, L., Zhao, S. Z., Zhao, C. Z., Xia, H., Li, P., Zhang, Y., Bian, X. T., Wang, X. J. (2016): Global Analysis of WRKY Genes and Their Response to Dehydration and Salt Stress in Soybean. – Front. Plant Sci. 7: 9.

[21] Srivastava, R., Kumar, S., Kobayashi, Y., Kusunoki, K., Tripathi, P., Kobayashi, Y., Koyama, H., Sahoo, L. (2018): Comparative genome-wide analysis of WRKY transcription factors in two Asian legume crops: Adzuki bean and Mung bean. – Rep. Sci. 8(1): 16971.

[22] Sun, X., Zhang, L., Wong, D. C. J., Wang, Y., Zhu, Z. F., Xu, G. Z., Wang, Q. F., Li, S. H., Liang, Z. C., Xin, H. P. (2019): The ethylene response factor VaERF092 from Amur

http://www.aloki.hu ● ISSN 1589 1623 (Print) ● ISSN1785 0037 (Online)
DOI: http://dx.doi.org/10.15666/aeer/2001_221233

grape regulates the transcription factor VaWRKY33, improving cold tolerance. – Plant J. Sci. 99(5): 988-1002.

[23] Wei, Z. P., Ye, J. F., Zhou, Z. Q., Chen, G., Meng, F. J., Liu, Y. F. (2021): Isolation and characterization of PoWRKY, an abiotic stress-related WRKY transcription factor from *Polygonatum odoratum*. – Physiol Mol Biol Plants 27: 1-9.

[24] Yokotani, N., Sato, Y., Tanabe, S., Chujo, T., Shimizu, T., Okada, K., Yamane, H., Shimono, M., Sugano, S., Takatsuji, H., Kaku, H., Minami, E., Nishizawa, Y. (2013): WRKY76 is a rice transcriptional repressor playing opposite roles in blast disease resistance and cold stress tolerance. – J. Exp Bot. Sci. 64(16): 5085-5097.

[25] Zhang, Y., Yu, H., Yang, X., Li, Q., Ling, J., Wang, H., Gu, X., Huang, S., Jiang, W. (2016): CsWRKY46, a WRKY transcription factor from cucumber, confers cold resistance in transgenic-plant by regulating a set of cold-stress responsive genes in an ABA-dependent manner. – Plant Physiol. Biochem. Sci. 108: 478-487.

[26] Zhang, L., Zhao, T., Sun, X., Wang, Y., Du, C., Zhu, Z., Gichuki, D. K., Wang, Q. F., Li, S. H., Xin, H. P. (2019): Overexpression of *VaWRKY12*, a transcription factor from *Vitis amurensis* with increased nuclear localization under low temperature, enhances cold tolerance of plants. – Plant. Mol Biol. Sci. 100(1-2): 95-110.

[27] Zhao, P., Zhao, C., Li, X., Gao, Q. Z., Huang, L. Q., Xiao, P. G., Gao, W. Y. (2018): The genus *Polygonatum*: A review of ethnopharmacology, phytochemistry and pharmacology. – J. Ethnopharmacol. Sci. 214: 274-291.

APPENDIX

Supplementary material

Table S1. *Details of primers used in this study*

Name	Forward Primer (5′-3′)	Reverse Primer (5′-3′)	Involved in the process
WRKY-C	GGTC(A/G)AAA(G/A/C)AC(G/A)GT(G/T)AA(G/A)GGGA	TAC(C/T)TT(C/T)TGCCC(A/G)TA(T/C)TTTC	Cloning of the conserved sequences of WRKY genes
5P1	---	ACCTCTCGACCTTCTTCTTGGTC	5'RACE
5P2	---	TACGTGCACTTGTAGTAGCTC	
5P3	---	CGTCTTTTGACCATATTCCTCC	
3P1	GATATTCTTGACGATGGATATA	---	3'RACE
3P2	GAAAATACGGGCAGAAAGTA	---	
β-actin	CGGGGAAACTTACCAGGTCC	TCCACCAACTAAGAACGGCC	Primers of the reference gene for qRT-PCR
WRKY-qRT	CGAAAACAGCAACATGGGCA	TCTTCTTGGTCGGGCAGTTC	Expression analysis by qRT-PCR
WRKY-OE	GGACTAGTATGGCTTCTTCAACTGGGA	GGGGTACCTCAACATAGCAGCGATTCG	Construction of eukaryotic expression vector for over-expressing

http://www.aloki.hu ● ISSN 1589 1623 (Print) ● ISSN1785 0037 (Online)
DOI: http://dx.doi.org/10.15666/aeer/2001_221233

Table S2. *The submitted sequences of WRKY transcription factors with Genbank accession No. for construction of phylogenetic tree*

Gene name	Genbank accession No.	Size of putative protein (residues)	Level of similarity with PsWRKY1 (%)	Plant source
PsWRKY1	MK256764	510	100	*Polygonatum sibiricum*
AcWRKY24	XP_020101951	537	54.46	*Ananas comosus*
AoWRKY24	XP_020271607	487	72.88	*Asparagus officinalis*
CcWRKY24	XM_020356797	523	54.22	*Cajanus cajan*
CsWRKY24	XP_028051918	557	42.22	*Camellia sinensis*
CarWRKY26	XP_004500327	502	36.75	*Cicer arietinum*
CeWRKY24	XP_027175580	565	40.88	*Coffea eugenioides*
CmWRKY24	XP_022964929	559	39.89	*Cucurbita moschata*
DoWRKY	AHF55741	542	44.44	*Dendrobium officinale*
EgWRKY24	XP_019706087	570	47.58	*Elaeis guineensis*
EgrWRKY26	XP_018724852	549	40.31	*Eucalyptus grandis*
LrWRKY33	ART33472	549	47.86	*Lilium regale*
LaWRKY24	XP_019418126	535	37.04	*Lupinus angustifolius*
McWRKY24	XP_022154851	424	32.19	*Momordica charantia*
MaWRKY24	XP_009383300	519	41.88	*Musa acuminata*
PhWRKY24	XP_025819311	552	36.61	*Panicum hallii*
PeWRKY26	XP_020596685	554	43.02	*Phalaenopsis equestris*
PdWRKY24	XP_026663206	549	45.73	*Phoenix dactylifera*
SiWRKY25	XP_011080757	542	38.32	*Sesamum indicum*
SgWRKY6	AZU90760	402	30.91	*Siraitia grosvenorii*
SbWRKY24	XP_021310889	556	37.18	*Sorghum bicolor*
VcWRKY33	AXR71208	392	32.05	*Vaccinium corymbosum*
VrWRKY24	XP_014489595	526	50.18	*Vigna radiata*
ZmWRKY	NP_001354299	555	37.75	*Zea mays*

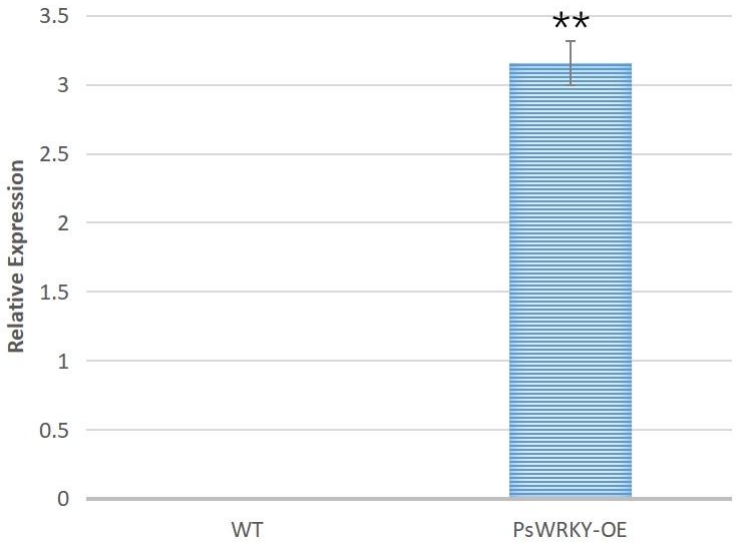

Figure S1. *qRT-PCR for confirming PsWRKY1 transgenic plants. Asterisks indicate a significant difference compared to WT by Student's t test (**P<0.01)*

http://www.aloki.hu ● ISSN 1589 1623 (Print) ● ISSN1785 0037 (Online)
DOI: http://dx.doi.org/10.15666/aeer/2001_221233

RHIZOPHAGUS INTRARADICES AND TOMATO-BASIL COMPANIONSHIP AFFECT ROOT MORPHOLOGY AND ROOT EXUDATE DYNAMICS IN TOMATO UNDER FUSARIUM WILT DISEASE STRESS

RAZA, S. M. J.[1] – AKHTER, A.[1*] – WAHID, F.[2] – HASHEM, A.[3,4] – ABD_ALLAH, E. F.[5]

[1]*Department of Plant Pathology, Faculty of Agricultural Sciences, University of the Punjab, Quaid-i-Azam Campus, PO Box 54590, Lahore, Pakistan*

[2]*Department of Agriculture, University of Swabi, Khyber Pakhtunkhwa, Pakistan*

[3]*Botany and Microbiology Department, College of Science, King Saud University, PO Box 2460, Riyadh 11451, Saudi Arabia*

[4]*Mycology and Plant Disease Survey Department, Plant Pathology Research Institute, ARC, Giza 12511, Egypt*

[5]*Plant Production Department, College of Food and Agricultural Sciences, King Saud University, PO Box 2460, Riyadh 11451, Saudi Arabia*

**Corresponding author*
e-mail: adnanakhter.iags@pu.edu.pk; phone: +92-322-602-3186; fax: +92-429-923-1846

(Received 18th Jul 2021; accepted 1st Oct 2021)

Abstract. Combining the benefits of intercropping with arbuscular mycorrhizal fungi (AMF) can be an additional tool for managing the soil-borne diseases in sustainable land management systems. The present study was designed to investigate the influence of basil (*Ocimum basilicum* L.) as an intercropping partner and arbuscular mycorrhizal fungi (*Rhizophagus intraradices*: AMF) on tomato (*Solanum lycopersicum* L.) root morphology and exudation both in the presence and absence of Fusarium wilt (*Fusarium oxysporum* f. sp. *lycopersici,* FOL) disease stress. Experiments were conducted in a root compartment system. Our results indicated that intercropping tomato with basil did not only increase the plant biomass but also significantly reduced disease severity in tomatoes. Moreover, tomato plants intercropped with basil and co-inoculated with AMF and FOL had higher root lengths, volume and surface areas as compared to the plants in tomato-tomato combination. *In vitro* studies of FOL microconidia germination in tomato root exudates revealed significantly lower germination rate in the root exudates of AMF colonized tomatoes intercropped with basil than in exudates of tomato intercropped with tomato. In conclusion, intercropping basil with tomato successfully alleviates Fusarium wilt stress even without direct root contact. The addition of AMF increases the tolerance of the host plant towards Fusarium wilt by affecting tomato root morphology and exudation dynamics.
Keywords: *interspecific communication, soil fungi, intercropping, arbuscular mycorrhiza, biological control*

Introduction

Fusarium wilt is a potent devastating factor for tomato (*Solanum lycopersicum* L.) cultivation all over the world. The wilting of tomato caused by a soil borne fungus *Fusarium oxysporum* f. sp. *lycopersici* (FOL) is responsible for massive crop losses all over the world. Yield losses due to Fusarium wilt vary between tomato cultivation systems and may reach up to 45%, as recently reported in India (Ramyabharathi et al., 2012). As a result, sound and effective disease management strategies are needed to ensure maximum tomato production and protection without harming the environment.

Intercropping or co-cultivation of two crops together has been utilized as a mean of subsistence farming in Asia, Latin and North America, Europe and Africa. It is being

http://www.aloki.hu ● ISSN 1589 1623 (Print) ● ISSN 1785 0037 (Online)
DOI: http://dx.doi.org/10.15666/aeer/2001_235249

largely practiced to promote organic gardening, increasing land use efficiency and as a part of integrated pest management strategies (Bomford, 2009). The emphasis of farmers and environmentalists on the chemical free approaches to control diseases by utilizing companion crops with stimulating and suppressing effects on plant growth and disease development, respectively, is growing as well (Fu et al., 2015). Intercropping different plant species has been proposed to offer benefits including increase in yield, protection from pest and diseases (Son et al., 2018); however, the scientific backing of these proposed benefits is lacking due to the small number of studies in this regard.

The selection of a proper cropping partner is very important to avoid negative effects on the main crop. Basil (*Ocimum basilicum* L.) is an aromatic herb, when intercropped with tomato is suggested to improve tomato growth, yield and flavor, whereas other members of the family *Brassicaceae*, for instance Brussels sprout (*Brassica oleracea* L.) and tomato are antagonistic to each other (Riotte, 1975; Bomford, 2009). Salehi et al. (2018) reported an increase in water use efficiency of tomatoes growing with basil in the intercrop setting. Rice (1984) has termed the phenomenal influence of intercrops on each other by plant secondary metabolites or through the by-products of main metabolic pathways as allelopathy. There are also reports concerning allelochemicals acting as natural pesticides against fungal and bacterial pathogens (Farooq et al., 2011). For example, two allelochemicals 5,7,40-trihydroxy-30,50-dimethoxyflavone and 3-isopropyl-5-acetoxycyclohexene-2-one-1 has been isolated from rice, which inhibited the germination of spores of two fungal pathogens *Rhizoctonia solani* and *Pyricularia oryzae* (Kong et al., 2004). However, the knowledge is limited about the consequences of companion crops such as basil on the main crop tomato in terms of protection against FOL.

Arbuscular mycorrhizal fungi (AMF) form a symbiosis with approximately 80% of all land plants and thereby exhibit positive effects on their host plant (Brundrett, 2002; Smith and Read, 2008). The mycorrhizal association with tomato plant roots modifies root morphology, facilitates absorption of nutrients and most importantly induces systemic resistance against *Fusarium oxysporum* f. sp. *lycopersici* (Dehne and Schönbeck, 1979; Scheffknecht et al., 2006). Combining the positive effects of the proper intercropping partner with the application of AMF might be a promising additional tool in sustainable disease management strategies. Increased Fusarium wilt suppression in tomato using basil as intercropping partner has already been demonstrated (Hage-Ahmed et al., 2013a). However, root morphological traits and root exudation dynamics in the tomato-basil intercropping setting and their putative contribution to less diseased plants remain to be elucidated. Thus, in this work a root compartment system separated by a fine mesh (Ø 60 µm) allowing AM hyphae to pass was used to evaluate root morphological traits and their contribution to Fusarium wilt suppression in the tomato-basil intercropping setting.

Materials and methods

Plant material

Tomato (*Solanum lycopersicum* L. cv. Roma) and basil (*Ocimum basilicum* L. cv. Genovese) seeds were surface sterilized by soaking in 50% commercial bleach (3.5% NaOCl) for 10 min, followed by rinsing with sterilized distilled water thrice. Afterwards, seeds were sown in a tray containing sterilized sandy loam soil having clay, silt and sand (18-23%, 52-57% and 23-25%, respectively). The trays were covered with polythene bags

http://www.aloki.hu ● ISSN 1589 1623 (Print) ● ISSN 1785 0037 (Online)
DOI: http://dx.doi.org/10.15666/aeer/2001_235249

to maintain humidity for optimum germination at 24 °C. Tap water was used for irrigating the pots. The seedlings were grown for four weeks before transplanting.

Fungal culture

Fusarium oxysporum f. sp. *lycopersici* isolate was provided by the First fungal culture bank of Pakistan, University of the Punjab Lahore, Pakistan. The fungus was cultivated at 24 °C for 15 days on Potato dextrose Agar medium (Merck KGaA, Darmstadt, Germany) in the dark. Microconidia suspension of FOL was prepared by flooding the culture plates with sterilized distilled water and rubbing the mycelium with spatula. The suspension was filtered through three layers of filter paper (filters, 150 µm pore diameter). For plant inoculation, the final concentration was adjusted to 1×10^5 microconidia ml^{-1} by using a haemocytometer. For AMF inoculation, a commercially available inoculum containing *Rhizophagus intraradices* (Xtreme Gardening, HGC721205 Mykos Pure Mycorrhizal Inoculant) was used.

Experimental design

Pre-cultivated seedlings of tomato and basil were transferred to a modified compartment system (rhizobox) adopted from Vierheilig et al. (2000). Each rhizobox made up of wooden material and comprised of two compartments separated by a nylon membrane of 60 µm mesh size fixed on a dissector. The membrane can be passed by AM hyphae but excludes the roots. So, each box had two sub-compartments allowing only one intercropping combinations per rhizobox. The rhizoboxes were filled with an autoclaved mixture of sand, and soil at the ratio of 1:1 (v/v). The experimental setup consisted of two plant combinations (tomato-tomato and tomato-basil), along with the inoculation of plants with *R. intraradices* and *F. oxysporum* f. sp. *lycopersici*. The treatment plan was as followed: 1) tomato-tomato combination (TT), 2) tomato-tomato with AMF (TTM), 3) tomato-basil (TB) and 4) tomato-basil with AMF (TBM). The treatments were either inoculated with *F. oxysporum* f. sp. *lycopersici* (+Fol) or un-inoculated (–Fol). The experiment was done in a random design with six replicates in two repeats for each treatment. The experiment was conducted at the greenhouse facility of Faculty of Agricultural Sciences, University of the Punjab (Lahore, Pakistan).

For the AMF inoculation, 4 ml of the inoculum was mixed with the soil around the planting hole before seedling transplantation. In case of *F. oxysporum* f. sp. *lycopersici* inoculation, only tomato plants were inoculated by dipping the slightly clipped roots in conidial suspension (1×10^5 microconidia ml^{-1}) for 5 min before transplanting, whereas in case of AMF inoculation, both tomato and basil transplants received the inoculum. The rhizoboxes with the plantlets were placed in the greenhouse for 6 weeks. The plants were irrigated with water according to the moisture requirements and fertilized once a week with a nutrient solution (Steinkellner et al., 2005).

Plant assays

For harvesting, the plants were gently uprooted after 6 weeks. The roots were washed with running tap water. Tomato roots were submerged in autoclaved acetate buffer (25 mM; pH = 5.5) for 6 h to collect root exudates. For each exudate two plants were pooled. The concentration of the exudates was adjusted according to 20 ml buffer per one gram of root fresh weight, filtered through 0.22 µm sterile filters (Thomas Scientific, USA) and stored at –80 °C. Thereafter, root and shoot fresh weights were

http://www.aloki.hu ● ISSN 1589 1623 (Print) ● ISSN 1785 0037 (Online)
DOI: http://dx.doi.org/10.15666/aeer/2001_235249

determined. The disease severity and incidence was assessed both visually and by incubating a 0.5 cm long slice from the shoot base on potato dextrose agar media plates amended with 10 mg L-1 of streptomycin (Akhter et al., 2016; Hage-Ahmed et al., 2013b). For mycorrhizal assessment, the root samples of 1 cm length were collected 2 cm below the base of shoot. To assess AMF root colonization, root samples were cleared by boiling with 10% KOH and stained afterwards with a 5% ink-vinegar solution (Vierheilig et al., 1998). The percentage of root colonization was determined according to the gridline intersect method (Newman, 1966; Giovannetti and Mosse, 1980). Roots morphological parameters (root diameter, surface area, cumulative root length and volume) were determined with the software WinRHIZO PRO (Regent Instruments QC, Canada). For this purpose, the digitized root images were obtained using an optical scanner. Specific root length depicting a ratio between root length and mass was calculated as well.

In vitro effect of root exudates on F. oxysporum f. sp. lycopersici

The 96-well plates were used to determine the *F. oxysporum* f. sp. *lycopersici* microconidia germination rate in the root exudates. For each treatment six root exudates were analyzed in three replicates. To each well of a plate 175 µl of root exudates were poured along with 35 µl of a conidial spore suspension (1×10^7 microconidia ml^{-1}). The plates were incubated without light on a rotary shaker at 200 rpm for 20 h, at 24 °C. Microconidia germination rate (%) was determined microscopically after 20 h by observing 200 spores for the presence of germ tubes from each well.

Statistical analysis

The data analysis was performed by using PASW Statistics 18 (Version 18.0.0, IBM, Armonk, NY, USA) software. A one-way analysis of variance (ANOVA) was used to determine the treatment effects. Equality of variance was tested by the Levene's test. The percentage data was transformed before analysis. The treatment means were compared using Tukey's honestly significant difference (HSD) test, at a significance level of 5%.

Results

Plant growth assessment

It became evident through data that tomato plant growth has been significantly increased by the intercropping partner. The details of statistical analysis have been summarized in *Table 1*. We documented an increase in root and shoot dry weight for tomato plants intercropped with basil (*Fig. 1a, b*). The tomato-basil combination has produced maximum root and shoot dry weights (1.25 and 1.97 g, respectively) in un-inoculated control treatments. In addition, the plants cope with *F. oxysporum* f. sp. *lycopersici* induced reduction in plant growth better, when tomato plants were intercropped with basil. Among *F. oxysporum* f. sp. *lycopersici* inoculated plants, root and shoot dry weights of the TB combinations increased by 40% and 43.80%, respectively, compared to plants from the TT combinations. Co-inoculation of AMF and *F. oxysporum* f. sp. *lycopersici* showed a significant average increase of 31% in plant growth in the TB combination as compared to the TT combination. Moreover, tomato plants had produced higher shoot lengths in the TB combination with the maximum of 31 cm and 28.9 cm in un-inoculated and *F. oxysporum* f. sp. *lycopersici* inoculated

http://www.aloki.hu ● ISSN 1589 1623 (Print) ● ISSN 1785 0037 (Online)
DOI: http://dx.doi.org/10.15666/aeer/2001_235249

treatments, respectively (*Fig. 1*c). However, in the TT combination shoot length was minimum in *F. oxysporum* f. sp. *lycopersici* inoculated plants and plants received AMF and *F. oxysporum* f. sp. *lycopersici* together (21 cm and 23.5 cm, respectively).

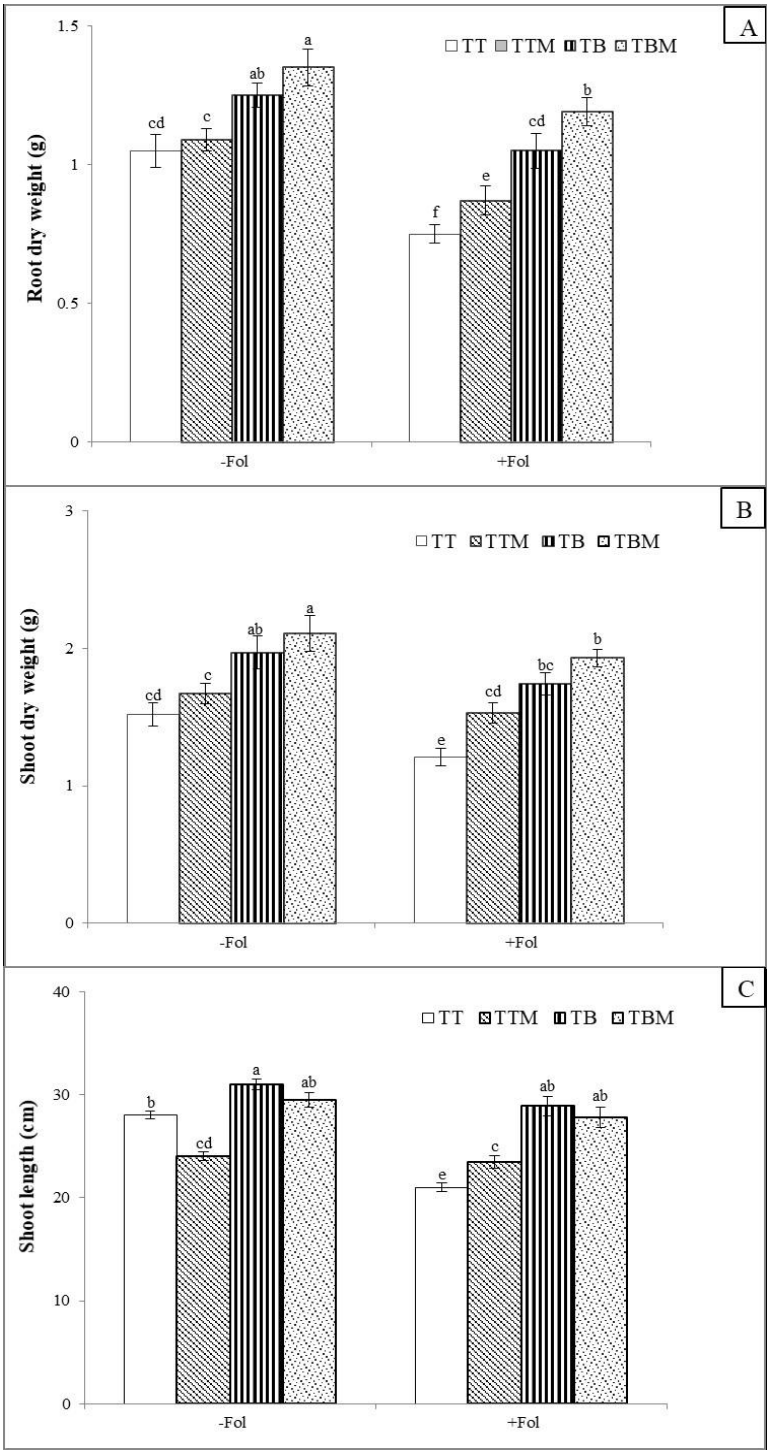

Figure 1. *Effect of cropping partner and AMF on root dry weight (a), shoot dry weight (b) and shoot length (c) of tomato plants intercropped with tomato (TT) and basil (TB), either inoculated with F. oxysporum f. sp. lycopersici (+Fol) or un-inoculated (–Fol) and/or with the AMF 'R. intraradices' (M) (mean ± S.E.). Bars with different letters show significant differences according to Tukey's HSD test ($P < 0.05$)*

http://www.aloki.hu ● ISSN 1589 1623 (Print) ● ISSN 1785 0037 (Online)
DOI: http://dx.doi.org/10.15666/aeer/2001_235249

Table 1. *ANOVA results presented as degrees of freedom (DF), F and P values for tomato plant growth, disease severity, mycorrhizae root colonization and Fusarium oxysporum f. sp. lycopersici microconidia germination assay*

Parameters	DF	F	P
Root dry weight	7	12.1	**
Shoot dry weight	7	15.3	**
Shoot height	7	25.3	**
Root diameter	7	4.75	**
Root volume	7	38.1	**
Root surface area	7	27.1	**
Root length	7	37.2	**
Specific root length	7	2.41	*
Disease severity	3	15.4	**
Mycorrhizal root colonization	3	29	**
Fol microconidia germination	4	135	**

*$P \leq 0.05$; **$P < 0.001$

Root morphology assessment

The intercropping partner as well as AMF had no significant effect on root diameter (*Fig. 2*a). However, both minimum (0.68 cm) and maximum (0.99 cm) root diameter was recorded in TT combination received no inoculation and co-inoculated with AMF and *F. oxysporum* f. sp. *lycopersici,* respectively. Apart from root diameter, other root morphological parameters such as root volume, surface area and root length were significantly altered depending on the intercropping partner as well as on the inoculation of AMF and *F. oxysporum* f. sp. *lycopersici* (*Fig. 2b, c, d; Table 1*). Intercropping tomato with basil had a positive impact on the root surface area, volume and length when *F. oxysporum* f. sp. *lycopersici* was not present. The incorporation of AMF in the TT combination (in the absence of *F. oxysporum* f. sp. *lycopersici*) resulted in the reduction of the root volume, surface area and length. On the contrary, in the TB combination with AMF the root surface area and volume remained unaltered; however, a significant reduction in root length was recorded. In the TT combination, plants inoculation with *F. oxysporum* f. sp. *lycopersici* has decreased root surface area, volume and length in comparison with their un-inoculated counterparts. The inoculation with *F. oxysporum* f. sp. *lycopersici* in the TT combination reduced root volume and root surface area compared to the un-inoculated TT combination, in the absence of AMF. Moreover, addition of AMF had a non-significant impact on minimizing the *F. oxysporum* f. sp. *lycopersici* induced reduction in above mentioned root morphological measurements in TT combination. However, the tomato plants in the TB combination co-inoculated with AMF and *F. oxysporum* f. sp. *lycopersici* had sustained higher root volume (0.72 cm^3), than plants from the TB combination without AMF (root volume; 0.55 cm^3).

The minimum specific root length (0.68 cm/mg) was recorded in plants of TB combination in the presence of *F. oxysporum* f. sp. *lycopersici*; however, no significant differences were observed in specific root length of tomato plants grown in combination with either tomato or basil, in the absence of *F. oxysporum* f. sp. *Lycopersici*, both with and without AMF (*Fig. 3*).

http://www.aloki.hu ● ISSN 1589 1623 (Print) ● ISSN 1785 0037 (Online)
DOI: http://dx.doi.org/10.15666/aeer/2001_235249

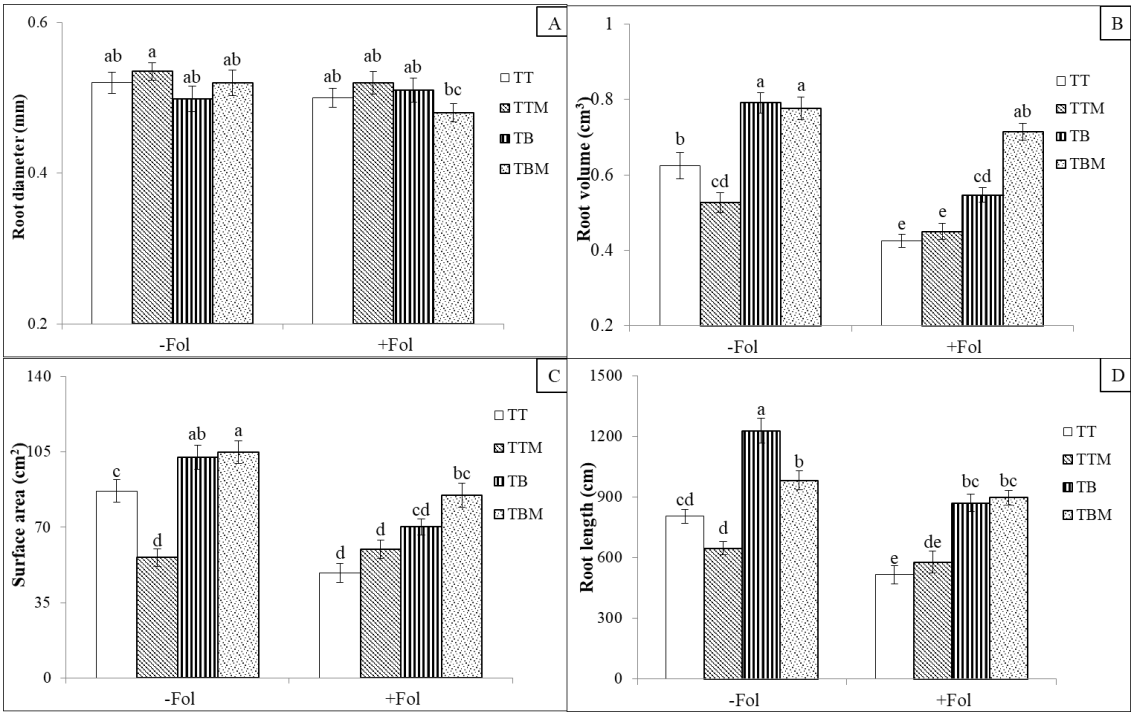

Figure 2. *Effect of cropping partner and AMF on root diameter (a), volume (b), surface area (c) and root length (d) of tomato plants intercropped with tomato (TT) and basil (TB), either inoculated with F. oxysporum f. sp. lycopersici (+Fol) or un-inoculated (–Fol) and/or with the AMF 'R. intraradices' (M) (mean ± S.E.). Bars with different letters show significant differences according to Tukey's HSD test (P < 0.05)*

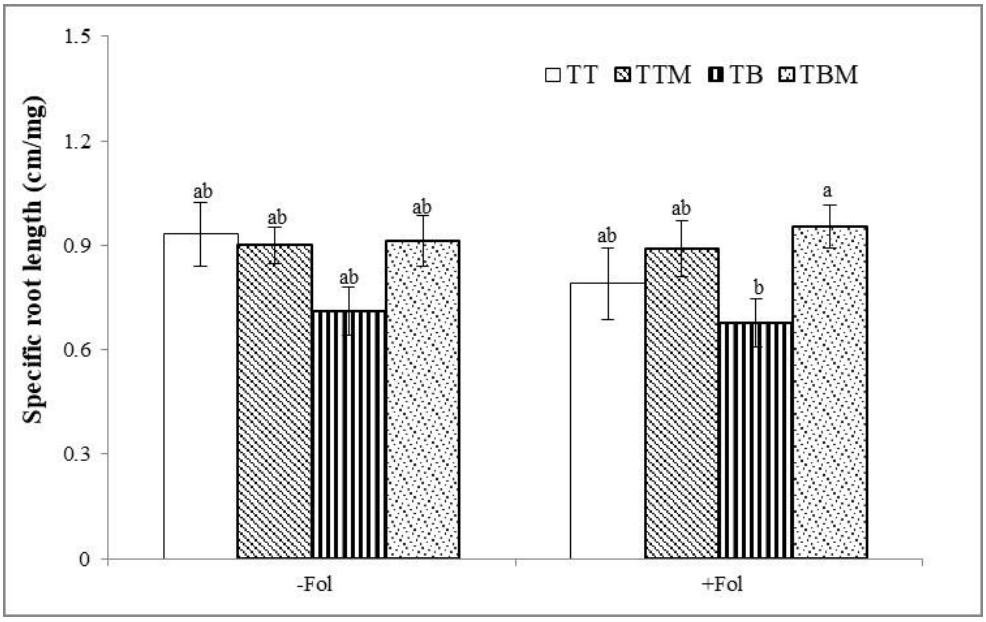

Figure 3. *Effect of cropping partner and AMF on the specific root length of tomato plants intercropped with tomato (TT) and basil (TB), either inoculated with F. oxysporum f. sp. lycopersici (+Fol) or un-inoculated (–Fol) and/or with the AMF 'R. intraradices' (M) (mean ± S.E.). Bars with different letters show significant differences according to Tukey's HSD test (P < 0.05)*

http://www.aloki.hu ● ISSN 1589 1623 (Print) ● ISSN 1785 0037 (Online)
DOI: http://dx.doi.org/10.15666/aeer/2001_235249

Mycorrhizal root colonization

Six weeks after plantation, plants were harvested and root sections were stained to assess the root colonization (*Fig. 4*). Mycorrhizal root colonization of tomato plants was higher in TB than TT combination. Maximum root colonization (46.33 and 43.83%) was observed in TB, where plants were inoculated with FOL and TB combination in the absence of FOL, respectively. However, *F. oxysporum* f. sp. *lycopersici* inoculated plants from TT combination has the lowest (25.85%) rate of root colonization. Basil plants were also assessed for root colonization; an increase in basil root colonization was observed when corresponding tomato plants received co-inoculation of AMF and *F. oxysporum* f. sp. *lycopersici* as compared to basil grown with *–Fol* tomato plants (data not shown).

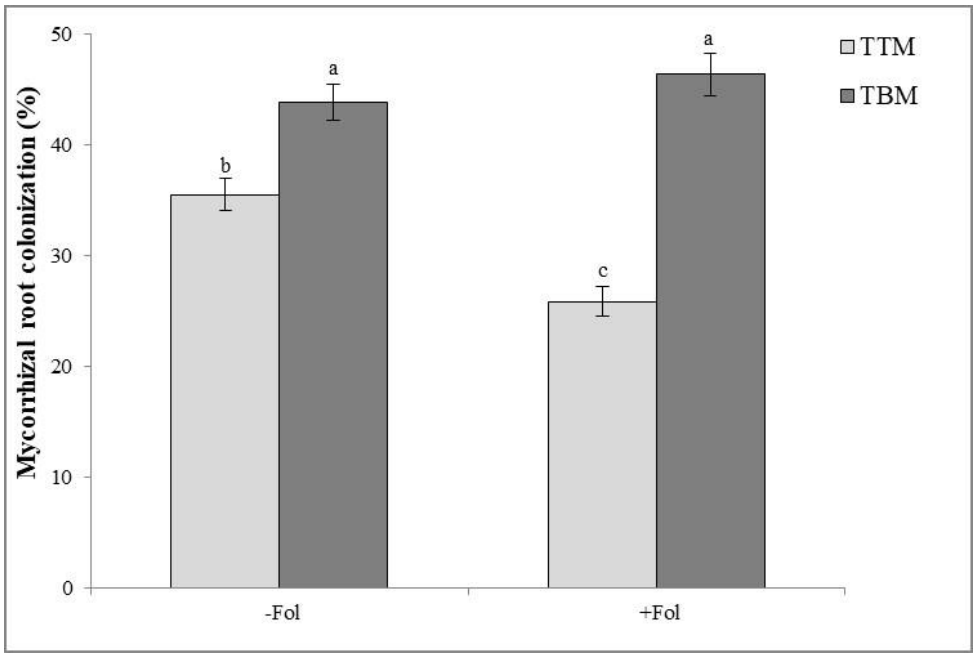

Figure 4. *AMF colonization rate of tomato plants intercropped with tomato (TT) and basil (TB), inoculated with F. oxysporum f. sp. lycopersici (+Fol) or un-inoculated (–Fol) (mean ± S.E.). Bars with different letters show significant differences according to Tukey's HSD test ($P < 0.05$)*

Disease assessment

Table 2 summarizes the FOL disease incidence and severity on tomato plants. The pathogen *F. oxysporum* f. sp. *lycopersici* successfully infected the plants either grown in combination of TT or TB but the degree of infection varied depending on intercropping partner. For the plants grown in TT combination, there was maximum disease incidence and disease severity (91.67 and 32.75 ± 8.95%, respectively). However, with the incorporation of AMF, a trend in reduction (26.82 ± 6.46%) in disease severity was recorded in TT combination. The disease incidence of tomato plants intercropped with basil was 66.67 and 58.33% in the *F. oxysporum* f. sp. *lycopersici* only and co-inoculated (AMF with FOL) treatments, respectively. Disease incidence in TB combination was lower than in TT combination. The co-inoculation of plants with AMF and *F. oxysporum* f. sp. *lycopersici* resulted in a significant reduction in disease severity (59.61%) as compared to the co-inoculated plants of TT combination.

http://www.aloki.hu ● ISSN 1589 1623 (Print) ● ISSN 1785 0037 (Online)
DOI: http://dx.doi.org/10.15666/aeer/2001_235249

Table 2. *F. oxysporum f. sp. lycopersici disease incidence and severity on tomato plants intercropped with tomato (TT) and basil (TB). +AMF' corresponds to the plants inoculated with R. intraradices (mean ± S.D.)*

		Disease incidence[1] (%)	Disease severity[2] (%)
TT + Fol	–AMF	91.67	32.75 ± 8.95^{a}
TB + Fol	–AMF	66.67	19.21 ± 3.57^{bc}
TT + Fol	+AMF	75	26.82 ± 6.46^{ab}
TB + Fol	+AMF	58.33	10.83 ± 3.28^{d}

[1]Disease incidence was calculated for the total number of plants in each treatment
[2]Mean values with different letters show significant differences according to Tukey's HSD test ($P < 0.05$)

Microconidia germination of Fusarium oxysporum f. sp. lycopersici in root exudates

The *F. oxysporum* f. sp. *lycopersici* microconidia germination rate in tomato root exudates and PDA broth are shown in *Figure 5*. Potato dextrose broth control has shown maximum (69.65%) microconidia germination rate. The pH of root exudates was in the range of 5.65 to 5.83. The tomato root exudates had a variable influence on microconidia germination depending on the cropping partner and AMF. The exudates from AMF colonized plants from TT (+M) combination showed a higher germination rate (61.50%) in comparison to respective non-mycorrhizal counterparts [TT (–M); 35.75%]. However, there was a reduction of 24% in germination rate in the exudates from mycorrhizal plants in TB (+M) combination as compared to the non-mycorrhizal (–M) plants of the same combination. The lowest germination rate (34.48 and 35.75%) was recorded in TB (+M) and TB (–M) combination, respectively.

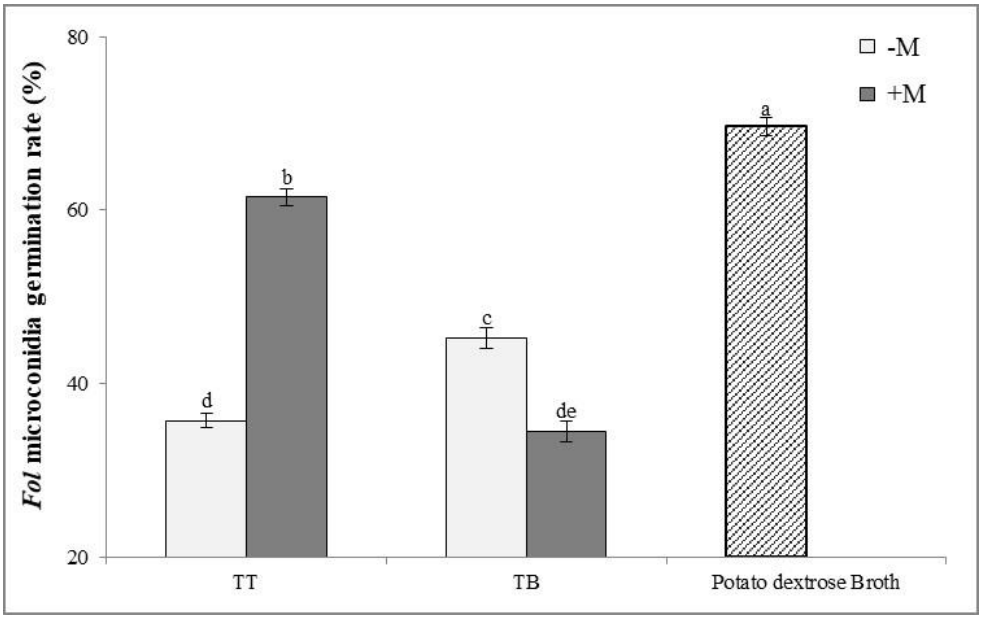

Figure 5. *F. oxysporum f. sp. lycopersici (Fol) microconidia germination rate (%) in the root exudates of tomato plants intercropped with tomato (TT) and basil (TB), inoculated with 'R. intraradices' (+M) or un-inoculated (–M). Bar with pattern represents microconidia germination in Potato dextrose broth (PDA broth; control) (mean ± S.E.). Bars with different letters show significant differences according to Tukey's HSD test (P < 0.05)*

http://www.aloki.hu ● ISSN 1589 1623 (Print) ● ISSN 1785 0037 (Online)
DOI: http://dx.doi.org/10.15666/aeer/2001_235249

Discussion

In this study a tomato-basil intercropping setting was investigated for its impact on Fusarium wilt suppression, root morphology and exudation by using a rhizobox compartment system.

Our greenhouse experiment has shown that intercropping basil with tomato significantly reduced the development of Fusarium wilt in tomatoes compared to tomato intercropped with tomato. Previous studies have documented as well the suppressive effect of interspecific plant interactions against soil borne pathogens (Yang et al., 2014; Ren et al., 2008). Earlier, Fu et al. (2015) reported that companion cropping of tomatoes with potato and onion has reduced the incidence and severity of tomato Verticillium wilt (*Verticillium dahliae*). The reduction of disease incidence and severity in intercropping settings could be attributed to many factors such as changes in the rhizospheric microbial communities, activation of host defense mechanisms along with allelopathic inhibition of pathogens by root exudates and other signaling compounds from the intercropping partner or by the antifungal activity of host root exudates (Fierro-Coronado et al., 2013; Gómez-Rodrıguez et al., 2003; Fu et al., 2015). While, Kadoglidou et al. (2020) reported that even the soil incorporation of aromatic spearmint enhanced the tomatoes tolerance against wilt inducing FOL and *Verticillium dahliae*.

In contrast to the AMF - *Fusarium oxysporum* f. sp. *basilici* interaction (Toussaint et al., 2008), AMF did not confer a clear bioprotective effect against FOL. In this work, the addition of AMF did not reduce disease severity further but alleviated negative effects of *Fusarium oxysporum* f. sp. *lycopersici* on tomato root morphology. Root morphology parameters provide important information about plant physiology and nutrient uptake efficiency (Marques et al., 2016) and are therefore valuable additional indicators for the vitality status of plants challenged by soil-borne pathogens. The alterations in root morphology in response to AMF are not always comparable (Schroeder and Janos, 2005; Berta et al., 1993). AMF induced reduction in root volume, surface area and cumulative root length in the tomato-tomato combination might be due to the competition of AMF with roots for nutrients (Berta et al., 1993). In addition to that the AMF ability to take over the root function of nutrient retention from the soil can also contribute to the alterations in the root architecture (Hetrick, 1991). However, in the tomato-basil combination no greater changes in root morphology were observed in the absence of *F. oxysporum* f. sp. *lycopersici*. The influence of AMF on root morphological traits (root diameter, length, volume and surface area) was more prominent in *F. oxysporum* f. sp. *lycopersici* inoculated plants indicating disease alleviating effects. Earlier, Morauf and Steinkellner (2015) attributed any reduction in the root surface area, volume, length and weight to the *F. oxysporum* f. sp. *lycopersici* inoculation in tomato plants. These alterations critically influence the ability of the plant to acquire nutrients from soil (Hodge et al., 2009). Among co-inoculated plants, tomato plants intercropped with basil had higher root length, volume and surface area as compared to their respective controls indicating greater access to nutrient reservoirs in the soil (Casper and Jackson, 1997).

Furthermore, plant biomass was increased when tomato was intercropped with basil even under disease stress as compared to tomato-tomato combination. The addition of AMF did not significantly impact on tomato plant biomass. Previous studies are contradictory concerning the influence of AMF on plant growth in intercropping settings (Hage-Ahmed et al., 2013a; Schroeder-Moreno and Janos, 2008; Lee et al., 2014). Hashem et al. (2021) reported an increase in photosynthetic and anti-oxidant

http://www.aloki.hu ● ISSN 1589 1623 (Print) ● ISSN 1785 0037 (Online)
DOI: http://dx.doi.org/10.15666/aeer/2001_235249

activity of tomato plants with enhanced growth and resistance against FOL. While, Schroeder-Moreno and Janos (2008) documented the negative effect of AMF on chili, maize and zucchini plant biomass in inter- as well as intra-specific density settings, whereas, Lee et al. (2014) found that AMF inoculum consisting of a mixture of *Glomus*, *Gigaspora*, and *Scutellospora* sp. has significantly improved the *Microstegium vimineum* biomass production and P uptake. Van der Heijden et al. (2003) showed the dependence of the outcome of interspecific plant competition on the diversity of AMF species. Different AMF species depict contrasting ability of N and P uptake (George et al., 1995) and these differences become more prominent at genus rather than at species level (van der Heijden et al., 2003). Our results also indicate that the plant growth response was dependent on the intercropping partner but not on AMF, which contrasts with the findings of Hage-Ahmed et al. (2013a). This might be due to the fact that, in this study, we utilized a different experiment setup than Hage-Ahmed et al. (2013a) i.e. by employing a nylon membrane to avoid direct root contact of intercropping partners with each other and AMF inoculum consisting of only one species (*R. intraradices*) instead of six different species. Thus, competition for nutrients and space for the development of roots has been minimized between intercropping partners. Therefore, allelopathic influence of basil root exudates on disease suppression and tomato plant growth promotion is likely.

Using a rhizobox compartment system also offers the possibility to study AMF colonization preferences between the different intercropping partners, indirect effects mediated by common mycorrhizal networks (CMNs) and putative influence on root exudation. Tomato intercropped with basil has shown an increase in AM root colonization in comparison to plants from the tomato-tomato (– *F. oxysporum* f. sp. *lycopersici*) and tomato-tomato (+*F. oxysporum* f. sp. *lycopersici*) combination by 32.57% and 166.23%, respectively. The plants under stress not only modify their root exudate chemistry which in turn attracts beneficial soil microflora by following a cry out for help hypothesis as proposed by Rolfe et al. (2019). Interestingly, we also found a higher rate of AM root colonization of basil (data not shown) when neighboring tomato plants were inoculated with *F. oxysporum* f. sp. *lycopersici*, suggesting a possible mechanism of belowground communication between plants through CMNs or root exudates. Such CMNs may contribute to the more efficient transfer of signaling and root exudate compounds from basil to tomato plants which might result into activation of induced systemic resistance against Fusarium wilt of tomato. The activation of secondary metabolic pathways in response to plant –AMF interaction contribute significantly in alleviating the effects of biotic as well as abiotic elements faced by the plants (Kaur and Suseela, 2020). Song et al. (2010) revealed that the CMNs established by AMF induced the expression of defense related genes in un-infected tomato plants neighboring *Alternaria solani* infected tomato plants. However, further experiments are necessary to clarify the role of CMNs in this tomato-basil intercropping setting.

In addition to CMNs, root exudates play a crucial role in determining the fate of below ground plant–microbe as well as plant–plant interactions (De-la-Pena et al., 2008; Haichar et al., 2014). Alterations in the composition of root exudates are dependent on the plant species, soil type and environment. Root exudates not only influence but also determine the outcome of tripartite plant–microbe–plant interactions (Badri and Vivanco, 2009; Xu et al., 2015). Presumably, plant species in intercropping settings depict root exudates-mediated allelopathic effects on the nearby plants and also influence the microbial communities in the rhizosphere (Ainalidou et al., 2021; Farooq

http://www.aloki.hu ● ISSN 1589 1623 (Print) ● ISSN 1785 0037 (Online)
DOI: http://dx.doi.org/10.15666/aeer/2001_235249

et al., 2011). Recently, it has been shown that wheat root exudates have antifungal properties against *F. oxysporum* f. sp. *niveum* in wheat-watermelon companion cropping (Xu et al., 2015), and in another study Yu (1999) reported that the tomato intercropped with Chinese chive (*Allium tuberosum* L.) inhibits *Pseudomonas solanacearum*. While, Li et al. (2021), documented the bio-protective effect of AMF against *Ralstonia solanacearum* in tomatoes through enhanced production of phenolic compounds and defense associated enzymes in the rhizosphere.

In this study, *F. oxysporum* f. sp. *lycopersici* microconidia germination was not only influenced by the root exudates of tomato plants but also by the intercropping partner (basil). We found that there was a strong inhibition of microconidia germination in tomato (intercropped with basil) root exudates co-inoculated with *F. oxysporum* f. sp. *lycopersici* and AMF; however, no such inhibition was observed in the tomato-tomato combination and in the tomato-basil combination in the absence of AMF. Hage-Ahmed et al. (2013b) associated the *F. oxysporum* f. sp. *lycopersici* microconidia germination inhibition to the *F. oxysporum* f. sp. *lycopersici* and AMF co-inoculation of tomato plants intercropped with cucumber. Fu et al. (2015) also documented the *V. dahliae* spore germination inhibition in tomato root exudates grown with potato onion. Our results suggest that apart from *F. oxysporum* f. sp. *lycopersici* and AMF, the intercropping partner also significantly contributes to the plant response and the pathogen behavior in the root exudates.

Conclusion

In conclusion, intercropping basil with tomato successfully alleviates Fusarium wilt stress even without direct root contact. The addition of AMF increases the tolerance of the host plant towards Fusarium wilt further by affecting tomato root morphology and exudate dynamics. Thus, the combination of intercropping and AMF application represent an additional tool in sustainable agricultural management practices to reduce the soil-borne pathogen *F. oxysporum* f. sp. *lycopersici*. Further studies are required to analyze the variations in the tomato root exudate chemistry in response to different intercropping partners and to determine the consequence of interaction between plant (tomato)-plant (basil)-AMF and *F. oxysporum* f. sp. *lycopersici* and other rhizosphere inhabitants.

Acknowledgements. The authors would like to extend their sincere appreciation to the Researchers Supporting Project Number (RSP-2021/134), King Saud University, Riyadh, Saudi Arabia.

REFERENCES

[1] Ainalidou, A., Bouzoukla, F., Menkissoglu-Spiroudi, U., Vokou, D., Karamanoli, K. (2021): Impacts of decaying aromatic plants on the soil microbial community and on tomato seedling growth and metabolism: suppression or stimulation? – Plants 10(9): 1848.

[2] Akhter, A., Hage-Ahmed, K., Soja, G., Steinkellner, S. (2016): Potential of *Fusarium* wilt-inducing chlamydospores, in vitro behaviour in root exudates and physiology of tomato in biochar and compost amended soil. – Plant and Soil 406: 425-440.

[3] Badri, D. V., Vivanco, J. M. (2009): Regulation and function of root exudates. – Plant, Cell and Environment 32: 666-681.

http://www.aloki.hu ● ISSN 1589 1623 (Print) ● ISSN 1785 0037 (Online)
DOI: http://dx.doi.org/10.15666/aeer/2001_235249

[4] Berta, G., Fusconi, A., Trotta, A. (1993): VA mycorrhizal infection and the morphology and function of root systems. – Environmental and Experimental Botany 33: 159-173.
[5] Bomford, M. K. (2009): Do tomatoes love basil but hate Brussels sprouts? Competition and land-use efficiency of popularly recommended and discouraged crop mixtures in biointensive agriculture systems. – Journal of Sustainable Agriculture 33: 396-417.
[6] Brundrett, M. C. (2002): Coevolution of roots and mycorrhizas of land plants. – New Phytologist 154: 275-304.
[7] Casper, B. B., Jackson, R. B. (1997): Plant competition underground. – Annual Review of Ecology, Evolution and Systematics 28: 545-570.
[8] Dehne, H. W., Schönbeck, F. (1979): Influence of endotrophic mycorrhiza on plant diseases. II. Phenol metabolism and lignification. – Journal of Phytopathology 95: 210-216.
[9] De-la-Pena, C., Lei, Z., Watson, B. S., Sumner, L. W., Vivanco, J. M. (2008): Root-microbe communication through protein secretion. – Journal of Biological Chemistry 283: 25247-25255.
[10] Farooq, M., Jabran, K., Cheema, Z. A., Wahid, A., Siddique, K. H. (2011): The role of allelopathy in agricultural pest management. – Pest Management Science 67: 493-506.
[11] Fierro-Coronado, R. A., Castro-Moreno, M. G., Ruelas-Ayala, R. D., Apodaca-Sánchez, M. Á., Maldonado-Mendoza, I. E. (2013): Induced protection by *Rhizophagus intraradices* against *Fusarium* wilt of tomato. – Interciencia 38: 48-53.
[12] Fu, X., Wu, X., Zhou, X., Liu, S., Shen, Y., Wu, F. (2015): Companion cropping with potato onion enhances the disease resistance of tomato against *Verticillium dahliae*. – Frontiers in Plant Science 6: 726.
[13] George, E., Marschner, H., Jakobsen, I. (1995): Role of arbuscular mycorrhizal fungi in uptake of phosphorus and nitrogen from soil. – Critical Reviews in Biotechnology 15: 257-270.
[14] Giovannetti, M., Mosse, B. (1980): An evaluation of techniques for measuring vesicular arbuscular mycorrhizal infection in roots. – New Phytologist 84: 489-500.
[15] Gómez-Rodrıguez, O., Zavaleta-Mejıa, E., Gonzalez-Hernandez, V. A., Livera-Munoz, M., Cárdenas-Soriano, E. (2003): Allelopathy and microclimatic modification of intercropping with marigold on tomato early blight disease development. – Field Crop Research 83: 27-34.
[16] Hage-Ahmed, K., Krammer, J., Steinkellner, S. (2013a). The intercropping partner affects arbuscular mycorrhizal fungi and *Fusarium oxysporum* f. sp. *lycopersici* interactions in tomato. – Mycorrhiza 23: 543-550.
[17] Hage-Ahmed, K., Moyses, A., Voglgruber, A., Hadacek, F., Steinkellner, S. (2013b): Alterations in root exudation of inter-cropped tomato mediated by the arbuscular mycorrhizal fungus *Glomus mosseae* and the soil borne pathogen *Fusarium oxysporum* f. sp. *lycopersici*. – Journal of Phytopathology 161: 763-773.
[18] Haichar, F. Z., Santaella, C., Heulin, T., Achouak, W. (2014): Root exudates mediated interactions belowground. – Soil Biology and Biochemistry 77: 69-80.
[19] Hashem, A., Akhter, A., Alqarawi, A. A., Singh, G., Almutairi, K. F., Abd_Allah, E. F. (2021): Mycorrhizal fungi induced activation of tomato defense system mitigates Fusarium wilt stress. – Saudi Journal of Biological Sciences 1-9.
[20] Hetrick, B. A. D. (1991): Mycorrhizas and root architecture. – Cellular and Molecular Life Sciences 47: 355-362.
[21] Hodge, A., Berta, G., Doussan, C., Merchan, F., Crespi, M. (2009): Plant root growth, architecture and function. – Plant and Soil. 321: 153-187.
[22] Kadoglidou, K., Chatzopoulou, P., Maloupa, E., Kalaitzidis, A., Ghoghoberidze, S., Katsantonis, D. (2020): Mentha and oregano soil amendment induces enhancement of tomato tolerance against soilborne diseases, yield and quality. – Agronomy 10(3): 406.
[23] Kaur, S., Suseela, V. (2020): Unraveling arbuscular mycorrhiza-induced changes in plant primary and secondary metabolome. – Metabolites 10(8) 335.

http://www.aloki.hu ● ISSN 1589 1623 (Print) ● ISSN 1785 0037 (Online)
DOI: http://dx.doi.org/10.15666/aeer/2001_235249

[24] Kong, C., Liang, W., Xu, X., Hu, F., Wang, P., Jiang, Y. (2004): Release and activity of allelochemicals from allelopathic rice seedlings. – Journal of Agricultural and Food Chemistry 52: 2861-2865.
[25] Lee, M. R., Tu, C., Chen, X., Hu, S. (2014): Arbuscular mycorrhizal fungi enhance P uptake and alter plant morphology in the invasive plant *Microstegium vimineum*. – Biological Invasions 16: 1083-1093.
[26] Li, M., Hou, S., Wang, J., Hu, J., Lin, X. (2021): Arbuscular mycorrhizal fungus suppresses tomato (*Solanum lycopersicum* Mill.) Ralstonia wilt via establishing a soil–plant integrated defense system. – Journal of Soils and Sediments 1-13.
[27] Marques, D. J., da Silva, E. C., Ferreira, M. M., Paglis, C. M., de Souza, T. C., Maluf, W. R. (2016): Differential responses of root system and gas exchange in contrasting tomato genotypes under phosphorus starvation. – Australian Journal of Crop Science 10: 101-110.
[28] Morauf, C., Steinkellner, S. (2015): *Fusarium oxysporum* f. sp. *lycopersici* and compost affect tomato root morphology. – European Journal of Plant Pathology 143: 385-398.
[29] Newman, E. I. (1966): A method of estimating the total length of root in a sample. – Journal of Applied Ecology 3: 139-145.
[30] Ramyabharathi, S. A., Meena, B., Raguchander, T. (2012): Induction of chitinase and β-1,3- glucanase PR proteins in tomato through liquid formulated *Bacillus subtilis* EPCO 16 against Fusarium wilt. – Journal of Today's Biological Sciences 1: 50-60.
[31] Ren, L., Su, S., Yang, X., Xu, Y., Huang, Q., Shen, Q. (2008): Intercropping with aerobic rice suppressed Fusarium wilt in watermelon. – Soil Biology and Biochemistry 40: 834-844.
[32] Rice, E. L. (1984): Allelopathy. Second Ed. – Academic Press, Orlando.
[33] Riotte, L. (1975): Carrots Love Tomatoes: Secrets of Companion Planting for Successful Gardening. – Storey Books, Pownal.
[34] Rolfe, S. A., Griffiths, J., Ton, J. (2019): Crying out for help with root exudates: adaptive mechanisms by which stressed plants assemble health-promoting soil microbiomes. – Current Opinion in Microbiology 49: 73-82.
[35] Salehi, Y., Zarehaghi, D., Dabbagh Mohammadi Nasab, A., Neyshabouri, M. R. (2018): The Effect of intercropping and deficit irrigation on the water use efficiency and yield of tomato (*Lycopersicon esculentum* mill) and Basil (*Ocimum basilicum*). – Journal of Agricultural Science and Sustainable Production 28(3): 209-220.
[36] Scheffknecht, S., Mammerler, R., Steinkellner, S., Vierheilig, H. (2006): Root exudates of mycorrhizal tomato plants exhibit a different effect on microconidia germination of *Fusarium oxysporum* f. sp. *lycopersici* than root exudates from non-mycorrhizal tomato plants. – Mycorrhiza 16: 365-370.
[37] Schroeder, M. S., Janos, D. P. (2005): Plant growth, phosphorus nutrition, and root morphological responses to arbuscular mycorrhizas, phosphorus fertilization, and intraspecific density. – Mycorrhiza 15: 203-216.
[38] Schroeder-Moreno, M. S., Janos, D. P. (2008): Intra- and inter-specific density affects plant growth responses to arbuscular mycorrhizas. – Botany. 86: 1180-1193.
[39] Smith, S. E., Read, D. J. (2008): Mycorrhizal Symbiosis. Third Ed. – Academic Press, London.
[40] Son, D., Somda, I., Legreve, A., Schiffers, B. (2018): Effect of plant diversification on pest abundance and tomato yields in two cropping systems in Burkina Faso: farmer practices and integrated pest management. – International Journal of Biological and Chemical Sciences 12(1): 101-119.
[41] **S**ong, Y. Y., Zeng, R. S., Xu, J. F., Li, J., Shen, X., Yihdego, W. G. (2010): Interplant communication of tomato plants through underground common mycorrhizal networks. – PLoS ONE 5: 13324.

http://www.aloki.hu ● ISSN 1589 1623 (Print) ● ISSN 1785 0037 (Online)
DOI: http://dx.doi.org/10.15666/aeer/2001_235249

[42] Steinkellner, S., Mammarler, R., Vierheilig, H. (2005): Microconidia germination of tomato pathogen *Fusarium oxysporum* in the presence of root exudates. – Journal of Plant Interactions 1: 23-30.
[43] Toussaint, J. P., Kraml, M., Nell, M., Smith, S. E., Smith, F. A., Steinkellner, S., Schmiderer, C., Vierheilig, H., Novak, J. (2008): Effect of Glomus mosseae on concentrations of rosmarinic and caffeic acids and essential oil compounds in basil inoculated with *Fusarium oxysporum* f. sp. *basilici*. – Plant Pathology 57: 1109-1116.
[44] Van der Heijden, M., Wiemken, A., Sanders, I. (2003): Different arbuscular mycorrhizal fungi alter coexistence and resource distribution between co-occuring plant. – New Phytologist 157: 569-578.
[45] Vierheilig, H., Coughlan, A. P., Wyss, U., Piché, Y. (1998): Ink and vinegar, a simple staining technique for arbuscular-mycorrhizal fungi. – Applied and Environmental Microbiology 64: 5004-5007.
[46] Vierheilig, H., Garcia-Garrido, J. M., Wyss, U., Piché, Y. (2000): Systemic suppression of mycorrhizal colonization on barley roots already colonized by AM fungi. – Soil Biology and Biochemistry 32: 589-595.
[47] Xu, W., Liu, D., Wu, F., Liu, S. (2015): Root exudates of wheat are involved in suppression of Fusarium wilt in watermelon in watermelon-wheat companion cropping. – European Journal of Plant Pathology 141: 209-216.
[48] Yang, M., Zhang, Y., Qi, L., Mei, X., Liao, J., Ding, X. (2014): Plant-plant-microbe mechanisms involved in soil-borne disease suppression on a maize and pepper intercropping system. – PLoS ONE 9: e115052.
[49] Yu, J. Q. (1999): Allelopathic suppression of *Pseudomonas solanacearum* infection of tomato (*Lycopersicon esculentum*) in a tomato- Chinese chive (*Allium tuberosum*) intercropping system. – Journal of Chemical Ecology 25: 2409-2417.

http://www.aloki.hu ● ISSN 1589 1623 (Print) ● ISSN 1785 0037 (Online)
DOI: http://dx.doi.org/10.15666/aeer/2001_235249

SOIL PROPERTIES OF SHOLA FORESTS INVADED BY BLACK WATTLE (*ACACIA MEARNSII*) IN THE WESTERN GHATS OF TAMIL NADU, INDIA

SURYA PRABHA, A. C.[1*] – ARULMANI, K.[1] – SENTHIVELU, M.[2] –VELUMANI, R.[1] – PRAGADEESH, S.[1]

[1]*Silviculture and Forest Management Division, Institute of Forest Genetics and Tree Breeding, Coimbatore, Tamil Nadu 641002, India*

[2]*Department of Oilseeds, Tamil Nadu Agricultural University, Coimbatore, Tamil Nadu, India*

**Corresponding author*
e-mail: acsuryaprabha19@gmail.com; phone: +91-94-8746-8371

(Received 20th Jul 2021; accepted 28th Oct 2021)

Abstract. The Australian Black Wattle (*A. mearnsii)* threatens native habitats by outcompeting indigenous vegetation for water, soil nutrients and organic matter. The present investigation was conducted to study the soil properties of shola forests invaded by *A. mearnsii* plantations in the Kodaikanal Forest Division of the Western Ghats of Tamil Nadu, India. Soil samples were collected from *A. mearnsii* invaded shola forests of Poombarai forest range in the Kodaikanal Forest Division. For comparison purposes, soil samples were collected from shola forests, *A. mearnsii* plantation, grass land and pine plantations. Soil pH (5.02), organic carbon (5.82%), available nitrogen (201.6 kg ha^{-1}) and available potassium (334.5 kg ha^{-1}), exchangeable calcium (3.79 meq/100 g) and exchangeable magnesium (5.18 meq/100 g) were highest under *A. mearnsii* invaded shola forest at 0-30 cm depth. Available P was highest under *A. mearnsii* plantation (21.5 kg ha^{-1}). The control plot (shola forest), registered a pH of 3.94, organic carbon (5.80%), available nitrogen (180.4 kg ha^{-1}), available phosphorus (21.0 kg ha^{-1}), available potassium (318.3 kg ha^{-1}), exchangeable calcium (3.59 meq/100 g) and exchangeable magnesium (5.08 meq/100 g). The baseline data generated from the study can be utilized for undertaking appropriate decision making in the management of forests to control the invasion menace of *A. mearnsii* thereby improving the soil quality.
Keywords: *invasion ecology, habitat modification, invasive species, soil characteristics*

Introduction

A collective of Tropical Montane, evergreen forests locally known as sholas is situated in the higher mountain tracts of the Western Ghats, at an altitude above 1500 m interspersed with rolling grasslands. Shola forests have high ecological significance in protecting the headwaters of rivers by holding back water received by precipitation like a sponge, thus preventing rapid run-off. These diverse forests and grasslands were converted into commercially valuable plantations to meet the fuel wood requirement of tea industry during British period. Some of the introduced species like *A. mearnsii* have become invasive alien species in this ecosystem and became a serious threat to this high-altitude ecosystem (Myers et al., 2000).

The Australian Black Wattle (*A. mearnsii)* was introduced during the 1960s in State Forest lands located in the upper altitudes of the Palani hills- an eastern offshoot of the Western Ghats, a mountain range that runs parallel to the southwest coast of Peninsular India near the hill station of Kodaikanal (Mitchell, 1972; Mathew et al., 1975). *A. mearnsii,* a small to large, evergreen, single stemmed or multi branched tree threatens native habitats by outcompeting indigenous vegetation for water, soil nutrients and organic matter (Moyo and Fatunbi, 2010). Invasive alien plants alter the invaded

http://www.aloki.hu ● ISSN 1589 1623 (Print) ● ISSN 1785 0037 (Online)
DOI: http://dx.doi.org/10.15666/aeer/2001_251263

community by shifting native biodiversity through a reduction in light penetration, changes in soil nutrients and hydrology and then modifying ecosystem functionality (Vardien et al., 2012). There are various mechanisms whereby invasive alien plants can alter soil ecosystems (Tererai et al., 2015). Studies have reported the mass of the leaf litter in areas invaded by *A. mearnsii* to be greater than that of un-invaded areas, thereby the dense layer inhibits the establishment of native seedlings (Pandey et al., 2014). Between 1849 and 1992, in the Nilgiris Biosphere Reserve, the sholas decreased from 8600 ha to 4225 ha and grasslands from 29875 ha to 4700 ha (Kumar, 1993).

Soil is the major source of nutrients for the growth of plants and determining the degree of soil physico-chemical characteristics are very necessary to evaluate the soil fertility. The nutrient transformation and its availability in soils depend on pH, clay minerals, cation and anion exchange capacity (Reddy and Reddy, 2010). Soils exhibit difference in properties in relation to the vegetation changes and vary spatially primarily in response to rooting and litter fall characteristics of the perennial vegetation on more or less the same soil material (Balagopalan et al., 1993). Invasive plant species can modify physical or chemical attributes of soil, including inputs and cycling of nitrogen and other elements (Ehrenfeld, 2003; Haubensaket al., 2004 and Hawkes et al., 2005; Tererai et al., 2015). The amount of soil nutrients especially soil nitrogen, phosphorus and carbon, soil pH, microbial N and P, decomposition rates and soil water repellents can be increased due to invasive alien plants compared to the natural site (Fan et al., 2010; Ruwanza et al., 2013; Ruwanza and Shackleton, 2016). However, in some studies, they may show the reverse trends (Ehrenfeld, 2003; Tererai et al., 2015). Nutrient dynamics may also become altered as a result of changes in the physical properties of the soil caused by the introduction of new species.

Studies on the properties of soil in invaded shola forests are required for proper management of the forests and utilization of resources. Studies on the assessment of soil properties under shola forests invaded by *A. mearnsii* in the Western Ghats of Kodaikanal are scanty. Therefore, the present study was proposed with an aim to study the soil properties of shola forests invaded by *A. mearnsii* plantations in the Western Ghats of Kodaikanal, Tamil Nadu, India.

Materials and methods

Location and site description

The present study was carried out in the Western Ghats of Tamil Nadu covering the Poombarai Range of the Kodaikanal Forest Division, Tamil Nadu, India (*Fig. 1*). Kodaikanal Forest Division lies within 10°6' and 10°21' North latitudes and 77°16' and 77°42' East longitudes and is surrounded by Kerala state in West, Indira Gandhi Wild life sanctuary, Pollachi in North-west, Dindigul forest division on the North-east and Theni revenue district in South. The altitude varies from 300 to 2654 m and this area experiences an average yearly rainfall of 165 cm. The average annual temperature in Kodaikanal 20.8 °C.

Soil sampling and analysis

Soil samples were collected from the different study plots *viz*, shola forests invaded by *A. mearnsii*, shola forests, *A. mearnsii* plantation, grass land and pine plantations during 2016-2018 (*Fig. 2*). At each of the study plot, soil samples were collected from three sites and at four depths *viz.*, 0-30, 30-50, 50-80 and 80-100 cm. Sites within each

http://www.aloki.hu ● ISSN 1589 1623 (Print) ● ISSN 1785 0037 (Online)
DOI: http://dx.doi.org/10.15666/aeer/2001_251263

invasion treatment were approximately 200 m apart to provide a measure of independence (Galatowitsch and Richardson, 2005).

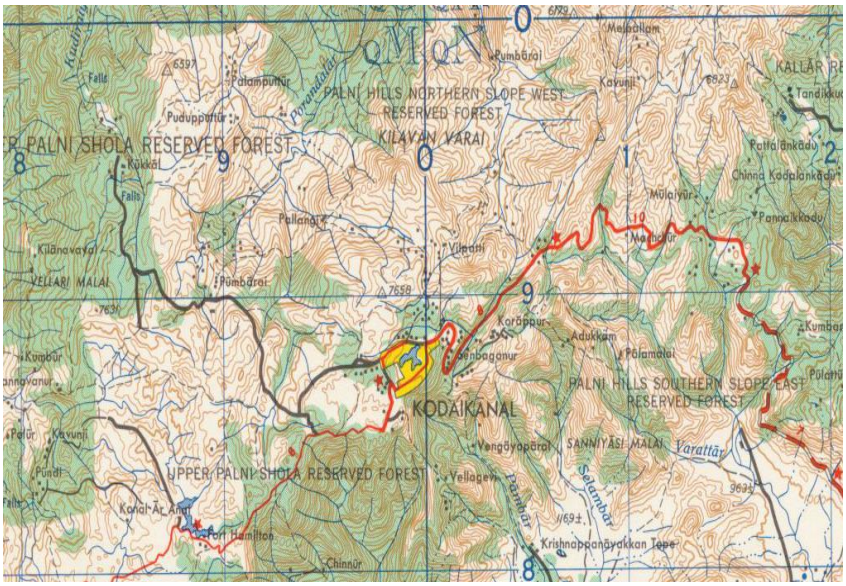

Figure 1. *Map showing the study area*

(a)

(b)

(c)

http://www.aloki.hu ● ISSN 1589 1623 (Print) ● ISSN 1785 0037 (Online)
DOI: http://dx.doi.org/10.15666/aeer/2001_251263

(d)

Figure 2. *(a) Acacia mearnsii invaded shola forests. (b) Acacia mearnsii plantation. (c) A. mearnsii invaded grassland; Evergreen shola forest (d) Soil sampling in Acacia mearnsii invaded sites*

At each sampling point, an area of 0.5 m × 0.5 m was removed and a pit of 50 cm wide, 50 cm in length and 100 cm deep was dug. The soil was scrapped from three sides of the pit with the help of a kurpee at each depth. The soil was mixed thoroughly and transferred to a polythene bag with proper labeling. The samples were air-dried and sieved to pass through 2 mm mesh sieve for physico-chemical analysis. The pH of soil was determined using an aqueous suspension of soil (soil and water in 1:2.5 ratio) using a digital micro controller based pH meter with electrode, Make: Systronics (Jackson, 1973). Soil organic carbon was estimated by standard Chromic acid wet oxidation method (Walkley and Black, 1934). The available nitrogen in the soil was estimated by the alkaline permanganate method using Automatic Nitrogen Analyzer, Make: Pelican (Subbiah and Asija, 1956).

The concentration of available phosphorus was determined by Olsen, Bray 1 and Kurtz extraction methods using UV-Vis Spectrophotometer, Make: Shimadzu (Olsen et al., 1954; Bray and Kurtz, 1945). Available potassium was estimated by neutral normal ammonium acetate extraction using Flame Photometer, Make: Systronics (Stanford and English, 1949). The contents of exchangeable bases (Ca and Mg,) were determined by Versenate titration after extraction using 1 N ammonium acetate adjusted to pH 7.0 (Cheng and Bray, 1951). Available micronutrients *viz,* Fe, Mn, Zn and Cu were extracted using Diethylene Triamine Penta Acetic acid reagent and the micronutrients content were estimated using Atomic Absorption Spectrophotometer, Make: Shimadzu (Lindsay and Norvell, 1978).

Statistical analysis

The data obtained were subjected to statistical analysis in SPSS ® 19.0 version statistical software. One-way ANOVA was also applied to analyse and to compare the mean significant difference between each parameter under different sites. During the ANOVA test the soil properties were the dependent variables while sampling sites were the independent variables.

Results

Acacia mearnsii invasion on soil properties

Analysis of variance (ANOVA) testing the effects of *A. mearnsii* on soil properties among the study plots of Poombarai forest range at 0 to 30 cm depth is given in *Table 1*. The soils in all the sites were acidic in general and soil pH was highest under *A.*

http://www.aloki.hu ● ISSN 1589 1623 (Print) ● ISSN 1785 0037 (Online)
DOI: http://dx.doi.org/10.15666/aeer/2001_251263

mearnsii invaded shola forest ($p < 0.001$)) at 0-30 cm depth and was followed by grassland. Shola forest registered the lowest pH (3.94) at 0-30 cm depth. At 30-50 cm, 50-80 cm and 80-100 cm, soil pH was highest under *A. mearnsii* invaded shola forest at (*Tables 2, 3* and *4*).

Table 1. *Analysis of variance (ANOVA) testing the effects of Acacia mearnsii on soil properties among the study plots of Poombarai forest range at 0 to 30 cm depth*

Soil properties	Study plots					F-value	p-value
	***A. mearnsii* invaded shola**	***A. mearnsii* plantation**	**Grassland**	**Pine forest**	**Shola forest**		
Soil pH	5.02 ± 0.03	4.13 ± 0.02	4.39 ± 0.02	4.15 ± 0.02	3.94 ± 0.02	296.68	< 0.001
Electrical conductivity (dS m^{-1})	0.42 ± 0.03	0.62 ± 0.06	0.41 ± 0.03	0.30 ± 0.03	0.36 ± 0.03	954.78	< 0.001
Organic carbon (%)	5.82 ± 0.03	3.97 ± 0.02	4.3 ± 0.02	5.54 ± 0.03	5.8 ± 0.03	835.15	< 0.001
Available nitrogen (kg ha^{-1})	201.6 ± 1.16	168.6 ± 0.97	164 ± 0.95	145.6 ± 0.84	180.4 ± 1.04	429.87	< 0.001
Available phosphorus (kg ha^{-1})	19.9 ± 0.11	21.5 ± 0.12	20.6 ± 0.12	20.1 ± 0.11	21.0 ± 0.12	29.97	< 0.001
Available potassium (kg ha^{-1})	334.5 ± 1.93	183.6 ± 1.06	164.8 ± 0.95	139.2 ± 0.80	318.3 ± 1.84	4262.04	< 0.001
Exchangeable calcium (meq/100 g)	3.79 ± 0.04	1.99 ± 0.02	3.59 ± 0.03	3.39 ± 0.02	3.59 ± 0.03	587.56	< 0.001
Exchangeable magnesium (meq/100 g)	5.18 ± 0.04	4.78 ± 0.04	4.09 ± 0.03	4.68 ± 0.04	5.08 ± 0.04	106.06	< 0.001
DTPA-Cu (ppm)	2.99 ± 0.03	1.2 ± 0.01	2.79 ± 0.03	0.6 ± 0.01	5.58 ± 0.05	4717.02	< 0.001
DTPA-Zn (ppm)	1.00 ± 0.01	0.5 ± 0.01	0.8 ± 0.01	0.3 ± 0.0	1.2 ± 0.01	2386.24	< 0.001
DTPA-Mn (ppm)	2.4 ± 0.01	0.6 ± 0.01	0.4 ± 0.0	0.2 ± 0.0	2.6 ± 0.02	14442.85	< 0.001
DTPA-Fe (ppm)	10.4 ± 0.06	7.6 ± 0.05	6.4 ± 0.03	5.9 ± 0.03	20.1 ± 0.11	8117.2	< 0.001

Table 2. *Analysis of variance (ANOVA) testing the effects of Acacia mearnsii on soil properties among the study plots of Poombarai forest range at 30 to 50 cm depth*

Soil properties	Study plots					F-value	p-value
	***A. mearnsii* invaded shola**	***A. mearnsii* plantation**	**Grassland**	**Pine forest**	**Shola forest**		
Soil pH	5.04 ± 0.03	4.23 ± 0.02	4.56 ± 0.02	4.23 ± 0.02	3.95 ± 0.02	266.12	< 0.001
Electrical conductivity (dS m^{-1})	0.4 ± 0.00	0.54 ± 0.06	0.38 ± 0.00	0.28 ± 0.00	0.38 ± 0.00	1302.0	< 0.001
Organic carbon (%)	5.11 ± 0.03	3.89 ± 0.02	4.25 ± 0.02	4.87 ± 0.03	5.6 ± 0.03	589.80	< 0.001
Available nitrogen (kg ha^{-1})	168 ± 0.97	154.2 ± 0.88	150.2 ± 0.87	124.2 ± 0.72	164.8 ± 0.95	384.59	< 0.001
Available phosphorus (kg ha^{-1})	19.7 ± 0.11	20.8 ± 0.12	20.4 ± 0.11	20.3 ± 0.11	20.6 ± 0.12	12.46	< 0.001
Available potassium (kg ha^{-1})	326.3 ± 1.88	152.8 ± 0.88	152.8 ± 0.88	130.2 ± 0.75	302.6 ± 1.75	5008.86	< 0.001
Exchangeable calcium (meq/100 g)	3.2 ± 0.02	2.0 ± 0.01	3.2 ± 0.02	2.8 ± 0.02	3.4 ± 0.02	1170.0	< 0.001
Exchangeable magnesium (meq/100 g)	4.8 ± 0.03	4.5 ± 0.02	3.6 ± 0.02	4.6 ± 0.03	4.7 ± 0.03	314.06	< 0.001
DTPA-Cu (ppm)	2.6 ± 0.02	1.0 ± 0.01	2.6 ± 0.02	0.4 ± 0.0	4.5 ± 0.03	9822.97	< 0.001
DTPA-Zn (ppm)	0.6 ± 0.01	0.3 ± 0.0	0.6 ± 0.01	0.2 ± 0.0	1.0 ± 0.01	4900.00	< 0.001
DTPA-Mn (ppm)	2.0 ± 0.01	0.4 ± 0.0	0.2 ± 0.0	0.1 ± 0.0	2.0 ± 0.01	17775.00	< 0.001
DTPA-Fe (ppm)	8.2 ± 0.05	6.7 ± 0.04	6.2 ± 0.03	4.6 ± 0.03	14.6 ± 0.09	5645.86	< 0.001

http://www.aloki.hu ● ISSN 1589 1623 (Print) ● ISSN 1785 0037 (Online)
DOI: http://dx.doi.org/10.15666/aeer/2001_251263

Table 3. *Analysis of variance (ANOVA) testing the effects of Acacia mearnsii on soil properties among the study plots of Poombarai forest range at 50 to 80 cm depth*

Soil properties	Study plots					F-value	p-value
	***A. mearnsii* invaded shola**	***A. mearnsii* plantation**	**Grassland**	**Pine forest**	**Shola forest**		
Soil pH	5.32 ± 0.03	4.35 ± 0.02	4.78 ± 0.03	4.85 ± 0.03	3.88 ± 0.02	416.25	< 0.001
Electrical conductivity (dS m^{-1})	0.34 ± 0.00	0.58 ± 0.01	0.49 ± 0.00	0.20 ± 0.00	0.21 ± 0.00	4264.5	< 0.001
Organic carbon (%)	4.25 ± 0.02	3.42 ± 0.01	4.02 ± 0.02	4.56 ± 0.03	5.23 ± 0.03	736.69	< 0.001
Available nitrogen (kg ha^{-1})	156.8 ± 0.90	150.6 ± 0.87	126.4 ± 0.73	118.6 ± 0.68	152.4 ± 0.88	442.38	< 0.001
Available phosphorus (kg ha^{-1})	18.2 ± 0.10	20.4 ± 0.11	18.2 ± 0.10	19.3 ± 0.11	19.4 ± 0.11	72.88	< 0.001
Available potassium (kg ha^{-1})	276.5 ± 1.59	145.2 ± 0.84	146.7 ± 0.85	126.4 ± 0.72	286.4 ± 1.65	4239.96	< 0.001
Exchangeable calcium (meq/100 g)	2.8 ± 0.02	1.2 ± 0.01	2.4 ± 0.01	2.6 ± 0.02	2.7 ± 0.02	2006.2	< 0.001
Exchangeable magnesium (meq/100 g)	4.6 ± 0.03	3.8 ± 0.02	3.2 ± 0.01	4.1 ± 0.02	4.5 ± 0.03	562.53	< 0.001
DTPA-Cu (ppm)	2.2 ± 0.01	0.6 ± 0.01	1.9 ± 0.01	0.2 ± 0.0	3.4 ± 0.02	13816.6	< 0.001
DTPA-Zn (ppm)	0.57 ± 0.01	0.2 ± 0.0	0.3 ± 0.0	0.1 ± 0.0	0.84 ± 0.01	6796.5	< 0.001
DTPA-Mn (ppm)	1.4 ± 0.01	0.4 ± 0.0	0.3 ± 0.0	0.1 ± 0.0	1.8 ± 0.01	16950.00	< 0.001
DTPA-Fe (ppm)	6.8 ± 0.04	4.3 ± 0.02	5.8 ± 0.03	4.2 ± 0.02	10.2 ± 0.06	4116.82	< 0.001

Table 4. *Analysis of variance (ANOVA) testing the effects of Acacia mearnsii on soil properties among the study plots of Poombarai forest range at 80 to 100 cm depth*

Soil properties	Study plots					F-value	p-value
	***A. mearnsii* invaded shola**	***A. mearnsii* plantation**	**Grassland**	**Pine forest**	**Shola forest**		
Soil pH	5.28 ± 0.03	4.38 ± 0.02	4.69 ± 0.03	4.73 ± 0.03	3.86 ± 0.02	379.44	< 0.001
Electrical conductivity (dS m^{-1})	0.36 ± 0.00	0.41 ± 0.00	0.32 ± 0.00	0.24 ± 0.00	0.14 ± 0.00	-	-
Organic carbon (%)	3.41 ± 0.02	2.84 ± 0.02	3.64 ± 0.02	3.92 ± 0.02	4.86 ± 0.03	1107.7	< 0.001
Available nitrogen (kg ha^{-1})	134.4 ± 0.77	140.7 ± 0.81	116.4 ± 0.67	104.8 ± 0.61	130.6 ± 0.76	399.86	< 0.001
Available phosphorus (kg ha^{-1})	19.0 ± 0.11	18.6 ± 0.10	18.0 ± 0.10	19.4 ± 0.11	18.8 ± 0.11	22.74	< 0.001
Available potassium (kg ha^{-1})	240.8 ± 1.39	133.4 ± 0.77	130.2 ± 0.75	118.6 ± 0.68	274.6 ± 1.59	4329.71	< 0.001
Exchangeable calcium (meq/100 g)	2.0 ± 0.01	1.0 ± 0.01	1.9 ± 0.01	2.2 ± 0.01	2.3 ± 0.01	2355.88	< 0.001
Exchangeable magnesium (meq/100 g)	3.7 ± 0.02	3.4 ± 0.01	2.9 ± 0.01	3.8 ± 0.02	4.0 ± 0.02	415.90	< 0.001
DTPA-Cu (ppm)	1.6 ± 0.01	0.4 ± 0.0	2.0 ± 0.01	0.1 ± 0.0	4.0 ± 0.02	15012.5	< 0.001
DTPA-Zn (ppm)	0.4 ± 0.01	0.2 ± 0.0	0.1 ± 0.0	0.1 ± 0.01	0.62 ± 0.01	7542.0	< 0.001
DTPA-Mn (ppm)	1.8 ± 0.01	0.2 ± 0.0	0.1 ± 0.0	0.2 ± 0.0	1.2 ± 0.01	17400.00	< 0.001
DTPA-Fe (ppm)	5.7 ± 0.03	2.9 ± 0.02	5.0 ± 0.03	3.1 ± 0.02	8.4 ± 0.05	5262.58	< 0.001

Soil organic carbon (SOC) content in the Poombarai range was significantly influenced by *A. mearnsii* invasion (*Fig. 3*). SOC content in the study plots varied significantly ($p < 0.001\%$ by ANOVA) at different soil depths. Soil organic carbon was highest under *A. mearnsii* invaded shola forest (5.82%) and was on par with shola forest

http://www.aloki.hu ● ISSN 1589 1623 (Print) ● ISSN 1785 0037 (Online)
DOI: http://dx.doi.org/10.15666/aeer/2001_251263

(5.80%) at 0-30 cm depth. This was followed by pine forest (5.54%), and grassland (4.30%). The lowest SOC was recorded in *A. mearnsii* plantation (3.97%).

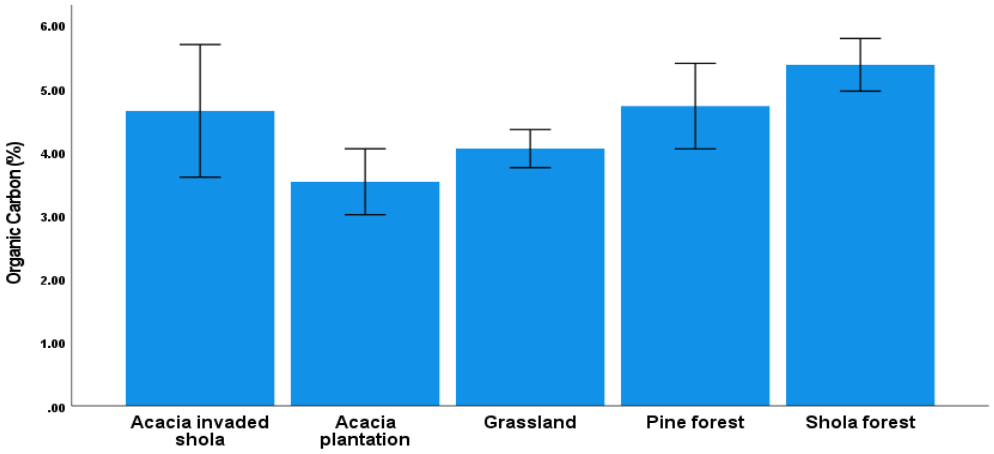

Figure 3. *A. mearnsii invasion on soil organic carbon (%) in Poombarai range*

The available nitrogen (kg ha^{-1}) in the different study plots of Poombarai range is presented in *Figure 4*. At different soil depths, the available nitrogen varied significantly ($p < 0.001\%$ by ANOVA) among the study plots. *A. mearnsii* invaded shola forest recorded the highest available nitrogen ($p < 0.001\%$) at 0-30 cm depth (201.6 kg ha^{-1}) and was followed by shola forest (180.4 kg ha^{-1}), and *A. mearnsii* plantation (168.6 kg ha^{-1}). The lowest available nitrogen was recorded in pine forest (145.6 kg ha^{-1}) at 0-30 cm depth (*Table 1*). With respect to soil depth, maximum available nitrogen was registered at 0-30 cm depth. The available nitrogen showed a decreasing trend with soil depth in all the study plots of Poombarai range. At 30-50 cm, 50-80 cm and 80-100 cm nitrogen availability was highest under *A. mearnsii* invaded shola forest ($p < 0.001\%$).

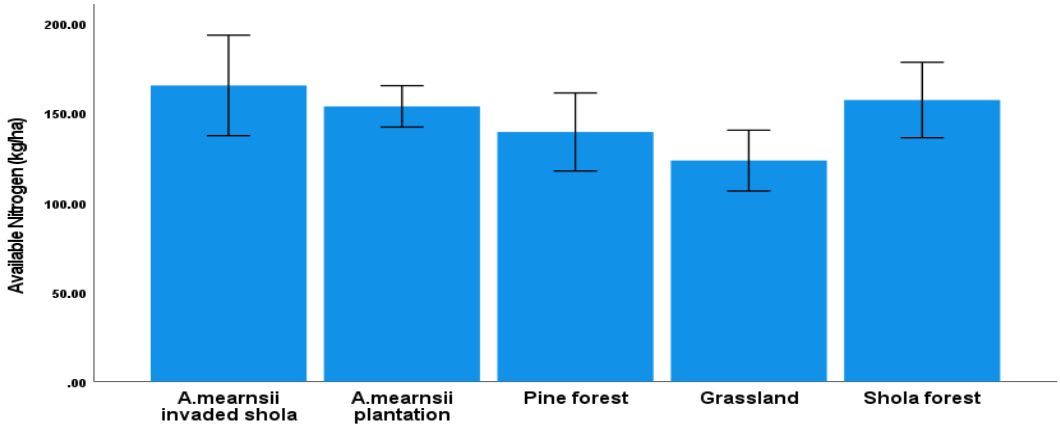

Figure 4. *A. Mearnsii invasion on available nitrogen (kg ha^{-1}) in Poombarai range*

Available phosphorus was highest under *A. mearnsii* plantation (21.5 kg ha^{-1}) at 0-30 cm depth. This was on par with shola forest (21.0 kg ha^{-1}) and was followed by pine

http://www.aloki.hu ● ISSN 1589 1623 (Print) ● ISSN 1785 0037 (Online)
DOI: http://dx.doi.org/10.15666/aeer/2001_251263

forest, and grassland (*Table 1*). Available phosphorus was lowest in *A. mearnsii* invaded shola forest (19.9 kg ha^{-1}). At 30-50 cm and 50-80 cm, *A. mearnsii* plantation recorded the highest Available Phosphorus ($p < 0.001$) and was on par with shola forest (*Table 2* and 3). Pine forest registered greater available P (<0.001) at 80-100 cm (*Table 4*). The available potassium (kg ha^{-1}) in the different study plots of Poombarai range is presented in (*Fig. 5*). Available potassium varied significantly ($p < 0.001\%$) among the study plots. *A. mearnsii* invaded shola forest recorded the highest available potassium (334.5 kg ha^{-1}) at 0-30 cm depth and was followed by shola forest (318.3 kg ha^{-1}). The lowest available potassium was recorded in pine forest (139.2 kg ha^{-1}) at 0-30 cm depth. With respect to soil depth, maximum available potassium was registered at 0-30 cm depth. The available potassium showed a decreasing trend with soil depth in all the study plots (*Table 1*).

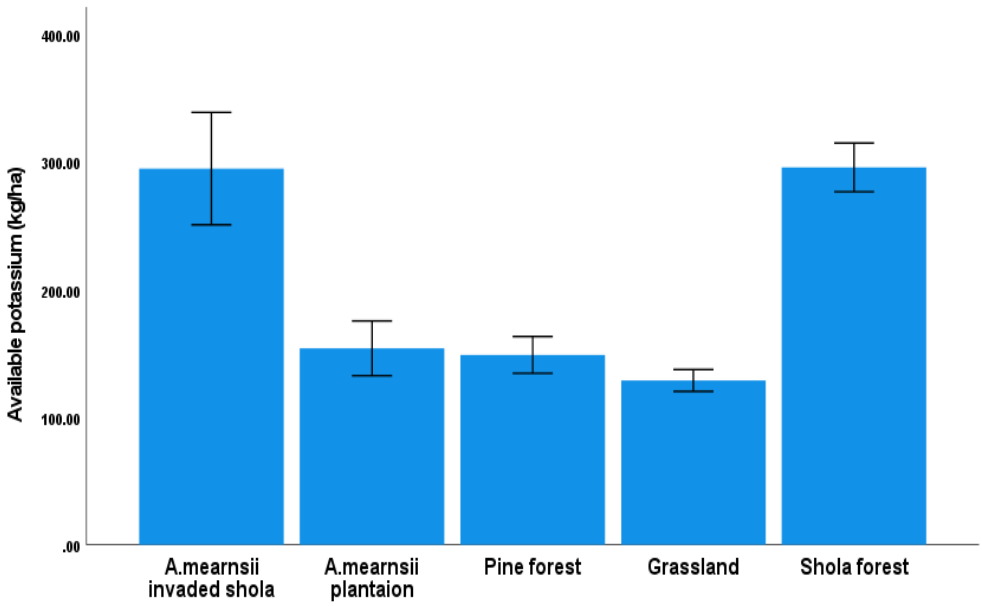

Figure 5. *A. Mearnsii invasion on available potassium (kg ha^{-1}) in Poombarai range*

The effects of *A. mearnsii* invasion on soil exchangeable calcium in the Poombarai range at 0 -30 cm is presented in (*Table 1*). The exchangeable calcium varied from 0.3 to 0.62 meq/100 g. The exchangeable calcium was highest under *A. mearnsii* invaded shola forest (3.8 meq/100 g) at 0-30 cm depth. This was followed by shola forest (3.6 meq/100 g) and grassland (3.6 meq/100 g). *A. mearnsii* plantation registered the lowest exchangeable calcium (2.0 meq/100 g) at 0-30 cm depth. Exchangeable calcium availability was highest ($p < 0.001\%$) under shola forest and was on par with *A. mearnsii* invaded shola forest at 30-50 cm (*Table 2*).

The perusal of data on exchangeable magnesium in the different study plots revealed that, at 0-30 cm depth, *A. mearnsii* invaded shola forest recorded the highest exchangeable magnesium (5.2 meq/100 g). This was found to be on par with the shola forest (5.2 meq/100 g). The exchangeable magnesium showed a decreasing trend with soil depth in all the study plots (*Table 1*). At 30-50 cm and 50-80 cm, *A. mearnsii* invaded shola forest registered higher exchangeable magnesium ($p < 0.001$) and was on par with shola forest (*Tables 2* and *3*).

http://www.aloki.hu ● ISSN 1589 1623 (Print) ● ISSN 1785 0037 (Online)
DOI: http://dx.doi.org/10.15666/aeer/2001_251263

Micronutrients availability

Among the different study plots, shola forests recorded the highest DTPA-Cu (5.6 ppm), DTPA-Zn (1.2 ppm), DTPA-Mn (2.6 ppm), DTPA-Fe (20.1 ppm) at 0-30 cm depth (*Table 1*; *Fig. 6*) and was followed by *A. mearnsii* invaded shola forest (3.0, 1.0, 2.4 and 10.4 ppm), and grassland (2.8, 0.8, 0.4 and 6.4 ppm). The lowest DTPA-Cu (0.6 ppm), DTPA-Fe (5.9 ppm), DTPA-Mn (0.2 ppm) and DTPA-Zn (0.3 ppm) was recorded in pine forest at 0 to 30 cm depth. At 30-50 and 50-80 cm, shola forest registered the highest DTPA-Cu, DTPA-Mn and DTPA-Fe ($p < 0.001$). Pine forest recorded the lowest availability of micronutrients with respect to copper, iron manganese and zinc (*Tables 2* and *3*). DTPA-Cu, DTPA-Zn and DTPA-Fe availability was highest ($p < 0.001$) under shola forest at 80-100 cm (*Table 4*).

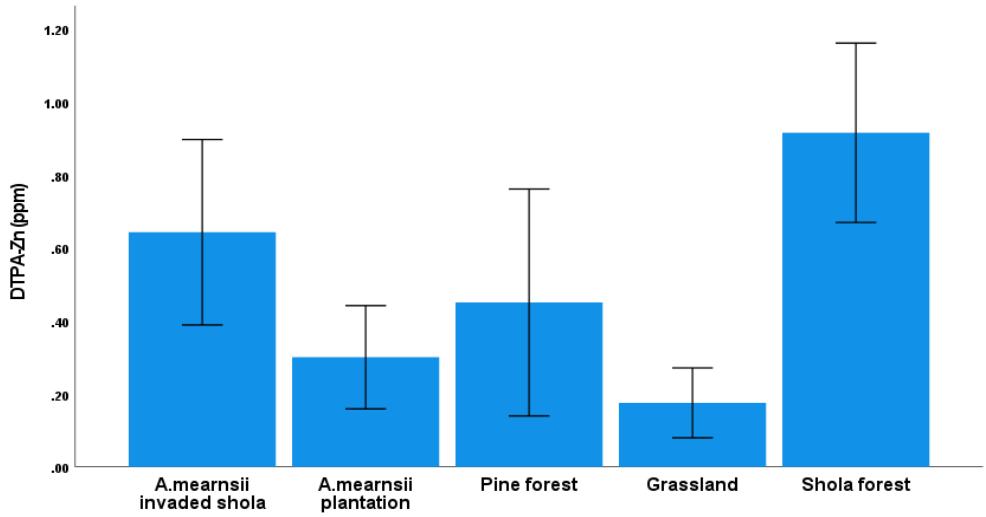

Figure 6. *A. mearnsii invasion on DTPA-Zn (ppm) in Poombarai range*

Discussion

Introduced plants affect soil nutrient dynamics by differing from native species in tissue chemistry, plant morphology and phenology (Ehrenfeld, 2003). Soil properties such as pH and the amount of base cations available in the soil differ greatly under trees of different species and when invading trees are compared with native vegetation (Dijkstra et al., 2001). The present study revealed higher pH under *A. mearnsii* invaded shola forest. Similar results were reported for *L. camara* infested soils by Fan et al. (2010) and Olusegun and Perrett (2011). High soil pH accelerated litter decomposition and thus plays a crucial role in regulating nutrient availability. Due to the high soil cation exchange process, soil cations are available in the root rhizosphere of the invasive species compared to native species resulting in high soil pH in the invaded sites. (Simba et al., 2013; Debnath et al., 2018). However, both increases and decreases in pH following plant invasion have been equally reported in the literature (Ehrenfeld, 2003).

Soil organic carbon was highest under *A. mearnsii* invaded shola forest. The results are concurrent with many other studies (Picone et al., 2003; Cheng et al., 2013). The combined effect of low temperature and high rainfall in shola forests restricts biochemical decomposition of organic residues in these soils and thus help maintain

http://www.aloki.hu ● ISSN 1589 1623 (Print) ● ISSN 1785 0037 (Online)
DOI: http://dx.doi.org/10.15666/aeer/2001_251263

high organic carbon percentage, which in turn becomes responsible for the high cation exchange capacity and base saturation of these soils (Balagopalan, 1993). However, Debnath et al. (2018) reported equal amount of soil organic carbon in both invaded and natural sites. Available nitrogen, exchangeable calcium and magnesium were highest under *A. mearnsii* invaded shola forest. The increase in available nitrogen and exchangeable calcium and magnesium in *A. mearnsii* invaded sites could be due to decrease in nutrient sequestration following native shola species displacement. *A. mearnsii* drops a lot of litter beneath it and this probably account for the elevated nitrogen levels when the litter decays. These findings are consistent with the findings by Ehrenfeld (2003), who reported an increase in soil nitrate following *Lantana camara* invasion. Jovanovic et al. (2009) also reported an increase in nitrogen where *A. saligna* invaded Sand Plain Fynbos. Dusanka et al. (2021) also reported that soil in mixed plots (those populated with *Amorpha fruticosa, Fraxinus pennsylvanica* and *Acer negundo*) contained much higher levels of nitrifying bacteria (NB), organic matter (Om), nitrogen (N), and carbon (C) as well as lower carbon to nitrogen ratio (C:N) levels, compared to single species invaded plots and control plots.

In our study, *A. mearnsii* plantation recorded the highest available phosphorus and was on par with shola forest. Musil and Midgley (1990) found similar results on Sand Plain Fynbos. *Acacia saligna* infestation doubled the average concentration of calcium, magnesium, potassium, total nitrogen, manganese, boron and zinc. Burnt plots showed a significant increase for soil pH, calcium, manganese and available phosphorus.

Our findings revealed that, available potassium was highest under *A. mearnsii* invaded shola forest. The high soil cation exchange process might have resulted in increased soil cations availability in the root rhizosphere of the invasive species compared to native species and our results was supported by earlier findings of Simba et al. (2013), Ruwanza and Shackleton (2016) and Debnath et al. (2018). Similarly, a study on long-term invasive occupation by *Acacia longifolia* significantly altered soil properties, with increased levels of organic C, total N, and exchangeable cations (Ehrenfeld, 2003 and Fan et al. 2010). In the present study, the availability of micronutrients *viz,* DTPA-Cu, Zn Mn and Fe were higher under shola forest compared to other study plots.

Conclusion

For proper management of the environment and utilization of resources, studies on the properties of soil in invaded forest ecosystems are important. Without adequate knowledge of the dynamic interaction between soil, climate and forest management we cannot develop a proper soil management system. Soil properties such as pH, available nitrogen, available phosphorus, available potassium, exchangeable calcium and magnesium in the soil varied significantly under *A. mearnsii* invaded shola forests compared with native vegetation. Baseline data generated in the present study can be utilized by the State Forest Department for undertaking appropriate decision making in the eco-restoration of areas invaded by *A. mearnsii*. From a management point of view removal of *A. mearnsii* for restoration purposes, could reduce the effect of the invasive species on the soil properties. Therefore, appropriate methods for the management of *A. mearnsii* are necessary to circumvent potential threats to native biodiversity.

http://www.aloki.hu ● ISSN 1589 1623 (Print) ● ISSN 1785 0037 (Online)
DOI: http://dx.doi.org/10.15666/aeer/2001_251263

Acknowledgements. We are thankful to the Director General, Indian Council of Forestry Research and Education, Dehradun for providing financial support to undertake the project work.

REFERENCES

[1] Balagopalan, M., Jose, A. I. (1993): A comparative study on the properties of soils in relation to the vegetational types. – Journal of Tropical Agriculture 31: 167-173.
[2] Bray, R. H., Kurtz, L. T. (1945): Determination of total, organic and available forms of phosphorus in soils. – Soil Science 59: 39-45.
[3] Cheng, K. L., Bray, R. H. (1951): Determination of calcium and magnesium in soil and plant material. – Soil Science 72:449-458.
[4] Cheng, C. H., Chen, Y. S., Huang., C.-R., Chiou, C.-C., Lin, D., Oleg, V. M. (2013): Effects of repeated fires on ecosystem C and N stocks along a fire induced forest/grassland gradient. – Journal of Geophysical Research 118: 215-25.
[5] Debnath, A., Paul, R., Debnath, B. (2018): Effects of the invasive shrub, *Chromolaena odorata*, on soil properties in the Atharamur a forest ecosystem: Indian Himalayan state of Tripura, Northeast India. – Vegetos 31(2):77-90. DOI: 10.5958/2229-4473.2018.00059.9.
[6] Dijkstra, F. A. (2001): The effect of organic acids on base cation leaching from the forest floor under six North American tree species. – European Journal of Soil Science 52: 205-214.
[7] Dusanka, V., Gianalberto, L., Stanko, M., Dubravka, M. (2021): The impact of multiple species invasion on soil and plant communities increases with invader diversity. – Biorxiv. DOI: 10.1101/2021.04.30.442106
[8] Ehrenfeld, J. G. (2003): Effects of exotic plant invasions on soil nutrient cycling processes. – Ecosystems 6: 503-523.
[9] Fan, L., Chen, Y., Yuan, J., Yang, Z. (2010): The effect of Lantana camara Linn. invasion on soil chemical and microbiological properties and plant biomass accumulation in southern China. – Geoderma 154: 370-378.
[10] Galatowitsch, S., Richardson, D. M. (2005): Riparian scrub recovery after clearing of invasive alien trees in headwater streams of the Western Cape, South Africa. – Biological Conservation 122: 509-521.
[11] Haubensaket, K. A., D'Antonio, C. M., Alexander, J. (2004): Effects of nitrogen-fixing shrubs in Washington and coastal California. – Weed Technology 18: 1475-1479.
[12] Hawkes, C. V., Wren, I. F., Herman, D. J., Firestone, M. K. (2005): Plant invasion alters nitrogen cycling by modifying the soil nitrifying community. – Ecology Letters 8: 976-985.
[13] Jackson, M. L. (1973): Soil and Plant Analysis. – Prentice Hall of India Private Limited, New Delhi.
[14] Jovanovic, N. Z., Israel, S., Tredoux, G., Soltau, L., Le Maitre, D., Rusinga, F., Rozanov, A., Van der Merwe, N. (2009): Nitrogen dynamics in land cleared of alien vegetation (*Acacia saligna)* and impacts on groundwater at Riverlands Nature Reserve (Western Cape, South Africa). – Water Sa 35(1): 37-44.
[15] Kumar, S. (1993): Survey and mapping of shola forests and grasslands in the upper Nilgiri plateau and assessment of human utilization of the vegetation. – Report submitted to World Wide Fund for Nature India. WWF, Gland.
[16] Lindsay, W. L., Norvell, W. A. (1978): Development of DTPA soil test for zinc, iron, manganese and copper. – Soil Science Society of American Journal 42: 421-428.
[17] Mathew, K. M., Blasco, F., Ignacimuthu, S. (1975): Biological changes at Kodaikanal, 1949-1974. – Tropical Ecology 16: 147-162.
[18] Mitchell, N. (1972): The Indian hill-station: Kodaikanal. – University of Chicago Department of Geography Research, Paper No.141, University of Chicago, Chicago.
[19] Moyo, H. P. M., Fatunbi, A. O. (2010): Utilitarian perspective of the invasion of some South African biomes by *A. mearnsii.* – Global Journal of Environmental Research 4(1): 6-17.

http://www.aloki.hu ● ISSN 1589 1623 (Print) ● ISSN 1785 0037 (Online)
DOI: http://dx.doi.org/10.15666/aeer/2001_251263

[20] Musil, C. F. (1993): Effects of invasive Australian *acacias* on the regeneration, growth and nutrient chemistry of South African lowland Fynbos. – Journal of Applied Ecology 30: 361-372.
[21] Myers, N., Mittermeier, R. A., Mittermeier, C. G., Da Fonseca, G. A. B., Kent, J. (2000): Biodiversity hotspots for conservation priorities. – Nature 403: 853-858.
[22] Olsen, S. R., Cole, C. V., Watanabe, F. S., Dean, A. L. (1954): Estimation of available phosphorus in soils by extraction with sodium bicarbonate. – Circular No.: 939, USDFA, US Govt. Printing Office, Washington, DC.
[23] Olusegun, O. O., Perrett, C. (2011): Lantana camara L. (Verbenaceae) invasion effects on soil physico-chemical properties. – Biology and Fertility of Soils 47: 349-355.
[24] Pandey, S. K., Singh, H., Singh, J. S. (2014): Effect of environmental conditions on decomposition in eight woody species of a dry tropical forest. – Plant Biosystem 148: 410-418. https://doi.org/10.1080/11263504.2013.772923.
[25] Picone, L. I., Quaglia, G., Garcia, F. O., Laterra, P. (2003): Biological and chemical response of a grassland soil to burning. – Journal of Range Management 56(3): 291-97.
[26] Reddy, T. Y., Reddy, G. H. S. (2010): Principles of Agronomy. – Kalyani Publishers, New Delhi.
[27] Ruwanza, S., Shackleton, C. (2016): Effects of the invasive shrub, Lantana camara, on soil properties in the Eastern Cape, South Africa. – Weed Biology and Management 16: 67-79. https://doi.org/10.1111/ wbm.12094.
[28] Ruwanza, S., Gaertner, M., Richardson, D. M., Esler, K. J. (2013): Soil water repellency in riparian systems invaded by Eucalyptus camaldulensis: a restoration perspective from the Western Cape Province, South Africa. – Geoderma 200-201: 9-17. https://doi.org/10.1016/j.-Geoderma 2013.01.017.
[29] Simba, Y. R., Kamweya, A. M., Mwangi, P. N., Ochora, J. M. (2013): Impact of the invasive shrub Lantana camara L. on soil properties in Naibory National Park, Kenya. – International Journal of Biodiversity Conservation 5(12): 803-809. https://doi.org/10.5895/IJBC2013.0623.
[30] Stanford, G., English, L. (1949): Use of flame photometer in rapid soil test for K and Ca. – Agronomy Journal.41: 446-447.
[31] Subbiah, B. V., Asija, G. L. (1956): A rapid procedure for the estimation of available nitrogen in soils. – Current Science 25: 259-260.
[32] Tererai, F., Gaertner, M., Jacobs, S. M., Richardson, D. M. (2015): Eucalyptus camaldulensis invasion in riparian zones reveals few significant effects on soil physico-chemical properties. – River Res Appl 31: 590-601. https://doi.org/10.1002/rra.2762.
[33] Vardien, W., Richardson, D. M., Foxcroft, L. C., Thompson, G. D., Wilson, J. R. U. (2012): Invasion dynamics of Lantana camara L. (sensu lato) in South Africa. – African Journal of Botany 81: 81-94.
[34] Walkley, A., Black, C. A. (1934): An examination of the Degtjareff method for determining soil organic matter and a proposed modification of the chromic acid titration method. – Soil Science 40: 233- 243.

APPENDIX

Appendix 1. *Details of soil sample collection in Kodaikanal (Poombarai Range)*

S. No.	Soil depth	Location	GPS	Forest type
1	0-30 cm	Near Kundar Falls (**Kodaikanal**)	N 10° 12’ 54.3” E 077° 26’ 08.3” 2171 m	Pine forest plantation
2	30-50 cm			
3	50-80 cm			

http://www.aloki.hu ● ISSN 1589 1623 (Print) ● ISSN 1785 0037 (Online)
DOI: http://dx.doi.org/10.15666/aeer/2001_251263

4	80-100 cm			
5	0-30 cm	Near Kundar Falls (**Kodaikanal)**	N 10° 21’ 58.2” E 077° 43’ 62.7” 2171 m	Pine forest plantation
6	30-50 cm			
7	50-80 cm			
8	80-100 cm			
9	0-30 cm	Kundar Falls (**Kodaikanal)**	N 10° 13’ 02.7 “ E 077° 25’ 33.3” 2185 m	Grass land
10	30-50 cm			
11	50-80 cm			
12	80-100 cm			
13	0-30 cm	Kundar Falls (**Kodaikanal)**	N 10° 21’ 72.0” E 077° 42’ 67.1” 2131 m	Grass land
14	30-50 cm			
15	50-80 cm			
16	80-100			
17	0-30 cm	Krishnan Kovil (**Kodaikanal)**	N 10° 13’ 40.6” E077° 25’ 23.9” 2236 m	*Acacia mearnsii* plantation
18	30-50 cm			
19	50-80 cm			
20	80-100 cm			
21	0-30 cm	Krishnan Kovil (**Kodaikanal)**	N 10° 22’ 82.4” E077° 42’ 32.3” 2224 m	*Acacia mearnsii* plantation
22	30-50 cm			
23	50-80 cm			
24	80-100 cm			
25	0-30 cm	FDA thottam (TNFD) inside the Krishnan kovil (**Kodaikanal)**	N 10° 14’ 08.9” E077° 25’ 39.8” 2222 m	*Acacia mearnsii* invaded grass land
26	30-50 cm			
27	50-80 cm			
28	80-100 cm			
29	0-30 cm	FDA thottam (TNFD) inside the Krishnan kovil (**Kodaikanal)**	N 10° 23’ 53.7” E077° 42’ 78.0” 2213 m	*Acacia mearnsii* invaded grass land
30	30-50 cm			
31	50-80 cm			
32	80-100 cm			
33	0-30 cm	Near Water flow after Krishnan temple (**Kodaikanal)**	N 10° 14’ 23.3” E077° 25’ 20.1” 2193 m	Shola forest
34	30-50 cm			
35	50-80 cm			
36	80-100 cm			
37	0-30 cm	Near Water flow after Krishnan temple (**Kodaikanal)**	N 10° 24’ 02.4” E077° 42’ 22.9” 2201 m	Shola forest
38	30-50 cm			
39	50-80 cm			
40	80-100 cm			
41	0-30 cm	Near Mahalakshmi kovil (**Kodaikanal)**	N 10° 14’ 56.5” E077° 24’ 53.5” 2194 m	*Acacia mearnsii* invaded shola forest
42	30-50 cm			
43	50-80 cm			
44	80-100 cm			
45	0-30 cm	Near Mahalakshmi kovil (**Kodaikanal)**	N 10° 24’ 86.8” E077° 41’ 46.0” 2103 m	*Acacia mearnsii* invaded shola forest
46	30-50 cm			
47	50-80 cm			
48	80-100 cm			

http://www.aloki.hu ● ISSN 1589 1623 (Print) ● ISSN 1785 0037 (Online)
DOI: http://dx.doi.org/10.15666/aeer/2001_251263

STUDIES ON MICROBIAL MECHANISMS OF PERMAFROST CARBON CONVERSION TO CLIMATE WARMING: RETROSPECT AND PROSPECT

YU, S. P. – XU, N.* – DING, J. N. – SHI, C. Q.

Key Laboratory of Heilongjiang Province for Cold-Regions Wetlands Ecology and Environment Research, and School of Geography and Tourism, Harbin University, Harbin 150086, China

**Corresponding author*
e-mail: xunan0451@126.com

(Received 24th Jul 2021; accepted 28th Oct 2021)

Abstract. Recently, very active studies have been undertaken on the response and stability of permafrost carbon pool and key biogeochemical processes in permafrost regions to climate warming. By observing the significant differences in microbial community structure in regions of seasonal frost and permafrost, it is evident that microbes play key roles in the conversion of permafrost carbon. This paper reviews research progress at the cutting edges on the conversion and decomposition of permafrost carbon to climate warming and subsequent changes in microbial activities over the past decade. Findings indicated that: (1) Freeze-thaw cycles of soils in the active layer in permafrost regions showed an increasing annual trend and the existing survival patterns of permafrost microbes may be altered by the increasing freeze-thaw frequency; and (2) Soil microbes are an essential part of the cold-regions ecosystem and they play vital roles in soil carbon and nitrogen cycling, the mineralization and decomposition of soil organic matter. Thus, climate warming and subsequent permafrost degradation affect the conversion and decomposition of permafrost carbon, resulting in changes in CO_2 and CH_4 emissions, soil environmental factors, and soil microbial community structures. The laws for governing permafrost carbon conversion and the self-regulation mechanisms of soil microbes are important for natural ecosystems and environments in cold regions, and affect the strengths of greenhouse gas sources and sinks in permafrost regions.
Keywords: *frozen soils, degenerate, microorganisms, climate change, carbon cycle*

Introduction

Frozen soil generally refers to all kinds of rocks and soils with a temperature of 0℃ or below and is mainly found in high-latitude or high-altitude regions (Brown et al., 2002). Depending on its geographical distribution, pedogenesis, and diagnostic characteristics, frozen soil can be classified into tundra and frozen desert soil. Considering its geological history and impacts from climate change, permafrost is a geological entity formed through surface-atmosphere material and energy exchanges under the combined effect of geological structures, lithology, regional geographical environments, and other factors. It is also an essential component of the earth's cryosphere (Feng et al., 2004; Schmitt et al., 2008; Lawrence et al., 2015), covering about 24% of the exposed surface areas of the Northern Hemisphere. With its extensive distribution and unique hydrothermal properties, permafrost has become a very important environmental factor in regulating land surface processes (Bracho et al., 2016).

The occurrence conditions of permafrost are very fragile. Due to the strong influence of human activities such as climate warming and forest logging over the past century, most of the permafrost has begun to degrade, mainly manifested in the continuous northward movement of the south boundary of the permafrost, the gradual regression from south to north, the continuous reduction of the total area, the thinning of the thickness of the permafrost, the thickening of the active layer, the increase of the

http://www.aloki.hu ● ISSN 1589 1623 (Print) ● ISSN1785 0037 (Online)
DOI: http://dx.doi.org/10.15666/aeer/2001_265283

maximum seasonal melting depth The trend of melting and shrinking also intensifies. The original permafrost becomes seasonal permafrost, the continuous permafrost becomes discontinuous, and the multi-year Island permafrost disappears. It is estimated that the global permafrost area will decrease significantly in the next century (Camill and Clark, 2000). With the continuous warming of the climate, the area and speed of permafrost degradation may further increase in the next century. Subsequently, it will cause a series of ecological and hydrological changes, which will lead to changes in vegetation succession and productivity, and may also bring severe ecological and environmental problems in cold areas, that is, the common degradation of frozen soil, wetland and forest (Camill, 1999; Camill and Clark, 2000).

Climate warming has known effects on high-latitude permafrost zones (Natali et al., 2012; Song et al., 2014). According to the latest assessment, the global mean annual ground surface temperature rose by roughly 0.85℃ from 1880-2012 (IPCC, 2013). In the past century, the mean annual air temperature of the northern high-latitude region increased by more than 1℃, changing climatic, hydrological, and mass cycles in permafrost zones (Anisimov and Nelson, 1996; Feng et al., 2020). Permafrost degradation causes the decomposition of the soil organic carbon (SOC) stored in permafrost zones, accounting for 50% of the global SOC, which in turn feeds back and accelerates climate warming (Luo et al., 2007; Haeberli and Hohmann, 2008; Bracho et al., 2016; Guo et al., 2018; Feng et al., 2020). Studies have shown that very short-term climate warming of only 1.5 years can stimulate rapid decomposition of SOC in permafrost zones (as mediated by microbes), but does not affect soil microbial communities. However, experimental winter warming for a five-year period in the same place showed altered microbial communities (Zhou and Yang, 2020). There are intense interactions between thawing depth, community aggregation and interaction networks, which means that the climate-warming-induced acceleration of permafrost thawing has fundamentally reconstructed microbial communities (Huntington, 2006; Schmitt et al., 2008; Deane-Coe et al., 2015; Guo et al., 2018).

Under a warming climate, there is an increase in both the decomposition of carbon and the relative abundance of methanogenic genes, and their functional structures are closely related to ecosystem respiration or methane emission. This suggests that carbon cycling-related microbial responses may have produced positive feedbacks, thus accelerating the decomposition of SOC in permafrost zones. However, in most cases, the loss of SOC incurred by changes in the composition of microbial communities is unlikely to subside. This result is of great significance for the conversion of permafrost carbon and the interactive mechanisms of soil microbes (Jin et al., 2000; Friedlingstein et al., 2006; Shannon et al., 2010; Song et al., 2013). Microbes play a vital role in the biogeochemical cycling in permafrost regions, and can serve as early warning and sensitive bio-indicators of ecosystem changes in cold regions (Song et al., 2004; Bracho et al., 2016; Guo et al., 2018). In the context of global warming, the degradation of permafrost is bound to directly or indirectly affect soil microbial community structures and microbe-regulated soil ecological processes, further changing the structures and functions of permafrost ecosystems.

Based on the Science Citation Expanded (SCIE) database of the Web of Science platform, a quantitative analysis was carried out on the literature of SCI in the field of soil animals from 2010 to 2020, most geocryological studies have focused on soil microbial and environmental changes, a total of 883 relevant literatures (*Fig. 1*). As temperatures continuously rise, the active layer deepens. In this case, the large amount of SOC

http://www.aloki.hu ● ISSN 1589 1623 (Print) ● ISSN1785 0037 (Online)
DOI: http://dx.doi.org/10.15666/aeer/2001_265283

sequestered in permafrost may be released. On the other hand, as metabolic activity of the soil microbes is enhanced, the decomposition efficiency of organic carbon increases, resulting in large effluxes of greenhouse gases, such as CO_2, CH_4, and N_2O. This further enhances the positive feedback of permafrost degradation to climate warming, impacting all ecosystems in cold regions (Jin et al., 2007; Feng et al., 2007; Zhu et al., 2016). Thus, investigating permafrost microbes is scientifically relevant for further understanding of the degradation of biodiversity and permafrost ecosystems. In addition, studying the changes in soil microbial community structures and response mechanisms between them and various soil environmental factors in permafrost zones will further our ability to comprehensively and accurately predict and assess the impacts of future climate change on the functions and stability of permafrost ecosystems.

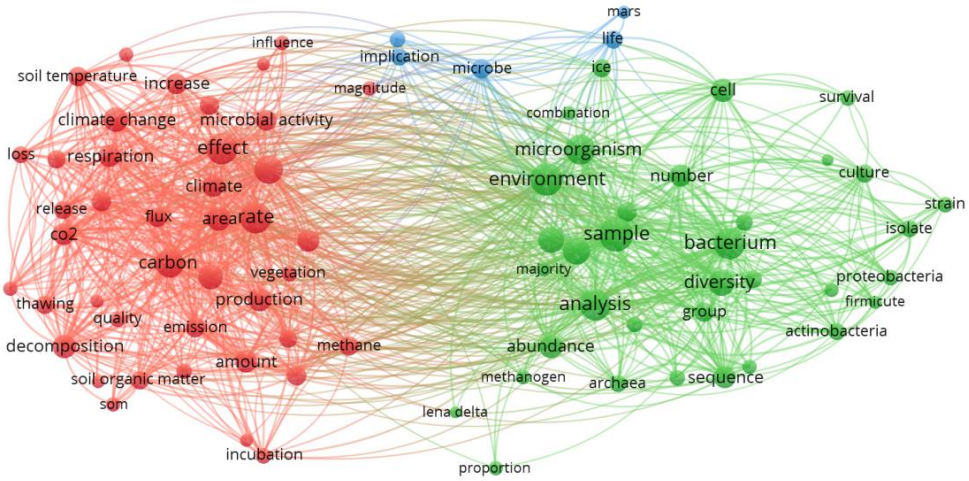

Figure 1. *Hotspot distribution of the geocryology research field. Notes: Each circle represents a technical term. The distribution of these terms is based on their occurrence frequency in titles and abstracts. Two terms co-occurring at a higher frequency are closer in the diagram. Each color represents a theme, and the size of a circle is directly proportional to the number of corresponding studies*

As one of the extreme environments in the cryosphere, frozen soil covers a large area and is widely distributed. It is sensitive to global climate change. Compared with the traditional terrestrial and aquatic ecosystems of forests, farmland, oceans, lakes, rivers and atmosphere, there are few studies on soil microbial communities in the frozen soil extreme environment that is sparsely populated and not polluted by modern industry (Simth et al., 1998; Dobbie and Simth, 2003). Permafrost distribution area is a sensitive area of global climate change. Permafrost degradation leads to the shrinkage of permafrost area, the decline of soil biodiversity function and the damage of ecological function, which has become one of the important ecological problems at present. The study of frozen soil microorganisms has become a hot field of international research. Over the years, the research on frozen soil in China has made great progress and has been in the leading position in the world. However, the research on frozen soil microorganisms has just started (Puser et al., 2006).

Due to the huge soil carbon storage in the multi-year frozen soil area and its vulnerability to climate warming, microorganisms are considered to be the key to regulate the effect of climate warming on soil carbon. Therefore, the microbial decomposition

http://www.aloki.hu ● ISSN 1589 1623 (Print) ● ISSN1785 0037 (Online)
DOI: http://dx.doi.org/10.15666/aeer/2001_265283

function of soil carbon is enhanced under the condition of global warming, which leads to the increase of soil respiration and methane emission, which in turn accelerates the loss of carbon in the tundra. since the soil temperature during the growing season remains unchanged, these observations may be caused by changes caused by winter warming treatment. For many years, it has been believed that thawing of frozen soil area has a profound influence on local hydrology, heat and dynamics. And found that warming increases the depth of thawing, which is associated with fine the most important factors associated with bacterial phylogeny, community composition, and network topology.

Effects of a warming climate on the conversion of permafrost carbon

Due to the effects of rising temperature on carbon cycling processes in terrestrial ecosystems (Ping et al., 2015), warming will exert a tremendous influence on global carbon cycling (Xu et al., 2007; Schaefer et al., 2014; Turetsky et al., 2020). Climate warming can affect terrestrial carbon cycling processes through the following mechanisms: affecting surface plant growth and community structures through changing the duration of phenological and growth periods (Walther et al., 2002; Nemani, 2003); influencing soil respiration and nutrient cycling through modifying the activity of soil microbial and the decomposition rate of SOC (Grogan et al., 2000; Johnson et al., 2000; Melillo et al., 2002; Singh et al., 2010) and ultimately impacting the growth and pattern of surface vegetation (Rustad et al., 2001; Walther et al., 2002; Welker et al., 2004); The carbon balance of the terrestrial ecosystem is mainly determined by two processes: photosynthesis and respiration of surface vegetation and soil (Nakatsubo et al., 2005; Grosse et al., 2016). The modification of the carbon cycling processes of the terrestrial ecosystem by warming will promote the above mentioned processes and change the initial carbon balance, creating a positive feedback to the warming process (Grosse et al., 2016). Such feed backs may accelerate the process of climate warming (Natali et al., 2015). Soil is also the largest carbon pool in the terrestrial ecosystem (Post et al., 1982; Wan et al., 2002), and any minor change to the soil carbon pool due to warming may end up a significant impact on the carbon balance of the terrestrial ecosystem. Climate warming accelerates the decomposition of SOC (Hayes et al., 2014) and soil respiration (Natali et al., 2015) (*Fig. 2*).

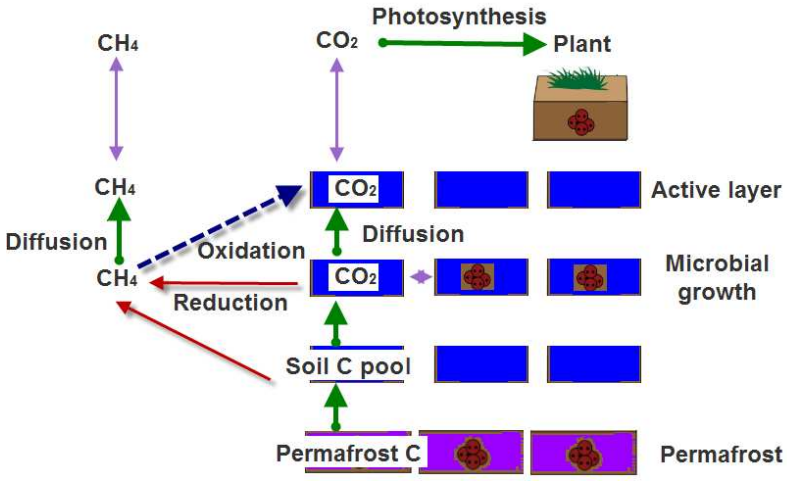

Figure 2. *Mechanism of carbon exchange between microbial community and soil*

http://www.aloki.hu ● ISSN 1589 1623 (Print) ● ISSN1785 0037 (Online)
DOI: http://dx.doi.org/10.15666/aeer/2001_265283

Existing earth system models mainly focus on how a warming climate affects the thickness and hydrological status of the active layer above the permafrost. Driven by warming, the thickness of the active layer in permafrost region sathigh-latitudes gradually increases. However, in regions with excess ground ice, ground surface settlement occurs during the degradation of permafrost, resulting in thermokarsting and modified hydrology (Merritt et al., 2020). The thickness of active layer in permafrost region is significantly correlated with soil temperature and moisture, thus affecting the carbon emission process of ecosystem (*Fig. 3*). When thawed soil is flooded, its carbon mineralization rate is inhibited, but its CH_4 yield is increased. Thus, ground thawing changes the permafrost carbon balance, leading to ecological succession (Merritt et al., 2020). On the millennial scale, thermokarst lakes can change from atmospheric carbon sources into sinks (Cox et al., 2000; Elberling et al., 2013; Webb et al., 2016; Pries et al., 2016).

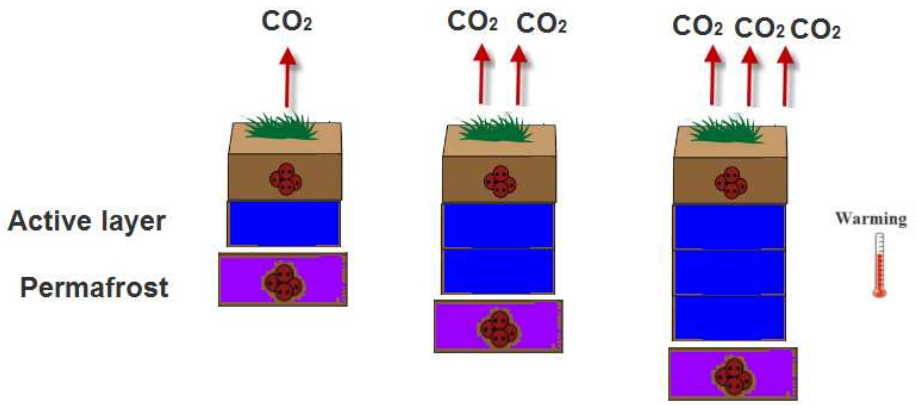

Figure 3. *A schematic diagram of effects of permafrost on ecosystem respirations*

As a warming climate continues to promote emissions of soil carbon, permafrost zones are likely to become huge carbon sources (Zak et al., 1999; Grosse et al., 2016). The huge carbon pools in high-latitude depermafrost ecosystems are susceptible to climate warming. This has always been a hotspot in research on climate change. The rapid warming of high-latitude and high-altitude regions is accelerating the decomposition of permafrost carbon and releasing large quantities of greenhouse gases into the atmosphere (Turetsky et al., 2020). Permafrost carbon is affected by ground thawing, and the resulting emissions load can be enormous. In fact, this has become focal point in climate negotiations (Merritt et al., 2020). Continuous monitoring showed that thermal melt slump resulted in enhanced respiration of exposed bare soil, and the ecosystem in the region changed from carbon sink to carbon source (Mu et al., 2017) (*Fig. 4*). At the same time, the transport of water, dissolved organic carbon and minerals due to thermal melt slump enhanced the methanogenic process and denitrification ability, which further accelerated and nitrous oxide emissions (Yang et al., 2018). Some of the soil carbon is converted into greenhouse gases and the other is released as surface runoff flows into rivers and lakes.

The increase of temperature has significantly degraded the frozen soil, mainly manifested in the deepening of the thickness of the active layer and the increasing frequency of freeze-thaw alternation. Freeze thaw alternation can promote the decomposition of organic debris and the mineralization of carbon and nitrogen, enhance the respiration of soil animals, plants and microorganisms, and increase the emission

http://www.aloki.hu ● ISSN 1589 1623 (Print) ● ISSN1785 0037 (Online)
DOI: http://dx.doi.org/10.15666/aeer/2001_265283

fluxes of CO_2, CH_4 and N_2O. The increase of temperature changes the physical and chemical characteristics of soil and enhances the activity of soil microorganisms, so as to enhance soil respiration and emit more CO_2. However, the CO_2 emission intensity caused by warming shows great differences due to different climatic conditions, surface vegetation, soil organisms and warming range (Yu et al., 2009; Li et al., 2011). Under the influence of temperature change, no matter whether the emission of CO_2, CH_4 and N_2O in frozen soil increases or decreases, its mechanism is mainly that the soil temperature change caused by climate warming changes the activity of key microbial flora (mainly including methanogens, methane oxidizing bacteria, nitrifying bacteria and denitrifying bacteria) in the process of carbon and nitrogen transformation, and promotes or inhibits the decomposition of soil nutrients by microorganisms, Then affect the fluxes of CO_2, CH_4 and N_2O. In addition, temperature changes can regulate soil physical, chemical and biological properties, delay or shorten the growth period of soil plants, and indirectly affect the changes of CO_2, CH_4 and N_2O fluxes (Wang et al., 2002; Geng et al., 2013).

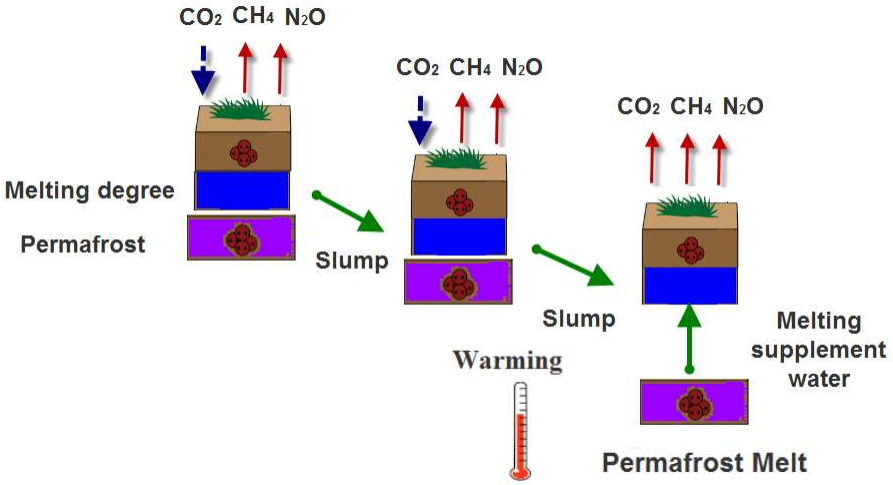

Figure 4. *Impacts of permafrost degradation on soil moisture, dissolved organic carbon and the release of greenhouse gases (CO_2, CH_4, N_2O) and the arrows indicate the direction and potential of ecosystem greenhouse gas exchange during the growing seasons*

Water conditions mainly affect the change of CH_4 flux from two aspects: CH_4 production and oxidation. In some studies, five gradients of 30%, 45%, 60%, 75% and 90% (field capacity) were set in to study the effects of different water conditions on CH_4 emission from alpine meadow (Wang et al., 2016). It was found that the soil water content was between 30% ~ 60% of field capacity, and the alpine meadow showed a sink of methane. At this time, the absorption of CH_4 was greater than the emission, but the absorption decreased gradually with the increase of water. This is because water filling the soil gap makes the gas difficult to diffuse and the CH_4 absorption flux decreases. At the same time, the increase of water affects the activity of soil microorganisms, gradually changing it from a good gas process to a bad gas process, and CH_4 oxidizing bacteria are limited (Wu et al., 2010; Wang et al., 2016). The soil water content is between 60% ~ 90% of the field water capacity, the CH_4 emission rate increases, and its emission increases with the increase of water content. The alpine meadow is the source of CH_4.

Soil is the main emission source of N_2O. Soil moisture directly affects nitrification and denitrification by affecting the content of O_2 in soil, and indirectly affects the production

http://www.aloki.hu ● ISSN 1589 1623 (Print) ● ISSN1785 0037 (Online)
DOI: http://dx.doi.org/10.15666/aeer/2001_265283

and emission of N_2O. When the water content is lower than the critical value of water and the soil permeability is strong, N_2O mainly comes from chemical action, and N_2O emission increases with the increase of water content. When the soil has accumulated water for a long time, the denitrification process is the main source of N_2O (Mikan and Schimel, 2002; Wu et al., 2010; Wang et al., 2016), but the O_2 supply decreases and the N_2 proportion increases, resulting in the reduction of N_2O emission with the increase of water content. Therefore, too low or too high soil water content is not conducive to N_2O emission. In forest ecosystem, the response of soil N_2O emission range to water content varies with forest type, which may be due to the different organic matter and other nutrients contained in different types of litter, resulting in different substrates in biochemical process (Wu et al., 2010; Geng et al., 2013; Wang et al., 2016). During the growing season, the alpine meadow ecosystem has abundant precipitation, enhanced microbial activities and promoted N_2O emission; The cold temperature in the non-growing season leads to the reduction of microbial activity, and part of N_2O is frozen in the soil and difficult to release to the outside world, inhibiting N_2O emission (Wu et al., 2010; Wang et al., 2016).

There are large differences in the response sensitivity of different ecosystem components to climate change (Vishnivetskaya et al., 2006; Hassan et al., 2016). Climate change affects the carbon cycle of Arctic terrestrial ecosystems by changing temperatures, precipitation, snow cover and growth season length. In the future trend of increasing temperature and precipitation, the biomass of most Arctic vegetation will increase, so that more carbon will enter the Arctic terrestrial ecosystem. and higher temperature usually accelerates SOC microbial decomposition and greenhouse gas release. This feedback can accelerate climate change, but the scale of greenhouse gas emissions and their impact on climate change remain uncertain (Wang et al., 2002; Geng et al., 2013; Wang et al., 2016). Some research temperature and moisture are considered to be the main drivers of organic carbon mineralization (Bergero et al., 1999; Hassan et al., 2016). However, some studies have suggested that the sensitivity of SOC to temperature is not strong, and the effect of temperature increase is mainly the soil inert organic carbon component (Wang et al., 2002; Geng et al., 2013; Wang et al., 2016; Hassan et al., 2016). However, the intensity of the effect of temperature and water content on SOC mineralization rate is still poorly understood. in addition, the multi-year frozen soil carbon loss associated with wildfire, river and coastal erosion may not be well addressed in the global model.

Microbial mechanisms of permafrost carbon conversion under a warming climate

Microbial activities under a warming climate

Permafrost not only contains a huge amount of organic carbon matter, it is also inhabited by a rich variety of microbial communities. As survivors, microorganisms can engage in metabolism and reproduction under harsh living conditions, such as oligotrophic status, low temperature, freeze-thaw cycles, ultraviolet and polar radiation (Deng et al., 2015; Zhang et al., 2015). Permafrost is also inhabited by large quantities of microbial communities of various kinds, which can metabolize and reproduce under similarly harsh conditions (Xue et al., 2016; Salmon et al., 2016). In the biogeochemical cycling in permafrost regions, soil microbes play vital roles. As key bonds in ecosystems, they are highly sensitive to climate change; they are capable of linking underground soil nutrient systems with surface vegetation, and; thus, they are sensitive biological indicators for early warning of ecosystem changes in cold regions. A significant positive

http://www.aloki.hu ● ISSN 1589 1623 (Print) ● ISSN1785 0037 (Online)
DOI: http://dx.doi.org/10.15666/aeer/2001_265283

correlation was observed between the NPP and atmospheric CO_2 concentration. The impact of permafrost degradation on NPP differed with regional environment. The NPP had a significant positive correlation with the mean annual ground temperature, but a negative correlation with the annual maximum permafrost depth (Mao et al., 2012; Hao et al., 2018; Feng et al., 2019).

Soil freezing and thawing occurs when the soil temperature changes around 0 ℃, and temperature is the dominant factor in the occurrence of freezing and thawing. Most studies show that there is a good correlation between forest soil respiration rate and soil surface temperature (Wu et al., 2010; Geng et al., 2013; Wang et al., 2016). Repeated freezing and thawing and a series of complex processes caused by it. The quantitative change of "living" microorganisms in frozen soil is consistent with the change characteristics of melting and freezing of frozen soil due to climate change. Many studies used pure culture method, selected two typical frozen soil soils of high latitude and high altitude frozen soil for bacterial isolation and culture, preliminarily obtained the community structure and diversity of culturable bacteria in the soil of high latitude and high altitude frozen soil areas in China, and compared the similarities and differences between them. The number of colonies isolated from soil in different frozen soil areas is different. The reason may be that the material basis necessary for the growth of soil microorganisms includes carbon source, nitrogen source, inorganic salt, growth factor and water (Mikan and Schimel, 2002; Puser et al., 2006), and the amount affects the number and species of soil microorganisms (Puser et al., 2006).

Seasonal freeze-thaw processes and soil physicochemical properties affect both the microbial quantities and species. Soil microbes are one of the most active components of soil system, and their biomass, activity, and community structures are strongly affected by changes in soil temperature, humidity, and micro-environment. Investigating the responses of soil microbes to a warming climate is crucial for predicting changes in the carbon stock of terrestrial ecosystems (Yao et al., 2006; Zhang et al., 2015; Das et al., 2017). Permafrost is featured by stable low temperature, low nutrient and continuous exposure to low level radiation. The metabolism of microorganisms in permafrost is at a relatively low level, with low frequency of gene mutation. Studying the characteristics of the microbial community structure in permafrost helps better understand the adaptive characteristics and genetic indicators of microorganisms in cold environment (*Table 1*).

Since the 1950s, researchers have studied mold in polar snow, mainly from *Thyronectria antarctica var.hyperantarctica, Coleroa turfosorum, Bryosphaeria megaspora, Epibryon chorisodontii, Microdochium nivale, Sclerotinia borealis* belonging to *Ascomycetes*. *Trichoderma polysporum; Typhula ishikariensis, Microbotryum bistortarum, Polygonum viviparum;* attributable to the *Basidiomycetes Rhizopus, Bryum antarcticum*; attributable to the *Oomycetes comnium palustre, Calliergon stramineum* and *Tomenthypnum nitens*. These fungi are mostly cold resistant species and have a variety of cold adaptation mechanisms (Tojo and Newsham, 2012). Up to now, fungal activities of fungi have been found in various elements of the cryosphere (*Table 2*). Hassan et al. (2016) conducted a comprehensive review of this research field.

In permafrost ecosystems, soil microbes promote the decomposition of organic matter and the conversion of soil nutrients, link underground soil nutrient systems with surface vegetation, and are highly sensitive to climate change (Yakushev et al., 2014; Zhou et al., 2017). So far, existing studies on permafrost microbes mainly concentrate on the following two aspects: 1) Effects of freeze-thaw action on soil microbes under a warming

http://www.aloki.hu ● ISSN 1589 1623 (Print) ● ISSN1785 0037 (Online)
DOI: http://dx.doi.org/10.15666/aeer/2001_265283

climate, and; 2) Correlations of the structures and diversity of permafrost microbial communities with various environmental factors. Facilitated by the rise of culture-independent molecular biological methods, researchers have made extensive and profound inquiries for exploring microbial communities in frozen soils. The structures and diversity of permafrost microbial communities have been found to be influenced by many diverse factors. For example, Fierer et al. (2006) found that across a wide area, soil pH was the primary influencing factor for microbial communities. This was further confirmed by Chu et al. (2010) after the investigations of the soil bacterial community structures at 29 tundra sites in Alaska and other Arctic regions.

Table 1. *Diversity and number of culturable microorganisms in permafrost*

Type	Microbe totality	Dominant microflora	Reference
(Arctic)			
Kolyma lowland	10^3~10^8 cell·gdw^{-1}	--	Gillchinsky et al., 1989
Spitsbergen, Northern	$1.7\times10^9\pm2.4\times10^8$ cell·gdw^{-1}	*Cellulomonas*	Hansen et al., 2007
Norway	$1.7\times10^9\pm2.4\times10^8$ cell·gdw^{-1}	*Arthrobacter*	
Eureka	10^1~10^4 cell·gdw^{-1}	*Acidobacteria,Gemmatimonadetes,*	Seven et al., 2007
	10^1~10^4 cell·gdw^{-1}	*Bacteroidetes,Plantomycetes,*	
	10^1~10^4 cell·gdw^{-1}	*Firmicutess,Proteobacteria*	
(Antarctica)			
Marble Point	$7.8\times10^7\pm1.3\times10^8$ cell·gdw^{-1}	*Bacteroidetes,*	Aislabie et al., 2006
	$7.8\times10^7\pm1.3\times10^8$ cell·gdw^{-1}	*Acidobacteria*	
Bull pass	10^6~2.3×10^7 cell·gdw^{-1}	*Bacteroidetes,*	
Vanda	3.6×10^7 ~1.2×10^8 cell·gdw^{-1}	*Bacteroidetes,*	
Mt.Fleming	< 10^6 cell·gdw^{-1}	*Arthrobacter,*	
	< 10^6 cell·gdw^{-1}	*γ-proteobacteria*	
South Shetland Archipelago	--	*Bacteroidetes,*	Ganzert et al., 2011
	--	*Acidobacteria*	
	10^3~10^8 cell·gdw^{-1}	*Actinobacteria,*	Horowitz et al., 1972
	10^3~10^8 cell·gdw^{-1}	*Firmicutess*	Cowan et al., 2002
(Tibetan Palteau)			
Beilu River Basin	ND	*Arthrobacter, Pseudomonas*	Zhang et al., 2007
Beilu River Basin	1.0×10^7 ~3.8×10^9 cell·gdw^{-1}	--	Fang et al., 2004
(Tianshan Mountains)			
Tianshan Mountains	2.5~6×10^5 CUF·gdw^{-1}	*Arthrobacter*	Bai et al., 2006

The continuous warming increases the thawing depth of the soil, resulting in a significant difference between the warming and the soil environment on the same ground, so the microbial community is unlikely to adapt to the warming. Because the temperature sensitivity of soil inert organic carbon is higher than that of unstable soil organic carbon, the higher microbial function of inert soil organic carbon decomposition under warming

http://www.aloki.hu ● ISSN 1589 1623 (Print) ● ISSN1785 0037 (Online)
DOI: http://dx.doi.org/10.15666/aeer/2001_265283

conditions will aggravate the soil carbon instability related to ecosystem respiration; while for deep soil, the warming effect of frozen soil area is often more significant, which contributes to ecosystem respiration. therefore, we predict that these microbial communities will continue to provide positive feedback for climate warming. Overall, the warming experiments significantly changed the bacterial composition and functional structure of the microbial community in the permafrost region and revealed its sensitivity to warming (*Tables 1, 2*). soil thawing depth is the most important factor affecting bacterial taxonomic composition, carbon decomposition potential and network topological properties, indicating that warming-induced thawing of permafrost regions basically reconstructs the associated bacterial communities. Therefore, we believe that the response of microorganisms to long-term warming will lead to positive feedback in the tundra region to promote carbon decomposition.

Table 2. *Fungal genus/species distributed in permafrost*

Type	Fungal genus/species	Reference
Franz Joseph Land	*Geomyces, Phialophora, Phoma, Acremonium,Thelebolus, Mortierella.*	Bergero et al., 1999
Northern Fennoscandia Arctic	*Anthracoiedea echinospora, Anthracoidea heterospora.*	Scholler et al., 2003
Western Beringia	*Acanthophysium, Mortierella, Bensingtonia, Cryptococcus*	Lydolph et al., 2005
Arctic	*Sordaria Phanerochaete, Phialocephala.*	Lydolph et al., 2005
Tyrolean Alps	*Cenococcum geophilum, Sebacina sp, Cortinarius sp.*	Muhlmann and Peintner, 2008
Cliff ledges	*Cenococcum geophilum, Thelephoraceae sp, Cortinarius sp.*	Ryberg et al., 2009
High Arctic	*Cryptococcus, Rhizosphaera, Mycopaoous, Melampsora, Mrakia, Tetracladium, Phaeosphaeria, Venturia, Leptosphaeria.*	Zhang and Yao, 2015
Antarctic Peninsula	*G. Pannorum, Thelebolus microspores. Mortierella sp. Firmicutess. Thielavia Antarctica, Apiosordaria antarctica.*	Goncalves et al., 2012
King George Island Antarctica	*Mucor hiemalis, Mortierella alpina, Umbelopsis isabellina, Penicillium chrysogenum.*	Stchigel et al., 2003
Damma Glacier	*Lemonniera, Tetracladium nainitalense, Thelebolus microspores.*	Brunner et al., 2011
Himalayan Glacier	*Phoma sclerotioides, P. antarctica, P. olivacea, P. lutea, Pseudogymnoascus, T. Psychrophilum, T. ellipsoideum, T. globosum.*	Hassan et al., 2016
Plateau Glacier	*Antrodia, Eupenicillium, Sporobolomyces, Candida, Cryptococcus, Trametes, Periconia, Thelebolus, Trichoderma, Pueraria,*	Wang et al., 2015
Kunlun Mountains Glacier	*Pseudogymnoascus, Beauveria, Pseudeurotium, Fontanospora, Cordyceps,*	Hassan et al., 2016

http://www.aloki.hu ● ISSN 1589 1623 (Print) ● ISSN1785 0037 (Online)
DOI: http://dx.doi.org/10.15666/aeer/2001_265283

Microbial mediation in permafrost carbon conversion under a warming climate

As an important part of the ecosystem, soil microorganisms participate in the cycling process of soil carbon elements and the mineralization process of soil organic matter, which play an important role in the global carbon cycle and in the decomposition and transformation of organic substance, the transformation and supply of nutrients. *Fig. 5* is a schematic diagram of the relationship between microorganisms and soil carbon cycle in permafrost areas. Studies have revealed the viability of microorganisms is frozen or greatly depressed/slowed in time, where the nutrients in unfrozen/liquid water films are used for growth and proliferation. For instance, Nataliet al. (2015) found that bacterial metabolism could still produce CO_2 at –39 ℃. Thawing of permafrost is closely correlated with the release of trace gases, and ground warming boosts the decomposition rate of organic matter, particularly that from ancient times (Coolen and Orsi, 2015), resulting in the enhanced production of CH_4 and CO_2 (Romanovsky et al., 2008). A study on Alaskan peatlands show that since thawing of permafrost beginning at 3 ka B. P., they are losing carbon sources at an annual net rate of 26 g/m^2. Although the carbon released from the ancient permafrost increases the carbon offset by plant growth, permafrost has become a giant carbon source (instead of carbon sink) in the biosphere under a warming climate. The emission of large amounts of greenhouse gases in turn promotes climate warming, positively feeding back to the climate system (Schuur et al., 2015; Natali et al., 2015). Thus, permafrost microbes participate in carbon cycling through metabolizing carbonaceous organic matter (Hultman et al., 2015).

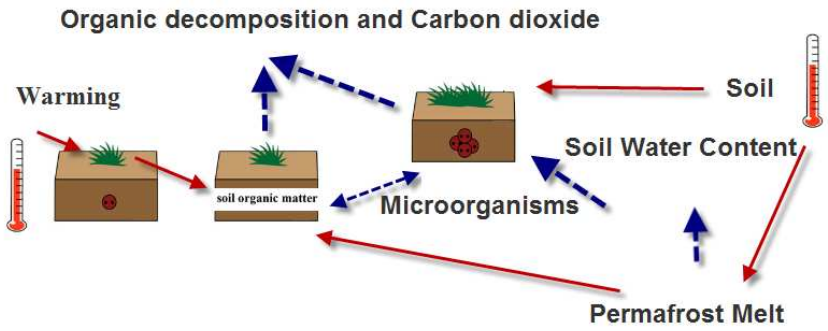

Figure 5. *Mechanism of carbon and nitrogen exchange between microbial community and soil. Notes: A solid line with an arrow indicates positive feedback; The solid line of the flat arrow indicates negative feedback, and; Dashed arrows indicate positive or negative feedback*

Based on previous studies, Zhou and Yang (2020) proposed the hypothesis that five-year warming yielded substantial changes in plant productivity, soil microclimate, and soil microbial community structures. Their results showed that, under a warming climate, the classification, composition, functional structures, and changes of soil microbial communities were both potential driving factors and ecological results. It was also discovered that climate warming greatly modified the composition and functional structures of permafrost bacterial communities. The thawing depth was the most significant influencing factor for bacterial classification and composition, carbon decomposition potential, and network topological properties. Permafrost was induced by climate warming fundamentally reconstructed those related bacterial communities. Thus, responses of microbes to long-term climate warming would create positive feed backs and promote carbon decomposition in permafrost zones.

http://www.aloki.hu ● ISSN 1589 1623 (Print) ● ISSN1785 0037 (Online)
DOI: http://dx.doi.org/10.15666/aeer/2001_265283

Conclusion and prospect

Permafrost carbon conversion has currently become a research hot spot. Summarizing latest research on the responses of permafrost carbon conversion to climate warming and the related microbial mechanisms, there are still several key problems await further investigations:

(1) Succession of vegetation communities in forest ecosystems: The degradation of permafrost induced by climate change gives rise to a series of environmental changes, such as increased activity layer thickness and hydrothermal instability, and alters forest ecosystems. For instance, the timberline of the main original constructive species of the Da Xing'anling Mountains in Northeast China (such as *Larixgmelinii* and *Pinus sylvestris*) has been elevated, and coniferous forests have experienced a succession towards deciduous mixed broad-leaved and coniferous forests. On account of in-situ monitoring conditions in the field, existing studies on climate change mostly resort to numerical simulations, which is fundamentally different from field in-situ experiments. Thus, it is still necessary to strengthen the continuous, long-term observation of permafrost experiment zones, especially in combination with changes in the biogeochemical cycling of soil carbon under a warming climate. In addition, existing studies have touched upon the effects of changing seasonal freeze-thaw processes on SOC, especially soil carbon fractions and soil carbon conversion characteristics.

(2) Shrinking permafrost wetlands: There is a symbiotic relationship between permafrost and wetlands, and the degradation of permafrost is accompanied by a rapid loss of soil water. As a consequence, the original wetlands on permafrost gradually shrink in areal extent due to the lack of water replenishment, and wetland ecosystems gradually change to meadow and farmland ecosystems. However, the interactions between wetlands and permafrost and the mechanisms by which they emit high levels of greenhouse gases still remain poorly known, and the monitoring of the effective substrates of soil activity is not adequately diversified. For this reason, efforts should be made to explore the microbial community structures and effective substrates of permafrost peatlands, and to analyze the structural characteristics and functional genes of the microbial communities playing dominant roles in the decomposition of soil organic matter, methanogensis, and other processes under a warming climate.

Due to the rapid expansion of human activities and industrialization process, greenhouse effect changes forest ecosystems at different scales. Over the next 40~50 years, if air temperature rises by 1.5 ℃, the southern/lower limit of permafrost will continue to move northwards/upwards. With the degradation of permafrost, continuous permafrost may degrade first into discontinuous permafrost, and then into seasonal frost, resulting in the decomposition of carbon sources fixed by microbes. This degradation process is also accompanied by the production of CO_2 through aerobic soil respiration or the emission of CH_4 under anaerobic microbial action. Jointly, these processes intensify the greenhouse effect, producing positive feed backs to climate warming. To provide a base line for accurately predicting the intensity of greenhouse gas sources and sinks in permafrost regions and more effectively protect forest ecosystems under a changing climate, it is necessary to explore the effects of global warming on the conversion of permafrost carbon. and discuss the mediating mechanism of microbes in the responses of the conversion of permafrost carbon to global warming.

Climate warming has led to significant degradation of permafrost as manifested by increased active layer thickness and altered seasonal freeze-thaw processes. More frequent seasonal freeze-thaw cycles promote the decomposition of fragmental organic

http://www.aloki.hu ● ISSN 1589 1623 (Print) ● ISSN1785 0037 (Online)
DOI: http://dx.doi.org/10.15666/aeer/2001_265283

matter and the mineralization of organic carbon and nitrogen, and strengthen the respiration of soil animals, plants, and microbes, and increase CO_2, N_2O and CH_4 effluxes. Ground warming also modifies soil physiochemical properties and enhances soil microbial activity, resulting in enhanced soil respiration and CO_2 emissions.

Frozen soil is a very important environmental factor on the earth's land surface. It is widely distributed and has unique hydrothermal characteristics. It is an extremely valuable natural resource. Bacteria account for a large proportion of many soil microorganisms, and make a great contribution to soil material circulation and energy flow. In the study of soil bacteria, there are many reports on agricultural areas, but there are few reports on soil bacteria in permafrost areas, especially in permafrost areas at high latitudes in China. As one of the extreme environments in the cryosphere, frozen soil covers a large area and is widely distributed. It is sensitive to global climate change. Compared with the traditional terrestrial and aquatic ecosystems of forests, farmland, oceans, lakes, rivers and atmosphere, there are few studies on soil microbial communities in the frozen soil extreme environment that is sparsely populated and not polluted by modern industry. Permafrost distribution area is a sensitive area of global climate change. The degradation of permafrost leads to the shrinkage of permafrost area, the decline of soil biodiversity function and the damage of ecological function, which is one of the important ecological problems we will study in the future.

Funding. This study was financially supported by China-Norway International Collaboration Project (Grant No.CHN-17/0019) and the project of Heilongjiang Province Key Laboratory of Cold Region Wetland Ecology and Environment Research of the Harbin University (No. 201910). The project of Young Doctoral Research of the Harbin University (No. 2020106).

REFERENCES

[1] Aislabie, J. M., Chhour, K. L., Saul, D. J., Miyauchi, S., Ayton, J., Paetzold, R. F., Balks, M. R. (2006): Dominant bacteria in soils of marble point and wright valley, Victoria land, Antarctica. – Soil Biology Biochemistry 38(10): 3041-3056.

[2] Anisimov, O. A., Nelson, F. E. (1996): Permafrost distribution in the northern hemisphere under scenarios of climatic change. – Global and Planetary Change 14: 59-72.

[3] Bai, Y., Yang, D., Wang, J., Xu, S., Wang, X., An, L. (2006): Phylogenetic diversity of culturable bacteria from alpine permafrost in the Tianshan Mountains, northwestern China. – Res Microbiol. 157: 741-751.

[4] Bergero, R., Girlanda, M., Varese, G. C., Intili, D., Luppi, A. M. (1999): Psychrooligotrophic fungi from arctic soils of Franz Joseph Land. – Polar Biology 21: 361-368.

[5] Bracho, R., Natali, S., Pegoraro, E., Crummer, K. G., Christina, S., Celis, G., Hale, L., Wu, L., Yin, H., Tiedje, J. M. (2016): Temperature sensitivity of organic matter decomposition of permafrost region soils during laboratory incubations. – Soil Biology and Biochemistry 97: 1-14.

[6] Brown, J., Ferrians, O. J. Jr., Heginbottom, J. A., Melnikov, E. S. (2002): Circum-arctic map of permafrost and ground-ice conditions. – Version 2. Natl. Snow Ice Data Center/World Data Cent. Glaciol., Boulder, Co.

[7] Brunner, I., Plotze, M., Rieder, S., Zumsteg, A., Furrer, G., Frey, B. (2011): Pioneering fungi from the Damma glacier forefield in the Swiss Alps can promote granite weathering. – Geobiology 9: 266-279.

[8] Camill, P. (1999): Patterns of boreal permafrost peatland vegetation across environmental gradients sensitive to climate warming. – Canadian Journal of Botany 77(5): 721-733.

http://www.aloki.hu ● ISSN 1589 1623 (Print) ● ISSN1785 0037 (Online)
DOI: http://dx.doi.org/10.15666/aeer/2001_265283

[9] Camill, P., Clark, J. S. (2000): Long-term perspectives on lagged ecosystem responses to climate change: permafrost in boreal peat lands and the grassland/woodland boundary. – Ecosystems 3(6): 534-544.
[10] Chu, F. (2010): Soil bacterial diversity in the arctic is not fundamentally different from that found in other biomes. – Environmental Microbiology 12(11): 2998-3006.
[11] Coolen, M. J., Orsi, W. D. (2015): The transcriptional response of microbial communities in thawing Alaskan permafrost soils. – Frontiers in Microbiology 6(6): 197.
[12] Cowan, D. A., Russell, N., Mamais, A., Sheppard, D. M. (2002): Antarctic Dry Valley mineral soils contain unexpectedly high levels of microbial biomass. – Extremophiles 6: 431-436.
[13] Cox, P. M., Betts, R. A., Jones, C. D., Spall, S. A., Totterdell, I. J. (2000): Acceleration of global warming due to carbon-cycle feedbacks in a coupled climate model. – Nature 408(6809): 184-187.
[14] Das, S., Ganguly, D., Mukherjee, A., Chakraborty, S., De, T. K. (2017): Soil urease activity of Sundarban Mangrove Ecosystem, India. – Advances in Microbiology 7(8): 617-632.
[15] Deane-Coe, K. K., Mauritz, M., Celis, G., Salmon, V., Schuur, E. A. G. (2015): Experimental warming alters productivity and isotopic signatures of tundra mosses. – Ecosystems 18(6): 1070-1082.
[16] Deng, J., Gu, Y., Zhang, J., Kai, X., Zhou, J. (2015): Shifts of tundra bacterial and archaeal communities along a permafrost thaw gradient in Alaska. – Molecular Ecology 24(1): 222-234.
[17] Dobbie, K. E., Smith, K. A. (2003): Nitrous oxide emission factors for agricultural soils in Great Britain: The impact of soil water - filled pore space and other controlling variables. – Global Change Biology 9(2): 204-218.
[18] Elberling, B., Michelsen, A., Schädel, C., Schuur, E. A. G., Christiansen, H., Berg, L., Tamstorf, M. P., Sigsgaard, C. (2013): Long-term CO_2 production following permafrost thaw. – Nature Climate Change 3(10): 890.
[19] Feng, H., Ma, X., Zhang, G., Bai, Y., Fei, G. Q., Cheng, G. D., An, L. Z., Liu, G. X. (2004): Culturing and counting the microbial cells in permafrost on the Tibetan Plateau. – Journal of Glaciology and Geocryology 26(2): 182-187.
[20] Feng, R. F., Yang, W. Q., Zhang, J., Deng, R. J., Jian, Y., Lin, J. (2007): Effects of simulated elevated atmospheric CO_2 concentration and temperature on soil enzyme activity in the subalpine fir forest. – Acta Ecologica Sinica 27(10): 4019-4026.
[21] Feng, J., Penton, C. R., He, Z., Nostrand, J. D. V., Yuan, M. M., Wu, L. Y., Wang, C., Qin, Y. J., Shi, Z. J., Guo, X. (2019): Long-Term warming in Alaska Enlarges the diazotrophic community in deep soils. – mBio 10(1): e02521-18.
[22] Feng, J. J., Wang, C., Lei, J. S. (2020): Warming-induced permafrost thaw exacerbates tundra soil carbon decomposition mediated by microbial community. – Microbiome 8: 3. https://doi.org/10.1186/s40168-019-0778-3.
[23] Fierer, J. (2006): The diversity and biogeography of soil bacterial communities. – Proceedings of the National Academy of Science of the United States of America 103(3): 626.
[24] Friedlingstein, P., Cox, P., Betts, R., Bopp, L., Bloh, W. V., Brovkin, V., Cadule, P., Doney, S., Eby, M., Fung, I. (2006): Climate-carbon cycle feedback analysis: Results from the C^4MIP model inter comparison. – Journal of Climate 19(14): 3337-3353.
[25] Ganzert, L., Lipsk, A., Hubberten, H. W., Dirk, W. (2011): The impact of different soil parameters on the community structure of dominant bacteria from nine different soil located on Livingston island, South Shetland Archipelago, Antarcica. – Microbiology Ecology 76(3): 476-491.
[26] Geng, S. C., Chen, Z. J., Zhang, J. H., Lou, X., Wang, X. X., Dai, G. H., Han, S. J., Yu, D. D. (2013): Soil methane fluxes of three forest types in Changbai Mountain of northeast China. – Chinese Journal of Ecology 32(5): 1091-1096.

http://www.aloki.hu ● ISSN 1589 1623 (Print) ● ISSN1785 0037 (Online)
DOI: http://dx.doi.org/10.15666/aeer/2001_265283

[27] Gilichinsky, D. A., Khlebnikova, G. M., Zvyagintsev, D. G., Fedorov-Davydov, D. G., Kudryavtseva, N. N. (1989): Microbiology of sedimentary materials in the permafrost zone. – International Geology Review 31(8): 847-858.
[28] Goncalves, V. N., Vaz, A. B. M., Rosa, C. A., Rosa, L. H. (2012): Diversity and distribution of fungal communities in lakes of Antarctica. – FEMS Microbiology Ecology 82: 459-471.
[29] Grogan, P., Chapin Ⅲ, F. S. (2000): Initial effects of experimental warming on above-and belowground components of net ecosystemCO_2 exchange in Arctic tundra. – Oecologia 1250: 512-520.
[30] Grosse, G., Goetz, S., McGuire, A. D., Romanovsky, V. E., Schuur, E. A. G. (2016): Changing permafrost in a warming world and feedbacks to the Earth system. – Environmental Research Letters 11(4): 040201.
[31] Guo, X., Feng, J., Shi, Z., Zhou, X., Yuan, M., Tao, X., Lauren, H., Yuan, T., Wang, J., Qin, Y. (2018): Climate warming leads to divergent succession of grassland microbial communities. – Nature Climate Change 8(9): 813-818.
[32] Haeberli, W., Hohmann, R. (2008): Climate, glaciers and permafrost in the Swiss Alps 2050: Scenarios, consequences and recommendations. – In: Kane, D. L., Hinkel, K. M. (eds.) Proceedings, Ninth International Conference on Permafrost. Institute of Northern Engineering, University of Alaska Fairbanks: Alaska, USA, pp. 607-612.
[33] Hansen, A. A., Herbert, R. A., Mikkelsen, K., Jensen, L. L., Kristoffersen, T., Tiedje, J. M., Lomstein, B. A., Kai, W. F. (2007): Viability, diversity and composition of the bacterial community in a high Arctic permafrost soil from Spitsbergen, Northern Norway. – Environmental Microbiology 9(11): 2870-2884.
[34] Hao, Z., Li, L., Fu, Y., Liu, H. (2018): The influence of bioregenerative life-support systemdietary structure and lifestyle on the gut microbiota: a 105-day ground based space simulation in Lunar Palace 1. – Environmental microbiology 20(10): 3643-3656.
[35] Hassan, N., Rafiq, M., Hayat, M., Shah, A. A., Hasan, F. (2016): Psychrophilic and psychrotrophic fungi: a comprehensive review. – Reviews in Environmental Science and Biotechnology 15: 147-172.
[36] Hayes, D. J., Kicklighter, D. W., Mcguire, A. D., Chen, M., Zhuang, Q., Yuan, F., Melillo, J. M., Wullschleger, S. D. (2014): The impacts of recent permafrost thaw on land-atmosphere greenhouse gas exchange. – Environmental Research Letters 9: 45005.
[37] Horowitz, N. H., Cameron, R. E., Hubbard, J. S. (1972): Microbiology of the dry valleys of Antarctica. – Science 176: 242-245.
[38] Hultman, J., Waldrop, M. P., Mackelprang, R., David, M. M., McFarland, J., Blazewicz, S. J., Harden, J., Turetsky, M. R., Mcguire, A. D., Shah, M. B. (2015): Multi-omics of permafrost, active layer and thermokarst bog soil microbiomes. – Nature 521(7551): 208.
[39] Huntington, T. G. (2006): Evidence for intensification of the global water cycle: Review and synthesis. – Journal of Hydrology 319(1): 83-95.
[40] IPCC (2013): Climate Change 2013: The Physical Science Basis. – Contribution of Working Group I to Fifth Assessment Report of the Intergovernmental Panel on Climate Change.
[41] Jin, H. J., Li, S. X., Cheng, G. D., Wang, S. L., Xin, L. (2000): Permafrost and climatic change in China. – Global and Planetary Change 26(4): 387-404.
[42] Jin, H. J., Yu, Q. H., Guo, D. X., Li, Y. (2007): Degradation of permafrost in the Xing'anling Mountains, Northeastern China. – Permafrost and Periglac Process 18: 245-258.
[43] Johnson, L. C., Shaver, U. R., Cades, D. H., Rastetter, E., Nadelhoffer, K., Giblin, A., Stanley, L. A. (2000): Plant carbon-nutrient interactions control CO_2 exchange in Alaskan wet sedge tundra ecosystems. – Ecology 81(2): 453-469.
[44] Lawrence, D. M., Koven, C. D., Swenson, S. C., Riley, W. J., Slater, A. G. (2015): Permafrost thaw and resulting soil moisture changes regulate projected high-latitude CO_2 and CH_4 emissions. – Environmental Research Letters 10(9): 094011.

http://www.aloki.hu ● ISSN 1589 1623 (Print) ● ISSN1785 0037 (Online)
DOI: http://dx.doi.org/10.15666/aeer/2001_265283

[45] Li, L., Lei, G. C., Gao, J. Q., Lv, S., Zhou, Y., Jia, Y. F., Yang, M., Duoerji, S. (2011): Effect of water table and soil water content on methane emission flux at Carex muliensis marshes in Zoigê Plat-Eau. – Wetland Science 9(2): 173-178.
[46] Luo, Y. (2007): Terrestrial carbon-cycle feedback to climate warming. – Annual Review of Ecology, Evolution and Systematics 38(1): 683-712.
[47] Lydolph, M. C., Jacobsen, J., Arctander, P., Gilbert, M. T. P., Gilichinsky, D. A., Hansen, A. J., Willerslev, E., Lange, L. (2005): Beringian paleocology inferred from permafrost-preserved fungal DNA. – Applied and Environmental Microbiology 71: 1012-1017.
[48] Mao, D. H., Wang, Z. M., Luo, L., Han, J. X. (2012): Dynamic changes of vegetation net primary productivity in permafrost zone of Northeast China in 1982-2009 in response to global change. – Chinese Journal of Applied Ecology 23(6): 1511-1519.
[49] Melillo, J. M., Steudler, P. A., Aber, J. D., Newkirk, K., Morrisseau, S. (2002): Soil warming and carbon-cycle feedbacks to the climate system. – Science 298(5601): 2173-2176.
[50] Mikan, C. J., Schimel, J. P., Doyle A P. (2002): Temperature controls of microbial respiration in arctic tundra soils above and below freezing. – Soil Biology and Biochemistry 34(11): 1785-1795.
[51] Mu, C. C., Abbott, B. W., Zhao, Q., Wang, S. F., Wu, Q. B., Zhang, T. J. (2017): Permafrost collapse shifts alpine tundra to a carbon source but reduces N_2O and CH_4 release on the northern Qinghai-Tibetan Plateau. – Geophysical Research Letters 44(17): 8945-8952.
[52] Muhlmann, O., Peintner, U. (2008): Mycobionts of Salix herbacea on a glacier forefront in the Austrian Alps. – Mycorrhizae 18: 171-180.
[53] Nakatsubo, T., Bekku, Y. S., Uchida, M., Muraoka, H., Kume, A., Ohtsuka, T., Masuzawa, T., Kanda, H., Koizumi, H. (2005): Ecosystem development and carbon cycle on a glacier foreland in the high Arctic, Ny-Alesund, Sralbard. – J Plant Res 118(3): 173-179.
[54] Natali, S. M., Schuur, E. A. G., Rubin, R. L. (2012): Increased plant productivity in Alaskantundra as a result of experimental warming of soil and permafrost. – Journal of Ecology 100(2): 488-498.
[55] Natali, S. M., Schuur, E. A. G., Mauritz, M., Schade, J. D., Celis, G., Crummer, K. G., Johnston, C., Krapek, J., Pegoraro, E., Salmon, V. G. (2015): Permafrost thaw and soil moisture driving CO_2 and CH_4 release from upland tundra. – Journal of Geophysical Research Biogeosciences 120(3): 525-537.
[56] Nemani, R. R. (2003): Climate driven increases in global terrestrial net primary production from 1982 to 1999. – Science 300(5625): 1560-1563.
[57] Parkinson, S. V. D. (2009): Soil biological criteria as indicators of soil quality: Soil microorganisms. – American Journal of Alternative Agriculture 7(1): 33-37.
[58] Ping, C. L., Jastrow, J. D., Jorgenson, M. T., Michaelson, G. J., Shur, Y. L. (2015): Permafrost soils and carbon cycling. – Soil Discussions 1(1): 147-171.
[59] Post, W. M., Emanuel, W. R., Zinke, P. J., Stangenberger, A. G. (1982): Soil carbon pools and world life zones. – Nature 298(5870): 156-159.
[60] Pries, C. E. H., Schuur, E. A., Natali, S. M., Crummer, K. (2016): Old soil carbon losses increase with ecosystem respiration in experimentally thawed tundra. – Nature Climate Change 6(2): 214.
[61] Puser, R., Flessah, H., Russow, R., Schmidt, G., Buegger, F., Munch, J. C. (2006): Emission of N_2O, N_2 and CO_2 from soil fertilized with nitrate: Effect of compaction, soil moisture and rewetting. – Soil Biology and Biochemistry 38(2): 263-274.
[62] Qin, Y., Yi, S. H., Li, N. J. (2012): Advance in studies of carbon cycling on alpine grasslands of the Qinghai-Tibetan Plateau. – Acta Prata culturae Sinica 21(6): 275-285.
[63] Rustad, L., Campbell, J., Marion, G., Norby, R., Mitchell, M., Hartley, A., Cornelissen, J., Gurevitch, J. (2001): A meta-analysis of the response of soil respiration, net nitrogen mineralization, and aboveground plant growth to experimental ecosystem warming. – Oecologia 126(4): 513-562.

http://www.aloki.hu ● ISSN 1589 1623 (Print) ● ISSN1785 0037 (Online)
DOI: http://dx.doi.org/10.15666/aeer/2001_265283

[64] Ryberg, M., Larsson, E., Molau, U. (2009): Ectomycorrhizal diversity on Dryas octopetala and Salix reticulata in an alpine cliff ecosystem. Arctic. – Antarctic and Alpine Research 41: 506-514.
[65] Salmon, V. G., Soucy, P., Mauritz, M., Celis, G., Natali, S. M., Mack, M. C., Schuur, E. A. G. (2016): Nitrogen availability increases in a tundra ecosystem during five years of experimental permafrost thaw. – Global Change Biology 22(5): 1927-1941.
[66] Schaefer, K., Lantuit, H., Romanovsky, V. E., Schuur, E. A. G., Witt, R. (2014): The impact of the permafrost carbon feedback on global climate. – Environmental Research Letters 9(8): 085003.
[67] Schmitt, A., Glaser, B., Borken, W., Schuur, E. A. G., Witt, R. (2008): Repeated freeze-thaw cycles changed organic matter quality in a temperate forest soil. – Journal of Plant Nutrition and Soil Science 171: 707-718.
[68] Scholler, M., Schnittler, M., Piepenbring, M. (2003): Species of Anthracoidea (Ustilaginales, Basidiomycota) on Cyperaceae in Arctic Europe. – Nova Hedwigia 76: 415-428.
[69] Schuur, E. A. G., Mcguire, A. D., Schädel, C., Grosse, G., Harden, J. W., Hayes, D. J., Hugelius, G., Koven, C. D., Kuhry, P., Lawrence, D. M., Natali, S. M., Olefeldt, D., Romanovsky, V. E., Schaefer, K., Turetsky, M. R., Treat, C. C., Vonk, J. E. (2015): Climate change and the permafrost carbon feedback. – Nature 520(7546): 171.
[70] Shannon, M. H., Bhavaraju, L., Jorge, L. M. R., Corien, B., Gilichinsky, D. A., Tiedje, J. M. (2010): Characterization of abacterial community from a Northeast Siberianseacoast permafrost sample. – Microbiology Ecology 74(1): 103-113.
[71] Singh, B. K., Bardgett, R. D., Smith, P., Reay, D. S. (2010): Microorganisms and climate change: terrestrial feedbacks and mitigation options. – Nature Reviews Microbiology 8(11): 779-790.
[72] Smith, K. A., Thomson, P. E., Clayton, H., McTaggart, I. P., Conen, F. (1998): Effects of temperature, water content and nitrogen fertilization on emissions of nitrous oxide by soils. – Atmospheric Environment 32(19): 3301-3309.
[73] Song, C. C., Wang, X. W., Miao, Y. Q. (2013): Effects of permafrost thaw on carbon emissions under aerobic and anaerobic environments in the Great Hing'an Mountains China. – Science of the Total Environment 487(1). http://dx.doi.org/10.1016/j.scitotenv.09.083.
[74] Song, C. C., Wang, Y. Y., Wang, Y. S., Zhao, Z. C. (2014): Dynamics of CO_2, CH_4 and N_2O emission fluxes from mires during freezing and thawing season. – Environmental Science 26(4): 7-12.
[75] Stchigel, A. M., Guarro, J., Cormack, W. M. (2003): Apiosordaria antarctica and Thielavia antarctica, two new ascomycetes from ntarctica. – Mycologia 95: 1218-1226.
[76] Steven, B., Briggs, G., McKay, C. P., Pollard, W. H., Greer, C. W., Whyte, L. G. (2007): Characterization of the microbial diversity in a permafrost sample from the Canadian high Arctic using culture-dependent and culture-independent methods. – FEMS Microbiology Ecology 59: 513-523.
[77] Turetsky, M. R., Abbott, B. W., Jones, M. C., Anthony, K. W., Olefeldt, D., Schuur, E. A. G., Grosse, G., Kuhry, P., Hugelius, G., Koven, C. (2020): Carbon release through abrupt permafrost thaw. – Nature Geoscience 13: 138-143.
[78] Vishnivetskaya, T. A., Petrova, M. A., Urbance, J., Ponder, M., Moyer, C. L., Gilichinsky, D. A., Tiedje, J. M. (2006): Bacterial community in ancient Siberian permafrost as characterized by culture and culture-independent methods. – Astrobiology 6(3): 400-414.
[79] Vorobyova, E., Soina, V., Gorlenko, M., Minkovskaya, N., Zalinova, N., Mamukelashvili, A., Gilichinsky, D., Rivkina, E., Vishnivetskaya, T. (1997): The deep cold biosphere: facts and hypothesis. – FEMS Microbiol Reviews 20(3-4): 277-290.
[80] Walther, G. R., Post, E., Convey, P., Menzel, A., Parmesan, C., Beebee, T. J. C., Fromentin, J., Hoegh-Guldberg, O., Bairlein, F. (2002): Ecological responses to recent climate change. – Nature 416(6879): 389-395.

http://www.aloki.hu ● ISSN 1589 1623 (Print) ● ISSN1785 0037 (Online)
DOI: http://dx.doi.org/10.15666/aeer/2001_265283

[81] Wan, S., Luo, Y., Wallace, I. L. (2002): Changes in microclimate induced by experimental warming and clipping in tallgrass prairie. – Global Change Biology 8(8): 754-768.
[82] Wang, C. R., Huang, G. H., Liang, Z. B., Wu, J., Xu, G. Q., Yue, J., Shi, J. (2002): Advances in the research on sources and sinks of CH_4 and CH_4 oxidation (uptake) in soil. – Chinese Journal of Applied Ecology 13(12): 1707-1712.
[83] Wang, M., Jiang, X., Wu, W., Hao, Y., Su, Y., Cai, L., Xiang, M., Liu, X. (2015): Psychrophilic fungi from the world's roof. – Persoonia 34: 100-112.
[84] Wang, D. X., Gao, Y. H., An, X. J., Wang, R., Xie, Q. Y. (2016): Responses of greenhouse gas emissions to water table fluctuations in an alpine wetland on the Qinghai-Tibetan Plateau. – Acta Prataculturae Sinica 25(8): 27-35.
[85] Webb, E. E., Schuur, E. A. G., Natali, S. M., Oken, K. L., Bracho, R., Krapek, J. P., Risk, D., Nickerson, N. R. (2016): Increased wintertime CO_2 loss as a result of sustained tundra warming. – Journal of Geophysical Research: Biogeosciences 121(2): 249-265.
[86] Welker, J. M., Fahnestock, J. T., Henry, G. H. R., O'Dea, K. W., Chimner, R. A. (2004): CO_2 exchange in three Canadian High Arctic ecosystems; response to long-term experimental warming. – Global Change Biology 10(12): 1981-1995.
[87] Wu, X., Brggemann, N., Gasche, R., Shen, Z. Y., Wolf, B., Butterbach-Bahl, K. (2010): Environmental controls over soil atmosphere exchange of N_2O, NO and CO_2 in a temperate Norway spruce forest. – Global Biogeochemical Cycles 24(2): 1-16.
[88] Xu, X. F., Tian, H. Q., Wan, S. Q. (2007): Climate warming impacts on carbon cycling in terrestrial ecosystems. – Journal of Plant Ecology 31(2): 175-188.
[89] Xue, K., Yuan, M. M., Shi, Z. J., Qin, Y., Deng, Y., Cheng, L., Wu, L., He, Z., Nostrand, V., Nostrand, J. D. V., Bracho, R., Natali, S., Schuur, E. A. G., Luo, C., Konstantinidis, K. T., Wang, Q., Cole's, J. R., Tiedje, J. M., Luo, J. Q., Zhou, J. Z. (2016): Tundra soil carbon is vulnerable to rapid microbial decomposition under climate warming. – Nature Climate Change 6(6): 595.
[90] Yakushev, A. V., Kuznetsova, I. N., Blagodatskaya, E. V., Blagodatsky, S. A. (2014): Temperature dependence of the activity of polyphenol peroxidases and polyphenol oxidases in modern and buried soils. – Eurasian Soil Science 47(5): 459-465.
[91] Yang, G., Peng, Y., Olefeldt, D., Chen, Y., Wang, G., Li, F., Zhang, D., Wang, J., Liu, L., Qin, S., Sun, T., Yang, Y. (2018): Changes in methane flux along a permafrost thaw sequence on the Tibetan Plateau. – Environmental Science & Technology 52(3): 1244-1252.
[92] Yao, X. H., Min, H., Lu, Z. H., Yuan, H. P. (2006): Influence of acetamiprid on soil enzymatic activities and respiration. – European Journal of Soil Biology 42: 120-126.
[93] Yu, J. B., Liu, J. S., Sun, Z. G., Wang, J., Yang, J., Meixner, F. X. (2009): N_2O and CH_4 fluxes and influencing factors in fresh marshes in northeastern China. – Science in China Press (Ser. D Earth Sciences) 39(2): 177-187.
[94] Zak, D. R., Holmes, W. E., Macdonald, N. W., Pregitzer, K. S. (1999): Soil Temperature, Matric Potential, and the Kinetics of Microbial Respiration and Nitrogen Mineralization. – Soil Science Society of America Journal 63(3): 575-584.
[95] Zhang, G., Ma, X., Niu, F., Dong, M., Feng, H., An, L., Cheng, G. (2007): Diversity and distribution of alkaliphilic psychrotolerant bacteria in the Qinhai-Tibet Plateau permafrost region. – Exteremophiles 11: 415-424.
[96] Zhang, T., Yao, Y. F. (2015): Endophytic fungal communities associated with vascular plants in the high Arctic zone are highly diverse and hostplant specific. – PLOS One 10(6): e0130051.
[97] Zhang, Y., Ling, J., Yang, Q., Wen, C., Yan, Q., Sun, H., Nostrand, J. D. V., Shi, Z., Zhou, J., Dong, J. (2015): The functional gene composition and metabolic potential of coral-associated microbial communities. – Scientific reports 5: 16191.
[98] Zhou, X., Wang, S. J., Chen, C. (2017): Modeling the effects of tree species and temperature on soil's extracellular enzyme activity in 78-year-old tree plantations. – Biogeosciences 14: 5393-5402.

http://www.aloki.hu ● ISSN 1589 1623 (Print) ● ISSN1785 0037 (Online)
DOI: http://dx.doi.org/10.15666/aeer/2001_265283

[99] Zhou, J. Z., Yang, Y. F. (2020): Warming-induced permafrost thaw exacerbates tundrasoil carbon decomposition mediated by microbial community. – Microbiome. On line.
[100] Zhu, J. T., Chen, N., Zhang, Y. J., Liu, Y. J. (2016): Effects of experimental warming on net ecosystem CO_2 exchange in northern Xizang alpine meadow. – Chinese Journal of Plant Ecology 40(12): 1219-1229.

http://www.aloki.hu ● ISSN 1589 1623 (Print) ● ISSN1785 0037 (Online)
DOI: http://dx.doi.org/10.15666/aeer/2001_265283

ANALYSIS OF THE EFFECTS OF SOME ECOLOGICAL FACTORS ON UDDER HEALTH BY USING NONLINEAR REGRESSION MODELS

ÖZTÜRK, I.

Department of Animal Science, Biometry Genetics Unit, Agricultural Faculty, Harran University, Şanlıurfa, Turkey
(e-mail: ozirfan23@yahoo.com; phone: +90-505 665 7583; fax: phone: +90-414-318-1431)

(Received 30th Jul 2021; accepted 28th Oct 2021)

Abstract. Mastitis is an important udder disease causing loss of yield in dairy cattle farming and environmental factors that play a significant role in the emergence of the disease. Factors, such as infectious diseases, live weight, cattle breed, nutritional status, environment and milking hygiene, which are thought to affect the presence of mastitis disease were discussed in the study. The data of the study was obtained randomly from the records of veterinarians and small and medium-sized enterprises operating in the two provinces of Turkey. Based on these results, we found that the environment and milking hygiene, and adequate and balanced nutrition would lead to a 6.2%, 11.3%, and 94.9% lower risk on mastitis, respectively. Of the other hand, it was determined that cattle with various symptoms of infectious diseases had a 4.3 times greater risk of mastitis than healthy cattle. It was concluded that taking into account the impact rates of factors affecting the risk of mastitis of enterprises, it can contribute to the prevention of milk yield losses.
Keywords: *mastitis, milking hygiene, environmental factors, Probit and Logit regression*

Introduction

Mastitis disease is one of the biggest problems that cause yield losses in milk production enterprises. It is reported that more than 130 microorganisms cause the occurrence of mastitis (Lakew et al., 2009; Tel et al., 2009). Mastitis is observed in two ways depending on the clinical course. The first is subclinical mastitis, which is not taken seriously by farmers because it is invisible to the eye and can be described as a latent disease, while the other is clinical mastitis, which is manifested by symptoms such as hardening, swelling, flushing in the udder tissue (Ndahetuye et al., 2020; Cobirka et al., 2020). Mastitis disease causes milk yield losses both directly and indirectly. The direct effect of mastitis is the milk yield loss caused by the damages in udder tissue over time. On other hand, losses that it causes in reproductive performance and increases that it causes in treatment expenses can be shown as examples of the indirect effect of mastitis (Özyurt, 2013).

Research results noted a negative correlation between mastitis and reproductive performance (Chebel et al., 2004). This may indirectly affect milk yield losses in cases where there is failure to conceive or due to delayed insemination. Guimaraes et al. (2017) reported that cattle might suffer from milk loss up to 77% due to mastitis during the lactation period. In the studies conducted in different periods in Turkey, mastitis findings showing differences between 5% and 60% by provinces were encountered (Sabuncuoğlu et al., 2003; Kılıç and Keskin, 2019). Mastitis is not only a problem in the undeveloped countries, but also always an important risk factor in modern dairy farming enterprises in developed countries. In a study conducted in the Netherlands, as a developed country on dairy cattle breeding, it was found that 38% of dairy cattle (Rougoor et al., 1999) had mastitis, while in another study conducted in dairy farming enterprises in France, it was

http://www.aloki.hu ● ISSN 1589 1623 (Print) ● ISSN1785 0037 (Online)
DOI: http://dx.doi.org/10.15666/aeer/2001_285299

reported that 29% of cows had mastitis (Longo et al., 2001; Sabuncuoğlu and Çoban, 2006).

Given the large economic losses caused by mastitis disease in dairy farming enterprises, it is clear that the impact rates of the factors causing mastitis should be determined by appropriate regression models. The presence of mastitis disease discussed here and some of the factors affecting it are qualitative (categorical) variables, and some are continuous variables. Since qualitative variables indicate the presence or absence of a characteristic, the way to digitize these characteristics is to create dummy variables that take values of 0 and 1 (Gujarati and Porter, 2009; Güneri and Durmuş, 2020). In the model created in this study, like independent variables, dependent variables include Bernoulli random variables consisting of categorical data with two options (1/0).

The risk of mastitis in cattle is not only microbial, but also under the influence of some environmental factors. For example, this disease can also develop due to many environmental factors such as weather conditions, age, weight, nutrition and care status of the animal (Mekonnen et al., 2017; Jamali et al., 2018; Özenç, 2019). In order to model mastitis findings under the influence of these factors, instead of the least-squares (LS) method, it is necessary to take advantage of approaches that better explain binary dependent variables (Long and Freese, 2014; Mert, 2016). For this purpose, by using Logit and Probit regression models, it was attempted to explain the impact rates of factors that could cause the presence of mastitis disease leading to a significant loss of yield in dairy cattle. In this way, it is aimed to draw attention to the effect rates of some environmental factors that will reduce mastitis to the lowest incidence.

Materials and Methods

The research was carried out in 2020 in Adıyaman (37.763650; 38.277259, GPS: 37° 45' 49.14" N 38° 16' 38.132" E) and Şanlıurfa (37.167404; 38.795515; GPS: 37° 10 '2.654" N 38° 47' 43.854 " E) provinces taking place in the Southeastern Anatolia region of Turkey. The data were obtained randomly from some small (1 to 10 head) and medium-sized (11 to 100 head) cattle enterprises located in the rural area in question. For this purpose, the records of veterinarians serving in the region were also used. In the records, information such as cattle's earring numbers, breeds, farms in which they are located, disease symptoms, body weight, age, and artificial insemination was reached. Cattle with missing registration information and some variables were eliminated, and data obtained from the remaining 180 dairy cattle were used. By visiting the 69 enterprises where the cattle in question were registered, feeding conditions, and environment and milking hygiene of cattle were observed. In addition, as a result of a survey conducted with owners of the enterprises, factors related to the environment and milking hygiene were scored with values between 0 and 100 points. Descriptions related to the dependent and independent variables to be included in the regression model are given in *Table 1*.

The presence of mastitis in dairy cattle in the enterprises was defined as a dependent variable (Y). Whether there was mastitis (1) or not (0) was coded as a binary categorical variable. The live weight of cattle, which were considered as independent variable, was defined by X_1 and its unit was kg. Environmental hygiene (X_2) and milking hygiene (X_3) in the enterprises were scored between zero and one hundred (0-100).

http://www.aloki.hu ● ISSN 1589 1623 (Print) ● ISSN1785 0037 (Online)
DOI: http://dx.doi.org/10.15666/aeer/2001_285299

Table 1. *Descriptions of dependent and independent (explanatory) variables*

Variables	Meaning of the variable	Description	Codding
Dependent (Y)	Mastitis	Whether or not there is mastitis in cattle in randomly determined enterprises	Mastitis yes=0 (Reference) Mastitis no=1
Independent			
(X_1)	Live weight	Live weight of the cattle (Continuous variable)	kg
(X_2)	Environmental hygiene	Hygiene status of the enterprise: scored between 0 and 100	Low score = poor hygiene High score = good hygiene
(X_3)	Milking hygiene	Whether attention is paid to milking hygiene: scored between 0 and 100.	Low score = poor hygiene High score= high hygiene
(X_4)	Infectious disease	Whether cattle have any infectious diseases (categorical variable)	No disease=0 (reference) Have disease = 1
(X_5)	Nutrition	Balanced nutritional status of dairy cattle	Malnutrition =0 (Reference) Adequate Nutrition = 1
(X_6)	Cattle breed	Breeds of cattle in the enterprises (categorical variable)	Local breed = 1(Reference) Holstein friesian = 2 Simmental = 3

A low score indicates that hygiene is poor and bad, while a high score indicates that hygiene conditions are good. Environmental and milking hygiene scores were categorized as in *Table 2*. As can be seen in *Table 2*, 20 points were given for each operation performed by farmers in terms of environmental and milking hygiene; thus, the enterprise performing all expected operations earned a score of 100.

Table 2. *Classification of scores given for environmental and milking hygiene procedure.*

	Hygiene procedure	
Scores	**Environmental hygiene**	**Milking hygiene**
1-(20%)	Dry base	Simple udder and teat cleaning
2-(40%)	Material hygiene	Application of disinfectant to teats before milking
3-(60%)	Periodic environmental disinfection	Cleaning with disposable cloths
4-(80%)	Disinfecting shoes at the entrance to the enterprise	Cleaning milk residues at the end of milking
5-(100%)	Outsiders are not allowed to enter into the enterprise and milking households	Applying teat dipping at the end of milking

Whether the cattle in question had any infectious diseases was defined by X_4. Cattle that had disease were coded by "1", while cattle that did not have disease were accepted as references and coded by "0". The nutritional status defined as X_5 was coded by "1" if the cattle were fed with an adequate and balanced ration, and by "0" if they were fed insufficiently and with haphazard feed. Cattle breeds in the enterprises (X_6) were coded as local breed (1), Holstein (2), and Simmental (3). Local breed was accepted as the reference. In the region in general, as a local breed, there is South Anatolian Red (SAR), which is adapted to hot climatic conditions.

In short, as seen in *Table 1*, the dependent variable is a binary variable, while the independent variables are categorical, binary categorical, and continuous variables. In regression model estimations to be made by LS method, problems such as the occurrence

http://www.aloki.hu ● ISSN 1589 1623 (Print) ● ISSN1785 0037 (Online)
DOI: http://dx.doi.org/10.15666/aeer/2001_285299

of the problem of changing variance, non-normal distribution of residues, or the loss of the importance of the coefficient of determination (R^2) can be encountered due to the fact that the dependent variable is a binary categorical variable. Therefore, it is more convenient to use the logistic model whose parameters are estimated iteratively by the maximum likelihood method (Mert, 2016).

In Logit and Probit regression approaches, assumptions that are in the LS method are not sought. The only assumption is that the dependent variable is a binary categorical variable such as successful-unsuccessful and sick-healthy (1 and 0). For independent variables, there is not any restriction. In other words, independent variables can be nominal, ordinal, or continuous. The most basic difference between the Logit model and the Probit model is that while the Logit model uses the logistic odds ratio (the odds ratio is the probability obtained by dividing the probability of an event occurring by the probability of it not occurring), the Probit model uses the Gaussian distribution function. In logistic regression, the probability of the interested event is P_i, and the dependent variable is shown as ln (P_i/(1-P_i)) and it is defined as a Logit function (İnal et al., 2006; Mert, 2016).

Logit regression model

In logistic regression analysis, as in other model configuration methods, the goal is to create the best prediction model with minimum independent variables. As in linear regression, in logistic regression analysis, estimates are tried to be made based on some variables. However, in linear regression, the value of the dependent variable is tried to be estimated by using independent variables, while in logistic regression, the probability of occurrence of one of the values that the dependent variable can take is calculated (Montgomery et al., 2012).

Logistic regression is a powerful alternative method that could be used in conditions where the assumptions of other methods cannot be met. Moreover, Nusinovici et al. (2020) reported that the estimation performance of the logistic regression was at least as good as machine learning techniques in some studies. Logistic regression refers to models that reveal the shape of the relationship between weak-scale (categorical) variables.

The basis of the logistic regression model is based on the odds ratio. The odds ratio is obtained by dividing the probability of an event occurring by the probability of the event not occurring. By taking the natural logarithm of the ratio in question (odds), the parameters of the logistic regression model are estimated using the Maximum Likelihood method (Gujarati and Porter, 2009).

Signs of the coefficients belonging to the independent variables in the estimated model show the direction of the relationship. A positive coefficient indicates that the probability of occurring of an event will increase, and a negative coefficient indicates that it will decrease. Another meaning of negative coefficients is that the odds ratio is less than 1 and its probability is less than 0.5. The fact that the coefficient is zero means that the probability of occurring of an event will not change (Mert, 2016).

In binary logistic regression analysis, the functions given in *Eq.1* and *Eq.2* are used.

$$P(Y) = \frac{e^z}{1+e^z} = \frac{1}{1+e^{-z}} \quad \text{(Eq.1)}$$

$$P(Y) = \frac{e^{\beta_0+\beta_1 X}}{1+e^{\beta_0+\beta_1 X}} = \frac{1}{1+e^{-(\beta_0+\beta_1 X)}} \quad \text{(Eq.2)}$$

http://www.aloki.hu ● ISSN 1589 1623 (Print) ● ISSN1785 0037 (Online)
DOI: http://dx.doi.org/10.15666/aeer/2001_285299

In case of multivariate model, Z value in *Eq.1* is written as in *Eq.3*

$$Z = \beta_0 + \beta_1 X_1 + \beta_2 X_2 + \cdots + \beta_p X_p \quad \text{(Eq.3)}$$

Beta (β_i) parameters in *Eq.3*; $\beta_0, \beta_1, \beta_2, \ldots, \beta_P$ are the coefficients of the logistic regression.

Calculation of logistic regression parameter coefficients is performed as follows.

If *Q(Y)=1-P(Y)*, the odds ratio is found as:

$$\frac{P(Y)}{Q(Y)} = \frac{P(Y)}{1-P(Y)} = \frac{\frac{e^Z}{(1+e^Z)}}{1-\frac{e^Z}{(1+e^Z)}} = e^Z = e^{\beta_0+\beta_1 X_1+\beta_2 X_2+\cdots+\beta_p X_p} \quad \text{(Eq.4)}$$

If the natural logarithm of both sides of the odds ratio equation (*Eq.4*) is taken, *Eq.5* is obtained;

$$\ln \frac{P(Y)}{Q(Y)} = \beta_0 + \beta_1 X_1 + \beta_2 X_2 + \cdots + \beta_p X_p \quad \text{(Eq.5)}$$

If the ratio of two separate odds values to each other is calculated, the odds ratio (OR) is obtained:

$$OR = \frac{P(Y)}{Q(Y)} = e^Z = e^{\beta_0+\beta_1 X_1+\beta_2 X_2+\cdots+\beta_p X_p} = Exp(\beta) \quad \text{(Eq.6)}$$

In *Eq.6*, the *Exp(β)* values of each parameter are taken as values of the odds ratio. Thus, *Exp (β)* indicates how likely (or how many % more) the variable *Y* is observed under the influence of the variable X_P. The significance of the coefficient β_P is also considered as the significance of $OR_P = Exp(\beta_P)$ (Uzmay et al., 2001; Montgomery et al., 2012; Güneri and Durmuş, 2020).

Probit regression model

Probit analysis, as an alternative to logistic regression, is a model used to find the effect of one or more explanatory variables on a binary categorical response variable (alive-dead, working-not working, sold or not sold, etc.). Both logistic and probit regression analyses are quite similar to each other and the obtained probability estimates are close to each other. Log-odds are used in logistic regression analysis, while cumulative normal distribution is used in probit regression. In other words, the probit is the opposite of the cumulative standard normal distribution (Caffo and Griswold, 2006).

The assumption underlying the probit model is that the response function is in the form of $Y_i = \alpha + \beta X_i + U_i$. Here, X_i is a variable that can be observed but Y_i is a variable that cannot be observed. If $Y_i > 0$, $Y_i=1$, but if $Y_i < 0$, $Y_i = 0$. When assigning the result of the Y_i variable, the c value used as the threshold value is usually taken as zero (0), but another number value can also be used instead of zero (Demaris, 2004). If the cumulative normal distribution function *Φ (z)* is defined as *Φ (z) = P (Z≤z)* for the normal standard variable Z, it can be expressed as:

$$P(Yi = 1) = P(U_i > -\propto -\beta X_i) = 1 - \emptyset(\frac{-\propto -\beta X_i}{\sigma}) \quad \text{(Eq.7)}$$

http://www.aloki.hu ● ISSN 1589 1623 (Print) ● ISSN1785 0037 (Online)
DOI: http://dx.doi.org/10.15666/aeer/2001_285299

$$P(Yi = 0) = P(U_i \leq -\propto -\beta X_i) = \emptyset(\frac{-\propto -\beta X_i}{\sigma}) \quad \text{(Eq.8)}$$

When there is more than one explanatory variable in the Probit model, it is defined as Pr(Y=1/X) = ∅(Xβ). Here, Φ is the standard normal probability distribution. βX is called Probit score or index and has a normal distribution. Probit coefficient (β) refers to an increase that a unit increase in the estimate will make in the Probit score. The Probit coefficient measures the effect that the independent variable will have on the standard z-value of the dependent variable. The numerical magnitudes of these coefficients have no importance and no special interpretation; they only determine the direction and degree of the relationship (MacKinnon et al., 2007; Kulendran and Wong, 2011).

Results and Discussion

Description of dependent and independent variables belonging to 180 cattle randomly determined from the enterprises and their descriptive statistics are given in *Table 3*. In the table, the distribution of each variable by breeds, their means, standard deviations, standard errors, and the confidence interval values (limits) are summarized.

Table 3. *Descriptive statistics for dependent and independent variables*

Variable	(X_6) *Breed	Total Cow	Cow with mastitis	Proportion	SD	95% CI for p Lower - Upper
(Y) Mastitis	1	41	23	0.561	-	0.407-0.715
	2	67	32	0.477	-	0.357-0.598
	3	72	30	0.417	-	0.302-0.531
(X_4) Infectious diseases	1	41	23	0.561	-	0.407-0.715
	2	67	34	0.508	-	0.387-0.628
	3	72	38	0.528	-	0.412-0.644
(X_5) Nutrition	1	41	17	0.415	-	0.262-0.567
	2	67	29	0.433	-	0.313-0.552
	3	72	38	0.528	-	0.412-0.644
				Mean	**SD**	**95% CI for μ**
(X_1) Live weight	1	41	-	465.76	31.83	456.2- 475.3
	2	67	-	580.90	34.09	573.4- 588.4
	3	72	-	603.96	27.14	596.8- 611.2
(X_2)Environmental hygiene	1	41	-	43.05	24.05	36.05- 50.05
	2	67	-	49.57	20.98	44.09- 55.04
	3	72	-	53.47	23.48	48.19- 58.76
(X_3) Milking hygiene	1	41	-	52.39	20.74	46.02- 58.76
	2	67	-	55.24	20.60	50.25- 60.22
	3	72	-	58.85	20.71	54.04- 63.66

(X_6) = * Breed was coded as "1, 2, and 3": 1. Local breed, Southern Anatolian Red (SAR), 2. Holstein Friesian and 3. Simmental, SD: standard deviation, CI: confidence interval

Data of the study were analyzed and evaluated by using the Stata (2018) package program. The data were analyzed according to both the probit and logistic models. The fit statistics of the statistical results of the probit model obtained from the definition

http://www.aloki.hu ● ISSN 1589 1623 (Print) ● ISSN1785 0037 (Online)
DOI: http://dx.doi.org/10.15666/aeer/2001_285299

interval in the *Eq.7* and *Eq.8* are given in *Table 4*. Similarly, some fit statistics of the logit model are given in the same table for comparison.

Table 4. *Some goodness of fit statistics for Logistic and Probit regressions*

Goodness of fit criteria	Probit regression	P	Logit regression	P
LR CHI^2 (DF=7)	177.480	0.000	**179.770**	0.000
AIC	0.519	-	**0.507**	-
PSEUDO R^2	0.7128	-	**0.722**	-
Cragg & Uhler's R^2	0.837	-	**0.843**	-
Mckelvey and Zavoina's R^2	0.845	-	**0.859**	-
Log Likelihood	-35.749	-	**-34.605**	-
Hosmer Lemeshow CHI^2 (DF=8)	-	-	**12.212**	0.142

AIC: Akaike information criterion, LR chi^2: likelihood ratio chi-square test, DF: Degrees of freedom, P: probability

In general, the Probit and Logit regression analyses gave results close to each other. However, since we had to choose one of them in the interpretation of variables, it was required to look at the adaptation criteria. As can be seen in *Table 4*, all goodness of fit criteria and test criteria mainly point to the logit model. For example, the fact that the AIC value of the logit model is lower than the probit (0.519>0.507) indicates that logit is a better model. In addition, the fact that the Log Likelihood value of the logit model is higher than the probit model (-35.749<-34.605) again indicates that the logit model should be preferred. Moreover, the value of LR chi2 (179.77), which again plays an important role in the choice of the model, should be large and significant ($p<0.01$). Taking into account other criteria like these, it was decided to prefer the logit model and make evaluations on the results of this model.

The results obtained by running the following command in Stata (2018) program are given in *Table 5*. In addition, OR (Odds ratio Exp(B)) values obtained from *Eq.6* are given in the same *Table 5*:

$$Logit\ Y\ (X_1)\ (X_2)\ (X_3)\ i.(X_4)\ i.(X_5)\ i.(X_6)$$

Here, the infectious disease variable (X4) was significant at the level of $p<0.05$, while all other independent variables were significant at the level of $p<0.01$. This indicates that the independent variables are adequate in explaining the dependent variable.

Table 5. *Parameter estimates for the Logistic regression model*

Variables	Coefficient B	SEM	Wald	df	P	Odds ratio Exp(B)	95% CI for Exp(B)	
							Lower	Upper
(X_1) Live weight	0.043	0.012	12.721	1	0.000	1.044	1.019	1.068
(X_2)Environmental hygiene	-0.064	0.016	16.292	1	0.000	0.938	0.909	0.968
(X_3) Milking hygiene	-0.120	0.023	27.952	1	0.000	0.887	0.848	0.927
(X_4) Infectious disease (1)	1.449	0.671	4.659	1	0.031	4.257	1.143	15.859
(X_5) Nutrition (1)	-2.975	0.710	17.550	1	0.000	0.051	0.013	0.205
(X_6) Breed			9.643	2	0.008			
(X_6) Holstein(2)	-4.927	1.622	9.226	1	0.002	0.007	0.000	0.174
(X_6) Simmental(3)	-5.632	1.855	9.215	1	0.002	0.004	0.000	0.136
Constant	-9.915	5.256	3.559	1	0.059	0.000		

SEM: standard error of means, df: degrees of freedom, P: probability, CI: confidence interval

http://www.aloki.hu ● ISSN 1589 1623 (Print) ● ISSN1785 0037 (Online)
DOI: http://dx.doi.org/10.15666/aeer/2001_285299

Whether there is a specification error in the created logistics model can be understood by entering the 'linktest' command in the Stata (2018) program. The obtained results are given in *Table 6*, and the '*hatsq*' statistic was not found significant (p>0.05). This indicates that there is no specification error in the model. That is, there is no missing variable to be included in the model or an unnecessary variable to be removed from the model. Here, the variable '*hat*' shows the estimated values of the dependent variable. '*hatsq*', on the other hand, shows the variable $\widehat{Y}_i^2$, consisting of the square of estimated values (Mert, 2016).

Table 6. *Test results for the specification error*

Mastitis	Coefficient	Standard error	Z	P	[95% Conf. Interval]
hat	1.050	0.172	6.08	0.000	0.712 - 1.389
hatsq	0.051	0.046	1.11	**0.267**	- 0.039 - 0.142
constant	-0.219	0.379	-0.58	0.562	-0.963 - 0.523

Z: Z test statistic, P: probability

Before interpreting the logistic model, the '*collin*' command was used to check whether there was multicollinearity between continuous variables in the regression model. For this, the following command was run in the Stata (2018) and the results showing the vif values were obtained (*Table 7*):

collin X_1 X_2 X_3

Here, the fact that vif values for the live weight(X_1), milking hygiene(X_2), and environmental hygiene (X_3) are below five (vif<5) indicates that there is not any multicollinearity. Since there can be no multicollinearity between categorical variables, there is no need to calculate vif values.

Table 7. *Collinearity diagnostics*

Variable	VIF	SQRT VIF	Tolerance	R-Squared
(X_1) Live weight	1.02	1.01	0.9791	0.0209
(X_2) Envir. hygiene	1.07	1.04	0.9309	0.0691
(X_3) Milking hygiene	1.05	1.03	0.9498	0.0502
Mean VIF	1.05			

SQRT VIF: square root of the variance inflation factor

When the parameters obtained based on the logistic model are given in *Table 5*. It was observed that the coefficients of the live weight variable and the infectious disease variable were positive and the coefficients of the other independent variables were negative. In this case, looking at the odds ratio of the live weight variable, it can be interpreted that a one-unit increase in live weight increases the likelihood of mastitis by 1.044 times. In other words, the probability of getting mastitis increases by 4.4%. As the age of the animal's increases, also, there is a natural increase in body weight, milk yield and udder tissues. Due to the fact that the udder tissues, especially the nipples are close to the ground and contact surface with the bedding material and feces increases and this situation reveals the risk of mastitis (Kuczaj, 2003).

http://www.aloki.hu ● ISSN 1589 1623 (Print) ● ISSN1785 0037 (Online)
DOI: http://dx.doi.org/10.15666/aeer/2001_285299

The coefficient of environmental hygiene is negative, and by looking at its odds ratio, it can be interpreted that a one-unit increase in environmental hygiene scores leads to a 6.2% (1-0.938) decrease in the likelihood of being mastitis. Similarly, it can be also interpreted that a one-unit increase in milking hygiene scores will reduce the likelihood of being mastitis by 11.3% (1-0.887). Ndahetuye et al. (2020) stated that paying attention to environment and milking hygiene may reduce the risk of mastitis in dairy cows with a high rate of subclinical mastitis. In addition, many researchers reported that the dryness of the bedding material that cattle are in constant contact with reduces the rate of contamination in the udder tissue. The reduction of mastitis pathogen risk in dry bedding material supports the results of the current study (Jobim et al., 2010; Lago et al., 2011; Oliveira and Ruegg, 2014; Fávero et al., 2015).

It has been reported that streptococci which cause infectious diseases, are one of the main causes of subclinical mastitis in cattle herds (Jobim et al., 2010; Oliveira and Ruegg, 2014). In this study, statistics of data (*Table 5*) show that cattle showing signs of infectious disease are 4.257 times more at risk of mastitis than healthy cattle. Alpay and Yeşilbağ (2009) and Zadoks et al. (2001) reported that there is a high degree of positive correlation between infectious diseases caused by many microorganisms and mastitis. In addition, these investigators stated that many secretions and spills such as nose, eyes, saliva, stool, semen and vaginal discharge and milk of infected animals, and placenta and fetal tissues play an important role in the spread of the virus to environment. This situation, explains why the risk of mastitis is high in cattle with symptoms of infectious disease.

Cattle fed adequately with a good and balanced ration are 94.9% (1 - 0.051) less likely to get mastitis compared to cattle fed inadequately and unbalanced (*Table 5*). Ingvartsen and Moyes (2013) stated that feeding with a balanced ration may prevent sudden changes in body condition score, so, it increases resistance against diseases by keeping immune cell functions at a high level. Inadequate nutrition in terms of vitamin E and selenium can lead to an increase in infections in cows (Cengiz, 2009). In addition, Spears and Weiss (2008) stated that the incidence of mastitis was reduced by 37% and clinical symptoms by 62%, by giving oral selenium and vitamin E (740 IU/day) for 3 weeks before delivery. This supports the finding of how effective nutrition is on mastitis.

In *Table 3*, mastitis rates of each breed are given. Here, the highest incidence of mastitis is in local breeds (56.1%). This is followed by Holstein (47.7%) and Simmental (41.7%), respectively. The reason for this is that farmers give more attention to care for cultural breeds, and it has been observed that they behave more carefully towards them. In this experiment, local breed (SAR) was accepted as a reference, however, it was statistically insignificant ($p>0.05$), so, local breed didn't compare with Holstein and Simmental breed's mastitis occurrence. However, the possibility of mastitis occurrence for each breed are given in *Table 9* and have been interpreted separately.

In *Table 8*, the classification of cows according to whether they have mastitis are given. The predictive power of the Logit model can be seen in this classification table. In the *Table 8*, out of a total of 95 cows without mastitis disease, 87 were classified correctly and 8 were classified incorrectly, which indicates that estimation is carried out at a 91.6% accuracy level. Similarly, out of the total 85 cows with mastitis disease, 80 were correctly classified and 5 were incorrectly classified, which shows that the correct estimate rate is 94.1%. Overall, it can be said that the model has a high estimation rate (92.8%).

http://www.aloki.hu ● ISSN 1589 1623 (Print) ● ISSN1785 0037 (Online)
DOI: http://dx.doi.org/10.15666/aeer/2001_285299

Table 8. *Classification table*

		Mastitis		Percentage correct
		No	Yes	
Mastitis	No	87	8	91.6
	Yes	5	80	94.1
Overall percentage				92.8

To estimate the impact rates of each of the categorical variables (infectious disease (X_4), nutrition(X_5), and breed (X_6)) on mastitis disease, the following 'margins' command was used in the Stata (2018) program, and the results given in *Table 9* were obtained:

margins X_4 X_5 X_6, at means

It is seen in the *Table 9* that all factors except the local breed factor have a significant ($p<0.05$) impact rate on mastitis.

Table 9. *Risk probabilities of categorical independent variables that are effective in the mastitis disease*

Categorical variable	Impact rate margin	Delta-method Std. Err.	Z	P	95% confidence interval	
(X_4) Infectious Dis.					Lower	Upper
0	0.217	0.089	2.42	0.015	0.041	0.393
1	0.541	0.107	5.03	0.000	0.330	0.753
(X_5) Nutrition						
0	0.705	0.097	7.26	0.000	0.514	0.895
1	0.108	0.050	2.15	0.032	0.009	0.208
(X_6) Breed						
(1) Local (SAR)	0.972	0.071	1.59	0.113	-0.026	0.252
(2) Holstein	0.204	0.091	2.24	0.025	0.025	0.383
(3) Simmental	0.112	0.036	26.82	0.000	0.901	1.043

Z: Z test statistic, P: probability

As can be seen in *Table 9*, the probability of getting mastitis in cows without any infectious disease (0) is 21.7%, while the probability of getting mastitis in cows with symptoms of any infectious disease increases to 54.1%. Since the body resistance of cattle fed inadequately with a poor and unbalanced ration (0) weakened, the probability of getting mastitis is estimated as 70.5%. However, in cattle fed balanced with a ration (1) whose nutrients, minerals, and vitamins balance is well-adjusted, the probability of getting mastitis decreases to 10.8%. These results are consistent with the study of Sundrum (2015) who stated that the incidence of mastitis increased up to 60% in herds with poor care, feeding and adverse environmental conditions throughout the world. On the other hand, in an experiment carried out in the same region (Tel et al., 2009), rate of mastitis was quite high (72.4%) compared to other parts of Turkey. The researchers claimed that this was due to the lack of environmental and milking hygiene and dry period treatment habits, especially in small scale family farms.

When the breed factor was considered, the probability of getting mastitis was 11.2% in the Simmental breed, while the rate increased to 20.4% in the Holstein breed (*Table 9*).

http://www.aloki.hu ● ISSN 1589 1623 (Print) ● ISSN1785 0037 (Online)
DOI: http://dx.doi.org/10.15666/aeer/2001_285299

Koç (2016) states that, the somatic cell count of the Simmental breed in raw milk is 70 to 80% lower than the Holstein breed, and Simmental breeds are more resistant against to mastitis. Tel et al. (2009) reported that the incidence of mastitis in Simmental cows in Turkey was 15.78%. This data supports the research findings obtained from the region. In local breeds, this rate was found to be 97.2%, but it was not significant ($p>0.05$). When the reason of this was investigated, it was understood that farmers are take care more to cultural breeds that are more economically valuable, but they ignored many factors, such as environmental conditions, care, milking hygiene, and nutrition, for local breeds because they approach these cattle traditionally. This leads to a decrease in cows' milk yields by increasing the likelihood of developing subclinical mastitis that farmers cannot see by eye. Tel et al. (2009) recommended that for overcome of these problems the breeders in that region should be trained.

In order to estimate the impact rates of milking (X_3) and environmental hygiene (X_2) on mastitis, it is necessary to categorize the variables (*Table 10*). Since scores are not categorical variables, they must be categorized by classifying first (Schreiner and Ruegg, 2003; Mert, 2016). Then, it is possible to obtain the impact probability of the score value of each created class on mastitis by using the 'margins' command. For environmental hygiene (X_2) and milking hygiene (X_3), the following commands were run respectively in the Stata 14.2 program:

margins, at(X_2 =(20(20)100)) vsquish
margins, at(X_3 =(20(20)100)) vsquish

Here, the environment and milking hygiene, divided into 5 classes at 20 point intervals, were categorized, and the impact rates (margins) of each category on mastitis disease are obtained as in *Table 10.*

Table 10. *Impact rates of environmental and milking hygiene scores on mastitis*

Class scores	Impact rate margin	Delta-method Std. Err.	Z	P	95% confidence interval	
Environmental hygiene					Lower	Upper
1-(20%)	0.609	0.038	15.99	0.000	0.534	0.683
2-(40%)	0.518	0.026	19.89	0.000	0.467	0.569
3-(60%)	0.424	0.028	15.13	0.000	0.369	0.479
4-(80%)	0.324	0.046	7.00	0.000	0.233	0.415
5-(100%)	0.220	0.065	3.35	0.001	0.091	0.349
Milking hygiene						
1-(20%)	0.862	0.053	16.17	0.000	0.758	0.967
2-(40%)	0.643	0.043	14.67	0.000	0.557	0.729
3-(60%)	0.397	0.036	10.99	0.000	0.326	0.468
4-(80%)	0.179	0.057	3.12	0.000	0.066	0.291
5-(100%)	0.040	0.035	1.14	0.256	-0.029	0.111

Z: Z test statistic, P: probability

As seen in *Table 10*, the probability of getting mastitis is 60.9% in enterprises with the lowest environmental hygiene (20 points), while the risk of getting mastitis also decreases as scores increase. The probability of getting mastitis of cows in the enterprise that receives a 100 score from environmental hygiene falls to 22%. Similarly, while the probability of mastitis is 86.2% in enterprises that receive 20 points from milking hygiene,

http://www.aloki.hu ● ISSN 1589 1623 (Print) ● ISSN1785 0037 (Online)
DOI: http://dx.doi.org/10.15666/aeer/2001_285299

the risk of mastitis decreases in enterprises that pay more attention to the milking procedure. That is, in an enterprise that scores 80 by paying more attention to milking hygiene conditions, the probability of mastitis falls to 17.9% ($p<0.01$).

Mastitis may develop in the udder lobes of dairy cows inadequate care before and after milking and non-hygienic conditions. While mastitis can develop due to a single factor, it is inevitable that the risk of mastitis increases with the combination of negative factors.

Teat dipping solution before and after milking are important not only to reduce the possibility of mastitis but also to reduce the risk of bacterial contamination in milk (Zucali et al., 2011). Before milking, the teats should be dipped in an antiseptic solution and waited for at least 30 seconds, then the teats should be wiped with disposable paper napkins or towels and dried. If not dried, the remnants of the solution applied to the udder contaminate the milk. If the above-mentioned precautions are not taken before milking, microorganisms pass into the milk. In this case, since the quality of milk deteriorates, it causes odor, taste, structure and color changes in products obtained from milk, causing a decrease in product quality (Nelson and Trout, 1964).

Since the teats remain open for a while after milking, flies and microorganisms easily transmitted by animal manure increase the risk of mastitis. To protect from this contamination, after milking, teat dipping should be done, and the cows should be fed so that they can stand for at least half an hour.

The estimated logit model of factors affecting the mastitis disease was defined as follows, and it was determined that the model had a high prediction rate of 92.8%.

Model for mastitis = 1

$$\begin{aligned} Z = -9.914 + 0.043 * (\text{LiveW.}) - 0.064 * (\text{EnvirH.}) - 0.12 * (\text{MilkingH.}) \\ + 1.449 * (\text{Inf. Dis} = 1) - 2.975 * (\text{Nutrition} \\ = 1) - 4.927 * (\text{Breed} = 2) - 5.631 * (\text{Breed} = 3) \end{aligned}$$

It may be a little difficult for the model to be applied directly by the farmers in practice. However, it can be easily used by a veterinarian or zootechnist. The Z value is calculated by defining the relevant parameters in the *Eq.3* model, and by replacing them in *Eq.1*, estimation values in the range of $0 \leq P(Y) \leq 1$ could be obtained. The obtained value gives the probability of getting mastitis of the cow under the mentioned living conditions.

Conclusion and Recommendations

In conclusion, in this study, the impact rates of factors that directly and indirectly affect mastitis disease, which secretly gnaws on the udder lobes of dairy cows and causes a constant decrease in milk yield, was revealed. It was attempted to draw attention to the effects of these factors, which are ignored especially by small family enterprises, on mastitis. It should be told to enterprise managers that taking the necessary measures for the mentioned factors is a cheaper way than treating animals. In addition, it was concluded that although they were more adapted to environmental conditions, local breeds, which are fed poorly in pastures, are far from veterinary control and whose living and caring conditions were not paid attention, were at risk more in terms of mastitis.

In cases where the dependent variable is in a binary structure, the LS method is insufficient in estimating the relationships between the dependent and independent variables since it cannot provide the necessary assumptions. Therefore, it is necessary to resort to logistic regression analysis, which does not require the assumption of normality and continuity, and also offers a prediction performance as good as machine learning.

http://www.aloki.hu ● ISSN 1589 1623 (Print) ● ISSN1785 0037 (Online)
DOI: http://dx.doi.org/10.15666/aeer/2001_285299

When the study is applied to larger integrated farms in the future, it can ensure that measures are taken to minimize economic losses. However, there are many other factors that directly and indirectly affect the risk of mastitis. For example, these include disease types, ration content, number of lactations, genetic predisposition, milking number, periodic mastitis controls, environmental factors such as milk yields, climatic conditions, temperature, humidity, and technical factors such as the breeder's expertise and educational status. For this reason, it would be beneficial to conduct more comprehensive studies covering all factors by researchers.

REFERENCES

[1] Alpay, G., Yeşilbağ, K. (2009): The roles of viruses in mastitis. – Uludag Univ. J. Fac. Vet. Med. 28(1): 39-46.
[2] Caffo, B., Griswold, M. (2006): A user-friendly ıntroduction to link-probit-normal models. – The American Statistician 60(2): 139-145.
[3] Cengiz, M. (2009): The protective approaches against dry period mastitis in cows. – Atatürk Univ. Journal of Veterinary Sciences 4(3): 215-222.
[4] Chebel, R. C., Santos, J. E. P., Reynolds, J. P., Cerri, R. L. A., Juchem, S. O., Overton, M. (2004): Factors affecting conception rate after artificial insemination and embryonic loss in lactating dairy cows. – Anim. Reprod. Sci. 84: 239-255.
[5] Cobirka, M., Tancin, V., Slama, P. (2020): Epidemiology and classification of mastitis. – Animals 10(12): 2212.
[6] Demaris, A. (2004): Regression with Social Data: Modeling Continuous and Limited Response Variables. – John Wiley & Sons, Inc. Hoboken, New Jersey.
[7] Fávero, S., Portilho, F. V. R., Oliveira, A. C. R., Langoni, H., Pantoja, J. C. F. (2015): Factors associated with mastitis epidemiologic indexes, animal hygiene, and bulk milk bacterial concentrations in dairy herds housed on compost bedding. – Livestock Science 181: 220-230.
[8] Guimaraes, J. L., Brito, M. A., Lange, C. C., Silva, M. R., Ribeiro, J. B., Mendonça, L. C., Souza, G. N. (2017): Estimate of the economic impact of mastitis: A case study in a Holstein dairy herd under tropical conditions. – Prev Vet Med. 142: 46-50.
[9] Gujarati, D. N., Porter, D. C. (2009): Basic Econometrics. – 5th Edition, McGraw Hill Inc., New York.
[10] Güneri, Ö. İ., Durmuş, B. (2020): Dependent dummy variable models: An application of logit, probit and tobit models on survey data. – International Journal of Computational and Experimental Science and Engineering (IJCESEN) 6(1): 63-74.
[11] İnal, M. E., Topuz, D., Uçan, O. (2006): Linear probability and parameter estimation with Logit models. – Sosyoekonomi-1 3(3): 47-72.
[12] Ingvartsen, K. L., Moyes, K. (2013): Nutrition, immune function and health of dairy cattle. – Animal 7: 112-122.
[13] Jamali, H., Barkema, H. W., Jacques, M., Lavallée-Bourget, E. M., Malouin, F., Saini, V., Stryhn, H., Dufour, S. (2018): Invited review: Incidence, risk factors, and effects of clinical mastitis recurrence in dairy cows. – Journal of Dairy Science 101(6): 4729-4746.
[14] Jobim, M. B., Lopes, M. A., Costa, G. M. D., Demeu, F. A. (2010): Pathogens associated with bovine mastitis in dairy herds in the south region of Brazil. – Animal Industry Bulletin 67: 175-181.
[15] Kılıç, B., Keskin, İ. (2019): Determination of factors effective in diagnosis of mastitis in holstein cattle by logistic regression analysis. – Journal of Bahri Dagdas Animal Research 8(2): 46-55.
[16] Koç, A. (2016): A review on Simmental raising: 2. studies in Turkey. – Journal of Adnan Menderes University Agricultural Faculty 13(2): 103-112.

http://www.aloki.hu ● ISSN 1589 1623 (Print) ● ISSN1785 0037 (Online)
DOI: http://dx.doi.org/10.15666/aeer/2001_285299

[17] Kuczaj, M. (2003): Analysis of changes in udder size of high-yielding cows in subsequent lactations with regard to mastitis. – Electronic J. Pol. Agric. Univ., Ser. Anim. Husb. 6(1): 2-5.
[18] Kulendran, N., Wong, K. K. F. (2011): Determinants versus composite leading ındicators in predicting turning points in growth cycle. – Journal of Travel Research 50(4): 417-430.
[19] Lago, A., Godden, S. M., Bey, R., Ruegg, P. L., Leslie, K. (2011): The selective treatment of clinical mastitis based on on-farm culture results: I. Effects on antibiotic use, milk withholding time, and short-term clinical and bacteriological outcomes. – J. Dairy Sci. 94: 4441-4456.
[20] Lakew, M., Tolosa, T., Tigre, W. (2009): Prevalence and major bacterial causes of bovine mastitis in Asella, South Eastern Ethiopia. – Tropical Animal Health and Production 41(7): 1525-1530.
[21] Long, J. S., Freese, J. (2014): Regression Models for Categorical Dependent Variables Using Stata. – Third Edition, College Station: Stata Press, USA.
[22] Longo, F., Salat, O., Van Gool, F. (2001): Incidence of clinical mastitis in French dairy herds, epidemiological data and economic costs. – Folia Veterinaria 45: 45-46.
[23] MacKinnon, D. P., Lockwood, C. M., Brown, C. H., Wang, W., Hoffman, J. M. (2007): The ıntermediate endpoint effect in logistic and probit regression. – Clinical Trials 4(5): 499-513.
[24] Mekonnen, S. A., Koop, G., Melkie, S. T., Getahun, C. D., Hogeveen, H., Lam, T. J. G. M. (2017): Prevalence of subclinical mastitis and associated risk factors at cow and herd level in dairy farms in North-West Ethiopia. – Prev Vet Med. 145: 23-31.
[25] Mert, M. (2016): SPSS-STATA Horizontal Cross-Section Data Analysis Computer Applications. – Detay Yayıncılık, Ankara.
[26] Montgomery, D. C., Peck, E. A., Vining, G. G. (2012): Introduction to Linear Regression Analysis. – 5th Edition, Wiley, New York.
[27] Ndahetuye, J. B., Twambazimana, J., Nyman, A. K., Karege, C., Tukei, M., Ongol, M. P., Persson, Y., Båge, R. (2020): A cross sectional study of prevalence and risk factors associated with subclinical mastitis and intramammary infections, in dairy herds linked to milk collection centers in Rwanda. – Prev. Vet. Med. 179: 1-9.
[28] Nelson, J. A., Trout, G. H. (1964): Judging Dairy Products. – The Olsen Publishing Co. Milwaukee 12, Wis. U.S.A.
[29] Nusinovici, S., Zhang, L., Chai, X., Zhou, L., Tham, Y. C., Vasseneix, C., Majithia, S., Sabanayagam, C., Wong, T. Y., Cheng, C. Y. (2020): Machine learning to determine relative contribution of modifiable and non-modifiable risk factors of major eye diseases. – British Journal of Ophthalmology, doi: 10.1136/bjophthalmol-2020-317454.
[30] Oliveira, L., Ruegg, P. L. (2014): Treatments of clinical mastitis occurring in cows on 51 large dairy herds in Wisconsin. – J. Dairy Sci. 97: 5426-5436.
[31] Özenç, E. (2019): Determination of risk factors associated with subclinical mastitis as detected by california mastitis test in smallholder dairy farms in Afyonkarahisar. – Kocatepe Veterinary Journal 12(3): 277-283.
[32] Özyurt, A. (2013): Effects on reproductive performance of mastitis cases in postpartum period in Holstein Friesian dairy cows. – Journal of Animal Production 54(1): 21-29.
[33] Rougoor, C. W., Hanekamp, W. J. A., Dijkhuizen, A. A., Nielen, M., Wilmink, J. B. M. (1999): Relationships between dairy cow mastitis and fertility management and farm performance. – Prev Vet Med. 39: 247-264.
[34] Sabuncuoğlu, N., Çolak, A., Akbulut, Ö., Tüzemen, N., Bayram, B. (2003): Relationships between CMT scores and some milk yield traits in Holstein Friesian and brown Swiss cows. – Atatürk University Journal of Agricultural Faculty 34(2): 139-143.
[35] Sabuncuoğlu, N., Çoban, Ö. (2006): Mastitis Economy. – Atatürk University J. Vet. Sci. 1(1): 1-5.
[36] Schreiner, D. A., Ruegg, P. L. (2003): Relationship between udder and leg hygiene scores and subclinical mastitis. – J. Dairy Sci. 86: 3460-3465.

http://www.aloki.hu ● ISSN 1589 1623 (Print) ● ISSN1785 0037 (Online)
DOI: http://dx.doi.org/10.15666/aeer/2001_285299

[37] Spears, J. W., Weiss, W. P. (2008): Role of antioxidants and trace elements in health and immunity of transition dairy cows. – Vet J. 176: 70-76.
[38] Stata (2018): STATA 14.2. – StataCorp LLC 4905 Lakeway Drive College Station, TX 77845 USA.
[39] Sundrum, A. (2015): Metabolic disorders in the transition period indicate that the dairy cows' ability to adapt is overstressed. – Animals 5: 978-1020.
[40] Tel, O. Y., Keskin, O., Zonturlu, A. K., Arserim Kaya, N. B. (2009): Subclinical mastitis prevalance and determination of the antibiotics susceptibility in Şanliurfa region. – Fırat Univ. Veterinary Journal of Health Sciences 23(2): 101-106.
[41] Uzmay, C., Kaya, A., Kaya, İ., Akbaş, Y. (2001): Studies on prevalence of mastitis and factors affecting prevalence in herds of İzmir Holstein breeders association. 2. relationships between managerial practices and subclinical mastitis. – Journal of Agricultural Faculty of Ege Univ. 38(2-3): 71-78.
[42] Zadoks, R. N., Allore, H. G., Barkema, H. W., Sampimon, O. C., Wellenberg, G. J., Gröhn, Y. T., Schukken, Y. H. (2001): Cow and quarter level risk factors for Streptoccus uberis and Staphylococcus aereus mastitis. – J. Dairy Sci. 84: 2649-2663.
[43] Zucali, M., Bava, L., Tamburini, A., Brasca, M., Vanoni, L., Sandrucci, A. (2011): Effects of season, milking routine and cow cleanliness on bacterial and somatic cell counts of bulk tank milk. – Journal of Dairy Research 78(4): 436-441.

http://www.aloki.hu ● ISSN 1589 1623 (Print) ● ISSN1785 0037 (Online)
DOI: http://dx.doi.org/10.15666/aeer/2001_285299

EXPLORATION OF IMPORTANT ENVIRONMENTAL DETERMINANTS OF FLOWERING PHENOLOGY IN THE WESTERN HIMALAYAN FORESTS OF DHIRKOT, AZAD JAMMU AND KASHMIR, PAKISTAN

KHALID, N.[1] – KHAN, A. M.[1,2*] – QURESHI, R.[1] – SAQIB, Z.[3] – ZAHID, N.[4] – BUSSMANN, R. W.[5]

[1]*Department of Botany, Pir Mehr Ali Shah Arid Agriculture University, Rawalpindi, Pakistan*

[2]*Department of Botany, Govt. Hashmat Ali Islamia Associate College Rawalpindi, Pakistan*

[3]*Department of Environmental Science, International Islamic University, Islamabad, Pakistan*

[4]*Department of Botany, Mirpur University of Science & Technology, 10250 Mirpur, AJ&K, Pakistan*

[5]*Department of Ethnobotany, Institute of Botany, Ilia State University, Tbolisi, Georgia*

[*]*Corresponding author*
e-mail: arshadbotanist@gmail.com; phone: +92-333-521-7235

(Received 1st Aug 2021; accepted 28th Oct 2021)

Abstract. The flowering phenology of plants is influenced by the unique set of environmental variations, and therefore, elucidation of important driving factors is important. The study area of Dhirkot (western Himalaya, Pakistan) is explored to record the interactions among the flowering phenology of the vascular plants and current climate along the temporal gradient from March-2015 to February-2018. A total of 38 randomly selected representative sites were visited to record the timing of flowering response and compared with mean monthly climatic data. Multivariate classification and ordination tools were used to analyze the data. The results revealed that majority (185 spp; 68%) of plant species passes through thier flowering phase in the month of July. Canonical correspondence analysis (CCA) results depicted that about 63.7% of the phenological variations were explained by the monthly explanatory climatic variables, and mean minimum temperature, precipitation, wind speed and soil moisture were significantly (p-adj. <0.05) important. Pseudo-canonical correlation of the first three CCA axes was found higher than 0.8 which depicted that the selected variables were important determinants. This study concluded that predicted future temperature increase might alter the phenological responses, and prove to be devastating for valuable plant species of this unique and very delicate western Himalayan ecosystem.
Keywords: *floral diversity, life forms, climatic variations, flowering events, multivariate analysis*

Introduction

The word phenology is derived from the Greek word *phainomai*, which means "to appear". It is the study of the timing of life events of plants (Vashistha et al., 2009). Phenological events attract special attention when the normal pattern deviates, e.g. out of season flowering. Phenological studies are important to understand the interaction of species and community function, just like many other temporal and spatial aspects (Fenner, 1998). Flowering phenological studies observe the duration and timing of flowering, and temporal and spatial variations in the number of flowers in response to different environmental gradients (Rathcke and Lacey, 1985). The term phenology is used in ecology more generally to designate the period of any seasonal or cyclic phenomena, including the dates of last appearance (Menzel et al., 2006; Mier, 2007).

http://www.aloki.hu ● ISSN 1589 1623 (Print) ● ISSN 1785 0037 (Online)
DOI: http://dx.doi.org/10.15666/aeer/2001_301337

Changes in phenological events are closely related to climatic variations (Bertin, 2008) and such changes can alter the functioning of ecosystem (Parmesan, 2006; Calinger et al., 2013) and ecological interactions such as those amongst plants and pollinators (Forrest, 2015; Kharouba and Vellend, 2015) or plants and migratory birds (Both et al., 2006). Selection pressure is considered as long-term cause of timing of a life history event, which is the cause of plants idiosyncratic phenology. These pressures vary from biotic types such as seasonal presence of pollinators, dispersers and predators to abiotic constraints such as seasonally unfavorable temperatures and unpredictable rainfall (Fenner, 1998; Badeck et al., 2004; Neil and Wu, 2006).

Phenology is an extremely delicate indicator (Peñuelas et al., 2004; Williams and Abberton, 2004), and thermoperiodic and photoperiodic responses affect flowering time variations from species to species (Holway and Ward, 1965; Khan et al., 2018). Phenological and phenomenological differences of plants are due to the interaction between environment and genotype (Raunkiaer, 1934; Mooney and Billings, 1960; Khan et al., 2019a,b). The ability of some plant species to grow in either early or late growth seasons indicate their ability to survive in harsh environment say least water availability, and low or high temperature (Vashistha et al., 2009; Patel et al., 2010). Any species not responding to climate change might have a risk of shorter growing season as compared to active competitors (Cleland et al., 2012). It has been shown that species not responding to temperature variations have declined significantly in abundance over the past 150 years (Willis et al., 2008), while species adaptive in their phenology with increase of warming have better chance of survival (Cleland et al., 2012). This clearly indicates that temperature variations influence species' capacity of survival (Wang et al., 2018).

According to an estimate, a rise of about 0.74°C is detected in global surface temperature over the past century by International Panel on Climate Change (IPCC, 2007), and resulting glaciers melt, decrease of snow cover, rise in sea level and change in patterns of temperature, wind and rainfall. These fluctuations have likely profound biological effects affecting many taxa in the different geographical regions of the world (Parmesan and Yohe, 2003; Menzel et al., 2006; Parmesan, 2006). For instance, many spring plants now show early leafing and flowering time across the world (Chambers et al., 2013; Schwartz et al., 2013; Ge et al., 2015), while changes in autumn phenological phases are often less obvious, but might have far reaching effects (Menzel et al., 2006; Gill et al., 2015). These studies have shown that the plant phenology phases are important biological indicators of the climate change, and influence all including terrestrial ecosystems (Rosenzweig, 2007).

The Himalayan mountain range is described as ‘‘Water Tower of Asia’’, and its melting glaciers recharge the eight largest rivers in Asia. When compared to the rest of the world, the Himalayan region is facing a relatively more pronounced rise of temperature (Khan et al., 2018) and has been declared the most vulnerable region in the world (Shrestha et al., 2012). These climatic changes are one of the main causes for loss and changes in biodiversity, species composition, shifting of geographical ranges of species, high glacier melting, increase in number of glacial lakes, and associated socioeconomic changes (Chaudhary et al., 2011). The Kashmir Himalaya is well known all over the world for its pleasing beauty. It has been referred to as a ‘Terrestrial Paradise’ (Vigne, 1842). One of the dominant features contributing to the global distinction of Kashmir is the rich biodiversity that embellishes its entrancing landscapes (Lawrence, 1895). Various studies (Shaheen et al., 2011; Nazir et al., 2012; Faiz et al., 2014; Khan et al., 2015, 2016, 2018, 2019a,b) have reported the distribution pattern of plant species and

http://www.aloki.hu ● ISSN 1589 1623 (Print) ● ISSN 1785 0037 (Online)
DOI: http://dx.doi.org/10.15666/aeer/2001_301337

communities, life forms, leaf size spectra and flowering phenology of the western Himalayan forests in different parts of Azad Jammu and Kashmir (AJ&K), Pakistan. However, the western Himalayan forests of Dhirkot, AJ&K, Pakistan have remained unexplored, especially related to plant species traits, including life forms, leaf size spectra, and flowering phenology and its determinants. Therefore, documentation of existing interaction among the prevailing climate and flowering phenology of Dhirkot area would help in saving the biodiversity, and explore the following un-answered questions:

1. What about the plant species richness, and composition of major floristic groups, and pattern of biological and leaf size spectra distribution?
2. When majority of vascular plant species enter in flowering phase?
3. How the vascular plant species flowering response is correlated with the current climate?
4. What are the number of statistically significant temporal groups linked to flowering phenological response of the vascular plant species?
5. Which climatic variables are the most influential determinants of the plant species flowering phenological response?

Materials and Methods

Study area

The study area of Dhirkot is a Tehsil of District Bagh, AJ&K, Pakistan, in the western Himalayas, and located 132 km from the capital city of Islamabad. It lies between 73.50-73.69 East longitude and 33.90-34.13 North latitude, covering an area of 231 km^2. The elevation ranges from 603 to 2639 m above sea level (masl). Dhirkot borders district Muzaffarabad in the north, district Poonch in the south, tehsil Harighel of district Bagh in the east, and the river Jhelum in the west (*Fig. 1*). The entire area is a mountainous terrain with generally sloping orientation from North-East to South-West, and covered with thick, green coniferous forests.

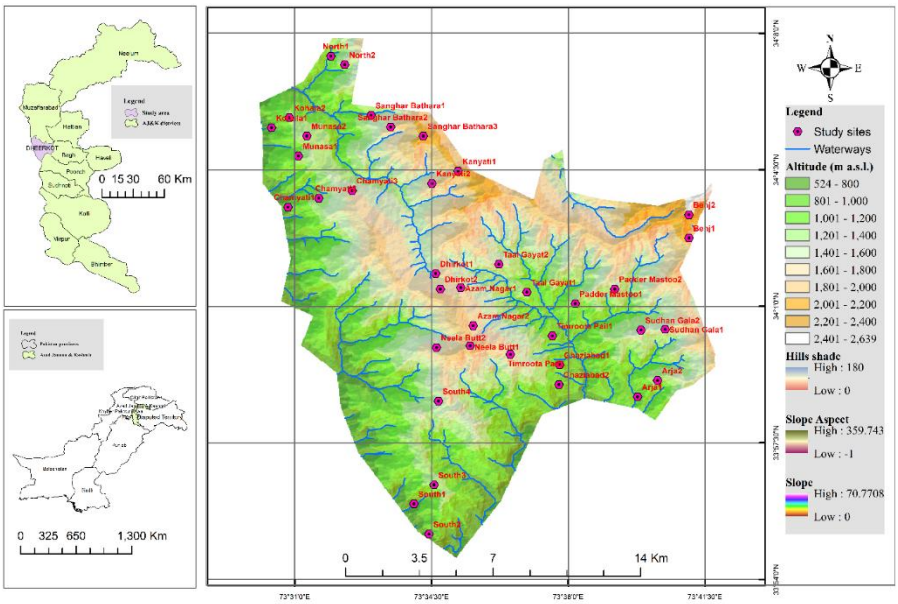

Figure 1. *Map of the study area displaying study locations and topographic variations*

http://www.aloki.hu ● ISSN 1589 1623 (Print) ● ISSN 1785 0037 (Online)
DOI: http://dx.doi.org/10.15666/aeer/2001_301337

The forest vegetation of the study area is comprised of western Himalayan mixed temperate forests with dominance of *Pinus wallichiana* (Blue Pine) and *Cedrus deodara* (Deodar). The humid subtropical zone harbors *Pinus roxburghii* (Chir Pine) as abundant species (*Fig. 2*). A total of 15 bird and 20 mammal species are commonly encountered, including globally threatened species like leopard (Khan, 2002). The human population of the area is 36270 based on the population census results of 2017 (Anonymous, 2017). The majority of local communities has inadequate income resources and depends on agro-based activities for their livelihoods. The most important crops include maize, wheat and vegetables, with a major share of tomatoes and potatoes. As the study area is mountainous, terrace cultivation techniques are adopted, and the yield is significantly linked to rainfall patterns in the area.

Figure 2. *Diverse landscape of two elevation zones representing sampled microhabitats (a: subtropical broad leaved evergreen forest zone; b: subtropical evergreen coniferous forest zone; c-d: Himalayan moist temperate forest zone*

Floristic and phenological data collection

A total of 38 randomly selected sites (*Fig. 1*) of the study area are visited on monthly basis (Dates: 11^{th}-20^{th}) from March 2015 to February 2018 (36 months) for collection of plant specimens, and to record the temporal variations in flowering response. The applied observation frequency is appropriate, and the same was also used by Khan et al. (2018). At each site, 3 plots of varying sizes (herbs: 2×1 m; shrubs: 10×5 m; tree: 20×10 m) were laid, and the presence/absence of each plant species (criterion; if more than 50% individuals of any recorded species are found passing through their flowering phase in

http://www.aloki.hu ● ISSN 1589 1623 (Print) ● ISSN 1785 0037 (Online)
DOI: http://dx.doi.org/10.15666/aeer/2001_301337

the considered plot/month subsequently counted as present otherwise absent.) were recorded. All the collected plant specimens were pressed, dried and mounted on the standard sized herbarium sheets, followed by identification using *Flora of Pakistan* (http://www.efloras.org/) and other floristic literature (Nasir and Ali, 1970-1989; Ali and Nasir, 1989-1991; Ali and Qaiser, 1993-1995, 2000-2014). After identification, the binomials of each plant species and their family names were copied from the plant list (TPL) ver. 1.1 (http://www.theplantlist.org/) (TPL 2013) to avoid the use of illegitimate and synonymous binomials (Khan et al., 2015, 2016, 2018). The determined voucher specimens were deposited in the herbarium of Department of Botany, Pir Mehr Ali Shah Arid Agriculture University Rawalpindi, Pakistan for future reference and record. Additional information, including local names, Raunkiaer's biological spectra or life forms (Batalha and Martins, 2002; Khan et al., 2019b) and leaf size spectra (Cain and Castro, 1959) were also recorded for each plant species. Additionally, native or introduced status of each species is recorded along with thier abundance (frequency of occurrence among the studied sites) status and invassive-noninvassive capabilities.

Monthly flowering response (timing and duration) of each plant species is calculated by using the formula conveyed by Khan et al. (2015), and presented in *Eq.1*.

$$SFR\ (\%)\ = \frac{Species\ found\ in\ flowering\ in\ a\ month\ at\ all\ studied\ sites}{Total\ species\ found\ in\ flowering\ in\ all\ months\ and\ sites} \times 100 \quad \text{(Eq.1)}$$

Where SFR is the monthly species flowering response of the studied plants. Subsequently, monthly responses were averaged to calculate the seasonal flowering response of each plant species say winter (November-February), spring (March-April), summer (May-mid July), monsoon (mid July-mid September), and autumn (mid September-October).

Family richness (FR) was calculated by using the formula (*Eq.2*) as conveyed by Khan et al. (2018).

$$FR\ (\%) = \frac{Species\ belong\ to\ a\ plant\ family}{Total\ species\ recorded\ in\ all\ months\ and\ sites} \times 100 \quad \text{(Eq.2)}$$

Climate data collection

The climate of the area varies considerably on temporal scales. The month of January was recorded as the coldest month in the study area, and minimum temperature varied between -0.35-2 °C during 2015-2018, whereas the month of June was the hottest and maximum temperature varied from 31.32-34.04 °C. The minimum precipitation received in the month of December (varied between 2.79-55.87 mm) and the July was recorded as the wettest receiving maximum (381.29-625.72 mm) (*Supplementary Data Table 2*). The remote sensing based monthly climate data of precipitation, maximum and minimum temperature, specific humidity, soil moisture, wind speed, and short & longwave radiation (36 months) of the study area (Dhirkot) was acquired from the United States National Centers for Environmental Prediction (US-NCEP) Climate Forecast System Reanalysis (CFSR) by using climate engine (https://app.climateengine.org/). The data source was CFSv2 19200 m (1/5-deg) daily reanalysis dataset, National Oceanic and Atmospheric Administration (NOAA) (*Supplementary Data Table 2*). The majority of study area receives precipitation in the form of snowfall from December to mid-March (Khan et al., 2018).

http://www.aloki.hu ● ISSN 1589 1623 (Print) ● ISSN 1785 0037 (Online)
DOI: http://dx.doi.org/10.15666/aeer/2001_301337

Statistical analyses

The events of sporogenesis in pteridophytes, strobili development in gymnosperms and flowering in angiosperms were treated as flowering response during each of 36 months at 38 ranodomly selected sites. This response data was entered in Microsoft excel spreadsheets (species vs. month/seasons) as binary data matrix. The total number of plant species found in flowering in each month at all the study sites was calculated and correlated with remote sensing based climatic data by using R statistical package (R Core Team, 2015) to develop pairwise correlation, distribution and scatterplots (Khan et al., 2015, 2018). Hierarchical clustering (Distance: Correlation, Linkage: Ward) was developed using the package "*pvclust*" in the R statistical package. As the species flowering respose data is of binary (presence/absence) nature, detrended correspondence analysis (DCA), a unimodal unconstrained model, was selected to seek the gradient length in the binary compositional response data whereas CCA (a constrained unimodal ordination model) was performed to explore; how much variations in the response data were explained by the studied predictors, and what is their order of importance. Multicollinearity in the climatic variables was detected by observing the variance inflation factor values (VIFs) of each climatic variable, and a threshold value of <5 was selected to remove the highly collinear explanatory variables. If the overall CCA model results found significant (p-value < 0.002), subsequently all the explanatory variables were further tested for their significance and order of importance by using permutation test via both simple (marginal) and conditional (net) term effects testing. All the p-values were corrected by using false discovery rate method. The ordination was performed by using Canoco software (Ter Braak and Smilauer, 2012).

Results

Floristic categorization

A total of 287 vascular plant species belonging to 219 genera and 77 plant families were recorded in the study area. The results of species categorization into major taxonomic groups depicted that there were 8 species (2.79%) of pteridophytes, and distributed in 5 genera (2.28%) and 3 families (3.9%). A total of four species (1.39%) of gymnosperms were recorded, and belong to 3 genera (1.37%) and 2 families (2.6%). The majority of plant species (275 species; 95.8%) belong to angiosperms, and found distributed in 211 genera (96.34%) and 72 plant families (93.5%). Within the latter group, 59 plant species (20.56%) belong to monocotyledons, and distributed in 46 genera (21%) and 6 plant families (7.8%) whereas, 216 species (75.26%) belong to dicotyledons, and distributed in 165 genera (75.34%) and 66 plant families (85.7%) (*Table 1*).

Table 1. *Floral composition of the major plant taxa in the study area*

Taxa	Families (percent)	Genera (percent)	Species (percent)
Pteridophytes	03 (3.9%)	05 (2.28%)	08 (2.79%)
Gymnosperms	02 (2.6%)	03 (1.37%)	04 (1.39%)
Monocots	06 (7.8%)	46 (21%)	59 (20.56%)
Dicots	66 (85.7%)	165 (75.34%)	216 (75.26%)
Total	77	219	287

http://www.aloki.hu ● ISSN 1589 1623 (Print) ● ISSN 1785 0037 (Online)
DOI: http://dx.doi.org/10.15666/aeer/2001_301337

The study area was dominated by herbs (212 species; 73.86%), followed by shrubs (33 species; 11.49%), trees (32 species; 11.15%), and climbers group (10 species; 3.48%) (*Supplementary Data Table 1*). The family richness (FR) results showed that Poaceae was the leading family with 41 species (14.28%), followed by Compositae (34 species, 11.84%), Lamiaceae (22 species, 7.66%), Leguminosae (14 species, 4.87%), Cyperaceae (11 species, 3.83%), Rosaceae (10 species, 3.48%), Amaranthaceae and Polygonaceae (8 species each, 2.79%), and Solanaceae (7 species, 2.44%), whereas the remaining plant families were represented by ≤ 6 species (*Supplementary Data Table 1*).

The results of biological (life form) classification of recorded plant species showed the dominance of therophytes with 106 species (36.93%), followed by hemicryptophytes (67 species, 23.34%), phanerophytes (65 species, 22.99%), geophytes (22 species, 7.66%), chamaephytes (16 species, 5.57%), and lianas (10 species, 3.48%). The phanerophytes were further distributed into nanophanerophytes (29 species, 10.10%), mesophanerophytes (21 species, 7.32%), microphanerophytes (10 species, 3.48%), and megaphanerophytes (6 species, 2.09%) (*Fig. 3*). The leaf size spectrum of the recorded vascular flora was dominated by microphylls (137 species, 47.74%), followed by mesophylls (69 species, 24%), nanophylls (56 species, 19.51%), leptophylls (19 species, 6.62%), and macrophylls (6 species, 2.09%) (*Fig. 4*).

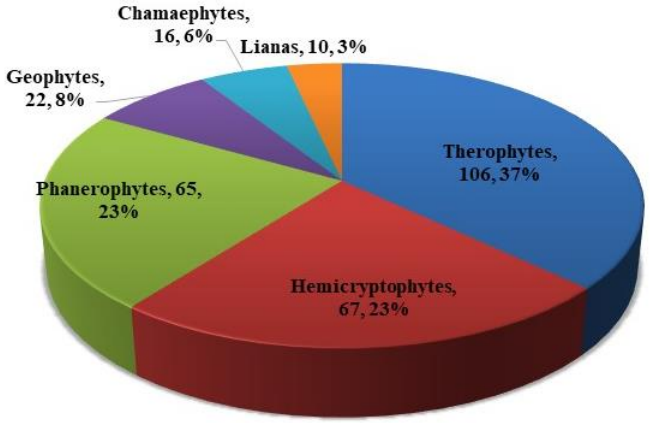

Figure 3. *Graph depicting the distribution of recorded vascular plant species into different life form classes*

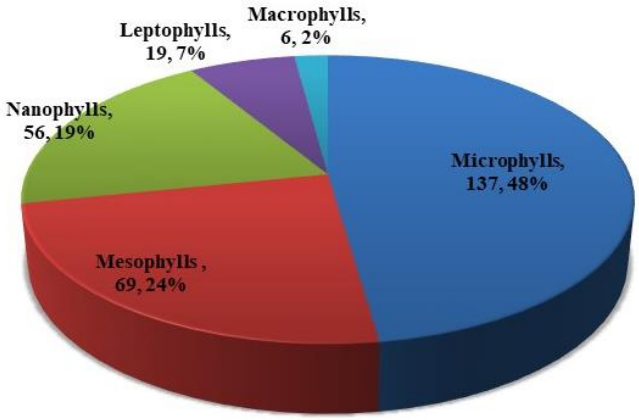

Figure 4. *Graph depicting the distribution of recorded vascular plant species into different leaf size classes*

http://www.aloki.hu ● ISSN 1589 1623 (Print) ● ISSN 1785 0037 (Online)
DOI: http://dx.doi.org/10.15666/aeer/2001_301337

A total of 234 plant species (81.5%) were native of the area, and 53 (18.5%) are introduced ones. Similarly, on the basis of frequency of occurrence of the recorded plant species among the studied sites, 110 (38.3%) were very common, 101 (35.2%) were common, 55 (19.2%) were rare, and 21 (7.3%) were very rare. A total 48 plant species (16.7%) were recorded as highly invassive in the study area (*Supplementary Data Table 1*).

Flowering phenology

The results of flowering response of the recorded plant species showed that majority of plant species (185 species, 64.46%) were in flowering phase during the month of July, followed by August (182 species, 63.41%), June (167 species, 58.19%), and September (145 species, 50.52%). The least response was observed in the month of December (14 species, 4.88%) and January (13 species, 4.53%) (*Fig. 5*). The flowering phenology response results indicated that most of the plant species go through their initial reproductive phase (flowering) from March to October.

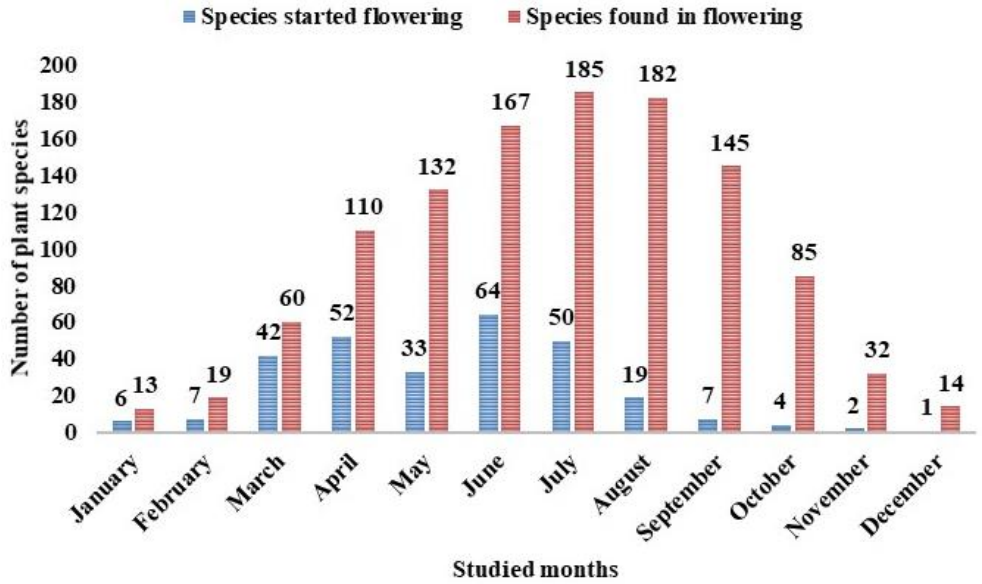

Figure 5. *Graph depicting the variations in flowering phenology of the recorded vascular plant species during studied months (each monthly value represent the cumulative number of 36 studied months/3 years: March-2015 to February-2018)*

As far as the results of initiation of flowering event during the studied months are concerned, majority of plant species were entered in flowering phase in the month of June (64 species, 22.3%), followed by April (52 species, 18.12%), July (50 species, 17.42%), and March (42 species, 14.63%), whereas, least species were found entering in their flowering phase in the month of December (1 species, 0.35%), followed by November (2 species, 0.7%), October (4 species, 1.39%), and January (6 species, 2.09%) (*Fig. 5*).

The results of Pearson's correlation and its significance depicted that the total plant species found in flowering phase in different months (SFR%) was strongly correlated ($r > 0.8$) with the mean monthly values of five different climatic variables. These includes mean minimum temperature ($r = 0.93$), shortwave radiation ($r = 0.93$), longwave radiation ($r = 0.92$), mean maximum temperature ($r = 0.89$), and mean specific humidity ($r = 0.88$).

http://www.aloki.hu ● ISSN 1589 1623 (Print) ● ISSN 1785 0037 (Online)
DOI: http://dx.doi.org/10.15666/aeer/2001_301337

Similarly, precipitation was found moderately positively correlated (r = 0.49). A strong negative correlation was observed with wind speed (r = -0.69), whereas no correlation of flowering abundance was observed with the soil moisture of the study area (*Fig. 6*).

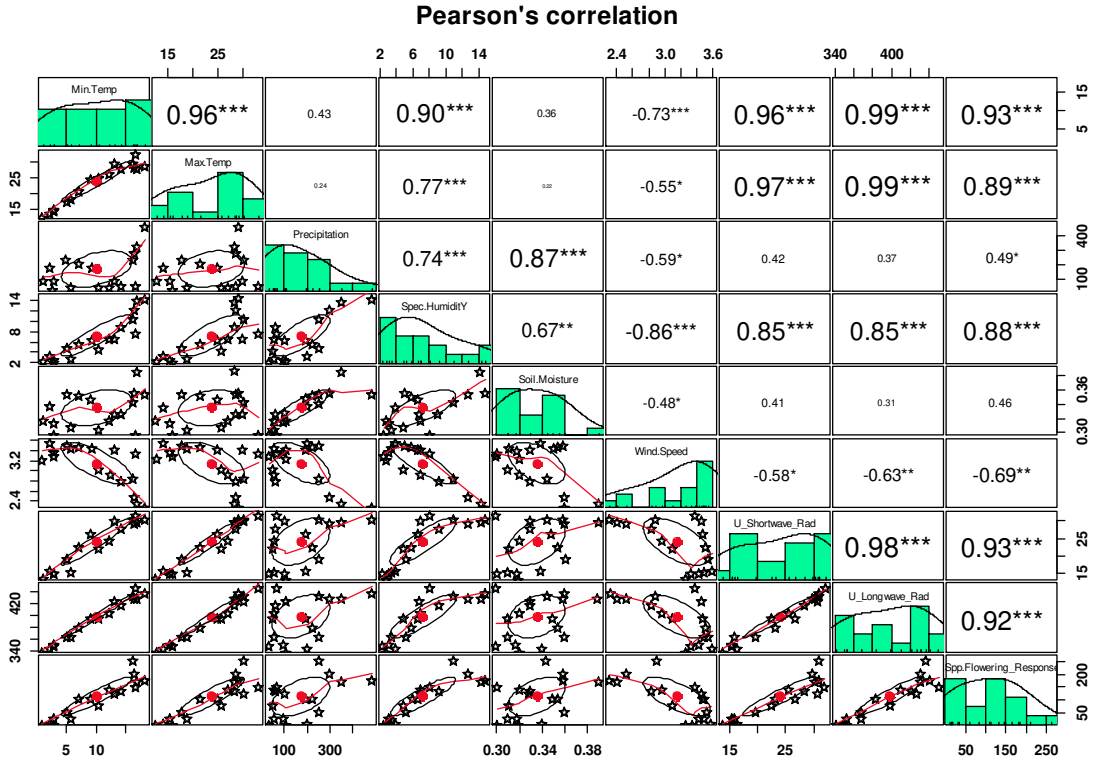

Figure 6. *Pearson correlation and its significance of climatic and SFR (n = 17; months = 12 & seasons = 5) variables. The distribution of each studied variable is shown on the diagonal, the bottom of the diagonal has bivariate scatter plots with a fitted line, and ellipses are displayed. Top of the diagonal has the correlation values coupled with significance levels as stars, representing p-values ("***" ≤ 0.001; "**" ≤ 0.01; "*" ≤ 0.05; " " > 0.05)*

Similarly, the month of June is found strongly correlated with the summer season on the basis of plant species flowering response. The months of July and August were detected as representative of monsoon season when the majority of flowering responses were observed. April was the main representative of the spring season which last from March to May. The winter season with least flowering response was primarily comprised of the months from November to February (*Fig. 7*).

Hierarchical clustering of months and seasons results were closely related to the pairwise correlation (*Fig. 7*). The dendrogram tree depicted that there were four significantly (p-value <0.05) different groups of months and seasons in the study area based on timing of plant species flowering response. The values given in green and red font colour above each cluster represent the approximately bootstrapped probability (BP %) and unbiased (AU %) p-values respectively. Likewise, the grey colored values below each cluster show the order of clustering (*Fig. 8*).

http://www.aloki.hu ● ISSN 1589 1623 (Print) ● ISSN 1785 0037 (Online)
DOI: http://dx.doi.org/10.15666/aeer/2001_301337

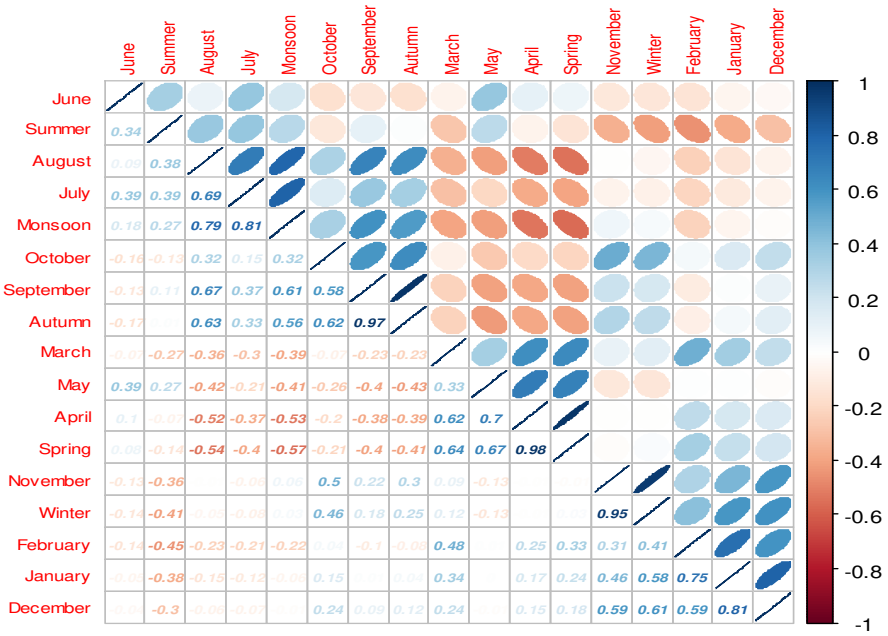

Figure 7. *Pairwise correlation plot of months and seasons based on plant species flowering phenological response (n = 287 plant species)*

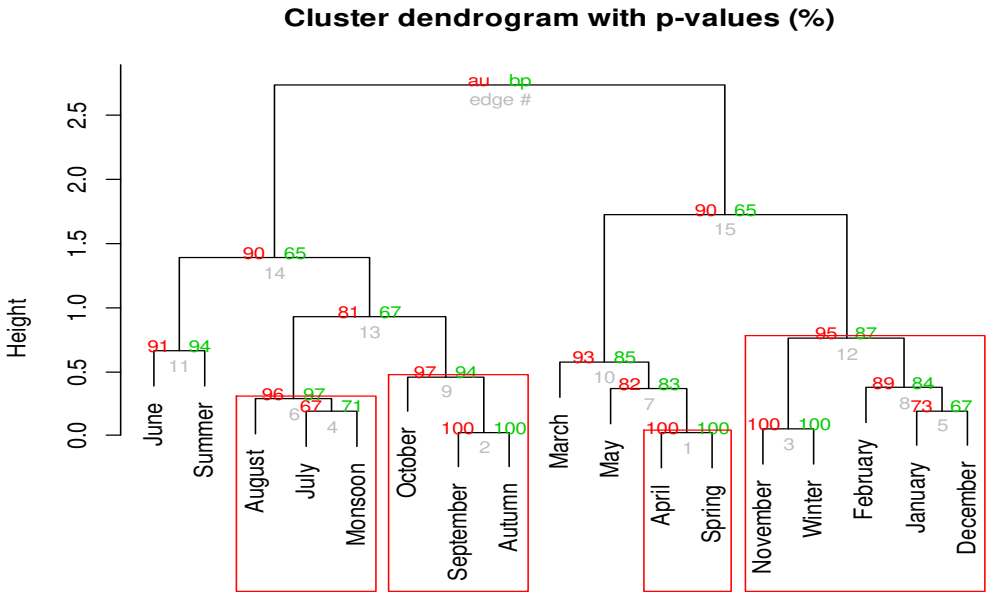

Figure 8. *Hierarchical clustering tree of months and seasons (distance method: correlation; linkage method: Ward) with AU/BP% values based on plant species flowering phenological response (Red colored rectangle around the clusters represents significant (p-value ≤ 0.05) response difference)*

Ordination analysis

The DCA results showed that the gradient length in the response data was above 4 SD (standard deviation of species turnover) for the first two DCA axes, hence, depicted that

http://www.aloki.hu ● ISSN 1589 1623 (Print) ● ISSN 1785 0037 (Online)
DOI: http://dx.doi.org/10.15666/aeer/2001_301337

use of a unimodal like DCA is more appropriate in this study than say principal component analysis (PCA: a linear model). The DCA results also confirmed the results of hierarchical clustering, and the same four groups are found well distincntly distributed in the ordination space. After removal of highly collinear, final CCA model is comprised of four predictors, including minimum temperature, wind speed, precipitation, and soil moisture (25 cm below the soil surface). A total inertia of 1.38 was recorded in the flowering phenology response data, and about 63.7% (R^2: 0.637) variations were explained by the explanatory variables, and the adjusted explained variations were 51.6% (adjusted R^2: 0.516). The first two CCA axes cumulatively explained about 55% variations. A significantly high pseudo-canonical correlation ($r > 0.8$) value was observed for the first three CCA axes which depict that the selected predictors were important determinants, and there is no single important climatic gradient rather all the four were important in one way or another.

The overall CCA model results were significant (pseudo-F: 2.7; p-value < 0.002), and based on simple term effects testing, the mean minimum temperature was detected as leading driver (explained variations: 27.2%; p-value [adj]: 0.004) of the flowering phenological response. It was followed by wind speed, precipitation and soil moisture. In case of conditional (unique) term effect testing, precipitation surpassed wind speed in order of importance. The study area received maximum precipitation in the months July and August during monsoon, and the same months/season were found highly suitable for flowering by the vascular plant species. These results are confirmed by CCA, and precipitation was detected as second most important determinant followed by wind speed which might be another important determinant as prerequisite for successful pollination of many species. Similarly, soil moisture was another influential determinant. The CCA numerical and graphical results are presented in *Table 2* and *Fig. 9*, respectively. The CCA biplot of months/seasons and climatic predictors showed that minimum temperature was highly correlated with the months of June, July and August, and Monsoon season, whereas wind speed was relatively higher than the average for spring season including March and April months (*Fig. 9*).

Table 2. *Summary of canonical correspondence analysis results and contribution of climatic variables in driving of flowering phenological response*

Statistic	**Axis 1**	**Axis 2**	**Axis 3**	**Axis 4**
Eigenvalues	0.4545	0.3134	0.0598	0.0529
Explained variation (cumulative)	32.86	55.51	59.84	63.67
Pseudo-canonical correlation	0.9781	0.9449	0.8159	0.7173
Explained fitted variation (cumulative)	51.61	87.2	93.99	100
Simple Term Effects:				
Name	Explains %	pseudo-F	P	P(adj)
Min. Temp (°C)	27.2	5.6	0.002	0.004
Wind speed (m/sec)	23.5	4.6	0.002	0.004
Precipitation (mm)	7	1.1	0.33	0.438
Soil moisture (25cm; in fraction)	5.8	0.9	0.438	0.438
Conditional Term Effects:				
Name	Explains %	pseudo-F	P	P(adj)
Min. Temp (°C)	27.2	5.6	0.002	0.008
Precipitation (mm)	15.9	4.9	0.004	0.008
Wind speed (m/sec)	14.6	3.5	0.008	0.01067
Soil moisture (25cm; in fraction)	6	2	0.028	0.028

http://www.aloki.hu ● ISSN 1589 1623 (Print) ● ISSN 1785 0037 (Online)
DOI: http://dx.doi.org/10.15666/aeer/2001_301337

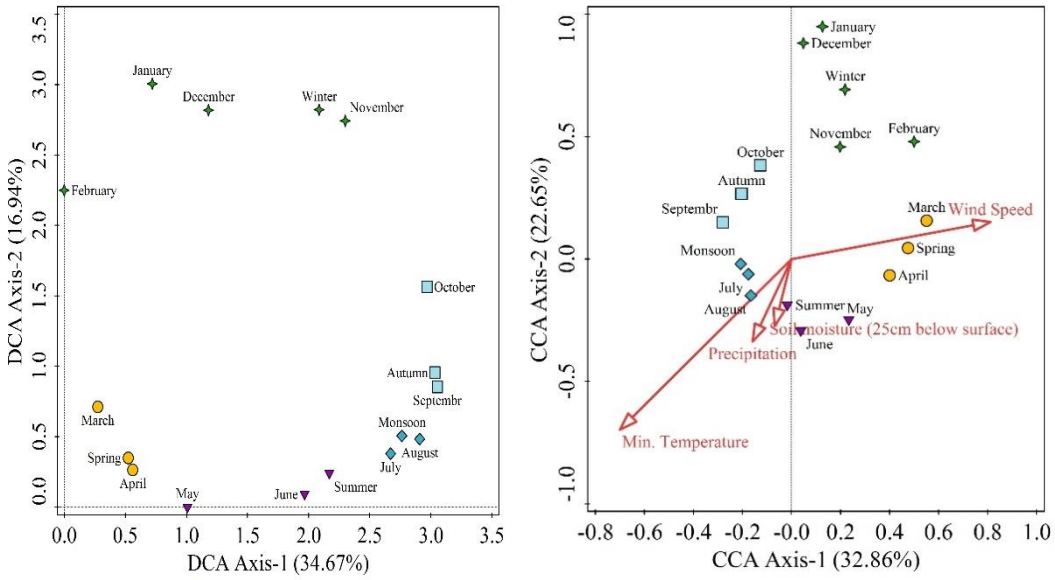

Figure 9. *DCA scatterplot and CCA biplot presenting the distribution pattern of months and seasons based on flowering response of plant species, and role of climatic variations respectively*

Discussion

Floristic classification and its importance

The study area of Dhirkot (AJ&K), Pakistan is a mountainous terrain, part of western Himalaya, and rich in floristic diversity. The present study was conducted to record the floristic composition of the area along with various attributes including biological spectra, leaf size spectra, flowering phenology and flowering phenological response of the vascular plant species along the prevailing climatic gradients.

A total of 287 vascular plant species were documented, and Poaceae was the leading family followed by Compositae and Lamiaceae. The present work showed a striking similarity with the floristic composition of Qalagai hills, Kabal valley, Swat (Ilyas et al., 2013) who also reported Poaceae (22 spp.) as dominant plant family followed by Compositae (16 spp.) and Lamiaceae (14 spp.). Similarly, Shaheen et al. (2015) also reported the same order of family richness from the western Himalayan subtropical forest stands of Kashmir. Other results similar to our findings include the work of Khan et al. (2014) from Shahbaz Garhi, district Mardan, Pakistan, Tanvir et al. (2014) from district Bagh, AJ&K, Pakistan, Khan et al. (2015) from district Kotli, AJ&K, Pakistan, and Khan et al. (2017) from Swat Ranizai, district Malakand, Khyber Pakhtunkhwa, Pakistan. The dominance of Poaceae and Compositae are due to their wide ecological amplitude within diverse habitat (Ibrahim et al., 2019). The common presence of grazing animals contributes to the spread of grasses. Grasses often quickly colonize any area (Attenborough, 1984). Similarly, Compositae is the largest family within angiosperms and possibly it is the most successful in evolutionary traits. Plant species of Compositae and Lamiaceae are economically and medicinally important in the western Himalaya, so people might transport them from one place to another resulting their quick spread to newly available habitats.

http://www.aloki.hu ● ISSN 1589 1623 (Print) ● ISSN 1785 0037 (Online)
DOI: http://dx.doi.org/10.15666/aeer/2001_301337

Biological spectra and its significance

The biological (life form) classification results depicted the dominance of therophytes followed by hemicryptophytes, phanerophyte, geophytes, Chamaephytes, and lianas. These results closely resemble with the results of Qalagai hills, Kabal valley, Swat-Pakistan (Ilyas et al., 2013), who reported therophytes as dominant followed by hemicryptophytes and macrophanerophytes. Other similar results include the studies conducted by Khan et al. (2014) from Shahbaz Garhi, district Mardan, Pakistan, Shaheen et al. (2015) from the western Himalayan subtropical forests of Kashmir, Khan et al. (2019c) from Mandan, district Bannu, Pakistan, Ishaq et al. (2019) from Derikot Selai Pattay district Malakand, Pakistan, and sililarly match with many otheres (Malik, 1986; Malik and Malik, 2004; Ajaib et al., 2008; Nazir et al., 2014). Although, life form can be used as an indicator or response towards the climate, Raunkiaer (1934) suggested that anthropogenic disturbances also contribute towards life form variations. Therophytes are usually considered as characteristics of harsh environmental conditions and hemicryptophytes as indicators for the temperate region with cold humid climate (Cain and Castro, 1959; Shimwell, 1971; Batalha and Martins, 2002). Hence, the dominance of therophytes in the study area may also be due to population pressure, over grazing, land modification for terrace cultivation and deforestation (Shehzad et al., 1999; Ilyas et al., 2013). In addition, winter drought might be an important factor continuously pushing plant species to a therophytes life form, and the presence of perennating structures just under the soil surface (hemicryptophytes) to pass the unfavorable environment is also common. The dominance of hemicryptophytes might be due to the extreme cold environment in winter, as well as heavy biotic stress due to overgrazing and deforestation (Nazir et al., 2014). On the other hand, the reasonable contribution of phanerophytes showed that the study area provide an ample environment for Himalayan forest tree species, e.g., *Pinus wallichiana* A.B. Jacks., *Pinus roxburghii* Sarg., *Cedrus deodara* (Roxb. ex D. Don) G. Don, *Quercus baloot Griff., Quercus incana Bartram, Acacia nilotica (*L.*) Delile* (Khan et al., 2017). Overall the thero-hemicryptophytic flora of the study area shows adaptations to avoid the harsh and long winter season, although the conifers and few sclerophyllous plant species remain active around the year (Ilyas et al., 2013).

Leaf size spectra and its significance

The leaf size spectrum of the vascular flora was dominated by microphylls, followed by mesophylls, nanophylls, leptophylls, and macrophylls. Our results resemble with the study conducted in Swat Ranizai, district Malakand, Khyber Pakhtunkhwa, Pakistan (Khan et al., 2017). Similarly, Khan et al. (2011) reported the dominance of microphylls followed by mesophylls and nanophylls from Darra Adam Khel, Khyber Pakhtonkhwa, Pakistan. In addition, Ishaq et al. (2019) from Derikot Selai Pattay district Malakand, Pakistan, Khan et al. (2014) from Shahbaz Garhi, district Mardan, Pakistan also reported the dominance of microphylls, and in many other studies (Amjad, 2012; Ilyas et al., 2013; Ibrahim et al., 2019). Leaf sizes of microphylls, mesophylls and nanophylls classes dominate in the flora of Dhirkot. Large sized leaves (mesophylls and macrophylls) are characteristic of wet warmer climates coupled with high precipitation, while the dominancy of small sized leaves (microphylls) are common in degraded dry habitats coupled with cold climates. The appearance of microphylls and nanophylls in the study area might be an adaptation to arid conditions. The majority of study area faces a long

http://www.aloki.hu ● ISSN 1589 1623 (Print) ● ISSN 1785 0037 (Online)
DOI: http://dx.doi.org/10.15666/aeer/2001_301337

drought period, especially during autumn and winter). Leaf size generally increases with increasing rainfall and declines with increasing irradiance and elevation (Khan et al., 2014). Therefore, the dominance of microphylls was positively associated with the increasing altitude, as also found by (Dewald and Steiner, 1986; Khan, 2013). Microphylls and nanophylls are the features of temperate regions (Cain and Castro, 1959; Shimwell, 1971), and climatically the study area of Dhirkot is also situated in the temperate zone. The dominance of mesophylls may be due to reasonable monsoon rainfall, and some unique microhabitats harboring rare and valuable plant species in the area (*Fig. 10*).

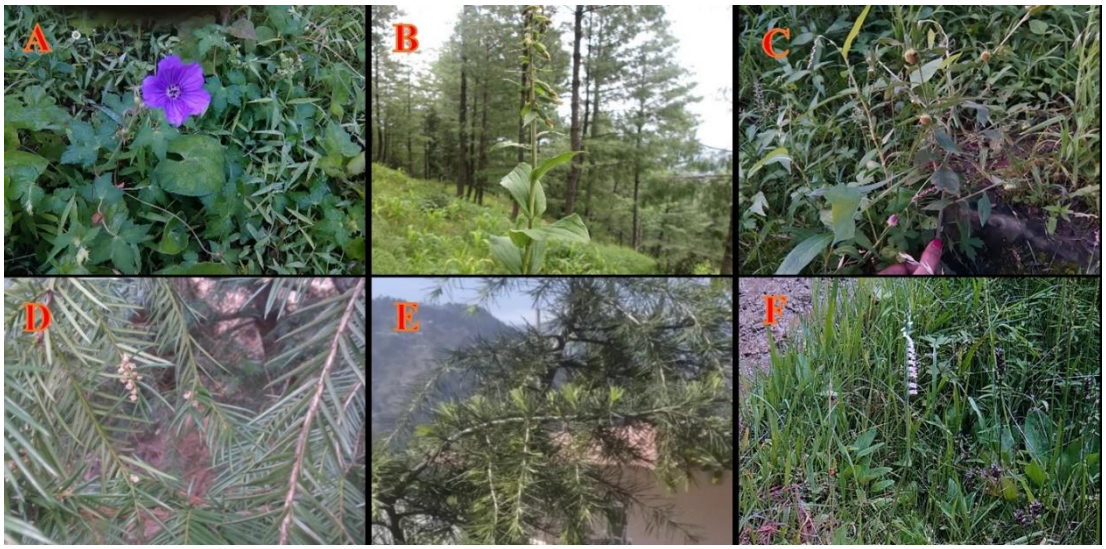

Figure 10. *A figure displaying some rare vascular plants in flowering phase (A) Geranium wallichianum (B) Epipactis helleborine (C) Carpesium cernuum (D) Taxus wallichiana and (E) Cedrus deodara (F) Spiranthes sinensis in the study area*

Climatic determinants of flowering phenology

The flowering phenology results showed that a majority of species were found in flowering phase during the month of July, followed by August, June, and September. Our results match with Vashistha et al. (2009) and Khan et al. (2018) who conveyed that majority of plant species pass through their flowering phase during July and August in the Western Himalayan regions of India and Muzaffarabad, AJ&K, Pakistan respectively. The results of this study are positively associated with the temporal climatic variations (especially temperature and monsoon rainfall) of the study area. CCA (simple term effects testing) results depicted the significant importance of four predictors including minimum temperature, wind speed, precipitation, and soil moisture (25 cm below the soil surface), whereas conditional (unique) term effects testing suggested the order of importance as mean minimum temperature followed by precipitation, wind speed and soil moisture. Many workers detected the importance and significance of temperature to the plant phenological responses (Dewald and Steiner, 1986; Badeck et al., 2004; Peñuelas et al., 2004; Ahas and Aasa, 2006; Estrella and Menzel, 2006) particularly in high altitude areas. Similarly, Khan et al. (2018) concluded that variations in the minimum temperature are more important than the maximum temperature in driving the flowering phenological variations. Precipitation was the second important determinant of the flowering

http://www.aloki.hu ● ISSN 1589 1623 (Print) ● ISSN 1785 0037 (Online)
DOI: http://dx.doi.org/10.15666/aeer/2001_301337

phenological response in the study area, and Pearson (2019) reported the similar effect of precipitation on both spring and fall-flowering events from Southeast USA. Wind plays an important role in the dispersal of winged seeds over long distance (Heydel et al., 2015), and was also observed as a central factors. Our findings are alike to Khan et al. (2018) in this regard. The majority of plant species flowers in summer (July, August and June) season, so it is predicted that the months of May and June provide the essential prerequisite photo-thermic stimulus. The highest flowering phenological response of plant species from July to August can also be correlated with maximum precipitation in these months (monsoon season) resulting in higher soil moisture which in turn might resulted in required resource mobilization in the soil of the study area. A few plant species were also found in flowering stage in December to February (in winters) months depicting their unique evolutionary capabilities.

This study found that western Himalayan forests are richly diverse, and lead by Poaceae, Compositae, and Lamiaceae members. Similalrly, there is dominancy of therophytic life form and microphyllous leaf size characteristics of the vascular plant species in the study area. July and August months or monsoon season was detected as the most suitable time for plant species to pass their flowering phase, and SFR was found strongly correlated with the current climate of the study area. Intiation of flowering response was bimodal, first peak is detected in the month of April and second one in June. There were four significant groups of months/seasons linked to SFR, and monsoon season is the leading one. Mean minimum temperature, precipitation, wind speed and soil moisture in order were detected as leading drivers of flowering phenological response of the recorded plant species in the study area.

Conclusions and Recommendations

The study area (Dhirkot, AJ&K Pakistan) harbors high plant species richness characteristics of the floristically rich and highly diverse western Himalaya of Pakistan. The dominancy of therophytic and microphyll classes suggested that the study area is under heavy anthropogenic pressure and harbors unique climatic conditions. Minimum temperature, precipitation, wind speed and soil moisture (in order) were the most important climatic determinants of flowering phenology of the recorded plant species. Based on these findings we further predict that any change especially in temperature and precipitation in the area will change flowering phenological response which might prove detrimental. The resultant negative impact on many extremely rare, endangered and endemic flora including *Cedrus deodara, Taxus wallichiana, Notholirion thomsonianum, Epipactis helleborine, Aristolochia punjabensis, Jurinea dolomiaea, Swertia chirayita, Mimosa himalayana, Paeonia emodi* and *Skimmia laureola* might result in biodiversity loss. The study area needs effective management and conservation plans for sustainable development, and future studies that focus on determination of ecological niche variations of valuable plant species under predicted climate change scenarios are required. The population of invasive alien plant species like *Ailanthus altissima, Broussonetia papyrifera, Erigeron bonariensis, Lantana camara,* and *Parthenium hysterophorus* needed to be continuously monitored in the study area.

http://www.aloki.hu ● ISSN 1589 1623 (Print) ● ISSN 1785 0037 (Online)
DOI: http://dx.doi.org/10.15666/aeer/2001_301337

Acknowledgments. The authors thankfully acknowledge the local residents of the study area for sharing common names of the plant species. Authors are also thankful to the members of the herbarium of PMAS-Arid Agriculture University, Rawalpindi, Pakistan for giving direct access to plant specimens for comparison and identification.

Author contributions. NK was involved in field data collection, and preparation of the preliminary draft; AMK developed study design, and did multivariate data analyses, results interpretation, revision and formating, NZ was involved in methodology, ZS did literature search, RWB did language editing and corrections, and RQ conceived the idea and overall supervised all the research activities.

Competing interests and funding. The author of this study have no competing interests, and this study was not financially supported by any funding agency/organization/institute etc.

REFERENCES

[1] Ahas, R., Aasa, A. (2006): The effects of climate change on the phenology of selected Estonian plant, bird and fish populations. – Int. J. Biometeorol. 51: 17-26.
[2] Ajaib, M., Khan, Z., Muhammad, S., Mahmood, R. (2008): Biological spectra of Saney Baney hills district Kotli Azad Jammu and Kashmir. – Philippine J. Sci. 60: 53-58.
[3] Ali, S. I., Nasir, Y. J. (1989-1991): Flora of Pakistan (Fascicle series). – Department of Botany, University of Karachi, Pakistan.
[4] Ali, S. I., Qaiser, M. (1993-1995 & 2000-2014): Flora of Pakistan (Fascicle series). – Department of Botany, University of Karachi, Pakistan.
[5] Amjad, M. S. (2012): Life form and leaf size spectra of vegetation in Kotli hills, Azad Jammu and Kashmir (Pakistan). – Greener J. Agri. Sci. 2: 345-350.
[6] Anynomous. (2017): City Population. – URL: <http://www.citypopulation.de/AzadKashmir.html> access on 06 May 2020.
[7] Attenborough, D. (1984): The living planet. – British Broadcasting Corporation, 320p.
[8] Badeck, F. W., Bondeau, A., Böttcher, K., Doktor, D., Lucht, W., Schaber, J., Sitch, S. (2004): Responses of spring phenology to climate change. – New phytologist 162: 295-309.
[9] Batalha, M. A., Martins, F. R. (2002): Life-form spectra of Brazilian cerrado sites. – Flora 197: 452-460.
[10] Bertin, R. I. (2008): Plant phenology and distribution in relation to recent climate change. – J. Torrey. Bot. Soc. 135: 126-146.
[11] Both, C., Bouwhuis, S., Lessells, C. M., Visser, M. E. (2006): Climate change and population declines in a long-distance migratory bird. – Nature 441: 81-83.
[12] Cain, S. A., Castro, G. M. D. (1959): Manual of vegetation analysis. – Harpers and Brothers publishers, New York, pp. 225-325.
[13] Calinger, K. M., Queenborough, S., Curtis, P. S. (2013): Herbarium specimens reveal the footprint of climate change on flowering trends across North-central North America. – Ecol. Lett. 16: 1037-1044.
[14] Chambers, L. E., Altwegg, R., Barbraud, C., Barnard, P., Beaumont, L. J., Crawford, R. J., Durant, J. M., Hughes, L., Keatley, M. R., Low, M., Morellato, P. C. (2013): Phenological changes in the southern hemisphere. – PloS One 18(10): e75514. https://doi.org/10.1371/journal.pone.0075514.
[15] Chaudhary, P., Rai, S., Wangdi, S., Mao, A., Rehman, N., Chettri, S., Bawa, K. S. (2011): Consistency of local perceptions of climate change in the Kangchenjunga Himalaya landscape. – Curr. Sci. 101: 504-513.
[16] Cleland, E. E., Allen, J. M., Crimmins, T. M., Dunne, J. A., Pau, S., Travers, S. E., Zavaleta, E. S., Wolkovich, E. M. (2012): Phenological tracking enables positive species responses to climate change. – Ecology 93: 1765-71. https://doi.org/10.1890/11-1912.1.
[17] Dewald, L. E., Steiner, K. C. (1986): Phenology, height increment and cold tolerance of

http://www.aloki.hu ● ISSN 1589 1623 (Print) ● ISSN 1785 0037 (Online)
DOI: http://dx.doi.org/10.15666/aeer/2001_301337

Alnus glutinosa population in a common environment. – Silvae Genet. 35: 205-211.
[18] Estrella, N., Menzel, A. (2006): Responses of leaf coloring in four deciduous tree species to climate and weather in Germany. – Clim. Res. 32: 253-267.
[19] Faiz, A. H., Ghufarn, M. S., Mian, A., Akhtar, T. (2014): Floral diversity of Tolipir National Park, Azad Jammu and Kashmir, Pakistan. – Biologia (Pakistan) 60: 43-55.
[20] Fenner, M. (1998): The phenology of growth and reproduction in plants. – Perspectives in Plant Ecology, Evolution and Systematics 1: 78-91.
[21] Forrest, J. R. K. (2015): Plant-pollinator interactions and phonological change: what can we learn about climate impacts from experiments and observations? – Oikos 124: 4-13.
[22] Ge, Q., Wang, H., Rutishauser, T., Dai, J. (2015): Phenological response to climate change in China: A meta-analysis. – Glob. Chang. Biol. 21: 265-274. https://doi.org/10.1111/gcb.12648.
[23] Gill, A. L., Gallinat, A. S., Sanders-DeMott, R., Rigden, A. J., Short Gianotti, D. J., Mantooth, J. A., Templer, P. H. (2015): Changes in autumn senescence in northern hemisphere deciduous trees: a meta-analysis of autumn phenology studies. – Annals of botany 116: 875-88. https://doi.org/10.1093/aob/mcv055.
[24] Heydel, F., Cunze, S., Bernhardt-Römermann, M., Tackenberg, O. (2015): Seasonal synchronization of seed release phenology promotes long-distance seed dispersal by wind for tree species with medium wind dispersal potential. – J. Veg. Sci. 26: 1090-1101.
[25] Holway, J. G., Ward, R. T. (1965): Phenology of alpine plants in Northern Colorado. – Ecology 46: 73.
[26] Ibrahim, M., Khan, M. N., Sajjad, A., Razaq, A., Zaman, A., Iqbal, M., Jan, F. (2019): Floristic composition and species diversity of plant resources of rural area "Takht Bhai" district Mardan, Khyber Pakhtunkhwa, Pakistan. – Med. Aromat. Plants (Los Angeles) 8: 338. http://doi.org/10.35248/2167-0412.19.8.338.
[27] Ilyas, M., Qureshi, R., Shinwari, Z. K., Arshad, M., Mirza, S. N., Haq, Z. U. (2013): Some ethnobotanical aspects of the plants of Qalagai hills, Kabal valley, Swat Pakistan. – Int. J. Agric. Biol. 15: 801-810.
[28] IPCC. (2007): International panel on climate change: The physical science basis-summary for policymakers. – 10th Session of Working Group I of the IPCC, Paris.
[29] Ishaq, M., Alam, Z., Rahim, F. (2019): Floristic list and their ecological characteristics, of plants at village Derikot Selai Pattay district Malakand Khyber Pakhtunkhwa Pakistan. – University of Chitral Journal of Botany 1: 93-105.
[30] Khan, R. N. (2002): Distribution and habitat preference of small mammals in Dhirkot, AJK. – Masters Thesis, University of AJ&K, Muzaffarabad, Pakistan.
[31] Khan, M., Hussain, F., Musharaf, S., Imdadullah (2011): Floristic composition, life form and leaf size spectra of the coal mine area vegetation of Darra Adam Khel, Khyber Pakhtonkhwa, Pakistan. – J. Biodiv. Environ. Sci. 1: 1-6.
[32] Khan, M. (2013): Dimension and composition of plant life in tehsil Takht-e-Nasrati, district Karak, Khyber Pakhtunkhawa, Pakistan. – PhD Thesis, University of Peshawar, Peshawar, Khyber Pakhtunkhawa, Pakistan.
[33] Khan, M., Hussain, F., Musharaf, S. (2014): Floristic composition and ecological characteristics of Shahbaz Garhi, District Mardan, Pakistan. – Glob. J. Sci. Front. Res. 14: 7-17.
[34] Khan, A. M., Qureshi, R., Qaseem, M. F., Munir, M., Ilyas, M., Saqib, Z. (2015): Floristic checklist of district Kotli, Azad Jammu & Kashmir. – Pak. J. Bot. 47: 1957-1968.
[35] Khan, A. M., Qureshi, R., Qaseem, M. F., Ahmad, W., Saqib, Z., Habib, T. (2016): Status of basic taxonomic skills in botanical articles related to Azad Jammu and Kashmir, Pakistan: A review. – J. Bioreso. Manag. 3: 22-54.
[36] Khan, A., Khan, N., Ali, K., Rahman, I. U. (2017): An assessment of the floristic diversity, life-forms and biological spectrum of vegetation in Swat Ranizai, district Malakand, Khyber Pakhtunkhwa, Pakistan. – Sci. Technol. Dev. 36: 61-78.
[37] Khan, A. M., Qureshi, R., Arshad, M., Mirza, S. N. (2018): Climatic and flowering

http://www.aloki.hu ● ISSN 1589 1623 (Print) ● ISSN 1785 0037 (Online)
DOI: http://dx.doi.org/10.15666/aeer/2001_301337

phenological relationships of western Himalayan flora of Muzaffarabad district, Azad Jammu and Kashmir Pakistan, Pak. – J. Bot. 50: 1093-1112.

[38] Khan, A. M., Qureshi, R., Saqib, Z., Munir, M., Shaheen, H., Habib, T., Dar, M. E. U. I., Fatimah, H., Afza, R., Hussain, M. A., (2019a): A first ever detailed ecological exploration of the western Himalayan forests of Sudhan Gali and Ganga summit, Azad Jammu and Kashmir, Pakistan. – Appl. Ecol. Env. Res. 17: 15477-15505. http://dx.doi.org/10.15666/aeer/1706_1547715505.

[39] Khan, A. M., Qureshi, R., Saqib, Z. (2019b): Multivariate analyses of the vegetation of the western Himalayan forests of Muzaffarabad district, Azad Jammu and Kashmir, Pakistan. – Ecol. Indic. 104: 723-736. https://doi.org/10.1016/j.ecolind.2019.05.048.

[40] Khan, T. Y., Badshah, L., Ullah, S., Ali, A. (2019c): Floristic evaluation and ecological attributes of plants resources of Mandan, district Bannu, Pakistan. – Int. J. Bot. St. 4: 185-190.

[41] Kharouba, H. M., Vellend, M. (2015): Flowering time of butterfly nectar food plants is more sensitive to temperature than the timing of butterfly adult flight. – J. Anim. Ecol. 84: 1311-1321.

[42] Lawrence, W. R. (1895): The valley of Kashmir. – Chinar Publishing House, Srinagar.

[43] Malik, Z. H. (1986): Phytosociological studies on the vegetation of Kotli Hills, Azad Jammu and Kashmir. – M. Phil. Thesis, University of Peshawar, Peshawar, Pakistan.

[44] Malik, N. Z., Malik, Z. H. (2004): Present status of sub-tropical chir pine vegetation of Kotli hills, Azad Jammu and Kashmir. – J. Scientometric Res. 15: 85-90.

[45] Menzel, A., Sparks, T. H., Estrella, N., Koch, E., Aasa, A., Ahas, R., Alm-Kübler, K., Bissolli, P., Braslavská, O. G., Briede, A., Chmielewski, F. M. (2006): European phenological response to climate change matches the warming pattern. – Global Change Biology 12: 1969-76. https://doi.org/10.1111/j.1365-2486.2006.01193.

[46] Mier, N. (2007): Grape harvest records as a proxy for Swiss April to August temperature reconstructions. – Doctoral dissertation, University of Bern, Switzerland, pp. 12-25.

[47] Mooney, H. A., Billings, W. D. (1960): The annual carbohydrate cycle of alpine plants as related to growth. – Am. J. Bot. 47: 594-598.

[48] Nasir, E., Ali, S. I. (1970-1989): Flora of Pakistan (Fascicle series). – Department of Botany, University of Karachi, Pakistan.

[49] Nazir, A., Malik, R. N., Ajaib, M. (2012): Phytosociological studies of the vegetation of Sarsawa Hills District Kotli, Azad Jammu and Kashmir. – Biologia (Pakistan) 58: 123-133.

[50] Nazir, A., Malik, R. N., Shaheen, H. (2014): Floristic composition, life form and leaf spectra of plant communities recorded at Sarsawa hills district Kotli, Azad Kashmir. – Afr. J. Soil Sci. 2: 077-078.

[51] Neil, K., Wu, J. (2006): Effects of urbanization on plant flowering phenology: A review. – Urban Ecosyst. 9: 243-257.

[52] Parmesan, C., Yohe, G. (2003): A globally coherent fingerprint of climate change impacts across natural systems. – Nature 421: 37-42. https://doi.org/10.1038/nature01286.

[53] Parmesan, C. (2006): Ecological and evolutionary responses to recent climate change. – Annu. Rev. Ecol. Evol. Syst. 37: 637-669.

[54] Patel, H., Jain, B. K., Dabgar, Y. B. (2010): Life form and phyto climate of Sebhargog region, North Gujarat, India. – Plant Arch. 10: 965-966.

[55] Pearson, K. D. (2019): Spring- and fall-flowering species show diverging phenological responses to climate in the Southeast USA. – Int. J. Biometeorol. 63: 481-49.

[56] Peñuelas, J., Filella, I., Zhang, X., Llorens, L., Ogaya, R., Lloret, F., Comas, P., Estiarte, M., Terradas, J. (2004): Complex spatiotemporal phenological shifts as a response to rainfall changes. – New Phytologist 161: 837-46.

[57] R Core Team (2015): R: A language and environment for statistical computing. – R Foundation for Statistical Computing, Vienna, Austria. URL: http://www.R-project.org/.

[58] Rathcke, B., Lacey, E. P. (1985): Phenological patterns of terrestrial plants. – Ann. Rev. Ecol. System. 16: 179-214.

http://www.aloki.hu ● ISSN 1589 1623 (Print) ● ISSN 1785 0037 (Online)
DOI: http://dx.doi.org/10.15666/aeer/2001_301337

[59] Raunkiaer, C. (1934): The life form of plants and statistical plant geography. – The Clarendon Press, Oxford, 632p.
[60] Rosenzweig, C., Casassa, G., Karoly, D. J., Imeson, A., Liu, C., Menzel, A., Rawlins, S., Root, T. L., Seguin, B., Tryjanowski, P., Parry, M. L. (2007): Assessment of observed changes and responses in natural and managed systems. – In: Climate change 2007: Impacts, adaptation and vulnerability. Contribution of Working Group II to the Fourth Assessment Report of the Intergovernmental Panel on Climate Change, Cambridge University Press, pp. 79-131.
[61] Schwartz, M. D., Ault, T. R., Betancourt, J. L. (2013): Spring onset variations and trends in the continental United States: Past and regional assessment using temperature-based indices. – Int. J. Climatol. 33: 2917-2922.
[62] Shaheen, H., Malik, N. M., Dar, M. E. U. I. (2015): Species composition and community structure of subtropical forest stands in western Himalayan foothills of Kashmir. – Pak. J. Bot. 47: 2151-2160.
[63] Shaheen, H., Qureshi, R. A., Shinwari, Z. K. (2011): Structural diversity, vegetation dynamics and anthropogenic impact on Lesser Himalayan subtropical forests of Bagh District, Kashmir. – Pak. J. Bot. 43: 1861-1866.
[64] Shehzad, K. R., Malik, Z. H., Qureshi, R. A. (1999): Phytosociological survey of Samahni valley Bhimber, Azad Kashmir. – Pak. J. For. 49: 91-98.
[65] Shimwell, D. W. (1971): The description and classification of vegetation. – Sedgwick and Jackson, London, 322p.
[66] Shrestha, U. B., Gautam, S., Bawa, K. S. (2012): Widespread climate change in the Himalayas and associated changes in local ecosystems. – Plos One 7: e36741.
[67] Tanvir, M., Murtaza, G., Ahmad, K. S., Salman, M. (2014): Floral diversity of District Bagh, Azad Jammu and Kashmir Pakistan. – Universal J. Plant Sci. 2: 1-13.
[68] Ter Braak, C. J. F., Smilauer, P. (2012): Canoco 5, Windows release (5.00), [Software for canonical community ordination]. – Microcomputer Power, Ithaca, NY, USA.
[69] TPL. (2013): The Plant List. Version 1.1. – Avaialble at <http://www.theplantlist.org/> access on 15 April 2020.
[70] Vashistha, R. K., Rawat, N., Chaturvedi, A. K., Nautiyal, B. P., Prasad, P., Nautiyal, M. C. (2009): An exploration on the phenology of different growth forms of an alpine expanse of North-West Himalaya, India. – New York Science Journal 2(6): 29-41.
[71] Vigne, G. T. (1842): Travels in Kashmir, Ladak and Iskardo (1835-1839). – Henry Colburn, London.
[72] Wang, H., Dai, J., Rutishauser, T., Gonsamo, A., Wu, C., Ge, Q. (2018): Trends and variability in temperature sensitivity of lilac flowering phenology. – J. Geophys. Res. Biogeo. 123: 807-817.
[73] Williams, T. A., Abberton, M. T. (2004): Earlier flowering between 1962 and 2002 in agricultural varieties of white clover. – Oecologia 138: 122-126.
[74] Willis, C. G., Ruhfel, B., Primack, R. B., Miller-Rushing, A. J., Davis, C. C. (2008): Phylogenetic patterns of species loss in Thoreau's woods are driven by climate change. – Proceedings of the National Academy of Sciences of the United States of America 105: 17029-17033. https://doi.org/10.1073/pnas.0806446105.

http://www.aloki.hu ● ISSN 1589 1623 (Print) ● ISSN 1785 0037 (Online)
DOI: http://dx.doi.org/10.15666/aeer/2001_301337

APPENDIX

Supplementary Data Table 1. *Floristic list of the vascular plants species of Dhirkot, district Bagh, and their various attributes*

Family	Species names and Voucher No.	Local name	Habit	Life forms	Leaf spectra	Phenology	Status
Pteridophytes							
Aspleniaceae	*Asplenium dalhousiae* Hook. / NK98	Alaf jarhi	H	G	Mep	Jun-Dec	Native [Ra, NI]
Dryopteridaceae	*Dryopteris ramosa* (C. Hope) C. Chr. / NK99	Kunji	H	G	Map	Jun-Sep	Native [Ra, NI]
Pteridaceae	*Adiantum capillus-veneris* L. / NK100	Kakwai	H	G	Mip	May-Aug	Native [Ra, NI]
	Adiantum raddianum C. Presl / NK101	Parsoshan	H	G	Mep	Jun-Sep	Introduced [Ra, NI]
	Adiantum venustum D. Don / NK102	Kakwai	H	G	Mip	May-Aug	Native [VC, NI]
	Onychium japonicum (Thunb.) Kunze / NK103	Kunji	H	G	Map	Jun-Sep	Introduced [Ra, NI]
	Pteris cretica L. / NK104	Nanoor	H	Hc	Map	Jun-Aug	Native [Co, NI]
	Pteris vittata L. / NK105	Nanoor	H	G	Map	Jun-Aug	Native [Co, NI]
Gymnosperms							
Pinaceae	*Cedrus deodara* (Roxb.ex D. Don) G.Don / NK106	Deyaar	T	Mp	Lep	Oct-Nov	Native [Ra, NI]
	Pinus roxburghii Sarg. / NK107	Chir	T	Mp	Lep	Mar-Apr	Native [VC, NI]
	Pinus wallichiana A.B.Jacks. / NK108	Beyaarh	T	Mp	Lep	Apr-Jun	Native [VC, NI]
Taxaceae	*Taxus wallichiana* Zucc. / NK109	Tooni	T	Ms	Lep	Feb-Mar	Native [Ra, NI]
Monocotyledons							
Araceae	*Arisaema jacquemontii* Blume / NK110	Sap booti, Cobra plant	H	G	Mep	Jun-Jul	Native [Ra, NI]
	Sauromatum venosum (Dryand. ex Aiton) Kunth / NK111.	Adbees	H	G	Mep	Apr-May	Native [Co, NI]

http://www.aloki.hu ● ISSN 1589 1623 (Print) ● ISSN 1785 0037 (Online)
DOI: http://dx.doi.org/10.15666/aeer/2001_301337

Family	Species names and Voucher No.	Local name	Habit	Life forms	Leaf spectra	Phenology	Status
Commelinaceae	*Commelina benghalensis* L. / NK112	Kanteri, Chura	H	Th	Mip	Jun-Sep	Native [Co, NI]
Cyperaceae	*Carex brunnea* Thunb. / NK113	Kangri malla	H	Th	Nap	Jul-Aug	Native [Ra, NI]
	Cyperus arenarius Retz. / NK114	Unavailable	H	G	Nap	Mar-May	Native [Co, NI]
	Cyperus compressus L. / NK115	Elegant sedge	H	Th	Lep	Jul-Oct	Native [C0, NI]
	Cyperus difformis L. / NK116	Daila	H	Hc	Nap	Jul-Oct	Native [Co, NI]
	Cyperus iria L. / NK117	Bhoian	H	Th	Mip	May-Oct	Native [VR, NI]
	Cyperus niveus Retz. / NK118	Snow white	H	Hc	Nap	Apr-Jun	Native [Ra, NI]
	Cyperus rotundus L. / NK119	Nagarmotha	H	G	Nap	Apr-Oct	Native [Co, In]
	Cyperus serotinus Rottb. / NK120	Unavailable	H	Th	Nap	Jul-Sep	Native [Ra, NI]
	Eriophorum comosum (Wall.) Nees / NK121	Babya	H	Hc	Mip	Jul-Sep	Native [VC, NI]
	Fimbristylis bisumbellata (Forssk.) Bubani / NK122	Choti bhuini	H	Th	Nap	Jul-Oct	Native [Co, NI]
	Fimbristylis dichotoma (L.) Vahl / NK123	Choti bhuini	H	G	Nap	Aug-Oct	Native [Co, NI]
Liliaceae	*Notholirion thomsonianum* (Royle) Stapf / NK124	Hazara lily	H	G	Mip	Apr-May	Native [Ra, NI]
	Tulipa clusiana DC. / NK125	Kakarh mula	H	G	Mip	Mar-May	Native [Co, NI]
Orchidaceae	*Epipactis helleborine* (L.) Crantz / NK126	Koka maki	H	G	Mip	Jun-Aug	Native [Ra, NI]
	Spiranthes sinensis (Pers.) Ames / NK127	Chitti batti	H	G	Nap	May-Sep	Introduced [VR, NI]
Poaceae	*Agrostis canina* L. / NK128	Kaah	H	Th	Nap	Jul-Aug	Native [VC, NI]
	Agrostis gigantea Roth / NK129	Kaah	H	Hc	Mip	Jun-Aug	Native [VC, NI]
	Apluda mutica L. / NK130	Ghagari	H	Hc	Nap	Aug-Nov	Native [Co, NI]
	Aristida funiculata Trin. & Rupr. / NK131	Lamb	H	Th	Mip	Jun-Sep	Native [Co, NI]

http://www.aloki.hu ● ISSN 1589 1623 (Print) ● ISSN 1785 0037 (Online)
DOI: http://dx.doi.org/10.15666/aeer/2001_301337

Family	Species names and Voucher No.	Local name	Habit	Life forms	Leaf spectra	Phenology	Status
	Arundinella nepalensis Trin. / NK132	Garali	H	G	Mip	Sep-Nov	Native [VC, NI]
	Arundo donax L. / NK133	Nari	H	Hc	Map	Jun-Oct	Native [Co, In]
	Avena fatua L. / NK134	Jwaan seela	H	Th	Nap	May-Aug	Native [VC, NI]
	Brachiaria ramosa (L.) Stapf / NK135	Kanderi	H	Th	Mip	Jul-Oct	Native [Co, NI]
	Brachypodium sylvaticum (Huds.) P. Beauv. / NK136	Bitkaai	H	Th	Mip	Jun-Sep	Native [VC, NI]
	Bromus catharticus Vahl / NK137	Tank	H	Hc	Mip	Apr-Jun	Introduced [VC, NI]
	Chrysopogon gryllus (L.) Trin. / NK138	Bari kaah	H	Hc	Nap	Jun-Aug	Native [VC, NI]
	Chrysopogon serrulatus Trin. / NK139	Jargi kaah	H	Hc	Nap	Jun-Aug	Native [Co, NI]
	Cymbopogon jwarancusa (Jones) Schult. / NK140	Khawi	H	Hc	Nap	Mar-May	Native [Ra, NI]
	Cynodon dactylon (L.) Pers. / NK141	Khabbal	H	Hc	Lep	Whole year	Native [VC, NI]
	Dactylis glomerata L. / NK142	Samaki	H	Hc	Mip	Jul-Aug	Native [Co, NI]
	Dactyloctenium aegyptium (L.) Willd. / NK143	Madhani kaah	H	Th	Nap	Jul-Oct	Native [Ra, NI]
	Dichanthium annulatum (Forssk.) Stapf / NK144	Murgha kaah	H	Hc	Lep	Mar-Oct	Native [Co, NI]
	Digitaria sanguinalis (L.) Scop. / NK145	Tarakhni malla	H	Hc	Mip	Jul-Sep	Native [VC, NI]
	Digitaria violascens Link / NK146	Tarakhni malla	H	Hc	Mip	Jul-Aug	Native [VC, NI]
	Echinochloa colona (L.) Link / NK147	Malla kaah	H	Th	Mip	May-Sep	Native [Co, NI]
	Eleusine indica (L.) Gaertn. / NK148	Goose grass	H	Th	Mip	Jun-Aug	Native [Co, NI]
	Eragrostis pilosa (L.) P. Beauv. / NK149	Barboori	H	Th	Mip	Jul-Oct	Native [VC, NI]

http://www.aloki.hu ● ISSN 1589 1623 (Print) ● ISSN 1785 0037 (Online)
DOI: http://dx.doi.org/10.15666/aeer/2001_301337

Family	Species names and Voucher No.	Local name	Habit	Life forms	Leaf spectra	Phenology	Status
	Heteropogon contortus (L.) P. Beauv. ex Roem. & Schult. / NK150	Sureli	H	Hc	Mip	Jun-Oct	Native [VC, NI]
	Leptochloa panicea (Retz.) Ohwi / NK151	Kaah	H	Th	Mip	Sep-Nov	Native [VC, NI]
	Oplismenus compositus (L.) P.Beauv. / NK152	Malla	H	Hc	Mip	Aug-Sep	Native [Co, NI]
	Oplismenus undulatifolius (Ard.) Roem. & Schult. / NK153	Malla	H	Hc	Mip	Aug-Sep	Native [VC, NI]
	Paspalidium flavidum (Retz.) A.Camus / NK154	Kangna	H	Hc	Mip	Jul-Oct	Native [Co, NI]
	Paspalum distichum L. / NK155	Daila	H	Hc	Nap	Apr-May	Introduced [Ra, NI]
	Pennisetum flaccidum Griseb. / NK156	Manehra kaah	H	Hc	Mip	Jun-Oct	Native [VC, NI]
	Pennisetum glaucum (L.) R. Br. / NK157	Phulai	H	Hc	Mip	Jun-Aug	Introduced [Co, NI]
	Pennisetum orientale Rich. / NK158	Phulai	H	Hc	Mip	Apr-Oct	Native [Co, NI]
	Phalaris minor Retz. / NK159	Dumbi sitti	H	Th	Mip	Mar-May	Native [Co, NI]
	Piptatherum munroi (Stapf ex Hook. f.) Mez / NK160	Smilo grass	H	Hc	Mip	Jun-Sep	Native [VC, NI]
	Poa annua L. / NK161	Kaah	H	Th	Mip	Mar-Sep	Native [VC, NI]
	Polypogon viridis (Gouan) Breistr. / NK162	Pochar	H	Hc	Mep	May-Aug	Native [VC, NI]
	Saccharum spontaneum Linn. / NK163	Kamath	H	Hc	Mip	Jul-Sep	Native [VC, NI]
	Setaria pumila (Poir.) Roem. & Schult. / NK164	Kangri mallo	H	Th	Mip	Jun-Oct	Native [VC, In]
	Setaria viridis (L.) P. Beauv. / NK165	Kangrel	H	Th	Mip	Jun-Sep	Native [VC, NI]
	Sorghum halepense (L.) Pers. / NK166	Barru kaah	H	G	Mip	May-Oct	Native [VC, In]

http://www.aloki.hu ● ISSN 1589 1623 (Print) ● ISSN 1785 0037 (Online)
DOI: http://dx.doi.org/10.15666/aeer/2001_301337

Family	Species names and Voucher No.	Local name	Habit	Life forms	Leaf spectra	Phenology	Status
	Themeda anathera (Nees ex Steud.) Hack. / NK167	Samaki	H	Hc	Nap	Jun-Oct	Native [VC, NI]
	Tragus berteronianus Schult. / NK168	Unavailable	H	Th	Nap	Nov-Apr	Native [Ra, NI]
		Dicotyledons					
Acanthaceae	*Dicliptera bupleuroides* Nees / NK169	Somni	H	Hc	Nap	Jun-Oct	Native [VC, NI]
	Dicliptera paniculata (Forssk.) I. Darbysh. / NK170	Toot tallo	H	Th	Mip	Dec-Feb	Native [VC, NI]
	Justicia adhatoda L. / NK171	Bekarh	S	Np	Mep	Jul-Oct	Native [VC, NI]
	Strobilanthes urticifolia Wall. ex Kuntze / NK172	Bekarhi	H	Ch	Mep	Jun-Oct	Native [VC, In]
Adoxaceae	*Viburnum grandiflorum* Wall. ex DC / NK173	Guch	S	Np	Mep	Nov-Jun	Native [VC, NI]
Amaranthaceae	*Achyranthes aspera* L. / NK174	Puth kanda	H	Ch	Mip	Jul-Oct	Native [VC, In]
	Alternanthera pungens Kunth / NK175	Bakharha	H	Th	Mip	Aug-Oct	Introduced [Co, NI]
	Amaranthus caudatus L. / NK176	Baghi ganehr	H	Th	Mep	May-Aug	Introduced [Co, NI]
	Amaranthus hybridus L. / NK177	Surkh ganehr	H	Th	Mip	Jul-Oct	Introduced [VC, In]
	Amaranthus retroflexus L. / NK178	Ganehr	H	Th	Mip	Jul-Sep	Introduced [Co, NI]
	Amaranthus viridis L. / NK179	Ganehr	H	Th	Mip	Mar-Oct	Introduced [VC, In]
	Chenopodium album L. / NK180	Bathwa	H	Th	Mip	May-Oct	Native [VC, In]
	Digera muricata (L.) Mart. / NK181	Tandla	H	Th	Mip	Aug-Sep	Native [Co, NI]
Anacardiaceae	*Cotinus coggygria* Scop. / NK182	Pann	S	Np	Mip	Apr-May	Native [Co, NI]
Apiaceae	*Bupleurum falcatum* L. / NK183	Patti	H	Hc	Nap	Jun-Oct	Native [Co, NI]

http://www.aloki.hu ● ISSN 1589 1623 (Print) ● ISSN 1785 0037 (Online)
DOI: http://dx.doi.org/10.15666/aeer/2001_301337

Family	Species names and Voucher No.	Local name	Habit	Life forms	Leaf spectra	Phenology	Status
	Conium maculatum L. / NK184	Morkach	H	Hc	Mip	Jun-Aug	Native [Co, NI]
	Foeniculum vulgare Mill. / NK185	Saunf	H	Hc	Nap	Aug-Oct	Native [VR, NI]
	Pimpinella stewartii Nasir / NK186	Unavailable	H	Ch	Nap	Jun-Aug	Native [Co, NI]
Apocynaceae	*Nerium oleander* L. / NK187	Kaneera	S	Np	Mip	Apr-Oct	Native [VC, In]
Araliaceae	*Hedera helix* L. / NK188	Batkal, Harhbamal	C	L	Mip	Oct-Apr	Native [Co, NI]
Aristolochiaceae	*Aristolochia punjabensis* Lace / NK189	Kutyari, kuttay booti	S	Np	Mip	Jun-Jul	Native [Ra, NI]
Balsaminaceae	*Impatiens edgeworthii* Hook. f. / NK224	Bantil	H	Th	Mep	Jul-Sep	Native [VC, NI]
Berberidaceae	*Berberis lycium* Royle / NK225	Sumbal	S	Np	Nap	Apr-Jun	Native [VC, NI]
Boraginaceae	*Cynoglossum lanceolatum* Forssk. / NK226	Churoon	H	Th	Mip	Jun-Aug	Native [VC, NI]
	Cynoglossum wallichii Var. *glochidiatum* (Wall. ex Benth.) Kazmi / NK227	Phulari jarhi	H	Th	Mip	May-Aug	Native [VC, NI]
Brassicaceae	*Capsella bursa-pastoris* (L.) Medik. / NK228	Ban paincha	H	Th	Mip	May-Jul	Native [VC, In]
	Conringia orientalis (L.) Dumort. / NK229	Ban sariyaan	H	Th	Mip	Apr-May	Native [Co, NI]
	Lepidium apetalum Willd. / NK230	Duda patti	H	Th	Mip	Apr-Jun	Native [VC, NI]
	Lepidium didymum L. / NK231	Jangli hallon	H	Th	Mip	Mar-Jun	Introduced [Ra, NI]
	Sinapis arvensis L. / NK232	Ban sariyaan	H	Th	Mip	Apr-Jun	Native [Co, NI]
	Sisymbrium irio L. / NK233	Ban hailyan	H	Th	Mip	Mar-May	Native [Co, NI]
Buxaceae	*Sarcococca saligna* (D. Don) Müll-Arg. / NK234	Nairi	S	Np	Mip	Sep-Apr	Native [VC, NI]
Campanulaceae	*Campanula pallida* Wall. / NK235	Beli flower	H	Th	Nap	Apr-Jul	Native [Ra, NI]

http://www.aloki.hu ● ISSN 1589 1623 (Print) ● ISSN 1785 0037 (Online)
DOI: http://dx.doi.org/10.15666/aeer/2001_301337

Family	Species names and Voucher No.	Local name	Habit	Life forms	Leaf spectra	Phenology	Status
Cannabaceae	*Cannabis sativa* L. / NK236	Bhang	H	Th	Mep	Apr-Sep	Native [VC, In]
	Celtis australis L. / NK237	Kharik	T	Ms	Mip	Mar-May	Native [Ra, NI]
Caprifoliaceae	*Valeriana jatamansi* Jones / NK238	Mushkbala	H	G	Mip	Mar-May	Native [Co, NI]
	Lonicera quinquelocularis Hard. / NK239	Phutt	S	Mc	Mip	Apr-Jul	Native [Co, NI]
Caryophyllaceae	*Silene conoidea* L. / NK240	Dabbri	H	Th	Nap	Mar-Apr	Native [Ra, NI]
	Stellaria media (L.) Vill. / NK241	Lausari	H	Th	Nap	Apr-Aug	Native [VC, In]
Celastraceae	*Gymnosporia royleana* Wall. ex M.A. Lawson / NK242	Patakhi	S	Np	Nap	Sep-Jan	Native [Ra, NI]
Compositae	*Achillea millefolium* L. / NK190	Sultan booti	H	Th	Mip	Jul-Sep	Native [VC, NI]
	Anaphalis triplinervis (Sims) Sims ex C.B. Clarke / NK191	Unavailable	H	G	Mip	Jul-Oct	Native [VR, NI]
	Artemisia absinthium L. / NK192	Chaoo	H	Ch	Mip	Jun-Sep	Native [Ra, NI]
	Artemisia scoparia Waldst. & Kitam. / NK193	Marua	H	Ch	Lep	Jul-Nov	Native [Ra, NI]
	Artemisia vulgaris L. / NK194	Chaoo	H	Ch	Mip	Aug-Nov	Native [Co, NI]
	Aster alpinus L. / NK195	Alpine aster	H	Th	Mip	May-Jun	Introduced [VR, NI]
	Aster flaccidus Bunge / NK196	Unavailable	H	Th	Nap	Jul-Sep	Native [Co, NI]
	Bidens bipinnata L. / NK197	Surela	H	Th	Mip	Jun-Oct	Introduced [VC, In]
	Bidens pilosa L. / NK198	Surela	H	Th	Mip	May-Oct	Introduced [VC, In]
	Carpesium abrotanoides L. / NK199	Unavailable	H	Np	Mep	Sep-Nov	Native [Co, NI]
	Carpesium cernuum L. / NK200	Unavailable	H	Th	Mep	Jun-Aug	Native [VC, NI]
	Cirsium arvense (L.) Scop. / NK201	Tattaar	H	Th	Mep	Aug-Oct	Native [Co, In]

http://www.aloki.hu ● ISSN 1589 1623 (Print) ● ISSN 1785 0037 (Online)
DOI: http://dx.doi.org/10.15666/aeer/2001_301337

Family	Species names and Voucher No.	Local name	Habit	Life forms	Leaf spectra	Phenology	Status
	Erigeron bonariensis L. / NK202	Neeli booti	H	Th	Nap	Jun-Nov	Introduced [VC, In]
	Erigeron trilobus (Decne.) Boiss. / NK203	Paleet	H	Th	Lep	Sep-Oct	Native [Ra, NI]
	Galinsoga parviflora Cav. / NK204	Gallant soldiers	H	Th	Mip	Jul-Oct	Introduced [VC, In]
	Gerbera gossypina (Royle) Beauverd / NK205	Phutkola	H	Hc	Mep	May-Jul	Native [VC, NI]
	Himalaiella heteromalla (D. Don) Raab-Straube / NK206	Gwaal mula	H	Hc	Mip	Jun-Aug	Native [VC, NI]
	Jurinea dolomiaea Boiss. / NK207	Gugal toof	H	Hc	Mip	Jul-Sep	Native [VR, NI]
	Kalimeris altaica (Willd.) Nees ex Fisch. Mey. & Ave-Lall. / NK208	Unavailable	H	Th	Nap	Jul-Oct	Native [Co, NI]
	Launaea nudicaulis Hook. f. / NK209	Dudhal	H	Th	Mep	Apr-Jun	Native [Ra, NI]
	Leontopodium himalayanum DC. / NK210	Silver star	H	Th	Nap	Jul-Oct	Native [VR, NI]
	Myriactis nepalensis Less. / NK211	Thuke phool	H	Th	Mip	Apr-Nov	Native [VC, NI]
	Myriactis wightii DC. / NK212	Thuke phool	H	Th	Mip	Jul-Nov	Native [Co, NI]
	Parthenium hysterophorus L. / NK213	Gandi booti	H	Th	Nap	Apr-Aug	Introduced [VC, In]
	Phagnalon rupestre (L.) DC. / NK214	Unavailable	H	Th	Mip	Mar-May	Native [VR, NI]
	Prenanthes brunoniana Wall. ex DC. / NK215	Duddal	H	Th	Mep	Aug-Sep	Native [VC, NI]
	Siegesbeckia orientalis L. / NK216	Yellow crown beared	H	Th	Mep	Oct-Nov	Native [Co, NI]
	Silybum marianum (L.) Gaertn. / NK217	Kandyari	H	Th	Mep	Feb-Apr	Native [VC, In]
	Solidago virgaurea L. / NK218	Woundwort	H	Hc	Mip	Jul-Oct	Native [Co, NI]
	Sonchus asper (L.) Hill / NK219	Dudhal	H	Th	Mep	Mar-Oct	Native [VC, NI]

http://www.aloki.hu ● ISSN 1589 1623 (Print) ● ISSN 1785 0037 (Online)
DOI: http://dx.doi.org/10.15666/aeer/2001_301337

Family	Species names and Voucher No.	Local name	Habit	Life forms	Leaf spectra	Phenology	Status
	Sonchus oleraceus (L.) L. / NK220	Dudhal	H	Th	Mep	Mar-Jun	Native [Co, NI]
	Tagetes minuta L. / NK221	Sadbarga	H	Th	Mip	Oct-Nov	Introduced [VC, In]
	Taraxacum campylodes G.E. Haglund / NK222	Hand	H	Hc	Mip	Mar-Sep	Introduced [VC, In]
	Xanthium strumarium L. / NK223	Kandeli	H	Th	Mep	Aug-Oct	Introduced [VC, In]
Convolvulaceae	*Convolvulus arvensis* L. / NK243	Do tilla	C	L	Mip	May-Sep	Native [VC, NI]
	Cuscuta australis R. Br. / NK244	Neela taari	C	L	Lep	Aug-Oct	Introduced [Ra, NI]
	Cuscuta reflexa Roxb. / NK245	Neela taari	C	L	Lep	Aug-Oct	Native [Co, NI]
	Ipomoea carnea Jacq. / NK246	Jangli bekarh	S	Np	Mep	Jul-Nov	Introduced [Ra, NI]
	Ipomoea purpurea (L.) Roth / NK247	Eerh	C	Th	Mep	Jul-Sep	Introduced [Co, NI]
Cornaceae	*Cornus macrophylla* Wall. / NK248	Qandar	T	Ms	Mep	Apr-Jun	Native [VR, NI]
Cucurbitaceae	*Solena amplexicaulis* (Lam.) Gandhi / NK249	Gwal khakhri	C	L	Mep	Apr-Jul	Native [VR, NI]
Ebenaceae	*Diospyros kaki* L.f. / NK250	Mota amlook	T	Ms	Mep	May-Aug	Introduced [Co, NI]
	Diospyros lotus L. / NK251	Amlook	T	Ms	Mep	May-Jun	Native [VC, NI]
Elaeagnaceae	*Elaeagnus umbellata* Thunb. / NK252	Kankoli	S	Mc	Mip	May-Jun	Native [Co, NI]
Euphorbiaceae	*Euphorbia granulata* Forssk. / NK253	Hazar dani	H	Th	Lep	Jun-Sep	Native [Co, NI]
	Euphorbia helioscopia L. / NK254	Dhudal	H	Th	Nap	Jan-Jul	Native [VC, In]
	Euphorbia heterophylla L. / NK255	Milk weed	H	Th	Mip	Aug-Sep	Introduced [Co, NI]
	Euphorbia hirta L. / NK256	Dudhali	H	Th	Nap	Jul-Dec	Introduced [Co, In]
	Euphorbia prostrata Aiton / NK257	Hazaar dani	H	Th	Lep	Apr-Oct	Introduced [Co, NI]
	Mallotus philippensis	Kamela	T	Mc	Mep	Mar-May	Native [Co, NI]

http://www.aloki.hu ● ISSN 1589 1623 (Print) ● ISSN 1785 0037 (Online)
DOI: http://dx.doi.org/10.15666/aeer/2001_301337

Family	Species names and Voucher No.	Local name	Habit	Life forms	Leaf spectra	Phenology	Status
	(Lam.) Müll.Arg. / NK258						
	Ricinus communis L. / NK259	Arind	H	Mc	Mep	Jun-Sep	Introduced [VC, In]
Fagaceae	*Quercus baloot* Griff. / NK274	Parungi	T	Ms	Mep	Apr-May	Native [VC, NI]
	Quercus incana Bartram / NK275	Reen	T	Ms	Mep	Apr-May	Native [VC, NI]
Gentianaceae	*Gentiana squarrosa* Ledeb. / NK276	Unavailable	H	Th	Nap	Apr-Sep	Native [VC, NI]
	Swertia angustifolia Buch.-Ham. ex D. Don / NK277	Choratta	H	Th	Mip	Jun-Nov	Native [VC, NI]
	Swertia chirayita (Roxb.) Buch.-Ham. ex C.B.Clarke / NK278	Choratta	H	Th	Mip	Jul-Oct	Native [Ra, NI]
Geraniaceae	*Geranium nepalense* Sweet / NK279	Rattan doi	H	Hc	Mip	Apr-Sep	Native [Co, NI]
	Geranium wallichianum D. Don ex Sweet / NK280	Rattan do	H	Th	Mip	Jul-Sep	Native [VC, NI]
Hypericaceae	*Hypericum perforatum* L. / NK281	Sharan gulab	H	Ch	Nap	Jun-Sep	Native [Co, NI]
Juglandaceae	*Juglans regia* L. / NK282	Akhor	T	Ms	Mep	Feb-Apr	Native [VC, NI]
Lamiaceae	*Ajuga integrifolia* Buch.-Ham / NK283	Ratti booti	H	Hc	Mip	Mar-Jun	Native [Ra, NI]
	Ajuga parviflora Benth. / NK284	Ratti booti	H	Th	Mep	Mar-Jun	Native [Co, NI]
	Callicarpa macrophylla Vahl / NK285	Ukkal	T	Ms	Mep	Jul-Nov	Native [Co, NI]
	Clinopodium debile (Bunge) Kuntze / NK286	Unavailable	H	Hc	Nap	Aug-Sep	Native [VR, NI]
	Clinopodium umbrosum (M. Bieb.) Kuntze / NK287	Unavailable	H	Hc	Nap	May-Jul	Native [VC, NI]
	Clinopodium vulgare L. / NK288	Unavailable	H	Th	Mip	Mar-Jul	Native [Co, NI]
	Isodon coetsa (Buch.-Ham. ex	Unavailable	H	Ch	Mip	Aug-Sep	Native [VC, NI]

http://www.aloki.hu ● ISSN 1589 1623 (Print) ● ISSN 1785 0037 (Online)
DOI: http://dx.doi.org/10.15666/aeer/2001_301337

Family	Species names and Voucher No.	Local name	Habit	Life forms	Leaf spectra	Phenology	Status
	D. Don) Kudo / NK289						
	Isodon rugosus (Wall. ex Benth.) Codd / NK290	Pissu maar	S	Np	Mip	Mar-Oct	Native [VC, NI]
	Mentha arvensis L. / NK291	Bareena	H	Hc	Mip	Jul-Sep	Native [Co, NI]
	Mentha longifolia (L.) L. / NK292	Pootna, chitta podina	H	Hc	Mip	May-Nov	Native [Co, NI]
	Micromeria biflora (Buch.-Ham. ex D. Don) Benth. / NK293	Jarhi	H	Hc	Lep	Mar-Nov	Native [VC, NI]
	Nepeta cataria L. / NK294	Cat mint	H	Hc	Mep	Jun-Jul	Native [Co, NI]
	Nepeta govaniana (Wall. ex Benth.) Benth. / NK295	Ladori	H	Hc	Nap	Jul-Sep	Native [Ra, NI]
	Nepeta laevigata (D. Don) Hand.-Mazz. / NK296	Unavailable	H	Hc	Mip	Jun-Aug	Native [Co, NI]
	Origanum vulgare L. / NK297	Maskanna	H	Hc	Nap	Jun-Oct	Native [VC, NI]
	Prunella vulgaris L. / NK298	Nariya	H	Hc	Mip	Jun-Aug	Native [Co, NI]
	Rydingia limbata (Benth.) Scheen & V. A. Albert / NK299	Chitta jand	S	Np	Mip	Apr-May	Native [Co, NI]
	Salvia canariensis L. / NK300	Kathra	H	Hc	Mip	Apr-Jul	Native [Co, NI]
	Salvia moorcroftiana Wall. ex Benth. / NK301	Kathra	H	Hc	Mep	May-Jun	Native [Ra, NI]
	Salvia nubicola Wall. ex Sweet / NK302	Noorchari	H	Hc	Mep	Jun-Oct	Native [Ra, NI]
	Scutellaria grossa Wall. / NK303	Mastiari	H	Hc	Mip	Jul-Sep	Native [Co, NI]
	Thymus linearis Benth. / NK304	Chikal	H	Ch	Lep	Jul-Aug	Native [Ra, NI]
Leguminosae	*Acacia nilotica* (L.) Delile / NK260	Kikar	T	Ms	Mip	Mar-Aug	Native [VC, In]
	Astragalus grahamianus Benth. / NK261	Kala kandyara	H	Ch	Mep	Apr-Aug	Native [Ra, NI]
	Crotalaria medicaginea Lam. / NK262	Sinji	H	Th	Mip	Mar-Aug	Native [Co, NI]

http://www.aloki.hu ● ISSN 1589 1623 (Print) ● ISSN 1785 0037 (Online)
DOI: http://dx.doi.org/10.15666/aeer/2001_301337

Family	Species names and Voucher No.	Local name	Habit	Life forms	Leaf spectra	Phenology	Status
	Dalbergia sissoo DC. / NK263	Tahli, Sheesham	T	Ms	Mip	Mar-May	Native [Co, NI]
	Desmodium elegans DC. / NK264	Chamkath	S	Np	Mep	Jun-Sep	Native [Ra, NI]
	Indigofera heterantha Brandis / NK265	Jandh	S	Np	Lep	May-Jul	Native [VC, In]
	Indigofera linifolia (L. f.) Retz. / NK266	Nikki kawati	H	Th	Nap	Jul-Oct	Native [Ra, NI]
	Lespedeza juncea var. *sericea* (Thunb.) Lace & Hauech / NK267	Jandi	H	Ch	Nap	Jul-Oct	Native [VC, NI]
	Lespedeza bicolor Turcz. / NK268	Chamkaath	S	Np	Mep	Jul-Sep	Native [Ra, NI]
	Lotus corniculatus L. / NK269	Peela palti	H	Hc	Nap	Apr-Aug	Native [Co, NI]
	Medicago polymorpha L. / NK270	Maina	H	Th	Mip	Mar-May	Native [VC, In]
	Mimosa himalayana Gamble / NK271	Arai	S	Np	Nap	Jun-Aug	Native [Ra, NI]
	Oxytropis lapponica (Wahlenb.) Gay / NK272	Jandi	H	Ch	Nap	Jun-Aug	Native [Ra, NI]
	Trifolium repens L. / NK273	Khatimal	H	Hc	Mip	Apr-Jul	Native [VC, In]
Linaceae	*Linum corymbulosum* Rchb. / NK305	Tangra	H	Ch	Mip	Mar-Jun	Native [Ra, NI]
Lythraceae	*Punica granatum* L. / NK306	Daarhu	S	Np	Mip	Apr-Jun	Native [VC, NI]
Malvaceae	*Corchorus tridens* L. / NK307	Unavailable	H	Th	Mip	Jul-Nov	Native [Ra, NI]
	Grewia optiva J.R. Drumm. ex Burret / NK308	Taman	T	Ms	Mep	Apr-Sep	Native [Co, NI]
	Malva neglecta Wallr. / NK309	Sonchal	H	Th	Mip	Jun-Sep	Native [Co, NI]
	Malvastrum coromandelianum (L.) Garcke / NK310	Gogi booti	H	Th	Mip	Jun-Sep	Introduced [Co, NI]
Meliaceae	*Melia azedarach* L. / NK311	Daraik	T	Ms	Mep	Mar-Apr	Introduced [VC, In]
Moraceae	*Broussonetia papyrifera* (L.)	Jangli toot	T	Ms	Mep	Mar-Aug	Introduced [VC, In]

http://www.aloki.hu ● ISSN 1589 1623 (Print) ● ISSN 1785 0037 (Online)
DOI: http://dx.doi.org/10.15666/aeer/2001_301337

Family	Species names and Voucher No.	Local name	Habit	Life forms	Leaf spectra	Phenology	Status
	L'Her. ex Vent. / NK312						
	Ficus carica L. / NK313	Teen patri phagwari	T	Mc	Mep	Apr-Dec	Native [Co, NI]
	Ficus palmata Forssk. / NK314	Phagwari	T	Ms	Mep	May-Sep	Native [VC, NI]
	Ficus sarmentosa Buch.-Ham. ex. Sm. / NK315	Dadday veil	C	L	Mip	May-Sep	Native [VR, NI]
	Morus alba L. / NK316	Shaitoot	T	Ms	Mep	Apr-Sep	Introduced [VR, NI]
	Morus nigra L. / NK317	Toot	T	Ms	Mep	Mar-Jul	Introduced [Ra, NI]
Oleaceae	*Jasminum humile* L. / NK318	Chamba	S	Np	Mep	Apr-Jun	Native [Co, NI]
	Olea ferruginea Wall. ex Aitch. / NK319	Kaoo	T	Ms	Nap	Apr-May	Native [VC, NI]
Onagraceae	*Oenothera rosea* L' Her. ex Aiton / NK320	Ratt mundia	H	Th	Mip	Apr-Sep	Introduced [VC, In]
Oxalidaceae	*Oxalis corniculata* L. / NK321	Khatti booti	H	Hc	Nap	Mar-Oct	Introduced [VC, In]
Paeoniaceae	*Paeonia emodi* Royle / NK322	Mameikh	H	G	Mep	May-Jun	Native [VR, NI]
Papaveraceae	*Fumaria indica* (Hausskn.) Pugsley / NK323	Shatra papra	H	Th	Mip	Mar-Jun	Native [Co, NI]
Passifloraceae	*Passiflora caerulea* L. / NK324	Garhi wala phool	C	L	Mep	Jul-Sep	Introduced [VR, NI]
Phyllanthaceae	*Leptopus cordifolius* Decne. / NK325	Karukni	S	Np	Mip	Jul-Oct	Native [VC, NI]
Phytolaccaceae	*Phytolacca latbenia* (Moq.) H. Walter / NK326	Parth, Kala kaath	T	Ms	Mep	Jun-Aug	Native [VR, NI]
Plantaginaceae	*Plantago lanceolata* L. / NK327	Batti	H	Hc	Mip	Jul-Sep	Native [VC, In]
	Plantago major L. / NK328	Isamgol	H	Hc	Mep	Aug-Sep	Native [VC, In]
	Veronica persica Poir. / NK329	Lazarh	H	Th	Mip	Feb-May	Introduced [Co, NI]
Platanaceae	*Platanus orientalis* L. / NK330	Chinaar	T	Ms	Mep	Apr-May	Introduced [VR, NI]
Polygalaceae	*Polygala abyssinica* R. Br. ex Fresen. / NK331	Unavailable	H	Ch	Nap	Mar-Sep	Native [Co, NI]

http://www.aloki.hu ● ISSN 1589 1623 (Print) ● ISSN 1785 0037 (Online)
DOI: http://dx.doi.org/10.15666/aeer/2001_301337

Family	Species names and Voucher No.	Local name	Habit	Life forms	Leaf spectra	Phenology	Status
Polygonaceae	*Persicaria amplexicaulis* (D. Don) Ronse Decr. / NK332	Masloon	H	Hc	Mep	Jun-Sep	Native [Co, NI]
	Persicaria barbata (L.) H. Hara / NK333	Nariya	H	Th	Mip	Jun-Sep	Native [VC, NI]
	Persicaria lapathifolia (L.) Delarbre / NK334	Pani ka malla	H	Th	Mip	Jun-Sep	Native [Co, NI]
	Persicaria nepalensis (Meisn.) Miyabe / NK335	Mezarh	H	Hc	Mip	Jun-Sep	Native [VC, In]
	Polygonum aviculare L. / NK336	Darubra	H	Th	Nap	Mar-Sep	Native [Co, NI]
	Polygonum plebeium R. Br. / NK337	Banali	H	Th	Lep	May-Aug	Native [Co, NI]
	Rumex nepalensis Spreng. / NK338	Hulla	H	Th	Mep	Jun-Sep	Native [VC, In]
	Rumex hastatus D. Don / NK339	Chukki, Chukhri	S	Ch	Mip	Jun-Oct	Native [Co, In]
Portulacaceae	*Portulaca oleracea* L. / NK340	Kulfa	H	Th	Nap	May-Aug	Native [Co, NI]
Primulaceae	*Anagallis arvensis* var *arvensis* L. / NK341	Billi booti	H	Th	Nap	Feb-May	Native [Co, NI]
	Anagallis arvensis var. caerulea (L.) Gouan / NK342	Billi booti	H	Th	Nap	Feb-May	Native [Co, NI]
	Androsace rotundifolia Hardwicke / NK343	Akh jarhi	H	Hc	Mip	Apr-Aug	Native [Co, NI]
	Myrsine africana L. / NK344	Khukhan	S	Np	Nap	Mar-May	Native [VC, NI]
Ranunculaceae	*Clematis grata* Wall. / NK345	Chitta jand	C	L	Mip	Aug-Sep	Native [Co, NI]
	Ranunculus laetus Wall. ex Hook. f & J.W. Thomson / NK346	Khandbarya, Chambal booti	H	Th	Mep	Jun-Jul	Native [VC, NI]
Rhamnaceae	*Ziziphus jujuba* Mill. / NK347	Barri	S	Mc	Mip	Jun-Jul	Introduced [Co, NI]
Rosaceae	*Agrimonia eupatoria* L. / NK348	Jalebi booti	H	Th	Mep	Jul-Aug	Introduced [Ra, NI]
	Cotoneaster roseus Edgew. / NK349	Loon	T	Mc	Nap	May-Jun	Native [Ra, NI]

http://www.aloki.hu ● ISSN 1589 1623 (Print) ● ISSN 1785 0037 (Online)
DOI: http://dx.doi.org/10.15666/aeer/2001_301337

Family	Species names and Voucher No.	Local name	Habit	Life forms	Leaf spectra	Phenology	Status
	Duchesnea indica (Andrews) Focke / NK350	Budi meva	H	Hc	Nap	Mar-Oct	Native VC, NI
	Fragaria vesca L. / NK351	Kanechi	H	Hc	Mip	Apr-Jun	Native VC, NI
	Prunus persica (L.) Batsch / NK352	Aaroon	T	Mc	Mip	Feb-Apr	Introduced VC, In
	Pyrus pashia Buch.-Ham. ex D.Don / NK353	Batangi	T	Mc	Mip	Apr-Jun	Native Co, NI
	Rosa webbiana Wall. ex Royle / NK354	Chahl	S	Np	Mep	Jun-Aug	Native VC, NI
	Rubus ellipticus Sm. / NK355	Peela akhra	S	Np	Mep	Apr-Jun	Native VC, NI
	Rubus niveus Thunb. / NK356	Pakanah	S	Np	Mep	Apr-Jun	Native VC, In
	Rubus ulmifolius Schott / NK357	Akhra	S	Np	Mip	Apr-Jul	Introduced VR, NI
Rubiaceae	*Galium divaricatum* Pourr. ex Lam. / NK358	Boora	H	Th	Lep	May-Jun	Native VC, NI
	Rubia manjith Roxb. ex Fleming / NK359	Khuratan	H	L	Mip	Jun-Nov	Native VC, NI
Rutaceae	*Skimmia laureola* Franch. / NK360	Challei	S	Np	Mip	Apr-Jun	Native VC, NI
	Zanthoxylum armatum DC. / NK361	Timbar	S	Mc	Mip	Mar-Apr	Native Co, NI
Salicaceae	*Populus deltoides* Marshall / NK362	Safeda	T	Mp	Mep	Apr-Jun	Native Co, In
	Salix alba L. / NK363	Beesa	T	Mp	Mip	Apr-May	Introduced Ra, NI
Sapindaceae	*Dodonaea viscosa* (L.) Jacq. / NK364	Sanatha	S	Np	Mip	Jan-Mar	Native VC, In
	Aesculus indica (Wall. ex Cambess.) Hook. / NK365	Bankhor	T	Ms	Mep	Apr-May	Native Ra, NI
Saxifragaceae	*Bergenia ciliata* (Haw.) Sternb. / NK366	Batt peya, Zakham e hayaat	H	Hc	Mep	Mar-May	Native Ra, NI
Scrophulariaceae	*Verbascum thapsus* L. / NK367	Jangli tambaku	H	Th	Mep	Jun-Aug	Native Co, In
Simaroubaceae	*Ailanthus altissima* (Mill.) Swingle / NK368	Darawiya	T	Mp	Map	May-Jun	Introduced VC, In

http://www.aloki.hu ● ISSN 1589 1623 (Print) ● ISSN 1785 0037 (Online)
DOI: http://dx.doi.org/10.15666/aeer/2001_301337

Family	Species names and Voucher No.	Local name	Habit	Life forms	Leaf spectra	Phenology	Status
Solanaceae	*Datura stramonium* L. / NK369	Datura	H	Np	Mep	Jun-Jul	Introduced VC, In
	Physalis minima L. / NK370	Jangli tamatar	H	Th	Mip	Aug-Oct	Introduced Co, NI
	Solanum americanum Mill. / NK371	Kach mach	H	Th	Mip	Jun-Oct	Introduced Ra, NI
	Solanum pseudocapsicum L. / NK372	Marcholi	S	Th	Mip	Apr-Jul	Introduced Ra, NI
	Solanum surattense Burm. f. / NK373	Kandiari	H	Hc	Mip	Whole year	Native Co, In
	Solanum villosum Mill. / NK374	Kach mach	H	Th	Mip	Jul-Sep	Native Co, NI
	Withania somnifera (L.) Dunal / NK375	Aksoon	H	Ch	Mep	Whole year	Native Ra, NI
Verbenaceae	*Glandularia aristigera* (S.Moore) Tronc. / NK376	Unavailable	H	Th	Lep	Sep-Apr	Introduced VR, NI
	Lantana camara L. / NK377	Panj phulli	S	Np	Mip	Whole year	Introduced Co, In
	Verbena officinalis L. / NK378	Pamukh	H	Th	Mip	Jun-Sep	Native Ra, NI
Violaceae	*Viola canescens* Wall. / NK379	Gul naqsh	H	Hc	Mip	Mar-Jun	Native VC, NI
	Viola odorata L. / NK380	Gul naqsh	H	Hc	Mip	Mar-Jul	Introduced Ra, NI
Vitaceae	*Vitis vinifera* L. / NK381	Daakh	C	L	Mep	May-Jul	Introduced VR, NI
Urticaceae	*Debregeasia saeneb* (Forssk.) Hepper & J.R.I. Wood / NK382	Sindhari	S	Np	Mep	Mar-Jun	Native Co, NI
	Parietaria judaica L. / NK383	Unavailable	H	Th	Mip	Jul-Aug	Native VR, NI
	Urtica dioica L. / NK384	Bichu booti	H	G	Mip	May-Sep	Native Ra, NI

Legend: *Habit: H= Herb, S= Shrub, T= Tree, C= Climber; **Life forms: Mp= Megaphanerophyte, Ms= Mesophanerophyte, Mc= Microphanerophyte, Np= Nanophanerophyte, Ch= Chaemephyte, Hc= Hemicryptophyte, G= Geophyte, Th= Therophyte; ***Leaf spectra: Lep= Leptophyll, Nap= Nanophyll, Mip= Microphyll, Mep= Mesophyll, Map= Macrophyll; ****Status: VC=Very Common (Frequency of occurrence =.75-100%), Co=Common (Frequency of occurrence =.50-75%), Ra=Rare (Frequency of occurrence =.25-50%), VR=Very Rare (Frequency of occurrence =.0-25%), IN=Invassive, NI=Noninvassive.

http://www.aloki.hu ● ISSN 1589 1623 (Print) ● ISSN 1785 0037 (Online)
DOI: http://dx.doi.org/10.15666/aeer/2001_301337

Supplementary Data Table 2. *Monthly temporal climatic variations (Mean ± SD (Min-Max)) in the study area from March-2015 to February-2018 (3 years)*

Months	Min. Temp (°C)	Max. Temp (°C)	PPT (mm)	Spe. Hum. (g/kg)	Soil Moist. (frac.)	Wind Speed (m/sec)	Shortwave Rad. (W/M²)	Longwave Rad. (W/M²)
January	1.1±0.99 (-0.35-2)	12.87±2.99 (9.68-16.4)	107.52±104.55 (4.26-264.45)	2.8±0.84 (1.7-3.59)	0.32±0.04 (0.27-0.34)	3.27±0.23 (3.03-3.52)	13.95±2.87 (10.62-17.11)	341.78±8.25 (331.65-350.65)
February	2.26±1.26 (0.04-2.99)	14.33±2.81 (10.16-17.18)	198.99±132.14 (69.82-415.55)	3.97±0.48 (3.36-4.47)	0.34±0.03 (0.3-0.38)	3.59±0.14 (3.42-3.79)	16.38±2.92 (13.89-20.85)	349.92±9.09 (334.85-357.26)
March	5.14±1.43 (3.64-6.95)	18.01±2.5 (16.35-22.35)	251.54±156.91 (93.49-508.13)	5.17±0.66 (4.23-6.01)	0.36±0.03 (0.31-0.38)	3.54±0.14 (3.36-3.71)	19.72±2.14 (18.03-23.06)	368.03±10.25 (361.12-384.95)
April	9.29±0.43 (8.8-9.86)	25.09±1.35 (22.75-26.01)	193.26±80.56 (118.46-284.41)	6.71±0.62 (6.27-7.68)	0.35±0.02 (0.33-0.38)	3.48±0.22 (3.22-3.79)	26.8±1.38 (25.27-28.62)	399.14±4.51 (391.62-402.74)
May	13.23±0.84 (12.32-14.24)	30.09±0.65 (29.38-30.98)	106.65±41.6 (60.53-163.46)	6.93±0.84 (6.14-8.09)	0.33±0.01 (0.32-0.34)	3.47±0.14 (3.27-3.6)	30.78±1.11 (28.85-31.68)	427.15±4.44 (422.75-434.19)
June	16.76±1 (15.58-17.86)	33.04±1.11 (31.32-34.04)	68.56±36.94 (32.69-117.61)	8.1±1.45 (6.24-9.61)	0.3±0.01 (0.29-0.31)	3.38±0.26 (3.19-3.74)	32.1±1.11 (30.34-33.33)	450.29±6.39 (440.07-456.16)
July	18.25±0.38 (17.88-18.83)	29.12±0.97 (27.66-30.25)	481.82±100.86 (381.29-625.72)	14.78±1.09 (13.28-16.31)	0.36±0.02 (0.35-0.38)	2.32±0.24 (1.96-2.6)	31.1±1.6 (29.36-33.23)	440.6±3.19 (436.13-444.57)
August	16.9±0.43 (16.5-17.59)	28.38±0.77 (27.21-29.22)	353.7±123.42 (200.57-528.17)	14.3±0.97 (13.02-15.09)	0.39±0.02 (0.37-0.4)	2.41±0.14 (2.25-2.61)	30.29±1.09 (28.79-31.37)	431.58±2.57 (428.56-434.94)
September	14.3±0.83 (13.17-15.37)	28.55±0.53 (28.12-29.42)	64.13±15.82 (45.86-89.15)	9.2±1.2 (7.8-10.33)	0.33±0.01 (0.32-0.35)	2.84±0.08 (2.75-2.94)	28.48±0.42 (28.19-29.16)	421.79±3 (417.79-424.79)
October	10.46±1.14 (8.92-11.8)	25.7±2.15 (24.06-28.3)	53.87±56.48 (1.23-133.12)	4.89±0.85 (3.85-5.68)	0.31±0.02 (0.29-0.33)	3.1±0.14 (2.94-3.31)	22.63±1.84 (20.39-24.59)	399.22±8.82 (389.85-410.34)
November	5.83±0.98 (5.01-7.46)	19±2.45 (16.81-22.08)	60.14±47.82 (10.37-117.96)	3.47±0.9 (2.46-4.28)	0.31±0.04 (0.27-0.35)	3.5±0.29 (3.02-3.72)	16.05±2.24 (14.07-19.14)	367.9±8.17 (361-379.58)
December	2.87±1.47 (1.74-5.35)	16.17±2.38 (14.63-20.33)	37.47±23.2 (2.79-55.87)	2.44±0.45 (1.8-3.03)	0.3±0.03 (0.27-0.33)	3.34±0.25 (3.08-3.74)	15.54±0.93 (14.71-17.02)	352.41±9.26 (345.56-368.11)

Legends: Min. Temp = Mean minimum temperature; Max. Temp. = Mean maximum temperature; PPT = Mean precipitation; Spe. Hum. = Mean specific humidity; Soil Moist. = Mean soil moisture (below 5cm); Shortwave/Longwave Rad. = Mean shortwave/longwave radiations

http://www.aloki.hu ● ISSN 1589 1623 (Print) ● ISSN 1785 0037 (Online)
DOI: http://dx.doi.org/10.15666/aeer/2001_301337

Supplementary Data Table 3. *GPS data of study locations*

No.	Study location	Longitude (East)	Latitude (North)
1	Arja1	73.66294867	33.97807
2	Arja2	73.67143619	33.98500396
3	Azam Nagar1	73.58753339	34.02468598
4	Azam Nagar2	73.59279973	34.00840741
5	Benj1	73.684812	34.045877
6	Benj2	73.68481246	34.0558
7	Chamyati1	73.51381315	34.0590691
8	Chamyati2	73.52695797	34.06288953
9	Chamyati3	73.54115746	34.06611085
10	Dhirkot1	73.57682243	34.03068903
11	Dhirkot2	73.57880889	34.02406129
12	Ghaziabad1	73.629676	33.991651
13	Ghaziabad2	73.62939449	33.98326068
14	Kanyati1	73.58634701	34.07441619
15	Kanyati2	73.57519198	34.0691501
16	Kohala1	73.5067886	34.09299635
17	Kohala2	73.5143939	34.09728174
18	Munasa1	73.51824205	34.08089177
19	Munasa2	73.52186825	34.08944362
20	Neela Butt1	73.591492	33.999812
21	Neela Butt2	73.57714147	33.99911363
22	North1	73.53210804	34.12355846
23	North2	73.5380138	34.11987237
24	Padder Mastoo1	73.63636299	34.0177996
25	Padder Mastoo2	73.65317164	34.02406422
26	Sanghar Bathara1	73.54928172	34.0982717
27	Sanghar Bathara2	73.55761023	34.09329579
28	Sanghar Bathara3	73.57150737	34.089422
29	South1	73.56751493	33.93229927
30	South2	73.57392639	33.91939993
31	South3	73.57610508	33.940425
32	South4	73.5779541	33.97623264
33	Sudhan Gala1	73.67467431	34.00685613
34	Sudhan Gala2	73.66437067	34.00651954
35	Taal Gayat1	73.61570527	34.02274768
36	Taal Gayat2	73.60374374	34.03465304
37	Timroota Pail1	73.62656789	34.00408794
38	Timroota Pail2	73.60862241	33.99616598

http://www.aloki.hu ● ISSN 1589 1623 (Print) ● ISSN 1785 0037 (Online)
DOI: http://dx.doi.org/10.15666/aeer/2001_301337

ENVIRONMENTAL DETERMINANTS OF VEGETATION IN DISTRICT MALAKAND, A SUB-TROPICAL ZONE OF THE OUTER HINDU KUSH MOUNTAIN RANGE

ALI, H.[1*] – MUHAMMAD, Z.[1] – AHMAD, Z.[2] – KHAN, S. M.[2]

[1]*Department of Botany, University of Peshawar, Peshawar, Pakistan*

[2]*Department of Plant Sciences, Quaid-i-Azam University, Islamabad-45320, Pakistan*

[*]*Corresponding author*
e-mail: hazratalibotanist@gmail.com; phone: +92-343-522-5380

(Received 3rd Aug 2021; accepted 1st Oct 2021)

Abstract. This study evaluates plant species composition, distribution pattern, formation of different plant associations and their respective indicators in relation to various environmental factors in the district Malakand, Hindu Kush Mountain. Quadrat quantitative ecological techniques were used for sampling vegetation. All the collected plant species and environmental data were analyzed using PC-ORD and CANOCO software. The present study explored 382 plant species belonging to 91 different families. Based on the number of species, Poaceae (sp., 48), therophytes (169 sp., 44.2%), and microphylls (185 sp., 48.4%) were the dominant family, life form and leaf form class, respectively. Cluster analysis and Two-way cluster analysis identified five plant associations i.e. (1) *Acacia-Ziziphus-Asphodelous* association (2) *Morus-Saccharum-Phalaris* association (3) *Salix-Debregeasia-Agrostis* association (4) *Monotheca-Rhazya-Aerva* association and (5) *Phoenix-Myrsine-Viola* association. CCA results showed that topographic and edaphic variables (altitude, aspect, landscape, soil texture, electrical conductivity, pH, total soluble solutes, calcium carbonates, organic matter, nitrogen, phosphorous and potassium) significantly influenced species distribution and vegetation structure. The present study can be utilized in ecology as a baseline for further research for analyzing vegetation structure and identifying its associated indicators.
Keywords: *vegetation structure, edaphic factors, plant association, multivariate analysis, Malakand, Hindu Kush range*

Introduction

Vegetation is the expression of several environmental factors in a specific time at a particular location (Khan et al., 2012; Manan et al., 2020). It is the outcome of the interaction of many factors, including biotic and non-biotic intervention (Rawat et al., 2020; Karami et al., 2021). Ecological studies are conducted to correlate abiotic and biotic components of the ecosystem (Rahman et al., 2016, Ye et al., 2020). Hence, the researcher checks and studies the distribution of species under the impact of environmental variables. Environmental factors play a dynamic role in plant growth (Wang et al., 2016). For example, physicochemical features of the soil influence species richness, abundance, and diversity. Site gradients influence the floristic composition, density, distribution, and diversity of the vegetation (Bernard-Verdier et al., 2012; Boulangeat et al., 2012; Zhuang et al., 2012). Similarly, vegetation is influenced by several natural and anthropogenic disturbances on local and broader scales (Ali et al., 2002; Bai et al., 2004; Dhyani et al., 2019; Tiwari et al., 2020).

Classifying vegetation into units (associations) was pioneered by Braun-Blanquet based on characteristics of species and floristic composition (Enright and Nuñez, 2013; Liu et al., 2020). The composition and structure of vegetation can be described based on several qualitative and quantitative features (Khare et al., 2019; Hauchhum et al., 2020;

http://www.aloki.hu ● ISSN 1589 1623 (Print) ● ISSN1785 0037 (Online)
DOI: http://dx.doi.org/10.15666/aeer/2001_339361

Paing et al., 2021). The quantitative analysis evaluates vegetation structure precisely (Singh et al., 2014). The quantitative vegetation analysis is a crucial criterion to plan and interpret long-term ecological research (Phillips et al., 2003). The multivariate techniques have been applied to expose the fundamental environmental factors responsible for shaping vegetation structure to remarkable effectiveness (Khan et al., 2013). Cluster and two-way cluster analysis classify the vegetation into different communities (Siddiqui et al., 2010). Canonical correspondence analysis (CCA) provides a better interpretation of ecological data underlying vegetation. Similarly, detrended correspondence analysis (DCA) provides more robust and interpretable results (Cazier and Ware, 2001).

In ecological studies, it is very crucial to investigate the environmental effect on the vegetation pattern using different statistic techniques (Ahmad et al., 2016; Adil et al., 2017; Iqbal et al., 2017; Khan et al., 2017b, 2018; Abdel Khalik et al., 2017). However, few studies have been available in the literature in terms of Hindu Kush mountain.

It is widely accepted since Humboldt's work on phytogeography in the 1800s that plant associations are affected by edaphic and climatic factors. District Malakand is a biological corridor in the great Hindu Kush mountain range. This sub-tropical zone is considered to be the hub to vegetation due to its favorable climatic parameters. The available literature on vegetation dynamics in relation to edaphic and topographic factors showed that this region is unexplored. Therefore, our research study aims to analyze the impact of various environmental factors on the vegetation dynamics using robust multivariate statistical techniques in the subtropical mountainous zone of the Hindu Kush range, District Malakand, Pakistan. The techniques used in the current investigation can be used as a baseline for further studies in ecology for the classification of different plant communities/associations and their respective indicator species.

Materials and Methods

Study area

District Malakand is located in the northern side of Khyber Pakhtunkhwa (KP) province, in the outer range of Hindu Kush Mountains of Pakistan. Because of its varied climate, the area possesses luxuriant vegetation and possesses elements of Sino-Japanese phytogeographical region (Rahman, 2012). Malakand has a total area of 952 sq. km with a population size of 720,295. It shares its boundaries with Swat, Dir, Buner, Charsadda, Mardan, Bajaur and Mohmand (*Figs. 1, 2*). Geographically, Malakand holds great importance as it connects Chitral, Bajaur, Dir and Swat with the province's main cities such as Peshawar, Mardan, Charsadda and Nowshera.

The landscape is represented by both plain as well as hilly regions. In the hilly terrain, Hazar Nao hill is the highest peak having an altitude of 2727 meters. The hills have many metallic, non-metallic and industrial minerals such as slate stone, marble, granite and chromite. The plain area is fertile and many types of crops are grown by farmers in the cultivated lands. River Swat irrigates these cultivated lands. The agriculture, horticulture and mining sectors present various opportunities to uplift the economy of the people. A significant portion of households depends on livestock for their livelihoods (Shah, 2019). Wheat, maize, rice and sugarcane are the main crops of this region. The district can become a major horticulture supplier of fruits as it is the third-highest producer in the province. The area is also suitable for olive tree cultivation to produce edible oil. The sampling stations in the present study had an altitude of 430 - 1072 meters that lie at a latitude of 34° 41' 92" to 34° 63' 65" North and longitude of 71° 66' 67" to 72° 19' 87"

http://www.aloki.hu ● ISSN 1589 1623 (Print) ● ISSN1785 0037 (Online)
DOI: http://dx.doi.org/10.15666/aeer/2001_339361

East. The sampled stations vary from each other by having differences in several edaphic and topographic features (*Table 1*).

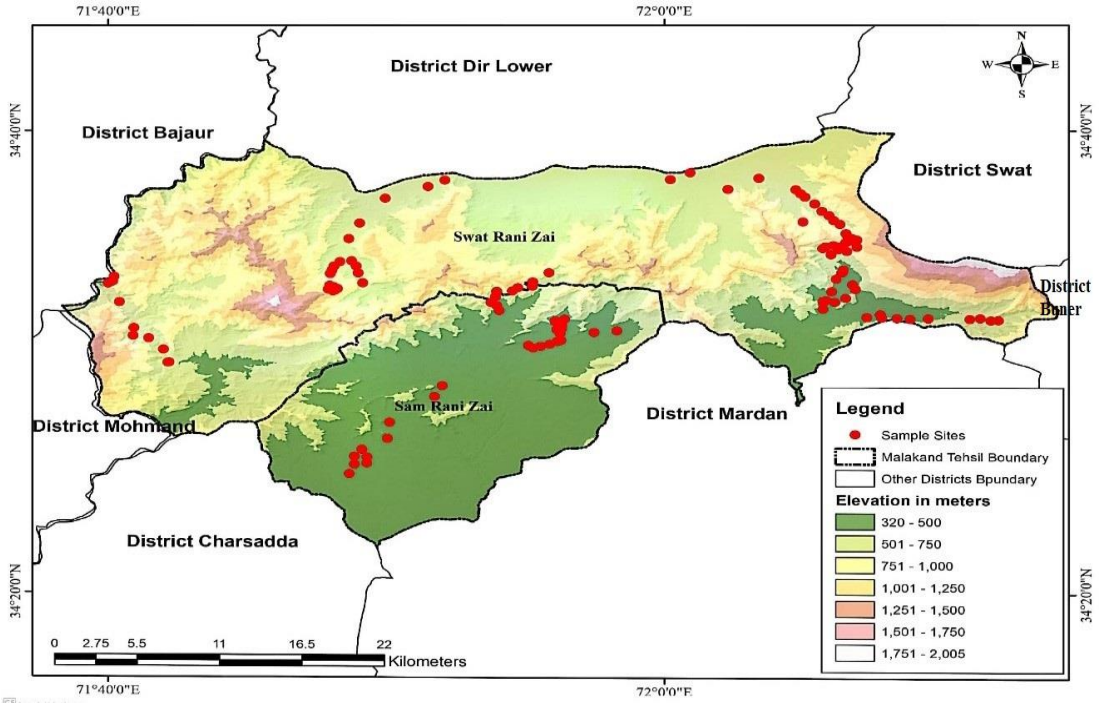

Figure 1. *Map of the research study area, District Malakand.*

Figure 2. *Pictorial view of the study area, (a) Lush green vegetation at station-7 (north aspect), (b) Thick vegetation at station-12 (south aspect), (c) View of vegetation at station-4 (north aspect) (d), Another look of vegetation at lower reaches of station-7*

http://www.aloki.hu ● ISSN 1589 1623 (Print) ● ISSN1785 0037 (Online)
DOI: http://dx.doi.org/10.15666/aeer/2001_339361

Table 1. *Landscape, altitude and geographic coordinates of the sampling sites*

Station No. & name	Landscape/ Aspect	Altitude (m)	Altitude type	Geographic coordinates	
				Latitude (N)	Longitude (E)
1. Palai	Plain	494-531	Low	34.538486-34.566793	72.094491-72.113713
2. Bazdara	Plain	496-660	Low	34.530209-34.534506	72.120600-72.198706
3. Palai-Thana	Hill (south)	625-1050	High	34.577700-34.586245	72.094303-72.114576
4. Palai-Thana	Hills (north)	765-1072	High	34.546316-34.605901	72.098013-72.114616
5. Thana	Plain	670-800	Middle	34.601248-34.636570	72.003585-72.093846
6. Totakan	Plain	612-675	Middle	34.556878-34.631025	71.805873-71.868756
7. Baika-Chapal	Hill (north)	690-1110	High	34.551081-34.568990	71.798991-71.804385
8. Malakand Pass	Hill (south)	534-829	Middle	34.537067-34.564329	71.896334-71.931110
9. Wartair	Plain	468-517	Low	34.510071-34.530854	71.918738-71.971611
10. Jaban-Dargai	Watercourse	463-520	Low	34.515374-34.529673	71.935134-71.938693
11. Palonao	Plain	430-454	Low	34.419211-34.482823	71.811648-71.867221
12. Dheri-Kandao	Hill (south)	501-688	Middle	34.49932-34.561230	71.666670-71.703456

Vegetation sampling

Several preliminary visits were conducted for sites selection during the years of 2019-20. As a complete result, the region was categorized into twelve sites. At each site, quadrats were taken randomly for the sampling of vegetation. Herbs, shrubs, and trees were quantitatively analyzed with 1 sq. meter, 5 sq. meter, and 10 sq. meter quadrats. Altitude and geographic coordinates were recorded for each stand using the Global Positioning System (GPS) (Yang et al., 2016). Various phytosociological approaches were applied for quantitative analyses of vegetation. Plant specimens were collected and preserved properly. According to the flora of Pakistan (Nasir and Ali, 1971-1989; Ali and Qaiser, 1991-2019) and other available literature, the plant specimens were identified. The biological spectrum was determined using the approach of Raunkiaer (1934).

Soil samples analyses

About 1 kg soil samples were collected from each site up to 15 cm in depth (Ahmad et al., 2019; Anwar et al., 2019; Manan et al., 2020). Soil samples were packed in plastic bags and were appropriately tagged. These samples were physicochemically analyzed in the Soil Science Laboratory of the Agricultural Research Institute (ARI), Tarnab, Peshawar, Pakistan. Soil texture was determined using a hydrometer method following the standard method of Brady (1990). Soil pH was determined by testing a 1:5 soil: water suspension with a pH meter (Jackson, 1992). Electrical conductivity (EC) was determined with a conductivity meter AD-3000 (Slavich and Petterson, 1993). Soil moisture content (MC) was determined by the gravimetric method, as indicated by Gardner (1986). The $CaCO_3$ was determined by acid neutralization method (Allison, 1965; Kalra, 1971). Organic matter (OM) was determined using the Walky-Black procedure (Rhoades, 1982). Total soluble solutes (TSS) were determined using method of AOAC (1984). Nitrogen (N) was determined using the Kjeldhal method (Bremner and Mulvaney, 1982) while Phosphorus (P) and Potassium (K) were determined using the methods described by Olsen & Sommers (1982) and Rhoades (1982), respectively.

http://www.aloki.hu ● ISSN 1589 1623 (Print) ● ISSN1785 0037 (Online)
DOI: http://dx.doi.org/10.15666/aeer/2001_339361

Data analyses

After completing eco-floristic data, data matrices were prepared in Excel for further analyses using PC-ORD (ver. 5) and CANOCO (ver. 4.5) software. The cluster analysis was used for the interpretation of the distribution of plant species. The CANOCO was used to analyze various environmental data i.e., altitude, aspect, soil texture (clay, silt, sand), pH, EC, TSS, organic matter, $CaCO_3$, N, P and K on plant species distribution. The ordination results were presented in the form of ordination graphs/plots. The species-area curve (SAC) was constructed using the Sorenson measure to assess adequacy of the sampled size. Plant associations were named based on the top three indicator plant species, identified by indicator species analysis (ISA), as suggested by Dufrêne and Legendre (1997).

Results

Floristic diversity

A total of 382 plant species were identified belonged to 289 genera of 91 different families from the subtropical zone of Hindu Kush mountainous range. Based on habit of plants, there were 290 (76%) species of herb, 46 (12%) shrubs, 39 (10%) trees and 7 (2%) shrubby climbers. The top 10 leading families based on possessing number of species were Poaceae (sp., 48) accompanied by Asteraceae (sp., 34), Papilionaceae (sp., 24), Lamiaceae (sp., 17), Brassicaceae (sp., 15), Amaranthaceae (sp., 13), Boraginaceae (sp., 13), Euphorbiaceae (sp., 11), Scrophulariaceae (sp., 11) and Cyperaceae (sp., 10).

Biological spectrum

The life form spectrum of the studied mountainous region showed that therophytes (169 sp., 44.2%) followed by hemicryptophytes (81 sp., 21.2%) and nanophanerophytes (39 sp., 10.2%) were the dominant leaf size classes. The other leaf size classes included chamaephytes (24 sp., 6.3%), mesophanerophytes (20 sp., 5.2%), microphanerophytes (13 sp., 3.4%), megaphanerophytes (18 sp., 4.7%) and geophytes (18 sp., 4.7%). The dominant leaf size spectrum was microphylls (185 sp., 48.4%) followed by nanophylls (107 sp., 28.0%) and mesophylls (61 sp., 16.0%). The other leaf size classes were leptophylls (21 sp., 5.5%) megaphylls (4 sp., 1.0%) and aphyllous (4 sp., 1.0%).

Classification of plant associations

Species area curve

Species area curve (SAC) was used to confirm the adequate sample size for assessing vegetation in the studied area. SAC showed that the maximum number of new plant species appearing high up to station/quadrat number 80. After that the curves become parallel, which comprehends adequate sampling in the mountainous region (*Fig. 3*).

Cluster Analysis (CA)

The CA of PC-ORD v.5 classified all the stations/quadrats and plant species into 5 major plant associations (*Fig. 4*). The detail description of each association along with their respective indicators and environmental gradient are as follows.

http://www.aloki.hu ● ISSN 1589 1623 (Print) ● ISSN1785 0037 (Online)
DOI: http://dx.doi.org/10.15666/aeer/2001_339361

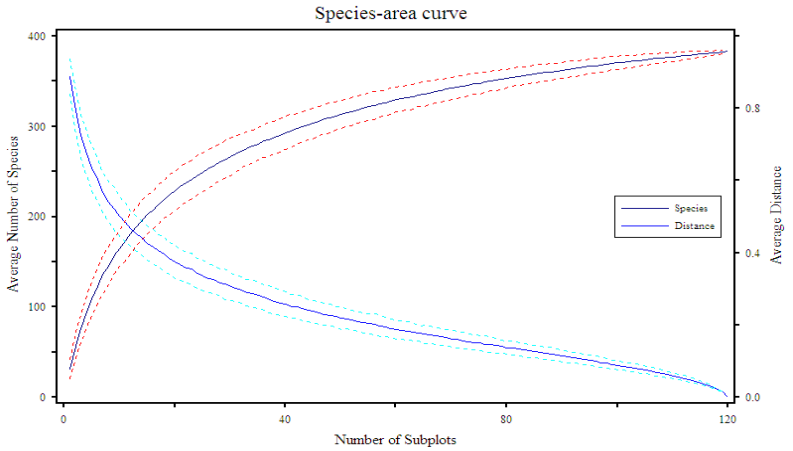

Figure 3. *Species area curve for 382 plant species in relation to sampling stations*

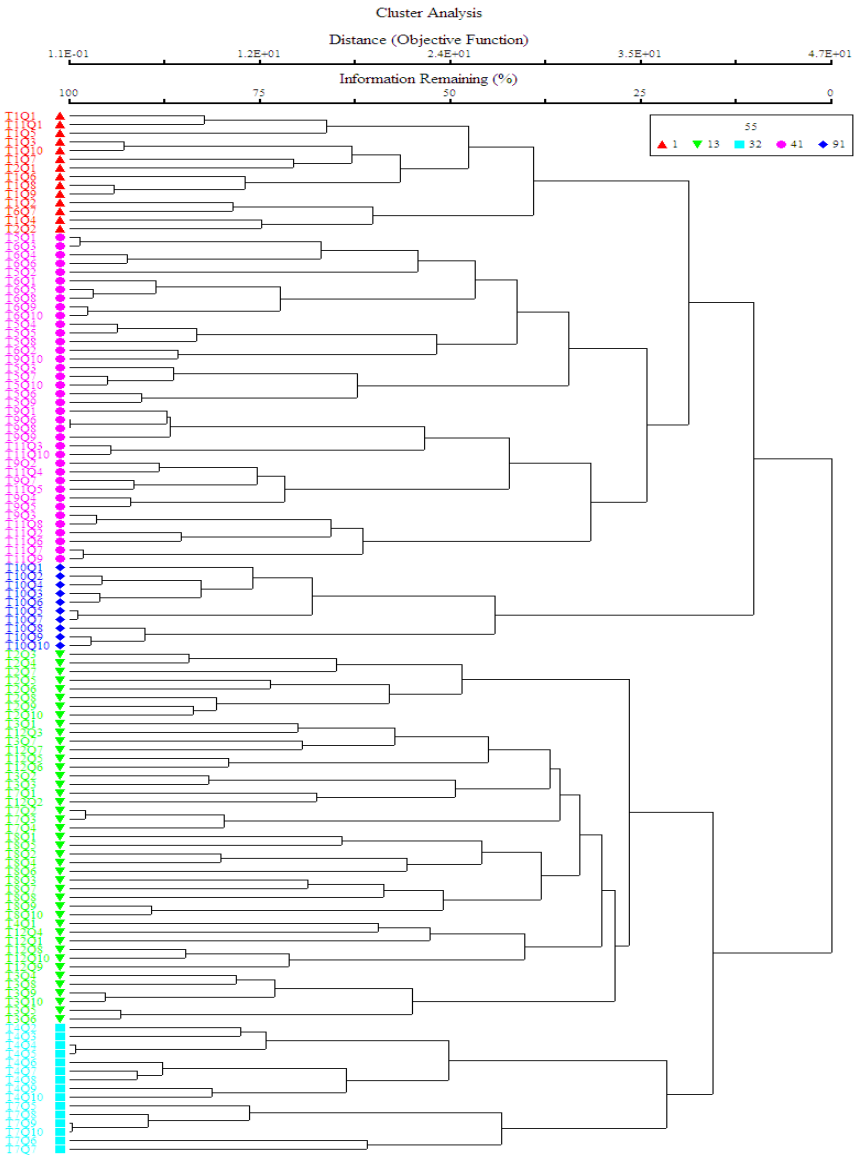

Figure 4. *Cluster Analysis dendrogram representing all the stations into 5 plant associations*

http://www.aloki.hu ● ISSN 1589 1623 (Print) ● ISSN1785 0037 (Online)
DOI: http://dx.doi.org/10.15666/aeer/2001_339361

Association-1 (Acacia-Ziziphus-Asphodelous association)

A total of 163 species of 4 different stations were clustered in this association. This association was developed in plain landscape at 430 - 675 m altitude. The topmost indicator species of this association were *Acacia nilotica, Ziziphus nummularia* and *Asphodelous tenuifolius* after the indicator species analysis (ISA) (*Fig. 5; Table 2*). The important environmental variables responsible for establishment this association were low pH and high amount of sand and phosphorous. Other characteristic herb species of this association were *Centaurea iberica*, *Malvastrum coromandelianum*, *Dactyloctenium aegyptium*, *Euphorbia prostrata* and *Cyperus rotundus*. The abundant shrub species of this association included *Lantana camara*, *Prosopis cineraria* and *Calotropis procera* while *Acacia nilotica* and *Melia azedarach* were the dominant tree species in the region.

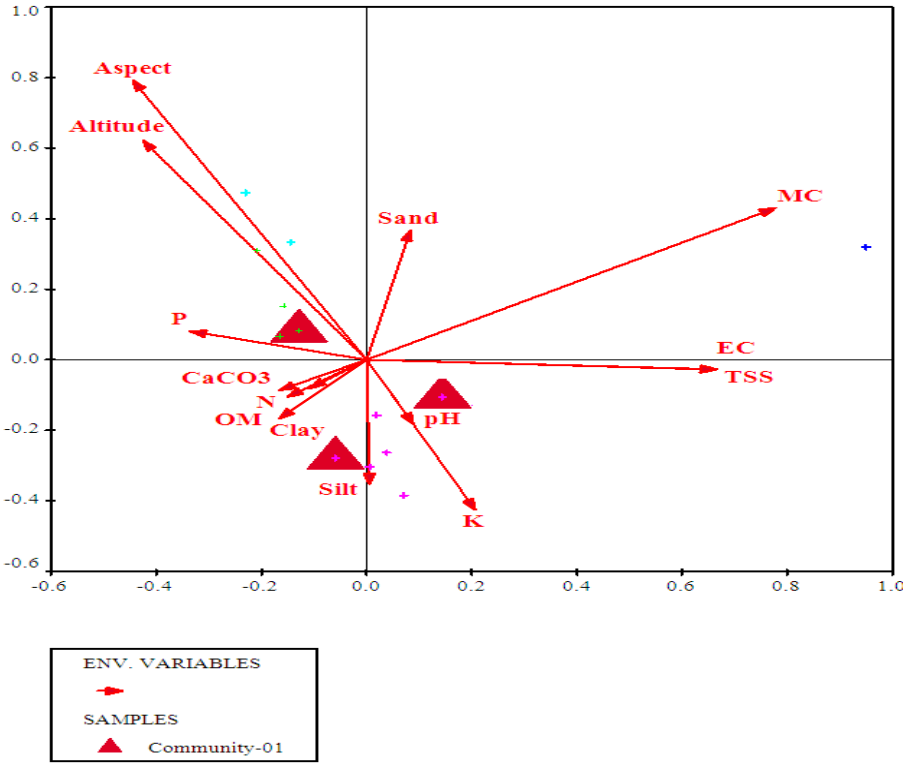

Figure 5. *Data attribute plot of Acacia nilotica (tree indicator species) of association-1 in relation to measured environmental variables*

Soil analyses of this association contained sand (52-58%), silt (36-44%), clay (2-4%) with pH ranged from 8.0 to 8.5, EC (0.11-0.20 dsm^{-1}), moisture (5.3-6.5%), TSS (0.035-0.064%), $CaCO_3$ (6.75-8.25%), OM (0.65-0.79%), N (0.032-0.039 mg kg^{-1}), P (8.0-15.4 mg kg^{-1}) and K (90-120 mg kg^{-1}) (*Table 3*).

Association-2 (Morus-Saccharum-Phalaris association)

A total of 197 plants, near to cultivated lands at altitude range of 430-800 m of 4 different stations clustered in this association. The top indicator species included *Morus nigra*, *Saccharum bengalense* and *Phalaris minor* after the ISA (*Fig. 6; Table 2*). The primary determinant environmental variables responsible for the formation of this

http://www.aloki.hu ● ISSN 1589 1623 (Print) ● ISSN1785 0037 (Online)
DOI: http://dx.doi.org/10.15666/aeer/2001_339361

association were low pH and high amount of $CaCO_3$ and clay. *Silybum marianum*, *Euphorbia helioscopia*, *Galium aparine*, *Parthenium hysterophorus*, *Achyranthes aspera*, *Torilis leptophylla*, *Poa annua*, *Digitaria sanguinalis*, *Cannabis sativa* and *Brachiaria ramosa* were the dominant herb species of this association. The important shrubs included *Dodonaea viscosa*, *Justicia adhatoda*, *Calotropis procera*, *Zizipus numularia*, and *Rosa multiflora* while *Broussonetia papyrifera*, *Melia azedarach*, *Populus nigra* and *Morus alba* were important tree species.

Table 2. *The topmost indicator species of each association, based on indicator species analysis (ISA)*

Associations	**Indicator species**	**Variables**	**MONTE CARLO test of significance (using ISA)**		
			Max. grp	IV	P* Values
Association-1	1. *Acacia nilotica*	pH	7	41.2	0.0462
	2. Ziziphus nummularia	Sand	54	41.2	0.0004
	3. *Asphodelous tenuifolius*	Phosphorus	15	60	0.0002
Association-2	1. *Morus nigra*	pH	7	60.7	0.0012
	2. *Saccharum bengalense*	Clay	10	34.5	0.0005
	3. *Phalaris minor*	$CaCO_3$	9	85.3	0.0002
Association-3	1. *Salix acmophylla*	Moisture	20	30	0.0026
	2. *Debregeasia salicifolia*	Moisture	20	31.2	0.0012
	3. *Agrostis viridis*	Moisture	20	100	0.0002
Association-4	1. *Monotheca buxifolia*	Altitude	73	56.2	0.0002
	2. *Rhazya stricta*	Phosphorus	19	32.5	0.0054
	3. *Aerva javanica*	Aspect (S)	2	42.3	0.0002
Association-5	1. *Phoenix sylvestris*	Aspect (N)	3	43.7	0.0114
	2. *Myrsine africana*	Aspect (N)	3	50.2	0.001
	3. *Viola canescens*	Altitude	105	33.6	0.0012

Table 3. *Physicochemical properties of soil of each association in the sub-tropical zone of Hindu Kush Mountain range*

Associations	**pH**	**EC**	**Clay**	**Silt**	**Sand**	**MC**	**$CaCO_3$**	**OM**	**TSS**	**N**	**P**	**K**
		(dsm^{-1})	---------- **%** ----------							**(mg^{-kg})** -----		
1	8.0-8.5	0.11-0.20	2-6	36-44	52-58	4.2-6.5	6.8-8.3	0.65-0.79	0.035-0.064	0.032-0.039	5.7-15.4	90-120
2	7.9-8.5	0.10-0.20	4-10	36-44	48-58	4.59.1	7.5-9.0	0.69-0.86	0.032-0.064	0.034-0.043	5.7-14.8	90-140
3	8.1	0.20	2	38	60	20.9	7.5	0.69	0.064	0.034	4	110
4	8.0-8.1	0.11	2-8	36-40	48-60	4.2-12.5	6.8-10.0	0.65-0.86	0.035-0.038	0.034-0.043	2.2-22.8	96-120
5	8.0	0.11	2-8	38-44	48-60	6.8-13	6.8-8.8	0.69-0.86	0.035	0.034-0.043	2.2-22.8	98-110

http://www.aloki.hu ● ISSN 1589 1623 (Print) ● ISSN1785 0037 (Online)
DOI: http://dx.doi.org/10.15666/aeer/2001_339361

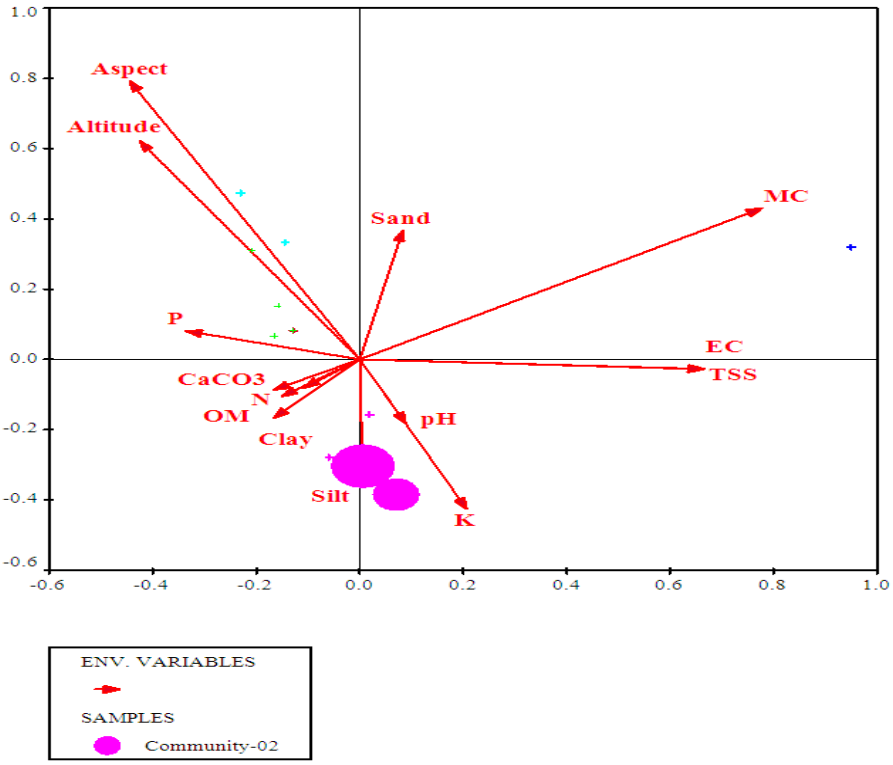

Figure 6. *Data attribute plot of Saccharum bengalense (shrub indicator species) of association-2 in relation to measured environmental variables*

This association was formed in alkaline soil having pH range from 7.9-8.5. The soil texture contained 8-58% sand, 36-44% silt and 4-10% clay with 4.5-9.1% moisture. EC varied from 0.10-0.20 dsm^{-1}, TSS 0.032-0.064%, $CaCO_3$ 7.5-9.0%, OM 0.69-0.86%, N 0.039-0.043 mg kg^{-1}, P 5.7-14.8 mg kg^{-1}, and K 90-140 mg kg^{-1} (*Table 3*).

Association-3 (Salix-Debregeasia-Agrostis association)

In streambeds at altitude of 463-520 m, a total of 89 plants belonging to single station clustered in this association. The ISA inveterate *Salix acmophylla*, *Debregeasia salicifolia* and *Agrostis viridis* as top indicators of this association showing their affinities with higher moisture contents (20.9%) (*Fig. 7; Table 2*). *Leucaena leucocephala, Eucalyptus camaldulensis, Broussonetia papyrifera* and *Ailanthus altissima* among trees while *Arundo donax, Debregeasia salicifolia, Saccharum ravennae Vitex negundo,* and *Nerium oleander* among shrubs were the dominant plant species. The herbaceous layer was dominated by *Nasturtium officinale*, *Persicaria maculosa, Paspalum paspaloides*, *Mentha longifolia*, *Arundo donax*, *Saccharum filifolium*, *Alternanthera sessilis*, *Persicaria hydropiper*, *Alopecurus myosuroides*, *Alternanthera philoxeroides*, *Cyperus alopecuroides*, *Kyllinga brevifolia* and *Ranunculus sceleratus*.

Soil texture of this association comprised of 60% sand, 38% silt and 2% clay with the highest amount of moisture contents (20.9%). The other soil variables included EC 0.20 dsm^{-1}, pH 8.1, TSS 0.064%, $CaCO_3$ 7.50%, OM 0.69%, N 0.034 mg kg^{-1}, P 4.0 mg kg^{-1} and K 110 mg kg^{-1} (*Table 3*).

http://www.aloki.hu ● ISSN 1589 1623 (Print) ● ISSN1785 0037 (Online)
DOI: http://dx.doi.org/10.15666/aeer/2001_339361

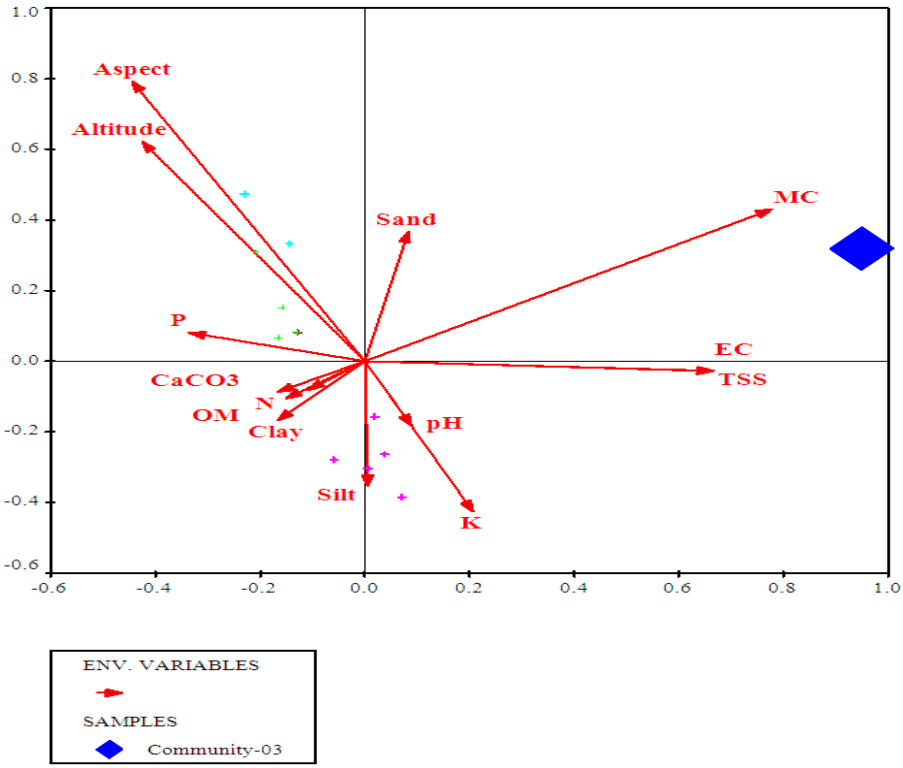

Figure 7. *Data attribute plot of Agrostis viridis (herb indicator species) of association-3 in relation to measured environmental variables*

Association-4 (Monotheca-Rhazya-Aerva association)

This association comprised a total of 243 plants, distributed in 6 different stations. This association was established in hilly landscape at 496-1072 m elevation at south aspect. The foremost indicator species were *Monotheca buxifolia, Rhazya stricta* and *Aerva javanica* (*Fig. 8; Table 2*). The indicator species of this association were influenced by altitude (higher), aspect (south) and high amount of phosphorous. These were the indicators of south aspect and lower altitude. Other important herb species included *Micromeria biflora*, *Arenaria serpyllifolia*, *Medicago minima*, *Cynodon dactylon*, *Lactuca dissecta*, *Ajuga bracteosa,* while in shrubs *Dodonaea viscosa* and *Justicia adhatoda* were the dominant shrubs. The other important tree species were *Acacia modesta* and *Olea ferruginea*.

Soil texture of this association contained 48-64% sand, 32-40% silt and 2-8% clay with 4.2-12.5% moisture. The soil pH varied from 8.0-8.1, EC 0.11-0.12 dsm^{-1}, TSS 0.035-0.038%, $CaCO_3$ 6.75-10.0%, OM 0.69-0.86%, N 0.032-0.043 mg kg^{-1}, P 2.2-22.8 mg kg^{-1} and K 95-120 mg kg^{-1} (*Table 3*).

Association-5 (Phoenix-Myrsine-Viola association)

This association comprised of 143 species, distributed in 2 stations. This association was formed at higher altitude (690-1072 m) at north aspect. *Phoenix sylvestris Myrsine africana* and *Viola canescens* were the indicator species of association-5 (*Fig. 9; Table 2*), showing its affinity with high altitude and north aspect. The dominant herb species included *Origanum vulgare*, *Scilla griffithii*, *Heteropogon contortus*, *Arabidopsis*

http://www.aloki.hu ● ISSN 1589 1623 (Print) ● ISSN1785 0037 (Online)
DOI: http://dx.doi.org/10.15666/aeer/2001_339361

thaliana, *Gagea elegans*, *Chrysopogon aucheri*, *Lespedeza juncea*, *Tulipa clusiana* while *Rubus fruticosus* and *Pinus roxburghii* were dominant shrub and tree species, respectively.

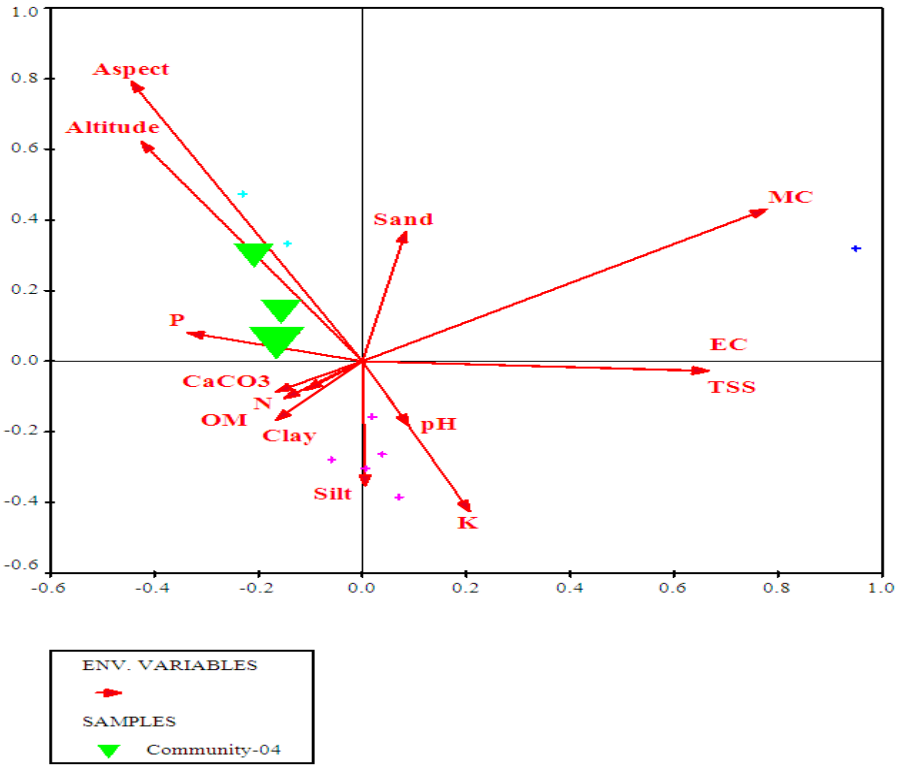

Figure 8. *Data attribute plot of Rhazya stricta (shrub indicator species) of association-4 in relation to measured environmental variables*

The soil texture of this association contained 48-60% sand, 38-44% silt and 2-8% clay, along with 6.8-12.5% moisture. The other soil features included 8.0 pH, 0.11 dsm^{-1} EC 0.035% TSS, 6.75-8.75% $CaCO_3$, 0.69-0.86% OM, 0.034-0.43 mg kg^{-1} N, 2.2-22.8 mg kg^{-1} P and 98-110 mg kg^{-1} K (*Table 3*).

Detrended Correspondence Analysis (DCA) of stations

DCA ordination tells about the pattern in complex data set. DCA was used to analyze the ordination of samples. The Eigen values for axis 1, 2, 3 and 4 were 0.619, 0.312, 0.246 and 0.198, respectively. The explained variations (cumulative) for the same axis were 5.7, 8.6, 10.9 and 12.7. The gradient length for axis 1, 2, 3 and 4 were 5.299, 3.300, 3.108 and 2.128, respectively (*Table 4*). DCA confirmed the plant association classified by CA. In DCA diagram, association-1 and association-2 occupied the center of the DCA diagram, having a partial overlapping of association-1 over association-2 because of the same topographic features and lower altitude. Association-3 clustered a distinct group on the right-hand side of the DCA diagram because of high moisture contents of soil (20.9%). Association-4 ordinated a separate group at lower left of DCA plot. The driving ecological factors for the clustering of this diverse group are aspect (south), similar low moisture contents (4.5-5.9%) and altitude. While plant species of higher altitude at north aspect were clustered in the top-left of the graph forming associations 5 (*Fig. 10*).

http://www.aloki.hu ● ISSN 1589 1623 (Print) ● ISSN1785 0037 (Online)
DOI: http://dx.doi.org/10.15666/aeer/2001_339361

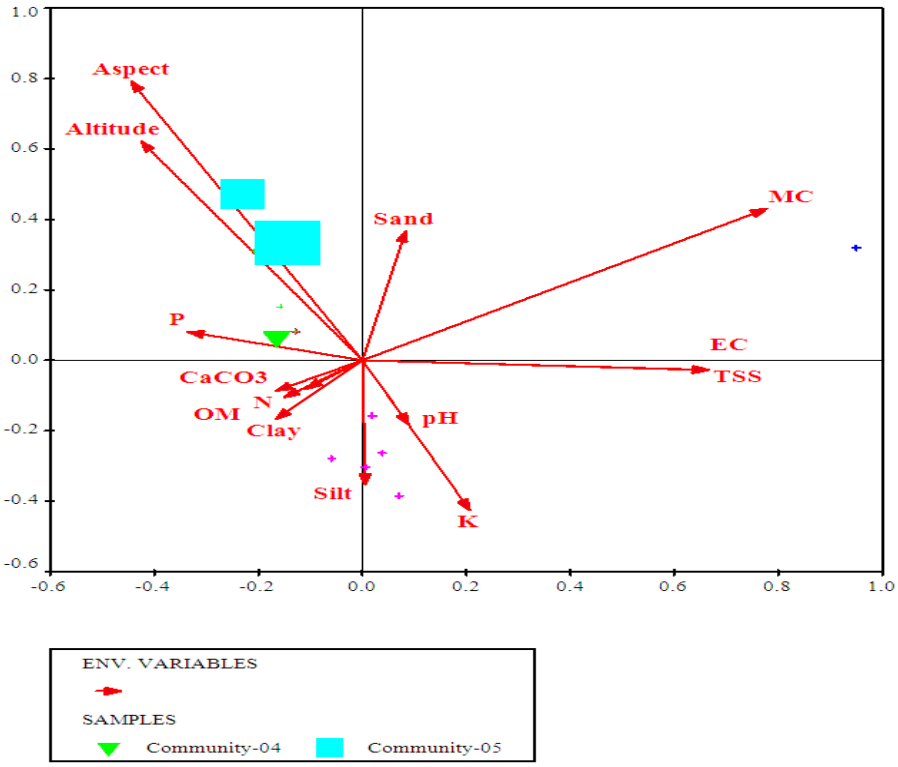

Figure 9. *Data attribute plot of Viola canescens (herb indicator species) of association-5 in relation to measured environmental variables*

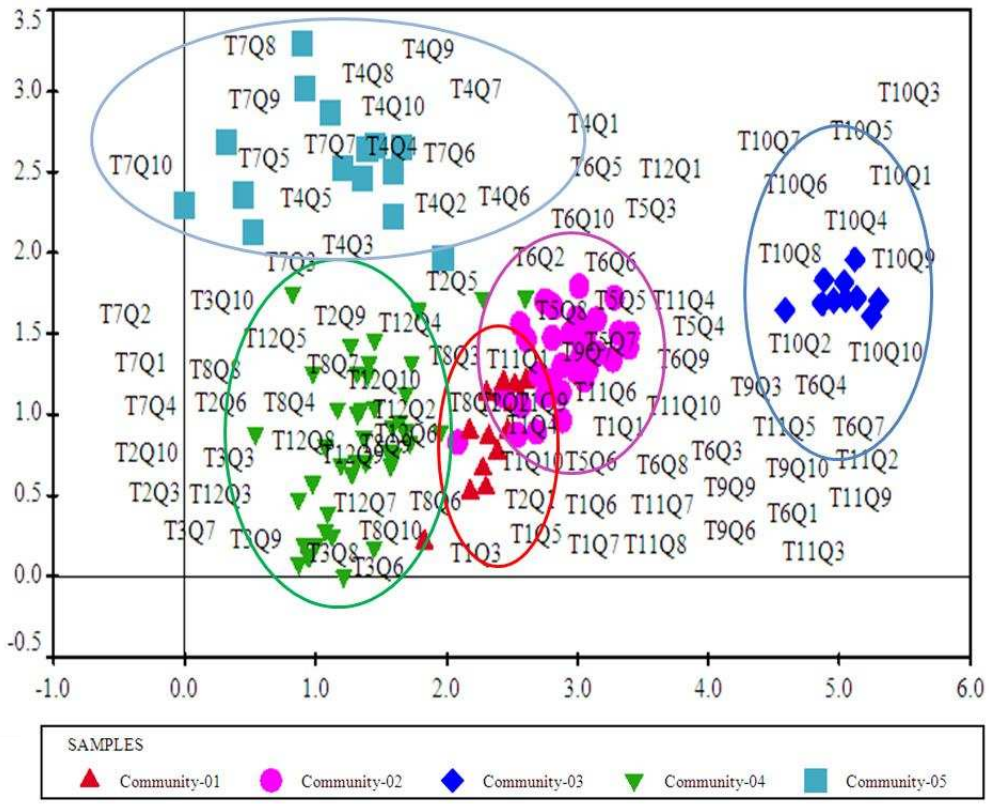

Figure 10. *DCA ordination plot of different stations in the study area*

http://www.aloki.hu ● ISSN 1589 1623 (Print) ● ISSN1785 0037 (Online)
DOI: http://dx.doi.org/10.15666/aeer/2001_339361

Table 4. *Description of the four axes of DCA ordination plot of different stations*

Axes	1	2	3	4	Total inertia
Eigen values	0.619	0.312	0.246	0.198	10.823
Lengths of gradient	5.299	3.300	3.108	2.128	
Cumulative percentage variance of species data	5.7	8.6	10.9	12.7	

Canonical Correspondence Analysis (CCA) of stations

In CCA ordination the maximum eigen value (0.600) was recorded for axis 1, followed by axis 2 (0.472), axis 3 (0.318) and axis 4 (0.231). Species-environment correlation was 0.987, 0.963, 0.919 and 0.931 for axis 1, 2, 3 and 4, respectively. Cumulative percentage variance of species data was 5.5, 9.9, 12.8 and 15.0 for axis 1, 2, 3 and 4 respectively. Species-environment relation for axis 1, 2, 3 and 4 was 23.9, 42.7, 55.4 and 64.6, respectively. The permutation test results for all axis were F (3.292) and P (0.0020) (*Table 5*).

Table 5. *Description of the four axes of the CCA for stations*

Axes	1	2	3	4	Total inertia
Eigen values	*0.600*	*0.472*	*0.318*	*0.231*	*10.823*
Species-environment correlation	0.987	0.963	0.919	0.931	
Cumulative percentage variance of species data	5.5	9.9	12.8	15.0	
Species-environment relation	23.9	42.7	55.4	64.6	
Sum of all eigenvalues					10.823
Sum of all canonical eigen values					2.510
Summary of Monte Carlo test (499 permutations under reduced model)					
Test of significance of first canonical axis		Test of significance of all canonical axes			
Eigen value	0.600	Trace	2.510		
F-ratio	6.398	F-ratio	3.292		
P-value	0.0020	P-value	0.0020		

The CCA bi-plot of stations (*Fig. 11*) showed that altitude, aspect and moisture contents were the strongest variable amongst the ecological factors. Moisture contents showed their strongest influence at first quadrant and strongly effected the vegetation at station-10 (high moisture contents), station-8 and station-2 (lower moisture contents). Altitude and aspect strongly influence the vegetation at station-4, station-7 (high altitude, north aspect), station-3, station-8 and station-12, (lower altitude, south aspect) at second quadrant. The 3rd and 4th quadrant showed the effect of different edaphic factors in the plains of the study area. The edaphic factors like calcium carbonate, organic matter, nitrogen and clayey nature of soil showed its effect at station-1 while pH, TSS, K showed their effects at stations 5, 6 and 9.

http://www.aloki.hu ● ISSN 1589 1623 (Print) ● ISSN1785 0037 (Online)
DOI: http://dx.doi.org/10.15666/aeer/2001_339361

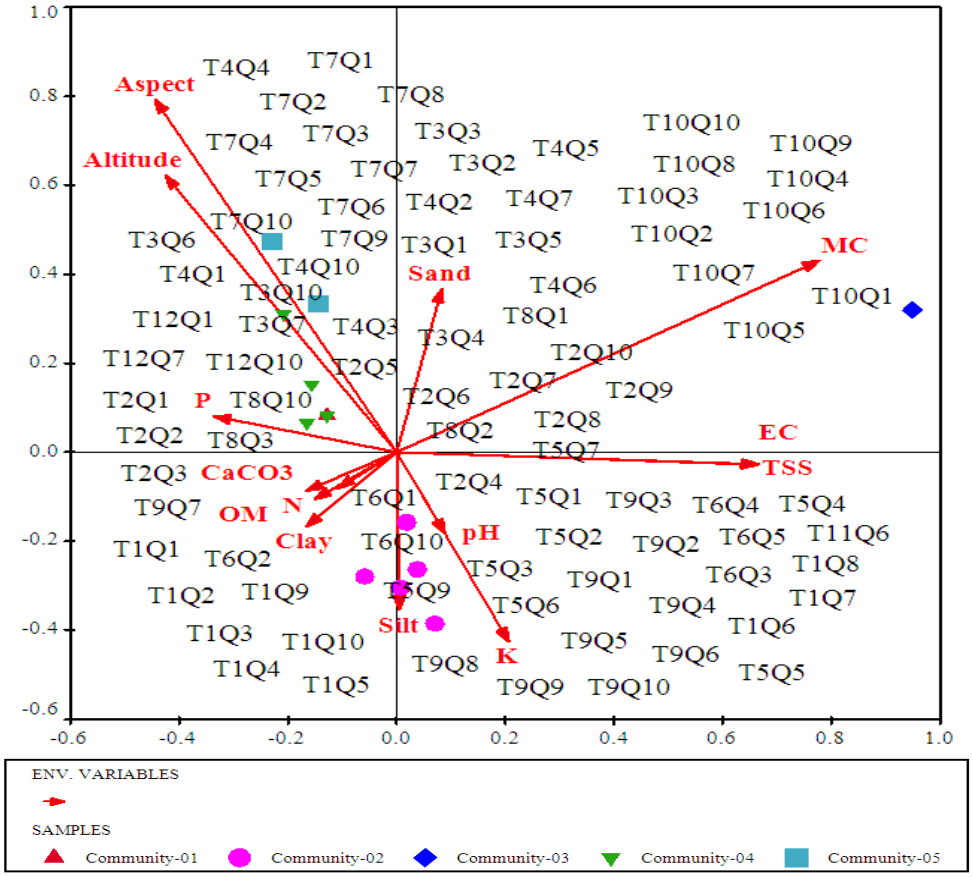

Figure 11. *CCA ordination plot the effect of environmental variables and sampled stations*

Canonical Correspondence Analysis (CCA) of herb species

CCA indicated that most of the plants were accumulated under the influence of moisture contents and sandy nature of soil. The species like *Oenothera rosea, Cheilanthes acrostica, Erioscirpus comosus, Alopecurus myosuroides, Paspalum paspaloides, Saccharum filifolium, Nasturtium officinale, Pycreus flavidus, Asplenium incisum, Mentha longifolia* and *Bidens tripartita* were affected by moisture contents. Species like *Cymbopogon jwarancusa, Conyza canadensis, Conyza bonariensis, Cerastium glomeratum, Boerhavia procumbens, Kickxia ramosissima, Forsskaolea tenacissima, Gagea elegans, Anisomeles indica, Scilla griffithii, Launaea procumbens, Lindenbergia indica, Teucrium stocksianum, Aerva sanguinolenta, Fagonia indica, Phagnalon niveum, Artemisia scoparia* and *Ajuga bracteosa* revealed their affinity to sandy nature of soil. *Chrysopogon aucheri, Heteropogon contortus, Aristida cyanantha, Micromeria biflora* and *Salvia aegyptiaca* were grouped under the influence of north aspect, higher altitude and phosphorous. Species like *Aerva javanica, Chenopodium botrys, Erodium malacoides, Triumfetta pentandra, Salvia aegyptica* showed their preference for lower altitude and south aspect. Phosphorous effected the distribution of *Plantago amplexicaulis* and *Sisymbrium irio*. Most of the species grouped around $CaCO_3$, N, OM, clayey and silty nature of soil. The existence of *Anagallis arvensis, Scandix pecten-veneris, Citrullus lanatus, Veronica biloba, Casia occidentalis Thymelaea passerina, Vicia sativa, Salvia moocroftiana, Parthenium hysterophorus, Chenopodium murale, Acrachne racemosa, Dichanthium annulatum, Raphanus raphanistrum* and *Cirsium*

http://www.aloki.hu ● ISSN 1589 1623 (Print) ● ISSN1785 0037 (Online)
DOI: http://dx.doi.org/10.15666/aeer/2001_339361

arvense depicted their affinity to $CaCO_3$, OM, N, clay and silt. *Filago hurdwarica, Atylosia scarabaeoides, Ranunculus muricatus, Cannabis sativa, Galium aparine, Xanthium strumarium, Rumex dentatus, Amaranthus graecizans, Euphorbia heterophylla, Lathyrus aphaca, Chenopodium album, Ipomoea pes-tigridis, Malvastrum coromandelianum, Lactuca serriola, Phalaris minor, Achyranthes aspera, Convolvulus arvensis, Setaria pumila, Imperata cylindrica, Ipomoea nil, Chrozophora tinctoria, Sorghum halepense, Coronopus didymus* and *Euphorbia helioscopia* showed their ecological amplitude with pH, TSS, K and EC (*Fig. 12*).

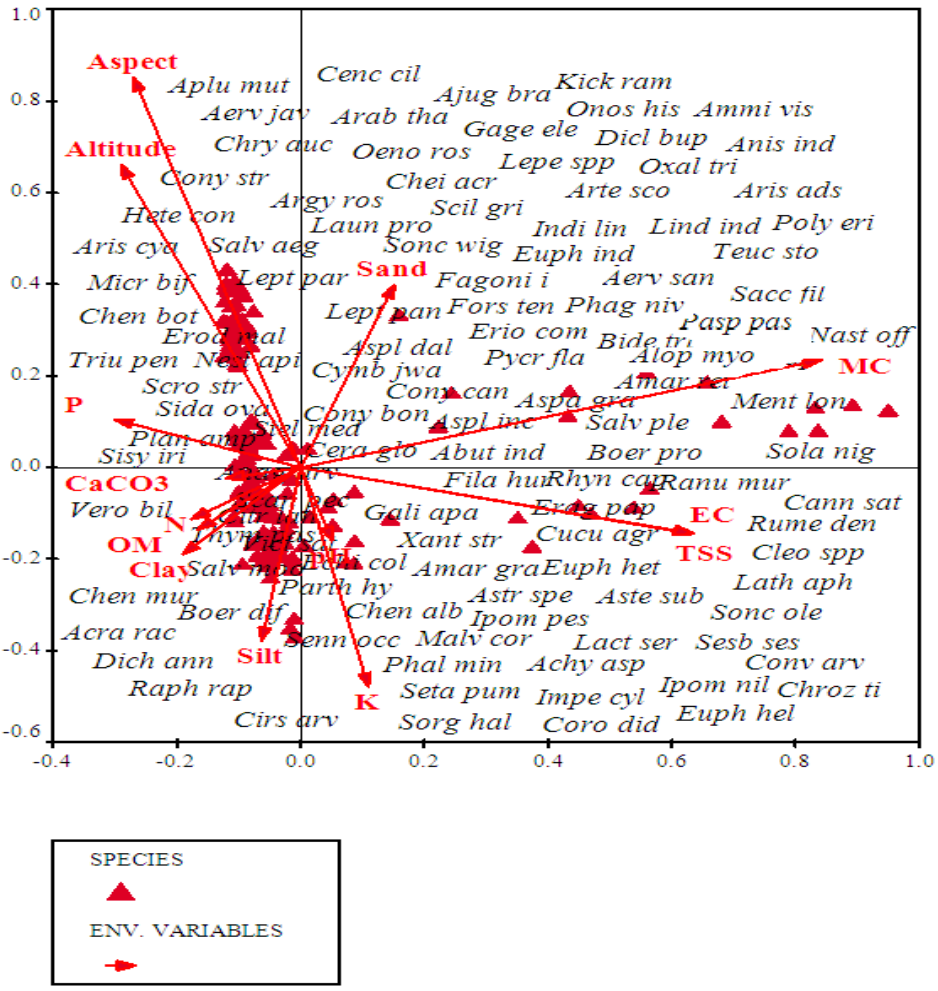

Figure 12. *CCA plot showing the distribution of herbs under the influence of environmental variables*

Canonical Correspondence Analysis (CCA) of shrubs and trees

CCA of shrubs and trees (Fig. 12) showed that altitude, aspect and moisture contents were the strong influencing factors among the environmental variables. The CCA showed that the aspect, altitude, organic matter, N and clayey nature of the soil influenced *Pinus roxburghii, Himalrandia tetrasperma, Rubus fruticosus, Daphne mucronata, Periploca aphylla, Ziziphus oxyphylla, Isodon rugosus* and *Mallotus phillipensis.* While *Phoenix sylvestris, Ficus racemosa, Olea ferruginea* and *Platanus orientalis* were associated with OM, N, P and clayey nature of soil. Soil moisture, electrical conductivity, K, TSS and

http://www.aloki.hu ● ISSN 1589 1623 (Print) ● ISSN1785 0037 (Online)
DOI: http://dx.doi.org/10.15666/aeer/2001_339361

silty nature of soil affected *Debregeasia salicifolia, Saccharum ravennae* and *Rosa multiflora plant* species distribution. Silt influenced the distribution of *Ricinus communis, Ailanthus altissima* and *Robinia pseudo-acacia. Morus nigra* and *Eucalyptus camaldulensis* showed their affinity with EC, TSS and K. Furthermore, the distribution of *Dalbergia sissoo, Ziziphus nummularia, Acacia nilotica* and *Parkinsonia aculeata* were influenced by soil pH in the region. While *Nerium oleander, Withania somnifera, Calotropis procera* and *Ziziphus mauritiana* showed correlation with pH and $CaCO_3$. Similarly, *Rhazya stricta, Maytenus royleanus, Saccharum griffithii, Justicia adhatoda, Cissampelos pareira, Berberis lycium, Colebrookea oppositifolia, Otostegia limbata, Woodfordia fruticosa, Albizia lebbeck, Ficus bengalensis* and *Tecomella undulata* were associated with sandy nature of soil (Fig. 13).

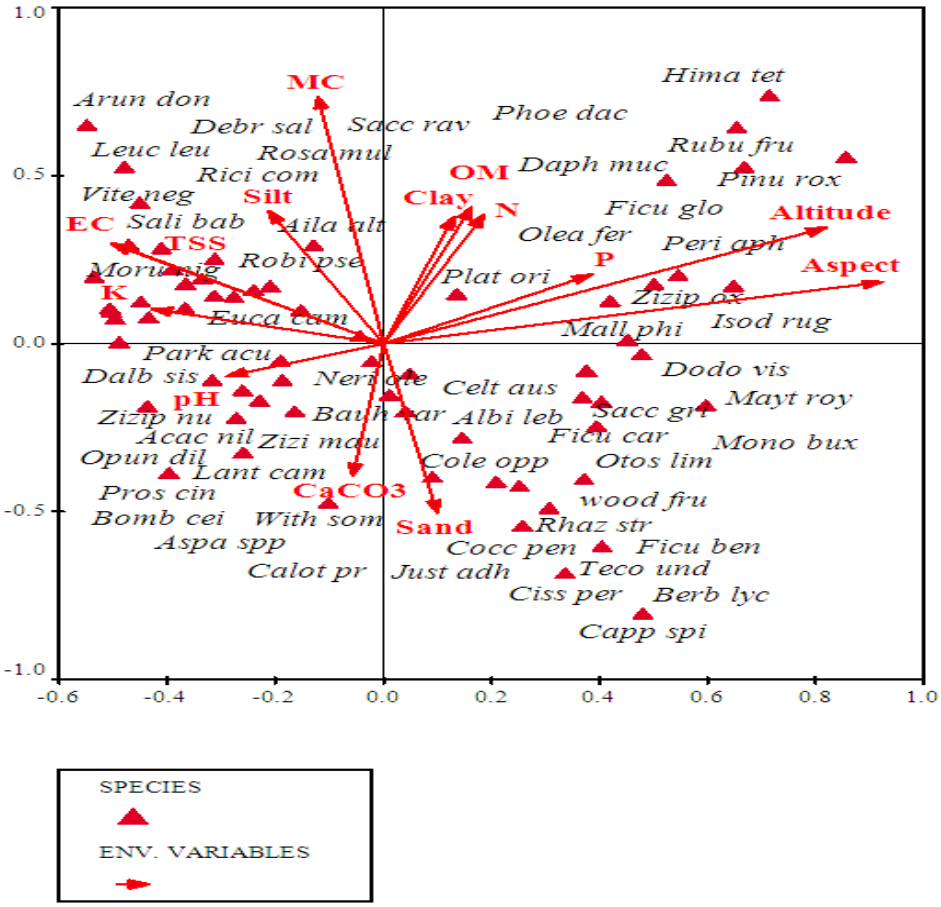

Figure 13. *CCA plot showing the distribution of shrubs and trees under the influence of environmental variables*

Discussion

The distribution pattern and composition of plants are usually attributed to edaphic and environmental factors. This research study indicated that the environmental variables significantly impact vegetation structure/dynamics and hence plant associations changed in response to different environmental gradients. In the current study, 382 species belonging to 289 genera of 91 families were recognized. The flora included a high number of herbaceous species (290 sp., 76%). It was followed by shrubs having 46 species (12%),

http://www.aloki.hu ● ISSN 1589 1623 (Print) ● ISSN1785 0037 (Online)
DOI: http://dx.doi.org/10.15666/aeer/2001_339361

trees 39 species (10%) and shrubby climbers 7 species (2%). The present results are similar to the previous studies (Shuaib et al., 2014; Qureshi et al., 2014) thus strengthening the present results.

The present study revealed that Poaceae (with 48 species), Asteraceae (sp., 34), Papilionaceae (sp., 24), Lamiaceae (sp., 17), Brassicaceae (sp., 15), Amaranthaceae (sp., 13), Boraginaceae (sp., 13), Euphorbiaceae (sp., 11), Scrophulariaceae (sp., 11) and Cyperaceae (sp., 10) were the most diverse families. As the families like Poaceae, Asteraceae, Lamiaceae and Brassicaceae are diverse due to their wide ecological amplitude, they are also dominant in the current area. Our findings are in line with Ilyas et al. (2013), Amjad et al. (2013), Saleem et al. (2013) and Qureshi et al. (2014) who also described Poaceae and Asteraceae as the leading families. Similarly, Jafari and Akhani (2008) reported Poaceae and Lamiaceae as the largest families in their study.

Life form spectrum of vegetation of the studied area disclosed that therophytes (169 sp., 44.2%) followed by hemicryptophytes (81 sp., 21.2%) and nanophanerophytes (39 sp.,10.2%) were the dominant leaf size classes. The other leaf size classes included chamaephytes (24 sp., 6.3%), mesophanerophytes (20 sp., 5.2%), megaphanerophytes (18 sp., 4.7%) and geophytes (18 sp., 4.7%) and microphanerophytes (13 sp., 3.4%). The dominancy of therophytes and hemicryptophytes were also noted by Tripathy et al. (2013), Badshah et al. (2013) and Hussain et al. (2015). The presence of a greater number of therophytes may respond to anthropogenic pressure and the harsh climate (Qureshi et al., 2011; Shahid and Joshi, 2015) because therophytes are better adapted to dry climate (Shah, 2013).

The results of biological spectrum revealed that the leaf size spectrum was dominated by microphylls (185 sp., 48.4%) followed by nanophylls (107 sp., 28.0%) and mesophylls (61 sp., 16.0%). The other leaf size classes were leptophylls (21 sp., 5.5%) megaphylls (4 sp., 1.0%) and aphyllous (4 sp., 1.0%). The presence of a greater number of microphylls and nanophylls may respond to anthropogenic pressure and the harsh climate because such species are better adapted to dry climate. Such type of results has been found by several workers. Haq et al. (2015) found microphylls as the dominant leaf size class while studying vegetation of subtropical forests in Battagram District. Sharma and Sharma (2020) also revealed microphyllous type of vegetation followed by nanophylls. In the study of Khan et al. (2016), microphylls, followed by leptophylls and nanophylls species were dominant. Similarly, in the study of Ullah and Badshah (2017) the leading leaf size classes were microphylls and nanophylls.

The CA clustered all the stations and plant species into 5 main associations and their distinctive indicators. In *Acacia-Ziziphus-Asphodelous* association (Association-1) a total of 163 species of 4 different stations were clustered. This association was developed in the plain landscape at 430 - 675 m altitude. The topmost indicator species of this association were *Acacia nilotica, Ziziphus nummularia* and *Asphodelous tenuifolius*. The important environmental variables responsible for establishment of this association were low pH, greater amount of sand and high quantity of phosphorous. A total of 197 plants clustered in *Morus-Saccharum-Phalaris* association (Association-2). The top indicator species included *Morus nigra*, *Saccharum bengalense* and *Phalaris minor*. This association was developed in the plain landscape at 430 - 800 m altitude. The primary determinant environmental variables, responsible for the formation of this association were low pH, high amount of clay and $CaCO_3$. A total of 89 plants clustered in *Salix-Debregeasia-Agrostis* association (Association-3) at altitude of 463-520 m. The ISA inveterate *Salix acmophylla*, *Debregeasia salicifolia* and *Agrostis viridis* as top indicator

http://www.aloki.hu ● ISSN 1589 1623 (Print) ● ISSN1785 0037 (Online)
DOI: http://dx.doi.org/10.15666/aeer/2001_339361

species of this association under the influence of higher moisture contents (20.9%). *Monotheca-Rhazya-Aerva* association (Association-4) comprised a total of 243 plants, distributed in 6 different stations. This association was established in higher altitude hills at 496-1072 m elevation at south aspect. The foremost indicator species were *Monotheca buxifolia, Rhazya stricta* and *Aerva javanica*. These were the indicators of south aspect and lower altitude. The indicator species of this association were influenced by high altitude, aspect (south) and high amount of phosphorous. *Phoenix-Myrsine-Viola* association (Association-5) comprised of 143 species, distributed in 2 stations. This association was formed at higher altitude (690-1072 m) at north aspect. *Phoenix sylvestris Myrsine africana* and *Viola canescens* were the indicator species with high altitude and north aspect.

Plant species are restricted to specific habitats due to the presence of optimum environmental factors. In the present study, five plant communities were established by using Cluster analysis (CA) and Two-Way Cluster Analysis (TWCA), which are same to the previous studies of Ahmad et al. (2016), Iqbal et al. (2017) and Khan et al. (2017b). They all found 5 various plant communities in their respective studied areas by using CA and TWCA. It is essential to know the environmental determinants of species (Rahman et al., 2021). Hence, in this study, vegetation was correlated with ecological variables using CCA. The environmental gradients (altitude, aspect, sand, silt, clay, pH, EC, MC, CaCO3, OM, N, TSS, P, K) showed significant effect on species distribution. Such impacts have also been studied by numbers of researchers (Khan et al., 2016, 2017 a, b; Anwar et al., 2019).

DCA ordination tells about the pattern in complex data set. DCA was used to analyze the ordination of stations. A DCA diagram of stations revealed the position of different stations along the axes and their association with the gradients. DCA resulted five distinct associations in the study area. The plant association classified by CA were confirmed by DCA. In DCA diagram, association-1 and association-2 occupied the center of the DCA diagram, having a partial overlapping of association-1 over association-2 because of the same topographic features and lower altitude. Association-3 clustered as a distinct group in the right-hand side of the DCA diagram because of high moisture contents of soil (20.9%). Association-4 ordinated a separate group at lower left of DCA plot. The driving ecological factors for the clustering of this diverse group are aspect (south), similar low moisture contents (4.5-5.9%) and altitude. While in association-5, plant species of higher elevation at north aspect were clustered in the top-left of the graph. In ecological terms, plant species of plain areas at lower altitudes are clustered in the middle of the graph (associations-1 & 2). Species of moist or aquatic environment are present at the right side in association-3. Plant species of south aspect with lower moisture were clustered in the lower-right of the graph (associations-4). Plant species of higher elevation at north aspect were clustered in in associations-5 at the top-left of the DCA diagram. The present DCA analysis strongly supporting the CCA results by revealing the same ecological factors like altitude, aspect, topography and edaphic characteristics are responsible for distribution of plants in various habitats in research area. The results of the present DCA analysis are similar with the results of Naqinezhad et al. (2008), Jabeen and Ahmed (2009) and Khan et al. (2017 b) as they also indicated the same ecological factors as the strong drivers for the distribution and composition of vegetation structure. CCA explains the relationship of measured environmental variables on species composition and distribution pattern. The tested environmental variables in the present study were altitude, aspect, clay, sand, silt, pH, moisture contents, electrical conductivity, organic matter, phosphorous, potassium,

http://www.aloki.hu ● ISSN 1589 1623 (Print) ● ISSN1785 0037 (Online)
DOI: http://dx.doi.org/10.15666/aeer/2001_339361

nitrogen and total soluble salts showed significant effect on plant species distribution of the region. Such impacts were also being study by numbers of authors in the neighboring habitats of Pakistan. In addition, any change in environmental variables and altitude cause significant effect in formation of communities (Dhyani et al., 2019; Manan et al., 2020; Rawat et al., 2020; Tiwari et al., 2020; Karami et al., 2021; Zeeshan et al., 2021).

Conclusion

It is concluded that the studied area is rich in term of species diversity. As a whole 382 species belonging to 289 genera of 91 families were recorded. Based on habit, maximum species were herbs, followed by shrubs, trees and shrubby climbers. The top leading families were Poaceae, Asteraceae, Papilionaceae, Lamiaceae and Brassicaceae. Biological spectrum showed that therophytes followed by hemicryptophytes and nanophanerophytes were the dominant life form classes while microphylls followed by nanophylls and mesophylls were the dominant leaf size classes. The quantitative data of plant species was further subjected to find out the effect of various edaphic and topographic variables, responsible for vegetation structure and species distribution. CA and resulted in five plant associations. DCA results further clarified five clusters revealing five types of association in the study area. CCA results revealed that several topographic and edaphic factors altitude, aspect, clay, silt, sand, moisture, pH, EC, TSS, organic matter, $CaCO_3$, N, P and K significantly influenced species distribution and vegetation structure. As the present study also highlights the severe biotic pressure on the vegetation as is evidenced by the presence of greater number of therophytes and microphyllous species in the study area. Hence, the biotic influences on the vegetation entails assessment to plan suitable measures for the conservation of all species in general and indicator and rare species in particular.

Acknowledgments. This paper is part of Ph. D thesis of the first author. The authors are grateful to the inhabitants of District Malakand for their guidance in the present work. Taxonomic support for identifying plant species, provided by the faculty of Herbarium, Department of Botany, University of Peshawar, is also acknowledged.

REFERENCES

[1] Abdel-Khalik, K., Al-Gohary, I., Al-Sodany, Y. (2017): Floristic composition and vegetation: environmental relationships of Wadi Fatimah, Mecca, Saudi Arabia. – Arid Land Research and Management 31(3): 316-334.

[2] Adil, S., Iqbal, Z., Khan, M. A., Ahmad, S., Iqbal, N., Adnan, W. A. (2017): Floristic composition and vegetation structure of Malam Jabba valley, District Swat. – J. Bio. Env. Sci. 11(4): 164-171.

[3] Ahmad, S., Khan, N., Hadi, F., Ali, M., Ahmad, W. (2016): Structure and natural dynamics of *Dodonaea viscosa* communities in Malakand division, Pakistan. – Journal of Biodiversity and Environmental Sciences 9(1): 257-273.

[4] Ahmad, Z., Khan, S. M., Ali, M. I., Fatima, N., Ali, S. (2019): Pollution indicandum and marble waste polluted ecosystem; role of selected indicator plants in phytoremediation and determination of pollution zones. – Journal of Cleaner Production 236: 117709.

[5] Ali, S. I., Qaiser, M. (1991-2019): Flora of Pakistan. – Department of Botany, University of Karachi, Pakistan.

http://www.aloki.hu ● ISSN 1589 1623 (Print) ● ISSN1785 0037 (Online)
DOI: http://dx.doi.org/10.15666/aeer/2001_339361

[6] Ali, R. J., Adams, D. M., McCarl, B. A. (2002): Projecting impacts of global climate change on the US forest and agriculture sectors and carbon budgets. – Forest Ecology and Management 169: 3-14.
[7] Allison, L. E. (1965): Organic Carbon. – In: Black, C. A. (ed.) Methods of Soil Analysis, Part 2: Chemical and Microbiological Properties. American Society of Agronomy, Madison, pp. 1367-1378.
[8] Amjad, M. S., Arshad, M., Qamar, I. A. (2013): Phytosociology of *Pinus-Qurecus* forest vegetation of Nikyal Hills, District Kotli, Azad Kashmir, Pakistan. – International Journal of Agriculture and Crop Sciences 5(24): 2952-2960.
[9] Anwar, S., Khan, S. M., Ahmad, Z., Ullah, Z., Iqbal, M. (2019): Floristic composition and ecological gradient analyses of the Liakot forests in the Kalam Region of District Swat, Pakistan. – Journal of Forestry Research 30(4): 1407-1416.
[10] AOAC. (1984): Official Methods of Analysis, 14th ed. – Association of Official Analytical Chemists, Washington, D.C.
[11] Badshah, L., Hussain, F., Sher, Z. (2013): Floristic inventory, ecological characteristics and biological spectrum of rangeland, District Tank, Pakistan. – Pak. J. Bot. 45(4): 1159-1168.
[12] Bai, Y., Broersma, K., Thompson, D., Ross, T. J. (2004): Landscape-level dynamics of grassland-forest transitions in British Columbia. – Rangeland Ecology & Management 57: 66-75.
[13] Bernard-Verdier, M., Navas, M. L., Vellend, M., Violle, C., Fayolle, A., Garnier, E. (2012): Community assembly along a soil depth gradient: contrasting patterns of plant trait convergence and divergence in a Mediterranean rangeland. – Journal Ecology 100: 1422-1433.
[14] Boulangeat, I., Lavergne, S., Van, E. J., Garraud, L., Thuiller, W. (2012): Niche breadth, rarity and ecological characteristics within a regional flora spanning large environmental gradients. – Journal Biogeography 39: 204-214.
[15] Brady, N. C. (1990): The nature and properties of soils, 10th ed. – Macmillan Publishing Co. New York, NY. 621p.
[16] Bremner, J. M., Mulvaney, C. S. (1982): Nitrogen-total. – In: Methods of soil analysis. Part 2: Chemical and microbiological properties, pp. 595-624.
[17] Cazier, P. W., Ware, S. (2001): Hardwood forest composition in the undissected lower coastal plain in Virginia. – Journal of the Torrey Botanical Society 128(4): 321-331.
[18] Dhyani, S., Maikhuri, R. K., Dhyani, D. (2019): Impact of anthropogenic interferences on species composition, regeneration and standard quality in moist temperate forest of Central Himalaya. – Tropical ecology 60: 539-551.
[19] Dufrêne, M., Legendre, P. (1997): Species assemblages and indicator species: the need for a flexible asymmetrical approach. – Ecol. Monogr. 67: 345-366.
[20] Enright, N. J., Nuñez, M. A. (2013): The Braun-Blanquet reviews in plant ecology: In honour of our founding editor, Josias Braun-Blanquet. – Plant Ecology 214(12): 1417-1418.
[21] Gardner, W. H. (1986): Water Content. – In: Methods of Soil Analysis, Part I: Physical and Mineralogical Methods, Chapter 21. American Society of Agronomy and Soil Science Society of America, Madison, WI, USA.
[22] Haq, F., Ahmad, H. Iqbal, Z. (2015): Vegetation description and phytoclimatic gradients of subtropical forests of Nandiar Khuwar catchment District Battagram. – Pak. J. Bot. 47(4): 1399-1405.
[23] Hauchhum, R., Singson, M. Z. (2020): Tree species composition and diversity in abandoned Jhum lands of Mizoram, North East India. – Tropical Ecology 61: 187-195.
[24] Hussain, F., Shah, S. M., Badshah, L., Durrani, M. J. (2015): Diversity and ecological characteristics of flora of Mastuj Valley, District Chitral, Hindu Kush Range, Pakistan. – Pak. J. Bot. 47(2): 495-510.

http://www.aloki.hu ● ISSN 1589 1623 (Print) ● ISSN1785 0037 (Online)
DOI: http://dx.doi.org/10.15666/aeer/2001_339361

[25] Ilyas, M., Qureshi, R., Shinwari, Z. K., Arshad, M., Mirza, S. N., Haq, Z. U. (2013): Some ethnoecological aspects of the plants of Qalagai Hills, Kabal Valley, Swat, Pakistan. – Int. J. Agric. Biol. 15: 801-810.
[26] Iqbal, M., Khan, S. M., Khan, M. A., Ahmad, Z., Abbas, Z. Khan, S. M. Khan, M. S. (2017): Distribution pattern and species richness of natural weeds of wheat in varying habitat conditions of district Malakand, Pakistan. – Pak. J. Bot. 49(6): 2371-2382.
[27] Jabeen, T., Ahmed, S. S. (2009): Multivariate analysis of environmental and vegetation data of Ayubia National Park, Rawalpindi. – Soil and Environment 28: 106-112.
[28] Jackson, M. A. (1992): Soil chemical analysis. – Constable and Co, Ltd., London.
[29] Jafari, S. M., Akhani, H. (2008): Plants of Jahan Nama protected area, Golestan Province, Iran. – Pak. J. Bot. 40(4): 1533-1554.
[30] Kalra, Y. (1971): Methods used for soil, plant and water analysis at the soil laboratory of the Manitoba-Saskatchewan Region 1967-1970. – AGRIS, 87p.
[31] Karami, P., Bandak, L., Karaji, M. G., Dragovich, D. (2021): Effect of seasonal grazing and annual moving on floristic composition and plant diversity in the Saral rangeland, Kurdistan, Iran. – Global Ecology and Conservation 27: e01515.
[32] Khan, S. M., Page, S., Ahmad, H., Harper, D. (2012): Anthropogenic influences on the natural ecosystem of the Naran valley in the western Himalayas. – Pak. J. Bot. 44: 231-238.
[33] Khan, N., Shaukat, S. S., Siddiqui, F. M. (2013): Vegetation-environment relationship in the forests of Chitral district Hindu Kush range of Pakistan. – Journal of Forestry Research 24: 205-216.
[34] Khan, W., Khan, S. M., Ahmad, H., Alqarawi, A. A., Shah, G. M., Hussain, M., Abd-Allah, E. (2016): Life forms, leaf size spectra, regeneration capacity and diversity of plant species grown in the Thandiani forests, district Abbottabad, Khyber Pakhtunkhwa, Pakistan. – Saudi J. Biol. Sci. 25(1): 94-100.
[35] Khan, M., Khan, S. M., Ilyas, M., Alqarawi, A. A., Ahmad, Z., Abd-Allah, E. F. (2017a): Plant species and communities' assessment in interaction with edaphic and topographic factors; an ecological study of the mount Eelum District Swat, Pakistan. – Saudi J. Biol. Sci. 24(4): 778-786.
[36] Khan, W., Khan, S. M., Ahmad, H., Shakeel, A., Page, S. (2017b): Ecological gradient analyses of plant associations in the Thandiani forestsof the Western Himalayas, Pakistan. – Turkish Journal of Botany 41: 253-264.
[37] Khan, K. R., Ishtiaq, M., Iqbal, Z., Alam, J., Bhatti, K. H., Shah, A. H., Farooq, M. (2018): Effects of edaphic and physiognomic factors on species diversity, distribution and composition in reserved forest of Sathan Gali (Mansehra), Pakistan. – Appl. Ecol. Environ. Res.16(2): 1085-1100.
[38] Khare, S. S., Shah, D. G. (2019): Structure and temporal changes in the mangrove vegetation of Jambusar Taluka of Gulf of Khambat, India. – Tropical Ecology 60(3): 447-454.
[39] Liu, H., Chen, Q., Liu, X., Xu, Z., Dai, Y., Liu, Y., Chen, Y. (2020): Variation pattern of plant composition/diversity in *Dacrydium pectinatum* communities and their deriving factors in a biodiversity hotspot on Hainan Island, China. – Global Ecology and Conservation 22: e01034.
[40] Manan, F., Khan, S. M., Ahmad, Z., Kamran, S., Haq, Z. U., Abid, F., Iqbal, M. (2020): Environmental determinants of plant association and evaluation of the conservation status of *Parratiopsis jacquemotiana* in Dir, the Hindu Kush range of mountains. – Tropical Ecology 61(4): 509-526.
[41] Naqinezhad, A., Hamzehée, B., Attar, F. (2008): Vegetation–environment relationships in the alderwood communities of Caspian lowlands, N. Iran (toward an ecological classification). – Flora-Morphology, Distribution, Functional Ecology of Plants 203(7): 567-577.
[42] Nasir, E., Ali, S. I. (1971-1989): Flora of Pakistan. – PARC, Islamabad, Pakistan.

http://www.aloki.hu ● ISSN 1589 1623 (Print) ● ISSN1785 0037 (Online)
DOI: http://dx.doi.org/10.15666/aeer/2001_339361

[43] Olsen, S. R., Sommers, L. E. (1982): Phosphorus. – In: Methods of soil analysis, part 2. 2nd ed. Madison, WI, USA, pp. 406-407.
[44] Paing, J. N., Gomez, R. A. (2021): Ecological distribution and soil-vegetation analysis of the indigenous vegetable panawil (*Leptosolena haenkei* C. Presl.) in specific areas of Benguet and Mountain province, Philippines. – Tropical Ecology 62: 107-115.
[45] Phillips, O. L., Vargas, P. N., Monteagudo, A. L., Cruz, A. P., Zans, E. C., Sánchez, W. G., Yli-Halla, M., Rose, S. (2003): Habitat association among Amazonian tree species: a landscape-scale approach. – J. Ecol. 91(5): 757-775.
[46] Qureshi, R., Bhatti, G. R., Shabbir, G. (2011): Floristic inventory of Pir Mehr Ali Shah Arid Agriculture University Research Farm at Koont and its surrounding areas. – Pak. J. Bot. 43(3): 1679-1684.
[47] Qureshi, R., Shaheen, H., Ilyas, M., Ahmed, W., Munir, M. (2014): Phytodiversity and plant life of Khanpur Dam, Khyber Pakhtunkhwa, Pakistan. – Pak. J. Bot. 46(3): 841-849.
[48] Rahman, M. U. (2012): Wild plants of Swat Pakistan. – Published by Government Jehanzeb Post Graduate College. Saidu Sharif Swat, 281p.
[49] Rahman, A. U., Khan, S. M., Khan, S., Hussain, A., Rahman, I. U., Iqbal, Z., Ijaz, F. (2016): Ecological assessment of plant communities and associated edaphic and topographic variables in the Peochar Valley of the Hindu Kush mountains. – Mountain Research and Development 36(3): 332-341.
[50] Rahman, A., Khan, S. M., Ahmad, Z., Alamri, S., Hashem, M., Ilyas, M., Aksoy, A., Dülgeroğlu, C., Khan, G., Ali, S. (2021): Impact of multiple environmental factors on species abundance in various forest layers using an integrative modeling approach. – Global Ecology and Conservation 29: e01712.
[51] Raunkiaer, C. (1934): The life forms of plants and statistical plant geography. – Oxford: Clarendon Press, 632p.
[52] Rawat, B., Negi, A. S. (2020): Plant diversity pattern along environmental gradients in Nanda Devi Biosphere Reserve, West Himalaya. – Tropical Ecology.
[53] Rhoades, J. (1982): Soluble salts. – Methods of soil analysis 2(2): 167-178.
[54] Saleem, H., Mehmood, S., Khan, R. U., Sherwani, S. K., Khan, S. U., Khan, A., Ullah, I. (2013): Conservation of native vascular plants of Township Campus, University of Science and Technology Bannu, Khyber Pakhtunkhwa, Pakistan. – International Journal of Herbal Medicine 1(3): 29-33.
[55] Shah, M. R. (2013): Phytosociological attributes and phytodiversity of Dheri Baba hill and Peer Taab Graveyard, District Swabi, Khyber Pakhtunkhwa, Pakistan. – P. J. Life Sci. 1(1): 1-16.
[56] Shah, T., Hayat, U., Bacha, M. S., Muhammad (2019): An empirical analysis of livestock activities of the model farm service center in Khyber Pakhtunkhwa. – Sarhad Journal of Agriculture 35(2): 557-564.
[57] Shahid, M., Joshi, S. P. (2015): Life-forms and biological spectrum of dry deciduous forests in Doon Valley, Uttarakhand, India. – International Journal of Environmental Biology 5(1): 1-10.
[58] Sharma, A., Sharma, N. (2020): Floristics, leaf size spectra and life-form distribution of Riparian Vegetation along a hill stream, Bhaderwah, Jammu and Kashmir, India. – Asian Journal of Plant Sciences 19: 91-106.
[59] Shuaib, M., Khan, I., Khan, R., Mubarik, S., Naz, R. (2014): Ethnobotanical studies of spring flora of District Dir (Lower), Khyber Pakhtunkhwa, Pakistan. – Pak. J. Weed Sci. Res. 20(1): 37-49.
[60] Siddiqui, F. M., Ahmed, M., Shaukat, S. S., Khan, N. (2010): Advance multivariate techniques to investigate vegetation-environmental complex of pine forests of moist area of Pakistan. – Pak. J. Bot. 42: 267-293.
[61] Singh, N., Tamta, K., Tewari, A., Ram, J. (2014): Studies on vegetational analysis and regeneration status of *Pinus roxburghii*, Roxb. and *Quercus leucotrichophora* forests of Nainital Forest Division. – Global Journal of Science Frontier Research 14: 41-47.

http://www.aloki.hu ● ISSN 1589 1623 (Print) ● ISSN1785 0037 (Online)
DOI: http://dx.doi.org/10.15666/aeer/2001_339361

[62] Slavich, P., Petterson, G. (1993): Estimating the electrical conductivity of saturated paste extracts from 1:5 soil, water suspensions and texture. – Soil Res. 31(1): 73-81.
[63] Tiwari, O. P., Sharma, C. M., Rana, Y. S. (2020): Influence of altitude and slope-aspect on diversity, regeneration and structure of some moist temperate forests of Garhwal Himalaya. – Tropical Ecology 61(2): 278-289.
[64] Tripathi, O. P., Tripathi, R. S., Pandey, H. N. (2013): Composition and structure of subtropical Vegetation of Meghalaya, Northeast India. – Journal of Ecology and the Natural Environment 5(6): 103-108.
[65] Ullah, S., Badshah, L. (2017): Floristic structure and ecological attributes of Jelar valley flora, district Upper Dir, Pakistan. – Journal of Biodiversity and Environmental Sciences 10(5): 89-105.
[66] Wang, J., Wang, H., Cao, Y., Bai, Z., Qin, Q. (2016): Effects of soil and topographic factors on vegetation restoration in opencast coal mine dumps located in a Loess area. – Sci. Rep. 6: 22058.
[67] Yang, Y., Shen, Z., Han, J., Zhongyong, C. (2016): Plant diversity along the eastern and western slopes of Baima Snow Mountain, China. – Forests 7(4): 89.
[68] Ye, R., Liu, G., Chang, H., Shan, Y., Mu, L., Wen, C., Te, R., Wu, N., Shi, L., Liu, Y., Wang, H. (2020): Response of plant traits of *Stipa breviflora* to grazing intensity and fluctuation in annual precipitation in a desert steppe, northern China. – Global Ecology and Conservation 24: e01237.
[69] Zeeshan, A., Khan, S. M., Page, S., Alamri, S., Hashem, M. (2021): Plants predict about mineral mines-a methodological approach of using indicator species for discovery of the mining sites. – Journal of Advanced Research. https://doi.org/10.1016/j.jare.2021.10.005.
[70] Zhuang, L., Tian, Z., Chen, Y., Li, W., Li, J., Lu, S. (2012): Community characteristics of wild fruit forests along elevation gradients and the relationships between the wild fruit forests and environments in the Keguqin Mountain region of Iii. – J. Mountain Sci. 9: 115-126.

http://www.aloki.hu ● ISSN 1589 1623 (Print) ● ISSN1785 0037 (Online)
DOI: http://dx.doi.org/10.15666/aeer/2001_339361

INFLUENCE OF ECOLOGICAL AND QUALITY CONCERNS ON THE ADOPTION INTENTION OF ENVIRONMENT-SMART AGRICULTURAL SYSTEMS

CHI, S. Y. – CHIEN, L.-H.*

Department of Applied Economics, National Chung Hsing University
145 Xinda Rd., Taichung City 40227, Taiwan

**Corresponding author*
e-mail: lhchien@nchu.edu.tw; phone: +886-4-2285-1541; fax: +886-4-2286-0255

(Received 3rd Aug 2021; accepted 28th Oct 2021)

Abstract. Within the framework of the theory of planned behavior, this paper explores whether farmers who plant high-priced tea accept an alternative farming system out of concern for the environment and product quality. In total, 253 tea farmers in Taiwan was interviewed, and their data were analyzed using partial least squares structural equation modeling. Statistical results indicated that the environmental concerns and quality considerations of tea farmers influence their behavioral intentions toward the adoption of new technology systems. Other social and economic variables, such as government subsidies, professional counseling, organization promotion, and community network, also affect their decision-making intention. Farmers with heterogeneous expectations of the new farming system must be considered in these analytical strategies. Based on the respondents' attitudes, effective promotion and implementation can be designed more specifically to target farmers' adoption intention by addressing ecological and product quality concerns.
Keywords: *decision analysis, theory of planned behavior, tea farming, heterogeneous expectations, behavioral intention*

Abbreviations: ESA, environment-smart agriculture; EC, ecological concerns; QC, quality concerns; TPB, theory of planned behavior; IA, intention to adopt ESA; AT, attitude toward the behavior; SN, subjective norms; PBC, perceived behavioral control; PLS-SEM, partial least squares structural equation modeling; AVE, average variance extracted; HTMT, heterotrait–monotrait ratio; FIMIX-PLS, finite mixture partial least squares; AIC, Akaike's information criterion; BIC, Bayesian information criterion; CAIC, consistent Akaike's information criterion; MDL, minimum description length; LnL, log-likelihood; EN, entropy statistic

Introduction

Environmental conservation and effective resource allocation have encouraged farmers to adopt more environmentally friendly technologies, and the efficient promotion of these ideas is crucial for agricultural policymakers. Many studies have integrated market demand, technological progress, and environmental concern to persuade farmers to adapt to environmental changes through the application and promotion of ecologically intelligent agricultural technology systems that also support the economic goals of farm management (Lalani et al., 2016; Pretty, 2008; Thornton et al., 2018). Rahman (2018) proposed the environment-smart agriculture (ESA) concept to consider the introduction of environmentally friendly farming devices under existing farming systems to minimize negative effects on the management habits and existing benefits of the operators. An ESA system collects field information through sensing technology, intelligent machines, and other related equipment and subsequently performs cloud computing with large data transmission or creative control of an expert database (Rahman, 2018). The system improves the quality of agricultural products by

http://www.aloki.hu ● ISSN 1589 1623 (Print) ● ISSN 1785 0037 (Online)
DOI: http://dx.doi.org/10.15666/aeer/2001_363381

enhancing the soil and water conditions of farms and reducing the harmful environmental and ecological effects of farm production (Zeweld et al., 2017).

Acceptance of a recommended ESA management plan implies that farmers must change their original experience-based management into an environmentally friendly expert information system, through which they can simultaneously conduct intensive commercial production and maintain a sustainable ecological business model (Lalani et al., 2016). Although ESA adoption has proven environmentally beneficial, ESA policies have yet to achieve desired results in terms of scale and long-term execution. Farmers are required to replant crops entirely or substantially convert existing farming systems and habits. The adoption of such drastic changes in production systems is difficult for small-scale farmers facing uncertain crop yields and inherent business risks (Rahman, 2018).

Many studies have applied econometric models to evaluate the implementation of similar smart agricultural systems, such as climate-smart agriculture; however, those studies have not explained why some farmers achieve less effective results when systems are implemented in areas with high potential for development (Osmond et al., 2015). Their estimations may be biased toward influential factors, creating confusion regarding actual behavioral intentions without accounting for the diverse of agricultural production.

Considerations and measures of whether the adoption of environmentally intelligent agricultural systems meets the needs of farms must be diversified. A comprehensive model describing a farmer's decision-making process requires information on adequate soil fertility levels and biomass production as well as farming practices, technology, finance, sales systems, and policies to achieve satisfactory results (Wall et al., 2013). Pannell et al. (2014) attempted to gauge framer perspectives on similar systems, arguing that farmers contemplating switching to a new system consider not only short-term economic benefits and cost concerns but also farm operations, such as training and system knowledge, the opinions of families and neighbors, pest management, the opportunity costs of crop rotation, public aid and regulations on the use of critical resources, interaction with local businesses, and financial and trade conditions. Therefore, by addressing these different dimensions and prioritizing farmers' decisions, an evaluation of their trade-offs and synergies warrants attention.

The establishment of ESA involves changes to the farming pattern by installing electronic sensors and equipment to collect and transmit farming data (Liao and Xu, 2019). Therefore, investment in these facilities and provision of technical support as well as mutual trust between farmers and stakeholders are critical factors in the initial stage of new smart system implementation and in determining whether the farmers can adopt this technology and adapt successfully (Makate et al., 2019; Nkala et al., 2011; Westermann et al., 2018). Social capital, personal effectiveness, training, and perceived usefulness also play key roles in the decision to adopt sustainable practices (Zeweld et al., 2017). Lalani et al. (2017) and Grabowski and Kerr (2014) have argued that if insufficient resources or commitment are provided to farmers during the system start-up stage, a low adoption rate occurs in the field and planned targets are not achieved; an ESA strategy's effectiveness is then limited to small plots of land, which farmers eventually abandon.

Many studies have indicated that government subsidy policies are essential for promoting environmentally friendly farming systems and have suggested that if the government does not provide continual financial support, they risk operational

http://www.aloki.hu ● ISSN 1589 1623 (Print) ● ISSN 1785 0037 (Online)
DOI: http://dx.doi.org/10.15666/aeer/2001_363381

instability as serious as that posed by natural environmental factors, leading to unsustainable agricultural systems and ineffectiveness throughout a region (Borges et al., 2014; Mittenzwei et al., 2017; Pannell et al., 2014). In addition, the farming systems of small-scale farms are highly heterogeneous, and the factors influencing decision-making behavior regarding ESA systems are complex (Makate et al., 2019).

Scholars have proposed that farmers' willingness to adopt a technology is affected by the following concerns: farmers' past behaviors, socioeconomic characteristics, farm characteristics, farmers' risk attitudes and information sources (Bamberg et al., 2003; Brown et al., 2018), organizational promotion (Lalani et al., 2016), membership in farmers' associations (Issa and Hamm, 2017), weather-based crop agroadvisories (Khatri-Chhetri et al., 2017), national agricultural policies and related economic incentives (Mittenzwei et al., 2017; Nkala et al., 2011; Pannell et al., 2014), and the effects of initiatives by nongovernmental organizations and consumer groups. Thus, psychological factors are essential in measuring and analyzing the factors influencing smallholders' adoption of sustainable business models and their participation in public policy. Selecting a farm with a willingness to participate in public policy is crucial for effectively promoting ESA operations and achieving consistent performance.

Daxini et al. (2019) reported that due to a lack of consideration of farmers' psychosocial responses and decision-making attitudes in policy planning, they may be less proactive in selecting environmentally beneficial technology in practical operation. Possible concerns for farmers are social pressure, peer influence, self-expectation, and the willingness to adopt (Borges and Oude Lansink, 2016). Ajzen (1991) and Madden et al. (1992) proposed the theory of planned behavior (TPB), suggesting that three independent facets influence the behavioral intention of individual decision-making, namely attitude, subjective norms (i.e., social pressure), and perceived behavioral control (the extent to which individuals can achieve their goals). The intentions and perceived behaviors of decision-makers are defined as the influencers of behavioral beliefs (equivalent to the driving factors of attitudes), normative beliefs (equivalent to the driving factors of subjective norms), and control beliefs (comparable to the driving factors of perceived behavioral control).

Studies have employed this model to assess farmers' decision-making on a range of agricultural technologies from social and psychological perspectives (Beedell and Rehman, 2000; Borges et al., 2014; García et al., 2012; Lalani et al., 2016; Senger et al., 2017b). This theory has been widely used to analyze farmer decision-making through the influence of their supporting behaviors and attitudes, subjective norms, and perceived behaviors (Senger et al., 2017a; Zeweld et al., 2017).

This study applied the TPB to present the potential behavioral intention in farmers' decisions to adopt new technology by considering these three facets. The sustainability concerns of environment and product quality are also considered to represent additional drivers of operational intents (Ciccullo et al., 2018). Farmers are concerned about production possibilities, social pressures, ability perceptions, and subsequent changes in their intent to adopt. Because new operating system adoption may be affected by the unobservable heterogeneity of the farmers, this study used finite mixture partial least squares (FIMIX-PLS) segmentation to categorize farmers with diverse ecological and product quality concerns. *Figure 1* represents the base concept and analytical processes.

The objectives of this study were as follows: 1) to identify notable differences among farmers' intentions to adopt ESA, 2) to identify the effects of the three TPB structural factors of behavioral intention in terms of different ecological and product quality

http://www.aloki.hu ● ISSN 1589 1623 (Print) ● ISSN 1785 0037 (Online)
DOI: http://dx.doi.org/10.15666/aeer/2001_363381

concerns, and 3) to analyze the characteristic effects of ecological factors and product quality concerns of farmers with different intentions.

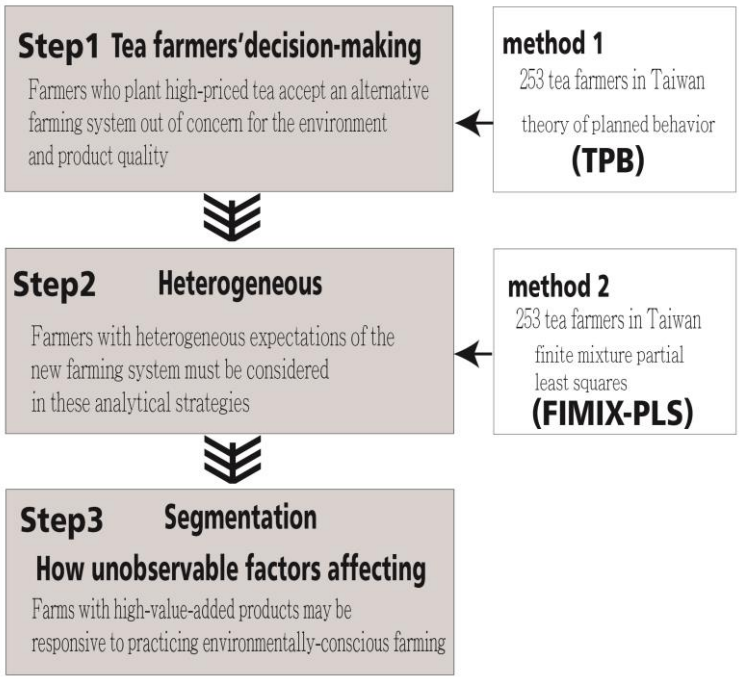

Figure 1. *Base concept and analytical processes*

Materials and methods

Theory of planned behavior: an introduction

According to the TPB, human social behavior is a reasonable stage process (Ajzen, 1991; Bamberg et al., 2003). The TPB maintains that behavior is psychologically driven by intentions (IA), which are influenced by the following three considerations: should I do this? (attitude, AT), do others think it should be done? (subjective norms, SN), and I think it can be done (perceived behavioral control, PBC). Perceived behavioral control emphasizes the ability of humans to control practices, and it may be an essential aspect of understanding farmers' agricultural decisions. Therefore, the role of behavioral intention in decision-making behavior is integrated in the TPB architecture through the consideration of perceived behavioral control (Lee et al., 2016; Madden et al., 1992; Mahindarathne and Gunaratne, 2015).

TPB has been widely used to understand farmers' decision-making and adoption behaviors in different agricultural areas. Policymakers can determine the role of intentions by grasping the underlying psychological factors that influence farmers' beliefs regarding the adoption of an ESA system (Borges et al., 2014; Lalani et al., 2016; Senger et al., 2017a, b; Zeweld et al., 2017). Research results have demonstrated that farmers' attitudes toward increasing production, reducing labor input, improving soil quality, and reducing critical cognitive drivers are the most influential factors affecting intent, in addition to social pressure and the opinions of family.

Attitudes are derived from an assessment of behavioral beliefs and their outcomes. Subjective norms originate from normative beliefs, which are formed by the normative

http://www.aloki.hu ● ISSN 1589 1623 (Print) ● ISSN 1785 0037 (Online)
DOI: http://dx.doi.org/10.15666/aeer/2001_363381

expectations and adherence motives of the subject. This study proposes that ecological and product quality concerns affect a farmer's farming philosophy. Perceived behavioral control stems from controlling beliefs, which in turn may promote or inhibit behavioral performance.

Behavioral factors can be promoted or inhibited and therefore, behavior, norms, and control have functions in the TPB. First, the sum of behavioral, normative, and control beliefs are indirect measures of attitude, subjective norms, and perceived behavioral control. These three factors further affect decision-making regarding the expected intentions of interviewed farmers. In addition, expected behaviors, norms, and control beliefs promote intentional attitudes, subjective norms, and perceived behavioral control through the formation of decision-making intentions and final decision behavior (Borges et al., 2014).

In the last 10 years, ecological and food safety concerns have markedly affected the production of high value agricultural products. Whether farmers' concern for these two factors affects their decision to adopt ESA is another focus of this article. This study explored whether the key factors of the TPB influence farmers' decisions regarding safe and environmentally friendly farming. Possible considerations in behavioral beliefs and concerns include increasing total production and product value, improving product quality, reducing manual input and material costs through precision fertilization, preventing soil erosion through precision irrigation management, and controlling farming procedures by receiving technological recommendations through their mobile phones. Possible factors for the normative beliefs aspect include government financial subsidies, professional counseling services, technological farming expansion, online stories of success, and support from family, neighbors, and friends. Adequate investment funds, professional and feasible levels of knowledge, and awareness of market access and marketing management are considered under the behavioral control category.

Partial least squares structural equation modeling

A structural equation modeling approach is effective for analyzing the causal relationship between indicator and latent variables (Ajzen, 2002a, b; Bamberg et al., 2003; Grabowski and Kerr, 2014; Han et al., 2010; Luhmann and Theuvsen, 2016) and the structural pathways of the TPB to measure related business behaviors (Bamberg et al., 2003; Borges et al., 2014; Han et al., 2010; Lalani et al., 2016; Senger et al., 2017b). With the convenience of fewer samples and no need to set sample distribution patterns in modeling (Hair et al., 2018), variance-based partial least squares structural equation modeling (PLS-SEM) provides a less restrictive exploration tool in the social sciences, and it is advantageous for its estimation of the potential values of observed variables (Chin, 2010; Hair et al., 2012; Henseler et al., 2009, 2015; Wold, 1975). This article comprises a prediction-oriented exploratory analysis on the effects of environmental concerns and product quality on farming technology behavior, using PLS-SEM for analysis (Hair et al., 2017a).

PLS-SEM consists of two models, namely the measurement and the structural model (Hair et al., 2019). For the measurement model, the reliability of the internal indicators and facets must be evaluated. First, the standardized factor loading must exceed a threshold of 0.7 in the internal consistency reliability analysis (Hair et al., 2012; Hulland, 1999). Second, the conventional indicator, Cronbach's α, must be greater than 0.7. Finally, the reliability test between the potential variables and the

http://www.aloki.hu ● ISSN 1589 1623 (Print) ● ISSN 1785 0037 (Online)
DOI: http://dx.doi.org/10.15666/aeer/2001_363381

observed variables requires a consideration of their composite reliability (Bagozzi and Yi, 1988), for which a value of ≥ 0.7 is acceptable (Fornell and Larcker, 1981; Hair et al., 2018).

The validity of the PLS-SEM model was measured using convergent and discriminant validity (Hair et al., 2016a). Convergent validity evaluates the average variance extracted (AVE) across all indicators with a specific construct. According to relevant research recommendations, the AVE across all potential indicators should exceed 0.5 (Bagozzi and Yi, 1988; Fornell and Larcker, 1981; Hair et al., 2006). This study used the Fornell–Larcker criterion (Fornell and Larcker, 1981; Götz et al., 2010) and the heterotrait–monotrait ratio (HTMT; Chin, 2010; Henseler et al., 2015; Rasoolimanesh et al., 2017) of correlations to indicate and assess discriminant validity (Hair et al., 2016a, b).

Path coefficients between facets were estimated using the bootstrap method (Dijkstra and Henseler, 2015). In total, 3,000 calculations were performed, and the statistical significance and explanatory power (R2) for hypothetical paths were estimated and examined (Hair et al., 2011).

Construct development and variables

Tea trees grow on hillsides; thus, soil management, such as water and soil conservation, is critical to tea farming in Taiwan. In recent years, consumers have begun to pay attention to the domestic tea they consume and whether tea plantations meet environmental and quality standards. New farming applications must ensure profitability by achieving lower costs or higher production; farmers, especially those with small-scale, lower-income plots, adopt new technology primarily for this reason (Lalani et al., 2016; Lee et al., 2016; Nguyen et al., 2019). Respondents measured their degree of agreement with statements on a 7-point Likert scale for each question. The major construct in this research was divided into two parts. First, the farmer's concern for ecology (EC) and product quality (QC) was included in terms of whether the farming management considers the effects on the environment and biodiversity and whether this ecological concern affects the quality requirements of products; then the effects of QC on AT, SN, and PBC were extended within the TPB model. Second, the structure of the TPB was emphasized by examining the influence of AT, SN, and PBC and analyzing how these three facets affect farmers' intention (IA) to adopt ESA. The relevant variables are listed in *Table 1*.

Structural model and path analysis

The relationship between the research structure and the causal path is based on the two-stage reference TPB model proposed by Ajzen (1991). The first stage confirms the effects of EC on QC (Kim et al., 2014) with hypothesis 1 (H1), and the effect of QC on the TPB three-pillar facet is examined through a review of hypotheses 2 to 4 (H2, H3, and H4) (McFadden and Huffman, 2017; Valeeva et al., 2004). The second stage then analyzes the effects of the three facets on each other and then on the behavioral intentions (IA) of farming decision-makers using the ESA system as hypotheses 5 to 9, which display as H5, H6, H7, H8, and H9.

In addition, many studies have adopted a multigroup analysis of partial least squares according to categorical variables to more accurately target the socioeconomic conditions of the respondents. However, decision-makers may be affected by other

http://www.aloki.hu ● ISSN 1589 1623 (Print) ● ISSN 1785 0037 (Online)
DOI: http://dx.doi.org/10.15666/aeer/2001_363381

unobservable heterogeneous attributes (Hair et al., 2016b). Therefore, the procedures do not include critical influencing factors, which may affect the validity of the inference. This study used the FIMIX-PLS approach (Hair et al., 2016a, b; Sarstedt and Ringle, 2010; Sarstedt et al., 2017) to examine the differences in the behaviors of tea farmers in different clusters by considering the characteristics of ESA (Hahn et al., 2002; Rigdon et al., 2011).

Table 1. *Research constructs and questionnaire items. (Source: this study)*

Latent construct	Descriptive definition and items
Ecological concerns (EC)	For me, caring for the environment and ecology is an attitude that must be valued and considered in agricultural management (Kim et al., 2014). ♦ An eco-friendly management model (EFMM) to manage tea farms can assist in the control and effective use of soil and water resources to protect the environment. ♦ Tea farms can be managed with EFMMs, which can sustain coexistence with surrounding flora and fauna.
Quality concerns (QC)	For me, the quality improvements in tea products that occur after adopting an EFMM will affect my decision-making attitude toward the system (McFadden and Huffman, 2017; Valeeva et al., 2004). ♦ Using an EFMM to manage the tea farm can ensure the quality of the tea and the peace of mind of the customers. ♦ Using an EFMM to manage the tea farm can ensure the stability of tea quality and enhance the level of tea production.
Attitude toward the behavior (AT)	Environment-smart agriculture (ESA) systems represent one popular local EFMM application. For me, adopting an ESA system to manage the tea farm would be a unique and comfortable decision. ♦ Therefore, considering the factors of "increasing the quantity of tea leaves harvested," "upgrading tea leaf quality," "saving labor," "performing precision fertilization," "mastering irrigation timing and precise water use," and "acquiring timely management suggestions" constitute my attitude toward implementing the ESA system.
Subjective norms (SN)	Most of the people I care about will support and encourage my subsequent adoption of the ESA system to manage the tea farm. ♦ Considerations such as "government grants," "agricultural organization and counseling promotion," "technology promotion," "successful experiences of the online community," and "recommendations of family, neighbors, or friends" will constitute the normative nature of my belief in adopting the ESA system.
Perceived behavioral control (PBC)	For me, it is easy to manage my tea farm using an ESA system with the following conditions: ♦ "Expertise in research and development," "operating capabilities of professional machinery and facilities," "sufficient funds," and "understanding of product markets" instill confidence toward using the ESA system.
Intention to adopt ESA (IA)	I will adopt the ESA system to manage the tea farm to achieve and maintain business goals. ♦ If the adoption of the ESA system can "increase the profitability of the tea farm," "generate public benefits to the tea industry," "promote new farming techniques," and "improve tea farm market visibility after adoption," my intention to adopt the ESA system will be constituted.

The FIMIX-PLS method proposed by Hahn et al. (2002) has been primarily used to determine optimal grouping by investigating the presence of unobservable heterogeneity in data. The procedures allow for estimates of the model parameters and the number of

http://www.aloki.hu ● ISSN 1589 1623 (Print) ● ISSN 1785 0037 (Online)
DOI: http://dx.doi.org/10.15666/aeer/2001_363381

classifications related to the interviewee. Furthermore, the method can evaluate the path model between different classifications according to its validity (Arenas-Gaitán et al., 2018; Hair et al., 2016a, b; Matthews et al., 2016). The statistical results from grouping characteristics can shape policy and managerial measures for improving the farming system and promoting the efficacy and expansion of tea operators in Taiwan.

Data collection and analysis

A total of 439 tea farmers in central Taiwan were interviewed between May and June 2019. The number of valid surveys was 253, with a completion rate of 57.6%. Approximately 62.5% of the respondents were male, and 37.5% were female (*Table 2*). Their average age was 43 years, and nearly 80% of the farmers surveyed were between 31 and 60 years old. Compared with the current average age of 64 for farmers in Taiwan (DGBAS, 2017), the respondents were younger. In addition, 56.1% were university graduates and nearly 10% held master's degrees. Moreover, 56% of respondents were members of specialized tea organizations. Fewer than half of the farmers owned their tea farms; rather, most of them jointly owned or rented them. Approximately 40.3% reported that their tea farm provided more than half of their household income, indicating that nearly 60% of the interviewed operators maintain family economic stability through additional part-time work.

Table 2. *Demographic description of participants (n = 253). (Source: computed by this study)*

Variables and characteristics	Frequency	Percentage (%)
Gender		
Male	158	62.5
Female	95	37.5
Age		
Below 30	37	14.6
31~40	91	36.0
41~50	61	24.1
51~60	50	19.8
61 and above	14	5.5
Education		
Junior high school diploma	16	6.3
Senior high school diploma	70	27.7
Bachelor's degree	142	56.1
Master's degree and above	25	9.9
Member of professional organization		
Yes	142	56.1
No	111	43.9
Ownership of the tea farm under operation		
Below and equal 50%	124	49.0
Above 50%	129	51.0
Tea farm income share for total household amount		
Below and equal 50%	151	59.7
Above 50%	102	40.3

http://www.aloki.hu ● ISSN 1589 1623 (Print) ● ISSN 1785 0037 (Online)
DOI: http://dx.doi.org/10.15666/aeer/2001_363381

Results

Evaluation of the measurement model and TPB structural path

Measurement indicators and textual descriptions of the research facets were developed after the relevant constructs of previous studies and tea industry practices were referenced; these facets are presented in *Table 1*. Cronbach's α for each index and the composite reliability value indicated that all latent variables had acceptable internal consistency and content reliability (Hair et al., 2012; Hulland, 1999). The statistical results demonstrate that the factor loadings of all indicators met the requirements (*Table 3*). For the testing of convergent validity, the AVE values of the seven latent variables satisfied the commonality analysis.

Table 3. *Index details for measurement models, reliability, and convergent validity*

Construct factors and items	α	CR	AVE	Loading
Ecological concerns (EC)	0.848	0.929	0.868	
Effective use of soil and water resources can protect the earth				0.936
Responsibility to maintain the sustainable coexistence of surrounding flora and fauna				0.927
Quality concerns (QC)	0.914	0.959	0.921	
ESA can ensure the stability of tea quality and satisfy processing requirements				0.961
ESA can ensure the safety of tea for customers to consume				0.959
Attitude toward using an environmental smart farming system (AT)	0.932	0.947	0.747	
I can master the timing and irrigation of tea farms using the precise amount of water				0.898
I can apply fertilizers systematically, effectively, and accurately				0.886
I can improve the quality of the tea				0.872
I can monitor tea tree growth by using mobile phones and obtain farming recommendations				0.866
I can increase the amount of tea leaves harvested				0.859
I can hire fewer workers and reduce workforce demands				0.804
Subjective norms (SN)	0.868	0.906	0.66	
Counseling and promotion by professional technical units				0.884
Counseling and promotion by local agricultural organizations				0.863
Financial support from government subsidies				0.820
Success stories from online social media				0.804
Suggestions from family, neighbors, or friends				0.673
Perceived behavioral control (PBC)	0.901	0.931	0.772	
Individuals must have sufficient knowledge of the system				0.923
Machine operation and facility requirements				0.878
Sufficient funds				0.868
Must increase market visibility of product				0.845
Intention to adopt ESA (IA)	0.89	0.924	0.753	
Adopting ESA can be considered a new technological improvement				0.904
Using ESA can generate public benefits that are also beneficial to the tea industry				0.897
Introducing ESA can be used as advertising to increase product popularity				0.863
Using ESA can increase the profitability of the tea farm				0.804

Alpha: Cronbach's α; CR: composite reliability; AVE: average variance extracted

http://www.aloki.hu ● ISSN 1589 1623 (Print) ● ISSN 1785 0037 (Online)
DOI: http://dx.doi.org/10.15666/aeer/2001_363381

The Fornell–Larcker criterion and the HTMT test of each primary construct exhibited significant differences in the paths of the model, indicating discriminant validity (*Table 4*). These statistical results indicated that the TPB framework and the potential paths between the primary constructs are appropriate for subsequent analysis with ecological and product quality concerns (Hair et al., 2017b, 2019).

Table 4. *Discriminant validity of constructs*

Constructs	Fornell-Larcker criterion						Heterotrait-Monotrait ratio (HTMT)				
	EC	QC	AT	SN	PBC	IA	EC	QC	AT	SN	PBC
EC	0.932										
QC	0.842	0.96					0.955				
AT	0.522	0.574	0.864				0.586	0.62			
SN	0.408	0.431	0.437	0.812			0.476	0.485	0.487		
PBC	0.434	0.432	0.356	0.583	0.879		0.492	0.473	0.386	0.658	
IA	0.865	0.854	0.526	0.483	0.501	0.868	0.993	0.944	0.573	0.552	0.557

EC: ecological concerns; QC: quality concerns; AT: attitude toward the behavior; SN: subjective norms; PBC: perceived behavioral control; IA: intention to adopt ESA

This study examined nine paths between EC, AT, SN, and PBC and the interactions among three primary constructs based on the TPB framework in *Figure 2*. The values of determinant coefficients between the major facets are listed in *Table 5*. The total effects of the major constructs were statistically significant ($P < 0.05$); therefore, the simulation results determined that the TPB structure was significantly supported by the statistical results. The findings revealed that farmers' concerns for the conservation of soil and water resources alters their attitudes toward the quality of their own tea products (H1: EC→QC, 0.842). Furthermore, concerns about tea quality affect the constructs of advantage evaluation (H2: QC→AT, 0.516), perceived expectations of others (H3: QC→SN, 0.220), and self-perception and perceived ability to enact the system (H4: QC→PBC, 0.432; see *Fig. 3*). All three constructs appreciably affected the intentions of the interviewed farmers to enact a new system (H7: AT→IA, 0.354; H8: SN→IA, 0.167; H9: PBC→IA, 0.278). Each path of the first group was significantly supported, demonstrating that the three fundamental constructs influence farmers' willingness to adopt an ESA system.

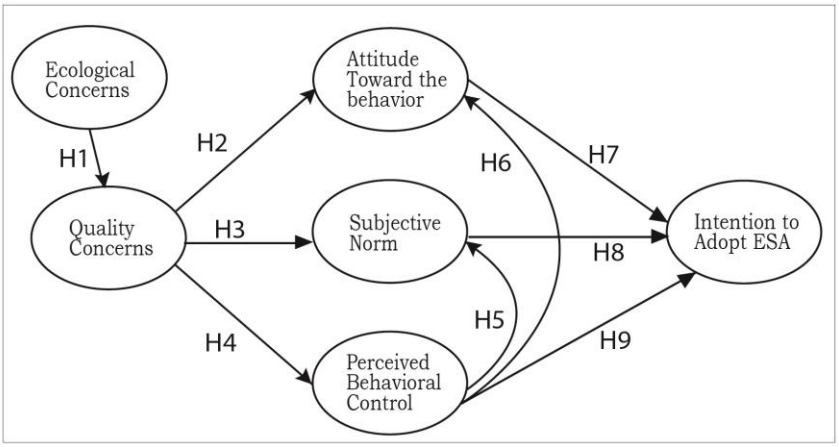

Figure 2. *Proposed research framework*

http://www.aloki.hu ● ISSN 1589 1623 (Print) ● ISSN 1785 0037 (Online)
DOI: http://dx.doi.org/10.15666/aeer/2001_363381

Table 5. *Path coefficients of the structural model*

Construct hypothesis and path	Path coef.	T statistics	P values	Result	R^2-adj
H1: EC → QC	0.842	27.367	**	Accepted	
H2: QC → AT	0.516	5.913	**	Accepted	
H3: QC → SN	0.220	2.867	**	Accepted	
H4: QC →PBC	0.432	5.563	**	Accepted	
H5: PBC → SN	0.488	5.936	**	Accepted	
H6: PBC → AT	0.133	1.443		Rejected	
TPB					
H7: AT → IA	0.354	4.276	**	Accepted	
H8: SN → IA	0.167	2.011	*	Accepted	
H9: PBC → IA	0.278	3.935	**	Accepted	
Determinant coefficients for the construct					
QC					0.708
AT					0.338
SN					0.374
PBC					0.184
IA					0.399

EC: ecological concerns; QC: quality concerns; AT: attitude toward the behavior; SN: subjective norms; PBC: perceived behavioral control; IA: intention to adopt ESA. *P < 0.05, **P < 0.01

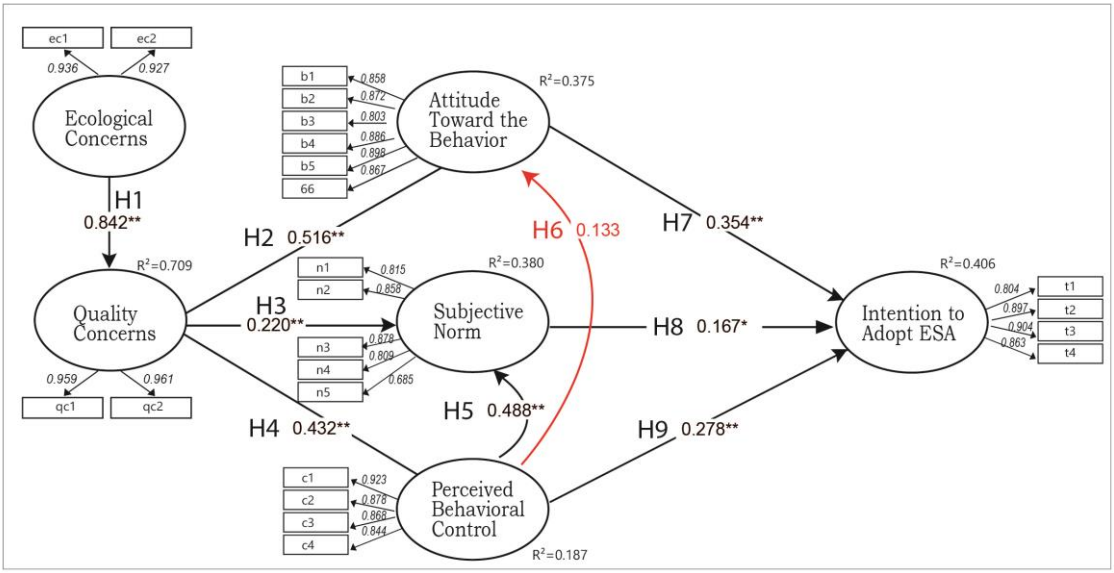

Figure 3. *PLS path modeling results. Note: Red line indicates the path with no significance*

Further analysis of the specific behavioral connotations was undertaken after the FIMIX-PLS grouping. This study used the K group verification indicators provided by Sarstedt et al. (2011) to examine potential unobservable heterogeneity in the data. *Table 6* presents the analysis results of K from 2 to 5 and four classification critera, include modified Akaike's information criterion with factor 3 (AIC_3), Bayesian information criterion (BIC), consistent Akaike's information criterion (CAIC),

http://www.aloki.hu ● ISSN 1589 1623 (Print) ● ISSN 1785 0037 (Online)
DOI: http://dx.doi.org/10.15666/aeer/2001_363381

minimum description length with factor 5 (MDL_5) (Groß, 2018; Hair et al., 2017a, b; Sarstedt et al., 2011). Many studies have proposed the entropy statistic (EN) to demonstrate the maximum value for the most significant separation between groups, and it can be used as the determinant of the classification number (Groß, 2018; Hair et al., 2017a, b). This study used K = 2 as the basis for classification to avoid parameter estimation bias for the path coefficient because of the small sample number (Hair et al., 2017a, b). Therefore, the sample was divided into two groups according to the highest EN results of 132 (52%) and 121 (48%).

Table 6. *Classification criteria for varying numbers of segments*

Criteria	No. of segments (k)				
	Complete	**k = 2**	**k = 3**	**k = 4**	**k = 5**
AIC_3	2908.62	2095.74	1955.99	1583.49	1574.99
BIC	2944.09	2169.21	2067.46	1732.96	1762.46
CAIC	2958.09	2198.21	2111.46	1791.96	1836.46
MDL_5	3253.96	2811.08	3041.34	3038.84	3400.34
LnL	-1433.31	-1004.37	-912.00	-703.25	-676.50
EN		0.92	0.91	0.90	0.92
Relative segment size					
1 group	1.00	0.52	0.52	0.52	0.40
2 group		0.48	0.40	0.26	0.27
3 group			0.08	0.12	0.15
4 group				0.10	0.10
5 group					0.08

AIC_3: modified AIC with factor 3; BIC: Bayesian information criterion; CAIC: consistent AIC; MDL_5: minimum description length with factor 5; LnL: log-likelihood; EN: entropy statistic (Normed)

The significance of the path coefficients of the two groups is detailed in *Table 7*. The results strongly indicated that the ecological concern of the farmers has an effect on achieving product quality, with significant coefficients for H1 (EC→QC) in both groups. EC and QC both significantly influenced the farmers' attitudes and their decision to adopt ESA for both groups.

An analysis of the influence of QC on facets of the model indicated that the three paths for the first group were all significant (H2: QC→AT = 0.673; H3: QC→SN = 0.584; H4: QC→PBC = 0.864), but the path of QC to AT was the only significant route for the second group. Three fundamental constructs influenced the farmers' willingness to adopt the ESA system for the first group, but attitude was the only factor affecting decision intention for the second group.

The effects of AT, SN, and PBC on IA were also supported; this supports the TPB model architecture and the connection between the concerns of EC and QC, which then affect AT, SN, PBC, and IA. The influence of EC on QC in the second group was less than that in the first group. For the overall TPB framework, the statistical results only supported the influence of QC on AT, and thus on IA, demonstrating that the EC and QC factors in this group only affect AT; AT to IA was the only significant path in the TPB framework. Farmers in this group were more concerned about what practical business results can be achieved using ESA. Unobserved variability was detected in the

http://www.aloki.hu ● ISSN 1589 1623 (Print) ● ISSN 1785 0037 (Online)
DOI: http://dx.doi.org/10.15666/aeer/2001_363381

data; regrouping the tea farmers with different behaviors is therefore essential when considering their heterogeneity.

Table 7. *Path coefficients and information for the two-segment solution*

Criteria	Segment 1 N = 132(52%)		Segment 2 N = 121(48%)		t[mgp], $\lvert\Delta_{12}\rvert$
Path coefficient					
H1:EC→QC	1.000**		0.730**		0.27**
H2:QC→AT	0.673**		0.419**		0.254
H3:QC→SN	0.584**		0.101		0.483
H4:QC→PBC	0.864**		0.107		0.757**
H5:PBC→SN	0.193		0.463**		0.27**
H6:PBC→AT	0.092		0.058		0.034
TPB					
H7:AT→IA	0.179*		0.322*		0.143
H8:SN→IA	0.163*		0.126		0.037
H9:PBC→IA	0.682**		0.077		0.605**
Reliability and validity	Segment 1		Segment 2		
	CR_1	AVE_1	CR_2	AVE_2	
EC	0.983	0.967	0.892	0.806	
QC	0.977	0.955	0.944	0.893	
AT	0.949	0.755	0.943	0.733	
SN	0.913	0.680	0.893	0.629	
PBC	0.947	0.816	0.919	0.740	
IA	0.945	0.810	0.904	0.703	

EC: ecological concerns; QC: quality concerns; AT: attitude toward the behavior; SN: subjective norms; PBC: perceived behavioral control; IA: intention to adopt ESA; t[MGP] $\lvert\Delta_{12}\rvert$: absolute difference between segment 1 and 2; t = value for multigroup comparison test; CR_i and AVE_i: composite reliability and average variance extracted, respectively, for segment *i*, with *i* = 1, 2

The clustering analysis distinguished the influence of ecological and quality concerns on the respondents' intentions between groups by measuring the unobserved variables in the categories, indicating that the respondents were heterogeneous. Researchers can consider the factors influencing the decision to adopt ESA for different operators and subsequently develop more effective coaching and marketing strategies. Additionally, the concerns of all interviewed farmers in EC and QC significantly influenced their willingness to adopt ESA, indicating that environmental concern increases farmers' product quality demands, thereby increasing their willingness to implement ESA technology. During the early stages of the promotion and introduction of an ESA system, operators with higher EC and QC responsiveness exhibit a willingness to adopt; thus, promotional activities directed at such farmers would yield favorable results.

Discussion

An agricultural farming system oriented toward scale and production can lead to environmental, ecological, and safety problems, resulting in excess inputs of fertilizer

http://www.aloki.hu ● ISSN 1589 1623 (Print) ● ISSN 1785 0037 (Online)
DOI: http://dx.doi.org/10.15666/aeer/2001_363381

and chemicals. With the adoption of an unknown farming system and input changes, framers may worry about the effects on tea quality and total yield. These considerations led to the development of environmentally friendly production systems that have become the focus of policy guidance (Daxini et al., 2019).

This study analyzed the data of 253 tea farmers in Taiwan to assess how ecological and product quality considerations affect their intentions to adopt a new system and their decision behavior within the TPB framework. This study was conducted with consideration for the high quality standards and the higher price for tea than for ordinary grains and horticultural crops in the market. This may encourage tea farmers located on hillsides with a sensitive soil environment to pay more attention to the development of new systems.

The results demonstrate that the TPB model is effective for analyzing the farmers' intention to adopt ESA and indicate that ecology and product quality concerns have positive effects on willingness to implement a new farming system. They also indicated that farmers who pay more attention to the environment and ecology may be more focused on product quality and thus more likely to adopt a new system. Through the monitoring of environmental factors such as soil and humidity through sensors and intelligent control, the application of ESA has indeed made significant changes to increase the yield of tea gardens and reduce management costs (Wu and Ke, 2020).

The study determined that ecological and quality concerns are associated with behavioral attitudes, subjective norms, and perceived behavioral control, which significantly affect adoption intention. The variables considered for each aspect exhibited the same reliability and validity, demonstrating that the questionnaire clearly presented the meaning of each potential concern. In summary, tea farmers with sensitive concerns in environment and product aspects will in turn affect their intent to adopt ESA. The validity and structure of the TPB model and its connections were supported by this study (Borges et al., 2014; Senger et al., 2017a, b; Issa and Hamm, 2017).

After FIMIX-PLS grouping, respondents were dividing into two groups with the specific behavioral connotations. If farmers concern on the environment and quality seriously, they also support the primary constructs in the TPB, such as self-expectation, social interactions, technical knowledge, communication patterns, and financial conditions, which in turn affect their willingness to adopt ESA.

The second group of farmers exhibited a relatively practical attitude toward considering ESA systems on their farms. Consultations with and support of the organizational network had less of an effect on their willingness to adopt, indicating that technical and financial support is not a large factor for consideration for these farmers.

The clustering result demonstrates that intention analysis must consider the heterogeneity of farmers' intentions (Hahn et al., 2002; Groß, 2018). This result provides statistical verification that the TPB indicators can be used to examine the intention of tea farmers, which can be used to adjust counseling measures. Understanding that tea farmers' different attitudes towards the environment and quality concerns will affect ESA application, differentiated strategies should be designed for different respondents to increase the adoption rate of the system.

Conclusion

This study demonstrated that both economic and noneconomic factors significantly influence farmers' intention to adopt ESA in lieu of their conventional farming systems.

http://www.aloki.hu ● ISSN 1589 1623 (Print) ● ISSN 1785 0037 (Online)
DOI: http://dx.doi.org/10.15666/aeer/2001_363381

Farmers concerned about product safety and production stability achieve more market recognition, which increases their willingness to adopt new environmentally friendly systems.

We considered the effectiveness of economic incentives and the influence of social networks in the propagation of new ESA technology. These findings strongly support the role of local farmers' organizations and technical consulting units. However, information disseminated through online social networking affects farmers' decision-making more than does information shared by neighbors and nearby friends, who had minimal influence in this case. Opinions from the virtual network community are key sources of farming information.

The communication methods of professional advisory services have gradually developed in rural areas, indicating that policy interaction and knowledge communication must change. With the prevalence of online communities and the popularity of mobile devices, public-sector counseling services and marketing schemes, which usually depended on traditional interpersonal patterns, must adapt.

Strong and continual technical and financial support from local organizations is a key factor in enticing farmers to adopt a new environmentally friendly system. If profitability for tea farmers can be achieved and environmental and product quality concerns addressed to the satisfaction of public interest, farms with high-value-added products may be responsive to practicing environmentally-conscious farming.

This study analyzed the characteristics of tea farming, with a focus on the influence of unobservable factors affecting farmers' intention to adopt green technology instead of traditional socioeconomic-based systems. According to the results, concerns about the environment and product quality are highly influential aspects for the behavior of farmers in the high-value product market. The scope of system implementation can be extended by considering farmers' diversified responses toward greener farming technology. This study has successfully learned through the TPB model that tea farmers' decision to adopt ESA will be determined by their own concern about tea planting conditions and product quality. Therefore, a segmentation strategy should be adopted to promote high-interest groups for effective system application with consistent performance.

Acknowledgements. Authors are very grateful for the research funding provided by the Ministry of Science and Technology of Taiwan and the advice provided by Professor Shen Yuan from National Chung Hsing University of Taiwan during the project.

REFERENCES

[1] Ajzen, I. (1991): The theory of planned behavior. – Organizational Behavior and Human Decision Processes 50: 179-211.

[2] Ajzen, I. (2002a): Perceived behavioral control, self-efficacy, locus of control, and the theory of planned behavior. – Journal of Applied Social Psychology 32: 665-683.

[3] Ajzen, I. (2002b): Residual effects of past on later behavior: habituation and reasoned action perspectives. – Personality and Social Psychology Review 6: 107-122.

[4] Arenas-Gaitán, J., Rondán-Cataluña, F. J., Ramírez-Correa, P. E. (2018): Modelling the success of learning management systems: application of latent class segmentation using FIMIX-PLS. – Interactive Learning Environments 26: 135-147.

http://www.aloki.hu ● ISSN 1589 1623 (Print) ● ISSN 1785 0037 (Online)
DOI: http://dx.doi.org/10.15666/aeer/2001_363381

[5] Bagozzi, R. P., Yi, Y. (1988): On the evaluation of structural equation models. – Journal of the Academy of Marketing Science 16: 74-94.
[6] Bamberg, S., Ajzen, I., Schmidt, P. (2003): Choice of travel mode in the theory of planned behavior: the roles of past behavior, habit, and reasoned action. – Basic and Applied Social Psychology 25: 175-187.
[7] Beedell, J., Rehman, T. (2000): Using social-psychology models to understand farmers' conservation behaviour. – Journal of Rural Studies 16: 117-127.
[8] Borges, J. A. R., Oude Lansink, A. G. J. M., Ribeiro, C. M., Lutke, V. (2014): Understanding farmers' intention to adopt improved natural grassland using the theory of planned behavior. – Livestock Science 169: 163-174.
[9] Borges, J. R. A., Oude Lansink, A. G. J. M. (2016): Identifying psychological factors that determine cattle farmers' intention to use improved natural grassland. – Journal of Environmental Psychology 45: 89-96.
[10] Brown, B., Llewellyn, R., Nuberg, I. (2018): Global learnings to inform the local adaptation of conservation agriculture in Eastern and Southern Africa. – Global Food Security 17: 213-220.
[11] Chin, W. W. (2010): How to Write Up and Report PLS Analyses. – In: Vinzi, V. E., Chin, W. W., Henseler, J., Wang, H. (eds.) Handbook of Partial Least Squares: Concepts, Methods and Applications. Springer, Berlin.
[12] Ciccullo, F., Pero, M., Caridi, M., Gosling, J., Purvis. L. (2018): Integrating the environmental and social sustainability pillars into the lean and agile supply chain management paradigms: a literature review and future research directions. – Journal of Cleaner Production 172: 2336-2350.
[13] Daxini, A., Ryan, M., O'Donoghue, C., Barnes, A. P. (2019): Understanding farmers' intentions to follow a nutrient management plan using the theory of planned behaviour. – Land Use Policy 85: 428-437.
[14] Directorate General of Budget, Accounting and Statistics (DGBAS) (2017): Statistics of the 2015 census of agriculture in Taiwan. – https://www.dgbas.gov.tw/public/Attachment/711301712205LGQ425T.pdf.
[15] Dijkstra, T. K., Henseler, J. (2015): Consistent partial least squares path modeling. – MIS Quarterly 39: 297-316.
[16] Fornell, C., Larcker, D. F. (1981): Evaluating structural equation models with unobservable variables and measurement error. – Journal of Marketing Research 18: 39-50.
[17] García, C. G. M., Dorward, P., Rehman, T. (2012): Farm and socio-economic characteristics of smallholder milk producers and their influence on technology adoption in Central Mexico. – Tropical Animal Health and Production 44: 1199-1211.
[18] Götz, O., Liehr-Gobbers, K., Krafft, M. (2010): Evaluation of Structural Equation Models Using the Partial Least Squares (PLS) Approach. – In: Vinzi, V. E., Chin, W. W., Henseler, J., Wang, H. (ed.) Handbook of Partial Least Squares: Concepts, Methods and Applications. Springer, Berlin.
[19] Grabowski, P. P., Kerr, J. M. (2014): Resource constraints and partial adoption of conservation agriculture by hand-hoe farmers in Mozambique. – International Journal of Agricultural Sustainability 12: 37-53.
[20] Groß, M. (2018): Heterogeneity in consumers' mobile shopping acceptance: a finite mixture partial least squares modelling approach for exploring and characterising different shopper segments. – Journal of Retailing and Consumer Services 40: 8-18.
[21] Hahn, C., Johnson, M. D., Herrmann, A., Huber, F. (2002): Capturing customer heterogeneity using a finite mixture PLS approach. – Schmalenbach Business Review 54: 243-269.
[22] Hair, J. F., Black, W. C., Babin, B. J., Anderson, R. E., Tatham, R. L. (2006): Multivariate Data Analysis. 6th Ed. – Prentice-Hall, New Jersey.

http://www.aloki.hu ● ISSN 1589 1623 (Print) ● ISSN 1785 0037 (Online)
DOI: http://dx.doi.org/10.15666/aeer/2001_363381

[23] Hair, J. F., Ringle, C. M., Sarstedt, M. (2011): PLS-SEM: Indeed a silver bullet. – Journal of Marketing theory and Practice 19: 139-152.
[24] Hair, J. F., Sarstedt, M., Ringle, C. M., Mena, J. A. (2012): An assessment of the use of partial least squares structural equation modeling in marketing research. – Journal of the Academy of Marketing Science 40: 414-433.
[25] Hair, J. F., Hult, Y., Ringle, C., Sarstedt, M. (2016a): A Primer on Partial Least Squares Structural Equation Modeling (PLS-SEM). 2nd Ed. – Sage Publications, Thousand Oaks.
[26] Hair, J. F., Sarstedt, M., Matthews, L. M., Ringle, C. M. (2016b): Identifying and treating unobserved heterogeneity with FIMIX-PLS: Part I–method. – European Business Review 28: 63-76.
[27] Hair, J. F., Matthews, L. M., Matthews, R., Sarstedt, M. (2017a): PLS-SEM or CB-SEM: updated guidelines on which method to use. – International Journal of Multivariate Data Analysis 1: 107-123.
[28] Hair, J. F., Sarstedt, M., Ringle, C. M., Gudergan, S. P. (2017b): Advanced Issues in Partial Least Squares Structural Equation Modeling. – Sage Publications, Thousand Oaks.
[29] Hair, J. F., Black, W. C., Babin, B. J., Anderson, R. E. (2018): Multivariate Data Analysis. – Cengage Learing EMEA, London.
[30] Hair, J. F., Risher, J. J., Sarstedt, M., Ringle, C. M. (2019): When to use and how to report the results of PLS-SEM. – European Business Review 31: 2-24.
[31] Han, H., Hsu, L-T. J., Sheu, C. (2010): Application of the theory of planned behavior to green hotel choice: testing the effect of environmental friendly activities. – Tourism Management 31: 325-334.
[32] Henseler, J., Ringle, C. M. R., Sinkovics, R. R. (2009): The Use of Partial Least Squares Path Modeling in International Marketing. – In: Sinkovics, R. R., Ghauri, P. N. (eds.) New Challenges to International Marketing. Emerald Group Publishing Limited, Binley.
[33] Henseler, J., Ringle, C. M., Sarstedt, M. (2015): A new criterion for assessing discriminant validity in variance-based structural equation modeling. – Journal of the Academy of Marketing Science 43: 115-135.
[34] Hulland, J. (1999): Use of partial least squares (PLS) in strategic management research: a review of four recent studies. – Strategic Management Journal 20: 195-204.
[35] Issa, I., and Hamm, U. (2017): Adoption of organic farming as an opportunity for Syrian farmers of fresh fruit and vegetables: an application of the theory of planned behaviour and structural equation modelling. – Sustainability 9: 2024.
[36] Khatri-Chhetri, A., Aggarwal, P. K., Joshi, P. K., Vyas, S. (2017): Farmers' prioritization of Climate-Smart Agriculture (CSA) technologies. – Agricultural Systems 151: 184-191.
[37] Kim, Y. G., Jang, S. Y., Kim, A. K. J. (2014): Application of the theory of planned behavior to genetically modified foods: moderating effects of food technology neophobia. – Food Research International 62: 947-954.
[38] Lalani, B., Dorward, P., Holloway, G., Wauters, E. (2016): Smallholder farmers' motivations for using conservation agriculture and the roles of yield, labour and soil fertility in decision making. – Agricultural Systems 146: 80-90.
[39] Lalani, B., Dorward, P., Holloway, G. (2017): Farm-level economic analysis. Is conservation agriculture helping the poor? – Ecological Economics 141: 144-153.
[40] Lee, S., Nguyen, T. T., Poppenborg, P., Shin, H.-J., Koellner, T. (2016): Conventional, partially converted and environmentally friendly farming in South Korea: profitability and factors affecting farmers' choice. – Sustainability 8: 704.
[41] Liao, Y., and Xu, K. (2019): Traceability system of agricultural product based on block-chain and application in tea quality safety management. – Paper presented at the Journal of Physics: Conference Series 1288, the 5th Annual International Conference on Network and Information Systems for Computers (ICNISC2019), Wuhan, China.
[42] Luhmann, H., Theuvsen, L. (2016): Corporate social responsibility in agribusiness: literature review and future research directions. – Journal of Agricultural & Environmental Ethics 29: 673-696.

http://www.aloki.hu ● ISSN 1589 1623 (Print) ● ISSN 1785 0037 (Online)
DOI: http://dx.doi.org/10.15666/aeer/2001_363381

[43] Madden, T. J., Ellen, P. S., Ajzen, I. (1992): A comparison of the theory of planned behavior and the theory of reasoned action. – Personality and Social Psychology Bulletin 18: 3-9.
[44] Mahindarathne, P., Gunaratne, L. (2015): Entrepreneurial orientation of organic farmers: a case of organic vegetable farmers in the Badulla district of Sri Lanka. – Journal of International Food & Agribusiness Marketing 27: 324-336.
[45] Makate, C., Makate, M., Mango, N., Siziba, S. (2019): Increasing resilience of smallholder farmers to climate change through multiple adoption of proven climate-smart agriculture innovations. Lessons from Southern Africa. – Journal of Environmental Management 231: 858-868.
[46] Matthews, L. M., Sarstedt, M., Hair, J. F., Ringle, C. M. (2016): Identifying and treating unobserved heterogeneity with FIMIX-PLS. – European Business Review 28: 208-224.
[47] McFadden, J. R., Huffman, W. E. (2017): Consumer valuation of information about food safety achieved using biotechnology: evidence from new potato products. – Food Policy 69: 82-96.
[48] Mittenzwei, K., Persson, T., Höglind, M., Kværnø, S. (2017): Combined effects of climate change and policy uncertainty on the agricultural sector in Norway. – Agricultural Systems 153: 118-126.
[49] Nguyen, A. T., Trinh, Q.-A., Pham, V. T., Le, B. B., Nguyen, D. T., Hoang, Q. N., Pham, H. T., Luu, V. N., Hens, L. (2019): Farmers' intention to climate change adaptation in agriculture in the red river delta biosphere reserve (Vietnam): a combination of Structural Equation Modeling (SEM) and Protection Motivation Theory (PMT). – Sustainability 11: 2993.
[50] Nkala, P., Mango, N., Zikhali, P. (2011): Conservation agriculture and livelihoods of smallholder farmers in Central Mozambique. – Journal of Sustainable Agriculture 35: 757-779.
[51] Osmond, D. L., Hoag, D. L., Luloff, A. E., Meals, D. W., Neas, K. (2015): Farmers' use of nutrient management: lessons from watershed case studies. – Journal of Environmental Quality 44: 382-390.
[52] Pannell, D. J., Llewellyn, R. S., Corbeels, M. (2014): The farm-level economics of conservation agriculture for resource-poor farmers. – Agriculture, Ecosystems & Environment 187: 52-64.
[53] Pretty, J. (2008): Agricultural sustainability: concepts, principles and evidence. – Philosophical Transactions of the Royal Society B: Biological Sciences 363: 447-465.
[54] Rahman, S. (2018): Environment-smart agriculture and mapping of interactions among environmental factors at the farm level: a directed graph approach. – Sustainability 10: 1-17.
[55] Rasoolimanesh, S. M., Ringle, C. M., Jaafar, M., Ramayah, T. (2017): Urban vs. rural destinations: residents' perceptions, community participation and support for tourism development. – Tourism Management 60: 147-158.
[56] Rigdon, E. E., Ringle, C. M., Sarstedt, M., Gudergan, S. P. (2011): Assessing Heterogeneity in Customer Satisfaction Studies: Across Industry Similarities and within Industry Differences. – In: Sarstedt, M., Schwaiger, M., Taylor, C. R. (eds.) Measurement and Research Methods in International Marketing. Emerald Group Publishing Limited, Bingley.
[57] Sarstedt, M., Ringle, C. M. (2010): Treating unobserved heterogeneity in PLS path modeling: a comparison of FIMIX-PLS with different data analysis strategies. – Journal of Applied Statistics 37: 1299-1318.
[58] Sarstedt, M., Becker, J.-M., Ringle, C. M., Schwaiger, M. (2011): Uncovering and treating unobserved heterogeneity with FIMIX-PLS: which model selection criterion provides an appropriate number of segments? – Schmalenbach Business Review 63: 34-62.

http://www.aloki.hu ● ISSN 1589 1623 (Print) ● ISSN 1785 0037 (Online)
DOI: http://dx.doi.org/10.15666/aeer/2001_363381

[59] Sarstedt, M., Ringle, C. M., Hair, J. F. (2017): Treating Unobserved Heterogeneity in PLS-SEM: A Multi-Method Approach. – In: Latan, H., Noonan, R. (eds.) Partial Least Squares Path Modeling. Springer International Publishing AG, Cham.
[60] Senger, I., Borges, J. A. R., Machado, J. A. D. (2017a): Using structural equation modeling to identify the psychological factors influencing dairy farmers' intention to diversify agricultural production. – Livestock Science 203: 97-105.
[61] Senger, I., Borges, J. A. R., Machado, J. A. D. (2017b): Using the theory of planned behavior to understand the intention of small farmers in diversifying their agricultural production. – Journal of Rural Studies 49: 32-40.
[62] Thornton, P. K., et al. (2018): A framework for priority-setting in climate smart agriculture research. – Agricultural Systems 167: 161-175.
[63] Valeeva, N. I., Meuwissen, M. P. M., Huirne, R. B. M. (2004): Economics of food safety in chains: a review of general principles. – NJAS-Wageningen Journal of Life Sciences 51: 369-390.
[64] Wall, P. C., Thierfelder, C., Ngwira, A., Govaerts, B., Nyagumbo, I., Baudron, F. (2013): Conservation agriculture in Eastern and Southern Africa. – In: Jat, R. A., Sahrawat, K. L., Kassam, A. H. (eds.) Conservation Agriculture Global Prospectives and Challenges. CAB International, Oxfordshire.
[65] Westermann, O., Förch, W., Thornton, P., Körner, J., Cramer, L., Campbell, B. (2018): Scaling up agricultural interventions: case studies of climate-smart agriculture. – Agricultural Systems 165: 283-293.
[66] Wold, H. (1975): Path Models with Latent Variables: The NIPALS Approach. – In: Blalock, H. M., Aganbegian, A., Borodkin, F. M., Boudon, R., Capecchi, V. (eds.) Quantitative Sociology. Academic Press Inc, New York.
[67] Wu, M.-Y., and Ke, C.-K. (2020): Development and application of intelligent agricultural planting technology. The case of tea. – Paper presented at the 2020 International Symposium on Computer, Consumer and Control (IS3C), IEEE, Taiwan.
[68] Zeweld, W., Van Huylenbroeck, G., Tesfay, G., Speelman, S. (2017): Smallholder farmers' behavioural intentions towards sustainable agricultural practices. – Journal of Environmental Management 187: 71-81.

http://www.aloki.hu ● ISSN 1589 1623 (Print) ● ISSN 1785 0037 (Online)
DOI: http://dx.doi.org/10.15666/aeer/2001_363381

ONION MEAL AND ONION EXTRACTS (*Allium cepa* L.) AS NATURAL GROWTH PROMOTERS FOR USE IN POULTRY PRODUCTION: A REVIEW

MALEMATJA, E. – NG'AMBI, J. W. – CHITURA, T.* – NEMAULUMA, M. F. D. – KOLOBE, S. D. – MANYELO, T. G.

Department of Agricultural Economics and Animal Production, University of Limpopo, Private Bag X1106, Sovenga 0727, South Africa

**Corresponding author*
e-mail: teedzai.chitura@ul.ac.za

(Received 5th Aug 2021; accepted 1st Oct 2021)

Abstract. The objective of this paper is to present a comprehensive understanding of the potential use of onion extracts (*Allium cepa* L.) as growth promoters in poultry production. The threat of antibiotic residues in poultry meat products to the human population, prohibit the use of antibiotics as feed additives and calls for the need to explore alternatives to synthetic growth promoters. Some attempt has been made to improve poultry performance and health condition through feeding the animal root tubers such as garlic, onions, and ginger. Root tubers contain various phytochemical compounds, flavonoids, and phenolic acids with confirmed anti-inflammatory, antibacterial, antioxidant, and growth promoting properties. Bioactive compounds in root tubers influence animal growth performance through enhanced digestibility and by altering gut health. The use of these tubers and their extracts has been shown to have non-toxic and non-pathogenic effects on birds; hence these tubers could be an alternative to antibiotics. Therefore, the onion bulb shows a tremendous potential as a natural growth promoter and a phytogenic natural feed additive alternative to synthetic growth promoters.
Keywords: *antibiotics, growth performance, carcass quality, gut morphology, bioactive compounds, root tubers*

Introduction

High feed costs which are partially attributable to the price fluctuations of feed ingredients present a major challenge to successful poultry production. This often results in the use of feed ingredients and feed additives that are cheap and of low quality in an effort to improve nutrient exploitation by the bird (Mammo, 2012; Mulugeta et al., 2019). Adding feed additives (synthetic or organic) to poultry diets maximizes nutrient exploitation by the bird thereby improving growth performance and feed conversion efficiency (Mulugeta et al., 2019). Synthetic additives have been used in poultry production for several decades and their over-usage resulted in the emergence of drug-resistant microorganisms in both poultry production and in the human population (Casewell et al., 2003; Yadav et al., 2016). Researchers are currently challenged with finding alternative ways of synchronizing the growth performance in poultry production to substitute synthetic drugs using organic growth promoters while minimizing the cost of production as well as adverse effects on human health (Iji et al., 2001; Khaidem et al., 2019). Medicinal plants or herbal extracts almost meet the nutrients required by the animals and contain unique organic phytochemicals that are believed to promote optimum health in birds (Yousuf et al., 2013). Several studies have reported positive effects of onion extracts on poultry production in terms of feed efficiency and weight gain (Guo et al., 2000; Demir et al., 2003; Ahmad et al., 2008; Mulugeta et al., 2019). These observations press a high demand for natural growth promoters as feed ingredients in the

http://www.aloki.hu ● ISSN 1589 1623 (Print) ● ISSN1785 0037 (Online)
DOI: http://dx.doi.org/10.15666/aeer/2001_383396

future. Therefore, this review aimed to provide a comprehensive understanding of the potential use of onion extracts as alternative natural growth promoters in poultry production.

Source of data

The data used in this review was acquired from recent articles that were published in different journals. Databases were accessed using electronic data sources such as Research gate, Science direct, and Google scholar. In addition, the citations included in articles from the databases were used to search for other relevant articles. In the search process, the key words were "Onion meal', "Onion extracts", and "poultry".

Structure and growth requirements of the onion bulb

Allium cepa commonly known as an onion is a vegetable crop that belongs to the family *Liliaceae*. It originated from central Asia and is now being cultivated throughout the world, Asia and North America being the most producing continents (Ebesunum et al., 2007; Obasi et al., 2009; Iqbal and Bayram, 2019). Onion is a short duration horticultural crop, and its cultivars differ from biannual to perennial cultivar (Brewster, 2008). The onion crop has green tubular leaves and a bulb with shallow adventitious fibrous roots (Pareek et al., 2017). The crop goes through three growth stages, namely germination, bulb initiation, and flowering stages. It is planted by seeds or bulbs (Brewster, 2008). Although the crop is cultivated under various temperatures, it does not do well under extremely hot or cold conditions (Brewster, 2008). The onion crop is planted on the field for 4 – 6 months under rainfall or irrigated conditions, through seed or propagations (Bulb) (Abdissa et al., 2011). Onion bulbs produce a smell when crushed and the bulb is the commonly used portion of the plant (Liguori et al., 2017; Pareek et al., 2017). It can be used in the form of onion-extracts or powder (Pareek et al., 2017). The nutritive and energy value of onions depend on their origin, cultivars, harvesting stage as well as the period of storage (Pareek et al., 2017). Although onion bulbs appear in different colours, their taste is not influenced by the colour, but by the cultivar (Kandoliya et al., 2015).

Nutritional values and the chemical compositions of onion bulbs

Proximate analysis reveals that raw onion bulbs contain high moisture levels (89.11%), less fibre (1.7%), ash (0.35%), carbohydrates (0.35%), and very little proteins (1.1%), fats (0.1%), and energy content (40 kcal) (Pareek et al., 2017). Bhattacharjee et al. (2013) reported a low ash level (0.25%), protein content (1.49%) in the Indian and Bangladeshi varieties of onion respectively. The Ash content of the feed provides the level of mineral elements that are present in the feedstuff (Edeogu et al., 2007). Onion has a low-fat content (0.7%), as well as low dietary fibre (1.92%) and calories. However, it is a good source of minerals and vitamins (Kandoliya et al., 2015; Ogbonna et al., 2016). High moisture level makes the onion to be more prone to deterioration, however, it helps the animal body to use less of its fluid for digestion (Bhattacharjee et al., 2013). Dietary fibre in the onion bulb helps in the digestion and regulation of oxidants in feed ingredients (Bhattacharjee et al., 2013). Energy and aromatic amino acids are derived from sugars and carbohydrates contained in the onion bulb (Kandoliya et al., 2015). Carbohydrates

http://www.aloki.hu ● ISSN 1589 1623 (Print) ● ISSN1785 0037 (Online)
DOI: http://dx.doi.org/10.15666/aeer/2001_383396

are also suggested to be an alternative source of glucose (Bhattacharjee et al., 2013). Onion bulbs are regarded as a good source of antioxidants and phytonutrients (Kandoliya et al., 2015). Nutritional values and chemical compositions of onion bulbs are presented in *Table 1*.

Table 1. *Nutritional values and the chemical compositions of raw onion bulbs (in percentages)*

Nutrient	Composition	References
Proximate		
Moisture	89.11	Pareek et al. (2017)
Protein	1.1	Pareek et al. (2017)
	1.489	Bhattacharjee et al. (2013)
	1.27	Kandoliya et al. (2015)
Lipids	0.1	Pareek et al. (2017)
	0.17	Ogbonna et al. (2016)
Ash	0.248	Bhattacharjee et al. (2013)
	0.66	Ogbonna et al. (2016)
	0.35	Pareek et al. (2017)
Carbohydrates	0.35	Pareek et al. (2017)
	14.772	Bhattacharjee et al. (2013)
	6.91	Ogbonna et al. (2016)
Fiber	1.7	Pareek et al. (2017)
	1.659	Bhattacharjee et al. (2013)
	1.92	Ogbonna et al. (2016)
Energy	40	Pareek et al. (2017)

Bioactive compounds in onion bulbs

Phytochemicals are biologically active compounds produced by plants to prevent infections (in roots, stem, leaves, flowers, or seeds) and are known to be beneficial to human and animal health (Rao, 2003; Saxena et al., 2013). Phytochemicals are present in a wide range of vegetables, grains, root tubers, herbs, and spices (Moorachian, 2000; Saxena et al., 2013). Bioactive phytochemicals mainly come from medicinal plants and root tubers such as onions and garlic which are common sources of phytochemicals and their concentration levels vary among plant species and cultivars, the growing environment, and the applied method of processing (Edeoga et al., 2005; Saxena et al., 2013). Onion bulbs have been characterised to contain plethora bioactive compounds such as organosulfur compounds, polysaccharides, saponins, fructants, and phenolic compounds (Saxena et al., 2013). Organosulfur compounds are the main bioactive compounds in onion bulbs and sulfur-containing compounds such as cysteine sulfoxides, quercetin, quercetin glucosides, and allicin are the major organosulfur compounds in onion bulbs (Kothari et al., 2019; Zhao et al., 2021). Organosulfur compounds are associated with antioxidants and antimicrobial activities (Kothari et al., 2019). Antioxidant compounds include polyphenolic, flavonoids, carotenoids, tocopherols, and ascorbic acid. whereas antimicrobial compounds include terpenoids, alkaloids, and phenolic which exert their effects through the stimulation of the immune system to fight against infections (Saxena et al., 2013; Kothari et al., 2019). Saponins in onion bulbs have been validated to contain biological properties such antifungal as well as anti-inflammatory properties (Kothari et al., 2019). These compounds stimulate and improve growth performance and health condition of birds through appetizing and stimulation of

http://www.aloki.hu ● ISSN 1589 1623 (Print) ● ISSN1785 0037 (Online)
DOI: http://dx.doi.org/10.15666/aeer/2001_383396

the digestive system and immune response (Guo et al., 2000). Phytochemical compounds enhance growth through induced nutrient utilization by the animal (Noman et al., 2015). Other phytochemical compounds include non-starch polysaccharides (cellulose, hemicellulose, pectins, and lignins) which delay the process of nutrient absorption, bind toxins, and bile acids (Saxena et al., 2013).

Utilisation of onion meal or onion extracts in poultry production reared under stress free environment

Among domesticated animals, poultry convert feed more efficiently than other animals. The maintenance of high feed conversion is crucial for birds to grow faster and reach the market weight early (Diaz et al., 2019). Medicinal plants and other plant extracts have been used as digestion stimulants as well as growth promoters in livestock production (Frankic et al., 2009). Lampe (1999), Aji et al. (2011) and Goodarzi et al. (2013) reported a positive effect of onion meal dietary inclusion on the growth performance of chickens. Onion possesses phytochemical compounds such as antioxidant properties, antimicrobial effect, and anti-inflammatory properties and there is evidence indicating that onion bulbs could improve the growth performance of birds when mixed in their diets. Goodarzi et al. (2013) further stated that onion bulbs or their extracts exert an influence on growth performance in chickens. It has been reported that onion powder in livestock feed or onion extracts in drinking water have growth promoting as well as anti-pathogen activities (Goodarzi and Nanekarani, 2014). Aditya et al. (2017) reported that the inclusion of onion meal or onion extracts at appropriate levels could improve broiler performance and productivity. There is evidence indicating that onion meal inclusion in the diets of broiler chickens could improve feed intake due to the favourable taste of processed onions and this in turn can improve the bodyweight of the chickens (Aditya et al., 2017). Metabolism systems in poultry species are similar, therefore, the influence of onion extracts on performance is the same throughout the poultry species (Keohavong and Bounyavong, 2018). Aditya et al. (2017) reported that onion inclusion level of 5 or 7.5 g into broiler diets improved overall feed intake and body weight of broiler chickens with unaffected feed conversion ration over a four-week trial period, however, its positive effect seemed to disappear when the supplementation levels are too high. Onion extracts supplementation of up to 1% in drinking water could improve average daily feed without affecting feed conversion ratio of broiler chickens during the stater and grower period (Goodarzi and Nanekarani, 2014). According to Aji et al. (2011), supplementing 25 mg of onion per kg DM increased body weight gain while no effects were observed on daily feed and water intake, however, increasing onion supplementation level to 100 mg of onion per kg DM had increased feed and water intake, feed conversion ratio, and live weight of broiler chickens at 21 days. Al-Ramamneh (2018) observed that adding 2.5 kg/t or 2.5% in basal diet or drinking water improved live weights of broiler chickens, while no effect was observed on feed intake until the fourth and fifth week of age when the feed intake was reduced compared to control group. In another study, Al-Ramamneh et al. (2017) reported increased feed intake and daily weight gain in broiler chickens fed diets having 2.5, 5 or 7.5 kg of onion per ton DM. Ibrahiem et al. (2004) reported increased feed conversion ratio, live body weight, and bodyweight gain in Muscovy ducks fed diets with of 1% of onion meal. However, Keohavong and Bounyavong (2018) observed that supplementing onion at 1 or 2% level did not produce effects on the overall growth performance of Muscovy ducks aged 4-8 weeks. Goodarzi

http://www.aloki.hu ● ISSN 1589 1623 (Print) ● ISSN1785 0037 (Online)
DOI: http://dx.doi.org/10.15666/aeer/2001_383396

et al. (2013) reported that adding 10 or 30 g of fresh onion bulbs into basal diets reduced feed conversion ratio without affecting body weight in broiler chickens during the starter and grower period. However, supplementing 30 g of fresh onion bulb per kg DM increased daily feed intake throughout the experiment as well as body weight at 42 days (Goodarzi et al., 2013). Olusola et al. (2018) reported improved feed conversion ratio was well as an increased body weight gain and final body weight in broiler chickens fed diets with 30 or 100 g of onion kg per DM. Waleed et al. (2021) also observed an increased body weight in Japanese quail hens fed diets with 800 g of dried onion per kg DM. However, An et al. (2015) observed no effect in feed intake, feed conversion ratio and body weight in white mini broiler chickens supplemented with 0.3 or 0.5% of onion extracts in basal diets. Effects of dietary onion on poultry production are presented in *Table 2*.

Effect of onion meal or onion extracts on bird's immune responses

Allium species have been characterized to contain numerous bioactive compounds such as organosulfur compounds, saponins, fructans, and polyphenols with proven antibacterial, antiviral, and immunostimulatory (Hanieh et al., 2010; Kothari et al., 2019). Bioactive compounds have beneficial effects on the humoral immune responses in animals and onion bulbs or extracts have been validated to have plethora effect on the humoral immune response in chickens (Hanieh et al., 2010; Omar et al., 2020). Immune responses play an important role in protection against various disease (Korpraditskul et al., 2009). Goodarzi et al. (2013) observed that adding 10 or 30 g of fresh onion bulbs in basal diets did not influence antibody titers against Newcastle virus in broiler chickens aged 14 and 21 days. Similar findings were made by Waleed et al. (2021) who reported that supplementing that onion supplementation of 800g per kg did not enhance humoral immune responses in Japanese quail hens as compared to control group. Hanieh et al. (2010) observed improved immune response against Newcastle disease virus in white leghorn chickens fed diets with 10g of onion powder per kg. Moreover, Korpraditskul et al. (2009) and Iqbal and Bayram (2019), reported enhanced humoral immune response against Newcastle virus in broiler and babcock hens fed 2% of onion extracts or juice in drinking. Omar et al. (2020) also reported an increased in immune responses in broiler chickens fed diets containing 3 g of phenolic-rich onion extracts per kg DM. Effects of onion meal or onion extracts inclusion in poultry diets on immune responses under controlled environment (*Table 3*).

Effects of onion meal or onion extracts in poultry diets on meat quality and sensory evaluation

Visual appearance and the texture of meat are the major factors that attract consumers to buy meat (Yang and Jiang, 2005). Research on the potential of plant extracts as alternatives to antibiotic growth promoters is popular in the poultry production industry due to consumers' high demand for meat from animals raised with no antibiotics (Yang and Jiang, 2005). Onion meal inclusion in chicken diets has been shown to improve gut morphology and carcass quality of poultry meat (Ur Rahman et al., 2017; Al-Ramamneh, 2018). Al-Ramamneh (2018) reported an increased in carcass weight with heavier meat organ part in broiler chickens fed basal diets with 2.5 kg/ton DM or 2.5% in drinking water.

http://www.aloki.hu ● ISSN 1589 1623 (Print) ● ISSN1785 0037 (Online)
DOI: http://dx.doi.org/10.15666/aeer/2001_383396

Table 2. *Effects of dietary onion on poultry growth performance*

Inclusion level	Diet formulation	Poultry species	Conclusion	Authors
5 or 7.5g/kg DM	Onion extracts in basal diet	Broiler chickens	Improved overall feed intake (2.457-2.478g/bird). No effects were observed on the feed conversion ratio over a four week trial period.	Aditya et al. (2017)
1.5, 2 or 2.5g /kg DM	Onion extracts in basal diet.	Broiler chickens	Improved body weight gain.	ur Rahman et al. (2017)
25 mg/kg DM	Onion powder in basal diet	Broiler chickens	No effects were observed on feed and water intake	Aji et al. (2011)
100 mg/kg DM	Onion powder in basal diet	Broiler chickens	Increased feed intake (1290g/bird/21 days) and water intake (2.88L/bird/21days) as well as feed conversion ratio and live weights of broiler chickens aged 21 days (2.57kg/bird).	Aji et al. (2011)
1%	Onion extracts in drinking water	Broiler chickens	Increased average daily feed intake with no change in feed conversion ratio during the starter and grower diet phases while feed conversion ratio was reduced during the finisher diet phase.	Goodarzi & Nanekarani, (2014)
1%	Onion meal in basal diet.	Muscovy ducks	Increased feed conversion ratio, live body weight, and bodyweight gain in Muscovy ducks.	Ibrahiem et al. (2004)
1or 2%	Onion extracts in basal diet.	Muscovy ducks	Did not affect the overall growth performance of Muscovy ducks aged 4-8 weeks.	Keohavong & Bounyavong, (2018)
25 or100 mg/kg	Onion powder in basal diet.	Broiler chickens	Increased body weight gains during the grower phase.	Aji et al. (2011)
10 or 30g/kg	Fresh onion bulbs in basal diet.	Broiler chickens	Did not affect body weight of broiler chickens aged 1 to 21 days. However, adding onion bulb into broiler diets reduced feed conversion ratio (1.51).	Goodarzi et al. (2013)
30g/kg	Fresh onion bulb in basal diet.	Broiler chickens	Increased daily feed (83g) throughout the experiment as well as body weight at 42 days.	Goodarzi et al. (2013)
2.5kg/t or 2.5%	Onion bulb in basal diets or onion extracts in drinking water.	Broiler chickens	Improved live weights (2177.1g/bird) while no effect was observed on feed intake until the fourth and fifth week of age when the feed intake was reduced (650.5 and 844.6g) compared to control group.	Al-Ramamneh, (2018)
30 or 100g /kg	Onion skin extracts or meal in basal diet.	Broiler chickens	Better feed conversion ratio and higher final body weight and weight gain.	Olusola et al. (2018)

http://www.aloki.hu ● ISSN 1589 1623 (Print) ● ISSN1785 0037 (Online)
DOI: http://dx.doi.org/10.15666/aeer/2001_383396

Inclusion level	Diet formulation	Poultry species	Conclusion	Authors
5 or 7.5 g/kg DM	Onion extracts in basal diet.	Broiler chickens	Improved body weight (1.694-1.727g/bird) however, its positive effect seemed to disappear when the supplementation levels are too high.	Aditya et al. (2017)
2.5, 5 or 7.5kg/ton	Onion extracts in basal diet.	Broiler chickens	Increased feed intake and daily weight gain.	Al-Ramamneh et al. (2017)
800g/kg	Dried onion with basal diet	Japanese quail hens	Supplementation of onion increased body weight compared to the control group.	Waleed et al. (2021)
0.3 or 0.5 %	Onion extract mixed with basal diet	White mini broilers	Similar body weight, no improvements feed intake, and feed efficiency were observed.	An et al. (2015)

Table 3. *Effects of onion meal or onion extracts inclusion in poultry diets on immune responses*

Inclusion level	Diet Formulation	Poultry species	Conclusion	Authors
10 or 30g/kg	Dietary treatments consisted of basal diet and fresh onion bulb	Broiler chickens	Did not influence antibody titers against Newcastle Disease Virus at 14 and 21 days of age	Goodarzi et al. (2013)
10g/kg	Onion powder in basal diets	White Leghorn chickens	Exerted enhancing effect on the humoral immune responses against Newcastle Disease Virus.	Hanieh et al. (2010)
2%	Onion tree extracts in drinking water	Arbor Acres Broiler chickens	Stimulated the humoral immune response against Newcastle Disease Virus.	Korpraditskul et al. (2009)
2%	Onion juice in drinking water	Babcock hens	Improved immune response against the Newcastle virus.	Iqbal & Bayram (2019
800g/kg	Dried onion with basal diet.	Japanese quail hens	Onion supplementation did not exert effect on humoral immune response.	Waleed et al. (2021)
3g/kg	Phenolic-rich onion extracts in basal diet	Broiler chickens	Significantly improved the immune response of birds.	Omar et al. (2020)

However, several studies reported no effect of onion extracts in basal diets or drinking water on carcass weight of chickens and Muscovy ducks (Aji et al., 2011; Goodarzi and Nanekarani, 2014; Keohavong and Bounyavong, 2018; Omar et al., 2020). An et al. (2015) observed no effects on meat pH and meat color of the breast meat among groups of white mini broiler chickens fed diets with 0.3 or 0.5% of onion extracts per kg DM, however, onion supplementation increased meat-shear force compared to the control group. Aditya et al. (2017) reported affected meat color lightness with the lower values from chickens fed 7.5 g of onion extracts per kg DM and red color of chickens fed onion extracts was lower throughout the treatment period. Keohavong and Bounyavong (2018)

http://www.aloki.hu ● ISSN 1589 1623 (Print) ● ISSN1785 0037 (Online)
DOI: http://dx.doi.org/10.15666/aeer/2001_383396

observed an improved breast meat of Muscovy ducks, in terms of cooking loss. Effect of onion meal or extracts inclusion on carcass characteristics and meat quality of broiler chicken (*Table 4*).

Table 4. *Effects of onion meal or onion extracts inclusion in poultry diets on meat quality*

Inclusion level	Diet Formulation	Poultry species	Conclusion	Authors
2.5kg/t or 2.5%	Onion bulb in basal diets or onion extracts in drinking water.	Broiler chickens	Increased carcass weight (1619.3g) with heavier breast-meat (577.8g), thigh (510.1g), wings (180.4), back (223.8g), and neck (96g) as compared to the control group.	Al-Ramamneh (2018)
25, 50 or 100 mg/kg DM	Onion powder in basal diet	Broiler chickens	No effects were observed on carcass yield of broiler chickens.	Aji et al. (2011)
0.3 or 0.5 %	Onion extracts in basal diet.	White mini broilers	No effects were observed on pH and meat color of the breast meat among groups, however, meat-shear force was increased (2.89-2.94) compared to the control group.	An et al. (2015)
1, 2 or 3 g/kg	Phenolic-rich onion extracts in basal diet.	Broiler chickens	Carcass weights were not affected by dietary onion extracts levels.	Omar et al. (2020)
5, 7.5 or 10g/kg DM	Onion extracts in basal diet.	Broiler chickens	Affected the meat color lightness with the lower values in the medium onion extracts group (49.50). The red color of chickens fed onion extracts was lower throughout the treatment period (0.95, 1.73, and 0.98).	Aditya et al. (2017)
1 or 2%	Basal diet with onion extracts	Muscovy ducks	Did not affect carcass yield and dressing percentage of Muscovy ducks	Keohavong & Bounyavong (2018)
1or 2%	Onion extracts in drinking water	Broiler chickens	Did not affect carcass yield.	Goodarzi & Nanekarani (2014)
5 kg/ton	Onion extracts in basal diet.	Broiler chickens	Increased the weight of edible parts such as breast-meat, thigh and wings, and other inedible parts such as the crop.	Al-Ramamneh et al. (2017)
2%	Basal diet with onion extracts	Muscovy ducks	Improved breast meat, in terms of cooking loss	Keohavong & Bounyavong (2018)

Effect of onion meal or extracts on gut morphology of poultry species

The structure and functionality of the gut microorganism are vital for the well-being of the bird through influences on nutrient digestion and intestinal integrity (Diaz et al., 2019). The onion bulb contains some compounds that prevent the accumulation of harmful bacterial in the gastrointestinal tract of the bird (Goodarzi and Nanekarani, 2014). Phytochemical compounds in onion change the gut microflora and the gut immune system and promote the proliferation of colonic and mucosal microflora which serve as a wall to prevent the access of bacteria to the gastrointestinal tract (Slavin, 2013). Fructans in onion

http://www.aloki.hu ● ISSN 1589 1623 (Print) ● ISSN1785 0037 (Online)
DOI: http://dx.doi.org/10.15666/aeer/2001_383396

bulb enhance gastrointestinal health through balancing the proportion between beneficial microbial and harmful microbial (Ogbonna et al., 2016). This could lead to efficient feed utilization, resulting in improved health conditions and performance (Bedford, 2000). Al-Ramamneh et al. (2017) reported no effects of onion meal supplementation level of 2.5, 5 or 7.5 kg per ton DM on the weight of the internal organs, including the digestive tract of broiler chickens, however, onion meal supplementation in diets had improved small intestinal lengths. Goodarzi and Nanekarani (2014) observed no effect on relative internal organ weight and affected abdominal fat in broiler chickens fed basal diets supplemented with 1 or 2% onion extracts in drinking water. However, Omar et al. (2020) reported no effect on abdominal fat weights and relative weight of liver, heart, and spleen in broiler chickens fed diets with 5, 7.5 or10 g of onion per kg DM. Adding 2.5 g of onion meal into broiler diets had increased the dimension, crypt depth, and the surface area of the duodenum, jejunum, and ileum of broiler chickens (Ur Rahman et al., 2017). Supplementing 2.5 kg per ton or 2.5% of onion into broiler diets increased liver weight, however, the abdominal fat and heart weight were negatively affected as compared to the control (Al-Ramamneh, 2018). Effect of onion meal or extracts inclusion on gut morphology of poultry species (*Table 5*).

Table 5. *Effect of onion meal or extracts on gut morphology of poultry species*

Inclusion level	Diet Formulation	Poultry species	Conclusion	Authors
2.5, 5 or 7.5kg/ton	Onion extracts in basal diet.	Broiler chickens	No effects were observed on the weight of the internal organs, including the digestive tract, however, small intestinal lengths were improved.	Al-Ramamneh et al. (2017)
1or 2% in drinking water	Onion extracts in drinking water	Broiler chickens	Did not affect relative organ weight, however, abdominal fat (2.15 and 1.95 %) was affected by onion supplementations.	Goodarzi & Nanekarani (2014)
2.5g/kg DM	Onion extracts in basal diet.	Broiler chickens	Increased the dimension, crypt depth, and the surface area of the duodenum, jejunum, and ileum of Ross 308 broiler chickens.	ur Rahman et al. (2017)
5, 7.5 or10 g/kg DM	Phenolic-rich onion extracts in basal diet	Broiler chickens	Abdominal fat weights and relative weight of liver, heart, and spleen were not affected by dietary onion extracts levels.	Omar et al. (2020)
1.5, 2, or 2.5g/kg DM	Onion extracts in basal diet.	Broiler chickens	It has been shown to have a positive effect on gut morphology.	ur Rahman et al. (2017)
2.5kg/t or 2.5%		Broiler chickens	Increased liver weight (55.7g). However, the abdominal fat (42.6) and heart weight (11.3g) were negatively affected as compared to the control group.	Al-Ramamneh, (2018)

http://www.aloki.hu ● ISSN 1589 1623 (Print) ● ISSN1785 0037 (Online)
DOI: http://dx.doi.org/10.15666/aeer/2001_383396

Effects of onion meal or onion extracts inclusion in poultry diets on egg quality of laying hens reared under stress free environment

Iqbal and Bayram (2019) reported that onion juice supplementation from 0.25 to 2% in drinking water did not improve egg weight as well as egg shell weight during 30 days storage at 4^0C. However, increasing onion juice supplementation level up to 2% had resulted in an increased egg production, while 0.5% onion juice in drinking water showed a remarkable improvement in egg weight whereas 0.25% of onion juice supplementation had negatively affected egg weight in babcock hens. Damaziak et al. (2017) observed improved egg weights from laying hens fed diets with 0.0032% of onion powder in diets, however, onion powder supplementation delayed laying process. Onion supplementation of 800 g per kg in basal diets did not produce effects on egg production rate as well as egg weight in Japanese quail hens (Waleed et al., 2021). Effects of onion meal or onion extracts inclusion in poultry diets on egg quality of laying hens (*Table 6*).

Table 6. *Effects of onion meal or onion extracts inclusion in poultry diets on egg quality of laying hens under controlled environment*

Inclusion level	Diet Formulation	Poultry species	Conclusion	Authors
0.25, 0.5,1or 2%	Onion juice in drinking water	Babcock hens	Adding onion juice in water had no effect on egg weight and shell weight throughout a 30 days storage at 4 ^{0}C.	Iqbal & Bayram (2019)
0.5%	Onion juice in drinking water	Babcock hens	Significantly increased egg weights (58.6g) as compared to other levels and control group.	Iqbal & Bayram (2019
0.25%	Onion juice in drinking water	Babcock hens	Egg weight was negatively affected (48.1g) by onion juice in drinking water.	Iqbal & Bayram (2019
2%	Onion juice in drinking water	Babcock hens	Egg production was increased by onion supplementation	Iqbal & Bayram (2019
0.0032%	Onion powder with basal diet	Laying hens	Onion meal inclusion in the diets improved egg weight (56g) as compared to control group. However, egg production was delayed.	Damaziak et al. (2017)
800g/kg	Dried onion powder with basal diet	Japanese quail hens	Onion supplementation did not affect laying rate as well the egg weight as compared to the control group.	Waleed et al. (2021)

Conclusions and recommendations

Due to the emergence of drug-resistant microorganisms as well as the threat of drug residues in poultry meat and meat products, attempts are being made to find alternative means to substitute synthetic growth promoters. Therefore, onions show significant potential to be used in poultry diets as natural growth promoters as well as possible

http://www.aloki.hu ● ISSN 1589 1623 (Print) ● ISSN1785 0037 (Online)
DOI: http://dx.doi.org/10.15666/aeer/2001_383396

alternative means of preventing infectious diseases through the enhanced immune response of birds. There is evidence that onion bulbs can be used as natural growth promoters to improve the growth performance and productivity of chickens. Onions contain various biological chemical compounds, flavonoids, and phenolic acids with verified antibacterial, antioxidant, and anti-inflammatory properties. Therefore, onions could be used as alternative and sustainable growth promoters in poultry feeds considering their inherent high nutritional values and high biosafety levels. Most researchers revealed that onion meal or extracts supplementation in basal diets improved growth performance in birds. However, more studies are recommended to establish the appropriate onion dosage or inclusion level, age of application and conditions under which onion meal or extracts can be applied.

Acknowledgements. Authors would like to acknowledge University of Limpopo, Department of Agricultural Economics and Animal Production for resources made available to conduct this paper.

REFERENCES

[1] Abdissa, Y., Tekalign, T., Pant, L. M. (2011): Growth, bulb yield and quality of onion (*Allium cepa* L.) as influenced by nitrogen and phosphorus fertilization on vertisol I. growth attributes, biomass production and bulb yield. – African Journal of Agricultural Research 6(14): 3252-3258.

[2] Aditya, S., Ahammed, M., Jang, S. H., Ohh, S. J. (2017): Effects of dietary onion (*Allium cepa*) extract supplementation on performance, apparent total tract retention of nutrients, blood profile, and meat quality of broiler chicks. – Asian-Australasian Journal of Animal Sciences 30(2): 229.

[3] Ahmad, T., Ansari, J. Z., Haq, A., Yousaf, M., Khan, S. (2008): Evaluation of different medicinal plants as growth promoters for broiler chicks. – Sarhad Journal of Agriculture 24(2): 323-329.

[4] Aji, S., Ignatius, K., Ado, A. Y., Nuhu, J. B., Abdulkarim, A., Aliyu, U., Numa, P. (2011): Effects of feeding onion (*Allium cepa*) and garlic (*Allium sativum*) on some performance characteristics of broiler chickens. – Research Journal of Poultry Sciences 4(2): 22-27.

[5] Al-Ramamneh, D., Almassed, M., Hussein, N. (2017): Effect of using onion as anticoccidial agent on broiler physiology and production. – Bulletin of Environment, Pharmacology, and Life Science 6: 87-92.

[6] Al-Ramamneh, D. (2018): Reduce Heat Stress in Broiler by Adding Onion. – Russian Agricultural Sciences 44(1): 92-96.

[7] An, B. K., Kim, J. Y., Oh, S. T., Kang, C. W., Cho, S., Kim, S. K. (2015): Effects of onion extracts on growth performance, carcass characteristics, and blood profiles of white mini broilers. – Asian-Australasian Journal of Animal Sciences 28(2): 247.

[8] Bedford, M. (2000): Removal of antibiotic growth promoters from poultry diets: implications and strategies to minimize subsequent problems. – World Poultry Science 56(4): 347-365.

[9] Bhattacharjee, S., Sultana, A., Sazzad, M. H., Islam, M. A., Ahtashom, M., Asaduzzaman, M. (2013): Analysis of the proximate composition and energy values of two varieties of onion (*Allium cepa* L.) bulbs of different origin: A comparative study. – International Journal of Nutrition and Food Sciences 2(5): 246-253.

[10] Brewster, J. L. (2008): Onions and Other Vegetable Alliums. – Wallingford, UK. -CAB international 15.

http://www.aloki.hu ● ISSN 1589 1623 (Print) ● ISSN1785 0037 (Online)
DOI: http://dx.doi.org/10.15666/aeer/2001_383396

[11] Casewell, M., Friis, C., Marco, E., McMullin, P., Phillips, I. (2003): The European ban on growth-promoting antibiotics and emerging consequences for human and animal health. – Journal of Antimicrobial Chemotherapy 52(2): 159-161.
[12] Damaziak, K., Riedel, J., Gozdowski, D., Niemiec, J., Siennicka, A., Róg, D. (2017): Productive performance and egg quality of laying hens fed diets supplemented with garlic and onion extracts. – Journal of Applied Poultry Research 26(3): 337-349.
[13] Demir, E., Sarica, Ş., Özcan, M. A., Sui Mez, M. (2003): The use of natural feed additives as alternatives for an antibiotic growth promoter in broiler diets. – British Poultry Science 44(1): 44-45.
[14] Diaz Carrasco, J. M., Casanova, N. A., Fernández Miyakawa, M. E. (2019): Microbiota, Gut Health, and Chicken Productivity; What Is the Connection? – Microorganisms 7(10): 374.
[15] Ebesunun, M. O., Popoola, O. O., Agbedana, E. O., Olisekodiaka, J. M., Onuegbu, J. A., Onyeagala, A. A. (2007): The effect of garlic on plasma lipids and lipoproteins in rats fed on high cholesterol-enriched diet. – Biochemistry 19(2): 53-58.
[16] Edeoga, H. O., Okwu, D. E., Mbaebie, B. O. (2005): Phytochemical constituents of some Nigerian medicinal plants. – African Journal of Biotechnology 4(7): 685-688.
[17] Edeogu, C. O., Ezeonu, F. C., Okaka, A. N. C., Ekuma, C. E., EIom, S. O. (2007): Proximate compositions of staple food crops in Ebonyi state, South Eastern Nigeria. – International Journal of Biotechnology & Biochemistry 3(1): 57-68.
[18] Frankic, T., Voljc, M., Salobir, J., Rezar, V. (2009): Use of herbs and spices and their extracts in animal nutrition. – Acta Agriculturae Slovenica 94: 95-102.
[19] Goodarzi, M., Nanekarani, S., Landy, N. (2013): Effect of dietary supplementation with onion (*Allium cepa* L.) on performance, carcass traits, and intestinal microflora composition in broiler chickens. – Asian Pacific Journal of Tropical Disease 4(1): 297-301.
[20] Goodarzi, M., Nanekarani, S. (2014): Effect of onion extract in drink water on performance and carcass traits in broiler chickens. – IERI Procedia 8: 107-112.
[21] Guo, F. C., Kwakkel, R. P., Verstegen, M. W. A. (2000): The use of Chinese herbs as alternative for growth promoters in broiler diets. – In: Proceedings of the 21st World's Poultry Congress (WPSA), Montreal, Canada.
[22] Hanieh, H., Narabara, K., Piao, M., Gerile, C., Abe, A., Kondo, Y. (2010): Modulatory effects of two levels of dietary Alliums on immune response and certain immunological variables, following immunization, in White Leghorn chickens. – Animal Science Journal 81(6): 673-680.
[23] Ibrahiem, A. I., Talib, A. E., Fathi, F. M. (2004): Effect of onion and/or garlic as feed additives on growth performance and immunity in broiler Muscovy ducks. – First Scientific Conference of Faculty of Veterinary Medicine, Benhar, pp. 236-247.
[24] Iji, P. A., Saki, A., Tivey, D. R. (2001): Body and intestinal growth of broiler chicks on a commercial starter diet. 1. Intestinal weight and mucosal development. – British Poultry Science 42(4): 505-513.
[25] Iqbal, A., Bayram, I. (2019): A Review-Use of onion juice and their product in animal nutrition and recent research of onion juice on laying hens. – The Journal of Animal and Plant Sciences 31(2): 377-385.
[26] Kandoliya, U. K., Bodar, N. P., Bajaniya, V. K., Bhadja, N. V., Golakiya, B. A. (2015): Determination of nutritional value and antioxidant from bulbs of different onion (Allium cepa) variety: A comparative study. – International Journal of Current Microbiology and Applied Sciences 4(1): 635-641.
[27] Keohavong, B., Bounyavong, S. (2018): Effects of Onion (*Allium cepa* L.) Extract on Growth Performance and Carcass Characteristics of Muscovy duck. – Department of Animal Science, Souphanouvong Journal University, Laos.
[28] Khaidem, A., Zuyie, R., Haque, N., Vidyarthi, V. K. (2019): Effect of garlic supplementation on performance, carcass traits, and blood profile of broiler chicken. – International Journal of Bio-resource and Stress Management 10(3): 292-297.

http://www.aloki.hu ● ISSN 1589 1623 (Print) ● ISSN1785 0037 (Online)
DOI: http://dx.doi.org/10.15666/aeer/2001_383396

[29] Korpraditskul, V., Kasornpikul, C., Chalorsantisakul, S. (2009): Effect of tree onion extracts as prebiotics on newcastle disease vaccine titer in broiler. – Journal of ISSAAS [International Society for Southeast Asian Agricultural Sciences] (Philippines).
[30] Kothari, D., Lee, W. D., Niu, K. M., Kim, S. K. (2019): The genus Allium as poultry feed additive: A review. – Animals 9(12): 1032.
[31] Lampe, J. W. (1999): Health effects of vegetables and fruits: Assessing mechanisms of action in human experimental studies. – American Journal of Clinical Nutrition 70(3): 475-490.
[32] Liguori, L., Califano, R., Albanese, D., Raimo, F., Crescitelli, A., Di Matteo, M. (2017): Chemical composition and antioxidant properties of five white onions (*Allium cepa* L.) landraces. – Journal of Food Quality, Article ID: 6873651.
[33] Mammo, M. (2012): The issue of feed-food competition and chicken production for the demands of foods of animal origin. – Asian Journal of Poultry Science 6(3): 31-43.
[34] Moorachian, M. E. (2000): Phytochemicals: Why and how. – Tastings 7: 4-5.
[35] Mulugeta, M., Worku, Z., Seid, A., Debela, L. (2019): Effect of garlic powder (*Allium sativum*) on performance of broiler chicken. – Livestock Research for Rural Development 31: 4.
[36] Noman, Z. A., Hasan, M. M., Talukder, S., Sarker, Y. A., Paul, T. K., Sikder, M. H. (2015): Effects of garlic extract on growth, carcass characteristics, and haematological parameters in broilers. – Bangladesh Veterinarian 32(1): 1-6.
[37] Obasi, K. O., Chineze, N. C., Duru, M. C. (2009): Studies on the bacteriocidal effects of garlic (*Allium sativum* linn) on selected pathogenic bacteria. – Environmental Health and Human Development 10(2).
[38] Ogbonna, O. J., Udia, P. M., Abe, P. N., Omoregha, C. U., Anele, E. I. (2016): Phytochemical and proximate analysis, mineral and vitamin compositions of *Allium Cepa* bulb extract. – Advances in Biomedicine and Pharmacy 3(4): 181-186.
[39] Olusola, O. O., Tella, A. K., Olasunkanmi, A. A. (2018): Performance and meat quality attributes of broiler chickens fed onion skin extract and onion skin meal supplemented diets at the finisher stage. – Journal of Experimental Agriculture 24(1).
[40] Omar, A. E., Al-Khalaifah, H. S., Mohamed, W. A., Gharib, H. S., Osman, A., Al-Gabri, N. A., Amer, S. A. (2020): Effects of Phenolic-Rich Onion (*Allium cepa* L.) Extract on the Growth Performance, Behavior, Intestinal Histology, Amino Acid Digestibility, Antioxidant Activity, and the Immune Status of Broiler Chickens. – Frontiers in Veterinary Science 7: 728.
[41] Pareek, S., Sagar, N. A., Sharma, S., Kumar, V. (2017): Onion (*Allium cepa* L.). Fruit and vegetable phytochemicals: chemistry and human health. – 2nd ed. Hoboken, NJ: Wiley Blackwell, pp. 1145-62.
[42] Rao, B. N. (2003): Bioactive phytochemicals in Indian foods and their potential in health promotion and disease prevention. – Asia Pacific Journal of Clinical Nutrition 12(1): 9-22.
[43] Saxena, M., Saxena, J., Nema, R., Singh, D., Gupta, A. (2013): Phytochemistry of medicinal plants. – Journal of Pharmacognosy and Phytochemistry 1(6): 168-182.
[44] Slavin, J. (2013): Fiber and prebiotics: mechanisms and health benefits. – Nutrients 5(4): 1417-1435.
[45] Swain, P., Sethy, K., Sahoo, P. R., Mishra, S. P., Nayak, S. M., Patro, P. (2017): Influence of Organic Dietary Supplementation on Physiological Performance in Japanese Quail (Coturnix japonica): A Critical Review. – International Journal of Pure and Applied Bioscience 5(5): 844-857.
[46] Ur Rahman, S., Khan, S., Chand, N., Sadique, U., Khan, R. U. (2017): *In vivo* effects of *Allium cepa* L. on the selected gut microflora and intestinal histomorphology in broiler. – Acta Histochemical 119(5): 446-450.
[47] Waleed, M. D., Hassan, S. Z., Mohamed, H. A., Soliman, M. Z., Maher, M. S., Nader, R. A., Abdel-Moneim, E., Taha, A. E., El-Tarabily, K. A., Mohamed, E. A. (2021): Impacts

http://www.aloki.hu ● ISSN 1589 1623 (Print) ● ISSN1785 0037 (Online)
DOI: http://dx.doi.org/10.15666/aeer/2001_383396

of onion and cinnamon supplementation as natural additives on the performance, egg quality and immunity in laying Japanese quail. – Poultry Science 100(12): 101482.

[48] Yadav, A. S., Kolluri, G., Gopi, M., Karthik, K., Singh, Y. (2016): Exploring alternatives to antibiotics as health promoting agents in poultry-A review. – Journal of Experimental Biology 4(3): 3-10.

[49] Yang, N., Jiang, R. S. (2005): Recent advances in breeding for quality chickens. – World's Poultry Science Journal 61(3): 373-381.

[50] Yousuf, M. N., Akter, S., Haque, M. I., Mohammad, N., Zaman, M. S. (2013): Compositional nutrient diagnosis (CND) of onion (*Allium cepa* L.). – Bangladesh Journal of Agricultural Research 38(2): 271-287.

[51] Zhao, X. X., Lin, F. J., Li, H., Li, H. B., Wu, D. T., Geng, F., Ma, W., Wang, Y., Miao, B. H., Gan, R. Y. (2021): Recent advances in bioactive compounds, health functions, and safety concerns of onion (*Allium cepa* L.). – Frontiers in Nutrition 8. DOI: 10.3389/fnut.2021.669805

http://www.aloki.hu ● ISSN 1589 1623 (Print) ● ISSN1785 0037 (Online)
DOI: http://dx.doi.org/10.15666/aeer/2001_383396

THE POTENTIAL OF JUTEORC (*CORCHORUS OLITORIUS* L.), A GEOTEXTILE MATERIAL, UNDER SALINE SOILLESS CULTURE CONDITIONS IN TURKEY

AKAT SARACOGLU, O.

Greenhouse Program, Bayindir Vocational School, Ege University, 35840 Bayindir-Izmir, Turkey (e-mail: ozlem.akat@ege.edu.tr; phone: +90-232-581-6317; fax: +90-232-581-7330)

(Received 5th Aug 2021; accepted 28th Oct 2021)

Abstract. The present study was conducted to determine the possibility of the employed of jute (*Corchorus olitorius* L.), a natural fiber used as geotextile cover material, under saline soilless culture conditions, which constitute of the biggest problems in agriculture. The effect of the jute material employed in Mexican marigold (*Tagetes erecta*) cultivation under saline soilless conditions was determined. For this purpose, the Mexican marigold cultivation was tested in a pot experiment under greenhouse conditions for two growth periods in İzmir, Turkey. The salinity levels in the experiment were compared based on whether the treatment included the jute material (G1) or did not include jute material (G0). The measured salinity level of Hoagland nutrient solution employed the irrigation and fertilization of plants was one of the studied factors and was considered as control (S1). The measured EC (electrical conductivity) level of Hoagland nutrient solution was increased by 1 dS m^{-1} (S2) and 2 dS m^{-1} (S3) with stock NaCl solution, and 3 salinity factors were tested. According to the results of the present study the highest salinity was observed in the G0 group without jute cover. It was demonstrated that the jute cover on the pot media reduced the mean salinity concentration in growth medium by 22.56%. This finding was associated with the ability of the jute material to hold the salt in the nutrient solution, preventing spread of the salinity around the root zone.
Keywords: *agrotextiles, root zone, salt removal, growth medium, electrical conductivity (EC)*

Introduction

Technical textile materials improve the yield, quality and safety of agricultural products due to their excellent environmental resistance, mechanical properties, easy processing and durability properties (Agrawal, 2013). Geotextile is a combination of the terms geo, meaning earth-soil, and textile. Geotextiles are permeable geosynthetic textile materials employed as foundation material in buildings and in geotechnical engineering as an integral part of projects, structures and systems along with soil and rock. Geotextile products are expected to possess at least one of five functions: separation, reinforcement, filtration, drainage and barrier. Geotextile products should have tensile, bearing and tear strength, a certain stiffness, resistance to elongation under load, air and water permeability, chemical and ultraviolet (UV) resistance (Horrocks and Anands, 2003). Geotextile products are generally employed in road construction, parks, railways, building foundations, concrete grounds, pavement applications, underground pipes and channels, storage areas, airports, ports and sports fields, drainage and filtration systems, drainage pipes, drainage channels, surface drainage, building drainage, hydraulic structures, coastal protection structures, dams, river beds and canal protection, artificial ponds, water dams and garbage and waste landfills (Mecit et al., 2007).

Jute is a geotextile material employed in various textile and industrial applications. Jute is not employed only in the traditional sense such as pulp and paper, but also in the manufacturing of other value-added products such as geo-textiles, composites and home textiles. Jute is an annually renewable energy source with high biomass production per

http://www.aloki.hu ● ISSN 1589 1623 (Print) ● ISSN 1785 0037 (Online)
DOI: http://dx.doi.org/10.15666/aeer/2001_397411

land unit. It is biodegradable and its byproducts could be easily disposed of without leading to environmental hazards (Islam and Ahmed, 2012). In addition to packaging material, jute is employed in the wood industry as flooring substitute, home furniture, and fiber composite, and in paper and automotive industries, soft suitcase production, and increasingly in garment industry (Chavan, 2001). In addition to environmental friendly and biodegradability properties, the employed of natural fibers such as flax, hemp, kenaf, jute and kapok as cost-effective synthetic fiber alternatives has increased (Çavuş et al., 2020).

All employed jute materials are biodegradable and recyclable. Jute, a vegetable material, decomposes in the soil when root and leaf residues are mixed with the soil and serves as organic macro and micronutrients for other plants; thus, reducing use of fertilizers, which are among important agricultural inputs (Islam and Ahmed, 2012). Jute is preferred in agricultural cultivation since it is environmentally friendly, does not produce toxic substances and all stages of production, employed and disposal are inexpensive (Sarkar, 2008). Geotextile materials have a significant potential in minimizing pre-harvest and post-harvest crop losses, increasing productivity and reducing costs in agricultural industry. Furthermore, the employed of these high value-added agricultural products significantly increases agricultural yield (İlhan, 2015). In recent years, geotextile material used for landscape design weed control does not restrict plant growth. By using geotextile cover, weed control is carried out, and water consumption by weeds is prevented by protecting the design. The water loss that will occur as a result of evaporation on the soil surface can also be minimized (Çakar et al., 2019; Çakar, 2021).

Salinity is a problem that limits vegetative production worldwide in agriculture and has the potential to reduce the visual quality of ornamental plants (Veatch-Blohm et al., 2014). As the most ornamental plants are produced in greenhouses in Turkey., the problem of salinity-limiting cultivation is an important matter (Akat et al., 2019). At least one third of the global agricultural land is saline (Carter et al., 2005; Cassaniti et al., 2009) and it is possible that the surface area affected by salinity increases every day (Munns and Tester, 2008; Shibli et al., 2007). Salty water is employed in irrigation where quality water is not sufficient for irrigation. Thus, the increase in soil salinity over time reduces plant growth, yield and product quality (Villora et al., 2000; Wahome et al., 2000). However, despite the fact that salinity inhibits plant growth, plants have a certain level of tolerance to salinity (Grattan, 1993). This is called salt tolerance and described as the ability of plants to withstand high salinity at the root zone. Salt tolerance of plants is affected by the nature of salinity, the plant, soil, climatic factors and the correlations between these variables, and was described as the proportional decrease in yield due to various salinity levels (Kotuby-Amacher et al., 2000). Salinity at concentrations that exceed the plant salt tolerance inhibits development, reduces flower quality (Sonneveld, 2000), leads to deformation and drying in leaves (Villarino and Mattson, 2011), and death in plant organs in later stages (Cassaniti et al., 2012). Similar to traditional cultivation, salinity problems arise in soilless growth systems, due to the accumulation of salt in the nutrient solution around plant roots over time (Sonneveld and Voogt, 2001). It is known that water used for solution preparation, other than nutrient solutions, often has high salinity (Sonneveld, 2000). Thus, due to the very small root volume in soilless culture, salt accumulation is faster in the root zone when compared to traditional agriculture and a serious salinity problem could be observed (Sonneveld et al., 1999). However, due to the employed of high-quality water in human

http://www.aloki.hu ● ISSN 1589 1623 (Print) ● ISSN 1785 0037 (Online)
DOI: http://dx.doi.org/10.15666/aeer/2001_397411

consumption in irrigated agriculture fields, it may be necessary to use bitter, saline or recycled water of insufficient quality and high electrical conductivity (EC) in agriculture (Villarino et al., 2011; Cassaniti et al., 2013). The availability of low-saline irrigation sources, the employed of alternatives such as recycled wastewater increased interest in the employed of innovative facilities and water management strategies to reduce the negative effects of salt and specific ions. It was emphasized that these types of low-quality water would not harm plant growth, yield and quality (Grive et al., 2013). Thus, the employed of techniques that reduce the effects of low-quality water and high salinity on plant growth became necessary. There are several methods and techniques that reduce the negative effects of salinity in agriculture (Kanber et al., 2005; Machado and Serralheiro, 2017; Karaoğlu and Yalçın; 2018). Soil reclamation is a technique that reduced salinity. This is perhaps the most effective and long-lasting way to minimize or even eliminate detrimental effects of salinity. However, besides being slow and expensive, the process requires large quantities of quality water and effective soil drainage. The other technique is maintenance leaching application. Leaching is absolutely necessary to achieve long-term successful irrigation. A leaching fraction (LF) of 15% to 20% is commonly recommended (Hoffman and Genuchten, 1983). The required leaching frequency depends on the degree of salinization and evaporation demand and the salt sensitivity of the crops. Another technique is irrigation method, management (irrigation and soil fraction) and soil cultivation, water use (WUE) and utilization, by influencing its salt and salt and water salinity, and to design and target water salinity from the front. Besides, the use of biofertilizers can also reduce salinity effects on vegetables and reduce soil salinity (Machado and Serralheiro, 2017). The present study aimed to present an alternative to the existing techniques that employed an innovative facility and water management strategy. Although jute is frequently employed in agriculture, there are no previous studies on the employed of this material in saline agricultural conditions. The present study aimed to develop an alternative method to reduce the salinity problem in the growth media or irrigation water, which is one of the most significant problems in agriculture, with an environment-friendly approach.

Materials and methods

The present study was conducted between 2018 and 2020, in a polyethylene (PE) greenhouse located at the Ege University Bayindir Vocational Training School in Izmir, Turkey (38 ° 12’ 09.9” N, 27 ° 40’ 20.8” E), during two consecutive production seasons to determine the possibility of the employed of jute, a geotextile material, in salinity growing conditions. To investigate the impact of salinity, jute, a natural geotextile material, was used since it does not lead to the accumulation of harmful chemical compounds in plant nutrients (Daira et al., 2020) and is an environment-friendly product (Annapoorani, 2018; Anonoymus, 2021). Certain properties of the jute fabric employed in the trials are presented in *Table 1*. Results given in *Table 1* were obtain from tests. Tests were done according to ISO 3801 and ISO 2060.

Table 1. *Jute material of properties*

Material	Weight	Warp count cm^{-1}	Weft count cm^{-1}
Jute	310 g m^{-2}	11	11

http://www.aloki.hu ● ISSN 1589 1623 (Print) ● ISSN 1785 0037 (Online)
DOI: http://dx.doi.org/10.15666/aeer/2001_397411

The plant material included Mexican marigold (Tagetes erecta 'Proud Mari Yellow') seedlings with moderate salt resistance (Sayyed et al., 2014) and 3-4 true leaves and procured from a seedling firm (*Fig. 1*).

Figure 1. *Mexican marigold seedlings*

Mexican marigold (*Tagetes erecta* 'Proud Mari Yellow') which has a high importance in trade because of its flowers, in landscape designs, medicine, cosmetics and textile industry, fowl breeding, keeps its flower during summer, annual, summer-growing plant (Patel et al., 2019). Plastic pots (measuring 75 cm × 25 cm × 16 cm, with a volume of 24 L) were used for the cultivation. The number of the pots is six in each treatment. A total of 108 plants were planted in balcony pots at a distance of 25 cm × 25 cm (3 plants per pot). Plants were cultivated under soilless culture conditions. A 1: 1 peat and perlite mixture, which is common in Turkey, was preferred as the plant growth media (*Fig. 2*).

Figure 2. *Growth media (perlite + peat)*

The study, where the effects of the certain parameters on jute material were investigated, was conducted in 3 replicates with a randomized blocks trial design in two cultivation seasons in two consecutive years. Plant nutrients required by plants were added to irrigation water as a nutrient solution (Maloupa, 2002; Sevgican, 2002). An irrigation controller (Rainbird, models ESP-RZX Indoor Controller) and electro moto-pomp was set up to operate drip irrigation system. Pressure regulator, manometer, meter, filter, electric (selenoid) valve were used at the pump output and an automation

http://www.aloki.hu ● ISSN 1589 1623 (Print) ● ISSN 1785 0037 (Online)
DOI: http://dx.doi.org/10.15666/aeer/2001_397411

control unit was created to provide automation of irrigation. This automated irrigation system was used in the distribution and application of the Hoagland nutrient solution (Hoagland and Arnon, 1950). For this purpose, a drip irrigation system with a pressure regulator dripper that provided 2.3 liters h^{-1} flow per plant on a 16 mm diameter polyethylene (PE) pipe was employed. Three nutrient solution tanks were used to provide 3 salinity levels in irrigation applications.

Three salinity levels were created to determine the effects of jute on plant growth in salinity conditions. In soilless cultivation, the measured electrical conductivity (EC) of the Hoagland nutrient solution prepared for the irrigation and fertilization of the plants was accepted as the control-K (S1) application as one of the salinity levels in the study. The content of the modified standard Hoagland nutrient solution (mM) included a combination of 12 N-NO3, 3.8 N-NH4, 2.8 P, 8.4 K 3.5 Ca, 1.4 Mg, 9.5 Na, 8.0 Cl, 2.7 S, 0.04 Fe chemicals (Alberici et al., 2008). The control salinity (C:S1) was increased by 1 and 2 dS m^{-1} for each application, respectively to obtain 2 salinity levels [C + 1 dS m^{-1} (S2), C + 2 dS m^{-1} (S3)]. Thus, a total of 3 salinity levels were tested in the study. To determine the reaction of jute to salinity, salinity levels in groups other than the control were obtained with a stock NaCl solution. The growth medium in the pots in the study area was covered with 25 cm x 75 cm jute clothes based on the pot size (*Fig. 3*).

Figure 3. *Jute cover material*

Small crevices were created on the jute cover at 25 cm intervals that equaled to the planting distance. Three plants were planted in each pot (*Fig. 4*).

Figure 4. *Covering the pots with jute*

http://www.aloki.hu ● ISSN 1589 1623 (Print) ● ISSN 1785 0037 (Online)
DOI: http://dx.doi.org/10.15666/aeer/2001_397411

The test area was organized by allowing the plants to pass through these crevices in the pots. Pot cultivation applications with (G1) and without jute cover were compared. In the study, to determine the effect of salinity on jute material, electrical conductivity (EC) and pH levels of the jute material were measured at the end of both cultivation periods. pH measurements were conducted based on ISO 3071:2005 and AATCC 81-2006 (Oktav Bulut and Akçalı, 2013). Salinity in the jute material was also measured based on ISO 3071:2005 and AATCC 81-2006 methods. At the end of both production periods, two whole cover samples were taken from each repetition of jute materials covering a total of 36 pots (the remaining 36 of the 72 pots are not covered with jute material). Geotextile material samples were collected from salinity groups at the end of the trial period and first divided into 1 g using a precision scale (Ohaus Adventurer Analytical Balance, models AR-1530). Acetic acid was added to samples to obtain pH 5.5 and they were transferred into 50 ml purified water. The samples were stirred for 30 min with a magnetic stirrer (WISD magnetic stirrer, models WiseStir MSH-20A) and filtered. pH was measured with a pH meter [WTW, Ph 3210 (330i) pH meter set (portable)] and EC (electrical conductivity) was measured with a conductivity meter (WTW, Cond 330i conductivity meter set).

To determine the salt accumulation in the growth medium, EC and pH levels were measured at the end of both cultivation periods. The cultivation medium samples were collected and purified water was added to the samples and they were stirred in a magnetic stirrer (WISD magnetic stirrer, models WiseStir MSH-20A) for 30 min and filtered. PH measurements were conducted with a calibrated pH measurement device [WTW, Ph 3210 (330i) pH meter set (portable)] and EC measurements were conducted with an electrical measurement device (WTW, Cond 330i conductivity meter set) (Riley, 1986; Çeltek, 1992).

In order to determine the effect of geotextile application on salinity levels, two-way anova analysis was used. In this analysis, the effect of two independent variables on one dependent variable was investigated. The dependent variable in this analysis is the EC value, which indicates the salt concentration. The independent variables are salinity levels (S1:Control, S2: Control + 1 dS m^{-1}, S3: Control + 2 dS m^{-1}) and geotextile usage conditions (1: without geotextile cover, 2: with geotextile cover). It was aimed to investigate the effect of both salinity levels and geotextile employed on EC value together with two-way anova analysis. The effect of independent variables on the dependent variable was determined by the interaction test. For this purpose, Partial Eta Squared values were examined. These values indicate the effect superiority of the independent variables. These values take the maximum value of 1. The fact that these values are close to the value of 1 indicates that this independent variable is so effective (Kalaycı, 2006).

The study datas were analyzed with the IBM SPSS Statistics (v21) software package program.

Results

The mean EC and pH levels were measured in the nutrient solutions that were administered to obtain various salinity levels in the trial groups in different cultivation periods (*Table 2*).

It was determined that the measured EC of the Hoagland nutrient solution added to the irrigation water, and the salinity concentrations in S1 (control), and S2 and S3 groups, the salinity applications for which were obtained by increasing the salt

http://www.aloki.hu ● ISSN 1589 1623 (Print) ● ISSN 1785 0037 (Online)
DOI: http://dx.doi.org/10.15666/aeer/2001_397411

concentration of the control group by 1 dS m^{-1} and 2 dS m^{-1}, respectively, in both cultivation periods were at recommended levels. According to *Table 2,* the mean EC levels in the nutrient solution remained between 1.70 dS m^{-1} and 3.70 dS m^{-1}, and pH levels remained between 6.20 and 6.66. The salt application was 59% more in S2 and 118% more in S3 when compared to the control group (S1).

Table 2. *The mean EC and pH levels in nutrient solutions administered to obtain various salinity levels in the trial groups in different cultivation*

Salinity application	Salinity (EC: dS m^{-1})	pH
S1 (Control)	1.70	6.40
S2 (Control + 1 dS m^{-1})	2.70	6.60
S3 (Control + 2 dS m^{-1})	3.70	6.20

The jute material EC (*Fig. 5*) and the jute material pH (*Fig. 6*) were measured after the jute cover material was removed from the pot media after each cultivation period for different salinity concentrations. According to one-way ANOVA analysis, there is a significant difference at the 5% significance level in terms of EC values compared to different salt concentration media (F = 9.987, p = 0.000).

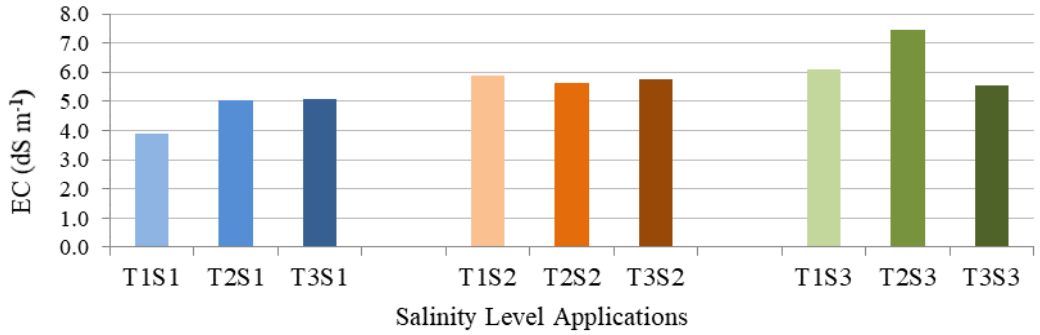

Figure 5. *The jute material EC measurements in salinity applications*

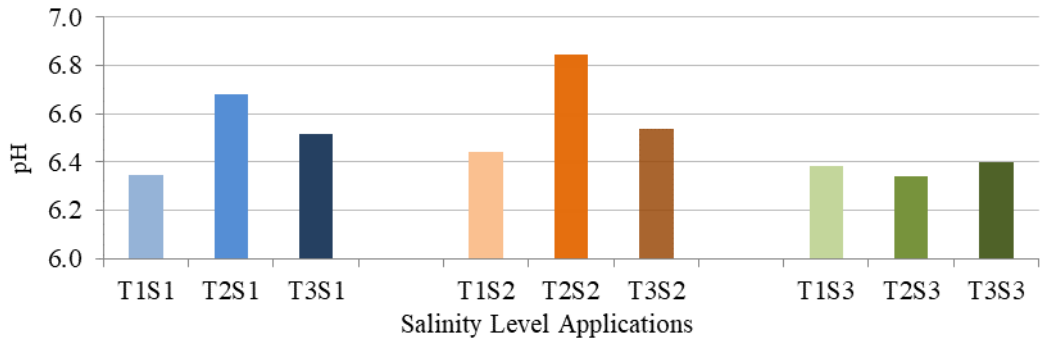

Figure 6. *The jute material pH measurements in salinity applications*

The review of the *Figure 5* would reveal that the lowest EC measurements were observed in S1 (control) group jute material samples, and the highest measurements were observed in the S3 group with the highest salinity. The mean jute cover material

http://www.aloki.hu ● ISSN 1589 1623 (Print) ● ISSN 1785 0037 (Online)
DOI: http://dx.doi.org/10.15666/aeer/2001_397411

EC measurements were 4.68 dS m^{-1}, 5.76 dS m^{-1}, 6.36 dS m^{-1} in S1, S2 and S3 groups, respectively. The EC measurements conducted on the jute cover material on the salt administered growth media in the were 28% higher in the S2 and 36% higher in the S3 groups when compared to the control.

The review of the *Figure 6* would demonstrate that the mean jute material pH scores for different trial groups varied between 6.38 and 6.61. These pH measurements conducted on the jute material were similar to the mean pH score for the saline nutrient solution administered to the trial groups (6.20-6.66). According to one-way ANOVA analysis, there is a significant difference at the 5% significance level in terms of pH values compared to different salt concentration medias ($F = 6.524$, $p = 0.004$).

To determine whether the geotextile cover material had an impact on the reduction of the salinity in the medium, the salinity concentrations (EC: dS m^{-1}) were measured in the growth media. The two-way analysis of variance (ANOVA) was conducted to determine whether there were statistically significant differences between the salinity (EC: dS m^{-1}) of different growth media based on salinity applications and the employed of the geotextile cover material.

Descriptive statistics were made that demonstrate the mean salinity levels for both cultivation periods in plant growth media on salinity applications (*Table 3*).

Table 3. *Salinity levels of plant growth media based on cultivation periods*

Dependent variable: EC2 (dS m^{-1})				
Salinity-II (S2)	**Geotextile cover**	**Mean**	**Std. deviation**	**N**
S1 (Control)	Without cover **(G0)**	4.1117	.89076	6
	With cover **(G1)**	3.1183	.59314	6
	Total	3.6150	.88864	12
S2 (Control + 1 dS m^{-1})	Without cover **(G0)**	5.9433	1.19928	6
	With cover **(G1)**	4.6233	1.16011	6
	Total	5.2833	1.31936	12
S3 (Control + 2 dS m^{-1})	Without cover **(G0)**	6.8417	1.78599	6
	With cover **(G1)**	5.3333	1.57853	6
	Total	6.0875	1.78969	12
Total	Without cover **(G0)**	5.6322	1.72076	18
	With cover **(G1)**	4.3583	1.46122	18
	Total	4.9953	1.70076	36

According to *Table 3,* the lowest mean salinity levels in growth media with geotextile cover material were 4.11 dS m^{-1}, 4.62 dS m^{-1}, and 5.33 dS m^{-1} for S1, S2 and S3 groups, respectively. Based on the mean cultivation period figures, the highest salinity was 5.63 dS m^{-1} in G0 group without geotextile cover and the lowest salinity was 4.36 dS m^{-1} in G1 group with geotextile cover. Thus, the mean salinity in the growth media decreased by 22.56% with the application of jute cover material. It was determined that in all growth medium salinity applications (S1, S2 and S3 groups), the employed of geotextile cover material over the pots led to lower salinity concentrations when compared to groups without geotextile material covers. However, two-way ANOVA revealed that the differences were not statistically significant. Before the analysis, the assumption of equality of variances was investigated (*Table 4*). Since p was greater than 0.05 as seen in *Table 3,* the assumption of equality of variances was confirmed.

http://www.aloki.hu ● ISSN 1589 1623 (Print) ● ISSN 1785 0037 (Online)
DOI: http://dx.doi.org/10.15666/aeer/2001_397411

Table 4. *Levane's test of equality of error variances*[a]

Dependent variable: EC2 (dS m^{-1})			
F	**df1**	**df2**	**P (Sig.)**
.837	5	30	.534*

*Statistically significant at 5% significance level (p > 0.05)

According to the statistical analysis results that revealed the correlation between the salt applications and the employed of jute cover material on salinity of the growth media; based on the sig. values presented in the table, both salt application (group 2) and the employed of geotextile cover material had statistically significant effects on salinity (*Table 5*). On the other hand, the interaction between the salinity applications and jute cover employed (group2-Jtex) did not have a statistically significant effect on salinity in the growth media. In other words, the variables alone had a significant impact on salinity. Based on the Partial Eta Squared analysis, it was determined that different salinity levels had greater effects on salinity in the growth media.

Table 5. *Intra-group effect tests*

Dependent variable: EC2 (dS m^{-1})						
Source	**Type III sum of squares**	**df**	**Mean square**	**F**	**Sig.**	**Partial eta squared**
Corrected model	53.186[a]	5	10.637	6.641	.000	.525
Intercept	898.301	1	898.301	560.800	.000*	.949
group2	38.173	2	19.087	11.916	.000*	.443
JTex	14.605	1	14.605	9.118	.005*	.233
group2 * JTex	.407	2	.204	.127	.881	.008
Error	48.055	30	1.602			
Total	999.541	36				
Corrected total	101.240	35				

*Statistically significant at 5% significance level (p > 0.05)

The mean, standard deviation and confidence intervals for salinity determined based on salt administrations to the growth media are presented in *Table 6*.

Both the averages and confidence intervals revealed that the lowest salinity was determined in S1 (control) group, followed by S2 (control + 1 dS m^{-1}) and S3 (control + 2 dS m^{-1}) groups.

Table 6. *The mean values based on salt applications*

Salinity media-II				
Dependent variable: EC2 (dS m^{-1})				
Salinity media-II	**Mean**	**Std. error**	**95% Confidence interval**	
			Lower bound	**Upper bound**
S1 (Control)	3.615	.365	2.869	4.361
S2 (Control + 1 dS m^{-1})	5.283	.365	4.537	6.029
S3 (Control + 2 dS m^{-1})	6.088	.365	5.341	6.834

http://www.aloki.hu ● ISSN 1589 1623 (Print) ● ISSN 1785 0037 (Online)
DOI: http://dx.doi.org/10.15666/aeer/2001_397411

The mean salinity, the standard deviation and confidence intervals for the growth media based on geotextile cover employed are presented in *Table 7*.

Table 7. *The mean values based on geotextile cover employed*

Dependent variable: EC2 (dS m^{-1})				
Salinity media-II	**Mean**	**Std. error**	**95% Confidence interval**	
			Lower bound	**Upper bound**
Without geotextile (G0)	5.632	.298	5.023	6.241
With geotextile (G1)	4.358	.298	3.749	4.968

Based on both averages and confidence intervals, the mean salinity was lower in growth media covered with geotextile material when compared to growth media without geotextile cover material. In other words, the employed of geotextile cover material in cultivation reduced salinity in the growth media around the roots.

The mean salinity, standard deviation and confidence intervals based on the interaction between the growth media with different salinity levels and the employed of geotextile cover material are presented *Table 8*.

Table 8. *The mean values based on the interaction between salinity applications and geotextile employed*

Salinity media-II * Geotextile employed					
Dependent variable: EC2 (dS m^{-1})					
Salinity media-II	**Geotextile employed**	**Mean**	**Std. error**	**95% Confidence interval**	
				Lower bound	**Upper bound**
S1 (Control)	Without geotextile **(G0)**	4.112	.517	3.056	5.167
	With geotextile **(G1)**	3.118	.517	2.063	4.174
S2 (Control + 1 dS m^{-1})	Without geotextile **(G0)**	5.943	.517	4.888	6.999
	With geotextile **(G1)**	4.623	.517	3.568	5.679
S3 (Control + 2 dS m^{-1})	Without geotextile **(G0)**	6.842	.517	5.786	7.897
	With geotextile **(G1)**	5.333	.517	4.278	6.389

As seen in *Table 8,* The effect of the interaction between the salinity media and geotextile cover material (group2-Jtex) on salinity levels (EC: dS m^{-1}) was not statistically significant. Although the salinity was lower in the groups with geotextile cover in each salinity media, it was determined that the confidence intervals intersected. Thus, the impact of the jute cover material was statistically more significant.

Discussion

The present study findings demonstrated that the highest salinity was observed in the G0 group without jute cover and the lowest salinity was observed in the G1 group with jute cover. It was demonstrated that the jute cover on the pot media reduced the mean salinity concentration in growth medium by 22.56%. The salinity in growth media was reduced by 24.17% in the S1 group, 22.21% in the S2 group, and 22.05%

http://www.aloki.hu ● ISSN 1589 1623 (Print) ● ISSN 1785 0037 (Online)
DOI: http://dx.doi.org/10.15666/aeer/2001_397411

in the S3 group when the pot growth media was covered with jute material when groups with and without cover material were compared. This finding was associated with the ability of the jute material to hold the salt in the nutrient solution, preventing the salinity around the root zone. Although there are no previous on the control of salinity with geotextile material under soilless growth conditions, few studies reported the retention of salinity by geotextile material in conventional agriculture. The results of these existing few studies seem to support the results obtained from this study. In a study conducted in saline soil conditions, the ability of various fabric types (nylon, cotton, geotextile and gauze) to remove soil salinity was investigated based on the correlations between desalination, evaporation loss and structural fabric properties, which are the main factors that affect desalination efficiency. The findings demonstrated that the fabric cover on the soil surface was significantly affected by desalination efficiency, fabric structure, and hydrophilicity/hydrophobicity. Furthermore, it was reported that among the four investigated fabric types, geotextile material had the highest desalination effect. The authors emphasized that further studies were required to determine the desalination properties of geotextile materials based on the spatial heterogeneity of soil texture, soil salinity and climatic conditions (Xu et al., 2021). In another study conducted on orange tree cultivation with geotextile cover material in saline conditions, the water and salinity distribution in sandy soil irrigated with a sprinkler system was investigated with mulch mats developed with geotextile cover. The findings demonstrated that the employed of geotextile material in reclaimed agricultural fields led to higher water distribution and lower soil salinity in the root zones (Derbala and Elmetwalli, 2015). As observed in the findings reported in both studies, geotextile material reduced salinity, consistent with the present study findings. According to the results of several other similar studies, plastic and organic mulching has favorable effects on reduction of soil evaporation and improvement of saline soils (Heydarzadeh et al., 2014; Wang et al., 2019).

Several methods are employed to desalinate the growth medium in agriculture (Ayers and Westcot, 1989; Burn et al., 2015). The most common methods to improve the soil affected by salinity in Turkey include the employed of various drainage systems, washing processes, chemicals, physical and cultural treatments with organic and inorganic substances, and bio-treatment plants (plant-based improvement). In addition to the fact that several of these methods are expensive, they have disadvantages such as excessive water use in washing applications and the inability to discharge the drainage water, and the exploitation of nutrients in the growth medium (Hanay et al., 2013; Temel et al., 2013). To provide an alternative to known salinity removal techniques, the present study aimed to provide an alternative method where jute cover material is used for agricultural purposes, different from its original intended use. The study provided certain findings that would improve the comprehension of the effectiveness of jute cover material under various salinity conditions in greenhouse conditions, which are commonly used in agriculture in certain locations based on climatic conditions. The findings on the desalination potential of the material suggested that jute was a promising material to prevent salt accumulation in growth media. The present study findings would contribute to the literature for the development of innovative facilities and water management strategies to reduce the negative effects of salinity and specific ion concentrations that lead to salinity.

http://www.aloki.hu ● ISSN 1589 1623 (Print) ● ISSN 1785 0037 (Online)
DOI: http://dx.doi.org/10.15666/aeer/2001_397411

Conclusion

It was concluded that the plant root zone salinity could be reduced when jute geotextile material is employed as cover in soilless culture. According to the results of the present study the highest salinity was observed in the G0 group without jute cover. It was demonstrated that the jute cover on the pot media reduced the mean salinity concentration in growth medium by 22.56%. It was determined that in all growth medium salinity applications (S1, S2 and S3 groups), the employed of geotextile cover material over the pots led to lower salinity concentrations when compared to groups without geotextile material covers. However, as an alternative to known desalination methods, the method presented in the study should be analyzed economically and compared to other existing methods to precisely determine the of the jute material. Furthermore, the proposed alternative technique should be supported with economic analysis findings based on yield losses due to salinity, which is significant problem in soilless culture systems. Further similar studies should develop different soilless farming systems in different salinity levels for different salt-sensitive plant species to demonstrate the applicability of the technique by the farmers in large fields.

REFERENCES

[1] Agrawal, S. K. (2013): Application of textile in agriculture. – International Journal of Advance Research in Science and Engineering 2(7): 9-18.

[2] Akat, H., Akat Saracoglu, O., Cakar, H. (2019): Yield response of *Limonium sinuatum* cultivars under salinity stress. – Journal of Environmental Biology (JEB) Special Issue 41(2): 302-309.

[3] Alberici, A., Quattrini, E., Penati, L., Martinetti, M. L., Gallina, P. M., Ferrante, A., Schiavi, M. (2008): Effect of the reduction of nutrient solution concentration on leafy vegetables quality grown in floating system. – ISHS Acta Horticulture 801: 1167-1176.

[4] Annapoorani, S. G. (2018): Agro Textiles and Its Applications. – Woodhead Publishing India Pvt. Ltd., New Delhi.

[5] Anonoymus, 2021. Report of The Working Group on Textiles & Jute Industry for Eleventh Five Year Plan. – https://niti.gov.in/planningcommission.gov.in/docs/aboutus/committee/wrkgrp11/wg11_textiles.pdf (accessed on 05 October 2021).

[6] Ayers, R. S., Westcot, D. W. (1989): Water Quality for Agriculture. – FAO Irrigation and Drainage Paper 29. FAO, Rome.

[7] Burn, S., Hoang, M., Zarzo, D., Olewniak, F., Campos, E., Bolto, B., Barron, O. (2015): Desalination techniques—a review of the opportunities for desalination in agriculture. – Desalination 364: 2-16.

[8] Carter, C. T., Grieve, C. M., Poss, J. A., Suarez, D. L. (2005): Production and ion uptake of *Celosia argentea* irrigated with saline wastewaters. – Scienta Horticulturae 106: 381-394.

[9] Cassaniti, C., Leonardi, C., Flowers, T. J. (2009): The effects of sodium chloride on ornamental shrubs. – Scienta Horticulturae 122: 586-593.

[10] Cassaniti, C., Romano, D., Flowers, T. J. (2012): The Response of Ornamental Plants to Saline Irrigation Water. – In: Garcia-Garizabal, I. (ed.) Water Management Pollution and Alternative Strategies. InTech, Rijeka, pp. 131-158.

[11] Cassaniti, C., Romano, D. I., Hop, M. E. C. M., Flowers, T. J. (2013): Growing floricultural crops with brackish water. – Environmental and Experimental Botany 92: 165-175.

http://www.aloki.hu ● ISSN 1589 1623 (Print) ● ISSN 1785 0037 (Online)
DOI: http://dx.doi.org/10.15666/aeer/2001_397411

[12] Chavan, R. B. (2001): Indian Textile industry - Environmental issues. – Indian Journal of Fibre and Textile Research 26(1): 11-21. http://nopr.niscair.res.in/bitstream/123456789/24908/1/IJFTR%2026(1-2)%2011-21.pdf. (accessed on 19 April 2021).
[13] Çakar, H. (2021): The Influence of geoextile materials used for landscape design on the growth of plants. – Pakistan Journal Agriculture and Sciences 58(3): 771-777.
[14] Çakar, H., Akat Saraçoğlu, Ö., Kılıç, C. C., Akat, H., Yücel, Ö. (2019): The performance analysis of geotextile materials used for irrigation water and weed control in stone garden landscape design. – Textile and Apparel 29(3): 237-245.
[15] Çavuş, Z., Özen, M. S., Gençtürk, A., Evirgen, S., Akalın, M. (2020): Otomotiv iç mekânlarında kullanılan doğal elyaf takviyeli iğnelenmiş dokunmamış kumaşların ses yutum özellikleri. – Nonwoven Technical Textiles Technology 28 Aralık 2020, İstanbul. http://nonwoventechnology.com/tag/dogal-elyaf/ (accessed on 19 April 2021).
[16] Çeltek, M. (1992): Topraksız Kültür Ortamında Kullanılabilecek Harç Materyallerinin Özelliklerinin Belirlenmesi. – Master Thesis, Ege University, Institute of Graduate School of Natural and Applied Science, Izmir, Tukey.
[17] Daria, M., Krzysztof, L., Jakup, M. (2020): Characteristics of biodegradable textiles used in environmental engineering: a comprehensive review. – Journal of Cleaner Production 268(2020): 122129. https://doi.org/10.1016/J.JCLEPRO.2020.122129.
[18] Derbala, A., Elmetwalli, A. (2015): Using geotextile mats to enhance the distribution of water and salinity under sprinkling irrigation. – International Journal of Agronomy and Agricultural Research (IJAAR) 6(6): 68-74.
[19] Grattan, S. R. (1993): How Plants Respond to Salts. – In: Hanson, B., Grattan, S. R., Fulton, A. (eds.) Agricultural Salinity and Drainage. University of California Irrigation Program, University of California, Davis, pp. 3-5.
[20] Grive, C. M., Grattan, S. R., Mass, E. V. (2013): Plant Salt Tolerance. – In: Wallender, W., Tanji, K. (eds.) Agricultural Salinity Assessment and Management. Chapter 13. ASCE, Reston, pp. 405-459. https://ascelibrary.org/doi/10.1061/9780784411698.ch13.
[21] Hanay, A., Büyüksönmez, F., Kiziloglu, F. M., Canpolat, M. Y. (2013): Reclamation of saline sodic soils with gypsum and MSW Compost. – Compost Science & Utilization 12(2): 175-179.
[22] Heydarzadeh, M., Khorsandi, F., Mousavi, A. A. 2014. The effects of three types of lithic mulches on salinity and moisture conservation in a heavy textured soil. – Advances in Environmental Biology 8(811): 1168-1172.
[23] Hoagland, D. R., Arnon, D. I. (1950): The Water Culture Method Growing Plants Without Soil. – California Agriculture Experiment Station Circular, The College Of Agriculture University of California, Berkeley, pp. 34-39.
[24] Hoffman, G. J., Genuchten, M. T. V. (1983): Soil Properties and Efficient Water Use: Water Management for Salinity Control. – In: Taylor, H. M., Jordan, W. R., Sinclair, T. R. (eds.) Limitations to Efficient Water Use in Crop Production. Chapter 2C. ASA-CSSA-SSSA, Madison, WI, 73-85 pp.
[25] Horrocks, A. R., Anand, S. C. (2003): Technical Textiles Handbook. 2nd Ed. – Woodhead Publishing, Cambridge.
[26] Islam, M. S., Ahmed, S. K. (2012): The Impacts of jute on environment: an analytical review of Bangladesh. – Journal of Environment and Earth Science 2(5): 24-31.
[27] İlhan, İ. 2015. Textile products used in agricultural applications. – Journal of The Faculty of Engineering and Architecture 30(1): 183-196.
[28] Kalaycı, Ş. (2006): SPSS Uygulamalı Çok Değişkenli İstatistik Teknikleri. – Asil Yayın Dağıtım, Ankara, Türkiye.
[29] Kanber, R., Çullu, M. A., Kendirli, B., Antepli, S., Yılmaz, N. (2005): Sulama, Drenaj ve Tuzluluk. – www.zmo.org.tr/etkinlikler/6tk05/013ri zakanber.pdf (accessed on 29 September 2021).

http://www.aloki.hu ● ISSN 1589 1623 (Print) ● ISSN 1785 0037 (Online)
DOI: http://dx.doi.org/10.15666/aeer/2001_397411

[30] Karaoğlu, M., Yalçın, A. M. (2018): Soil salinity and sample of Iğdır plain. – Journal of Agriculture 1(1): 27-41.
[31] Kotuby-Amacher, J., Koenig, R., Kitchen, B. (2000): Salinity and Plant Tolerance, AG-SO-03. – Electronic Publishing, Utah State University.
[32] Machado, R. M. A., Serralheiro, R. P. (2017): Soil salinity: effect of vegetable crop growth. Management practices to prevent and mitigate soil salinization. – Horticulturae 3(2): 30. https://doi.org/10.3390/horticulturae3020030.
[33] Maloupa, E. (2002): Hydroponic Systems. – In: Savvas, D., Passam, H. (eds.) Hydroponic Production of Vegetables and Ornamentals. Embryo Publications, Athens, pp. 143-178.
[34] Mecit, D., Ilgaz, S., Duran, D., Başal, G., Gülümser, T., Tarakçıoğlu, I. (2007): Technical textiles and applications (Part: 2). – Textile and Apparel 17(3): 154-161.
[35] Munns, R., Tester, M. (2008): Mechanisms of salinity tolerance. – Annual Review of Plant Biology 59: 651-681.
[36] Oktav Bulut, M., Akçalı, K. (2013): The effects of storage conditions on performance properties of textile materials dyed with reactive dyestuffs and top white. – Erciyes University Journal of Institute of Science and Technology 30(1): 39-47.
[37] Patel, M. A., Chawla, S. L., Chavan, S. K., Shah, H. P., Patil, S. D. (2019): Genetic variability, heritability and genetic advance studies in marigold (*Tagetes Spp*.) Under the South Gujarat region. – Electronic Journal of Plant Breeding 10(1): 272-276.
[38] Riley, J. L. (1986): Laboratory Methods for Testing Peat. – Ontario Peatland Inventory Project. Open File Report 5572. Ontario Geological Survey, Ontario.
[39] Sarkar, S. (2008): Good practices for jute and allied fibre crops in Souvenir. – International Symposium on Jute and Allied Fibre Production, Utilization and Marketing, Organized by Indian Fibre Society (Eastern Region), pp. 1-3.
[40] Sayyed, A., Gul, H., Hamayun, M., Nangyal, H., Fazal, I. (2014): Influence of sodium chloride on growth and chemical composition of *Tagetes erecta*. – South Asian Journal of Life Sciences 2(2): 29-32.
[41] Sevgican, A. (2002): Örtüaltı Sebzeciliği (Topraksız Tarım) Cilt – II. Ege University Faculty of Agriculture Publishing, Izmir-Turkey.
[42] Shibli, R. A., Kushad, M., Yousef, G. G., Lila, M. A. (2007): Physiological and biochemical responses of tomato microshoots to induced salinity stress with associated ethylene accumulation. – Plant Growth Regulation 51: 159-169.
[43] Sonneveld, C. (2000): Effects of salinity on substrate grown vegetables and ornamentals in greenhouse horticulture. – Doctoral Thesis (Ph.D. Dissertation), Wageningen University, The Netherlands.
[44] Sonneveld, C., Voogt, W. (2001): Chemical analysis in substrate systems and hydroponics - use and interpretation. – Acta Horticulturae 548: 247-260.
[45] Sonneveld, C., Baas, R., Nijssen, H. H. M., De Hoog. J. (1999): Salt tolerance of flower crops grown in soilless culture. – Journal Plant Nutrition 22: 1033-1048.
[46] Temel, S., Şimşek, U., Keskin, B., Yılmaz, İ. H. (2013): Tuzlu Toprakların Düzeltilmesinde Biyo-İyileştirici Olarak Tuza Tolerans Dereceleri Farklı Buğdaygil Yem Bitkilerinin Etkisi. – X. Tarla Bitkileri Kongresi, 10-13 Eylül 2013, Konya-Türkiye, pp. 651-658.
[47] Veatch-Blohm, M. E., Sawch, D., Elia, N., Pinciotti, D. (2014): Salinity tolerance of three commonly planted *Narcissus* Cultivars. – HortScience 49(9): 1158-1164.
[48] Villarino, G. H., Mattson, N. S. (2011): Assessing tolerance to sodium chloride salinity in fourteen floriculture species. – HortTechnology 21: 539-545.
[49] Villora, G., Moreno, A., Pulgar, G., Romero, L. (2000): Yield Improvement in zucchini under salt stress: determining micronutrient balance. – Scientia Horticulturae 86: 175-183.
[50] Wahome, P. K., Jesch, H. H., Grittner, I. (2000): Effect of NaCl on the vegetative growth and flower quality of roses. – Journal of Applied Botany 74: 38-41.

http://www.aloki.hu ● ISSN 1589 1623 (Print) ● ISSN 1785 0037 (Online)
DOI: http://dx.doi.org/10.15666/aeer/2001_397411

[51] Wang, J., Liu, H., Wang, S., Liu, Y., Cheng, Z., Fu, G., Mo, F., Xiong, Y. (2019): Surface mulching and a sandy soil interlayer suppress upward enrichment of salt ions in salt-contaminated field. – Journal of Soils and Sediments 19: 116-127.
[52] Xu, Z., Mao, X., Adeloye, A. J., Hu, K., Zhu, Y., Ma, X. (2021): Geotextile covering: potential technique for farmland salinization control. – Land Degradation and Development 32(3): 2493-2508.

http://www.aloki.hu ● ISSN 1589 1623 (Print) ● ISSN 1785 0037 (Online)
DOI: http://dx.doi.org/10.15666/aeer/2001_397411

SEASONAL DYNAMICS OF NON-STRUCTURAL CARBOHYDRATES IN CLONAL PLANTS IN DIFFERENT HABITATS OF INLAND RIVER WETLANDS

ZHOU, Y.[1,2] – JIAO, L.[1,2*] – LIU, X. R.[1,2] – LI, F.[1,2]

[1]*College of Geography and Environmental Science, Northwest Normal University, Lanzhou 730070, China*

[2]*Key Laboratory of Resource Environment and Sustainable Development of Oasis, Gansu Province, China*

[*]*Corresponding author*
e-mail: jiaoliang@nwnu.edu.cn; phone: +86-139-1935-0195

(Received 6th Aug 2021; accepted 1st Oct 2021)

Abstract. Research on the temporal and spatial dynamics of non-structural carbohydrates (NSC) in plants and their distribution patterns in different modules will help understand the effects of environmental changes on plant growth and the ecological adaptation strategies of plants to heterogeneous environments. In this paper, *Phragmites australis* L., as a typical clonal plant in inland river wetlands, was analyzed to determine the characteristics of the variation in NSC and their compositions (soluble sugars: SS and starch: S) in early growth, mid-growth and later growth seasons at three habitats (wet, salt marsh, drought). The results showed that (1) the contents of NSC, SS and S in the whole plant and clonal modules of *P. australis* showed seasonal variations with gradually increasing trends in wet, salt marsh and drought habitats, but the SS contents of leaves displayed seasonal variations with decreasing trends; (2) there were differences in NSC's allocation strategies across clonal modules, showing that the NSC and SS were mainly invested in rhizomes and were transferred from leaves to stems, while S were mainly invested in stems and was transferred from rhizomes to roots during the transition from wet to drought habitat. The growth and survival strategies of clonal plants in inland river wetlands are dependent on the accumulation and allocation of NSC and their compositions. Meanwhile, these were the great significance guiding for the protection of inland river wetlands in the arid area.
Keywords: *wetlands, Phragmites australis, resource allocation trade-offs, seasonal differences, environmental stress*

Introduction

Non-structural carbohydrates (NSC) produced by plant photosynthesis are important energy supplies and temporary solute pools in plant growth and metabolism (Piper et al., 2017; Li et al., 2018). Variation in the NSC and the composition of their contents can reflect a balance between plant carbon absorption (photosynthesis assimilation) and carbon consumption (respiring and growth), indicating the trade-offs of carbohydrate distribution in plants (Shi et al., 2006). Many environmental factors in nature may limit plant growth and affect their normal physiological and metabolic functions of plants, which also change the carbohydrate contents in plants and the distribution of the proportions in different modules (Li et al., 2008). At present, most studies on the relationship between NSC contents and environmental factors focus on alpine woody plants (Michelot et al., 2012; Guo et al., 2016), drought mosses (Fernandez et al., 2018), and aquatic plants (Eklöf et al., 2009; Pramanik et al., 2016). However, research on NSC contents in clonal plants in inland river wetlands is relatively scarce. Therefore, analyzing the changes of NSC in clonal plants in inland river wetlands can help us to understand the

http://www.aloki.hu ● ISSN 1589 1623 (Print) ● ISSN 1785 0037 (Online)
DOI: http://dx.doi.org/10.15666/aeer/2001_413430

status the carbohydrate supply and provide important clues to reveal the adaptation mechanisms in particular habitats.

The different results related to the metabolic intensity and distribution proportions of NSC are caused by temporal and spatial interactions. Because of the different demands at different growth seasons, the contents of NSC and their composition in plants have seasonal periodic variation characteristics (Petrussa et al., 2018). However, the variation of NSC and their composition in different plants during different growing seasons showed diversity and complexity. For example, the starch contents in seedlings of *Picea rubens* in Vermont in the northeastern United States showed a decreasing trend by seasons (Schaberg et al., 2000). The NSC in the rhizomes of *P. australis* and *Typha latifolia* in Kahramanmaras¸Turkey, showed a first increasing and then decreasing trend with season (Tursun et al., 2011). In addition, the NSC in *Arisarum italicum* and *Atrophoderma maculatum* in northeast Italy, *P. australis* and *Spartina alterniflora* in the Chongming Dongtan wetland in eastern China and *Syntrichia caninervis* in the Gurbantunggut Desert in northwest China showed gradually increasing trends with seasonal variations (Lv et al., 2013). There was no obvious seasonal variation in the leaf NSC contents of the main tree species in southwestern Basel of Switzerland (Hoch et al., 2003). Therefore, it is necessary to study the seasonal variations of NSC and their composition in different plants and diverse ecological systems.

Spatial heterogeneity resulting from different altitudes, drought and nutritional stress is also an important factor that restricts the distribution pattern of NSC resources in plants, which greatly affects plant growth and causes changes in the physiological and ecological adaptability of plants. The NSC contents of *Pinus cembra* in the Norbul Mountains of Switzerland and *Picea meyeri* in the Luliang Mountains of eastern China gradually increase with increasing altitude (Gričar et al., 2018). Under water stress, the starch contents of *Pinus sylvestris* in Scotland and *Picea abies* in Norway increased, and the soluble sugar contents of *Laurus nobilis* in southern Italy gradually decreased (Wang et al., 2015; Trifilò et al., 2017). Nutrient stress promoted the storage of carbohydrates of *Larix olgensis* in Northeast China, while it significantly reduced the total NSC contents of *Stipa granddis* and *Leymus chinensis* in western China (Ivanov et al., 2019). Therefore, the contents of NSC and their component in plants show different patterns in diverse habitats, which may be due to different adaptation mechanisms and strategies to adapt to different environments.

Clonal plants have strong environmental adaptability and wide distribution in natural ecosystems with the characteristics of infinite life, spatial mobility, reproductive diversity, resource sharing. In particular, clonal plants occupy an advantageous position and play a pivotal ecological role in grassland, tundra, wetlands, waters and other ecological systems (Ganie et al., 2015; Mudrák et al., 2017). At present, researches on clonal plants mostly focus on the integration and plasticity of clonal plants (Ooi et al., 2011; Wan et al., 2019), the trade-off between clonal growth and sexual reproduction (Xiao et al., 2015), the mechanism of resources sharing (Hutchings et al., 2008; Portela et al., 2018), and characteristics of life history and cloning diversity (Svensson et al., 2013). However, there is a paucity of researches on clonal plant NSC. The growth of Plant growth in natural systems is closely related to the accumulation and distribution of NSC (Lapointe, 2001; Douhovnikof et al., 2015). The doubling of CO_2 concentration promoted the accumulation of starch and NSC in the aboveground and root parts of *Bothriochloa ischaemum* in western China (Xiao et al., 2017). The NSC contents of *Ficus benjamina* and *Ficus binnendijkii* in southern Asia were relatively stable and did not show a

http://www.aloki.hu ● ISSN 1589 1623 (Print) ● ISSN 1785 0037 (Online)
DOI: http://dx.doi.org/10.15666/aeer/2001_413430

significant seasonal variation trend among modules (Veneklaas et al., 2005). The NSC contents of the roots of *Elymus nutans* on the Qinghai-Tibet Plateau significantly increased due to the delay in the chlorophyll degradation process with the warming autumn (Shi et al., 2015). Because of the complexity of the composition of non-structural carbohydrates in plants and the diversity of physiological activities involved, the dynamic changes of NSC contents will inevitably and significantly impact the structure and function of plant (Yin et al., 2009). However, the role of various NSC in clonal plants as signal substances in the ecosystem remains to be further explored.

Wetlands are ecosystems with many unique functions on earth, such as protecting biodiversity, regulating runoff, improving water quality and regulating the microclimate (Martyniuk et al., 2016; Finlayson et al., 2018). The ecosystems of inland river wetlands in special geographical locations could determine the high sensitivity of the area to environmental change and vulnerability to disturbance and destruction; these ecosystems are also difficult to re store to a balanced ecological status after destruction (Reis et al., 2017). *P. australis* is an advantageous plant in inland river wetlands with strong environmental adaptability and important ecological value; this species is a perennial root Poaceae clonal plant, which plays an irreplaceable role in maintaining the ecological balance, biodiversity and key zones of Earth's ecosystem (Liu et al., 2016; Atapaththu et al., 2017; Packer et al., 2017). To raise awareness of the trade-offs in *P. australis* resource allocation, extensive research has been carried out. Although some understanding of the resource allocation trade-offs for reeds has been developed, there has still been a lack of corresponding empirical studies. In this paper, *P. australis* individual in indifferent habitat gradients of inland river wetlands were taken as the research object, and the temporal and spatial variations in NSC were systematically explored. This paper aimed to solve two problems: (1) compare the temporal and spatial variations of NSC and composition contents in *P. australis* to clarify the adaptation strategies of plants to season and environment; (2) analyze of seasonal distribution of NSC and composition contents among the clonal modules of *P. australis* to explore the trade-offs of plant resource allocation. The research conclusions will have certain theoretical and applicable value for further understanding the ecological adaptation strategies of clonal plant populations and will provide a reference for ecological management in inland river wetlands of extremely arid areas.

Materials and Methods

Study Site

The Dunhuang Yangguan National Nature Reserve wetland is located in northwest China (93°53'–94°17'E, 39°39'–40°05'N) with a total area of 8.82×104 hm^2, an elevation of 1150-1500 m, and is surrounded by desert and Gobi (*Fig. 1*). The study regions have a typical continental arid climate with a large temperature difference between day and night. The annual mean temperature is 9.3°C. The annual total precipitation is 39 mm and the annual evaporation is 2465 mm. There are nearly 200 springs in the reserve, which are rare salt marsh wetlands in arid desert areas. The soil in the wetland is mainly sandy soils, brown desert soils and meadow soils. The main vegetation types are temperate desert vegetation, mainly *P. australis*, *Leymus secalinus*, *Lycium ruthenicum*, *Glycyrrhiza uralensis*, *Alhagi sparsifolia*, *Salicornia europaea* and other plants.

http://www.aloki.hu ● ISSN 1589 1623 (Print) ● ISSN 1785 0037 (Online)
DOI: http://dx.doi.org/10.15666/aeer/2001_413430

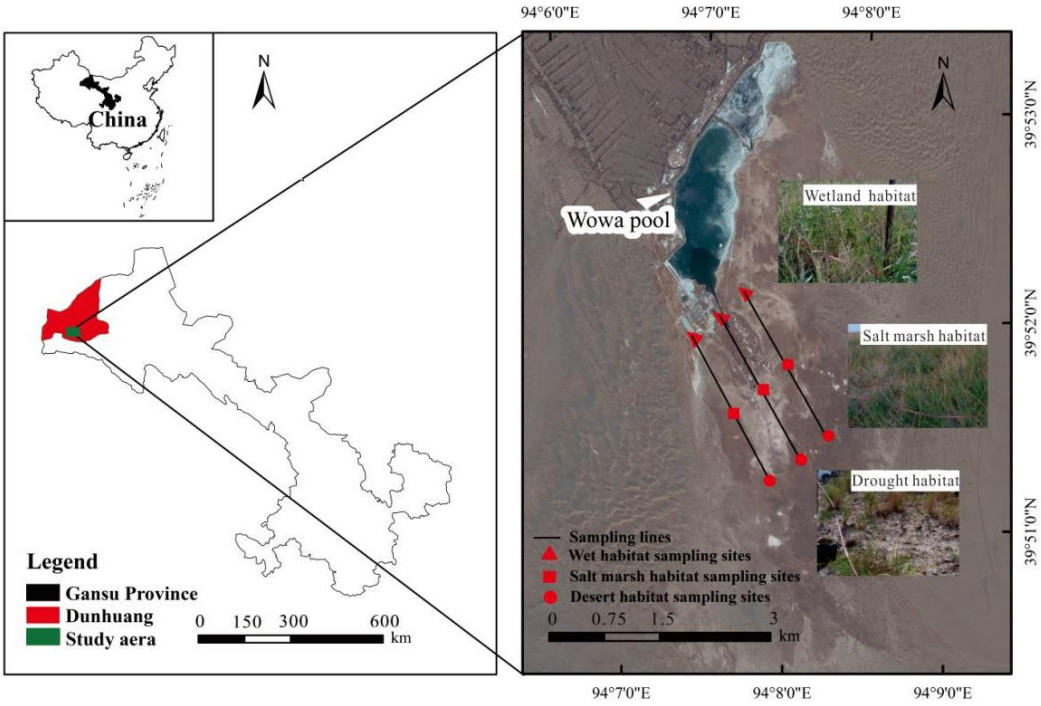

Figure 1. *Study area and sampling point distribution*

Experimental Design and Measurements

In May 2018 (early growth season), July (mid-growth season) and September (later growth season), three parallel sampling lines were set in the Dunhuang Yangguan National Nature Reserve along the direction from inside wetlands to outside droughts with distances of 500 m, 1500 m and 2500 m from the reservoir based on the coverage, density, frequency, height, and dry biomass of *P. australis* (*Table 1*). Three 5 m×5 m sample plots were set for each sampling line and the environmental factors such as altitude, latitude and longitude, geography and geomorphology of each sampling site were recorded (*Table 2*).

Table 1. *Characteristics of P. australis population in different habitats*

Habitat	Coverage (%)	Density (plants/m^2)	Frequency (%)	Height (cm)	Dry Biomass (g/m^2)
Wetland	84.2±6.36 a	94.3±7.65 a	100.00 a	137.6±7.25 a	2047.95±15.23 a
Salt marsh	58.8±6.58 b	37.9±10.40 b	70.3±4.48 b	74.5±4.84 b	424.20±15.77 b
Drought	24.2±1.67 c	8.40±3.93 c	40.7±6.72 c	22.49±2.84 c	35.55±7.78 c

Different lowercase letters indicate significant differences between environmental gradients ($p<0.05$)

Table 2. *Characteristics of sampling sites in different habitats*

Habitat	Longitude (°N)	Latitude (°E)	Altitude (a.s.l., m)	Sample Area（m）
Wetland	94°06′22″	39°52′07″	1125.67	5×5
Salt marsh	94°06′31″	39°52′25″	1121.12	5×5
Drought	94°06′46″	39°52′56″	1126.84	5×5

http://www.aloki.hu ● ISSN 1589 1623 (Print) ● ISSN 1785 0037 (Online)
DOI: http://dx.doi.org/10.15666/aeer/2001_413430

Based on the characteristics of the clonal plant community, we randomly selected three whole *P. australis* plants with identical growth conditions from each sample plot. All above-ground and underground parts of the selected plants were harvested according to the clonal module collection method of full digging using "tracking and digging" based on the direction of the rhizomes in each plot (Harper, 1977; Dong et al., 2011). To deactivate the enzymes, the collected plant samples were baked at 105°C for 30 minutes. Then, the plant materials were divided into clonal modules such as leaves, stems, rhizomes and roots with scissors, and all the samples were numbered uniformly. All the samples were dried to a constant weight at 75–80°C. The dried plant modules were crushed by a mixed ball mill (MM400, Retsch, Germany) and then sifted through a 100 mesh screen and immediately stored in a fridge (0–4°C).

Soluble sugar contents were determined according to the anthrone method (Quentin et al., 2015). Samples of *P. australis* (leaves, stems, rhizomes, and roots) were weighed out to 0.2 g each (Landhäusse et al., 2018). And samples were extracted with deionized water. The supernatants collected by centrifugation at 6000 rpm for 15 min were treated with 5% phenol and 98% sulfuric acid for 1 h. Starch contents were also determined using the anthrone method. The sediment from the extract was dried, weighed and boiled with deionized water, and the supernatant was used for the determination of starch contents. The total NSC concentration was calculated from the soluble sugars and starch contents, whose absorbance values were determined by Lamda 35 (PE, Waltham, USA) at a wavelength of 620 nm.

Data Analysis

The average soluble sugar and starch contents of each sample that were measured separately were tested for normal distribution and homovariance via Shapiro and Bartlett tests, and the non-normal and heteroscedastic samples were treated by variable transformation. The differences in NSC, soluble sugar and starch contents of the whole plant and its clonal modules in different growing seasons or habitats were tested by one-way ANOVA and Tukey-Kramer HSD, respectively, to compare their significant differences at $p < 0.05$ and $p < 0.01$. Linear mixed effect model was used to compare the effects of different plant modules, seasons and habitats on NSC and composition. ANOVA and Tukey-Kramer HSD were performed using SPSS 22.0 (SPSS Inc., Chicago, IL, USA). Linear mixed effect model was implemented by the “nlme” package in R 3.6.1 (R Core Team, 2015). All drawings were completed in Origin 8.0 (OriginLab Inc., Hampton, USA) software.

Results

Effect Factors of NSC and Compositions in P. australis

The effects of *P. australis* module, habitat, season and their interactions on NSC and compositions were different (*Table 3*). Among them, the effects of season, module and the interaction of habitat and module on NSC reached a highly significant level ($P<0.001$), the main effect of NSC variation was season, followed by modules and the interaction of habitat and module. Season, module, habitat and module-season interaction had significant effects on soluble sugars ($P<0.05$). Module and season were the most significant factors affecting soluble sugar variation. The effects of habitat, season and the interaction between habitat and module on starch reached a highly significant level

http://www.aloki.hu ● ISSN 1589 1623 (Print) ● ISSN 1785 0037 (Online)
DOI: http://dx.doi.org/10.15666/aeer/2001_413430

(P<0.001), the most important factors affecting starch variation were season and module-habitat interaction.

Table 3. *Linear mixed effect model results for effects of NSC and Compositions in P. australis*

Influencing factors	NSC			Soluble sugar			Starch		
	Standard error	*F*	*P*	*Standard error*	*F*	*P*	*Standard error*	*F*	*P*
Habitat	1.18	2.033	0.15	0.89	14.31	**<0.05**	0.88	13.56	**<0.05**
Season	1.17	79.66	**<0.001**	0.88	29.03	**<0.001**	0.87	44.99	**<0.001**
Module	0.93	29.86	**<0.001**	0.70	23.33	**<0.001**	0.69	0.02	0.88
Habitat×Season	0.54	0.52	0.60	0.41	0.01	0.95	0.41	0.533	0.47
Habitat×Module	0.43	39.06	**<0.001**	0.32	3.116	0.08	0.38	58.14	**<0.001**
Season×Module	0.42	3.788	**<0.05**	0.34	11.34	**<0.05.**	0.32	1.637	0.20
Habitat×Season×Module	0.20	0.69	0.68	0.15	0.148	0.70	0.15	0.01	0.94

Seasonal Variation of NSC Contents for P. australis in Different Habitats

Under the conditions in the wet, salt marsh, and drought habitats, *Fig. 2* shows that the NSC contents of the whole *P. australis* plant gradually increased with seasonal variations (wet: May 63.07% < July 67.75% < September 76.04%, $p < 0.05$; salt marsh: May 60.92% < July 67.69% < September 74.57%, $p < 0.05$; drought: May 61.10% < July 67.64% < September 74.97%, $p < 0.05$). The increase in NSC contents for the whole *P. australis* plant in the later growth season was significantly greater than that in the first two growth seasons.

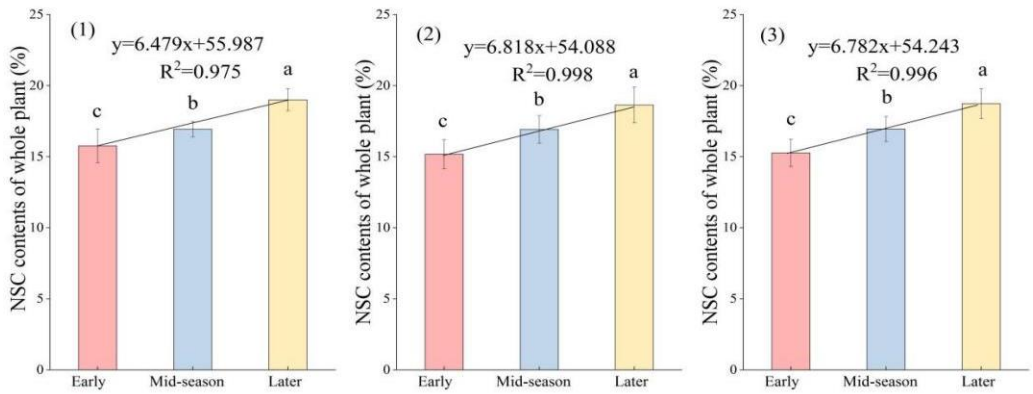

Figure 2. *Seasonal dynamics of NSC contents for P. australis in wet (1), salt marsh (2), drought (3) habitats. (Different lowercase letters from same column indicate significant differences between seasonal variations (p < 0.05)*

In wet, salt marsh, drought habitats, the NSC contents of the clonal modules showed increasing trends from the early growth season to the later growth season (*Fig. 3*). Meanwhile, under the condition in wet habitats, there were no significant differences in

http://www.aloki.hu ● ISSN 1589 1623 (Print) ● ISSN 1785 0037 (Online)
DOI: http://dx.doi.org/10.15666/aeer/2001_413430

the NSC contents of the leaf modules in the different growing seasons ($p > 0.05$), but there were significant differences in stem and root modules in the different growing seasons ($p < 0.05$). *Fig. 3* also shows that there were significant differences in the NSC contents of the rhizome modules between the later growth season and the first two growth seasons ($p < 0.05$). In salt marsh habitats, there were significant differences in the NSC contents of the leaf and rhizome modules in the later growth season and the first two growth seasons ($p < 0.05$), of stem modules in the early growth season and the mid- and later growth seasons ($p < 0.05$), and of root modules in each growth season ($p < 0.05$). In drought habitats, the NSC contents of the leaf modules were not significantly different in any of the growth seasons ($p > 0.05$), the stem and root modules were significantly different in each growth season ($p < 0.05$), and rhizomes were significantly different in the later growth season and the early and mid-growth seasons ($p < 0.05$). And the investment of NSC contents exhibited differences in the clonal modules among the three habitats, showing that the NSC were mainly invested in rhizomes and were transferred from leaves to stems from wet to drought habitats.

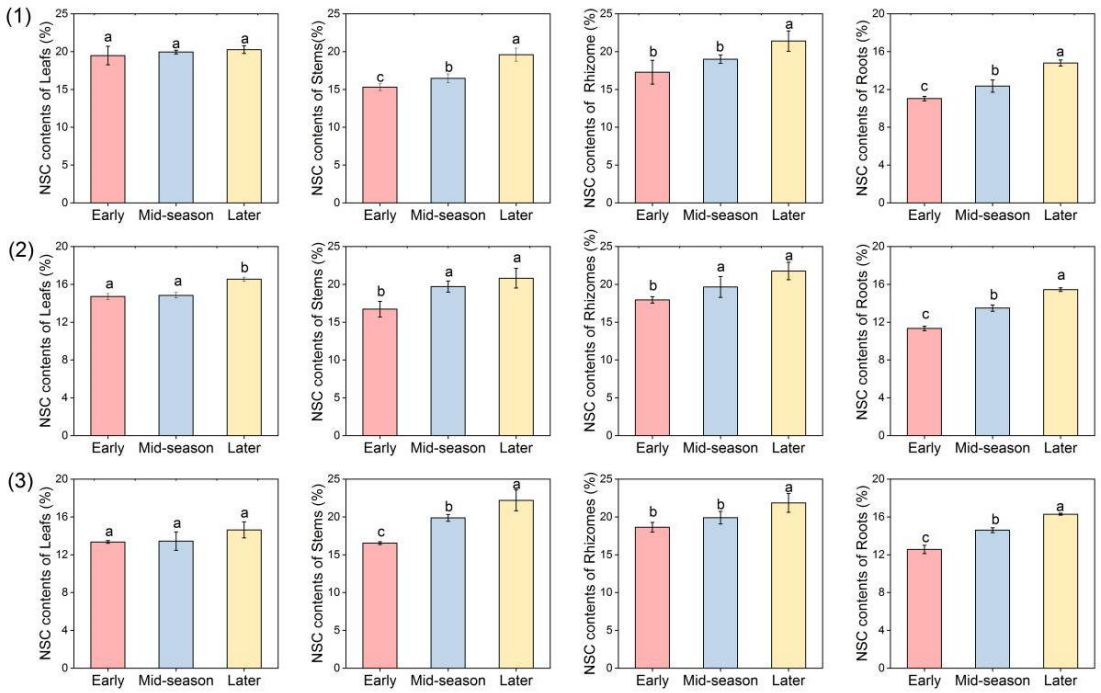

Figure 3. *Seasonal dynamics of NSC contents of clonal modules for P. australis in wet (1), salt marsh (2), drought (3) habitats (Different lowercase letters from same column indicate significant differences between seasonal variations ($p < 0.05$)*

Seasonal Dynamics of Soluble Sugar and Starch Contents for P. australis in Different Habitats

In the wet, salt marsh, and drought habitats, the soluble sugar contents and starch contents of the whole *P. australis* plant showed increasing trends with growing seasonal variations (*Figs. 4 and 5*). In the wet habitat, the main manifestations in the soluble sugar and starch contents were in the early growth season (sugar: 21.94% and starch: 41.13%) < mid-growth season (sugar: 24.21% and starch: 43.54%) < later growth season (sugar:

http://www.aloki.hu ● ISSN 1589 1623 (Print) ● ISSN 1785 0037 (Online)
DOI: http://dx.doi.org/10.15666/aeer/2001_413430

27.01% and starch: 49.03%). In the salt marsh habitat, the main manifestations in the soluble sugar and starch contents were in the early growth season (sugar: 22.53% and starch: 38.39%) < mid-growth season (sugar: 26.17% and starch: 41.52%) < later growth season (sugar: 29.29% and starch: 45.68%). In the drought habitat, the main manifestations were in the early growth season (sugar: 25.21% and starch: 35.89%) < mid-growth season (sugar: 29.13% and starch: 38.51%) < later growth season (sugar: 31.05% and starch: 43.92%). Under the conditions in the wet, salt marsh, and drought habitats, the soluble sugar contents of the whole plant were significantly different in each growth season ($p < 0.05$), but the starch contents of the whole plant were significantly different between the later growth season and the first two growth seasons ($p < 0.05$).

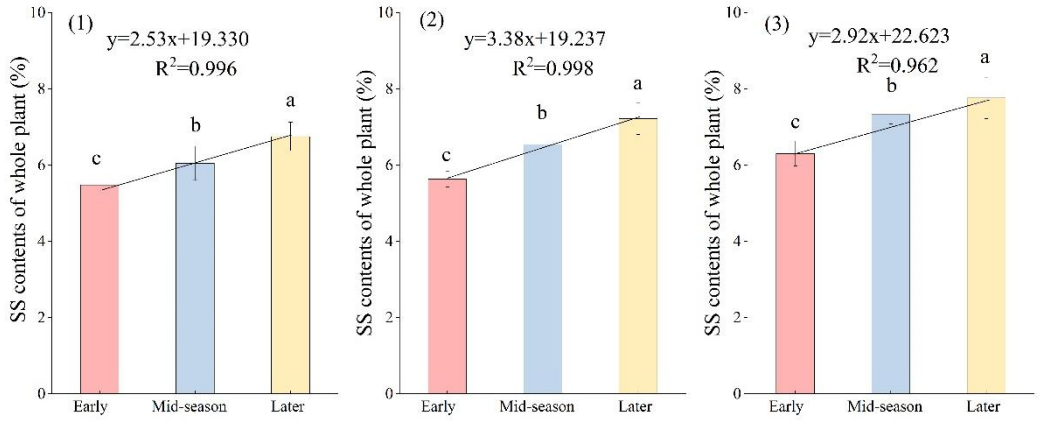

Figure 4. *Seasonal dynamics of soluble sugar contents for P. australis in wet (1), salt marsh (2), drought (3) habitats. (Different lowercase letters from same column indicate significant differences between seasonal variations ($p < 0.05$), and ss represent soluble sugar)*

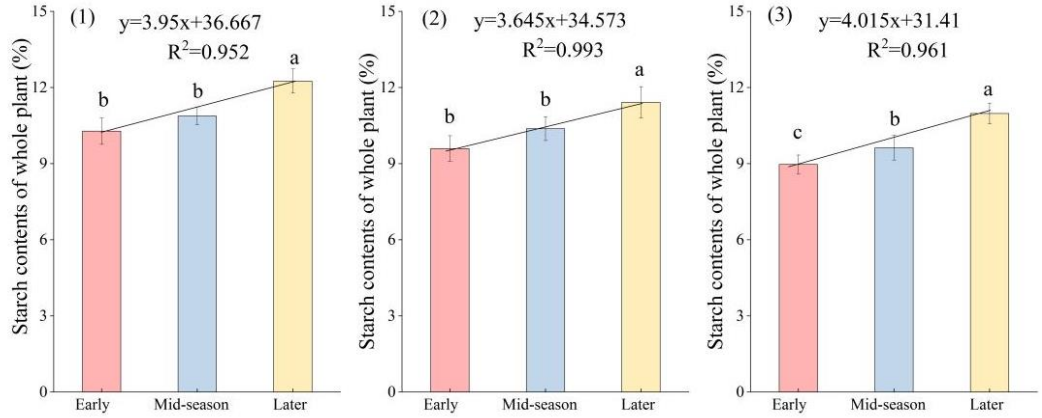

Figure 5. *Seasonal dynamics of starch contents for P. australis in wet (1), salt marsh (2), drough (3) habitats. ((Different lowercase letters from same column indicate significant differences between seasonal variations ($p < 0.05$)*

In the wet habitats, the content of soluble sugar in leaf modules showed increasing trends and starch showed decreasing trends with seasonal variations. The content of soluble sugar in the stem, rhizome and root modules showed an increasing trend with

http://www.aloki.hu ● ISSN 1589 1623 (Print) ● ISSN 1785 0037 (Online)
DOI: http://dx.doi.org/10.15666/aeer/2001_413430

seasonal variations. The soluble sugar contents invested in leaf and rhizome modules were significantly higher than those in stem and root modules. In the salt marsh habitats, the soluble sugar contents in leaf modules decreased trend. The contents of soluble sugar in stems, rhizomes and roots increased and exhibited variations. Meanwhile, the soluble sugar contents invested in leaf and rhizome modules were significantly higher than those in the stem and root modules. In the drought habitats, the contents of soluble sugar in leaf modules decreased and starch showed increasing trends with seasonal variations. The content of soluble sugar in the stem, rhizome and root modules increased with seasonal variations. Meanwhile, the soluble sugar contents invested in the stem and rhizome modules were significantly higher than those in the leaf and root module (*Fig. 6*).

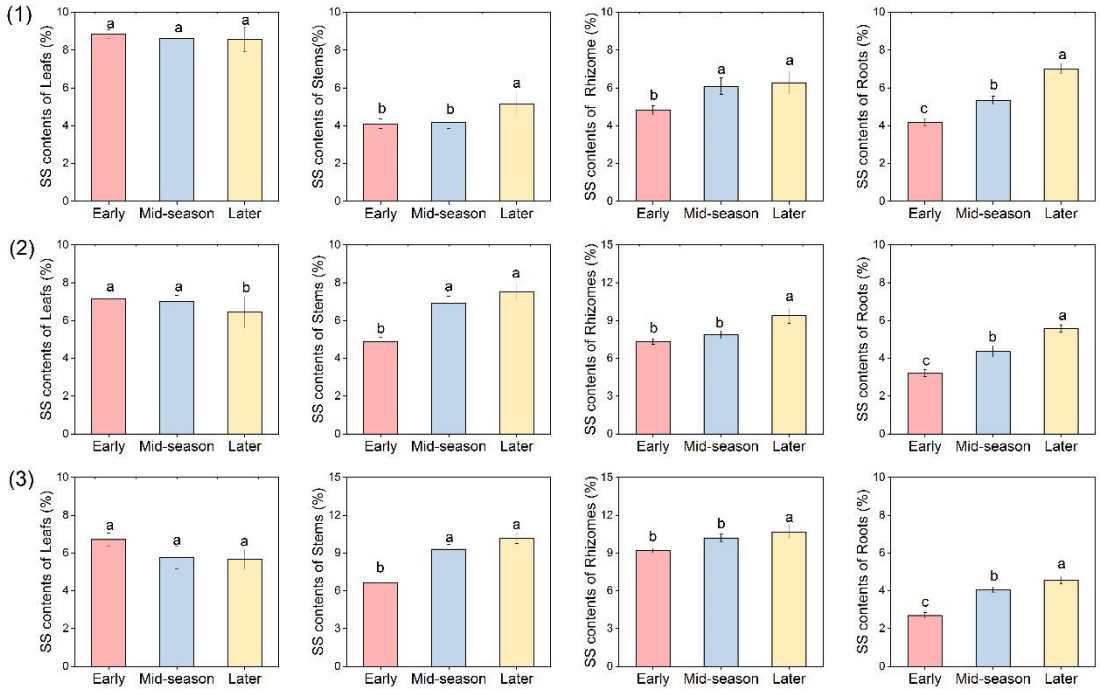

Figure 6. *Seasonal dynamics of soluble sugar contents of clonal modules for P. australis in wet (1), salt marsh (2), drought (3) habitats. (SS is soluble sugar, different lowercase letters from same column indicate significant differences between seasonal variations ($p < 0.05$))*

In the wet habitats, the content of starch in the stem, rhizome and root modules showed an increasing trend with seasonal variations. The starch content invested in the stem and rhizome modules were significantly higher than those in leaf and root modules. In the salt marsh habitats, the starch showed an increasing trend with seasonal variations. The content of starch in stem, rhizome and root modules increased and exhibited variations. Meanwhile, the starch content invested in the stem and rhizome modules were significantly higher than those in the leaf and root modules. In the drought habitats, the content of starch in leaf modules decreased and showed increasing trends with seasonal variations. The content of starch in the stem, rhizome and root modules increased with seasonal variations. Meanwhile, the starch contents in the stem and root modules were significantly higher than those in the leaf and rhizome modules (*Fig. 7*).

http://www.aloki.hu ● ISSN 1589 1623 (Print) ● ISSN 1785 0037 (Online)
DOI: http://dx.doi.org/10.15666/aeer/2001_413430

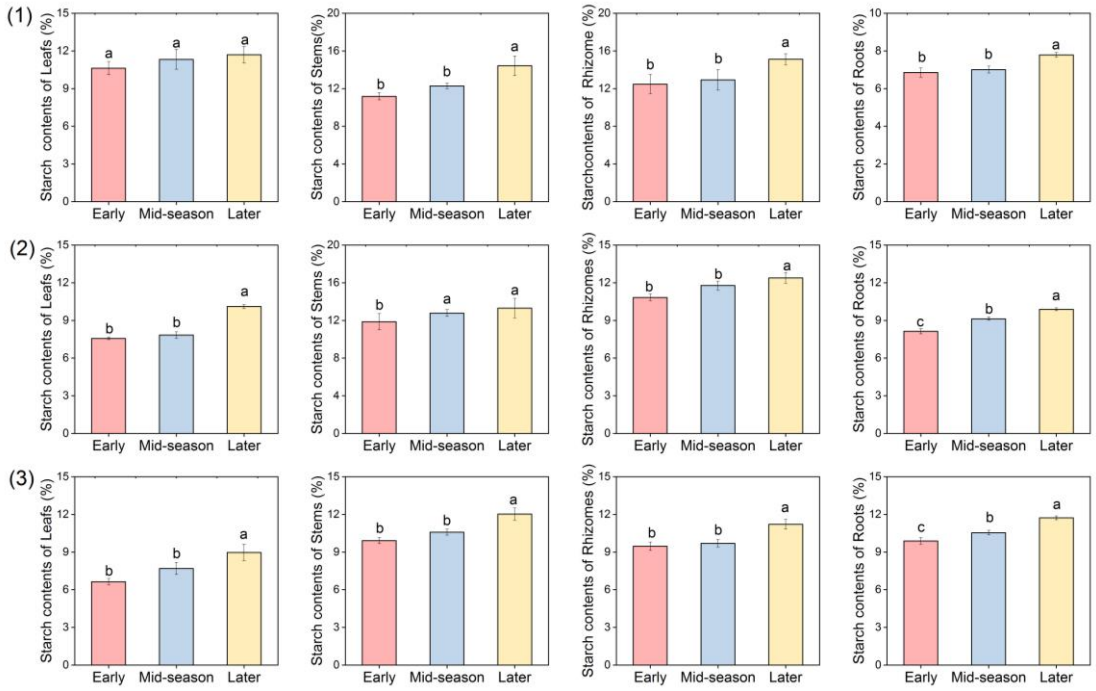

Figure 7. *Seasonal dynamics of starch contents of clonal modules for P. australis in wet (1), salt marsh (2), drought (3) habitats. Different lowercase letters from same column indicate significant differences between seasonal variations ($p < 0.05$)*

Discussion

Temporal and Spatial Variations of NSC and Compositions in P. australis

Non-structural carbohydrates (NSC) are the main energy source for plant growth, reproduction and survival (Sørensen et al., 2018). The NSC contents and concentrations can reflect the carbon supply status of plants, and represent the growth and survival ability of plants as well as their adaptability to external stress disturbances (Würth et al., 2004; Lloret et al., 2018). Recent studies have found that plants are highly sensitive to changes in environmental conditions and respond quickly to very small changes in physiological cell and molecular levels (Myers and Kitajima, 2007). The results of our study revealed that the contents of NSC, soluble sugar and starch in the whole and clonal modules of *P. australis* showed consistent seasonal trends in wet, salt marsh and drought habitats (*Figs. 2, 3, 4, 5, 6 and 7*). Environment heterogeneity has a uniform effect on the contents of NSC, soluble sugars and starch in plants. It shows an ecological adaptation strategy of plants under environmental stress.

The seasonal distribution pattern of NSC and the efficiency of transport integration affect the growth and survival of plants in the community. In wet, salt marshes and drought habitats, the NSC contents of the whole *P. australis* plant showed significant changes with seasonal variations, showing increasing trends (*Figs. 2, 4 and 5*). Increasing the storage of NSC is one of the strategies for plants to cope with adverse environments or potential stress (Chaves et al., 2008). This strategy is used because NSC, as the main energy and carbon supplier for plant growth, can act as a buffer when plant photosynthesis is insufficient (Loewe et al., 2000; Sala et al., 2012). At the end of growth, the NSC contents in plants reach the maximum at one year, which lays the material foundation for

http://www.aloki.hu ● ISSN 1589 1623 (Print) ● ISSN 1785 0037 (Online)
DOI: http://dx.doi.org/10.15666/aeer/2001_413430

the unfavorable weather conditions in winter and the formation of plant nodule germination and tillering in the subsequent year (Borrell et al., 1989; Orthen et al., 2004). NSC begins to be consumed in the early season of plant growth in the following year, and plants converted more photosynthesis products into fiber for the accumulation of plant biomass during the mid-growth season. The results of the study on the *P. australis* population in eastern China confirm this conclusion. At the same time, under the condition of habitat stress, the normal physiological metabolic activities of most plants are inhibited, manifesting as the restriction of carbohydrate synthesis into structural substances. In addition, environmental stress could also cause a barrier to the transmission of NSC, which would also reduce the availability of NSC used for metabolism and further affect the NSC contents (Yu et al., 2014). Therefore, the change of NSC contents in plants could represent a way of adapting to the heterogeneous environments.

Among NSC compositions, soluble sugar plays an important role in regulating osmotic pressure, while starch acts as organic storage and has effective functions in plant resistance to harsh environments, which can be transformed to each other when the environment changes (Nathan et al., 2010; Purdy et al., 2015). Our study results manifested that the contents of soluble sugar and starch in the whole plant of *P. australis* varied significantly with the seasons in the three habitats, showing the smallest contents (soluble sugar: 21.94%, 24.21%, 27.01%, starch: 35.89%, 38.51%, 43.92%) in the early growth season and the largest contents (soluble sugar: 25.21%, 29.13%, 31.05%, starch: 41.13%, 43.54%, 49.03%) in the later growth season (*Figs. 2, 4 and 5*). This result occurred because the photosynthesis of plants is sufficient during the early growth season and the contents of soluble sugar that are synthesized in plants are used for plant growth. At this time, a large amount of surplus starch was temporarily stored in plants as the seasons change and growth under these environmental conditions results in weakened photosynthesis and insufficient of photosynthetic supply, which was unbalanced with soluble sugar contents during the acquisition and expenditure. Additionally, starch could be transformed into soluble sugar to provide energy for plant growth and reproduction and maintain normal physiological function (Machado et al., 2017). This higher the distribution trade-off can make the plant growth and sustainable development due to the rational seasonal allocation of sugar and starch in plants. Therefore, plants are not only dependent on the total NSC content, but also need a balance dimension of sugar and starch to survive difficult environments and seasons. This finding indicates that the different distribution mechanisms of sugar and starch in plants are a positive adaptive response to environmental conditions, that is, the more difficult and harsh the habitat conditions are during plant growth, the more obvious and active the protection strategies of plants. In the course of long-term adaptive evolution, clonal plants have developed ecologically adaptive responses to effectively utilize heterogeneous resources and resist various environmental stresses.

Temporal and Spatial Variations of NSC and Compositions among Clonal Modules of P. australis

Variations in the location and contents of NSC in plants are associated with different seasons of growth and development. NSC metabolism, to a large extent, affects the growth and development of plants and their responses to the environment, showing seasonal distribution trade-offs of carbohydrate contents among different modules (Banerjee and Roychoudhury, 2016). Our study results showed that the NSC contents of clonal modules of *P. australis* exhibited different trends with seasonal dynamics, mainly

http://www.aloki.hu ● ISSN 1589 1623 (Print) ● ISSN 1785 0037 (Online)
DOI: http://dx.doi.org/10.15666/aeer/2001_413430

manifesting as the increasing trend of NSC contents in leaf, stem, rhizome and root modules (*Figs. 6 and 7*). This result was consistent with the conclusion of previous studies that revealed that plant carbon acquisition and consumption were seasonally dependent (Mataa et al., 1996). This result occurred because most of the NSC in plants were used during the growth of leaf modules in the early growth season. Plants gradually accumulate NSC into stems to maintain survival and improve the utilization efficiency of nutrients in the body by enhancing cell osmotic pressure and cell metabolic activity and promoting plant growth (Regier et al., 2010). Meanwhile, plant biomass was basically reached a stable level at the later stage of growth, and other clonal modules began to store large amounts of NSC for plant growth and development in the next year. Hence, a large amount of NSC accumulates in stems and rhizomes, asexual reproduction dependent on rhizomes was selected, plants invest more NSC in rhizome in order to escape from patches with poor resource levels to patches with better conditions (Sevanto et al., 2013). The same results were obtained from the study of NSC in roots, stems and leaves of *Zygophyllum xanthoxylon* in the Alaska region of China (Sun et al., 2020). Studies have confirmed that variation of the NSC contents and transfer between clonal modules in plants is most likely the signal generated by plants on environmental changes, which can control the expression of genes in plants, effectively mitigate the damage caused by environmental stress on plants, and further regulate the growth and development of plants (Li et al., 2018). Therefore, research on the seasonal dynamics and distribution trade-offs of NSC among clonal modules is of major importance for understanding the stability and survival of plants under different habitats and environmental stressors.

Sugar provides the carbon skeleton and energy for plants, and starch stores energy substances for a long time, which are the most important carbohydrate in plant storage modules. Therefore, the synthesis and decomposition of sugar and starch affect the whole process of plant growth and development (Savage et al., 2015; Kaur et al., 2016). Our study results showed that the soluble sugar and starch contents in clonal modules (except leaves) increased with seasonal variations in wet, salt marsh and drought habitats (*Figs. 6 and 7*). However, the contents of soluble sugar in leaves showed a decreasing trend, and starch contents showed an increasing trend. In the middle and later stages of growth, the decrease of sugar content in leaves was due to the obstruction of the photosynthesis process with the stomatal closure gradually increased and the gas exchange ability decreased between leaves and the outside in to prevent excessive water loss (Ge et al., 2012). At the same time, photosynthesis of plant leaves decreased during the mid and later growth seasons, and the soluble sugar used for growth was greatly inhibited. That was the soluble sugar contents invested in the growth of plant leaf modules would decrease and the starch contents would increase (Hinman and Fridley, 2018; Kleyer et al., 2018). In addition, our results also found that soluble sugar was transferred from leaves to stems, while starch was transferred from rhizomes to roots during the transition from wet to drought habitat. Allocate limited starch to roots to increase their ability to withstand stressful environments and induce root growth deeper into the soil to obtain more nutrients to adapt the harsh external environmental condition. The same results were obtained for the study of nutrient stoichiometry of *P. australis* in the northwest arid zone (Zhou et al., 2021). Therefore, the growth-priority strategy was selected depending on stems and roots types, which was a response trade-off to the stress environmental conditions (Jiao et al., 2020). Meanwhile, soluble sugars were transferred to stem modules and starch to root modules, which could allocate more photosynthetic products for growth, respiration and nutrient absorption based on the theory of optimal allocation of

http://www.aloki.hu ● ISSN 1589 1623 (Print) ● ISSN 1785 0037 (Online)
DOI: http://dx.doi.org/10.15666/aeer/2001_413430

resources (Klein et al., 2014). To carry out normal physiological activities under various habitat gradients to resist and adapt to environmental stress, clonal plants could regulate the osmotic potentials of cells in plants, maintain certain energy and maintain certain swelling pressure through the mutual transformation of soluble sugar and starch contents between plant modules during the growth process (Qin et al., 2013; Wang et al., 2015).

The distribution pattern of plant NSC and its components is the result of multiple ecophysiological processes, influenced by environmental factors, and closely related to the adaptation strategies of plants. In our study, season were the most important factors affecting NSC, soluble sugars, and starch (*Table 3*). The same results were obtained from the study of the seasonal dynamics of the non-structural carbohydrate content of *Syntrichia Caninervis* in different habitats (Zhu et al., 2017), indicating that the growing *P. australis* itself has a high capacity for nutrient utilization and a large variability in the elements required at different growth stages (Cullen et al., 2005). In addition, module also plays an important role in *P. australis* NSC variation. This may be due to the different degree of demand and limitation of NSC and its components in different modules (Martinez et al., 2016). The interaction of modules and habitats also played an important role in NSC and starch of *P. australis.* It due to the significant variation in soil nutrient status under different habitats, thus affecting the uptake of NSC and starch by *P. australis*.

Conclusion

NSC are the main energy substances for plant life activities and an important regulatory substance for plants in response to environmental changes, and play a leading role in plant growth, development and survival strategies. The results showed that the NSC contents of the whole plant and clonal modules of *P. australis* increased with seasonal variations in wet, salt marsh and drought habitats. Meanwhile, the soluble sugar and starch contents of the whole plant and stem, rhizome and root modules of *P. australis* increased with seasonal variations, but the soluble sugar contents decreased and the starch contents increased in leaves with seasonal variations. The investment of NSC and their compositions contents exhibited were differences in the clonal modules among the three habitats, showing that the NSC and soluble sugar were transferred from leaves to stems, while starch was transferred from rhizomes to roots during the transition from wet to drought habitats. These variation models reflect the physiological activities of plants and reveal the response and adaptation of plants to environmental changes, which can serve as a reference for the growth strategies and resource trade-offs of clonal plants in inland river wetlands. At the same time, research on the changing characteristics and response rules of non-structural carbohydrates in different seasons and habitats can further reveal the competition mechanism, enrich the competition theory and provide a theoretical basis for formulating and applying the restoration and reconstruction techniques of degraded vegetation and water resource shortages in extremely sensitive and fragile ecosystems.

Acknowledgements. This work was supported by the National Natural Science Foundation of China (Grant No. 41861006), the Natural Science Foundation of Gansu Province (No. 20JR10RA093), and the Research Ability Promotion Program for Young Teachers of Northwest Normal University (NWNU-LKQN2019-4). We also thank the anonymous referees for helpful comments on the manuscript.

http://www.aloki.hu ● ISSN 1589 1623 (Print) ● ISSN 1785 0037 (Online)
DOI: http://dx.doi.org/10.15666/aeer/2001_413430

REFERENCES

[1] Atapaththu, K. S. S., Asaeda, T., Yamamuro, M., Kamiya, H. (2017): Effects of water turbulence on plant, sediment and water quality in reed (*Phragmites australis*) community. – Ekologia Bratislava 6: 1-9.

[2] Banerjee, A., Roychoudhury, A. (2016): Group II late embryogenesis abundant (LEA) proteins: structural and functional aspects in plant abiotic stress. – Plant Growth Regulation 79: 1-17.

[3] Borrell, A. K., Incoll, L. D., Simpson, R. J., Dalling, M. J. (1989): Partitioning of Dry Matter and the Deposition and Use of Stem Reserves in a Semi-dwarf Wheat Crop. – Annals of Botany 63: 527-539.

[4] Chaves, M. M., Flexas, J., Pinheiro, C. (2008): Photosynthesis under drought and salt stress: regulation mechanisms from whole plant to cell. – Annals of Botany 103: 551-560.

[5] Cullen, B. R., Chapman, D. F., Quigley, P. E. (2005): Carbon resource sharing and rhizome expansion of *Phalaris aquatica* plants in grazed pastures. – Functional Plant Biology 32: 79-85.

[6] Dong, M., Yu, F. H., Chen, Y. F., Song, M. H., Liu, J., Chen, J. S., Li, J. M., Liu, F. H. (2011): Clonal plant ecology. – Beijing: science press.

[7] Douhovnikoff, V., Dodd, R. S. (2015): Epigenetics: a potential mechanism for clonal plant success. – Plant Ecology 216: 227-233.

[8] Eklöf, J. S., McMahon, K., Lavery, P. S. (2009): Effects of multiple disturbances in seagrass meadows: shading decreases resilience to grazing. – Marine and Freshwater Research 60: 1317-1327.

[9] Fernandez, E., Baird, G., Farías, D., Oyanedel, E., Olaeta, J. A., Brown, P., Zwieniecki, M., Tixier, M. A., Saa, S. (2018): Fruit load in almond spurs define starch and total soluble carbohydrate concentration and therefore their survival and bloom probabilities in the next season. – Scientia Horticulturae 237: 269-276.

[10] Finlayson, C. M., Everard, M., Irvine, K., McInnes, R. J., Middleton, B. A., Van Dam, A. A., Davidson, N. C. (2018): Preface: The wetland book. Vol. 1: Wetland structure and function, management, and method. – Springer, 2290p.

[11] Ganie, A. H., Reshi, Z. A., Wafai, B. A., Puijalon, S. (2015): Clonal growth architecture and spatial dynamics of 10 species of the genus potamogeton across different habitats in Kashmir Valley, India. – Hydrobiologia 767: 289-299.

[12] Ge, T. D., Sun, N. B., Bai, L. P., Tong, C. L., Sui, F. G. (2012): Effects of drought stress on phosphorus and potassium uptake dynamics in summer maize (*Zea mays*) throughout the growth cycle. – Acta Physiol Plant 34: 2179-2186.

[13] Gričar, J., Zavadlav, S., Jyske, T., Lavrič, M., Laakso, T., Hafner, P., Eler, K., Vodnik, D. (2018): Effect of soil water availability on intra-annual xylem and phloem formation and non-structural carbohydrate pools in stem of *Quercus pubescens*. – Tree Physiology 39: 222-233.

[14] Guo, Q. X., Li, J. Y., Zhang, Y. X., Zhang, J. X., Lu, D. L., Korpelainen, H., Li, C. Y. (2016): Species-specific competition and N fertilization regulation-structural carbohydrate contents in two Larix species. – Forest Ecology and Management 364: 60-69.

[15] Harper, J. L. (1977): Population Biology of Plant. – London and New York: Academic Press.

[16] Hinman, E. D., Fridley, J. D. (2018): To spend or to save? Assessing energetic growth-storage tradeoffs in native and invasive woody plants. – Oecologia 188: 659-669.

[17] Hoch, G., Richter, A., Körner, C. (2003): Non-structural carbon compounds in temperate forest trees. – Plant Cell & Environment 26: 1067-1081.

[18] Hutchings, M. J., Wijesinghe, D. K. (2008): Performance of a clonal species in patchy environments: effects of environmental context on yield at local and whole-plant scales. – Evolutionary Ecology 22: 313-324.

http://www.aloki.hu ● ISSN 1589 1623 (Print) ● ISSN 1785 0037 (Online)
DOI: http://dx.doi.org/10.15666/aeer/2001_413430

[19] Ivanov, Y. V., Kartashov, A. V., Zlobin, I. E., Sarvin, B., Stavrianidi, A. N., Kuznetsov, V. V. (2019): Water deficit-dependent changes in non-structural carbohydrate profiles, growth and mortality of pine and spruce seedlings in hydroculture. – Environmental and Experimental Botany 157: 151-160.
[20] Jiao, L., Zhou, Y., Liu, X., Wang, S., Li, F. (2020): Driving forces analysis of non-structural carbohydrates for *Phragmites australis* in different habitats of inland river wetland. – Water 12: 1700.
[21] Kaur, J., Thakur, S. S. (2016): Characterization of carbohydrates and proteins in phalaris minor seeds by cornell net carbohydrate and protein system. – Current Science A Fortnightly Journal of Research 110: 1324-1329.
[22] Klein, T., Hoch, G., Yakir, D., Korner, C. (2014): Drought stress, growth and nonstructural carbohydrate dynamics of pine trees in a semi-arid forest. – Tree Physiology 34: 981-992.
[23] Kleyer, M., Trinogga, J., Cebrián-Piqueras, M. A., Trenkamp, A., Fløjgaard, C., Ejrnaes, R., Blasius, B. (2018): Trait correlation network analysis identifies biomass allocation traits and stem specific length as hub traits in herbaceous perennial plants. – Journal of Ecology 107: 829-842.
[24] Landhäusser, S. M., Chow, P. S., Dickman, L. T., Furze, M. E., Kuhlman, I., Schmid, S. (2018): Standardized protocols and procedures can precisely and accurately quantify non-structural carbohydrates. – Tree Physiology 38: 1764-1778.
[25] Lapointe, L. (2001): How phenology influences physiology in deciduous forest spring ephemerals. – Physiologia Plantarum 113: 151-157.
[26] Li, M. H., Xiao, W. F., Wang, S. G., Cheng, G. W., Cherubini, P., Cai, X. H. (2008): Mobile carbohydrates in Himalayan treeline trees I. Evidence for carbon gain limitation but not for growth limitation. – Tree Physiology 28(8): 1287-1296.
[27] Li, L., Lan, Z., Chen, J., Song, Z. (2018): Allocation to clonal and sexual reproduction and its plasticity in *Vallisneria spinulosa* along a water-depth gradient. – Ecosphere 9: e02070.
[28] Li, T. T., Xue, J. Q., Wang, S. L., Xue, Y. Q., Hu, F. R., Zhang, X. X. (2018): Research advances in the metabolism and transport of non-structural carbohydrates in plants. – Plant Physiology Journal 54: 25-35.
[29] Liu, L. D., Jie, D. M., Liu, H. Y., Gao, G. Z., Gao, Z., Li, D. H., Li, N. N., Guo, J. X., Qiao, Z. H. (2016): Assessing the importance of environmental factors to phytoliths of *Phragmites communis* in north-eastern China. – Ecological Indicators 69: 500-507.
[30] Lloret, F., Sapes, G., Rosas, T., Galiano, L., Saura-Mas, S., Sala, A., Martínez-Vilalta, J. (2018): Non-structural carbohydrate dynamics associated with drought-induced die-off in woody species of a shrubland community. – Annals of Botany 121: 1383-1396.
[31] Loewe, A., Einig, W., Shi, L. B., Dizengremel, P., Hampp, R. (2000): Mycorrhiza formation and elevated CO_2 both increase the capacity for sucrose synthesis in source leaves of spruce and aspen. – New Phytologist 145: 565-574.
[32] Lv, Y. Y., Li, D. Z., Xu, J., Xu, L. L., Gao, J. J., Pan, Y., Zhao, M. X., Cheng, L. L., Wang, H., He, Y. Y. (2013): Spatial and Temporal Characteristics of Non-structural Carbohydrates Contents of *Phragmites australis* and *Spartina alterniflora* at Chongming Dongtan Wetland. – Journal of Northeast Forestry University 41: 85-89+121.
[33] Martinez-Vilalta, J., Sala, A., Asensio, D. (2016): Dynamics of non-structural carbohydrates in terrestrial plants: a global synthesis. – Ecological Monographs 86: 495-516.
[34] Martyniuk, C. J., Doperalski, N. J., Prucha, M. S., Zhang, J. L., Kroll, K. J., Conrow, R., Barber, D. S., Denslow, N. D. (2016): High contaminant loads in Lake Apopka's riparian wetland disrupt gene networks involved in reproduction and immune function in largemouth bass. – Comparative Biochemistry & Physiology Part D Genomics & Proteomics 19: 140-150.
[35] Mataa, M., Tominaga, S., Kozaki, I. (1996): Seasonal Changes of Carbohydrate Constituents in Ponkan (*Citrus reticulata Blanco*). – Engei Gakkai Zasshi 65: 513-523.

http://www.aloki.hu ● ISSN 1589 1623 (Print) ● ISSN 1785 0037 (Online)
DOI: http://dx.doi.org/10.15666/aeer/2001_413430

[36] Michelot, A., Simard, S., Rathgeber, C., Dufrene, E., Damesin, C. (2012): Comparing the intra-annual wood formation of three European species (*Fagus sylvatica*, *Quercus petraea* and *Pinus sylvestris*) as related to leaf phenology and non-structural carbohydrate dynamics. – Tree Physiology 32(8): 1033-1045.
[37] Mudrák, O., Fajmon, K., Jongepierová, I., Prach, K. (2017): Mass effects, clonality, and phenology but not seed traits predict species success in colonizing restored grasslands. – Restoration Ecology 26: 489-496.
[38] Myers, J. A., Kitajima, K. (2007): Carbohydrate storage enhances seedling shade and stress tolerance in a neotropical forest. – Journal of Ecology 95: 383-395.
[39] Nathan, G. M., Sevanto, S. (2010): The mechanisms of carbon starvation: how, when, or does it even occur at all? – New Phytologist 186: 264-266.
[40] Ooi, J. L. S., Kendrick, G. A., Van Niel, K. P. (2011): Effects of sediment burial on tropical ruderal seagrasses are moderated by clonal integration. – Continental Shelf Research 31: 1945-1954.
[41] Orthen, B., Wehrmeyer, A. (2004): Seasonal dynamics of non-structural carbohydrates in bulbs and shoots of the geophyte *Galanthus nivalis*. – Physiol Plantarum 120: 529-536.
[42] Packer, J. G., Meyerson, L., Skálová, H., Pyšek, P., Kueffer, C. (2017): Biological Flora of the British Isles: *Phragmites australis*. – Journal of Ecology 105: 1123-1162.
[43] Petrussa, E., Boscutti, F., Vianello, A., Casolo, V. (2018): 'Last In-First Out': Seasonal variations of non-structural carbohydrates, glucose-6-phospate and ATP in tubers of two Arum species. – Plant Biology 20: 346-356.
[44] Piper, F. I., Fajardo, A., Hoch, G. (2017): Single-provenance mature conifers show higher non-structural carbohydrate storage and reduced growth in a drier location. – Tree Physiology 37: 1001-1010.
[45] Portela, R., Barreiro, R., Roiloa, S. R. (2018): Biomass partitioning in response to resources availability: A comparison between native and invaded ranges in the clonal invader Carpobrotus edulis. – Plant Species Biology 34: 11-18.
[46] Pramanik, M. H. R., Shelley, I. J., Adhikary, D., Islam, M. O. (2016): Carbohydrate reserve and aerenchyma formation enhance submergence tolerance in rice. – Progressive Agriculture 27: 256-264.
[47] Purdy, S. J., Maddison, A. L., Cunniff, J., Donnison, I., Clifton-brown, J. (2015): Non-structural carbohydrate profiles and ratios between soluble sugars and starch serve as indicators of productivity for a bioenergy grass. – Aob Plants 7: 032-042.
[48] Qin, X., Feng, L., Chen, X., Xie, Y. (2013): Growth responses and non-structural carbohydrates in three wetland macrophyte species following submergence and de-submergence. – Acta Physiol. Plant. 35: 2069-2074.
[49] Quentin, A. G., Pinkard, E. A., Ryan, M. G., Tissue, D. T., Baggett, L. S., Adams, H. D., Gibon, Y. (2015): Non-structural carbohydrates in woody plants compared among laboratories. – Tree Physiology 35: 1146-1165.
[50] Regier, N., Streb, S., Zeeman, S. C., Frey, B. (2010): Seasonal changes in starch and sugar content of poplar (*Populus deltoides* x nigra cv. Dorskamp) and the impact of stem girdling on carbohydrate allocation to roots. – Tree Physiology 30: 979-987.
[51] Reis, V., Hermoso, V., Hamilton, S. K., Ward, D., Fluet-Chouinard, E., Lehner, B., Linke, S. (2017): A global assessment of inland wetland conservation status. – Bioscience 67: 523-533.
[52] Sala, A., Woodruff, D. R., Meinzer, F. C. (2012): Carbon dynamics in trees: feast or famine? – Tree Physiology 32: 764-775.
[53] Savage, J. A., Clearwater, M. J., Haines, D. F., Klein, T., Mencuccini, M., Sevanto, S., Turgeon, R., Zhang, C. (2015): Allocation, stress tolerance and carbon transport in plants: how does phloem physiology affect plant ecology? – Plant Cell Environ 39: 709-725.
[54] Schaberg, P. G., Snyder, M. C., Shane, J. B., Donnelly, J. R. (2000): Seasonal patterns of carbohydrate reserves in red spruce seedlings. – Tree Physiology 20: 549-555.

http://www.aloki.hu ● ISSN 1589 1623 (Print) ● ISSN 1785 0037 (Online)
DOI: http://dx.doi.org/10.15666/aeer/2001_413430

[55] Sevanto, S., McDowell, N. G., Dickman, L. T., Pangie, R., Pockman, W. T. (2013): How do trees die? A test of the hydraulic failure and carbon starvation. – Plant Cell & Environment 37: 153-161.
[56] Shi, P. L., Körner, C., Hoch, G. (2006): End of season carbon supply status of woody species near the tree line in western China. – Basic & Applied Ecology 7: 370-377.
[57] Shi, C. G., Silva, L. C. R., Zhang, H. X., Zheng, Q. Y., Xiao, B. X., Wu, N., Sun, G. (2015): Climate warming alters nitrogen dynamics and total non-structural carbohydrate accumulations of perennial herbs of distinctive functional groups during the plant senescence in autumn in an alpine meadow of the Tibetan Plateau, China. – Agricultural and Forest Meteorology 200: 21-29.
[58] Sørensen, S. T., Campbell, M. L., Duke, E., Manley-Harris, M. (2018): A standard, analytical protocol for the quantitation of non-structural carbohydrates in seagrasses that permits inter-laboratory comparison. – Aquatic Botany 151: 71-79.
[59] Sun, X. M., He, M. Z., Zhou, B., Li, J. X., Chen, N. L. (2020): Non-structural carbohydrates and C:N:P stoichiometry of roots, stems, and leaves of *Zygophyllum xanthoxylon* in responses to xeric condition. – Arid Land Geography 44: 240-249.
[60] Svensson, B. M., Rydin, H., Carlsson, B. Å. (2013): Clonality in the plant community. – Veg Ecol Second Edition.
[61] Trifilò, P., Casolo, V., Raimondo, F., Petrussa, E., Boscutti, F., Gullo, M. A. L., Nardini, A. (2017): Effects of prolonged drought on stem non-structural carbohydrates content and post-drought hydraulic recovery in *Laurus nobilis* L.: The possible link between carbon starvation and hydraulic failure. – Plant Physiol Biochem 120: 232-241.
[62] Tursun, N., Seyithanoglu, M., Uygur, F. N. (2011): Seasonal dynamics of soluble carbohydrates in rhizomes of *Phragmites australis* and *Typha latifolia*. – Flora 206: 731-735.
[63] Veneklaas, E., J den Ouden, F. (2005): Dynamics of non-structural carbohydrates in two Ficus species after transfer to deep shade. – Environmental & Experimental Botany 54: 148-154.
[64] Wan, J. Z., Wang, C. J., Yu, F. H. (2019): Large-scale environmental niche variation between clonal and non-clonal plant species: Roles of clonal growth modules and ecoregions. – The Science of the Total Environment 652: 1071-1076.
[65] Wang, B., Jiang, Y., Wang, M. C., Dong, M. Y., Zhang, Y. P. (2015): Variations of non-structural carbohydrate concentration of *Picea meyeri* at different elevations of Luya Mountain, China. – Chinese Journal of Plant Ecology 39: 746-752.
[66] Wang, S., Ding, Y., Lin, S., Ji, X., Zhan, H. (2015): Seasonal changes of endogenous soluble sugar and starch in different developmental stages of *Fargesia yunnanensis*. – Journal of Wood Science 62: 1-11.
[67] Würth, M. K. R., Peláez-Riedl, S., Wright, S. J., Körner, C. (2004): Non-structural carbohydrate pools in a tropical forest. – Oecologia 143: 11-24.
[68] Xiao, Y. A., Dong, M., Wang, N., Lan, L. L. (2015): Effects of modules removal on trade-offs between sexual and clonal reproduction in the stoloniferous herb *Duchesnea indica*. – Plant Species Biology 31: 50-54.
[69] Xiao, L., Liu, G. B., Li, P., Xue, S. (2017): Responses of photosynthesis and non-structural carbohydrates of *Bothriochloa ischaemum* to doubled CO_2 concentration and drought stress. – Journal of Plant Nutrition and Fertilizer 23: 389-397.
[70] Yin, J. J., Guo, D. L., He, S. Y., Zhang, L. (2009): Non-structural carbohydrate, N, and P allocation patterns of two temperate tree species in a semi-arid region of Inner Mongolia. – Acta Scientiarum Naturalium Universitatis Pekinensis 45: 519-527.
[71] Yu, D. P., Wang, Q. W., Liu, J. Q., Zhou, W. M., Qi, L., Wang, X. Y., Zhou, L., Dai, L. M. (2014): Formation mechanisms of the alpine Erman's birch (*Betula ermanii*) treeline on Changbai Mountain in Northeast China. – Trees 28: 935-947.

http://www.aloki.hu ● ISSN 1589 1623 (Print) ● ISSN 1785 0037 (Online)
DOI: http://dx.doi.org/10.15666/aeer/2001_413430

[72] Zhou, Y., Jiao, L., Qin, H. J., Li, F. (2022): Effect of Environmental Stress on the Nutrient Stoichiometry of the Clonal Plant *Phragmites australis* in Inland Riparian Wetlands of Northwest China. – Frontiers in Plant Science 12: 705319.
[73] Zhu, B. J., Yin, B. F., Zhang, Y. M. (2017): Seasonal dynamics of non-structural carbohydrate contents of *Syntrichia caninervis* among different microhabitats. – Journal Desert Research 37: 268-275.

http://www.aloki.hu ● ISSN 1589 1623 (Print) ● ISSN 1785 0037 (Online)
DOI: http://dx.doi.org/10.15666/aeer/2001_413430

GRAIN STARCH ESTIMATION USING HYPERSPECTRAL DATA AND ITS RELATIONSHIP WITH LEAF WATER CONTENTS FOR BROOMCORN MILLET (*PANICUM MILIACEUM* L.)

WANG, J. J.[1] – TIAN, X.[1] – CHEN, L.[1] – WANG, H. G.[1] – CAO, X. N.[1] – QIN, H. B.[1] – LIU, S. C.[1] – FAHAD, S.[2] – QIAO, Z. J.[1*]

[1]*Center for Agricultural Genetic Resources Research, Shanxi Agricultural University/Key Laboratory of Crop Gene Resources and Germplasm Enhancement on Loess Plateau, Ministry of Agriculture/Shanxi Key Laboratory of Genetic Resources and Genetic Improvement of Minor Crops, Taiyuan, China*
(phone: +86-152-3404-0919)

[2]*Institute of Molecular Biology and Biotechnology, The University of Lahore, Lahore, Pakistan*

**Corresponding author*
e-mail: nkypzs@126.com; phone: +86-139-3422-3541

(Received 9th Aug 2021; accepted 23rd Nov 2021)

Abstract. The analysis of grain starch content is one of the main indices to determine crop quality. The experiment was performed using two broomcorn millet varieties (Neimi 2 and Ningmi 14) in northern China, having 5 different sowing dates. The prediction models for grain starch fraction were constructed by integrating the spectral models and grain starch content with leaf water content using the intersection approach. We have identified 468, 630, 806, and 1488 nm as characteristic bands of the first derivative spectrum having a positive correlation. The correlation coefficient between the vegetation index of 608 nm and 1488 nm was significantly higher than other characteristic bands regarding leaf water contents. It is therefore identified that RDVI (1488, 806) could be used effectively to monitor leaf water content of broomcorn millet under different sowing date treatments, $R^2 = 0.7075$, RMSE = 0.073, RPD = 1.430 in the calibration set, $R^2 = 0.8458$, RMSE = 0.042, RPD = 2.546 in the validation set. In addition, the monitoring models of RVI (1488, 806), RDVI (1488, 806), and PVI (1488, 806) were superior to other models, and RPD was 0.020, 1.978, and 1.904, respectively. Overall, the RDVI (1488, 806) monitoring model, due to its stability and higher accuracy provided precise data on the grain starch fraction of broomcorn millet.
Keywords: *sowing dates, vegetation index, crop, agronomic parameters, remote sensing*

Introduction

Prolonged or transient water stress negatively affects crop growth and development, leading to crop yield and quality reductions (Jackson et al., 1982; Gupta et al., 2020; Hunter et al., 2021; García-León et al., 2021). It has been reported that cereal crops under water stress conditions tend to accumulate compatible solutes of osmolytes to counter osmotic imbalance and reduce water potential (Shafiq et al., 2018). A significant part of photosynthates is diverted towards roots to counter water imbalance and to tolerate drought stress. The ultimate result is a reduction in starch accumulation and its composition due to imbalanced photoassimilate transport (Prathap et al., 2019). Therefore, the analysis of grain starch content is one of the important indexes to evaluate its quality. The grain starch content directly affects its taste quality and processing quality, such as flavor, gelatinization temperature, etc. With the improvement of people's living standards, people have higher and higher requirements for quality, so it is particularly important to study the starch content of broomcorn millet.

http://www.aloki.hu ● ISSN 1589 1623 (Print) ● ISSN 1785 0037 (Online)
DOI: http://dx.doi.org/10.15666/aeer/2001_431445

Broomcorn millet also called proso millet, is a minor cereal crop mainly cultivated in dry and nutrient-poor soils by poor farmers. It is essential to mention here that millets are small-seeded annual cereals. About 20 different species are cultivated globally for food, forage, and fuel purposes, feeding about one-third of the global population (Fuller, 2006; Amadou et al., 2013; Changmei and Dorothy, 2014). Millets can grow on relatively less productive soils and serve as an essential food source to counter food insecurity. The broomcorn millet (*Panicum miliaceum*) has a somewhat shorter growing season of about 60-100 days (Habiyaremye et al., 2017) and was a warm-season grass member from the PACCAD (Panicoideae, Arundinoideae, Chloridoideae, Centothecoideae, Aristidoideae, Danthonioiseae) clade (GPWG, 2001) and is domesticated in China sometime around 10,000 BP (Before Present). Because of its strong drought resistance, barren tolerance, and shorter life cycle, some growers tend to cultivate this crop to compensate for the economic losses (Ravi, 2004; Brahmachari et al., 2019). Besides, the sowing time range for broomcorn millet is relatively broad; it has become an increasing trend to quickly and accurately obtain the starch content of the broomcorn millet for commercial harvests.

Different physiological plant indices, including leaf water contents, can be determined using hyperspectral data or a remote sensing approach (Miao et al., 2015; Han et al., 2018; Wang et al., 2019). The use of spectral features allows a non-destructive approach (Ding et al., 2004). to determine quality parameters possibly in less time and through eco-friendly method without using toxic dyes and chemicals. Numerous reports reported remote sensing of leaf water contents and grain protein contents from different crops (Wang et al., 2012, 2018; Hansen et al., 2002; Li et al., 2005; Feng et al., 2007; Caporaso et al., 2008; Onoyama et al., 2017; Marek et al., 2019). The research of spectral monitoring of leaf water content and grain quality by scholars at home and abroad is mainly focused on staple crops, but less research on broomcorn millet. Of different spectral studies of leaf water content, Ndlovu et al. (2021) reported that EWT (equivalent water thickness) and FMC (fuel moisture content) yielded the highest predictive performance and were the most optimal indicators of maize leaf water content. CAO et al. (2015) studied the normalized ratio (ND) type index dND (1415, 1530) and the simple ratio (SR) type index dSR (1530, 1895) based on the first derivative, which were the best for monitoring the relative water content (RWC) of all species. R^2 values are 0.95 and 0.97, respectively. Zhang et al. (2021) showed extreme random trees-x-loading weight (ERT-x-Lw) and difference vegetation index (DVI) (R1185, R1307) can effectively predict wheat leaf water content.

Of different spectral studies of grain starch, Kjær et al. (2016) sampled 60 potatoes from 10 varieties and used the hyperspectral reflectance to predict the starch content of potatoes. Similarly, Lu et al. (2017) found reported that the support vector regression principal component analysis (SVR-PCA) model can accurately detect grain starch content of rice, and the predicted coefficient of Determination (R^2) and root mean square error (RMSEP) were 0.991 and 0.669%, respectively. Likewise, Tian et al. (2004) suggested that the SPAD value, ratio index R(1500,610) and R(1220,560) of wheat leaves could predict the accumulation of grain starch during different growth stages of wheat. A linear discriminant analysis (LDA) normalized by the short-wave infrared spectrum was used to determine starch contents in rice (SEO et al., 2020). Other methods and validation techniques include the use of remote sensing images NDVI and climate environment data (Li et al., 2007), use of near-infrared spectral data (Zhao et al., 2011), and through model of support vector machine (SVM), stepwise

http://www.aloki.hu ● ISSN 1589 1623 (Print) ● ISSN 1785 0037 (Online)
DOI: http://dx.doi.org/10.15666/aeer/2001_431445

multiple linear regression (SMLR) and partial least squares method (PLS), R-SVM models (Wang et al., 2019).

The sowing dates and un-even quality of starch grains are two significant aspects of this study that will facilitate agronomic practices regarding broomcorn millet cultivation and harvest. Grain starch contents were determined using a non-destructive remote sensing approach. The quantitative relationship between leaf water content with canopy spectral parameters and grain starch content of broomcorn millet at each growth period under different sowing is presented here. Hence, the study provides the theoretical basis and technical support for remote sensing technology in broomcorn millet quality monitoring, management, and regulation of production. These findings are valuable and provide the technical basis for the utilization of hyperspectral technology towards precision agriculture.

Materials and methods

Experimental conditions

This study is a two-year study conducted from July 2019 to October 2019 and from July 2020 to October 2020. The experiment was carried out in Dingxiang County, Xinzhou (38°33′N, 112°54′E), Shanxi Province, China. The area was situated at an altitude of 780 m. During the experimental span, the annual rainfall was approx. 430 mm, the annual average temperature was 8.7 °C, the frost-free period was about 158 days, the annual sunshine hours was up to 2 734.6 h, and the temperature, light and heat resources were suitable for the growth and development of broomcorn millet. The mineral nutrient composition of the experimental soil is as follows; N (0.080%), P (12.4 mg kg^{-1}), K (114 mg kg^{-1}), organic matter percentage (13.7 g kg^{-1}), and soil pH of 8.09.

Introduction of broomcorn millet

Broomcorn millet is a short-day crop with strong photoperiod sensitivity, which can mature when the active accumulated temperature of ≥ 10°C is about 1000 °C, but the plant is short and yield is extremely low. In ancient times, broomcorn millet was often used as a disaster relief crop, when other crops could not be sown due to natural disasters, broomcorn millet was finally selected to sow. In northern China, the sowing period of broomcorn millet is relatively wide, usually from May to July, Therefore, the research results obtained by setting different sowing periods are more widely representative.

Experimental design

Through continuous cultivation experiment of broomcorn millet in Dingxiang County for many years, it was concluded that 10^{th} June was the best sowing date, because its yield was the highest. Therefore, the experiment took June 10 as the central point and set four sowing dates before and after it. The experimental treatments included five sowing dates (Factor-1) viz. B1 (10^{th} May 2019), B2 (25^{th} May 2019), B3 (10^{th} June 2019), B4 (25^{th} June 2019), and B5 (15th July 2019); and the second source of variation (Factor-2) included two broomcorn millet varieties P1 (Neimi 2) and P2 (Ningmi 14) respectively. The planting density was 60×10^4 seedlings hm^{-2} with a plot area of 30 m^2 (5 × 6 m) with row spacing of 30 cm. The experiment conducted using a randomized complete block design (RCBD) with three replications per treatment. The amount of fertilization is 120 kg hm^{-2} for pure N, 120 kg hm^{-2} for pure P_2O_5, and

http://www.aloki.hu ● ISSN 1589 1623 (Print) ● ISSN 1785 0037 (Online)
DOI: http://dx.doi.org/10.15666/aeer/2001_431445

90 kg hm^{-2} as pure K_2O. The soil type is loam, which has good aeration, water permeability, water and fertilizer conservation, water and fertilizer supply, and cultivation performance. This experiment is mainly used for the establishment of the model. Under the B1 and B2 planting conditions, the height of the millet plant is high due to early sowing, which leads to partial lodging during the dough period of the grain. Spectral measurement and sampling cannot be performed in 5 plots. P1 lodging was more serious than P2. Therefore, 145 spectral data, 145 leaf water content data and 30 grain starch content data were obtained in 3 repetitions, 128 spectral data and 30 grain starch content data were obtained by removing abnormal values.

From June 2020 to October 2020, the experimental design is the same as those of the experiment in 2019. This experiment is mainly used for the validation of the model, the repeated data were measured at jointing stage, booting stage, heading stage and maturity stage, a total of 40 spectral data and 40 leaf water content data were obtained, and 25 spectral data and corresponding leaf water content data were obtained by removing abnormal values to verify the monitoring model. 20 spectral data, 20 leaf water content data and 20 grain starch content data of corresponding maturity stage were obtained by measuring 2 repeated data at filling stage. 15 spectral data and corresponding leaf water content and grain starch content data were obtained by removing abnormal values, which were used to verify the monitoring model of grain starch content.

Canopy spectral reflectance

The canopy spectral reflectance of broomcorn millet was measured at the jointing stage, booting stage, heading stage, filling stage, and maturity stage of 5 sowing dates. Five points were measured from each plot. The measurements from each plot repeated five times, and the leaf water contents were determined simultaneously.

Determination of spectral reflectance and eco-physiological indices

Canopy spectrum

Canopy reflectance spectra were recorded at the jointing stage, booting stage, heading stage, filling stage, and maturity stages. The FieldSpec-4 back-mounted field hyperspectral radiometer was used for this purpose (American Analytical Spectral Device (ASD), USA). The band range used was 350-2500 nm, and the field of view angle was 25°; 350-1000 nm with a spectral sampling interval of 1.4 nm. The spectral resolution is 3 nm; the 1000-2500 nm spectral sampling interval is 2 nm, and the spectral resolution is 10 nm. The instrument was calibrated using a white standard white plate once every quarter. The canopy spectral of broomcorn millet was recorded from 10:00 AM to 2:00 PM; the sensor probe was vertically downward, and the vertical height from the top of the canopy is about 1.0 m. The standard whiteboard correction was carried out before and after the observation of each group of targets. A total of five points were measured from each plot. In addition, the measurement of each point was repeated five times, and average values were processed. It is pertinent to mention here that this experiment was used for the establishment of the model. Under the B1 and B2 planting conditions, the height of the millet plant was higher due to early sowing, which caused partial lodging during the dough period of the grain. Spectral measurement and sampling could not be performed in 5 plots. P1 lodging was more severe than P2. In the determination of spectral data, the spectral data sometimes become abnormal due to the environment, the instrument itself, and lodging in the late stage of broomcorn millet

http://www.aloki.hu ● ISSN 1589 1623 (Print) ● ISSN 1785 0037 (Online)
DOI: http://dx.doi.org/10.15666/aeer/2001_431445

plant. Because the anomalous spectral values differ greatly from the standard spectral values, these data are removed. Therefore, 145 spectral data, 145 leaf water content data, and 30-grain starch content data were obtained in 3 repetitions, 128 spectral data and 30-grain starch content data were obtained by removing abnormal values.

Determination of leaf water content

Leaf water contents were calculated using the methodology of González and González-Vilar (2001). Fresh leaves from each treatment were selected, and fresh weight was recorded (FW). Afterward, the leaves were oven-dried at 105 °C for 30 min and dried at 75 °C for 24 h to constant weight. The leaf water contents were then calculated using this formula:

$$\text{Leaf water content} = (\text{leaf fresh weight} - \text{leaf dry weight}) / \text{leaf fresh weight} \times 100$$

Quantitative determination of grain starch using anthrone reagent

The soluble sugar and starch were separated by using 80% ethanol. After that, the starch was further decomposed into glucose by acid hydrolysis. The glucose content was determined using an anthrone reagent (Dubois et al., 1956) at 560 nm using a SP-756P UV-Vis spectrophotometer (Shanghai Spectrometer Co., Ltd).

Vegetation index

To enhance the sensitivity to biophysical parameters, biochemical parameters, and other ecological function parameters, many dual-channel or multi-channel spectral indices have been developed and successfully used for biomass, leaf area index, chlorophyll and nitrogen. We used previous analytical data/research results in the present study, combined with the instrument characteristics and the research focus to summarize several characteristic spectral parameters reported (*Table 1*).

Table 1. *Algorithm and references of different spectral parameters*

Spectral parameter	Abbreviation	Algorithm	Reference
Reflectance	R_λ	–	Cropscan (2000)
Ratio vegetation index	RVI	R_{NIR}/R_{Red}	Pearson et al (1972)
Difference vegetation index	DVI	$R_{NIR}-R_{Red}$	Jordan (1969)
Normalized difference vegetation index	NDVI	$R_{NIR}-R_{Red}/R_{NIR}+R_{Red}$	Rouse et al. (1974)
Perpendicular vegetation index	PVI	$(R_{NIR}-aR_{Red}-b)/\sqrt{1+a^2}$ a=10.489, b=6.604	Richardson et al. (1977)
Enhanced vegetation Index	EVI	$2.5\times(R_{NIR}-R_{Red})/(R_{NIR}+6.0R_{Red}-7.5R_{Blue}+1)$	Chen et al. (2005)
Soil adjusted vegetation index	SAVI	$(1+L)(R_{NIR}-R_{Red})/(R_{NIR}+R_{Red}+L)$ L=0.5	Huete et al. (1988)
Optimized soil-adjusted vegetation index	OSAVI	$(1+0.16)(R_{800}-R_{670})/(R_{800}-R_{670}+0.16)$	Ronddeaux et al. (1996)
Renormalized difference vegetation index	RDVI	$\sqrt{NDVI \times DVI}$	Roujean et al. (1995)

R is reflectance

http://www.aloki.hu ● ISSN 1589 1623 (Print) ● ISSN 1785 0037 (Online)
DOI: http://dx.doi.org/10.15666/aeer/2001_431445

Derivation and validation of statistical models

This experiment used 2019 test data to construct a monitoring model and used 2020 test data to test and verify the above monitoring models. The accuracy and applicability of the model were evaluated by the statistical parameters such as coefficient of Determination (R^2), root mean squared error (RMSE), and residual prediction difference (RPD) of the predicted and measured values. If the R^2 is closer to 1, the RMSE is smaller, indicating that the model has better prediction accuracy. When RPD > 2, the model has good prediction ability. When 1.4 < RPD < 2, the model has medium prediction ability, when RPD < 1.4, the model has poor prediction ability and vice versa. A 1:1 relationship diagram is drawn between the predicted value and the measured value to show the fit and reliability of the monitoring model visually.

$$R^2 = 1 - \frac{\sum_{i=1}^{n}(Y_i - Y_i')/(n-p-1)}{\sum_{i=1}^{n}(Y_i - Y_i')^2/(n-1)}$$

$$\mathrm{RMSE} = \sqrt{\frac{1}{n}\sum_{i=1}^{n}(Y_i - Y_i')^2}$$

$$\mathrm{RPD} = \frac{\mathrm{SD}}{\mathrm{RMSE}}$$

where n is the number of samples, p is the number of variables entering the model, Y_i' and Y_i are the predicted values and the measured values, respectively, SD (standard deviation) is the standard deviation of the measured values.

Statistical analyses

The collected data was initially processed to remove abnormal values and then analyzed using SPSS 19.0 software. The Matlab (7.0) software was used to analyze the correlation between the original and first-order differential bands and their relationship with the leaf water contents. Finally, the spectral data were processed by first-order differential and Savitsky Golay smoothing by unscrambler 9.7, and data for various figures was processed using MS Excel and Origin8.

Results

Spectral characteristic analysis

As the spectral vegetation index calculated by visible light and near-infrared light, the spectral band of 400-1500 nm was selected for data analysis. The sensitive area of the original spectrum was mainly concentrated in 400-500 nm, and the range is relatively narrow; the sensitive area of the first derivative is concentrated in the whole range of 400-1500 nm (*Fig. 1*). So the spectral band of the first derivative is selected to construct the vegetation index, and the bands with good correlation with leaf water content (LWC) were selected for data analysis. Following bands at 468, 630, 806, and 1488 nm were identified as the characteristic bands of the first derivative spectrum, the correlation coefficients were -0.548, - 0.518, - 0.724, and -0.5581, respectively.

http://www.aloki.hu ● ISSN 1589 1623 (Print) ● ISSN 1785 0037 (Online)
DOI: http://dx.doi.org/10.15666/aeer/2001_431445

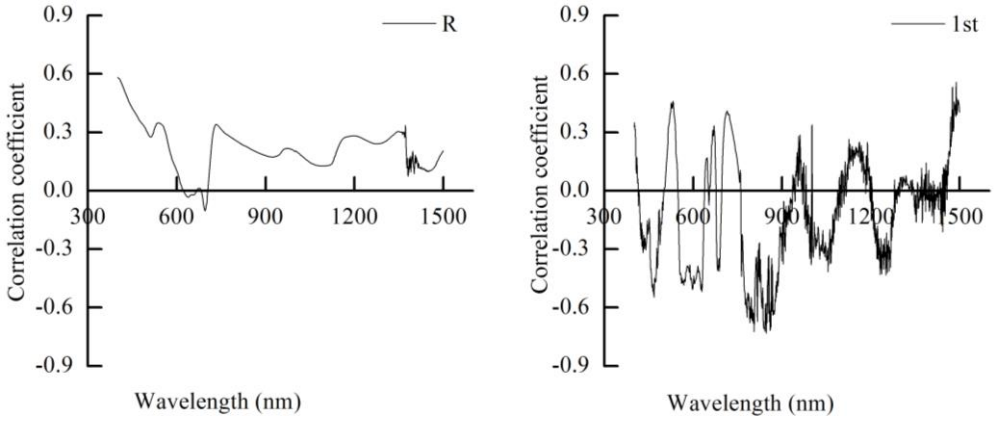

Figure 1. *Relationship between leaf water content and canopy spectral reflectance of broomcorn millet - First derivative spectral*

Canopy spectral variation patterns of broomcorn millet

It can be seen from *Figure 2* that under different sowing dates (B1-B5), the comparative canopy spectral reflectance of both the two kinds of broomcorn millet varieties was the same. It varied significantly among different growth stages. *Figure 2A* shows the spectral reflectance of P1B3 in different growth periods. The canopy spectral reflectance of P1B3 indicated an absorption valley (lower reflectance) near 680 nm in the red light band, which is the absorption valley of photosynthetic pigments (*Fig. 2A*). A decrease in the absorption in this range would be an indicator of broomcorn millet reaching maturity. However, a smaller reflection peak near 540 nm could be evident due to the relatively small chlorophyll absorption. The canopy spectral reflectance at the heading stage was significantly higher than other growth stages (*Fig. 2A*). Besides, the canopy spectral reflectance of P1 and P2 varieties shows the same phenomenon. The canopy spectral reflectance of B2 was the highest and the B3 was the second, while the least values were recorded in B5 (*Fig. 2B, C*).

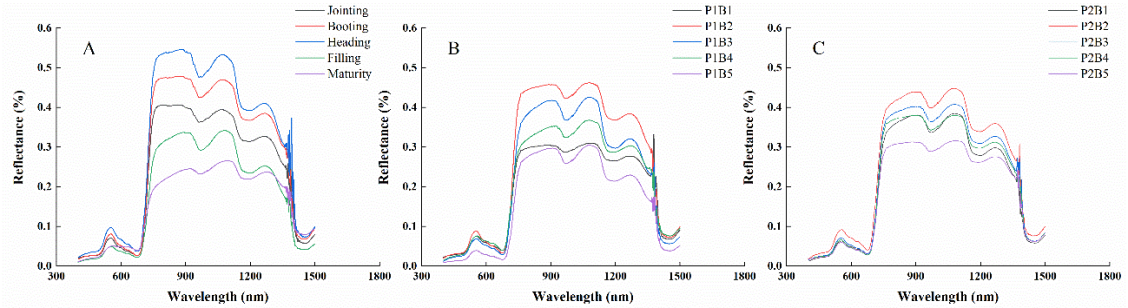

Figure 2. *Spectral characteristics of broomcorn millet at different sowing date and growing stage combinations*

Relationship between leaf water contents and canopy spectral parameters

Based on the calculation of leaf water content and corresponding different spectral indexes at the filling stage under five sowing dates, the RVI, DVI, NDVI, and some common vegetation indexes were used as the variable x. The leaf water content was

http://www.aloki.hu ● ISSN 1589 1623 (Print) ● ISSN 1785 0037 (Online)
DOI: http://dx.doi.org/10.15666/aeer/2001_431445

used as the variable y for correlation analysis. The results showed that the vegetation index composed of 806 and 1488 nm characteristic bands was better than other band combinations. The vegetation index composed of RVI, NDVI, SAVI, DVI, OSAVI, RDVI, EVI, and PVI significantly positively correlated with leaf water contents to sowing dates. The above spectral index and leaf water content were correlated and fitted; the spectral index, regression equation, R^2, RMSE, and RPD indicated good correlation (*Table 2*). Except for EVI and PVI, the vegetation index of RPD in the modeling set was higher than 1.4, indicating good prediction ability. The SAVI model was the best based on the R^2 value, which was higher than other models (the RMSE model exhibited lease value). The evaluation index parameters of RDVI model accuracy were not significantly different from SAVI. The RPD of SAVI, OSAVI, DVI, and RDVI were higher than 2.0, indicating that the model has good prediction ability, the RDVI model is the best, R^2 was 0.8458 and RMSE was the best 0.042. The results also depicted that RDVI (1488,806) could predict leaf water contents.

Table 2. *Fitting (n = 128) and validation (n = 25) models of hyperspectral in leaf water content*

Model type	Calibration set				Validation set			
	Equation	R^2	RMSE	RPD	Equation	R^2	RMSE	RPD
NDVI (1488,806)	y = 0.9331x + 0.0533	0.702	0.074	1.415	y = 1.0042x + 0.0002	0.7203	0.056	1.888
SAVI (1488,806)	y = 0.9161x + 0.0653	0.7121	0.073	1.434	y = 1x − 4E − 05	0.7665	0.051	2.069
OSAVI (1488,806)	y = 0.929x + 0.0555	0.7017	0.074	1.415	y = 1x + 9E − 06	0.7661	0.052	2.068
DVI (1488,806)	y = 0.939x + 0.0491	0.6984	0.074	1.408	y = 1x + 5E − 05	0.7664	0.051	2.069
RDVI (1488,806)	y = 0.9347x + 0.0514	0.7075	0.073	1.430	y = 1x + 6E − 06	0.8458	0.042	2.546
RVI (1488,806)	y = 0.9077x + 0.0736	0.7114	0.074	1.422	y = 0.9805x + 0.0195	0.7521	0.053	1.996
EVI (1488,806,468)	y = 0.9431x + 0.0476	0.6612	0.079	1.328	y = 1.0624x − 0.0471	0.7291	0.056	1.911
PVI (1488,806)	y = 0.9511x − 0.038	0.6506	0.080	1.316	y = 1x + 0.007	0.6843	0.060	1.768

Quantitative relationship between leaf water content and grain starch content of broomcorn millet

The delay in the sowing date caused a reduction in grain starch contents of the broomcorn millet (*Fig. 3*). The grain starch contents of P1B1 were 15.8% higher than P1B5, and of P2B1 were 13.6% higher than that of P2B5, respectively. A regression model is established that suggested a strong correlation between leaf water contents and grain starch contents at the grain filling stage (R^2 = 0.8125; *Table 3*).

Table 3. *Monitoring models of grain starch content based on leaf water content at different growth stages (n = 95)*

Growth stage	Equation	R^2
Jointing	Y = −451.59X + 1046.9	0.1998
Booting	Y = −349.95X + 951.77	0.2177
Heading	Y = −250.73X + 858.07	0.7472
Filling	Y = −214.55X + 805.2	0.8125
Maturity	Y = −231.14X + 803.47	0.7535

http://www.aloki.hu ● ISSN 1589 1623 (Print) ● ISSN 1785 0037 (Online)
DOI: http://dx.doi.org/10.15666/aeer/2001_431445

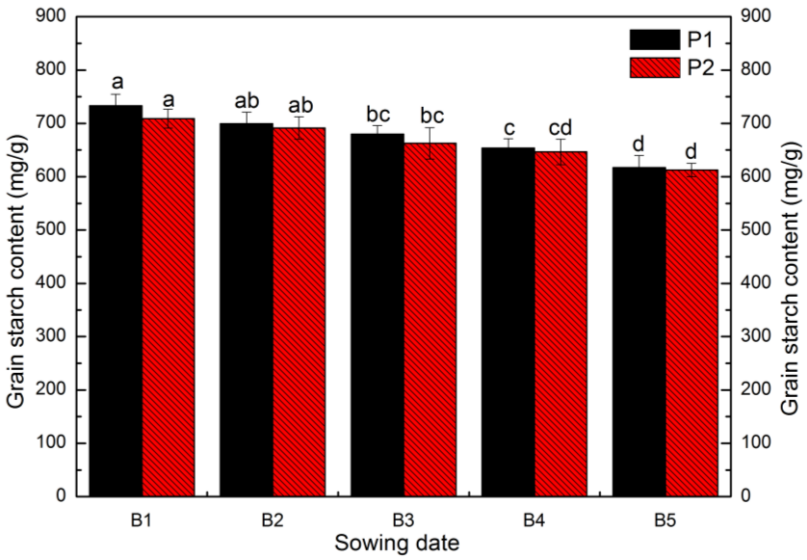

Figure 3. *The effects of different sowing dates on grain starch content of broomcorn millet varieties*

Validation of remote sensing monitoring model

The maximum correlation between leaf water content and grain starch content of broomcorn millet was recorded during the filling stage. In combination with the spectral monitoring model of leaf water content (*Tables 2* and *3*), the hyperspectral data were used to derive monitoring model equations for real-time Determination of grain starch contents (*Table 4*).

Table 4. *Forecasting models of grain starch content (y) to key spectral parameters (x) at leaf water content*

Model type	Equation
NDVI (1488,806)	$y = -214.55 \times (0.9331NDVI + 0.0533) + 805.2$
SAVI (1488,806)	$y = -214.55 \times (0.9161SAVI + 0.0653) + 805.2$
OSAVI (1488,806)	$y = -214.55 \times (0.929OSAVI + 0.0555) + 805.2$
DVI (1488,806)	$y = -214.55 \times (0.939DVI + 0.0491) + 805.2$
RDVI (1488,806)	$y = -214.55 \times (0.9347RDVI + 0.0514) + 805.2$
RVI (1488,806)	$y = -214.55 \times (0.9077RVI + 0.0736) + 805.2$
EVI (1488,806,468)	$y = -214.55 \times (0.9431EVI + 0.0476) + 805.2$
PVI (1488,806)	$y = -214.55 \times (0.9511PVI - 0.038) + 805.2$

The test data of the last growing season-2020 was used to validate the derived above equations using RMSE, $R^{2,}$ and RPD parameters. Finally, a linear relationship between the measured and predicted values was used to determine experimental indices (*Fig. 4*). Only the RPD of RVI (1488, 806) was 2.0, which indicated good predictive ability. The RMSE remained at least 15.656 and $R^2 = 0.8436$; the R^2 value of PVI was the largest, which is 0.8684, but the RPD value remained 1.904, which may be caused by the significant standard deviation between measured and predicted value. The RPD and

http://www.aloki.hu ● ISSN 1589 1623 (Print) ● ISSN 1785 0037 (Online)
DOI: http://dx.doi.org/10.15666/aeer/2001_431445

RMSE of RDVI (1488, 806) were 1.978 and 15.988, respectively, second only to RVI (1488 and 806); $R^2 = 0.7694$. Conclusively, the validation of the monitoring model, R^2 and RPD of different treatments were all above 0.65 and 1.4, respectively, which also indicated that it is feasible to predict the grain starch contents of broomcorn millet simply from the canopy spectrum using leaf water contents.

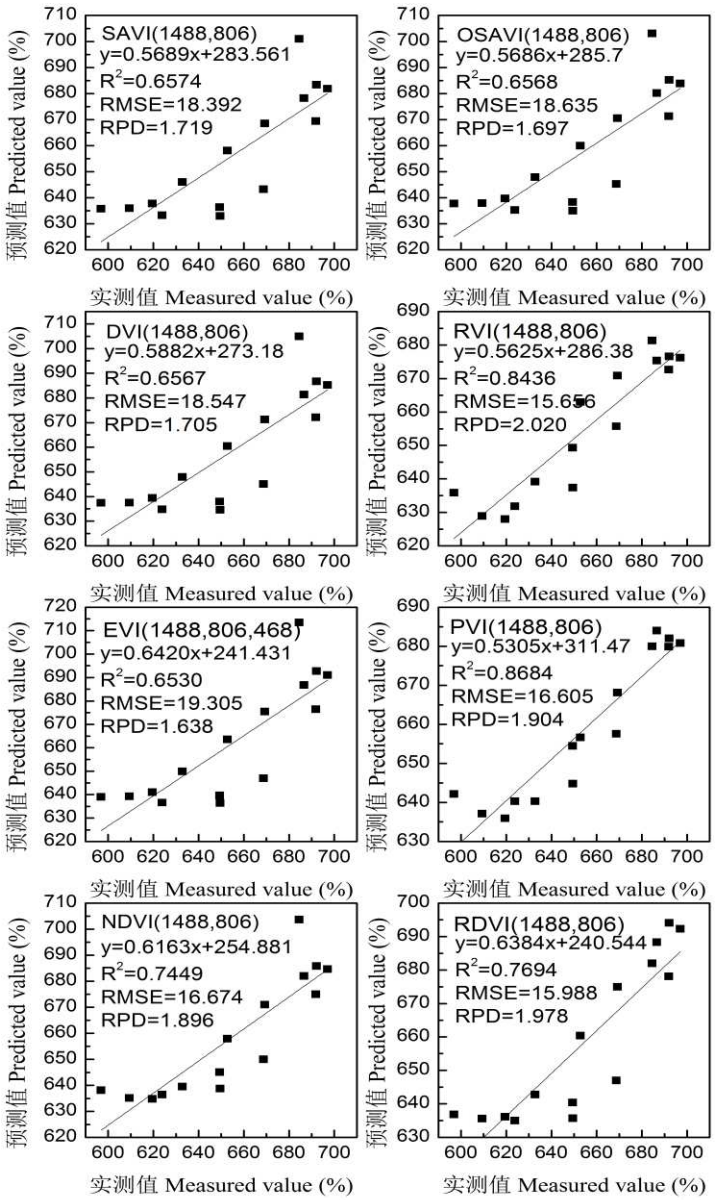

Figure 4. *The correlation between estimated and measured grain starch content with leaf water content (n = 25)*

Discussion

Remote sensing is an effective technology that enables fast, large-scale, and non-destructive testing with high spectral resolution through continuous wave band and imaging. In this study, the agronomic parameters were used as identification criteria to

http://www.aloki.hu ● ISSN 1589 1623 (Print) ● ISSN 1785 0037 (Online)
DOI: http://dx.doi.org/10.15666/aeer/2001_431445

integrate and predict grain starch contents of field-grown broomcorn millet via spectral remote sensing. A prediction model of grain starch content of broomcorn millet was established based on characteristic spectral parameters. The results showed that leaf water content could predict grain starch content accurately. The correlation between the first derivative and leaf water content was better than the original spectral band; the sensitive bands were 455~480 nm, 516~634 nm, 768~890 nm, and 1474~1500 nm. In this context of the recent development in chemometrics, accurately mining and correct extraction of spectral parameters is an important area in spectroscopy research. The derivative, least square method, normalization, baseline correction, and multivariate scattering correction methods are commonly used to correct the original spectral data. To a certain extent, the first derivative spectral band is better than the original spectral band, which is similar to previous results (Liang et al., 2013; Xie et al., 2020).

Leaf water content is an agronomic index to characterize the average growth and drought monitoring of plants. Among the spectral parameters related to leaf water content, the vegetation index constructed by visible light (400~780 nm) and near-infrared light (780~1350 nm) is used to monitor the leaf water content of plants. Recently, the DVI model used for the estimation of winter wheat leaf water content with an R^2 value of 0.886 was best compared with NDVI and RVI (Jin et al., 2020). Chen et al. (2020) also reported that the water content of leaf could be predicted using normalized difference (NDSI), ratio spectral index (RSI), partial least square regression (PLSR), and competitive adaptive reweighted sampling partial least square regression (CARS-PLSR). It was concluded that the accuracy and modeling accuracy of CARS-PLSR was highest, which quickly and accurately predicted leaf water contents of winter wheat. Various other studies used hyperspectral reflectance coupled with a modeling approach to predict leaf water contents (Xu et al., 2018; Hasan et al., 2018) using partial least squares regression (PLSR), BP neural network (ANN), RMSE, and RPD, respectively.

Xu et al. (2018) pointed out that the difference vegetation index DDV (833 and 236 nm) constructed by the first derivative could better predict the leaf water content of rice. Hasan et al. (2018) used the partial least squares regression (PLSR) model and BP neural network (ANN) model to monitor spring wheat leaf water content, partial least squares regression (PLSR) model. Based on the first derivative, could accurately monitor spring wheat leaf water content, and R^2, RMSE and RPD were 0.80, 0.55, and 2.01. It can be seen that the prediction accuracy of leaf water content in response to the vegetation index of the same crop or different crops under different treatment conditions is different. The results also depicted that the vegetation index RDVI (1488, 806) composed of 608 nm and 1488 nm could better predict the leaf water content of broomcorn millet under different sowing dates.

Nonetheless, the inconsistency of crop leaf water content monitoring models may be caused by different crop-specific leaf spectral reflectance, cultivation pattern measures, and edaphic factors. Therefore, different crop spectral monitoring models can be is crop and environment-specific. Here in this study, canopy spectral reflectance at the heading stage was significantly higher than that at other growth stages mainly because the population of broomcorn millet grew well at the flowering stage and was in the critical period of transformation from vegetative to reproductive growth. While the leaves at the maturity stage turned yellow and did not have the spectral characteristics of green vegetation, the reflectance was the lowest. Furthermore, the R^2 value of only 0.1998 at the jointing stage was recorded. In the early growth stage of broomcorn millet, obtained

http://www.aloki.hu ● ISSN 1589 1623 (Print) ● ISSN 1785 0037 (Online)
DOI: http://dx.doi.org/10.15666/aeer/2001_431445

nutrients only accumulate in the leaves and stem sheaths and cannot form an apparent relationship with the grain nutrients. With the continuous progress of the growth period, the vegetative growth is gradually transformed into reproductive growth, which gradually enhanced the correlation between the leaves and grain nutrients.

The vegetation index composed of 806 and 1488 nm characteristic bands was better than that of other band combinations, and there was a very significant positive correlation with leaf water content. RDVI (1488, 806) can better predict broomcorn millet leaf water content under different sowing dates. R^2 of the calibration set is 0.7075, RMSE = 0.073, RPD = 1.430; R^2 of the validation set is 0.8458, RMSE = 0.042, RPD = 2.546. The correlation between leaf water content and grain starch content was the best, $R^2 = 0.8125$, which could be used as a bridge to establish a hyperspectral monitoring model of grain starch content. Among the established models, the monitoring models of RVI (1488, 806), RDVI (1488, 806), and PVI (1488, 806) are better than other models, and the RPD were 0.020, 1.978, and 1.904, respectively.

In agreement with this study, amylase contents from rice can be accurately predicted using the difference vegetation index DVI and the ratio vegetation index RVI (Xie et al., 2012, 2020). Similarly, Wang et al. (2013) showed that NDVI (670,1200) accurately predicted starch accumulation in winter wheat ($R^2 = 0.9542$). Li et al. (2007) also showed that NDVI of satellite remote sensing images could accurately predict winter wheat grain starch content. It is essential to mention here that NDVI and DVI can indicate grain starch content of different crops than other vegetation plants, consistent with the optimal vegetation plant for monitoring grain starch content in this study. Our results showed that RDVI (1488, 806) monitoring model had strong stability and high accuracy, which quickly and non-destructively monitored grain starch content of broomcorn millet. The RDVI was calculated from the formula of NDVI and DVI, which represented the differences among all information data to a certain extent. Above all, the spectral vegetation indexes comprised of visible light and near-infrared light, NDVI, DVI, and RDVI can accurately, quickly, and non-destructively monitor grain starch content of different crops than other vegetation indexes.

Conclusions

The R^2, RMSE, and RPD of the hyperspectral monitoring model for leaf water content and grain starch content of broomcorn millet were positively connected. We conclude that the monitoring model of RDVI (1488, 806) had strong stability and high accuracy and could quickly and non-destructively monitor the leaf water content and grain starch content of broomcorn millet. This study mainly considered the effects of different sowing dates and varieties on broomcorn millet grain content but did not fully consider other elements such as fertilizers and water. So more comprehensive and more research is needed. Therefore, the monitoring model needs to be further tested and improved by multi-point experiments and large-scale planting to provide a more accurate theoretical basis for monitoring the leaf water content of broomcorn millet and grain starch content.

Acknowledgements. This work was supported by applied basic study plan of Shanxi Province (201901D21156), China Agriculture Research System of MOF and MARA, MOA Conservation and utilization of Crop Germplasm Resources Program (2019NWB036-20), National Crop Germplasm Resources Sharing Service Platform Shanxi crop germplasm resources platform (NCGRC-2020-26).

http://www.aloki.hu ● ISSN 1589 1623 (Print) ● ISSN 1785 0037 (Online)
DOI: http://dx.doi.org/10.15666/aeer/2001_431445

REFERENCES

[1] Amadou, I., Gounga, M. E., Le, G. W. (2013): Millets: nutritional composition, some health benefits and processing. A review. – Emirates Journal of Food & Agriculture 25: 501-508.
[2] Brahmachari, K., Sarkar, S., Santra, D. K., Maitra, S. (2019): Millet for food and nutritional security in drought prone and red laterite region of Eastern India. – Int J Plant Soil Sci 26(6): 1-7.
[3] Cao, Z. X., Wang, Q., Zheng, C. L. (2015): Best hyperspectral indices for tracing leaf water status as determined from leaf dehydration experiments. – Ecological Indicators 54: 96-107.
[4] Caporaso, N., Whitworth, M. B., Fisk, I. D. (2008): Protein content prediction in single wheat kernels using hyperspectral imaging. – Food Chemistry 240: 32-42.
[5] Changmei, S., and Dorothy, J. (2014): Millet - the frugal grain. – International Journal of Scientific Research and Reviews 3(4): 75-90.
[6] Chen, D., Huang, J. F., Jackson, T. J. (2005): Vegetation water content estimation for corn and soybeans using spectral indices derived from MODIS near and short wave infrared bands. – Remote Sensing of Environment 98(2/3): 225-236.
[7] Chen, X. Q., Yang, Q., Han, J. Y., Lin, L., Shi, L. S. (2020): Estimation of winter wheat leaf water content based on leaf and canopy hyperspectral date. – Spectroscopy and Spectral Analysis 40(3): 891-897.
[8] Cropscan, Inc. (2000): Data Logger Controller, User's Guide and Technical Reference. – CROPSCAN Inc, Rochester.
[9] Ding, S. Y., Li, H. M., Qian, L. X. (2004): Research advances in remote sensing techniques in estimation of vegetation biochemical material contents. – Chinese Journal of Ecology 23(4): 109-117.
[10] Dubois, M., Gilles, K. A., Hamilton. J. K., Rebers, P., Smith, F. (1956): Colorimetric method for determination of sugars and related substances. – Analytical Chemistry 28: 350-356.
[11] Feng, W., Yao, X., Tian, Y. C., Zhu, Y., Liu, X. J., Chao, W. X. (2007): predicting grain protein content with canopy hyperspectral remote sensing in wheat. – Acta Agronomica Sinica 33(12): 1935-1942.
[12] Fuller, D. Q. (2006): A Millet Atlas: Some Identification Guidance. – University College London, London.
[13] García-León, D., Standardi, G., Staccione, A. (2021): An integrated approach for the estimation of agricultural drought costs. – Land Use Policy 100: 104923.
[14] González, L., González-Vilar, M. (2001): Determination of Relative Water Content. – In: Roger, M. J. R. (ed.) Handbook of Plant Ecophysiology Techniques. Springer, Dordrecht, pp. 207-212.
[15] GPWG (Grass Phylogeny Working Group), Barker, N. P., Clark, L. G., Davis, J. I., Duvall, M. R., Guala, G. F., Hsiao, C., Kellogg, E. A., Linder, H. P., Mason-Gamer, R. J., Mathews, S. Y., Simmons, M. P., Soreng, R. J., Spangler, R. E. (2001): Phylogeny and subfamilial classification of the grasses (Poaceae). – Annals of the Missouri Botanical Garden 88(3): 373-457.
[16] Gupta, A., Rico-Medina, A., Caño-Delgado, A. I. (2020): The physiology of plant responses to drought. – Science 368(6488): 266-269.
[17] Habiyaremye, C., Matanguihan, J. B., D'Alpoim Guedes, J., Ganjyal, G. M., Whiteman, M. R., Kidwell, K. K., Murphy, K. M. (2017): Proso millet (Panicum miliaceum L.) and its potential for cultivation in the Pacific Northwest US. A review. – Frontiers in Plant Science 7: 1961.
[18] Han, H. K., Miao, J. Y., Zhang, Y. Y., Zhang, D. Z., Zong, G. H., Gong, X. W., Li, J., Feng, B. L. (2018): Estimating chlorophyll content of proso millet canopy by hyperspectral reflectance. – Agricultural Research in the Arid Areas 36(1): 164-170.

http://www.aloki.hu ● ISSN 1589 1623 (Print) ● ISSN 1785 0037 (Online)
DOI: http://dx.doi.org/10.15666/aeer/2001_431445

[19] Hansen, P. M., Jorgensen, J. R., Thomsen, A. (2002): Predicting grain yield and protein content in winter wheat and spring barley using repeated canopy reflectance measurements and partial least squares regression. – Journal Agricultural Science 139(3): 307-318.
[20] Hasan, U., Sawut, M., Kasin, N., Taxipulati, N., Wang, J. Z., Ablat, I. (2018): Hyperspectral estimation model of leaf water content in spring wheat based on grey relational analysis. – Spectroscopy and Spectral Analysis 38(12): 3905-3911.
[21] Huete, A. R. (1988): A soil-adjusted vegetation index (SAVI). – Remote Sensing of Environment 25(3): 295-309.
[22] Hunter, M. C., Kemanian, A. R., Mortensen, D. A. (2021): Cover crop effects on maize drought stress and yield. – Agriculture, Ecosystems & Environment 311: 107294.
[23] Jackson, R. D. (1982): Canopy temperature and crop water stress. – Advanced Irrigation 25(1): 43-85.
[24] Jin, N., Zhang, D. Y., Li, Z. H., He, L. (2020): Evaluation of water status of winter wheat based on simulated reflectance of multispectral satellites. – Transactions of the Chinese Society for Agricultural Machinery 51(11): 243-252.
[25] Jordan, C. F. (1969): Derivation of leaf area index from quality of light on the forest floor. – Ecology 50(4): 663-666.
[26] Kjær, A., Nielsen, G., Søren Stærke, S., Clausen, M. R., Edelenbos, M., Jørgensen, B. (2016): Prediction of starch, soluble sugars and amino acids in potatoes using hyperspectral imaging, dielectric and LF-NMR methodologies. – Potato Research 59(4): 357-374.
[27] Li, Y. X., Zhu, Y., Tian, Y. C., You, X. T., Zhou, D. Q., Cao, W. X. (2005): Relationship of grain protein content and relevant quality traits to canopy reflectance spectra in wheat. – Scientia Agricultura Sinica 38(7): 1332-1338.
[28] Li, W. G., Wang, J. H., Zhao, C. J., Liu, L. Y., Guo, W. S. (2007): Study on monitoring starch content in winter wheat grain using land-sat TM image. – Journal of Yunnan Agriculture University 22(3): 365-369.
[29] Liang, L., Zhang, L. P., Li, C. M., Yang, M. H. (2013): Estimating canopy leaf water content in wheat based on derivative spectra. – Scientia Agricultura Sinica 46(1): 18-29.
[30] Lu, X. Z., Sun, J., Mao, H. P., Wu, X. H., Gao, H. Y. (2017): Quantitative determination of rice starch based on hyperspectral imaging technology. – International Journal of Food Properties 20(1): 1037-1044.
[31] Marek, K., Marian, B., Oksana, S., Viliam, B., Pavol, H., Marek, Z. (2019): Evaluation of hyperspectral reflectance parameters to assess the leaf water content in soybean. – Water 11(3): 443.
[32] Miao, J. Y., Zhang, Y. Y., Wang, M., Zhang, P. P., Li, X., Han, H. K., Liu, F. Q., Feng, B. L. (2015): Characteristics of hyper-spectral reflectance of broomcorn millet canopy in semi-arid region. – Journal of Heilongjiang Bayi Agricultural University 27(5): 6-9.
[33] Ndlovu, H. S., John, O., Mbulisi, S., Onisimo, M., Alistair, C., Chimonyo, V. G. P., Tafadzwanashe, M. (2021): A comparative estimation of maize leaf water content using machine learning techniques and unmanned aerial vehicle (UAV)-based proximal and remotely sensed data. – Remote Sensing 13(20): 4091-4091.
[34] Onoyama, H., Ryu, C., Suguri, M., Iida, M. (2017): Estimation of rice protein content before harvest using ground based hyperspectral imaging and region of interest analysis. – Precision Agriculture 19(4): 721-734.
[35] Pearson, R. L., Miller, D. L. (1972): Remote mapping of standing crop biomass for estimation of the productivity of the short grass prairie. – Proceedings of the Eighth International Symposium on Remote Sensing of Environment, Ann Arbor, Michigan, pp. 1357-1381.
[36] Prathap, V., Ali, K., Singh, A., Vishwakarma, C., Krishnan, V., Chinnusamy, V., Tyagi, A. (2019): Starch accumulation in rice grains subjected to drought during grain filling stage. – Plant Physiology and Biochemistry 142: 440-451.

http://www.aloki.hu ● ISSN 1589 1623 (Print) ● ISSN 1785 0037 (Online)
DOI: http://dx.doi.org/10.15666/aeer/2001_431445

[37] Ravi, S. B. (2004): Neglected millets that save the poor from starvation. – Leisa India 6(1): 1-8.
[38] Richardson, A. J., Wiegand, C. L. (1977): Distinguishing vegetation from soil back ground information. – Photogramm Engineering and Remote Sensing 43(12): 1541-1552.
[39] Rondeaux, G., Steven, M., Baret, F. (1996): Optimization of soil-adjusted vegetation indices. – Remote Sensing of Environment 55(2): 95-107.
[40] Roujean, J. L., Breon, F. M. (1995): Estimating PAR Absorbed by vegetation from bidirectional reflectance measurements. – Remote Sensing of Environment 51(3): 375-384.
[41] Rouse, J. W., Haas, R. H., Schell, J. A., Deering, D. W. (1974): Monitoring the vernal advancement and retro gradation (green wave effect) of natural vegetation. – NASA/GSFCT Type Ⅲ Final Report. Greenbelt, MD, USA, pp. 309-317.
[42] Seo, Y., Lee, A., Kim, B., Lim, J. (2020): Classification of rice and starch flours by using multiple hyperspectral imaging systems and chemometric methods. – Applied Sciences 10(19): 6724.
[43] Shafiq, F., Raza, S. H., Bibi, A., Khan, I., Iqbal, M. (2018): Influence of proline priming on antioxidative potential and ionic distribution and its relationship with salt tolerance of wheat. – Cereal Research Communications 46(2): 287-300.
[44] Tian, Y. C., Zhu, Y., Cao, W. X., Fan, X. M., Liu, X. J. (2004): Monitoring protein and starch accumulation in wheat grains with leaf SPAD and canopy spectral reflectance. – Scientia Agricultura Sinica 37(6): 808-813.
[45] Wang, Y. J., Cheng, J. H. (2018): Rapid and non-destructive prediction of protein content in peanut varieties using near-infrared hyperspectral imaging method. – Grain & Oil Science and Technology 1(1): 40-43.
[46] Wang, Q., Li, P. H. (2012): Identification of robust hyperspectral indices on forest leaf water content using PROSPECT simulated dataset and field reflectance measurements. – Hydrological Processes 26(8): 1230-1241.
[47] Wang, C., Feng, M. C., Wang, J. J., Xiao, L. J., Yang, W. D. (2013): Monitoring grain starch accumulation in winter wheat via spectral remote sensing. – Chinese Journal of Eco-Agriculture 21(4): 440-447.
[48] Wang, J. J., Chen, L., Wang, H. G., Cao, X. N., Liu, S. C., Tian, X., Qin, H. B., Qiao, Z. J. (2019): Effects of hyperspectral prediction on nitrogen content and the grain protein content of broomcorn millet. – Scientia Agricultura Sinica 52(15): 2593-2603.
[49] Xie, X. J., Li, B. B., Zhu, H. X. (2012): Estimating contents of crude protein and amylose content in rice grain by hyper-spectral under different high temperature stress. – Research of Agricultural Modernization 33(4): 481-484.
[50] Xie, L. L., Wang, F. M., Zhang, Y., Huang, J. F., Hu, J. H., Wang, F. L., Yao, X. P. (2020): Monitoring of amylose content in rice based on spectral variables at the multiple growth stages. – Transactions of the Chinese society of agricultural engineering 36(8): 165-173.
[51] Xu, Q., Ma, Y., Jiang, Q., Tong, C. Y., Zhao, Z. Y. (2018): Estimation of rice leaf water content based on hyperspectral remote sensing. – Remote Sensing Information 33(5): 1-8.
[52] Zhao, T. T., Zhang, L. Z., Zheng, S. H., Yang, L. L., Feng, N. H., Liu, G. K. (2011): Analysis of starch of Panicum miliaceum L. seed by near infrared transmittance spectroscopy. – Acta Agriculture Boreali-Sinica 26(1): 234-238.
[53] Zhang, J. J., Zhang, W., Xiong, S. P., Song, Z. X., Tian, W. Z., Shi, L., Ma, X. M. (2021): Comparison of new hyperspectral index and machine learning models for prediction of winter wheat leaf water content. – Plant Methods 17(1): 1-14.

http://www.aloki.hu ● ISSN 1589 1623 (Print) ● ISSN 1785 0037 (Online)
DOI: http://dx.doi.org/10.15666/aeer/2001_431445

MICROBIAL ACTIVITY REGULATION OF VOLATILE ORGANIC COMPOUNDS WITH POTENTIAL FUEL OXYGENATE WITHIN EAST TAIJINAR SALT LAKE, CHINA

LU, X. H.[1,2,3] – ZHANG, Y. S.[4] – YI, L.[1,2] – SU, W. G.[1,2] – MA, Z.[1,2,3] – HAN, F. Q.[1,2*]

[1]*Key Laboratory of Comprehensive and Highly Efficient Utilization of Salt Lake Resources, Qinghai Institute of Salt Lakes, Chinese Academy of Sciences, Xining, Qinghai 810008, China*

[2]*Qinghai Provincial Key Laboratory of Geology and Environment of Salt Lakes, Xining, Qinghai 810008, China*

[3]*University of Chinese Academy of Sciences, Beijing 100049, China*

[4]*The Third Geological Exploration Institute of Qinghai Province, Xining, Qinghai 810000, China*

[*]*Corresponding author*
e-mail: hanfq@isl.ac.cn

(Received 13th Aug 2021; accepted 28th Oct 2021)

Abstract. There is still limited information on the microbial communities and volatile organic compounds of different sediment types within salt lakes such as the East Taijinar Salt Lake, China. This study determined the variability in the ecogenomics and volatile organic compounds (VOCs) with fuel oxygenate potential of the different sediment types of the lake; clay sediment (NT), sandstone sediment (FS) and salt bearing sediment (SY) were examined to provide insight on the nature of bacterial communities and related VOCs in different forms of sediment. The results indicated distinct variability in microbial communities' diversity and metabolic functions between the different sediment types of the East Taijinar Salt Lake. Operational taxonomic Units (OTUs) were found to overlap more between the TN and FS types, and NT sediment type had the highest number of unique OTUs while SY had the least. The current study also reported the most highly abundant phylum group to be the proteobacteria, followed by firmicutes and then actinobacteria. *Niveispirillum* was shown to be the most abundant genus group and was recorded to have the highest abundance within the SY sediment type and the lowest within the NT sediment type. According to the results of the ACE, CHAO1, Shannon and Simpson indices, it was shown that higher diversity values occurred within the NT type and the lowest values were recorded within the SY sediment. Membrane transport, amino acid metabolism and carbohydrate metabolism were the major molecular activities across the sediment types causing ethanol to be the most abundant, while n-Hexyl acetate was the least abundant VOC across all the sediment types.
Keywords: *microbial community diversity, molecular activities, salt lake eco-genomics, salt lake environment, sediment type*

Introduction

Salt lakes, as their name indicates, are aquatic systems having significantly extreme environmental conditions, including higher salinity and other mineral content. Indeed, some of these salty aquatic ecosystems have been noted to have a moderately higher concentration of salt than sea water (Baxter, 2018). At the point when water vanishes from these lakes through evaporation or seepage, the accumulation of salt occurs, making salt lakes an incredible spot for deposition of salt particles. Moreover, as the point where the evaporation of water becomes higher than the amount flowing in, the accumulation of the deposited salts will steadily persist resulting in unique and extraordinary

http://www.aloki.hu ● ISSN 1589 1623 (Print) ● ISSN1785 0037 (Online)
DOI: http://dx.doi.org/10.15666/aeer/2001_447464

environmental conditions. Therefore, the extreme and unique climatic characteristics that dominate the salt lakes shape the life forms to develop adaptation strategies that enable them to withstand the existing physico-chemical parameters such as pH, temperature, salinity etc. (Tazi et al., 2014). In most of the times the surrounding climatic and physico-chemical parameters may result in the creation of acidic conditions with pH of <5, alkalinity condition with pH of >9, hyper condition with saltiness of >35%, low pressure condition of >0.1 MPa, high temperature condition of >40 °C, low temperature condition of <5 °C, and water pressure of <0.80 (Baxter, 2018). These conditions enable the survival of biotic communities that are extremophiles in nature, and they continue to develop and get duplicated with time (Han et al., 2017). In China, the salt lakes are described by their outstandingly rich properties such as higher temperatures, stronger radiation, high values of phosphates and carbonate deposits (Williams, 1991; Mianping et al., 1993; Zheng, 2011). Most salt lakes also have extreme conditions of environments that form in closed drainage basins exposed to high rate of evaporation processes. Due to their unique environment, most salty lakes develop high levels of carbonate and chloride salts, with pH range being predominant between 8 to > 12 (Jones et al., 1998; Kambura et al., 2016).

A reasonable difference exists in the organization of prokaryotic groups within the hypersaline lakes with NaCl levels of > 15% w/v and highly diluted waters with NaCl measures of about 5% w/v. Under this condition photosynthetic process stands to be the main mechanism that takes up the formed nutrient compounds, with all the vigorous microbial networks that are mostly anaerobic in nature being the major trophic gatherings liable for cycling of carbon and sulfur (Lin et al., 2017). Precise scientific studies have demonstrated that the microorganisms are alkaliphilic and several of them fall under closely related taxa, while a few others portray no solid linkages to major known groups of prokaryotes. These alkaliphiles are boundless and in this manner appears to be extraordinary to the hypersaline lakes, and continue to occur independently within the created climatic condition (Yu and Kuenen, 2005). Despite the current salty lakes being geographically young, they have most likely existed since archaean occasions, allowing them to advance into free networks of alkaliphiles (Jones et al., 1994; Yu and Kuenen, 2005; Grant and Sorokin, 2011).

Investigations of hypersaline biological systems regularly yield novel organic entities and add to better comprehension of extreme conditions (Hollister et al., 2010). Halophiles are moderately unexplored as possible sources of novel species. Furthermore, little is thought about the culturable bacterial variety with flourishing capacity in hypersaline lakes (Guan et al., 2020). Present day studies on the microbiology of Great Salt Lake have contributed to molecular methodologies and provided proper understanding of the surrounding environment. The investigation of Great Salt Lake by researchers depicting these small occupants of the saline solution enlighten the bigger terminal lake with its numerous aspects, human driven impacts, and consistently changing shorelines (Baxter, 2018). Halophilic and halotolerant forms of microorganisms stand out as dependable sources of salt-lenient enzymatic resources with potential use in different bio-based technological measures where high salinity ranges would somehow hinder enzymatic changes. Indeed, some salty lakes have been found to harbor different promising types of microorganisms that can readily create mechanically important enzymatic materials (Ruginescu et al., 2020). Indeed, the limiting osmotic conditions occurring in hypersaline conditions bring about diminishing metabolic variety with expanding saltiness and different microbial digestion systems have been depicted to occur even at high salt conditions (Oren et al., 1994). This creates the need to have proper geochemical

http://www.aloki.hu ● ISSN 1589 1623 (Print) ● ISSN1785 0037 (Online)
DOI: http://dx.doi.org/10.15666/aeer/2001_447464

understanding and to know the existing control mechanisms on microbial biology in saline-based lake conditions (Dong et al., 2006).

Biological systems experience exchange in significant atmospheric trace gases, incorporating volatile organic compounds (VOCs), which are a little but exceptionally receptive piece of the carbon cycle. Majority of the formed VOCs are produced by microorganisms, making it necessary to undertake in-depth studies to provide detailed information on the relationships between microorganisms and the major compounds (Insam and Seewald, 2010). VOCs have natural beneficial properties that contributes to the function and stability of the environment (Mellouki et al., 2015; Wu et al., 2020). VOCs are useful portion of the ecosystem that ensure the availability of supplements for the development of most cellular micro-organisms and intervene in coordination and interactions within the cells. Nonetheless, barely any investigations have zeroed in on the impacts of VOCs on prokaryotic varieties and surrounding environment. There is limited information on the influence of VOCs on the variety, creations, and organization of prokaryotic networks in saline silt (Ding et al., 2020). Indeed, it has been shown that water and sediments of different lakes can harbor unique and novel prokaryotic diversity (Mesbah et al., 2007).

Salt Lake environments such as the East Taijinar Salt Lake, China are important parts of the ecosystems (Last, 2002). Notwithstanding their raised salinities, saline lakes undertake numerous functions that form the foundation of economically productive source of mineral and other ecosystem functions (Chindapana et al., 2018). It is the interaction between the biological, chemical, and physical parameters that dictates the nature and amount of salt ions and minerals within the salt lake environment (Britannica, 2019). Despite this, more studies have only focused on the location, morphology and chemical characteristics, with much focus on the types of salts but less attention on the biological components such as microbial communities under related VOC characteristics (Boggsa et al., 2006; Freire et al., 2014). Therefore, this study was purposed to undertake ecogenomics and volatile organic compounds studies on different sediment types of East Taijinar Salt Lake to provide holistic insight on the nature of bacterial communities and related VOC at different sediment types for future management exploitation of the resources within the salt like regimen.

Materials and methods

Study area

The study was undertaken at the East Taijinar Salt Lake located at 37°21′54″–37°36′05″N and 93°45′33″–94°06′48″W (*Figure 1*). It is positioned in the middle of the Qaidam Basin, distributed in the direction of NW-SE, with an area of 121.5 km^2 and a depth of 0.6 m. It is an inland Salt Lake, which is mainly supplied by the East Taijinar River from the Kunlun Mountains in the southwest and excreted by evaporation. The brine is a magnesium sulfate subtype with a pH of 7.9, and is rich in lithium, boron, potassium, and magnesium. Due to the paleoclimate, neotectonic movement and provenance replenishment, the formation conditions of the lake sediments are relatively complex. There are two halite deposits in different periods, the upper layer is the Holocene sedimentary and the lower is Pleistocene sedimentary.

http://www.aloki.hu ● ISSN 1589 1623 (Print) ● ISSN1785 0037 (Online)
DOI: http://dx.doi.org/10.15666/aeer/2001_447464

Sampling site and procedure

The sediment samples used in this study were obtained from a depth profile within the middle of the dry salt flats at a location of 93°57′04″N and 37°27′46W using a polyvinyl chloride corer. A total of nine samples per site were taken from three different lithologic strata; clay (NT1-NT3), sandstone (FS1-FS3), and salt-bearing (SY1-SY3). The samples were kept in ice and transported to the Key Laboratory of Comprehensive and Highly Efficient Utilization of Salt Lake Resources, Qinghai Institute of Salt Lakes, Chinese Academy of Sciences for further processing and analysis.

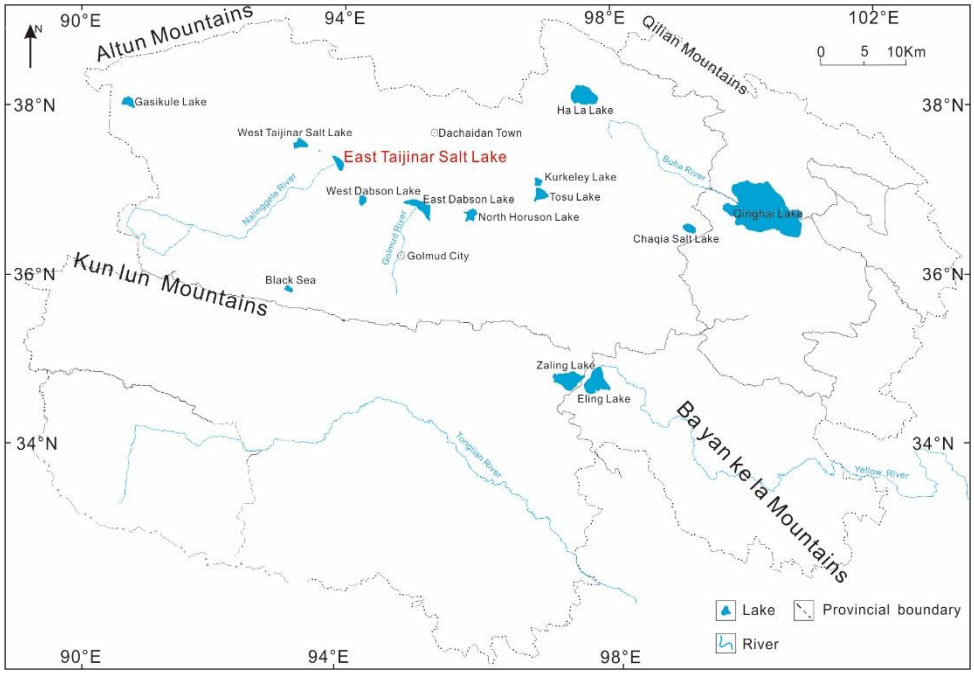

Figure 1. *Map of the study area showing East Taijinar Salt Lake*

DNA isolation and metagenomic sequencing

The extraction of the total genomic DNA from the sediment samples was carried out with CTAB/SDS method. The DNA purity and concentration monitoring were accomplished on 1% agarose gels. Based on the concentration, the dilution of DNA was made to 1ng/µl using sterile water. For the generation of amplicon, primer 16S V3-V4: 341F-806R, 18S V9: 1380F-1510R, ITS1: ITS1F- ITS2R were used. 16S /18S rRNA genes were subjected to amplification by applying the specific barcoded primers. The entire PCR reactions were accomplished in 30µL reactions having Phusion®High-Fidelity of 15 µL, Master Mix for PCR (New England Biolabs); of 0.2 µM for both the forward and reverse primers, and estimated 10 ng template DNA. The thermal cycling consisted of the initial denaturation which occurred within a temperature of 98 °C for a time period of 1 minute, followed by 30 cycles of denaturation within 98 °C for 10 seconds, then annealing within 50 °C for 30 seconds, and elongation at 72 °C for 60 seconds and final step was carried out at 72 °C for 5 minutes.

Quantification and qualification of the products of Polymerase chain reaction (PCR) involved same volume of 1X loading buffer (contained SYB green) that was added to the product of PCR and then electrophoresis was carried out on 2% agarose gel for the

http://www.aloki.hu ● ISSN 1589 1623 (Print) ● ISSN1785 0037 (Online)
DOI: http://dx.doi.org/10.15666/aeer/2001_447464

purpose of identification. Samples that possessed main strip which were bright and of between 400-450 bp were selected for further experimental analysis. For PCR products addition and purification, the PCR products were added together in equal density ratios. After that, the purification of the PCR products was undertaken by using AxyPrepDNA Gel Extraction Kit (AXYGEN). Preparation of library and sequencing was then achieved by generating sequencing libraries using NEB Next®Ultra™DNA Library Prep Kit (NEB, USA) taking note of the manufacturer's directives, with addition of index codes. The assessment of the quality of the library was accomplished on the Qubit@ 2.0 Fluorometer (Thermo Scientific) and Agilent Bioanalyzer 2100 system. Sequencing process was undertaken on an Illumina Miseq/HiSeq2500 platform where 250 bp/300 bp paired-end reads were produced.

Analysis of metagenomic data

For matched paired end reads congregations, the combined paired-end reads from the first Deoxyribonucleic Acid (DNA) pieces were consolidated utilizing FLASH to blend combined end-reads when probably a portion of the reads covered the read created from the opposite edge of a similar DNA section. Matched end reads were relegated to each example as per the special barcodes. For Operational Taxonomic Unit (OUT) grouping and species comment, successions of investigation was undertaken using the UPARSE programming bundle utilizing the UPARSE-OTU and UPARSE-OTUref calculations. For investigation of alpha (inside examples) and beta (among tests) variety within-house Perl scripts were applied. Arrangements with ≥97% similitude were assigned to similar OTUs. The agent successions for each OTU were then picked and utilized in the RDP classifier to clarify ordered data for every delegate grouping. To process Alpha Diversity, the table of the OTU was checked and determined with three measurements: ACE, CHAO1, Shannon and Simpson were used to appraise the abundance of species; number of Species observed was used to assess the measure of novel OTU that exists in each category (Barker et al., 2010; Chao and Chiu, 2016; Thukral, 2017).

For Phylogenetic distance and community dissemination investigation, graphical portrayal of the overall variety of bacterial abundance at phylum unit to species unit was pictured utilizing Krona outline. Group investigation was done before principal component analysis (PCA), which was incorporated to decrease the element of the first factors utilizing the QIIME programming bundle which computes both the weighted and unweighted unifrac distance as phylogenetic proportions of beta variety. Unweighted unifrac distance was utilized in the process of Principal Coordinate Analysis (PCoA) method as well as the Unweighted Pair Group Method with Arithmetic mean (UPGMA) Clustering. PCoA assisted with getting main arranges and envision them from unpredictable, multidimensional information. Then again, UPGMA Clustering was utilized to describe the distance grid.

Speciation and quantification of volatile organic compounds using GC-IMS

Ionization of the VOC values were determined using the headspace-gas chromatography-ion mobility spectrometry (HS-GC-IMS) instrument (FlavorSpec® H1-00053, Gesellschaft für Analytische Sensorsysteme mbH (G.A.S.), Dortmund, Germany). This analytical work was undertaken within the G.A.S. Department of the Shandong HaiNeng Science Instrument Co., Ltd. (Shandong, China). The chromatographs separation was undertaken with an FS-SE-54-CB-1 capillary column (15 m, ID: 0.53 mm), a radioactive ionization source (tritium; 6.5 KeV), and a

http://www.aloki.hu ● ISSN 1589 1623 (Print) ● ISSN1785 0037 (Online)
DOI: http://dx.doi.org/10.15666/aeer/2001_447464

heated spitless injector for auto-direct acquisition of the headspace volatile compounds samples from the samples and moved into the inside of the GC-IMS instrument. Before the GC-IMS analysis, the sample (1 g) was subjected to heating at temperature of eighty degrees Celsius for twenty minutes in a box for incubation to form volatile elements. The injection volume was set at five hundred μL, the injection speed setting was 0.6 mL s^{-1}, and the injection temperature was set at 80 °C. The temperature for the automatic headspace sampler was adjusted to 85 °C within the time duration of 15 minutes. After injection of the sample, the VOCs were introduced into the multi-capillary column through the carrier gas for timely separation. Chromatographic separation was performed at 60 °C: the initial placement of the rate of the carrier gas flow was put at 2 mL min^{-1} for 2 minutes; the flow was then raised in linear trend till it achieved 15 mL min^{-1} over a time period of 8 minutes; it was raised up to a volume of 80 mL min^{-1} for a time duration of 10 minutes; and for the end, the flow acquired 150 mL min^{-1} within a time period of 5 minutes. The total run time took a time duration of 40 min so that it could achieve a better separation output. In consequence to the division within the capillary column at 60 °C, the headspace was pushed into the ionization section for prior ionization, then forcefully pushed into the drift region by a shutter grid, and lastly moved into the IMS detector. The condition for working of the IMS were: 5 cm length of the drift tube and functioned at the same voltage of 400 V cm^{-1}; 45 °C drift tube temperature with nitrogen of 99.999% purity and 150 mL min^{-1} for the rate of flow. Every sample was introduced to two tier analysis procedure using GC-IMS. The experimental results were given as the average value to reduce errors.

Statistical analysis

To affirm contrasts in the quantity of individual scientific groups, STAMP programming was used. LEfSe was utilized for the quantitative based examination of biomarkers inside the various groups to dissect information wherein the quantity of species was a lot higher than the quantity of tests and to give biological group clarifications to set up measurable importance, organic consistency, and impact size assessment of anticipated biomarkers. To distinguish contrasts of microbial networks within the two categories, ANOSIM and ADONIS were undertaken dependent on the Bray-Curtis uniqueness distance grids. The means for VOC information were compared through SPSS version 12, with 95% as level of significance and P value of 0.05.

Results

Operational taxonomic unit analysis and distribution

Analysis of common and unique bacterial Operational Taxonomic Units (OUTs) between different sediment types are provided in *Fig. 2*. The results indicated that more numbers of OTUs overlapped between the clay sediment (TN) and sandstone sediment (FS) types. The NT also had the highest number of unique OTUs while salt bearing sediment (SY) had the least.

UPGMA cluster tree

The result on the similarity between different samples is provided in *Fig. 3*. From this result, the highly abundant phylum group was the proteobacteria, followed by firmicutes and then actinobacteria.

http://www.aloki.hu ● ISSN 1589 1623 (Print) ● ISSN1785 0037 (Online)
DOI: http://dx.doi.org/10.15666/aeer/2001_447464

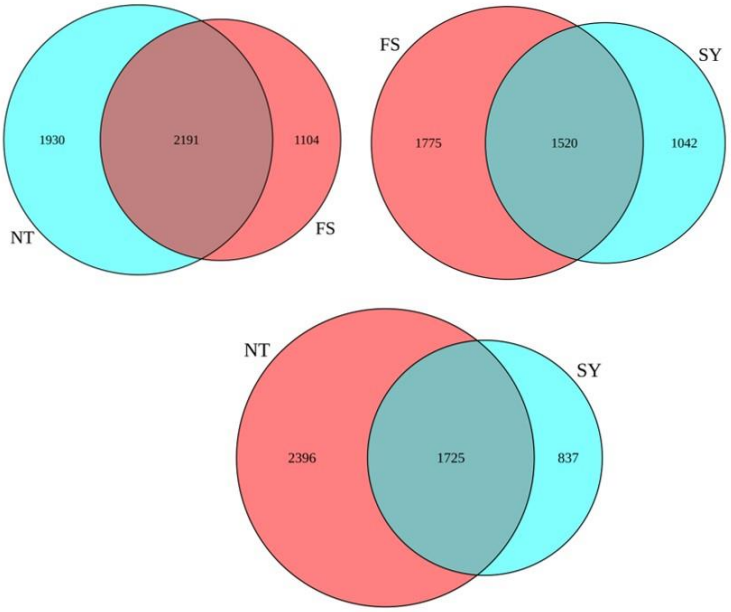

Figure 2. *OTU relationship between the sediment types (NT is clay sediment, FS is sandstone sediment and SY is salt bearing sediment) through Venn*

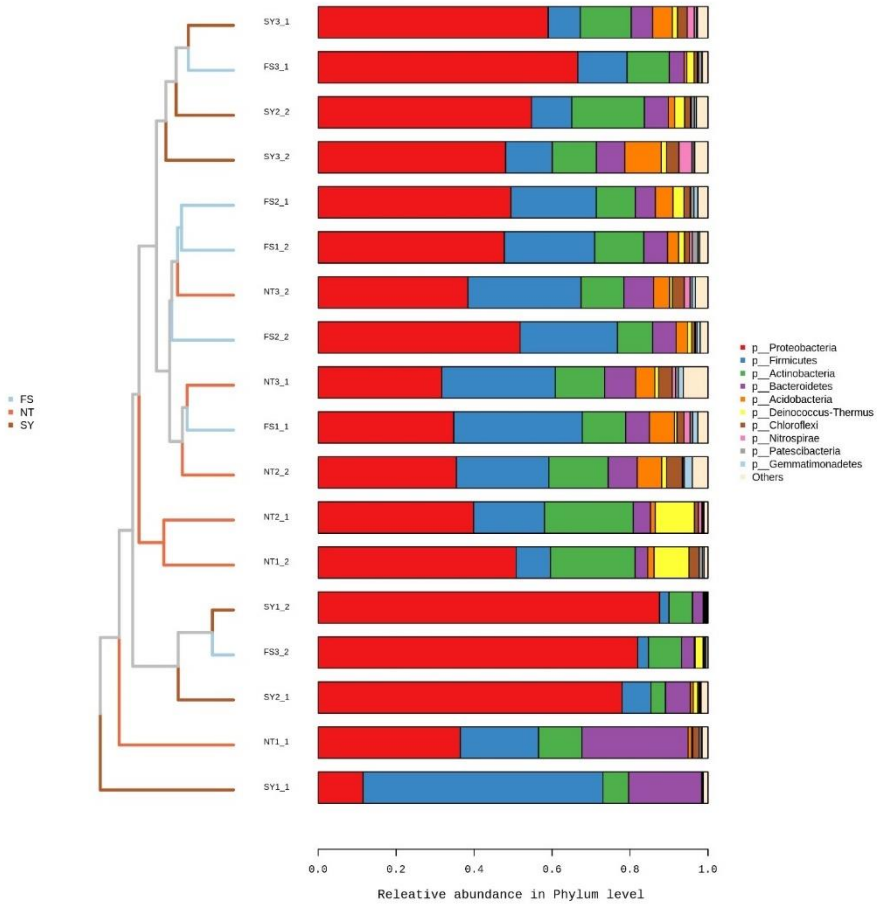

Figure 3. *UpGMA cluster trees and community structure bar charts based on Unweighted Unifrac distance*

http://www.aloki.hu ● ISSN 1589 1623 (Print) ● ISSN1785 0037 (Online)
DOI: http://dx.doi.org/10.15666/aeer/2001_447464

Analysis of species composition

Based on the results of *Fig. 4*, the most dominant bacterial genus was *Niveispirillum*, its abundance was the highest within the salt bearing sediment (SY) and the lowest within the clay sediment (NT).

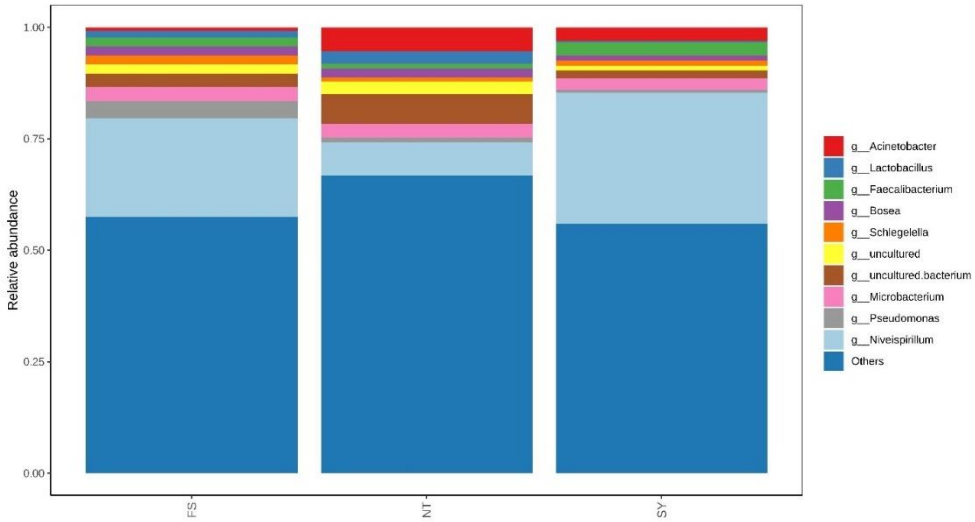

Figure 4. *Graph of relative abundance of top ten genus at each sediment type*

Community heatmap graph

Result on abundance of various genera based on heatmap analysis is provided in *Fig. 5*. The result indicated higher abundance of the dominant genera in NT sediment type and the lowest abundance in FS sediment type.

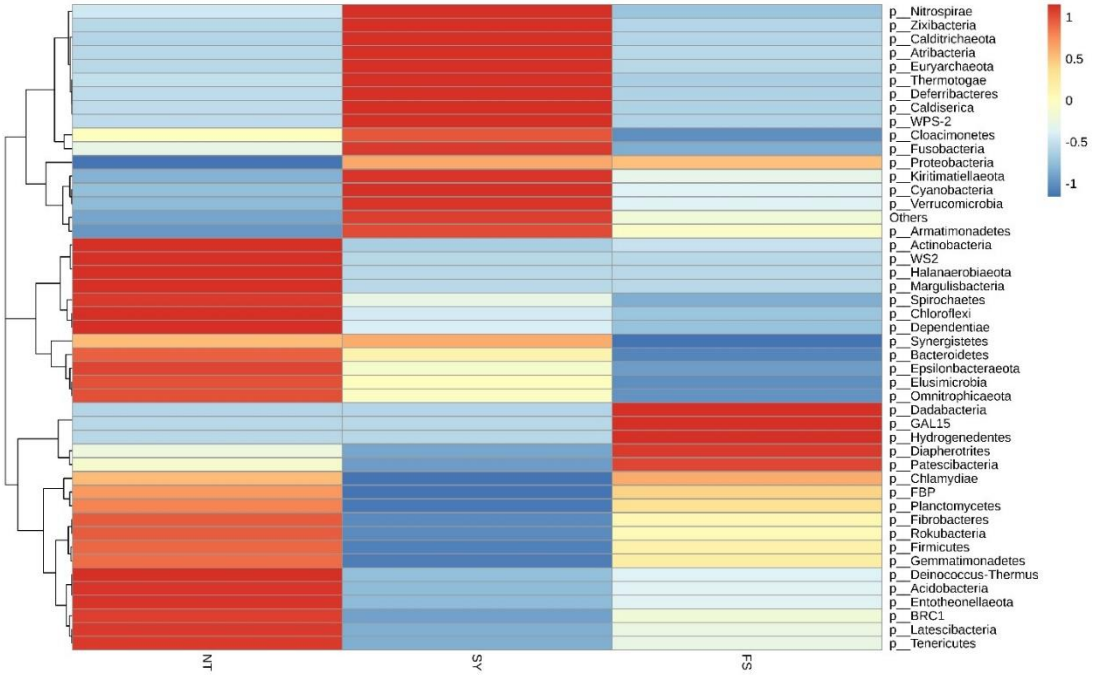

Figure 5. *Cluster heat map of species abundance at each group gate level*

http://www.aloki.hu ● ISSN 1589 1623 (Print) ● ISSN1785 0037 (Online)
DOI: http://dx.doi.org/10.15666/aeer/2001_447464

Species diversity analysis

Result on Alpha diversity index based on ACE, CHAO1, Shannon and Simpson are provided in *Fig. 6*. Based on this result, highest diversity occurred within the clay sediment (NT) and the lowest occurred within the salt bearing sediment (SY).

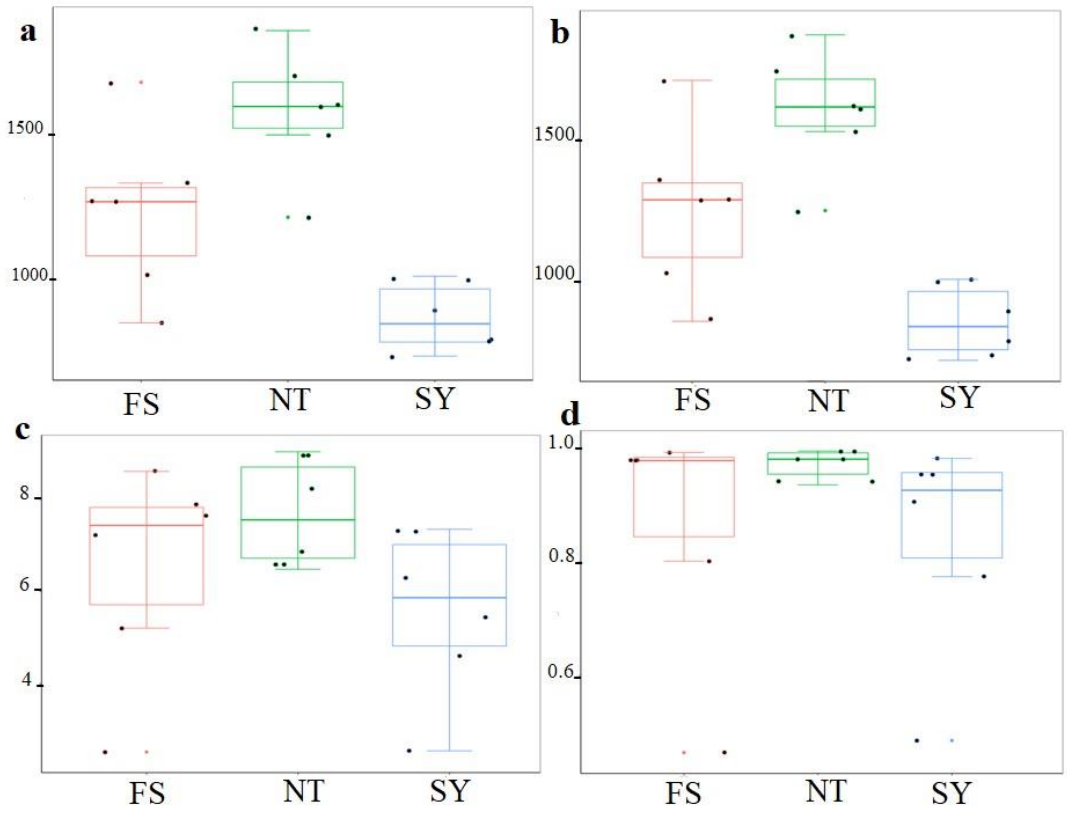

Figure 6. *Box whisker plots for Alpha diversity index based on ACE (a), CHAO1 (b), Shannon (c) and Simpson (d) indices across the different sediment types (FS is sand stone sediment, NT is clay sediment and SY is salt bearing sediment*

Functional feature prediction

The Kyoto Encyclopedia of Genes and Genomes (KEGG) functional prediction analysis was used to study the metabolic function changes of community samples at different sediment types. The result on biological pathways through KEGG is provided in *Fig. 7*. The Clusters of Orthologous Groups (COGs) was used to complement KEGG to compare the protein sequences of complete genomes at different sediment types. The results on functional prediction through Clusters of Orthologous Groups (COGs) are provided in *Fig. 8*. LEfSe analysis based on taxonomical composition of samples according to different grouping conditions for linear discrimination analysis (LDA), was used to find out the classification of samples and feature entries with significant differences. Result on group means for the functional genes through the LDA scores is provided in *Fig. 9*.

http://www.aloki.hu ● ISSN 1589 1623 (Print) ● ISSN1785 0037 (Online)
DOI: http://dx.doi.org/10.15666/aeer/2001_447464

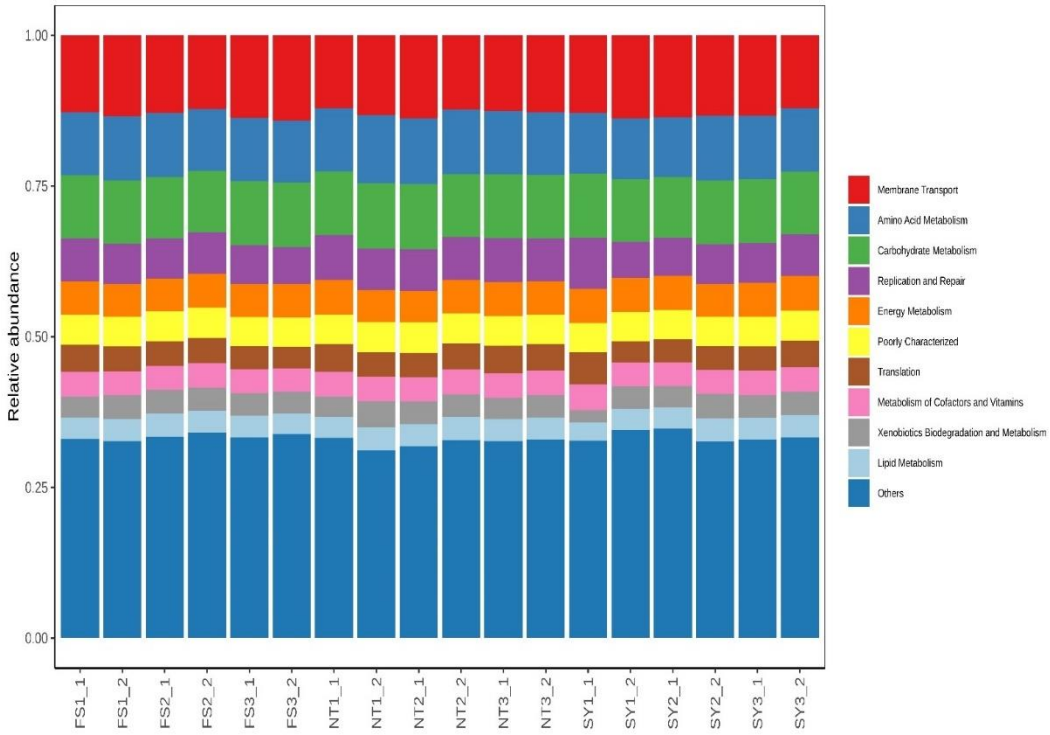

Figure 7. *Bar graph of biological activities through KEGG (Kyoto Encyclopedia of Genes and Genomes)*

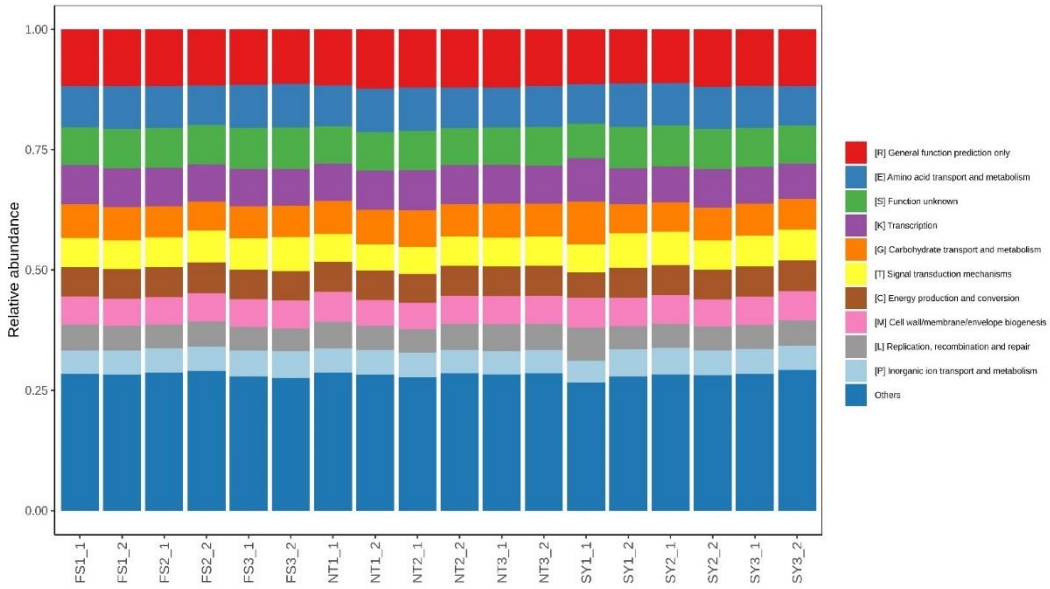

Figure 8. *Bar graph for functional prediction through Clusters of Orthologous Groups (COGs)*

Volatile organic compound (VOC)

Results on the values of volatile organic compound (VOC) across the different sediment types are provided in *Table 1*. From the results, it was shown that values for ethanol, 1-Butanol M, 2-Octanol and n-Hexyl acetate were relatively the highest within

http://www.aloki.hu ● ISSN 1589 1623 (Print) ● ISSN1785 0037 (Online)
DOI: http://dx.doi.org/10.15666/aeer/2001_447464

the clay sediment, the values for Cyclohexanone, 5-Methyl-3-heptanone, formic acid, ethyl propionate, propyl butanoate M, hexanal M and Benzaldehyde were relatively the highest within the sand stone sediment while values for Acetone, ethyl acetate M, Butyl butyrate M, Furfural M, Heptanal, Octanal, Nonanal M and Nonanal D were the highest within the salt bearing sediment. Across all the sediment types, ethanol was the most abundant while n-Hexyl acetate was the least abundant VOC.

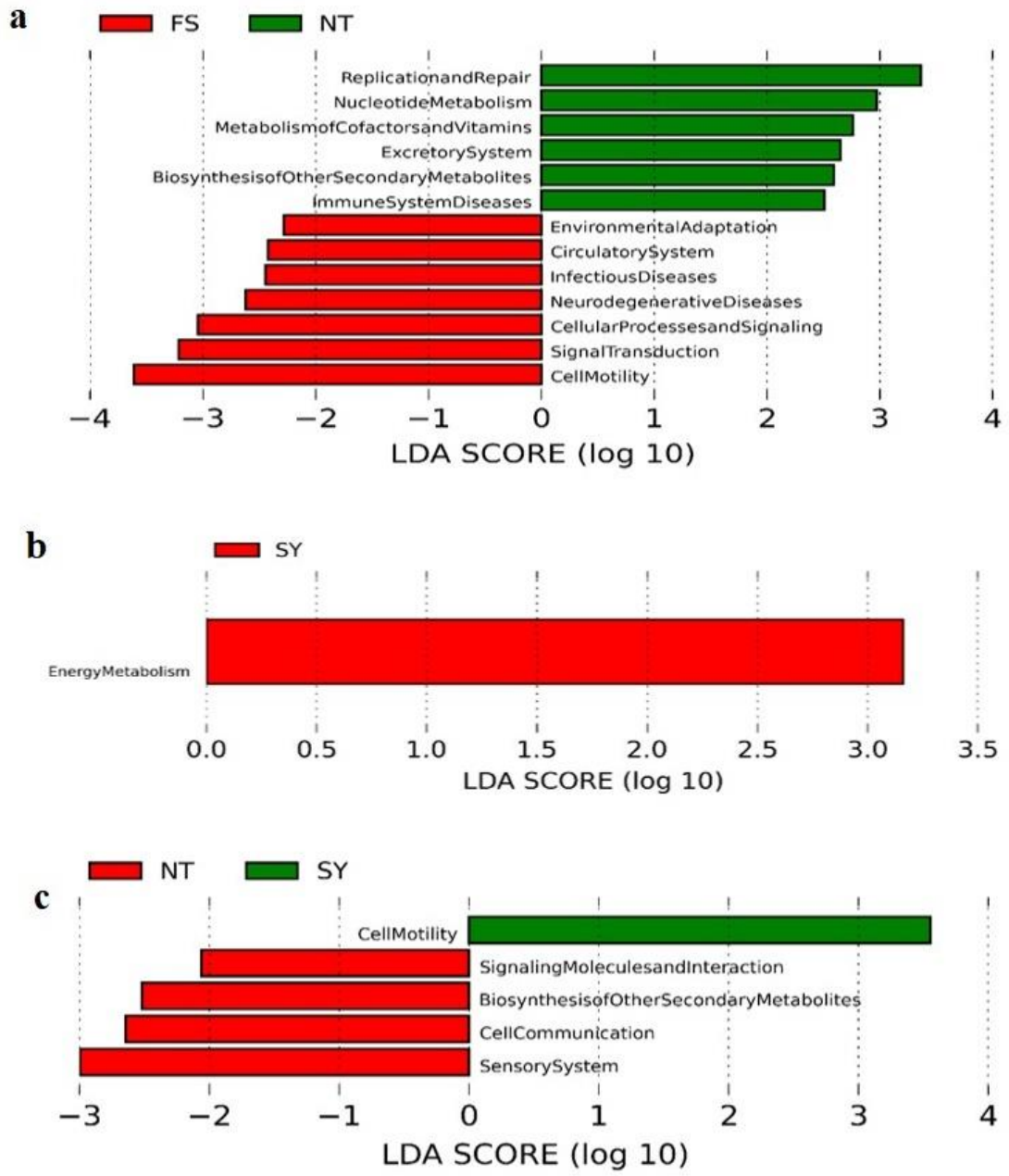

Figure 9. *Graph of means for the functional genes through the LDA scores for different groups FS vs NT (a), SY vs SF (b) and NT vs SY (c)*

http://www.aloki.hu ● ISSN 1589 1623 (Print) ● ISSN1785 0037 (Online)
DOI: http://dx.doi.org/10.15666/aeer/2001_447464

Table 1. *Spatial variation in the values of volatile organic compound (VOC) across the different sediment types (NT is clay sediment, FS is sandstone sediment and SY is salt bearing sediment, values followed by the different letter across the column are significantly different at P=0.05)*

VOC	NT	FS	SY	P-value
ethanol	0.1584±0.11a	0.1318±0.09b	0.0676±0.02c	0.0442
1-Butanol M	0.0706±0.02a	0.0361±0.03b	0.0674±0.01a	0.0015
2-Octanol	0.0103±0.011a	0.0078±0.01b	0.0024±0.00b	0.0224
n-Hexyl acetate	0.0103±0.01a	0.0038±0.00b	0.0038±0.00b	0.0042
Cyclohexanone	0.0066±0.01a	0.0320±0.03b	0.0022±0.00c	0.0001
5-Methyl-3-heptanone	0.0142±0.02a	0.0571±0.05b	0.0011±0.00c	0.0028
formic acid	0.0202±0.01a	0.0308±0.01a	0.0161±0.00a	0.0645
ethyl propionate	0.0250±0.03a	0.0473±0.01b	0.0045±0.00c	0.0037
propyl butanoate M	0.0445±0.00a	0.1129±0.04b	0.0486±0.01a	0.0019
hexanal M	0.0398±0.02a	0.0665±0.03b	0.0453±0.01a	0.0036
Benzaldehyde	0.0205±0.02a	0.0498±0.04b	0.0153±0.01a	0.0044
Acetone	0.0209±0.01a	0.0184±0.01a	0.0281±0.02a	0.0721
ethyl acetate M	0.0137±0.01a	0.0021±0.00b	0.0304±0.01c	0.0046
Butyl butyrate M	0.0344±0.01ab	0.0234±0.04b	0.0418±0.00a	0.0013
Furfural M	0.0047±0.00a	0.0057±0.01a	0.0216±0.01b	0.0035
Heptanal	0.0106±0.01a	0.0087±0.00b	0.0135±0.00a	0.0042
Octanal	0.0091±0.01a	0.0102±0.01b	0.0140±0.00b	0.0018
Nonanal M	0.0412±0.03a	0.0934±0.06b	0.0283±0.01c	0.0034
Nonanal D	0.0059±0.01a	0.0016±0.00a	0.0093±0.01a	0.0001

Discussion

Bacterial community structure

The study aimed at unlocking the characteristics of different sediment types within the East Taijinar Salt Lake based on the microbial community assemblage and types and concentrations of the volatile organic compounds. Halophiles are moderately neglected yet they are significant sources of novel species. Be that as it may, little is also understood about the culturable bacterial variety that flourish in hypersaline lakes despite groups such as *Rhodothermaeota* having been linked to these unique ecosystems (Ventosa et al., 2015; Guan et al., 2020). Moreover, the current acknowledged model of local area structure in hypersaline conditions is that the archaeal groups *Haloquadratum waslbyi*, the bacteroidete *Salinibacter ruber* and nanohaloarchaea are dominant members at higher levels of salinity, while more assorted archaeal and bacterial groups are seen in natural surroundings with moderate salt conditions. Metagenomic examination provides understanding into the detachment and portrayal of the major microorganisms in saline environment. For instance, a study had identified and described gammaproteobacterium *Spiribacter salinus* as a principal microbe of saline lake sediment. Based, on the current study, it was demonstrated through analysis of common and unique operational taxonomic units (OTUs) between different sediment types that more OTUs overlapped between the clay sediment (TN) and sandstone sediment (FS) types. Additionally, the NT also had the highest number of unique OTUs while salt bearing sediment (SY) had the least. This pointed out the influence of salt within the sediment on the survival of bacteria.

http://www.aloki.hu ● ISSN 1589 1623 (Print) ● ISSN1785 0037 (Online)
DOI: http://dx.doi.org/10.15666/aeer/2001_447464

Indeed, it highlighted that the salt bearing sediment as having unique environment to that of clay and sand sediment, hence had a more distinct OTUs from the other two forms of sediment types. This also agrees with a study by Kasper et al. (2007) which indicated that the growth performance of most bacteria isolates depends very much on the salinity levels of the ecosystem and only few and unique members can thrive in such ecosystems with extreme conditions.

Salty sediments have been shown to harbor a diverse bacterial community that differs spatially and temporary, and based on sediment characteristics (Rasuk et al., 2016). These conditions can turn out to be very hypersaline when dry, proposing that this variation in condition changes based on the occurrence of both flooding and high saltiness conditions (Vogt et al., 2017). It has also been shown that the salt tolerant microbial networks are overwhelmed by normal halotolerant to halophilic microorganisms, which may encounter shifts in community structure, richness, and variety along the ecological gradient. Through this shift, the exceptionally adjusted specialized groups may predominantly be found at the extremes, while less specialized groups with wide resilience reaches may dominate within the areas with moderate conditions. This demonstrated that the bacterial lavishness and variety may increment from the areas with higher salinities to areas with lower salinities (Rasuk et al., 2016). The current study also reported that most phylum group with high abundance were proteobacteria, followed by firmicutes and then actinobacteria, which were both more dominant across all the sediment types. The outcome of this study gives an exhaustive perspective on microbial survival specialization based on salt content within the lake sediments as had also been confirmed by Beazley et al. (2012).

A study on the most geochemically extreme salty lakes on Earth such as Lake Magic in Australia demonstrated that the bacterial group of the lake water was minimally different than that of both the groundwater and the sediment, and was dominated by a solitary OTU that was associated with *Salinisphaera*. In addition, pathways that had close relation with halotolerance were identified in the metagenomes, as were genes related with biological based synthesis of defensive carotenoids (Zaikova et al., 2018). The current study identified bacterial *Niveispirillum* as the most abundant genus group. Specifically, it was recorded in the highest abundance within the salt bearing sediment (SY) and the lowest within the clay sediment (NT). The Niveispirillum genus with members such as the *Niveispirillum cyanobacteriorum* sp. Nov has been associated with extreme environments where they enhance the restoration of the degraded sediment (Cai et al., 2015). Indeed, through heatmap analysis, it was confirmed that clay sediment types had the highest abundance of the dominating genera. Other similar studies have also recorded that aerobic anoxygenic phototrophic bacteria communities, including genus *Niveispirillum* are some of the overlooked drivers in promoting the production of bio-based sediment crusts (Beazley et al., 2012; Tang et al., 2018).

Microbial diversity

It is turning out to be obvious that the bacterial phyla co-happening at a given site possess a similar natural specialty and the spatial variability can demonstrate the presence of various levels in the dissemination of some major ecological components, including the saltiness levels. Through this, it has been clear that the connection of certain groups of microbes to the level of saltiness is by all accounts an important condition for the expansion of the species having a place with those specific groupings (Canfora et al., 2014). The current study also indicated that Alpha diversity index from the ACE,

http://www.aloki.hu ● ISSN 1589 1623 (Print) ● ISSN1785 0037 (Online)
DOI: http://dx.doi.org/10.15666/aeer/2001_447464

CHAO1, Shannon and Simpson had higher values within the clay sediment type and the lowest values within the salt bearing sediment. This also demonstrated the influence of salt levels within the sediment on the occurrence and distribution of bacterial communities.

Metabolic function analysis

The Kyoto Encyclopedia of Genes and Genomes (KEGG) functional prediction analysis has been applied on studies of the metabolic function changes of community samples at different sediment types. Additionally, the Clusters of Orthologous Groups (COGs) has been used to complement KEGG to compare the protein sequences of complete genomes of different types of samples (Nho et al., 2018). The current study also employed KEGG and COG to provide an understanding on metabolomic functions and the protein sequence comparison. The study result pointed out membrane transport, amino acid metabolism, carbohydrate metabolism as the major molecular activities across the sediment types. Through COG and LEfSe analysis based on taxonomical composition of samples according to different grouping conditions for linear discrimination analysis (LDA), there was less variation in the metabolomic functions of groups between the sandstone sediment and the clay sediment types, but more variation between the salt bearing sediment to the other sediment types.

Volatile organic carbon content

Soils may serve as sources or sinks of VOCs. VOCs assume a basic part in the guideline of the variety, syntheses, and network designs of bacterial networks in saline conditions and are additionally significant natural elements since they supply supplements for microbial cells and intervene in intercellular collaborations (Ding et al., 2020). The current study finding on the VOCs across the different sediment indicated that values for ethanol, 1-Butanol M, 2-Octanol and n-Hexyl acetate were relatively the highest within the clay sediment, the values for Cyclohexanone, 5-Methyl-3-heptanone, formic acid, ethyl propionate, propyl butanoate M, hexanal M and Benzaldehyde were relatively the highest within the sandstone sediment while values for Acetone, ethyl acetate M, Butyl butyrate M, Furfural M, Heptanal, Octanal, Nonanal M and Nonanal D were the highest within the salt bearing sediment. Within the clay sediment, Ethanol was the most abundant VOC, the most abundant VOC within the sandstone sediment was propyl butanoate M, while Butyl butyrate M was the most abundant. Across all the sediments types, ethanol was the most abundant while n-Hexyl acetate was the least abundant VOC. Ambient concentrations of volatile alcohols such as ethanol and methanol had been determined in saline environments leading to hypothesis that they could be having a common source. The biogeochemistry of ethanol in sediments points to the possible functional achievement of ethanol in the worldwide carbon cycle (Roebuck et al., 2016).

Conclusions and recommendations

From the study findings, it can be concluded that;

- There exists a distinct variability in microbial communities' diversity and metabolic functions between the different sediment types of the East Taijinar Salt Lake. The OTUs overlapped more between the clay sediment (TN) and sand stone sediment

http://www.aloki.hu ● ISSN 1589 1623 (Print) ● ISSN1785 0037 (Online)
DOI: http://dx.doi.org/10.15666/aeer/2001_447464

(FS) types, and NT sediment type had the highest number of unique OTUs while salt bearing sediment (SY) had the least.

- Most abundant phylum group was the Proteobacteria, thereafter Firmicutes followed by Actinobacteria. *Niveispirillum* was shown to be the most abundant genus group and specifically, it was recorded in the highest abundance within the salt bearing sediment (SY) and the lowest within the clay sediment (NT).
- Through the four indices, ACE, CHAO1, Shannon and Simpson, the highest diversity values occurred within the clay sediment type and the lowest values within the salt bearing sediment.
- Membrane transport, amino acid metabolism, carbohydrate metabolism were the major molecular activities across the sediment types and ethanol was the most abundant while n-Hexyl acetate was the least abundant VOC across all the sediment types.

As a recommendation, there is a need for in-depth study on the relationship between the salt lake microbial communities and the economically potential VOCs for further insert in the management and use of the lake resources.

Data availability statement. The data obtained from this study is available on reasonable request forwarded through the corresponding author.

Acknowledgement. This work was supported by the Natural Science Foundation of Qinghai Province (Grant number: 2019-ZJ-911).

REFERENCES

[1] Barker, M. S., Dlugosch, K. M., Dinh, L., Challa, R. S., Kane, L. C., King, M. G., Rieseberg, L. H. (2010): EvoPipes.net: Bioinformatic Tools for Ecological and Evolutionary Genomics. – Evolutionary Bioinformatics 6: 143-149. https://doi.org/10.4137/EBO.S5861.

[2] Baxter, B. K. (2018): Great Salt Lake microbiology: a historical perspective. – Int Microbiol. 21(3): 79-95. https://doi.org/10.1007/s10123-018-0008-z.

[3] Beazley, M. J., Martinez, R. J., Rajan, S., Powell, J., Piceno, Y. M., Tom, L. M., Andersen, G. L., Hazen, T. C., Van Nostrand, J. D., Zhou, J., Mortazavi, B., Sobecky, P A. (2012): Microbial community analysis of a coastal salt marsh affected by the Deepwater Horizon oil spill. – PloS one 7(7): e41305. https://doi.org/10.1371/journal.pone.0041305.

[4] Boggsa, D. A., Boggs, G. S., Eliota, I., Knott, B. (2006): Regional patterns of Salt Lake morphology in the lower Yarra Yarra drainage system of Western Australia. – Journal of Arid Environments 64(1): 97-115. https://doi.org/10.1016/j.jaridenv.2005.04.010.

[5] Britannica. (2019): Great Salt Lake. – Encyclopedia Britannica, https://www.britannica.com/place/Great-Salt-Lake. Accessed 1 May 2021.

[6] Cai, H., Wang, Y., Xu, H., Yan, Z., Jia, B., Maszenan, A. M., Jiang, H. (2015): Niveispirillum cyanobacteriorum sp. nov., a nitrogen-fixing bacterium isolated from cyanobacterial aggregates in a eutrophic lake. – International Journal of Systematic and Evolutionary Microbiology 65(8): 2537-2541. https://doi.org/10.1099/ijs.0.000299.

[7] Canfora, L., Bacci, G., Pinzari, F., Lo Papa, G., Dazzi, C., Benedetti, A. (2014): Salinity and Bacterial Diversity: To What Extent Does the Concentration of Salt Affect the Bacterial Community in a Saline Soil? – PLoS One: 9(9): e106662. https://doi.org/10.1371/journal.pone.0106662.

[8] Chao, A., Chiu, C. (2016): Species Richness: Estimation and Comparison. – Wiley StatsRef: Statistics Reference Online, pp. 1-26.

http://www.aloki.hu ● ISSN 1589 1623 (Print) ● ISSN1785 0037 (Online)
DOI: http://dx.doi.org/10.15666/aeer/2001_447464

[9] Chindapana, N., Niamnuyb, C., Devahastin, S. (2018): Physical properties, morphology and saltiness of salt particles as affected by spray drying conditions and potassium chloride substitution. – Powder Technology 326: 265-271. https://doi.org/10.1016/j.powtec.2017.12.014.
[10] Ding, X., Liu, K., Gong, G., Tian, L., Ma, J. (2020): Volatile organic compounds in the salt-lake sediments of the Tibet Plateau influence prokaryotic diversity and community assembly. – Extremophiles 24(2): 307-318. https://doi.org/10.1007/s00792-020-01155-3.
[11] Dong, H., Zhang, G., Jiang, H., Yu, B., Chapman, L. R., Lucas, C. R., Fields, M. W. (2006): Microbial diversity in sediments of saline Qinghai Lake, China: linking geochemical controls to microbial ecology. – Microb Ecol. 51(1): 65-82. https://doi.org/10.1007/s00248-005-0228-6.
[12] Freire, P., Andrade, C., Viveiros, F., Silva, C., Coutinho, R., Cruz, J. (2014): Mineral water occurrence and geochemistry in the Azores volcanic archipelago (Portugal): insight from an extended database on water chemistry. – Environmental Earth Sciences 73: 2749-2762. https://doi.org/10.1007/s12665-014-3157-1.
[13] Grant, W. D., Sorokin, D. Y. (2011): Distribution and Diversity of Soda Lake Alkaliphiles. – In: Horikoshi, K. (ed.) Extremophiles Handbook. Springer, Tokyo, pp. 27-54. https://doi.org/10.1007/978-4-431-53898-1_3.
[14] Guan, T. W., Lin, Y. J., Ou, M. Y., Chen, K. B. (2020): Isolation and diversity of sediment bacteria in the hypersaline aiding lake, China. – PloS one 15(7): e0236006. https://doi.org/10.1371/journal.pone.0236006.
[15] Han, R., Zhang, X., Liu, J., Long, Q., Chen, L., Liu, D., Zhu, D. (2017): Microbial community structure and diversity within hypersaline Keke Salt Lake environments. – Can. J. Microbiol. 63(11): 895-908. https://doi.org/10.1139/cjm-2016-0773.
[16] Hollister, E. B., Engledow, A. S., Hammett, A. J., Provin, T. L., Wilkinson, H. H., Gentry, T. J. (2010): Shifts in microbial community structure along an ecological gradient of hypersaline soils and sediments. – ISME 4(6): 829-38. https://doi.org/10.1038/ismej.2010.3.
[17] Insam, H., Seewald, M. S. A. (2010): Volatile organic compounds (VOCs) in soils. – Biol Fertil Soils 46: 199-213. https://doi.org/10.1007/s00374-010-0442-3.
[18] Jones, B. E., Grant, W. D., Collins, N. C., Mwatha, W. E. (1994): Alkaliphiles: Diversity and Identification. – In: Priest, F. G., Ramos-Cormenzana, A., Tindall, B. J. (eds.) Bacterial Diversity and Systematics. Federation of European Microbiological Societies Symposium Series, 75: Springer, Boston, MA. https://doi.org/10.1007/978-1-4615-1869-3_12.
[19] Jones, B. E., Grant, W. D., Duckworth, A. W., Owenson, G. G. (1998): Microbial diversity of soda lakes. – Extremophiles 2(3): 191-200. https://doi.org/10.1007/s007920050060.
[20] Kambura, A. K., Mwirichia, R. K., Kasili, R. W., Karanja, E. N., Makonde, H. M., Boga, H. I. (2016): Bacteria and Archaea diversity within the hot springs of Lake Magadi and Little Magadi in Kenya. – BMC Microbiology 16(1): 136. https://doi.org/10.1186/s12866-016-0748-x.
[21] Kasper, U. K., Alexander, L., Trine, F. J., Trine, R. T., Michael, W., Kjeld, I. (2007): Diversity of sulfate-reducing bacteria from an extreme hypersaline sediment, Great Salt Lake (Utah). – FEMS Microbiology Ecology 60(2): 287-298. https://doi.org/10.1111/j.1574-6941.2007.00288.x.
[22] Last, W. M. (2002): Geolimnology of salt lakes. – Geosci. J. 6: 347-369. https://doi.org/10.1007/BF03020619.
[23] Lin, Q., Xu, L., Hou, L., Liu, Z., Jeppesen, E., Han, B. (2017): Responses of trophic structure and zooplankton community to salinity and temperature in Tibetan lakes: Implication for the effect of climate warming. – Water Research 124: 618-629. https://doi.org/10.1016/j.watres.2017.07.078.
[24] Mellouki, A., Wallington, T., Chen, J. (2015): Atmospheric Chemistry of Oxygenated Volatile Organic Com pounds (OVOCs): Impacts on Air Quality and Climate. – Chemical

http://www.aloki.hu ● ISSN 1589 1623 (Print) ● ISSN1785 0037 (Online)
DOI: http://dx.doi.org/10.15666/aeer/2001_447464

Reviews, American Chemical Society 115(10): 3984-4014. https://doi.org/10.1021/cr500549nff.

[25] Mesbah, N. M., Abou-El-Ela, S. H., Wiegel, J. (2007): Novel and unexpected prokaryotic diversity in water and sediments of the alkaline, hypersaline lakes of the Wadi an Natrun, Egypt. – Microb. Ecol. 54(4): 598-617. https://doi.org/10.1007/s00248-006-9193-y.

[26] Mianping, Z., Jiayou, T., Junying, L., Fasheng, Z. (1993): Chinese saline lakes. – In: Hurlbert, S. H. (ed.) Saline Lakes V. Developments in Hydrobiology 87. Springer, Dordrecht. https://doi.org/10.1007/978-94-011-2076-0_3.

[27] Nho, S. W., Abdelhamed, H., Paul, D., Park, S., Mauel, M. J., Karsi, A., Lawrence, M. L. (2018): Taxonomic and Functional Metagenomic Profile of Sediment from a Commercial Catfish Pond in Mississippi. – Front. Microbiol. 9: 2855. https://doi.org/10.3389/fmicb.2018.02855.

[28] Oren, A., Fischel, U., Aizenshtat, Z., Krein, E. B., Reed, R. H. (1994): Osmotic adaptation of microbial communities in hypersaline microbial mats. – In: Stal, L. J., Caumette, P. (eds.) Microbial Mats. NATO ASI Series (Series G: Ecological Sciences), Vol 35. Springer, Berlin, Heidelberg. https://doi.org/10.1007/978-3-642-78991-5_14.

[29] Rasuk, M. C., Fernández, A. B., Kurth, D., Contreras, M., Novoa, F., Poiré, D., Farías, M. E. (2016): Bacterial Diversity in Microbial Mats and Sediments from the Atacama Desert. – Microb Ecol. 71(1): 44-56. doi: https://doi.org/10.1007/s00248-015-0649-9.

[30] Roebuck, J. A., Avery, G. B., Felix, J. D., Kieber, R. J., Mead, R. N., Skrabal, S. A. (2016). Biogeochemistry of Ethanol and Acetaldehyde in Freshwater Sediments. – Aquat Geochem. 22: 177-195. https://doi.org/10.1007/s10498-015-9284-9.

[31] Ruginescu, R., Gomoiu, I., Popescu, O., Cojoc, R., Neagu, S., Lucaci, I., Batrinescu-Moteau, C., Enache, M. (2020): Bioprospecting for Novel Halophilic and Halotolerant Sources of Hydrolytic Enzymes in Brackish, Saline and Hypersaline Lakes of Romania. – Microorganisms 8(12): 1903. https://doi.org/10.3390/microorganisms8121903.

[32] Tang, K., Jia, L., Yuan, B., Yang, S., Li, H., Meng, J., Zeng, Y., Feng, F. (2018): Aerobic Anoxygenic Phototrophic Bacteria Promote the Development of Biological Soil Crusts. – Frontiers in microbiology 9: 2715. https://doi.org/10.3389/fmicb.2018.02715.

[33] Tazi, L., Breakwell, D. P., Harker, A. R., Crandall, K. A. (2014): Life in extreme environments: microbial diversity in Great Salt Lake, Utah. – Extremophiles 8(3): 525-35. https://doi.org/10.1007/s00792-014-0637-x.

[34] Thukral, A. K. (2017): A review on measurement of Alpha diversity in biology. – Agricultural Research Journal 54(1): 1-10.

[35] Ventosa, A., de la Haba, R. R., Sánchez-Porro, C., Papke, R. T. (2015): Microbial diversity of hypersaline environments: a metagenomic approach. – Curr Opin Microbiol. 25: 80-87. https://doi.org/10.1016/j.mib.2015.05.002.

[36] Vogt, J. C., Abed, R. M. M., Albach, D. C., Palinska, K. A. (2017): Bacterial and Archaeal Diversity in Hypersaline Cyanobacterial Mats Along a Transect in the Intertidal Flats of the Sultanate of Oman. – Microb Ecol. 75(2): 331-347. https://doi.org/10.1007/s00248-017-1040-9.

[37] Williams, W. D. (1991): Chinese and Mongolian saline lakes: a limnological overview. – Hydrobiologia 210: 39-66. https://doi.org/10.1007/BF00014322.

[38] Wu, C., Wang, C., Wang, S., Wang, W., Yuan, B., Qi, J., Wang, B., Wang, H., Wang, C., Song, W., Wang, X., Hu, W., Lou, S., Ye, C., Peng, Y., Wang, Z., Huangfu, Y., Xie, Y., Zhu, M., Zheng, J., Wang, X., Jiang, B., Zhang, Z., Shao, M. (2020): Measurement report: Important contributions of oxygenated compounds to emissions and chemistry of volatile organic compounds in urban air. – Atmos. Chem. Phys. 20: 14769-14785. https://doi.org/10.5194/acp-20-14769-2020.

[39] Yu, D., Kuenen, J. G. (2005): Chemolithotrophic haloalkaliphiles from soda lakes. – FEMS Microbiology Ecology 52(3): 287-295. https://doi.org/10.1016/j.femsec.2005.02.012.

http://www.aloki.hu ● ISSN 1589 1623 (Print) ● ISSN1785 0037 (Online)
DOI: http://dx.doi.org/10.15666/aeer/2001_447464

[40] Zaikova, E., Benison, K. C., Mormile, M. R., Johnson, S. S. (2018): Microbial communities and their predicted metabolic functions in a desiccating acid Salt Lake. – Extremophiles 22(3): 367-379. https://doi.org/10.1007/s00792-018-1000-4.
[41] Zheng, M. (2011): Resources and eco-environmental protection of salt lakes in China. – Environ Earth Sci. 64: 1537-1546. https://doi.org/10.1007/s12665-010-0601-8.

http://www.aloki.hu ● ISSN 1589 1623 (Print) ● ISSN1785 0037 (Online)
DOI: http://dx.doi.org/10.15666/aeer/2001_447464

MOLECULAR CHARACTERIZATION OF THE PATHOGEN CAUSING GREY MOLD IN STRAWBERRY AND ITS MANAGEMENT

JAMEEL, S.[1] – REHMAN, A.[1*] – RAJPUT, N. A.[1] – SADIA, B.[2]

[1]*Department of Plant Pathology, University of Agriculture Faisalabad, Pakistan*

[2]*Centre of Agriculture Biochemistry and Biotechnology, University of Agriculture Faisalabad, Pakistan*

**Corresponding author*
e-mail: arb041@gmail.com

(Received 16th Aug 2021; accepted 23rd Nov 2021)

Abstract. Strawberry is an important fruit crop, it has been attacked by a number of pathogens. Grey mold for strawberry is commonly caused by Botrytis cinerea, which is an important fungal pathogen causing diseases in many crops. Strawberry samples affected by grey mold showing typical symptoms like browning of the fruit part, ripening berries and rotted fruit with grey mold growth were collected from different strawberry growing areas of Punjab and The National Agriculture Research Center (NARC). The associated pathogens were isolated, purified and their morphological features were observed. Pathogenicity test was conducted on fruits and were re-isolated from inoculated portions. The fungal DNA was isolated from diseased samples by using CTAB protocol. To identify the pathogens on the molecular basis PCR products were attained and amplified through universal primers. The sequence of associated pathogens were analyzed by constructing phylogenetic tree and the identified pathogens were organized into specific clades including other similar species. Different groups of fungicides, antagonistic microorganisms and plant extracts were also evaluated in-vitro against isolated fungal pathogens through poisoned food technique. Among fungicides, antagonists and plant extracts dicarboximide & benzimidazole, Trichoderma spp., Allium sativum and Mentha spicata can showed promising results against mycelial growth of B. cinerea.
Keywords: *Fragaria ananassa, Botrytis. cinerea, fungicides, antagonists, plant extract*

Introduction

Strawberry (*Fragaria ananassa* Duchesne) is a cherished fruit product all over the world (Basu et al., 2014). Its yields are drastically reduced each year owing to the attack of a wide number of fungal, viral and bacterial pathogens (Giampieri et al., 2015). Fungal infections are most common and damaging especially the gray mold caused by *Botrytis cinerea* as they attack the plant and fruit in field, storage and during transportation, making it quite unlikable for producers, buyers and consumers equal (Hasan et al., 2019). The pathogen B. *cinerea* causes serious losses in more than 200 crop species worldwide. Under wet conditions without application of fungicides, it can cause massive production losses of up to 80% (Petrasch et al., 2019). Diseased samples of grey mold of strawberry showing typical symptoms like browning or blackening of the fruit part, light brown lesions usually develop on the stem grey, dusty looking fungal growth on ripening berries and rotted fruit with velvety grey mold growth (Bertetti et al., 2008). The classification of *Botrytis* genus is largely depended on cultural and morphological characteristics. Morphological characteristics are important to ascertain the biology of pathogens but variability in growth, spore size and shape and pathogenicity has been reported in genus Botrytis. The molecular investigations

http://www.aloki.hu ● ISSN 1589 1623 (Print) ● ISSN 1785 0037 (Online)
DOI: http://dx.doi.org/10.15666/aeer/2001_465478

confirmed the traditional identification methods. Characteristics like colony color, texture, conidium size etc. are useful in describing some species (Staats et al., 2007). Along with the morphological characters, molecular characterization is also very important. Being an important pathogenic fungus, it is important to find out the genetic diversity of B. *cinerea* through latest molecular tools. Some gene specific primers are also available that had been used in B. *cinerea* identification at species level (Rigotti et al., 2002). Ribosomal internal transcribed spacer (ITS) region had been formerly used. With the ease of genome sequencing and use of other online software for genomic analyses, more information is available nowadays (Elad et al., 2009). Globally based on latest investigations, B. *cinerea* ranked second due to its economic and scientific importance. Among the list of top 10 fungal plant pathogens. Nowadays, the major way to manage grey mold rot caused by B. *cinerea* is the use of chemical fungicides, which may be about 8% of all the world fungicide market (Dean et al., 2012). In recent years, concerns about pesticide residues in food crops and fungicide-resistant pathogens have led to a demand for alternative methods to control plant pathogens such as B. *cinerea* (Fillinger and Elad, 2016). A lot of information about prevalence and incidence of the disease in different strawberry producing countries is available but in Pakistan very limited information is available. Therefore, this work is planned to find out the pathogens associated with grey mold of strawberry, their morphological and molecular identification and their management using different approaches. This study will provide basis for the development of integrated disease management strategies in future (Grover and Moore, 1962).

Materials and methods

The survey was conducted during December to March of 2018-2019 in strawberry fields which were on fruiting stage. Different strawberry growing areas of Punjab province Narowal, and NARC Pakistan were surveyed for the collection of typical grey mold diseased samples. From every field, different leaves, flowers and fruits samples were collected.

Isolation, purification and morphological identification

A total of 50 samples of rotted fruits were collected in the month of Dec-Mar, 2018-2019 from each of the field and assessed for presence of Botrytis cinerea fungi at the Plant Disease Diagnostic Laboratory, University of Agriculture, Faisalabad. Collected infected strawberry fruits were cut into small pieces (1 to 2 cm) and plating on potato dextrose agar (PDA). The resulted fungal pathogens were then purified using the hyphal tips technique (Tuite, 1969) on the PDA medium followed by preparation of fungal slants on PDA medium for further future studies. The germinating spore and fruiting body of pathogen were examined and observed using microscope (Nikon AZ100), at 10, 40 and 100 X magnification and images were captured by using a digital camera.

Pathogenicity test

Healthy fruits were disinfected by using 70% alcohol and washed with distilled water. The fruits were then flooded in 1% hypochlorite and again rinsed with distilled water. All fruits were pierced with a sterile needle and, then, scattered with the spore suspension. The interspersed fruits were kept in humid chambers at the room

http://www.aloki.hu ● ISSN 1589 1623 (Print) ● ISSN 1785 0037 (Online)
DOI: http://dx.doi.org/10.15666/aeer/2001_465478

temperature, with observations taken every 24 h. Symptoms of the inoculated strawberry fruits were observed on daily basis until development of typical grey mold appearance. Moreover, re-isolation was also done from the inoculated fruits to confirm the Koch's postulate (Park et al., 2008).

Molecular identification of grey mold of strawberry

DNA extraction and gel electrophoresis examination

The DNA of fungal pathogen was extracted by modified CTAB method (Möller et al., 1992). Extracted DNA samples of associated pathogen were examined by electrophoresis, 1.0% (weight/volume) agarose gels were added in (0.5X TBE buffer) along with (100 µg/ml) of ethidium bromide (100 µg/ml). The associated DNA samples of pathogen were examined by electrophoresis in 1.0% (w/v) agarose gels (0.5X TBE buffer) and DNA bands of associated pathogen were viewed on computerized Gel DocEZimager and pictured the image of DNA band (Shih et al., 2002).

PCR amplification

PCR Amplification is done through ITS. ITS regions of rDNA of associated pathogen will be amplify by using ITS1 (5′TCCGTAGGTGAACCTGCGG 3′) and ITS4 (5′ TCCTCCGCTTATTGATATGC 3′) respectively. A total of 15 isolates were tested for this purpose. Optimum conditions for PCR amplification will maintain and final step of Polymerase Chain Reaction amplification were completed by Green master mix (2X Dream Taq Green PCR) at volume of 15 µl. (Green Master mix) is a composition of (4 mM MgCl2) and 0.4 mM of dNTPs, (dATP, dCTP, dGTP and dTTP). Specific forward and reverse (ITS1 and ITS4) primers at volume (0.1-1.0 µM) were used for amplification DNA templates and finally (1-10 µl) of nuclease free water was added to complete the volume of PCR reaction.

Sequencing and phylogenetic analysis

The amplified PCR product were sequenced (Sanger et al., 1977) method and phylogenetic tree was constructed by using the MEGA 7.0 software (Kumar et al., 2016). Sequences were then submitted at NCBI database and were further analyze by BLAST analysis.

Management of grey mold of strawberry

In-vitro evaluation of different groups of fungicides

Fungicides Benzimidazole (1,3-benzodiazole), Dicarboximide (N-octylbicycloheptene), Anilide (Aniline), Triazole (Metconazole + Propiconazole) Anilinopyrimidine (Cyprodinil + Pyrimethanil) and Pyrazole (4-hydroxypyrazole) were tested in-vitro to evaluate suppression of mycelial growth of grey mold pathogen using the "poisoned food technique". 50, 100, 150, 200 and 250 µg/mL concentrations were made for each fungicide. Percent mycelial growth inhibition was calculated as given below:

$$\text{Mycelial growth inhibition} = \frac{X-Y}{X} \times 100 \qquad \text{(Eq.1)}$$

where: X = radial growth of control plate; Y = radial growth of fungicide treated plate.

http://www.aloki.hu ● ISSN 1589 1623 (Print) ● ISSN 1785 0037 (Online)
DOI: http://dx.doi.org/10.15666/aeer/2001_465478

In-vitro management of grey mold through plant extracts

Different plant extracts were evaluated in-vitro under different concentrations to determine the most efficient one. *Table 1* showed the plant extracts that were used with their scientific and common names, families and plant parts that were used against grey mold of strawberry. Three concentrations were used with 7 treatments along with distilled water as negative control and 3 replications were done.

Table 1. *List of different plant extracts used against grey mold of strawberry*

Sr. no	Scientific name	Common name	Family	Plant part used
1	*Allium sativum*	Garlic	Amaryllidaceae	Pods
2	*Mentha* spp.	Mint	Lamiaceae	Leaves
3	*Rosmarinu sofficinalis* L.	Rosemary	Lamiaceae	Leaves
4	*Achillea millefolium*	Yarrow	Asteraceae	Leaves
5	*Tagetes patula*	Marygold	Asteraceae	Leaves
6	*Syzygium cumini*	Jambolan	Myrtaceae	Leaves

Preparation of plant extracts

Plant parts after collections were surface sterilized and dried under shade conditions. After this, these samples were grind thoroughly using liquid nitrogen and extracted (48 h) in a Soxhlet apparatus by using with absolute ethanol and methanol solvents. These solvents were removed separately using a rotary evaporator (Heidolph VV2000) under reduced pressure at <50 °C. Resulted crude extracts were kept at 20 °C for storage until assayed. Stock solutions and serial dilutions of extracts were prepared in dimethyl sulphoxide (DMSO) (Fillinger and Elad, 2016). For control, DMSO was used.

Antifungal activity of selected medicinal plants *Allium sativum, Mentha* spp., *Rosmarinus officinalis*., *Achillea millefolium, Tagetespatula* and *Syzygium cumini* was evaluated against grey mold associated pathogen using an agar well diffusion method (Perez et al., 1990). PDA media was prepared for this purpose and petri plates were poured with 20 ml media after sterilization in autoclave at 15 psi and 121 °C. After solidification of media, four wells of 6 mm dia. were made in each petri plate with the help of sterilized cork borer. 5, 15, 25 and 50 µg/mL concentrations were prepared in DMSO and applied in each well using a micropipette. A purified colony of fungus (5 mm) was placed in the center of each petri plate and incubated at 25 °C. Three replications were used. Control treatment was performed by using DMSO with the same concentration used to test the extracts.

$$\text{Diameter of inhibition zone} = \frac{\text{diameter of sample} - \text{diameter of control}}{\text{diameter of control}} \qquad \text{(Eq.2)}$$

In-vitro management of grey mold through antagonistic microbes

Following are the antagonistic microbes that were used. List of different antagonists are shown in *Table 2*.

Three concentrations were used with 7 treatments along with sterile water as negative control and 3 replications were performed for each treatment. All the in-vitro experiments were conducted using Poisoned Food Technique.100, 200 and 300 µg/mL

http://www.aloki.hu ● ISSN 1589 1623 (Print) ● ISSN 1785 0037 (Online)
DOI: http://dx.doi.org/10.15666/aeer/2001_465478

concentrations were made for each antagonist. Percent mycelial growth inhibition was calculated as given below:

$$\text{Mycelial growth inhibition} = \frac{X-Y}{X} \times 100 \quad \text{(Eq.3)}$$

where: X = radial growth of control plate; Y = radial growth of antagonist treated plate.

Table 2. *List of different antagonists used against grey mold of strawberry*

Sr. no	Antagonists	Organism type
1	*Colletotrichum gloeosporioides*	Fungi
2	*Bacillus subtilis*	Bacteria
3	*Burkholderia cepacian*	Bacteria
4	*Aspergillus fumigatus*	Fungi
5	*Trichoderma* spp.	Fungi
6	*Penicillium* spp.	Fungi

Statistical analysis

CRD was used for conducting all the experiments which were executed twice. There was no significant interaction between the two tests applied for any treatment used in experiments. After that, all the results were compiled for the final analysis from duplicate tests. Statistix® 8.1 software was used for data analysis statistically. Overall significance of data was checked by ANOVA and differences among the treatment means were compared by using Tukey's test ($P \leq 0.05$) (Steel et al., 1997).

Results

Isolation, purification and morphological identification of grey mold pathogen

Isolation of fungal pathogens from district Narowal and NARC

Multiple samples of diseased plants (i.e., infected fruit parts) were collected from various strawberry fields, each of these samples were treated on following standard procedures and pure fungal mycelia were grown under optimum conditions, each of these fully grown cultures were compared with previously reported cultures, all purified cultures gave a typical greyish-brownish culture growth when compared after 6 and 10 days of culturing which was a positive response for grey mold pathogen (i.e., Botrytis cinerea). The maximum (7.05%) fungi were collected from fruits followed by leaves (2.56%) and flowers (1.43%) from district Narowal (*Table 3a*). Whilst from NARC, the maximum (6.91%) fungi were collected from fruits followed by leaves (2.55%) and flowers (1.76%) (*Table 3b*). Data of the colonization of isolated fungal pathogens from rotted fruit revealed that almost all the field samples were colonized by three or more pathogens. From Kanjroor (Narowal) samples, the frequency of fungi with the highest incidence from district Narowal was *Botrytis cinerea* with the mean frequency of (9.14%) followed by *Alternaria alternate* (5.79%), *Macrophomina* (4.41%), *Rhizoctonia* (3.56%), *Mucor* (2.54%), *Curvularia* (1.12%), *Rhizopus* (1.70%) and *Aspergillus* (0.75%) (*Table 3a*). From NARC samples, the pathogen with the highest incidence from rotted fruits was *Botrytis cinerea* with the mean frequency

http://www.aloki.hu ● ISSN 1589 1623 (Print) ● ISSN 1785 0037 (Online)
DOI: http://dx.doi.org/10.15666/aeer/2001_465478

of (10.09%) followed by *Alternaria alternate* (6.07%), *Macrophomina* (4.27%), *Rhizoctonia* (3.49%), *Mucor* (3.21%), *Rhizopus* (1.05%), *Curvularia* (0.79%), and *Aspergillus* (0.91%) (*Table 3b*).

Table 3a. *Frequency of fungi (per cent) isolated from different plant parts of strawberry collected from district Narowal*

Fungi	Plant parts			
	Leaves	**Fruits**	**Flowers**	**Mean**
Botrytis cinerea (Nar)	5.87	18.05	3.52	9.14
Alternaria alternata	4.26	11.03	2.09	5.79
Aspergillus niger	0.16	1.91	0.18	0.75
Macrophomina spp.	3.11	9.06	1.06	4.41
Rhizoctonia spp.	2.50	7.19	1.00	3.56
Curvularia spp.	1.11	2.12	0.14	1.12
Mucor spp.	1.21	5.16	1.26	2.54
Rhizopus spp.	1.03	1.91	2.17	1.70
Means	2.56	7.05	1.43	

Table 3b. *Frequency of fungi (per cent) isolated from different plant parts of strawberry collected from district NARC*

Fungi	Plant parts			
	Leaves	**Fruits**	**Flowers**	**Mean**
Botrytis cinerea	5.67	19.15	5.45	10.09
Alternaria alternata	4.62	12.01	1.60	6.07
Aspergillus niger	0.51	1.32	0.92	0.91
Macrophomina spp.	3.21	8.65	0.96	4.27
Rhizoctonia spp.	2.52	6.76	1.21	3.49
Curvularia spp.	1.25	0.82	0.31	0.79
Mucor spp.	1.42	5.56	2.66	3.21
Rhizopus spp.	1.21	0.95	1.01	1.05
Means	2.55	6.91	1.76	

Data presented in *Table 3a* and *b* is presented as stacked bar chart in *Figure 1*. Incidence of fungal pathogens associated with strawberry plant from different sources of inoculum collected from different fields of NARC and district Narowal in Pakistan shows in *Figure 1*.

Followed by culture morphological identification, physical identification of growing conidiophores was carried out via a compound microscope. For the purpose lab microscope was utilized at all given magnification powers starting from the lowest up to maximum power of 100X, under maximum magnification a conidiophore containing a tuft or cluster of egg-shaped, ellipsoidal conidia was easily observed confirming the presence of grey mold pathogen as shown in *Figure 2.*

Pathogenicity test

Followed by morphological identification a pathogenicity test was conducted in order to confirm the infection causing agent following the protocol given by Koch (Park

http://www.aloki.hu ● ISSN 1589 1623 (Print) ● ISSN 1785 0037 (Online)
DOI: http://dx.doi.org/10.15666/aeer/2001_465478

et al., 2008). For the trial healthy plants were grown in green house followed by division of plan in to an experimental and a control group, where the experimental group was inoculated by purified pathogen suspension (4 × 106 per mL) and the control group was kept un-inoculated. Each of the group was grown under controlled optimal environment (i.e., temperature 21 °C and RH > 90%) for next 28 days, after seven days the experimental group plants began to show signs of infection with soft rot observed all over the plant body, after 10 days the collapse of functional parenchyma tissues was evident which indicated rapid increase in the rate of infection and was in line with the typical infectious pattern of B. *cinerea*, after 15 days fruit organs appeared shriveled and collapsed due to infection with evident growth of fungus observed on the surface of plant organs, after 21 days complete collapse of fruits was evident along with greyish fungal growth on the surface and pale yellow spots easily seen all over the adjacent leaves. In comparison to this the control group was completely protected from the infection with no appearance of any symptoms on them. Significant reduction in yield of the experimental (ranging around 24-25%) was also observed in comparison to the control group. Comparison between pathogenicity of Narowal and NARC isolates are shown in *Table 4*. Pathogenicity test were perform only to see the presence and confirmation of pathogen but not for the yield reduction.

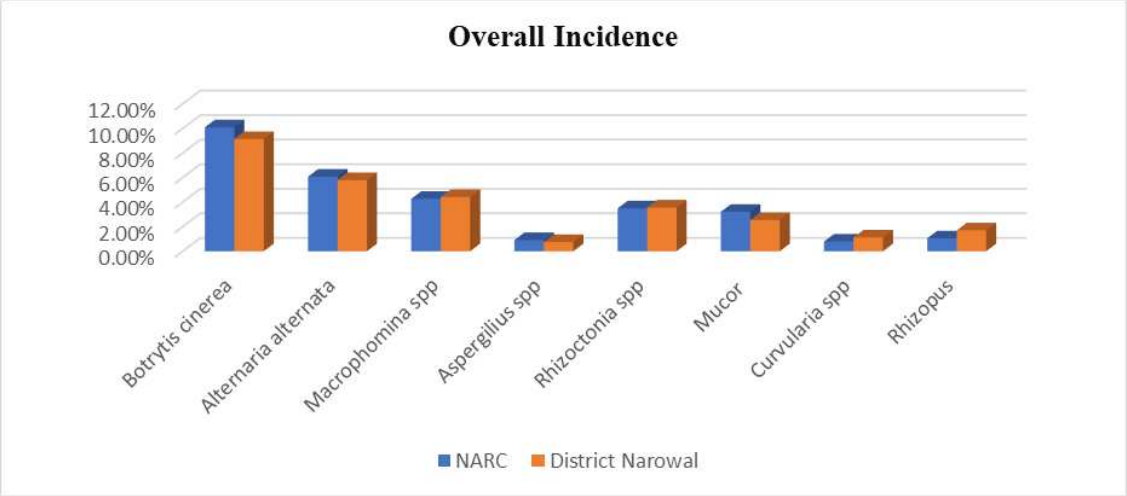

Figure 1. *Overall incidence of colonization of fungal pathogens associated with strawberry plant from different sources of inoculum collected from different fields of NARC and district Narowal in Pakistan*

Table 4. *Comparison between pathogenicity of Narowal and NARC isolate*

Days	Infection stage	Experimental group		Control group
		NARC isolate	Narowal isolate	
7	Visible Soft rot	Yes	Yes	No
10	Collapse of parenchyma cells	Yes	Yes	No
15	Shriveled fruit	Yes	Yes	No
21	Greyish fungal growth	Yes	Yes	No

http://www.aloki.hu ● ISSN 1589 1623 (Print) ● ISSN 1785 0037 (Online)
DOI: http://dx.doi.org/10.15666/aeer/2001_465478

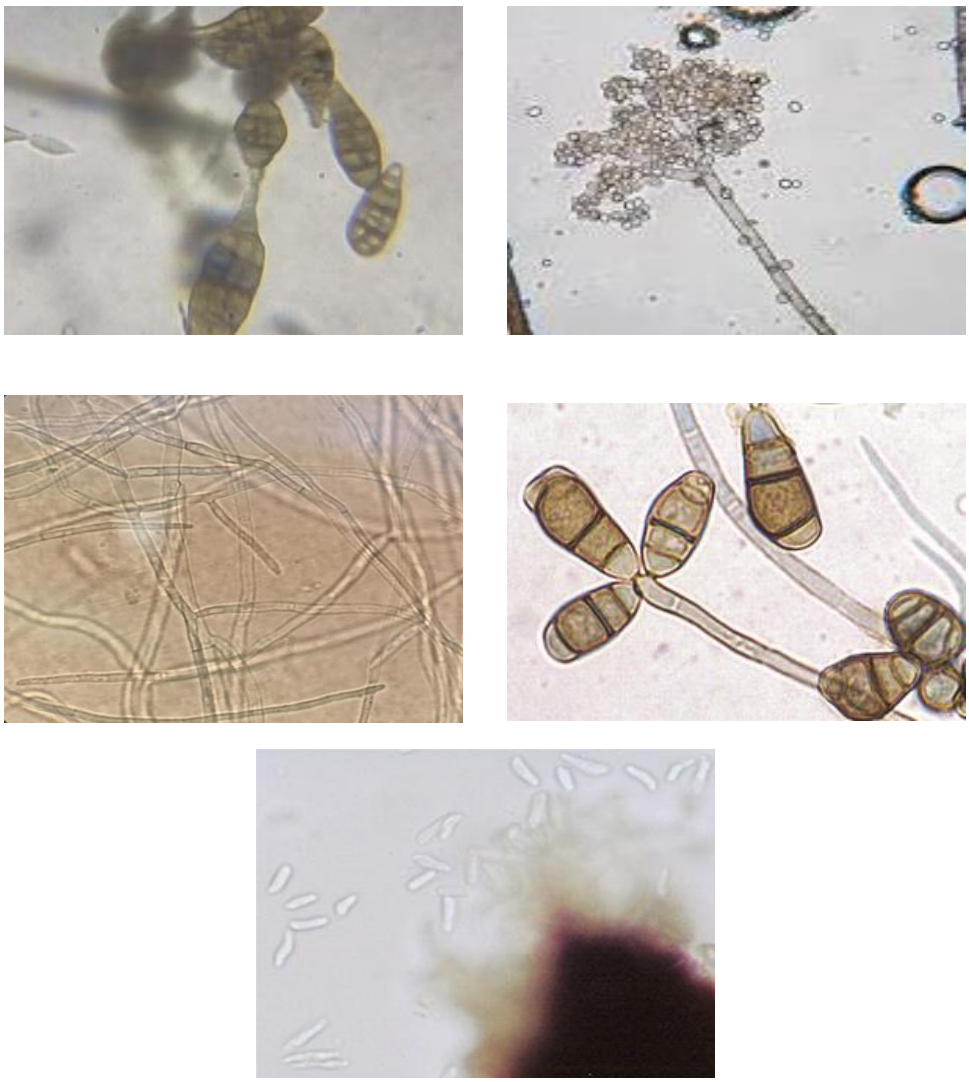

Figure 2. *Microphotographs of isolates isolated from different disease samples infected (a) Alternaria, (b) Rhizopus spp, (c) Rhizoctonia spp), (d) Curbvularia spp, (e) Macrophomina spp*

Molecular identification and phylogenetic analysis: identification on the basis of gapA gene

As illustrated from above experiments (the incidence of colonization of fugal pathogen) it is clarified that Botrytis cinerea were the only pathogen involved in the grey mold disease of strawberry, therefore we selected Botrytis cinerea for further studies. For genetic identification ITS region of 18S rRNA gene was amplified for the 5 representative B. cineria isolates by using ITS 1 and ITS 4 primer (explained in materials and methods). The BLAST searches using NCBI (http://www.ncbi.nlm.nih.gov) and phylogenetic analyses using Maximum likelihood method (Mega7) revealed that the nucleotide sequences of all 5 isolates were identical to B. cinerea (WBD, 2018) Phylogenetic trees of all the strains are shown in *Figure 3.*

These five sequences were submitted to GenBank with the following accession numbers SUB8901212 Seq1 MW485211, SUB8901212 Seq2 MW485212, SUB8901212 Seq3 MW485213, SUB8901212 Seq4 MW485214, SUB8901212 Seq5 MW485215.

http://www.aloki.hu ● ISSN 1589 1623 (Print) ● ISSN 1785 0037 (Online)
DOI: http://dx.doi.org/10.15666/aeer/2001_465478

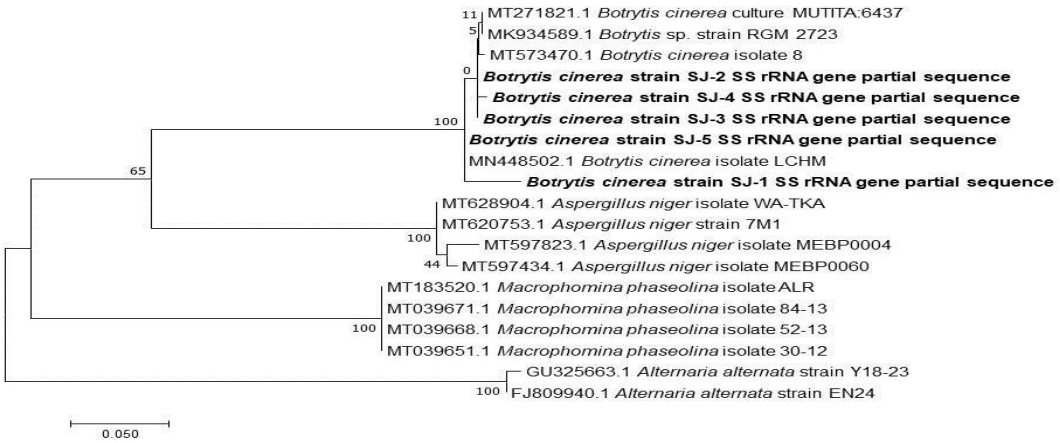

Figure 3. *Molecular phylogenetic analysis by maximum likelihood method*

The evolutionary history was inferred by using the Maximum Likelihood method based on the Tamura-Nei model. The analysis involved 19 nucleotide sequences. There were a total of 656 positions in the final dataset. Evolutionary analyses were conducted in MEGA7 (Kumar et al., 2016). Aspergillus niger, Macrophomina phaseolina and Alternaria alternate species were used as out-group species for rooting the tree.

In-vitro evaluation of various fungicides, antagonists and plant extracts on the mycelial growth of Botrytis cinerea NARC and Narowal isolate

The mean square values for various fungicides, antagonists and plant extracts showed significant effects on mycelia growth of Botrytis cinerea from samples collected from two different locations i.e., NARC and Narowal. In comparison to the control all fungicides treatments gave a significant response against the fungal growth with Dicarboximide giving best result followed by Benzimidazole, Anilinoptrimidine, Trizole, Pyrazole and anilide at both locations i.e., NARC and Narowal (*Table 5*). This massive difference of growth values between control and each of the treatments give a general view of the fact that each of these treatments has a significant inhibitory effect on the growth of pathogen. Certain of these chemicals gave slightly better results against Narowal isolates than the NARC isolates where as some showed a slight increase in the overall growth of the pathogen, this anomaly can be due to fungus natural ability to develop a certain degree of resistance against the chemicals. A trial was conducted with the technical evaluation of antagonist's inhibitory effect carried out against two isolates of strawberry grey mold to estimate the overall efficacy of antagonist agents, a total of seven treatments; with six antagonists and one control were applied on to the fungus under in-vitro conditions and the final results were evaluated. The application of antagonists against NARC and Narowal isolates showed that each of the antagonist treatments gave a significant response in reducing the growing ability of the pathogen in reference to the control, which shows ability to reduce pathogen infection in host plants. In case of NARC and Narowal isolates, among all antagonist treatments, *Trichoderma* spp. gave best results followed by *Bacillus subtilis*, *Penicillium* spp., *Burkholderia* spp., *Aspergillus* spp., and *Colletotrichum* spp.

http://www.aloki.hu ● ISSN 1589 1623 (Print) ● ISSN 1785 0037 (Online)
DOI: http://dx.doi.org/10.15666/aeer/2001_465478

respectively Plant extracts is also considered to be one of the eco-friendly methods to inhibit the growth of certain pathogens. For the purpose of evaluating various extracts against Botrytis cinerea an experiment was carried out for estimating the effectiveness of plant extracts on growth reduction of two isolates. A total of six plant extracts and a control were evaluated against the pathogen. The application of different plant extracts against NARC and Narowal isolates revealed that *Allium sativum* was most effective followed by *Mentha spicata*, *Tagetes patula, Syzygium cumini, Rosmarinus officinalis*, and *Achillea millefolium*. This massive difference of growth values between control and each of the treatments give a general view of the fact that each of these treatments has a significant inhibitory effect on the growth of pathogen.

Table 5. *Mean square values for In-vitro evaluation of various fungicide, antagonists and plant extracts on the mycelia growth of Botrytis cinerea*

Source	DF	Fungicides NARC	Fungicides Narowal	Antagonists NARC	Antagonists Narowal	Plant extracts NARC	Plant extracts Narowal
Rep	2	2.741	0.181	4.274	0.557	1.268	5.676
Treatment	6	860.471*	955.340*	507.759*	531.314*	396.912*	445.723*
Error	12	0.552	0.694	1.321	1.702	0.497	0.397
Total	20						

CV = 4.37

Response of different groups of treatments on mycelial growth of Botrytis cinerea

In order to estimate a group-based effectiveness of various chemicals being utilized for inhibiting the growth and infection of fungus we ultimately compared the values of growth under various treatments against the NARC and Narowal isolate. The overall comparison of different groups of treatments shows that each of the treatment type has particularly positive response in inhibiting the growth of fungus and thus preventing the infection. Among the treatments fungicidal treatments were most effective in reducing the infection followed by antagonists and plant extracts. Overall comparison of three groups of treatments over two-year time period is shown in *Figure 4*.

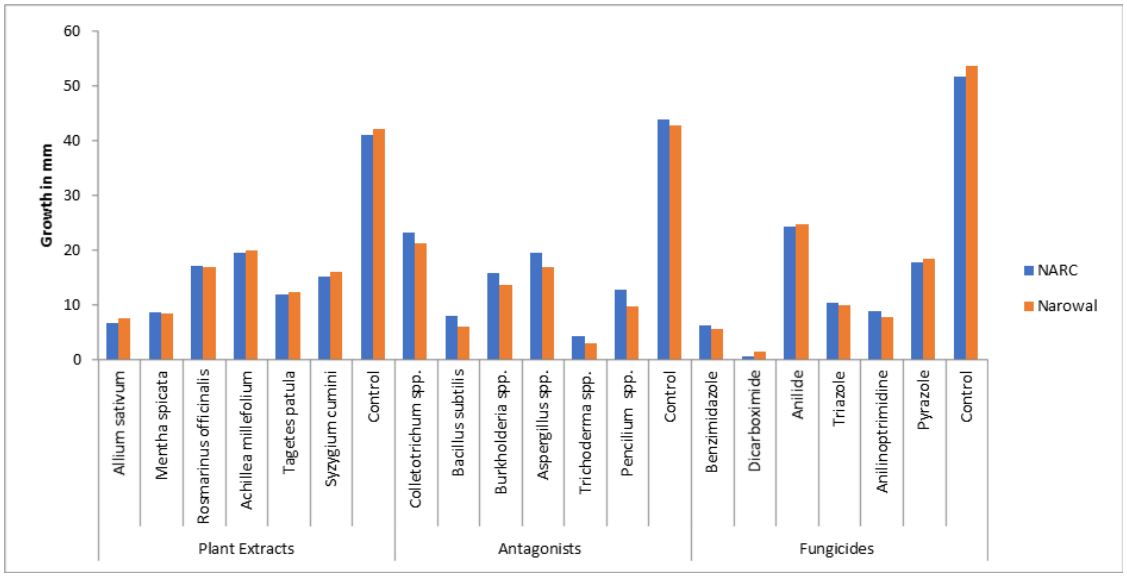

Figure 4. *Response of different groups of treatments on mycelial growth of Botrytis cinerea*

http://www.aloki.hu ● ISSN 1589 1623 (Print) ● ISSN 1785 0037 (Online)
DOI: http://dx.doi.org/10.15666/aeer/2001_465478

Response of individual treatments on Botrytis cinerea

For estimating the individual treatment effectiveness response against the fungal pathogen all treatment data for inhibition of growth against the two isolates (i.e., NARC and Narowal isolate) was collected together and plotted on a graph (*Fig. 5*). The plotted data carefully shows level of effectiveness for each of the individual treatment in comparison to the control group, all of the treatments turn out to be effective having a significant reducing effect on pathogen indicating each of these can be made a part of well-designed broad range integrated management plan for combating the disease. Among the effective treatment the most effective of all is Dicarboximide which is a chemical based fungicidal treatment and remains the most effective over the entire experimental duration maintaining its efficacy. Second most effective treatment is the *Trichoderma* spp. based antagonists approach used for combating the disease by utilizing the competitive and counters active natural ability of the antagonists against the pathogen. Third best of all the treatments was the plant extract of *Allium sativum*, among all the treatments Anillide gave least effective result against both isolates but notably it was still far more effective in comparison to the control as it gave significantly lower growths of fungus in comparison to the control group.

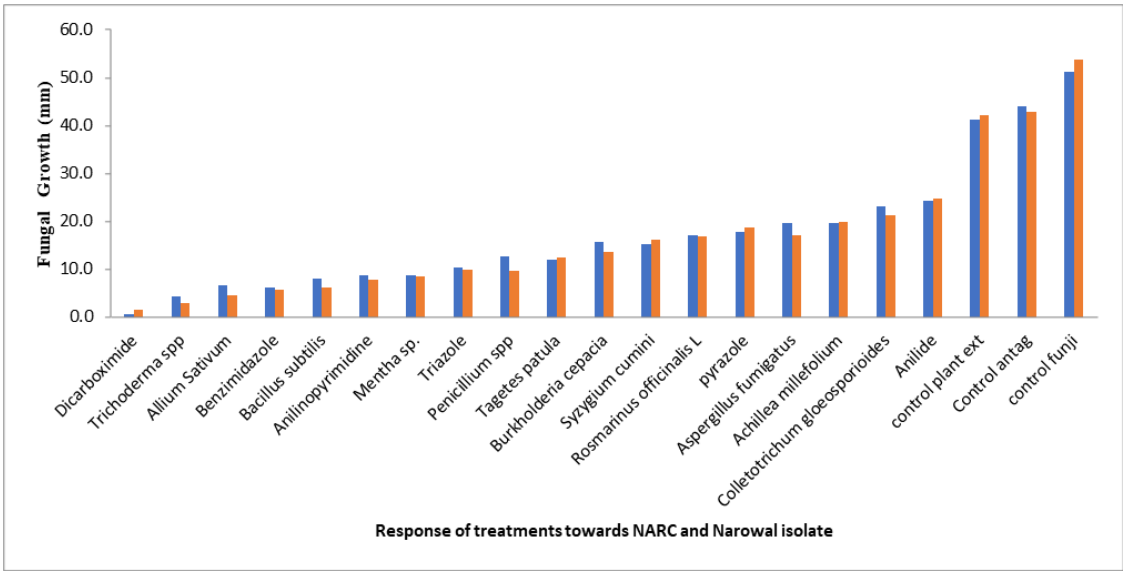

Figure 5. *Response of individual treatments on Botrytis cinerea*

Discussion

The fungal pathogen Botrytis cinerea causes grey mold, a commercially damaging disease of strawberry (Petrasch et al., 2019). During the first stage of the study, we carefully studied various symptoms of disease and conducted survey for visual analysis, we collected certain infected plant samples showing collapsed plant organs and parenchyma cells with watery soaked surfaces and greyish mold like appearances on collapsed fruit surfaces as all these symptoms matched with the one earlier explained by Barnes and Shaw The growing fungus from purified sample was carefully examined under microscope and results were in line. Initially different areas of Narowal and NARC were surveyed for the collection of typical grey mold diseased samples. The disease occurrence was more in NARC as compared to Narowal is attributed to high

http://www.aloki.hu ● ISSN 1589 1623 (Print) ● ISSN 1785 0037 (Online)
DOI: http://dx.doi.org/10.15666/aeer/2001_465478

relative humidity during survey period (Hassan et al., 2019). The similar results were also reported by Card (2005). In this study, isolates of B. cinerea exhibited variation in cultural and morphological aspects. These differences were found to be due to geographical distribution of the studies isolates. Different studies also used cultural and morphological characters for tentative identification of B. *cinerea* (Fernández-Ortuño et al., 2012). Management of this disease to prevent yield losses is an extremely important process, for this purpose we carried out a series of trials under in-vitro conditions to estimate the effectiveness of wide range of fungicidal chemicals, antagonists and plant extracts for disease control. A total of six different fungicides were evaluated, each of them gave a significant response in counter acting the effect of fungus. Dicarboximide was the most effective fungicide followed by benzimidazole among all fungicides. Various studies reported that B. cinerea had developed resistance to dicarboximide, benzimidazole (Shao et al., 2021), Anilide (Stehmann and de Waard, 1996) Triazole (Stehmann and de Waard, 1996) and many other group of fungicide (Maia et al., 2021). Due to simultaneous resistance development against multiple fungicides and environmental concerns plant scientists are focusing on other integrative practices from last decades including biological and agricultural practice (Shao et al., 2021). Antagonistic microorganisms as a biological control agents have been suggested as a practicable approach to lessen the manifestation of various diseases on strawberries (Spadaro and Droby, 2016). In our study, invitro evaluation of six different antagonists were done to assess their efficacy against the pathogen. Each of them gave a significant response against the pathogen with the *Trichoderma* spp. giving best results of all followed by *Bacillus subtilis*, *Pencillium* spp., *Burkholderia* spp., and *Colletotrichum* spp. The results of our study are in line with the findings of Chen et al. (2019).

Under in-vitro conditions, six different extracts were prepared and evaluated, in general each of the extract gave a significant response against pathogens in comparison with the control group. The extract of *Allium sativum* revealed maximum inhibitory activities, followed by *Mentha spicata*, *Tagetes patula*, *Syzygium cumini*, *Rosmarinus officinalis* and *Achillea millefolium* respectively. The overall impact of *Allium sativum* extract on to the pathogen were promising and showed the potential of being used as an alternate to conventional chemicals, the results of our study are also supported by previous recorded results of Fufa and Kutawa. Both pre and postharvest practices and procedures are imperative in the ultimate control of fungal pathogens responsible for Grey mold disease. Based on our results, we recommend fungicides dicarboximide and benzimidazole showed promising results. Exploitable potential of extracts derived from *Allium sativum* and *Mentha spicata* can be used as an alternative to synthetic fungicides to control grey mold disease. Encouraging results were showed by *Trichoderma* spp. and *Bacillus subtilis* which is another biological control to avoid chemical possessions (Perez et al., 1990).

Conclusions

In conclusion, we showed the effectiveness of various group of fungicides, antagonists and plant extracts against mycelial growth of *B. cinerea*. Among fungicides, antagonists and plant extracts dicarboximide and benzimidazole, *Trichoderma* spp., *Allium sativum* and *Mentha spicata* can showed promising results against mycelial growth of *B. cinerea*. Our results provide basic information on the chemical and biological control of *B. cinerea* and are expected to contribute to future work. By using

http://www.aloki.hu ● ISSN 1589 1623 (Print) ● ISSN 1785 0037 (Online)
DOI: http://dx.doi.org/10.15666/aeer/2001_465478

these management practices grey mold in strawberries could be controlled near future. These will also control post-harvest diseases in fruit crops.

REFERENCES

[1] Basu, A., Nguyen, A., Betts, N. M., Lyons, T. J. (2014): Strawberry as a functional food: an evidence-based review. – Critical Reviews in Food Science and Nutrition 54(6): 790-806.

[2] Bertetti, D., Garibaldi, A., Gullino, M. (2008): Resistance of Botrytis cinerea to fungicides in Italian vineyards. – Communications in Agricultural and Applied Biological Sciences 73(2): 273-282.

[3] Card, S. D. (2005): Biological control of Botrytis cinerea in lettuce & strawberry crops. – A thesis submitted in partial fulfillment of the requirements for the Degree of Doctor of Philosophy at Lincoln University, Canterbury, New Zealand.

[4] Chen, X., Wang, Y., Gao, Y., Gao, T., Zhang, D. (2019): Inhibitory abilities of Bacillus isolates and their culture filtrates against the gray mold caused by Botrytis cinerea on postharvest fruit. – The Plant Pathology Journal 35(5): 425.

[5] Dean, R., Van Kan, J. A., Pretorius, Z. A., Hammond-Kosack, K. E., Di Pietro, A., Spanu, P. D., Rudd, J. J., Dickman, M., Kahmann, R., Ellis, J. (2012): The Top 10 fungal pathogens in molecular plant pathology. – Molecular Plant Pathology 13(4): 414-430.

[6] Fernández-Ortuño, D., Li, X., Wang, F., Schnabel, G. (2012): First report of gray mold of strawberry caused by Botrytis caroliniana in North Carolina. – Plant Disease 96(6): 914-914.

[7] Giampieri, F., Forbes-Hernandez, T. Y., Gasparrini, M., Alvarez-Suarez, J. M., Afrin, S., Bompadre, S., Quiles, J. L., Mezzetti, B., Battino, M. (2015): Strawberry as a health promoter: an evidence based review. – Food & Function 6(5): 1386-1398.

[8] Hassan, I., Mehmood, N., Riaz, A., Naz, F. (2019): Geographical distribution and morpho-molecular characterization of pre-harvest gray mold of strawberry in Punjab, Pakistan. – Mycopath 15(2).

[9] Kumar, S., Stecher, G., Tamura, K. (2016): MEGA7: molecular evolutionary genetics analysis version 7.0 for bigger datasets. – Molecular Biology and Evolution 33(7): 1870-1874.

[10] Maia, J. N., Beger, G., Pereira, W. V., De Mio, L. L. M., Duarte, H. d. S. S. (2021): Gray mold in strawberries in the Paraná state of Brazil is caused by Botrytis cinerea and its isolates exhibit multiple-fungicide resistance. – Crop Protection 140: 105415.

[11] Möller, E., Bahnweg, G., Sandermann, H., Geiger, H. (1992): A simple and efficient protocol for isolation of high molecular weight DNA from filamentous fungi, fruit bodies, and infected plant tissues. – Nucleic Acids Research 20(22): 6115.

[12] Park, D., Shafer, O. T., Shepherd, S. P., Suh, H., Trigg, J. S., Taghert, P. H. (2008): The Drosophila basic helix-loop-helix protein DIMMED directly activates PHM, a gene encoding a neuropeptide-amidating enzyme. – Molecular and Cellular Biology 28(1): 410-421.

[13] Petrasch, S., Knapp, S. J., Van Kan, J. A., Blanco-Ulate, B. (2019): Grey mould of strawberry, a devastating disease caused by the ubiquitous necrotrophic fungal pathogen Botrytis cinerea. – Molecular Plant Pathology 20(6): 877-892.

[14] Rigotti, S., Gindro, K., Richter, H., Viret, O. (2002): Characterization of molecular markers for specific and sensitive detection of Botrytis cinerea Pers.: Fr. in strawberry (Fragaria× ananassa Duch.) using PCR. – FEMS Microbiology Letters 209(2): 169-174.

[15] Sanger, F., Nicklen, S., Coulson, A. R. (1977): DNA sequencing with chain-terminating inhibitors. – Proceedings of the National Academy of Sciences 74(12): 5463-5467.

[16] Shao, W., Zhao, Y., Ma, Z. (2021): Advances in understanding fungicide resistance in Botrytis cinerea in China. – Phytopathology 111(3): 455-463.

http://www.aloki.hu ● ISSN 1589 1623 (Print) ● ISSN 1785 0037 (Online)
DOI: http://dx.doi.org/10.15666/aeer/2001_465478

[17] Shih, M., Ambady, N., Richeson, J. A., Fujita, K., Gray, H. M. (2002): Stereotype performance boosts: the impact of self-relevance and the manner of stereotype activation. – Journal of Personality and Social Psychology 83(3): 638.
[18] Spadaro, D., Droby, S. (2016): Development of biocontrol products for postharvest diseases of fruit: the importance of elucidating the mechanisms of action of yeast antagonists. – Trends in Food Science & Technology 47: 39-49.
[19] Staats, M., Van Baarlen, P., Schouten, A., Van Kan, J. A. (2007): Functional analysis of NLP genes from Botrytis elliptica. – Molecular Plant Pathology 8(2): 209-214.
[20] Stehmann, C., de Waard, M. A. (1996): Factors influencing activity of triazole fungicides towards Botrytis cinerea. – Crop Protection 15(1): 39-47.
[21] Tuite, J. (1969): Plant Pathological Methods. Fungi and Bacteria. – Burgess Publishing Company, Minneapolis, MN.
[22] Fufa, B. K. (2019): Anti-bacterial and anti-fungal properties of garlic extract (Allium sativum): a review. – Inter. J. Microbiol. Res. DOI: 10.9734/mrji/2019/v28i330133.
[23] Kutawa, A. B., Danladi, M. D., Haruna, A. (2018): Antifungal activity of garlic (Allium sativum) extract on some selected fungi. – J. Medi. Herbs Entho. Medi. DOI: https://doi.org/10.25081/jmhe.2018.v4.3383.
[24] Barnes, S., Shaw, M. (2003): Infection of commercial hybrid primula seed by Botrytis cinerea and latent disease spread through the plants. – Phyto. Pathol. 93: 573-578.
[25] Steel, R. G. D., Torrie, J. H., Deekey, D. A. (1997): Principles and Procedures of Statistics. A Biometrical Approach. 3rd Ed. – McGraw Hill Book Co. Inc, New York.
[26] Elad, Y., Williamson, B., Tudzynski, P., Delen, N. (2009): Botrytis spp. and diseases they cause in agricultural systems. An intro. – Botrytis. Bio. Pathol. Control. Springer, pp.1-8.
[27] Fillinger, S., Elad, Y. (2016): Botrytis: The Fungus, the Pathogen and Its Management in Agricultural Systems. – In: Elad, Y., Williamson, B., Tudzynski, P., Delen, N. (eds.) Botrytis: Biology, Pathology and Control. Springer, Dordrecht.
[28] Grover, R. K., Moore, J. D. (1962): Toximetric studies of fungicides against the brown rot organisms, Sclerotinia fructicola and S. laxa. – Phytopathology 52: 876-879.
[29] Perez, C., Paul, M., Bazerque, P. (1990): An antibiotic assay by agar well diffusion method. – Acta Biol. Med. Exp. 15: 113-115.

http://www.aloki.hu ● ISSN 1589 1623 (Print) ● ISSN 1785 0037 (Online)
DOI: http://dx.doi.org/10.15666/aeer/2001_465478

CROP YIELD PREDICTION BASED ON GROWTH AND ENVIRONMENTAL FACTORS: A CASE STUDY OF ORIENTAL MELONS (*CUCUMIS MELO* L. VAR. *MAKUWA* MAKINO) IN SEONGJU REGION

MOON, S. H.[1] – NA, M. H.[2] – KIM, T. Y.[3] – PARK, M. S.[4*]

[1]*Research Institute of Future Medicine, Samsung Medical Center, 81 Irwon-ro, Gangnam-gu, Seoul 06351, Republic of Korea*

[2]*Department of Statistics, Chonnam National University, 77 Yongbong-ro, Buk-gu, Gwangju 61186, Republic of Korea*

[3]*Department of Statistics, Keimyung University, 1095 Dalgubeol-daero, Dalseo-gu, Daegu 42601, Republic of Korea*

[4]*Department of Information and Statistics, Chungnam National University, 99 Daehak-ro, Yuseong-gu, Daejeon 34134, Republic of Korea*

**Corresponding author*
e-mail: minsu.park51@gmail.com; phone: +82-42-821-5431; fax: +82-42-822-0260

(Received 23rd Aug 2021; accepted 23rd Nov 2021)

Abstract. In the Republic of Korea, Gyeongsangbuk-do accounts for 95% of the total oriental melon (*Cucumis melo* L. var. *makuwa* Makino) cultivation area and 91% of the yield. Recently, a smart farm system has been introduced that improves efficiency in farm management by collecting information on the growth and environmental factors for each facility farm. This study aimed to identify the factors that influence the increase in the crop yield of Seongju oriental melon through oriental melon information obtained from such a smart farm system, and to construct crop yield prediction models. The data used in the study was collected from four Seongju oriental melon facility farms measured from 2018 to 2019. To predict the crop yield of each farm per week, this study used principal component analysis, distributed-lag model, and auto-regressive integrated moving average with explanatory variables model (ARIMAX) based on growth and environmental variables. ARIMAX with principal components provided stable predictability. We expect the results of this study to be useful in developing optimal farming techniques that can improve the crop yield for farms cultivating Seongju oriental melon in facilities.
Keywords: *Seongju oriental melon, harvest, smart farm, ARIMAX model, principal component analysis*

Introduction

Agriculture was at the center of the first human settlements, enabling them to wait for harvest and cultivate nature to secure a stable food supply beyond hunting and gathering. Large quantities of high-quality agricultural products were harvested through efforts such as maintaining adequate solar radiation and temperature. In addition, the crop yield was increased by using appropriate fertilizers or by administering nutrients for specific agricultural products to remove harmful plants or insects around agricultural products and supply the nutrients necessary for growth.

However, climate change, manifesting in heat waves, abnormal temperatures, droughts, and heavy rains, acts as a factor that hinder the sustainable production of crops. Agriculture in particular is more affected by these environmental factors than other industries. Various studies and technological developments have been steadily

http://www.aloki.hu ● ISSN 1589 1623 (Print) ● ISSN 1785 0037 (Online)
DOI: http://dx.doi.org/10.15666/aeer/2001_479497

carried out to grow agricultural products under certain environmental conditions and thereby cope with such climate changes (Bindi and Olesen, 2011; Deschênes and Greenstone, 2007; Lee et al., 2012).

One such effort in response to these environmental changes is the use of smart farm systems. The smart farm system combines information and communications technologies (ICTs), such as the internet of things (IoT), big data, and artificial intelligence. The smart farm system improves yield and quality by maintaining and providing the environmental factors, such as temperature, solar radiation, humidity, and carbon dioxide, that are most suitable for the cultivation and growth of crops and livestock. In addition, the smart farm system enables automatic and remote management, and can be applied to reduce labor, increase productivity and convenience, and manage crops efficiently, leading to an increasing trend of farmers introducing smart farms (Shin and Jeon, 2020). Not only does it properly maintain the appropriate growing environment for agricultural products but it also reduces instability in agricultural product cultivation by detecting and reporting risks to users and reflecting important characteristics in agriculture. Through these smart farms, humans can cultivate and harvest plants stably regardless of the season by providing a suitable environment that is optimal for the growth and cultivation of each plant.

Table A1 (see *Appendix*) is the National Statistical Office's data on the area and yield of vegetable production (fruit) from 2017 to 2019. *Table A1* shows that more production per area is produced in facility farms than in outdoor farms. The crop yield of oriental melon (*Cucumis melo* L. var. *makuwa* Makino) was less than that of other fruits and vegetables. As of 2019, watermelons accounted for the largest harvest at 20.29%; tomato, 18.59%; cucumber, 16.84%; strawberry, 12.09%; pumpkin, 8.59%; and oriental melon, 7.62%. In the case of oriental melon, which has a lower yield than other fruits and vegetables, studies analyzing data collected from smart farms have been insignificant. Therefore, among fruits and vegetables, this study focused on oriental melon harvested in Seongju, Gyeongsangbuk-do, Republic of Korea, to identify the most suitable environment for the growth of Seongju oriental melon and predict crop yield.

Oriental melon is one of the *Cucurbitaceae* family in terms of total production and harvestable area worldwide (Shin et al., 2017). *Cucurbitaceae* family crops, such as oriental melons, cucumbers and pumpkins, mostly use grafting methods. Among them oriental melons can be grafted onto *Cucurbita* spp., bottle gourd, and C. *melo* rootstocks (King et al., 2010).

Grafting is to connect a scion to a rootstock and make it into a single plant. Grafting not only alleviates the damage caused by inadequate environmental factors and illnesses, but also increases growth speed, yields and affects quality improvements (Goldschmidt, 2014). *Figure 1* describes the growth factors of oriental melons associated with grafting.

In addition to growth factors, oriental melons with poor quality values such as cracking, fermentation, and deformation may be harvested depending on environmental factors, and yields will decrease. Fruit cracking is a phenomenon in which fruit cracks due to a large difference in growth velocity between the surface and the interior of the fruit. Fruit cracking usually occurs in dry soil and in humid environments in the air at the time of fruit formation (Hwang et al., 1999). Fermented fruit is a phenomenon in which pulp is browned and water is filled inside. It is caused by complex environmental factors and cultivation conditions, such as sudden supply of moisture while the soil is

http://www.aloki.hu ● ISSN 1589 1623 (Print) ● ISSN 1785 0037 (Online)
DOI: http://dx.doi.org/10.15666/aeer/2001_479497

dry or lack of sunlight. Therefore, sufficient solar radiation must be provided during periods of fruit growth, and the soil must maintain constant humidity and lower airborne humidity at night (Hwang et al., 1999). Deformation fruit is a fruit that grows in a different shape from normal, resulting from a lack of solar radiation at a time when the fruit grows. As such, growth factors and yield are subject to many environmental factors. Therefore, it is necessary to control through optimal environmental factors using smart farm systems.

Figure 1. *Description of the growth factors of oriental melons (from 'nongsaro' homepage: http://nongsaro.go.kr)*

Using advanced facilities, farms that cultivate fruits and vegetables, such as cucumber, pepper, tomato, and olive, have introduced smart farms to increase production; optimal environmental analysis has helped identify the factors influencing production (Galán et al., 2004; Kang et al., 2020; Lee et al., 2020, 2019). As such, smart farms are being actively introduced for producing fruits and vegetables with a high production weight and analysis studies are being actively conducted accordingly.

Early studies on crop yields using smart farm data in Republic of Korea have focused mainly on fruits and vegetables with a high proportion, such as watermelon, strawberry, and tomato. Lee et al. (2019) used environmental factor variables to explore the factors that affect the growth of plant cucumbers through multiple linear regression analysis. Their results showed that internal cumulative temperature, night average internal relative humidity, and maximum soil humidity, maximum soil moisture tension influence the production. Kang et al. (2020) predicted the production of pepper by region using multiple linear and nonlinear regression analyses using environmental factors, growth factors, and variables with or without irrigation facilities. In determining the yield of red pepper, the study revealed that plant height, main length, length, and branches are significant factors, and the presence or absence of irrigation facilities is a particularly important factor.

Galán et al. (2004) developed a multi-regression model to predict future olive fruit yields for effective and optimized agricultural management. At this study, rainfall five months before the forecast and pollen emissions eight months before the forecast had a significant impact on fruit yields. Choudhury and Jones (2014) predicted crops harvested over different periods in the same region using several time series methods to demonstrate a more robust time series model than smoothing techniques. In this study, auto-regressive moving average showed higher decision coefficients compared with

http://www.aloki.hu ● ISSN 1589 1623 (Print) ● ISSN 1785 0037 (Online)
DOI: http://dx.doi.org/10.15666/aeer/2001_479497

other time series models, such as simple, double, and attenuation trend linear exponential smoothing. The problem of variable crop yields within a region could thus be avoided over time. Bertin and Génard (2018) reviewed several models to simulate tomato growth and quality using Process-based simulation models and investigated the potential application of ideas design of ideotypes, such as conceptual plants, which are expected to be performed in a particular environment. Di Vittori et al. (2018) defines an objective concept of strawberry quality and summarizes the key pre-harvest factors affecting the quality of the fruit. It was analyzed that climate variables such as soil conditions, production cycles, and factors related to cultivation systems such as traditional or soil-free cultivation affect the final quality of strawberry fruits.

In this study, we aim to explore the environmental and growth factors with high yield obtained from smart farms for relatively unstudied oriental melons due to lower yields than other fruits and vegetables, and provide models for crop yield prediction.

Materials and methods

Data description

We collected crop yield, environmental, and growth data for oriental melon from four facility farms that cultivate oriental melons in Seongju. The GPS coordatinates for four farms are 35°56’34.0”N 128°13’09.0”E, 35°55’16.0”N 128°16’12.0”E, 35°57’20.0”N 128°17’51.0”E, and 35°56’15.0”N 128°13’21.0”E, respectively. The data used for the analysis were provided by the Rural Development Administration, Republic of Korea, and the response variable was defined as oriental melon yield per 10a (kg/10a). Moreover, the growth and facility farm environmental variables were used as explanatory variables. We measured the oriental melon yield per 10a (kg/10a) and growth variables every week from December 19, 2018 to July 9, 2019, and the environmental variables of facility farms were collected in minutes, from January 24, 2019 to June 4, 2019. Therefore, we used common data obtained from January 24, 2019 to June 4, 2019, or a total of 19 weeks.

Initially, we considered 8 growth and 28 environmental variables. Some variables were created through averages or cumulates to expand specifically the growth and environmental variables. Growing degree day (GDD) variable was defined by taking the average of the daily maximum and minimum temperatures compared to the base temperature of the oriental melon. For factors related to temperature in environmental variables, we used the following: average, maximum, minimum, daily average, nighttime average, GDD, and daily temperature range.

Data in each facility farm showed no outlier. Therefore, the average value of 10 oriental melon trees in each facility farm was used to represent them as one data. *Table 1* describes the response and explanatory variables. For additional information on the measurement methods and experimental conditions of the listed variables in *Table 1* collected through smart farm technology, we can refer to sites of the Rural Development Administration (*http://www.nongsaro.go.kr*) and the Korea Agency of Education, Promotion and Information Service in Food, Agriculture, Forestry and Fisheries (*https://www.epis.or.kr/main/view*). Because similar variable exist, we separately marked the variables used in our model (“†” and “‡” in *Table 1*) by removing semantically redundant variables. Furthermore, we used the reduced variables marked “†” in the prediction models without principal components (PCs) in consideration of multicollinearity between explanatory variables (*Table 1*).

http://www.aloki.hu ● ISSN 1589 1623 (Print) ● ISSN 1785 0037 (Online)
DOI: http://dx.doi.org/10.15666/aeer/2001_479497

Table 1. *Description of variables*

Variable name	Explanation	Unit
Response variable		
yield 10a	Weekly cumulative yields area of 10a	kg/10a
Explanatory variables: growth		
ll	Leaf length	cm
lw	Leaf width	cm
sd rs †, ‡	Stem diameter of rootstock	cm
sd s †	Stem diameter of scion	cm
sd gp	Stem diameter of grafting point	cm
sd	Stem diameter	cm
crp	Chlorophyll	-
angel †, ‡	Angle of growing point	°
Explanatory variables: environment		
cumulate sun †	Cumulate of solar radiation	W/m^2
mean sun †, ‡	Average of solar radiation	W/m^2
mean ltemp †	Average of leaf temperature	℃
daymean ltemp †	Day average of leaf temperature	℃
nightmean ltemp	Night average of leaf temperature	℃
max ltemp	Highest leaf temperature	℃
min ltemp	Lowest leaf temperature	℃
mean 2h sunrise ltemp	Average leaf temperature at two hours before and after sunrise	℃
mean temp †	Average of temperature	℃
daymean temp †	Day average of temperature	℃
nightmean temp	Night average of temperature	℃
max temp	Highest temperature	℃
min temp	Lowest temperature	℃
mean 2h sunrise temp	Average temperature at two hours before and after sunrise	℃
GDD temp	Growing degree day temperature	℃
DIF temp †, ‡	Daily temperature range	℃
mean stemp †	Average of soil temperature	℃
daymean stemp	Day average of soil temperature	℃
nightmean stemp †	Night average of soil temperature	℃
max stemp †, ‡	Highest soil temperature	℃
min stemp †	Lowest soil temperature	℃
mean 2h sunrise stemp †	Average soil temperature at two hours before and after sunrise	℃
GDD stemp †, ‡	Growing degree day soil temperature	℃
mean mois	Average of moisture	%
daymean mois	Day average of moisture	%
nightmean mois †, ‡	Night average of moisture	%
max mois	Highest moisture	%
min mois	Lowest moisture	%

† = variables used to generate principal component; ‡ = variables considering multicollinearity

Workflow

This study aimed to identify the significant factors that affect the crop yield of oriental melon between farms and estimate prediction models for crop yield. The response variable was defined as the crop yield per 10a (kg/10a) of oriental melon calculated as the weekly cumulative yield. The explanatory variables consisted of the average growth and environmental variables for that week. To construct prediction models, we examined whether the explanatory variables of the past lag and response variable of the current time were correlated with Pearson's correlation coefficients. The

http://www.aloki.hu ● ISSN 1589 1623 (Print) ● ISSN 1785 0037 (Online)
DOI: http://dx.doi.org/10.15666/aeer/2001_479497

lag with the explanatory variable having the most influence on the response variable was then selected. The variables were expanded into eight-week lags from the past to the current time, and the correlation coefficients with the response variable were measured and compared. Finally, the optimal lag was selected using the largest average of the absolute correlation coefficient values of all farms. Prediction models were constructed according to the following procedure:

1. Select optimal lag for each explanatory variable, called a lagged variable.
2. Construct time-series models based on lagged variables or PCs of lagged variables.
   A. In the lagged variable-based models, only nine lagged variables (marked "‡" in *Table 1*) are used, excluding variables with high similarity in consideration of multicollinearity.
   B. In the PCs-based models, all lagged variables (marked "†" in *Table 1*) are used.
3. Compare the performance measures of estimated models.

All statistical analyses with a significance level of 0.05 for a two-sided test were performed using R version 4.0.3 (R Foundation for Statistical Computing, Vienna, Austria).

Statistical methods

Principal component analysis

When the number of explanatory variables is greater than the number of observations in measured data and multicollinearity between explanatory variables is high, then the number of variables needs to be reduced using principal component analysis (PCA). In multivariate data of size, PCA is a method of extracting important information and generating new variables ($PC^T = (PC_1, \cdots, PC_k)$), which are new variables independent of one another, through a linear combination of correlated $x^T = (x_1, \cdots, x_k)$ variables (Hotelling, 1933). PCA can solve the multicollinearity problem and reduce the number of variables.

Distributed-lag model

The distributed-lag model (DLM) is a method for analyzing linear relationships with time-dependent variables by including past lags of explanatory variables as explanatory variables (Pesaran et al., 2001). The general form of DLM for the dependent variable is expressed as

$$Y_t = \alpha + \sum_{i=1}^{k} \sum_{j=1}^{h_i} \beta_{i,j} X_{i,t-j} + \varepsilon_t, \qquad \text{(Eq.1)}$$

where α is a constant term, k are the number of explanatory variables, h_i are the lag of the i-th explanatory variable X_i, $\beta_{i,j}$ are the coefficient of X_i at the j-th lag, and ε_t is an error term at time t. In this study, h_i were used as the optimal with the largest correlation coefficient for the response variable among lags of X_i.

http://www.aloki.hu ● ISSN 1589 1623 (Print) ● ISSN 1785 0037 (Online)
DOI: http://dx.doi.org/10.15666/aeer/2001_479497

Auto-regressive integrated moving average model

Auto-regressive integrated moving average with explanatory variables model (ARIMAX) is a linear combination of an auto-regressive (AR) model and a moving average (MA) model with explanatory variables (Box et al., 2015). The general form of ARIMAX for Y_t is represented as

$$\Delta^d Y_t = \alpha + \sum_{i=1}^{p} \phi_i \Delta^d Y_{t-i} + \sum_{j=1}^{q} \theta_j \varepsilon_{t-j} + \sum_{m=1}^{k} \beta_m X_{m,t} + \varepsilon_t, \quad \text{(Eq.2)}$$

where α is a constant term, p is the autoregressive order. ϕ's are the autoregressive coefficients, q is the moving average order, θ's are the moving average coefficients, ε_t is an error term at time t, k is the number of explanatory variables, β's are the regression coefficients, and X's are the lagged explanatory variables. In this study, we set $d = 0$ for simplicity. Thus, the final model can be expressed as ARIMA($p, 0, q$)-lagged X model. Here, the orders ($p, 0, q$) are automatically determined using the auto.arima function of the R package {forecast}, which selects the order that minimizes Akaike information criterion (AIC).

Model performance

The predicted models were evaluated using root mean square error (RMSE), root mean absolute error (RMAE), and mean magnitude of relative error (MMRE) measures. These model performance measures are defined by

$$RMSE = \sqrt{\frac{1}{n}\sum_{t=1}^{n}(y_t - \hat{y}_t)^2}, \quad \text{(Eq.3)}$$

$$RMAE = \sqrt{\frac{1}{n}\sum_{t=1}^{n}\left|y_t - \hat{y}_t\right|}, \quad \text{(Eq.4)}$$

$$MMRE = \frac{1}{n}\sum_{t=1}^{n}\left|\frac{y_t - \hat{y}_t}{y_t}\right|. \quad \text{(Eq.5)}$$

Here, n is the number of measured data, t is the measurement time point, y_t is the actual value at time t, and $\hat{y}_t$ is the predicted value at time t. As the error decreases, the values of the evaluation indicators RMSE, RMAE, and MMRE decrease. Therefore, the smaller the value of the model performance measures, the better the estimated model predicts the response variable.

Results

In this study, to find and predict the factors affecting the weekly yield per 10a (kg/10a) of oriental melon, we used the growth and environmental variables measured at four Seongju oriental melon facility farms in 2019.

http://www.aloki.hu ● ISSN 1589 1623 (Print) ● ISSN 1785 0037 (Online)
DOI: http://dx.doi.org/10.15666/aeer/2001_479497

Statistics of variables

Prior to the analysis, basic statistics on the yield, growth factors and environmental factors of the response variable oriental melon were measured on a farm-by-farm basis. *Figure 2* showed basic statistics of the yield of oriental melon by farm. *Figure 2* show that the highest yield is 124.8 kg/10a, which is confirmed in Farm2. Farm3 had a lower yield than other farms, with a peak yield of 63.7 kg/10a. *Table 2* measures basic statistics for each facility farms growth factors and environmental factors.

Table 2. *Statistics of explanatory variables*

Variable	Mean ± SD	Min~Max	Median(Q1, Q3)
Farm1			
sd rs	1.2 ± 0.3	0.8~2.0	1.2(1.1, 1.4)
sd s	0.8 ± 0.2	0.5~1.4	0.7(0.7, 0.8)
angle	35.3 ± 5.1	22.9~53.2	34.1(33.4, 37.2)
mean temp	20.5 ± 4.4	7.6~25.8	21.1(19.3, 23.2)
daymean temp	25.2 ± 5.5	9.3~31.7	25.9(23.8, 28.9)
DIF temp	22.5 ± 5.7	8.2~32.0	23.1(20.5, 25.9)
mean stemp	19.7 ± 4.0	7.1~24.4	20.2(19.0, 21.9)
night mean stemp	19.9 ± 4.1	7.1~24.4	20.4(19.1, 22.3)
min stemp	18.4 ± 3.7	6.7~23.2	18.8(17.6, 20.5)
max stemp	21.2 ± 4.4	7.5~25.7	21.6(20.5, 23.8)
mean 2h sunrise stemp	18.8 ± 3.9	6.8~23.6	19.2(18.0, 20.9)
mean ltemp	18.9 ± 3.9	6.8~23.4	19.5(18.0, 21.2)
daymean ltemp	22.9 ± 4.8	8.3~27.8	23.4(21.8, 26.3)
nightmean mois	88.6 ± 18.6	24.7~112.7	91.1(84.2, 97.2)
mean sun	141.5 ± 47.9	60.0~226.4	137.1(104.6, 181.2)
cumulate sun	20237.0 ± 6921.0	7944.3~32597.5	19742.2(15041.7, 26095.3)
GDD stemp	84.9 ± 23.6	34.4~125.0	86.5(69.7, 99.0)
Farm2			
sd rs	1.1 ± 0.2	0.6~1.4	1.1(1.1, 1.2)
sd s	0.7 ± 0.1	0.4~1.0	0.7(0.7, 0.8)
angle	30.3 ± 7.0	18.5~46.2	30.3(23.8, 35.2)
mean temp	19.6 ± 4.2	9.6~25.1	19.5(18.6, 21.7)
daymean temp	24.7 ± 5.2	11.8~32.1	24.9(23.6, 28.5)
DIF temp	23.0 ± 5.3	10.0~32.5	23.3(21.5, 24.5)
mean stemp	20.1 ± 4.1	9.8~26.1	20.2(18.7, 22.3)
night mean stemp	20.3 ± 4.1	10.0~26.4	20.4(18.9, 22.7)
min stemp	19.1 ± 3.8	9.2~24.4	19.2(18.0, 20.9)
max stemp	21.2 ± 4.3	10.4~27.6	21.3(19.7, 23.7)
mean 2h sunrise stemp	19.5 ± 3.9	9.4~25.1	19.6(18.3, 21.4)
mean ltemp	18.3 ± 3.7	8.9~23.2	18.4(17.3, 20.5)
daymean ltemp	22.2 ± 4.5	10.8~28.8	22.3(21.3, 25.5)
nightmean mois	92.1 ± 18.5	33.2~114.6	95.0(92.0, 101.7)
mean sun	139.0 ± 49.2	46.3~221.2	134.2(98.6, 177.7)
cumulate sun	19898.6 ± 7126.0	6283.4~31852.1	19326.3(14204.0, 25588.3)
GDD stemp	86.9 ± 21.1	43.3~121.0	86.9(75.9, 97.2)

Variable	Mean ± SD	Min~Max	Median(Q1, Q3)
Farm3			
sd rs	1.1 ± 0.2	0.5~1.5	1.2(1.1, 1.2)
sd s	0.7 ± 0.2	0.3~1.4	0.7(0.6, 0.8)
angle	33.5 ± 6.8	13.5~42.4	35.3(30.5, 37.9)
mean temp	20.7 ± 2.8	12.6~24.3	20.8(20.4, 22.9)

http://www.aloki.hu ● ISSN 1589 1623 (Print) ● ISSN 1785 0037 (Online)
DOI: http://dx.doi.org/10.15666/aeer/2001_479497

daymean temp	25.1 ± 3.4	15.3~29.3	25.2(24.4, 27.1)
DIF temp	22.3 ± 3.9	12.9~31.4	22.4(20.4, 24.0)
mean stemp	22.2 ± 3.0	13.5~25.9	22.8(22.1, 23.8)
night mean stemp	22.1 ± 3.0	13.6~25.7	22.4(21.9, 23.9)
min stemp	20.3 ± 2.8	12.4~23.5	21.1(20.2, 21.6)
max stemp	24.4 ± 3.3	14.6~29.5	25.1(24.0, 25.6)
mean 2h sunrise stemp	20.7 ± 2.9	12.7~24.0	21.4(20.6, 22.1)
mean ltemp	20.3 ± 2.8	11.4~24.4	20.7(19.8, 21.8)
daymean ltemp	23.7 ± 3.2	13.6~27.1	23.9(23.0, 26.5)
nightmean mois	87.5 ± 14.6	43.3~110.8	89.5(84.6, 95.5)
mean sun	125 ± 35.9	49.1~197.1	121.1(98.6, 150.1)
cumulate sun	17930.6 ± 5120.0	7075.5~27670.1	17436.0(14199.1, 21613.2)
GDD stemp	102.5 ± 15.8	66.5~128.6	105.7(96.6, 112.7)
Farm4			
sd rs	1.3 ± 0.3	0.6~2.1	1.2(1.0, 1.5)
sd s	0.9 ± 0.2	0.5~1.5	0.9(0.8, 1.0)
angle	34.6 ± 4.9	15.7~41.9	35.3(33.2, 36.7)
mean temp	22.9 ± 3.5	18.1~32.2	22.2(20.4, 24.6)
daymean temp	25.6 ± 3.5	19.5~35.0	25.4(23.7, 27.9)
DIF temp	14.0 ± 3.8	8.5~22.9	13.2(11.2, 16.3)
mean stemp	23.0 ± 3.2	17.9~31.6	22.9(20.9, 24.9)
night mean stemp	22.7 ± 3.3	17.5~31.6	22.2(20.5, 24.4)
min stemp	20.8 ± 3.4	15.6~29.5	20.0(18.5, 21.8)
max stemp	25.6 ± 3.0	21.0~33.4	24.9(23.5, 27.2)
mean 2h sunrise stemp	21.2 ± 3.4	15.9~30.1	20.5(18.8, 22.2)
mean ltemp	22.8 ± 3.5	18.0~32.5	22.2(20.4, 24.5)
daymean ltemp	26.7 ± 3.3	22.0~36.5	26.4(24.4, 28.7)
nightmean mois	78.6 ± 8.7	60.2~97.3	80.8(71.4, 83.9)
mean sun	132.3 ± 43.4	49.1~203.4	134.2(101.7, 165.4)
cumulate sun	18943.0 ± 6245.6	7075.5~28288.8	19331.9(14648.7, 23813.1)
GDD stemp	106.0 ± 21.3	70.4~156.0	102.5(91.2, 118)

SD = standard deviation; Q1 = 1st quartile; Q3 = 3rd quartile

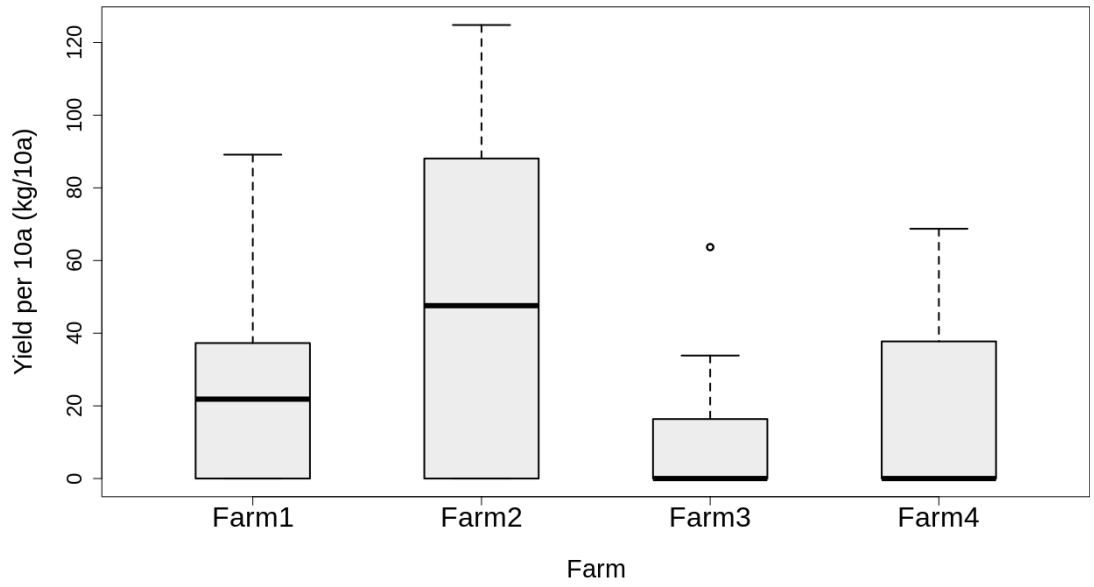

Figure 2. *Statistics of response variable over the entire period*

http://www.aloki.hu ● ISSN 1589 1623 (Print) ● ISSN 1785 0037 (Online)
DOI: http://dx.doi.org/10.15666/aeer/2001_479497

Correlation analysis

To confirm the relation between the explanatory (growth and environmental) variables with lags and crop yield, we conducted a correlation analysis. *Table A2* represents the average correlation coefficient of the farm between lagged covariates and yield of oriental melon per 10a (kg/10a). For each selected lag, the lagged covariates affecting crop yield were mostly 2- or 6-week lags (*Table A2*). In the growth variables, the stem diameters of rootstock and stem diameters of scion at the time of lag 2 were strongly correlated with crop yield. In addition, angle of growing point, a growth variable, and temperature related variables, which were environmental variables, showed a strong correlation with crop yield at the time of lag 6. Therefore, as above, we used the covariate at the selected time point where the correlation with the crop yield was large to construct the model. The lags of night average of moisture, average of solar radiation, cumulate of solar radiation, and GDD soil temperatures, all environmental variables, were determined to be 2, 3, 0, and 7, respectively.

Next, the correlation analysis between the explanatory variables of the four farms, shown in *Table A3*, confirmed potential multicollinearity issues. Among the growth variables, in all farms, reception diameter and stock tree diameter showed a high correlation. Among the environmental variables, most of those related to solar radiation, soil temperature, and night average humidity were highly correlated. In addition, the average soil temperature had correlation coefficient values close to 1 with other temperature-related variables. Finally, we determined the explanatory variables that could be used in the prediction model with covariates, marked with "‡" in *Table 1*.

Prediction models

We performed PCA to solve the problem of multicollinearity in lagged explanatory variables. First of all, All variables used were standardized in the PCA process. The number of PCs was determined to include a dimension that accounted for up to 99% of the cumulative variance over the total data. We found that eight PCs could be used for each farm. Finally, based on the lagged variables and selected PCs, we identified and predicted the factors affecting oriental melon yield per 10a (kg/10a) using DLM and ARIMAX, respectively. When explanatory variables are used directly in the model without PCA, some variables with multicollinearity were excluded. In addition, in the case of using PCs, the prediction model was constructed using all explanatory variables, and the explanatory variables used in each approach are represented (*Table 1*).

As a result of selecting the order of the model that minimizes AIC, in ARIMA with covariates, the auto-regressive and moving average orders were selected as 1, respectively, and thus the ARIMA(1,0,1) model was used. Similarly, in ARIMA with PCs, the orders were selected in the same way, and the ARIMA(1,0,3) model was used. To test whether the residuals from the ARIMA model had no autocorrelation, we used the Ljung–Box test. The Ljung–Box test results confirmed that the significance probability value of all models in the four farms was over 0.05, indicating the absence of serial autocorrelation (*Table A4*).

The results of the comparison between the actual and predicted values for each farm using the four models are shown in *Figure 3*. In this figure, the black solid lines are the actual yield values across weeks. The green, blue, yellow, and green dotted lines represent the fitted values for DLM and ARIMAX(1,0,1) with covariates and DLM and

http://www.aloki.hu ● ISSN 1589 1623 (Print) ● ISSN 1785 0037 (Online)
DOI: http://dx.doi.org/10.15666/aeer/2001_479497

ARIMAX(1,0,3) with PCs, respectively. Based on these results, the predicted values (red dotted line) obtained from ARIMAX(1,0,3) with PCs were closest to the actual values, compared with other models. Thus, yield predictability improved when all covariates were used and their multicollinearity was controlled.

Estimated models that could predict oriental melon yield were compared through the following evaluation measurements: RMSE, RMAE, and MMRE. The comparison results of the model performance confirmed that the RMSE, RMAE, and MMRE of ARIMAX with PCs had the lowest values in all farms (*Table 3*). Therefore, ARIMAX(1,0,3) with PCs performed better than other prediction models.

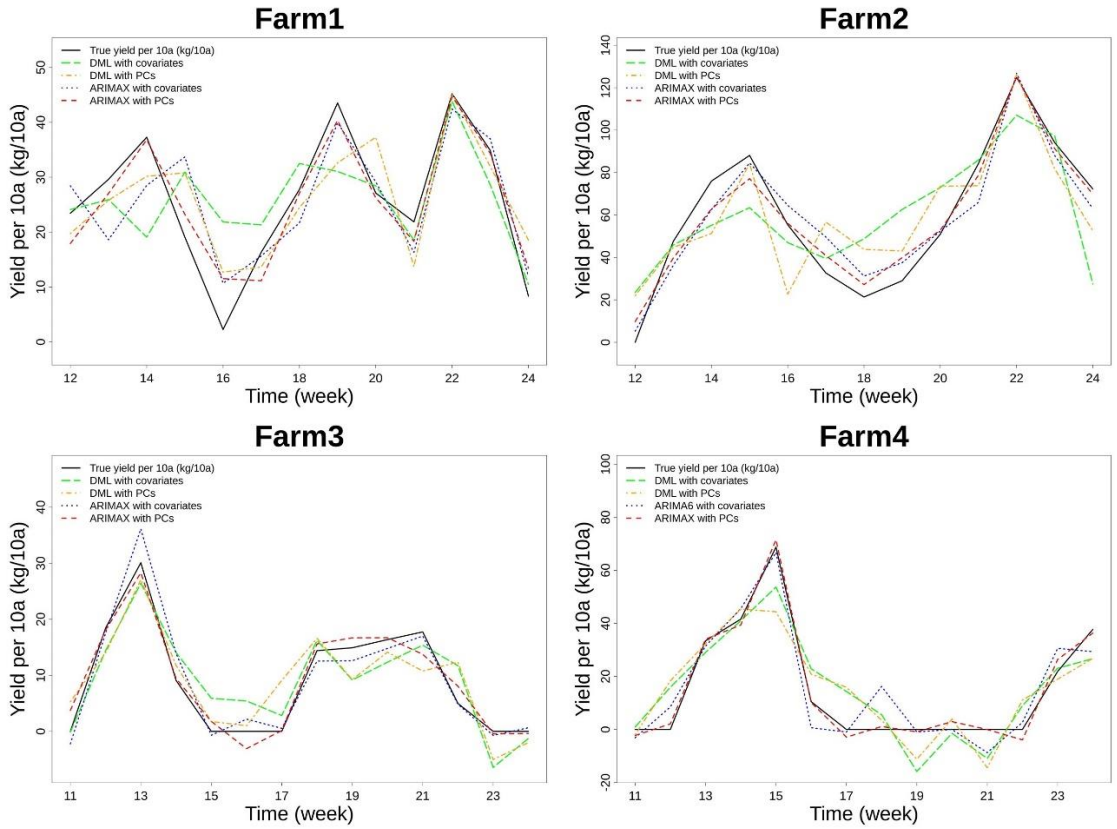

Figure 3. *Prediction results of yield per 10a (kg/10a) in four farms (1 to 4)*

Table 3. *Comparison of predictability between estimated models*

Farm	Model	Measurement		
		RMSE	**RMAE**	**MMRE**
Farm1	DLM with covariates	9.326	2.640	0.8732
	DLM with PCs	7.569	2.560	0.6385
	ARIMAX(1,0,1) with covariates	6.894	2.389	0.5021
	ARIMAX(1,0,3) with PCs	**4.093**	**1.788**	**0.4538**
Farm2	DLM with covariates	22.207	4.264	2.0864
	DLM with PCs	18.859	4.049	1.9467
	ARIMAX(1,0,1) with covariates	10.187	2.974	0.7916
	ARIMAX(1,0,3) with PCs	**7.423**	**2.486**	**0.5081**

http://www.aloki.hu ● ISSN 1589 1623 (Print) ● ISSN 1785 0037 (Online)
DOI: http://dx.doi.org/10.15666/aeer/2001_479497

Farm3	DLM with covariates	4.419	1.988	1.7927
	DLM with PCs	4.817	2.049	1.8119
	ARIMAX(1,0,1) with covariates	2.450	1.347	0.8906
	ARIMAX(1,0,3) with PCs	**2.080**	**1.266**	**0.7061**
Farm4	DLM with covariates	10.237	2.911	5.286
	DLM with PCs	11.717	3.091	5.724
	ARIMAX(1,0,1) with covariates	7.060	2.332	3.207
	ARIMAX(1,0,3) with PCs	**2.384**	**1.413**	**1.325**

RMSE = root mean square error; RMAE = root mean absolute error; MMRE = mean magnitude of relative error; DLM = distributed-lag model; PC = principal component; ARIMAX = auto-regressive integrated moving average with explanatory variables

Table 4 shows the ARIMAX model for each farm using the PCs in the models. In these models, standardized angle of growing point, standardized stem diameters of scion and standardized day average of leaf temperature showed relatively higher coefficients compared with other variables. These coefficients were recalculated using the weights for each PC.

Table 4. *Estimated model equation for ARIMAX with PCs in each farm*

Estimated models for ARIMAX(1,0,3) with PCs	
Farm1	$\hat{Y}_t = -197.15 - 0.56 \times ar_1 - 0.11 \times ma_1 + 0.11 \times ma_2 - 1.0 \times ma_3$ $+ 14.73 \times sd\ rs_{t-2} + 24.22 \times sd\ s_{t-2} + 3.74 \times angle_{t-6} - 1.02 \times mean\ temp_{t-6}$ $- 3.69 \times daymean\ temp_{t-6} + 0.14 \times DIF\ temp_{t-6} + 0.79 \times mean\ stemp_{t-6}$ $+ 0.95 \times night\ mean\ stemp_{t-6} + 4.76 \times min\ stemp_{t-6} - 2.60 \times max\ stemp_{t-6}$ $+ 4.66 \times mean\ 2h\ sunrise\ stemp_{t-6} - 2.19 \times mean\ ltemp_{t-6} - 2.83 \times daymean\ ltemp_{t-6}$ $+ 0.79 \times nightmean\ mois_{t-2} - 0.09 \times mean\ sun_{t-3} + 0.001 \times cummulate\ sun_t$ $+ 0.38 \times GDD\ stemp_{t-7}$
Farm2	$\hat{Y}_t = 21.33 - 0.71 \times ar_1 + 0.91 \times ma_1 - 0.91 \times ma_2 - 1.0 \times ma_3$ $+ 0.04 \times sd\ rs_{t-2} + 1.39 \times sd\ s_{t-2} + 1.62 \times angle_{t-6} - 0.83 \times mean\ temp_{t-6}$ $+ 1.78 \times daymean\ temp_{t-6} + 4.79 \times DIF\ temp_{t-6} - 1.45 \times mean\ stemp_{t-6}$ $- 0.67 \times night\ mean\ stemp_{t-6} - 2.54 \times min\ stemp_{t-6} - 0.66 \times max\ stemp_{t-6}$ $- 2.17 \times mean\ 2h\ sunrise\ stemp_{t-6} - 3.35 \times mean\ ltemp_{t-6} + 1.27 \times daymean\ ltemp_{t-6}$ $+ 0.002 \times nightmean\ mois_{t-2} + 0.021 \times mean\ sun_{t-3} - 0.001 \times cummulate\ sun_t$ $+ 0.498 \times GDD\ stemp_{t-7}$
Farm3	$\hat{Y}_t = -86.55 - 0.87 \times ar_1 - 0.91 \times ma_1 - 0.91 \times ma_2 + 1.0 \times ma_3$ $- 0.80 \times sd\ rs_{t-2} - 1.96 \times sd\ s_{t-2} - 0.77 \times angle_{t-6} - 0.91 \times mean\ temp_{t-6}$ $- 0.30 \times daymean\ temp_{t-6} + 1.47 \times DIF\ temp_{t-6} + 0.55 \times mean\ stemp_{t-6}$ $+ 0.40 \times night\ mean\ stemp_{t-6} + 0.41 \times min\ stemp_{t-6} + 0.80 \times max\ stemp_{t-6}$ $+ 0.25 \times mean\ 2h\ sunrise\ stemp_{t-6} + 0.46 \times mean\ ltemp_{t-6} + 0.94 \times daymean\ ltemp_{t-6}$ $+ 0.18 \times nightmean\ mois_{t-2} + 0.07 \times mean\ sun_{t-3} - 0.001 \times cummulate\ sun_t$ $+ 0.33 \times GDD\ stemp_{t-7}$

http://www.aloki.hu ● ISSN 1589 1623 (Print) ● ISSN 1785 0037 (Online)
DOI: http://dx.doi.org/10.15666/aeer/2001_479497

Farm4	$\hat{Y}_t = -390.2 - 0.87 \times ar_1 - 0.77 \times ma_1 + 2.73 \times ma_2 - 0.99 \times ma_3$ $- 1.55 \times sd\ rs_{t-2} - 0.94 \times sd\ s_{t-2} - 0.50 \times angle_{t-6} + 0.11 \times mean\ temp_{t-6}$ $+ 0.78 \times daymean\ temp_{t-6} + 0.83 \times DIF\ temp_{t-6} - 0.01 \times mean\ stemp_{t-6}$ $+ 0.15 \times night\ mean\ stemp_{t-6} + 0.22 \times min\ stemp_{t-6} - 0.14 \times max\ stemp_{t-6}$ $+ 0.12 \times mean\ 2h\ sunrise\ stemp_{t-6} - 0.44 \times mean\ ltemp_{t-6} + 0.92 \times daymean\ ltemp_{t-6}$ $+ 0.31 \times nightmean\ mois_{t-2} + 0.79 \times mean\ sun_{t-3} - 1.99 \times cummulate\ sun_t$ $+ 0.21 \times GDD\ stemp_{t-7}$

ARIMAX = auto-regressive integrated moving average with explanatory variables; PC = principal component

Discussion

Oriental melon is mainly cultivated in Republic of Korea, Japan, and northern China in Central Asia (Hendryanti et al., 2020). The Republic of Korea, it is cultivated mainly in Seongju, in Gyeongsangbuk-do. Using smart farm data obtained from the Rural Development Administration, factors affecting the yield of Seongju oriental melon were identified and the predictive models were established. Through the results of this study, it is shown that the growth variables angle of growing point, stem diameters of scion and the day average of leaf temperature have a major effect on the yield of oriental melon in common in four farms. Also, the ARIMAX model with PCs has been proposed as an alternative model for Seongju oriental melon.

Growing points form organs such as root and stem through cell division. Clark and Burge (2002) tested plants by tubers size, and found that growing points had a significant relationship between the weights of tubers. The larger the weight of the tubers, the greater the size of the growing point. In the case of tubers of the same size, the larger the growing point, the better the plant grows. Mngrsquo et al. (2012) reviewed that plant growth is active when the gripping system diameters of scion is thicker. Stem diameters of scion found that thick trees grew faster and larger than other trees and produced much more. When the temperature is high, the stomata of the leaves close and the surface temperature of the leaves increases. Glenn et al. (2001) confirmed that the daytime air temperature was below 25 ℃ and that the daytime leaf surface temperature was low, increasing Carbon assimilation and statistical conductance, and increasing plant yields. Environmental variables such as day average of temperature and highest soil temperature were also identified as factors that increase the crop yield.

In addition, Liu et al. (2017) and Kim and Ferris (2002) found that the environment in which oriental melons are grown is dry, and soil moisture is grown in a relatively constant environment throughout the growth period. It has a better impact on oriental melons growth and therefore need to manage environmental factors. Shin et al. (2005) showed that when oriental melon is grown at a low temperature, the initial growth is delayed and the early yield decreases, which affects the production quantity and quality. In addition, the higher the heat retention, the faster the flowering and the shorter the number of harvesting days, the higher the fruit weight and sugar content.

In terms of lag time, the yield showed a high correlation with the environmental variables temperature, soil temperature, and leaf temperature 6 weeks before harvesting. In the oriental melon cultivation process, as shown in *Figure 4*, 6 weeks before harvesting is the fruiting setting season.

http://www.aloki.hu ● ISSN 1589 1623 (Print) ● ISSN 1785 0037 (Online)
DOI: http://dx.doi.org/10.15666/aeer/2001_479497

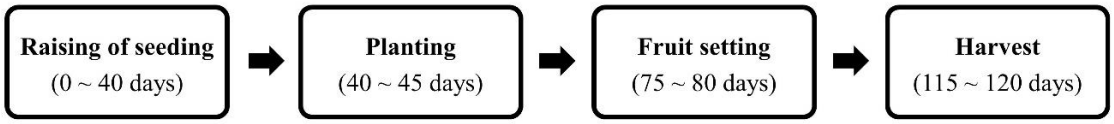

Figure 4. *The process and duration of melon cultivation (from Seongju-gun homepage: https://sj.go.kr/S0007/)*

The fruiting season of oriental melon is the time when the fruit is opened, and it is necessary to reduce the fall of the oriental melon and provide an environment suitable for the fruit to open, such as arranging vines and leaves, removing pests, and controlling environmental factors to improve the yield at harvest time. Also, excessively high temperatures interfere with fruiting and must be controlled. When the humidity is too high, the fruit becomes soft, and when the humidity is too low, the fruit may become malformed. Therefore, it is necessary to manage environmental factors during the fruiting season, 6 weeks before the oriental melon is harvested.

When the optimum temperature, humidity, soil temperature, and plant growth factors are identified for each crop and applied to the smart farm, it will be possible to increase the yield of not only oriental melon but also other crops and harvest high-quality crops. In particular, if the angle of growing point and day average of leaf temperature are managed 6 weeks before harvesting and stem diameters of scion 2 weeks before harvesting, high yields with high sugar content and high quality are expected to be obtained.

Conclusion

This study constructed models for predicting the yield of oriental melon produced from Seongju. We examined what growth and environmental variables affected the crop yield of oriental melon and modeled them using these covariates based on a comparison of the predictability of the models. When checking the performance of models based on three measurements, ARIMAX with PCs showed the best results, which demonstrated effectiveness in utilizing highly correlated covariates, such as growth and environmental variables. Therefore, the ARIMAX with PCs model could be a new alternative for predicting crop yield. In addition, we confirmed that angle of growing point, stem diameters of scion, and day average of leaf temperature had a significant effect on the prediction model of the Seongju oriental melon yield.

The operation of the smart farm system in farms calls for the collection of various growth and environmental variables, which in turn necessitates the construction of a precise model that takes into account these variable characteristics. Therefore, studies such as ours can be expected to contribute to progressive changes in the improvement of crop yield in the future.

Acknowledgments. This work was supported by the National Research Foundation of Korea (NRF) grant funded by the Korea government (MIST) (No. 2019R1C1C100315412 and No. 2021R1C1C1009976) and the Research Program of Rural Development Administration (No. PJ0153372021).

REFERENCES

[1] Bertin, N., Génard, M. (2018): Tomato quality as influenced by preharvest factors. – Scientia Horticulturae 233: 264-276.

http://www.aloki.hu ● ISSN 1589 1623 (Print) ● ISSN 1785 0037 (Online)
DOI: http://dx.doi.org/10.15666/aeer/2001_479497

[2] Bindi, M., Olesen, J. E. (2011): The responses of agriculture in Europe to climate change. – Regional Environmental Change 11(1): 151-158.
[3] Box, G. E., Jenkins, G. M., Reinsel, G. C., Ljung, G. M. (2015): Time Series Analysis: Forecasting and Control. – John Wiley & Sons, Hoboken, NJ.
[4] Choudhury, A., Jones, J. (2014): Crop yield prediction using time series models. – Journal of Economics and Economic Education Research 15(3): 53-68.
[5] Clark, G. E., Burge, G. K. (2002): Effects of apical growing point size and tuber weight on production in Sandersonia aurantiaca. – Scientia Horticulturae 94(3-4): 323-332.
[6] Deschênes, O., Greenstone, M. (2007): The economic impacts of climate change: evidence from agricultural output and random fluctuations in weather. – American Economic Review 97(1): 354-385.
[7] Di Vittori, L., Mazzoni, L., Battino, M., Mezzetti, B. (2018): Pre-harvest factors influencing the quality of berries. – Scientia Horticulturae 233: 310-322.
[8] Galán, C., Vázquez, L., García-Mozo, H., Domínguez, E. (2004): Forecasting olive (olea europaea) crop yield based on pollen emission. – Field Crops Research 86(1): 43-51.
[9] Glenn, D. M., Puterka, G. J., Drake, S. R., Unruh, T. R., Knight, A. L., Baherle, P., Prado, E., Baugher, T. A. (2001): Particle film application influences apple leaf physiology, fruit yield, and fruit quality. – Journal of the American Society for Horticultural Science 126(2): 175-181.
[10] Goldschmidt, E. E. (2014): Plant grafting: new mechanisms, evolutionary implications. – Frontiers in Plant Science 5: 727.
[11] Hwang, J. M., Um, J. S., Yi, Y. K. (1999): Survey of physiological disorders in greenhouse fruit vegetables in Kyungbuk province. – Horticultural Science & Technology 17(6): 737-741.
[12] Hendryanti, D. N., Jeong, H., Kim, J. Y., Kwon, O. (2020): Serine protease in a bred variety of oriental melon (*Cucumis melo* L. var. *makuwa*) curtails vascular thrombosis by balancing hemostasis and fibrinolysis in a rodent model. – Journal of Functional Foods 68: 103925.
[13] Hotelling, H. (1933): Analysis of a complex of statistical variables into principal components. – Journal of Educational Psychology 24(6): 498-520.
[14] Kang, S. R., Cho, W. H., Na, M. H., Choi. D. W. (2020): Consideration of environmental factors and growth factors and watering facilities for prediction of pepper production. – Journal of the Korean Data Analysis Society 22(1): 177-188.
[15] Kim, D. G., Ferris, H. (2002): Relationship between crop losses and initial population densities of Meloidogyne arenaria in winter-grown oriental melon in Korea. – Journal of Nematology 34(1): 43-49.
[16] King, S. R., Davis, A. R., Zhang, X., Crosby, K. (2010): Genetics, breeding and selection of rootstocks for Solanaceae and Cucurbitaceae. – Scientia Horticulturae 127(2): 106-111.
[17] Lee, K. K., Ko, K. K., Lee, J. W. (2012): Correlation analysis between meteorological factors and crop products. – Journal of Environmental Science International 21(4): 461-470.
[18] Lee, J. E., Kang. S. R., Ok. Y. J., Chun, M. H., Na, M. H. (2019): A study on the optimal environmental factors affecting the growth of facility cucumbers. – Journal of the Korean Data Analysis Society 21(6): 2913-2920.
[19] Lee, H., Hong, K. H., Kwon, D. H., Cho, M. C., Lee, J. G., Hwang, I., Ahn, Y. K. (2020): Changes of growth and yield by using rootstocks in tomato. – Protected Horticulture and Plant Factory 29(4): 456-463.
[20] Liu, S., Liu, Y., Huang, X., Yang, W., Hu, W., Pan, S. (2017): Effect of ultrasonic processing on the changes in activity, aggregation and the secondary and tertiary structure of polyphenol oxidase in oriental sweet melon (*Cucumis melo* var. *makuwa* Makino). – Journal of the Science of Food and Agriculture 97: 1326-1334.

http://www.aloki.hu ● ISSN 1589 1623 (Print) ● ISSN 1785 0037 (Online)
DOI: http://dx.doi.org/10.15666/aeer/2001_479497

[21] Mngrsquo, S. A., Sileshi, G. W., Jamnadass, R., Akinnifesi, F. K., Mhango, J. (2012): Scion and stock diameter size effect on growth and fruit production of Sclerocarya birrea (Marula) trees. – Journal of Horticulture and Forestry 4(9): 153-160.
[22] Pesaran, M. H., Shin, Y., Smith, R. J. (2001): Bounds testing approaches to the analysis of level relationships. – Journal of Applied Econometrics 16(3): 289-326.
[23] Shin, B. H., Jeon, H. K. (2020): ICT-based smart farm design. – Journal of Convergence for Information Technology 10(2): 15-20.
[24] Shin, Y. S., Park, S. D., Do Han, W., Bae, S. G., Kim, J. H., Kim, B. S. (2005): Effect of double layer nonwoven fabrics on the growth, quality and yield of oriental melon (*Cucumis melo* L. Var. *makuwa* Mak.) under vinyl house. – Protected Horticulture and Plant Factory 14(1): 22-28.
[25] Shin, A. Y., Kim, Y. M., Koo, N., Lee, S. M., Nahm, S., Kwon, S. Y. (2017): Transcriptome analysis of the oriental melon (*Cucumis melo* L. var. *makuwa*) during fruit development. – PeerJ 5: e2834.

APPENDIX

Table A1. *Area and yield of vegetable production (fruit) from 2017 to 2019*

Item		2017		2018		2019	
		Outdoors	**Facility**	**Outdoors**	**Facility**	**Outdoors**	**Facility**
Watermelon	Area (ha)	2,726 (6.50%)	9,935 (23.69%)	2,367 (5.63%)	9,447 (22.45%)	2,648 (6.21%)	9,325 (21.88%)
	Yield (ton)	92,736 (4.90%)	413,735 (21.88%)	76,543 (4.1%)	400,091 (21.3%)	84,469 (4.38%)	391,346 (20.29%)
	Yield/Area	34.02	41.64	32.34	42.35	31.90	41.97
Strawberry	Yield (ton)	124 (0.30%)	5,783 (13.79%)	93 (0.22%)	5,969 (14.19%)	41 (0.10%)	6,421 (15.06%)
	Area (ha)	2,473 (0.13%)	206,226 (10.91%)	1,745 (0.09%)	181,894 (9.67%)	934 (0.05%)	233,291 (12.09%)
	Yield/Area	19.95	35.66	18.85	30.47	22.83	36.33
Tomato	Area (ha)	0 (0.00%)	5,782 (13.78%)	0 (0.00%)	6,058 (14.40%)	0 (0.00%)	5,706 (13.39%)
	Yield (ton)	0 (0.00%)	355,107 (18.78%)	0 (0.00%)	388,657 (20.66%)	0 (0.00%)	358,580 (18.59%)
	Yield/Area	0.00	61.42	0.00	64.15	0.00	62.84
Cucumber	Yield (ton)	1,113 (2.65%)	3,805 (9.07%)	1,160 (2.76%)	4,164 (9.90%)	999 (2.34%)	3,963 (9.30%)
	Area (ha)	44,888 (2.37%)	296,476 (15.68%)	48,849 (2.59%)	342,365 (18.20%)	41,250 (2.13%)	324,815 (16.84%)
	Yield/Area	40.33	77.92	42.12	82.22	41.29	81.96
Oriental melon	Area (ha)	127 (0.30%)	3,454 (8.23%)	145 (0.34%)	3,469 (8.24%)	159 (0.37%)	3,488 (8.18%)
	Yield (ton)	2,298 (0.12%)	163,983 (8.67%)	3,104 (0.16%)	127,424 (6.77%)	3,194 (0.16%)	147,040 (7.62%)
	Yield/Area	18.09	47.48	21.38	36.74	20.07	42.15
Pumpkin	Yield (ton)	6,177 (14.73%)	2,919 (6.96%)	6,299 (14.97%)	2,907 (6.91%)	6,814 (15.99%)	3,060 (7.18%)
	Area (ha)	158,508 (8.38%)	154,182 (8.15%)	172,052 (9.15%)	138,166 (7.34%)	177,795 (9.22%)	165,716 (8.59%)
	Yield/Area	25.66	52.83	27.31	47.53	26.09	54.16

This data is from National Statistical Office of Republic of Korea

http://www.aloki.hu ● ISSN 1589 1623 (Print) ● ISSN 1785 0037 (Online)
DOI: http://dx.doi.org/10.15666/aeer/2001_479497

Table A2. *Average correlation coefficients of farms between lagged covariates and yield of oriental melon per 10a (kg/10a)*

Variable		lag0	lag1	lag2	lag3	lag4	lag5	lag6	lag7	lag8
Growth	sd rs	0.470	0.573	**0.610**	0.490	0.390	0.440	0.533	0.483	0.273
	sd s	0.553	0.630	**0.633**	0.495	0.380	0.425	0.560	0.528	0.350
	angle	0.158	0.295	0.315	0.185	0.270	0.348	**0.450**	0.440	0.233
Environment	mean temp	0.433	0.305	0.335	0.223	0.258	0.473	**0.593**	0.470	0.263
	daymean temp	0.438	0.295	0.310	0.213	0.203	0.400	**0.568**	0.463	0.260
	DIF temp	0.235	0.133	0.178	0.153	0.115	0.305	**0.480**	0.370	0.238
	mean stemp	0.365	0.303	0.328	0.175	0.208	0.440	**0.563**	0.475	0.325
	nightmean stemp	0.373	0.303	0.328	0.195	0.225	0.453	**0.580**	0.478	0.315
	min stemp	0.385	0.303	0.350	0.210	0.250	0.483	**0.563**	0.470	0.275
	max stemp	0.325	0.278	0.285	0.135	0.128	0.353	**0.518**	0.448	0.353
	mean 2h sunrise stemp	0.380	0.300	0.345	0.210	0.250	0.478	**0.565**	0.473	0.283
	mean ltemp	0.345	0.338	0.378	0.205	0.235	0.473	**0.535**	0.410	0.283
	daymean ltemp	0.375	0.320	0.323	0.158	0.183	0.415	**0.533**	0.403	0.268
	nightmean mois	0.108	0.240	**0.353**	0.203	0.198	0.085	0.178	0.213	0.208
	mean sun	0.455	0.265	0.263	**0.455**	0.365	0.438	0.444	0.410	0.318
	cumulate sun	**0.453**	0.265	0.245	0.438	0.363	0.440	0.445	0.410	0.315
	GDD stemp	0.400	0.350	0.260	0.323	0.328	0.375	0.415	**0.445**	0.295

http://www.aloki.hu ● ISSN 1589 1623 (Print) ● ISSN 1785 0037 (Online)
DOI: http://dx.doi.org/10.15666/aeer/2001_479497

Table A3. *Average correlation coefficients of farms between selected lagged covariates and the yield of oriental melon per 10a (kg/10a), and significance of the correlation coefficient*

	Yield per 10a	**sd rs_2**	**sd s_2**	**angle1_6**	**mean temp_6**	**daymean temp_6**	**DIF temp_6**	**mean stemp_6**	**nightmean stemp_6**	**min stemp_6**	**max stemp_6**	**mean 2h sunrise stemp_6**	**mean ltemp_6**	**daymean ltemp_6**	**nightmean mois_2**	**mean sun_3**	**cumulate sun_0**	**GDD stemp_7**
Yield per 10a	1	0.61	0.63	0.45	0.59	0.57	0.48	0.56	0.58	0.56	0.52	0.57	0.54	0.53	0.35	0.46	0.45	0.44
sd rs_2	*	1	0.94	0.32	0.38	0.45	0.45	0.36	0.38	0.36	0.28	0.36	0.32	0.35	0.27	0.43	0.43	0.38
sd s_2	*	*	1	0.33	0.47	0.52	0.52	0.41	0.43	0.41	0.34	0.42	0.40	0.42	0.18	0.41	0.43	0.52
angle1_6	*		*	1	0.67	0.71	0.57	0.71	0.71	0.72	0.65	0.72	0.60	0.65	0.45	0.35	0.27	0.22
mean temp_6	*	*	*	*	1	0.94	0.54	0.96	0.96	0.95	0.93	0.95	0.96	0.94	0.42	0.25	0.22	0.43
daymean temp_6	*	*	*	*	*	1	0.78	0.90	0.92	0.87	0.87	0.87	0.87	0.96	0.46	0.26	0.28	0.38
DIF temp_6	*	*	*	*	*	*	1	0.57	0.58	0.50	0.55	0.51	0.49	0.70	0.36	0.48	0.30	0.30
mean stemp_6	*	*	*	*	*	*	*	1	1	0.99	0.98	0.99	0.96	0.93	0.37	0.16	0.16	0.40
nightmean stemp_6	*	*	*	*	*	*	*	*	1	0.98	0.97	0.99	0.96	0.94	0.38	0.16	0.17	0.41
min stemp_6	*	*	*	*	*	*	*	*	*	1	0.94	1	0.94	0.90	0.38	0.17	0.14	0.39
max stemp_6	*	*	*	*	*	*	*	*	*	*	1	0.94	0.94	0.92	0.31	0.18	0.15	0.38
mean 2h sunrise stemp_6	*	*	*	*	*	*	*	*	*	*	*	1	0.95	0.90	0.38	0.18	0.14	0.40
mean ltemp_6	*	*	*	*	*	*	*	*	*	*	*	*	1	0.92	0.32	0.13	0.20	0.38
daymean ltemp_6	*	*	*	*	*	*	*	*	*	*	*	*	*	1	0.36	0.20	0.30	0.38
nightmean mois_2	*			*	*	*	*	*	*	*	*	*	*	*	1	0.48	0.06	0.33
mean sun_3	*	*	*	*		*	*							*	*	1	0.36	0.19
cumulate sun_0	*	*	*													*	1	0.33
GDD stemp_7	*	*	*	*	*	*	*	*	*	*	*	*	*	*	*			1

upper right = average correlation coefficients; lower left = significance of the correlation coefficient; * = $p < .05$; covariate name = covariate name_lag

http://www.aloki.hu ● ISSN 1589 1623 (Print) ● ISSN 1785 0037 (Online)
DOI: http://dx.doi.org/10.15666/aeer/2001_479497

Table A4. *Results of the Ljung-Box Test for prediction models*

Model	DLM with covariates	DLM with PCs	ARIMAX(1,0,1) with covariates	ARIMAX(1,0,3) with PCs
Farm1	0.696	0.539	0.759	0.828
Farm2	0.193	0.644	0.177	0.147
Farm3	0.496	0.605	0.194	0.252
Farm4	0.756	0.346	0.455	0.051

DLM = distributed-lag model; PC = principal component; ARIMAX = Auto-regressive integrated moving average with explanatory

http://www.aloki.hu ● ISSN 1589 1623 (Print) ● ISSN 1785 0037 (Online)
DOI: http://dx.doi.org/10.15666/aeer/2001_479497

THE EFFECTS OF DRYING METHODS ON TOTAL PHENOLIC AND FLAVONOID SUBSTANCES AND ANTIOXIDANT CAPACITY OF REDSTEM FILAREE (*ERODIUM CICUTARIUM)*

ERGÜN, F.

Kırşehir Ahi Evran University, Faculty of Health Sciences, Kirsehir, Turkey
(e-mail: fatma.ergun@ahievran.edu.tr; phone: +90-505-678-4110)

(Received 24th Aug 2021; accepted 28th Oct 2021)

Abstract. In this study, the effects of some drying techniques on antioxidant activity of the Erodium cicutarium (L.) L'Her plant, which has ethnobotanical and medical importance, were investigated. The plant samples were divided into three groups; the group dried in sunlight (SD), the group dried in a thermostatic oven at 55 °C (OD) and the group dried in the shade (DS). Total phenolic substance amounts were determined as 41.27 ± 2.93 mg GAE/g in DS, 15.14 ± 2.25 mg GAE/g in SD and 14.60 ± 0.86 mg GAE/g in OD, respectively. The highest amount of flavonoid substance was determined as 71.99 ± 2.24 mg QE/g in the OD group. The IC_{50} value, from smallest to largest, was found to be 49.47 ± 2.69 µg/mL in DS, 71.90 ± 1.69 µg/mL in SD, and 89.81 ± 3.42 µg/mL in OD. In addition, it was determined that the highest 1,1-diphenyl-2-picrylhydrazil (DPPH) radical scavenging activity and the highest Fe^{3+}-Fe^{2+} reducing capacity were in DS at all concentrations. As a result, it was revealed that the use of shade drying technique would be advantageous in case the E. cicutarium plant was stored by drying, and the total amount of flavonoid substances was affected by the drying time
Keyword: *erodium cicutarium, antioxidant, dried in sunlight, dried in the shade, dried in a thermostatic oven*

Introductıon

Edible plants are one of our main food sources. In addition to basic nutrients such as carbohydrates, fats and vitamins, there are bioactive compounds in plants. The most important type of bioactive compounds in plants are flavonoids and phenolic acids (Demir and Akpınar, 2020). The presence of these compounds affects the antioxidant activity of plants. It has been reported that antioxidants have a preventive effect against cancer, cholesterol problems, diabetes and old age-related diseases (Erlund et al., 2008; Abdolahi, 2018). There are plenty of antioxidants in many plant species, especially cereals, legumes, fruits, and medicinal plants (Foo and Porter, 1981). Some of the species belonging to the *Erodium* genus are natural plants with these characteristics.

There are 74 species belonging to the genus *Erodium*, which can be found in many regions, especially in the Mediterranean basin (Fiz et al., 2006). The most common of these species is *E. cicutarium*. This species is a naturally self-growing five-leaved herbaceous plant with pink blooms in spring (Latimer et al., 2019; Pieroni and Cattero, 2019) (*Fig. 1*). Although this species is consumed as fresh and dried vegetable in the regions where it grows, it is widely used for traditional medicine (Duke, 2001). *E. cicutarium* is used as a traditional medicine in many diseases, especially in diseases such as dysentery, uterine bleeding, constipation and diabetes (Molares et al., 2009; Munekata et al., 2019; Tene et al., 2007; Lis-Balchin, 1993; De-la-Cruz et al., 2007; Özgen et al., 2012; Rajaei and Mohamadi, 2012; Asadi-Samani et al., 2016; Safa et al., 2012). The fresh form of the plant is mostly used as a vegetable, and the dry form of the plant is used as a traditional medicine.

http://www.aloki.hu ● ISSN 1589 1623 (Print) ● ISSN 1785 0037 (Online)
DOI: http://dx.doi.org/10.15666/aeer/2001_499509

Figure 1. *Erodium cicutarium plant*

One of the important methods for post-harvest preservation of bioactive compounds and nutritive properties in the plant is drying. Müller (2007) stated in his study that drying is the most appropriate method especially for the preservation of medicinal and aromatic plants. In addition, the drying process provides ease of pharmaceutical use for medicinal and aromatic plants as well as storage (Lorenzi and Matos, 2002). However, the bioactive components and pharmaceutical properties of plants are affected by the drying process (Zhu et al., 2014).

A significant amount of work has been done on the effect of drying methods on the nutritional properties of fruits and vegetables (Deng et al., 2019; Harguindeguy and Fissore, 2020; Martysiak-Żurowska et al., 2020; Thamkaew et al., 2020; Guclu et al., 2021). However, there are very few studies showing how naturally grown herbs are affected by drying methods. In this study, it was aimed to investigate the effects of three different drying techniques on phenolic and flavonoid substance amounts and antioxidant capacity of natural *E. cicutarium* plant samples collected from Kırşehir region of Turkey.

Materials and methods

Collecting samples and forming groups

The study was planned as three groups: sun dried group (DS), shade dried group (SD), and oven dried group (OS). Self-growing *E. cicutarium* plant specimens (total 3 kg) from three different locations (39°06’37°N’34°11’05″E 1047 m/39°08’08°N’34°12’39″E 1151 m/39°08’58°N’34°06’10″E 1082 m) in Kırşehir region of Turkey were manually collected from above-ground parts in May 2021. In the selection of the examples, attention was paid to the fact that the vegetation period and plant sizes were similar. The samples were washed first with tap water and then with distilled water in order to be free from physical impurities. All samples collected after filtration were divided into three groups equally (750 g for each group) and representatively.

Drying process

The samples divided into groups were subjected to three different drying methods without waiting.

http://www.aloki.hu ● ISSN 1589 1623 (Print) ● ISSN 1785 0037 (Online)
DOI: http://dx.doi.org/10.15666/aeer/2001_499509

Drying in the sun

The samples were distributed on the glass tray as a whole. It was dried in 2 days (day length 12 h) under direct sunlight at temperatures between 16 °C and 20 °C in May 2021 (Quispe-Fuentes et al., 2018).

Oven drying

The samples were distributed as a whole on a glass tray and dried in a thermostatic oven (Elektro-Mag M 420 BP, Turkey) at 55 °C for 12 h (Jafari et al., 2016; Kamel et al., 2013).

Drying in the shade

The samples were distributed as a whole on a glass tray and drying was carried out in the shade with natural airflow and ambient temperature (21 ± 5 °C) (Pirbalouti et al., 2017).

The drying period in this study were determined as the moment when the samples reached constant weight. After drying, the samples were stored in polyethylene containers at + 4 °C in the dark.

Preparation of extracts

Merck and Sigma brand chemicals were used in the study. Plant extracts were prepared using methanol. For this, 10 g of plant samples from each group were weighed separately, ground in a grinder and placed in three 1-liter closed flasks separately. Then, twenty times of methanol (200 mL) was added to the samples and mixed in a magnetic stirrer. The resulting methanol extracts were filtered. This process was repeated three times at regular intervals for each group separately. The obtained extracts were removed at 45 °C with the help of methanol evaporator and the extracts were stored at +4 °C for study (Ergün, 2021a).

Preparation of stock solutions

Stock solutions were prepared from SD, OS and DS extracts using methanol at a concentration of 1000 ppm and stored at +4 °C for the study.

Determination of total phenolic substance

Total phenolic substance determination of the groups was made according to the Folin-Ciocaltaeu method (Slinkard and Singleton, 1977). A standard graph was prepared using gallic acid. 50 µL of the prepared stock solutions were taken, and their volume was completed to 1840 µL with distilled water. 40 µL of Folin-Ciocalteu reagent (FCR) was added to the mixtures separately. After waiting for 3 min at room temperature, 120 µL of 2% (w/v) Na_2CO_3 solution was added to them. The resulting mixtures were incubated for 2 h at room temperature. The absorbances of the samples were read at 760 nm against a blank with distilled water instead of the sample (Optima SP-3000, Tokyo/Japan). Three parallel studies were performed for the measurements. The total phenolic contents of the extracts were determined as equivalent to gallic acid (mg GAE/g) using the equation obtained from the standard gallic acid graph.

Determination of total flavonoid substance

The flavonoid contents of the groups were determined as equivalent to quercetin using the aluminum nitrate method (Nieva Moreno et al., 2000). Quercetin was used to

http://www.aloki.hu ● ISSN 1589 1623 (Print) ● ISSN 1785 0037 (Online)
DOI: http://dx.doi.org/10.15666/aeer/2001_499509

prepare standard graphics. 50 µL of the stock solutions were taken and the volume was made up to 1920 µL with methanol. 40 µL of 1 M potassium acetate was added and after 1 min 40 µL of 10% aluminum nitrate was added. Absorbance was read at 415 nm (Optima SP-3000, Tokyo/Japan) after an incubation period of 40 min. Three parallel studies were performed for the measurements. The total flavonoid contents of the extracts were determined as equivalent to quercetin using the equation obtained from the standard quercetin graph (mg QE/g).

Determination of DPPH• free radical scavenging activity

The free radical scavenging activities of the groups were determined using the Blois (1958) method. 1,1-diphenyl-2-picrylhydrazil (DPPH•) (0.1 mM) solution was used as the free radical and 2,6-di-t-butyl-1-hydroxytoluene (BHT) (1000 ppm) as a standard. 20, 40, 60, 80 and 100 µL of SD, OS, DS and BHT stock solutions were taken and their volumes were made up to 400 µL with methanol. Then, 1600 µL of DPPH• solution was added. Control was prepared using methanol under the same conditions. After incubation of the prepared solutions for 30 min in the dark at room temperature, the absorbance changes at 517 nm were measured against methanol (Optima SP-3000, Tokyo/Japan). Decreased absorbances gave the remaining amount of free DPPH• solution, i.e., free radical scavenging activity (Jaradat et al., 2017).

The % DPPH• radical scavenging activity was calculated with the formula given below:

$$\% \text{ DPPH• radical scavenging activity} = [(A_0 - A_1) / A_0] \times 100 \qquad \text{(Eq.1)}$$

where A_0: absorbance of control reaction, A_1: absorbance of plant extracts and standard solutions.

Determination of ferric reducing power

The determination of the Fe^{3+} reducing power of the groups was made according to Oyaizu (1986). BHT was used as a standard. BHT and stock solutions were placed in a tube with a concentration of 10, 20, 30, 40 and 50 µg/mL. Pure water was added to make a total volume of 1.0 mL. On top of these solutions, 2.5 mL of phosphate buffer (0.2 M pH 6.6) and potassium ferricyanide (1%) solution were added and kept in a water bath at 50 °C for 20 min. Then 2.5 mL of 10% trichloroacetic acid (TCA) was added and vortexed. 2.5 mL ultrapure water and 0.5 mL iron (III) chloride (0.1%) were added to 2.5 mL samples from vortexed tubes and the absorbance was read at 700 nm against the blank (Optima SP-3000, Tokyo/Japan). Results were calculated as ascorbic acid equivalent using the equation obtained from the standard graph (µg AAE/mL) (Ergün, 2021b)

Statistical analysis

The data obtained in the study were analyzed using SPSS 15.0 and Windows statistical software programs, and the effect of drying methods was investigated. In the study, which was planned as three groups and three replicates, one-way analysis of variance and DUNCAN test were used to compare groups. All results were given as mean ± standard deviation. Significance test was performed according to $P < 0.05$ and the results were evaluated accordingly.

http://www.aloki.hu ● ISSN 1589 1623 (Print) ● ISSN 1785 0037 (Online)
DOI: http://dx.doi.org/10.15666/aeer/2001_499509

Results and discussion

Natural plants, which date back to centuries and are named differently by the peoples of the region, are very important for sustainable life. Among them, there are plants that have medicinal properties as well as nutritional properties. In addition, the increasing interest in natural nutrition and alternative medicine has increased the importance of such plants. *E. cicutarium*, a member of the *Geraniaceae* family, is a herbaceous plant with medicinal plant properties as well as nutritional properties. It grows naturally. Its leaves are consumed fresh and dried, raw or cooked. In this study, total phenolic and flavonoid substance content, DPPH• radical scavenging activities and Fe^{+3} reducing power capacity were determined in the samples belonging to SD, OD, DS groups.

The Folin-Ciocaltaeu method was used to determine the amount of phenolic substances. Gallic acid was calculated as equivalent to gallic acid using the standard graph ($y = 0.0745x - 0.0011$). In terms of phenolic substance amounts, it was found that SD and OD groups were similar among themselves, and the difference between them and the DS group was significant ($P < 0.05$).

The amounts of phenolic substances were determined as 41.27 ± 2.93 mg GAE/g in DS, 15.14 ± 2.25 mg GAE/g in SD, and 14.60 ± 0.86 mg GAE/g in OD, respectively (*Table 1*). In studies conducted on *Erodium* species, phenolic substance amounts were reported as 25.40 ± 2.07 mg GAE/g in *Erodium bryoniifolium* (El-Hela et al., 2013), 10.8 mg GAE/g in *Erodium bryoniifolium* Boiss (Alali et al., 2007), 248.08 ± 2 mg GAE/mL in *Erodium glaucophyllum*, 180 ± 4.02 mg GAE/mL in *Erodium hirtum*, and 124 ± 6 mg GAE/mL in *Erodium guttatum* (Hamza et al., 2018).

While the values we found are similar to *E. bryoniifolium* and *E. bryoniifolium* Boiss, they are lower than the values found in other species. This result we found proves that the phytochemical structures of plants differ between species. It was concluded that the difference between the groups was due to the drying technique applied. Because phytochemical properties are affected depending on the heat applied during drying. (Thamkaew et al., 2020). In addition, the applied heat may be perceived by the plant as a stress factor and cause the production of phenolic compounds by the plant in response (Cooper and Rao, 1992).

Table 1. *The amount of phenolic substances belonging to the groups ($P < 0.05$)*

Groups	The amount of total phenolic (mg GAE/g)
SD	15.14 ± 2.25^{b}
OD	14.60 ± 0.86^{b}
DS	41.27 ± 2.93^{a}

The total amount of flavonoid substance was calculated as equivalent to quercetin using the standard graph of quercetin ($y = 0.0574\ x + 0.0387$). The differences between the groups in terms of total flavonoid content were found to be significant at the $P < 0.05$ level and it was detected that the highest value was 71.99 ± 2.44 mg QE/g in OD and the lowest value was 19.61 ± 1.25 mg QE/g in SD (*Table 2*).

In similar studies conducted in different species, the total amount of flavonoids was reported as 34 ± 1 mg QE/g in *Erodium glaucophyllum* (Bakari et al., 2018), 91.97 ± 1.56 mg RE/g in *Erodium glaucophyllum*, 63 ± 4.1 mg RE/g in *Erodium hirtum*, and 52 ± 2.3 mg RE/g in *Erodium guttatum* (Hamza et al., 2018).

http://www.aloki.hu ● ISSN 1589 1623 (Print) ● ISSN 1785 0037 (Online)
DOI: http://dx.doi.org/10.15666/aeer/2001_499509

This result we found proves that the phytochemicals in plants are affected differently by the drying process (Hossain et al., 2010). In addition, failure to adjust the heat to be applied well may cause deterioration of phytochemicals (Orphanides et al., 2013).

Table 2. *The amount of flavonoid substance belonging to the groups (P < 0.05)*

Groups	The amount of total flavonoid (mg QE/g)
SD	19.61 ± 1.25^{c}
OD	71.99 ± 2.24^{a}
DS	27.16 ± 1.91^{b}

DPPH• free radical and BHT as a standard were used to determine the free radical scavenging activity of the groups. DPPH• radical scavenging activities of the extracts and BHT were calculated (%) (*Table 3*). Parallel to the increase in concentration (20–100 µg/mL), it was observed an increase in DPPH• radical scavenging activities in both groups and BHT. The differences between the groups were significant at the $P < 0.05$ level. The highest activity value was detected in DS at all concentrations. In addition, the activity values in DS were higher than the value of BHT used as a standard. In a similar study on *E. glaucophyllum*, the activities detected in ethyl acetate and chloroform extracts were higher than the values we found (Radhia et al., 2018).

Table 3. *% DPPH radical scavenging activities of groups and BHT (P < 0.05)*

Extracts/standard	20 µg/mL	40 µg/mL	60 µg/mL	80 µg/mL	100 µg/mL
SD	7.54 ± 2.05^{c}	25.07 ± 2.12^{c}	42.10 ± 0.82^{c}	57.09 ± 2.14^{c}	70.96 ± 2.68^{c}
OD	0.47 ± 0.14^{d}	17.54 ± 0.81^{d}	27.99 ± 7.19^{d}	44.14 ± 2.39^{d}	56.56 ± 0.25^{d}
DS	19.31 ± 1.85^{a}	46.91 ± 1.62^{a}	63.03 ± 1.10^{a}	79.13 ± 6.26^{a}	83.58 ± 0.15^{a}
BHT	13.20 ± 3.25^{b}	42.01 ± 1.42^{b}	55.50 ± 2.34^{b}	65.81 ± 3.51^{b}	79.95 ± 2.34^{b}

The concentration of the extract and standard substance that inhibited 50% of DPPH• radical removal was determined as IC_{50}. This value was calculated using the graphs obtained by placing the % DPPH• radical scavenging activity values against the studied concentrations (*Table 4*). There is an inverse correlation between the IC_{50} value and the DPPH• radical scavenging activity. A low IC_{50} value means a high radical scavenging activity.

Table 4. *IC_{50} values of groups and BHT (P < 0.05)*

Extracts and standard	IC_{50} (µg/mL)
SD	71.90 ± 1.69^{b}
OD	89.81 ± 3.42^{a}
DS	49.47 ± 2.69^{d}
BHT	58.34 ± 0.86^{c}

The difference between the groups in terms of IC_{50} value was found to be significant ($P < 0.05$). The IC_{50} value order of the groups was detected as 71.90 ± 1.69

http://www.aloki.hu ● ISSN 1589 1623 (Print) ● ISSN 1785 0037 (Online)
DOI: http://dx.doi.org/10.15666/aeer/2001_499509

µg/mL in SD, 89.81 ± 3.42 µg/mL in OD and 49.47 ± 2.69 µg/mL in DS. In similar studies, the IC_{50} value was 38.8 ± 0.2 µg/mL in *E. glaucophyllum* flowers and 79.2 ± 0.6 µg/mL in its leaves, 20.29 ± 2.64 µg/mL in *E. glaucophyllum*, 49.1 ± 3.6 µg/mL in *E. hirtum* and 56.9 ± 3.3 µg/mL in *E. guttatum* (Hamza et al., 2018; Bakari et al., 2018). In addition, in a similar study conducted on *Kappaphycus alvarezii*, it was reported that the highest IC_{50} value was in the Oven-dried 40 °C group, and the lowest value was in the Sun-dried group (Ling et al., 2015). The Fe^{3+}-Fe^{2+} reducing capacity of SD, OD and DS extracts and BHT was determined by using the method of Oyaizu (1986). In the measurements of Fe^{3+} reducing capacity, absorbances at 700 nm were determined and a graph was obtained by placing the absorbance values against the concentration (*Fig. 2*). In this graph, increasing absorbance values show the reducing power capacity.

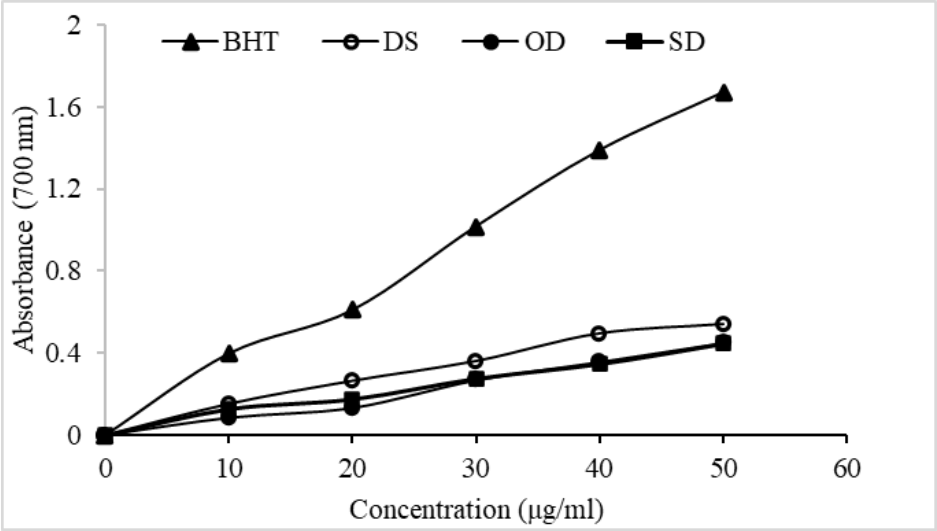

Figure 2. *Comparison of the Fe^{3+}-Fe^{2+} reducing capacity of the extracts of the groups with BHT (20-50 µg/mL)*

In addition, the Fe^{3+}-Fe^{2+} reducing power of the groups was calculated as ascorbic acid equivalent (µg AAE/mL) using the ascorbic acid standard graph (*Table 5*). The differences between the groups were found to be significant ($P < 0.05$). Similarity was found between SD and OD and DS. Respectively, it detected as 1231.01 ± 4.83 µg AAE/mL in BHT, 129.43 ± 6.80 µg AAE/mL in DS, 116.59 ± 4.90 µg AAE/mL in SD and 83.29 ± 4.12 µg AAE/mL in OD. In the study conducted by Jaradat et al., in 2017 on the same species, the values they found to be equivalent to trolox and the values we found were similar (Jaradat et al., 2017).

Table 5. *Fe^{3+}-Fe^{2+} reducing capacity of groups and BHT ($P < 0.05$)*

Extracts and standard	µg AAE/mL
SD	116.59 ± 4.90^{bc}
OD	83.29 ± 4.12^{c}
DS	129.43 ± 6.80^{b}
BHT	1231.01 ± 4.83^{a}

http://www.aloki.hu ● ISSN 1589 1623 (Print) ● ISSN 1785 0037 (Online)
DOI: http://dx.doi.org/10.15666/aeer/2001_499509

Conclusion

Recently, an increase has been observed in studies on the effects of drying techniques on phytochemicals. For this purpose, studies have been carried out on many foodstuffs (Osae et al., 2019; Al-juhaimi et al., 2018; Arvaniti et al., 2019; Mustafa, et al., 2019; Zahoor et al., 2019). Plants perceive the drying process as a stress factor. This affects the amount of antioxidants in plants, depending on the application (Guclu et al., 2021). Green plants are more affected by this condition than woody plants (Yousif et al., 1999). In this study, it was observed that the phytochemical structure of the *E. cicutarium* plant was affected by drying in sunlight, drying in a thermostatic oven at 55 °C and drying in the shade. It was determined that the shade drying method was advantageous in terms of total phenolic substance content, % DPPH radical removal activities, IC_{50} value and Fe^{3+}-Fe^{2+} reducing capacity, and the method of drying in a thermostatic oven at 55 °C was advantageous in terms of total flavonoid substance content. Results in this study were similar to those found results by Fernandes et al., 2011 and Jang et al., 2020. As a result, it was concluded that there is a need for new studies on the determination of the compounds responsible for the antioxidant activity of the *E. cicutarium* plant, which is valuable in terms of phytochemicals, its usability as a natural antioxidant and the kinetics of the drying process. In addition, it is recommended to develop new drying techniques that will least affect the existing properties of plant resources.

Funding. This research did not receive any specific grant from funding agencies in the public, commercial, or not-for-profit sectors.

REFERENCES

[1] Abdolahi, N., Soltani, A., Mirzaali, A., Soltani, S., Balakheyli, H., Aghaei, M. (2018): Antibacterial and antioxidant activities and phytochemical properties of *Punica granatum* flowers in Iran. – Iranian Journal of Science and Technology, Transactions A: Science 42: 1105-1110.

[2] Alali, F. Q., Tawaha, K., El-Elimat, T., Syouf, M., El-Fayad, M., Abulaila, K., Nielsen, S. J., Wheaton, W. D., Falkinham, J. O., Oberlies, N. H. (2007): Antioxidant activity and total phenolic content of aqueous and methanolic extracts of Jordanian plants: an ICBG project. – Natural Product Research 21: 1121-1131.

[3] Al-juhaimi, F., Ghafoor, K., Özcan, M. M., Jahurul, M. H. A., Babiker, E. E., Jinap, S., Zaidul, I. S. M. (2018): Effect of various food processing and handling methods on preservation of natural antioxidants in fruits and vegetables. – Journal of Food Science and Technology 55(10): 3872-3880.

[4] Arvaniti, O. S., Samaras, Y., Gatidou, G., Thomaidis, N. S., Stasinakis, A. S. (2019): Review on fresh and dried figs: chemical analysis and occurrence of phytochemical compounds, antioxidant capacity and health effects. – Food Research International 119: 244-267.

[5] Asadi-Samani, M., Moradi, M. T., Bahmani, M., Shahrani, M. (2016): Antiviral medicinal plants of Iran: a review of ethnobotanical evidence. – International Journal of PharmTech Research 9: 427-434.

[6] Bakari, S., Hajlaoui, H., Daoud, A., Mighri, H., Ross-Garcia, J. M., Gharsallah, N., Kadri, A. (2018): Phytochemicals, antioxidant and antimicrobial potentials and LC-MS analysis of hydroalcoholic extracts of leaves and flowers of *Erodium glaucophyllum* collected from Tunisian Sahara. – Food Science and Technology 38: 310-317.

http://www.aloki.hu ● ISSN 1589 1623 (Print) ● ISSN 1785 0037 (Online)
DOI: http://dx.doi.org/10.15666/aeer/2001_499509

[7] Blois, M. S. (1958): Antioxidant determinations by the use of a stable free radical. – Nature 181: 1199-1200.
[8] Cooper, J. E., Rao, R. (1992): Localised changes in flavonoid biosynthesis in roots of *Lotus pendiculatus* after infection by *Rhizobium loti*. – Plant Physiology 100: 444-450.
[9] De-la-Cruz, H., Vilcapoma, G., Zevallos, P. A. (2007): Ethnobotanical study of medicinal plants used by the Andean people of Canta, Lima, Peru. – Journal of Ethnopharmacology 111: 284-294.
[10] Demir, T., Akpınar, Ö. (2020): Biological activities of phytochemicals in plants. – Turkish Journal of Agriculture-Food Science and Technology 8(8): 1734-1746.
[11] Deng, L. Z., Mujumdar, A. S., Zhang, Q., Yang, X. H., Wang, J., Zheng, Z. A., Gao, Z. J., Xiao, H. W. (2019): Chemical and physical pretreatments of fruits and vegetables: effects on drying characteristics and quality attributes. A comprehensive review. – Critical Reviews in Food Science and Nutrition. 59(9): 1408-32.
[12] Duke, J. A. (2001): (Ed.) Handbook of Edible Weeds. – CRC Press, Boca Ratón, FL.
[13] El-Hela, A. A., Abdel-Hady, N. M., Dawoud, G. T., Hamed, A. M., Morsy, T. A. (2013): Phenolic content, antioxidant potential and Aedes aegyptii ecological friend larvicidal activity of some selected Egyptian plants. – Journal of the Egyptian Society of Parasitology 43: 215-234.
[14] Ergün, F. (2021a): *Lonicera iberica* M. Bieb.: investigation antioxidant activity and bioactive chemicals. – Turkish Journal of Agriculture - Food Science and Technology 9(6): 1124-1128.
[15] Ergün, F. (2021b): *Cotoneaster Transcaucasicus* Pojark. Determination of bioactive component amounts and antioxidant activities in fruit extracts. – Turkish Journal of Agriculture - Food Science and Technology 9(7): 1258-1263.
[16] Erlund, I., Koli, R., Alfthan, G., Marniemi, J., Puukka, P., Mustonen, P., Mattila, P., Jula, A. (2008): Favorable effects of berry consumption on platelet function, blood pressure, and HDL cholesterol. – Am. J. of Clin. Nutrition 87(2): 323-331.
[17] Fernandes, L., Casal, S., Pereıra, J. A., Saraıva, J. A., Ramalhosa, E. (2018): Effects of different drying methods on the bioactive compounds and antioxidant properties of edible Centaurea (*Centaurea cyanus*) petals. – Brazilian Journal of Food Technology 21(0): 1-10.
[18] Fiz, O., Vargas, P., Alarcon, M. L., Aldasoro, J. J. (2006): Phylogenetic relationships and evolution in *Erodium* (*Geraniaceae*) based on trnL-trnF sequences. – Systematic Botany 31(4): 739-763.
[19] Foo, L. Y., Porter, L. J. (1981): The structure of tannins of some edible fruits. – Journal Science Food Agricaltural 32: 711-716.
[20] Guclu, G., Keser, D., Kelebek, H., Keskin, M., Şekerli, Y. E., Soysal, Y., Selli, S. 2021: Impact of production and drying methods on the volatile and phenolic characteristics of fresh and powdered sweet red peppers. – Food Chemistry 338: 128129.
[21] Hamza, G., Emna, B. H., Yeddes, W., Dhouafli, Z., Moufida, T. S., El Akrem, H. (2018): Chemical composition, antimicrobial and antioxidant activities data of three plants from Tunisia region: *Erodium glaucophyllum*, *Erodium hirtum* and *Erodium guttatum*. – Data Brief 19: 2352-2355.
[22] Harguindeguy, M., Fissore, D. (2020): On the effects of freeze-drying processes on the nutritional properties of foodstuff: a review. – Drying Technology 38: 846-868.
[23] Hossain, M. B., Barry-Ryan, C., Martin-Diana, A. B., Brunton, N. P. (2010): Effect of drying method on the antioxidant capacity of six Lamiaceae herbs. – Food Chemistry 123(1): 85-91.
[24] Jafari, S. M., Azizi, D., Mirzaei, H., Dehnad, D. (2016): Comparing quality characteristics of oven-dried and refractance window-dried kiwifruits. – Journal of Food Processing and Preservation 40: 362-372.

http://www.aloki.hu ● ISSN 1589 1623 (Print) ● ISSN 1785 0037 (Online)
DOI: http://dx.doi.org/10.15666/aeer/2001_499509

[25] Jang, M., Kim, K. H., Kim, G. H. (2020): Antioxidant capacity of thistle (*Cirsium japonicum*) in various drying methods and their protection effect on neuronal PC12 cells and Caenorhabditis elegans. – Antioxidants 9(3): 200.
[26] Jaradat, N., Al-Masri, M., Zaid, A. N., Othman, D. G. (2018): Pharmacological and phytochemical screening of Palestinian traditional medicinal plants *Erodium laciniatum* and Lactuca orientalis. – Journal of Complementary and Integrative Medicine 15(1): 1-16.
[27] Kamel, S. M., Thabet, H. A., Algadi, E. A. (2013): Influence of drying process on the functional properties of some plants. – Chemistry and Materials Research 3: 1-8.
[28] Latimer, A. M., Jacobs, B. S., Gianoli, E., Heger, T., Salgado-Luarte, C. (2019): Parallel functional differentiation of an invasive annual plant on two continents. – AoB Plants 11: 1-16.
[29] Ling, A. L. M., Yasir, S., Matanjun, P., Abu Bakar, M. F. (2015): Effect of different drying techniques on the phytochemical content and antioxidant activity of Kappaphycus alvarezii. – Journal of Applied Phycology. 27: 1717-1723.
[30] Lis-Balchin, M. (1993): The essential oils of *Pelargonium grossularioides* and *Erodium cicutarium* (*Geraniaceae*). – Journal of Essential Oil Research 5: 317-318.
[31] Lorenzi, H., Matos, F. J. A. (2002): Plantasmedicinais no Brasil: Nativasexóticas. – Instituto Plantarum, Nova Odessa.
[32] Martysiak-Żurowska, D., Rożek, P., Puta, M. (2020): The effect of freeze-drying and storage on lysozyme activity, lactoferrin content, superoxide dismutase activity, total antioxidant capacity and fatty acid profile of freeze-dried human milk. – Drying Technology 1-11.
[33] Molares, S., Ladio, A. (2009): Ethnobotanical review of the Mapuche medicinal flora: use patterns on a regional scale. – Journal of Ethnopharmacology 122(2): 251-260.
[34] Munekata, P. E. S., Alcántara, C., Collado, M. C., Garcia-Perez, J. V., Saraiva, J. A., Lopes, R. P., Barba, F. J., do Prado Silva, L., Sant′Ana, A. S., Fierro, E. M., Lorenzo, J. M. (2019): Ethnopharmacology, phytochemistry and biological activity of *Erodium* species: a review. – Food Research International 126: 108659.
[35] Mustafa, I., Chin, N. L., Fakurazi, S., Palanisamy, A. (2019): Comparison of phytochemicals, antioxidant and anti-inflammatory properties of sun-, oven- and freeze-dried ginger extracts. – Foods 8: 456.
[36] Müller, J. (2007): Convective drying of medicinal, aromatic and spice plants: a review. – Stewart Postharvest Review 3(4): 1-6.
[37] Nieva Moreno, M. I., Isla, M. I., Sampieto, A. R., Vattuone, M. A. (2000): Comparison of the free radical-scavenging activity of propolis from several regions of Argentina. – Journal of Ethnopharmacology 71: 109-114.
[38] Orphanides, A., Goulas, V., Gekas, V. (2013): Effect of drying method on the phenolic content and antioxidant capacity of spearmint. – Czech Journal of Food Sciences 31: 509-513.
[39] Osae, R., Zhou, C., Xu, B., Tchabo, W., Tahir, H. E., Mustapha, A. T., Ma, H. (2019): Effects of ultrasound, osmotic dehydration, and osmosonication pretreatments on bioactive compounds, chemical characterization, enzyme inactivation, color, and antioxidant activity of dried ginger slices. – Journal of Food Biochemistry 43(5): e12832.
[40] Oyaizu, M. (1986): Studies on products of browning reactions: antioxidative activities of products of browning reaction prepared from glucosamine. – Japanese Journal of Nutrition 44: 307-315.
[41] Özgen, U., Kaya, Y., Houghton, P. (2012): Folk medicines in the villages of Ilıca District (Erzurum, Turkey). – Turkish Journal of Biology 36: 93-106.
[42] Pieroni, A., Cattero, V. (2019): Wild vegetables do not lie: comparative gastronomic ethnobotany and ethnolinguistics on the Greek traces of the Mediterranean diet of southeastern Italy. – Acta Botanica Brasilica 33: 198-211.

http://www.aloki.hu ● ISSN 1589 1623 (Print) ● ISSN 1785 0037 (Online)
DOI: http://dx.doi.org/10.15666/aeer/2001_499509

[43] Pirbalouti, A. G., Salehi, S., Craker, L. (2017): Effect of drying methods on qualitative and quantitative properties of essential oil from the aerial parts of coriander. – Journal of Applied Research on Medicinal and Aromatic Plants 4(1): 35-40.
[44] Quispe-Fuentes, I., Vega-Gálvez, A., Aranda, M. (2018): Evaluation of phenolic profiles and antioxidant capacity of maqui (*Aristotelia chilensis*) berries and their relationships to drying methods. – Journal of the Science of Food and Agriculture 98(11): 4168-4176.
[45] Radhia, A., Hanen, N., Abdelkarim, B. A., Mohamed, N. (2018): Phytochemical screening, antioxidant and antimicrobial activity of *Erodium glaucophyllum* (L.) L'Hérit. – Journal of Biomedical Sciences 7: 13.
[46] Rajaei, P., Mohamadi, N. (2012): Ethnobotanical study of medicinal plants of Hezar mountain allocated in south east of Iran. – Iranian Journal of Pharmaceutical Research 11: 1153-1167.
[47] Safa, O., Soltanipoor, M. A., Rastegar, S., Kazemi, M., Dehkordi, K. N., Ghannadi, A. R. (2012): An ethnobotanical survey on Hormozgan province, Iran. – Avicenna Journal of Phytomedicine 3: 64-81.
[48] Slinkard, K., Singleton, V. L. (1977): Total phenol analyses: automation and comparison with manual methods. – American Journal of Enology and Viticulture 28: 49-55.
[49] Tene, V., Malagón, O., Finzi, P. V., Vidari, G., Armijos, C., Zaragoza, T. (2007): An ethnobotanical survey of medicinal plants used in Loja and Zamora-Chinchipe, Ecuador. – Journal of Ethnopharmacology 111(1): 63-81.
[50] Thamkaew, G., Sjöholm, I., Galindo, F. G. (2020): A review of drying methods for improving the quality of dried herbs. – Critical Reviews in Food Science and Nutrition 18: 1-24.
[51] Yousif, A. L., Scaman, C. H., Durance, T. D., Girard, B. (1999): Flavor volatiles and physical properties of vacuum-microwave and airdried sweet basil (*Ocimum basilicum* L.). – Journal of Agricultural and Food Chemistry 47: 4777-4781.
[52] Zahoor, I., Khan, M. A. (2019): Microwave assisted convective drying of bitter gourd: drying kinetics and effect on ascorbic acid, total phenolics and antioxidant activity. – Journal of Food Measurement and Characterization 3(3): 2481-90.
[53] Zhu, Y., Pu, B., Xie, G. (2014): Dynamic changes of flavonoids contents in the different parts of rhizome of Belamcanda chinensis during the thermal drying process. – Molecules 19(7): 10440-10454.

http://www.aloki.hu ● ISSN 1589 1623 (Print) ● ISSN 1785 0037 (Online)
DOI: http://dx.doi.org/10.15666/aeer/2001_499509

COMPARATIVE STUDY ON THE LEAD ADSORPTION CHARACTERISTICS OF MODIFIED CORN STALK BIOCHAR

XU, H. Y.[1] – MA, X. L.[1*] – WANG, B.[1] – YUAN, M. Z.[1] – SU, J. H.[1] – WANG, Y. J.[1*] – GAO, H. J.[2]

[1]*College of Resources and Environment, Jilin Agricultural University, Changchun 130118, Jilin, China*

[2]*Institute of Agricultural Environment and Resources Research, Jilin Academy of Agriculture Sciences, Changchun 130033, Jilin, China*

**Corresponding authors*
e-mail/phone/fax: 491277643@qq.com/+86-180-0442-2753/+86-431-8453-1264 (X. Ma); wyj0431@126.com/+86-135-0441-9456/+86-431-8453-1264 (Y. Wang)

(Received 1st Sep 2021; accepted 23rd Nov 2021)

Abstract. In this study, corn straw and modified corn straw impregnated with Potassium hydroxide（KOH）were used as raw materials to prepare biochar (BC) and modified biochar (K-BC). SEM, FTIR, EDS and other analytical methods were used to study the structure of BC and K-BC, and the equilibrium adsorption method was used to compare and study the characteristics of BC and K-BC adsorbing Pb. The results show that when the solution is weakly acidic (pH 5), Quasi-second-order kinetics can accurately describe the adsorption process of Pb ($R^2 > 0.9875$); the Langmuir model fits well, indicating that Pb adsorption by biochar is mainly a single-layer adsorption; the results of thermodynamic tests $\Delta H^\circ > 0$, $\Delta S^\circ > 0$, $\Delta G^\circ < 0$ indicate that the adsorption of Pb by biochar is a spontaneous, endothermic, and disorderly increase process. Combining elemental analysis, specific surface area pore size determination, SEM, and EDS for the characterization of materials before and after adsorption, it can be seen that the difference between BC and K-BC adsorption of Pb comes from the difference between the specific surface areas, pore structures and aromatic structures of the materials, accompanied by the ion exchange effect.
Keywords: *corn stalk, biomass char, pH, alkali modification, lead, material characterization*

Introduction

Lead (Pb) is one of the three major heavy metal pollutants and is a heavy metal element that seriously harms human health. The ideal lead content in the human body is zero (Abdallah et al., 2019). Humans often bring lead into the human body by ingesting food and drinking tap water (Park et al., 2018). Lead poisoning is cumulative. After the long-term intake of lead, it will cause serious damage to the blood system and nervous system of the body, with the irreversible effects on children's health and intelligence (Dai and Jia, 2019). The lead production of China ranks first in the world. In recent years, the unreasonable extent of heavy metal mining and smelting, sewage irrigation, solid waste stacking, pesticides and fertilizers during the industrial development process has caused a large amount of heavy metals to enter the atmosphere, water bodies, and soil (Paranavithana et al., 2016). Heavy metals have become a global environmental pollution problem. At present, the main methods for removing heavy metals in water include chemical precipitation, ion exchange, adsorption, physical filtration and bioremediation (Abdelhafez et al., 2016). Adsorption method is a common method to remove heavy metals in wastewater (Deng et al., 2017). Due to the variety of adsorbent materials, the process is simple, and it is widely used in heavy metal polluted water bodies.

http://www.aloki.hu ● ISSN 1589 1623 (Print) ● ISSN 1785 0037 (Online)
DOI: http://dx.doi.org/10.15666/aeer/2001_511525

Biomass char is produced by pyrolysis of biomass raw materials under oxygen-limited conditions. Biochar has rich oxygen-containing functional groups, large porosity, and high pH. It has a good adsorption effect on heavy metals in water and soil, and has attracted widespread attention as a new material (Zhang et al., 2019a). Bio-carbon raw materials have wide sources, low prices, and no secondary pollution, and are widely used for heavy metal pollution treatment (Xiao et al., 2018). The adsorption performance of biochar depends not only on the size of the pore structure of biochar, but also on the surface chemical properties of chemical functional groups and surface heteroatoms on the surface of biochar (Komnitsas et al., 2016; Zhao et al., 2020). Biochar can be modified by oxidative modification (Shen et al., 2018), load-bearing substance modification (Li et al., 2019), acid-base modification (Mahdi et al., 2019), etc. To modify its surface chemical properties and thus enhance its adsorption capacity. Cheng et al. (Cao et al., 2018) used biochar made from corn stover to remove Pb at a rate of 98.62%. Cao et al. (Chi et al., 2017) found that the adsorption amount of Pb by wheat straw biochar is 2.58 times that of wheat straw. China is a large agricultural country. It produces about 243 million tons of corn stalks every year, which are discarded or burned at will, which has caused serious pollution to the environment (She et al., 2016). Using corn stalks as raw materials for preparing biomass charcoal can realize the resource utilization of agricultural wastes (Fahmi et al., 2018; Wang et al., 2019).

In this paper, corn straw (collected from Changchun, Jilin Province, China) was used as raw material to prepare biochar, and KOH soaked corn straw to prepare modified biochar. The adsorption characteristics of lead are studied in order to lay a foundational theory and provide technical reference for solving the pollution of heavy metal lead in wastewater.

Materials and methods

Instruments

SX2-4-10N muffle furnace (Shanghai Yetuo Instrumentation Co., Ltd.); LC-LX-HL210D high-speed desktop centrifuge (Shanghai Decheng Instrument Factory); TAS-990 atomic absorption spectrophotometer (Beijing General Analysis General Instrument Co., Ltd.); Vario-EL-Ⅲ Elemental Analyzer (Elementar Company, Germany); 3H-2000P Specific Surface Area, Aperture Analyzer (Beijing Best Company); Scanning Electron Microscope/X-Ray Energy Dispersion Analyzer (Japan Shimadzu Corporation); IRTracer-100 infrared spectrum (Japan Shimadzu Corporation), etc.

Reagents and materials

Main reagents

Cu $(NO_3)_2$, Pb $(NO_3)_2$, KOH, NaOH, $NaNO_3$ (all analytical reagents, Beijing Chemical Plant). Corn stalks come from Changchun, Jilin Province, China.

Preparation of biochar

Corn stalks passed through a 20-mesh sieve as raw materials, pyrolyzed at 450 °C for 2 h in a muffle furnace, cooled to room temperature, passed through a 60-mesh sieve, and marked as BC.

http://www.aloki.hu ● ISSN 1589 1623 (Print) ● ISSN 1785 0037 (Online)
DOI: http://dx.doi.org/10.15666/aeer/2001_511525

Preparation of alkali-modified biochar

Put 10 g of corn stalk passed through a 20 mesh sieve into a 250 mL beaker, add 150 mL of 15% KOH and stir every 8 h, let stand for 24 h, filter, and rinse the straw with deionized water. The KOH remaining on the surface was dried at 385 °C, then pyrolyzed at 450 °C for 2 h in a muffle furnace, cooled to room temperature, passed through a 60-mesh sieve, and marked as K-BC.

Test design

Structural characterization and physical and chemical characteristics

Refer to the "Charcoal and Charcoal Test Method" (GB/T17664-1999) for biochar asha content and pH; the content of C, N, H, and O on the surface of biochar shall be determined by elemental analyzer. Among them, O is obtained by subtractive method (Chen et al., 2014) specific surface area and pore structure are measured by specific surface area and pore size analyzer; functional groups on the surface of biochar are measured by infrared spectrometer (Gao et al., 2016); the microstructure of biochar is characterized by scanning electrons Microscopy/X-ray energy dispersive analysis was performed (Liang et al., 2015).

Adsorption test

Adsorption tests were performed under constant temperature and light, 150 $r \cdot min^{-1}$ air-bath shaking conditions; 0.01 $mol \cdot L^{-1}$ $NaNO_3$ was used as the background electrolyte solution; the amount of biochar was 1.25 $g \cdot L^{-1}$, and the pH of the background solution. It was adjusted with 0.01 $mol \cdot L^{-1}$ HNO_3 and NaOH solution.

Adsorption kinetics test

Add 0.0625 g of BC and K-BC samples to a 50 mL polyethylene centrifuge tube, add pH 5.0, and the initial concentration is 400 $mg \cdot L^{-1}$ lead nitrate solution, 25 °C constant temperature shaking, sampled at 0, 5, 10, 30, 60, 120, 240, 480, 720, 1440 min, centrifuged at 10000 $r \cdot min^{-1}$ for 10 min, and used the supernatant for Atomic absorption spectrophotometer measures the concentration of Pb.

Adsorption thermodynamic test

Add 0.0625 g of BC and K-BC to 50 mL polyethylene centrifuge tubes, add nitric acid with a pH value of 5.0 and an initial concentration of 50, 100, 200, 400, 600, 800 $mg \cdot L^{-1}$ Salt lead was placed under the conditions of 15 °C, 30 °C and 45 °C, shaken for 360 min, centrifuged at 10000 $r \cdot min^{-1}$ for 10 min, the supernatant was taken and the concentration of Pb was determined by atomic absorption spectrophotometer.

Effect of pH of background solution on Pb adsorption

Add 0.0625 g of BC and K-BC to a 50 mL polyethylene centrifuge tube. The pH of the background solution is 2.0, 3.0, 4.0, 5.0, 6.0, and the initial concentration is 400 $mg \cdot L^{-1}$ lead nitrate solution was shaken at 25 °C for 6 h, centrifuged at 10000 $r \cdot min^{-1}$ for 10 min, and the supernatant was measured by atomic absorption spectrophotometer.

http://www.aloki.hu ● ISSN 1589 1623 (Print) ● ISSN 1785 0037 (Online)
DOI: http://dx.doi.org/10.15666/aeer/2001_511525

Data analysis

The adsorption capacity of the solution is calculated using the mass balance equation (*Eq. 1*):

$$q_t = \frac{(C_0 - C_t)V}{m} \quad \text{(Eq.1)}$$

where qt is the adsorption capacity of Pb at time t ($mg \cdot g^{-1}$); C0 is the initial Pb concentration ($mg \cdot L^{-1}$); Ct is the equilibrium concentration of Pb at time t ($mg \cdot L^{-1}$); V is nitric acid Volume of lead solution (mL); m is the amount (mg) of the adsorbent BC and K-BC added.

Adsorption kinetics was fitted using quasi-first-order kinetic equations (*Eq. 2*) and quasi-second-order kinetic equations (*Eq. 3*).

$$q_t = Q_{e,1}(1 - e^{-k_1 t}) \quad \text{(Eq.2)}$$

$$q_t = \frac{Q_{e,2}^2 k_2 t}{1 + Q_{e,2} k_2 t} \text{ (non-linear form)} \quad \text{(Eq.3)}$$

in the formula: qt is the adsorption capacity of Pb at time t ($mg \cdot g^{-1}$); Qe, 1 and k1 are quasi-first-order kinetic constants, which represent the adsorption equilibrium amount ($mg \cdot g^{-1}$) and adsorption rate constant of Pb (min^{-1}); $Q_{e,2}$ and k_2 are quasi-second-order kinetic constants, which represent the adsorption equilibrium amount ($mg \cdot g^{-1}$) and adsorption rate constant ($g \cdot mg^{-1} \cdot min^{-1}$) of Pb, respectively.

The adsorption isotherm data was fitted using Langmuir equation (*Eq. 4*) and Freundlich equation (*Eq. 5*):

$$q_t = \frac{Q_{e,2}^2 k_2 t}{1 + Q_{e,2} k_2 t} \text{ (non-linear form)} \quad \text{(Eq.4)}$$

$$q_e = K_F C_t^{1/n} \text{ (non-linear form)} \quad \text{(Eq.5)}$$

where qe is the equilibrium adsorption amount ($mg \cdot g^{-1}$) of Pb; qm and K_L are parameters of the Langmuir model, which respectively represent the maximum adsorption amount ($mg \cdot g^{-1}$) and adsorption energy ($L \cdot mg^{-1}$) of Pb; K_F and n are parameters of the Freundlich model, and represent the adsorption capacity ($mg \cdot g^{-1} \cdot (mg \cdot L^{-1})^{-1/n}$) and adsorption strength of Pb, respectively.

The adsorption thermodynamic parameters are standard free energy change (ΔG˚, $kJ \cdot mol^{-1}$), standard enthalpy change (ΔH°, $kJ \cdot mol^{-1}$), and standard entropy change (ΔS˚, $J \cdot mol^{-1} \cdot K^{-1}$).

Thermodynamic equation calculation:

$$K_d = \frac{(C_0 - C_t)V}{C_r m} \quad \text{(Eq.6)}$$

$$\ln K_d = \frac{\Delta S°}{R} - \frac{\Delta H°}{RT} \quad \text{(Eq.7)}$$

http://www.aloki.hu ● ISSN 1589 1623 (Print) ● ISSN 1785 0037 (Online)
DOI: http://dx.doi.org/10.15666/aeer/2001_511525

$$\Delta G = \Delta H° - T\Delta S° \quad \text{(Eq.8)}$$

where Kd is the thermodynamic equilibrium constant ($mL \cdot g^{-1}$), R is the ideal gas constant (8.314 $J \cdot mol \cdot K^{-1}$), T is the reaction temperature (K), and the ΔH° and ΔS° values are $\ln K_d$-T^{-1} The slope and intercept of the straight line in the 1 diagram.

Results and discussion

BC and K-BC structural characterization and properties

Infrared spectral characterization

Figure 1 shows the ir spectra of BC and K-BC. As can be seen from *Figure 1,* the main peaks of BC and K-BC at 3400 cm^{-1} do not show significant deviation, but the intensity of K-BC peak decreases significantly. Through semi-quantitative analysis of the relative intensity of main absorption peaks of BC and K-BC, it decreases from 0.2755 to 0.1372. Compared with BC, the main adsorption peaks on the surface of K-BC have changed: the -OH stretching vibration peaks of alcohols and phenols associated with intermolecular hydrogen bonding at 3400 cm^{-1} are weakened; the asymmetric aliphatic CH and The stretching vibration absorption peak of -CH_2- symmetric aliphatic CH at 2850 cm^{-1} was weakened; the stretching vibration peaks of C = C, C = O of benzene ring or aromatic heterocycle between 1620 cm^{-1} and 1400 cm^{-1} increased, and 1425 cm^{-1}. The absorption peak of the stretching vibration of aromatic C = C is obviously enhanced and merges with the absorption peak of -OH in-plane bending vibration of the alcohol at 1362 cm^{-1}; Si-O bonds are characterized at 1038 cm^{-1} and 780 cm^{-1} The absorption peaks of the stretching vibrations are also enhanced.

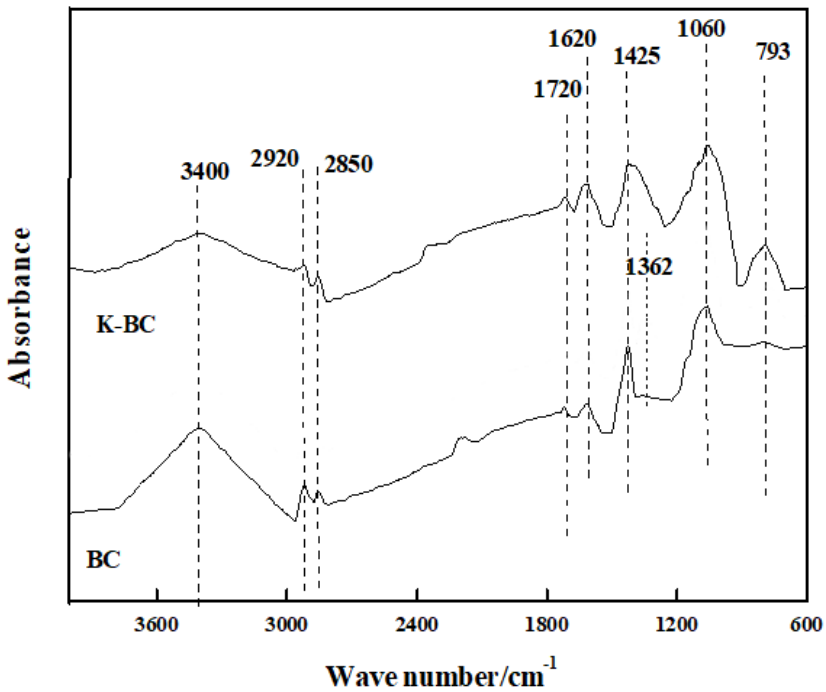

Figure 1. *BC and K-BC infrared spectra. (a) K-BC; (b) BC. The picture shows the infrared spectrum of Pb after adsorption*

http://www.aloki.hu ● ISSN 1589 1623 (Print) ● ISSN 1785 0037 (Online)
DOI: http://dx.doi.org/10.15666/aeer/2001_511525

Table 1 shows the results of semi-quantitative analysis of the relative intensities of the main absorption peaks of BC and K-BC, and the number of functional groups can be compared quantitatively. Among them, (2920 + 2850)/(1620 + 1425) can reflect the aromatic strength of biochar. It can be seen from *Table 1* that compared with BC, the (2920 + 2850)/(1620 + 1425) ratio of K-BC is significantly reduced, indicating that the carbonyl groups and aromatic structures contained in K-BC are increased, while the relative content of aliphatic CH is decreased. It means that the alkali-soaked corn stalk can promote the increase of K-BC aromatization degree and selectively retain some of its oxygen-containing groups. Li et al. (Wang et al., 2016) found that the cation-π action is one of the main mechanisms for biochar adsorption of heavy metals, that is, the higher the aromaticity of the biochar surface, the more π-conjugated aromatic structures, the stronger the cation-π action, and the cation-π. The greater the contribution of action to heavy metal adsorption. In this study, K-BC has a higher degree of aromaticity than BC and can provide more active adsorption sites for cation-π interactions. Therefore, the contribution of cation-π interactions to Pb2 + in K-BC may be higher than that of BC. Studies have shown that the inorganic mineral component SiO2 on the surface of biochar has an important contribution to the adsorption of heavy metals (Jian et al., 2015). At the same time, the absorption peaks of the Si-O bond stretching vibration in K-BC have been enhanced, indicating that the amount of SiO2 on the surface of K-BC More than BC.

Table 1. *Influence of the relative intensity of the main absorption peaks of the infrared spectra of BC and K-BC (semi-quantitative)*

Treatment	Relative strength /%							
	3400 /cm^{-1}	2920 /cm^{-1}	2850 /cm^{-1}	1620 /cm^{-1}	1425 /cm^{-1}	1362 /cm^{-1}	1060 /cm^{-1}	793 /cm^{-1}
BC	0.2755 ± 0.0061 a	0.0555 ± 0.0057 a	0.0287 ± 0.0062 a	0.0528 ± 0.0054 a	0.1651 ± 0.0056 a	0.0534 ± 0.0066	0.2348 ± 0.0069 a	0.1029 ± 0.0052 a
K-BC	0.1372 ± 0.0077 b	0.0513 ± 0.0060 a	0.0192 ± 0.0063 a	0.1269 ± 0.0071 ab	0.2343 ± 0.0068 ab	—	0.2538 ± 0.0053 a	0.1192 ± 0.0065 a

Treatment	Ratio	
	(2920 + 2850)/1620	(2920 + 2850)/(1620 + 1425)
BC	1.5946	0.3864
K-BC	0.5556	0.1952

"—" means not detected. The data in the table are mean plus or minus standard deviation. Different letters after data in the same column indicate significant difference between different soil samples (P < 0.05)

Determination of specific surface area, pore volume and pore size

As can be seen from *Table 2,* the K-BC specific surface area of the modified biochar (28.8272 m2·g^{-1}) is 9.6 times that of the unmodified biochar BC (3.0065 m2·g^{-1}); the micropore volume (0.0116 mL·g^{-1}) is 11.6 times the pore volume of BC (0.0010 mL·g^{-1}); the average particle size of K-BC (0.6878) is much smaller than the average particle size of BC (1.2030). It is shown that during the process of corn stalks being alkalized and impregnated and then cracked and carbonized, the number of micropores is larger and the specific surface area is larger, which is consistent with the SEM analysis result of *Figure 2*. The specific surface area of biochar will affect its ability to adsorb heavy metals (Wang et al., 2017a; Peng et al., 2017) Studied that the specific surface area of

http://www.aloki.hu ● ISSN 1589 1623 (Print) ● ISSN 1785 0037 (Online)
DOI: http://dx.doi.org/10.15666/aeer/2001_511525

biochar is a key factor affecting its adsorption to heavy metals. The larger the specific surface area of biochar, the number of micropores. The more adsorption points that can be provided, the stronger the electrostatic adsorption capacity for heavy metals. Therefore, the reason why K-BC adsorbs Pb better than BC is because K-BC has a larger specific surface area and more microporous structure, which provides more adsorption sites for Pb.

Table 2. *Specific surface area and pore structure parameters of BC and K-BC*

Treatment	Pore structure parameter			
	BET specific surface area /($m^2 \cdot g^{-1}$)	**Total pore volume /($mL \cdot g^{-1}$)**	**Micropore volume /($mL \cdot g^{-1}$)**	**The average particle size /(nm)**
BC	3.0065 a	0.0015 a	0.0010 a	1.2030 a
K-BC	28.8272 b	0.0136 b	0.0116 b	0.6878 b

Different letters after data in the same column indicate significant difference between different soil samples ($P < 0.05$)

Electron microscopy and energy spectrum analysis

It can be seen from *Figure 2* that the pore structures on the BC and K-BC surfaces have obvious differences. BC has a small number of pores and a relatively disordered distribution, and there are a small number of debris particles fused on the surface of the pores. The surface shape of K-BC is relatively smooth, and there are more pore structures with honeycomb shape and relatively orderly arrangement.

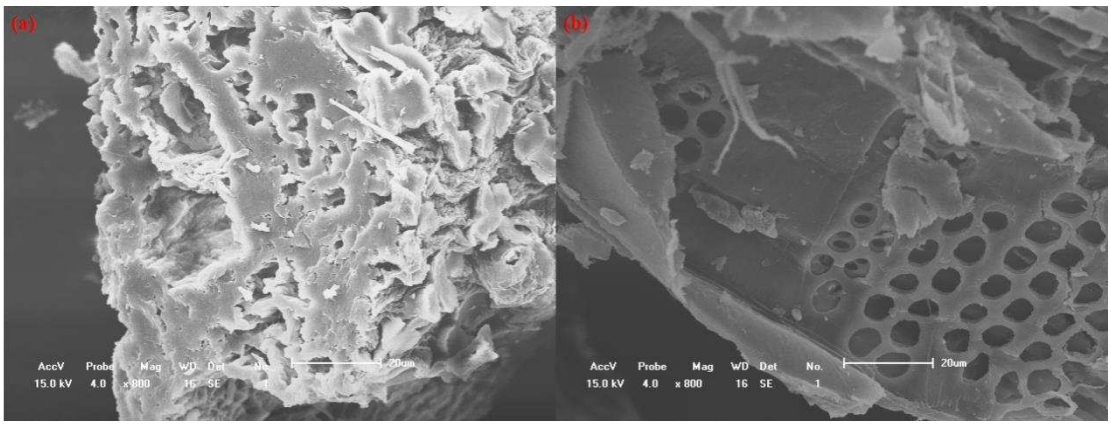

Figure 2. *SEM images of initial biochar BC and alkalized biochar K-BC. (A) BC; (b) K-BC*

As can be seen from *Figure 3,* the mass ratios of Mg, K, C, and O in BC are 4.44%, 2.08%, 33.69%, and 45.93%, and the mass ratios of Mg, K, C, and O in K-BC are 3.23%, 2.99%, 46.37%, 35.56%. It can be seen from *Figure 4* that when K-BC adsorbs Pb, the peaks of Mg, O, K, and C are significantly reduced, indicating that the process of adsorbing Pb is related to the loss of substances such as Mg, O, K, and C; the decrease in O peak may be due to In the biochar, carbonates reacted with Pb, resulting in a decrease in the O content; due to the lower adsorption rate of K-BC to Pb, the peak of Pb appeared smaller; the mass fractions of elements such as Na, Mg, and K There are

http://www.aloki.hu ● ISSN 1589 1623 (Print) ● ISSN 1785 0037 (Online)
DOI: http://dx.doi.org/10.15666/aeer/2001_511525

obvious changes, indicating that ion exchange has an important effect on the adsorption process (Zhang et al., 2019b).

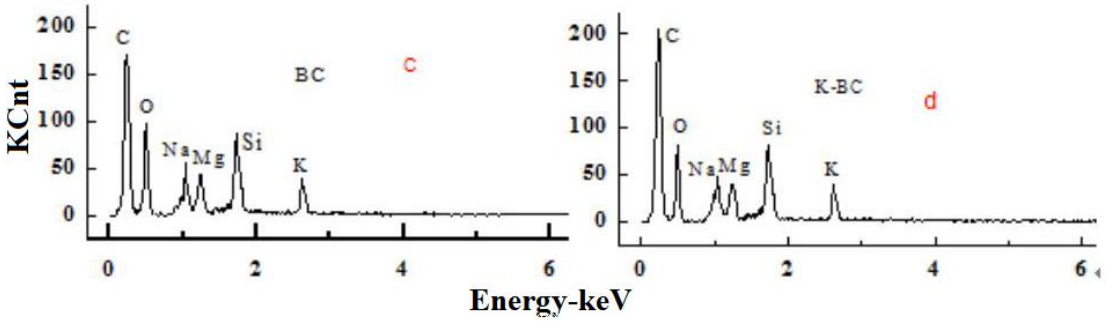

Figure 3. *EDS diagram of BC and K-BC. EDS diagrams for BC and K-BC. (c) BC; (d) K-BC. As shown in the figure, both modified and unmodified biochar contain high content of C and O and trace mineral composition (Na, Mg, Si, K) on the surface*

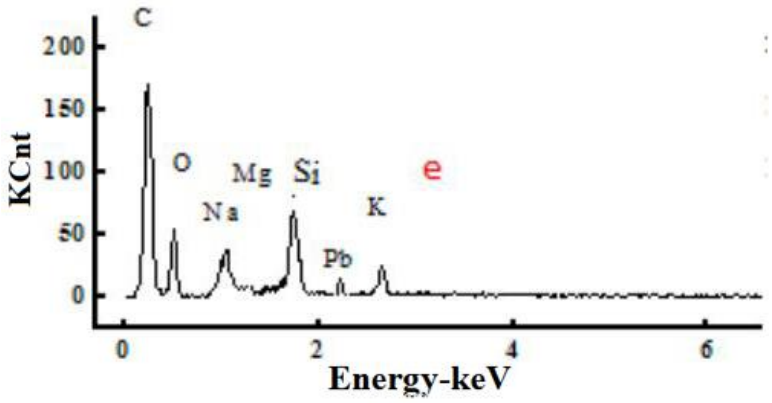

Figure 4. *EDS diagram of Pb adsorption by K-BC. As shown in the figure, the content of C and O in the adsorbed K-BC decreased significantly, and the trace element K also decreased*

Study on the adsorption characteristics of BC and K-BC to Pb

Study on the adsorption kinetics of Pb

The time-varying curve of BC and K-BC's adsorption of Pb is shown in *Figure 5*. It can be seen from *Figure 5* that the adsorption process of Pb by BC and K-BC is similar, 0-30 min is the rapid adsorption stage, BC and K-BC provide a large number of adsorption sites for Pb at the initial adsorption stage, and BC and K-BC are adsorbed at 30 min. adsorption of Pb was 111.72 $mg \cdot g^{-1}$ and 120.99 $mg \cdot g^{-1}$, accounting for 93.18% and 92.45% of the total adsorption; with the increase of the adsorption time, the adsorption sites on the surface of biochar tend to be saturated, Pb diffuses into the interior of the biochar, the diffusion resistance increases, and the adsorption amount stabilizes. It is a slow adsorption process within 30~360 min; the adsorption equilibrium at 360 min, the maximum adsorption amounts of BC and K-BC to Pb are 119.89 $mg \cdot g^{-1}$ and 130.87 mg $\cdot g^{-1}$. After the biochar was modified with alkali, the basic groups increased, which promoted the chemisorption of Pb (Kalderis et al., 2017), and the adsorption amount of K-BC increased by 9.16% compared with that of BC.

http://www.aloki.hu ● ISSN 1589 1623 (Print) ● ISSN 1785 0037 (Online)
DOI: http://dx.doi.org/10.15666/aeer/2001_511525

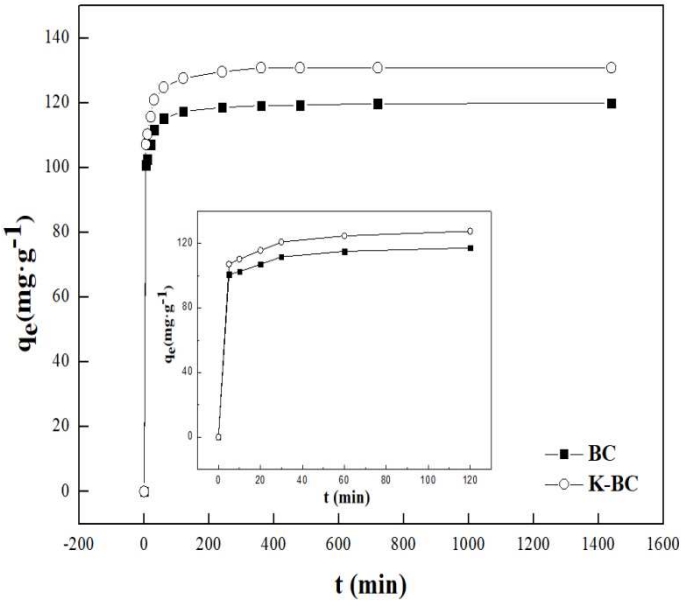

Figure 5. *The adsorption kinetic curve qe of BC and K-BC is the amount of lead adsorbed at time t, mg ·g^{-1}. Take t as 0, 5, 15, 30, 60, 100, 200, 600, 800, 1000, 1200, 1400 and 1600 min to draw the adsorption curve*

The BC and K-BC adsorption kinetics of Pb were fitted with quasi-first-order kinetic equations and quasi-second-order kinetic equations. The fitting parameters are shown in *Table 3*. In general, the better the model is, the greater the R value is. As can be seen from *Table 3,* the adsorption correlation coefficients of Pb in BC and K-BC by the quasi-second-order kinetic equation are 0.9969 and 0.9964, respectively, which are larger than those of the quasi-first-order kinetic equation (r is 0.9878 and 0.9854, respectively). The fitted equilibrium adsorption capacities of 118.2 mg·kg^{-1} and 129.2 mg·kg^{-1} were close to the experimental values.

Therefore, it can be inferred that the adsorption of BC and K-BC on Pb pair is a multiple adsorption process of external liquid film diffusion, surface adsorption and internal particle diffusion, rather than a single adsorption process. and the fitted equilibrium adsorption amounts of 118.2 mg·g^{-1} and 129.2 mg·g^{-1} were close to the experimental values.

It is inferred that the adsorption of Pb pairs by BC and K-BC is a multiple adsorption process of external liquid film diffusion, surface adsorption, and particle internal diffusion (Wang et al., 2017b), and is not a single adsorption process.

Table 3. *Adsorption kinetic parameters of BC and K-BC for Pb*

Treatment	Quasi-first order kinetic equation			Quasi-second order kinetic equation		
	$Q_{e,1}$/ mg·g^{-1}	K_1/ g·mg^{-1}·h^{-1}	R	$Q_{e,2}$/ mg·g^{-1}	K_2/ g·mg^{-1}·h^{-1}	r
BC	115.7	0.369	0.988**	118.2	0.007	0.997**
K-BC	126.0	0.337	0.985**	129.2	0.006	0.996**

$Q_{e,1}$ and $Q_{e,2}$ are the theoretical equilibrium adsorption capacity (mg·g^{-1}), K_1, K_2 and the primary and secondary adsorption rate constant (g·mg^{-1}·h^{-1}). ** indicates a very significant correlation ($p \leq 0.001$). r means the correlation coefficient between Quasi-first order kinetic equation and Quasi-second order kinetic equation

http://www.aloki.hu ● ISSN 1589 1623 (Print) ● ISSN 1785 0037 (Online)
DOI: http://dx.doi.org/10.15666/aeer/2001_511525

Study on the thermodynamics of Pb adsorption by BC and K-BC

In the test temperature range (15 °C, 30 °C, 45 °C), the adsorption isotherms of BC and K-BC on Pb are shown in *Figure 6*. It can be seen from *Figure 6* that when the initial concentration of Pb is less than 400 $mg \cdot L^{-1}$, the equilibrium adsorption of Pb by BC and K-BC increases with the increase of the initial concentration of the solution, and when the concentration of Pb is greater than 400 $mg \cdot L^{-1}$, the equilibrium. The adsorption amount remained basically unchanged, indicating that the adsorption equilibrium was reached when the Pb concentration was 400 $mg \cdot L^{-1}$. Giles et al. (Sing et al., 1985) divided the adsorption isotherm into four types of curves: "S, L, H, C" according to the initial slope of the adsorption isotherm. The adsorption isotherms of Pb by BC and K-BC were "L" Type, which belongs to the case of monolayer adsorption. With the increase of the reaction temperature, the adsorption amount of Pb by BC and K-BC also increased, indicating that the adsorption process is an endothermic process, and the increase in temperature is favorable for the adsorption of Pb.

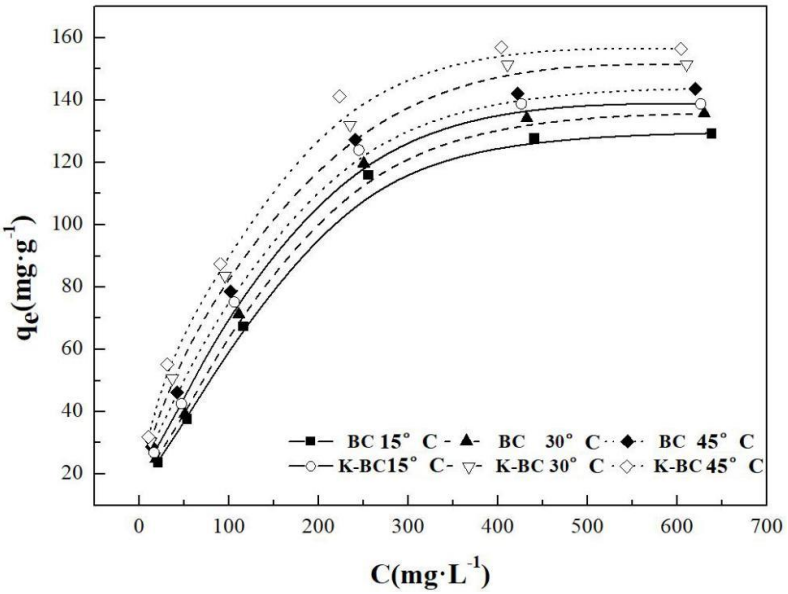

Figure 6. *Adsorption isotherms of Pb by BC and K-BC. Adsorption isotherm curves of lead in BC and K-BC. qe is the lead adsorption capacity mg $\cdot g^{-1}$; C is the mass concentration of lead in the equilibrium solution system, mg $\cdot L^{-1}$. The initial concentrations of Pb were 20, 50, 100, 150, 200, 250, 300, 350, 400, 450, 500, 550, 600 and 650 mg $\cdot L^{-1}$, and the test temperatures were 15 °C, 30 °C and 45 °C*

The Langmuir model and Freundlich model can describe the distribution behavior between adsorbent and adsorbent at a certain temperature (Zhu et al., 2015). The fitting parameters of the adsorption isotherms of BC and K-BC adsorbing Pb are shown in *Table 4*. It can be seen from *Table 4* that the Langmuir model ($0.986 < r < 0.991$) is more suitable for fitting BC and K-BC to Pb adsorption process than the Freundlich model ($0.953 < r < 0.970$). From the Langmuir model, we can know that K-BC to Pb The adsorption capacity of Pb is higher than that of Pb by BC, which indicates that the adsorption of Pb by biochar is more similar to that of single molecular layer. The dimensionless parameter separation factor KL ($0 < K_L < 1$) indicates that the adsorption of Pb by BC and K-BC is spontaneous.

http://www.aloki.hu ● ISSN 1589 1623 (Print) ● ISSN 1785 0037 (Online)
DOI: http://dx.doi.org/10.15666/aeer/2001_511525

Table 4. *BC and K-BC adsorption isotherm parameters*

Treatment	Temperature (°C)	Langmuir parameters			Freundlich parameters		
		q_m/ mg·g^{-1}	K_L/ L·mg^{-1}	r	n	K_f	r
BC	15	168.3	0.007	0.986**	2.282	8.448	0.953**
	30	175.1	0.007	0.989**	2.299	9.067	0.958**
	45	174.2	0.009	0.990**	2.564	12.831	0.954**
K-BC	15	174.1	0.008	0.989**	2.442	10.988	0.957**
	30	179.2	0.011	0.991**	2.675	15.072	0.970**
	45	180.9	0.013	0.987**	2.862	18.351	0.965**

Kf is the Freundlich equilibrium constant; n is the constant characterizing the adsorption strength, ** indicates extremely significant correlation ($p \leq 0.001$); r means correlation coefficient for the Freundlich and Langmuir equation; qm is the theoretical maximum adsorption amount, (mg·g^{-1}); KL is the adsorption affinity coefficient, (L·mg^{-1})

Table 5 shows the thermodynamic parameters of BC and K-BC adsorption of Pb. It can be seen from *Table 5* that at the test concentration (50~800 mg·L^{-1}) and test temperature (15 °C, 30 °C, 45 °C), $\Delta H^\circ > 0$ indicates that BC and K-BC adsorb Pb as an endothermic process, and increasing the temperature is beneficial The progress of the adsorption process indicates that the adsorption is a process of chemical bonding; $\Delta S^\circ > 0$ indicates that the adsorption is an irreversible process; ΔG° can reflect the driving force of the adsorption process (Liu et al., 2019), $\Delta G^\circ < 0$ indicates that BC and K-BC adsorb Pb The process is spontaneous, and the absolute value of ΔG° gradually increases, indicating that the temperature increase promotes the reaction.

Table 5. *Thermodynamic parameters of BC and K-BC adsorption of Pb*

Treatment	C (mL·g^{-1})	ΔH (kJ·mol^{-1})	ΔS (J·mol^{-1}·K^{-1})	ΔG (kJ·mol^{-1})		
				15 °C	30 °C	45 °C
BC	50	13.38	103.56	-16.44	-18.00	-19.55
	100	10.41	89.25	-15.29	-16.63	-17.97
	200	6.85	75.48	-14.89	-16.02	-17.15
	400	3.63	62.33	-14.32	-15.25	-16.19
	600	3.64	58.73	-13.28	-14.16	-15.04
	800	3.30	54.63	-12.44	-13.26	-14.07
K-BC	50	20.86	131.63	-17.05	-19.02	-20.00
	100	16.59	113.19	-16.01	-17.71	-19.41
	200	7.64	80.04	-15.42	-16.62	-17.82
	400	5.52	69.79	-14.58	-15.62	-16.67
	600	4.43	62.51	-13.58	-14.51	-15.45
	800	3.89	57.52	-12.67	-13.54	-14.40

C is the concentration; ΔG is the Gibbs free energy, (kJ·mol^{-1}); ΔH is the standard enthalpy change, (kJ·mol^{-1}); ΔS is the standard entropy change, (kJ·mol^{-1}·K^{-1})

Effect of different pH of background solution on Pb adsorption

pH can affect the adsorption of heavy metals by biochar by affecting the surface charge of biochar, the dissolution of mineral components, and the presence of heavy

http://www.aloki.hu ● ISSN 1589 1623 (Print) ● ISSN 1785 0037 (Online)
DOI: http://dx.doi.org/10.15666/aeer/2001_511525

metal ions (Yang et al., 2019) (*Fig. 7*). Changes in the amount of Pb adsorbed by BC and K-BC under different pH conditions in the background. It can be seen from *Figure 7* that in the test pH range (2.0~6.0), the adsorption amount of Pb by BC and K-BC increased first and then decreased. When the pH was 5, the adsorption amount of Pb by BC and K-BC reached the maximum. For 120.01 $mg \cdot g^{-1}$ and 131.53 $mg \cdot g^{-1}$. Different initial pH of the background solution have a greater effect on the adsorption of Pb by biochar. This is because when the pH value is low, a large amount of H^+ in solution will compete with Pb for adsorption (Liang et al., 2015). The negative charge relies on electrostatic adsorption of H^+, which reduces the adsorption efficiency of Pb on biochar. With the increase of pH, the concentration of H^+ in the solution gradually decreases, and the adsorption points on the surface and pore structure of biochar are fully exposed. Increasing the surface negative charge density provides more binding space for Pb, thereby increasing the amount of adsorption.

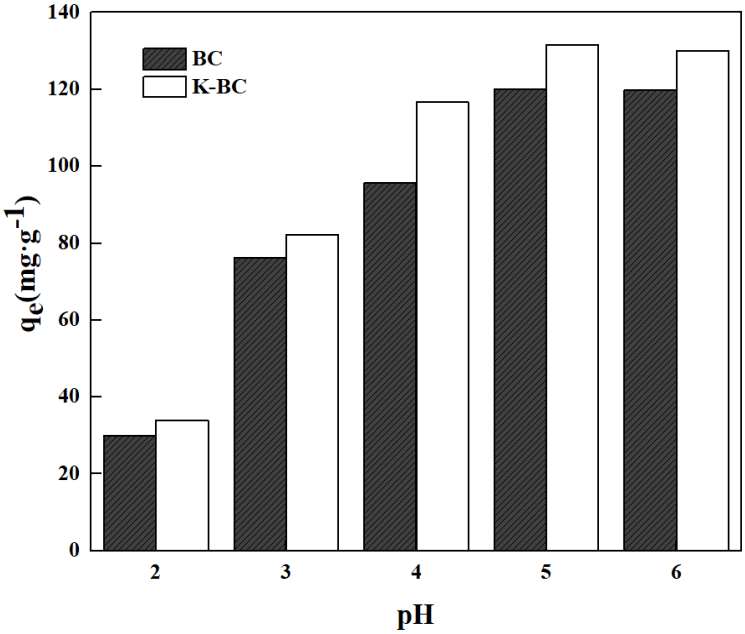

Figure 7. *Adsorption of Pb by BC and K-BC under different pH conditions. BC and K-BC adsorb Pb in equilibrium at different initial pH values. qe is the adsorption capacity $mg \cdot g^{-1}$ at equilibrium. The initial concentration of Pb was 400 $mg \cdot L^{-1}$, and the initial pH value was 2.0, 3.0, 4.0, 5.0 and 6.0. The test temperature was 15 °C and the reaction time was 360 min*

Conclusion

In this study, corn stalks and KOH were used to impregnate corn stalks to prepare biochar. The adsorption characteristics of biochar on Pb were studied.

The research shows that:

(1) The adsorption process of Pb by BC and K-BC is divided into two stages: fast and slow reaction. The adsorption equilibrium is reached in 360 min. The quasi-second-order kinetics can better evaluate the adsorption process.

The actual value is close.

With the increase of temperature, the adsorption of Pb by BC and K-BC also increases. The Langmuir equation fits the adsorption effect optimally. The adsorption is spontaneous, endothermic and irreversible.

http://www.aloki.hu ● ISSN 1589 1623 (Print) ● ISSN 1785 0037 (Online)
DOI: http://dx.doi.org/10.15666/aeer/2001_511525

When pH was 5, the adsorption of Pb by BC and K-BC reached the maximum.

(2) According to the structural characterization and physicochemical properties of BC and K-BC, the specific surface area of corn stalk charcoal was increased to 28.8272 $m^2 \cdot g^{-1}$ by KOH modification. The total pore volume increased to 0.0136 mL g^{-1}. The average particle size increased to 0.6878 nm. It can be seen that the larger the specific surface area, the richer the pore structure, the more adsorption sites provided, the stronger the electrostatic adsorption capacity for Pb; the higher the degree of aromatization, π The more conjugated aromatic structures, the stronger the cation-π interaction, and the greater the contribution rate to adsorption.

(3) Corn stalk biochar has a good adsorption effect on Pb. Within the temperature and pH range designed in the experiment, the adsorption capacity of the two biochar for Pb is K-BC > BC and KOH modification can increase the adsorption amount of Pb on corn straw charcoal. This experiment lays the foundation theory and provides technical reference for the resource utilization of waste corn straw and the solution of heavy metal lead pollution in wastewater.

Acknowledgements. The Technological Development Project of Jilin Province (20200402013NC).

Conflict of interests. The authors declare no conflict of interests.

Data availability declarations. The authors state that [all other] data supporting the findings of this study can be found in the article [and its supplementary information files].

REFERENCES

[1] Abdallah, M. M., Ahmad, M. N., Walker, G. (2019): Batch and continuous systems for Zn, Cu, and Pb metal ions adsorption on spent mushroom compost biochar. – Industrial & Engineering Chemistry Research. https://doi.org/10.1021/acs.iecr.9b00749.

[2] Abdelhafez, A. A., Li, J. H. (2016): Removal of Pb（Ⅱ） from aqueous solution by using biochars derived from sugar cane bagasse and orange peel. – Journal of the Taiwan Institute of Chemical Engineers 61: 367-375.

[3] Cao, Y., Xiao, W., Shen, G. (2018): Carbonization and ball milling on the enhancement of Pb(II) adsorption by wheat straw: competitive effects of ion exchange and precipitation. – Bioresource Technology. DOI: 10.1016/j.biortech.2018.10.065.

[4] Chen, J., Zhang, D., Wu, M. (2014): Elemental composition and thermal stability of two different biochar. – Environmental Chemistry 33(3): 417-422.

[5] Chi, T., Zuo, J., Liu, F. (2017): Performance and mechanism for cadmium and lead adsorption from water and soil by corn straw biochar. – Frontiers of Environmental Science & Engineering. https://doi.org/10.1007/s11783-017-0921-y.

[6] Dai, C., Jia, P. (2019): Chlorogenic acid relieves lead-induced cognitive impairments and hepato-renal damage via regulating the dysbiosis of the gut microbiota in mice. – Food & Function. https://doi.org/10.1039/C8FO01755G.

[7] Deng, J., Liu, Y., Liu, S. (2017): Competitive adsorption of Pb(II), Cd(II) and Cu(II) onto chitosan-pyromellitic dianhydride modified biochar. – Journal of Colloid and Interface Science 506: 355-364.

[8] Fahmi, A. H., Samsuri, A. W., Jol, H. (2018): Physical modification of biochar to expose the inner pores and their functional groups to enhance lead adsorption. – RSC Adv 8(67): 38270-38280.

[9] Gao, K., Jian, M., Yu, H. (2016): Effect of pyrolysis temperature on the biochars and its surface functional groups made from rice straw and rice busk. – Environmental Chemistry 35(8): 1663-1669.

http://www.aloki.hu ● ISSN 1589 1623 (Print) ● ISSN 1785 0037 (Online)
DOI: http://dx.doi.org/10.15666/aeer/2001_511525

[10] Jian, M., Gao, K., Yu, H. (2015): Comparison of surface characteristics and cadmium solution adsorption capacity of un-acidified or acidified bio-chars prepared from rice straw under different temperatures. – Ecology and Environmental Sciences 24(8): 1375-1380.
[11] Kalderis, D., Kayan, B., Akay, S., Kulaksız, E., Gözmen, B. (2017): Adsorption of 2,4-dichlorophenol on paper sludge/wheat husk biochar: process optimization and comparison with biochars prepared from wood chips, sewage sludge and hog fuel/demolition waste. – Journal of Environmental Chemical Engineering S2213343717301768.
[12] Komnitsas, K., Zaharaki, D., Bartzas, G. (2016): Efficiency of pecan shells and sawdust biochar on Pb and Cu adsorption. – Desalination & Water Treatment 57(7): 3237-3246.
[13] Li, M., Wei, D., Liu, T., Yan, L., Wei, Q., Du, B., Xu, W. (2019): EDTA functionalized magnetic biochar for Pb(II) removal: adsorption performance, mechanism and SVM model prediction. – Separation & Purification Technology 227. https://doi.org/10.1016/j.seppur.2019.115696.
[14] Liang, L., Wang, Y., Yan, Y. (2015): Adsorption property of Cr(VI) from aqueous solution by corncob and the SEM-EDS analysis on its characters. – Ecology and Environmental Sciences 24(2): 305-309.
[15] Liu, L., Huang, Y., Zhang, S. (2019): Adsorption characteristics and mechanism of Pb(II) by agricultural waste-derived biochars produced from a pilot-scale pyrolysis system. – Waste Management 287-295.
[16] Mahdi, Z., Hanandeh, A. E., Yu, Q. J. (2019): Preparation, characterization and application of surface modified biochar from date seed for improved lead, copper, and nickel removal from aqueous solutions. – Journal of Environmental Chemical Engineering 7(5).
[17] Paranavithana, G. N., Kawamoto, K., Inoue, Y. (2016): Adsorption of Cd^{2+} and Pb^{2+} onto coconut shell biochar and biochar-mixed soil. – Environmental Earth Sciences 75(6): 484.
[18] Park, J. H., Wang, J. J., Kim, S. H. (2018): Lead sorption characteristics of various chicken bone part-derived chars. – Environmental Geochemistry and Health. DOI: 10.1007/s10653-017-0067-7.
[19] Peng, C., Xiao, T., Li, Z. (2017): Effects of pyrolysis temperature on structural properties of sludge-based biochar and its adsorption for heavy metals. – Research of Environmental Sciences. DOI: 10.13198/j.issn.1001-6929.2017.02.95.
[20] She, S., Huang, H., Guan, C. (2016): Study on the carbon sink function of crop production in typical agricultural areas of China. – Engineering sciences 18(1): 106.
[21] Shen, Z., Zhang, J., Hou, D. (2018): Synthesis of MgO-coated corncob biochar and its application in lead stabilization in a soil washing residue. – Environment International 122: 357-362.
[22] Sing, K. S. W., Everett, D. H., Haul, R. A. W. (1985): Reporting physisorption data for gas/solid systems with special reference to the determination of surface area and porosity. – Pure & Appl. Chem. 57(4): 603-619.
[23] Wang, L., Zhao, B., Ma, F. (2016): Effects of biochar derived from potato straw on adsorption of Cd(Ⅱ) onto loess. – Environmental Chemistry 5(7): 1422-1430 (in Chinese).
[24] Wang, Z., Fei, S., Shen, D. (2017a): Immobilization of Cu^{2+} and Cd^{2+} by earthworm manure derived biochar in acidic circumstance. – Journal of Environmental Science 53(3): 293-300.
[25] Wang, T., Ma, J., Qu, D. (2017b): Characteristics and mechanism of copper adsorption from aqueous solutions on biochar produced from sawdust and apple branch. – Environmental Science 38(5): 2161-2171.

http://www.aloki.hu ● ISSN 1589 1623 (Print) ● ISSN 1785 0037 (Online)
DOI: http://dx.doi.org/10.15666/aeer/2001_511525

[26] Wang, W., Ma, X., Sun, J. (2019): Adsorption of enrofloxacin onacid/alkali-modified corn stalk biochar. – Spectroscopy Letters 52(7): 367-375.
[27] Xiao, X., Chen, B., Chen, Z. (2018): insight into multiple and multilevel structures of biochars and their potential environmental applications: a critical review. – Environmental Science & Technology 52(9): 5027-5047.
[28] Yang, W., Wang, Z., Song, S. (2019): Adsorption of copper (II) and lead(II) from seawater using hydrothermal biochar derived from Enteromorpha. – Marine Pollution Bulletin 149: 110586.
[29] Zhang, L., Liu, X., Huang, X. (2019b): Adsorption of Pb^{2+} from aqueous solutions using Fe-Mn binary oxides-loaded biochar: kinetics, isotherm and thermodynamic studies. – Environmental Technology 40(13-16): 1853-1861.
[30] Zhang, L., Tang, S., He, F. (2019a): Highly efficient and selective capture of heavy metals by poly(acrylic acid) grafted chitosan and biochar composite for wastewater treatment. – Chemical Engineering Journal. https://doi.org/10.1016/j.cej.2019.122215.
[31] Zhao, M., Dai, Y., Zhang, M. (2020): Mechanisms of Pb and/or Zn adsorption by different biochars: biochar characteristics, stability, and binding energies. – Science of the Total Environment 717: 136894.
[32] Zhu, J., Baig, S. A., Sheng, T. T. (2015): Fe_3O_4 and MnO_2 assembled on honeycomb briquette cinders (HBC) for arsenic removal from aqueous solutions. – Journal of Hazardous Materials 286: 220-228.

http://www.aloki.hu ● ISSN 1589 1623 (Print) ● ISSN 1785 0037 (Online)
DOI: http://dx.doi.org/10.15666/aeer/2001_511525

INTEGRATED MANAGEMENT OF *FUSARIUM* SPP. ASSOCIATED WITH CHICKPEA (*CICER ARIETINUM* L.) WILT DISEASE IN THE PUNJAB, PAKISTAN

FATIMA, K.[1] – HABIB, A.[1*] – SAHI, S. T.[1] – CHEEMA, H. M. N.[2]

[1]*Department of Plant Pathology, University of Agriculture, Faisalabad, Pakistan*

[2]*Department of Plant Breeding & Genetics, University of Agriculture, Faisalabad, Pakistan*

**Corresponding author*
e-mail: amer.habib@uaf.edu.pk; phone: +92-333-650-4965

(Received 1st Sep 2021; accepted 23rd Nov 2021)

Abstract. Chickpea (*Cicer arietinum* L.) is the third most significant crop grown in Pakistan. This crop is a rich source of protein and carbohydrates. In developing countries, civilians are facing dietary protein shortage problems due to limited resources. Animals' products, including beef, fish, meat and eggs are major sources of proteins which are too expensive to buy for the poor. In Pakistan, it is mostly cultivated in arid/semi-arid areas of the Thal region of Punjab province. These areas are totally dependent on rainfall for water requirements. Fortunately, chickpea is a drought tolerant crop but some biotic factors are also involved in low production of chickpea crop. Gram wilt disease is one of the major threats to this crop. Considering the current situation, it is necessary to develop sustainable management strategies. This study was planned with the aim of long-term management strategies against fungal pathogen associated with wilt disease including determination of resistant resources among the available genetic material, among three biocontrol agents *Trichoderma harzianum* showed maximum inhibition under in vitro and in vivo conditions and among ten chemicals, score showed maximum inhibition of *Fusarium* spp. which was followed by Topsin M and Baviston under in vitro and in vivo conditions.
Keywords: *resistant resources, biocontrol, chemical control, T. harzianum, score*

Introduction

Chickpea (*Cicer arietinum* L.) is a nutritive pulse crop that is grown under arid and semi-arid conditions worldwide (Millan et al., 2006). Legume crops enhance the fertility of soil by fixing the atmospheric nitrogen with the help of rhizobia which are present inside the nodules. Soybean, pea, bean, alfalfa, clover and chickpea are included concerning legumes. Legumes play important roles in several factors like salt tolerance, nitrogen fixation and soil fertility (Graham and Vance, 2003). Chickpea fulfills 80% of nitrogen requirement of crop and fixes 140 kg air nitrogen/hectare through symbiotic relationship with rhizobia, and is the major source of nitrogen for the consequent crops. Chickpea also increases organic matter in soil and results in the long-standing fertility of soil and plays a vital role in the sustainability of the ecosystem. Chickpea has now specialty in to the restaurants and health shops. It is now used in occasional stuffs in restaurants and has widened its range. Kabuli chickpea is an obligatory part of bean salad and salad bars in North America. Chickpea's huge amount is mainly used for several types of dishes in Mediterranean region, India and Burma. Mostly vegetarians use chickpea as food intake. Almost ninety percent losses in the yield are caused by root based diseases as well as by pathogens like fungi (Zamani et al., 2004: Haware, 1990; Sharma and Muehlbauer, 2007). Pathogenic fungi that affect roots include mainly *Fusarium oxysporum, Macrophomina phaseolina, Fusarium solani* and *Rhizoctonia solani*. The pathogens remain active even in the absence of its host for a period of more

http://www.aloki.hu ● ISSN 1589 1623 (Print) ● ISSN 1785 0037 (Online)
DOI: http://dx.doi.org/10.15666/aeer/2001_527541

than six years although they are seed borne (Haware et al., 1996; Ayyub et al., 2003). Fungal diseases are causing more disaster in chickpea crop due to the production of constant mycotoxins. Therefore, to reduce the chickpea disasters, it is necessary to control the fungal growth (Yan et al., 2015). Fusarium wilt is a serious disease of Pakistan, Nepal, Burma, Spain and Maxico. Chickpea wilt causes 61% damage at seedling stage and 43% at flowering stage (Nema et al., 1973). This disease causes 10-50% loss in chickpea production in Pakistan every year (Khan et al., 2002). Seeds of early wilted crop are lighter in weight and have dull appearance as compare to healthy crop (Haware and Nene, 1980). During reproductive and vegetative stage, chickpea wilt causes complete destruction of grain production (Navas et al., 2000). The pathogen of chickpea wilt disease mainly spread through soil in plant and can also be transmitted through seed. This pathogen survives in soil for six years without host (Haware et al., 1986). *Fusarium oxysporum* is difficult to control but resistant varieties are used for this purpose. Resistant varieties become susceptible to new races of pathogen after few years due to which this management strategy is difficult to use. Because the pathogen remains viable for long period of time and preparation of new resistant variety takes time to enter in market and losses becomes obvious. So, use of fungicides is most suitable for Fusarium wilt management (Gupta et al., 1988).

Materials and methods

Chickpea fields were visited in Thal region of Punjab, Pakistan for finding the diseased plants infected with *Fusarium spp.* associated with chickpea roots. *Fusarium* spp. were isolated from diseased sample and were stored in double ionized distilled water for further studies and most aggressive isolate after pathogenicity and molecular characterization was used for implementation of management strategies. For the completion of all experiments, field, greenhouse and laboratories of the department of plant pathology and CABB in the University of Agriculture, Faisalabad was used in 2017-2018.

Chickpea germplasm collection for resistance/susceptibility evaluation

Collection of chickpea varieties from seed agencies and from local markets was done to find out the most resistant cultivars (that can be used by farmers to get more production by growing these varieties in field). These varieties were under examination for two years. These plants were inoculated with *Fusarium* spp. and resistance of chickpea varieties was observed. 10 ml inoculum was added in soil near root zone of plants and these plants were stored in greenhouse at 25 °C for 3 weeks. Data was recorded after 1st, 2nd and 3rd week of inoculation in green house.

In vivo and in vitro management of Fusarium spp. by using fungal antagonists:

Three fungal antagonists *Trichoderma harzianum, Trichoderma viride* and *Trichoderma virens* were evaluated against *Fusarium* spp. associated with chickpea wilt by using dual culture technique (Atta et al., 2009). In petri dish containing PDA, 9 mm culture of both *Fusarium spp.* and antagonists were placed in petri dish at the distance of 5 mm from the edge of plate and control plate had only fungal pathogen. Three replications of each treatment were used with one control. Experiment was repeated three times. These plates were incubated at 25 ± 2 °C. Data was recorded after 24, 48 and 96 h of inoculation. Following formula was used for percent inhibition (Vincent, 1947):

http://www.aloki.hu ● ISSN 1589 1623 (Print) ● ISSN 1785 0037 (Online)
DOI: http://dx.doi.org/10.15666/aeer/2001_527541

$$\text{Percent Growth Inhibition (PI)} = \frac{C - T}{C} \times 100$$

where: C = Colony growth in control plate; T = Colony growth in treated plate.

In vivo evaluation of fungal antagonists (*Trichoderma harzianum, Trichoderma viride* and *Trichoderma virens*) was done under greenhouse conditions against most virulent *Fusarium spp.* soil was treated with these antagonists at the concentrations of 1×10^8 cfu/ml, 1×10^{16} cfu/ml and 1×10^{24} cfu/ml before one week of inoculation of *Fusarium* spp. Cultures were prepared on PDA. Four treatments were used with three replications. Culture suspension 1×10^7 cfu/ml of *Fusarium* spp. was prepared for inoculation of soil and was applied by using soil drenching technique in the greenhouse.

In vivo and in vitro management of Fusarium spp. by using fungicides

In this experiment 10 different systemic and contact fungicides were used with 3 replications and 1 control. Ten fungicides Score, Topsin M, Baviston, Chlorothalonil, Stump, Big Time, Champion, Velvet, Curzate M8 and Co-oxy were checked out against *Fusarium* spp. by using Poison Food Technique (Nene and Thapliyal, 1982). These ten fungicides were evaluated at three concentrations (100, 150 and 200 ppm):

Sr. No.	Chemical name	Trade name	Active ingredients	Mode of action	Formulation	Manufacturing company
1	Score	Score	Difenoconazole	Systemic	250 SC	Syngenta Pakistan
2	Topsin-M	Nativo	Trifloxystrobin + tebuconazole	Systemic	75%WG	Bayer Pakistan
3	Baviston	Baviston	Carbendazim	Systemic	50%DF	KANZO
4	Chlorothalonil	Chlorothalonil	Chlorothalonil	Contact	75%WP	Synenta Pakistan
5	Stump	Stump	Propineb	Contact	70% WP	FMC
6	Big Time	Big Time	Mancozeb, Dithane M-45	Systemic	80% WP	Arysta Life Science
7	Champion	Champion	Copper hydro oxide	Contact	77%WP	Jaffar Agros
8	Velvet	Velvet	Fosetyl-aluminium + mancozeb	Systemic	80% WP	Welcone
9	Curzate-M8	Curzate-M8	Mencozeb + cymoxanil	Protective	72.5%WDG	Arysta Life Science
10	Co-oxy	Co-oxy	Copper oxychloride	Contact	50% WP	Swat Agro Chemicals

Pure culture *Fusarium* spp. was used for evaluation. Stock solutions were prepared to get different concentrations (100, 200 and 300 ppm) according to active ingredient of fungicides followed by the method used by Rehman et al. (2018) and then were added in 200 ml of potato dextrose agar. All the procedure was completed in laminar flow cabinet (ESCO) to avoid contamination. 20 ml of prepared PDA containing fungicides at different concentrations was poured in 90 mm petri dishes. Control plates were also prepared by pouring 20 ml PDA without fungicides in petri plates. After solidification of PDA in petri plates, these petri dishes were inoculated by 4 mm block of PDA having pure culture of *Fusarium* spp. (7 days old culture). with the help of sterilized cork borer and these dishes were incubated at 25 ± 2 °C in an incubator. Radial culture growth (mm) of different *Fusarium spp.* was recorded after 7, 14 and 21 days of inoculation. Percent inhibition growth was calculated by above given formula. In vivo management was done by using most effective fungicides (Score, Topsin M and Baviston) at different concentration like 100, 200 and 300 ppm with three replications and one control in green house. Seeds were surface sterilized and soaked in distilled water for overnight to soften the seed coat for facilitation of pathogen penetration, Autoclaved pots were filled with disinfected soil, this soil was infested with most virulent *Fusarium* spp. by mixing soil with mass culture of

http://www.aloki.hu ● ISSN 1589 1623 (Print) ● ISSN 1785 0037 (Online)
DOI: http://dx.doi.org/10.15666/aeer/2001_527541

fungus. And 5 autoclaved seeds were sown 2 to 3 cm deep in each pot containing soil. All these experimental materials were laid down under CRD (Complete Randomized Design) in factorial arrangement with three replications. Aqueous suspension of most effective fungicides was added in pots by drenching the soil. Data was recorded after 40 days of application of fungicide and analyzed to find out the difference between treatments by using the statistic software version 8.1.

Results

Screening of chickpea germplasm against most aggressive Fusarium spp.

Twenty varieties were screen out against fusarium wilt of chickpea under greenhouse condition for two years. Data recorded during 2017 and 2018 showed that no variety was found immune against fusarium wilt. During 1st year two varieties incidence exhibited highly resistant response, while six varieties showed resistant response against fusarium wilt. Four varieties showed moderately resistant response whereas five varieties gave susceptible response against fusarium wilt. However, three varieties were highly susceptible (*Table 1*.). Study, during 2nd year, revealed that same three varieties were highly susceptible like first year. Five varieties exhibited susceptible response. Four varieties showed moderately resistant response. Six varieties showed resistant response against fusarium wilt. Two varieties gave highly resistant response (*Table 1*).

Table 1. *Two years response of chickpea germplasm against most aggressive isolate (NK32, Fusarium oxysporum (FOK1) from Layyah) (HR = highly resistant, R = resistant, MR = moderately resistant, S = susceptible and HS = highly susceptible)*

Variety	Year 1		Year 2	
	Disease incidence (%)	Response	Disease incidence (%)	Response
Dasht	54.667 B	HS	55.667 A	HS
Thal 2006	53.000 B	HS	52.000 B	HS
AUG-424	57.667 A	HS	56.667 A	HS
Balkasar	0.1667 M	HR	0.2333 J	HR
Bittle 98	5.6667 KL	R	6.6667 HI	R
CMC211S	14.667 HI	MR	15.667 F	MR
CM-98	13.667 I	MR	12.667 G	MR
CM-88	12.333 I	MR	12.667 G	MR
C-44	4.3333 L	R	5.0000 I	R
C-727	0.3000 M	HR	0.4333 J	HR
Punjab-91	4.6667 KL	R	5.3333 I	R
AUG-785	5.3333 KL	R	4.3333 I	R
Parbat	45.000 C	S	43.667 C	S
Noor-91	17.333 H	MR	17.667 F	MR
PB-1	40.667 D	S	42.333 C	S
C-235	7.3333 JK	R	6.3333 HI	R
PB200	36.000 E	S	35.333 D	S
DC1	30.000 F	S	28.667 E	S
CM72	8.6667 J	R	8.3333 H	R
ILC95	25.333 G	S	27.667 E	S
LSD ($p \leq 0.05$)	2.85**		2.70**	

http://www.aloki.hu ● ISSN 1589 1623 (Print) ● ISSN 1785 0037 (Online)
DOI: http://dx.doi.org/10.15666/aeer/2001_527541

In vivo and in vitro disease management by using fungal antagonists

In the greenhouse study, various antagonists viz. *Trichoderma harzianum, Trichoderma viride* and *Trichoderma virens* applied at various concentrations significantly ($p \leq 0.05$) reduced the disease incidence (%) with respect to different days. Disease incidence (%) was maximum (15.50%) in case of *Trichoderma virens* followed by *Trichoderma viride* (13.98%) and *Trichoderma harzianum* (12.48%) over control (35.06%). Regarding various concentrations, maximum disease incidence (20.98%) was observed where 1×10^{24} (cfu/ml) concentration was applied as compared to 1×10^{16} (cfu/ml) (19.71%) and 1×10^{8} (cfu/ml) (17.06%). Disease incidence was at its peak at day 3rd (20.41%), whereas, minimum disease incidence was at day 1 (18.51%) (*Table 2*). Regarding interaction between treatments and concentrations revealed that maximum reduction in disease incidence (%) was assessed in case of *Trichoderma harzianum* (10.77%, 12.83%, 13.83%), while, minimum reduction in disease incidence was exhibited in case of control (31.54%, 35.87%, 37.76%) at 1×10^{8} (cfu/ml), 1×10^{16} (cfu/ml) and 1×10^{24} (cfu/ml) concentrations respectively. Interaction between concentrations and days revealed that maximum reduction in disease incidence (%) was assessed in case of 1×10^{8} (cfu/ml) (15.2%, 16.85%, 19.14%), while, minimum reduction in disease incidence was exhibited in case of 1×10^{24} (cfu/ml) (20.51%, 21.11%, 21.31%) at 1st, 2nd and 3rd day respectively. Interaction between treatments, concentrations and days showed that disease incidence (%) (10.33%) was minimum where *Trichoderma harzianum* applied with 1×10^{8}(cfu/ml) concentrations at 1st, 2nd and 3rd day. Disease incidence (%) was maximum in control as compared to all other treatments at various days. Indication of variation within treatments to nullify the error chances within treatments presents as error bars (*Figs. 1-3*).

Table 2. *Impact of various concentrations of Trichoderma spp. against Fusarium spp. under greenhouse condition*

Treatments (T)	Disease incidence (%)	LSD ($p \leq 0.05$)
Trichoderma harzianum	12.48 D	0.85
Trichoderma viride	13.98 C	
Trichoderma virens	15.50 B	
Control	35.06 A	
Concentration (C)		
1×10^{8}(cfu/ml)	17.06 C	0.74
1×10^{16}(cfu/ml)	19.71 B	
1×10^{24}(cfu/ml)	20.98 A	
Days (D)		
1	18.51 B	0.74
2	18.83 B	
3	20.41 A	
LSD ($p \leq 0.05$)		
T×C	**	
T×D	NS	
C×D	**	
T×C×D	**	

Any two means within a column followed by same letters are not significant at $p \leq 0.05$. * = Significant at $p \leq 0.05$; ** = Significant at $p \leq 0.01$; NS = Non-significant

http://www.aloki.hu ● ISSN 1589 1623 (Print) ● ISSN 1785 0037 (Online)
DOI: http://dx.doi.org/10.15666/aeer/2001_527541

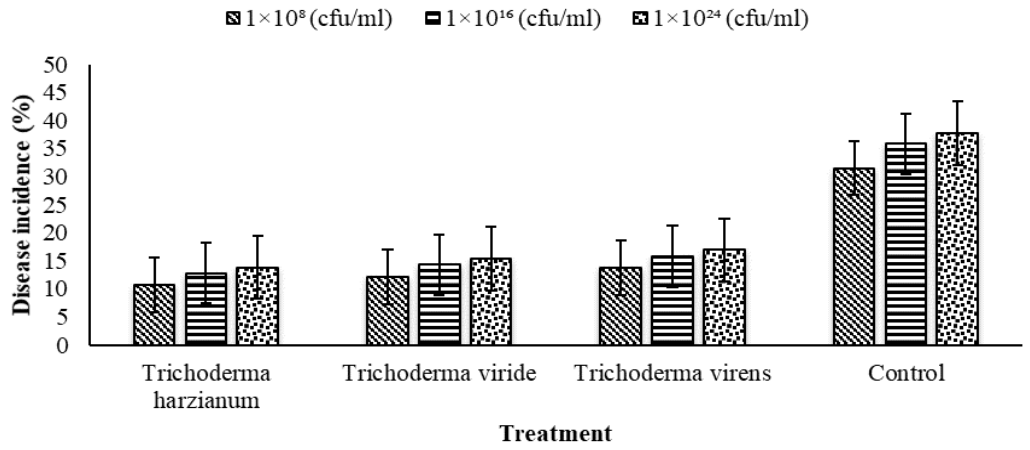

Figure 1. *Variation in disease incidence (%) with application of different concentrations of Trichoderma spp. against Fusarium spp. under greenhouse conditions*

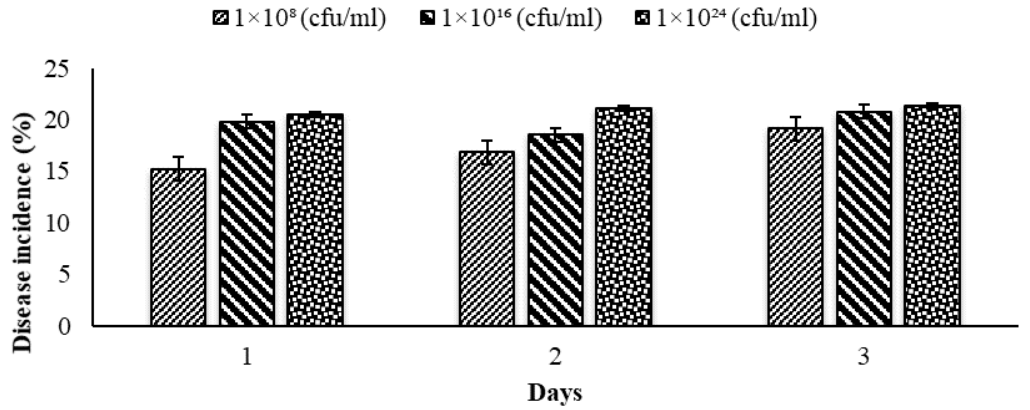

Figure 2. *Variation in disease incidence after the application of Trichoderma spp. against Fusarium spp. under greenhouse conditions at various days*

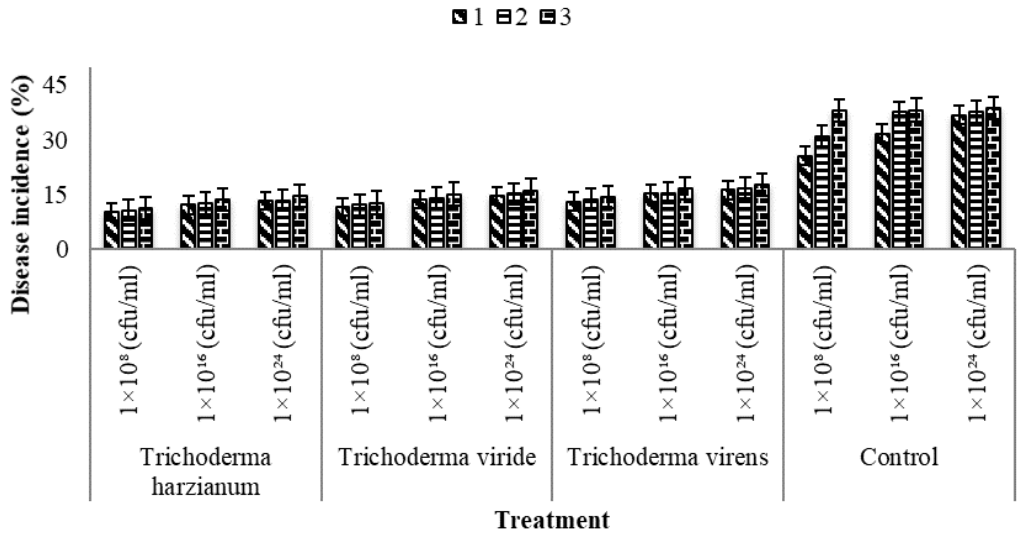

Figure 3. *Variation in disease incidence (%) with different treatments of Trichoderma spp. against Fusarium spp. under greenhouse conditions*

http://www.aloki.hu ● ISSN 1589 1623 (Print) ● ISSN 1785 0037 (Online)
DOI: http://dx.doi.org/10.15666/aeer/2001_527541

Impact of various antagonists on gram wilt under in vitro conditions

In lab study, various antagonists viz. *Trichoderma harzianum, Trichoderma viride* and *Trichoderma virens* significantly ($p \leq 0.05$) inhibit (%) the fungal growth with respect to different time intervals. Inhibition (%) was minimum (11.96%) in case of *Trichoderma virens* followed by *Trichoderma viride* (10.50%) and *Trichoderma harzianum* (8.96%) as compared to control. Regarding various time intervals, maximum disease inhibition (8.41%) was observed. Disease inhibition (%) was at its peak at day 96 h (8.41%), whereas, minimum disease inhibition (%) was at 24 h (7.41%) (*Table 3*). Non-significant ($p \leq 0.05$) interaction was observed between treatments and time interval over inhibition of fungal growth.

Table 3. *Impact of Trichoderma spp. against Fusarium spp. under lab condition*

Treatments (T)	**% Inhibition**	**LSD ($p \leq 0.05$)**
Trichoderma harzianum	8.96 C	0.66
Trichoderma viride	10.50 B	
Trichoderma virens	11.96 A	
Control	0.00 D	
Hours (h)		
24	7.41 B	0.57
48	7.73 B	
96	8.41 A	
LSD ($p \leq 0.05$)		
T×H	NS	

Any two means within a column followed by same letters are not significant at $p \leq 0.05$. * = Significant at $p \leq 0.05$; ** = Significant at $p \leq 0.01$; NS = Non-significant

In vivo and in vitro disease management by using fungicides

Impact of various fungicides on gram wilt under in vitro conditions

In in vitro study, ten fungicide chemicals from different chemical groups viz. Score, Topsin-M and Bavistan, Chlorothalonil, Stump, Big time, Champion, Valvet, Curzate-MS and Co-Oxy applied at various concentrations significantly ($p \leq 0.05$) reduced the fungal growth (mm) with respect to different days. Fungal growth (mm) was minimum (6.46) in case of Score followed by Topsin-M (8.00), Bavistan (9.46), Chlorothalonil (11.00), Stump (12.50), Big time (14.00), Champion (15.46), Valvet (16.96), Curzate-MS (18.46) and Co-Oxy (19.96) over control (42.37). Regarding various concentrations, maximum reduction in fungal growth (14.24) was observed where 100 ppm concentration was applied as compared to 200 ppm (16.07) and 300 ppm (17.30). Reduction in fungal growth was at its peak at day 1st (15.30), whereas, minimum reduction in fungal growth was at day 3 (16.59) (*Table 4*). Regarding interaction between treatments and concentrations revealed that maximum reduction in fungal growth (mm) was assessed in case of score (4.72, 6.83, 7.83), while, minimum reduction in fungal growth (mm) was exhibited in case of control (41.55, 42, 43.55) at 100 ppm, 200 ppm and 300 ppm concentrations respectively. Interactive effect of treatments and days revealed that maximum reduction in fungal growth (mm) was assessed in case of score (5.88, 6.27, 7.22), while, minimum reduction in fungal growth

http://www.aloki.hu ● ISSN 1589 1623 (Print) ● ISSN 1785 0037 (Online)
DOI: http://dx.doi.org/10.15666/aeer/2001_527541

(mm) was exhibited in case of control (41.22, 42.61, 43.27) at 1st, 2nd and 3rd day respectively. Interaction between concentrations and days revealed that maximum reduction in fungal growth (mm) was assessed in case of 100 ppm (13.57, 14.24, 14.92), while, minimum reduction in fungal growth (mm) was exhibited in case of 300 ppm (16.69, 17.19, 18.03) at 1st, 2nd and 3rd day respectively (*Figs. 4-6*).

Table 4. *Impact of different fungicides against wilt fungal pathogen under lab condition*

Treatments (T)	**Fungal growth (mm)**	**LSD ($p \leq 0.05$)**
Score	6.46 K	
Topsin-M	8.00 J	
Bavistan	9.46 I	
Chlorothalonil	11.00 H	
Stump	12.50 G	
Big time	14.00 F	0.16
Champion	15.46 E	
Valvet	16.96 D	
Curzate-M8	18.46 C	
Co-Oxy	19.96 B	
Control	42.37 A	
Concentration (C)		
100 ppm	14.24 C	
200 ppm	16.07 B	0.08
300 ppm	17.30 A	
Days (D)		
1	15.30 C	
2	15.72 B	0.08
3	16.59 A	
LSD ($p \leq 0.05$)		
T×C	**	
T×D	**	
C×D	**	
T×C×D	NS	

Any two means within a column followed by same letters are not significant at $p \leq 0.05$. * = Significant at $p \leq 0.05$; ** = Significant at $p \leq 0.01$; NS = Non-significant

Ten fungicides Score, Topsin M, Baviston, Chlorothalonil, Stump, Big Time, Champion, Velvet, Curzate M8 and Co-oxy were checked out against *Fusarium spp.* by using Poison Food Technique (Nene and Thapliyal, 1982). These ten fungicides were evaluated at three concentrations (100, 200 and 300 ppm). Effectiveness of fungicides was tested in inhibiting fungus growth. There was a significant decrease in mycelial growth with an increase in concentration of fungicide. Score followed by Topsin-M, and Bavistan was observed most effective fungicide and Curzate M8 and Co-oxy were found least effective fungicides against all the isolates in decreasing the fungus radial growth. Intermediate response in suppressing *F. oxysporum* growth was observed by the use of Chlorothalonil, Stump, Big Time, Champion and Velvet. In field study, various

http://www.aloki.hu ● ISSN 1589 1623 (Print) ● ISSN 1785 0037 (Online)
DOI: http://dx.doi.org/10.15666/aeer/2001_527541

antagonists viz. Score, Topsin-M and Bavistan applied at various concentrations significantly ($p \leq 0.05$) reduced the disease incidence (%) with respect to different days. Disease incidence (%) was minimum (8.46%) in case of Score followed by Topsin-M (10.00%) and Bavistan (11.46%) over control (44.37%). Regarding various concentrations, maximum reduction in disease incidence (17.16%) was observed where 100 ppm concentration was applied as compared to 200 ppm (18.61%) and 300 ppm (19.94%). Reduction in disease incidence was at its peak at day 1st (17.84%), whereas, minimum reduction in disease incidence was at day 3 (19.36%) (*Table 5*). Regarding interaction between treatments and concentrations revealed that maximum reduction in disease incidence (%) was assessed in case of score (6.72%, 8.83%, 9.83%), while, minimum reduction in disease incidence was exhibited in case of control (43.55%, 44%, 45.55%) at 100 ppm, 200 ppm and 300 ppm concentrations. Interactive effect of treatments and days revealed that maximum reduction in disease incidence (%) was assessed in case of score (7.88%, 8.27%, 9.22%), while, minimum reduction in disease incidence was exhibited in case of control (43.22%, 44.61%, 45.27%) at 1st, 2nd and 3rd day. Interaction between concentrations and days revealed that maximum reduction in disease incidence (%) was assessed in case of 100 ppm (16.29%, 17.25%, 17.95%), while, minimum reduction in disease incidence was exhibited in case of 300 ppm (19.33%, 19.83%, 20.66%) at 1st, 2nd and 3rd day. Interaction between treatments, concentrations and days showed that disease incidence (%) (6.16%) was minimum where score applied with 100 ppm concentration at 1st, 2nd and 3rd day. Disease incidence (%) was maximum in control as compared to all other treatments at various days (*Figs. 7-10*).

Table 5. *Impact of various fungicides against fungal pathogen under field condition*

Treatments (T)	**Disease incidence (%)**	**LSD ($p \leq 0.05$)**
Score	8.46 D	0.15
Topsin-M	10.00 C	
Bavistan	11.46 B	
Control	44.37 A	
Concentration (C)		
100 ppm	17.16 C	0.13
200 ppm	18.61 B	
300 ppm	19.94 A	
Days (D)		
1	17.84 C	0.13
2	18.51 B	
3	19.36 A	
LSD ($p \leq 0.05$)		
T×C	**	
T×D	**	
C×D	*	
T×C×D	**	

Any two means within a column followed by same letters are not significant at $p \leq 0.05$. * = Significant at $p \leq 0.05$; ** = Significant at $p \leq 0.01$; NS = Non-significant

http://www.aloki.hu ● ISSN 1589 1623 (Print) ● ISSN 1785 0037 (Online)
DOI: http://dx.doi.org/10.15666/aeer/2001_527541

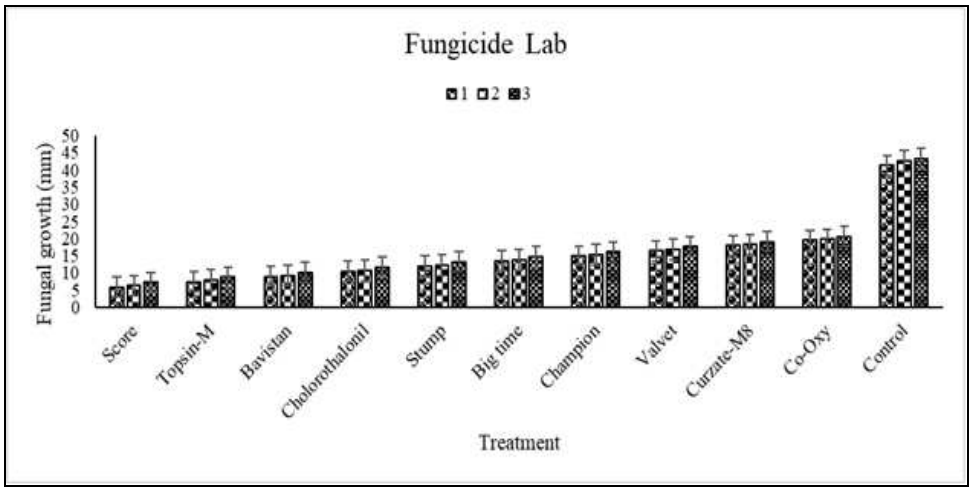

Figure 4. *Variation in growth inhibition with different treatments of ten fungicides against fungal pathogen under lab conditions*

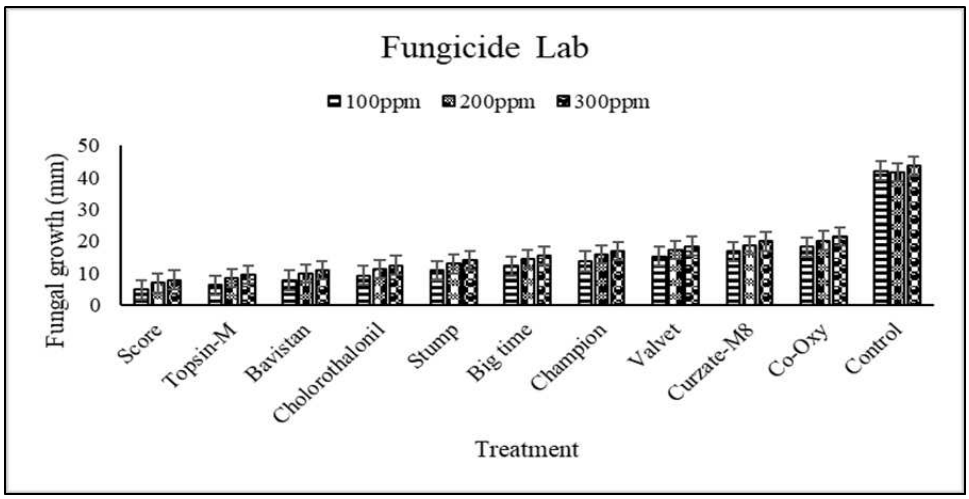

Figure 5. *Variation in growth inhibition with different concentrations of fungicides against fungal pathogen under lab conditions*

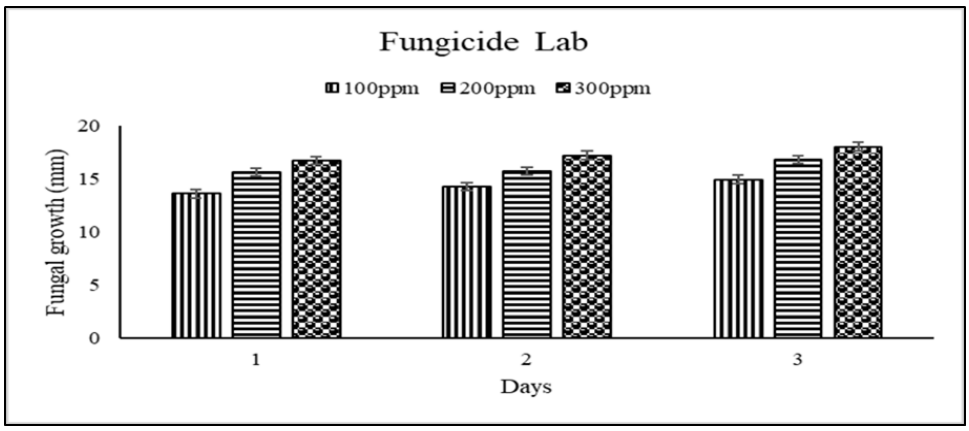

Figure 6. *Variation in growth inhibition after different days (1 = 7, 2 = 14 & 3 = 21) of application fungicides against fungal pathogen under lab conditions*

http://www.aloki.hu ● ISSN 1589 1623 (Print) ● ISSN 1785 0037 (Online)
DOI: http://dx.doi.org/10.15666/aeer/2001_527541

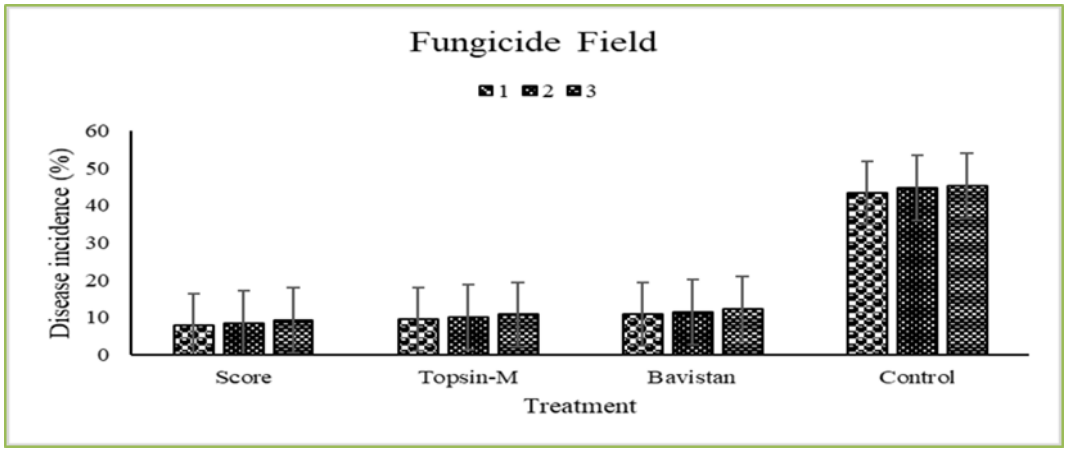

Figure 7. *Variation in disease incidence with different concentrations of fungicides against fungal pathogen under field conditions*

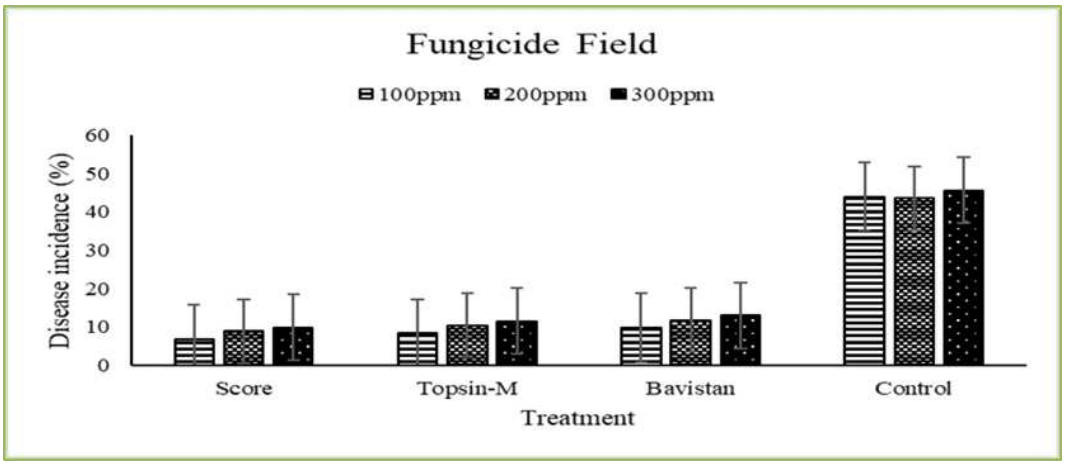

Figure 8. *Variation in disease incidence with different treatments of fungicides against fungal pathogen under field conditions*

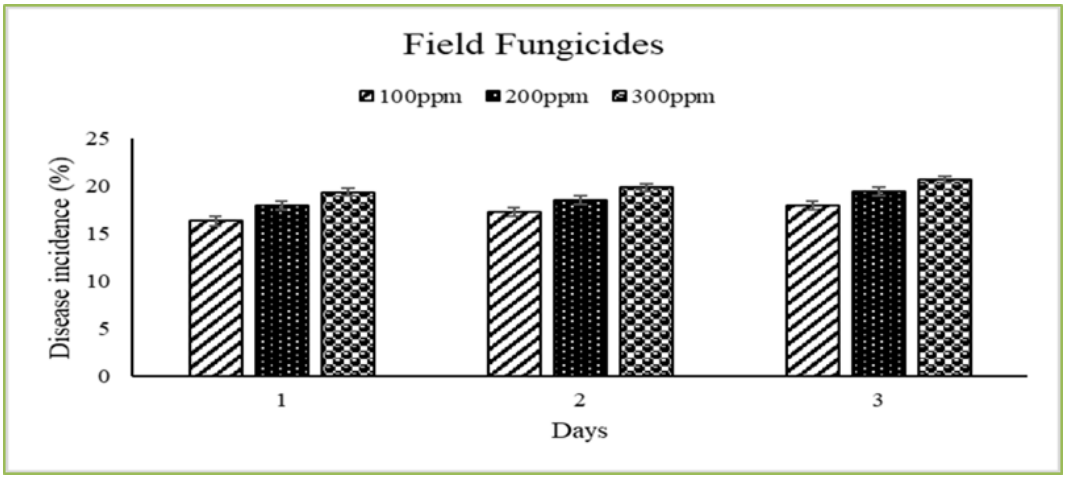

Figure 9. *Variation in disease incidence after different days (1 = 7, 2 = 14 & 3 = 21) of application of most effective fungicides against fungal pathogen under field conditions*

http://www.aloki.hu ● ISSN 1589 1623 (Print) ● ISSN 1785 0037 (Online)
DOI: http://dx.doi.org/10.15666/aeer/2001_527541

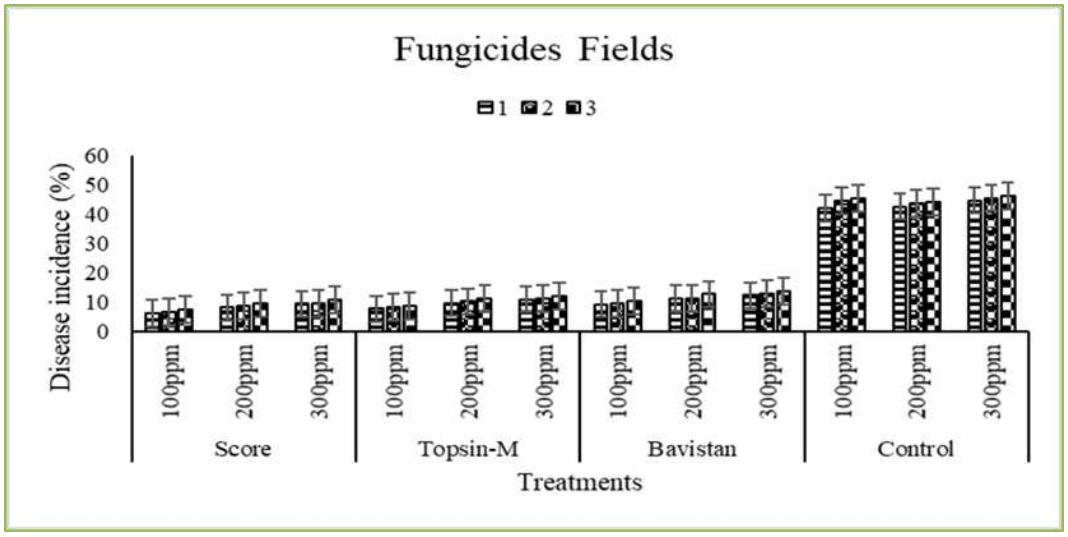

Figure 10. *Variation in disease incidence with different treatments fungicides against fungal pathogen under field conditions*

Discussion

Screening of 20 chickpea germplasms was done to find out the most resistant varieties against *Fusarium* spp. in 2017 and 2018. Two varieties (Balkasar and C-727) were highly resistant, six lines were resistant, four lines were moderately resistant, five varieties were susceptible and three varieties were highly susceptible. Such type of results has also been shown by another worker (Chaudhry et al., 2006, 2007; Infantino et al., 2006). The best procedure to infect the lines at seedling stage is by infestation of the soil with Fusarium inoculum and completely covers the surface of soil in the pots. By this method pathogen grows and infects the host more sharply (Gurha and Dubey, 1982). This technique is time saving and most effective as compare to other procedures. This technique was followed by (Sugha et al., 1991). Three fungal antagonists (*Trichoderma harzianum, Trichoderma viride* and *Trichoderma virens*) were evaluated against virulent pathogens in which *Trichoderma harzianum* showed maximum inhibition under lab and field conditions. My results showed similarity with the results of Akrami et al. (2013). These results also have synchronization with other researches (Jayalakshmi et al., 2009). Most competitive pathogens grow near the rootzone of chickpea and increase their colonies due to which fungal antagonists help to inhibit their action on plant (Benhamou et al., 2002). *Tricoderma spp.* is very beneficial against fungal pathogens because of their multiple actions. My results are also close to this research which shows that *Trichoderma harzianum* is very effective biocontrol agent because of its production of antibics, production of enzymes chitinase, has ability to solubilize inorganic compounds and also inactivate pathogenic enzymes (Harman, 2006). Ten fungicides (Score, Topsin M, Baviston, Chlorothalonil, Stump, Big Time, Champion, Velvet, Curzate M8 and Co-oxy) were evaluated against virulent pathogens in which Score showed maximum inhibition of isolates of *Fusarium spp.* which were followed by Topsin M and Baviston under lab conditions while on the other hand Score inhibited maximum fungal growth under field conditions. Response of my systemic fungicides showed relatedness with the results of Dahal and Shrestha (2018) in which sensitivity of *Fusarium spp.* was evaluated by using different fungicides like

http://www.aloki.hu ● ISSN 1589 1623 (Print) ● ISSN 1785 0037 (Online)
DOI: http://dx.doi.org/10.15666/aeer/2001_527541

carbendazim, chlorothalonil and dithane M-45. Maximum mycelial growth was inhibited by carbendazim which was up to 98.23% at all concentrations 100, 150, 200 ppm. Minimum inhibition was obtained by dithane M-45 which was up to 27.43% at 150 ppm. Intermediate inhibition was observed chlorothalonil (65.78%) at 150 ppm concentration. My results also correlate with the following references. Dithane M-45 is least effective as compare to the other examined fungicides. Some fungicide acts systemically in pathogens has more efficacy like carbendazim as compare to other non-systemic chemicals like mancozeb (Khola et al., 2016). Carbendazim is very effective against fusarium which causes wilt in chickpea at every concentration Luz et al. (2007), Maheshwari et al. (2008), Singh et al. (2010), and Somu et al. (2014). Carbendazim also inhibits the growth of *F. solani* (Narayanan et al., 2015). Some researcher used carbendazim for the reduction of *Foc* (Subhani et al., 2011) and some used it for complete inhibition of *Foc* (Maitlo et al., 2014). Chlorothalonil is least effective as compare to carbendazim and more effective as compare to dithane M-45. Chlorothalonil at 0.1% inhibits fusarium growth in less than carbendazim at 0.2% (Manasa et al., 2017). Chlorothalonil binds to proteins to inhibit the catalytic activity of enzyme. This chemical binds to glyceraldehyde-3-phosphate (GAP) and reacts with sulfhydryl which plays an important role in binding to GAP (Long and Siegel, 1975). Mancozeb inhibits the mycelia growth up to 66% by using 200 ppm (Singh et al., 2010). In some other researches it is reported that dithane M-45 fully inhibits the growth of *Fusarium* spp. at 200 ppm concentration (Dabbas et al., 2008).

Conclusion

Integrated disease management of chickpea wilt helped in finding out the appropriate management strategies against *Fusarium* spp. associated with chickpea wilt. Growing of resistant varieties would increase the chickpea yield by reducing the disease incidence. The future management strategies of this pathogen would be better with the combination of biological and chemical control.

Acknowledgments. The researcher and her team thankful for financial assistance under the project funded by USPCAS-AFS ≠ 935 at UAF and this article is a part of PhD dissertation of Kaneez Fatima, a PhD Scholar at Department of Plant Pathology, UAF.

REFERENCES

[1] Ayyub, M., Khan, S., Ahmad, R., Iftikhar, K. (2003): Screening of chickpea germplasm for the sources of resistance against chickpea wilt (*Fusarium oxysporum* f. sp. *ciceris*). – Pakistan Journal Phytopathology 15: 25-7.

[2] Akrami, M., Khiavi, H. K., Shikhlinski, H., Khoshvaghtei, H. (2013): Bio controlling two pathogens of chickpea *Fusarium solani* and *Fusarium oxysporum* by different combinations of *Trichoderma harzianum*, *Trichoderma asperellum* and *Trichoderma virens* under field condition. – International Journal of Microbiology Research 1(2): 052-055.

[3] Atta, B. M., Shah, T. M. (2009): Stability analysis of elite chickpea genotypes tested under diverse environments. – Australian Journal of Crop Science 3: 249-256.

http://www.aloki.hu ● ISSN 1589 1623 (Print) ● ISSN 1785 0037 (Online)
DOI: http://dx.doi.org/10.15666/aeer/2001_527541

[4] Benhamou. N., Garand, C., Goulet, A. (2002): Ability of nonpathogenic *Fusarium oxysporum* strain Fo47 to induce resistance against *Pythium ultimum* infection in cucumber. – Applied and Environmental Microbiology 68(8): 4044-4060.
[5] Chaudhry, M. A., Muhammad, F., Afzal, M. (2006): Screening of chickpea germplasm against fusarium wilt. – J. Agric. Res. 44(4).
[6] Chaudhry, M. A., Ilyas, M. B., Muhammad, F., Ghazanfar, M. U. (2007): Sources of resistance in chickpea germplasm against Fusarium wilt. – Mycopath 5(1): 17-21.
[7] Dahal, N., Shrestha, R. K. (2018): Evaluation of efficacy of fungicides against *Fusarium oxysporum* f. sp. Lentis in vitro at Lamjung, Nepal. – Journal of the Institute of Agriculture and Animal Science 35: 105-112.
[8] Dabbas, M., Srivastava, J., Rai. M. (2008): IDM for wilt disease of table pea. – Annals of Plant Protection Sciences 16: 156-158.
[9] Gupta, R. P., Katiyar, R. P., Singh, D. P. (1988): Seed treatment with Bavistin and Rhizobium and its effect on wilt incidence, nodulation and yield of chickpea. – Pesticides 22: 9-10.
[10] Gurha, S. N., Kamthan, K. P., Misra, D. P. (1982): Reaction of some exotic and indigenous cultivars of chickpea (*C. arietinum* L.) against *Sclerotium rolfsii* Sacc. – Madras Agric. J. 69: 471-473.
[11] Graham, P. H., and Vance, C. P. (2003): Legumes: importance and constraints to greater use. – Plant Physiology 131: 872-877.
[12] Harman, G. E. (2006): Overview of mechanisms and uses of *Trichoderma spp.* – Phytopathology 96: 190-194.
[13] Haware, M. P. (1990): Fusarium wilt and other important diseases of chickpea in the Mediterranean area. – Options Méditerranéennes Série A: Séminaires Méditerranéens 61.
[14] Haware, M. P., Nene, Y. L. (1980): Influence of wilt at different stages on the yield loss in chickpea. – Tropical Grain Legume Bulletin 19: 38-44.
[15] Haware, M. P., Nene, Y. L., Mathur, S. B. (1986): Seed borne diseases of chickpea. – Technical Bulletin. No.1, ICRISAT.
[16] Haware, M. P., Nene, Y. L., Natarajan, M. (1996): Survival of *Fusarium oxysporum* f. sp. *ciceri*. – Plant Disease 66: 809-810.
[17] Infantino, A., Kharrat, M., Riccioni, L., Clarice Coyne, J., Kevin, E., McPhee, J., Niklaus., Grünwald. (2006): Screening techniques and sources of resistance to root diseases in cool season food legumes. – Euphytica 147: 1-2, 201.
[18] Jayalakshmi. S. K., Raju, S., Usha-Rani, S., Benagi, V. I., Sreeramulu, K. (2009): *Trichoderma harzianum* L1 as a potential source for lytic enzymes and elicitor of defense responses in chickpea (*Cicer arietinum* L.) against wilt disease caused by *Fusarium oxysporum* f. sp. *ciceri*. – Australian Journal of Crop Science-3(1): 44-52.
[19] Khan, I. A., Alam, S. S., Haq, A., Jabbar, A. (2002): Selection for resistant to wilt in relation with phenols in Chickpea. – International Chickpea and Pigeonpea Newsletter 9: 19-20.
[20] Khola, R., Chaudhary, A. R., Farah, N., Ghulam. S. (2016): Management of vascular wilt of lentil through host plant resistance, biological control agents and chemicals. – Pakistan Journal of Botany 48(5): 2085-2092.
[21] Long, J. W., Siegel, M. R. (1975): Mechanism of action and fate of the fungicide chlorothalonill (2, 4, 5, 6-tetrachoroisophthalonitrile) in biological systems. 2. In vitro reactions. – Chemico-Biological Interactions 10(6): 383-394.
[22] Luz, C., Netto, M. C. B., Rocha, L. F. N. (2007): In vitro susceptibility to fungicides by invertebrate- pathogenic and saprobic fungi. – Mycopathologia 164: 39-47.
[23] Maheshwari, S. K., Bhat, N. A., Masoodi, S. D., Beig, M. A. (2008): Chemical Control of Lentil Wilt caused by *Fusarium oxysporum* f. sp. lentis. – Annual Plant Protection Science 16(2): 419-421.

http://www.aloki.hu ● ISSN 1589 1623 (Print) ● ISSN 1785 0037 (Online)
DOI: http://dx.doi.org/10.15666/aeer/2001_527541

[24] Maitlo, S. A., Syed, R. N., Rustamani, M. A., Khuhro, R. D., Lodhi, A. M. (2014): Comparative efficacy of different fungicides against fusarium wilt of chickpea (*Cicer arietinum* L.). – Pakistan Journal of Botany 46(6): 2305-2312.
[25] Nema, K. G., Khare, M. N. (1973): A conspectus of wilt Bengal gram in Madhya Pradesh. Symposium on wilt problem and breeding for wilt resistance in Bengal gram. – Indian Agricultural Research Institute, New Dehli (Abst).
[26] Manasa, B. G., Somashekara, Y. M., Shankara, K., Swamy, C. (2017): Efficacy of fungicides in control of *Fusarium oxysporum* f. sp. dianthi, the cause of wilt in carnation. – International Journal of Current Microbiology and Applied Sciences 6(10): 2559-2565.
[27] Millan, T., Clarke, H. J., Siddique, K. H., Buhariwalla, H. K., Gaur, P. M., Kumar, J., Gil, J., Kahl, G., Winter, P. (2006): Chickpea molecular breeding: new tools and concepts. – Euphytica147: 81-103.
[28] Narayanan, P., Vanitha, S., Rajalakshmi, J., Parthasarathy, S., Arunkumar, K., Nagendran, K., Karthikeyan, G. (2015): Efficacy of bio-control agents and fungicides in management of mulberry wilt caused by *Fusarium solani*. – Journal of Biological Control 29(2): 107-114.
[29] Navas-Cortes, J. A., Hau, B., Jimenez-Diaz, R. M. (2000): Yield loss in chickpea in relation to development to Fusarium wilt epidemics. – Phytopathololology 90: 1269-1278.
[30] Nene, Y. L., Thaplyal, P. N. (1982): Fungicides in plant disease control. – Oxford and IBH Publ. Comp., New Delhi.
[31] Rehman, A., Imran, M., Mehboob, S., Khan, N. A., Alam, W., Riaz, K. (2018): Etiology, pathogenicity and management of collar rot in cockscomb (*Celosia aregentea*). – Int. J. Agric. Biol., 17: 9-14.
[32] Sharma, K. D., Muehlbauer, F. J. (2007): Fusarium wilt of chickpea: physiological specialization, genetics of resistance and resistance gene tagging. – Euphytica 157: 1-14.
[33] Singh, V. K., Naresh, P., Biswas, S. K., Singh, G. P. (2010): Efficacy of fungicides for management of wilt disease of lentil caused by *Fusarium oxysporum* f sp. lentis. – Annals of Plant Protection Sciences 18(2): 411-414.
[34] Somu, R., Thammaiah, N., Swami, G. S. K., Kulkarni, M. S., Devappa, V. (2014): In vitro evaluation of fungicides against *Fusarium oxysporum* f. sp. cubense. – International Journal of Plant Protection 7(1): 221-224.
[35] Subhani, M. N., Sahi, S. T., Hussain, S., Ali, A., Iqbal, J., Hameed, K. (2011): Evaluation of various fungicides for the control of gram wilt caused by *Fusarium oxysporum* f. sp. ciceri. – African Journal of Agricultural Research 6: 4555-4559.
[36] Sugha, S. K., Sharma, B. K., Tyagi, P. D. (1991): A modified technique for screening chickpea (*Cicer arietinum*) varieties against collar rot caused by *Scerotium rolfsii*. – Indian J. Agric. Sci. 61(4): 289-290.
[37] Vincent, J. M. (1947): Distortions of fungal hyphae in the presence of certain inhibitors. – Phytopathology 48: 268-270. Crossref.
[38] Yan, J., Yuan, S., Jiang, L., Ye, X., Bun, T., Wu, Z. (2015): Plant antifungal proteins and their applications in agriculture. – Appl. Microbiol. Biotechnol. 99: 4961-4981.
[39] Zamani, M., Motallebi, M., Rostamian, A. (2004): Characterization of Iranian isolates of *Fusarium oxysporum* on the basis of RAPD analysis, virulence and vegetative compatibility. – Journal of Phytopathology 152: 449-53.

http://www.aloki.hu ● ISSN 1589 1623 (Print) ● ISSN 1785 0037 (Online)
DOI: http://dx.doi.org/10.15666/aeer/2001_527541

GROWTH, AND YIELD CHARACTERISTICS AS WELL AS PESTS AND DISEASES SUSCEPTIBILITY OF CHILI PEPPER (*Capsicum annuum* L.) UNDER DIFFERENT PLANT DENSITIES AND PRUNING LEVELS

SETIAWATI, W.[1] – MUHARAM, A.[2] – HASYIM, A.[1] – PRABANINGRUM, L.[1] – MOEKASAN, T. K.[1] – MURTININGSIH, R.[1] – LUKMAN, L.[3] – MEJAYA, M. J.[4*]

[1]*Indonesian Vegetable Research Institute, Jl. TangkubanParahu No. 517, Lembang Bandung Barat 40391, Indonesia*

[2]*Indonesian Center for Agricultural Technology Assessment and Development, Indonesia (ICATAD), Jl. Tentara Pelajar No. 10 Bogor 16111, West Java, Indonesia*

[3]*Directorate General of Horticulture, Ministry of Agriculture, Republic of Indonesi, Jl. AUP no. 3 Pasar Minggu, Jakarta Selatan, Indonesia*

[4]*Indonesian Legumes and Tuber Crops Research Institute (ILETRI), Jl. Raya Kendakpayak Km. 8 PO Box 66, Malang 65101, East Java, Indonesia*

[*]*Corresponding author*
e-mail: mmejaya@yahoo.com; phone: +62-341-806-074

(Received 2nd Sep 2021; accepted 23rd Nov 2021)

Abstract. The field experiments were conducted at Indonesian Vegetable Research Institute (IVEGRI) West Java, Indonesia during the period of July 2018 to February 2019. The objective of the study was to determine the effect of three plant densities (20,000, 30,000 and 40,000 plants ha^{-1}) and four stem pruning levels (control, 3 stems, 4 stems, and shoot pruning) on growth and yield parameters as well as pest and diseases incidences for chili pepper. Split plot experiment was performed using a randomized block design with three replications. The recommended cultural practices were done for better crop growth and good yields. Results showed no interactions between plant density and pruning for any of the variables measured. Chili pepper growth, yield, and quality and incidence of pest and diseases can be effectively manipulated by plant density and pruning. Increasing of plant population from 20,000 to 30,000 plants ha^{-1} resulted in the increased of total fruit yield to 52.58%, however, total fruit yield declined up to 34.09% at 40,000 plant/ha. Pruning significantly affected fruit yield from 4.65 to 20.33%. Shoot pruning produced higher number of branches, and resulted in maximum yield per ha^{-1} due to higher number of shoots contributing to the production of more number of fruits. Growing chili pepper at a density of 30,000 plant ha^{-1} was better than the conventional methods, and it combination with shoot pruning in nurseries could be used as an alternative method to increase the production of chili pepper.
Keywords: *plant population, branches, susceptibility, fruit quality, production*

Introduction

Chili pepper (*Capsicum annuum* L.) is one of important spices and vegetable crops in the world. FAOSTAT (2020) reported that world production of chili pepper was 42.282 million tons in both dry and green fruits from 3.718 million hectares of land. Indonesia is currently ranked fourth in chili production after China, Mexico and Turkey and account for about 5 percent of global annual chili production (Kementan, 2020). An average production, however, is low (8.46 t ha^{-1}) compared to its potential yields of 12 to 20 t ha^{-1}. It attributed to a combination of various bottlenecks in production constraints such as climate change, poor cultivation practices, high production costs for

http://www.aloki.hu ● ISSN 1589 1623 (Print) ● ISSN 1785 0037 (Online)
DOI: http://dx.doi.org/10.15666/aeer/2001_543553

seeds, fertilizers, and pesticides, as well as high pests and diseases attacks (Setiawati et al., 2021).

Successful of crop production could be affected by various factors including transplanting age, fertilization, pest and diseases management, pruning and plant density. Plant density and plant arrangement influenced plant development, plant dry weight, stem diameter, plant width, growth and marketable yield of chili pepper. Planting density, which can be maintained by adjusting row spacing and plant spacing, is a strong determinant of yield in various crops, including chili pepper.

Yield of sweet pepper was depended on the number of plants accommodated per unit area of land (Maboko and Plooy, 2008; El Naim and Jabereldar, 2010; Islam et al., 2011). Plant density of chili pepper for double population increased production up to 67%, and plant density of 40,000 plants ha^{-1} increased productivity by 123% compared to the conventional technology (9,570 plants ha^{-1}) (Adams et al., 2001; O'Keefe and Palada, 2002). The chili variety used did not affect the productivity. A number of studies have indicated a linear increase in fruit yield when plant density is increased (Jovicich et al., 2003, 2004; Mavengahama et al., 2009) and then declined as plant population increased up to a point (Akintoye, 2009; Mavengahama et al., 2009).

Chili pepper plants have a branching habit, therefore, fruit development is controlled by restricting the branching pattern to 1, 2, 3 and 4 main branches (Alsadon et al., 2013). The reasons for pruning sweet pepper are to train plant growth to facilitate light penetration throughout the leaf canopy for more efficient interception of light (Jovicich et al., 2004). Pinching of marigold plants resulted in an increased number of branches per plant (Chauhan et al., 2005). Pruning to two or three stems was reported to be effective in increasing yield and reducing fruit size of cherry tomatoes to a more acceptable marketable size (Dasgan and Abak, 2003). Chili pepper plants are commonly infested by numerous insect pests that attack at its various growth stages. Plant density and pruning had a significant effect on the presence of pests. Plant density and pruning are very important for the optimization of plant spacing per unit area (El Naim et al., 2010). Many factors influence the optimum plant population for a crop such as availability of water, nutrients and sunlight, length of growing season, potential plant size, and the plant's capacity to change its form in response to varying environmental conditions (morphological plasticity). By determining optimum plant population under suitable environment, it is possible to get optimum yield.

Majority of the chili growers in Indonesia have little knowledge about the advantage of pruning in chili production. Usually the farmers of Indonesia cultivate chili without pruning and even they do not maintain proper plant density and plant population. Populations vary from 15 000 to 20 000 plants ha^{-1}. The objective of this study was to evaluate the effect of different plant density and pruning systems on the growth and yield characteristics as well as the pest and diseases susceptibility for chili pepper in open field condition.

Methodology

Place and time of study

The study was conducted in the research field station of the Indonesian Vegetables Research Institutes (IVEGRI), Lembang, Bandung, West Java Province, Indonesia from July 2018 to February 2019. This site is 1,250 m above sea level and located at 60° 30' S and – 107° 30' E. Soil type in this location is mainly Andisol with the average pH of 5.0

http://www.aloki.hu ● ISSN 1589 1623 (Print) ● ISSN 1785 0037 (Online)
DOI: http://dx.doi.org/10.15666/aeer/2001_543553

– 6.0. This area experiences average temperature of 19-24°C, humidity ranges from 34-90% and average rainfall of 2,207 mm/year.

Research design

A complete randomized block with split-plot arrangement and three replications was established up to achieve the goal. The main plot was population density (a) consisting of (a1) 20,000 plants ha^{-1} (one plant per hole), (a2) 30,000 plants ha^{-1} (one and two plants per hole), and (a3) 40,000 plants ha^{-1} (two plants per hole). The pruning system was applied as subplot, and there were four subplots set up in the field i.e. (b1) control or upruned plants, (b2) three branches remaining after pruning, (b3) four branches remaining after pruning, and (b4) shoot pruning or pinching.

The chili pepper variety of Kencana was used in the experiment. Seedlings were raised in the protected nursery to minimize pests and diseases attacks. Seedling pruning for shoot pruning treatment were conducted in the nursery. Three weeks old seedlings were pruned using sterile scissor right under the first leaf shoots. Two weeks after pruning, seedlings were transplanted in to the field as per experiment layout (*Figure 1*). As for other treatments i.e., b2, and b3, five weeks old seedlings were transplanted in to the field and pruned at the base of main stem on the 30 days after transplanting (DAT) to follow the treatments.

a) Shoot pruning

b) Chili seedlings ready to be transplanted

c) Zigzag transplanting system

d) shoot pruning crop performance on 90 DAT

Figure 1. *Shoot pruning treatment*

http://www.aloki.hu ● ISSN 1589 1623 (Print) ● ISSN 1785 0037 (Online)
DOI: http://dx.doi.org/10.15666/aeer/2001_543553

An area of 88 m x 136 m was divided into three equal blocks. There were 36 plots altogether in the experiment. The size of each plot was 13 m x 14 m (700 plants per plot) and the plots were arranged in spacing 50 cm x 70 cm in a zigzag system to avoid competition in light, distribution of roots and nutrients contents The distance within blocks and plots were 1 m and 0.5 m, respectively. Organic materials consisting of mature compost were applied as a basal fertilizer along with NPK composite fertilizers. The dose of organic materials and NPK was 30 t ha^{-1} and 1 t ha^{-1}, respectively. The chemical characteristics of Andisol soil and mature compost are presented on *Tables 1 and 2*, respectively.

Tabel 1. *Chemical characteristics of Andisol soil*

Chemical characteristics*	Analysis values	Criteria
pH (H_2O)	5.80	Acid
pH (KCl)	4.70	Acid
C-rganik (%)	5.80	Very high
N-total (%)	0.72	High
C/N	9.0	Low
P_2O_5 – Bray 1 (ppm)	3.50	Very low
K – Morgan (ppm)	135.50	Medium
Ca (cmol(+)/kg)	2.80	Low
Mg (cmol(+)/kg)	0.27	Very low

*IVEGRI's Integrated Testing Laboratory (2018)

Table 2. *Chemical characteristics of mature compost*

Chemical characteristics	Mature compost (made of enrichment stable manure + plant residues compost)
pH (H_2O)	7.67
pH (KCl)	7.31
Kadar air (%)	48.46
C-organik (%)	10.71
N-total (%)	0.57
C/N	19.0
P_2O_5 (%)	0.58
K_2O (%)	0.45
CaO (%)	0.71
MgO (%)	0.26
Fe (ppm)	8878.0
Mn (ppm)	423.0
Cu (ppm)	32.0
Zn (ppm)	55.0
Pb (ppm)	20.09

*IVEGRI's Integrated Testing Laboratory (2018)

The beds were covered with silvery plastic mulch. The land was cleared manually started with plugging and making beds.

Data analysis

Growth of plant and percentage of plant damage due to pests and diseases attack were recorded. Ten sample plants from each plot were randomly selected in each

http://www.aloki.hu ● ISSN 1589 1623 (Print) ● ISSN 1785 0037 (Online)
DOI: http://dx.doi.org/10.15666/aeer/2001_543553

observation day. Assessments were conducted throughout the growing season in weekly interval started from 30 Days After Planting (DAP).

Plant damage due to thrips was measured using to follow Equation 1 formula as follow:

$$I = \frac{\sum (n \times v)}{N \times z} \times 100\% \quad \text{(Eq.1)}$$

Notes:
I, damage levels (%)
v, the value of damage category
n, number of plants that have same v value
Z, the value of highest damage category
N, number of observed plants

Category of plant damage value (v) is determined based on the percentage of leaf area damage i.e.:

0, if there is no damage leaf area
1, if there is > 0 – ≤ 20% leaf area damage
3, if there is > 20 – ≤ 40% leaf area damage
5, if there is > 40 – ≤ 60% leaf area damage
7, if there is > 60 – ≤ 80% leaf area damage
9, if there is > 80 – ≤ 100% leaf area damage.

The incidence of anthracnose was observed from total harvested fruit. The intensity of anthracnose attack on chili fruit was measured using *Equation 2* as follow:

$$Disease\ incidence = \frac{\sum infected\ fruits}{\sum observed\ fruits} \times 100\% \quad \text{(Eq.2)}$$

Yield assessment: Data collected were fruit length (cm), fruit diameter (cm), individual fruit weight (g). Chili pepper fruit per plot were weighed for each treatment to observe the total yield. Data are presented as expected weight t ha^{-1}. The percent increase in yield over control in various treatments was calculated to follow *Equation 3*.

$$\%\ of\ increasing\ yield = \frac{yield\ in\ treatment - yield\ in\ control}{yield\ in\ control} \times 100\% \quad \text{(Eq.3)}$$

Statistical analysis

The data were subjected to two ways ANOVA (SAS Program). Significantly different means ($P < 0.05$) were separated using Duncan Multiple Range Test (DMRT) at 5% probability. Count data were transformed by square root of (x + 0.5), and transformation of percentage data by arcsine-square root.

Results and Discussion

There was no significant interaction between plant density and pruning for all parameter observed ($p \geq 0.05$), showing that these factors took action independently on variables of plant height, number of flowers per plant, fruit length, fruit diameter, number of fruits per plant, individual fruit weight, pest and diseases, and chili yield.

http://www.aloki.hu ● ISSN 1589 1623 (Print) ● ISSN 1785 0037 (Online)
DOI: http://dx.doi.org/10.15666/aeer/2001_543553

Vegetative growth parameters

Plant density and pruning system gave significant effects on chili plant height ($p \leq 0.05$). The plant height ranged between 63.03 and 71.41 cm. Plant height increased linearly in response to increased plant densities at all observations (*Table 3*). This was due to intra-specific competition for the sunlight (El Naim, 2010; Edgar et al., 2017). Plant height showed significant variation at different days after transplanting (DAT) due to pruning. At 93 DAT the maximum plant height (69.34 cm) was obtained from (b3) which was statistically similar to b0 and b1, while the minimum (65.30 cm) was recorded from (b4). This was probably caused to the fact that competition between plants for available water, nutrients and light was less in one branch system than in 3 or 4 branches systems. Shoots pruning/pinching (b4) significantly reduced the plant height in comparison with the other treatments. Decreased plant height and increased number of branches could reduce vertical plant growth, resulting in translocation of photosynthates to leaf axils, hence increased number of axillary (Kumar et al., 2014; Singh et al., 2015; Setiawati et al., 2021).

Table 3. *The average of plant height on chili pepper at different treatments*

Treatments	(Plant height at plant ages) ……. (DAP)									
	30	**37**	**44**	**51**	**58**	**65**	**72**	**79**	**86**	**93**
Population density										
a1.20,000 plants ha^{-1}	10.02^{b}	12.96b	16.43b	19.81c	26.71c	34.18c	43.03c	51.64c	57.46c	63.03b
a2.30,000 plants ha^{-1}	11.18^{a}	13.98b	17.92ab	22.76b	29.48b	38.12b	47.90b	57.11b	62.45b	69.25a
a3.4,000 plants ha^{-1}	12.20^{a}	15.69a	19.31a	25.15a	34.82a	43.87a	53.82c	60.58a	65.82a	71.41a
LSD 5%	1.05	1.46	1.95	1.84	2.63	2.96	3.16	2.34	2.36	2.53
Pruning system										
b1. Control (upruned plants)	11.63a	14.73a	18.00a	23.19a	31.73a	39.70a	49.22a	56.92a	61.71ab	69.29a
b2. Three branches remaining	11.87a	14.51a	18.71a	23.39a	30.82a	39.56a	49.16a	57.04a	62.42ab	67.90ab
b3. Four branches remaining	11.09a	16.57a	20.5a	25.38a	33.11a	41.81a	50.96a	58.09a	63.90a	69.34a
b4. Shoot pruning	9.21b	12.47b	15.41b	19.80b	27.08b	35.33b	45.37b	54.20b	60.16b	65.30b
LSD 5%	1.21	1.69	2.26	2.13	3.04	3.42	3.65	2.70	2.73	2.92

Means followed by the same letter in the column are not significantly different according to Duncan's Multiple Range Test at $\alpha = 0.05$

Pests and diseases incidence on chili pepper

The lowest plant damage occurred in plant density of 20,000 plants ha^{-1}, followed by density of 30,000 and 40,000 plants ha^{-1}. In the pruning treatment, the lowest plant damage occurred in shoot pruning (b4), followed by b1, b2 and highest was presented in b3. There was no significant effect of plant density on the plant damage in most of observation days. However, on the 44 until 93 DAP plant damage due to thrips attack in the 40,000 plants ha^{-1} plot were significantly higher compared to other treatments (*Table 4*). Other studies suggested that there might be an inverse relationship between the attack rates and the number of branches. Shivute (2005) reported that pruned tomatoes were less prone to pest attack than those, which were not pruned.

http://www.aloki.hu ● ISSN 1589 1623 (Print) ● ISSN 1785 0037 (Online)
DOI: http://dx.doi.org/10.15666/aeer/2001_543553

Tabel 4. *Plant damage (%) due to thrips attack*

Treatments	Plant damage (%) at DAP									
	30	**37**	**44**	**51**	**58**	**65**	**72**	**79**	**86**	**93**
Populations density										
a1. 20,000 plants ha^{-1}	0.00	1.48a	1.02ab	2.50a	6.02b	7.32b	6.39a	12.96a	5.83a	4.54a
a2. 30,000 plants ha^{-1}	0.00	1.57a	0.83b	3.24a	7.13ab	8.33b	6.39a	12.59a	4.72a	4.91a
a3. 40,000 plants ha^{-1}	0.00	0.93a	1.94a	2.50a	9.28a	11.39a	6.21a	13.24a	4.81a	4.81a
Pruning system										
b1.Control (upruned plants)	0.0	1.23a	0.99a	2.47a	6.67bc	9.88a	6.42a	12.84a	4.57b	4.69ab
b2. Three branches remaining	0.0	0.99a	1.11a	3.21a	8.15ab	8.64ab	6.05a	13.09a	4.94ab	4.20b
b3. Four branches remaining	0.0	3.21a	2.22a	3.33a	9.88a	11.48a	6.67a	13.83a	6.05a	5.43a
b4. Shoot pruning	0.0	0.86a	1.11a	1.97a	5.21c	6.05b	6.30a	12.22a	4.94ab	4.32b

Means followed by the same letter in the column are not significantly different according to Duncan's Multiple Range Test at $\alpha = 0.05$

Plant density and pruning had a significant effect on incidence of anthracnose diseases. Plant density of 20,000 plants ha^{-1} and pruning (b1 and b4) had decreased the incidence of this diseases compared to the other treatments (*Table 5*). Pruning made the sunlight freely illuminates the parts of plants and the leaves more productive in carbohydrates production, this situation provides benefits to the plant because it could reduce the infestation level of pests and diseases (Setiawati et al., 2021).

Table 5. *Effects of populations density and pruning on total yields incidence of Anthracnose diseases on fruit of chili pepper*

Treatments	Total fruit yield (t ha^{-1})	% Increasing yield	% Incidence of Anthracnose diseases on fruit
Populations density			
a1. 20,000 plants ha^{-1}	12.38 ^{c}	-	37.17 ^{b}
a2. 30,000 plants ha^{-1}	18.89 ^{a}	52.58	37.29 ^{b}
a3. 40,000 plants ha^{-1}	16.60 ^{b}	34.09	38.82 a
Pruning system			
b1.Control (upruned plant)	15.05 ^{b}	-	37.97 ^{a}
b2. Three branches remaining	16.01 ^{b}	6.38	35.77 ^{c}
b3. Four branches remaining	15.75 ^{b}	4.65	37.97 ^{a}
b4. Shoot pruning	18.11 ^{a}	20.33	35.90 ^{b}

Means followed by the same letter in the column are not significantly different according to Duncan's Multiple Range Test at $\alpha = 0.05$

Physical fruit characteristics

Number of fruits plant^{-1} and number flower plant^{-1} increased significantly with the increase of plant density. Different plant densities showed significant variation on number of fruits plant^{-1} and number flower plant^{-1}. The highest number of fruits plant^{-1}

http://www.aloki.hu ● ISSN 1589 1623 (Print) ● ISSN 1785 0037 (Online)
DOI: http://dx.doi.org/10.15666/aeer/2001_543553

and number flower plant^{-1} was found from a2 which was followed by a3 and the lowest number was found for a1. This is a direct effect of plant competition. Green pepper fruit number and weight per hectare increased as plant population as well (Buler and Mika, 2009).

Different levels of pruning showed significant variation on fruits plant^{-1} and number flower plant^{-1}. The highest number of fruits plant^{-1} and number flower plant^{-1} (445.45) was observed for b4 which was followed by b2 (406.24), b3 (405.04) and the lowest number (381.02) was found for b1 (no stem pruning) (*Table 6*). Number of fruits per plant affected by pruning (Thakur et al., 2005). Fruit size parameters such as weight, length and diameter fruit of chili were affected by pruning as well. An influence on a number of tree physiological processes connected with the growth, yield and quality of fruits (Buler and Mika, 2009). Pruning decreased total yield, yield plant^{-1}, plant weight and number of fruits plant^{-1}, but it increased fruit weight. Branch numbers plant^{-1} ranged from 11.27 to 14.37, by which significant differences in branch numbers plant^{-1} occurred between the plant density of 20,000 plants ha^{-1} and two others (30,000 and 40,000 plants ha^{-1}). Generally, an increase in plant densities led to significantly lower branching. Low density resulted in an increased number of branches plant^{-1}. This was consistent with the findings of Islam et al. (2011) who reported that there is a relationship between the number of branches and plant population density. The denser the plant population, the less the number of branches produced and will delay the flowering time of plants (Karuppaiah and Krishna, 2005; Mane et al., 2006). Generally, increasing the plant population increased competition among plants for soil moisture, nutrient, light and carbon dioxide (El Naim and Jabereldar, 2010).

Table 6. *Yield components of chili pepper*

Treatments	Branch number / Plant	Flower number / Plant	Fruit number / Plant	Fruit length (cm)	Fruit weight (g)	Fruit diameter (cm)
Populations density						
a1. 20,000 plants ha^{-1}	14.37^{a}	151.43^{b}	216.02^{b}	13.10 ^{a}	5.04 ^{a}	0.85 ^{a}
a2. 30,000 plants ha^{-1}	11.42^{b}	166.75^{ab}	278.63^{a}	13.42 ^{a}	4.97 ^{a}	0.83 ^{a}
a3. 40,00 plants ha^{-1}	11.27^{b}	180.37^{a}	235.12^{b}	13.32 ^{a}	5.10 ^{a}	0.83 ^{a}
Pruning system						
b1. Control (upruned plants)	12.31^{a}	150.31^{b}	230.71^{b}	12.85 ^{b}	4.86 ^{b}	0.80 ^{b}
b2. Three branches remaining	12.62^{a}	163.53^{ab}	242.71^{ab}	13.51 ^{a}	5.16 ^{a}	0.85 ^{a}
b3. Four branches remaining	12.13^{a}	171.51^{a}	233.53^{b}	13.48 ^{a}	5.03 ^{ab}	0.84 ^{a}
b4. Shoot pruning	12.33^{a}	179.38^{a}	266.07^{a}	13.29 ^{a}	5.10 ^{ab}	0.82 ^{a}

Means followed by the same letter in the column are not significantly different according to Duncan's Multiple Range Test at $\alpha = 0.05$

Yield characteristics

Yield increase as plant density increased (*Table 5*). The highest total yield obtained was 18.89 t ha^{-1} from the second highest plant density (30,000 plants ha^{-1}) and 18.11

http://www.aloki.hu ● ISSN 1589 1623 (Print) ● ISSN 1785 0037 (Online)
DOI: http://dx.doi.org/10.15666/aeer/2001_543553

t ha^{-1} from shoots pruning in nursery while the lowest yield per hectare (12.38 t ha^{-1}) was recorder at density 20,000 plants ha^{-1}. Increasing plant densities resulted in a greater yield of hot chili pepper and bell pepper (Jovicich et al., 2004), and "Spanish" pepper, Jalapeno chili peppers and other plants (Russo, 2003; Jovicich et al., 2003; Khasmakhi-Sabet et al., 2009; Mavengahama et al., 2009).

This was probably due to the increasing in the number of plants per unit area, which might contribute to the production of extra yield per unit area leading to the high yield. However, as plant population was increased to 40,000 plants ha^{-1}, total fruit yield was decreased up to 34.09%. The production per plant doubled when one and two plants per hole left (30,000 plant ha^{-1}) compared with two plants per hole (40,000 plant ha^{-1}). This shows that the yield per plant lost when was two plants were left per hole was offset by another plant in the same hole.

Yield per unit area tends to increase as plant density increase up to a point and then declines (Akintoye et al., 2009), however, Aminifard et al. (2010) reported that yield per unit area tends to increase as plant density increase. This may be due to better availability of nutrients and better translocation of photosynthesis, such as competition for various environmental resources, availability of water, nutrients and sunlight (Mavengahama, 2009). Plant population increased from 20,000 up to 30,000 plants/ha, total fruit yield was also increased to 52.58%, however, yield declined up to 34.09% at 40,000 plant/ha. Pruning significantly affected fruit yield from 4.65 to 20.33%. Shoot pruning produced more number of branches resulted in maximum yield per ha due to more number of shoots contributed in producing more number of fruits. Planting chili pepper at plant density of 30,000 plant/ ha was an optimum plant density which was better than the two others (20,000 and 40,000 plants ha^{-1}). Plant density of 30,000 plant/ ha and together with shoot pruning in nurseries increased total fruit yield productivity of chili pepper.

Conclusions

Chili pepper growth, yield and quality, as well as the pest and diseases incidence can be effectively managed through plant density and pruning manipulation. The fruit yield can be increased up to 52.58% by adding plant population from 20,000 up to 30,000 plants/ha. However, adding plant population up to 40,000 plant ha^{-1} reduced 34.09% of yield. Pruning could significantly improve yield from 4.65 to 20.33%. Shoot pruning can add more branches on the plant and consequently more fruits can be produced to eventually resulting maximum yield ha^{-1}. The plant density of 30,000 plant ha^{-1} with zigzag transplanting system and shoot pruning/pinching in nursery application was considered as powerful method to boost higher productivity and quality. Therefore, this pruning technology practice could be recommended to chili farmers to obtain higher marketable yield in chili pepper. There is further research needed to determine the upper limit for plant population, particularly on the basis of economic viability.

Acknowledgments. We deeply thank to Prof. Dr. *B.M. Shepard* (Professor Emeritus at Clemson University, South Carolina, United State) who gave comments and corrected English grammar of the manuscripts.

http://www.aloki.hu ● ISSN 1589 1623 (Print) ● ISSN 1785 0037 (Online)
DOI: http://dx.doi.org/10.15666/aeer/2001_543553

REFERENCES

[1] Adams, H. V., Lauckner, F. B., Sisnett, D. D. (2001): Effects of high plant population densities on yields, plant and fruit characters of the hot pepper cultivar, West Indies Red. – Proceedings of the Caribbean Food Crop Society 37: 197-201.

[2] Akintoye, H. A., Kintomo, A. A., Adekunle, A. A. (2009): Yield and fruit quality of watermelon in response to plant population. – International Journal of Vegetable Science 15: 369-380.

[3] Alsadon, A., Wahb-Allah, M., Abdel-Razzak, H., Ibrahim, A. (2013): Effects of pruning systems on growth, fruit yield and quality traits of three greenhouse-grown bell pepper (*Capsicum annuum* L.) cultivars. – Australian Journal of Crop Science 7(9): 1309-1316.

[4] Aminifard, M. H., Aroiee, H., Karimpour, S., Nemati, H. (2010): Growth and Yield Characteristics of paprika pepper (*Capsicum annuum* L.) in response to plant density. – Asian Journal of Plant Sciences 9(5): 276-280.

[5] Buler, Z., Mika, A. (2009): The influence of canopy architecture on light interception and distribution in 'Samion' apple trees. – Journal of Fruit and Ornamental Plant Research 17(2): 45-52.

[6] Chauhan, S., Singh, C. N., Singh, A. K. (2005): Effect of vermicompost and pinching on growth and flowering in marigold cv. Pusa Narangi Gainda. – Progressive Horticulture 37(2): 419-422.

[7] Dasgan, H. Y., Abak, K. (2003): Effects of plant density and number of shoot on yield and fruit characteristics of peppers grown in glasshouses. – Turkish Journal of Agricultural Forestry 27: 29-35.

[8] Edgar, O. N., Gweyi-Onyango, J. P., Korir, N. K. (2017): Plant Row Spacing Effect on Growth and Yield of Green Pepper (*Capsicum annuum* L.) in Western Kenya. – Archives of Current Research International 7(3): 1-9.

[9] El Naim, A. M., Jabereldar, A. A. (2010): Effect of Plant density and Cultivar on Growth and Yield of Cowpea (*Vigna unguiculata* L. Walp). – Australian Journal of Basic and Applied Sciences 4(8): 3148-3153.

[10] El Naim, A. M., Eldouma, M. A., Abdalla, A. E. (2010): Effect of weeding frequencies and plant density on vegetative growth characteristic in groundnut (*Arachis hypogaea* L.) in North Kordofan of Sudan. – International Journal of Applied Biology and Pharmaceutical Technology 1(3): 1889-1893.

[11] FAOSTAT. (2020): FAOSTAT online. – Rome: United Nations Food and Agriculture Organization. http://faostat.fao.org/default/aspx?lang-en.

[12] Islam, M., Saha, S., Akand, H., Rahim, A. (2010): Effect of spacing on the growth and yield of sweet pepper (*Capsicum annuum* L.). – Journal of Central European Agriculture 12(2): 328-335.

[13] Jovicich, E., Cantliffe, D. J., Stofella, P. J. (2003): Spanish pepper trellis system and high plant density can increase fruit yield, fruit quality and reduced labour in hydroponic, passive-ventilated greenhouse crop. – Acta Horticulturae (ISHS) 614: 255-262.

[14] Jovicich, E., Cantliffe, D. J., Stofella, P. J. (2004): Fruit yield and quality of greenhouse-grown bell pepper as influenced by density, container and trellis system. – Hort. Technology 14: 507-513.

[15] Karuppiah, P., Krishna, G. (2005): Response of spacings and nitrogen levels on growth flowering and yield characters of French marigold (*Tagetes patula* Linn.). – Journal of Ornamental Horticulture 8(2): 96-99.

[16] Kementan. (2020): Outlook cabai. Komoditas Pertanian Sub Sektor Hortikultura. – Pusat Data dan Sistem Informasi Pertanian. Kementrian Pertanian, 70p. file:///C:/Users/USER/Downloads/Outlook%20Cabai%20Besar%202020.pdf.

[17] Khasmakhi-Sabet, A., Sedaghathoor, S., Mohammady, J., Olfati, J. A. (2009): Effect of plant density on bell pepper yield and quality. – International Journal of Vegetable Science 15: 264-271.

http://www.aloki.hu ● ISSN 1589 1623 (Print) ● ISSN 1785 0037 (Online)
DOI: http://dx.doi.org/10.15666/aeer/2001_543553

[18] Kumar, R., Sood, S., Sharma, S., Kasana, R. C., Pathania, V. L., Singh, B., Singh, R. D. (2014): Effect of plant spacing and organic mulch on growth, yield and quality of natural sweetener plant Stevia and soil fertility in western Himalayas. – International Journal of Plant Production 8(3): 311-334.
[19] Maboko, M. M., Du Plooy, C. P. (2008): Effect of pruning on yield and quality of hydroponically grown cherry tomato (*Lycopersicon esculentum*). – South African Journal of Plant and Soil 25(3): 178-181.
[20] Mane, P. K., Bankar, G. H., Makne, S. S. (2006): Effect of spacing, bulb size and depth of planting on growth and bulb production in tuberose (*Polianthes tuberosa*) cv. Single. – Indian Journal of Agricultural Research 40(1): 64-67.
[21] Mavengahama, S., Ogunlela, V. B., Mariga, I. K. (2009): Agronomic performance of paprika (*Capsicum annuum* L.) in Response to Varying Plant Populations and Arrangement in the Small holder Sector Zimbabwe. – Asian Journal of Crop Science 1(2): 96-104.
[22] O'Keefe, D. A., Palada, M. C. (2002): In-row plant spacing affects growth and yield of four hot pepper cultivars. – Proceedings of the Caribbean Food Crop Society 38: 162-168.
[23] Russo, V. M. (2003): Planting date plant density affect yield of pungent and no pungent Jalapeno peppers. – HortScience 38(4): 520-523.
[24] Setiawati, W., Udiarto, B. K., Hasyim, A. (2021): Manipulation of chili plant architecture to enhance productivity and pests control. – IOP Conference Series: Earth and Environmental Science 752: 012059.
[25] Shivute, B. K. L. (2005): Influence of pruning on tomato production under controlled environments. – Agricultura Tropica Et Subtropica 38(2): 79-81.
[26] Singh, A. K., Singh, S. V., Sisodia, A., Hembrum, R. (2015): Effect of pinching and nitrogen on growth flowering and seed yield of African marigold cv. Pusa Narangi Gainda. – Environmental & Ecology 33(4B): 1876-1879.
[27] Thakur, M. C., Shyam, L., Arun, J. (2005): Effect of different training systems and spacing on yield and quality characters and its impact on economics of tomato production. – Horticulure Journal 18(1): 64-68.

http://www.aloki.hu ● ISSN 1589 1623 (Print) ● ISSN 1785 0037 (Online)
DOI: http://dx.doi.org/10.15666/aeer/2001_543553

TEMPORAL DROUGHT ASSESSMENT USING VARIOUS INDICES OF THE SEYHAN AND CEYHAN BASINS, TURKEY

ALKAN, A.* – TOMBUL, M.

Department of Civil Engineering, Eskisehir Technical University, Eskisehir 26555, Turkey

**Corresponding author*
e-mail: alialkan18@gmail.com

(Received 6th Sep 2021; accepted 23rd Nov 2021)

Abstract. Drought is a natural phenomenon with various social, environmental, and economic effects. Adverse impacts of drought at a regional and global scale have become more evident with climate change. The Seyhan and Ceyhan basins were chosen as study areas in Turkey. Drought analyses were performed using data from 14 meteorological stations gathered between January 1989 and July 2020 in Standardized Precipitation Index (SPI) and Standardized Precipitation Evapotranspiration Index (SPEI), based on 3-4-6-12 monthly scales. SPI and SPEI are common indices used for drought tracking. The coefficient of determination (R^2) was found to be 0.954 and used to analyze the regression between the annual SPI and SPEI. According to SPI and SPEI annual analyses results of study area, the driest year was found to be 2014. SPEI determined more arid periods than SPI for the same time scales. Analyses reveal that the dry period in basins has increased in the last decade and the region is facing a risk of drought. Analyses were made to predict and evaluate risks and to help the efficient use of agricultural lands and water resources in the study area during dry periods.
Keywords: *drought analysis, drought tracking, standardized precipitation index (SPI), standardized precipitation evapotranspiration index (SPEI), precipitation indices*

Introduction

Drought is a climatic event that occurs during periods of insufficient rainfall and has significant negative effects on ecosystems and societies. The phenomenon of drought cannot be explained only as insufficient precipitation in a particular region, precipitation distribution and temperature-related evaporation should also be taken into account (Ahsan, 2020a). The increase in temperatures and the changes in the amount of precipitation shows that drought is intertwined with climate change and should address the phenomenon caused by global warming in recent years (Ahsan, 2020b).

In terms of water resources, drought can be thought of as a quantitative factor arising from the basin response time. In addition to effects on soil moisture, hydrological responses in river and groundwater discharge, factors such as crops and native vegetation affect response times; therefore, analyses should be done on time scales (Lorenzo-Lacruz et al., 2010). Drought types are divided into meteorological, agricultural, hydrological droughts according to time periods. Meteorological, hydrological and agricultural drought are analyzed respectively by considering 1-, 3-, 6- and 12- month period. Therefore, it is essential to classify droughts according to specific time scales and to determine and evaluate drought severity accordingly (Homdee et al., 2016).

There are some scientific discussions about the importance of climate parameters in determining the intensity of drought. Parameters such as precipitation, temperature and evapotranspiration affect the drought severity. The importance of precipitation is inevitable for explaining drought variability, but there is no consensus on the necessity of this variable in calculating any drought indices. Nevertheless, neglecting a variant,

http://www.aloki.hu ● ISSN 1589 1623 (Print) ● ISSN 1785 0037 (Online)
DOI: http://dx.doi.org/10.15666/aeer/2001_555569

such as evapotranspiration that takes into account climatic water demand is not generally admitted as its impact on drought-related conditions is not understood (Alley, 1984; Chang and Kleopa, 1991). Evapotranspiration rate is mainly affected by evaporation caused by the increase in atmospheric temperature and the effect of heat waves. In most semi-dry and dry zones of the world, potential evapotranspiration is higher than annual rainfall (Beguería et al., 2014). Several studies have shown that other factors that define the magnitude, duration and intensity of precipitation and droughts also should be taken into account. A study comparing different drought indices reveals that indices which use just rainfall data to define climate droughts suggest the best choice (Olukayode Oladipo, 1985).

Droughts are usually classified according to their features as meteorological, agricultural and hydrological (Wilhite and Glantz, 1985). With reduced precipitation, meteorological drought is the most intuitive among them as it is an extreme climatic event that has a more human and social aspect than other droughts. Meteorological droughts are directly related to other droughts types (Zhang and Jia, 2013; Wang et al., 2019). It is difficult to identify and assess the characteristics of drought because of the complexity and severity of the drought. Therefore, in recent years many drought indices have been advanced for monitoring and evaluating drought events.

Most indices and indicators for drought analysis in the literature use rainfall alone or in combination with other meteorological elements as input. Drought indices are variables that show the duration, extent and spatial extent of drought, determined by hydrological and meteorological variables. Standardized Precipitation Index (SPI) and Standardized Precipitation Evapotranspiration Index (SPEI) have multi time scale characteristics that can show types of drought and better express differences in characteristics of drought (Mishra and Singh, 2010). SPI and SPEI are similar, but there are apparent differences in terms of the parameters used when calculating SPI and SPEI. The SPI ensures the calculation of time-related drought in a particular area, considering only precipitation (Zhou et al., 2013; Tao et al., 2014). McKee et al. (1993) developed SPI for monitoring drought, which is an essential tool for determining periodic meteorological droughts using specific time-precipitation data as input parameters. Vicente-Serrano et al. (2010) developed SPEI to evaluate the severity of drought by taking into account evaporation in the environment in which the plant is located. SPEI is counted basis on the cumulative difference between Precipitation (P) and Potential Evapotranspiration (PET). However, temperature rise and evaporation associated with global warming cannot be ignored to evaluate drought; therefore, SPEI appears to be better than SPI in terms of drought monitoring (Mathbout et al., 2018).

This study aimed to investigate the temporal variation of drought events of the Seyhan and Ceyhan basins in Turkey, based on data from 14 meteorological stations gathered between January 1989 and July 2020, using Standardized Precipitation Index and Standardized Precipitation Evapotranspiration Index.

Materials and Methods

Study Area

The Seyhan and Ceyhan basins lie between 35°.40′ to 39°.25′ N latitudes and 34°.40′ to 37°.80′ E longitudes with an area of 43.840 km^2. In particular, Cukurova delta plain is located in the south of these basins, which the biggest delta plain of Turkey. Therefore, drought analysis is of great importance in these basins (Gumus and Algin,

http://www.aloki.hu ● ISSN 1589 1623 (Print) ● ISSN 1785 0037 (Online)
DOI: http://dx.doi.org/10.15666/aeer/2001_555569

2017). The northern parts of the Seyhan basin are in the Central Anatolia Region, the central and southern parts are in the Mediterranean Region (*Figure 1*). The most important settlements in the Seyhan basin are the cities of Kayseri, Nigde, Sivas, Mersin and Adana. The Seyhan basin is adjacent to Kizilirmak, Konya and the Eastern Mediterranean basins in the west, the Ceyhan and Euphrates River in the east (Republic of Turkey Ministry of Forestry and Water Affairs, 2017). The Ceyhan basin is neighbour to Seyhan Basin in the northwest, the Asi basin which is in the south and the Euphrates River basin which is in the northeast. The Gulf of Iskenderun surrounds the south part of the Seyhan basin. The Ceyhan basin area covers three main provinces (Kahramanmaras, Osmaniye and Adana). The Seyhan-Ceyhan Basins have similar climate conditions (Tanriverdi et al., 2010). In the lower parts of these basins, the climate is mainly the Mediterranean, while in the central and upper parts of the basins, the climate is mainly continental.

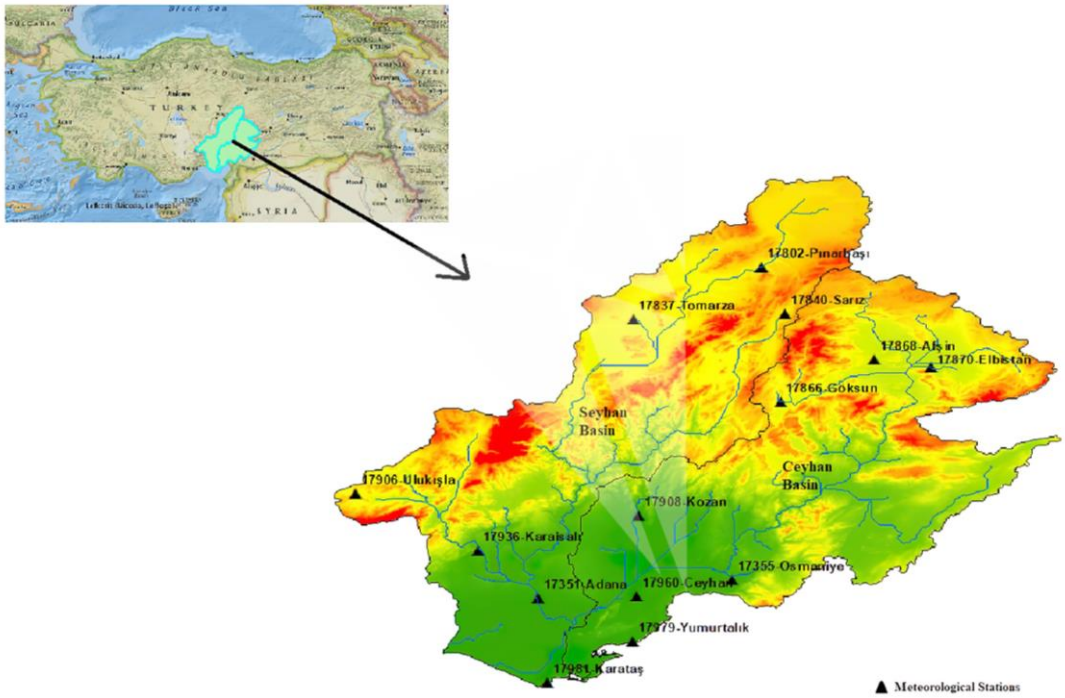

Figure 1. *The Seyhan-Ceyhan basins' geographical locations and distribution of the spatial meteorological stations*

Data Used

Drought analyses were performed using monthly data collected from 14 meteorological stations. Meteorological data were obtained from the Ministry of Agriculture and Forestry and General Directorate of Meteorology. The missing data was filled with the help of CRU-TS 4.04 (Climatic Research Unit Timeseries). As presented in *Table 1*, the geographical characteristics of meteorological stations, observation periods, monthly average temperatures and annual average precipitation values were considered in the drought analyses. SPI and SPEI analyses were conducted using observation data from January 1989 to July 2020.

http://www.aloki.hu ● ISSN 1589 1623 (Print) ● ISSN 1785 0037 (Online)
DOI: http://dx.doi.org/10.15666/aeer/2001_555569

Table 1. *Geographical features of meteorological stations, monthly average temperatures and annual average precipitation values for meteorological stations selected between January 1989 and July 2020*

Station ID	Station name	Altitude (m)	Latitude (N)	Longitude (E)	Monthly average Tmin (°C)	Monthly average Tmax (°C)	Annual average rainfall (mm)
Seyhan Basins Stations							
17351	Adana	23	37.0041	35.3443	14.6	25.5	655
17802	Pinarbasi	1542	38.7224	36.3924	1.2	15	392
17837	Tomarza	1402	38.4522	35.7912	0.6	16.2	380
17840	Sariz	1599	38.4781	36.5035	0.9	14.8	485
17936	Karaisali	240	37.2505	35.0628	14.1	24.3	862
17981	Karatas	22	36.5683	35.3894	15.5	23.5	777
17906	Ulukisla	1453	37.548	34.4867	4.4	16.4	326
Ceyhan Basins Stations							
17355	Osmaniye	94	37.1021	36.2539	12.7	24.7	811
17960	Ceyhan	48	37.0132	35.8055	12.6	25	719
17979	Yumurtalik	34	36.7801	35.7903	15.2	24.3	791
17866	Goksun	1344	38.024	36.4823	2.3	16.5	555
17868	Afsin	1230	38.2405	36.919	4.4	17.6	415
17870	Elbistan	1137	38.2038	37.1892	4.4	18.6	379
17908	Kozan	112	37.4337	35.8188	15.1	25.7	796

Methods

Standardized Precipitation Index

SPI is a drought index designed by McKee et al. (1993) and it is an essential tool in identifying periodic meteorological droughts using specific time-precipitation data as input parameter. SPI drought classes are obtained from precipitation series with (standard normal distribution) Gauss distribution (Gurler, 2017). Nevertheless, the probability distribution function of precipitation and data series does not usually match the normal distribution. The probability distribution that performs best on rainfall data is the Gamma probability distribution. According to McKee et al. (1993), distribution functions obtained from precipitation data are converted to Gamma probability distribution functions in the SPI method. The precipitation prediction probabilities derived from the Gamma probability distribution function are converted into normalized standard precipitation series with the help of the reverse standard normal distribution function. As a result, Standardized Precipitation Index is calculated using mean and variance.

SPI is measured as the ratio of the difference between the current and the average precipitation amounts to the standard deviation at a given time (McKee et al., 1993):

$$\mathrm{SPI} = \frac{x_i - x_j}{\sigma} \qquad \text{(Eq.1)}$$

where,
x_i : Current Precipitation
x_j : Average Precipitation
σ : Standart Deviation

http://www.aloki.hu ● ISSN 1589 1623 (Print) ● ISSN 1785 0037 (Online)
DOI: http://dx.doi.org/10.15666/aeer/2001_555569

Table 2 summarizes possible explanations for wet or dry conditions using the cumulative probabilities for the various SPI / SPEI values and the resulting SPI / SPEI values.

Table 2. *Classification of SPI / SPEI values*

SPI-SPEI	Classification
≥ 2.00	Extremely Wet
1.5 to 1.99	Severely Wet
1.0 to 1.49	Moderately Wet
0.5 to 0.99	Slightly Wet
-0.49 to 0.49	Near Normal
-0.99 to -0.5	Mild Dry
-1.49 to -1.0	Moderately Dry
-1.99 to -1.5	Severely Dry
≤ -2.00	Extremely Dry

Standardized Precipitation Evapotranspiration Index

SPEI is designed by Vicente-Serrano et al. (2010). SPEI method provides the point and spatial distribution by including the temperature, evaporation and perspiration parameters in addition to the drought calculations made using only precipitation data as the SPI method does. Thus, converting the original values to standard units, it provides spatial-temporal comparison and evaluation as a multi-temporal structure (Lorenzo-Lacruz et al., 2010; Vicente-Serrano et al., 2010; Beguería et al., 2014).

SPEI method, developed to overcome the limitations of the SPI method, can include factors like Palmer Drought Severity Index (PDSI), temperature and evaporation. The multiple-temporal structure of SPI method also allows inspections in long-term (6-12-24 month periods) projections (Republic of Turkey Ministry of Forestry and Water Affairs General Directorate of Water Management Department of Flood and Drought Management, 2015). The variation in rainfall is specified using the log-logistical distribution as standard (Liu et al., 2015). In applications performed in many parts of the world, a good relationship was between log-logistic distribution and rainfall variation series in different time scales and climatic areas. This is important for the effective use of the SPEI method (Vicente-Serrano et al., 2010).

SPEI standardizes the difference between Potential Evapotranspiration (PET) and precipitation (P), defining the degree of distortion of humid or dry conditions. SPEI is calculated by the potential evaporation data collected in specific periods with the difference between weekly or monthly rainfall and corresponding to a probability distribution function (Beguería et al., 2014). SPEI can effectively identify the water deficit with several time scales reflecting the lag relationship of different water sources, rainfall and evaporation (Liu et al., 2015).

The deficiency difference between rainfall, evapotranspiration and humidity cannot be positive. This is common in semi-dry and dry zones where the difference in moisture deficiency is negative. So, a three-parameter distribution is required to model open values (Hernandez and Uddameri, 2014). Three-parameter log-logistic distribution is more generally preferred than the normal distribution (Vicente-Serrano et al., 2010; Zambreski, 2016). While negative values of SPEI express aridity, positive values express above-average humidity and normal conditions.

http://www.aloki.hu ● ISSN 1589 1623 (Print) ● ISSN 1785 0037 (Online)
DOI: http://dx.doi.org/10.15666/aeer/2001_555569

Calculating SPEI:

(1) SPEI is measured as the difference (*D*) between Potential Evapotranspiration (PET) and Precipitation (*P*) on a monthly (or weekly) basis. PET is computed by the Hargreaves equation with limited data requirements and has no internal limitations of the Thornthwaite equation, which is similar to the standard Food and Agriculture Organization – Penman-Monteith Method (FAO PM) equation (Hargreaves, 1994; Hargreaves and Allen, 2003):

$$D_i = P_i - PET_i \tag{Eq.2}$$

where D_i is the water surplus or deficit for the analyzed month *i*.

(2) The next step is to compute the cumulative difference in different time scales between Precipitation (*P*) and PET. The computed D_i values are collected at different time scales with the same method as that for the SPI. For example, the cumulative difference can be calculated for one month in a specific year on a 12-month time scale as:

$$\text{If } j < k \; X_{i,j}^{k} = \sum_{l=13-k+j}^{12} D_{i-1,l} + \sum_{l=1}^{j} D_{i,l} \tag{Eq.3}$$

$$\text{If } j \geq k \; X_{i,j}^{k} = \sum_{l=j-k+1}^{j} D_{i,l} \tag{Eq.4}$$

where $D_{i,l}$ is the P − PET difference at the first month of year i, in millimeter and $X_{i,j}^{k}$ is the cumulative difference for a given *k* timescale in month *j* and year *i.*

(3) Normalization of $X_{i,j}^{k}$; because data can have negative values of $X_{i,j}^{k}$ in the unique data array. Therefore, the three parameters log-logistics probability capacity distribution is used by SPEI. The cumulative function *F(x)* of the logistic probability distribution for the data series of all time scales (Beguería et al., 2014).

$$F(x) = \left[1 + \left(\frac{a}{x - \gamma} \right)^{\beta} \right]^{-1} \tag{Eq.5}$$

The log-logistic distribution parameters could be computed by several methods. Among them, the process of possible-weighted moments is the most dependable and easily applicable method. Log-logistics parameters are necessary for realistic drought analysis and observations, as they provide temporal and spatial comparability of drought indices (Yu et al., 2014). α, β and γ are scale, shape and origin parameters, respectively and these could be computed with the equations used by Vicente-Serrano et al. (2010) SPEI calculation equations as *P* value are as follows:

$$P = 1 - F(x) \tag{Eq.6}$$

http://www.aloki.hu ● ISSN 1589 1623 (Print) ● ISSN 1785 0037 (Online)
DOI: http://dx.doi.org/10.15666/aeer/2001_555569

where P is the probability of exceeding a determined $X_{i,j}^{k}$ value is exceeded.

$$\text{If } P \le 0.5,\ W = \sqrt{-2\ln(P)}, \qquad \text{SPEI} = W - \frac{C_0 + C_1 W + C_2 W^2}{1 + d_1 W + d_2 W^2 + d_3 W^3} \qquad \text{(Eq.7)}$$

$$\text{If } P > 0.5,\ W = \sqrt{-2\ln(1-P)},\ \text{SPEI} = \frac{C_0 + C_1 W + C_2 W^2}{1 + d_1 W + d_2 W^2 + d_3 W^3} - W \qquad \text{(Eq.8)}$$

where the variables $C_0 = 2.515517$, $C_1 = 0.802853$, $C_2 = 0.010328$, and $d_1 = 1.432788$, $d_2 = 0.189269$, $d_3 = 0.001308$ are constants (Vicente-Serrano et al., 2010).

The computed values of SPEI in the basin are used to examine the characteristics of dry and wet events in the basin according to their occurrence time, severity and frequency of occurrence. These values are categorized as in *Table 2*. The threshold ranges used are SPEI ≤ -1 for the dry event and SPEI ≥ 1 for the wet event. The period of an event is the time (months) during which the SPEI is equal to or less than the consecutive cut-off level (Gao et al., 2017; Polong et al., 2019).

Results and Discussion

Drought analysis was performed using meteorological data in the Seyhan-Ceyhan basins. SPI and SPEI are calculated for 3-, 4-, 6-, 12-month periods using meteorological data from January 1989 to July 2020. While calculating SPI only precipitation data was used but SPEI was calculated using precipitation data, values of minimum and maximum temperature. SPI and SPEI values were evaluated according to the drought classes in *Table 2*. However, since the direct evaporation data of the stations in the basins are not complete and there are no continuous data records, SPEI analysis was done with temperature data. Distributions of SPI and SPEI according to 3-, 4-, 6- and 12-month analyses are shown in *Figures 2 and 3*. The climatic conditions of the basins generally reveal similar characteristics and the yearly-based SPI and SPEI values appear to be consistent as shown *Figure 3*. Due to the compatibility of the topographic features and precipitation data of these basins, a joint evaluation was made for basins.

The coefficient of determination (R^2) between annual SPI and SPEI drought indices was found to be 0.954 for the analysis of approximately 30 years' meteorological data of the Seyhan and Ceyhan basins (*Figure 4*).

Considering period between January 1989 and July 2020, the highest degree of drought values was found between March and July 1989 in the SPI and SPEI evaluations calculated for 3-month periods. Continuous long-term drought was observed between November 2013-June 2014. As a result of the drought assessments using SPI values calculated based on 3-months periods indicated that 3.7%, 3.4%, 7.7% and 16.4% of the periods were to be Extremely Dry, Severely Dry, Moderately Dry, Mild Dry. The same assessment for SPEI showed 1.6%, 4.2%, 10.6% and 15.4% of the whole period were to be Extremely Dry, Severely Dry, Moderately Dry, Mild Dry. When the SPI was evaluated for each season, it was found that 20 months between September 2011 and July 2014 and 15 months between November 2015 and December 2017 were dry. Seasonal SPEI assessments were found to be dry for 21 months between

http://www.aloki.hu ● ISSN 1589 1623 (Print) ● ISSN 1785 0037 (Online)
DOI: http://dx.doi.org/10.15666/aeer/2001_555569

September 2011 and July 2014 and for 18 months between November 2015 and December 2017.

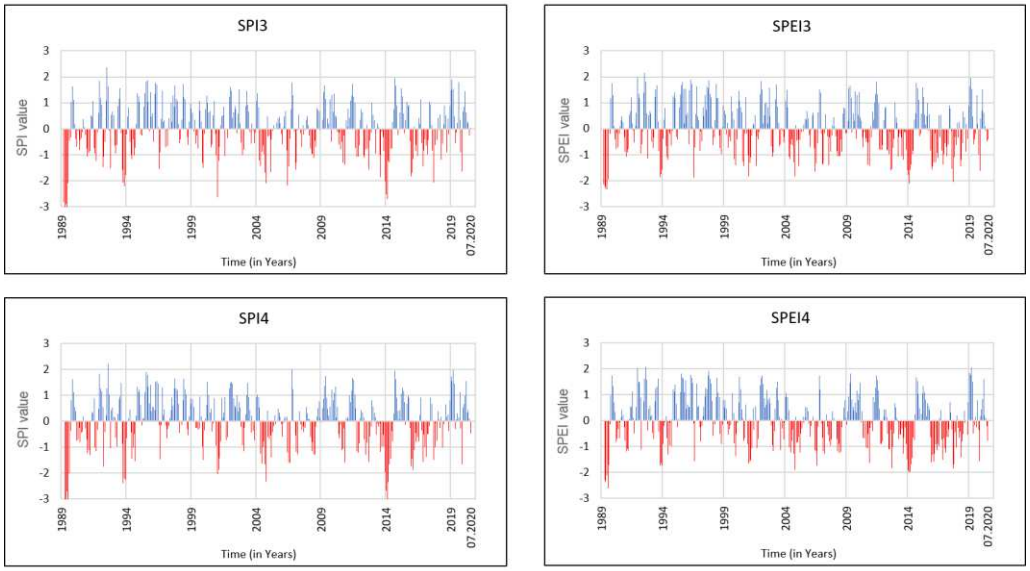

Figure 2. *Result of SPI and SPEI values at 3-month, 4-month time scales between January 1989 and July 2020 time frame in study area*

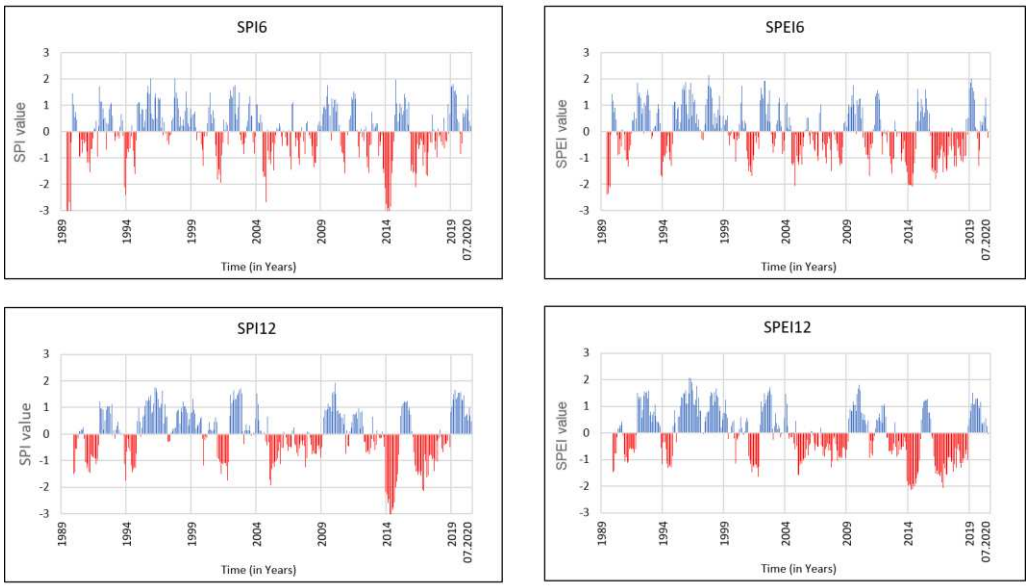

Figure 3. *Result of SPI and SPEI values at 6-month, 12-month time scales between January 1989 and July 2020 time frame in study area*

When the SPI and SPEI values were evaluated by taking 4-month periods, it was determined that the period with the highest degree of drought was between April and August 1989. When the SPI is calculated by taking 4-month periods and drought analyses are made, 3.5%, 4.0%, 9.3% and 10.9% of the time period was determined as Extremely Dry, Severely Dry, Moderately Dry and Mild Dry, respectively when

http://www.aloki.hu ● ISSN 1589 1623 (Print) ● ISSN 1785 0037 (Online)
DOI: http://dx.doi.org/10.15666/aeer/2001_555569

compared to the total time examined. Analyses using the same periods for SPEI showed that 1.3%, 5.9%, 9.6% and 16.5% of the total time were determined as Extremely Dry, Severely Dry, Moderately Dry and Mild Dry, respectively. In the 4-month evaluations of the SPI, it was found that it was dry for 17 months between May 2012-July 2014 and dry for 15 months between December 2015-December 2017. In the 4-month evaluations of SPEI, it was determined that 19 months between May 2012 and July 2014 and 18 months between December 2015 and December 2017 were dry.

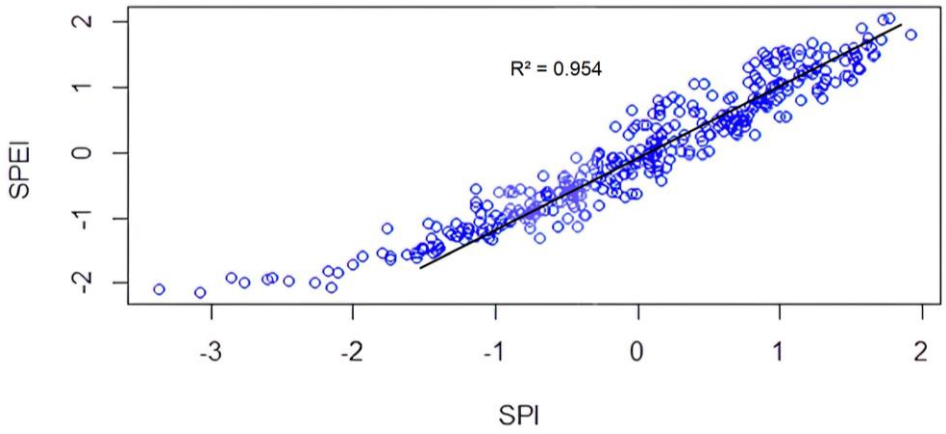

Figure 4. *Scatter plot showing linear relationship between annual SPI and SPEI*

6-month based evaluations of SPI and SPEI revealed that the period with the highest severity of drought was between June-September 1989. SPI values calculated for 6-month periods further showed that 3.7%, 4.5%, 5.9% and 13.1% of the time interval examined within the scope of the project were Extremely Dry, Severely Dry, Moderately Dry and Mild Dry months, respectively and between October 2013-July 2014 were determined as the period with the highest degree of drought. Based on SPEI's 6-month-based assessment, the longest continuous dry months are from December 2015 to April 2017. According to the calculated SPEI values, 2.4%, 4.0%, 10.7% and 15.8% of all months were found to be Extremely Dry, Severely Dry, Moderately Dry and Mild Dry months, respectively. For SPI, 24 months between July 2004 and September 2008, 13 months between July 2012 and July 2017 and 13 months between December 2015 and April 2017 were determined as dry months. When the same evaluation was made for 12-month periods for SPI, 27 months between January 2005-2009, 19 months between June 2012-December 2014 and 24 months between February 2016-May 2018 were observed as dry periods.

In the evaluations of SPI with 12-month data, the highest drought severity range was found between December 2013-2014. As a result of SPI's 12-month drought evaluations, when it is compared with the total number of months, 3.3%, 3.3%, 10.1% and 13.3% of the months were determined as Extremely Dry, Severely Dry, Moderately Dry and Mild Dry, respectively. On the other hand, according to the evaluation made for SPEI with the same data, the long continuous dry months are the months between February 2016 and October 2017. SPEI's 12-month data assessments showed that the largest drought severity was between November 2013 and December 2014. As a result of SPEI's 12-month drought evaluations, 0.8%, 5.2%, 12.0% and 18.2% of the months were determined as Extremely Dry, Severely Dry, Moderately Dry and Mild Dry,

http://www.aloki.hu ● ISSN 1589 1623 (Print) ● ISSN 1785 0037 (Online)
DOI: http://dx.doi.org/10.15666/aeer/2001_555569

respectively. Also, the longest dry months, according to SPEI, are from February 2016 to November 2018.

The ratio of dry periods to total periods in the drought evaluations of the study area, in the 3-month evaluations SPI-3 31.2% and SPEI-3 31.8%, in the 4-month evaluations SPI-4 27.7% and SPEI-4 33.3%, in the 6-month evaluations SPI-6 27.2% and SPEI-6 32.9%, in 12-month evaluations SPI-12 30.0% and SPEI-12 36,2% were determined. According to the monthly evaluations, it was seen that SPI determined the number of extremely dry months higher than SPEI. On the other hand, SPEI found the total number of dry months higher than SPI. In some years, differences were observed between SPI and SPEI regardless of time scale. SPEI has identified longer drought periods than SPI. The fact that SPEI determines the drought duration longer than SPI can be explained by the fact that evapotranspiration places demand on available water and its effect is felt most under water scarcity conditions. The results show that although decreased precipitation is the main driver of drought, the effect of temperature through evaporative water demand plays a role in determining droughts. Moreover, an increase in the number of Severely Dry, Moderately Dry, Mild Dry months was observed in the SPEI assessments. When the evapotranspiration effect was calculated, it was observed that the total number of dry months was high. Compared to SPEI, drought thresholds peak on more SPI graphs. Most of the wet months in these time frames are months that are classified as slightly and moderately wet. In the long-term drought analysis, SPEI reflects the drought impacts more successfully than SPI.

Vicente-Serrano et al. (2010) proved that SPI could not determine the role of temperature rise in future drought conditions. They explained the potential impacts of temperature changes and excessive temperatures in terms of global warming. Although determining the effect of evapotranspiration in drought conditions is very complex, they emphasized its inclusion in drought index calculations. Considering the additional data requirements of SPEI, it is more likely that SPI can be used to identify, analyze and monitor droughts in any climatic zone of the world (Vicente-Serrano et al., 2010; Beguería et al., 2014). Mathbout et al. (2018) confirmed the effect of PET index in calculating the severity of drought compared to the SPEI analysis. Stagge et al. (2014) stated in their research that the SPI proposed by the World Meteorological Organization (WMO) has significant potential as a variant of the SPEI meteorological drought index. As a justification, they showed that SPEI provides a more comprehensive water asset measurement and uses climatic water balance. Li et al. (2015) characterized drought conditions in southwestern China using SPEI and SPI in their study. In their study, they performed a correlation analysis between two remote sensing-based drought indices to study the performance of SPEI and SPI. They also found that SPEI gave better results than SPI. Nedealcov et al. (2015) compared the SPEI and SPI indices for the temporal and spatial distributions of drought in three and six-month periods for Moldova between 1980-2014 time scale. They stated that both indices gave similar shapes in temporal distributions, but there were differences between the two indices due to the fact that the SPEI values in terms of drought duration and severity use not only precipitation but also evapotranspiration. Danandeh Mehr and Vaheddoost (2020) stated that they observed similar drought events in their short-term (3-month) analysis between SPI and SPEI. In particular, SPI and SPEI found inconsistency between each other at 6 and 12 month time frames. Tefera et al. (2019) revealed that SPI can be used instead of SPEI at all time scales in their study. Therefore, they indicated that it is safer to use the SPI to

http://www.aloki.hu ● ISSN 1589 1623 (Print) ● ISSN 1785 0037 (Online)
DOI: http://dx.doi.org/10.15666/aeer/2001_555569

assess the drought in the study area at all studied time scales in the absence of temperature data and/or appropriate analysis tools to performing the SPEI.

Considering the annual values for SPI-12 and SPEI-12, 2014 was the driest year compared to the years examined in the drought classification. Drought intensity and the number of dry months in 2014 are remarkable in both indices. According to the SPI-12 and SPEI-12 annual drought classification results shown in *Figure 3*, the analysis results of the driest and wettest years are given in detail in *Table 3a-b*. In SPI-12 analyses, the driest years after 2014 were observed as 2005, 2016, 2001 and 2017, respectively. For SPEI-12, the driest years after 2014 were observed as 2016, 2017, 2001, 2005, respectively.

Table 3-a. *Classification of the driest years to their months' drought characteristic according to SPI-12 and SPEI-12 analysis of study area between January 1989 and July 2020*

SPEI-12 Analysis Result of the Driest Years					
Year	Extremely Dry	Severely Dry	Moderately Dry	Mild Dry	Near Normal
2014	2	8	2		
2016	1	5	4	1	1
2017		2	6	4	
2001		1	9	1	1
2005		2	4	4	2
SPI-12 Analysis Result of the Driest Years					
Year	Extremely Dry	Severely Dry	Moderately Dry	Mild Dry	Near Normal
2014	9	2		1	
2005	2	5	4	1	
2016	2	2	5	2	1
2001		2	7	3	
2017		2	3	6	1

Table 3-b. *Classification of the wettest years to their months' drought characteristic according to SPI-12 and SPEI-12 analysis of study area between January 1989 and July 2020*

SPEI-12 Analysis Result of the Wettest Years					
Year	Extremely Wet	Severely Wet	Moderately Wet	Slightly Wet	Near Normal
1996	2	3	6	1	
1992		4	5	3	
2019		1	8	3	
2002		3	6	2	1
1998		2	6	3	1
SPI-12 Analysis Result of the Wettest Years					
Year	Extremely Wet	Severely Wet	Moderately Wet	Slightly Wet	Near Normal
2019		5	7		
2002		5	6		1
1996		4	4	3	1
2015			6	5	1
2009		2	3	5	2

http://www.aloki.hu ● ISSN 1589 1623 (Print) ● ISSN 1785 0037 (Online)
DOI: http://dx.doi.org/10.15666/aeer/2001_555569

SPI-12 annual data identified 2019 as the wettest year among the years analyzed in the drought classification. Except for 2019, the wettest years were observed as 2002, 1996, 2015 and 2009, respectively. According to SPEI-12, 1996 was the wettest year compared to the years examined in the drought classification. Other than 1996, the wettest years were 1992, 2019, 2002 and 1998, respectively. SPI and SPEI differed in annual estimates when evaporation was calculated based on the temperature factor and sorted by rainy and dry years. Both indices found the same dry years but found the wettest years mildly different from each other.

The use of potential evapotranspiration in SPEI represents the water balance of a zone and therefore the severity of drought better than SPI. The weakness of analysis with SPEI is that it may not respond immediately to rapidly developing and short-term drought events. The strongest aspect of the SPI method is that it can be computed using just rainfall data. The SPI is partially inefficient as it uses only precipitation data as input and does not take into account the total water balance of a region and the temperature component that is important to water use. SPEI and SPI indices should be analyzed by comparing drought monitoring maps produced using remote sensing methods. In this way, a more comprehensive analysis can be made with both temporal and spatial drought analysis.

Conclusions

In this study, multiple monthly-based (3-, 4-, 6-, 12- month based) drought analyses were conducted based on SPI and SPEI drought indices calculated from meteorological data of the Seyhan and Ceyhan basins between January 1989 and July 2020 and the calculated SPI and SPEI results were compared. Drought indices used in the study are widely used throughout the world as a tool in hydrological, meteorological and agricultural drought analyses, defining long-term drought events, determining the beginning and ending times and measuring the severity. These analyses reveal that increase of dry months' number and duration after the 2000s is remarkable. The results of these analysis show that there is a significant drought risk when analyzed on an annual basis. The non-dry years in the basins are mainly in the moderately wet class. Calculated drought indices reveal that 2014 was the driest year on an annual basis. Other factors affecting the increase in drought in the last decade should be investigated and the environmental, economic and social effects of drought need to be determined in detail. A drought mitigation plan is needed in the area to promote the sustainable use of agricultural and natural water resources and mitigate the effects of future drought events. In order to determine regional droughts, analyses should be continued with remote sensing images and input parameters measured at stations, e.g., humidity, solar radiation.

REFERENCES

[1] Ahsan, M. M. (2020a): Desertification in the OIC Member Countries: Factors, Challenges and the Way Forward. – Journal of Bartin Faculty of Forestry 22(2): 642-653. DOI: 10.24011/barofd.731741.

[2] Ahsan, M. M. (2020b): Climate Change Adaptation-Based Strategies on Water and Its Security: A Study on Dhaka and Ankara. – The Journal of Security Sciences Special

http://www.aloki.hu ● ISSN 1589 1623 (Print) ● ISSN 1785 0037 (Online)
DOI: http://dx.doi.org/10.15666/aeer/2001_555569

Volume (International Security Congress Special Issue), pp. 79-93. DOI: 10.28956/gbd.695924.

[3] Alley, W. M. (1984): The Palmer Drought Severity Index: Limitations and Assumptions. – Journal of Climate and Applied Meteorology 23(7): 1100-1109. DOI: 10.1175/1520-0450(1984)023<1100:tpdsil>2.0.co;2.

[4] Beguería, S., Vicente-Serrano, S. M., Reig, F., Latorre, B. (2014): Standardized precipitation evapotranspiration index (SPEI) revisited: parameter fitting, evapotranspiration models, tools, datasets and drought monitoring. – International Journal of Climatology 34(10): 3001-3023. DOI: 10.1002/joc.3887.

[5] Chang, T. J., Kleopa, X. A. (1991): A Proposed Method for Drought Monitoring. – Journal of the American Water Resources Association 27(2): 275-281. DOI: 10.1111/j.1752-1688.1991.tb03132.x.

[6] Danandeh Mehr, A., Vaheddoost, B. (2020): Identification of the trends associated with the SPI and SPEI indices across Ankara, Turkey. – Theoretical and Applied Climatology 139(3-4): 1531-1542. DOI: 10.1007/s00704-019-03071-9.

[7] Gao, X., Zhao, Q., Zhao, X., Wu, P., Pan, W., Gao, X., Sun, M. (2017): Temporal and spatial evolution of the standardized precipitation evapotranspiration index (SPEI) in the Loess Plateau under climate change from 2001 to 2050. – Science of The Total Environment 595: 191-200. DOI: 10.1016/j.scitotenv.2017.03.226.

[8] Gumus, V., Algin, H. M. (2016): Meteorological and hydrological drought analysis of the Seyhan−Ceyhan River Basins, Turkey. – Meteorological Applications 24(1): 62-73. DOI: 10.1002/met.1605.

[9] Gurler, C. (2017): Beysehir and Konya-Cumra-Karapinar Sub-Basins. – Hydrological Drought Assessment with the Standardized Indices Approach. Publication in Turkish.

[10] Hargreaves, G. H. (1994): Defining and Using Reference Evapotranspiration. – Journal of Irrigation and Drainage Engineering 120(6): 1132-1139. DOI: 10.1061/(asce)0733-9437(1994)120:6(1132).

[11] Hargreaves, G. H., Allen, R. G. (2003): History and Evaluation of Hargreaves Evapotranspiration Equation. – Journal of Irrigation and Drainage Engineering 129(1): 53-63. DOI: 10.1061/(asce)0733-9437(2003)129:1(53).

[12] Hernandez, E. A., Uddameri, V. (2014): Standardized precipitation evaporation index (SPEI)-based drought assessment in semi-arid south Texas. – Environmental Earth Sciences 71(6): 2491-2501. DOI: 10.1007/s12665-013-2897-7.

[13] Homdee, T., Pongput, K., Kanae, S. (2016): A comparative performance analysis of three standardized climatic drought indices in the Chi River basin, Thailand. – Agriculture and Natural Resources 50(3): 211-219. DOI: 10.1016/j.anres.2016.02.002.

[14] Li, X., He, B., Quan, X., Liao, Z., Bai, X. (2015): Use of the Standardized Precipitation Evapotranspiration Index (SPEI) to Characterize the Drying Trend in Southwest China from 1982–2012. – Remote Sensing 7(8): 10917-10937. DOI: 10.3390/rs70810917.

[15] Liu, X., Wang, S., Zhou, Y., Wang, F., Li, W., Liu, W. (2015): Regionalization and Spatiotemporal Variation of Drought in China Based on Standardized Precipitation Evapotranspiration Index (1961–2013). – Advances in Meteorology. DOI: 10.1155/2015/950262.

[16] Lorenzo-Lacruz, J., Vicente-Serrano, S. M., López-Moreno, J. I., Beguería, S., García-Ruiz, J. M., Cuadrat, J. M. (2010): The impact of droughts and water management on various hydrological systems in the headwaters of the Tagus River (central Spain). – Journal of Hydrology 86(1-4): 13-26. DOI: 10.1016/j.jhydrol.2010.01.001.

[17] Mathbout, S., Lopez-Bustins, J. A., Martin-Vide, J., Bech, J., Rodrigo, F. S. (2018): Spatial and temporal analysis of drought variability at several time scales in Syria during 1961–2012. – Atmospheric Research 200: 153-168. DOI:10.1016/j.atmosres.2017.09.016.

http://www.aloki.hu ● ISSN 1589 1623 (Print) ● ISSN 1785 0037 (Online)
DOI: http://dx.doi.org/10.15666/aeer/2001_555569

[18] McKee, T. B., Doesken, N. J., Kleist, J. (1993): The relationship of drought frequency and duration to time scales. – Paper presented at 8th Conference on Applied Climatology, Am. Meteorol. Soc., Anaheim, California, pp. 17-22.
[19] Mishra, A. K., Singh, V. P. (2010): A review of drought concepts. – Journal of Hydrology 391(1-2): 202-216. DOI: 10.1016/j.jhydrol.2010.07.0121.
[20] Nedealcov, M., Răileanu, V., Sîrbu, R., Cojocari, R. (2015): The Use of Standardized Indicators (SPI and SPEI) In Predicting Droughts Over the Republic Of Moldova Territory. – Present Environment and Sustainable Development 9(2): 149-158. DOI: 10.1515/pesd-2015-0032.
[21] Olukayode Oladipo, E. (1985): A comparative performance analysis of three meteorological drought indices. – Journal of Climatology 5(6): 655-664. DOI: 10.1002/joc.3370050607.
[22] Polong, F., Chen, H., Sun, S., Ongoma, V. (2019): Temporal and spatial evolution of the standard precipitation evapotranspiration index (SPEI) in the Tana River Basin, Kenya. – Theoretical and Applied Climatology 138(1-2): 777-792. DOI: 10.1007/s00704-019-02858-0.
[23] Republic of Turkey Ministry of Forestry and Water Affairs (2017): Project on Preparation of Seyhan Basin Sectoral Water Allocation Plan. – Publication in Turkish.
[24] Republic of Turkey Ministry of Forestry and Water Affairs General Directorate of Water Management Department of Flood and Drought Management (2015): Akarcay Basin Drought Management Plan Drought Indices, Indicators and Threshold Values Detection Report. – publication in Turkish.
[25] Stagge, J. H., Tallaksen, L. M., Xu, C. Y., Van Lanen, H. A. J. (2014): Standardized precipitation-evapotranspiration index (SPEI): Sensitivity to potential evapotranspiration model and parameters. – In: IAHS-AISH Proceedings and Reports 363: 367-373.
[26] Tanrıverdi, Ç., Alp, A., Demirkıran, A. R., Üçkardeş, F. (2009): Assessment of surface water quality of the Ceyhan River basin, Turkey. – Environmental Monitoring and Assessment 167(1-4): 175-184. DOI: 10.1007/s10661-009-1040-4.
[27] Tao, H., Borth, H., Fraedrich, K., Su, B., Zhu, X. (2013): Drought and wetness variability in the Tarim River Basin and connection to large-scale atmospheric circulation. – International Journal of Climatology 34(8): 2678-2684. DOI: 10.1002/joc.3867.
[28] Tefera, A. S., Ayoade, J. O., Bello, N. J. (2019): Comparative analyses of SPI and SPEI as drought assessment tools in Tigray Region, Northern Ethiopia. – SN Applied Sciences 1(10): 1265. DOI: 10.1007/s42452-019-1326-2.
[29] Vicente-Serrano, S. M., Beguería, S., López-Moreno, J. I. (2010): A Multiscalar Drought Index Sensitive to Global Warming: The Standardized Precipitation Evapotranspiration Index. – Journal of Climate 23(7): 1696-1718. DOI: 10.1175/2009jcli2909.1.
[30] Wang, Y., Liu, G., Guo, E. (2019): Spatial distribution and temporal variation of drought in Inner Mongolia during 1901–2014 using Standardized Precipitation Evapotranspiration Index. – Science of The Total Environment 654: 850-862. DOI: 10.1016/j.scitotenv.2018.10.425.
[31] Wilhite, D. A., Glantz, M. H. (1985): Understanding: The Drought Phenomenon: The Role of Definitions. – Water International 10(3): 111-120. DOI: 10.1080/02508068508686328.
[32] Yu, M., Li, Q., Hayes, M. J., Svoboda, M. D., Heim, R. R. (2014): Are droughts becoming more frequent or severe in China based on the Standardized Precipitation Evapotranspiration Index: 1951-2010? – International Journal of Climatology 34(3): 545-558. DOI: 10.1002/joc.3701.
[33] Zambreski, Z. T. (2016): A Statistical Assessment of Drought Variability and Climate Prediction for Kansas. – Master of Science Thesis, Department of Agronomy, Kansas State University, Manhattan, Kansas.

http://www.aloki.hu ● ISSN 1589 1623 (Print) ● ISSN 1785 0037 (Online)
DOI: http://dx.doi.org/10.15666/aeer/2001_555569

[34] Zhang, A., Jia, G. (2013): Monitoring meteorological drought in semiarid regions using multi-sensor microwave remote sensing data. – Remote Sensing of Environment 134: 12-23. DOI: 10.1016/j.rse.2013.02.023.

[35] Zhou, Y., Li, N., Ji, Z., Gu, X., Fan, B. (2013): Temporal and Spatial Patterns of Droughts Based on Standard Precipitation Index (SPI) in Inner Mongolia during 1981-2010. – Journal of Natural Resources 28(10): 1694-1706. DOI: 10.11849/zrzyxb.2013.10.005.

http://www.aloki.hu ● ISSN 1589 1623 (Print) ● ISSN 1785 0037 (Online)
DOI: http://dx.doi.org/10.15666/aeer/2001_555569

DISTRIBUTION OF MARINE DEBRIS DURING COVID-19 PANDEMIC AT A PRISTINE ISLAND ON THE ANDAMAN SEA, THAILAND

SORNPLANG, K.[1,2] – NITIRATSUWAN, T.[3] – TOWATANA, P.[1,2] – PRADIT, S.[1,2*]

[1]*Coastal Oceanography and Climate Change Research Center, Faculty of Environmental Management, Prince of Songkla University, Hat Yai, Songkhla, 90110, Thailand*

[2]*Marine and Coastal Resources Institute, Faculty of Environmental Management, Prince of Songkla University, Hat Yai, Songkhla, 90110, Thailand*

[3]*Faculty of Science and Fisheries Technology, Rajamangala University of Technology Srivijaya, Trang Campus, Sikao, Trang,-92150, Thailand*

**Corresponding author*
e-mail: siriporn.pra@psu.ac.th

(Received 23rd Sep 2021; accepted 23rd Nov 2021)

Abstract. The study was conducted with an exploratory study design to explore the amount of debris around beaches on Libong Island, Thailand. Libong Island is one of the significant tourist attractions in Trang Province. The study was conducted by collecting samples from 4 areas during February, June, September and December 2020. The findings from the study showed that 1,580 items of debris were found with a total weight of 44,744 g. The most common debris found included hard plastic glass, fabric, and fibre, respectively. Thung Ya Kha Beach was the beach where the highest amount of debris was found. The largest quantity of debris (692 items) was found in June, followed by 404 items in February, 274 items in September, and 210 items in December. Based on this study, the outstanding debris was comprised of plastic, including 87 types of plastic, both hard and soft varieties, totaling 805 items. No COVID-19 related products were found on the beach, possibly due to a government emergency declaration. Regarding the closure of beaches and the country's lockdown, there were few Thai tourists. There were no foreign tourists in June or September. The result of the waste separation that the major activity causing waste was shoreline and recreation activity.
Keywords: *marine litter, microplastic, seagrass, plastic, tourist*

Introduction

The amount of waste around the world is constantly increasing as a result of human production and consumption. Seas and oceans play an important role in the long-distance transport of substances and materials, governing the substance and material budget among all the continents. Oceans not only transport heat and chemical compounds but also solid objects and particles floating on or near the surface of water or suspended solids including the spread of life (Maximenko et al., 2019). Seas and oceans are currently threatened by anthropogenic activities resulting in ocean changes, such as rising ocean temperatures and sea level, ocean acidification, biodiversity loss including various pollutants especially plastic pollution (Cauwenberghe et al., 2013). By the middle of the 20th century, there was an increase in commercial plastic production (Geyer et al., 2017; Maximenko et al., 2019). There are 4.8-12.7 million tons of plastic waste transferred from land into the sea (Jambeck et al., 2015). Most of the waste is plastic. It has spread to different areas from the influence of ocean currents and accumulate in the environment, open oceans, coasts and islands, as well as in the deep

http://www.aloki.hu ● ISSN 1589 1623 (Print) ● ISSN 1785 0037 (Online)
DOI: http://dx.doi.org/10.15666/aeer/2001_571586

sea (Barnes et al., 2009). This affects the economy, environment, creatures on the coast and in the sea and poses danger to human health (Cauwenberghe et al., 2013; Sheavly, 2007). Over time, these plastic wastes are broken into small pieces. These fragmented plastic wastes are called microplastics (Claessens et al., 2013).

At present, marine debris and microplastics are a major global problem which was mentioned in the Decade of Ocean Science for Sustainable Development (2021–2030) (UNESCO, 2019), proclaimed by the United Nations. As for the Sustainable Development Goals Goal 14.1 aims to prevent and reduce marine pollution of all kinds including marine debris by 2025 (United Nations, 2019). Which prioritizes regional maritime work and collaborating with the G20 Action Plan on Marine Litter. In Thailand, policy recommendations have been made on urgent issues of national interest at sea. Recommendations on marine waste management were presented, which were divided into three main areas: prevention, problem solving and education including: 1) Increasing the capacity of waste collection. The government has to increase waste collection services by waste sorting thoroughly in all communities, both on land and coast, as well as collect garbage on time and regularly, etc. 2) Promoting education. The government must create awareness among the people by publicizing the serious situation of land and marine waste. Marine debris has to be studied and collected in accordance with international principles such as the International Coastal Clean-up (ICC). The obtained information will be definitely used for efficient waste management. Studies on the sources, effects and solutions to the microplastic problem should be carried out as well. People need to be trained on marine debris and microplastics, etc. (Marine Knowledge Database, 2018). In addition, Thailand's roadmap on plastic waste management 2018–2030 to reduce and stop using some types of plastic and recycle them as much as possible (Pollution Control Department, 2018).

However, measures to reduce the amount of plastic waste have changed. Due to the COVID-19 outbreak, the WHO Emergency Committee declared a global health emergency on January 30, 2020, following the high rates of COVID-19 cases in China and other countries. Global Increase (Velavan and Meyer, 2020). Therefore, it is expected that the problem of plastic waste will become more severe both from excessive use and the consumption of single-use plastics (Silva et al., 2021), as well as an increase in the demand for personal protective equipment (PPE) such as masks, rubber gloves, etc., which will also be accompanied by PPE waste after consumption (Okuku et al., 2021). As for Thailand, the first case of COVID-19 was reported on January 12, 2020 (Department of Disease Control, 2020). Therefore, the country has been locked with the government declaring a state of emergency follow by Regulation Issued under Section 9 of the Emergency Decree on Public Administration in Emergency Situations B.E. 2548 (2005) (No. 1). Announced on 25 March 2020 consists of measures do not enter the risk area closing of places that are at risk of disease, such as service places natural attractions, etc., closing the channel into the kingdom. People who are at high risk to stay in housing including refraining from traveling across areas, etc. (Royal Thai Government Gazette, 2020) and canceling measures on 29 May 2020

Libong Island, Trang province, is a coastal community living on fishery resources. Sources of the biggest seagrass beds in Thailand are near the island. It is a significant tourist attraction of Trang province. This is the first study conducted in Thailand around coastal areas of the island having the important ecosystem seagrass and tourist attractions with and without owners, where coastal community-based are located. Therefore, the researchers were interested in studying the type, amount and abundance

http://www.aloki.hu ● ISSN 1589 1623 (Print) ● ISSN 1785 0037 (Online)
DOI: http://dx.doi.org/10.15666/aeer/2001_571586

of marine debris on the beaches of Libong Island annually. During the COVID-19 situation of Thailand, since before the lockdown after and before the new wave of COVID-19 outbreak in early 2021. The study result would certainly provide valuable basic information about waste which leads to finding ways to manage marine debris and microplastics in an island ecosystem to prevent and reduce their impacts on fragile ecosystems and living things.

Materials and methods

Selection of the study area

Libong Island is located in Thailand at latitude 07°14'-07°17' N and longitude 99° 22'-09° 27' E, in Trang Province, roughly 2-3 km from the mainland coast. It is an important tourist attraction in Trang Province. There is a large seagrass source which is the food of the dugong around the island. Libong Island is currently in the Libong Islands Non-Hunting Area, Department of National Parks, Wildlife, and Plant Conservation. Thus, different study areas of four beaches were selected for marine debris collection in this investigation, comprising two to the east and two to the west of Libong Island (*Fig. 1*).

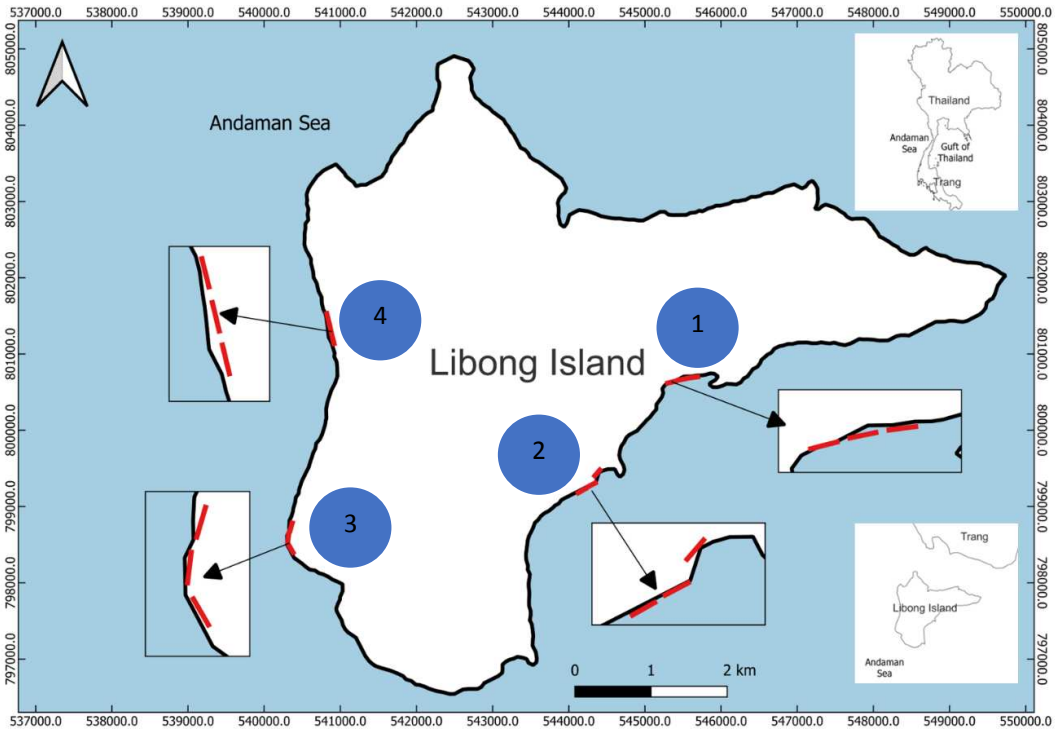

Figure 1. *Map of Libong Island with the location of the marine debris collection area: 1 Thung Chin Beach, 2 Libong Camp, 3 Ban Lung Khao and 4 Thung Ya Kha Beach*

(1) Thung Chin Beach

Thung Chin Beach (latitude 7°14'35.961"N longitude 99°24'43.395"E) is to the east of Libong Island, 1 km away to the east of the Ban Khok Sathon Village with a coastline about 1 km long. The coastline is sand mixed with shell fragments and next to

http://www.aloki.hu ● ISSN 1589 1623 (Print) ● ISSN 1785 0037 (Online)
DOI: http://dx.doi.org/10.15666/aeer/2001_571586

the sandy beach into the sea is a mud beach. There are mangroves growing in this area and next to the muddy beach into the sea is a seagrass area, which is 200 m to 1,500 m away from the coastline. It covers a total area of 2,616.8 ha. One unregulated waste disposal site is located approximately 500 m before reaching Thung Chin Beach. Villagers use the beach as a passageway for local fishing (lobster, shellfish, crab nets) around the seagrass area.

(2) Libong Camp

Libong Camp (latitude 7°14'35.961"N longitude 99°24'43.395"E) is on the east side of Libong Island, next to Thung Chin Beach to the south of the island with a 1-km coastal length. The coastline is sand mixed with shell debris. Next to the sandy beach into the sea are rocky and muddy beaches. Next to the mud beach is seagrass (Pradit et al., 2020a,b), with the beachhead area being residential and vacant. In the middle of the beach is the Libong Camp hostel, while at the end of the beach is a cove for a small fishing port in conjunction with a residential area. In addition, villagers use this area for local fishing (collecting shellfish) in the seagrass area.

(3) Ban Lung Khao

Ban Lung Khao (latitude 7°13'28.291"N longitude 99°21'54.657"E) is to the west of Libong Island. It has a coastline length of about 800 m. The coastline is sandy. The beach area is a residential area and a small fishing port, which tends to be influenced by high sea waves, causing coastal erosion. Hence, bamboo pole breakwater has been constructed all along the beachhead. In the middle and the end of the beach are hotels and homestays for tourists. The coast is used for leisure activities by tourists during the summer, such as swimming, sunbathing, etc. In addition, villagers take advantage by finding shellfish nearby and on the rocky beaches during low tide.

(4) Thung Ya Kha Beach

Thung Ya Kha Beach (latitude 7°14'58.019"N longitude 99°22'12.728"E) is on the west side of Libong Island and is located in the north of Ban Lung Khao with a coastline length of about 800 m. The coastline is a fine sandy beach. The coast is used for leisure activities by tourists during the summer including walking, taking pictures, etc. The steep slope of the beach is generated by the strong waves of the sea and therefore makes it unsuitable for swimming.

Survey method

Four sampling periods were conducted to cover all seasons in 2020. The Andaman coast is influenced by the southwest monsoon. May to mid-October experiences heavy rain, waves, and strong winds in the sea and therefore is not suitable for tourism, whereas mid-October to February is the tourist season for Libong Island (Department of Marine and Coastal Resources, 2013). Due to the COVID-19 pandemic, Thailand had a nationwide lockdown from April to May 2020. Thus, the researchers had to postpone the collection of samples. The actual samples were collected during February (before lockdown), June (after lockdown), September (after lockdown) and December 2020 (before the COVID-19 pandemic in 2021). Samples at each station were collected from the shoreline with three transects lined up, each being 100 m long and 1 m wide at the

http://www.aloki.hu ● ISSN 1589 1623 (Print) ● ISSN 1785 0037 (Online)
DOI: http://dx.doi.org/10.15666/aeer/2001_571586

highest tide. Each survey was carried out by collecting all visible garbage excluding compostable waste, while buried garbage and large pieces/areas of garbage were photographed without collecting. The sample location was defined using the freeware program QGIS and then exported to a KML file for use. The exported file was opened with an application on a mobile phone called MAPinr. Subsequently, the garbage samples were collected along the defined lines.

Classification of marine debris

Marine waste collected was recorded in a data sheet modified from NOAA (Lippiatt et al., 2013). The collected waste was classified, counted, and weighed. The marine waste was divided into nine categories including hard plastic, thin plastic, fabric and fibre, foam, polymer compounds, glass and ceramics, metals, paper, etc. (unclassifiable/mixed materials). Furthermore, marine debris was also divided according to its origin into 6 sources, namely coastal activities and leisure, marine activities, smoking activity, sanitary equipment (including COVID–19 related such as gloves, masks, liquid hand wash and alcohol-based sanitiser bottles, etc.), large-scale debris disposal activity and other activities (Ocean Conservancy Start a Sea Change, 2009).

Results and discussion

Type and amount of marine debris

The survey results of marine debris on the coast of Libong Island showed a total amount of marine debris from all categories of 1,580 items at a total weight of 47,744 g. The largest quantity of marine debris was found in June (692 items), followed by February (404 items), September (274 items) and December (210 items). The areas where samples were collected and had the largest quantity of marine debris during the study were Thung Ya Kha Beach (568 items), followed by Ban Lung Khoa (444 items), Libong Camp (440 items) and Thung Chin Beach (128 items). The study results in each area of study during each month found that Thung Ya Kha Beach had the largest amount of marine debris in June (389 items), February (111 items), and September (51 items). Ban Lung Khoa had the largest quantity of marine debris in September (142 items), February (121 items) and December (103 items), Libong Camp: June (167 items), February (124 items), December (76 items), Thung Chin Beach: June (52 items), February (48 items) and December (14 items).

The total number of hard plastics was 709 items, weighing 10,278 g, followed by 240 items of glass with the highest weight of 10,714 g, and fabric and fibre (123 items) weighing 10,667 g (*Fig. 2*). The highest quantity of hard plastic was found on Thung Chin Beach almost every month, comprising 50.785% overall, followed by thin plastic (13.285%), and an equal quantity of fabric and fibre and metal (11.725%), except during September, when fabric and fibre and foam were found in equal amounts. Glass was found the most every month in Libong Camp (33.185% overall), followed by hard plastic (23.865%) and polymer (12.505%). In June, hard plastic was found the most. During December, unidentified debris was found in Ban Lung Khoa the most, but the largest quantity of hard plastic was found overall (31.535%), followed by glass (15.325%), and unidentified debris (13.515%). The largest quantity of hard plastic was found each month in Thung Ya Kha Beach, totalling 70.255%, followed by foam (10.745%), and fabric and fibre (6.345%).

http://www.aloki.hu ● ISSN 1589 1623 (Print) ● ISSN 1785 0037 (Online)
DOI: http://dx.doi.org/10.15666/aeer/2001_571586

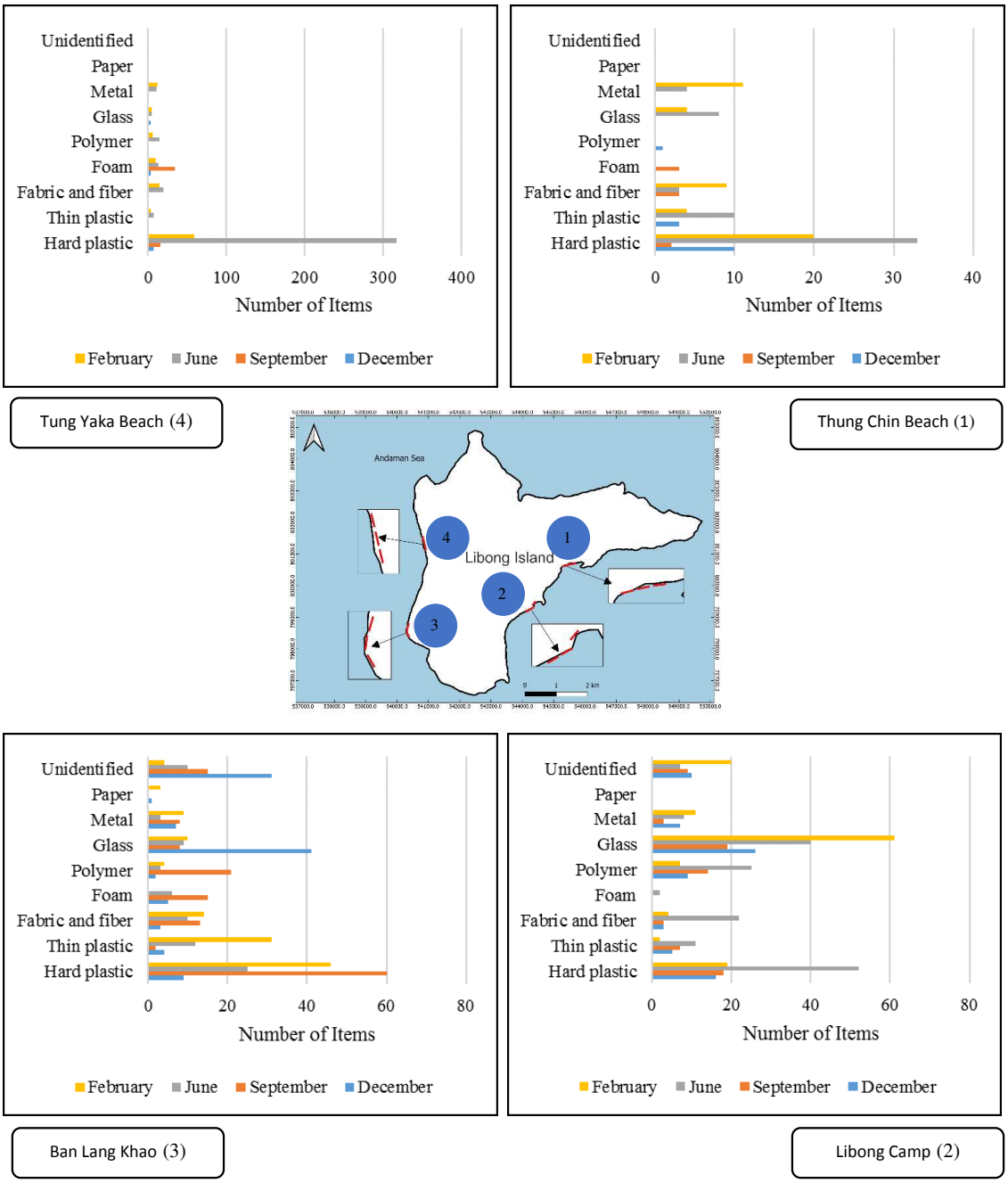

Figure 2. *Type and amount of marine debris found in the study area during the whole year*

The most common type of marine debris found at almost all the sample stations was hard plastic, except for Libong Camp, at which the most found type was glass. Since Libong Camp has communities located near it, glass found included decomposed glass from drinking bottles in clear, amber, and green colours, totalling 127 items. The study results supported a previous study conducted by Pradit et al. (2020b) on marine debris during May-August 2019 on the beach of Libong Camp, which found that glass was the most outstanding marine debris in the area totalling 699 items. The accumulation of marine debris on beaches results from various factors, including currents in the areas and coastal currents, the slope and length of beaches, levels of current and flowing wind

http://www.aloki.hu ● ISSN 1589 1623 (Print) ● ISSN 1785 0037 (Online)
DOI: http://dx.doi.org/10.15666/aeer/2001_571586

(Mobilik et al., 2016). Debris swept into the ocean will partially sink immediately and accumulate wherever it went into the ocean for the first time. However, there is a large quantity of marine debris floating on the ocean surface that perhaps gets moved out of old places (Gonulal et al., 2016; Mobilik et al., 2016). This study found that plastic debris tends to be lightweight. Strong wind and waves from the ocean may sweep plastic debris from the ocean or nearby coasts to beaches, while decomposed glass and ceramic sink into the sand. When weather conditions do not facilitate strong winds or rain, the glass will get dug and scatter on coasts (Simeonova and Chuturkova, 2019). In addition, wind may sweep fabric into the ocean for areas of the study located near communities. Once fabric gets wet, it will absorb water and sink into the ocean.

Distribution of marine debris per area

Seasonal marine debris distribution at each surveyed beach was determined. The coastline of Libong Island is presented in *Figure 3*. The results revealed that the highest density of marine debris was in June. Thung Ya Kha Beach had 6.1297 items/100 m^2, followed by Libong Camp at 67.55 items/100 m^2, Ban Lung Khao at 26.00 items/100 m^2 and Thung Chin Beach at 19.33 items/100 m^2. Libong Camp showed the highest density of marine debris in February with 41.33 items/100 m^2. For Ban Lung Khao, the highest density of marine debris was found during September and December at 47.33 items/100 m^2 and 34.33 items/100 m^2, respectively. During June, every station had the highest density of marine debris almost every month except Ban Lang Khoa since it was the period that Thailand had just cancelled the lockdown measures due to the COVID-19 situation, so a small number of tourists were found in the area. The density of marine debris during the COVID-19 situation was small compared to the density of marine debris during the COVID-19 situation in Kenya on beaches in urban areas, which ranged between 0.00 and 3.8 × 10^2 items m^2 and on beaches in distant areas that ranged between 0.00 and 5.6 × 10^2 items m^2 (Okuku et al., 2021). A study conducted by Pradit et al. (2020b) reported that the clean coastal index (CCI) of the sandy beach of Libong Island was classified as moderately clean, while the mud beach was classified as very clean.

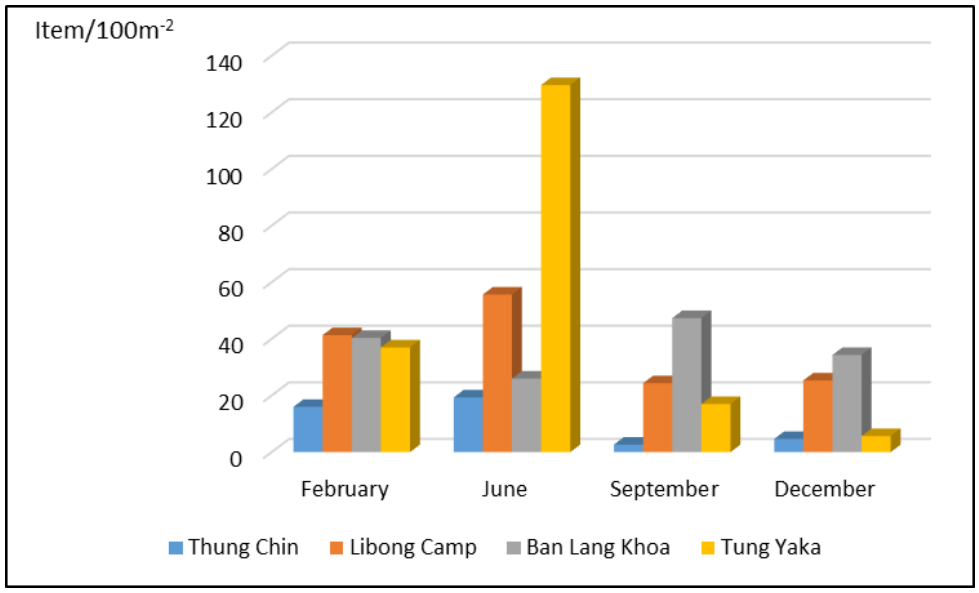

Figure 3. *Distribution of marine debris in the study area*

http://www.aloki.hu ● ISSN 1589 1623 (Print) ● ISSN 1785 0037 (Online)
DOI: http://dx.doi.org/10.15666/aeer/2001_571586

Source of marine debris

The collected marine waste was divided into six categories, as reported by the ICC (2009) (*Fig. 4*). Shoreline and recreational are the largest sources of marine debris and the most prominent sources of marine debris among all the study stations on the Libong coast, which amounted to 64.875% and weight accounting for 62.825%, followed by 16.525% of other activities. Weight accounted for 4.905% and ocean and waterway amounted to 8.805% and weight accounted for 18.535%. Here, 5outstanding types of marine debris are presented according to activities. Some activities produce only 3 types of marine debris found in the areas of study and were conducted during the study, as shown in *Table 1*. As for shoreline and recreational activities, the most commonly found marine debris is glass, followed by food packages such as snack bags, foam food containers, etc, and bottle caps/stoppers such as water bottle caps, seasoning, or spice bottle caps, etc. An example of the marine debris found in the study areas is shown in *Figure 5*.

Table 1. *Outstanding marine debris classified by sources of origin at Libong Island in 2020*

	Thung Chin Beach	**Libong Camp**	**Ban Lung khao**	**Thung Ya Kha Beach**	**Total (item)**
1. Shoreline and recreational					
1.1 Glass bottle	11	127	55	11	204
1.2 Food package	19	25	57	46	147
1.3 Bottle cap/stopper	6	5	10	89	110
1.4 Household consumption product	3	60	30	15	108
1.5 Plastic bag	16	24	49	11	100
2. Ocean and waterway					
2.1 Rope/fish net/seine	9	7	20	22	58
2.2 Buoy	0	2	3	16	21
2.3 Battery	0	8	1	0	9
2.4 Sponge	0	1	0	7	8
2.5 Fertilizer sack/coated sack	2	1	4	1	8
3. Smoking related					
3.1 Lighter	0	1	3	21	25
3.2 Cigarette pack	0	0	1	1	2
3.3 Tobacco pack	0	0	1	0	1
4. Medical and personal hygiene					
4.1 Medicine plastic pack	1	0	7	6	14
4.2 Medicine glass bottle	0	1	1	2	4
4.3 Diaper	0	2	0	0	2
5. Large-scale debris disposal activity					
5.1 Construction material	0	44	59	1	104
5.2 Zinc roofing sheet	0	1	1	0	2
5.3 Vehicle tire	1	0	0	0	1
6. Other					
6.1 Plastic scrap	4	16	21	124	165
6.2 Foam scrap	3	2	23	48	76
6.3 Rubber scrap	0	5	5	3	13
6.4 Wire	0	3	3	1	7
6.5 Sack scrap	0	1	1	1	3

http://www.aloki.hu ● ISSN 1589 1623 (Print) ● ISSN 1785 0037 (Online)
DOI: http://dx.doi.org/10.15666/aeer/2001_571586

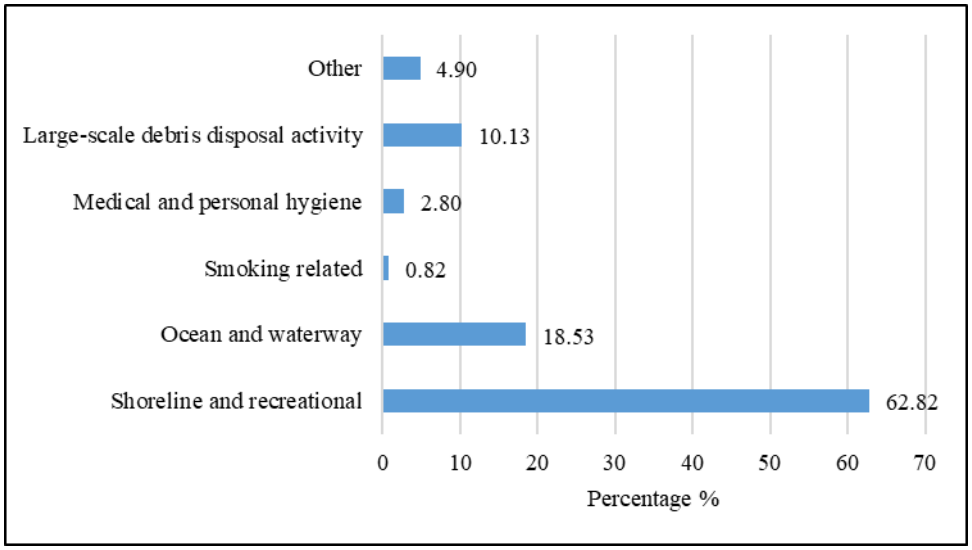

Figure 4. *Sources of marine debris*

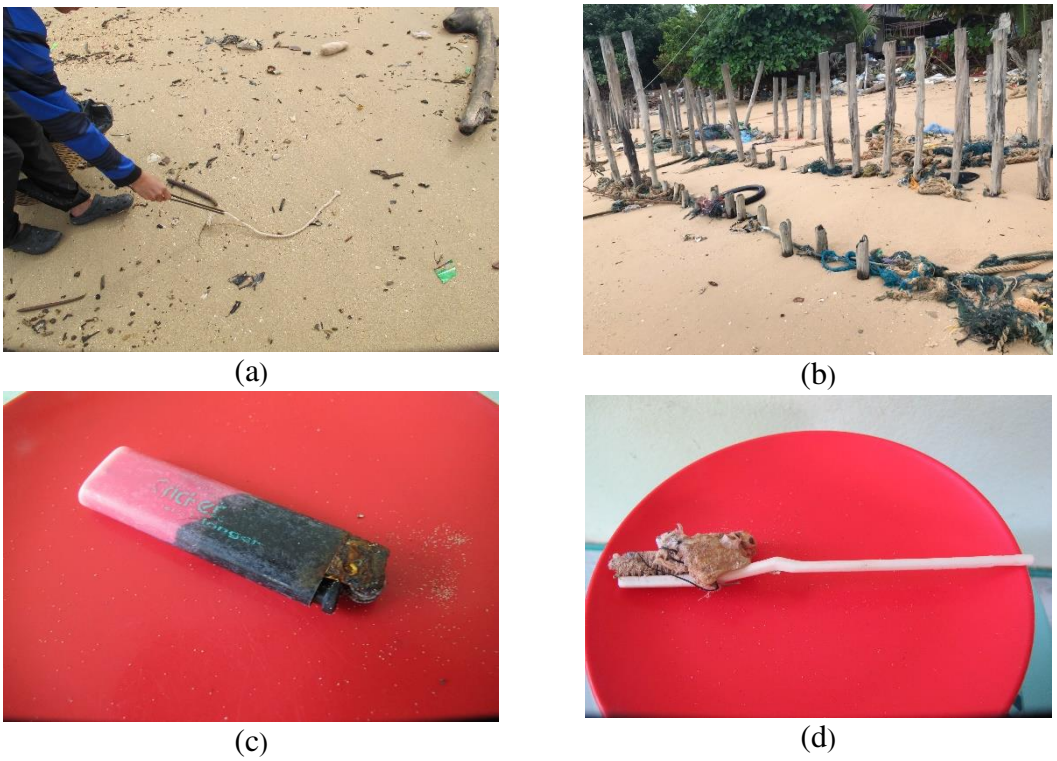

Figure 5. *Example of marine debris found in the study areas*

In the areas of study, no waste related to COVID-19 was found such as masks, bottles of hand sanitiser, and alcohol-based sanitiser bottles. A study on the density of marine debris during the COVID-19 situation conducted by Okuku et al. (2021) showed that such types of debris were not found in some areas of study. As for large-scale debris disposal activity, the most outstanding debris are construction materials such as brick scraps, cement waste, gypsum board scraps, and other waste that cannot be

http://www.aloki.hu ● ISSN 1589 1623 (Print) ● ISSN 1785 0037 (Online)
DOI: http://dx.doi.org/10.15666/aeer/2001_571586

identified types of activity such as hard plastic scraps, foam scraps, and rubber scraps. According to previous studies, sources of marine debris were shoreline and recreational activities (Pervez et al., 2020). A study conducted by Kumar et al. (2016) revealed that the sources of marine debris from shoreline and recreational activities accounted for 74.465%. Shoreline activities and tourism play an important role in producing coastal debris resulting from waste disposal behaviours (Pervez et al., 2020; Kumar et al., 2016).

Based on this study, outstanding marine debris are plastics, 87 types of both hard and soft plastics, totalling 805 items. A comparison of the top 20 marine debris calculated from the number of items (*Table 2*) indicated that the marine debris with the highest distribution were hard plastics (types of plastic could not be identified), 160 items (23.055%), which were found the most in June, followed by September and February. The second was plastic carrier bags at 102 items (14.705%), which were found the most in June, followed by February with similar items, and December respectively. Third place was the same number of plastic water bottles and bottle caps, 59 items (8.505%), which were found the most in June, followed by plastic water bottles, which were found in September, and February and December at the same number, followed by water bottle caps, which were found in February and September. The fourth was seasoning or spice bottle caps at 45 items (6.485%), which were found the most in June, followed by September. Comparison with the 2019 study results of Pradit et al. (2020b) around beaches, stone beaches, and mud beaches in Libong Island, other plastics (30.085%) were found the most, followed by plastic bags (25.965%), and plastic bottles (15.685%), respectively.

Comparing marine plastic waste to previous studies by Pradit et al. (2020b) in the Libong Island area during the COVID-19 outbreak in Thailand, only marine debris that can be classified will be discussed. The predominant plastic waste in the area was plastic bags, which were found in both previous studies and at the beginning of this study. Every time there is a survey, it will observe that condiment caps peaked in June, with very few in other months. This corresponds to the period after the lockdown that more people are staying at home. As a result, there is also an increase in household cooking.

From this study, an overview study of marine debris on the coast of Koh Libong, Trang Province during the COVID-19 situation of 2020 can be summarised as shown in *Table 3*. It was found that the amount of marine debris during June, after the lockdown announcement, the amount of waste was found to be higher than the previous month (February) because it was the time when everyone was at home. Consequently, consumption increases, so it may be garbage that accumulates during the lockdown period. In addition, the COVID-19 situation in 2020 resulted in a shortage of masks and, thus, more expensive prices. Other PPE products also saw similar situations, so most people used cloth masks as they tended to be cheap and could be used many times. Therefore, it may be one of the reasons that PPE waste was not found in the study area, including the country's lockdown measures (lockdown period) affecting Trang Province in June and September. During the COVID-19 outbreak in Thailand with the government lockdown order, there was no inter-provincial travel and no activity of both private and government organisations for approximately 3 months. Thus, this certainly changed people's lifestyles by causing them to stay at home and work from home, resulting in more laundry activities, releasing more cloth fibres into the drain water, and finally entering the environment (Pradit et al., 2021). Compared to the amount of

http://www.aloki.hu ● ISSN 1589 1623 (Print) ● ISSN 1785 0037 (Online)
DOI: http://dx.doi.org/10.15666/aeer/2001_571586

marine debris found at Libong Camp beach before COVID-19 pandemic (June 2019) while the number of tourists remained unrestricted, there were 579 items (Pradit, 2020b), but in June 2020 (this study) 167 items of marine debris were found on the same beach, which a decrease of about five times.

Table 2. *The top 20 marine debris along the coasts of Libong Island in 2020*

No.	List	February	June	September	December	Total	Percentage
1	Hard plastic (types of plastic could not be identified)	14	118	22	6	160	23.05
2	Plastic carrier bag	40	44	8	10	102	14.70
3	Water bottle	11	24	13	11	59	8.50
4	Water bottle cap	14	36	6	3	59	8.50
5	Seasoning or spice bottle cap	1	39	4	1	45	6.48
6	Clear plastic bag	21	14	0	1	36	5.19
7	Plastic straw	10	15	4	0	29	4.18
8	Clear plastic glass	13	12	1	0	26	3.75
9	Lighter	3	19	2	1	25	3.60
10	Fruit juice bottle	10	11	2	1	24	3.46
11	Toy	0	15	6	1	22	3.17
12	Fork and spoon	2	18	1	0	21	3.03
13	Coca-Cola bottle	3	13	1	1	18	2.59
14	Plastic jelly cup	4	8	4	0	16	2.31
15	Plastic label	1	1	12	1	15	2.16
16	Plastic pendulum/buoy	4	6	0	0	10	1.44
17	Plastic sack	3	4	1	1	9	1.30
18	Plastic medicine bottle	1	6	1	0	8	1.15
19	Food container	0	2	2	1	5	0.72
20	Medicine sachet, medicine pack	0	0	5	0	5	0.72
Total		155	405	95	39	694	100

Only for Thai tourists by June, there were fewer Thai tourists. Compared to the same period the previous year (2019), 92 per cent had no income from foreign tourists. The income from Thai tourists accounted for 93.5 per cent compared to the monsoon season, it was found June was the period where the largest quantity of marine debris was found since June is the beginning of southwest monsoon season, strong wind and high wave sweep debris in the ocean to coasts but in September, a monsoon period, the small amount of marine debris is found since strong wind and wave in the ocean sweep most of the debris to the lines of beach morning glory above line transect where samples were collected.

http://www.aloki.hu ● ISSN 1589 1623 (Print) ● ISSN 1785 0037 (Online)
DOI: http://dx.doi.org/10.15666/aeer/2001_571586

Table 3. *The situation of COVID-19 in 2020 and the occurrence of marine debris on the coast of Libong Island*

Factor	February 2020 (before lockdown)	June 2020 (after lockdown)	September 2020 (after lockdown)	December 2020 (before new lockdown)
Amount of marine debris (this study)	↑↑ 404 items	↑↑↑ 692 items	↑ 274 items	↓ 210 items
COVID-19 pandemic (2020)	**Face masks**			
	• No face mask used	• Face masks are in short supply and expensive	• Face masks are in short supply and expensive	• Face masks are in short supply and expensive
	Tourists*			
	• Thai (down from the previous year by 12.9%) • Foreigner (decrease from the previous year 29.9%)	• Thai (down from the previous year by 92.0%) • Foreigner (none)	• Thai (down from the previous year by 34.3%) • Foreigner (none)	• Thai (down from the previous year by 52.0%) • Foreigner (decrease from the previous year 99.7%)
	Income from tourists*			
	• Thai (down from the previous year by 12.9%) • Foreigner (decrease from the previous year 29.89%)	• Thai (down from the previous year by 93.5%) • Foreigner (none)	• Thai (down from the previous year by 37.9%) • Foreigner (none)	• Thai (down from the previous year by 52.43%) • Foreigner (decrease from the previous year 99.9%)
Monsoon season	Pre monsoon	Before monsoon	Inter monsoon	Post monsoon

*Ministry of Tourism and Sports, 2020

A study conducted by Alvarez et al. (2020) helped to confirm the information that the areas with the greatest marine debris accumulation comprise areas that are higher than the highest water level and where the tide is at its highest level. In December, there is a small quantity of marine debris as it is a post-monsoon period. The wind blows from the northeast direction and sweeps marine debris from the coasts into the ocean. Villagers living in Libong Island call this wind “Lom oak” (wind blows from the coast to sea). Although Thung Ya Kha Beach is located far from communities, the largest quantity of marine debris was found since Thung Ya Kha Beach is located on the west coast of the island. It is an open beach influenced by the southwest monsoon the most as well as Ban Lung Khoa is located on the west coast of the island. However, since Ban Lung Khoa is located near communities, some parts of marine debris are from communities. This study found construction materials such as floor tile scraps, roof tile scraps, louvre glass scraps, cement waste, and ceramic ware scraps. A small quantity of marine debris was found on the beaches in front of hotels since they are cleaned by hotel staff every day. Libong Camp and Thung Chin Beach are located on the east coast of the island. They look like coves and are less likely to be influenced by the southwest monsoon. Both beaches are quite clean with numerous natural features. They have restrictions for access, making them have low pressure from humans (Alvarez et al., 2020; Pradit et al., 2020b).

The model of wind flow in the areas of the study is similar to that of Malaysia. A study conducted by Mobilik et al. (2016) found a large quantity of marine debris was found during the southwest monsoon period compared to the northeast monsoon period in conjunction with the movement of ocean current in the form of anti-clockwise direction that slightly circulates during the northeast monsoon period but moves in the form of clockwise direction during the southwest monsoon period. The movement of wind and waves is a factor distributing marine debris; previous studies help support this

http://www.aloki.hu ● ISSN 1589 1623 (Print) ● ISSN 1785 0037 (Online)
DOI: http://dx.doi.org/10.15666/aeer/2001_571586

subject very well. Comparison of data related to the quantity of marine debris of any beach to the prevalence of marine debris from other beaches in the world seems to be difficult due to different methods and random sampling techniques including other causes such as closeness with inhabited areas. The quantity of debris or waste is related to the congestion of the population, the number of tourists (Gonulal et al., 2016; Pervez et al., 2020), and recreational activities. The quantity of waste is in contrast to the distance of inhabited areas (Veerasingam et al., 2020), environmental factors especially wind velocity and sociological factors such as environmental awareness of beach users (Mobilik et al., 2016).

As there are large seagrass beds nearby Libong Island, the accumulation of plastics in the seagrass bed will have an impact on marine animals in the shallow water ecosystem if the level of marine debris accumulation is high (Bonanno and Orlando-Bonaca, 2020). It is a severe threat to marine mammals, sea turtles, and sea birds (Alshawafi et al., 2017; Bonanno and Orlando-Bonaca, 2020; Haram et al., 2020; Mobilik et al., 2016; Veerasingam et al., 2020). A study conducted by Veerasingam et al. (2020) identified that regular beach activity and long-term marine debris monitoring could help reduce marine debris along the coastlines. Therefore, long-term marine debris monitoring along the coastlines of Libong Island would be useful for collecting data related to a tendency of marine debris accumulation along coastlines, which will help improve national policies and measures on marine debris management to be consistent with the future goal of reducing plastic waste in Thailand's roadmap on plastic waste management 2018–2030. Rayon-Vina et al. (2019) proposed a guideline to solve marine debris problems, starting from raising people's awareness. Everyone must be aware that they are a part of the problems and problem-solving guidelines.

Conclusion

Thung Ya Kha Beach is where the most marine debris found and found the highest amount of marine debris in June. Though it is a beach where tourism activities were more reduced than the previous year due to COVID-19 situations and the country lockdown, the period going to enter southwest monsoon season is the period having a higher quantity of marine debris than monsoon period, the same period when the country lockdown was eased. In this study, no COVID-19 related waste was found. Most of marine debris came from shoreline and recreational activities. A campaign raising people's awareness aims to adjust people's attitudes towards environment. Emphasis should be placed on making understanding of beach status in their locality in order to help encourage people to see how important beaches are before implementing activities together. Local administrative organizations probably consider data from this study for planning management and raising a campaign to make Libong Island become a significant tourist attraction in conjunction with prosperous natural resources – seagrass beds and primitive way of life of coastal community for facilitating tourists in the future. Since the floating waste can be transferred by the streams and waving and the landing of the waste materials on the beaches is influenced mainly by weather conditions (wind direction) and wave direction. Further study should include those factors for better understand the source and transport of marine debris.

Acknowledgements. This study was funded by the graduate school, Prince of Songkla University, for thesis research grants on the topic of community solutions in 2020 and Coastal Oceanography and

http://www.aloki.hu ● ISSN 1589 1623 (Print) ● ISSN 1785 0037 (Online)
DOI: http://dx.doi.org/10.15666/aeer/2001_571586

Climate Change Research Center. Researcher are thankful to the Department of National Parks, Wildlife and Plant Conservation for allowing us to conduct the research at Libong Island. Thank you to all the research team who helped collect the samples. We express many thanks to reviewers for assisting us to improve the quality of manuscript.

REFERENCES

[1] Alshawafi, A., Analla, M., Alwashali, E., Aksissou, M. (2017): Assessment of marine debris on the coastal wetland of Martil in the North-East of Morocco. – Marine Pollution Bulletin 117: 302-310.

[2] Alvarez, S., Gestoso, I., Herrera, A., Riera, L., Canning-Clode, J. (2020): A comprehensive first baseline for marine litter characterization in the Madeira Archipelago (NE Atlantic). – Water, Air & Soil Pollution 231(4): 182.

[3] Barnes, D. K. A., Galgani, F., Thompson, R. C., Barlaz, M. (2009): Accumulation and fragmentation of plastic debris in global environments. – Philosophical Transactions of the Royal Society B 364: 1985-1998.

[4] Bonanno, G., Orlando-Bonaca, M. (2020): Marine plastics: what risks and policies exist for seagrass ecosystems in the Plasticene? – Marine Pollution Bulletin 158: 111425.

[5] Cauwenberghe, L. V., Claessens, M., Vandegehuchte, M. B., Mees, J., Janssen, C. R. (2013): Assessment of marine debris on the Belgian Continental shelf. – Marine Pollution Bulletin 73: 161-169.

[6] Claessens, M., Cauwenberghe, L. V., Vandegehuchte, M. B., Janssen, C. R. (2013): New techniques for the detection of microplastics in sediments and field collected organisms . –Marine Pollution Bulletin 70: 227-233.

[7] Department of Disease Control (2020): Daily COVID-19 report, Thailand information. – https://data.go.th/dataset/covid--19daily (accessed 9 September 2021).

[8] Department of Marine and Coastal Resources (2013): Coastal Hydrographic. – https://km.dmcr.go.th/th/c_51/d_1130. (Accessed 25 July 2021).

[9] Geyer, R., Jambeck, J. R., Law, K. L. (2017): Production, use, and fate of all plastics ever made. – Science Advances 3: 1-5.

[10] Gonulal, O., Oz, I., Gurasen, S. O., Qzturk, B. (2016): Abundance and composition of marine litter around Gokceada Island (Northern Aegean Sea). – Aquatic Ecosystem Health & Management 19(4): 461-467.

[11] Haram, L. E., Carlton, J. T., Ruiz, G. M., Maximenko, N. A. (2020): A plasticene lexicon. – Marine Pollution Bulletin 150(110714).

[12] Jambeck, J. R., Geyer, R., Wilcox, C., Siegler, T. R., Perryman, M., Andrady, A., Narayan, R., Law, K. L. (2015): Plastic waste inputs from land into the ocean. – Science 347(6223): 768-771.

[13] Kumar, A. A., Sivakumar, R., Reddy, Y. S. R., Bhagya Raja, M. V., Nishanth, T., Revanth, V. (2016): Preliminary study on marine debris pollution along Marina beach, Chennai, India. – Regional Studies in Marine Science 5: 35-40.

[14] Lippiatt, S., Opfer, S., Arthur, C. (2013): Marine Debris Monitoring and Assessment. – NOAA Technical Memorandum NOS-OR&R-46.

[15] Marine Knowledge Database (2018): Brief policy recommendations situations and preventive approaches to solve marine and coastal waste problems. Documents under the project "Preparing a Brief Policy Recommendation on Urgent Issues on the National Maritime Interests of Thailand." –

http://www.aloki.hu ● ISSN 1589 1623 (Print) ● ISSN 1785 0037 (Online)
DOI: http://dx.doi.org/10.15666/aeer/2001_571586

http://mrpolicy.trf.or.th/LinkClick.aspx?fileticket=TqcNIuZ6E7g%3D&tabid=65&mid=401 (Accessed 9 July 2021).

[16] Maximenko, N., Corradi, P., Law, K. L., Van Sebille, E., Garaba, S. P., Lampitt, R. S., Galgani, F., Martinez-Vicente, V., Goddijn-Murphy, L., Veiga, J. M., Thompson, R. C., Maes, C., Moller, D., Löscher, C. R., Addamo, A. M., Lamson, M. R., Centurioni, L. R., Posth, N. R., Lumpkin, R., Vinci, M., Martins, A. M., Pieper, C. D., Isobe, A., Hanke, G., Edwards, M., Chubarenko, I. P., Rodriguez, G., Aliani, S., Arias, M., Asner, G. P., Brosich, A., Carlton, J. T., Chao, Y., Cook, A. M., Cundy, A. B., Galloway, T. S., Giorgetti, A., Goni, G. J., Guichoux, Y., Haram, L. E., Hardesty, B. D., Holdsworth, N., Lebreton, L., Leslie, H. A., Macadam-Somer, I., Mace, T., Manuel, M., Marsh, R., Martinez, E., Mayor, D. J., Le Moigne, M., Jack, M. E. M., Mowlem, M. C., Obbard, R. W., Pabortsava, K., Robberson, B., Rotaru, A. E., Ruiz, G. M., Spedicato, M. T., Thiel, M., Turra, A., Wilcox, C. (2019): Toward the integrated marine debris observing system. – Frontiers in Marine Science 6(447).

[17] Ministry of Tourism and Sports. (2020): Domestic Tourism Statistics (Classify by region and province 2020). – https://mots.go.th/more_news_new.php?cid=594 (accessed 9 September 2021).

[18] Mobilik, J. M., Ling, T. Y., Husain, M. L., Hassan, R. (2016): Type and quantity of shipborne garbage at selected tropical beaches. – The Scientific World 2016(5126951).

[19] Ocean Conservancy Start a Sea Change (2009). Guide to Marine Debris and International Coastal Cleanup. – Department of Marine and Coastal Resources (translator to Thai).

[20] Okuku, E., Kiteresi, L., Owato, G., Otieno, K., Mwalugha, C., Mbuche, M., Gwada, B., Nelson, A., Chepkemboi, P., Achieng, Q., Wanjeri, V., Ndwiga, J., Mulupi, L., Omire, J. (2021): The impacts of COVID-19 pandemic on marine litter pollution along the Kenyan Coast: A synthesis after 100 days following the first reported case in Kenya. – Marine Pollution Bulletin 162(111840).

[21] Pervez, R., Wang, Y., Mahmood, Q., Zahir, M., Jattak, Z. (2020): Abundance, type, and origin of litter on No. 1 Bathing Beach of Qingdao, China. – Coastal Conservation 24(34).

[22] Pollution Control Department (2018): A Roadmap for Plastic Waste Management 2018–2030. – http://www.pcd.go.th/Info_serv/File/Plastic%20Roadmap.pdf (accessed 30 July 2021).

[23] Pradit, S., Towatana, P., Nitiratsuwan, T., Jualaong, T., Jirajarus, M., Sornplang, K., Noppradit, P., Darakai, Y., Weerawong, C. (2020a): Occurrence of microplastics on beach sediment at Libong, a pristine island in Andaman Sea, Thailand. – ScienceAsia 46(2020).

[24] Pradit, S., Nitiratsuwan, T., Towatana, P., Jualaong, T., Sornplang, K., Noppradit, P., Jirajarus, M., Darakai, Y., Weerawon, C. (2020b): Marine debris accumulation on the beach in Libong, a small island in Andaman Sea, Thailand. – Applied Ecology and Environmental Research 18(4): 5461-5474.

[25] Pradit, S., Noppradit, P., Goh, B. P., Sornplang, K., Ong. M. C., Towatana, P. (2021): Occurrence of microplastics and trace metals in fish and shrimp from Songkla Lake, Thailand During the COVID-19 pandemic. – Applied Ecology and Environmental Research 19(4): 1085-1106.

[26] Royal Thai Government Gazette (2020): Regulation Issued under Section 9 of the Emergency Decree on Public Administration in Emergency Situations. – B. E. 2548(2005) (No. 1).

http://www.aloki.hu ● ISSN 1589 1623 (Print) ● ISSN 1785 0037 (Online)
DOI: http://dx.doi.org/10.15666/aeer/2001_571586

[27] Rayon-Vina, F., Miralles, L., Fernandez-Rodrigues, S., Dopico, E., Garcia-Vazques, E. (2019): Marine litter and public involvement in beach cleaning: Disentangling perception and awareness among adults and children, Bay of Biscay, Spain. – Marine Pollution Bulletin 141: 112-118.
[28] Sheavly, S. B. (2007): National Marine Debris Monitoring Program: Final Program Report, Data Analysis and Summary. – Prepared for U. S. Environmental Protection Agency by Ocean Conservancy, Grant Number X83053401-02.
[29] Silva, A. L. P., Prata, J. C., Walker, T. R., Duarte, A. C., Ouyang, W., Barcelò, D., Rocha-Santos, T. (2021): Increased plastic pollution due to COVID-19 pandemic: Challenges and recommendations. – Chemical Engineering Journal 405(126683).
[30] Simeonova, A., Chuturkova, R. (2019): Marine litter accumulation along the Bulgarian Black Sea coast: categories and predominance. – Waste Management 84: 182-193.
[31] UNESCO (2019): United Nations Decade of Ocean Science for Sustainable Development (2021-2030). – https://en.unesco.org/ocean-decade (accessed 19 July 2021).
[32] United Nations (2019): Sustainable Development Goal 14. Conserve and sustainably use the oceans, seas and marine resources for sustainable development. – https://sustainabledevelopment.un.org/sdg14 (accessed 19 July 2021).
[33] Veerasingam, S., Al-Khayat, J. A., Aboobacker, V. M., Hamza, S., Vethamony, P. (2020): Sources, spatial distribution and characteristics of marine litter along the west coast of Qatar. – Marine Pollution Bulletin 159(111478).
[34] Velavan, T. P., Meyer, C. G. (2020): The COVID-19 epidemic. – Tropical Medicine and International Health 25(3): 278-280.

http://www.aloki.hu ● ISSN 1589 1623 (Print) ● ISSN 1785 0037 (Online)
DOI: http://dx.doi.org/10.15666/aeer/2001_571586

TWO KEY VOLATILES OF CHINESE WHITE PINE (*PINUS ARMANDII*) (PINALES: PINACEAE: PINOIDEAE) PHLOEM RESIST INVASION BY CHINESE WHITE PINE BEETLE (*DENDROCTONUS ARMANDII*) (COLEOPTERA: CURCULIONIDAE: SCOLYTINAE)

ZHAO, M.[1,2] – KANG, X.[3] – AN, H.[1] – LIU, B.[3] – CHEN, H.[1*]

[1]*State Key Laboratory for Conservation and Utilization of Subtropical Agro-Bioresources (South China Agricultural University), Guangdong Key Laboratory for Innovative Development and Utilization of Forest Plant Germplasm, College of Forestry and Landscape Architecture, South China Agricultural University, Guangzhou 510642, Guangdong, China*

[2]*Key Lab Vector Biol & Pathogen Control Zhejiang P, College of Life Science, Huzhou University, Huzhou, Zhejiang 313000, China*

[3]*College of Forestry, Northwest A&F University, Yangling, Shaanxi 712100, China*

**Corresponding author*
e-mail: chenhuiyl@163.com; phone: +86-20-8528-0256; fax: +86-20-8528-0256

(Received 20th Mar 2021; accepted 6th Dec 2021)

Abstract. *Pinus armandii* phloem is the key tissue in which *Dendroctonus armandii* live and breed. Although previous research examined the volatiles in *P. armandii* phloem, the dynamic changes and functions of these volatiles were never revealed. This study detected the changes in *P. armandii* phloem volatiles at each stage of infestation from healthy to dead trees and tested the toxicity of these volatiles against *D. armandii*. It revealed that (1) the weight of females was significantly greater than that of males, and females were more tolerant to host volatiles than males. (2) Limonene and myrtanol of *P. armandii* phloem volatiles played the key roles in resisting the invasion of *D. armandii*. The first increased the percentage of limonene together with other volatiles killing *D. armandii* in the resistant period of *P. armandii*, and the second synthesised myrtanol to further resist the invasion of *D. armandii* in the retreat period of *P. armandii*. These observations highlight the differences in the resistance of males and females to toxicity from the volatiles and the difference in the toxicity of different volatiles to *D. armandii*, revealing the defensive system of *P. armandii* phloem to provide a theoretical basis for the control and management of *D. armandii*.
Keywords: *host volatiles, toxicity, host defence, limonene, myrtanol*

Introduction

The Chinese white pine beetle (*Dendroctonus armandii*) is the most destructive forest pest in the Qinling Mountains and Ta-pa Mountains of China (Chen et al., 2010). Unlike red turpentine beetle (*Dendroctonus valens*) and mountain pine beetle (*Dendroctonus ponderosae*) that invade weakened pine trees, and only infest healthy trees during outbreaks (Sun et al., 2013; Krause et al., 2018), *D. armandii* is a primary pest of healthy Chinese white pine (*Pinus armandii*) (Hu et al., 2016). *D. armandii* has two generations per year at elevations lower than 1700 m a.s.l, three generations in two years between 1700 and 2150 m a.s.l, and one generation per year in areas higher than 2150 m a.s.l (Ning et al., 2019). Females invade first and overcome the tree's resistance, drill tunnels, and release pheromones to attract males (Dai et al., 2015). The successful invasion of *D. armandii* is often followed by colonization of secondary pests (such as *Ips acuminatus*,

http://www.aloki.hu ● ISSN 1589 1623 (Print) ● ISSN 1785 0037 (Online)
DOI: http://dx.doi.org/10.15666/aeer/2001_587600

Ips sexdentatus, *Hylurgops longipilis*, *Tomicus piniperda* and *Trypodendron lineatum*) in the weakened pines, and the infected *P. armandii* will die in two years (Chen et al., 2007). Since 1970, more than 3×10^8 m^3 of *P. armandii* trees (older than 30 years) have been harmed by *D. armandii* (Xie and Lv, 2012), and even young *P. armandii* trees were found to have been invaded by *D. armandii* (Chen et al., 2015).

Insect pheromones play a vital role in the management of bark beetles (Pureswaran et al., 2008; Perkins et al., 2015; Gillette et al., 2009). Integrated pest management measures focused on the identification of pheromones have been performed for *D. armandii* in recent years. Aggregation pheromones are considered to be a key factor in the success of insect invasion and colonization (Faccoli and Stergulc, 2008; Blazenec and Jakus, 2009). Frontalin + α-pinene is an aggregation pheromone released by virgin females and mated males of *D. armandii* (Zhao et al., 2017a), and myrtenal may be an aggregation pheromone produced by females of *D. armandii* to exert aggregation effects on other females (Zhao et al., 2019). The anti-aggregation pheromones of bark beetles, such as verbenone in *D. ponderosae* and *D. valens*, and toxic host terpene have been used to protect pine species from bark beetles (Gillette et al., 2006). Verbenone has been detected using gas chromatography and mass spectrometry (GC-MS) analyses of the hindguts of female beetles and the fumes emanating from *P. armandii* logs naturally attacked by *D. armandii* (Xie and Lv, 2012; Chen et al., 2015). In our previous study, verbenone was verified as an anti-aggregation pheromone based on electrophysiological (EAG) and Y-tube laboratory assays. In addition, field trials indicated that the addition of verbenone to the bait used to trap *D. armandii* significantly decreased the efficiency of field trapping (Zhao et al., 2017b). *trans*-Verbenol is a pheromone of western pine beetle (*Dendroctonus brevicomis*), southern pine beetle (*Dendroctonus frontalis*), *D. ponderosae* and Douglas-fir beetle (*Dendroctonus pseudotsugae*) (Byers et al., 1984; Chiu et al., 2018; Pureswaran et al., 2004), but it has not been found to have a clear role in the pheromone ecology of *D. armandii* (Zhao et al., 2017b). Quantities of potential semiochemicals identified in extracts of the hindguts of female *D. armandii*, include *cis*-verbenol, *trans*-verbenol, α-pinene, β-caryophyllene, 3-carene, verbenone, myrcene and limonene (Xie and Lv, 2012).

Leptographium qinlingensis is a symbiotic fungi of *D. armandii* that assists in the invasion of the host tree by blocking flow of water and resin, thereby reducing host defenses. Metabolites biosynthesized by *L. qinlingensis* that may be phytotoxic to *P. armandii* seedlings, include 6-methoxymethyleugenin, maculosin and cerevisterol (Li et al., 2012).

Some volatiles of *P. armandii* were tested and applied to traps in the field. Myrtenol was found to be a kind of *P. armandii* volatile and did not exhibit significant toxicity towards *D. armandii* (Zhao et al., 2019). Myrtanol was produced by infected *P. armandii* after *D. armandii* invasion and had significant toxicity towards *D. armandii*, especially females (Zhao et al., 2019). α-Pinene, camphene, β-pinene, myrcene, 3-carene, limonene and longifolene were detected from *P. armandii* logs with or without *D. armandii* attack (Chen et al., 2015).

The pine defence against bark beetles is multifaceted and temporally dynamic (Franceschi et al., 2005). Resin flow can kill invading bark beetles (Strom et al., 2002; Hood and Sala, 2015; Kane and Kolb, 2010). In addition, pines produce defence volatiles, such as monoterpenes, sesquiterpenes, diterpenes, and phenolics (Raffa et al., 2017), and the invasion of bark beetles can increase the concentration of host phloem volatiles (Kolb et al., 2019). Other defence measures include the physical defence

http://www.aloki.hu ● ISSN 1589 1623 (Print) ● ISSN 1785 0037 (Online)
DOI: http://dx.doi.org/10.15666/aeer/2001_587600

provided by bark and water (Arango-Velez et al., 2016; Erbilgin et al., 2017; Kolb et al., 2019). Resin flow and terpene release are known means of defence in response to bark beetles and their symbiotic fungi (Arango-Velez et al., 2018; Roth et al., 2018). For example, ponderosa pine can undergo induction of both resin flow and phloem terpenes in response to bark beetle attack (Kolb et al., 2019). Current research has mainly concentrated on *P. armandii* trees in a single state, such as a healthy or infested tree. The kinds of volatiles produced during different stages of host condition from fully healthy to fully infested is not clear. Whether new volatiles are synthesized specifically to resist insect invasion is also unknown. There has been no study on the dynamic changes of volatiles during the whole process of *P. armandii* resistance to bark beetle invasion. The purpose of this study was to examine the changes in host volatile production during the invasion process of *P. armandii* from healthy to dead and to test the toxicity of these volatiles against *D. armandii* to obtain more specific knowledge of the autonomic chemical defence process of *P. armandii*.

Materials and methods

Sampling

The study sites were located on the southern slope of the middle Qinling Mountains, Ningshan County, Shaanxi, China, and mainly occurred in Huoditang Forest Farm (33°18′-33°28′N, 108°21′-108°39′E) and Pingheliang Forest Farm (33°22′-33°34′N, 108°24′-108°36′E). The two forest farms were chosen because they were severely affected by *D. armandii*. The investigated *P. armandii* trees were distributed widely inside the two areas.

For convenience, the defence process of *P. armandii* against invasion by *D. armandii* was divided into four periods: healthy period, resistance period, retreat period and withered period. Healthy period was defined by the lack of resinous pitch tubes in *P. armandii* trunks. The resistance period was defined by resinous pitch tubes in *P. armandii* trunks; resinous pitch tubes are comprised of colloidal liquid containing some dead *D. armandii*. Dry frass is usually a sign of successful invasion by bark beetles (Gillette et al., 2006). The retreat period was defined by a change in the resinous pitch tubes to dry frass, and a change in the needles from green to yellow. The withered period was defined by *D. armandii* mating and production of the next generation, the needles becoming withered and yellow, and some limbs dropping out of the trees.

Phloem samples were collected from *P. armandii* trunks with a small sickle (length × width = 22 cm × 6 cm, custom-made by a blacksmith) in June 2019. Phloem was collected from healthy *P. armandii* and infested areas of different period (resistance, retreat and withered periods) of attacked trees, and the beetles and frass were cleared from the infested phloem. These phloem samples of every period were collected from five different trees of the period subjected to five repetitions. Glass culture dishes with phloem samples were placed in an outdoor cooler (4 ℃) and transported to the laboratory.

Collection and identification of host volatiles

We collected five 1.5 g samples of phloem from each of the four periods and placed each sample in a separate 50 ml vial for volatile collection. The volatiles released from these phloem samples were collected passively by headspace solid-phase microextraction (HS-SPME) (Chai et al., 2012; Keenan et al., 2012). An SPME fibre

http://www.aloki.hu ● ISSN 1589 1623 (Print) ● ISSN 1785 0037 (Online)
DOI: http://dx.doi.org/10.15666/aeer/2001_587600

coated with a 75-μm film of divinylbenzene/carboxen/polydimethylsiloxane (DVB/CAR/PDMS) (Supelco, Sigma-Aldrich, Bellefonte, PA, USA) was exposed to the headspace of each vial/phloem sample for 3 min. The split ratio of the phloem samples was 10:1. The fibre was selected due to its suitability for gases and compounds with a low molecular mass. Prior to use, the fibre was preconditioned in the injection port of the gas chromatograph at 270 ℃ for 60 min. Extracts were analysed using a DB-5 MS column (30 m × 0.25 mm × 0.25 μm) (Thermo Fisher Scientific Company, Shanghai, China). The SPME fibre was injected directly into the injection port at a temperature of 250 ℃ for 3 min. The temperature of the GC oven was maintained at 40 ℃ for 2.5 min, increased to 240 ℃ at a rate of 6 ℃/min and maintained at 240 ℃ for 10 min. The flow of helium (carrier gas) was 1.0 mL/min. Compounds were identified by comparison of their retention times and mass spectra with those in the NIST and Varian libraries. Furthermore, the retention times and mass spectra of α-pinene, β-pinene, myrcene, limonene, 3-carene and longifolene detected during the GC–MS analysis were also compared with the purchased standards.

Insects

P. armandii logs invaded by *D. armandii* larvae and pupae were felled in the Pingheliang Forest Farm (33°28′12.1″N, 108°29′26.2″E) in July and August 2019. The logs were transported to the Huoditang Forest Farm experiment base, placed in a greenhouse, covered by a thin stainless-steel net (bore diameter ≤ 0.8 mm) and watered to keep the bark moist. Once emerging beetles appeared in the net, active beetles were collected and analysed on the same day using toxicity assays (Light, 1983; Zhang et al., 2006).

Chemicals

The chemicals used in this study are listed in *Table 1*.

Table 1. *The purity of host volatiles and companies (with addresses) from which these chemicals were purchased*

Volatile	Purity	Company	Address
(-)-α-Pinene	≥ 99.0%	sigma	Shanghai, China
(+)-α-Pinene	Analytical standard	sigma	Shanghai, China
(-)-β-Pinene	Analytical standard	sigma	Shanghai, China
(+)-β-Pinene	Analytical standard	sigma	Shanghai, China
Myrcene	≥ 99.0%	Yuanye Bio-Technology Co., Ltd	Shanghai, China
S-(-)-limonene	Analytical standard	sigma	Shanghai, China
R-(+)-limonene	Analytical standard	sigma	Shanghai, China
(+)-3-carene	Analytical standard	sigma	Shanghai, China
(+)-longifolene	≥ 99.0%	Yuanye Bio-Technology Co., Ltd	Shanghai, China

Toxicity assays

Certain volatiles from the GC-MS analysis of *P. armandii* phloem were chosen for toxicity assays (*Table 1*). Camphene was in a solid state at room temperature and was not chosen for the toxicity assays. The toxic effects of *trans*-verbenol, verbenone, myrtenol, and myrtenal on *D. armandii* have previously been explored (Zhao et al., 2017b, 2019)

http://www.aloki.hu ● ISSN 1589 1623 (Print) ● ISSN 1785 0037 (Online)
DOI: http://dx.doi.org/10.15666/aeer/2001_587600

and were not examined in this study. The toxicity of (-)-α-Pinene, (+)-α-pinene, (-)-β-pinene, (+)-β-pinene, myrcene, *S*-(-)-limonene, *R*-(+)-limonene, (+)-3-carene and (+)-longifolene towards *D. armandii* was tested using a method used previously for *D. ponderosae* (Reid et al., 2017; Chiu et al., 2017). A 1.5 × 1.5 cm filter paper was placed in a 20 mL glass vial as the reagent carrier. Different dosages of the test volatiles were applied to the filter paper using a micro-dispenser. Beetles in the control group were exposed to untreated filter paper for 24 h. Each glass vial contained only one *D. armandii*, and the glass vials were sealed after the beetles were placed inside. Before the beetle was put into the glass bottle, they were weighed. Preliminary toxicity tests were conducted with each volatile to refine an intermediate range of dosages from lethal to non-lethal, to more accurately determine an LC_{50} (*Table 2*). The *D. armandii* beetles were maintained in glass vials for 24 h. After that, *D. armandii* were considered to have died if they showed no limb movements after the glass vial was shaken. Each *D. armandii* was weighed again to calculate their weight loss. Each concentration (contain all concentration in the preliminary experiments and the experiments of LC_{50}) of each tested volatile compound was tested with 40 *D. armandii* individuals (20 females and 20 males). To eliminate potential bias of different treatment in results, beetles collected at different times were used for all the assays in a completely random manner.

Table 2. *The determination doses of different volatiles for females and males*

Volatile	Sex	Volatile dosage (μL)									
		0	**0.2**	**0.4**	**0.7**	**1**	**1.5**	**2**	**4**	**10**	**15**
(-)-α-Pinene	Male	√		√		√	√	√			
	Female	√		√		√	√	√			
(+)-α-Pinene	Male	√		√	√	√		√			
	Female	√			√	√	√	√			
(-)-β-Pinene	Male	√		√		√	√	√			
	Female	√		√		√	√	√			
(+)-β-Pinene	Male	√		√		√	√	√			
	Female	√		√		√	√	√			
Myrcene	Male	√						√	√	√	√
	Female	√						√	√	√	√
S-(-)-limonene	Male	√		√	√	√		√			
	Female	√		√	√	√		√			
R-(+)-limonene	Male	√	√	√		√		√			
	Female	√		√	√	√		√			
(+)-3-carene	Male	√		√	√	√		√			
	Female	√		√	√	√		√			
(+)-longifolene	Male	√						√	√	√	√
	Female	√						√	√	√	√

Statistical analysis

The probit analysis method was used to determine the LC_{50}. One-way ANOVA was used to test for differences in the mean weights of males and females. Multiple comparisons (LSD-*t* test) were used to test the difference in mean % of limonene, mean weight loss, mean weight loss % and death rate %. The probit analysis, one-way ANOVA and multiple comparisons ($P < 0.05$) were run in SPSS (1999).

http://www.aloki.hu ● ISSN 1589 1623 (Print) ● ISSN 1785 0037 (Online)
DOI: http://dx.doi.org/10.15666/aeer/2001_587600

Results

Collection and identification of host volatiles

In the GC-MS analysis of the phloem during four different *P. armandii* periods (healthy period, resistance period, retreat period and withered period), eleven host volatiles were detected (*Table 3*). Eight host volatiles (α-pinene, camphene, β-pinene, myrcene, 3-carene, myrtenol, verbenone, longifolene) were detected in all four periods. *trans*-Verbenol was only detected in the resistance period, and myrtanol was only detected in the retreat period. The percentage of limonene in the total phloem volatiles was similar during the healthy and retreat periods, significantly increased during the resistance period, and absent in the withered period (*Fig. 1*). Over thirty volatiles (accounting for 18%-30%), including pentadecane, naphthalene, tetradecane, octadecane, and acenaphthene, were also detected. Because theses volatiles were not major volatiles (such as α-pinene) or were not markedly changed in the different periods (such as myrtanol) in the preliminary analysis, they were not subjected to further analysis.

Table 3. *Mean (SE) percentage composition of identified volatiles emitted from phloem of Pinus armandii during different stages of infestation by Dendroctonus armandii. Five replicate samples were analysed for each period*

	Healthy period (n = 5)	**Resistance period (n = 5)**	**Retreat period (n = 5)**	**Withered period (n = 5)**
α-Pinene	77.46 ± 3.72(5)	65.69 ± 24.71(5)	61.41 ± 11.34(5)	60.07 ± 9.41(5)
Camphene	1.74 ± 0.92(5)	1.45 ± 0.77(5)	10.72 ± 5.79(5)	21.31 ± 18.75(3)
β-pinene	5.10 ± 0.56(5)	11.42 ± 7.23(5)	13.35 ± 4.65(5)	11.99 ± 6.81(5)
Myrcene	5.44 ± 1.23(5)	5.17 ± 3.30(5)	2.1 ± 1.47(5)	8.06 ± 3.13(4)
Limonene	8.81 ± 2.65(5)	15.08 ± 5.53(5)	9.24 ± 4.22(5)	ND[b]
3-Carene	1.75 ± 1.61(5)	0.09 ± 0.02(5)	0.8 ± 0.74(5)	5.12 ± 4.16 （4）
trans-Verbenol	ND[b]	0.01 ± 0.01(5)	ND[b]	ND[b]
Myrtenol	0.025 ± 0.015(2)	0.02(1)	0.13 ± 0.11(2)	0.017 (1)
verbenone	0.028 ± 0.011(5)	0.03 ± 0.02(5)	0.14 ± 0.13(5)	0.044 ± 0.027(4)
Myrtanol	ND[b]	ND[b]	0.04 ± 0.03(3)	ND[b]
Longifolene	1.38 ± 0.72(5)	1.05 ± 1.02(5)	2.18 ± 1.02(5)	1.17 ± 0.69(5)

[a]The values shown are the means ± SE, and the values in parentheses are the number of samples in which the component was identified
[b]ND indicates that the pheromone was not detected

Toxicity assays

The mean weight (+/- SE) of female *D. armandii* (9.74 + /- 0.05) was marginally but significantly higher than that of males (9.17 + /- 0.05) (ANOVA, $F = 60.39$, df = 1798, $P < 0.01$). After the toxicity assays, each beetle was re-weighed and the percentage weight loss was calculated. There was a significant difference between the experiment group and the control group, the beetles exposed to host volatiles lost more mass than control beetles (*Fig. 2*). Although there was no significant difference between experiment females and males, the females lost more mass than males (*Fig. 2*). Males

http://www.aloki.hu ● ISSN 1589 1623 (Print) ● ISSN 1785 0037 (Online)
DOI: http://dx.doi.org/10.15666/aeer/2001_587600

(14.14 + /- 0.33) lost a higher percentage of weight than females (13.80 + /- 0.33), but the difference was not significant (LSD-*t*, *P = 0.467*). After 24 h of volatile treatment, the death rate was calculated for the experiment and control groups. The death rate of experiment males was significantly higher than that of control males, the death rate of experiment females was significantly higher than that of control females (*Fig. 3*). There was a significant difference between experiment females and experiment males, and the experiment males had a higher death rate than females (*Fig. 3*).

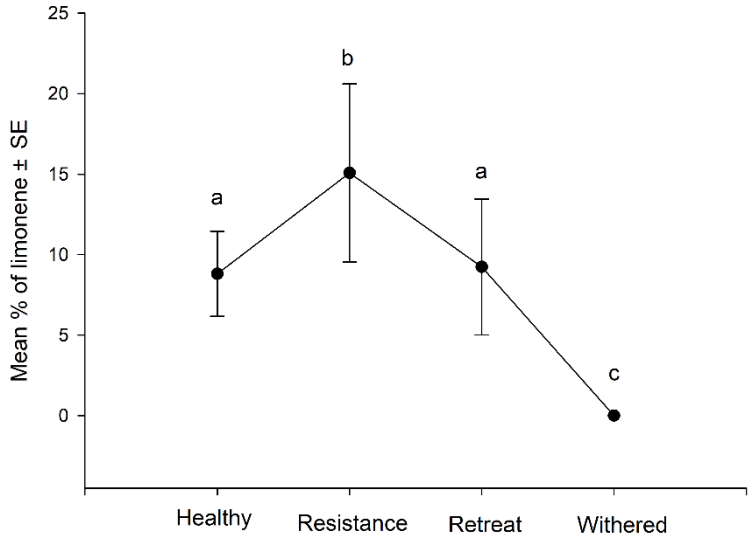

Figure 1. *Mean % ± SE of limonene in four P. armandii periods. Different letters indicate a significant difference (LSD; p < 0.01), and the same letter indicates no significant difference*

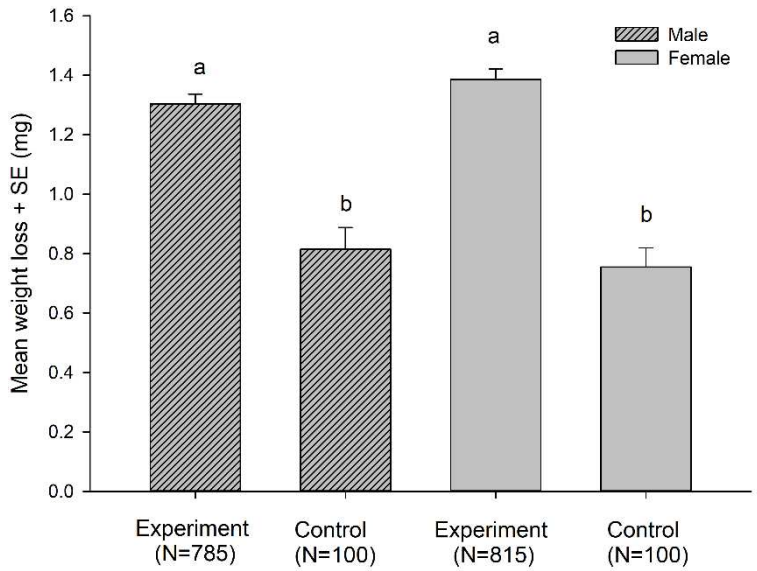

Figure 2. *Mean weight loss + SE (mg) of D. armandii males and females after 24 h exposure to various phloem volatiles on filter paper (experimental group) or untreated filter paper (control group). Means with different letters differed significantly (LSD, P < 0.01). Numbers in parentheses are the numbers of beetles measured*

http://www.aloki.hu ● ISSN 1589 1623 (Print) ● ISSN 1785 0037 (Online)
DOI: http://dx.doi.org/10.15666/aeer/2001_587600

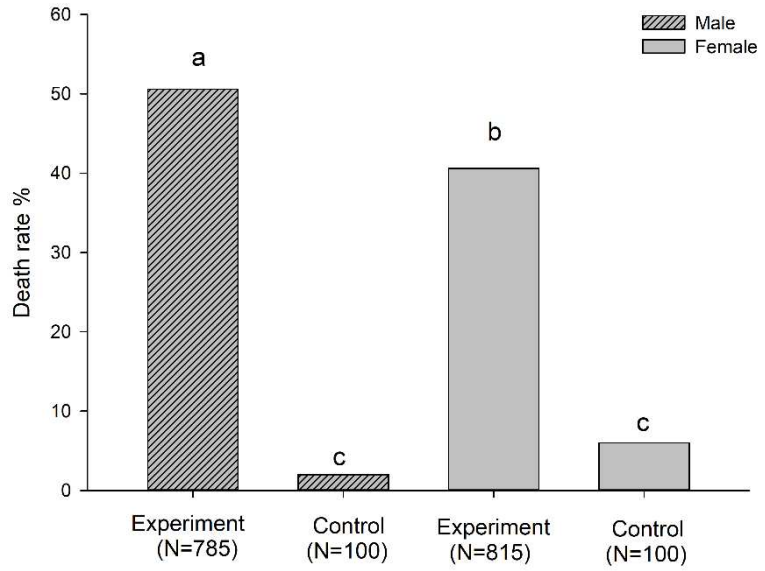

Figure 3. *Percentage mortality of D. armandii exposed for 24 h to various dosages of phloem volatiles on filter paper (experimental group) or untreated filter paper (control group). Percentage mortality with different letters differed significantly (LSD, $P < 0.01$). Numbers in parentheses are the numbers of beetles measured*

The LC_{50} values for nine host volatiles at 24 h of vapour exposure to *D. armandii* were measured. The range of LC_{50} values was from 17 to > 750, revealing the differences in toxicity of different host volatiles (*Table 4*). *R*-(+)-Limonene was the most toxic host volatile to both females and males, followed by (+)-3-carene and *S*-(-)-limonene. This ranking was consistent in females and males. The next most toxic volatiles were (+) and (-) of α-pinene and (+) and (-) of β-pinene. Myrcene and (+)-longifolene were the two lowest toxicity host volatiles. *R*-(+)-Limonene, (+)-3-carene, *S*-(-)-limonene, (-)-α-pinene, (+)-α-pinene, (+)-β-pinene and myrcene were more toxic to males than to females. (-)-β-Pinene and (+)-longifolene were more toxic to females than to males (*Table 4*).

Table 4. *The lethal concentration of elect phloem volatiles necessary to kill 50% of D. armandii males and females after 24 h exposure*

Male		**Female**	
Volatile	LC_{50} (μL/L)	Volatile	LC_{50} (μL/L)
R-(+)-limonene	17	*R*-(+)-limonene	32
(+)-3-carene	25	(+)-3-carene	39
S-(-)-limonene	42	*S*-(-)-limonene	49
(-)-α-Pinene	60	(+)-α-Pinene	68
(+)-α-Pinene	61	(-)-β-Pinene	70
(+)-β-Pinene	62	(+)-β-Pinene	74
(-)-β-Pinene	73	(-)-α-Pinene	82
Myrcene	399	Myrcene	507
(+)-longifolene	＞750	(+)-longifolene	682

The probit analysis method was used to determine the LC_{50} in SPSS (1999). Less than 50% of the males died at all test doses of (+)-longifolene

http://www.aloki.hu ● ISSN 1589 1623 (Print) ● ISSN 1785 0037 (Online)
DOI: http://dx.doi.org/10.15666/aeer/2001_587600

Discussion

Female *D. armandii* are responsible for locating and invading hosts, overcoming tree defence, building tunnels and oviposition, and males are mainly responsible for mating. Comparison of the body weights of male and female individuals revealed that the mean weight of female *D. armandii* was significantly higher than that of males. This is in line with their respective roles. Females take on more work and need more energy. After exposure to host volatiles, the weight loss (absolute values and percentages) of both sexes were significantly different between the experiment and control groups (*Fig. 2*). This demonstrated that the host volatiles have significant toxicity to female and male *D. armandii*. The death rate in the beetles exposed to host volatiles was significantly higher in males than in females, indicating that females are more resistant to the toxic effects of the tested pine volatiles. The LC_{50} values for 24 h of exposure to each tested host volatile except (+)-longifolene were higher in females than in males, further indicating that females are more resistant to the toxic effects of pine volatiles than males. Toxicity is usually affected by an individual organism's weight, and females were significantly larger than males; this could at least partially explain why the LC_{50}s for females were higher than those for males.

In previous research with *D. ponderosae*, beetle gender had no significant effects on body weight or toxicity of most monoterpenes (Chiu et al., 2017; Reid et al., 2017). A possible reason for the difference may be because at low population densities, *D. ponderosae* colonizes weakened pine and colonizes and kills healthy pine trees when beetle populations are at high densities (Krause et al., 2018; Coops et al., 2008). Whereas *D. armandii* mainly invades healthy pine greater than 30 years old (Chen et al., 2010). Due to the differences in the health status of these hosts, it can be concluded that female *D. armandii* consume more energy than female *D. ponderosae* to resist host pine resistance during invasion. At the same time, female *D. armandii* need stronger anti-host defence abilities than female *D. ponderosae* to ensure successful invasion. Female *D. armandii* have evolved significant differences from male *D. armandii*. In *D. valens*, the host defence chemicals, mainly volatile α-pinene, were found to influence its feeding behaviour and gut bacterial community structure (Xu et al., 2016). In other *Dendroctonus* spp. (*Dendroctonus rhizophagus*, *D. brevicomis*, *D. frontalis*, *Dendroctonus rufipennis*), although the host volatiles were identified and applied in behavioural research (Cano-Ramírez et al., 2012; Sullivan, 2005; Ryall et al., 2013), the toxicity of the host volatiles was not determined.

Pinus contorta and *Pinus banksiana* are hosts of *D. ponderosae*. Limonene was detected as one of the main volatiles in *P. contorta* and *P. banksiana*, accounting for 5.26 ± 0.85% and 4.77 ± 0.99% of the total volatiles (Clark et al., 2014). The toxicity of (-)-limonene to *D. ponderosae* was the strongest among a few test host volatiles, including ((-)-β-phellandrene, (+)-3-carene, myrcene, terpinolene, (-)-α-pinene, (+)-α-pinene, (-)-β-pinene, (+)-β-pinene, (-)-limonene and (+)-limonene), and (+)-limonene was the second most toxic (Chiu et al., 2017). The LC_{50} of (-)-limonene and (+)-limonene were 49 and 89 μL/L, respectively, for *D. ponderosae*. Compared with our research results (*Tables 3* and *4*), the percentage of limonene in healthy *P. armandii* was higher than in *P. contorta* and *P. banksiana*; at the same time, the LC_{50} of limonene was lower in *D. armandii* than in *D. ponderosae*. These results show that *P. armandii* has advantages in resisting bark beetle invasion compared with *P. contorta* and *P. banksiana*. Although limonene was not detected in more host survival states, limonene was the main volatile in the *D. ponderosae* host and was the most toxic host volatile.

http://www.aloki.hu ● ISSN 1589 1623 (Print) ● ISSN 1785 0037 (Online)
DOI: http://dx.doi.org/10.15666/aeer/2001_587600

The percentage dosage may increase in the host resistance period and increase host defence. However, this still needs further research. Limonene was also the main volatile found in *Picea abies* (the host of *Ips typographus*) (Persson et al., 1996), *Pinus tabuliformis* (the host of *D. valens*) (Chen et al., 2019), and *Pinus ponderosa* (the host of *D. brevicomis*) (Kolb et al., 2019). Adding limonene to the standard lure ([1:1:1 blend of (+)-alpha-pinene, (-)-beta-pinene, and (+)-3-carene]) decreased the response of *D. valens* but not significantly (Sun et al., 2004). While the toxicity and the existential state of limonene were not further considered in these studies, if limonene was the main host defence against invasion of *Dendroctonus* spp., more related data is needed for other bark beetle species.

Myrtenol was present in very low amounts (< 0.2%) during all periods of *P. armandii* invasion by *D. armandii* colonization (*Table 3*). (1R)-myrtenol was converted into both (1R)-myrtenal and (1R)-myrtanol using a *P. abies* suspension culture (Lindmark-Henriksson et al., 2004). Based on the research result, myrtenol may be the raw material of myrtanol in the retreat period of *P. armandii*. In our previous study, myrtanol was found to be toxic to *D. armandii*, especially females (Zhao et al., 2019). Myrtanol was produced in the retreat period of *P. armandii*; at this time, the resin flow stopped, and females released pheromones to attract males for mating. At the same time, the females were the most numerous sex, the number of males gradually increased. The toxicity of the generated myrtanol was stronger in females than in males (Zhao et al., 2019), this was consistent with the bark beetle population proportion in the retreat period of *P. armandii*.

Based on these studies, the chemical defence of *P. armandii* has gradually become clear. After the first female *D. armandii* tunnels into the *P. armandii* trunk, the tree responds with host defences (the resistance period). Two lines of defence in the *P. armandii* phloem were launched to resist the invasion of *D. armandii*. At first, *P. armandii* secreted resin to mount a physical attack on *D. armandii*. The concentration of host phloem volatiles was increased (Kolb et al., 2019), and at the same time, the % dosage of the key volatile limonene in the phloem rapidly increased, leading to *D. armandii* death. If the first defensive line was overcome, *P. armandii* entered the retreat period. The resin production was hindered by *L. qinlingensis,* and the % dosage of limonene was lowered. At this time, the second defensive line was initiated. *P. armandii* used volatiles (perhaps myrtenol) to synthesize the toxic compound myrtanol to resist *D. armandii*, especially females. If the second defensive line was overcome by *D. armandii*, limonene and myrtanol became absent in the phloem. *P. armandii* then entered the withered period and was unable to resist invasion.

Conclusion

In summary, this research provided evidence that females were stronger and were significantly better than males at resisting the toxicity of host volatiles. The differences between *D. armandii* and other *Dendroctonus* spp. shows that distinct bark beetle management must be used for the former. During the *D. armandii* invasion process, *P. armandii* phloem organized two defensive lines to resist the invasion of *D. armandii*. Furthermore, our results indicated that the percentage of limonene was elevated from the healthy period to the resistance period and decreased from the resistance period to the retreat period, while limonene was absent in the withered period. What triggers these changes in limonene is still not clear. Myrtanol was produced in the retreat period

http://www.aloki.hu ● ISSN 1589 1623 (Print) ● ISSN 1785 0037 (Online)
DOI: http://dx.doi.org/10.15666/aeer/2001_587600

and disappeared in the withered period. Myrtanol was produced after the first line of defence was broken, but the factors that resulted in its disappearance are not clear. Further research is needed to determine the biosynthetic mechanisms of limonene and myrtanol in *P. armandii*. Furthermore, whether limonene and myrtanol were toxic to the fungi carried by *D. armandii* was not clear. The defence of *P. armandii* against fungi is also worthy of further study.

Acknowledgements. This research was funded by the National Natural Science Foundation of China (31870636) and the National Key Research and Development Program of China (2017YFD0600104).

REFERENCES

[1] Arango-Velez, A., El Kayal, W., Copeland, C. C. J., Zaharia, L. I., Lusebrink, I., Cooke, J. E. K. (2016): Differences in defence responses of *Pinus contorta* and *Pinus banksiana* to the mountain pine beetle fungal associate *Grosmannia clavigera* are affected by water deficit. – Plant Cell and Environment 39: 726-744.

[2] Arango-Velez, A., Chakraborty, S., Blascyk, K., Phan, M. T., Barsky, J., El Kayal, W. (2018): Anatomical and chemical responses of eastern white pine (*Pinus strobus* L.) to blue-stain (*Ophiostoma minus*) inoculation. – Forests 9: 690.

[3] Blazenec, M., Jakus, R. (2009): Effect of (+)-limonene and 1-methoxy-2-propanol on *Ips typographus* response to pheromone blends. – Journal of Forest Research 20: 37-44.

[4] Byers, J. A., Wood, D. L., Craig, J., Hendry, L. B. (1984): Attractive and inhibitory pheromones produced in the bark beetle, *Dendroctonus brevicomis*, during host colonization: regulation of inter- and intraspecific competition. – Journal of Chemical Ecology 10: 861-877.

[5] Cano-Ramírez, C., Armendáriz-Toledano, F., Macías-Sámano, J. E., Sullivan, B. T., Zúñiga, G. (2012): Electrophysiological and behavioral responses of the bark beetle *Dendroctonus rhizophagus* to volatiles from host pines and conspecifics. – Journal of Chemical Ecology 38: 512-524.

[6] Chai, Q. Q., Wu, B. H., Liu, W. S., Wang, L. J., Yang, C. X., Wang, Y. J. et al. (2012): Volatiles of plums evaluated by HS-SPME with GC–MS at the germplasm level. – Food Chemistry 130: 432-440.

[7] Chen, H., Tang, M. (2007): Spatial and temporal dynamics of bark beetles in Chinese white pine in Qinling Mountains of Shaanxi Province, China. – Environmental Entomology 36: 1124-1130.

[8] Chen, H., Li, Z., Tang, M. (2010): Laboratory evaluation of flight activity of *Dendroctonus armandi* (Coleoptera: Curculionidae: Scolytinae). – Canadian Entomologist 142: 378-387.

[9] Chen, G. F., Song, Y. S., Wang, P. X., Chen, J. Y., Zhang, Z., Wang, S. M. et al. (2015): Semiochemistry of *Dendroctonus armandii* Tsai and Li (Coleoptera: Curculionidae: Scolytinae): both female-produced aggregation pheromone and host tree kairomone are critically important. – Chemoecology 25: 135-145.

[10] Chen, J. G., Bi, H. X., Yu, X. X., Fu, Y. L., Liao, W. C. (2019): Influence of physiological and environmental factors on the diurnal variation in emissions of biogenic volatile compounds from *Pinus tabuliformis*. – Journal of Environmental Sciences 81: 102-118.

[11] Chiu, C. C., Keeling, C. I., Bohlmann, J. (2017): Toxicity of pine monoterpenes to Mountain Pine Beetle. – Scientific Reports 7: 8858.

[12] Chiu, C. C., Keeling, C. I., Bohlmann, J. (2018): Monoterpenyl esters in juvenile mountain pine beetle and sex-specific release of the aggregation pheromone *trans*-verbenol. – PNAS 115: 3652-3657.

http://www.aloki.hu ● ISSN 1589 1623 (Print) ● ISSN 1785 0037 (Online)
DOI: http://dx.doi.org/10.15666/aeer/2001_587600

[13] Clark, E. L., Pitt, C., Carroll, A. L., Lindgren, B. S., Huber, D. P. W. (2014): Comparison of lodgepole and jack pine resin chemistry: implications for range expansion by the mountain pine beetle *Dendroctonus ponderosae* (Coleoptera: Curculionidae). – PeerJ 2: 240.

[14] Coops, N. C., Timko, J. A., Wulder, M. A., White, J. C., Ortlepp, S. M. (2008): Investigating the effectiveness of mountain pine beetle mitigation strategies. – International Journal of Pest Management 54: 151-165.

[15] Dai, L. L., Ma, M. Y., Wang, C. Y., Shi, Q., Zhang, R. R., Chen, H. (2015): Cytochrome P450s from the Chinese white pine beetle, *Dendroctonus armandi* (Curculionidae: Scolytinae): Expression profiles of different stages and responses to host allelochemicals. – Insect Biochemistry and Molecular Biology 65: 35-46.

[16] Erbilgin, N., Cale, J. A., Lusebrink, I., Najar, A., Klutsch, J. G., Sherwood, P. et al. (2017): Water-deficit and fungal infection can differentially affect the production of different classes of defense compounds in two host pines of mountain pine beetle. – Tree Physiology 37: 338-350.

[17] Faccoli, M., Stergulc, F. (2008): Damage reduction and performance of mass trapping devices for forest protection against the spruce bark beetle, *Ips typographus* (Coleoptera Curculionidae Scolytinae). – Annals of Forest Science 65: 309.

[18] Franceschi, V. R., Krokene, P., Christiansen, E., Krekling, T. (2005): Anatomical and chemical defenses of conifer bark against bark beetles and other pests. – New Phytologist 167: 353-375.

[19] Gillette, N. E., Stein, J. D., Owen, D. A., Webster, J. N., Fiddler, G. O., Mori, S. R. et al. (2006): Verbenone-releasing flakes protect individual *Pinus contorta* trees from attack by *Dendroctonus ponderosae* and *Dendroctonus valens* (Coleoptera: Curculionidae, Scolytinae). – Agricultural and Forest Entomology 8: 243-251.

[20] Gillette, N. E., Erbilgin, N., Webster, J. N., Pederson, L., Mori, S. R., Stein, J. D. et al. (2009): Aerially applied verbenone-releasing laminated flakes protect *Pinus contorta* stands from attack by *Dendroctonus ponderosae* in California and Idaho. – Forest Ecology and Management 257: 1405-1412.

[21] Hood, S., Sala, A. (2015): Ponderosa pine resin defenses and growth: metrics matter. – Tree Physiology 35: 1223-1235.

[22] Hu, X., Li, M., Zhang, F. P., Chen, H. (2016): Influence of starvation on the structure of gut-associated bacterial communities in the Chinese white pine beetle (*Dendroctonus armandi*). – Forests 7: 126.

[23] Kane, J. M., Kolb, T. E. (2010): Importance of resin ducts in reducing ponderosa pine mortality from bark beetle attack. – Oecologia 164: 601-609.

[24] Keenan, D. F., Brunton, N. P., Mitchell, M., Gormley, R., Butler, F. (2012): Flavour profiling of fresh and processed fruit smoothies by instrumental and sensory analysis. – Food Research International 45: 17-25.

[25] Kolb, T., Keefover-Ring, K., Burr, S. J., Hofstetter, R., Gaylord, M., Raffa, K. F. (2019): Drought-mediated changes in tree physiological processes weaken tree defenses to bark beetle attack. – Journal of Chemical Ecology 45: 888-900.

[26] Krause, A. M., Townsend, P. A., Lee, Y., Raffa, K. F. (2018): Predators and competitors of the mountain pine beetle *Dendroctonus ponderosae* (Coleoptera: Curculionidae) in stands of changing forest composition associated with elevation. – Agricultural and Forest Entomology 20: 402-413.

[27] Li, X. J., Gao, J. M., Chen, H., Zhang, A. L., Tang, M. (2012): Toxins from a symbiotic fungus, *Leptographium qinlingensis* associated with *Dendroctonus armandi* and their in vitro toxicities to *Pinus armandi* seedlings. – European Journal of Plant Pathology 134: 239-247.

[28] Light, D. M. (1983): Sensitivity of antennae of male and female *Ips paraconfusus* (Coleoptera: Scolytidae) to its pheromone and other behavior-modifying chemicals. – Journal of Chemical Ecology 9: 585-606.

http://www.aloki.hu ● ISSN 1589 1623 (Print) ● ISSN 1785 0037 (Online)
DOI: http://dx.doi.org/10.15666/aeer/2001_587600

[29] Lindmark-Henriksson, M., Isaksson, D., Vaněk, T., Valterová, I., Högberg, H. E., Sjödin, K. (2004): Transformation of terpenes using a *Picea abies* suspension culture. – Journal of Biotechnology 107: 173-184.
[30] Persson, M., Sjödin, K., Borg-Karlson, A. K., Norin, T., Ekberg, I. (1996): Relative amounts and enantiomeric compositions of monoterpene hydrocarbons in xylem and needles of *Picea abies*. – Phytochemistry 42: 1289-1297.
[31] Ning, H., Dai, L. L., Fu, D. Y., Liu, B., Wang, H. L., Chen, H. (2019): Factors influencing the geographical distribution of *Dendroctonus armandi* (Coleoptera: Curculionidae: Scolytidae) in China. – Forests 10: 425.
[32] Perkins, D. L., Jorgensen, C. L., Rinella, M. J. (2015): Verbenone decreases whitebark pine mortality throughout a Mountain Pine Beetle outbreak. – Forest Science 61: 747-752.
[33] Pureswaran, D. S., Borden, J. H. (2004): New repellent semiochemicals for three species of *Dendroctonus* (Coleoptera: Scolytidae). – Chemoecology 14: 67-75.
[34] Pureswaran, D. S., Hofstetter, R. W., Sullivan, B. T. (2008): Attraction of the southern pine beetle, *Dendroctonus firontalis*, to pheromone components of the western pine beetle, *Dendroctonus brevicomis* (Coleoptera: Curculionidae: Scolytinae), in an allopatric zone. – Environmental Entomology 37: 70-78.
[35] Raffa, K. F., Mason, C. J., Bonello, P., Cook, S., Erbilgin, N., Keefover-Ring, K. et al. (2017): Defence syndromes in lodgepole - whitebark pine ecosystems relate to degree of historical exposure to mountain pine beetles. – Plant Cell and Environment 40: 1791-1806.
[36] Reid, M. L., Sekhon, J. K., LaFramboise, L. M. (2017): Toxicity of monoterpene structure, diversity and concentration to Mountain Pine Beetles, *Dendroctonus ponderosae*: beetle traits matter more. – Journal of Chemical Ecology 43: 351-361.
[37] Roth, M., Hussain, A., Cale, J. A., Erbilgin, N. (2018): Successful colonization of lodgepole pine trees by mountain pine beetle increased monoterpene production and exhausted carbohydrate reserves. – Journal of Chemical Ecology 44: 209-214.
[38] Ryall, K. L., Silk, P., Thurston, G. S., Scarr, T. A., de Groot, P. (2013): Elucidating pheromone and host volatile components attractive to the spruce beetle, *Dendroctonus rufipennis* (Coleoptera: Curculionidae), in eastern Canada. – Canadian Entomologist 145: 406-415.
[39] Strom, B. L., Goyer, R. A., Ingram, L. L., Boyd, G. D. L., Lott, L. H. (2002): Oleoresin characteristics of progeny of loblolly pines that escaped attack by the southern pine beetle. – Forest Ecology and Management 158: 169-178.
[40] Sullivan, B. T. (2005): Electrophysiological and behavioral responses of *Dendroctonus frontalis* (Coleoptera: Curculionidae) to volatiles isolated from conspecifics. – Journal of Economic Entomology 98: 2067-2078.
[41] Sun, J. H., Miao, Z. W., Zhang, Z., Zhang, Z. N., Gillette, N. E. (2004): Red turpentine beetle, *Dendroctonus valens* LeConte (Coleoptera: Scolytidae), response to host semiochemicals in China. – Environmental Entomology 33: 206-212.
[42] Sun, J. H., Lu, M., Gillette, N. E., Wingfield, M. J. (2013): Red Turpentine Beetle: innocuous native becomes invasive tree killer in China. – Annual Review of Entomology 58: 293-311.
[43] Xie, S. A., Lv, S. J. (2012): An improved lure for trapping the bark beetle *Dendroctonus armandi* (Coleoptera: Scolytinae). – European Journal of Entomology 109: 569-577.
[44] Xu, L. T., Shi, Z. H., Wang, B., Lu, M., Sun, J. H. (2016): Pine defensive monoterpene α-pinene influences the feeding behavior of *Dendroctonus valens* and its gut bacterial community structure. – International Journal of Molecular Sciences 17: 1734.
[45] Zhang, L. W., Sun, J. H., Clarke, S. R. (2006): Effects of verbenone dose and enantiomer on the interruption of response of the red turpentine beetle, *Dendroctonus valens* LeConte (Coleoptera: Scolytidae), to its kariomones. – Environmental Entomology 35: 655-660.

http://www.aloki.hu ● ISSN 1589 1623 (Print) ● ISSN 1785 0037 (Online)
DOI: http://dx.doi.org/10.15666/aeer/2001_587600

[46] Zhao, M. Z., Dai, L. L., Fu, D. Y., Gao, J., Chen, H. (2017a): Electrophysiological and behavioral responses of *Dendroctonus armandi* (Coleoptera: Curculionidae: Scolytinae) to two candidate pheromone components: frontalin and *exo*-brevicomin. – Chemoecology 27: 91-99.

[47] Zhao, M. Z., Dai, L. L., Sun, Y. Y., Fu, D. Y., Chen, H. (2017b): The pheromone verbenone and its function in *Dendroctonus armandi* (Coleoptera: Curculionidae: Scolytinae). – European Journal of Entomology 114: 53-60.

[48] Zhao, M. Z., Liu, B., Sun, Y. Y., Wang, Y. Y., Dai, L. L., Chen, H. (2019): Presence and roles of myrtenol, myrtanol and myrtenal in *Dendroctonus armandi* (Coleoptera: Curculionidae: Scolytinae) and *Pinus armandi* (Pinales: Pinaceae: Pinoideae). – Pest Management Science 76: 188-197.

http://www.aloki.hu ● ISSN 1589 1623 (Print) ● ISSN 1785 0037 (Online)
DOI: http://dx.doi.org/10.15666/aeer/2001_587600

THE FULL-LENGTH TRANSCRIPTOME BY THE SINGLE-MOLECULE LONG-READ SEQUENCING REVEALS A HEAT-RESISTANT MECHANISM IN CAPER BUSH (*CAPPARIS SPINOSA* L.)

LIU, Z.[1] – ZHOU, K.[2] – WANG, L.[3,4] – LI, S.[1] – CHEN, G.[1] – SUN, Z.[5] – SUN, R.[2*] – QANMBER, G.[2*]

[1]*Zhengzhou Research Base, State Key Laboratory of Cotton Biology, School of Agricultural Sciences, Zhengzhou University, Zhengzhou, 450001 Henan, China*

[2]*State Key Laboratory of Cotton Biology, Institute of Cotton Research, Chinese Academy of Agricultural Sciences, Anyang, 455000 Henan, China*

[3]*State Key Laboratory of Desert and Oasis Ecology, Xinjiang Institute of Ecology and Geography, Chinese Academy of Sciences, 830011 Urumqi, China*

[4]*University of Chinese Academy of Sciences, 100049 Beijing, China*

[5]*Development Center for Science and Technology, Ministry of Agriculture and Rural Affairs, 100122 Beijing, China*

**Corresponding authors*
e-mail: sunruibin@caas.cn; gqkhan12@gmail.com

(Received 21st May 2021; accepted 20th Sep 2021)

Abstract. Recent global climate change affects the living conditions of many plant and animal species on Earth. *Capparis spinosa* L. is a perennial xerophytic shrub with significant adaptability to arid environments and a candidate species for the prevention of soil erosion. However, its reference genome or large-scale full-length cDNA sequences are still lacking. Here, we applied a combination of second and third-generation sequencing technologies to sequence the full-length transcriptome in *Capparis spinosa* L. In total, 14.96 GB of clean reads were generated, including 828,518 reads of insert (ROI) and 370,258 full-length non-chimeric (FLNC) reads. We reported 216,240 consensus isoforms by transcript clustering analysis. After removing redundant reads, we identified 191,599 non-redundant isoforms of which 171,893 were coding isoforms. Through second-generation sequencing (SGS), we obtained 434 differentially expressed genes (DEGs) from samples collected under different temperatures for further analysis. Among these DEGs, we found 29 transcription factors belonging to seven different TF families in which *CsMYB28* and *CsMYB73* were up-regulated as the temperature rose. Overall, this is the first study to perform SMRT sequencing of full-length transcriptome of *Capparis spinosa* L. Our results will contribute to increasing interest for *Capparis spinosa* L as a candidate crop for future environmental challenges.
Keywords: *global warming, Capparis spinosa, drought tolerance, SMRT, caper*

Introduction

In recent years, climate change has been reported as a factor that has adverse effects on biological survival around the world (Bellard et al., 2012). Climate change has a significant impact on biodiversity, especially on changes in the distribution of species (Peterson et al., 2004). As the environment changes more drastically, the distribution of species will become more uncontrollable (Lagouvardos and Kotroni, 2007). Moreover, climate change has significantly affected agricultural production. High temperature, heat and drought stress make it impossible to ensure global food security (Campbell,

http://www.aloki.hu ● ISSN 1589 1623 (Print) ● ISSN 1785 0037 (Online)
DOI: http://dx.doi.org/10.15666/aeer/2001_601617

2015). Environmental factors such as drought, salinity and extreme temperatures adversely affect plant growth and productivity.

However, the introduction of stress-tolerant crops and varieties into agricultural systems is not a rapid process. Xerophytic (drought-tolerant) plants are those that are able to adapt to drought and can grow, develop and reproduce as usual under such conditions (Henckel, 1964). Through the evolution, drought-tolerant plants acquired a series of morphological and biochemical changes in roots, stems and leaves in order to adapt to this stress. Such crops may be an effective way to promote sustainable agriculture (Thiry et al., 2016). This study pay attention to the crop that can adapt to heat stress namely caper (*Capparis spinosa* L.).

Capparis spinosa L. is a typical heat-tolerant plants, which could flourish under extremely high temperatures and poor soil conditions (Nabavi et al., 2016). It is usually grown on the sandy loam with low alkalinity. Since it has a deep and extensive root system that can grow in harsh environments, it is recommended to prevent land degradation and control soil erosion (Nabavi et al., 2016). *C. spinosa* is a dicotyledonous 20-30 cm tall shrub that is widely distributed in the Mediterranean countries such as Greece, Italy, Turkey, Morocco and Spain (Inocencio et al., 2000). In China, it is distributed in Xinjiang and Tibet especially in Turpan, Korla and Aksu areas of Xinjiang province. *C. spinosa* is also known as Caper, (wild watermelon in China), Cappero (in Italy) and Alcapparo (in Spain) (Tlili et al., 2011). *C. spinosa* is a winter-deciduous perennial and evergreen shrub, growing and flowering from May to October during summer (Rhizopoulou and Psaras, 2003). The flowers are open pollinated at night and die soon after sunrise (Rhizopoulou and Psaras, 2003). It withstands not only over 45 ℃ in summer and over 50 ℃ in the gravel Gobi, but also hurricanes with winds of about 40 days every year (Rhizopoulou and Psaras, 2003). Its main roots are flourishing which extend up to 30-40 m underground with well-developed vascular system, so the groundwater resources can be effectively utilized (Rhizopoulou and Psaras, 2003).

The adaptation of *C. spinosa* to drought is based on its osmotic adjustment, regulation of stomatal opening, modification of cell wall properties, and extensive root systems. The stomata remains open throughout the day, with a high transpiration rate, resulting in leaf temperature of 3.9 ℃ less than air temperature (Rhizopoulou and Psaras, 2003). The stomatal length of *C. spinosa* is 28 um, which is much larger than 134 desert plants (Gadgoli and Mishra, 1999). The stomatal density is also high among all desert plants (Gadgoli and Mishra, 1999). Dense root system and transport tissues enabled *C. spinosa* to adapt environmental stress. Further, the sugar and proline content are high in the *C. spinosa*, as both are important cell osmotic adjustment substance, and regulate the flow of water between the membranes and maintaining the balance of water in tissues (Rhizopoulou and Psaras, 2003). In *C. spinosa*, unsaturated fatty acids are the main components of lipids in petals, which affect the fluidity of the membrane. The solute and water potential of petals are low when flowing in the night, which keep enough water in cells while after sunrise, the water and solute potential begin to rise (Rhizopoulou et al., 2006). Strong drought resistance properties of *C. spinosa* play an important ecological and economic role in desert areas.

In the past years, structural and functional genomics have laid the foundation for exploring plant biology. In order to carry out these studies efficiently, it is necessary to obtain high quality genomic and transcriptome sequences (Margulies et al., 2005). Second-generation sequencing (SGS) technology has changed DNA sequencing and

http://www.aloki.hu ● ISSN 1589 1623 (Print) ● ISSN 1785 0037 (Online)
DOI: http://dx.doi.org/10.15666/aeer/2001_601617

genomic/transcriptome studies (Shendure and Ji, 2008). However, one of the disadvantages of SGS is that they have a shorter read length (i.e., hundreds of base pairs). As a result, shorter read length reduces the accuracy of sequence assembly and increase the difficulty of bioinformatics analysis in the future. Recently, a third-generation sequencing (TGS) platform of single-molecule real-time (SMRT) sequencing carries out in the PacBio RS (Pacific Biosciences of California) that is widely used in genome sequencing because of its long reads (average 4-8 kb) sequencing technology (Eid et al., 2009). TGS has long read length and contributes to the de novo genome and transcriptome assembly in higher organisms and makes TGS the best choice for full-length transcripts (Sharon et al., 2013). However, relatively high error rate of TGS may be problematic in sequence alignment and bioinformatics analysis. But this problem can be minimized and improved by high-accuracy of SGS (Li et al., 2014). Previously it has been shown that combining SGS and TGS technologies could provide high quality and more complete assembly in genomic and transcriptome studies (Sharon et al., 2013). Recently, transcriptome sequencing by SGS and TGS technologies has been widely applied in plant development and stress response research (Minio et al., 2019. Filichkin et al., 2018; Pan et al., 2020).

Though the excellent adaptation ability of *C. spinosa* to the extreme conditions, the molecular mechanisms were still unknown. In this study, we constructed a full-length cDNA library from *C. spinosa* derived from four different tissues (root, stem, leaves and shoots) by using SMRT sequencing. In addition, leaves collected at three different time points (8:00 am, 2:00 pm, 8:00 pm) of a day were used as sample for RNA sequencing. The annotation of full-length transcriptome analysis of *C. spinosa* helps to understand the complexity of the *C. spinosa* genome and provides a reference sequence for gene cloning and mechanism analysis of *C. spinosa*'s adaptation. This will help improve this species and develop more intensive research, especially in responding to climate change.

Methods

Sample collection, RNA extraction, library construction and sequencing

The roots, stems, leaves and shoots of *C. spinosa* (Specimen number 05SYIIM213:2) were taken from State Key Laboratory of Desert and Oasis Ecology, Xinjiang Institute of Ecology and Geography, Chinese Academy of Sciences, Urumqi, China. C. spinosa plants were sampled from Turfan desert in July, where is one of the most dry with 25-100 mm of annual precipitation and the hottest area in southern Xinjiang. At three different time points (8:00 am, 2:00 pm, 8:00 pm) we collected leaves and measured the temperature respectively. Total RNA was extracted by RNAprep Pure Plant Kit (TIANGEN), NanoDrop 2000 microvolume spectrophotometer instrument (Thermo Scientific, USA) was used to measure the purity and concentration of RNA. The quality and integrity of RNA was tested by agarose gel electrophoresis and Agilent Bioanalyzer 2100 system (Agilent Technologies, USA). Qualified RNA samples were used for following experiments. For SMRT sequencing, a portion of RNA samples were taken and mixed with equal molar ratio and oligo-dT magnetic beads were used to enrich mRNA. Reverse transcription PCR was conducted by using SMARTer™ PCR cDNA Synthesis Kit (Clontech, Japan) to synthesize full-length cDNA. BluePippin (Sage Science, USA) was used to select specific size of full-length cDNA for construction of library with specific size of insert cDNA. After re-amplification, and end repairing and

http://www.aloki.hu ● ISSN 1589 1623 (Print) ● ISSN 1785 0037 (Online)
DOI: http://dx.doi.org/10.15666/aeer/2001_601617

adenylation, adaptors with a hairpin loop structure were ligated to cDNA to obtain SMRT bell sequencing library. The constructed SMRT library was quantified by Qubit 2.0 (Thermo Scientific, USA), and quality assessed using Agilent Bioanalyzer 2100 system. The qualified SMRT library was sequenced by using a PacBio RSII sequencer (Pacific Biosciences, USA). For common Illumina transcriptome sequencing, purified mRNA was fragmented using the fragmentation agents and served as templates for cDNA synthesis primed by random hexamers. Then the end of cDNA fragments was repaired and added by single nucleotide A (adenine) to ligate with adaptors. By using agarose gel electrophoresis, about 250 bp were selected for constructing library. The amplified libraries were quantified and quality assessed by Qubit 2.0 and Agilent Bioanalyzer 2100 system.

Processing of SMRT sequencing data

The raw SMRT sequencing polymerase reads were processed into reads of insert (ROIs) by removing adapter sequences, ROIs with length of less than 50 bp and quality of less than 0.75 were discarded. During the SMRT library construction, some cDNA sequences may ligate directly with each other without adapter, this leads to some chimeric ROIs with sequencing primer existed in the inner part of sequence. These chimeric ROIs were discarded, only non-chimeric ROIs were further processed. Filtered non-chimeric ROIs within the 5′sequencing primer, 3′sequencing primer and poly A tail before 3′sequencing primer at terminals were recognized as full-length reads, while ROIs lacking one of these three elements were non-full-length reads. After removing terminal primer sequences, the full-length transcripts were used for iterative clustering and error correction referring non-full-length transcripts by ICE （isoform-level clustering for error correction）algorithm by using SMRT analysis 2.3.0 software. After error correction, the obtained polished full-length transcripts with accuracy > 99% were recognized as high quality. Further, the high-quality full-length transcripts were processed to eliminate redundancy using CD-HIT software (http://weizhong-lab.ucsd.edu/cdhit_suite/cgi-bin/index.cgi). The final non-redundancies high quality full-length transcripts were considered as full-length transcript isoforms.

Functional annotation

Transdecoder 3.0.0 software (https://portal.rc.fas.harvard.edu/p3/build-reports/TransDecoder%2F3.0.0-fasrc01) was used to identify candidate coding sequence regions and corresponding proteins of final non-redundancy full-length transcripts with default parameters and integrating the blast against Swissprot (https://web.expasy.org/docs/swiss-prot) and Pfam (https://pfam.xfam.org/) database search results. All obtained full-length transcripts were functionally annotated by mapping transcripts sequences to six sequence databases including GO, KEGG, KOG, NR, NT, and Swissprot.

Transcription factors (TFs) prediction and analysis

The corresponding protein amino acid sequences of full-length transcripts were submitted to iTAK database (http://itak.feilab.net/cgi-bin/itak/index.cgi) to predict genome-wide transcription factors (TFs) using iTAK online v1.6 program with default parameters. The resulted candidate TFs were classified into corresponding TF families automatically.

http://www.aloki.hu ● ISSN 1589 1623 (Print) ● ISSN 1785 0037 (Online)
DOI: http://dx.doi.org/10.15666/aeer/2001_601617

NGS sequencing reads mapping, transcripts quantification and differentially expressed genes (DEGs) analysis

Using non-redundancy high quality full-length transcripts as reference, NGS sequencing reads were mapped by Bowtie 2.1.0 software (Langmead et al., 2012), transcripts quantification was conducted using RSEM 1.2.15 software (Li et al., 2011) based on mapping results, expression level of transcripts were computed and represented with fragments per kilo base (kb) of transcript per million fragments mapped (FPKM) value. edgeR 3.14.0 software (Chen et al., 2014) was used for differentially expressed genes (DEGs) identification, and genes with absolute value of expression fold change (FC) > 2 and false discovery rate (FDR) < 0.05 were recognized as differentially expressed genes. The total DEGs were identified in different sample comparison pairs (8:00 am vs 2:00 pm, 8:00 am vs 8:00 pm and 2:00 pm vs 8:00 pm) that were used for subsequent analyses. Expression heatmap within hierarchy clustering of DEGs was drawn using R software package pheatmap based on log10-transformed FPKM values. GO and KEGG pathway enrichment analyses were conducted using topGO 2.24.0 (Alexa et al., 2016) and KOBAS 2.0 (Bu et al., 2021) software respectively.

Quantitative real-time PCR experiment

Remove genomic DNA from RNA samples and reverse cDNA using PrimeScript^{TM}RT reagent Kit with gDNA Eraser (Perfect Real Time) kit (Takara, Dalian, China). By a qRT-PCR experiment, Premix Ex Taq™ II (Takara) was used along with the LightCycler 480 system (Roche). The *CsUBQ6* (C. spinosa_1-6k_c193395/f1p19/1544) was used as the reference gene. The relative expression values were calculated by the $2^{-\Delta CT}$ method.

Results

General quality and data output of SMRT sequencing

C. spinosa is a shrub plant (*Fig. 1A, B*), and is found to be adapted well under drought and poor soil conditions. To obtain a full-length of *C. spinosa* transcriptome, we mixed different tissues for library sequencing. Full-length cDNA library with an insert size of 1-6 kb was sequenced with 2 SMRT cells. In total, we obtain 893869 polymerase reads with 14.96 Gb of clean reads after preprocessing (*Table 1*). A total of 828518 reads of insert (ROIs) were produced with full passes ≥ 50 and the predicted consensus accuracy > 0.75, including 44.69% (370528) of full-length non-chimeric reads and 4.98% of full-length chimeric reads. While, the remaining were non-full-length reads (50.33%) (*Table 2*). The mean length of ROI is 1820 bp, and the quality of 0.90 and 8 passes (*Table 2*). Similarly, we obtained 216240 consensus isoforms sequences and ICE (Isoform-level Clustering Algorithm) was used to cluster and polish the non-chimeric transcripts. After clustering and polishing, redundant transcripts were removed. Finally, we obtained 191599 non-redundant isoforms, of which 171893 were coding non-redundant isoforms. The average lengths of non-redundant andcoding non-redundant isoforms are 1674 bp and 985 bp, respectively (*Table 3*). Among non-redundant isoforms, most of them were mainly distributed in length from 1 k to 3 k and among these, 53.05% of the isoforms were 1-2 k in length. The percentage of isoforms of length in 2-3 k was 20.41%. Only very few isoforms were longer than 5 k (*Fig. 1C*).

http://www.aloki.hu ● ISSN 1589 1623 (Print) ● ISSN 1785 0037 (Online)
DOI: http://dx.doi.org/10.15666/aeer/2001_601617

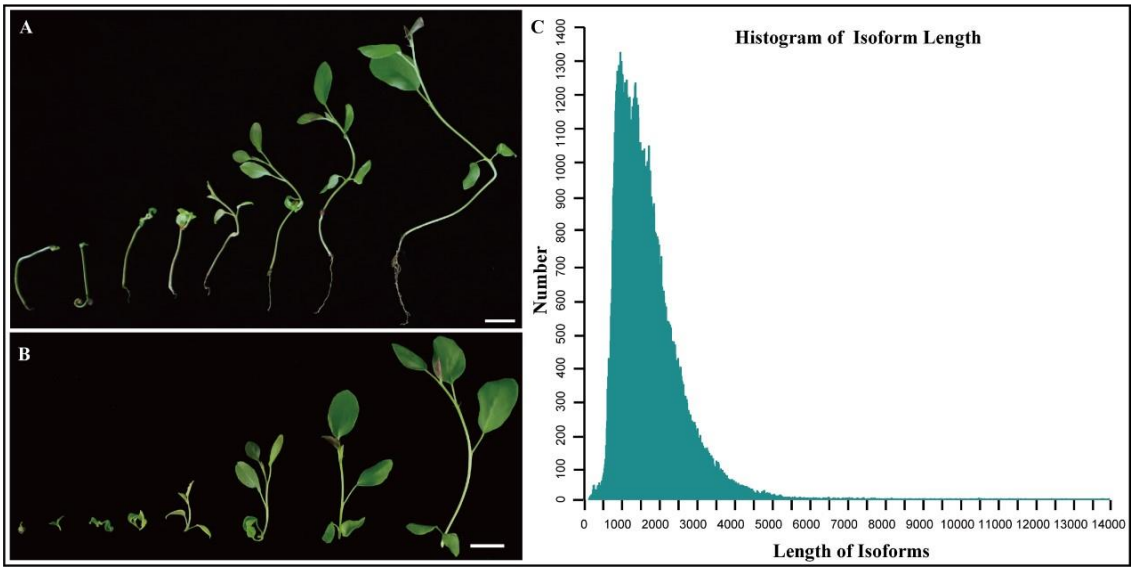

Figure 1. *(A, B) Phenotype of C. spinosa whole plant and shoots. (C) Length distribution of C. spinosa isoforms*

Table 1. *Statistics of polymerase reads*

Sample name	Cell ID	cDNA size	Polymerase read bases	Polymerase reads	Polymerase read N50	Polymerase read length
C. spinosa	A01	1-6 K	7.69 GB	387853	42750	19828
C. spinosa	B01	1-6 K	7.27 GB	506016	34750	14360

Table 2. *Statistics of reads of insert (ROI)*

Sample	*C. spinosa*
cDNA size	1-6 k
Reads of insert	828518
Read bases of insert	1508295266
Number of five prime reads	457118
Number of three prime reads	558636
Number of poly-A reads	503802
Number of filtered short reads	0
Number of non-full-length reads	416980
Number of full-length reads	411538
Number of full-length non-chimeric reads	370258
Full-length non-chimeric reads percentage (%)	44.69%
Mean read length of insert	1820
Mean read quality of insert	0.904459165655
Mean number of passes	8

http://www.aloki.hu ● ISSN 1589 1623 (Print) ● ISSN 1785 0037 (Online)
DOI: http://dx.doi.org/10.15666/aeer/2001_601617

Table 3. *Statistics of non-redundant isoforms*

Sample	*C. spinosa*
cDNA size	1-6 k
Number of consensus isoforms	216240
Number of non-redundant isoforms	191599
Average length of non-redundant isoforms	1674
Number of coding isoforms	171893
Average length of coding isoforms	985

Functional annotation and transcription factors analysis

To predict and analyze the function of 191,599 non-redundant isoforms, we used BLAST to perform functional annotation in GO, KEGG, KOG, NR, Swissprot databases. In total, 186840 isoforms were successfully annotated in at least one out of five subjected databases (*Table 4*), accounting 97.51% of the total isoforms. For functional classification of *C. spinosa* transcripts, GO annotation was performed using BLAST2GO, and transcripts divided into three categories (molecular function, cellular component, and biological process) (*Fig. 2*). In the classification of biological process, major categories were "cellular process" (104104, 18.77% of the total) and "metabolic process" (97177, 17.52% of the total). While in the category of cellular component, isoforms involved in the "cell" (131964, 22.17% of the total) and "cell part" (131635, 22.11% of the total) were main component in our analysis. However, the major subgroups of molecular function were "binding" (89893, 43.44% of the total) and "catalytic activity" (80841, 39.07% of the total).

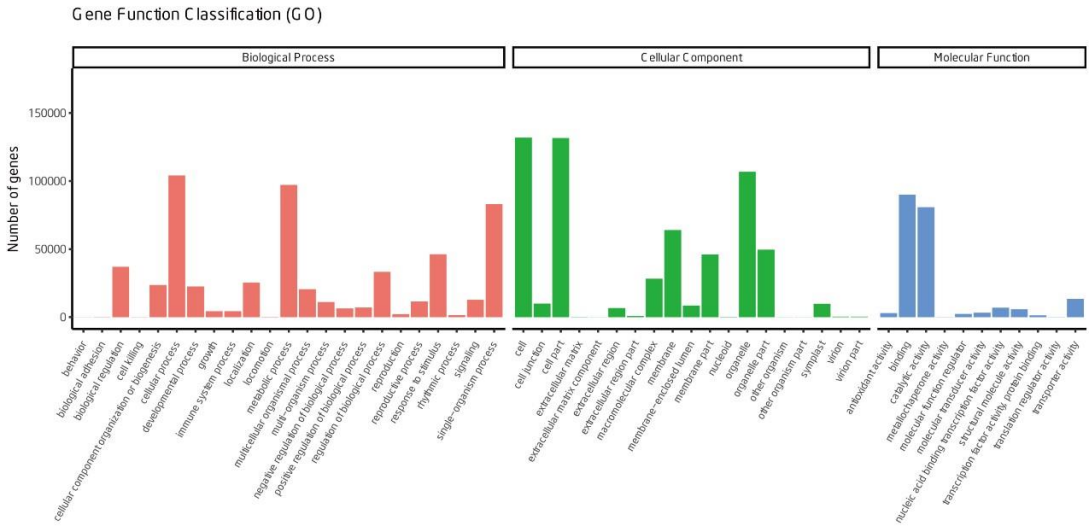

Figure 2. *Distribution of Gene Ontology (GO) terms of C. spinosa full-length transcriptome*

Further, to study the functions and interactions of isoforms in *C. spinosa*, we performed KEGG analysis. During KEGG analysis, a total of 92992 isoforms were annotated and divided into 19 functional categories (*Fig. 3*). Among these categories, the "carbohydrate metabolism" pathway contained a maximum number of isoforms accounting for a total of 12728 isoforms.

http://www.aloki.hu ● ISSN 1589 1623 (Print) ● ISSN 1785 0037 (Online)
DOI: http://dx.doi.org/10.15666/aeer/2001_601617

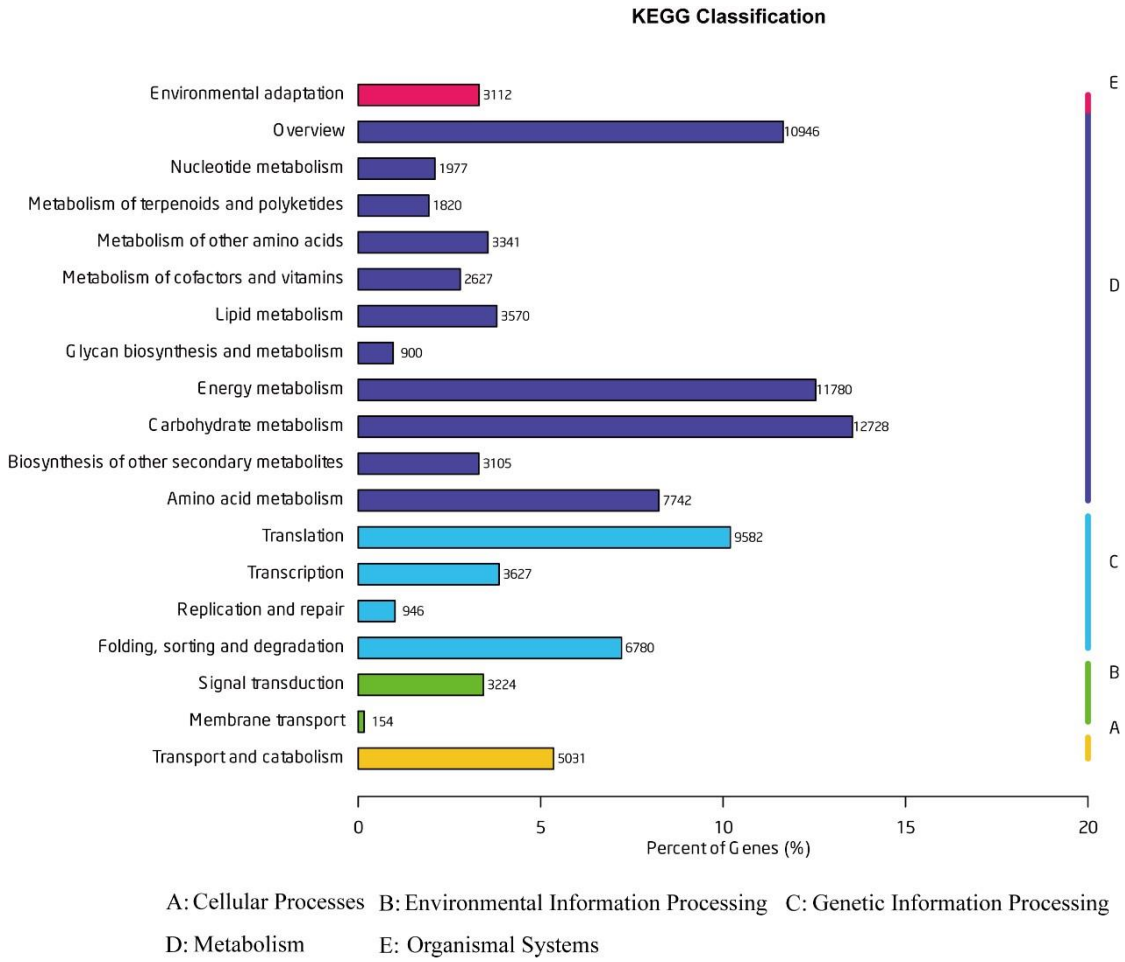

Figure 3. *KEGG pathway classification of C. spinosa full-length transcriptome*

Table 4. *Statistics of functional annotation of isoforms*

Anno_Database	Annotated_Number
GO	161075
KEGG	93966
KOG	82834
NR	182680
Swissprot	143370
All_Annotated	186840

For the prediction of transcription factor, we used full length transcripts and found that a total of 7188 transcripts were annotated as transcription factors belonging to 64 TF (transcription factor) families. AP2/ERF and bHLH were the two largest transcription factor families accounting for 10.2% and 6.6% of the genes, respectively. Similarly, other transcription factor such as C3H, bZIP, GRAS, MYB-related, C2H2, WRKY, NAC, and MYB accounted for 58.2% (each accounted for 3.7% to 8.4%) of the transcription factor genes (*Fig. 4*).

http://www.aloki.hu ● ISSN 1589 1623 (Print) ● ISSN 1785 0037 (Online)
DOI: http://dx.doi.org/10.15666/aeer/2001_601617

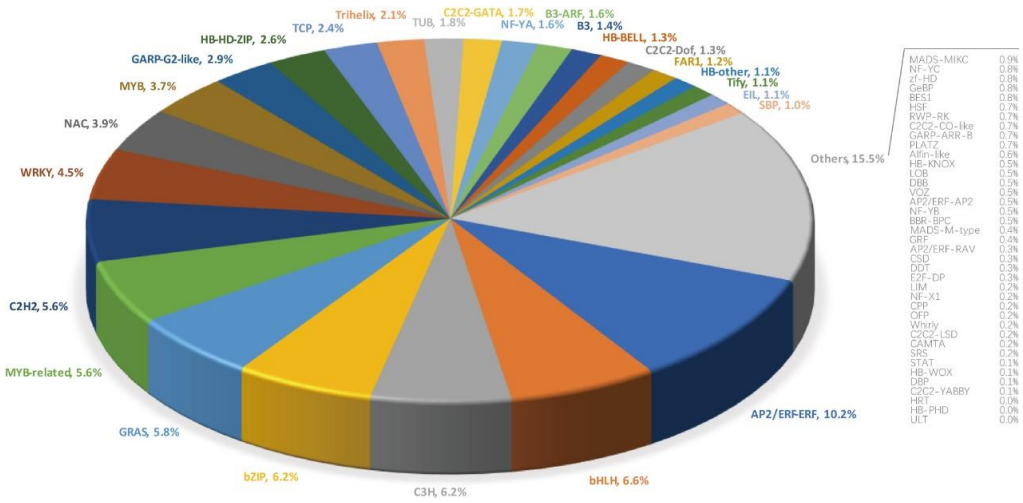

Transcription Factors Family Classification

Figure 4. *Distribution of different transcription factor in C. spinosa full-length transcriptome. The number represents the proportion of transcription factors*

Quality improvement and error correction of SMRT Isoforms by RNA-Seq reads

Since SMRT sequencing produces high error rates, it is necessary to perform error correction by using high quality SGS short read corrections. We filtered raw data and obtain a total of 737 million clean reads which were further used for gene expression analysis (*Table 5*). The RNA-Seq reads were aligned to the reference isoforms with the alignment ratio greater than 89% for whole alignment. Further, we identified differentially expressed genes (DEGs) between different comparative pairs (8:00 am vs 2:00 pm, 8:00 am vs 8:00 pm, 2:00 pm vs 8:00 pm) and 434 DEGs were obtained. The numbers of DEGs in three comparative pairs were shown in *Figure 5A*. In 8:00 am vs 8:00 pm and 2:00 pm vs 8:00 pm comparative pairs, more DEGs were up-regulated (10 and 100 genes respectively) than down-regulated (8 and 24 genes respectively), whereas, in 8:00 am vs 2:00 pm more genes were down-regulated (244 genes) than up-regulated genes (100 genes) (*Fig. 5A*). Moreover, *Figure 5A* showed the degree of overlap of DEGs between different comparative pairs. In 8:00 am vs 2:00 pm, 8:00 am vs 8:00 pm and 2:00 pm vs 8:00 pm comparative pairs, the number of DEGs were 344, 18, and 124 respectively (*Fig. 5A*).

Table 5. *Mapping rate of NGS RNA-sequencing reads to reference isoforms*

Sample	Total reads	Mapped reads (ratio)
8pm-1	101873366	92175720 (90.48%)
8pm-2	80236132	71433332 (89.03%)
8pm-3	70479896	63334948 (89.86%)
8am-1	84737406	75985496 (89.67%)
8am-2	80664968	72437594 (89.80%)
8am-3	79395082	71806346 (90.44%)
2pm-1	80060560	72265336 (90.26%)
2pm-2	72857102	65459946 (89.85%)
2pm-3	87460746	79245078 (90.61%)

http://www.aloki.hu ● ISSN 1589 1623 (Print) ● ISSN 1785 0037 (Online)
DOI: http://dx.doi.org/10.15666/aeer/2001_601617

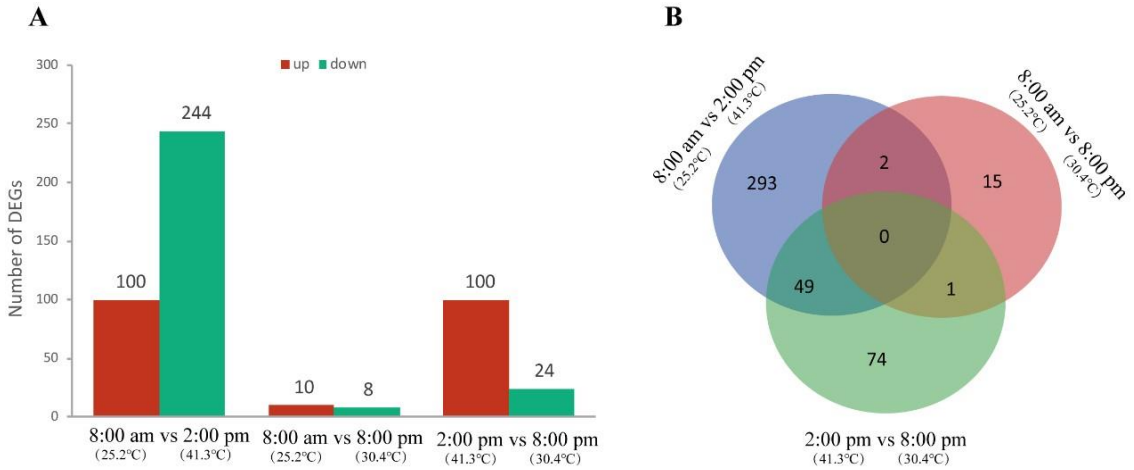

Figure 5. *DEGs between different comparative pairs (8:00 am vs 2:00 pm, 8:00 am vs 8:00 pm, 2:00 pm vs 8:00 pm). The numbers in brackets represent temperature of C. spinosa leaves. (A) The number of DEGs between different group. (B) Venn diagram showing overlapping areas in different group*

Additionally, we clustered the expression level of 434 DEGs. The results showed that almost half of the genes (190) hardly expressed in the "8:00 am" samples while expressed in the "2:00 pm" and "8:00 pm" samples. Similarly, 94 genes were expressed in the "8:00 am" samples, but hardly expressed in the "2:00 pm" and "8:00 pm" samples (*Fig. 6*).

GO and KEGG analysis of differentially expressed genes

We performed GO classification and enrichment analysis of 434 DEGs. GO analysis divided DEGs into three major functional categories: molecular function, cellular component, and biological process. In terms of molecular function, chlorophyll binding was most highly enriched category. Besides, DEGs were also enriched significantly in pigment binding, aldehyde dehydrogenase activity and transcription factor binding. Under cellular component category, DEGs were significantly enriched in the regulation of transcription. Most importantly, Abscisic acid and cold response process pathways were highly enriched (*Fig. 7*). Next, to explore the biological pathways, all DEGs were annotated from KEGG databases, and results indicated that most of DEGs showed enrichment in the microbial metabolism in diverse environments pathways, carbon metabolism, and circadian rhythm pathways (*Fig. 8*).

Expression pattern of transcription factors in DEGs

In all 434 DEGs, a total of 29 transcription factors were identified. These transcription factors were assigned to seven different TF families. Among these TFs, most of them around 14 members (48.27%) belonged to MYB family (*Fig. 9*; *Table 6*). However, TFs belonging to bHLH, bZIP, C2C2-CO-like, C2H2, DBB, GARP-G2-like families were also identified. Expression patterns analysis of these transcription factors shown two MYB genes C.spinosa_1-6k_c837860/f1p6/1454 and C.spinosa_1-6k_c571484/f1p41/1176 were up-regulated in "2:00 pm" and "8:00 pm" samples indicating these two MYB genes may respond to heat and drought stresses (*Fig. 9*).

http://www.aloki.hu ● ISSN 1589 1623 (Print) ● ISSN 1785 0037 (Online)
DOI: http://dx.doi.org/10.15666/aeer/2001_601617

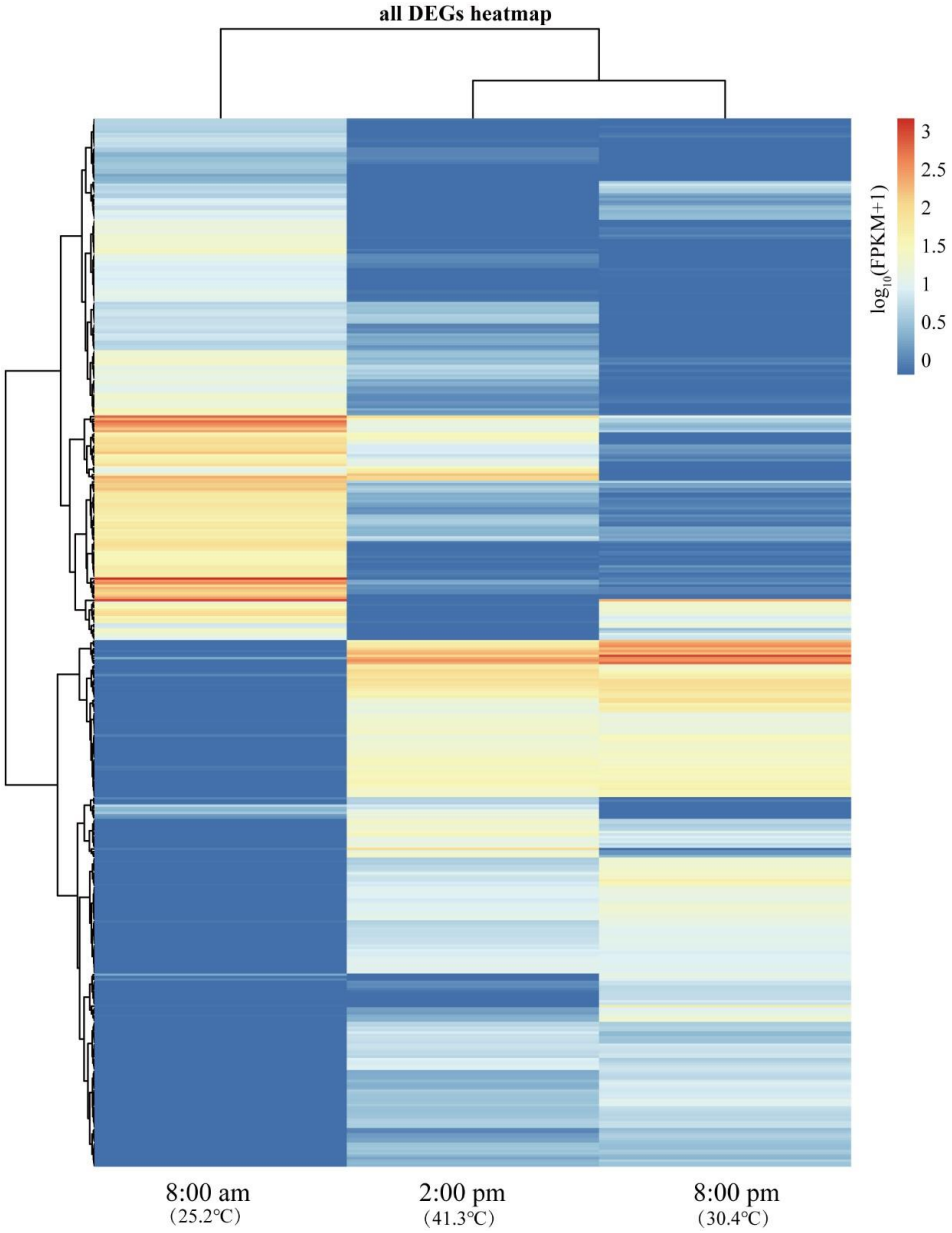

Figure 6. *The heatmap of 434 DEGs in "8:00 am", "2:00 pm" and "8:00 pm" samples. The $log_{10}FPKM + 1$ value was used to construct the heat map*

Table 6. *Statistics and classification of differentially expressed transcription factors*

Transcription factors name	Numbers
MYB->MYB-related	14
C2C2->C2C2-CO-like	5
DBB	4
C2H2	2
GARP-G2-like	2
bHLH	1
bZIP	1
Total	29

http://www.aloki.hu ● ISSN 1589 1623 (Print) ● ISSN 1785 0037 (Online)
DOI: http://dx.doi.org/10.15666/aeer/2001_601617

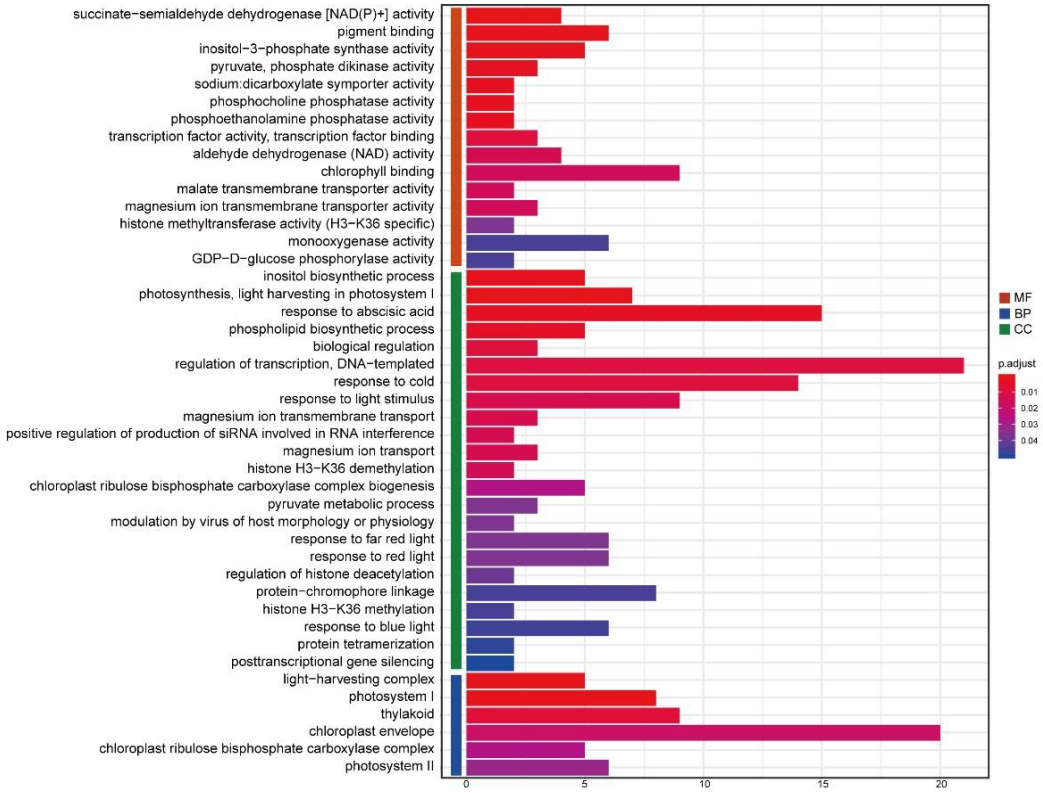

Figure 7. *GO Enrichment of DEGs. Molecular function (red color), biological process (blue color), and cellular component (green color)*

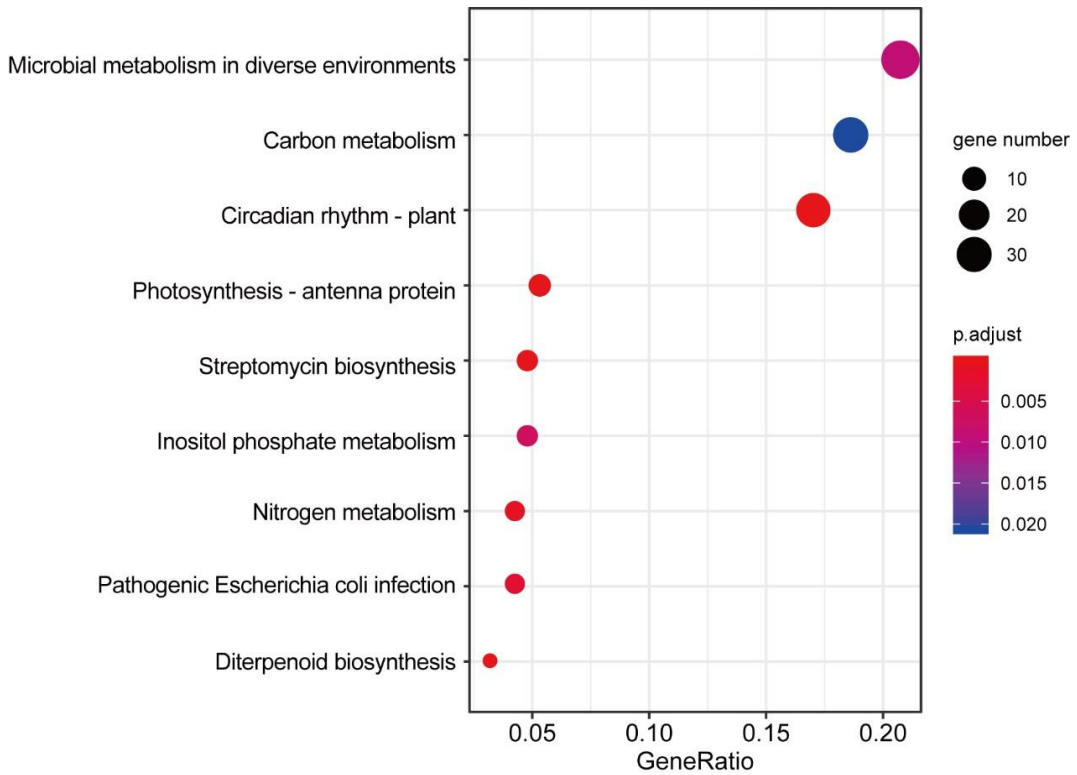

Figure 8. *KEGG pathway classification of C. spinosa DEGs*

http://www.aloki.hu ● ISSN 1589 1623 (Print) ● ISSN 1785 0037 (Online)
DOI: http://dx.doi.org/10.15666/aeer/2001_601617

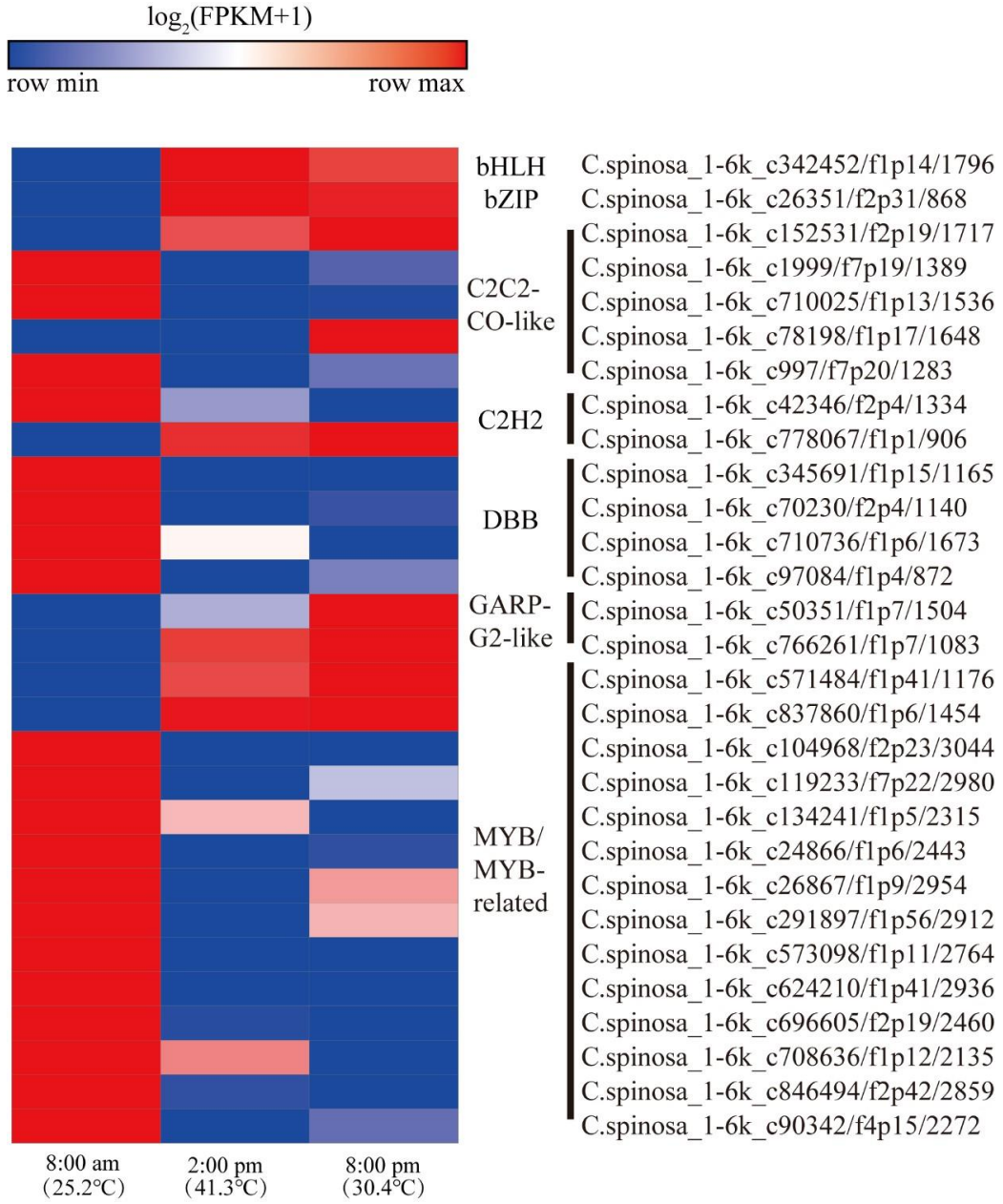

Figure 9. *Expression pattern of 29 transcription factors from DEGs in "8:00 am", "2:00 pm" and "8:00 pm" samples. The log_2FPKM + 1 value was used to construct the heat map*

Discussion

Climate change has adverse effects on biological survival and biodiversity especially in the distribution of species. Drastic environmental changes have affected the agricultural production. *C. spinosa* is an important source of secondary metabolites required by humans. Many biologically active chemical constituents were also identified from different parts (e.g. roots and seeds) of the *C. spinosa*. Therefore, some studies focused on the phytochemical and pharmacological properties of *C. spinosa* (Nabavi et al., 2016). *C. spinosa* is a shrub that has significant adaptability to harsh environments and an important source of candidate genes related to drought and heat resistance (Chedraoui et al., 2017). Nevertheless, since there was no reference genome

http://www.aloki.hu ● ISSN 1589 1623 (Print) ● ISSN 1785 0037 (Online)
DOI: http://dx.doi.org/10.15666/aeer/2001_601617

for *C. spinosa*, the progress of gene excavating and their functional study is slow. However, SMRT sequencing has been applied in many species with the advantage of obtaining full-length transcripts (Hoang et al., 2017). In this study, we provided a transcript-level reference genome for *C. spinosa* that laid the foundation for subsequent research on gene cloning and functional analysis. SMRT sequencing produced 14.96 Gb of clean data, including 828518 ROI and 370528 full-length non-chimeric reads. A total of 216240 consensus isoforms sequences were identified which included 191599 non-redundant isoforms. Previous studies demonstrated long reads sequencing ability of SMRT technology (Abdel-Ghany et al., 2016). In this study, the average size of non-redundant isoforms is 1678 bp. Besides this, Illumina-based RNA-seq is widely used in transcriptome analysis since RNA-seq has the advantages of highly accurate reads coupled with low costs (Li et al., 2017). However, the disadvantage of SGS is short reads. The SMRT sequencing can generate long reads (average 4-8 kb) without PCR amplification which usually represents full-length transcript. In this paper, we combined SMRT sequencing with SGS to obtain full-length transcripts of *C. spinosa* with high accuracy. Until now only one study was reported to clone a *CsHSP70* gene by using RACE (Luan and Dong, 2009). The *CsHSP70* gene contained a 1950 bp coding sequence (including the stop codon) encoding a 70-kDa protein with 650 amino acids. The study found that *CsHSP70* heterologous expressed in E. coli can increase tolerance to temperature stress both at 50 ℃ and 4 ℃ (Luan and Dong, 2009). We searched *CsHSP70L* (*CsHSP70*-Like) gene using *CsHSP70* protein sequence by Blastp in our protein database for *C. spinosa*. Finally, we found a sequence with highest similarity of 97.53% with *CsHSP70* (*Fig. 10B*) with the gene number C. spinosa_1-6k_c514583/f1p102/4431:160-2109(-) so we designated this gene as *CsHSP70L*. *CsHSP70L* contained a 1950 bp coding sequence (including the stop codon) encoding 650 amino acids. However, we were not found FPKM about this gene in the transcriptome data. We detected the expression of this gene by qRT-PCR. For qRT-PCR, we first used homologous alignment to identify reference genes in *caper CsUBQ6* which had high similarity with *AtUBQ6* (*Fig. 10A*). Our results show that this gene expressed highly in the "2:00 pm" samples (*Fig. 10E*). As the temperature in Xinjiang is very high at noon, high expression of *CsHSP70L* at noon indicated that it may be involved in response to heat.

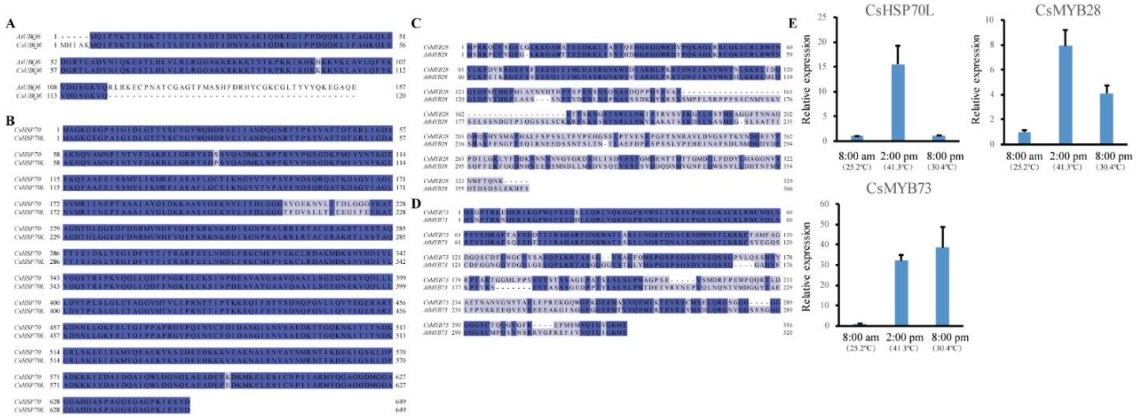

Figure 10. *Analysis of drought related genes in C. spinosa. (A) Alignment of AtUBQ6 with CsUBQ6 to confirm it as an internal control. (B) Alignment of CsHSP70 with CsHSP70L. (C) Alignment of CsMYB28 with AtMYB28. (D) Alignment of CsMYB73 with AtMYB73. (E) Relative expression pattern of CsHSP70L, CsMYB73 and CsMYB28 using qRT-PCR analysis*

http://www.aloki.hu ● ISSN 1589 1623 (Print) ● ISSN 1785 0037 (Online)
DOI: http://dx.doi.org/10.15666/aeer/2001_601617

The MYB family is one of the largest transcription factors family in plants. Some studies reported that MYB participated in heat and drought stress (Yu et al., 2016; Zhao et al., 2019). The RNA-seq data show two MYB genes (C. spinosa_1-6k_c837860/f1p6/1454 and C. spinosa_1-6k_c571484/f1p41/1176) were up-regulated in "2:00 pm" and "8:00 pm" samples (*Fig. 9*). We predicted their homologous genes of in *Arabidopsis* and found that *AtMYB28* and *AtMYB73* were their putative homologous gene pairs respectively (*Fig. 10C, D*). So, we designated these genes as *CsMYB28* and *CsMYB73* respectively. We found *CsMYB28* and *CsMYB73* increased in "2:00 pm" and "8:00 pm" samples by qRT-PCR (*Fig. 10E*). This result is consistent with transcriptome data. *AtMYB28* was previously reported to regulate the biosynthesis of aliphatic glucosinolates (Sønderby et al., 2007, 2010). Recently over-expression of *AtMYB28* showed hypersensitivity to exogenous ABA during seed germination, cotyledon greening and early seedling growth, suggesting that *AtMYB28* positively involved in response to ABA (Yu et al., 2016). *AtMYB73* is a negative regulator in response to salt stress in *Arabidopsis*. While, *GhMYB73* showed increased tolerance to salt stress in transgenic *Arabidopsis* (Zhao et al., 2019). In the present research, *CsMYB28* and *CsMYB73* were up-regulated in "2:00 pm" and "8:00 pm" samples which may indicate that these two genes participated in heat and drought stresses for *C. spinosa*. However, this speculation may need further research to investigate the function of *CsMYB28* and *CsMYB73*. Our results provide the possibility to isolate and clone the gene in *C. spinosa* which will help the functional and molecular studies of *C. spinosa* in future.

Conclusions

C. spinosa is known for its medicinal properties. Meanwhile it is a candidate species to maintain and promote agricultural development in extreme climate change and extreme drought areas. *C. spinosa* is a good candidate species for addressing climate risks. This is the significant ability of *C. spinosa* to adapt different climates. In this study, complete SMRT sequencing of the full-length transcriptome of *C. spinosa* was performed first time. Further, full-length isoforms improved *C. spinosa* transcriptome annotation a lot. Additionally, the full-length transcriptome provides a more accurate depiction of gene transcription. It provides a strong factual basis for the development and utilization of *C. spinosa* genes in the future. Our results help discover related functional genes in *C. spinosa* and to lay the foundation for screening heat-tolerant genotypes. It is of great practical value to obtain more stress-resistant species by genetic engineering.

Funding. This work was sponsored by State Key Laboratory of Cotton Biology Open Fund (No. CB2020A02).

Authors' contributions. RS and GQ conceived and designed the experiments; LW collected the samples; ZL, RS, SL and GC performed the experiments and analyzed the data; ZL, RS and GQ drafted the manuscript; KZ, LW, ZS, RS and GQ revised the manuscript. All authors have read and approved the final manuscript.

Conflict of interests. The authors declare that they have no competing interests.

Availability of data and materials. The datasets generated during the current study are available from the corresponding author on reasonable request.

http://www.aloki.hu ● ISSN 1589 1623 (Print) ● ISSN 1785 0037 (Online)
DOI: http://dx.doi.org/10.15666/aeer/2001_601617

REFERENCES

[1] Abdel-Ghany, S. E., Hamilton, M., Jacobi, J. L., Ngam, P., Devitt, N., Schilkey, F., et al. (2016): A survey of the sorghum transcriptome using single-molecule long reads. – Nat. Commun. 7: 1-11.
[2] Alexa, A., Rahnenfuhrer, J. (2016): topGO: enrichment analysis for Gene Ontology. – R package version 2.28. 0. Cranio.
[3] Bellard, C., Bertelsmeier, C., Leadley, P., Thuiller, W., Courchamp, F. (2012): Impacts of climate change on the future of biodiversity: biodiversity and climate change. – Ecol. Lett. 15: 365-377.
[4] Bu, D., Luo, H., Huo, P., Wang, Z., Zhang, S., He, Z., et al. (2021): KOBAS-i: intelligent prioritization and exploratory visualization of biological functions for gene enrichment analysis. – Nucleic Acids Res.
[5] Campbell, J. R. (2015): Development, global change and traditional food security in Pacific Island countries. – Reg Environ Change 15(7): 1313-1324.
[6] Chedraoui, S., Abi-Rizk, A., El-Beyrouthy, M., Chalak, L., Ouaini, N., Rajjou, L. (2017): Capparis spinosa L. in a systematic review: a xerophilous species of multi values and promising potentialities for agrosystems under the threat of global warming. – Front. Plant Sci. 8: 1845.
[7] Chen, Y., Lun, A. T., Smyth, G. K. (2014): Differential Expression Analysis of Complex RNA-seq Experiments Using edgeR. – In: Datta, S., Nettleton, D. (eds.) Statistical Analysis of Next Generation Sequencing Data. Springer, Cham, pp. 51-74.
[8] Eid, J., Fehr, A., Gray, J., Luong, K., Lyle, J., Otto, G., et al. (2009): Real-time DNA sequencing from single polymerase molecules. – Science 323: 133-138.
[9] Filichkin, S. A., Hamilton, M., Dharmawardhana, P. D., Singh, S. K., Sullivan, C., Ben-Hur, A., et al. (2018): Abiotic stresses modulate landscape of poplar transcriptome via alternative splicing, differential intron retention, and isoform ratio switching. – Front. Plant Sci. 9: 5.
[10] Gadgoli, C., Mishra, S. H. (1999): Antihepatotoxic activity of p-methoxy benzoic acid from Capparis spinosa. – J. Ethnopharmacol. 66: 187-192.
[11] Henckel, P. A. (1964): Physiology of plants under drought. – Annu. Rev. Plant Physiol. 15: 363-386.
[12] Hoang, N. V., Furtado, A., Mason, P. J., Marquardt, A., Kasirajan, L., Thirugnanasambandam, P. P., et al. (2017): A survey of the complex transcriptome from the highly polyploid sugarcane genome using full-length isoform sequencing and de novo assembly from short read sequencing. – BMC Genomics 18: 1-22.
[13] Inocencio, C., Rivera, D., Alcaraz, F., Tomás-Barberán, F. A. (2000): Flavonoid content of commercial capers (Capparis spinosa, C. sicula and C. orientalis) produced in Mediterranean countries. – Eur. Food Res. Technol. 212: 70-74.
[14] Lagouvardos, K., Kotroni, V. (2007): TRMM and lightning observations of a low-pressure system over the Eastern Mediterranean. – Bull. Am. Meteorol. Soc. 88: 1363-1368.
[15] Langmead, B., Salzberg, S. L. (2012): Fast gapped-read alignment with Bowtie 2. – Nat. Methods 9(4): 357-359.
[16] Li, B., Dewey, C. N. (2011): RSEM: accurate transcript quantification from RNA-Seq data with or without a reference genome. – BMC Bioinformatics 12(1): 1-16.
[17] Li, Q., Li, Y., Song, J., Xu, H., Xu, J., Zhu, Y., et al. (2014): High-accuracy de novo assembly and SNP detection of chloroplast genomes using a SMRT circular consensus sequencing strategy. – New Phytol. 204: 1041-1049.
[18] Li, Y., Dai, C., Hu, C., Liu, Z., Kang, C. (2017): Global identification of alternative splicing via comparative analysis of SMRT-and Illumina-based RNA-seq in strawberry. – Plant J. 90: 164-176.

http://www.aloki.hu ● ISSN 1589 1623 (Print) ● ISSN 1785 0037 (Online)
DOI: http://dx.doi.org/10.15666/aeer/2001_601617

[19] Luan, D., Dong, Y. (2009): Cloning and its prokaryotic expression of a 70 kD heat shock protein gene from Capparis spinosa. – Acta Bot. Boreali-Occident. Sin. 29: 1291-1297.
[20] Margulies, M., Egholm, M., Altman, W. E., Attiya, S., Bader, J. S., Bemben, L. A., et al. (2005): Genome sequencing in microfabricated high-density picolitre reactors. – Nature 437: 376-380.
[21] Minio, A., Massonnet, M., Figueroa-Balderas, R., Vondras, A. M., Blanco-Ulate, B., Cantu, D. (2019): Iso-Seq allows genome-independent transcriptome profiling of grape berry development. – G3-Gene Genom Genet 9(3): 755-767.
[22] Nabavi, S. F., Maggi, F., Daglia, M., Habtemariam, S., Rastrelli, L., Nabavi, S. M. (2016): Pharmacological effects of Capparis spinosa L. – Phytother. Res. 30: 1733-1744.
[23] Pan, C., Wang, Y., Tao, L., Zhang, H., Deng, Q., Yang, Z., et al. (2020): Single-molecule real-time sequencing of the full-length transcriptome of loquat under low-temperature stress. – PLoS One 15(9): e0238942.
[24] Peterson, A. T., Martínez-Meyer, E., González-Salazar, C., Hall, P. W. (2004): Modeled climate change effects on distributions of Canadian butterfly species. – Can. J. Zool. 82: 851-858.
[25] Rhizopoulou, S., Psaras, G. K. (2003): Development and structure of drought-tolerant leaves of the Mediterranean shrub Capparis spinosa L. – Ann. Bot. 92: 377-383.
[26] Rhizopoulou, S., Ioannidi, E., Alexandredes, N., Argiropoulos, A. (2006): A study on functional and structural traits of the nocturnal flowers of Capparis spinosa L. – J. Arid Environ. 66: 635-647.
[27] Sharon, D., Tilgner, H., Grubert, F., Snyder, M. (2013): A single-molecule long-read survey of the human transcriptome. – Nat. Biotechnol. 31: 1009-1014.
[28] Shendure, J., Ji, H. (2008): Next-generation DNA sequencing. – Nat. Biotechnol. 26: 1135-1145.
[29] Sønderby, I. E., Hansen, B. G., Bjarnholt, N., Ticconi, C., Halkier, B. A., Kliebenstein, D. J. (2007): A systems biology approach identifies a R2R3 MYB gene subfamily with distinct and overlapping functions in regulation of aliphatic glucosinolates. – PLoS One 2: e1322.
[30] Sønderby, I. E., Burow, M., Rowe, H. C., Kliebenstein, D. J., Halkier, B. A. (2010): A complex interplay of three R2R3 MYB transcription factors determines the profile of aliphatic glucosinolates in Arabidopsis. – Plant Physiol. 153: 348-363.
[31] Thiry, A. A., Chavez Dulanto, P. N., Reynolds, M. P., Davies, W. J. (2016): How can we improve crop genotypes to increase stress resilience and productivity in a future climate? A new crop screening method based on productivity and resistance to abiotic stress. – J. Exp. Bot. 67: 5593-5603.
[32] Tlili, N., Elfalleh, W., Saadaoui, E., Khaldi, A., Triki, S., Nasri, N. (2011): The caper (Capparis L.): Ethnopharmacology, phytochemical and pharmacological properties. – Fitoterapia 82: 93-101.
[33] Yu, Y.-T., Wu, Z., Lu, K., Bi, C., Liang, S., Wang, X.-F., et al. (2016): Overexpression of the MYB transcription factor MYB28 or MYB99 confers hypersensitivity to abscisic acid in Arabidopsis. – J. Plant Biol. 59: 152-161.
[34] Zhao, Y., Yang, Z., Ding, Y., Liu, L., Han, X., Zhan, J., et al. (2019): Over-expression of an R2R3 MYB Gene, GhMYB73, increases tolerance to salt stress in transgenic Arabidopsis. – Plant Sci. 286: 28-36.

http://www.aloki.hu ● ISSN 1589 1623 (Print) ● ISSN 1785 0037 (Online)
DOI: http://dx.doi.org/10.15666/aeer/2001_601617

EVALUATION OF SALT TOLERANT WHEAT VARIETIES CULTIVARS BY OBSERVING GROWTH AND PHYSIOLOGICAL RESPONSE UNDER DROUGHT STRESS

WANG, G.[1#] – LI, Y. P.[1#] – MAJEEDANO, A. Q.[1] – YU, Y. H.[1] – PU, S. R.[2] – WANG, G.[1*] – LIU, Q.[1] – GUO, Q.[1]

[1]College of Forestry, Sichuan Agricultural University, Chengdu 611130, Sichuan province, China (e-mail: nkdwg@126.com (Wang, G.); 755537960@qq.com (Li, Y. P.); aqmajeedano@outlook.com (Majeedano, A. Q.); 291842374@qq.com (Yu, Y. H.); 348011991@qq.com (Liu, Q.); 916588828@qq.com (Guo, Q.))

[2]Department of Landscape Plants, Sichuan Agricultural University, Chengdu 611130, Sichuan province, China (e-mail: 574803485@qq.com (Pu, S. R.))

[#]These authors contributed equally to this work.

[*]Corresponding author
e-mail: wanggang@sicau.edu.cn

(Received 25th May 2021; accepted 23rd Nov 2021)

Abstract. Generally, the yield of most crops relies the intensity of drought and the stage of plant growth period where it occurs. Various wheat genotypes viz. IBWSN-1010, IBWSN-1025 (Salt tolerant liens), TD-1, ESW-9526 (Hybrid lines) Khirman (Commercial cultivated cultivar) and Chakwal-86 (Drought tolerant) were evaluated to examine the growth and physiological responses to drought stress. Growth and water relations were investigated in the fourth leaf over a twenty-day timescale under drought and control conditions. The results were used to evaluate whether the salt tolerant cultivars IBWSN-1010 and IBWSN-1025 are also tolerant to drought stress. In the drought treatment, the cultivars Chakwal-86 (drought tolerant), IBWSN-1010, IBWSN-1025 (salt tolerant liens) and TD-1 and ESW-9525 (Lines) had a significantly higher number of live leaves, leaf and shoot fresh and dry mass, retained higher leaf and relative water content, and had a lower leaf mortality compared to Khirman. The salt and drought tolerant cultivars all showed significantly higher leaf water potential compared to the hybrid lines and Khirman. No significant differences were observed in soil water content and potential, meaning that all cultivars depleted soil water equally. Longer leaf longevity and greater fresh mass retention show that salt tolerant cultivars are also drought tolerant.
Keywords: *evaluation, salt tolerant, wheat, Triticum aestivum, cultivars, growth, physiological response, drought*

Introduction

Due to the rapid climatic change drought becomes abiotic constraint globally (Nariman et al., 2017). Abiotic stresses lead to desertification, loosing productive lands and severely limited growth and development (Chunthaburee et al., 2016). Insufficient availability of water to plants more precisely, when the amount of water is lost by evapotranspiration drought exceeds tremendously in the tissues (Aldesuquy et al., 2012). The effect of drought can be enhanced under conditions of low humidity and high temperatures. Chronic temperatures and light stresses highly affect the kernel filling stage and reduces the kernel dry weight (Tanaka and Gustavo, 2009). Globally, the production of wheat is progressively decreasing due to a shortage of irrigation water, and this is seriously influenced by global climatic change and an increasing shortage of irrigation resources (Shao et al., 2005; Saba et al., 2010; Monneveux et al., 2012). Once

http://www.aloki.hu ● ISSN 1589 1623 (Print) ● ISSN1785 0037 (Online)
DOI: http://dx.doi.org/10.15666/aeer/2001_619632

a plant is exposed to drought stress, it will be less resistant other types of stress. Abiotic stresses are major agriculture disasters affecting the vulnerability of wheat production, particularly in arid and semiarid regions of the world (Daryanto et al., 2016). Environmental stresses and their influences on plant growth and productivity are receiving a great deal of attention because of the potential impacts of climatic change on rainfall patterns, increasing temperatures and salinity (Verslues et al., 2006). Wang et al. (2014) have claimed that more crop losses are caused by abiotic stresses than any other factor. Major crops have reduced yield more than 50% compared with their yield potential.

Wheat is a major food crop with an annual production of 620 Mt worldwide; it supplies more than 20% of the total human food calories, Moreover, growth and yield of wheat significantly decrease under stressful environmental conditions. Salinity and drought together causes about 37% losses to the potential yield of crops. However, in the arid and semi-arid cropping systems, water stress caused by drought and salinity is the most important abiotic factor limiting plant growth and crop productivity (Zahid and Mohammad, 2016).

Among abiotic stresses drought and salinity are the major factors limiting the growth and yield of cereals (Tester and Bacic, 2005). Plant responses to drought and salt stress are closely related and the protection mechanisms overlap; for example salt stress reduces plant growth by reducing the ability of roots to take up water (Knipfer et al., 2020). It has been observed that drought stress and salt stress (Chaves et al., 2003; Jiang and Zhang, 2004; Liu and Baird, 2004; Shao et al., 2005) share similar physiological and biochemical processes (Chen et al., 2003; Zhu et al., 2004). Water stress in its broadest sense includes both drought and salt stresses (Kaur and Zhawar, 2015). During water stress some plants loose turgor when soil water potential is too low and are very sensitive to dry and saline conditions, but other plants are able to maintain their turgor during these same environmental stresses, and are considered tolerant.

Several hundred plants were obtained and tested for salt tolerance in a hydroponic culture (Al Hattab et al., 2018). The plant drought tolerance is complex involving diverse physiological and molecular mechanisms. These physiological responses vary to drought from phenological stage to another (Punia et al., 2011). Understanding the mechanisms of how these plants respond to drought stress should lead to the identification of new ways to optimize plant growth and productivity under dry conditions. Improvement of wheat growth and productivity under drought stress is therefore the main objective of research inferring the physiological behavior and tolerance of different wheat genotypes under drought. Salt stress significantly affected growth and yield attributes, as well as physiological traits of wheat genotypes (Mahboob et al., 2017).

Materials and methods

In our research trial the, ability of the six wheat cultivar s under water stressed, its particular focus was on leaf growth and mortality (%), leaf area, leaf water content, soil water content, relative water content, leaf water potential and soil water potential for six different wheat cultivars (IBWSN-1010, IBWSN-1025, TD-1, ESW-9525, Khirman and Chakwal-86). Different genotypes and their respective references are shown in *Table 1*. Seed were obtained from ARI Agriculture research institute, Sindh Agriculture University, Sindh, Pakistan. Seeds germinated on Whatman's filter paper in petri dishes

http://www.aloki.hu ● ISSN 1589 1623 (Print) ● ISSN1785 0037 (Online)
DOI: http://dx.doi.org/10.15666/aeer/2001_619632

moistened with distilled water (ddH_2O) for five days at growth room temperature 20 ± 15°C. A complete randomized design (CRD) was used in the whole series of experiments of growth and physiological responses. Statistical differences were evaluated between day zero and other days and also between genotypes on each selected day. A drought treatment was applied by withholding water when the fourth leaf was fully expanded, as indicated by ligule emergence. Sampling of the fully expanded fourth leaf was carried out at 0, 5, 10, 15, and 20 days of the drought treatment and controlled conditions (normal four irrigations). Only one plant was grown in each pot. Samples of the fully expanded fourth leaf (five replicates for each point) were harvested using a razor blade, immediately weighed, and then dried in an oven at 72˚C for 48 hours. Dry weight of samples was recorded to a precision of 0.001 g. Determination of water content was expressed as both a percentage of fresh and dry weights (Ali et al., 2014). Water potential of the fully expanded fourth leaf was measured using a pressure chamber, as described by Gomes et al. (2012). The number of live leaves and dead/senesced leaves were recorded on 0, 5, 10, 15, and 20 days of the drought stress and control. All the data were expressed as means of five replicates ± SE, calibrated using standard salt solutions (NaCl) of 0.1, 0.2, 0.5, and 1.0 m (molality) for to see the performance at salt stress. The data were expressed as means of five replicates ±SE on a cm^2 basis. Relative water content (RWC) was expressed as the percentage water content at a given time as related to the water content at full turgor: RWC (%) = [(FW-DW)/(TW-DW)] X 100. Where: FW= Fresh weight, TW= Turgid weight, and DW= Dry weight, Fresh weight and dry weight measurements. The TW was measured by keeping the leaves in ddH_2O over night (12 hours) at room temperature.

Table 1. *Different genotypes and their respective references*

S. No	Genotypes	References
1	IBWSN-1010	Abro et al., 2020
2	IBWSN-1025 (Salt tolerant liens)	Abro et al., 2019
3	TD-1	Malik et al., 2015
4	ESW-9526 (Hybrid lines)	
5	Khirman (Commercial cultivated cultivar)	
6	Chakwal-86 (Drought tolerant)	

Statistical analysis

The data recorded were subjected to analysis of variance to discriminate the superiority of treatment means and LSD test were applied to compare the means. Statistics 8.1 is the name of the statistical software which was used in this experiments data analysis.

Results

Leaf mortality

Leaf mortality increased with the severity of drought stress, and all the genotypes had significantly higher ($P<0.001$) leaf mortality rates under the drought treatment. The leaf mortality was greatest in the cultivar Khirman, which had a significantly ($P<0.05$) higher leaf mortality rate of 53% than the other genotypes, which had only up to 25%

http://www.aloki.hu ● ISSN 1589 1623 (Print) ● ISSN1785 0037 (Online)
DOI: http://dx.doi.org/10.15666/aeer/2001_619632

leaf mortality on the twentieth day of the drought treatment (*Fig. 1*). Under control conditions, all the genotypes showed a non-significant leaf mortality of up to 3%, excluding Chakwal-86, which showed statistically significant ($P<0.05$) leaf mortality of 13% on the twentieth day.

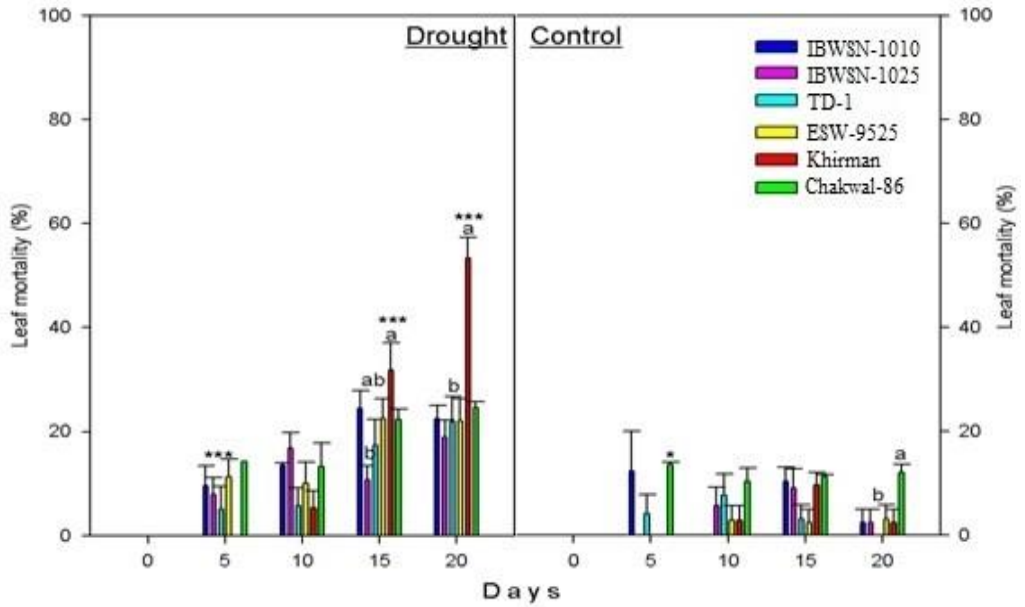

Figure 1. *The leaf mortality rate (%) ± SE (Standard Error) of six wheat genotypes (n=5) under drought stress and control conditions. Statistically significant differences between zero and the other days (ANOVA) are marked with an asterisk where ***, equals P=0.001; letters show significant differences (P<0.05) among genotypes on each selected day*

Mortality

The cultivar Khirman had a significantly ($P<0.001$) increased number of dead leaves on the twentieth day of the drought treatment compared to day zero. The same cultivar had a significant ($P<0.001$) decrease in number of living leaves under drought stress conditions on the twentieth day compared to day zero. These cultivars IBWSN-1010, IBWSN-1025, Chakwal-86, TD-1 and ESW-9525 had a significantly ($P<0.05$) higher number of living leaves compared to Khirman on the twentieth day of the drought. These cultivars also had a significantly ($P<0.05$) lower number of dead leaves on the twentieth day of the drought compared to Khirman (*Fig. 2*). Under control conditions, all the genotypes had a lower number of dead leaves except Chakwal-86 which had a significantly ($P<0.05$) higher number of dead leaves on the twentieth day of the drought treatment (*Fig. 2*).

Growth

A gradual, non-significant increase in shoot fresh weight was observed across all the cultivars during the first ten days of the drought treatment (*Fig. 3*). The cultivars IBWSN-1010, IBWSN-1025 and Chakwal-86 continued to significantly ($P<0.01$) increase in shoot fresh weight throughout the drought treatment period. However, there was a gradual decrease in shoot fresh weight in the cultivar Khirman starting after ten days, and in 5757-3 and 5746-20 after fifteen days of the drought treatment. The cultivars Chakwal-86, IBWSN-1025 and IBWNS-1010 had significantly ($P<0.05$)

http://www.aloki.hu ● ISSN 1589 1623 (Print) ● ISSN1785 0037 (Online)
DOI: http://dx.doi.org/10.15666/aeer/2001_619632

higher shoot fresh weight compared to Khirman, TD-1 and ESW-9525 under drought stress conditions. Under control conditions, all the cultivars had significantly (P<0.001) increased shoot fresh weight compared to day zero (*Fig. 3*). All the cultivars had significantly (P<0.05) increased shoot dry weight until fifteen days of the drought stress except Khirman, which stopped dry weight accumulation (*Fig. 3*). The cultivars Chakwal-86, IBWSN-1025 and IBWSN-1010 had significantly (P<0.01) increased shoot dry weight on the twentieth day of the drought stress. The cultivars Chakwal-86, IBWSN-1025 and IBWSN-1010 followed by TD-1 and ESW-9525 had significantly (P<0.05) higher shoot dry weight compared to Khirman on the twentieth day of the drought treatment. Under control conditions all the cultivars had significantly (P<0.001) increased shoot dry weight compared to day zero (*Fig. 3*).

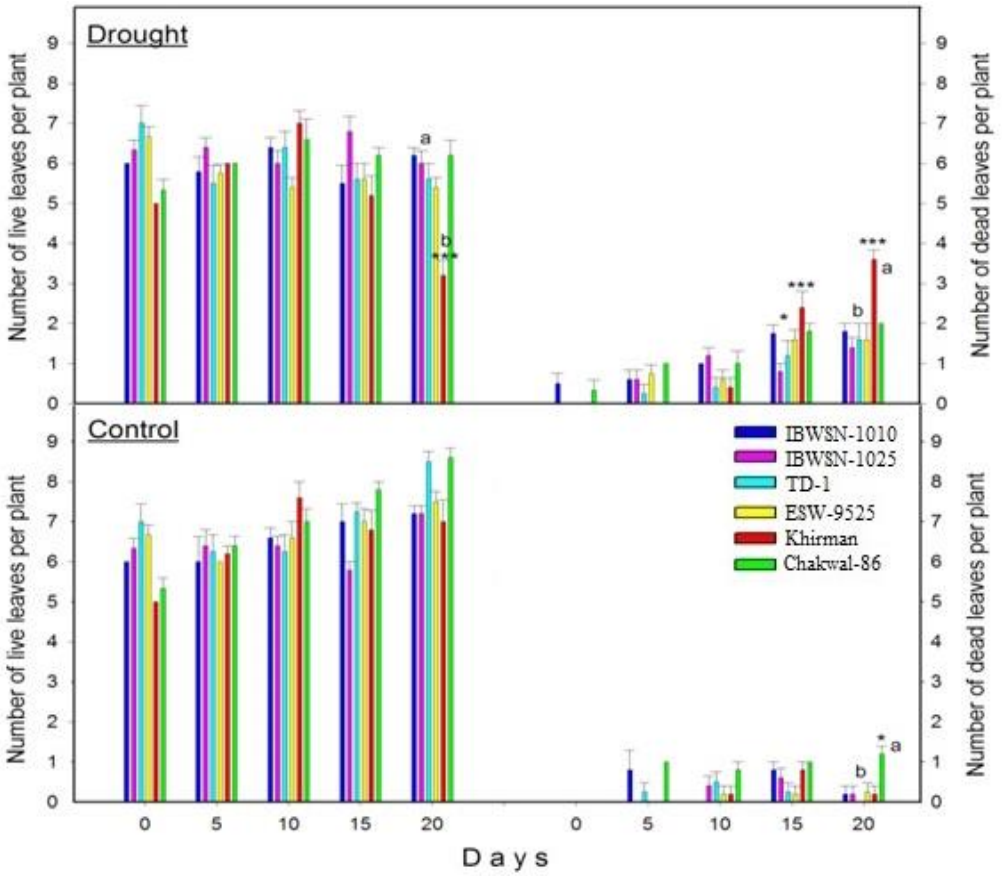

Figure 2. *Number of live leaves (left) and dead leaves (right) per plant ± SE (Standard Error) of six wheat genotypes (n=5) under drought stress and control conditions. Statistically significant differences between day zero and the other days (ANOVA) are marked with an asterisk where *, **, ***, equals P=0.05, P=0.01 and P=0.001; letters show significant differences (P<0.05) among genotypes on each selected day*

Leaf area increased in all genotypes until day ten of the drought stress (*Fig. 4*). However, it was significantly (P<0.001) decreased in Khirman on the twentieth day of the drought treatment compared to day zero. The genotypic differences were statistically significant (P<0.05), and the cultivar Khirman had significantly (P<0.05) smaller leaf area on the twentieth day of the drought treatment. No significant changes in leaf area were observed in any of the cultivars under control conditions (*Fig. 4*).

http://www.aloki.hu ● ISSN 1589 1623 (Print) ● ISSN1785 0037 (Online)
DOI: http://dx.doi.org/10.15666/aeer/2001_619632

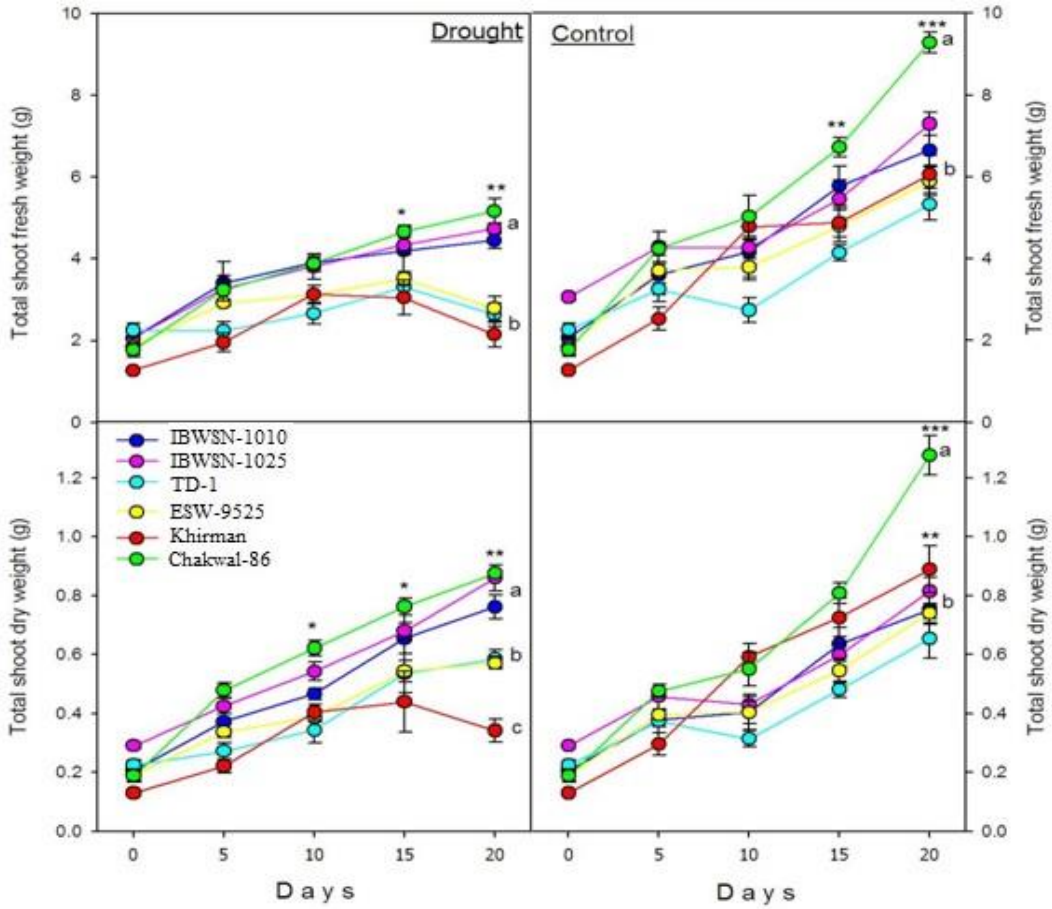

Figure 3. *Shoot fresh and dry weight ± SE (Standard Error) of six wheat genotypes (n=5) under drought stress and control conditions. Statistically significant differences between day zero and the other days (ANOVA) are marked with an asterisk where *, **, ***, equals P=0.05, P=0.01 and P=0.001; letters show significant differences (P<0.05) among genotypes on each selected day*

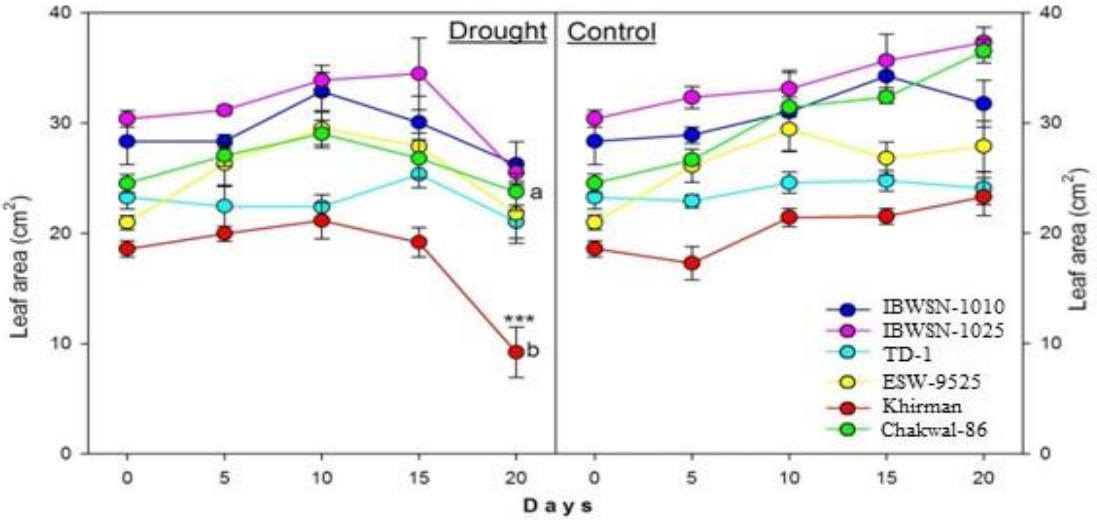

Figure 4. *Leaf area (cm^2) ± SE (Standard Error) of three wheat genotypes (n=5) under drought stress and control conditions. Statistically significant differences between day zero and the other days (ANOVA) are marked with an asterisk where ***, equals P=0.001; letters show significant differences (P<0.05) among genotypes on each selected day*

http://www.aloki.hu ● ISSN 1589 1623 (Print) ● ISSN1785 0037 (Online)
DOI: http://dx.doi.org/10.15666/aeer/2001_619632

Leaf water content

No significant decrease in leaf water content was recorded in the six genotypes until fifteen days of the drought treatment (*Fig. 5*). However, after fifteen days of the drought stress, the leaf water content significantly ($P<0.001$) decreased in Khirman by 17% and, to a lesser extent, in the cultivars ESW-9525, and TD-1 which decreased ($P<0.05$) by 8% and 6% in leaf water content, respectively. The remaining three cultivars did not show significant decreases in leaf water content during the drought treatment (*Fig. 5*), while according to the caption asterisks shows significant differences between day zero and the other days. The cultivars IBWSN-1010, IBWSN-1025 and Chakwal-86 had significantly higher leaf water content compared to Khirman on the twentieth day of the drought treatment. Under control conditions, the leaves of all the genotypes contained approximately 90% water, and remained the same throughout the experimental period (*Fig. 5*).

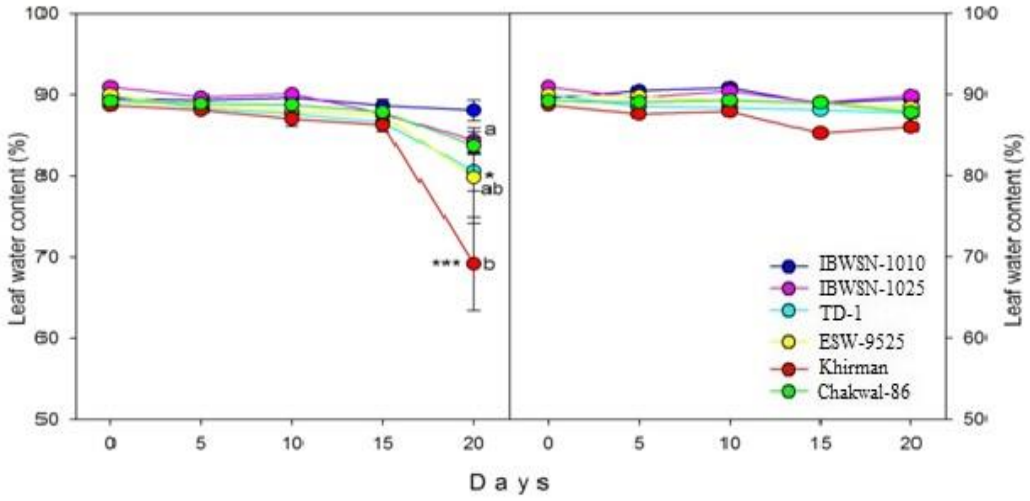

Figure 5. *Leaf water content (%) ± SE (Standard Error) of six wheat genotypes (n=5) under drought stress and control conditions. Statistically significant differences between day zero and the other days (ANOVA) are marked with an asterisk where *, ***, equals P=0.05 and P=0.001; letters show significant differences (P<0.05) among genotypes on each selected day*

Soil water content

All of the genotypes significantly ($P<0.001$) reduced the soil water content during the first five days of the drought treatment except Chakwal-86, where soil water was unchanged (*Fig. 6*). After five days, all the cultivars had significantly ($P<0.001$) decreased soil water content throughout the drought period but differed in the rate this occurred; the decreases were of 45%, 42%, 37%, 37%, and 28% in cultivars Khirman, ESW-9525, TD-1, Chakwal-86, IBWSN-1025 and IBWSN-1010 under drought stress period, respectively (*Fig. 3.14a*). Soil water content was approximately the same in all the cultivars under control conditions (*Fig. 6*). 33% was non-significant.

Soil and plant water relations

The relative water content decreased after ten days of the drought in all of the three cultivars (*Fig. 7*). The cultivar Khirman had significantly ($P<0.001$) lower RWC on the

http://www.aloki.hu ● ISSN 1589 1623 (Print) ● ISSN1785 0037 (Online)
DOI: http://dx.doi.org/10.15666/aeer/2001_619632

fifteenth day of the drought treatment. All of the other genotypes maintained steady RWC until fifteen days of the drought treatment. Overall decreases of 20%, 14%, and 7% were shown in cultivars IBWSN-1010, Chakwal-86, and IBWSN-1025 on the twentieth day of the drought. A significant ($P<0.001$) decrease in RWC of 52% compared to day zero was noted in Khirman from ten to twenty days of the drought treatment (*Fig. 2*). However, IBWSN-1010 and Chakwal-86 had shown significantly higher ($P<0.05$) RWC, whereas the cultivar Khirman had significantly lower RWC than other genotypes on the twentieth day of the drought treatment. All the genotypes had a relative water content of 97-100% under control conditions (*Fig. 7*).

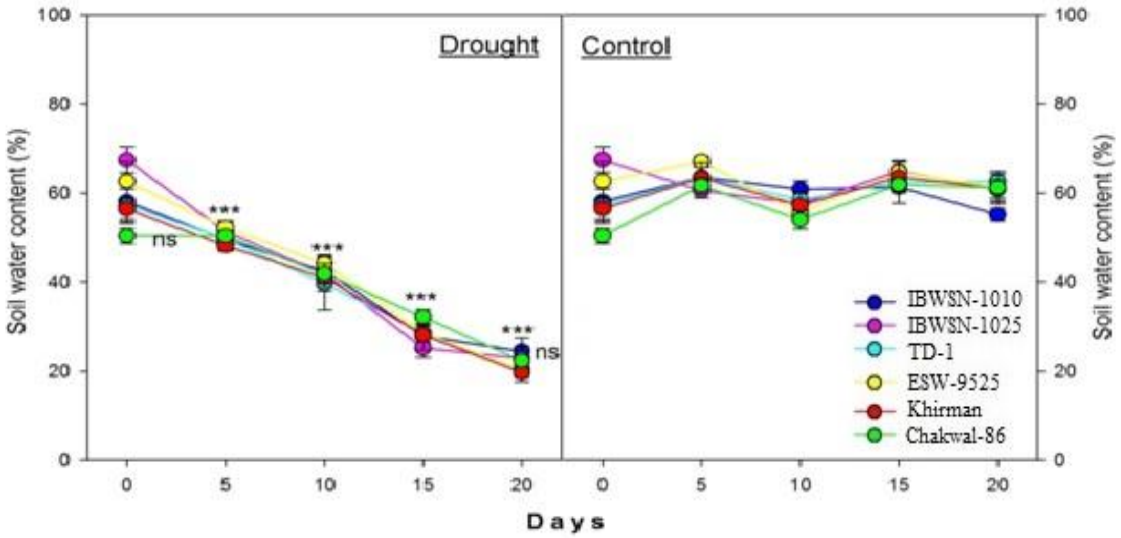

Figure 6. *Soil water content (%) ± SE (Standard Error) of six wheat genotypes (n=5) under drought stress and control conditions. Statistically significant differences between day zero and the other days (ANOVA) are marked with an asterisk where ***, equals P=0.001. ns= no significant. Ns=non-significant write in all fig description*

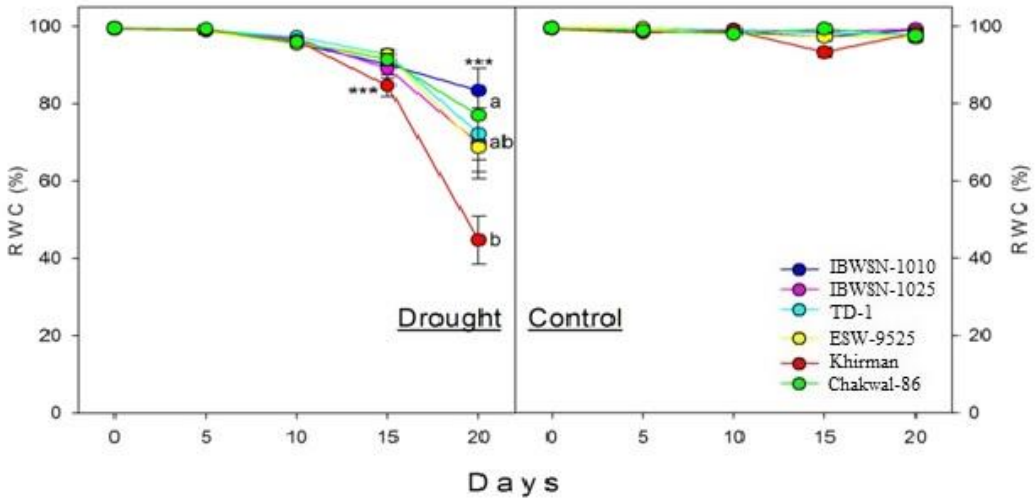

Figure 7. *Relative water content (%) ± SE (Standard Error) of three wheat genotypes (n=5) under drought stress and control conditions. Statistically significant differences between day zero and the other days (ANOVA) are marked with an asterisk where ***, equals P=0.001; letters show significant differences (P<0.05) among genotypes on each selected day*

http://www.aloki.hu ● ISSN 1589 1623 (Print) ● ISSN1785 0037 (Online)
DOI: http://dx.doi.org/10.15666/aeer/2001_619632

All the genotypes showed highly significant ($P<0.001$) decreases in soil Ψ_w on the fifteenth and twentieth days of the drought treatment (*Fig. 8*). Soil Ψ_w gradually decreased during the first ten days of the drought treatment, showing the largest decrease in 5757-3 (-3.0 MPa), Khirman (-2.3 MPa), followed by ESW-9525 (-2.2 MPa), IBWSN-1010, IBWSN-1025 and Chakwal-86 (-2.0 MPa) under drought stress conditions. Under control conditions, all the cultivars had approximately the same soil Ψ_w (*Fig. 8*). All the genotypes maintained their leaf Ψ_w until ten days of the drought stress then, from ten to fifteen days, leaf Ψ_w significantly ($P<0.001$) decreased in all the cultivars (*Fig. 8*). The cultivars Chakwal-86, IBWSN-1010, and IBWSN-1025 retained significantly higher ($P<0.05$) leaf Ψ_w than the genotype Khirman on the twentieth day of the drought treatment. No significant changes were recorded in leaf Ψ_w under control conditions in any of the cultivars (*Fig. 8*).

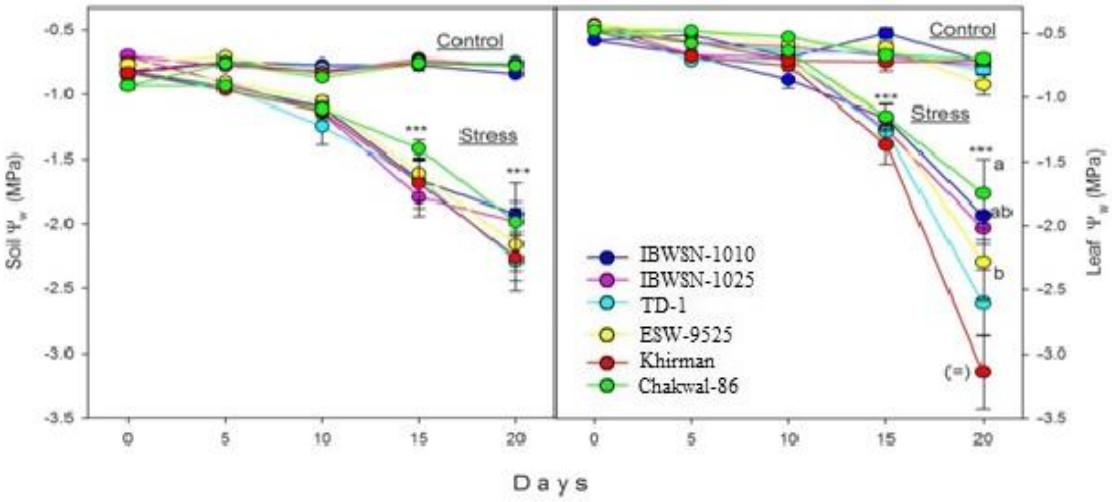

Figure 8. *Leaf water potential and soil water potential ± SE (Standard Error) of six wheat genotypes (n=5) under drought stress and control conditions. Statistically significant differences between day zero and the other days (ANOVA) are marked with an asterisk where ***, equals P=0.001; letters show significant differences (P<0.05) among genotypes on each selected day. (=): Only two replicates/leaves were alive out of five*

Discussion

Since the last decades drought has spread major areas of the world intensifying extreme loss to agriculture production (Daryanto et al., 2016). The response to stress creates wide variability at morphological, cellular, physiological, biochemical, and molecular level and the expression of key genes results in enhanced stress tolerance (Tas and Tas, 2007; Aprile et al., 2013). In the present study, the changes was observed from detrimental effects of the drought on the essential metabolic processes, leading to loss in growth, and slowing of crop development, which ultimately would have damaged crop quality and production. Drought stress restricts plant growth and crop production (Shao et al., 2005); it is therefore important for plants to continue growth during drought to avoid its influences. Tolerant cultivars Chakwal-86, IBWSN-1010 and IBWSN-1025 had significantly higher shoot fresh and dry masses under drought stress compared to the sensitive cultivar Khirman, suggesting that these cultivars were tolerant of drought stress. The results are in agreement with finding of Datta et al. (2011), and Tas and Tas (2007),

http://www.aloki.hu ● ISSN 1589 1623 (Print) ● ISSN1785 0037 (Online)
DOI: http://dx.doi.org/10.15666/aeer/2001_619632

who reported higher losses in fresh and dry masses in sensitive cultivar than tolerant under drought stress in wheat genotypes. Loss of leaf fresh weight was noted after the tenth day of the drought treatment in all the cultivars, suggesting that the severe phase of the drought started from the tenth day of withholding water (Demirevska et al., 2008). However, leaf fresh weight did not decrease in any of the cultivars in the de-tillering experiment except in Khirman, which significantly decreased its leaf fresh weight by 65% because soil water content decreased more slowly. Keles and Öncel (2004) also reported significant decrease of 40% in fresh weight in wheat under drought stress. The retention of higher leaf fresh weight suggested leaf longevity under drought stress in tolerant cultivars. Losses of fresh and dry weights under drought stress were associated with the leaf senescence and finally mortality in sensitive cultivar. Leaf senescence has importance under drought stress because it contributes to remobilization of leaf resources to other parts of the plant to ensure survival (Munné-Bosch, 2007; Qadir et al., 2019). Leaf senescence and leaf mortality had started after five days of the drought treatment in all of the cultivars. Leaf senescence progressed from the tip towards the base of the leaf, while leaf mortality was concomitant with continued shoot growth, indicating translocation of resources away from senescing tissues. Leaf mortality rates also increased with the severity of the drought and became a problem for the sensitive cultivar Khirman as most of its leaves died under drought stress conditions. All the cultivars had a significantly higher number of living leaves compared to Khirman under drought stress conditions. According to Liu and Li (2005), the drought sensitive cultivar (Khirman) is highly sensitive to severe drought stress than the moderate stress. Other cultivars intentionally reduce the leaf number to survive on available water resources and remobilization of leaf resources in the growing shoot tips, while Khirman does not managed these resources towards shoot tips.

Leaf water content (LWC) is considered as indicators of the water status of the plant (Zhou et al., 2021). LWC was significantly higher in tolerant cultivars compared to sensitive and hybrid cultivars under drought stress, suggesting that retaining higher water content in the leaf as the result of higher turgor potential. The results are in agreement with the finding of (Fresneau et al., 2007), who had observed a significant decrease in LWC under drought stress in wheat. Brown et al. (2010) and Nayyar et al. (2005) have suggested that leaf water potential (LWP) should be considered a reliable parameter to quantify plant response to drought stress, and can be used as a selectable marker for improving drought tolerance in different crops. Tolerant cultivars had significantly higher LWP under the drought treatment compared to the sensitive cultivar Khirman, which had only two leaves alive out of five replicates suggesting that the maintenance of higher LWP will enable tolerant cultivars to keep higher rate of photosynthesis and therefore maintain shoot growth under drought stress conditions. LWP was decreased significantly under the drought treatment in all the cultivars. Liu and Li (2005), and Tambussi et al. (2005) have observed significant decrease in LWP in wheat cultivars under drought stress conditions. Genotypic difference were reported by Subrahmanyam et al. (2006), and Tas (2007), who observed a significantly greater decreases in leaf water potential (leaf Ψ_w) in sensitive wheat cultivars compared to tolerant cultivars under drought stress conditions. Drought stress also significantly decreased leaf Ψ_w in other crop plants (Medeiros et al., 2012).

Leaf area only decreased in Khirman under the drought treatment. Maintenance of leaf area in the tolerant cultivars was associated with higher leaf water status, whereas loss of leaf area in the sensitive cultivar was associated with lower leaf water status under

http://www.aloki.hu ● ISSN 1589 1623 (Print) ● ISSN1785 0037 (Online)
DOI: http://dx.doi.org/10.15666/aeer/2001_619632

drought stress. Leaf area decreased significantly in all the cultivars under drought stress conditions suggesting leaf senescence had occurred. This could be a strategy to avoid further water loss or simply a response to insufficient water availability, because with greater leaf area, higher water losses occur. The results are in agreement with the finding of who observed leaf senescence and reported 36% of remobilization in a controlled pot experiment, while Da Ros and Mansfield (2020) reported leaf senescence and observed 57-79% remobilization of resources in field conditions. A decrease in leaf area under drought stress has also been shown in multiple crops (Chaves et al., 2002). Reductions in leaf area under the drought reduce both biomass and radiation interception by plants. Relative water content (RWC) is considered as indicators of the water status of the plant. Relative water content is an important characteristic for estimating tissue hydration and water status (Zhang et al., 2015). RWC was significantly decreased in the sensitive cultivar Khirman from the fifteenth day of the drought treatment, suggesting that it had lost water faster in early days of the drought treatment, and that this resulted in lower leaf turgor. Fresneau et al. (2007) have also reported a significant decrease in RWC after ten days of the drought stress in wheat. RWC was significantly decreased in all the cultivars under drought stress conditions. Similar results were reported by Medeiros et al. (2012), who observed significant decrease in RWC in four wheat cultivars subject to drought stress. RWC was significantly decreased under drought stress in all the cultivars in accordance with the findings of Fresneau et al. (2007), Huseynova et al., (2007), and Liu et al. (2006). A significant decrease in RWC was observed in different crops under drought stress conditions (Medeiros et al., 2012). The salt tolerant cultivars IBWSN-1010, IBWSN-1025 (salt tolerant liens), had significantly higher RWC compared to sensitive cultivar Khirman under the drought treatment, suggesting higher RWC helped to maintain photosynthesis and growth in these cultivars. Higher RWC was previously reported in tolerant and lower RWC in sensitive cultivars of wheat under drought stress (Subrahmanyam et al., 2006).

Plant water status is closely associated with the water status of the soil (Bellot and de Urbina, 2008). Soil water potential (SWP) and soil water content (SWC) are the measures of water availability to the plants and its abundance in the soil. SWP and SWC decreased significantly in all the cultivars under drought stress compared to day zero suggesting increasing drought stress caused a progressive decrease in soil water status. The results show that the drought treatment had worked properly. The results are in agreement with the findings of who observed a significant decrease in SWP in wheat cultivars under drought stress conditions. SWP also decreased significantly in a range of different crops subjected to drought stress (Volaire, 2003). SWC was significantly higher in Chakwal-86 and IBWSN-1010 on the fifth day of the drought treatment compared to remaining cultivars in tillering experiment. No genotypic difference was observed under drought stress conditions supporting the former explanation, and suggesting removal of tillers had worked, such as all the cultivars had the same available water. Similar results have been reported by Volaire (2003) and Xiong et al. (2006), who had observed significant decrease in SWC and SWP under drought stress conditions in wheat, but no genotypic differences were observed.

Conclusions

The preliminary results showed that different degrees of stability were shown by salt and drought tolerant cultivars under drought stress conditions. The drought tolerant

http://www.aloki.hu ● ISSN 1589 1623 (Print) ● ISSN1785 0037 (Online)
DOI: http://dx.doi.org/10.15666/aeer/2001_619632

cultivar Chakwal-86 was also found to be more tolerant to drought compared to the salt tolerant and intolerant lines. Under severe drought conditions, senescence of mature leaves reduced the leaf area and caused higher leaf mortality in Khirman, a typical drought sensitive variety, compared to tolerant lines, which showed lower leaf mortality. The cultivars Chakwal-86, IBWSN-1025 and IBWSN-1010 had significantly higher relative water content and leaf water potentials and lower decline in leaf water potential, while Khirman had significantly lower leaf water potential by the twentieth day of the drought. These results suggest that Chakwal-86, IBWSN-1010, and IBWSN-10250 retained more water and therefore had higher water use efficiency, which enables these genotypes to continue growth, as shown by the continued increase in plant biomass. The decrease in relative water content is an indication that a plant is facing osmotic stress; as a result, photosynthesis may be affected. Strong recommendations for future studies are also needed.

Acknowledgements. This study was supported by the Key Research and Development Projects of Sichuan Province (2018NZ0057), Sichuan Liangshan Science and Technology Plan Projects (21ZDFY0152).

REFERENCES

[1] Abro, A. A., Memon, S., Abro, S. A., Magsi, F. H., Soomro, A. A., Mahar, N. A., Chang, B. H. (2019): Influence of additional amino acids in growth of different wheat (*Triticum aestivum* L.) genotypes. – Journal of Plant Nutrition 42(19):2539-2551. DOI: 10.1080/01904167.2019.1659318.

[2] Abro, A. A., Memon, S., Abro, S. A., Sam, E. K., He, Ru-yu., Rind, M. H., Memon, S., Solangi, Z., Muhammad, T., Ali, B., Ahmed, W., Dev, W., Abro, M. A., Rajput, N., Nizamani, S., Nargis, M., Kumbhar, R. A. (2020): Evaluation of drought tolerance in wheat (*Triticum aestivum* L.) Cultivars at early seedling stage using polyethylene glycol induced osmotic stress. – The Journal of Animal & Plant Sciences 30(4):950-957.

[3] Abbas, Z. K., Mobin, M. (2016): Comparative growth and physiological responses of two wheat (*Triticum aestivum* L.) cultivars differing in salt tolerance to salinity and cyclic drought stress. – Archives of Agronomy & Soil Science 62(6): 745-758.

[4] Al Hattab, Z., Al-Ani, M., Al Gburi, R. J., Kh, S., Al Raheem, F. N., Hussain (2018): Coping with salinity: HANAA new salt tolerant wheat (*Triticum aestivum* L.) Cultivar. – Bioscience Research 15(2): 1020-1027.

[5] Aldesuquy, H. S., Baka, Z. A., El-Shehaby, O. A., Ghanem, H. E. (2012): Varietal differences in growth vigor, water relations, protein and nucleic acids content of two wheat varieties grown under seawater stress. – Journal of Stress Physiology & Biochemistry 8(1): 24-47.

[6] Ali, N., Chaudhary, B. L., Panwar, N. L. (2014): The fungal pre-treatment of maize cob heart and water hyacinth for enhanced biomethanation. – International Journal of Green Energy 11(1): 40-49.

[7] Aprile, A., Havlickova, L., Panna, R., Maré, C., Borrelli, G. M., Marone, D., Perrotta, C., Rampino, P., De Bellis, L., Curn, V., Mastrangelo, A. M., Rizza, F., Cattivelli, L. (2013): Different stress responsive strategies to drought and heat in two durum wheat cultivars with contrasting water use efficiency. – BMC genomics 14: 1.

[8] Bellot, J., de Urbina, J. O. (2008): Soil water content at the catchment level and plant water status relationships in a Mediterranean Quercus ilex forest. – Journal of Hydrology 357: 67-75.

[9] Chaves, M. M., Maroco, J. P., Pereira, J. S. (2003): Understanding plant responses to drought from genes to the whole plant. – Functional plant biology 30: 239-264.

http://www.aloki.hu ● ISSN 1589 1623 (Print) ● ISSN1785 0037 (Online)
DOI: http://dx.doi.org/10.15666/aeer/2001_619632

[10] Chen, C., Payne, W. A., Smiley, R. W., Stoltz, M. A. (2003): Yield and water-use efficiency of eight wheat cultivars planted on seven dates in northeastern Oregon. – Agronomy journal 95: 836-843.
[11] Chunthaburee, S., Dongsansuk, A., Sanitchon, J., Pattanagul, W., Theerakulpisut, P. (2016): Physiological and biochemical parameters for evaluation and clustering of rice cultivars differing in salt tolerance at seedling stage. – Saudi Journal of Biological Sciences 23: 467-477.
[12] Da Ros, L. M., Mansfield, S. D. (2020): Biotechnological mechanism for improving plant remobilization of phosphorus during leaf senescence. – Plant Biotechnology Journal 18(2): 470-478.
[13] Daryanto, S., Wang, L., Jacinthe, P. A. (2016): Global synthesis of drought effects on maize and wheat production. – PloS one 11: e0156362.
[14] Datta, J., Mondal, T., Banerjee, A., Mondal, N. (2011): Assessment of drought tolerance of selected wheat cultivars under laboratory condition. – Journal of Agricultural Science and Technology 7: 383-393.
[15] Demirevska, K., Simova-Stoilova, L., Vassileva, V., Vaseva, I., Grigorova, B., Feller, U. (2008): Drought-induced leaf protein alterations in sensitive and tolerant wheat varieties. – Gen Appl Plant Physiol 34: 79-102.
[16] Fresneau, C., Ghashghaie, J., Cornic, G. (2007): Drought effect on nitrate reductase and sucrose-phosphate synthase activities in wheat (*Triticum durum* L.): role of leaf internal CO2. – Journal of Experimental Botany 58: 2983-2992.
[17] Huseynova, I. M., Suleymanov, S. Y., Aliyev, J. A. (2007): Structural–functional state of thylakoid membranes of wheat genotypes under water stress. – Biochimica et Biophysica Acta (BBA)-Bioenergetics 1767: 869-875.
[18] Jiang, M-Y., Zhang, J-H. (2004): Abscisic acid and antioxidant defense in plant cells. – Acta Botanica Sinica-English Edition- 46: 1-9.
[19] Kaur, L., Zhawar, V. K. (2015): Phenolic parameters under exogenous aba, water stress, salt stress in two wheat cultivars varying in drought tolerance. – Indian Journal of Plant Physiology 20(2): 151-156.
[20] Keles, Y., Öncel, I. (2004): Growth and Solute Composition in Two Wheat Species Experiencing Combined Influence of Stress Conditions. – Russian Journal of Plant Physiology 51: 203-209.
[21] Knipfer, T., Danjou, M., Vionne, C., Fricke, W. (2020): Salt stress reduces root water uptake in barley (*Hordeum vulgare* L.) through modification of the transcellular transport path. – Plant, Cell & Environment 44(2).
[22] Liu, X., Baird, W. V. (2004): Identification of a novel gene, HAABRC5, from Helianthus annuus (Asteraceae) that is upregulated in response to drought, salinity, and abscisic acid. – American Journal of Botany 91: 184-191.
[23] Liu, H. S., Li, F. M. (2005): Root respiration, photosynthesis and grain yield of two spring wheat in response to soil drying. – Plant growth regulation 46: 233-240.
[24] Malik, S., Rahman, M., Malik, T. A. (2015): Genetic Mapping of Potential Qtls Associated with Drought Tolerance in Wheat. – The Journal of Animal & Plant Sciences 25(4): 1032-1040.
[25] Mahboob, W., Khan, M. A., Shirazi, M. U. (2017): Characterization of salt tolerant wheat (*Triticum aestivum*) genotypes on the basis of physiological attributes. – Int. J. Agric. Biol. 19: 726-734.
[26] Medeiros, D. B., Silva, E., Santos, H., Pacheco, C. M., Musser, R., Nogueira, R. (2012): Physiological and biochemical responses to drought stress in Barbados cherry. – Brazilian Journal of Plant Physiology 24(3): 181-192.
[27] Monneveux, P., Jing, R., Misra, S. C. (2012): Phenotyping for drought adaptation in wheat using physiological traits. – Frontiers in Physiology 3: 429.
[28] Munné-Bosch, S. (2007): Aging in perennials. – Critical Reviews in Plant Sciences 26: 123-138.

http://www.aloki.hu ● ISSN 1589 1623 (Print) ● ISSN1785 0037 (Online)
DOI: http://dx.doi.org/10.15666/aeer/2001_619632

[29] Nayyar, H., Kaur, S., Singh, K., Dhir, K., Bains, T. (2005): Water Stress-induced Injury to Reproductive Phase in Chickpea: Evaluation of Stress Sensitivity in Wild and Cultivated Species in Relation to Abscisic Acid and Polyamines. – Journal of Agronomy and Crop Science 191: 450-457.
[30] Punia, S., Shah, A. M., Ranwha, B. R. (2011): Genetic analysis for high temperature tolerance in bread wheat. – African Crop Science Journal 19: 149-163.
[31] Qadir, S., Ayub, I., Sarwat, M., John, R. (2019): Proteolytic Processes During Leaf Senescence. – Senescence Signalling and Control in Plants, pp. 165-185.
[32] Saba, J., Moghadam, M., Ghassemi, K., Nishabouri, M. (2010): Genetic properties of drought resistance indices. – Journal of Agricultural Science and Technology 3: 43-49.
[33] Shao, H., Liang, Z., Shao, M., Wang, B. (2005): Changes of some physiological and biochemical indices for soil water deficits among 10 wheat genotypes at seedling stage. – Colloids Surf B: Biointerfaces 42(2): 107-113.
[34] Subrahmanyam, D., Subash, N., Haris, A., Sikka, A. (2006): Influence of water stress on leaf photosynthetic characteristics in wheat cultivars differing in their susceptibility to drought. – Photosynthetica 44: 125-129.
[35] Tambussi, E. A., Nogués, S., Araus, J. L. (2005): Ear of durum wheat under water stress: water relations and photosynthetic metabolism. – Planta 221: 446-458.
[36] Tanaka, W., Maddonni, G. Á. (2009): Maize kernel oil and episodes of shading during the grain-filling period. – Crop Science 49(6): 2187-2197.
[37] Tas, S., Tas, B. (2007): Some physiological responses of drought stress in wheat genotypes with different ploidity in Turkiye. – World J Agric Sci 3: 178-183.
[38] Tester, M., Bacic, A. (2005): Abiotic stress tolerance in grasses. From model plants to crop plants. – Plant Physiology 137: 791-793.
[39] Verslues, P. E., Agarwal, M., Katiyar-Agarwal, S., Zhu, J., Zhu, J. K. (2006): Methods and concepts in quantifying resistance to drought, salt and freezing, abiotic stresses that affect plant water status. – The Plant Journal 45: 523-539.
[40] Volaire, F. (2003): Seedling survival under drought differs between an annual (Hordeum vulgare) and a perennial grass (Dactylis glomerata). – New Phytologist 160: 501-510.
[41] Xiong, Y-C., Li, F-M., Zhang, T. (2006): Performance of wheat crops with different chromosome ploidy: root-sourced signals, drought tolerance, and yield performance. – Planta 224: 710-718.
[42] Zhang, W. J., Huang, Z. L., Wang, Q., Guan, Y. N. (2015): Effects of low temperature on leaf anatomy and photosynthetic performance in different genotypes of wheat following a rice crop. – International Journal of Agriculture & Biology 17(6).
[43] Zhou, H., Zhou, G., He, Q., Zhou, L., Lv, X. (2021): Capability of leaf water content and its threshold values in reflection of soil-plant water status in maize during prolonged drought. – Ecological Indicators 124: 1470-1160.
[44] Zhu, J., Shi, H., Lee, B., Damsz, B., Cheng, S., Stirm, V., Zhu, J-K., Hasegawa, P. M., Bressan, R. A. (2004): An Arabidopsis homeodomain transcription factor gene, HOS9, mediates cold tolerance through a CBF-independent pathway. – Proceedings of the National Academy of Sciences of the United States of America 101: 9873-9878.

http://www.aloki.hu ● ISSN 1589 1623 (Print) ● ISSN1785 0037 (Online)
DOI: http://dx.doi.org/10.15666/aeer/2001_619632

EVALUATION AND APPLICATION OF THE ORYZA (v3) RICE MODEL UNDER DIFFERENT NITROGEN LEVELS IN LIAONING PROVINCE, CHINA

WU, Y. X.[1] – WANG, S.[1] – YIN, H.[1*] – JIA, B. Y.[1] – HUANG, Y. C.[1] – CHEN, P. S.[2] – GUO, Y. Y.[1]

[1]*College of Agronomy, Shenyang Agricultural University, Shenyang 110866, China*

[2]*Ecometeorology and Satellite Remote Sensing Center of Liaoning, Shenyang 110001, China*

**Corresponding author*
e-mail: snyinhong@syau.edu.cn

(Received 18th Aug 2021; accepted 23rd Nov 2021)

Abstract. Climate change and the growing-demand for food security force growers to identify ways to improve both food production and resource-utilization effectiveness. Liaoning province is one of the major rice (*Oryza sativa* L.) production regions of China (CL), accounting for about 10% of the total national japonica cultivation area. In this study, the experimental regions were divided into five rice agroecological zones based on the difference in the planting area and climate conditions. Four nitrogen (N) management levels were designed by the application amount of N fertilizer. ORYZA (v3) model was calibrated, validated and applied to simulate yields under four N fertilizer levels. The results showed that ORYZA (v3) can describe grain yield and above-ground biomass well, and it can be applied to simulate growth in CL region. Scenario-analysis indicated that the simulated grain-yield responded strongly to a low nitrogen level. However, there was no significant grain-yield increase under more N. Significant spatial variation in the grain-yield was observed at different levels. Compared to regions with limited temperature and light resources during the rice growing-periods, the regions with more optimal conditions showed higher grain-yields under all four N levels.
Keywords: *climate change, yield, fertilizer, agriculture, crop*

Introduction

Rice (*Oryza sativa* L.) is one of the most important staple food crops which feeds more than half of the world's population (Fan et al., 2016). China is an important rice production country, wherein the rice planting area accounted for 26.1% of the total grain-crop area, and the rice production accounts for 32.1% of the national total grain crop production (National Bureau of Statistics of China, 2016). Hence, rice production is vital for the food security in China. To meet the growing populational demand for food, people continuously improve the way of cultivation and management to increase rice yields.

Nitrogen (N) is the most important plant nutrient in crop yield determination and the fertilizer is the major N source for modern agricultural systems (Mae, 1997). To increase rice yields, farmers often apply excessive amount of N fertilizers. In China, the average N application-rate in rice production is approximately 180 kg ha^{-1}, which is higher than that in most countries and as much as 75% above the global average. Rice crops in China consume about 37% of the total N fertilizer used for rice production in the world (Buresh and Witt, 2002; Roelcke et al., 2004; Peng et al., 2010). However, excessive usage of N has greatly decreased the economic return and also placed a heavy economic burden on farmers (Zhang, 2007). It can cause many issues such as low N-efficiency in the soil, leaching, volatilization, nitrification of N, even destroying ecological balances and causing environmental hazards (Cheng et al., 2021). Moreover,

http://www.aloki.hu ● ISSN 1589 1623 (Print) ● ISSN1785 0037 (Online)
DOI: http://dx.doi.org/10.15666/aeer/2001_633651

over-application of N often induces rice lodging and pest damage resulting in yield and quality reduction. Further increase in N application to croplands is unlikely an effective method for increasing crop yield (Tilman et al., 2011).

Process-based crop models are important tools in modern agricultural research. The modeling method is time-saving and cost-effective and suitable for the extrapolation from site-specific experiments to larger spatial and temporal scales (Ling et al., 2019). ORYZA2000 is a robust model which provides reliable predictions for rice growth and yield in irrigated systems (Li et al., 2017) and has been widely used in modeling rice growth all over the world (Rani et al., 2011; Soundharajan and Sudheer, 2013; Kim et al., 2015). ORYZA (v3) is an advanced version of ORYZA2000. ORYZA series models can be influenced by environmental conditions, crop management, and cultivar characteristics (Li et al., 2013, 2016, 2017).

The Liaoning province is an important japonica rice production region in China. The rice planting area in Liaoning accounts for approximately 10% of the national japonica rice area (National Bureau of Statistics of China, 2016). Rice yield in this region can significantly influence the local food supplies. For the rice production in Liaoning, high-N fertilizer is applied at average levels of 200-300 kg ha^{-1} and even 350 kg ha^{-1} in some area (Yu et al., 2009). Until now, there has been no case-study on the application of ORYZA (v3) model under different N levels in the Liaoning province. The objectives of this study were to (a) calibrate and evaluate the performance of ORYZA (v3) for simulating rice development and yields under nitrogen-limited conditions in different agro-ecological zones in Liaoning and (b) apply ORYZA (v3) to investigate yield response to N-application rates.

Materials and methods

Study area

The study area includes the main rice-growing areas of Liaoning province (CL), which was divided into five distinct agro-ecological zones based on the difference in the planting area and climate conditions (*Figure 1*). Huanren (CL1), Donggang (CL2), Liaozhong (CL3), Kaiyuan (CL4), Dawa (CL5) were respectively selected as the rice planting-sites in each agro-ecological zone. Two-three study sites were chosen within each agro-ecological zone, and a total of 18 sites (five experimental sites and 13 representative sites) were selected in the end. The spatial distribution of these sites was shown in *Figure1*.

Data sources

The experimental data sets used to calibrate and validate the crop model were derived from field experiments conducted from 2017-2019 (presented in *Table 1*). In this study, five widely planted local high-yielding rice cultivars were used in these experiments and assumed to be area-specific (*Table 1*).

On this basis, a database was generated from a rice field study in different areas with four nitrogen fertility management practices. The database was used to evaluate the ORYZA (v3) model. On every test site, experiments were performed by a completely randomized block design (CRBD) with three replications. The area of each experimental plot was 6 m×1.8 m (length×width). To analyze surveyed yield-levels in different regions, the Stanford formula (*Eq.1-Eq.2*) was used to calculate the amount of

http://www.aloki.hu ● ISSN 1589 1623 (Print) ● ISSN1785 0037 (Online)
DOI: http://dx.doi.org/10.15666/aeer/2001_633651

N applied in five testing-points. Four nitrogen fertilizer levels, namely the basic yield level (Yck), farmers' yield level (Yfp), high-yield and efficient yield level (Yhh), and super-high-yield level (Ysh) were used in this study. A diverse distribution for a specific fertilization-treatment was identified among the five areas (*Table 2*). Base fertilizer was applied 1d before sowing, and the tiller and jointing fertilizer were applied at the corresponding periods. All other management practices were the same for all plots following local standards, including the control of plant diseases, insect pests and weeds etc.

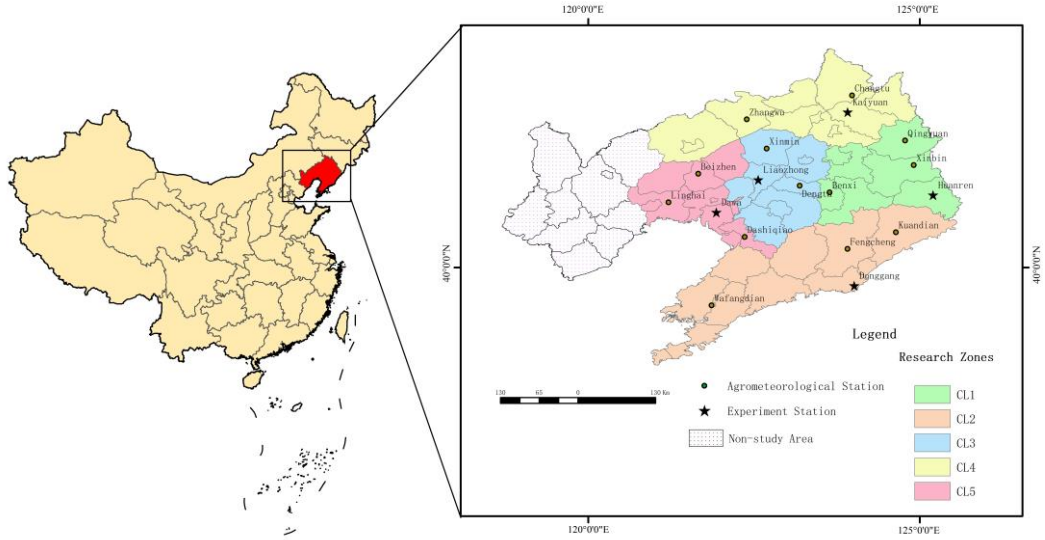

Figure 1. *Distribution of rice representative sites and agro-meteorological observation stations in each region of the study area. Among them, CL1 represents the rice cultivation area in the eastern hilly area, CL2 represents the rice cultivation area in the coastal plain, CL3 represents the rice cultivation area in the central plain, CL4 represents the rice cultivation area in northern plain and CL5 represents Liaohe Delta rice planting area*

Table 1. *The database was divided into two samples, calibration data set (I) and validation data set (II)*

Area	Experimental station	Cultivar	Calibration data set (I)	Validation data set (II)
CL1	Huanren	Shendao529	2017-2018	2019
CL2	Donggang	Shendao505	2017-2018	2019
CL3	Liaozhong	Beijing 1	2017-2018	2019
CL4	Kaiyuan	Tiejing 7	2017-2018	2019
CL5	Dawa	Yanfeng47	2017-2018	2019

At the end of April, the soil was tilled twice by the rotary machine, and then the puddling was used one week before transplanting. The basal fertilizers were applied onto the soil surface before tillage. All plots were separated from one other and each had its own inlet and outlet to irrigate and drain water. The water regime was followed by continuous flood with 15 to 20 cm depth and the paddy field was dried 10 d before harvesting. Except that the field was irrigated with underground water in Liaozhong

http://www.aloki.hu ● ISSN 1589 1623 (Print) ● ISSN1785 0037 (Online)
DOI: http://dx.doi.org/10.15666/aeer/2001_633651

County, the water sources of other four sites were rivers. The barnyard grass and broad-leaf grass were controlled by applying butachlor and bensulfuron-methyl 5 to 7 d after transplanting. The thiamethoxam was applied at early tillering stage to control rice borer and isoprothiolane applied 7 d before anthesis to control the rice blast. The pymetrozine was sprayed at filling stage to control plant hopper.

Table 2. *Models set different management measures for rice in five regions in Liaoning Province*

Region Cultivar	Yield level	Emergence Julia day	Seed-bed Duration (Days)	Nitrogen Regime (kg ha^{-1})		Irrigation Regime
				Amount	Ratios (TP-TL-JT)	
Dawa Yanfeng 47	Yck	111	40	0	0-0-0	flooded
	Yfp	111	40	250	62.5-12.5-25	flooded
	Yhh	111	40	270	45-20-35	flooded
	Ysh	111	40	290	45-20-35	flooded
Liaozhong Beijing 1	Yck	101	35	0	0-0-0	flooded
	Yfp	101	35	200	62.5-12.5-25	flooded
	Yhh	101	35	220	45-20-35	flooded
	Ysh	101	35	240	45-20-35	flooded
Kaiyuan Tiejing 7	Yck	111	40	0	0-0-0	flooded
	Yfp	111	40	180	62.5-12.5-25	flooded
	Yhh	111	40	200	45-20-35	flooded
	Ysh	111	40	220	45-20-35	flooded
Huanren Shendao 529	Yck	121	36	0	0-0-0	flooded
	Yfp	121	36	160	62.5-12.5-25	flooded
	Yhh	121	36	180	45-20-35	flooded
	Ysh	121	36	200	45-20-35	flooded
Donggang Shendao 505	Yck	116	41	0	0-0-0	flooded
	Yfp	116	41	160	62.5-12.5-25	flooded
	Yhh	116	41	180	45-20-35	flooded
	Ysh	116	41	200	45-20-35	flooded

Note: In the nitrogen fertilizer application schedule, TP, TL, and JT represent the nitrogen application at transplanting, tillering, and jointing. For irrigation schemes, "Flooded" means using an automatic irrigation system to maintain a water depth of 10-50 mm

The “leaf weight” method was used to measure leaf areas specifically at early growth, heading and full heading stages to obtain the leaf area index. Stem, leaf and panicle samples were taken at heading，full heading and mature stages and then dried to constant weight for measurements of dry matters. The yield was measured by threshing at the mature stage, and panicles were tested and analyzed in the laboratory. Through data extraction, we must collect important information from each trial and data records (phenological dates, leaf area index, above-ground biomass, and yield).

$$N_{\mathrm{f}} = \left(N_{\mathrm{y}} - N_{\mathrm{s}}\right) / E_{\mathrm{f}} \quad \text{(Eq.1)}$$

$$N_{\mathrm{y}} = \left(N_{\mathrm{frac}} \times \text{ Target Yield }\right) / \mathrm{NHI} \quad \text{(Eq.2)}$$

where N_{y} is the above ground N contained in a crop with a specified yield, N_{f} is the N fertilizer requirement, N_{s} is the amount of N supplied by the soil to the above ground

http://www.aloki.hu ● ISSN 1589 1623 (Print) ● ISSN1785 0037 (Online)
DOI: http://dx.doi.org/10.15666/aeer/2001_633651

portion of the crop, N_{frac} is the fraction of N in the grain and NHI is the nitrogen harvest index. The target yield is the yield we want to get in theory on a special nitrogen fertilizer amount.

Data from historical rice trials (year of 1981-2015) were collected on the agro-meteorological experimental stations, including yields and dates of emergence, transplantation, flowering, and physiological maturity.

The soil data-set for this study was mainly obtained from the Environmental & Ecological Science Data Center for West China, National Natural Science Foundation of China (http://westdc.westgis.ac.cn), and the Institute of Soil Science, Chinese Academy of Sciences (ISSCAS). The soil parameters in the model operation included the saturated water-content in different soil layers, field water-capacity, wilting-point water- content, saturated hydraulic-conductivity, bulk density (BD), texture (sand and clay content), pH, and soil organic-matter (SOM).

The weather data in this study was obtained from the climate data-sharing service system of the China Meteorological Administration (CMA) (http://data.cma.cn) including sunshine hours (h; h d^{-1}), maximum temperature (TMMX; °C), minimum temperature (TMMN; °C), early morning vapor pressure (VP; kPa), and mean wind speed (WN; ms^{-1}) (Bouman and Laar, 2001). Since solar radiation measurements were not available from the stations, the sunshine hour was converted to solar radiation using the Ångström formula (*Eq.3-Eq.8*) (Angstrom, 1924; Black et al., 1954).

$$R_s = R_a \times \left(\mathrm{a} + \mathrm{b} \times \frac{n}{N} \right) \tag{Eq.3}$$

$$R_a = 37.59 \times d_r \times \left(\omega_s \sin\varphi \sin\delta + \cos\varphi \cos\delta \sin\omega_s \right) \tag{Eq.4}$$

$$d_r = 1 + 0.033 \times \cos\left(\frac{2\pi}{365} J \right) \tag{Eq.5}$$

$$\delta = 0.409 \times \sin\left(\frac{2\pi}{365} J - 1.39 \right) \tag{Eq.6}$$

$$\omega_S = \arccos(-\tan\varphi \tan\delta) \tag{Eq.7}$$

$$N = \frac{24}{\pi} \omega_s \tag{Eq.8}$$

where R_s is the solar radiation (MJ m^{-2} d^{-1}), R_a is the extraterrestrial radiation (MJ m^{-2} d^{-1}), a and b are the regression constant, empirical coefficient expressing the fraction of extraterrestrial radiation reaching the earth on overcast days, N is the maximum possible duration of sunshine or daylight hours(hour), n is the actual duration of sunshine (hour), d_r is the inverse relative distance Earth-sun, ω_s is the sunset hour angle(rad), φ is the latitude (rad), δ is the solar decimation (rad), J is the number of the day in the year.

http://www.aloki.hu ● ISSN 1589 1623 (Print) ● ISSN1785 0037 (Online)
DOI: http://dx.doi.org/10.15666/aeer/2001_633651

The ORYZA (v3) crop model

The ORYZA model series are widely used in the world for crop growth and yield stimulation of different varieties under different environmental conditions (Belder et al., 2004; Arora, 2005; Feng et al., 2007). Leading research institutes on these models include the International Rice Research Institute (IRRI) and the University of Wageningen (WUCR) in the Netherlands (Bouman and Laar, 2001). These models can follow the daily dry-matter accumulation of plant organs and dynamically and quantitatively describe rice growth and development and yield formation of a rice crop under situations of potential production (ORYZA1), water limitations (ORYZA-W), nitrogen limitations (ORYZA-N), soil moisture and N dynamic changes. These models have two sub-routines (NCROP and NSOIL) to simulate the crop-soil N dynamics. When the experimental data file (NITROENV) was set 'NITROGEN BALANCE', NCROP and NSOIL were called by the model. NCROP is used to calculate the N demand, uptake, distribution and transport in the crop canopy and the N-restriction stress-factors. The level of N-stress a rice plant experiences depends on the N-availability for uptake from soil. NSOIL is used to track daily N-availability in soil (Bouman and Laar, 2001). The models assume that the N is available on-demand, but actually the N-uptake is the lower than the maximum uptake capacity of a given cultivar on the total available soil mineral N. Also a simple sub-routine (NCROP) for the calculation of the leaf N concentration (LNC) may allow the determination of the rice production. The ORYZA (v3) model is the latest version of the series of models, which has a stronger capability to simulate rice growth and development dynamics. In this version, N-uptake and water-uptake are coupled (Li et al., 2017). The ORYZA (v3) model adds parameters such as the critical temperature and the date of rice-growth for better controls on the plant growth. Additional features are added for large-scale simulation, automatic parameter adjustment, carbon and nitrogen cycle, and the impact of greenhouse gases on climate change. Meanwhile, the soil-nutrient-content and irrigation-measure settings have been improved to increase the accuracy of simulating rice physiological processes, irrigation management measures, and dynamic changes of soil moisture (Guo et al., 2017).

Model calibration and validation

In this study, we selected a representative cultivar from each region to specify crop coefficients using ORYZA (v3) calibration. To evaluate model performance, we split the experimental data into two parts: training and validation data sets (*Table 1*). Previous empirical researches have convincingly showed that most crop-specific parameters are generic (Bouman and Laar, 2001; Li et al., 2017). Therefore, the bulk of our model parameters were taken from IR72 and were not adjusted during model identification. However, several parameters such as development rates, partitioning factors, relative leaf growth rate, specific leaf area, and the fraction of stem reserves (about 10% in the ORYZA (v3) model) needed to be adjusted specifically for the variety and environment to obtain an optimal model. Consistent with previous studies, we used DRATES and PARAM to determine development rates and other parameters (Kropff et al., 1994). Then we validated, trained, and improved the ORYZA (v3) model parameters in a trial and error process until the satisfactory performance achieved. Thereafter, one out-of-sample test by applying the calibrated model was performed to confirm the validation of the model.

http://www.aloki.hu ● ISSN 1589 1623 (Print) ● ISSN1785 0037 (Online)
DOI: http://dx.doi.org/10.15666/aeer/2001_633651

The crop model calibration approach consists of three stages: 1) calculating the mean absolute difference (d_a) (*Eq.9*) between the observed and the simulated values. The d_a is defined as an index that measures the average magnitude of errors in a set of forecasts and accuracy for continuous variables (Cao et al., 2006). It should be a pre-condition for validation of the ORYZA (v3) model; 2) calculating the root mean square errors (RMSE) (*Eq.10*) and normalized root mean square error (NRMSE) (*Eq.11*), which are defined as a quadratic scoring rule that measures the average magnitude of the error (Stockle et al., 1994; Evers et al., 2005); 3) measuring the intercept (α), slope (β), and coefficient of determination (R^2), at the same time plotting 1:1 diagram. The Model validation is mainly based on plotting comparison of theory and field measurement, including the weights of leaves (WLVG; kg ha^{-1}), stems (WST; kg ha^{-1}), storage organs (WSO; kg ha^{-1}), leaf area index (LAI), and grain yield. In this study, a student t-test was used to test differences in quantitative data among different groups. Ideally, the statistical parameters values of β, R^2 should be close to 1. Data were analyzed by spss6.0 using Student t-test (P(t*)) and results were considered significant when $p<0.05$. Excel 2019 and Origin 2018 were the main tools for analyzing data and drawing figures.

$$d_a = \frac{1}{n}\sum_{i=1}^{n}\left(Y_i - X_i\right) \quad \text{(Eq.9)}$$

$$RMSE = \sqrt{\frac{1}{n}\sum_{i=1}^{n}\left(Y_i - X_i\right)^2} \quad \text{(Eq.10)}$$

$$NRMSE = 100\frac{\sqrt{\sum_{i=1}^{n}\left(Y_i - X_i\right)^2 / n}}{\overline{x}} \quad \text{(Eq.11)}$$

where n is the number of samples, and Y_i and X_i represent the simulated and measured values. The root mean square error ($RMSE$) and the normalized root mean square error ($NRMSE$) reflect the magnitude of the simulated error. The mean of the values reflects the overall simulation effect. $NRMSE$ <15%, 15% ≤ $NRMSE$ <30% and $NRMSE$ > 30% indicate that the model simulation residuals are small, medium and large (Gaiser et al., 2010; Liu et al., 2011).

Scenario analyses

Validated ORYZA (v3) model was used to simulate the grain yield of rice concerning four critical N-fertilizer management practices employing weather data of Liaoning province from 1981 to 2015 (CMA). In scenario analyses, model runs with different emergence day (EMD) of the five stations were set as the 111th day (Dawa), 101th day (Liaozhong), 111th day (Kaiyuan), 121th day (Huanren), 116th day (Donggang) of the year. The settings of other management practices were the same with those for the field experiments (*Table 2*). The simulation continued until plant-death or the physiological mature-stage.

http://www.aloki.hu ● ISSN 1589 1623 (Print) ● ISSN1785 0037 (Online)
DOI: http://dx.doi.org/10.15666/aeer/2001_633651

Results

Calibration and validation of ORYZA (v3)

Determination of model parameters

The life cycle of the rice crop can be divided into four main phenological phases: the basic vegetative phase (BVP), photoperiod-sensitive phase (PSP), panicle formation phase (PFP), and grain-filling phase (GFP). The corresponding development-rate constants are development-rate in the juvenile phase (DVRJ), development-rate in photoperiod-sensitive phase (DVRI), development-rate in panicle development (DVRP), development-rate in the reproductive phase (DVRR). Adjusted model development parameters were listed in *Table 3*. *Table 4* showed the distribution of assimilation distribution coefficients and specific leaf-area parameters describing that the total daily dry-matter increment was partitioned to the various plant organ groups according to fractions which were a function of the development stage (Bouman and Laar, 2001). It was reflecting a rather high degree of regional specificity.

Table 3. *Corrected values of rice development rate in five test sites in Liaoning Province*

Development stage	Huanren Shendao 529	Donggang Shendao 505	Liaoning Beijing 1	Kaiyuan Tiejing 7	Dawa Yanfeng 47
DVRJ	0.0007932	0.0008890	0.0008969	0.0007960	0.0008860
DVRI	0.0008976	0.0008076	0.0007696	0.0008976	0.0007576
DVRP	0.0004741	0.0005630	0.0008544	0.0005990	0.0005420
DVRR	0.0019309	0.0016590	0.0019500	0.0016710	0.0013030

Calibration and validation of the model

The comparison of simulated and observed "key phenology days after transplantation" was showed in *Table 5*. The relative errors between the simulated value and measured value were 0-3 d for the flowering stage, and the average simulation error was about 2 d. The relative simulation error for the mature period was 0-5 d, and the average simulation error was about 2.5 d. Furthermore, according to the linear regression analysis, the coefficient of determination (R^2) was between 0.96 to 0.98 (*Table 6*). Thus, the measured values of the growth period showed a good agreement with the simulated values.

Leaf area index (LAI) is widely used to measure the growth of plants. Graphical comparisons of simulated and measured LAI over time were provided in *Figure 2 (a2-e2)*. Although we observed LAI variation in different areas, there was a satisfactory agreement between simulated and measured LAIs. The root mean square error and R^2 were 9% and 0.93, respectively, and there was no significance by a t-test. The testing of the model indicated that the model could well simulate the change in the dynamics of LAI.

In the calibration stage of 2017 (I), the simulated values of above-ground biomass revealed a statistically acceptable level of agreement with their observed values (*Figure 2 (a1-e1)*). The statistical analysis result showed that there was no significant difference between measured and observed above-ground biomass values (p=0.37 to 0.50, t-test), linear regression coefficients ranging from 0.79 to 0.96, and that the intercept was greater than zero possibly due to the higher estimation of rice growth by

http://www.aloki.hu ● ISSN 1589 1623 (Print) ● ISSN1785 0037 (Online)
DOI: http://dx.doi.org/10.15666/aeer/2001_633651

the model in the early growth stage. The normalized root mean square errors (NRMSE) of WST, WLVG, WSO were 10%, 24%, and 12%, respectively. Generally, in comparison with the 5 experiment sites observed in 2019 (Ⅱ), the model simulation was well performed. As shown in *Table 5*, the results of the t-test were ranged from 0.44 to 0.48 (no significance difference), the linear regression coefficient αwas close to 1, and the regression equation was significant (R^2 was 0.95 to 0.96). Both the simulated and measured above-ground biomass errors were under a reasonable range, which proved that the model was performing well.

Table 4. *Corrected values of assimilation distribution coefficient and specific leaf area parameters in five test sites in Liaoning Province*

Location	Assimilation coefficient				Specific leaf area	
	DVS	FSTTB	FLVTB	FSOTB	DVS	SLA
Huanren	0.00	0.60	0.40	0.00	0.16	0.0055
	0.50	0.60	0.40	0.00	0.33	0.0040
	0.75	0.85	0.05	0.10	0.65	0.0028
	1.00	0.11	0.00	0.89	0.79	0.0025
	1.20	0.00	0.00	1.00	2.10	0.0025
Donggang	0.00	0.31	0.69	0.00	0.16	0.0036
	0.50	0.33	0.67	0.00	0.33	0.0035
	0.75	0.55	0.15	0.3	0.65	0.0033
	1.00	0.02	0.00	0.98	0.79	0.0032
	1.20	0.00	0.00	1.00	2.10	0.0024
Liaozhong	0.00	0.42	0.58	0.00	0.16	0.0054
	0.50	0.43	0.57	0.00	0.33	0.0047
	0.75	0.65	0.25	0.10	0.65	0.0038
	1.00	0.085	0.00	0.915	0.79	0.0038
	1.20	0.00	0.00	1.00	2.10	0.0026
Kaiyuan	0.00	0.31	0.69	0.00	0.16	0.0040
	0.50	0.33	0.67	0.00	0.33	0.0035
	0.75	0.55	0.15	0.30	0.65	0.0033
	1.00	0.02	0.00	0.98	0.79	0.0032
	1.20	0.00	0.00	1.00	2.10	0.0024
Dawa	0.00	0.62	0.38	0.00	0.16	0.0045
	0.50	0.62	0.38	0.00	0.33	0.0030
	0.75	0.85	0.05	0.10	0.65	0.0026
	1.00	0.11	0.00	0.89	0.79	0.0026
	1.20	0.00	0.00	1.00	2.10	0.0023

NOTE: Table of the fraction of shoot dry matter partitioned to the leaves (FLVTB), Table of the fraction of shoot dry matter partitioned to the stems (FSTTB), Table of the fraction of shoot dry matter partitioned to the panicles (FSOTB). Emergence stage (DVS = 0.00), panicle initiation stage (DVS = 0.65), flowering stage (DVS = 1.00), and physiological maturity stage (DVS = 2.00)

The simulated and measured results of yield were illustrated in *Figure 3* with a great agreement. In the calibration stage (Ⅰ), the resulting values were distributed around 1:1 lined (b). According to the statistical analysis (*Table 6*), the linear regression coefficients α was 1.08 (proximity near one), the intercept β of the linear regression through the data was -806, which indicated that the model underestimated the yield of

http://www.aloki.hu ● ISSN 1589 1623 (Print) ● ISSN1785 0037 (Online)
DOI: http://dx.doi.org/10.15666/aeer/2001_633651

rice. In the calibration stage (Ⅱ), the points got much closer to the 1:1 line distribution (a). And the model had a higher coefficient of determination (R^2) and NRMSE was 4%. In addition, there were no significant differences as determined by Student's t-test (*Table 7*). These values were considered to be within acceptable limits.

Table 5. *Comparison between simulated and measured values of the key phenology days*

Location	Flowering				Maturity				Flowering		Maturity	
	Simulated value		Observed value		Simulated value		Observed value		Difference between simulation and observation			
	2017	2018	2017	2018	2017	2018	2017	2018	2017	2018	2017	2018
Huanren	78	77	76	75	128	125	129	127	2	2	1	2
Donggang	76	78	75	75	148	146	145	144	1	3	3	2
Liaozhong	90	88	91	90	146	146	148	149	1	2	2	3
Kaiyuan	77	76	78	77	131	130	133	133	1	1	2	3
Dawa	80	78	78	75	150	152	155	156	2	3	5	4

Table 6. *The statistical test results on the calibration data set (Ⅰ), including LAI, biomass, and yield*

Year	Crop variable	N	X_{obs}	*SD Xobs*	X_{sim}	*SD Xsim*	P(t*)	a	b	R^2	RMSE	RMSE (%)
											absolute	normalized
2017	The key phenology days (d)	10	110.4	32.78	110.8	33.94	0.49	0.96	3.59	0.98	1.8	1.62
	Biomass of green leaves (kg ha^{-1})	16	1058	2095	2220	1165	0.37	0.810	555	0.79	528	24
	Biomass of stems (kg ha^{-1})	16	4429	2631	4627	2638	0.42	0.970	-136	0.96	446	10
	Biomass of panicles (kg ha^{-1})	16	3972	4195	4086	4241	0.47	0.940	-43	0.95	477	12
	Leaf Area Index (-)	16	3.33	0.77	4.96	2.56	0.45	0.910	-0.55	0.93	0.49	9
	Yield (kg ha^{-1})	20	8914	2317	8980	2079	0.46	1.080	-806	0.94	400	4
2018	The key phenology days(d)	10	109.6	32.92	110.1	34.6	0.49	0.95	5.04	0.97	2.43	2.2
	Biomass of green leaves (kg ha^{-1})	16	2249	891	2284	891	0.46	1.040	-124	0.88	75	9
	Biomass of stems (kg ha^{-1})	16	7286	2079	7288	2152	0.50	0.960	268	0.96	104	2
	Biomass of panicles (kg ha^{-1})	16	3885	2834	4939	3858	0.44	0.960	16	0.94	69	4
	Leaf Area Index (-)	16	5.43	2.22	5.39	2.65	0.48	0.805	1.10	0.93	0.48	9
	Yield (kg ha^{-1})	20	8358	2675	8504	2559	0.43	1.020	-337	0.96	565	7

http://www.aloki.hu ● ISSN 1589 1623 (Print) ● ISSN1785 0037 (Online)
DOI: http://dx.doi.org/10.15666/aeer/2001_633651

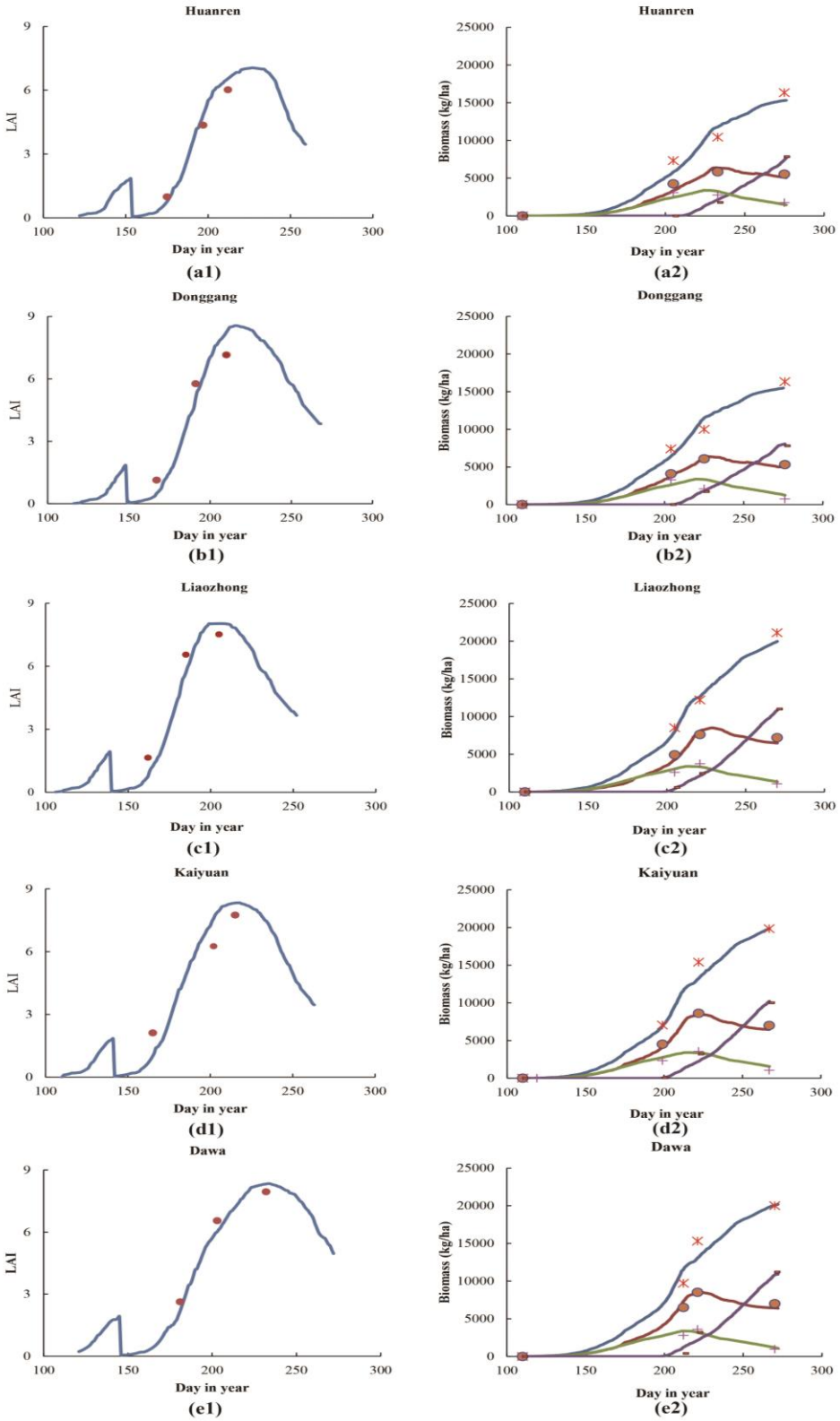

Figure 2. *Simulated (lines) and measured biomass of the whole crop (Ж), green leaves (+), stems (●), and panicles (−), and leaf area index (LAI) of rice in Huanren (a), Donggang (b), Liaozhong (c), Kaiyuan (d), Dawa (e), farmers' yield level N applied in 2017(calibration data set)*

http://www.aloki.hu ● ISSN 1589 1623 (Print) ● ISSN1785 0037 (Online)
DOI: http://dx.doi.org/10.15666/aeer/2001_633651

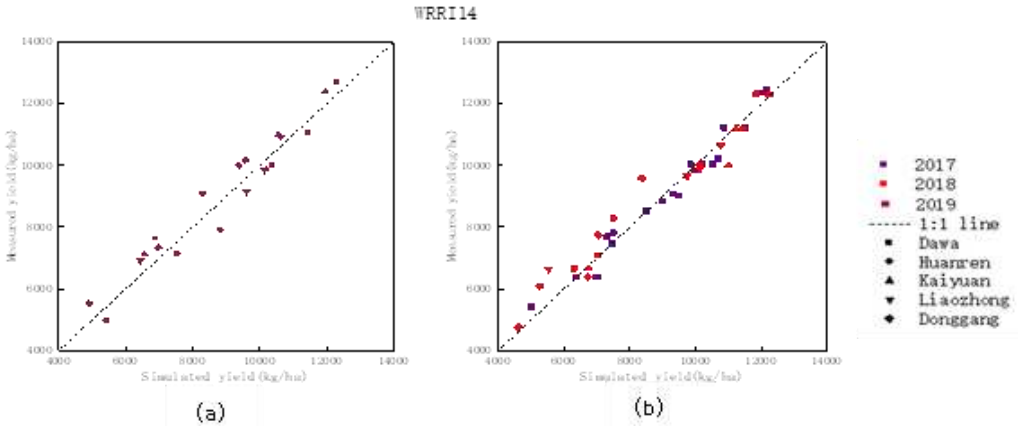

Figure 3. *Comparison between simulated and measured values of grain yield in rice at the regional scale using the ORYZA (v3) models. Subplots (a) and (b) represent the validation stage and the calibration stage value, respectively*

Table 7. *The statistical test results on the validation dataset (Ⅱ), including LAI, biomass, and yield*

Year	Crop variable	N	X_{obs}	*SD Xobs*	X_{sim}	*SD Xsim*	P(t*)	a	b	R^2	RMSE	RMSE (%)
											absolute	normalized
2019	The key phenology days(d)	10	108.9	33.61	110.1	34.6	0.47	0.97	2.34	0.96	3.21	2.92
	Biomass of green leaves (kg ha^{-1})	16	1907	1626	1961	1691	0.44	0.930	61	0.96	349	18
	Biomass of stems (kg ha^{-1})	16	5422	4213	5470	4245	0.48	0.950	91	0.96	798	15
	Biomass of panicles (kg ha^{-1})	16	1926	1496	1969	1546	0.47	0.930	69	0.95	244	12
	Leaf Area Index (-)	16	5.49	2.46	5.39	2.57	0.46	0.890	0.57	0.90	0.49	9
	Yield (kg ha^{-1})	20	8514	2868	8999	2110	0.45	1.010	-729	0.95	328	4

Scenario analyses

The calibrated and validated ORYZA (v3) model was applied to predict growth and production in rice, using weather data from 1981 to 2015. The cumulative probability distribution of grain-yield in five rice-growing areas under different N fertilizer management were shown in *Figure 4 (a-d)*. ORYZA (v3) simulated similar trend of grain-yields trends in different rice-growing areas showing that higher grain-yields with increasing N fertilization as Ysh>Yhh>Yfp>Yck. Among compared growing-areas, the yield differences across years were larger with a high N rate. The lowest yield was obtained at CL2 under the Yck level, and the median (with 50% probability of exceedance) of simulated grain yield was 4500 kg ha^{-1}. In addition, in the CL1 area which lacked thermal resources the simulated data had a lower value with Yfp to Ysh levels. From the Yfp to Ysh level, the median (with 50% probability of exceedance) of

http://www.aloki.hu ● ISSN 1589 1623 (Print) ● ISSN1785 0037 (Online)
DOI: http://dx.doi.org/10.15666/aeer/2001_633651

simulated grain yields were 6500 kg ha^{-1}, 7500 kg ha^{-1}, 8750 kg ha^{-1}, respectively. On the contrary, in CL5 where the region of adequate thermal resources, all four yield levels were expressed at higher values. From the Yck to the Ysh level, the median of simulated grain yield was 6700 kg ha^{-1}, 9600 kg ha^{-1}, 10500 kg ha^{-1}, 11700 kg ha^{-1}, respectively. The difference in simulated yields in different areas over the years was mainly attributed by differences in temperature and solar radiation, and high N rates enhanced the variation.

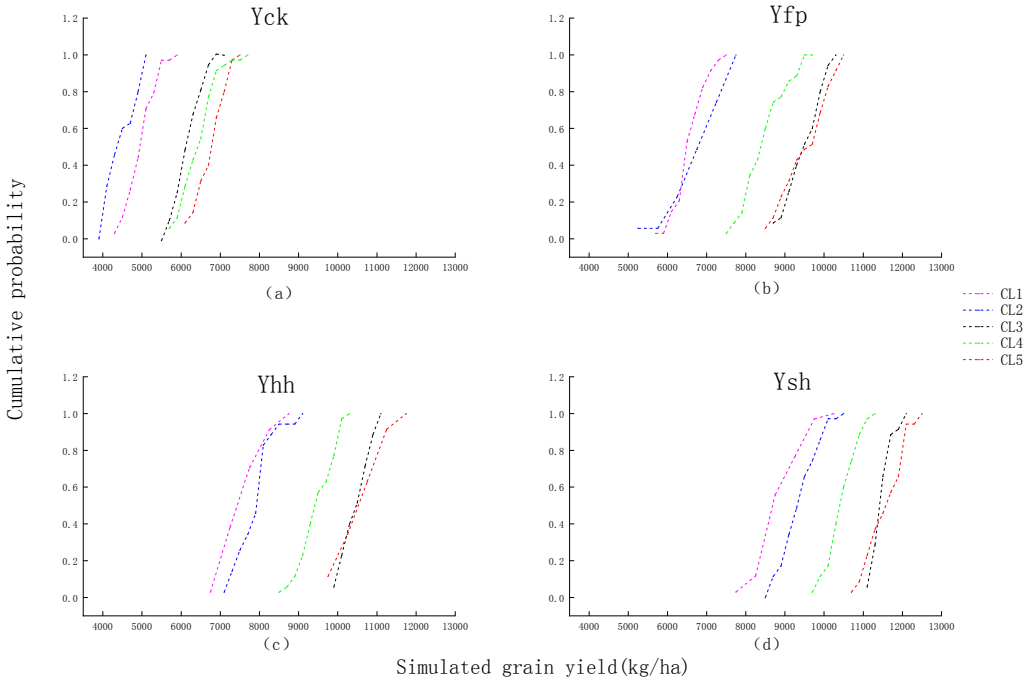

Figure 4. *Cumulative probability distribution curves of simulated grain yield from 1981 to 2015 under four N application*

Figure 5 (a-e) showed the detailed changes of simulated grain yield from 1981 to 2015. Spatial distribution characteristics could be obviously identified in different regions. The average simulated grain-yield over 35 years under four N fertilizers application were also exhibited in *Figure 5 (f)*. The yields at four levels in CL1 and CL2 regions were generally lower than those in CL3-CL5 regions. However, regardless of the regions, N significantly increased the grain-yields. From the N-level perspective, different fertilizer levels showed different influences on the rice yield. From the *Figure 5* that, the increase of yield was significant from Yck to Yfp with a lower N level. The increase of yield was also significant in CL3 and CL5 regions but relatively small in CL1 region. For Yhh and Ysh levels, an increasing trend in yield was identified with increasing N applied. As N fertilizer continued increasing, the increase of yield trend had obviously slowed down which was indicated by the slope of the increase. With high N levels, the grain-yield increase in the CL1 region was large while that in the CL4 regions were relatively small. The grain-yield increased from Yhh to Ysh in CL1 to CL5 were 747 kg ha^{-1}, 795 kg ha^{-1}, 705 kg ha^{-1}, 252 kg ha^{-1}, 643 kg ha^{-1}, respectively. Therefore, scenario analyses suggested that N fertilization posted great effects on the rice yield, especially with the low N level. Also the response of rice yield

http://www.aloki.hu ● ISSN 1589 1623 (Print) ● ISSN1785 0037 (Online)
DOI: http://dx.doi.org/10.15666/aeer/2001_633651

to N application declined with an increase in the N application rate to the level of Yhh. The five regions showed significant differences in rice yield and the application of N fertilizer increased the regional differences.

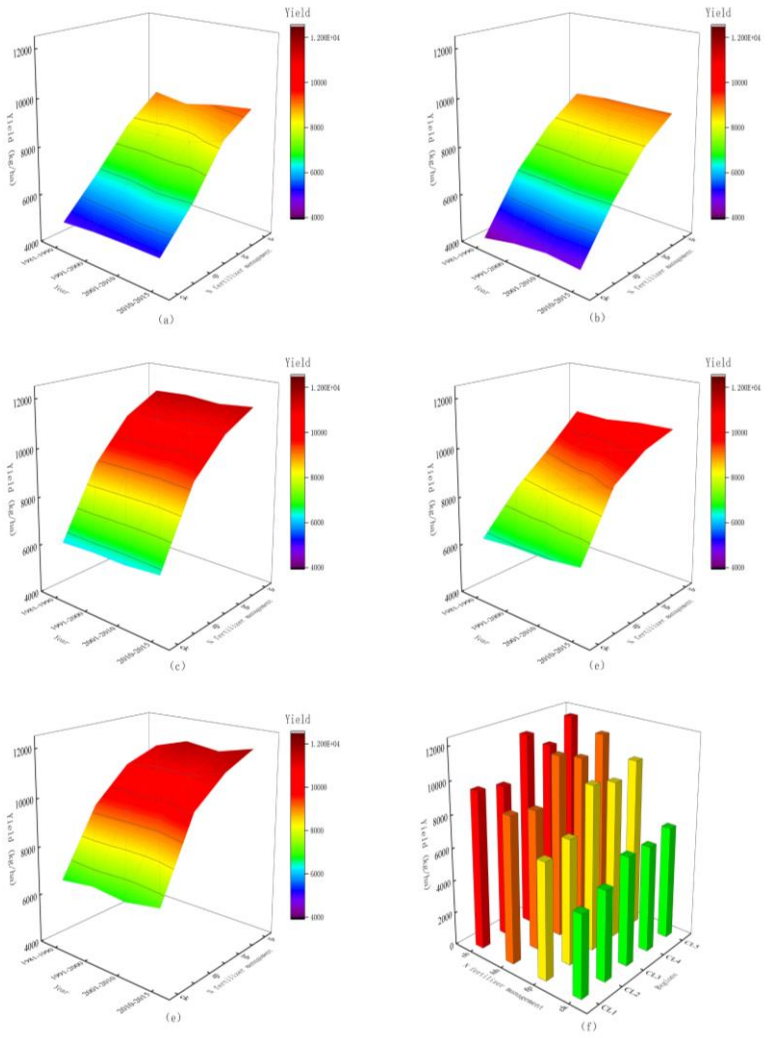

Figure 5. *Simulated yield change (1981-2015) in different levels for five regions, respectively (a–e), meanwhile, shows the average simulated yield in different regions of 35 years under four N fertilizer management (f)*

Discussion

In this study, we integrated examined field test data to study localized and regionalized of the ORYZA (v3) model and obtained the parameters of growth and development in different regions in Liaoning province, which were clearly distinguished from its cultivar parameters (IR72). The model evaluation was an important procedure before the model application. By comparing with the experimental data of the key phenology days in five regions, it was verified that the error of simulation data was less than 5 d. Additionally, the value passed the test of significance, which also proved the rationality of the model. The statistical parameters and scatter diagrams showed a relatively close agreement between measured and simulated biomass in the calibration

http://www.aloki.hu ● ISSN 1589 1623 (Print) ● ISSN1785 0037 (Online)
DOI: http://dx.doi.org/10.15666/aeer/2001_633651

data set (Ⅰ) and validation data set (Ⅱ). The other parameter was NRMSE in which the predicted value was relatively deviated from the real value. The lower value of NRMSE indicated a better precision and reliability of the simulation-performance, while a higher NRMSE value indicated a poor performance (Confalonieri et al., 2016). The NRMSE of WLVG, WST, and WSO in 2017-2019 were 9%-24%, 2%-15%, and 4%-12%, respectively. The simulation results also showed that the simulated values of WSO and WST performed better than the value of WLVG, and an acceptable coefficient of determination (R^2) values was obtained in all cases (R^2>0.9). Besides, simulated grain-yields were also in agreement with observation from five regions in Liaoning province. Its R^2 ranged from 0.95 to 0.96 and the α was close to 1. Nevertheless, for simulated LAI, the effect was not better than other indexes, which was consistent with previous studies (Bouman and Laar, 2004; Li et al., 2017). This might result from the calculation method of the model which calculates leaf area (LA) with a specific leaf area (SLA). This calculation method involved some disadvantages, including the lack of mechanistic explanations of the environmental-factors and management-measures influences, which could lead to certain errors between the simulated and the measured values. In general, these simulation results were in good qualitative agreement with experimental observations in Liaoning province. It also provided a basis for further applications of the model to resource-utilization analysis and climate-change-impact researches.

Scenario analyses indicated that N fertilizer application method could significantly influence grain-yields and the N fertilizer requirement varied with the yield level. The yield increased with an increase in the amount of N fertilizer applied as shown by Ysh>Yhh>Yfp>Yck. No matter in which area, the changes in Yfp to Yhh were all greater than the changes in Yhh to Ysh since the extent of the grain-yield increase decreased as the N fertilizer increased. This finding was consistent with results from previous researches (Wang et al., 2010; York et al., 2016; Wang, 2017). Several studies have shown that the reason that fertilizer usage does not guarantee a higher yield is because of declining returns (Shen et al., 1994; Liu et al., 2000; Chen et al., 2011), which is also consistent with our conclusion in this paper. Excessive fertilization not only leads to a decrease in N utilization-efficiency but also causes a series of adverse environmental reactions (Mao et al., 2005). However, it was found that N fertilization showed different influences on grain-yields in different growing-zones. With the N-fertilizer increase, the grain-yield increased significantly in the central plain, northern plain and Liaohe Delta rice planting area. This was because of the good thermal resource and sufficient solar radiation in the growing season in these rice planting regions. The improvement of rice grain-yield and N use-efficiency depended on the good weather conditions. At higher N fertilizer levels, lower gains were observed in the eastern hilly area and the coastal plain. The eastern hilly area is a cold region with fewer heat resources during the growing season, where the availability of N fertilizers is frequently limiting. On the other hand, although there are enough heat resources, there are problems such as excessive precipitation and insufficient sunshine in the coastal plain. These issues in a way would be prone to cause lodging, plant diseases and insect pests with higher N fertilizer level. So, only by jointing efforts of breeding new resistant cultivars, changing the irrigation patterns, and reducing fertilizer N input we could improve the yield in these coastal plains (Chen et al., 2019). Nitrogen use-efficiency has not been calculated in this paper, and future research needs to carry out correlation analysis in this aspect to better study the relationship between nitrogen fertilizer and yield.

http://www.aloki.hu ● ISSN 1589 1623 (Print) ● ISSN1785 0037 (Online)
DOI: http://dx.doi.org/10.15666/aeer/2001_633651

On the regional-scale level, our simulation results fitted well with the experimental results, which indicated that the model was suitable for Liaoning province. However, this paper did not take into account of actual spatial variability of the soil and the rice varieties. Using the same parameter datasets in each region would make the data simulation less certain. Besides, the uncertainties of human factors, the randomness of data collection and regional heterogeneity of the initial conditions could lead to greater uncertainty of the simulation results. This realization required us to take careful management measures and control variables in the field experiment in order to ensure the consistency of the unified treatments and reduce the influence of human factors. We should also take more extreme weather events on the growth and yield into consideration, such as high temperature and drought. To circumvent these issues, the integration monitoring data with remote-sensing and climate-change models could further help to reduce the model uncertainties.

Conclusion

In this study, the ORYZA (v3) model was regionalized for Liaoning province. Both graphical and statistical tools were used to test for the model. It was indicated that the performance of the ORYZA (v3) model was overall satisfactory in simulating grain yield and biomass dynamics for rice in Liaoning province. However, the simulation of LAI was sub-optimal, which still needed to be improved in the future research. The scenario analyses using historical weather data from the last 35 years suggested that the N-application rates had greater impacts on rice yield. For Yck to Yfp, the grain yields were increased by 2061 kg ha^{-1}, 2118 kg ha^{-1}, 3439 kg ha^{-1}, 3168 kg ha^{-1}, 3480 kg ha^{-1} in CL1-CL5, respectively. However, the increased amplitude declined with the application of N fertilizer. In addition, different effects on grain-yield by N fertilizer were clearly associated with the regional characteristics. Areas with obvious increasing yield-trends were areas under better conditions of thermal resources and sunshine. Application of N fertilizer is crucial to obtaining appropriate crop yields without unnecessary expenses and waste of resources. Reasonable nitrogen application rate is preferable from the environmental and economic viewpoints. Current agriculture requires further research on how to make nitrogen fertilizer input more reasonable to achieve optimal crop management. This study can provide more valuable insights into future N fertilizer management analysis.

Acknowledgments. This study was supported by the National Key Research and Development Project of China (2016YFD0300104), Scientific research project of Liaoning Provincial Department of Education (LSNJC201905) and the National Natural Science Foundation of China (31771673).

REFERENCES

[1] Angstrom, A. (1924): Solar and terrestrial radiation. Report to the international commission for solar research on actinometric investigations of solar and atmospheric radiation. – Quarterly Journal of the Royal Meteorological Society 50(210): 121-126.
[2] Arora, V. K. (2005): Application of a rice growth and water balance model in an irrigated semi-arid subtropical environment. – Agricultural Water Management 83: 51-57.

http://www.aloki.hu ● ISSN 1589 1623 (Print) ● ISSN1785 0037 (Online)
DOI: http://dx.doi.org/10.15666/aeer/2001_633651

[3] Belder, P., Bouman, B. A. M., Cabangon, R., Lu, G., Quilang, E. J. P., Li, Y., Spiertz, J. H. J., Tuong, T. P. (2004): Effect of water-saving irrigation on rice yield and water use in typical lowland conditions in Asia. – Agricultural Water Management 65: 193-210.
[4] Black, J. N., Bonython, C. W., Prescott, J. A. (1954): Solar radiation and the duration of sunshine. – Quarterly Journal of the Royal Meteorological Society 80: 231-235.
[5] Bouman, M., van Laar, H. H. (2001): ORYZA2000: modeling lowland rice. – Los Baños: International Rice Research Institute, & Wageningen: Wageningen University & Research Centre, 235 Pp + Cd-rom.
[6] Bouman, B. A. M., van Laar, H. H. (2004): Description and evaluation of the rice growth model ORYZA2000 under nitrogen-limited conditions. – Agricultural Systems 87(3): 249-273.
[7] Buresh, R., Witt, C. (2002): Challenge and Opportunity in Improving Fertilizer-nitrogen Use Efficiency of Irrigated Rice in China. – Agricultural Sciences in China 7: 67-76.
[8] Cao, H. X., Zhang, C. L., Li, G. M., Zhang, B. J., Zhao, S. L., Wang, B. Q., Jin, Z. Q. (2006): Researches of simulation models of rape (*Brassica napus* L.) growth and development. – Acta Agronomica Sinica 32: 1530-1536.
[9] Chen, J., Huang, Y., Tang, Y. (2011): Quantifying economically and ecologically optimum nitrogen rates for rice production in south-eastern China. – Agriculture Ecosystems & Environment 142: 195-204.
[10] Chen, W., Liu, L., Liu, G. Y., Tai, E., Jin, F., Jia, G. (2019): Experimental study on alternate dry-wet irrigation of rice in middle area of Liaoning Province. – Hydro Science and Cold Zone Engineering 2: 6-11.
[11] Cheng, W., Lv, J., Xie, J., Yu, J., Li, J., Zhang, J., Tang, C., Niu, Bakpa, E. (2021): Effect of slow-release fertilizer on soil fertility and growth and quality of wintering Chinese chives (Allium tuberm Rottler ex Spreng.) in greenhouses. – Scientific reports 11 (1): 8070.
[12] Confalonieri, R., Bregaglio, S., Acutis, M. (2016): Quantifying uncertainty in crop model predictions due to the uncertainty in the observations used for calibration. – Ecological Modelling 328: 72-77.
[13] Evers, J. B., Vos, J., Fournier, C., Andrieu, B., Chelle, M., Struik, P. C. (2005): Functional-Structural Plant Modelling ‖ Towards a Generic Architectural Model of Tillering in Gramineae, as Exemplified by Spring Wheat (*Triticum aestivum* L.). – New Phytologist 166: 801-812.
[14] Fan, X. R., Tang, Z., Tan, Y. W., Zhang, Y., Luo, B. B., Yang, M., Lian, X. M., Shen, Q. R., Miller, A. J., Xu, G. H. (2016): Overexpression of a pH-sensitive nitrate transporter in rice increases crop yields. – Proceedings of the National Academy of Sciences 113: 7118-7123.
[15] Feng, L. P., Bouman, B. A. M., Tuong, T. P., Cabangon, R. J., Li, Y. L., Lu, G. A., Feng, Y. H. (2007): Exploring options to grow rice using less water in northern China using a modelling approach: I. Field experiments and model evaluation. – Agricultural Water Management 88: 1-13.
[16] Gaiser, T., de Barros, I., Sereke, F., Lange, F-M. (2010): Validation and reliability of the EPIC model to simulate maize production in small-holder farming systems in tropical sub-humid West Africa and semi-arid Brazil. – Agriculture, Ecosystems & Environment 135(4): 318-327.
[17] Guo, E. J., Yang, X. G., Wang, X. Y., Zhang, T. Y., Huang, W. H., Liu, Z. Q., Li, T. (2017): Spatial-Temporal Distribution of Double Cropping Rice's Yieldr Gap in Hunan Province. – Scientia Agricultura Sinica 50: 399-418.
[18] Kim, J., Sang, W., Shin, P., Cho, H., Kim, K. S. (2015): Evaluation of regional climate scenario data for impact assessment of climate change on rice productivity in Korea. – Journal of Crop Science Biotechnology 18: 257-264.

http://www.aloki.hu ● ISSN 1589 1623 (Print) ● ISSN1785 0037 (Online)
DOI: http://dx.doi.org/10.15666/aeer/2001_633651

[19] Kropff, M. J., van Laar, H. H., Matthews, R. B. (1994): ORYZA1: An ecophysiological model for irrigated rice production. – DLO-Research Institute for Agrobiology and Soil Fertility, Wageningen. ISBN 9789073384231. https://edepot.wur.nl/297737
[20] Li, T., Raman, A. K., Marcaida, M., Kumar, A., Angeles, O., Radanielson, A. M. (2013): Simulation of genotype performances across a larger number of environments for rice breeding using ORYZA2000. – Field Crops Research 149: 312-321.
[21] Li, T., Jauhar, A., Manuel, M., Olivyn, A., Johann, F. N., Edrian, R. J., Emmali, M., Edilberto, R. A., Xu, J., Li, Z. (2016): Combining Limited Multiple Environment Trials Data with Crop Modeling to Identify Widely Adaptable Rice Varieties. – Plos One 11: e0164456.
[22] Li, T., Angeles, O., Marcaida, M., Manalo, E., Manalili, M. P., Radanielson, A., Mohanty, S. (2017): From ORYZA2000 to ORYZA (v3): An improved simulation model for rice in drought and nitrogen-deficient environments. – Agricultural & Forest Meteorology 237-238: 246-256.
[23] Ling, X., Zhang, T., Deng, N., Yuan, S., Huang, J. (2019): Modelling rice growth and grain yield in rice ratooning production system. – Field Crops Research 241: 107574.
[24] Liu, J. L., Song, J. J., Li, F. L., Liu, S. Q. (2000): Effects of Nitrogen application amount on soil fertility and plant nutrient content and yield of paddy rice. – Agriculture and Technology 4: 8-12.
[25] Liu, H. L., Yang, J. Y., Drury, C. F., Reynolds, W. D., Tan, C. S., Bai, Y. L., He, P., Jin, J. (2011): Using the DSSAT-CERES-Maize model to simulate crop yield and nitrogen cycling in fields under long-term continuous maize production. – Nutrient Cycling in Agroecosystems 89: 313-328.
[26] Mae, T. (1997): Physiological nitrogen efficiency in rice: Nitrogen utilization, photosynthesis, and yield potential. – Plant Soil 196: 201-210.
[27] Mao, X. Y., Sun, K. J., Wang, D. H., Liao, Z. W. (2005): Controlled-release fertilizer (CRF): a green fertilizer for controlling non-point contamination in agriculture. – Journal of environmental sciences (China) 17: 181-184.
[28] National Bureau of Statistics of China (2016): China Statistical Yearbook. – China Statistics Press, Beijing.
[29] Peng, S., Buresh, R. J., Huang, J., Zhong, X. (2010): Improving nitrogen fertilization in rice by sitespecific N management. A review. – Agronomy for Sustainable Development 30: 649-656.
[30] Rani, Y. S., Jayasree, G., Sesha Sai, M. V. R., Reddy, M. D. (2011): Impact of Climate Change on Rice Production in Nalgonda District, Andhra Pradesh using ORYZA 2000 Model. – Journal of Rice Research 4: 21-26.
[31] Roelcke, M., Yong, H., Schleef, K. H., Zhu, J. G., Gang, L., Cai, Z. C., Richter, J. (2004): Recent Trends and Recommendations for Nitrogen Fertilization in Intensive Agriculture in Eastern China. – Pedosphere 14: 449-460.
[32] Shen, Y. Z., Zhang, Z. L., Qian, X. Q., Wu, J. Y., Dong, K. J., Liu, B. X., Jiang, S. Q., Li, J. (1994): Nitrogen nutrition characteristics and fertilization in high yield rice. – Chinese Journal of Soil Science 2: 78-80.
[33] Soundharajan, B., Sudheer, K. P. (2013): Sensitivity analysis and auto-calibration of ORYZA2000 using simulation-optimization framework. – Paddy and Water Environment 11: 59-71.
[34] Stockle, C. O., Martin, S. A., Campbell, G. S. (1994): CropSyst, a cropping systems simulation model: water/nitrogen budgets and crop yield. – Agricultural Systems 46: 335-359.
[35] Tilman, D., Balzer, C., Hill, J., Befort, B. L. (2011): Global food demand and the sustainable intensification of agriculture. – Proceedings of the National Academy of ences of the United States of America 108: 20260-20264.
[36] Wang, Y. (2017): Analysis of rice yield and fertilizer utilization rate under conventional fertilization in Liaoning Province. – China Agricultural Technology Extension 33: 36-39.

http://www.aloki.hu ● ISSN 1589 1623 (Print) ● ISSN1785 0037 (Online)
DOI: http://dx.doi.org/10.15666/aeer/2001_633651

[37] Wang, Y. H., Han, X. R., Wang, L., Yu, X. H. (2010): Study of Fertilizers' Effect on Rice and Function Models of Fertilizer Recommendation in the Panjin District of China. – Chinese Journal of Soil Science 41: 373-378.
[38] York, L. M., Silberbush, M., Lynch, J. P. (2016): Spatiotemporal variation of nitrate uptake kinetics within the maize (*Zea mays* L.) root system is associated with greater nitrate uptake and interactions with architectural phenes. – Journal of experimental botany 67(12): 3763-75.
[39] Yu, G. X., Sui, G. M., Peng, S. B., Hou, S. G., Chen, Y. (2009): Effects of site-specific nitrogen management techniques on rice growth and nitrogen utilization rate. – Liaoning Agricultural Sciences, 1-4.

http://www.aloki.hu ● ISSN 1589 1623 (Print) ● ISSN1785 0037 (Online)
DOI: http://dx.doi.org/10.15666/aeer/2001_633651

UNDERSTANDING SPATIAL DRIVERS OF DEFORESTATION IN THE LUKI BIOSPHERE RESERVE, DEMOCRATIC REPUBLIC OF CONGO

OPELELE, O. M.[1,2,3] – YU, Y.[1,2*] – FAN, W.[1,2*] – LUBALEGA, T.[4,5] – CHEN, C.[1,2] – KACHAKA, S. K.[3]

[1]*School of Forestry, Northeast Forestry University, Harbin 150040, Heilongjiang, P. R. China*

[2]*Key Laboratory of Sustainable Forest Ecosystem Management-Ministry of Education, School of Forestry, Northeast Forestry University, Harbin 150040, Heilongjiang, P. R. China*

[3]*Department of Natural Resources Management, Faculty of Agricultural Sciences, University of Kinshasa, 117 Kinshasa XI, Mont-Amba/Lemba, Democratic Republic of Congo*

[4]*Institut National pour l'Étude et la Recherche Agronomiques (INERA/Luki), Antenne de Gestion et Conservation des Ressources Naturelles, Province Kongo Central, Luki, Democratic Republic of Congo*

[5]*Université de Kikwit. Faculté des Sciences Agronomiques, Département de Phytotechnie, BP 76 Kikwit, Democratic Republic of Congo*

[*]*Corresponding authors*
e-mail: fanwy@163.com or yuying4458@163.com; phone: +861-394-605-5384

(Received 18th Aug 2021; accepted 23rd Nov 2021)

Abstract. Understanding factors that are driving land use/land cover change is one of the major steps that should be rationally addressed for the purpose of sustainable management of natural resources. The present study examines four spatial drivers affecting deforestation in the Luki Biosphere Reserve over the last three decades (1987-2020), where forest resources are prone to multiple human pressures compromising their sustainability. These are: distance from the nearest road; population density; elevation; and slope. Change detection analysis was performed on classified Landsat images to generate the Boolean map with two categories including forest change and no change. GIS and topographic data were used to compute spatial drivers of deforestation. Additionally, the logistic regression model was used to assess the effect of the spatial drivers on forest conversion, and determine the drivers that significantly influence forest conversion. The study results revealed a major change in the landscape that led to the loss of forest land, and gain in other land use classes. However, the regression model was statistically significant ($p < 0.01$), suggesting that all the spatial drivers (independent variables) were significantly related to forest conversion. Distance to roads and population density have been identified as the most significant spatial drivers of deforestation over the last three decades. However, although slope and elevation also significantly affected forest conversion, but when compared to two other variables, their effects were moderate. It has been noted that the impact of these spatial drivers was spatially related to socioeconomic and demographic aspects. This study provides valuable information that could benefit the managers, policy-makers, and local authorities in their decision-making processes, especially for the purpose of environmental monitoring.
Keywords: *logistic regression, spatial drivers, land use/ land cover change, Luki Biosphere Reserve, Democratic Republic of Congo*

Introduction

The concept of land cover is defined by the type of natural area on the land, while land use relates to the type of human activities carried out on the land or the current use of the land (Lambin, 2006; Rawat and Kumar, 2015; McConnett, 2015). Forest conversion has

http://www.aloki.hu ● ISSN 1589 1623 (Print) ● ISSN 1785 0037 (Online)
DOI: http://dx.doi.org/10.15666/aeer/2001_653670

become a global concern due to the major role of forest resources in not only providing several resources for survival of human population, but also in their role for the mitigation of the climate change effects. Land use change constitutes an important source of carbon emissions due to human activities (Henders et al., 2015; Li et al., 2017; Zhou et al., 2021); and can lead to natural ecosystem degradation (Foley et al., 2005; Moghadasi et al., 2017; Sharma et al., 2019), fragmentation of habitats (Sun and Southworth, 2013; Adhikari and Hansen, 2018; Diuk-Wasser et al., 2021; Opelele et al., 2021), and loss of wildlife corridors (Nandy et al., 2007; Sharma et al., 2018; Powers and Jets, 2019). Also, ecosystem services such as biodiversity maintenance, food production, and climate regulation can be significantly affected by land use and land cover change (Verburg and Overmars, 2009; González et al., 2012; Al Kafy et al., 2021; Opelele et al., 2021). Therefore, factors driving land use change should be fully examined to provide a good understanding of their effect in order to provide valuable information to decision-makers. The drivers of land use/land cover change are multidimensional and can be derived from different facets including socioeconomic factors, institutional factors, and human-environment systems (Geist and Lambin, 2001; Overmars and Verburg, 2005).

Several studies have been conducted to examine the effects of spatial drivers (i.e. proximity to town and roads, elevation, slope, population density, and rainfall) on land use/land cover change (Lambin et al., 2001; Sulieman, 2018; Maitima et al., 2010). These studies have provided the data necessary for improving our comprehension of factors that drive land use/land cover change, and for planning land use for sustainable development of local communities. However, studies regarding the effects of spatial drivers on land use/land cover change in the Luki Biosphere Reserve are yet to be conducted. Given the spatio-temporal dynamic nature of the drivers of land use/land cover change, it is crucial to further examine them to obtain more accurate information that can support the decision-making process.

Meanwhile, the expansion of human activities has negatively impacted land use/land cover in the Luki Biosphere Reserve and its surroundings for a long time. The land use/land cover change process in this reserve continues to reduce the extent or area of different natural ecosystems, including forest lands, hence impacting the related ecosystem services. Several studies have noted that the proliferation of villages around the Reserve, added to this the increase in the population, of which the majority depends on forest resources for their survival, are the main causes of deforestation and forest degradation in the Luki Biosphere Reserve (Doumenge, 1990; Pendje and Mbaya, 1992; Gata, 1997; Nyange, 2014). However, the spatial drivers of land use/land cover change in this region are poorly studied and less understood.

In this research, the distance from roads, elevation, slope, population density was considered as spatial drivers of land use change in the Luki biosphere reserve. In fact, the distance to roads indicates the accessibility to natural resources by road, and subsequently their utilization. In addition, population density determines the forest clearance rate to establish cropland, and the magnitude of usage of forest resources in terms of providing various forest products (Kamwi et al., 2015). In another way, slope and elevation are often key with regards to the potential of the land use. For instance, areas reserved for construction are preferably allocated on flat land with good traffic conditions and water supply, while steeper land is mostly occupied by forest lands (Olaya, 2009; Buckley, 2010). Qasim et al. (2013) reported that changes observed in the landscape are also caused by physical factors, including slope and altitude. According to the authors, the choice of land use activity may be determined by the slope and altitude of an area. For example,

http://www.aloki.hu ● ISSN 1589 1623 (Print) ● ISSN 1785 0037 (Online)
DOI: http://dx.doi.org/10.15666/aeer/2001_653670

agricultural areas are often allocated to the low elevation land because of the accessibility to the facility. With the recurrent change in socioeconomic, demographic, institutional and political conditions in the region, it could be evident to expect for certain changes in the spatial drivers. Despite the fact that the aforementioned drivers have been revealed to be significant in the process of land use change, their applicability in the current land use change process in the Luki biosphere reserve has not been proved yet, in order to support decision-making process.

In this context, the present study intended to examine how spatial drivers including, population density, distance from roads, slope, and elevation influenced deforestation in the Luki Biosphere Reserve during the last three decades, by using logistic regression techniques. In fact, the logistic regression model has been successfully used to evaluate land use changes and its related drivers (Loza, 2004; Siles, 2009; Arekhi, 2011; Mustafa et al., 2018; Wang et al., 2019; Buya et al., 2020). Thus, forest cover change was regarded as the dependent variable in the logistic regression and the distance from roads, elevation, slope, population density, were considered as explanatory variables. The findings of the present study will provide new understandings of spatial drivers associated with land use change in the Luki biosphere reserve, in order to support the establishment of sustainable land management strategies for the Luki biosphere reserve.

Materials and Methods

Study area

This study was conducted in the Luki Biosphere Reserve, the Democratic Republic of Congo (DRC) (*Figure 1*). According to Angoboy et al. (2019), Luki covers an area of about 33000 hectares. It was created in 1937 and was recognized by UNESCO as a Biosphere Reserve in 1979. The Luki Biosphere Reserve is located at the eastern boundary of the Mayombe forest, and remains a sample relic of the Mayombe vegetation (Lubini, 1997). The annual average rainfall ranges from 1150 mm to 1500 mm. The annual average temperature ranges between 25°C and 30°C (Lubalega et al., 2018). The region is located within a humid tropical climate Aw5 according to the Köppen classification (Peel et al., 2007). The soils are generally ferrallitic and acidic (Sénéchal et al., 1998). Additionally, these soils are characterized by a low content of cations. Presently, the Luki Reserve is conserved with the support of the DRC government institutions and other partners including the WWF. Nevertheless, the natural resources of the Luki Reserve are prone to tremendous anthropogenic pressures, mainly due to local population activities, such as slash-and-burn agriculture, wood energy, bush fires, fuelwood, illegal logging, etc. This compromises the sustainability of natural resources in the Reserve.

The *Figure 2* shows the temporal variation of temperature and precipitation over the last ten decades.

Land use/land cover classification

Landsat images and Digital Elevation Model were downloaded from google earth engine (https://code.earthengine.google.com) and United States Geological Survey (USGS) Earth Resources Observation Systems (EROS) Data Center (EDC) (http://glovis.usgs.gov). Road maps were downloaded from the OpenStreetMap website (https://www.openstreetmap.org/). Landsat images used in the present study are described in *Table 1*.

http://www.aloki.hu ● ISSN 1589 1623 (Print) ● ISSN 1785 0037 (Online)
DOI: http://dx.doi.org/10.15666/aeer/2001_653670

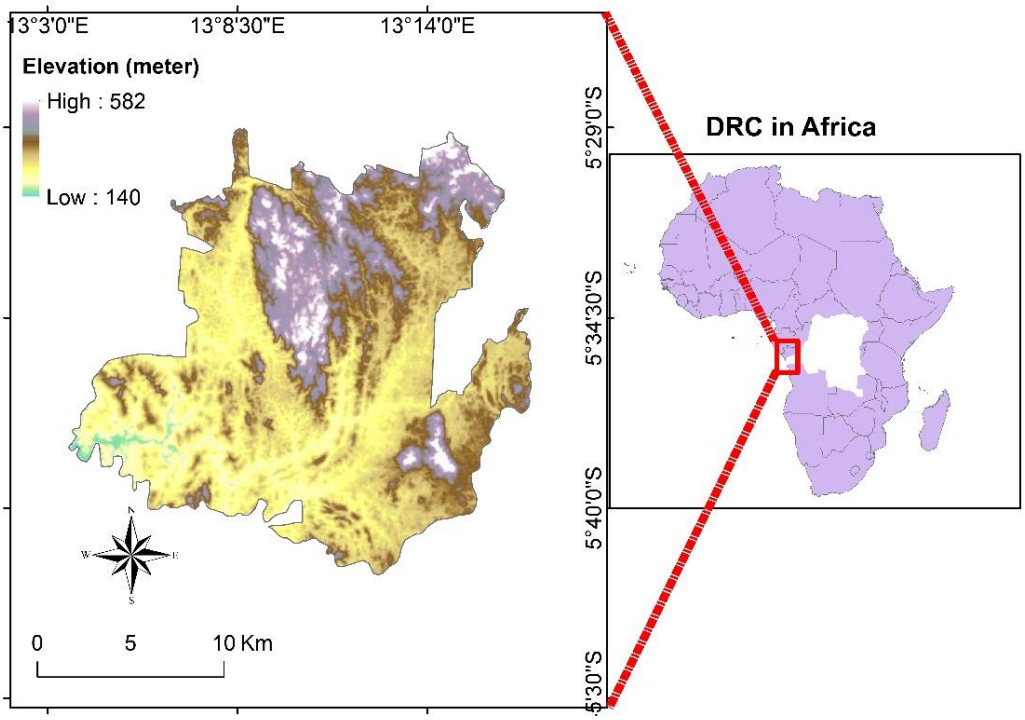

Figure 1. *Location of the Luki Biosphere Reserve*

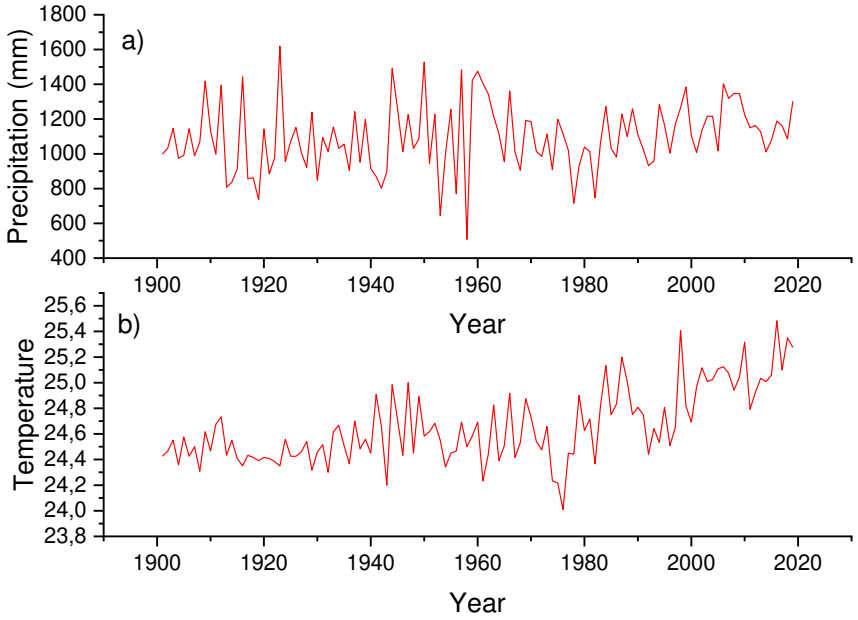

Figure 2. *Annual temperature (in degree Celsius) and precipitation variation, from the year 1901 to 2019 (Harris et al., 2020)*

We used the FLAASH method to perform radiometric and atmospheric correction for the Landsat images of the years 1987, 2002, and 2020. Then, the Luki's landscape was classified into different land use/land cover classes of which, forest land, complex of degraded and young secondary forest, fallow land and fields, savanna, and built-up area.

http://www.aloki.hu ● ISSN 1589 1623 (Print) ● ISSN 1785 0037 (Online)
DOI: http://dx.doi.org/10.15666/aeer/2001_653670

These land use/land cover classes were grouped into two categories including forest land that comprises the complex of degraded and young secondary forest and forest land. The second category was the non-forest land that comprises fallow land and fields, savanna, and built-up area. Field data were collected in 2020 for the purpose of creating the testing and training data for each land use/land cover class. Then the maximum likelihood algorithm was used to carry out the supervised classification on the two images. It has been reported that this algorithm provides better land use/land cover classification results (Vadrevu, 2013). Kappa statistics and overall accuracy were computed to evaluate the image classification accuracy (Congalton and Mead, 1983; Pijanowski et al., 2005; Keshtkar et al., 2017).

Table 1. *Description of Landsat data*

Data Type	Name	Pixel Size	Wavelength	Description	Year
Landsat 4 TM	B1	30 m	0.45–0.52 µm	Blue	1987
	B2	30 m	0.52–0.60 µm	Green	
	B3	30 m	0.63–0.69 µm	Red	
	B4	30 m	0.76–0.90 µm	Near infrared	
	B5	30 m	1.55–1.75 µm	Shortwave infrared 1	
	B6	30 m	10.40–12.50 µm	Thermal Infrared 1.	
	B7	30 m	2.08–2.35 µm	Shortwave infrared 2	
Landsat 8 OLI/TIRS	B1	30 m	0.43–0.45 µm	Coastal aerosol	2020
	B2	30 m	0.45–0.51 µm	Blue	
	B3	30 m	0.53–0.59 µm	Green	
	B4	30 m	0.64–0.67 µm	Red	
	B5	30 m	0.85–0.88 µm	Near infrared	
	B6	30 m	1.57–1.65 µm	Shortwave infrared 1	
	B7	30 m	2.11–2.29 µm	Shortwave infrared 2	
	B8	15 m	0.52–0.90 µm	Band 8 Panchromatic	
	B9	15 m	1.36–1.38 µm	Cirrus	
	B10	30 m	10.60–11.19 µm	Thermal infrared 1	
	B11	30 m	11.50–12.51 µm	Thermal infrared 2	

Spatial analysis

From the three land use/land cover maps produced for the years 1987, 2002 and 2020, a change map in each category (forest and non-forest land) was created using TerrSet software. Boolean maps (0=no change, 1=change) were then created for two periods (1987-2002 and 2002-2020), for the purpose of implementing the logistic regression model. The logistic regression model was used to map the probability of occurrence for forest lands to non-forest land. However, for this study, we used distance to roads, population density, elevation, and slope as independent variables (*Table 2*). Although these factors have been considered to drive land use change processes, there are still no studies that have examined the impact of these variables on the land use change in the Luki Biosphere Reserve. In this study, these factors were selected and used to perform logistic regression with each land use/land cover conversion being considered as dependent variable. The choice of independent variables depended on data availability. Also, these independent variables were selected because they represented the process believed to drive the land use/land cover change in the region.

http://www.aloki.hu ● ISSN 1589 1623 (Print) ● ISSN 1785 0037 (Online)
DOI: http://dx.doi.org/10.15666/aeer/2001_653670

Table 2. *Independent variables used in the logistic regression model*

Variable	Description	Sources
Population density	Population density in square km	Bas-fleuve district surveys
Distance to roads	Distance in (km) from a middle of a pixel to the nearest road	Field data and OpenStreetMap
Digital elevation model	The elevation value (in meter) for each pixel	USGS
Slope	The maximum rate of change in elevation from a given cell to its neighbors	

Roads vector data was converted into raster data, and the distance from roads map was created using the proximity tools in QGIS (version 2.18). The nearest distance was computed by evaluating the shortest distance between the random pixels and near roads. Additionally, the population density map was created through the interpolation tool using the IDW technique. Population data was collected during our survey in each village located within the Luki Biosphere Reserve. The slope map was computed from elevation data using spatial tool analysis in ArcGIS 10.1. The extract function in R software was used to extract all image attributes related to each of the land use/land cover conversion. Further steps were followed to map the predicted probabilities of occurrence and produce probability maps. These maps are important in highlighting the relationship between spatial distribution of land use/land cover and the spatial drivers. R (version 3.6.1 (2019-07-05)) and SPSS (version 20)) software were used to perform all analyses related to variable extraction and regression model.

Logistic regression implementation to assess spatial drivers of land use/land cover change

Here, the logistic regression was performed to measure the relationship between the derived spatial variables and LULC change outcome. Logistic regression is a powerful tool that can allow the simultaneous analysis of several explanatory variables, while avoiding the effect of confounding factors (Sperandei, 2014). The binary logistic regression was used since the outcome variable (forest change) had two categories (no change=0, change=1). The magnitude of strength between spatial drivers and forest conversion was measured by computing the odds ratio. A statistically significant association (p-value less than 0.05) between spatial drivers and the dependent variable was then considered. To avoid problems induced by multicollinearity in the estimation of regression coefficients, we computed Pearson's correlation to examine the correlation between the spatial variables. Finally, the Variance Inflation Factor (VIF) and tolerance (I/VIF) were computed to analyze the collinearity among the spatial drivers (Field, 2013). The workflow of the present research is illustrated in *Figure 3*. The basic logistic regression model can be presented as follows:

$$\text{Logit(P)} = \ln\left(\frac{P}{1-p}\right) = \beta_0 + \beta_1 x_1 + \beta_2 x_2 + \beta_3 x_3 + \beta_4 x_4 \qquad \text{(Eq.1)}$$

where β0 is the intercept, βi are the regression coefficients, and xi represents the set of independent variables.

http://www.aloki.hu ● ISSN 1589 1623 (Print) ● ISSN 1785 0037 (Online)
DOI: http://dx.doi.org/10.15666/aeer/2001_653670

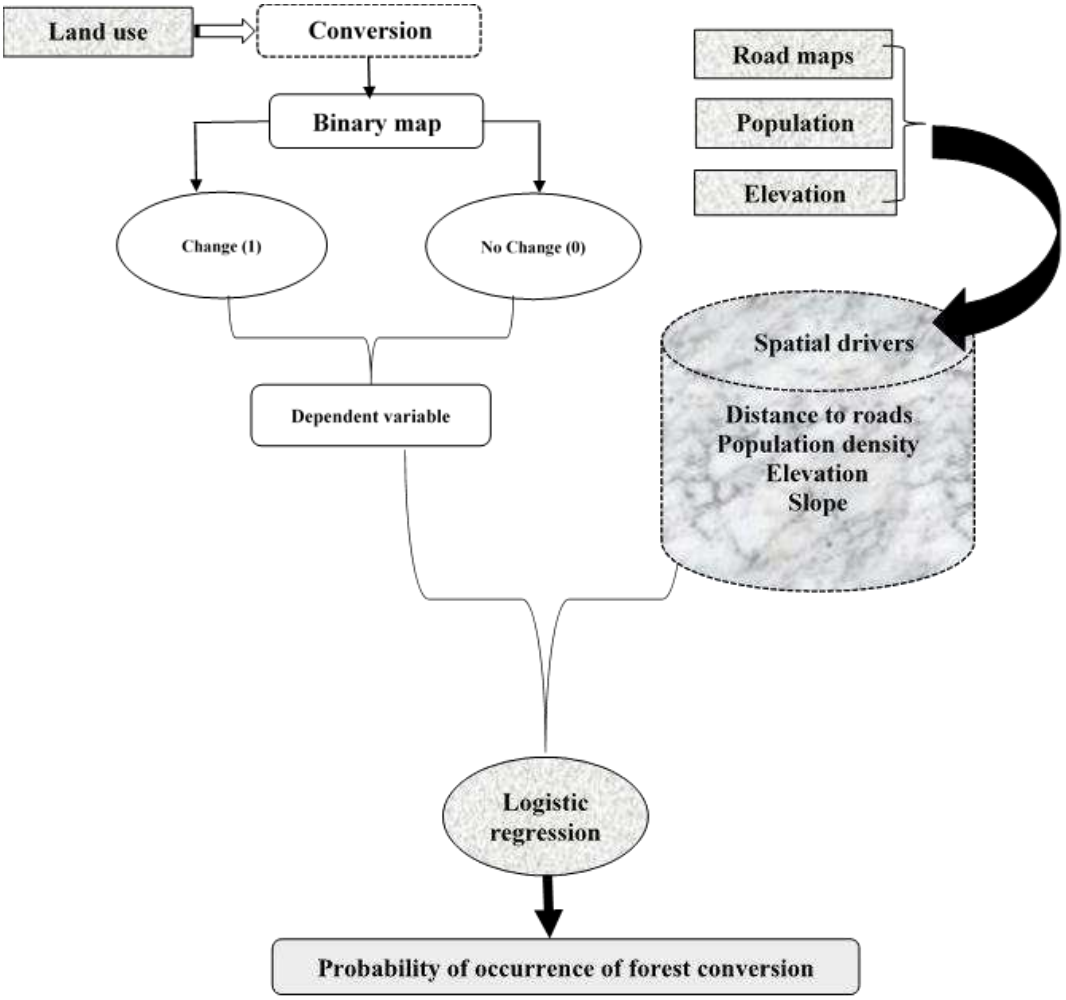

Figure 3. *The workflow of the training and simulation processes*

The area under the curve method was analyzed to evaluate the performance of the model (Metz, 1978; Hanley et al., 1983). *Table 2* illustrates the independent variables used to examine the house-hold forest dependency in the Luki Biosphere Reserve.

Results

Land Use/Land Cover conversion from 1987 to 2020

Change detection method was used to analyze the past land use/land cover change (1987–2020) in the Luki Biosphere Reserve. For all classified images, the estimated overall accuracy was more than 80% (*Table 3*).

The results of land use/land cover change from the year 1987 to 2020 are shown in *Figure 4 and Table 4*. The Luki's landscape was found to have undergone major changes during the period under study. This is because all the land use/land cover classes experienced either an increase or a decrease in terms of their area. There was a decrease in forest land, while savannah, the complex of degraded and young secondary forest, built-up and fallow land and fields experienced an increase. However, the fallow land and fields' class received the greatest increase, although the built-up area also doubled in size.

http://www.aloki.hu ● ISSN 1589 1623 (Print) ● ISSN 1785 0037 (Online)
DOI: http://dx.doi.org/10.15666/aeer/2001_653670

Table 3. *Image classification accuracy*

LULC Categories	1987		2002		2020	
	Producer's Accuracy (%)	User's Accuracy (%)	Producer's Accuracy (%)	User's Accuracy (%)	Producer's Accuracy (%)	User's Accuracy (%)
Forest land	90.7	91.9	93.9	96.3	99.05	98.05
Savannah	86.7	86.7	93.3	91.3	89.28	97.16
Complex of degraded and young secondary forest	89.7	90.2	91.1	94.2	92.3	94.1
Fallow land and fields	92.3	90.6	94.7	92.3	96.19	75.75
Builtup area	90.3	90.3	91.7	91.7	98.48	66.41
Overall accuracy (%)	89.16		93.6		97.17	
Kappa coefficient	0.86		0.91		0.92	

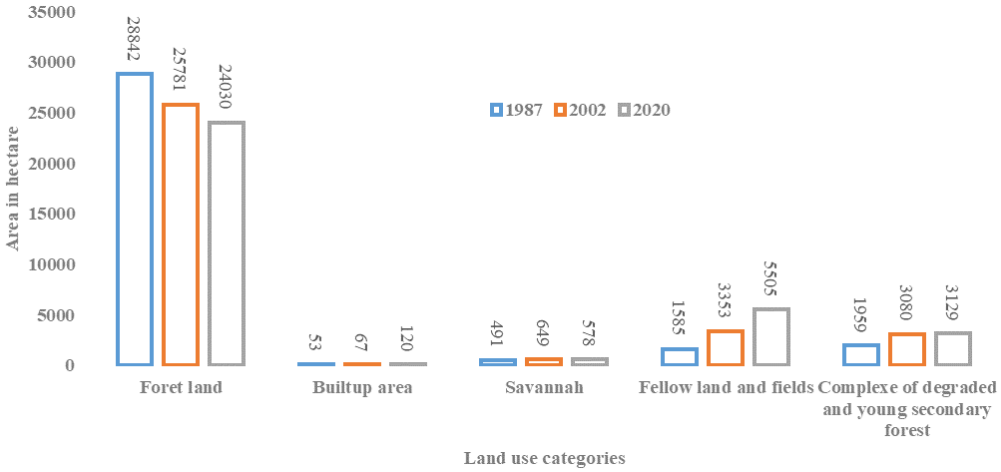

Figure 4. *Land use/land cover statistics from 1987 to 2020*

Table 4. *Transition matrix (in %) in the Luki's landscape*

	Land Use Class	Forest land	Complex of degraded and young Secondary forest	Savannah	Fallow Land	Built-up Area
1987 to 2020	Forest land	82.12	4.06	0.48	13.26	0.08
	Complex of degraded and young Secondary forest	0.005	90.88	0.799	7.865	0.45
	Savannah	0.000	7.9824	83.449	1.556	7.012
	Fallow land	0.267	7.46	0.346	91.418	0.510
	Built-up area	0.0000	2.555	9.000	0.852	87.5639

The transition matrix (*Table 5*) offers the full pattern of change for all land use/land cover categories in the Luki Biosphere Reserve. From 1987 to 2020, the forest land lost the greatest amount of area. Also, the biggest forest land area was transformed into fallow land and fields, followed by the complex of degraded and young secondary forest, savannah, and built-up area.

http://www.aloki.hu ● ISSN 1589 1623 (Print) ● ISSN 1785 0037 (Online)
DOI: http://dx.doi.org/10.15666/aeer/2001_653670

Table 5. *Land use/land cover statistics (in hectare) from 1987 to 2020 in the Luki's landscape*

Land Use Class	1987	2002	2020
Forest land	30818.71	28876.17	26812.69
Non-forest	2128.59	4071.12	6132.72

In fact, due to the expansion of human activities, particularly agriculture, more than 13.26% of forest land was transformed into fallow land and fields. Further, the fallow land and field class has been identified as the class that gained the biggest area, principally transformed from forest land, the complex of degraded and young secondary forest (7.8%), savannah (1.5%), and built-up area (0.8%). Nevertheless, the absence of human activities in the fallow land (4%) converted from forest land, has led to the natural evolution of this class to young secondary forest. Moreover, the overexploitation of forest land areas (0.48%) over a long period has been resulted in their transformation into savannah class.

However, after grouping land use classes in two groups for the purpose of implementing the logistic regression model, it has revealed a decrease in forest land while the non-forest land increased from 1987 to 2020, as shown in *Table 5 and Figure 5*.

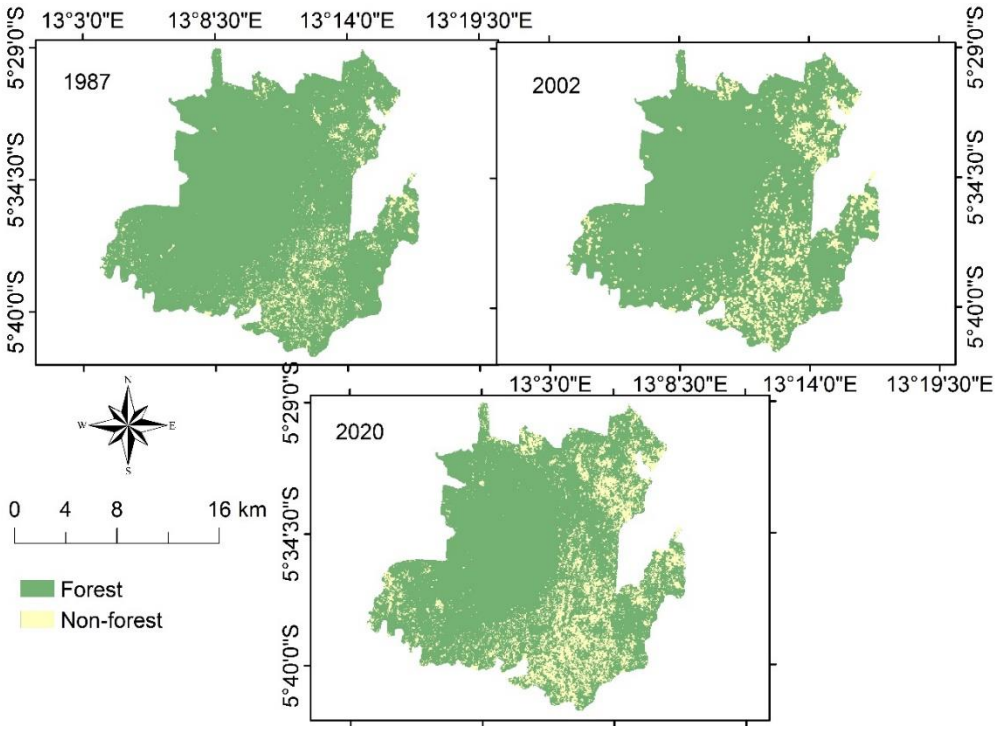

Figure 5. *Land use/land cover change*

Multicollinearity and correlation analyses between the drivers for different LULC conversions

In this study, the Pearson method was used to examine the correlation between different drivers selected to perform the logistic regression. As shown in *Figure 6*, all the explanatory variables were weakly correlated, and none of them had correlation values greater than 0.5. All the drivers were positively correlated to other variables except for

http://www.aloki.hu ● ISSN 1589 1623 (Print) ● ISSN 1785 0037 (Online)
DOI: http://dx.doi.org/10.15666/aeer/2001_653670

the population density that was negatively correlated. A strong correlation between elevation and slope was observed, although it did not reach the value of 0.5 for both periods under study (1987-2002 and 2002-2020). The variance inflation factor (VIF) was used to test the multicollinearity of independent variables. Meanwhile, different authors have demonstrated that, variables with VIF values greater than 10 are not suitable for modelling analysis (Field, 2013). In this study, the VIF values for all independent variables ranged from 1.054 to 1.097 (*Table 6*). These values were acceptable, thus, all drivers were included in the model. Finally, the tolerance value that expresses the percentage of variation related to the variable was found to be greater than 0.8 for all the independent variables, suggesting that multicollinearity was not a limitation when computing the variable coefficients using the logistic regression model.

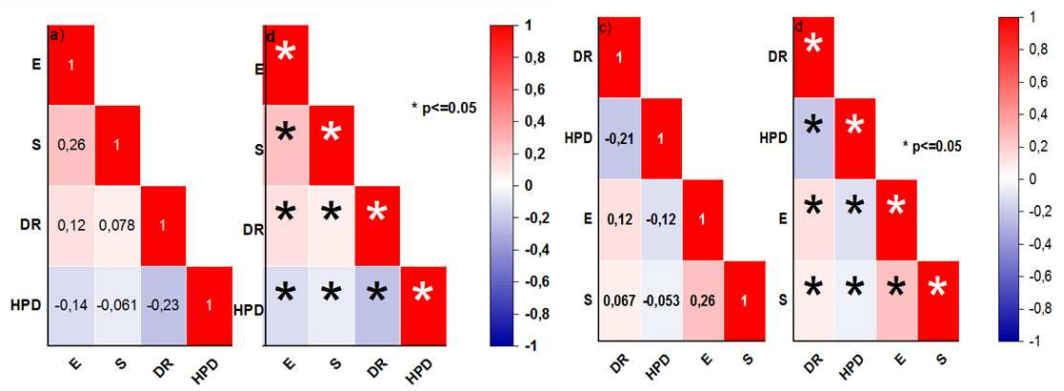

Figure 6. *Correlation analysis of drivers for; a) 1987-2002 b) significance level c) 2002-2020 d) significance level. (E: elevation, S: slope, DR: distanceto roads, HPD: human population density)*

Table 6. *Multicollinearity analysis of drivers for different LULC conversions*

LULC conversions	Variables	Tolerance	VIF
Forest lands to others 1987-2002	Elevation	0.912	1.097
	Slope	0.931	1.074
	Distance to roads	0.939	1.065
	Population density	0.936	1.063
Forest lands to others 2002-2020	Elevation	0.917	1.091
	Slope	0.933	1.072
	Distance to roads	0.946	1.057
	Population density	0.949	1.054

Modelling LULC change based logistic regression

Odds ratios (ORs) were used to measure the effects of spatial drivers of deforestation in the Luki Reserve as illustrated in *Table 7*. During the period under study, major changes have been observed in forest land, leading to the decrease of forest land area. Thus, the effects of underlying variables that had driven the observed changes were thoroughly analysed. These variables include distance from roads, slope, and elevation and population density. Based on the obtained results, it was evident that all the explanatory

http://www.aloki.hu ● ISSN 1589 1623 (Print) ● ISSN 1785 0037 (Online)
DOI: http://dx.doi.org/10.15666/aeer/2001_653670

variables had significantly impacted the forest change during the period under study, with p-value being less than 0.05. The proximity to roads significantly increased the conversion probability of forest land to other land use types by 2.569 and 2.768 (p-value < 0.05), respectively from 1987-2002 and 2002-2020. In addition, an increase in population density significantly increased the conversion probability of forest lands to other land use types by 2.191 and 2.357 (p-value<0.05), respectively from 1987-2002 and 2002-2020. It is worth noting that these two independent variables (proximity to roads and population density) were found to be the most important drivers that strongly affected the process of deforestation in the Luki biosphere reserve during the period under study.

Table 7. *Drivers affecting the conversion of LULC categories in the Luki biosphere reserve*

LULC conversion	Independent variables	Odd ratio	p-value
Forest lands to others 1987-2002	Distance to roads	2.569*	<0.05
	Elevation	1.120*	<0.05
	Slope	0.976*	<0.05
	Population density	2.191*	<0.05
Forest lands to others 2002-2020	Distance to roads	2.768*	<0.05
	Elevation	1.235*	<0.05
	Slope	0.998*	<0.05
	Population density	2.357*	<0.05

The selected drivers were found to affect forest conversion process in the Luki Biosphere Reserve between 1987 and 2020. Areas closer to roads experienced significant change, especially the conversion from primary forest to fallow land and fields. Similarly, the closer the area to highly populated areas, the higher the conversion probability from forest land to other land use categories. These two drivers (proximity to roads and areas with high population density) were the most significant contributors of forest conversion in the Luki biosphere reserve. Meanwhile, slope and elevation also significantly impacted the conversion of forest land to other land use types, but when compared to proximity to roads and population density, their effects were moderate. Areas with low slope were expected to experience a high probability of conversion, compared to areas with high slope.

Discussion

The present research examined the spatial drivers of deforestation in the Luki Biosphere Reserve during the last three decades (1987-2020). Remote sensing data and modeling techniques were used to perform land use/land cover change and examine the pattern of spatial drivers (distance to roads, population density, elevation and slope) affecting this change.

From our analysis, major landscape changes were found to have occurred during the study period, leading to forest loss and the expansion of agricultural land and built-up area, as reported by other studies done in other regions (Lambin et al., 2001; Bamba, 2010; Mpoyi et al., 2013; Ciza et al., 2015; Ngabinzeke et al., 2016; Kyale et al., 2019; Opelele et al., 2020). Numerous spatial variables have been known to play a significant role in driving the land use/land cover changes (Ouedraogo et al., 2010).

http://www.aloki.hu ● ISSN 1589 1623 (Print) ● ISSN 1785 0037 (Online)
DOI: http://dx.doi.org/10.15666/aeer/2001_653670

However, in the Luki Biosphere Reserve, the observed changes have been significantly induced by spatial drivers such as population density, distance to roads, as well as elevation and slope. Of these, population density and proximity to roads were the most significant spatial drivers of deforestation in the Luki Biosphere Reserve; and their relative importance did not change according to the two periods chosen for the present study. Furthermore, the proximity to roads and high population led to massive conversion of forest land to other land use/land cover types. This conversion increased with high population density and proximity to roads, then with elevation and slope. Our findings are consistent with previous reports (van Gils and Loza, 2006; Mhawish and Saba, 2008; Siles, 2009; Buckley, 2010; Kyale et al., 2019) which demonstrated the impact of population density and road network in the land use/land cover change process. These drivers increase the susceptibility of forest lands to conversion into other land use types due to the dependency of local community on forest resources, and promotion of intense trade of forest products. According to Mhawish and Saba (2016) and Verburg and Overmars (2009), the population density is one of the main drivers of land use/land cover change that can influence change from local to large scale. Also, among five explanatory variables (distance from roads and settlements, topography, land tenure, and soil texture), Loza (2004) has revealed a high significant relationship between distance from roads and forest conversion. In fact, the population growth and economic development of surrounding cities of the Luki forest led to the increase of land and natural resource demands, thus acting as significant drivers of deforestation and forest degradation. Meanwhile, agriculture is the main source of livelihoods for the local communities. As such, crop fields have been established in areas closer to roads and human settlements. This has increased the impact of these two drivers on land use conversion.

With respect to slope and elevation, major conversion types were found to mostly occur in flatter zones in our study area. These findings were consistent with reports from previous studies (Mertens and Lambin, 1997; Qasim et al., 2013). These studies showed that low elevation is more associated to agriculture and agglomeration expansion due to the high accessibility, while steeper areas are suitable for forest lands (Mertens and Lambin, 1997; Qasim et al., 2013). The present study revealed the significant role of accessibility variables on forest change, compared to topographical variables. Our results corroborate with previous studies in other regions (Linkie et al., 2004; Mas et al., 2004; Lesschen et al., 2005).

The area under curve, as presented in *Figure 7*, was estimated at 76.5% and 81.9% for the period 1987-2002 and 2002-2020, respectively. This provides 76.5% and 81.9% of accuracy of our prediction results. Loza (2004) and Siles (2009), in their studies on examining the effects of spatial drivers on forest conversion, have estimated the area under curve at 71.50% and 87%, respectively.

The approach of the logistic regression applied in the present research has been found to be most suitable technique to examine spatial dimension of the spatial drivers of deforestation, approving its potential in the field of regression analysis for binary dependent variables (Huang et al., 2009). Therefore, it is essential to properly analyze landscape changes and the factors that induce them in order to predict their future evolutions and subsequently support the decision-making processes from a perspective of multiple scenarios. The present study considered only four variables in the model since data for other variables such as temperature, soil type and precipitation were not available for this research. Thus, it would be important for future studies to include other variables in the model to further improve its precision.

http://www.aloki.hu ● ISSN 1589 1623 (Print) ● ISSN 1785 0037 (Online)
DOI: http://dx.doi.org/10.15666/aeer/2001_653670

However, Huang et al. (2009) pointed out that in a model of land use change, the use of a limited number of variables is very useful to providing a better understanding of land use/land cover change involving complex processes, as revealed in this study. Finally, with spatial resolution as low as 30 m, the use of Landsat images in this study may have had an impact on the pattern of change observed in the Luki landscape. Images of low spatial resolution often induce mixed pixel problems when used in the classification of heterogeneous vegetation. Thus, the use of high spatial resolution can solve the problem of mixed pixels, as we used Landsat images that had coarse resolution.

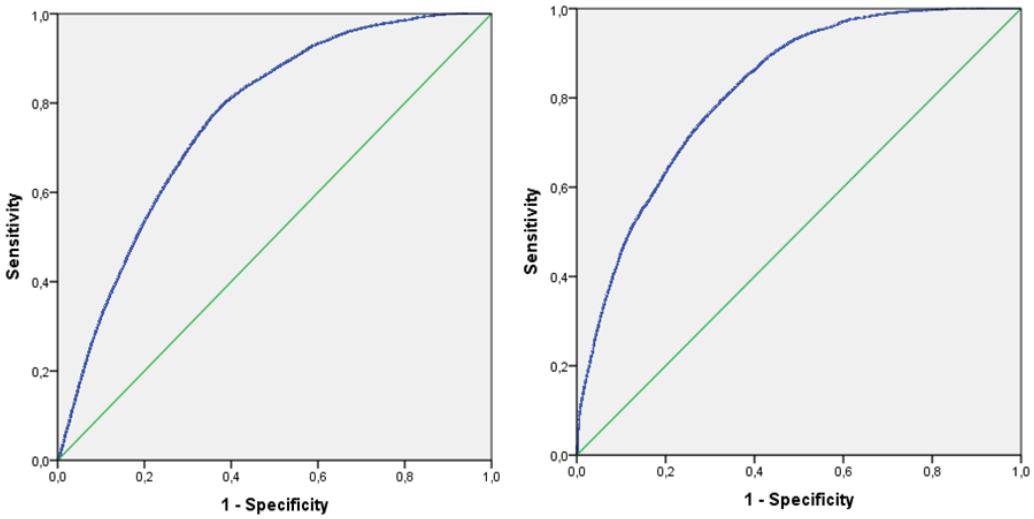

Figure 7. *Validation of the logistic regression model prediction (AUC/ROC). A) 1987-2002, and b) 2002-2020*

Conclusions

The present study revealed an enormous decrease in area of forest land in the Luki Biosphere Reserve during the studied period (1987-2020). A number of human pressures such as agriculture, illegal logging, village expansion has mainly caused forest losses in the study area. It has been found that these changes have been significantly associated with factors such as distance from roads, population density, slope, and elevation. However, it was noted that population density and distance from roads were the most important spatial drivers of deforestation in the region. Indeed, areas closer to roads and highly populated villages are expected to experience the higher probability of forest conversion. The logistic regression model has been found to be an efficient tool to model spatial drivers associated with deforestation and facilitated in examining their relative importance on the deforestation process. The present study provides reliable information that managers, policy-makers and local authorities should include in their decision making processes for the purpose of environmental monitoring and planning, prediction analysis and impact assessment at local level. However, considering the limitation of data related to intensification of farming, future studies should incorporate this variable when establishing the model. Household surveys could also be conducted to provide socio-economic data related to household forest dependence for developing decision models for sustainable land management.

http://www.aloki.hu ● ISSN 1589 1623 (Print) ● ISSN 1785 0037 (Online)
DOI: http://dx.doi.org/10.15666/aeer/2001_653670

Funding. This study was supported by The Fundamental Research Funds for the Central Universities (2572019CP12).

REFERENCES

[1] Adhikari, A., Hansen, A. J. (2018): Land use change and habitat fragmentation of wildland ecosystems of the North Central United States. – Landscape and Urban Planning 177: 196-216. https://doi.org/10.1016/j.landurbplan.2018.04.014.

[2] Al Kafy, A., Abdullah-Al, F., Al Rakib, A., Abdullah Al, R., Shaleha, K. A., Zullyadini, A. R., Dewan, A. J., Gangaraju, S., Opelele, O. M., Abhishek, B. (2021): The operational role of remote sensing in assessing and predicting land use/land cover and seasonal land surface temperature using machine learning algorithms in Rajshahi, Bangladesh. – Applied Geomatics 13: 793-816.

[3] Angoboy, I. B., Beeckman, H., Ouédraogo, D. Y., Bourland, N., De Mil, T., Van Den Bulcke, J., Van Acker, J., Couralet, C., Ewango, C., Hubau, W., Toirambe, B., Doucet, J. L., Fayolle, A. (2019): Une forte saisonnalité du climat et de la phénologie reproductive dans la forêt du Mayombe: l'apport des données historiques de la Réserve de Luki en République démocratique du Congo. – Bois et Forêts des Tropiques 341: 39-53. https://doi.org/10.19182/ bft2019.341.a31753.

[4] Arekhi, S. (2011): Modeling spatial pattern of deforestation using GIS and logistic regression: a case study of northern Ilam forests, Ilam province, Iran. – Afr. J. Biotechnol. 10(72): 16236-16249.

[5] Bamba, I. (2010): Anthropisation et dynamique spatio-temporelle de paysages forestiers en République démocratique du Congo. – Available online at: https://www.congoforum.be/Upldocs/Forets%20These_finale_IBAMBA.pdf (accessed on 7 May 2021).

[6] Buckley, A. (2010): ESRI ArcGIS Blog. – Understanding curvature rasters.

[7] Buya, S., Tongkumchum, P., Owusu, B. E. (2020): Modelling of land-use change in Thailand using binary logistic regression and multinomial logistic regression. – Arabian Journal of Geosciences 13(12). https://doi.org/10.1007/s12517-020-05451-2.

[8] Ciza, S. K., Mikwa, J. F., Malekezi, A. C., Gond, V., Bosela, F. B. (2015): Identification des moteurs de déforestation dans la région d'Isangi, République démocratique du Congo. – Bois Forets des Tropiques 324: 29-38. https://doi.org/10.19182/bft2015.324.a31264.

[9] Congalton, R. G., Mead, R. A. (1983): A quantitative method to test for consistency and correctness in photo-interpretation. – Photogrammetric Engineering and Remote Sensing 49(1): 69-74.

[10] Diuk-Wasser, M. A., Vanacker, M. C., Fernandez, M. P. (2021): Impact of Land Use Changes and Habitat Fragmentation on the Eco-epidemiology of Tick-Borne Diseases. – Journal of Medical Entomology 58(4): 1546-1564. https://doi.org/10.1093/jme/tjaa209.

[11] Doumenge, C. (1990): La Conservation des Écosystèmes Forestiers du Zaïre. – UICN: Gland, Switzerland, 242p.

[12] Field, A. (2013): Discovering statistics using IBM SPSS statistics. Statistics (58). – SAGE Publications Ltd.

[13] Foley, J. A., DeFries, R., Asner, G. P., Barford, C., Bonan, G., Carpenter, S. R., Chapin, S., Coe, M. T., Daily, G. C., Gibbs, H. K., Helkowski, J. H., Holloway, T., Howard, E. A., Kucharik, C. J., Monfreda, C., Patz, J. A., Prentice, I. C., Ramankutty, N., Snyder, P. K. (2005): Global consequences of land use. – Science 309: 570-574.

[14] Gata, D. (1997): Etudes des Impacts Humains, Estimation De Degré de Péril de la Biodiversité et Principes Directeurs pour une Gestion Durable des Ressources Disponibles. – MAB: Kinshasa, Democratic Republic of Congo, 37p.

http://www.aloki.hu ● ISSN 1589 1623 (Print) ● ISSN 1785 0037 (Online)
DOI: http://dx.doi.org/10.15666/aeer/2001_653670

[15] Geist, H. J., Lambin, E. F. (2001): What Drives Tropical Deforestation? A meta-analysis of proximate and underlying causes of deforestation based on subnational case study evidence. – LUCC International Project Office 5: 207-210.
[16] González, M. G., Martínez, M., Lithgow, D., Pérez-Maqueo, O., Simonin, P. (2012): Land use change and its effects on the value of ecosystem services along the coast of the Gulf of Mexico. – Ecol. Econ 82: 23-32. https://doi.org/10.1016/j.ecolecon.2012.07.018.
[17] Hanley, J. A., McNeil, B. J. (1983): A method of comparing the areas under receiver operating characteristic curves derived from the same cases. – Radiology 148: 839-843.
[18] Harris, I., Osborn, T. J., Jones, P., Lister, D. H. (2020): Version 4 of the CRU TS monthly high-resolution gridded multivariate climate dataset. – Sci. Data 7: 109.
[19] Henders, S., Persson, U. M., Kastner, T. (2015): Trading forests: Land-use change and carbon emissions embodied in production and exports of forest-risk commodities. – Environmental Research Letters 10: 12. https://doi.org/10.1088/1748-9326/10/12/125012.
[20] Huang, B., Zhang, L., Wu, B. (2009): Spatiotemporal analysis of rural-urban land conversion. – Int. J. Geogr. Inf. Sci. 23(3): 379-398. https://doi.org/10.1080/13658810802119685.
[21] Kamwi, J. M., Chirwa, P. W. C., Manda, S. O. M., Graz, F. P., Kätsch, C. (2015): Livelihoods, land use and land cover change in the Zambezi Region, Namibia. – Popul. Environ. 37(2): 207-230. https://doi.org/10.1007/s11111-015-0239-2.
[22] Keshtkar, H., Voigt, W., Alizadeh, E. (2017): Land-cover classification and analysis of change using machine learning classifiers and multi-temporal remote sensing imagery. – Arabian Journal of Geosciences 10: 6. https://doi.org/10.1007/s12517-017-2899-y.
[23] Kyale, K. J., Wardell, D. A., Mikwa, J. F., Kabuanga, J. M., Monga Ngonga, A. M., Oszwald, J., Doumenge, C. (2019): Dynamique de la déforestation dans la Réserve de biosphère de Yangambi (République démocratique du Congo): variabilité spatiale et temporelle au cours des 30 dernières années. – Bois et Forêts des Tropiques 341: 15. https://doi.org/10.19182/bft2019.341.a31752.
[24] Lambin, E. F., Turner, B. L., Geist, H. J., Agbola, S. B., Angelsen, A., Bruce, J. W., Coomes, O. T., Dirzgo, R., Fischer, G., Folke, C., George, P. S., Homewood, K., Imbernon, J., Leemans, R., Li, X., Moran, E. F., Mortimore, M., Ramakrishnan, P. S., Xu, J. (2001): The Causes of Land-Use and Land-Cover Change: Moving Beyond the Myths. – Glob. Environ. Change 11(4): 261-269. https://doi.org/10.1016/S0959-3780(01)00007-3.
[25] Lambin, E. (2006): Land Cover Assessment and Monitoring. Encyclopedia of Analytical Chemistry. – John Wiley & Sons, Ltd. https://doi.org/10.1002/9780470027318.a2311.
[26] Lesschen, J. P., Verburg, P. H., Staal, S. J. (2005): Statistical Methods for Analysing the Spatial Dimension of Changes in Land Use and Farming Systems. – LUCC Focus 3 Office and ILRI.
[27] Li, W., Ciais, P., Peng, S., Yue, C., Wang, Y., Thurner, M., Saatchi, S., Arneth, A., Avitabile, V., Carvalhais, N., Harper, A., Kato, E., Koven, C., Liu, Y., Nabel, J., Pan, Y., Pongratz, J., Poulter, B., Pugh, T., Santoro, M., Sitch, S., Stocker, B., Viovy, N., Wiltshire, A., Yousefpour, R., Zaehle, S. (2017): Land-use and land-cover change carbon emissions between 1901 and 2012 constrained by biomass observations. – Biogeosciences 14(22): 5053-5067. https://doi.org/10.5194/bg-14-5053-2017.
[28] Linkie, M., Smith, R. J., Leader-Williams, N. (2004): Mapping and predicting deforestation patterns in the lowlands of Sumatra. – Biodivers. Conserv. 13: 1809-1818.
[29] Loza, A. V. (2004): Spatial logistic model for tropical forest conversion : a case study of Carrasco province (1986–2002), Bolivia. – International Institute for Geoinformation Science and Earth Observation, Enschede, The Netherlands.
[30] Lubalega, T. K., Mananga, P. M. (2018): Évaluation de la biodiversité spécifique ligneuse des cultures agricoles sous couvert arboré à Patu, dans le Mayombe, en République Démocratique du Congo (RDC). – CongoSciences 6: 2.
[31] Lubini, A. (1997): La végétation de la Réserve de Biosphère de Luki au Mayombe (RD Congo). – Opera Botanica Belgica 10: 155.

http://www.aloki.hu ● ISSN 1589 1623 (Print) ● ISSN 1785 0037 (Online)
DOI: http://dx.doi.org/10.15666/aeer/2001_653670

[32] Maitima, J. M., Olson, J. M., Mugatha, S. M., Mugisha, S., Mutie, T. (2010): Land use changes, impacts and options for sustaining productivity and livelihoods in the basin of Lake Victoria. – J. Sustain. Dev. Afr. 12(3): 1520-5509.
[33] Mas, J. F., Puig, H., Palacio, J. L., Sosa-López, A. (2004): Modelling deforestation using GIS and artificial neural networks. – Environ. Model. Softw. 19: 461-471.
[34] McConnell, W. J. (2015): Land Change: The Merger of Land Cover and Land use Dynamics. – International Encyclopedia of the Social & Behavioral Sciences (Second Edition). Oxford: Elsevier, 220-3.
[35] Mertens, B., Lambin, E. F. (1997): Spatial modeling of tropical deforestation in southern Cameroon: spatial disaggregation of diverse deforestation processes. – Appl. Geogr. 17: 143-162.
[36] Metz, C. E. (1978): Basic principles of ROC analysis. – Seminars in Nuclear Medicine 8: 283-298.
[37] Mhawish, Y. M., Saba, M. (2016): Impact of Population Growth on Land Use Changes in Wadi Ziqlab of Jordan between 1952 and 2008. – International Journal of Applied Sociology 6(1): 7-14. Retrieved from http://journal.sapub.org/ijas.
[38] Moghadasi, N., Karimirad, I., Sheikh, V. (2017): Assessing the impact of land use changes and rangeland and forest degradation on flooding using watershed modeling system. – Journal of Rangeland Science 7(2): 93-106. https://doi.org/10.5772/intechopen.77041.
[39] Mpoyi, A. M., Nyamwoga, F. B., Kabamba, F. M., Assembemvondo, S. (2013): Le contexte de la REDD+ en République Démocra-tique du Congo Causes, agents et institutions. – CIFOR, Bogor. https://doi.org/10.17528/cifor/004094.
[40] Mustafa, A., Rienow, A., Saadi, I., Cools, M., Teller, J. (2018): Comparing support vector machines with logistic regression for calibrating cellular automata land use change models. – European Journal of Remote Sensing 51(1): 391-401. https://doi.org/10.1080/22797254.2018.1442179.
[41] Nandy, S., Kushwaha, S. P. S., Mukhopadhyay, S. (2007): Monitoring Chilla-Motichur corridor using geospatial tools. – J. Nat. Conserv. 15(4): 237-244.
[42] Ngabinzeke, J. S., Linchant, J., Quevauvillers, S., Muhongya, J. M. K., Lejeune, P., Vermeulen, C. (2016): Cartographie de la dynamique de terroirs villageois à l'aide d'un drone dans les aires protégées de la République démocratique du Congo. – Bois Forets des Tropiques 315: 21-28. https://doi.org/10.19182/bft2016.330.a31320.
[43] Nyange, N. M. (2014): Participation des communautés locales et gestion durable des forêts: Cas de la réserve de la biosphère de Luki en République Démocratique du Congo. – Ph.D. Thesis, Université Laval Québec, Québec, QC, Canada, 227p. Available online: https://corpus.ulaval.ca/jspui/bitstream/20.500.11794/25349/1/30892.pdf (accessed on 2 May 2021).
[44] Olaya, V. (2009): Basic land-surface parameters. – Developments in Soil Science 33: 141-169. https://doi.org/10.1016/S0166-2481(08)00006-8.
[45] Opelele, O. M., Fan, Y., Yu, Y., Kachaka, S. K. (2020): Analysis of land use/land cover change and its prediction in the Mambasa sector, Democratic Republic of Congo. – Applied Ecology and Environmental Research 18(4): 5627-5644. https://doi.org/10.15666/aeer/1804_56275644.
[46] Opelele, O. M., Ying, Y., Fan, W., Chen, C., Kachaka, S. K. (2021): Examining Land Use/Land Cover Change and Its Prediction Based on a Multilayer Perceptron Markov Approach in the Luki Biosphere Reserve, Democratic Republic of Congo. – Sustainability 13: 6898.
[47] Opelele, O. M., Yu, Y., Fan, W., Lubalega, T., Chen, C., Kachaka, S. K. (2021): Analysis of the Impact of Land-Use/Land-Cover Change on Land-Surface Temperature in the Villages within the Luki Biosphere Reserve. – Sustainability 13(20): 11242. https://doi.org/10.3390/su132011242.

http://www.aloki.hu ● ISSN 1589 1623 (Print) ● ISSN 1785 0037 (Online)
DOI: http://dx.doi.org/10.15666/aeer/2001_653670

[48] Ouedraogo, I., Tigabul, M., Savadogo, P., Compaore, H., Odén, P. C., Ouadba, J. M. (2010): Land cover change and its relation with population dynamics in Burkina Faso,West Africa. – Land Degrad. Dev. 21(5): 453-462. https://doi.org/10.1002/ldr.981.
[49] Overmars, K. P., Verburg, P. H. (2005): Analysis of land use drivers at the watershed and household level: Linking two paradigms at the Phillipine forest fringe. – Int. J. Geogr. Inf. Sci. 19: 125-152. https://doi.org/10.1080/13658810410001713380.
[50] Peel, M. C., Finlayson, B. L., Mcmahon, T. A. (2007): Updated world map of the Köppen–Geiger climate classification. – Hydrology and Earth System Sciences 11: 1633-1644. https://doi.org/10.5194/hess-11-1633-2007.
[51] Pendje, G., Mbaya, M. (1992): La réserve de Biosphère de Luki, Patrimoine Floristique et Faunique en Péril. – UNESCO: Paris, France, 62p.
[52] Pijanowski, B. C., Pithadia, S., Shellito, B. A. (2005): Calibrating a neural network-based urban change model for two metropolitan areas of the Upper Midwest of the United States. – International Journal of Geographical Information Science 19(2): 197-215. https://doi.org/10.1080/13658810410001713416.
[53] Pontius Jr., R. G., Schneider, L. C. (2001): Land-cover change model validation by an ROC method for the Ipswich watershed, Massachusetts, USA. – Agric. Ecosyst. Environ. 85(1-3): 239-248.
[54] Pontius Jr., R. G., Malanson, J. (2005): Comparison of the structure and accuracy of two land change models. – Int. J. Geogr. Inf. Sci. 19(2): 243-265.
[55] Powers, R. P., Jetz, W. (2019): Global habitat loss and extinction risk of terrestrial vertebrates under future land-use-change scenarios. Nature Climate Change. – Nature Publishing Group. https://doi.org/10.1038/s41558-019-0406-z.
[56] Qasim, H., Klaus, H., Termansen, M., Fleskens, L. (2013): Modelling Land Use Change across Elevation Gradients in District Swat, Pakistan. – Regional Environmental Change 13(3): 567-581. https://doi.org/10.1007/s10113-012-0395-1.
[57] Rawat, J. S., Kumar, M. (2015): Monitoring land use/cover change using remote sensing and GIS techniques: A case study of Hawalbagh block, district Almora, Uttarakhand, India. – The Egyptian Journal of Remote Sensing and Space Science 18: 77-84. https://doi.org/10.1016/j.ejrs.2015.02.002.
[58] Sénéchal, J., Kabala, M., Fournier, F. (1989): Revue des connaissances sur le Mayombe. – Paris, France, Unesco, 343p.
[59] Sharma, R., Nehren, U., Rahman, S. A., Meyer, M., Rimal, B., Seta, G. A., Baral, H. (2018): Modeling land use and land cover changes and their effects on biodiversity in Central Kalimantan, Indonesia. – Land 7(2). https://doi.org/10.3390/land7020057.
[60] Sharma, R., Rimal, B., Baral, H., Nehren, U., Paudyal, K., Sharma, S., Rijal, S., Ranpal, S., Alenazy, A., Kandel, P. (2019): Impact of land cover change on ecosystem services in a tropical forested landscape. – Resources 8(1). https://doi.org/10.3390/resources8010018.
[61] Siles, N. J. S. (2009): Spatial Modelling and prediction of tropical for-est conversion in the Isiboro Secure National Park and Indigenous Territory(TIPNIS), Bolivia. – International Institute for Geoinformation Science and Earth Observation, Enschede, The Netherlands.
[62] Sperandei, S. (2014): Understanding logistic regression analysis. – Biochemia Medica 24(1): 12-18. https://doi.org/10.11613/BM.2014.003.
[63] Sulieman, H. M. (2018): Exploring divers of forest degradation and fragmentation in Sudan: The case of Erawashda Forest and its surrounding community. – Science of the Total Environment 621: 895-904. https://doi.org/10.1016/j.scitotenv.2017.11.210.
[64] Sun, J., Southworth, J. (2013): Remote sensing-based fractal analysis and scale dependence associated with forest fragmentation in an Amazon tri-national frontier. – Remote Sens. 5: 454-472.
[65] Vadrevu, K. P. (2013): Introduction to Remote Sensing. Fifth Ed. – In: Campbell, J. B., Wynne, R. H. (eds.) The Photogrammetric Record. Guilford Press New York.
[66] van Gils, H. A. M. J., Loza Armand Ugon, A. V. (2006): What drives conversion of tropical forest in Carrasco province, Bolivia? – Ambio 35(2): 81-85.

http://www.aloki.hu ● ISSN 1589 1623 (Print) ● ISSN 1785 0037 (Online)
DOI: http://dx.doi.org/10.15666/aeer/2001_653670

[67] Verburg, P. H., Overmars, K. P. (2009): Combining top-down and bottom-up dynamics in land use modeling: Exploring the future of abandoned farmlands in Europe with the Dyna-CLUE model. – Landscape Ecology 24(9): 1167-1181. https://doi.org/10.1007/s10980-009-9355-7.

[68] Wang, M., Cai, L., Xu, H., Zhao, S. (2019): Predicting land use changes in northern China using logistic regression, cellular automata, and a Markov model. – Arabian Journal of Geosciences 12(24). https://doi.org/10.1007/s12517-019-4985-9.

[69] Zhou, Y., Chen, M., Tang, Z., Mei, Z. (2021): Urbanization, land use change, and carbon emissions: Quantitative assessments for city-level carbon emissions in Beijing-Tianjin-Hebei region. – Sustainable Cities and Society 66. https://doi.org/10.1016/j.scs.2020.102701.

http://www.aloki.hu ● ISSN 1589 1623 (Print) ● ISSN 1785 0037 (Online)
DOI: http://dx.doi.org/10.15666/aeer/2001_653670

EFFECTS OF ACTIVATED BRACKISH WATER IRRIGATION ON THE GROWTH AND WATER USE EFFICIENCY OF MATURE FRAGRANT PEAR (*PYRUS PYRIFOLIA* L.)

ZHANG, J. H.[1] – WEI, K.[1*] – WANG, Q. J.[1*] – HALIMAMU, J.[1] – GUO, Y.[1] – LIU, Y.[1] – WANG, K.[1] – CAO, L.[2]

[1]*State Key Laboratory of Eco-hydraulics in Northwest Arid Region of China, Xi'an University of Technology, Xi'an 710048, China*

[2]*Shaanxi Fengxi Xincheng Investment Development Co., Ltd, Xi'an 710048, China*

[*]*Corresponding authors*
e-mail: 18291869766@163.com, wquanjiu@163.com

(Received 9th Aug 2021; accepted 23rd Nov 2021)

Abstract. Understanding the effect and mechanism of activated brackish water irrigation on fruit tree growth is of great significance to improve the utilization efficiency of brackish water in Xinjiang, China. In this study, Korla fragrant pear (*Pyrus pyrifolia* L.) was taken as the research object, and a two-year field irrigation experiment was carried out using brackish water (B), magnetized brackish water (MB) and ionized brackish water (IB) to study the effects of activated brackish water on the growth of new shoots, fruit shape, yield and quality, and water use efficiency of mature fragrant pear. The results showed that the rhizosphere soil water content increased somewhat under the activated brackish water irrigation. Compared to treatment B, the average soil water content under MB and IB irrigation increased by 13.07%-14.90% and 28.15%-28.55%, respectively. In addition, the activated brackish water irrigation could effectively promote the growth and fruit development of fragrant pear trees. Compared with treatment B, the maximum new shoot lengths increased by 17.87%-28.33 and 48.79%-51.12%, the fruit shape index increased by 9.62%-11.68% and 9.58%-10.66%, respectively, the volume of fragrant pear increased by 8.96%-11.96% and 11.89%-15.54%, respectively, the yield of fragrant pear increased by 11.20%-22.22% and 12.47%-25.08%, respectively, and water use efficiency increased by 12.97%-25.24% and 14.15%-26.21%, respectively. Furthermore, the single fruit weight and soluble solid content of fragrant pear significantly increased ($P < 0.05$), while the hardness and total acid content significantly decreased ($P < 0.05$). In conclusion, activated brackish water irrigation can effectively improve the yield and water use efficiency of fragrant pear, and ameliorate the shape and quality of fragrant pear fruit, alleviate the negative effects of brackish water.
Keywords: *magnetized brackish water, ionized brackish water, fragrant pear, yield and quality*

Introduction

Fragrant pear (*Pyrus pyrifolia* L.) is well-known inside and outside of China for its thin skin, thin meat, crisp and sweet juice and strong flavor (Niu et al., 2019). It has become one of the important high-earning export agricultural products in southern Xinjiang, China (Chen et al., 2020a). However, due to the large water consumption of fragrant pear and the extreme shortage of fresh water resources in Xinjiang, the sustainable development of forest and fruit industry in this area is seriously restricted (Li et al., 2020b). The development and utilization of brackish water resources has become an adaptation strategy for drought resistance and yield increase in fruit tree cultivation in freshwater deficient areas (Han et al., 2019). However, there are salt ions in the brackish water. During irrigation, the water enters the soil, causing the accumulation of salt, resulting in the deterioration of the environment in the rhizosphere of fruit trees (Yuan et al., 2019), hindering the absorption of water and nutrients by the roots of fruit trees, thus

http://www.aloki.hu ● ISSN 1589 1623 (Print) ● ISSN 1785 0037 (Online)
DOI: http://dx.doi.org/10.15666/aeer/2001_671683

reducing their productivity (Chen et al., 2018). Therefore, the continuous search for new technologies to improve the quality of brackish water has become a hot topic.

Activated water treatment technology mainly includes magnetized and ionized water treatment methods (Mu et al., 2019). After activation treatment, the physical and chemical properties of water change, the surface tension decreases, the viscosity and half peak width of 17O-NMR increase, and the associated water molecules decompose (Al-Bayar et al., 2020). When the activated brackish water enters the soil through irrigation, the proportion of soil exchangeable sodium ions decreases, and the substitution amount of calcium ions and magnesium ions increases, which changes the exchange characteristics and ion composition of soil base ions (Hamza, 2019), so as to ameliorate soil physical and chemical properties, improve the availability of soil nutrients, provide more ionic nutrients for crop growth, and promote the growth and development of crops (Abdel-Kader et al., 2020). Wang et al. (2021) showed that activated water irrigation could improve wheat root activity, improve root configuration, enhance leaf chlorophyll content and improve wheat yield. Turker et al. (2007) applied a stable magnetic field perpendicular to the gravity field of sunflower and found that both chlorophyll a and chlorophyll b of sunflower increased. Maheshwari and Grewal (2009) found that magnetized water improved the growth and physiological indexes of crops, such as the SPDA value of crop leaves, leaf area index and relative water content of plant leaves. Zhou et al. (2021) pointed out that the cotton yield under irrigation with 300 mT magnetized water increased by 28.8%-31.69%, and the water use efficiency increased by 27.4%-42.8%. Surendran et al. (2016) believed that when the water flowed through the magnetic field, the positive and negative ions in the water were forced to separate. After entering the soil, the nutrient ions were easier to move, and the water molecules were easier to adhere to the soil pores and. It played a role in maintaining the water in the root zone of crops and promoting the growth of peas. Zhao et al. (2021) pointed that the yield of wheat irrigated with magnetized water and ionized water increased by 10.1% and 13.9%, respectively, and the water use efficiency increased by 8.8% and 7.9%, respectively.

At present, there has been extensive research on the activated brackish water irrigation of grain and economic crops, but there is little research on the activated water irrigation of fruit trees. Korla fragrant pear, as a unique variety in China, the impact of activated brackish water irrigation on the growth of fragrant pear fruit trees has not been reported publicly. Therefore, taking the mature fragrant pear fruit trees as the research object, through a two-years of field experiment, this paper analyzed the effects of activated brackish water on the growth, fruit shape, quality, yield and water use efficiency of fragrant pear trees, so as to provide a theoretical basis for the application of activated brackish water in fruit tree irrigation.

Materials and methods

Experimental site description

From 2018 to 2019, the experimental study was carried out in a pear garden (41°45'N, 86°10'E, 901 m a.s.l.) of water conservancy Research Institute of Tarim River Basin Authority, Korla City, Xinjiang, China. Located in the hinterland of the Eurasian continent, the experimental site is a typical temperate continental arid climate area, with an average annual temperature of 11.6 ℃. The average annual precipitation is 58.6 mm, the average annual evaporation is 2257.2 mm, the frost free period is 226 d, and the

http://www.aloki.hu ● ISSN 1589 1623 (Print) ● ISSN 1785 0037 (Online)
DOI: http://dx.doi.org/10.15666/aeer/2001_671683

average annual sunshine hours is 2769.8 h (Wang et al., 2019b). The meteorological elements during the growth period of fragrant pear in 2018 and 2019 were shown in *Fig. 1*. The cumulative reference crop evapotranspiration (ET_0) during the growth period of fragrant pear in 2018 is 1050 mm, and the cumulative rainfall (R) was 60 mm. In 2019, ET_0 during the growth period of fragrant pear was 1025.8 mm, and the cumulative rainfall (R) was 42.9 mm. Before the test, the basic physical and chemical properties of the soil in the 0-100 cm soil layer of the test site were measured. According to the soil texture classification of the U.S. Department of agriculture, the soil in the test area is sandy loam (50.2% sand, 46.0% silt and 3.8% clay), with an average unit weight of 1.56 $g \cdot cm^{-3}$, a saturated volume water content of 0.43 $cm^3 \cdot cm^{-3}$, a field water capacity of 0.25 $cm^3 \cdot cm^{-3}$, a wilting coefficient of 0.05 $cm^3 \cdot cm^{-3}$, a pH value of 7.8, a total nitrogen content of 0.84 $g \cdot kg^{-1}$ and an organic matter content of 13.24 $g \cdot kg^{-1}$ (Chen et al., 2020b). The content of alkali hydrolyzable nitrogen is 57.46 $mg \cdot kg^{-1}$, the content of available phosphorus is 9.85 mg kg^{-1}, and the content of available potassium is 136.52 $mg \cdot kg^{-1}$ (Li et al., 2019). From 2018 to 2019, the average buried depth of underground level is 6.5 m. The brackish water comes from underground well water, and its salinity is 1.83-2.74 $g \cdot L^{-1}$. *Fig. 1* showed the main meteorological factors during the growth period of fragrant pear.

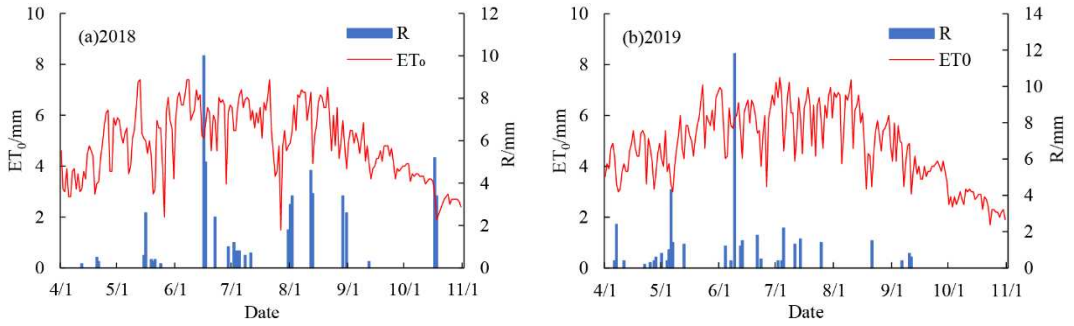

Figure 1. *Main meteorological elements in growth period of fragrant pear. ET0 and R represent the reference crop evapotranspiration and rainfall, respectively*

Magnetizer and magnetized water device

The test started in early April and ended in mid-September every year. The tested materials were 15-year-old fragrant pear trees with a row spacing of 4 m × 6 m (417 trees $\cdot hm^{-2}$). 3 rows of fragrant pear trees with similar tree shape were selected, and divided into 9 communities. Each community was 12 m long and 6 m wide, including 5 fragrant pear trees. Taking different irrigation water treatments as influencing factors, three groups of treatments were set up, namely brackish water (B), magnetized brackish water (MB) and ionized brackish water (IB). Each treatment controlled the irrigation of 5 fragrant pear trees, repeated for 3 times and arranged randomly. Both the magnetized water processor and the ionized water processor were installed on the irrigation water diversion pipeline. The magnetized water processor adopted the pipeline magnetizer (XS300) with a magnetization of 300 mT produced by Urumqi Water-saving Equipment Research and Development Center, Xinjiang, China. The ionized water processor (W600DELF) is produced by Korea Yameihua (Beijing) environmental technology Development Co., Ltd, China. According to the research of Wang et al. (2016), the technical parameters of the equipment were adjusted and controlled. The irrigation method was small tube outflow. 4mm capillary was used to arrange 4 small tubes around

http://www.aloki.hu ● ISSN 1589 1623 (Print) ● ISSN 1785 0037 (Online)
DOI: http://dx.doi.org/10.15666/aeer/2001_671683

the fragrant pear tree, and the small tube flow was 8 $L \cdot h^{-1}$. The irrigation quota was 5625 $m^3 \cdot hm^{-2}$. Irrigation had been started since April 22, and the irrigation cycle was 10 days. A total of 15 times of irrigation had been carried out during the growth period, and the irrigation quota was 375 $m^3 \cdot hm^{-2}$. The fertilization method was ditch application. During the growth period, 652 $kg \cdot hm^{-2}$ urea (containing 46% N), 543 $kg \cdot hm^{-2}$ heavy superphosphate (containing 46% P_2O_5) and 118 $kg \cdot hm^{-2}$ potassium sulfate (containing 51% K_2O) were applied. Other field management of each treatment group was consistent during the experiment. The old bark of fragrant pear fruit trees should be pruned and scraped before the end of February every year, meanwhile, the orchard should be clean. The chemicals should be sprayed before budding to reduce the base number of diseases and pests. When applying fertilizer, the root with a diameter of 0.5 cm should be careful not to hurt.

Determination index and method

Soil water content

PR2 soil water monitoring system (Davis instruments, California, USA) was adopted to determine the soil water content. Three trees with similar growth and healthy were randomly selected for each treatment. A PR2 pipe with a depth of 100 cm was buried at 50 cm and 100 cm in four directions along the East, West, North, South of each tree. There were 8 water monitoring points for each tree and 24 water monitoring points for each treatment. The soil water content was measured every 20 days at the depths of 10, 20, 30, 40, 60 and 100 cm, respectively. The soil moisture content determined by PR2 was calibrated according to the regression equation given by Liang et al. (2019).

Shoot length

According to the actual growth status of fragrant pear trees, 3 fragrant pear trees with uniform growth were selected for each treatment. During the germination period of fragrant pear trees, 4 new shoots with strong growth were randomly selected from the East, West, North and south directions around the crown as markers, and the length and diameter of new shoots were measured with steel tape and vernier caliper. They were measured every 7 days for 6 consecutive cycles.

Fruit shape, yield and quality

The yield of fragrant pear was measured in the first ten days of October every year. Three fragrant pear trees were randomly selected for each treatment, and the total number of fruits produced by each fragrant pear tree was accurately counted. 10 fragrant pear fruits are randomly picked on each fragrant pear tree. The longitudinal diameter (D_Z, mm) and transverse diameter (D_H, mm) were measured with vernier caliper, and the fruit shape index (Wang et al., 2020) ($SI = D_Z/D_H$) and volume (Wu et al., 2012) ($V = 0.002\ D_Z^{\ 1.864}\ D_H^{\ 0.803}$, cm^3) were calculated. The single fruit weight of fragrant pear was measured with an electronic scale with an accuracy of 0.01 g. The product of the single fruit weight and the total number of fruits was taken as the average yield per plant, and the total yield was obtained by area conversion based on the yield per plant. Two samples were selected from four directions of each fragrant pear tree, East, West, North and South, a total of 8 samples were selected to determine the fruit quality. The fruit hardness was determined by GY-2 fruit hardness tester (Vetus Instruments, USA), the soluble solid content was determined by WYT-4 handheld sugar meter (Guangzhou Mingrui Co., Ltd, China), the total acid

http://www.aloki.hu ● ISSN 1589 1623 (Print) ● ISSN 1785 0037 (Online)
DOI: http://dx.doi.org/10.15666/aeer/2001_671683

content was determined by NaOH titration, and the vitamin C content was determined by dichloroindophenol titration.

Meteorological data

The Vantage Pro2-6152c meteorological station produced by Davis company of the United States was used to monitor the meteorological data such as maximum temperature, minimum temperature, sunshine time, 2 m wind speed, air humidity and rainfall during the growth period of fragrant pear.

Calculation of water consumption and water use efficiency

The water consumption in the growth period of fragrant pear fruit trees is calculated by water balance:

$$ET = SWC + I + R + U - D - R_0 \quad \text{(Eq.1)}$$

where, *ET* represents the water consumption of fragrant pear tree (mm). *SWC* represents the water storage in the main root zone of fragrant pear fruit tree (mm). *I* represents the amount of irrigation, mm. *R* represents the rainfall (mm). *U* represents the recharge of groundwater (mm). *D* represents the deep leakage (mm). R_0 is the surface runoff (mm). Since the buried depth of groundwater is greater than 6m, *U* could be ignored. In this test, small pipe outflow is adopted, the irrigation quota is small, there will be no leakage, so *D* can be ignored. The irrigation quota is small, there will be no surface runoff, so R_0 can be ignored;

Since *U*, *D* and R_0 are negligible, Eq. (1) can be simplified as:

$$ET = SWC + I + R \quad \text{(Eq.2)}$$

The water storage in the main root zone of fragrant pear can be calculated according to the measured soil water content data:

$$SWC = 1000H(\theta_{t_2} - \theta_{t_1}) \quad \text{(Eq.3)}$$

where, *H* represents the depth of main root zone of fragrant pear (m). θ_{t1}, θ_{t2} represent the average water content of soil at the depth of 0-100cm in the main root zone at t_1 and t_2.

The water use efficiency (*WUE*) of fragrant pear fruit trees can be expressed as:

$$WUE = 100Y / ET \quad \text{(Eq.4)}$$

where, *WUE* represents the water use efficiency of fragrant pear trees ($kg \cdot m^{-3}$). *Y* represents the yield of fragrant pear ($t \cdot hm^{-2}$).

Data processing and analysis

The data were recorded in Excel 2019 and analyzed using SPSS 22.0 software (IBM Corp. USA). Duncan method was used for significance test and analysis of variance ($P < 0.05$).

http://www.aloki.hu ● ISSN 1589 1623 (Print) ● ISSN 1785 0037 (Online)
DOI: http://dx.doi.org/10.15666/aeer/2001_671683

Results and Discussion

Effect of activated brackish water irrigation on soil water content

The water content of 0-100 cm soil under the irrigation of activated brackish water during the growth period is shown in *Fig. 2*. The soil water content fluctuated in the whole growth period, which was mainly related to irrigation, rainfall, evaporation and other factors (Tan et al., 2017). The soil water content under activated brackish water irrigation was significantly higher than that under brackish water control, while the soil water content under IB irrigation was slightly higher than MB. In 2018, the average soil water content under MB irrigation increased by 14.90% compared with control B, and the average soil water content under IB irrigation increased by 28.55% compared with control B. In 2019, the average soil water content under MB irrigation increased by 13.07% compared with control B, and the average soil water content under IB irrigation increased by 28.15% compared with control B. The experimental results of the two years were slightly different, but they were consistent with the results of Wang et al. (2021). The results indicate that activated brackish water irrigation con effectively improve the soil water content during the growth period of fragrant pear. This is mainly because the associated water molecular cluster and contact angle become smaller after the activation treatment of brackish water (Chibowski and Szcześ, 2018), and the water is easier to enter the small soil pores, which can store a large amount of water in the soil effective pores and reduce the evaporation loss (Shan et al., 2021). As a result, the soil water content of 0-100 cm under activated brackish water irrigation is higher as a whole.

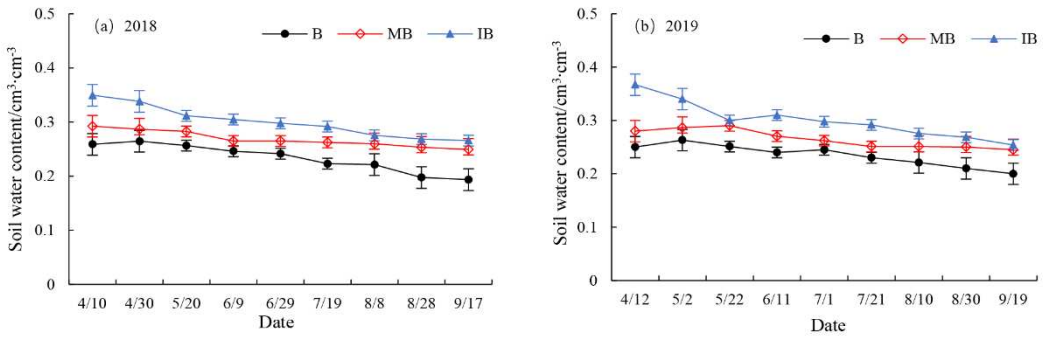

Figure 2. *Soil water content of fragrant pear during growth period under activated brackish water irrigation. B, MB and IB represent brackish water, magnetized brackish water and ionized brackish water, respectively. The error bars represent standard deviations*

Effect of activated brackish water irrigation on new shoot length of fragrant pear trees

New shoots and branches are the basic unit of flowering and fruiting of fragrant pear tree. The length of new shoots is directly related to the transmission efficiency of nutrients and fruit development of fragrant pear tree (Wu et al., 2012). *Fig. 3* showed the change process of new shoot length of fragrant pear tree under activated brackish water irrigation at leaf spreading stage. During the leaf development period of fragrant pear, the length of new shoots and branches of each treatment increased with the advance of growth time. In 2018, the maximum shoot length of fragrant pear fruit trees irrigated with B, MB and IB was 43.55 cm, 51.33 cm and 64.80 cm, which increased by 17.87% and 48.79% compared with control B. In 2019, the maximum shoot length of fragrant pear fruit trees irrigated

http://www.aloki.hu ● ISSN 1589 1623 (Print) ● ISSN 1785 0037 (Online)
DOI: http://dx.doi.org/10.15666/aeer/2001_671683

with B, MB and IB was 41.55 cm, 53.32 cm and 62.79 cm, which increased by 28.33% and 51.12% compared with control B. Wang et al. (2019a) showed that the shoot growth of grapes irrigated with magnetized brackish water increased by 25.56%, and Wang et al. (2021) showed that the dry matter mass of wheat irrigated with ionized water increased by 29.7%, which were consistent with this study. Therefore, the activated brackish water irrigation is beneficial to promote the growth of new shoots of fragrant pear fruit trees and effectively increase the biomass of fragrant pear fruit trees. On the one hand, the activated brackish water irrigation improves the soil water storage in the main root layer of fragrant pear trees and provides sufficient water for the growth of new shoots of fragrant pear trees (Zhao et al., 2021), on the other hand, the water quality performance of activated brackish water is improved (the reducing of surface tension (Liu and Cao, 2021) and the increase of dissolved oxygen and solubility (Wang et al., 2018)), salt activity is reduced (Bu et al., 2010), and the carrying capacity of nutrient elements is improved (Liu et al., 2020), which provides sufficient nutrients for the growth of new shoots of fragrant pear fruit trees, resulting in faster growth of new shoots of fragrant pear trees.

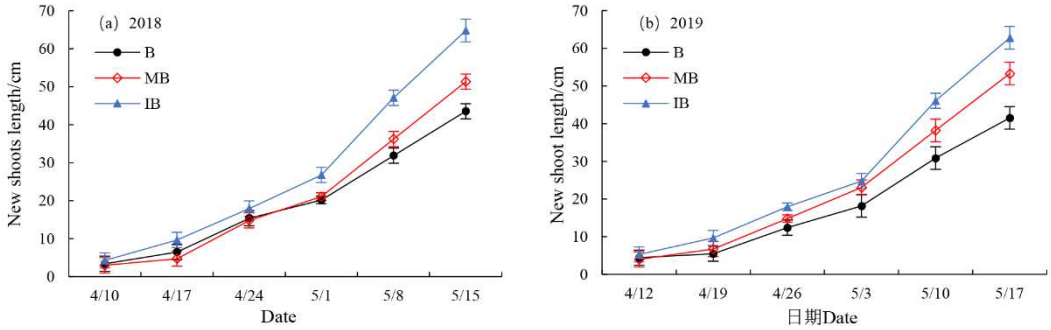

Figure 3. *New shoot lengths of fragrant pear tree under activated brackish water irrigation. B, MB and IB represent brackish water, magnetized brackish water and ionized brackish water, respectively. The error bars represent standard deviations*

Effect of activated brackish water irrigation on fruit shape of fragrant pear

The fruit shape of fragrant pear is one of the important indicators that determine whether its commodity value is competitive in the high-end international pear market (Chen et al., 2020). As can be seen from *Table 1*, activated brackish water irrigation had significant effect on fruit shape of fragrant pear ($P < 0.05$). Compared with control B treatment, the longitudinal diameter of fragrant pear irrigated with MB and IB increased by 6.76%, 7.22% (2018) and 7.25%, 8.83% (2019), the transverse diameter decreased by 4.40%, 2.16% (2018) and 2.17%, 1.65% (2019), the fruit shape index increased by 11.68%, 9.58% (2018) and 9.62%, 10.66% (2019), and the volume of fragrant pear increased by 8.96%, 11.89% (2018) and 11.96%, 15.54% (2019). Li et al. (2011) showed that the fruit shape of fragrant pear with fruit shape index less than 1.12 was nearly round, and that greater than 1.29 was long oval. The fruit shape between 1.12 and 1.29 was oval, and the oval was better. The fruit shape of fragrant pear treated with control B was mostly nearly round, while the fruit shape of fragrant pear irrigated with MB and IB was mostly oval and upright. The results indicate that activated brackish water can not only effectively improve the volume of fragrant pear fruit, but also improve the fruit shape of

http://www.aloki.hu ● ISSN 1589 1623 (Print) ● ISSN 1785 0037 (Online)
DOI: http://dx.doi.org/10.15666/aeer/2001_671683

fragrant pear to a certain extent, which may be due to the fact that activated brackish water irrigation could play a role similar to plant growth hormone to some extent (Boe and Salunkhe, 1963; Qiu et al., 2011), and can effectively regulate the improvement of fruit shape of fragrant pear.

Table 1. *Fruit shape of fragrant pear irrigated with activated brackish water. B, MB and IB represent brackish water, magnetized brackish water and ionized brackish water, respectively*

Year	Treatment	Longitudinal diameter (mm)	Transverse diameter (mm)	Fruit shape index	Fruit tree volume (cm^3)
2018	B	63.46b	56.55a	1.12b	116.98b
	MB	67.75a	54.06c	1.25a	127.45a
	IB	68.04a	55.33b	1.23a	130.89a
2019	B	64.53b	58.24a	1.11b	123.57c
	MB	69.21a	56.98b	1.21a	138.34b
	IB	70.23a	57.28b	1.23a	142.77a
Significance					
Treatment		**	***	**	***
Year		*	**	*	***
Treatment×Year		**	***	**	***

Different letters within a column indicate significant differences among all treatments at $P < 0.05$. *, **And *** represent significant differences at the levels of $P < 0.05$, $P < 0.01$ and $P < 0.01$, respectively

Effects of activated brackish water irrigation on yield and water use efficiency of fragrant pear

Fig. 4 showed the yield and water use efficiency of fragrant pear under activated brackish water irrigation. The activated brackish water irrigation could significantly improve the yield and water use efficiency of fragrant pear ($P < 0.05$). Compared with control B treatment, the yield of fragrant pear irrigated with MB and IB increased by 11.20%, 12.47% (2018) and 22.22%, 25.08% (2019), and water use efficiency increased by 12.97%, 14.15% (2018) and 25.24%, 26.21% (2019). Zhang et al. (2020) showed that the yield of winter wheat irrigated with magnetized water increased by 8.99% and the water use efficiency increased by 5.07%, and Zhu and Li (2020) found that the yield of single tomato irrigated with ionized water increased by 19.87% and the irrigation water use efficiency increased by 37.69%, which were consistent with the results of this study. The results indicate that activated brackish water irrigation can effectively improve the yield and water use efficiency of fragrant pear. On the one hand, activated brackish water irrigation can improve the availability of soil water and nutrients (Li et al., 2020a), which is conducive to the absorption and utilization of the roots of fragrant pear fruit trees (Mostafa et al., 2016), on the other hand, activated brackish water improves the water molecular activity. It is beneficial to promote the absorption and utilization of light energy by fragrant pear leaves (Liu et al., 2019), promote the transformation of photosynthetic substances (Liu et al., 2016), and finally improve the yield and water use efficiency of fragrant pear.

Effect of activated brackish water irrigation on quality of fragrant pear

The quality grade of fragrant pear is determined by the single fruit weight, hardness, soluble solid content, total acid content and vitamin C content of fragrant pear. As can be seen from *Table 2*, activated brackish water irrigation had a significant effect on the quality of fragrant pear ($P < 0.05$). Under activated brackish water irrigation, the fruit

http://www.aloki.hu ● ISSN 1589 1623 (Print) ● ISSN 1785 0037 (Online)
DOI: http://dx.doi.org/10.15666/aeer/2001_671683

surface of fragrant pear was smooth, the peel was fine, the stem was intact, and the fruit was yellow-green. The single fruit weight of fragrant pear irrigated with brackish water was less than 120 g, which could only reach the standard of first-grade fragrant pear, while the single fruit weight of fragrant pear irrigated with activated brackish water was between 120 g and 160 g, which reached the standard of super-grade fragrant pear. Compared with control B treatment, the single fruit weight of fragrant pear irrigated with MB and IB increased by 15.96%, 19.07% (2018) and 20.33%, 22.62% (2019), hardness decreased by 21.69%, 23.90% (2018) and 20.65%, 21.61% (2019), soluble solids increased by 4.41%, 4.25% (2018) and 8.48%, 8.64% (2019), total acid decreased by 13.01%, 12.33% (2018) and 16.78%, 17.72% (2019), and the content of vitamin C decreased slightly, but not significantly ($P > 0.05$). This result is consistent with the result of Jia et al. (2019) using magnetized water to irrigate Lingwu winter jujube. Thus, activated brackish water irrigation can effectively improve the fruit soluble solid content, reduce the total acid content and improve the taste of fragrant pear to a certain extent. This is mainly because activated brackish water irrigation can improve the utilization rate of light energy of fragrant pear fruit trees, affect the allocation of photosynthetic products (Cai et al., 2020), and then improve the sugar acid balance inside the fruit (Wei et al., 2020).

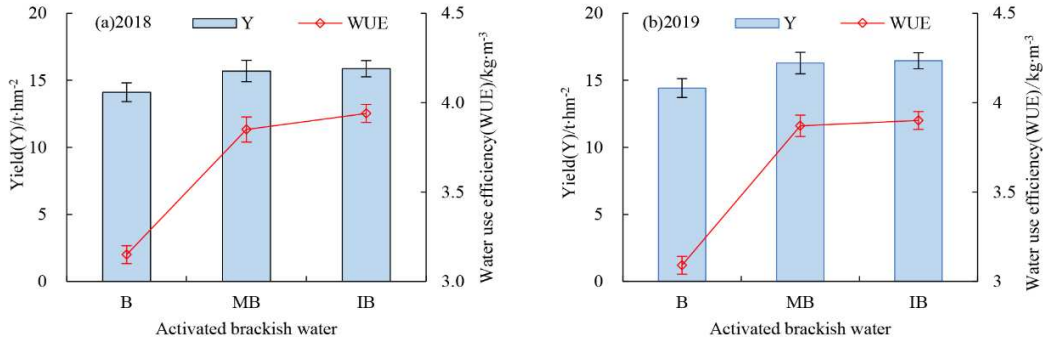

Figure 4. *Yield and water use efficiency of fragrant pear under activated brackish water irrigation. B, MB and IB represent brackish water, magnetized brackish water and ionized brackish water, respectively. The error bars represent standard deviations*

Table 2. *The fruit quality index of fragrant pear under activated brackish water irrigation. B, MB and IB represent brackish water, magnetized brackish water and ionized brackish water, respectively*

Year	Treatment	Single fruit weight (g)	Solidity (kg·cm^{-2})	Soluble solids (%)	Total acidity (%)	Vitamin C (mg·kg^{-1})
2018	B	113.76b	5.44a	12.24b	0.44a	6.10a
	MB	131.92a	4.26b	12.78a	0.38b	6.05a
	IB	135.45a	4.14b	12.76a	0.38b	6.07a
2019	B	118.43b	5.23a	12.38b	0.43a	6.50a
	MB	142.51a	4.15b	13.43a	0.36b	6.42a
	IB	145.22a	4.10b	13.45a	0.35b	6.45a
Significance						
Treatment		**	**	**	**	NS
Year		*	*	**	*	NS
Treatment×Year		***	**	***	**	NS

Different letters within a column indicate significant differences among all treatments at $P < 0.05$. *, **And *** represent significant differences at the levels of $P < 0.05$, $P < 0.01$ and $P < 0.01$, respectively, and NS represents no significant difference ($P > 0.05$)

http://www.aloki.hu ● ISSN 1589 1623 (Print) ● ISSN 1785 0037 (Online)
DOI: http://dx.doi.org/10.15666/aeer/2001_671683

Conclusions

In this study, the effects of activated brackish water irrigation on the growth, fruit shape, yield, quality and water use efficiency of fragrant pear trees aged 15 years were studied through a two-year field irrigation experiments. The main conclusions are as follows:

(1) The activated brackish water irrigation can effectively improve the soil water content. During the growth period, the soil water content of the main root of fragrant pear fruit trees increases by 13.07%-28.15%.

(2) The maximum new shoot length of fragrant pear fruit trees irrigated with activated brackish water increased by 17.87%-51.12%, the fruit volume increased by 8.96%-15.54%, and the fruit shape of fragrant pear tended to be oval.

(3) Activated brackish water irrigation can not only improve the yield and water use efficiency of fragrant pear, but also improve the soluble solid content, reduce the total acid content and improve the taste of fragrant pear.

Generally speaking, in arid areas where fresh water is scarce, using activated brackish water instead of brackish water to irrigate fragrant pear can obtain a higher yield and quality. However, the optimal amount of irrigation and fertilization of fragrant pear irrigated with activated brackish water need to be further studied.

Acknowledgements. This study was funded by the National Natural Science Foundation of China (41830754 and 52179042).

REFERENCES

[1] Abdel-Kader, H. H., El-Saady, W. A., Zaky, H. A. (2020): Effect of magnetized water and NPK fertilization treatments on growth and field performance of gladiolus. – Journal of Plant Production 11(7): 627-632.

[2] Al-Bayar, M. A., Mahmood, R. M., Saieed, A. Y. (2020): Magnetic treated water, reality and applications: A review. – Plant Archives 20(2): 732-737.

[3] Boe, A. A., Salunkhe, D. K. (1963): Effects of magnetic fields on tomato ripening. – Nature 199: 91-92.

[4] Bu, D. S., Feng, W. G., Cai, L. H., Zhou, L. (2010): Effects of magnetization water on desalinization in cotton farmland of under-film dripping irrigation in XinJiang Province. – Transactions of the Chinese Society of Agricultural Engineering 26(3): 163-166. (in Chinese with English abstract).

[5] Cai, M. L., Li, Y. Y., Fan, J. (2020): Effects of magnetized water on growth, photosynthesis and nutrient uptake of cucumber seedlings under different soil moisture contents. – Agricultural Research in the Arid Areas 38(5): 94-100. (in Chinese with English abstract).

[6] Chen, W., Jin, M., Ferré, T. P. A., Liu, Y., Xian, Y., Shan, T., Ping, X. (2018): Spatial distribution of soil moisture, soil salinity, and root density beneath a cotton field under mulched drip irrigation with brackish and fresh water. – Field Crops Research 215(4): 207-221.

[7] Chen, J., Lü, J., He, Z., Zhang, F., Zhang, S., Zhang, H. (2020a): Investigations into the production of volatile compounds in Korla fragrant pears (*Pyrus sinkiangensis* Yu). – Food chemistry 302(3): 125337.

[8] Chen, W., Jin, M., Ferré, T. P. A., Liu, Y., Huang, J., Xian, Y. (2020b): Soil conditions affect cotton root distribution and cotton yield under mulched drip irrigation. – Field Crops Research 249: 107743.

http://www.aloki.hu ● ISSN 1589 1623 (Print) ● ISSN 1785 0037 (Online)
DOI: http://dx.doi.org/10.15666/aeer/2001_671683

[9] Chibowski, E., Szcześ, A. (2018): Magnetic water treatment–A review of the latest approaches. – Chemosphere 203(2): 54-67.
[10] Hamza, J. N. (2019): Investigation on using magnetic water technology for leaching high saline-sodic soils. – Environmental monitoring and assessment 191(8): 1-11.
[11] Han, S., Yang, Y., Li, H., Yang, Y., Wang, J., Cao, J. (2019): Determination of crop water use and coefficient in drip-irrigated cotton fields in arid regions. – Field Crops Research 236(2): 85-95.
[12] Jia, H., Li, L., Cao, B. (2019): Effects of magnetized water irrigation on vegetative growth and fruit quality of lingwuchangzao. – Journal of Nuclear Agricultural Sciences 33(11): 2280-2286. (in Chinese with English abstract).
[13] Li, F., Wu, J., Hu, R., Ma, B. X. (2011): Quantitative analysis and classification of fruit shape in Korla fragrant pear. – Journal of Shihezi University (Natural Science) 29(04): 514-517. (in Chinese with English abstract).
[14] Li, M., Du, Y., Zhang, F., Bai, Y., Fan, J., Zhang, J., Chen, S. (2019): Simulation of cotton growth and soil water content under film-mulched drip irrigation using modified CSM-CROPGRO-cotton model. – Agricultural Water Management 218: 124-138.
[15] Li, J., Fan, J., Zhu, Z. M. (2020a): Effects of activated water irrigation on growth characteristics of soybean under drought stress. – Chinese Journal of Applied Ecology 31(11): 3711-3718. (in Chinese with English abstract).
[16] Li, N., Lin, H., Wang, T., Li, Y., Liu, Y., Chen, X., Hu, X. (2020b): Impact of climate change on cotton growth and yields in Xinjiang, China. – Field Crops Research 247(4): 107590.
[17] Liang, J., Shi, W., He, Z., Pang, L., Zhang, Y. (2019): Effects of poly-γ-glutamic acid on water use efficiency, cotton yield, and fiber quality in the sandy soil of southern Xinjiang, China. – Agricultural Water Management 218: 48-59.
[18] Liu, X., Wang, H. T., Wang, Y. P., Ma, F. Y., Wang, L., Wan, X. (2016): Analysis of magnetic salinity water irrigation promoting growth and photosynthetic characteristics of Populus×euramericanna '*Neva*'. – Transactions of the Chinese Society of Agricultural Engineering 32(1): 1-7. (in Chinese with English abstract).
[19] Liu, X., Zhu, H., Meng, S., Bi, S., Zhang, Y., Wang, H., Song, C., Ma, F. (2019): The effects of magnetic treatment of irrigation water on seedling growth, photosynthetic capacity and nutrient contents of Populus× euramericana '*Neva*'under NaCl stress. – Acta Physiologiae Plantarum 41(1): 1-13.
[20] Liu, X., Wang, L., Wei, Y., Zhang, Z., Zhu, H., Kong, L., Meng, S., Song, C., Wang, H., Ma, F. (2020): Irrigation with magnetically treated saline water influences the growth and photosynthetic capability of *Vitis vinifera L.* seedlings. – Scientia Horticulturae 262: 109056.
[21] Liu, J., Cao, Y. (2021): Experimental study on the surface tension of magnetized water. – International Communications in Heat and Mass Transfer 121: 105091.
[22] Maheshwari, B. L., Grewal, H. S. (2009): Magnetic treatment of irrigation water: Its effects on vegetable crop yield and water productivity. – Agricultural water management 96(8): 1229-1236.
[23] Mostafa, M. F. M., El-Boray, M. S. S., Shalan, A. M. N., Ghaffar, A. H. (2016): Effect of magnetized irrigation water levels and compost on vegetative growth, leaf mineral content and water use efficiency of Washington navel orange trees. – Journal of Plant Production 7(2): 249-255.
[24] Mu, Y., Zhao, G. Q., Zhao, Q. Q. (2019): Advances in the application of activated water irrigation. – Journal of Agricultural Resources and Environment 36(04): 403-411. (in Chinese with English abstract).
[25] Niu, Y., Chen, X., Zhou, W., Li, W., Zhao, S., Nasir, M., Dong, S., Zhang, S., Liao, K. (2019): Genetic relationship between the 'Korla fragrant pear' and local pear varieties in xinjiang based on floral organ characteristics. – Scientia Horticulturae 257: 108621.

http://www.aloki.hu ● ISSN 1589 1623 (Print) ● ISSN 1785 0037 (Online)
DOI: http://dx.doi.org/10.15666/aeer/2001_671683

[26] Qiu, N., Tan, Y., Shen, X., Han, R., Lin, Y., Ma, Z. (2011): Biological effects of magnetized water on seed germination, seedling growth and physiological characteristics of wheat. – Plant Physiology Communications 47(8): 803-810.
[27] Shan, Y. Y., Li, X. J., Wang, Q. J., Ma, C. G., Zhang, J. H., Wei, K. (2021): Analysis of one-dimensional horizontal absorption characteristics and water movement parameters of magnetized brackish water. – Transactions of the Chinese Society for Agricultural Machinery 52(2): 266-274. (in Chinese with English abstract).
[28] Surendran, U., Sandeep, O., Joseph, E. J. (2016): The impacts of magnetic treatment of irrigation water on plant, water and soil characteristics. – Agricultural water management 178: 21-29.
[29] Tan, S., Wang, Q., Xu, D., Zhang, J., Shan, Y. (2017): Evaluating effects of four controlling methods in bare strips on soil temperature, water, and salt accumulation under film-mulched drip irrigation. – Field Crops Research 214: 350-358.
[30] Turker, M., Temirci, C., Battal, P., Erez, M. E. (2007): The effects of an artificial and static magnetic field on plant growth, chlorophyll and phytohormone levels in maize and sunflower plants. – Phyton Ann. Rei Bot 46: 271-284.
[31] Wang, Q. J., Zhang, J. H., Men, Q., Tan. S., Zhou, L. W., Liu, X. Y. (2016): Experiment on physical and chemical characteristics of activated brackish water by magnetization or ionization. – Transactions of the Chinese Society of Agricultural Engineering 32(10): 60-66. (in Chinese with English abstract).
[32] Wang, Y., Wei, H., Li, Z. (2018): Effect of magnetic field on the physical properties of water. – Results in Physics 8: 262-267.
[33] Wang, L., Guo, J. Y., Bi, S. S., Zhang, Z. H., Wang, H. T., Liu, X. M., Zhu, H., Tang, J., Chen, S. Y., Cong, G. Z. (2019a): Effects of irrigation with magnetized saline water on Vitis vinifera growth and soil mineral nutrients. – Journal of Fruit Science 36(12): 1683-1692. (in Chinese with English abstract).
[34] Wang, Z., Wu, Q., Fan, B., Zheng, X., Zhang, J., Li, W., Guo, L. (2019b): Effects of mulching biodegradable films under drip irrigation on soil hydrothermal conditions and cotton (*Gossypium hirsutum* L.) yield. – Agricultural water management 213: 477-485.
[35] Wang, L. L., Wu, W. Y., Xiao, J., Huang, Q. N. (2020): The effects of spatial layout of drip irrigation belts on growth and water use efficiency of golden pear. – Journal of Irrigation and Drainage 39(5): 10-17. (in Chinese with English abstract).
[36] Wang, Y. H., Sun, H. W., Wei, C. H., Wang, L. (2021): Effects of activated water on growth and root activity of wheat. – ACTA Agriculturae Boreali-Sinica 36(1): 124-133. (in Chinese with English abstract).
[37] Wei, Y., Wang, L., Zhu, H. (2020): Effects of magnetized water irrigation on growth and photosynthetic characteristics of grape under nitrogen application. – Journal of Nuclear Agricultural Sciences 34(04): 849-859. (in Chinese with English abstract).
[38] Wu, Y., Wang, W., Huang, X. F., Ren, D. X., Su, L. Y., Liu, Z. H. (2012): Yield and root growth of mature Korla fragrant pear tree under deficit irrigation. – Transactions of the Chinese Society for Agricultural Machinery 43(09): 78-84. (in Chinese with English abstract).
[39] Yuan, C., Feng, S., Huo, Z., Ji, Q. (2019): Effects of deficit irrigation with saline water on soil water-salt distribution and water use efficiency of maize for seed production in arid Northwest China. – Agricultural water management 212: 424-432.
[40] Zhang, Y. Y., Song, N., Shan, Z. J., Liu, X. F., Ning, H. F., Wu, J. L., Chen, Z. F. (2020): Effects of magnetic treatment of irrigation water on yield and water use efficiency of winter wheat. – Journal of Irrigation and Drainage 39(6): 60-66. (in Chinese with English abstract).
[41] Zhao, G., Mu, Y., Wang, Y., Wang, L. (2021): Response of winter-wheat grain yield and water-use efficiency to irrigation with activated water on Guanzhong Plain in China. – Irrigation Science 39(2): 263-276.

http://www.aloki.hu ● ISSN 1589 1623 (Print) ● ISSN 1785 0037 (Online)
DOI: http://dx.doi.org/10.15666/aeer/2001_671683

[42] Zhou, B., Yang, L., Chen, X., Ye, S., Peng, Y., Liang, C. (2021): Effect of magnetic water irrigation on the improvement of salinized soil and cotton growth in Xinjiang. – Agricultural Water Management 248: 106784.
[43] Zhu, M., Li, B. (2020): Effects of irrigation with de-electronic water on yield, quality and water use efficiency of tomato grown in greenhouse. – Water Saving Irrigation 11: 20-24. (in Chinese with English abstract).

http://www.aloki.hu ● ISSN 1589 1623 (Print) ● ISSN 1785 0037 (Online)
DOI: http://dx.doi.org/10.15666/aeer/2001_671683

EFFECTS OF DROUGHT STRESS ON TASSEL GROWTH AND CHARACTERISTICS PHYSIOLOGICAL OF MAIZE VARIETIES

LI, J.[1,2†] – WANG, T.[1,2†] – WANG, C.[1,2] – CUI, R.[1,2] – ZHANG, X.[1,2] – FENG, Q.[1,2] – LIU, S.[1,2*] – XIE, Z.[3*]

[1]*College of Resources and Environment, Jilin Agricultural University, Changchun 130118, China*

[2]*Key Laboratory of Sustainable Utilization of Soil Resources in Commodity Grain Base of Jilin Province, Changchun 130118, China*

[3]*College of Plant Science, Jilin University, Changchun, 130062, China.*

[†]*These authors contributed equally.*

**Corresponding authors*
e-mail: liushuxia2005824@163.com, xiezl@jlu.edu.cn

(Received 21st Aug 2021; accepted 23rd Nov 2021)

Abstract. This study explored the effects of drought stress on the growth and characteristics physiological of different maize varieties. Three maize varieties with different levels of drought tolerance (strong drought tolerance JQ707, medium drought tolerance ND19 and weak drought tolerance FD16) were selected as test crops in a plot experiment while artificial rain shelters were used to control moisture and drought stress. This study was carried out under different degrees of drought stress at the ear stage of maize (Normal water supply, CK; mild drought stress, C1; moderate drought stress, C2; severe drought stress, C3). The results show that drought stress will significantly affect the growth and physiological characteristics of maize tassels. Among them, the anti-oxidant enzyme activity and the content of osmotic adjustment substances in the maize tassels of JQ707 reach the peak value at C2 treatment, which is used to resist the phenomenon of plant water shortage. The anti-oxidant system and osmotic adjustment ability of FD16 maize tassels were poor, and the external morphological structure was also relatively short. This study also found that appropriate stress is beneficial to promote the growth and development of maize tassels and the physiological reaction process. The conclusions of experiment can provide a certain theoretical basis for drought resistance and yield of maize planting in Northeast China.
Keywords: *water stress, maize tassels, morphological traits, physiological traits*

Introduction

Crop growth and development will be limited by environmental factors, such as drought is considered to be one of the important factors (Fathi and Barari, 2016). Maize (*Zea mays L.*) is not only one of the most widely planted crops in the world, but also an important food crop and economic crop in China. Northeast China is the main maize producing area in China. In recent years, the trend of drought in Northeast China became more and more serious, which poses a serious threat to maize yield (Yang et al., 2015; Zhang et al., 2011; Fu et al., 2020). The growth cycle of maize can be divided into seedling stage, ear stage, and flowering stage. The ear stage is the key period of maize water demand, and water deficit in this period will affect maize yield to a great extent (Jia et al., 2020; Li et al., 2019). As an important reproductive organ of maize, the development of tassel is closely related to the yield of maize. The tassels of a different maize varieties showed different adaptability to different arid environments, it is specifically reflected in the morphological structure and physiological function of tassels (Xu et al., 2012; Gage et al., 2018). Under drought stress, maize tassels will adapt to

http://www.aloki.hu ● ISSN 1589 1623 (Print) ● ISSN 1785 0037 (Online)
DOI: http://dx.doi.org/10.15666/aeer/2001_685697

drought stress through changes in morphology, antioxidant enzymes and osmotic regulation substances accumulation. The development of tassels plays an important role in coordinating the development of male and female tassels, even increasing grain yield in maize (Abdoul et al., 2016; Li et al., 2020). Drought stress will cause the maize tassels to become smaller, and the tassels will be drawn out slowly or even unable to be drawn out (Song et al., 2005). A large number of studies have been done on the effects of drought stress on the physiological characteristics of maize (Zhuang, 2007; Zhang et al., 2012; Liu, 2020; Gill and Tuteja, 2010). For example, maize plants would produce a large number of reactive oxygen species after drought stress (Fathi and Barari, 2016). Reactive oxygen molecules are prone to disrupt the balance of the cell's internal environment. Its excessive presence will lead to lipid reaction of the cell membrane and destroy the structure of protein and enzyme on the cell membrane (Dumanović et al., 2021). To avoid the disturbance of the internal cell environment caused by excessive drought, maize will produce a series of defense mechanisms (Sayadi et al., 2016; Zhao, 2016). The antioxidant system enzymes played a positive role in eliminating excessive oxygen free radicals (Guo et al., 2018); under drought stress, the presence of soluble protein, proline and soluble sugar could maintain the balance of intracellular osmotic pressure and improve the stress resistance of crops, which also play a key role in resisting adversity stress (Tahereh et al., 2011; Blum, 2017; Liu et al., 2011). Therefore, it is of great significance to explore the influence mechanism of different degrees of drought stress on the tassel of different maize varieties.

At present, many studies have demonstrated the effects of drought stress on the growth and physiological traits of maize, most of them, however, only discuss the effects on the growth morphology of maize plants and the physiological characteristics of ear leaves, there are few types of researches on the morphological and physiological characteristics of maize tassels. Therefore, to explore and clarify the effects of curing on tassel growth and physiological characteristics of different maize varieties, this experiment selected three different maize varieties for comparison at the same time and analyzed the morphology and structure of male panicle of different maize varieties, as well as the enzyme activity of the antioxidant system, the content of osmotic regulating substances and the content of malondialdehyde by setting different degrees of drought stress. It will provide a certain theoretical basis for drought resistance and yield protection of maize in Northeast China.

Materials and methods

Experimental design

The research was conducted in the Qiqihar Branch of Heilongjiang Academy of Agricultural Sciences, China (47°17'33"N, 123°43'20"E) (*Fig. 1A*). Details of climatic conditions of the maize growth cycle are shown in *Figure 1B*. The general situation of the test site and the growth of maize in the test are shown in *Figure 2*. The tested soil was chernozem and the basic characteristics of the soil (0-20 cm) were as follows: pH, 7.82; organic matter, 26.1 $g \cdot kg^{-1}$; available nitrogen, 102 $g \cdot kg^{-1}$; available phosphorus 15.9 $mg \cdot kg^{-1}$; available potassium, 130 $mg \cdot kg^{-1}$.

The tested crop was the three varieties of maize: Jinqing 707 (JQ707) with strong drought tolerance, Nendan 19 (ND19) with medium drought tolerance, and Fudan 16 (FD16) with weak drought tolerance. A total of 12 plots were set up in the experiment, each with an area of 12 m^2 (4 m × 3 m). In order to simulate natural drought conditions,

http://www.aloki.hu ● ISSN 1589 1623 (Print) ● ISSN 1785 0037 (Online)
DOI: http://dx.doi.org/10.15666/aeer/2001_685697

open the mobile rain-proof shelter in rainy days to control soil moisture, and close the shelter in sunny days to make maize photosynthesis normally.

The experiment was conducted in maize period different degrees of drought stress, set up to deal with four different moisture gradient, normal water supply as control (CK, keep the soil moisture content is more than 80% of field capacity), mild drought stress (C1, keep the soil moisture maintained at 70%-80% of field capacity), moderate drought stress (C2, keep the soil moisture maintained at 60%-70% of field capacity) and severe drought stress (C3, keep the soil moisture maintained at 50%-60% of field capacity). During the stress period, a soil moisture content analyzer (Instrument model: TZS-1K-G) was used to regularly detect the soil moisture content, and water was supplemented according to the measured moisture content to ensure that the soil moisture content during the stress period was within the set soil moisture content range. A one-time application of fertilizer 30 kg, N: P: K = 22:14:6. Each treatment was repeated three times with a normal water supply as control (CK), and each repeat contains three maize plants.

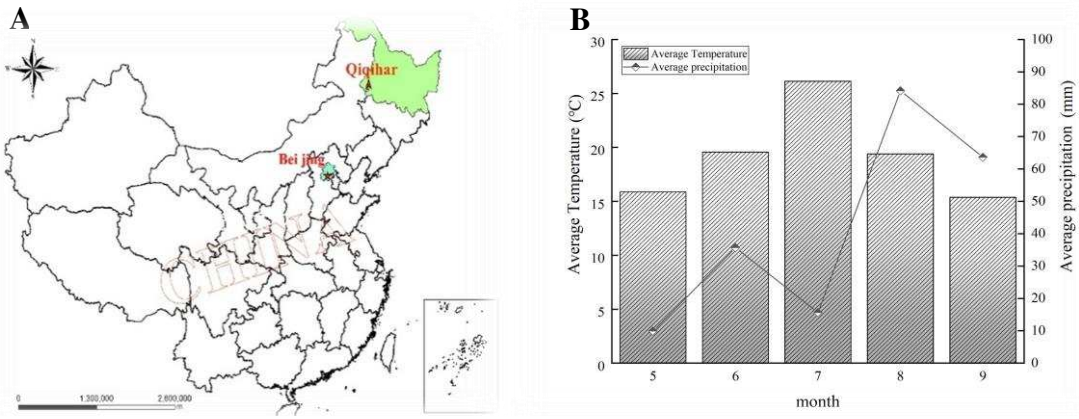

Figure 1. *Experimental location and climatic conditions of maize growth cycle*

Figure 2. *Overview of the test site and the growth of maize in the test*

Determination of morphological index in tassel of maize

Tassel size = tassel spindle length + average branch length × branching number.

Spindle length of tassel was measured with a tape measure. The spindle diameter is measured with a vernier caliper. Dry matter weight was determined by the drying method.

http://www.aloki.hu ● ISSN 1589 1623 (Print) ● ISSN 1785 0037 (Online)
DOI: http://dx.doi.org/10.15666/aeer/2001_685697

Determination of physiological index in tassel of maize

The enzyme activities of the antioxidant system were detected by the ELISA detection kit. Weigh 1 g tassel sample, cut it into pieces, put it into a mortar, add 10 ml PBS buffer solution and grind it fully, after centrifugation at 4000 $r \cdot min^{-1}$ for 15 min, and then take the supernatant. The enzymatic activities of SOD, CAT, and POD in a tassel of maize were determined by an enzymatic plate analyzer. The content of proline was determined by sulfosalicylic acid method; Soluble sugar content was determined by anthrone colorimetry; Soluble protein content was determined by coomassie bright blue method; The content of malondialdehyde was determined by thiobarbituric acid method; The methods were based on Zou (2003).

Data analysis

All data were produced using Microsoft Excel 2016 software. The experimental data are all used SPSS 21.0 software for one-way statistical analysis of variance, and Origin 2018 software for plotting.

Results

Effects of drought stress on morphological traits in tassel of different maize varieties

To explore the effect of drought stress on the morphological structure of the tassel of different maize varieties, the following analysis from four aspects were made: tassel size, spindle length, spindle diameter, and dry matter weight (*Table 1*).

Table 1. *Effects of drought stress on the morphological structure of tassels of different maize varieties*

Treatment	Maize variety	Tassel size (cm)	Spindle length (cm)	Coarse spindle (mm)	Tassel dry weight (g)
CK	JQ707	188.17 ± 8.61a	38.67 ± 3.06a	6.00 ± 0.50a	3.09 ± 0.08a
	ND19	187.70 ± 13.79a	35.67 ± 2.52a	5.93 ± 0.81a	3.14 ± 0.13a
	FD16	156.60 ± 7.86b	35.33 ± 1.53a	6.30 ± 0.82a	2.98 ± 0.06a
C1	JQ707	179.33 ± 10.68a	35.19 ± 0.76a	4.83 ± 0.76a	3.23 ± 0.22a
	ND19	178.79 ± 8.28a	31.33 ± 2.93a	5.17 ± 0.29a	3.21 ± 0.08a
	FD16	143.68 ± 12.71b	32.17 ± 0.76a	4.83 ± 0.29a	3.03 ± 0.02b
C2	JQ707	163.42 ± 3.85a	35.05 ± 0.93a	5.00 ± 0.87a	2.53 ± 0.02a
	ND19	153.91 ± 12.06a	31.17 ± 0.76b	4.37 ± 0.71a	3.02 ± 0.03a
	FD16	121.81 ± 6.10b	31.51 ± 0.77b	4.50 ± 0.50a	2.21 ± 0.27a
C3	JQ707	148.36 ± 7.29a	34.83 ± 0.76a	4.67 ± 0.76a	2.28 ± 0.02a
	ND19	137.23 ± 12.97a	31.23 ± 0.71b	4.43 ± 0.81a	2.89 ± 0.12a
	FD16	111.37 ± 13.86b	29.50 ± 0.50c	4.13 ± 1.21a	1.89 ± 0.08a

Data in the table are mean ± standard deviation, and different lowercase letters after data in the same column indicate significant difference ($P < 0.05$)

As can be seen from *Table 1,* with the increase of drought stress, the tassel size of different maize varieties decreased to different degrees, tassel spindle length, and diameter of tassel spindle shortened to different degrees, and the effects of drought on

http://www.aloki.hu ● ISSN 1589 1623 (Print) ● ISSN 1785 0037 (Online)
DOI: http://dx.doi.org/10.15666/aeer/2001_685697

different varieties were different. Among all the drought stress treatments, JQ707 was the least affected. Under normal water supply, the tassel size of FD16 was smaller than that of JQ707 and ND19, but there was no significant difference in the length and diameter of its main axis. Under severe drought stress, the tassel size, spindle length and spindle diameter of the tested maize varieties were the lowest values relative to CK. The main shaft length of the tassel of JQ707, ND19, and FD16 was shortened by 11.02%, 14.22%, and 19.76%, and the main shaft diameter of the tassel was reduced by 28.48%, 33.86%, and 52.54%, respectively.

With the increase of drought stress, the dry matter weight of different maize tassels showed a trend of first increasing and then decreasing. Mild drought stress can promote the accumulation of dry matter in tassels. Compared with CK, the dry matter weight of JQ707, ND19, and FD16 increased by 4.33%, 2.18%, and 1.65%, respectively. Moderate and severe drought stress was not conducive to dry matter accumulation in the tassels of maize. The dry matter weight of the three varieties of maize decreased compared with that of CK. The dry matter accumulation was the order of ND19 > JQ707 > FD16.

Effects of drought stress on physiological characteristics of different maize varieties

Effects of drought stress on enzyme activity of antioxidant system and malondialdehyde content in tassel of different maize varieties

To investigate the effects of drought stress on the contents of antioxidant enzymes and MDA in a different tassel of maize, the following analysis was conducted: as shown in *Figure 2A,* there was no significant difference in SOD content of tassel under different drought stress, but SOD had a higher content in tassels. The SOD content in the tassels of the weak drought-tolerant variety FD16 can be maintained above 800 $U \cdot g^{-1}$, and the content of strong drought-tolerant variety JQ707 and medium drought-tolerant variety ND19 can be maintained above 1000 $U \cdot g^{-1}$. This indicates that SOD plays an important role in the tassel of maize, and its role is to decompose excessive $O^{2\cdot -}$ in the body so as to prevent the subsequent formation of hydrogen peroxide and hydroxyl radicals. The change of SOD content can also indicate that its secretion level did not change significantly with the degree of drought. The enzyme activity of FD16 was the highest under moderate drought stress, which was 22.95% higher than that of CK, and its activity returned to the level of CK under severe drought stress. Under moderate drought stress, the enzyme activities of JQ707 and ND19 were 29.38% and 22.80%, which were higher than those of CK, respectively, and under severe drought stress, the enzyme activities were also 9.67% and 6.66%, which were also higher than those of CK, respectively. Therefore, we can see the difference of SOD activity in tassel between drought-tolerant maize and drought-resistant maize under drought conditions.

As shown in *Figure 2B* and *C,* the activity change trend of CAT and POD is different from SOD. The activities of CAT and POD were significantly affected by drought stress. The overall trend of CAT is that the enzyme activity reaches its peak under moderate drought stress and decreased under severe drought stress. Under mild and moderate drought stress, the most significant change was CAT in JQ707 and ND19, the CAT secretion of them was more than twice that CK treatment, and under severe drought stress, it was also increased by 38.45% and 35.92%, respectively. However, for the weak drought-tolerant variety FD16, the changes in CAT activity in

http://www.aloki.hu ● ISSN 1589 1623 (Print) ● ISSN 1785 0037 (Online)
DOI: http://dx.doi.org/10.15666/aeer/2001_685697

its tassels are not significant. The activity of SOD under mild drought stress was 36.04% higher than that of CK, while its secretion volume under severe drought stress was not significantly different from that of CK. The reason why the content of CAT in the tassels changes so significantly was probably due to the excessive formation of superoxide free radicals in the tassel cells under drought conditions and the secretion of SOD did not change much. Therefore, excessive oxygen free radicals will induce the production of H_2O_2, and the maize tassels will secrete excessive CAT to eliminate H_2O_2. The POD exists in the CAT enzyme body, the secretion of CAT increased and POD also increased, and the mode of action of POD was to use hydrogen peroxide as the electron acceptor to catalyze the oxidation of the substrate, thereby, removing harmful substances produced in plants due to adversity, such as hydrogen peroxide, oxidized phenols, and amines. This also indirectly explained the drought tolerance of the three maize varieties.

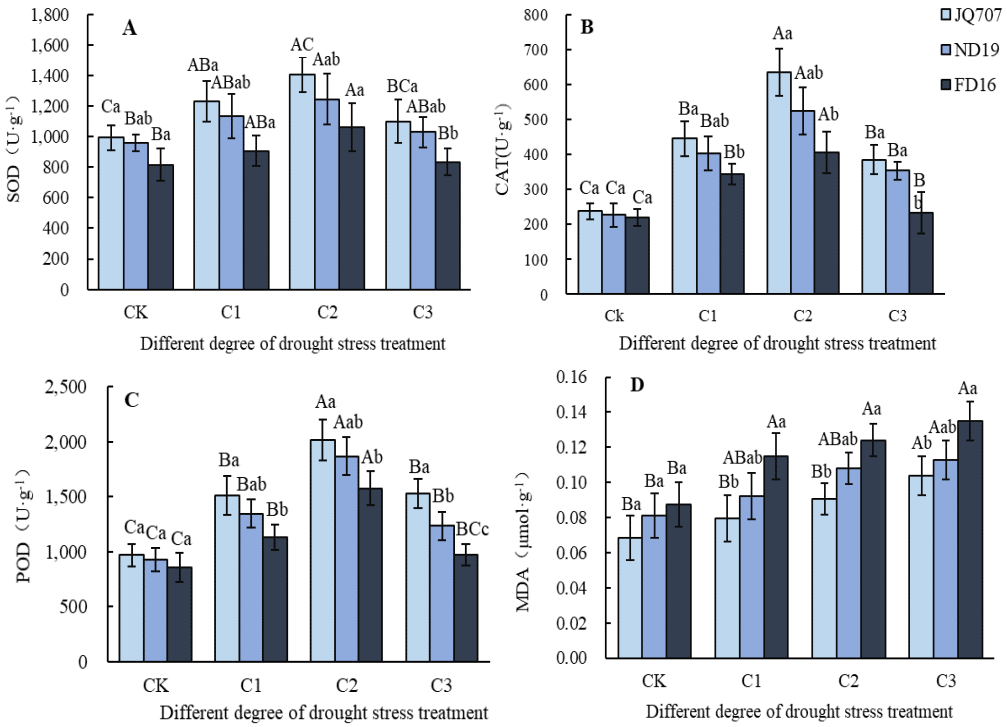

Figure 2. *Effects of drought stress on the activities of antioxidant enzymes (SOD, POD and CAT) and MDA content in tassels of different maize varieties. The error column shown in the figure is the positive and negative deviation of the standard deviation of antioxidant enzyme data of different maize tassels under the same drought treatment. Capital English letters represent the significant difference of antioxidant enzyme activity between different drought stress treatments under the same maize variety, and small letters represent the significant difference of antioxidant enzyme activity data of different maize tassels under the same drought stress treatment*

As shown in *Figure 2D,* the content of MDA increased significantly with the increase of drought. The growth rates of JQ707, ND19, and FD16 were 11.8%, 11.1%, and 15.2%, respectively. Under severe drought stress, the MDA content in the tassels of the three maize varieties all reached a peak. The MDA content of FD16 increased by 35.16% compared with CK under severe drought stress, and the secretion of FD16

http://www.aloki.hu ● ISSN 1589 1623 (Print) ● ISSN 1785 0037 (Online)
DOI: http://dx.doi.org/10.15666/aeer/2001_685697

increased significantly compared with JQ707 and ND19. This was because the secretion of SOD, CAT, and POD in the tassel of FD16 returned to a low level under severe drought stress, unable to decompose too many harmful substances, resulting in a sharp increase in MDA content, while the changing trend of JQ707 and ND19 was less obvious. Since MDA can be used as a criterion for judging the degree of cell damage, the change in its content can show the stress resistance of maize ears, which also proves to a certain extent that these two maize varieties, JQ707 and ND19, have strong resistance to stress.

Effects of drought stress on the content of osmotic regulating substances in tassel of different maize varieties

In order to explore the effect of drought stress on the osmotic mechanism of different maize tassels, the following analysis was conducted: as shown in *Figure 3A,* the specific expression of Pro secretion in a tassel of maize was as follows: the growth rate of Pro in tassels of JQ707 and FD16 was higher under mild drought, which increased by 20.8% and 17.73% compared with CK, respectively, and slightly lower at moderate levels, while the changing trend of ND19 was opposite to the two. Under severe drought stress, the secretion rate of Pro in the three maize tassels all decreased, but the secretion of JQ707 was still the highest among the three. The reason was probably that the regulation mechanism of proline in different maize tassels was different under mild and moderate drought. JQ707 and FD16 had higher Pro secretion in the early drought period. These maize varieties paid more attention to osmotic pressure regulation in the early drought period so that they could pass through the middle drought period smoothly, while ND19 paid more attention to the regulation in the middle drought period. Under severe drought, ND19 and FD16 increased tassel cell damage and decreased Pro secretion, but the Pro secretion of JQ707 did not decrease but increased, which proved its strong drought resistance to a certain extent.

As shown in *Figure 3B,* under mild and moderate drought stress, the accumulation of SP in the tassels of the three varieties increased rapidly, and the secretion growth rate reached 60%, 37%, and 32%, respectively, while under severe drought, the secretion rate of the three varieties all decreased. Although the SP secretion rate in FD16 tassels under severe drought exceeded 20%, the SP content in tassels was only 5.67 $mg \cdot g^{-1}$, which was the same as that of JQ707 under mild drought. This also proved the reason for the strong drought resistance of JQ707.

As shown in *Figure 3C,* the change of SS content in tassels also increased with the increase of drought degree, but there was no significant difference among the treatments. Compared with JQ707 and ND19, the secretion rate of SS in tassels of FD16 was always low, and its highest content was only 3.35 $mg \cdot g^{-1}$, which was equivalent to the content of JQ707 and ND19 under mild and moderate drought, indicating that the secretion ability of SS in maize tassel of FD16 was poor. Under mild drought, SS accumulation in male panicles of ND19 was higher, but under moderate and severe drought, SS secretion rate in male panicles of ND19 was significantly reduced, which indicated that SS regulation ability of ND19 was stronger under mild drought. For all treatments, the accumulation of SS in the tassels of JQ707 was at a higher level. Under severe drought stress, the SS secretion rate in the tassels was 3-4 times higher than that of ND19 and FD16, and the SS content in the tassels could reach 4.22 $mg \cdot g^{-1}$. This showed that JQ707 SS had a strong secretion ability and good stress resistance.

http://www.aloki.hu ● ISSN 1589 1623 (Print) ● ISSN 1785 0037 (Online)
DOI: http://dx.doi.org/10.15666/aeer/2001_685697

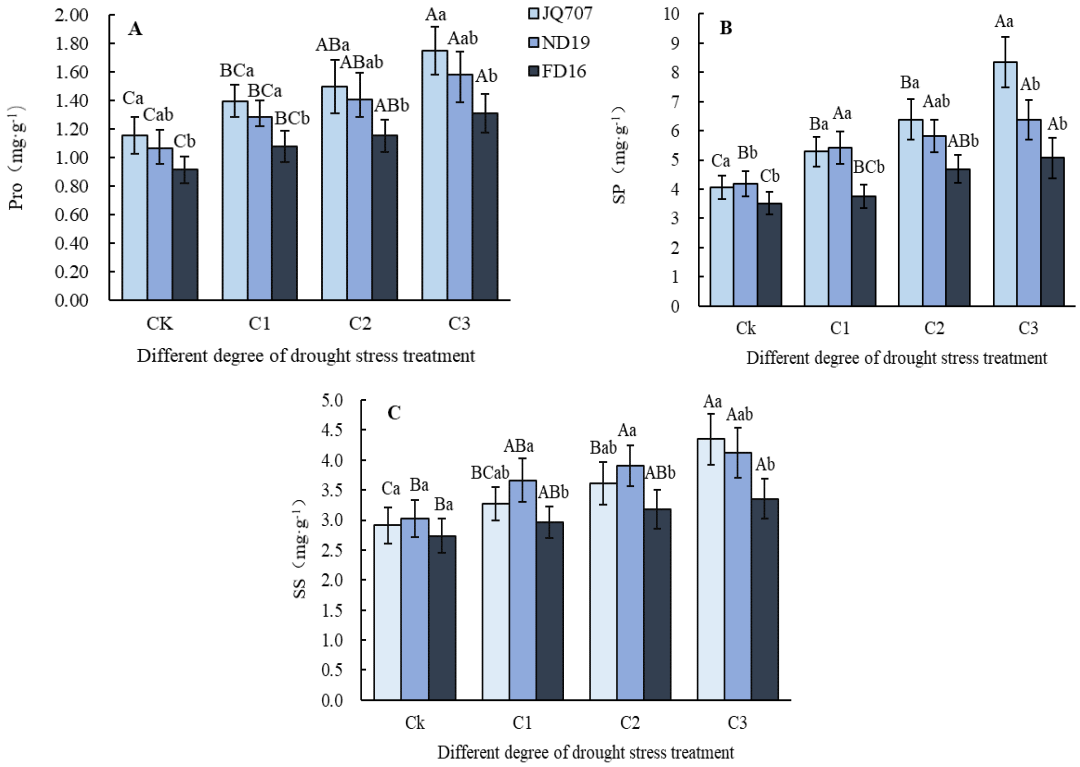

Figure 3. *Effect of drought stress on osmotic adjustment substances (Pro, SP and SS) in tassels of different maize varieties. The error column shown in the figure is the positive and negative deviation of the standard deviation of osmotic adjustment substances data of different maize tassels under the same drought treatment. Capital English letters represent the same maize variety, and the contents of osmotic adjustment substances in different drought stress treatments are significantly different, while small letters represent the same drought stress treatment, and the contents of osmotic adjustment substances in different maize tassels are significantly different*

Discussion

In this experiment, the poor performance of weak drought-tolerant varieties was due to the poor secretion ability of antioxidant enzymes compared with the other two varieties, and during severe drought, the antioxidant system enzymes in the tassels cannot be excessively secreted, their secretions return to normal levels, unable to eliminate the excessive harmful substances produced in the tassels. Medium drought-tolerant varieties have higher antioxidant system enzyme activity than weak drought-tolerant varieties, which can decompose excessive oxygen free radicals and harmful substances in the tassels to improve the stress resistance of the tassels. In all treatments, the strong drought-tolerant varieties have higher secretion of antioxidant system enzymes and strong cell activity, and the tassels have strong stress resistance and perform well under drought stress. Previous studies in other plants have also found that drought-tolerant plant varieties have a strong antioxidant enzyme system to effectively control the content of active oxygen in the body (Hou et al., 2018; Zhang et al., 2018; Xu et al., 2014).

The possible mechanism of the antioxidant system in maize tassels as shown in *Figure 4A:* under drought conditions, maize cells will lose water, then it will produce a

http://www.aloki.hu ● ISSN 1589 1623 (Print) ● ISSN 1785 0037 (Online)
DOI: http://dx.doi.org/10.15666/aeer/2001_685697

large number of reactive oxygen molecules. These oxygen free radicals can cause oxidative damage to the cell membrane, induce its lipidation, and produce a large amount of malondialdehyde (MDA). A large number of reactive oxygen species and MDA could change the fluidity and permeability of cell membranes. Finally, damage the structure and function of cells. This excessive damage encourages the endocrine of the maize tassel to secrete antioxidant system enzymes (such as SOD, POD, and CAT) to eliminate this side effect. For example, SOD eliminates $O^{2\cdot-}$in the cell, thereby generating H_2O and O_2, which can avoid subsequent oxidation reactions. The POD and CAT mainly eliminate the H_2O_2 molecules in the maize tassel and also produce water and O_2, reducing the active oxygen content in the tassels to a balanced state, and the water and oxygen produced will be used by the tassels, which can compensate to a certain extent. In this way, the damage caused by drought can be compensated, and then the resistance of tassels can be enhanced.

Combined with the analysis of the mechanism of osmotic adjustment, the reason for the poor performance of weak drought-tolerant varieties under drought conditions is that the secretion ability of tassel osmotic adjustment substances is reduced and the overall content is less. Compared with the weak drought tolerant varieties, the osmotic adjustment ability of the medium drought-tolerant tassel was stronger, and the osmotic adjustment substance content in the tassel increased significantly under mild and moderate drought, but the secretion rate decreased under severe drought. The reason for strong drought-tolerance of tassel of maize may be that: (1) In the early period of drought, the internal osmotic adjustment substance accumulation in the tassel is sufficient, so the secretion rate in the later period was slow; (2) Due to severe drought, the cells lose water and their activity decreases, resulting in a decrease in the secretion rate of osmotic substances.

In this study, the change of osmotic adjustment substance content and the changing trend of antioxidant system enzymes are basically the same. This indicates that osmotic regulation can protect the enzyme activity that is beneficial to the removal of active oxygen under drought conditions, which is basically consistent with the results of previous studies (Xu et al., 2014).

The possible mechanism of osmotic adjustment in maize tassels is shown in *Figure 4B:* under drought conditions, maize cannot normally absorb water from the soil and lose water, which leads to the inconsistency of osmotic pressure inside and outside the cell and further leads to cell shrinkage and activity reduction. Under this condition, a large number of osmotic adjustment substances (such as pro, SS, and SP) will be secreted and accumulated inside the tassel, so as to reduce the cell water potential and maintain the same osmotic pressure inside and outside the cell. Finally, the tassel can grow normally and complete the late pollination.

Although maize tassels can improve their drought resistance by secreting antioxidant enzymes and osmotic adjustment substances, the peroxidation and osmotic imbalance caused by drought still have a serious impact on the external morphological structure of maize tassels. The results showed that the ability of antioxidant system enzyme and osmotic adjustment substance secretion of weak drought-tolerance maize tassel was weak, and its stress resistance was poor. Therefore, compared with the other two kinds of drought-tolerant maize, the development of weak drought tolerant maize tassels is slower, and the length of tassels and the number of branches are shortened most significantly. This is similar to the previous results (Jia et al., 2019).

http://www.aloki.hu ● ISSN 1589 1623 (Print) ● ISSN 1785 0037 (Online)
DOI: http://dx.doi.org/10.15666/aeer/2001_685697

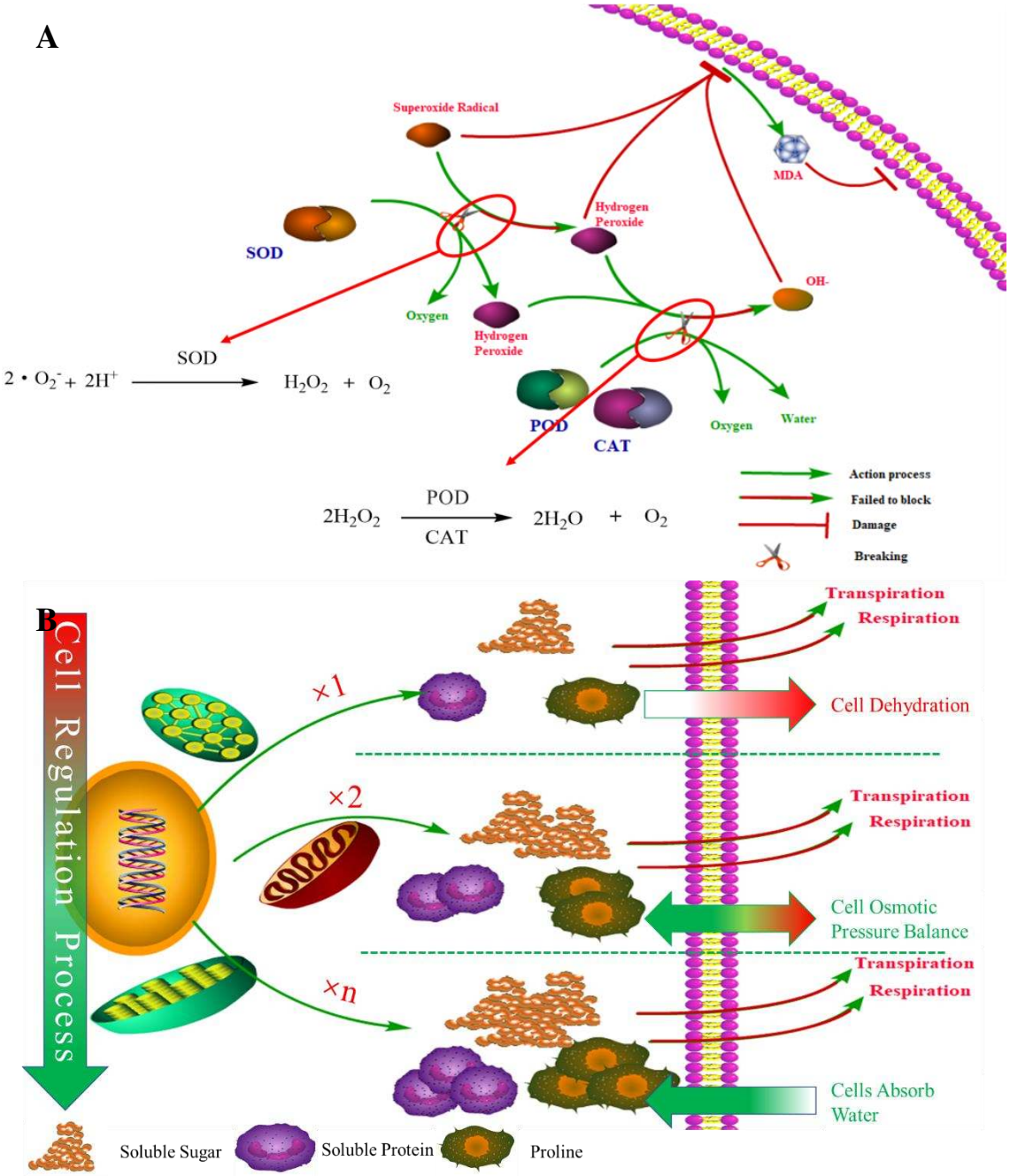

Figure 4. *Schematic diagram of physiological function in maize under drought stress. (A) Schematic diagram of the physiological effects of antioxidant system enzymes and malondialdehyde in maize ears under drought. (B) Schematic diagram of the physiological effects of osmotic adjustment substances in maize ears under drought*

In conclusion, from the analysis of drought degree, appropriate drought is conducive to the normal development of maize tassels, and can promote the secretion of antioxidant enzymes and osmotic adjustment substances. However, excessive drought or prolonged drought stress are not conducive to the development of tassels, which will cause excessive accumulation of harmful substances in maize tassels and irreversible damage to maize tassels. From the analysis of drought tolerance of maize varieties,

http://www.aloki.hu ● ISSN 1589 1623 (Print) ● ISSN 1785 0037 (Online)
DOI: http://dx.doi.org/10.15666/aeer/2001_685697

under drought stress, the internal physiological response of maize tassels with strong drought tolerance will be more active to resist the harmful substances produced by drought stress. The maize varieties with weak drought tolerance not only have weak internal physiological response of tassels, but also have a greater impact on the external morphological structure.

Conclusion

The study found that drought stress would seriously affect the growth and physiological characteristics of maize tassels. The results showed that the strong drought-tolerant varieties had a strong antioxidant enzyme system and osmotic adjustment ability. The changes of antioxidant enzyme activity and osmotic adjustment substance content in tassel were consistent, which indicated that osmotic adjustment could coordinate the protective enzyme activity to a certain extent. Under severe drought conditions, there was a negative correlation between the activity of antioxidant enzymes and the content of MDA, which indicated that MDA in tassels would destroy the stability of membrane structure and hinder the secretion of antioxidant enzymes. Maize tassel is an important reproductive organ of maize. Therefore, this study suggests that drought tolerant varieties suitable for local climate should be selected in the process of maize planting, and appropriate drought stress can be carried out. In maize breeding, we can consider increasing the density of SOD regulatory genes in maize to improve the drought resistance of maize.

Acknowledgements. We thank two anonymous reviewers for their comments on an earlier draft of this manuscript.

Data availability. The data used in this study is available from the corresponding author upon request.

Funding. This work is a contribution Jilin Provincial Key Research and Development Program (20200403069SF); Cultivation Project of “Interdisciplinary Integration and Innovation” of Jilin University: The research on the integration innovation system of Rural Revitalization promoting the protection of black land, agricultural transformation and income multiplication in Northeast China.

REFERENCES

[1] Blum, B. (2017): Osmotic adjustment is a prime drought stress adaptive engine in support of plant production. – Plant, Cell Environment 40(1).
[2] Dumanović, J., Nepovimova, E., Natić, M., Kuča, K., Jaćević, V. (2021): The Significance of reactive oxygen species and antioxidant defense system in plants: a concise overview. – Frontiers in Plant Science. https://doi.org/10.3389/fpls.2020.552969.
[3] Fathi, A., Barari, D. (2016): Effect of drought stress and its mechanism in plants. – International Journal of Life Sciences 10(1).
[4] Fu, C., Zhang, Y., Mi, N., Ming, H., Zhang, S., Zhang, H., Zhao, X. (2020): Maize (Zea mays L.) physiological responses to drought and rewatering, and the associations with water stress degree. – Agricultural Water Management 241.
[5] Gage, J. L. (2018): Tassel Morphology in Zea Mays: Novel Phenotyping Tools and Signatures of Selection. – The University of Wisconsin, Madison.
[6] Gill, S. G., Tuteja, N. (2010): Reactive oxygen species and antioxidant machinery in abiotic stress tolerance in crop plants. – Plant Physiology and Biochemistry 48(12).

http://www.aloki.hu ● ISSN 1589 1623 (Print) ● ISSN 1785 0037 (Online)
DOI: http://dx.doi.org/10.15666/aeer/2001_685697

[7] Guo, Y. Y., Liu, J., Zhu, Y. L., Bai, Y. W., Li, H. J., Xue, J. Q., Zhang, R. H. (2018): The response of maize leaf photosynthesis and antioxidant enzyme activities to drought stress. – Plant Physiology 54(12): 1839-1846.
[8] Hou, J. (2018): Physiological Mechanism of Different Drought-Resistant Wheat Varieties in Response to Drought Differences. – The Agricultural University of Henan, Henan.
[9] Jia, S., Wang, N., Hao, X., Zong, Y., Zhang, D., Li, P. (2019): Effects of different drought stress treatments on growth and stress physiology of Soybean. – Acta Agriculturae Sinica 34(05): 137-144
[10] Jia, S. J., Li, H. W., Jiang, Y. P., Zhao, G. Q., Wang, H. Z., Yang, S. J., Yang, Q. H., Guo, J. M., Shao, R. X. (2020): Effects of drought stress on leaf photosynthetic characteristics and ear development characteristics of maize. – Acta Ecologica Sinica 40(03): 854-863.
[11] Li, W., Hao, Z., Pang, J., Zhang, M., Wang, N., Li, X., Li, W., Wang, L., Xu, M. (2019): Effect of water-deficit on tassel development in maize. – Gene 681
[12] Li, H. W., Jiang, Y. P., Jia, S. J., Zhao, G. Q., Wang, Y. C., Yang, Q. H., Liu, T. X., Li, C. H., Shao, R. X. (2020): Advances in studies on effects of drought stress on ear development of maize. – Journal of Maize Science 28(02): 90-95.
[13] Liu, C., Liu, Y., Guo, K., Fan, D., Li, G., Zheng, Y., Yu, L., Yang, R. (2011): Effect of drought on pigments, osmotic adjustment and antioxidant enzymes in six woody plant species in karst habitats of southwestern China. – Environmental and Experimental Botany 71(2).
[14] Liu, G. (2020): Physiological and Biochemical Characteristics of Drought Resistance in Maize and Analysis of Differentially Expressed Genes. – The Agricultural University of Hebei, Hebei.
[15] Sayadi, A., Zou, M., Tu, J., Qiu, J., Liu, Z. (2016): Breeding for drought tolerance in maize (Zea mays L.). – American Journal of Plant Sciences 7(14)
[16] Song, F. B., Dai, J. Y. (2005): The response and adaptability of maize to drought stress Ⅱ. The growth and development of maize ears and tassels in response to drought stress. – Journal of Jilin Agricultural University 01: 1-5 + 10.
[17] Tahereh, Z.-A., Naser, B., Mohammad, S.-H. (2016): Physiological and morphological response to drought stress in seedlings of ten citrus. – Trees 30(3).
[18] Xu, H. W., Song, F. B., Tong, S. Y. (2012): Advances in development and physiological characteristics of male and female ears in maize. – Guangdong Agricultural Sciences 39(03): 22-24.
[19] Xu, H., Lu, Y., Xie, Z., et al. (2014): Changes in nitrogen metabolism and antioxidant enzyme activities of maize tassel in black soils region of northeast China. – Frontiers in Plant Science 5.
[20] Yang, R. Z. (2015): Temporal and spatial characteristics and risk comprehensive assessment of main agrometeorological disasters of maize in Northeast China. – PhD Dissertation, Chinese Academy of Meteorological Sciences.
[21] Zhang, S. J., Zhang, Y. S., Ji, R. P., Cai, F., Wu, J. W. (2011): Analysis of Distributional Characteristics and Primary Causes of Maize Drought in Northeast China 29(01): 231-236.
[22] Zhang, R., Guo, D., Zhang, X., Lu, H., Liu, J., Li, F., Hao, Y., Xue, J. (2012): The effect of drought stress during the spinning period on maize physiological characteristics and material production. – Acta Agronomica Sinica 38(10): 1884-1890.
[23] Zhang, C., Shi, S., Wu, F. (2018): Effects of drought stress on root growth and physiological characteristics of different drought-resistant alfalfa varieties. – Chinese Agricultural Sciences 51(05): 868-882.
[24] Zhao, W. S. (2016): Response of stomatal development of maize leaves to drought and effects of repeated drought on photosynthesis and drought resistance of maize. – PhD Dissertation, Northwest A & F University.

http://www.aloki.hu ● ISSN 1589 1623 (Print) ● ISSN 1785 0037 (Online)
DOI: http://dx.doi.org/10.15666/aeer/2001_685697

[25] Zhuang, Y. L. (2007): Effects of drought on gene expression of male and female ears of maize and cloning and analysis of glutamate decarboxylase gene. – PhD Dissertation, The University of Shandong.
[26] Zou, Q. (2003): Experimental Guidance of Plant Physiology. – China Agricultural Press, Beijing.

http://www.aloki.hu ● ISSN 1589 1623 (Print) ● ISSN 1785 0037 (Online)
DOI: http://dx.doi.org/10.15666/aeer/2001_685697

MICROPROPAGATION PROTOCOL OF RABBIT FOOT FERN *DAVALLIA FEJEENSIS* HOOK

NOFAL, E. M. S.[1] – SAYED, S. S.[2] – HASSAN, H. H. M.[2*]

[1]*Hort. Dept., Fac. Agric, Kafr El-Sheikh Univ., Kafr El-Sheikh, Egypt*

[2]*Ornamental Plants Res. Dept., Hort. Res. Inst., Agric Res. Center, Giza, Egypt*

**Corresponding author*
e-mail: heba.khder456@gmail.com

(Received 21st Aug 2021; accepted 23rd Nov 2021)

Abstract. This work was carried out in the Tissue Culture Laboratory, Horticulture Research Institute (HRI), Agricultural Research Center, Giza, Egypt during the years of 2018 and 2019 on the commercially important fern *Davallia fejeensis* Hook as an effort to establish a protocol to propagate this plant as much as possible in a relatively short time. For sterilization stage, the statistical analysis of data revealed that sterilization of explant with 0.1% mercuric chloride (MC) for 15 min is the suitable concentration and time for contamination-free and survival% explant. During the multiplication stage, the greatest leaf number, shootlet number and heaviest weight were observed in explants cultured in MS (Murashige and Skoog) medium supplemented with kinetin at 1.0 ppm. The highest value of total chlorophyll was achieved in the medium containing 0.5 ppm kinetin + NAA (1-Naphthaleneacetic acid) while carotenoid content rose to the highest content in medium free of plant growth regulators (control), 0.5 ppm BAP (6-Benzylaminopurine) or kinetin. For rooting stage, MS medium containing 4.0 ppm NAA produced the highest root number/plantlet, rhizome number and longest rhizome. Plants cultured in peat moss + sand + perlite produced the longest plant, greatest leaf number, fresh weight, greatest root number, longest root, greatest rhizome and longest rhizome number
Keywords: *MS-medium, ferns, mass multiplication, 6-benzylaminopurine, sterilization*

Introduction

Davallia fejeensis Hook commonly called rabbit foot fern belongs to the Davalliaceae family (Frohlich and Lau, 2008). It has furry rhizomes which cover the surface of the potting mixture as well as root down into it. The frond is triangular in shape and around 45 cm long and 30 cm wide. It divides into three to four pinnae which divide into many pinnules (Paul and Garber, 2015).

Ferns have been used extensively in the ornamental plant industry for landscaping and indoor. The beauty of their gently sloping leaflets makes an ideal accent in any setting. Most ferns like the shade, so it becomes an important accent to the darker portions of home and garden. Micropropagation of ferns *in vitro* has been tried using spores or vegetative parts. It can be applied especially for ferns that are hard to propagate conventionally for the benefit of the ornamental plant industry (Anico-Parr, 2000).

The ornamental plant is conventionally propagated by seeds and cutting, while propagation through seeds renders undesirable variation whereas shoot cuttings of many genotypes do not respond to root inducing medium (Lambardi and Rugini, 2003). In this regard, using micropropagation technique may be useful. Plant tissue culture is a tool for obtaining rapid, mass multiplication, diseases free and true to type plant material (Singh, 2003).

The first step in surface sterilization is the preparation of healthy explant for tissue culture because explants taken from field are highly exposed to microbial contamination

http://www.aloki.hu ● ISSN 1589 1623 (Print) ● ISSN 1785 0037 (Online)
DOI: http://dx.doi.org/10.15666/aeer/2001_699709

(Sameer and Nabeel, 2016). Regardless of its serious health effect, mercury chloride is frequently utilized for surface sterilization for mitigating microbial contamination in sugarcane tissue culture (Tilahun et al., 2013).

Type and concentration of cytokinins were the most important factors affecting on shoot multiplication, (Romano et al., 2002). Cytokinins have important physiological effects for stimulating cell division as well as cell elongation by activating RNA synthesis and stimulating protein synthesis and enzyme activity (Kulaeva and Skoog, 1980). No clear stimulatory effect of zeatin riboside, and 2-iP effect on the nodes produced per explant of the fern *Marsilea quadrifolia* was reported when compared with hormone-free condition. On the contrary, the micropropagation of rhizome explant was inhibited, the inhibition decreased with the reducing strength of cytokinins (Rolli et al., 2015). The importance of auxin and its transport have been implicated in many physiological processes of roots, such as the regulation maintenance of root meristem and zonation (Luijten and Heidstra, 2009).

There is no micropropagation review on *Davallia fejeensis* Hook despite its aesthetic and coordination importance. Therefore, it was important to establish a protocol for micropropagation of *Davallia fejeensis* Hook.

Materials and methods

This work was carried out in the Tissue Culture Laboratory, Horticulture Research Institute (HRI), Agricultural Research Center; Giza, Egypt over two years from 2018 to 2019. This study was carried out to establish a protocol for micropropagation of *Davallia fejeensis* Hook.

Plant material

One specimen of the fern *Davallia fejeensis* Hook was obtained from the greenhouse of the Gene Bank, Genetic Engineering Institute, Agricultural Research Center (*Fig. 1*).

Figure 1. *Davallia fejeensis Hook*

Culture medium and incubation condition

The survived contamination-free explants were cultured in 250 ml/jar containing 25 ml of MS (Murashige and Skoog, 1962) basal medium supplemented with 30 g/l

http://www.aloki.hu ● ISSN 1589 1623 (Print) ● ISSN 1785 0037 (Online)
DOI: http://dx.doi.org/10.15666/aeer/2001_699709

sucrose and solidified with 7 g/l agar. The medium pH was adjusted to 5.7 ± 0.1 with NaOH or HCl before sterilization by autoclaving at 121 °C for 20 min. The Plant growth regulators (PGR) were used according the experimental stage: benzylaminopurine (BAP), 6-Furfuryl-aminopurine (kinetin or kin), naphthalene acetic acid (NAA) or indole butyric acid (IBA). All cultures were incubated in room chamber at 24 ± 1 °C, under fluorescent illumination of 2000-2500 lux at 16\8 day\night fluctuation.

Sterilization stage

Pieces of the rhizomes were excised, washed with soap and water thoroughly for 15 min, rinsed under running water for 30 min. The explants were taken to aseptic conditions under the laminar air flow cabinet and soaked in either clorox at 5% (v/v) or mercuric chloride $HgCl_2$ (MC) at 0.1%, each for 5, 10, 15 or 20 min, with a few drops of Tween-20, followed by 3 rinses using distilled sterilized water. These pieces were divided to 1.5-2.0 cm long segments (explants) before being inoculated individually in MS medium free hormone for three weeks. Each treatment contained nine explants for three replicates. At the end of sterilization period contamination-free% and survived explants were calculated.

Multiplication stage

The survived contamination-free explants obtained from the new rhizomes were used in a multiplication experiment. These explants were inoculated on MS medium augmented with BAP or kin at (0.0, 0.5, 1.0, 2.0, 3.0, 4.0 or 5.0 ppm), without or with NAA at (0.2 ppm). In each treatment nine explants with three replicates were cultured for three months (three subcultures). At the end of the 3rd subculture data were recorded] leaf number/cluster, shootlet number/explant, cluster height (cm), fresh weight (g), total chlorophyll and carotenoids (mg/g) fw)]. For pigments determination, the ethanolic extractions were submitted to procedures to determine the endogenous chlorophyll and carotenoids (mg/g fw) (Saric et al., 1967).

Rooting stage

Shootlets obtained from the new rhizomes developed *in vitro* in the previous multiplication experiment were used to investigate the effect of two auxins, namely NAA or IBA applied separately at 0.0, 1.0, 2.0, 3.0, 4.0 or 5.0 ppm on rooting of these shootlets for one month. Data were calculated at the end of this period [root number/plantlet, root length (cm), rhizome number/plantlet and rhizome length (cm)]. Each treatment contained nine shootlets in three replicates.

Acclimatization stage

Transplants (rooted plantlets) were transferred to plastic pots containing peat moss: sand: perlite (1:1:1 v/v/v), Peat moss: perlite (1:1 v/v) or perlite alone. These treatments were irrigated with solution of 0.1% rezolix fungicide and covered by transparent polyethylene bags. Each treatment contained nine plantlets in three replicates. The acclimatized transplants were out of door for two months. Plant height (cm), leaf number/plant, root number/plant, root length (cm), rhizome number/plant and rhizome length (cm) were measured.

http://www.aloki.hu ● ISSN 1589 1623 (Print) ● ISSN 1785 0037 (Online)
DOI: http://dx.doi.org/10.15666/aeer/2001_699709

Statistical analysis

The design of experiments for starting, multiplication and rooting stage were factorial (two factor). While acclimatization experiment was one factor. The lay-out of the experiments was designed in complete randomized design and tests with program M-Stat. Least Significant Differences (L.S.D.) at $p \leq 0.05$ were used for the comparison means according to Steel and Torrie (1980).

Results and discussion

Sterilization stage

Effect of exposure to clorox and mercuric chloride (MC) for different times (min) on contamination-free% and survival% of Davallia fejeensis Hook

As shown in *Table 1,* there were significant fluctuations of exposure of clorox and mercuric chloride (MC) for different times and their interaction. For sterilization with clorox and MC, immersed explants in 0.1% MC recorded high percentage of contamination-free and survival % (47.25 and 66.75%, respectively) compared with using 5% (v/v) clorox for sterilization which gave 0.00% contamination- free and 52.75 survival%.

For different immersed times, explants immersed for 15 or 20 min gave high contamination-free % (27.83 or 39.00%) but reduced survival percentage to 44.33 or 38.67%. On the other hand, immersing explants for 5 or 10 min produced high % of survival (83.50 or 72.50%, respectively).

For the interaction between disinfection and times, 0.1% MC in all times gave suitable percentage of contamination-free% and survival %, while with 5% clorox all explants were contaminated in all times.

In this regard, Shekhawat and Manokari (2015) used mature rhizomes of *Marsilea quadrifolia* as explants and were successfully sterilized using 0.1% $HgCl_2$ for the establishment of cultures. Golamaully et al. (2015) reported that sterilization with 0.1% mercuric chloride resulted in minimal contamination levels but no germination of *Diplazium proliferum* spores were observed at all. Mercuric chloride at 0.05% was efficient for sterilization and the germination rate was 51%.

Table 1. *Effect of exposure in clorox and MC for different times on contamination-free% and survival% of Davallia fejeensis Hook*

Min	Contamination-free %			Survival %		
	Clorox (5%)	MC (0.1%)	Mean B	Clorox (5%)	MC (0.1%)	Mean B
5	0.00	11.00	5.50	78.00	89.00	83.50
10	0.00	44.33	22.17	67.00	78.00	72.50
15	0.00	55.67	27.83	33.00	55.67	44.33
20	0.00	78.00	39.00	33.00	44.33	38.67
Mean A	0.00	47.25		52.75	66.75	
$LSD_{0.05}$ A	11.96			13.52		
B	16.92			19.13		
A×B	23.93			27.05		

L.S.D. at 0.05 = Least Significant Different at 0.05 level of probability

http://www.aloki.hu ● ISSN 1589 1623 (Print) ● ISSN 1785 0037 (Online)
DOI: http://dx.doi.org/10.15666/aeer/2001_699709

Multiplication stage

Effect of PGR concentration and type on leaf number/cluster and shootlet number/explant of Davallia fejeensis Hook

The illustrated data in *Table 2* showed a significant fluctuation in behavior of shooting (leaf number/cluster and shootlet number/explant). For types of PGR using kin either alone or with 0.2 NAA induced the greatest leaf and shootlet number (52.35 or 52.79 leaf/cluster and 10.33 or 10.75 shootlet/explant, respectively). However, the lowest record was a result of using BAP + NAA (28.12 leaf/cluster and 5.91 shootlet/explant, respectively).

For concentration of PGR, the greatest leaf number and shootlet number (48.83 leaf/cluster and 9.75 shootlet/explant) were produced when culturing explants on 1.0 ppm. The lowest number of leaves and shootlets resulted when using cytokinins at 4.0 or 5.0 ppm (36.50 or 35.75 leaf/cluster and 7.33 or 7.33 shootlet/explant, respectively).

For the interaction between PGR concentration and type, the greatest leaf and shootlet number in this concern belonged to explants treated with kin at 1.0 ppm (63.67 leaf/cluster and 12.67 shootlet/explant, respectively). The lowest record in the same regard was induced by the BAP + NAA at 4.0 or 5.0 ppm (19.33 or 14.67 leaf/cluster, and 4.00 or 3.66 shootlet/explant, respectively).

In this respect, Ravi et al. (2015) found that the highest number of *Pteris tripartita* sporophytes was induced by 4 mg/l BAP, while the lowest values were obtained by kinetin. Shekhawat and Manokari (2015) observed that maximum number of *Marsilea quadrifolia* shoots was achieved on MS medium augmented with 0.5 mg/l BAP.

Table 2. *Effect of PGR concentration and type on leaf number/cluster and shootlet number/explant of Davallia fejeensis Hook*

	Leaf number/cluster					**Shootlet number/explant**				
Conc. (ppm)	**BAP**	**BAP + NAA**	**Kin**	**Kin + NAA**	**Mean B**	**BAP**	**BAP + NAA**	**Kin**	**Kin + NAA**	**Mean B**
0.0	45.00	45.17	41.33	41.17	43.17	9.33	9.67	9.00	9.00	9.280
0.5	45.00	39.00	48.00	46.67	44.67	10.00	8.67	9.67	9.00	9.333
1.0	45.00	31.33	63.67	55.3	48.83	9.33	6.00	12.67	11.00	9.750
2.0	33.33	27.00	56.67	61.00	44.50	6.67	5.00	10.00	12.00	8.417
3.0	28.67	20.33	51.67	59.00	39.92	6.00	4.33	1.33	11.67	8.083
4.0	21.67	19.33	54.00	51.00	36.50	4.67	4.00	10.33	10.33	7.333
5.0	21.67	14.67	51.33	55.33	35.75	4.33	3.67	10.33	11.00	7.333
Mean A	34.33	28.12	52.38	52.78		7.190	5.905	10.33	10.57	
$LSD_{0.05}$ A			2.323					0.5627		
B			3.073					0.2625		
A×B			6.146					1.489		

L.S.D. at 0.05 = Least Significant Different at 0.05 level of probability

Effect of PGR concentration and type on cluster height (cm) and cluster fresh weight (g) on Davallia fejeensis Hook

The results shown in *Table 3* demonstrated that high significant differences were obtained for PGR type, concentration and their interaction on cluster height and cluster

http://www.aloki.hu ● ISSN 1589 1623 (Print) ● ISSN 1785 0037 (Online)
DOI: http://dx.doi.org/10.15666/aeer/2001_699709

fresh weight. For PGR type, using kin or kin + NAA gave the tallest cluster and largest cluster fresh weight (2.512 or 2.567 cm and 2.307 or 2.492 g, respectively) compared to those produced in the presence of BAP or BAP + NAA (2.086 or 2.108 cm and 1.668 or 1.420 g, respectively).

PGR concentration affected cluster height and cluster fresh weight significantly, the tallest cluster and largest fresh weight (4.184 cm and 2.499 g, respectively) were noticed when no PGR were used (control). The shortest cluster and lowest fresh weight were a result of applying PGR at 5 ppm (1.772 cm and 1.635 g, respectively).

For the interaction between PGR concentration and type the tallest cluster resulted when explants were cultured on medium free hormone (control) (4.233, 4.167, 4.167 or 4.170 cm, respectively) while the heaviest fresh weight was produced when adding kin at 1.0 ppm or kin + NAA at 1.0, 2.0 or 3.0 ppm to culture medium which gave 2.65, 2.79, 2.76 or 2.76 g, respectively. On the other hand, the shortest cluster were observed when BAP at 5.0 ppm or BAP + NAA at 4.0 ppm were used which gave 1.58 or 1.45 cm, respectively while the lowest value of cluster fresh weight was recorded by BAP at 4.0 or 5.0 ppm or BAP + NAA at 4.0 or 5.0 ppm (0.92, 0.93, 0.94 or 0.85 g, respectively).

Findings of some workers were in harmony with our findings. Haddad and Bayerly (2014) mentioned that the longest stems of *Asplenium nidus* were observed when BAP 2.0 mg/l and IBA 0.3 mg/l were added. Ravi et al. (2015) found that the longest *Pteris tripartita* sporophytes were induced by 4 mg/L BAP, while the shortest ones were obtained by kin.

Table 3. *Effect of PGR concentration and type on plantlet height (cm) and plantlet fresh weight (g) on Davallia fejeensis Hook*

	Cluster height (cm)					**Cluster fresh weight (g)**				
Conc. (ppm)	**BAP**	**BAP + NAA**	**Kin**	**Kin + NAA**	**Mean B**	**BAP**	**BAP + NAA**	**Kin**	**Kin + NAA**	**Mean B**
0.0	4.23	4.17	4.17	4.17	4.184	2.74	2.74	2.21	2.30	2.499
0.5	1.63	2.07	2.92	3.27	2.473	2.02	1.69	1.90	1.97	1.896
1.0	1.83	1.78	2.58	2.57	2.192	2.03	1.36	2.65	2.79	2.207
2.0	1.67	1.72	2.05	2.45	1.971	1.54	1.24	2.30	2.76	1.960
3.0	1.60	1.68	1.93	1.95	1.791	1.51	1.11	2.54	2.76	1.978
4.0	2.05	1.45	2.25	1.63	1.847	0.92	0.94	2.20	2.44	1.627
5.0	1.58	1.88	1.69	1.93	1.772	0.93	0.85	2.34	2.43	1.635
Mean A	2.086	2.108	2.512	2.567		1.668	1.420	2.307	2.492	
$LSD_{0.05}$ A	0.1957					0.1907				
B	0.2588					0.2523				
A×B	0.5177					0.5046				

L.S.D. at 0.05 = Least Significant Different at 0.05 level of probability

Effect of PGR concentration and type on total chlorophyll and carotenoids content (mg/g fw) of Davallia fejeensis Hook

Data presented in *Table 4* showed the effect of PGR types, concentrations and their interaction. For the effect of PGR type, no significant differences in total chlorophyll were obtained by using different types of PGR while adding BAP raised the content of carotenoids compared to BAP + NAA, kin or kin + NAA.

http://www.aloki.hu ● ISSN 1589 1623 (Print) ● ISSN 1785 0037 (Online)
DOI: http://dx.doi.org/10.15666/aeer/2001_699709

For concentration of PGR, the highest content of total chlorophyll was observed by adding 0.5 ppm (0.7930 mg/g fw) while the carotenoids raised in medium free hormone (control) or with 0.5 ppm which gave 0.3588 or 0.3327 mg/g fw, respectively.

For the effect of the interaction between PGR concentration and type achieved the highest position of total chlorophyll in medium containing 0.5 ppm kin + NAA while carotenes raised to the highest contents in medium free PGR (control), 0.5 ppm BAP or kin. The lowest contents of total chlorophyll were a result of applying kin at 2.0 ppm while carotenoids were the lowest when using kin at 5.0 ppm to MS medium.

In this respect, Gao *et a*l. (2000) on *Carthamus tinctorius* revealed that different concentrations of cytokinins and auxins had a significant effect on the chlorophylls and carotenoids formation capacity. In the same trend, Sayed and El-Kareim (2007) on *Cotoneaster horizontalis* studied the effect of different concentrations of cytokinins on the formation capacity of chlorophyll-a,-b and carotenoids. They observed that the production of such pigments was negatively related with the concentrations of the other cytokinins examined.

Table 4. *Effect of PGR concentration and type on total chlorophyll and carotenoids content (mg/g f.w.) of Davallia fejeensis Hook*

	Total chlorophyll content (mg/g fw)					**Carotenoids content (mg/g fw)**				
Conc. (ppm)	**BAP**	**BAP + NAA**	**Kin**	**Kin + NAA**	**Mean B**	**BAP**	**BAP + NAA**	**Kin**	**Kin + NAA**	**Mean B**
0.0	0.588	0.579	0.578	0.586	0.5826	0.360	0.359	0.359	0.357	0.3588
0.5	0.843	0.7413	0.684	0.904	0.7930	0.360	0.287	0.365	0.320	0.3327
1.0	0.524	0.411	0.318	0.475	0.4321	0.204	0.081	0.169	0.128	0.1455
2.0	0.349	0.397	0.187	0.237	0.2931	0.206	0.207	0.117	0.094	0.559
3.0	0.303	0.411	0.319	0.304	0.3343	0.233	0.104	0.097	0.061	0.1238
4.0	0.236	0.292	0.271	0.245	0.2610	0.146	0.135	0.030	0.090	0.1003
5.0	0.258	0.246	0.272	0.269	0.2611	0.157	0.203	0.014	0.088	0.1156
Mean A	0.4430	0.4396	0.3758	0.4315		0.2379	0.1967	0.1645	0.1625	
$LSD_{0.05}$ A	NS					0.04375				
B	0.08966					0.05788				
A×B	0.1793					0.1158				

L.S.D. at 0.05 = Least Significant Different at 0.05 level of probability (NS: non significant)

Rooting stage

Effect of auxin type and concentration on number of roots/plantlet and root length (cm) of Davallia fejeensis Hook

Data in *Table 5* show, significant differences between type, concentrations, and interaction of auxins with root number/plantlet and root length (cm). For type of auxins no significant differences were obtained for using NAA or IBA on root number/plantlet and root length (cm).

The effect of concentrations of auxins, MS medium containing 4.0 ppm produced the highest number of roots/plantlet (22.83 root/plant let) while the longest root length was recorded when using 0.0, 1.0, 3.0 or 4.0 ppm which gave 2.70, 2.642, 2.692 or 2.695 cm, respectively. On the other hand, using 5.0 ppm recorded the lowest root number and shortest root length (12.83 root/plantlet and 1.783 cm, respectively).

http://www.aloki.hu ● ISSN 1589 1623 (Print) ● ISSN 1785 0037 (Online)
DOI: http://dx.doi.org/10.15666/aeer/2001_699709

For the interaction between concentrations and type of auxins, MS medium containing 4.0 ppm NAA or IBA produced the highest root number/plantlet (23.00 or 24.67 root/plantlet). In the same trend using 4.0 ppm IBA recorded the longest root length (3.40 cm). The lowest value for root number and root length was observed when using MS medium augmented with 5.0 ppm NAA which recorded 10.33 root/plantlet and 1.70 cm, respectively.

In this respect, Seyyedyousefi et al. (2013) on *Alstroemeria* (Alstroemerieae, ex. Liliaceae), Haddad and Bayerly (2014) on fern *Asplenium nidus*, Salem (2016) on *Aglaonema commutatum* and *Alocasia cucullata* and Badawy et al. (2020) on *Calathea medallion* reported that the highest number of roots and the longest roots were produced on medium with NAA.

Table 5. *Effect of auxin type and concentration on root number/plantlet and root length (cm) of Davallia fejeensis Hook*

	Root number/plantlet			**Root length (cm)**		
Conc. (ppm)	**NAA**	**IBA**	**Mean B**	**NAA**	**IBA**	**Mean B**
0	14.33	14.17	14.25	2.72	2.68	2.700
1	19.33	13.33	16.33	3.08	2.20	2.642
2	19.00	17.33	18.17	2.13	2.57	2.350
3	14.00	18.00	16.00	2.75	2.63	2.692
4	23.00	24.67	23.83	2.45	3.40	2.925
5	10.33	15.33	12.83	1.70	1.87	1.783
Mean A	16.67	17.14		2.472	2.558	
$LSD_{0.05}$ A		NS			NS	
B		1.832			0.8068	
A×B		2.590			1.141	

L.S.D. at 0.05 = Least Significant Different at 0.05 level of probability (NS: non significant)

Effect of auxin type and concentration on rhizome number (cm) and rhizom length (cm) of Davallia fejeensis Hook

Data presented in *Table 6* showed the effect of auxin type, concentration, and their interaction with number of rhizome/plantlet and rhizome length (cm). For auxin type, no significant differences were obtained between NAA or IBA on rhizome number/plantlet and rhizome length (cm).

The effect of auxin concentrations, medium augmented with 4.0 ppm has the highest rhizome number and longest rhizome length (9.00 rhizome/plantlet and 1.767 cm, respectively).

The interaction between auxin concentration and type, showed that the medium containing 4.0 ppm NAA recorded the highest number of rhizome and longest rhizome (10.00 rhizome/plantlet and 2.07 cm, respectively).

Acclimatization stage

Effect of media type on acclimatization for plant behaviour of Davallia fejeensis Hook

All rooted plantlets were transferred to different culture media of peat moss + sand + perlite, peat moss + perlite or perlite alone under ex vitro conditions. Data in *Table 7*

http://www.aloki.hu ● ISSN 1589 1623 (Print) ● ISSN 1785 0037 (Online)
DOI: http://dx.doi.org/10.15666/aeer/2001_699709

indicated that, the media investigated gave significant differences in acclimatization on plant behavior. Cultured plants in peat moss + sand + perlite produced the longest plant, greatest leaf number, heaviest fresh weight, greatest root number, longest root, greatest rhizome number and longest rhizome (10.90 cm, 23.0 leaf/plant, 2.70 g 19.33 root/plant, 3.47 cm, 7.67 rhizome/plant and 3.33 cm, respectively). However, culturing in peat moss + perlite recorded the longest plant, root and rhizome (9.57, 4.68 and 3.73 cm, respectively). On the other hand, culturing plants in perlite depressed to minimum values recorded for growth of plant behavior. These results may be attributed to the high nutrition value of peat moss which can permit the *in vitro* plant to grow up in higher length comparing to the poor nutrition value of perlite or sand. In this regard, Sayed et al. (2005) on *Cereus peruvianus*, using peat moss alone or in combination with sand at 1:1 (v:v) allowed the stem of the *in vitro* acclimatized plants to grow up to the highest value.

Table 6. *Effect of auxin type and concentration on rhizome number/plantlet and rhizome length (cm) of Davallia fejeensis Hook*

	Rhizome number/plantlet			**Rhizome length (cm)**		
Conc. (ppm)	**NAA**	**IBA**	**Mean B**	**NAA**	**IBA**	**Mean B**
0	5.00	4.83	4.917	1.32	1.27	1.292
1	5.00	4.67	4.833	1.72	1.0	1.408
2	6.00	6.00	6.000	1.00	1.50	1.250
3	4.33	5.67	5.000	1.65	1.50	1.575
4	10.00	8.00	9.000	2.07	1.67	1.767
5	5.67	6.67	6.167	1.07	1.32	1.192
Mean A	6.000	5.972		1.496	1.358	
$LSD_{0.05}$ A		NS			NS	
B		1.662			0.4432	
A×B		2.351			0.6268	

L.S.D. at 0.05 = Least Significant Different at 0.05 level of probability (NS: non significant)

Table 7. *Effect of media type on acclimatization for plant behavior of Davallia fejeensis Hook*

	Plant height (cm)	**Leaf number**	**Fresh weight (g)**	**Root number**	**Root length (cm)**	**Rhizome number**	**Rhizome length (cm)**
Beat + sand + perlite	10.90	23.00	2.70	19.33	3.47	7.67	3.33
Beat + perlite	9.57	15.33	2.03	15.33	4.68	4.00	3.73
Perlite	6.57	17.33	1.35	6.00	1.65	2.33	1.28
$LSD_{0.05}$	1.628	5.902	0.7787	3.023	1.14	2.449	1.487

L.S.D. at 0.05 = Least Significant Different at 0.05 level of probability

Conclusion

Using 0.1% mercuric chloride (MC) for 15 min proved to be the suitable time and disinfection for contamination-free and survival% explant. For multiplication stage, adding 1.0 ppm kin to MS medium produce the greatest shooting behavior. During rooting stage, MS medium containing 4.0 ppm NAA showed the highest root

http://www.aloki.hu ● ISSN 1589 1623 (Print) ● ISSN 1785 0037 (Online)
DOI: http://dx.doi.org/10.15666/aeer/2001_699709

number/plantlet, rhizome number and longest rhizome. Moreover, plants cultured in peat moss + sand + perlite produced good growth of plantlet (*Fig. 2*).

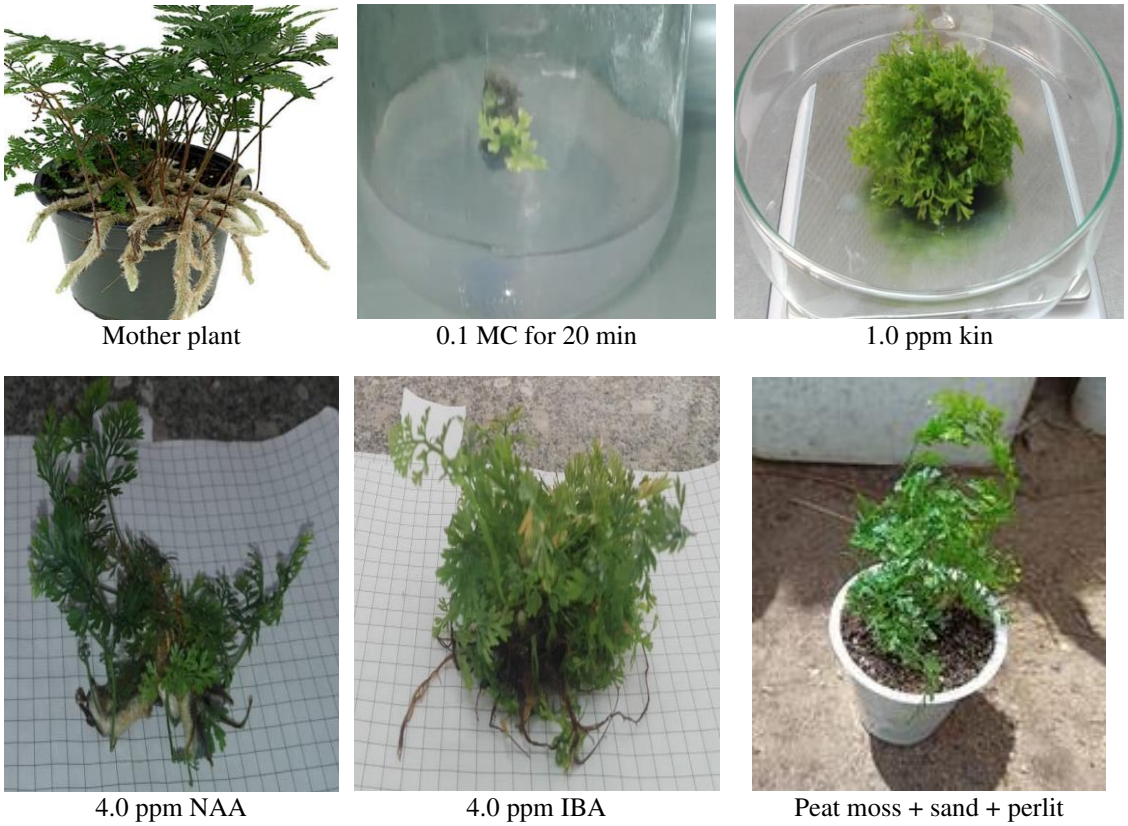

Figure 2. *Different stages on micropropagation of Davallia fejeensis Hook*

REFERENCES

[1] Anico-Parr, A. J. (2000): Micropropagation of ferns: *Pteris vittata* spores and *Nephrolepis biserrata* runners. – An undergraduate thesis in partial fulfillment for the B.Sc. biology degree. Institute of Biology, College of Science, Univ. of the Philippines.

[2] Badawy, E. M., El-Meadawy, E. E., El-Ezawy, W. H. (2020): Micropropagation of *Calathea* medallion, an ornamental plant. – Plant Archives 20(1): 1483-1489.

[3] Frohlich, D., Lau, A. (2008): New plant records from Oahu for 2007. – Bishop Mus. Occ. 100: 3-12.

[4] Gao, W. Y., Fan, L., Paek, K. Y. (2000): Yellow and red pigment production by cell cultures of *Carthamus tinctorius* in a bioreaction. – Plant Cell, Tissue & Organ Culture 60(2): 95-100.

[5] Golamaully, Z. M., Bhoyroo, V., Nazurally, N., Gopal, V. (2015): *In vitro* culture as an aid to conservation of indigenous ferns: *Diplazium proliferum.* – Intl. J. Plant Biol. 6: 33-36.

[6] Haddad, S., Bayerly, R. (2014): *In vitro* propagation of ferns (*Asplenium nidus*) via spores culture. – Jordan J. Agric. Sci. 10(1): 144-153.

[7] Kulaeva, O. N., Skoog, F. (1980): Plant Growth Substances. – Springer-Verlag, Berlin, pp. 119-128.

[8] Lambardi, M., Rugini, E. (2003): Micropropagation of Woody Trees and Fruits. – Kluwer Academic Publishers, The Netherlands, pp. 621-646.

http://www.aloki.hu ● ISSN 1589 1623 (Print) ● ISSN 1785 0037 (Online)
DOI: http://dx.doi.org/10.15666/aeer/2001_699709

[9] Luijten, M., Heidstra, R. (2009): Arabidopsis Root Development. – Beeckman, T. (ed.) Annual Plant Reviews Vol. 37: Root Development. Wiley-Blackwell, Oxford, UK, pp. 1-38.
[10] Murashige, T., Skoog, F. (1962). A revised medium for rapid growth and bio-assay with tobacco tissue culture. – Physiolgia Plantarum 15: 473-497.
[11] Paul, A. T., Garber, M. P. (2015): Growing ferns extension. – Horticulturists Bulletin 737, The University of Georgia.
[12] Ravi, B. X., Varuvel, G. V. A., Kilimas, R., Robert, J. (2015): Apogamous sporophyte development through spore reproduction of a South Asia's critically endangered fern: *Pteris tripartita* Sw. – Asian Pacific J. Reproduction 4(2): 135-139.
[13] Rolli, E., Brunoni, F., Marieschi, M., Torelli, A., Ricci, A. (2015): *In vitro* micropropagation of the aquatic fern *Marsilea quadrifolia* L. and genetic stability assessment by RAPD markers. – Plant Biosystems 149(1): 7-14.
[14] Romano, A., Barros, S., Martins-Loução, M. A. (2002): Micropropagation of the Mediterranean tree *Ceratonia siliqua*. – Plant Cell, Tissue and Organ Culture 68: 35-41.
[15] Salem, M. M. M. A. (2016): Micropropagation of some pot plants. – Ph.D. thesis, Horticulture Department, Faculty of Agric., Zagazig University.
[16] Sameer, N. M., Nabeel, K. A. (2016): Effect of different sterilization methods on contamination and viability of nodal segments of *Cestrum nocturnum* L. – Inter. J. of Res. Studies in Biosc. (IJRSB) 4(1): 1-9.
[17] Saric, M.; Kostrori, R.; Cupina, T. and Geric, I. (1967): Chlorophyll determination. – Univ. Noven Sadu Prakitikum is kiziologize Bilijaka Beogard, Haucana, Anjiga.
[18] Sayed, S. S., El-Kareim, G. S. (2007): Propagation of *Cotoneaster horizontalis* Decne through *in vitro* culture. – Annals of Agri. Sci., Mostohor 45(2): 761-772.
[19] Sayed, S. S., Abou-Dahab, T. A., Youssef, E. M. A. (2005): *In vitro* propagation of cactus (*Cereus peruvianus* L.). – Arab J. Biotech. 8(1) 169-176.
[20] Seyyedyousefi, S. R., Kaviani, B., Dehkaei, N. P. (2013): The effect of different concentrations of NAA and BAP on micropropagation of *Alstroemeria*. – European J. Exper. Biol. 3(5): 133-136.
[21] Shekhawat, M. S., Manokari, M. (2015): Direct organogenesis from rhizome explants in Marsilea *quadrifolia* L.: a threatened fern species. – Advances in Bio. 2015: 1-6.
[22] Singh, R. (2003): Tissue culture studies of sugarcane. – M.Sc. Thesis, Thapar Institute of Engineering and Technology, Patiala, India.
[23] Steel, R. G. D., Torrie J. H. (1980): Principles of Statistics. A Biometrical Approach. Second Ed. – Mc Graw-Hill, Kogakusha, Ltd, Tokyo.
[24] Tilahun, M., Mulugeta, D., Manju, S. (2013): An alternative safer and cost effective surface sterilization method for sugarcane (*Saccharum officinarum* L.) explants. – African J. Biol. 12(44): 6282-6286.

http://www.aloki.hu ● ISSN 1589 1623 (Print) ● ISSN 1785 0037 (Online)
DOI: http://dx.doi.org/10.15666/aeer/2001_699709

DRIVING FACTORS OF PHYTOPLANKTON COMMUNITY AND ASSESSMENT OF THE WATER QUALITY IN A SMALL EUTROPHIC WUXING LAKE, NORTHEAST CHINA

HOU, W. J.[1] – LIU, M. H.[1] – MING, X. Y.[1] – LIU, J. M.[1] – XU, L.[1] – CUI, X. B.[2] – YU, H. Y.[1*]

[1]*Department of Ecology, College of Wildlife and Protected Area, Northeast Forestry University, Harbin 150040, China*
(e-mail: wenjiu2678@163.com; phone: +86-139-4168-7523 – W. J. Hou)

[2]*Heilongjiang Naolihe National Nature Reserve Administration, Shuangyashan 155100, China*

**Corresponding author*
e-mail: china.yhx@163.com; phone: +86-131-0096-0911

(Received 31st Aug 2021; accepted 23rd Nov 2021)

Abstract. The community structure, spatiotemporal variation and influencing factors of phytoplankton accompanied with water quality in Wuxing Lake, northeast China were studied during spring, summer and autumn from summer 2019 to spring 2020. Our purpose was to reveal the driving factors influencing phytoplankton community, combined with water quality, discussing methods on improving water quality in the lake.112 species of phytoplankton including 8 phyla and 74 genera were identified. The phytoplankton community structure demonstrated obvious seasonal and spatial variation. 20 dominant species were selected during three seasons. Redundancy analysis (RDA) result showed that transparency (SD), total phosphorous (TP), chemical oxygen demand (COD_{Cr}), turbidity (Tur), dissolved oxygen (DO) and conductivity (EC) were main factors influencing the abundance of dominant species. Results of Shannon-Wiener index (*H'*) and Pielou's evenness index (*J'*) indicating slight to light pollution in the lake. Considering the risk of deterioration of water quality is still a possibility, measures to improve SD may be effective to prevent Cyanophyta blooms in summer. Our findings will provide a reference for water quality protection and management in small eutrophic lakes similar to Wuxing Lake.
Keywords: *Wuxing Lake, temporal and spatial succession, dominant species, diversity index, water quality, redundancy analysis (RDA)*

Introduction

Water eutrophication affecting rivers, lakes, reservoirs et cetera caused by human activities is becoming a global problem (Vincon-Leite and Casenave, 2019; Wang et al., 2019; Bouraï et al., 2020). Input of large amount of nutrients (mainly nitrogen and phosphorus) into freshwater ecosystems caused the proliferation of phytoplankton which eventually leads to algal blooms (especially harmful cyanobacteria) (Barcante et al., 2020). Algal blooms consume the majority of the dissolved oxygen in the water and release algal toxins, leading to the destruction of ecological functions (such as diversity protection, drinking water supply and recreation etc.) and sustainable development of aquatic ecosystem (Sakamoto et al., 2021; Preece et al., 2017; Huisman et al., 2018). Phytoplankton is main primary producer of aquatic ecosystems and plays an important role in material flow and energy cycle (Jiang et al., 2014). Due to sensitivity to environmental factors, phytoplankton community were widely used to evaluate water quality and predict changes of water quality in freshwater bodies (Yang et al., 2016; Boyer et al., 2009; Thiebaut et al., 2006). Various characteristics of phytoplankton with numbers types destined the result that algae surviving in environment consistent with

http://www.aloki.hu ● ISSN 1589 1623 (Print) ● ISSN 1785 0037 (Online)
DOI: http://dx.doi.org/10.15666/aeer/2001_711725

ecological demand and be eliminated when the environment was inappropriate, which leading the diversity of phytoplankton community under diversified types of environmental, namely, the temporal and spatial heterogeneity of phytoplankton community structure (Padisák et al., 2003). Studies showed that nutrients, light condition, physical factors (water temperature, transparency, dissolved oxygen etc.), climate change (precipitation, water level fluctuation, monsoon, hydrological connectivity etc.) were factors influencing the spatiotemporal variation of phytoplankton community structure (Liu et al., 2021; Cao et al., 2018; Liu et al., 2019; Xiao et al., 2011; Yuan et al., 2018). Which were different due to features of water environment.

Wuxing Lake is located in the experimental area of Naolihe National Nature Reserve in Heilongjiang Province which is surrounded by paddy. Drainage from paddy production was directly injected into the lake, resulting in high nutrient concentrations of water. Cyanobacteria blooms were observed in summer during recent years in the lake, indicating water quality is deteriorating. However, studies on phytoplankton community structure and their relationship with environmental factors in the lake have not been reported up to now. In this study we investigated characteristics of phytoplankton community and environmental factors in Wuxing Lake during one year. Our purposes were to (1) reveal the spatiotemporal succession of phytoplankton and their driving factors;(2) evaluate of water quality and offer proposals on improving water quality.

Materials and methods

Study area

Wuxing Lake locates in hinterland of Sanjiang plain, Heilongjiang Province, China (132°22′29″-134°13′45″E,46°30′22″-47°24′32″N) (*Fig. 1; Table 1*) and could be summarized as small eutrophic lake with a surface area 250 hectares and high centration of nutrients due to dewatering of surrounding farmland (mainly rice fields) (*Table 2*). Water depth is shallow with an average of 2 m and maximum no more than 3 m. The lake contains rich wildlife resources with great economic value including mammal, bird, fish and benthic macroinvertebrate and plays important role in preservation of biodiversity. The annual distribution of precipitation is mainly in summer (June to August), accounts for 64.5% of total annual rainfall while spring and autumn accounted for 14.3% and 18.7%, respectively.

Table 1. *Nine sampling sites coordinates in Wuxing Lake*

Sampling sites	Latitude	Longitude
1#	N46°48′41.8212″	E132°59′31.3008″
2#	N46°48′37.6884″	E132°59′56.3100″
3#	N46°48′37.6956″	E132°59′44.8332″
4#	N46°48′39.4092″	E132°59′35.4084″
5#	N46°48′12.1680″	E132°59′17.0556″
6#	N46°48′30.5316″	E132°59′12.2208″
7#	N46°48′51.1632″	E132°59′24.2664″
8#	N46°49′5.9700″	E132°59′45.4380″
9#	N46°49′2.2620″	E133°0′8.1684″

http://www.aloki.hu ● ISSN 1589 1623 (Print) ● ISSN 1785 0037 (Online)
DOI: http://dx.doi.org/10.15666/aeer/2001_711725

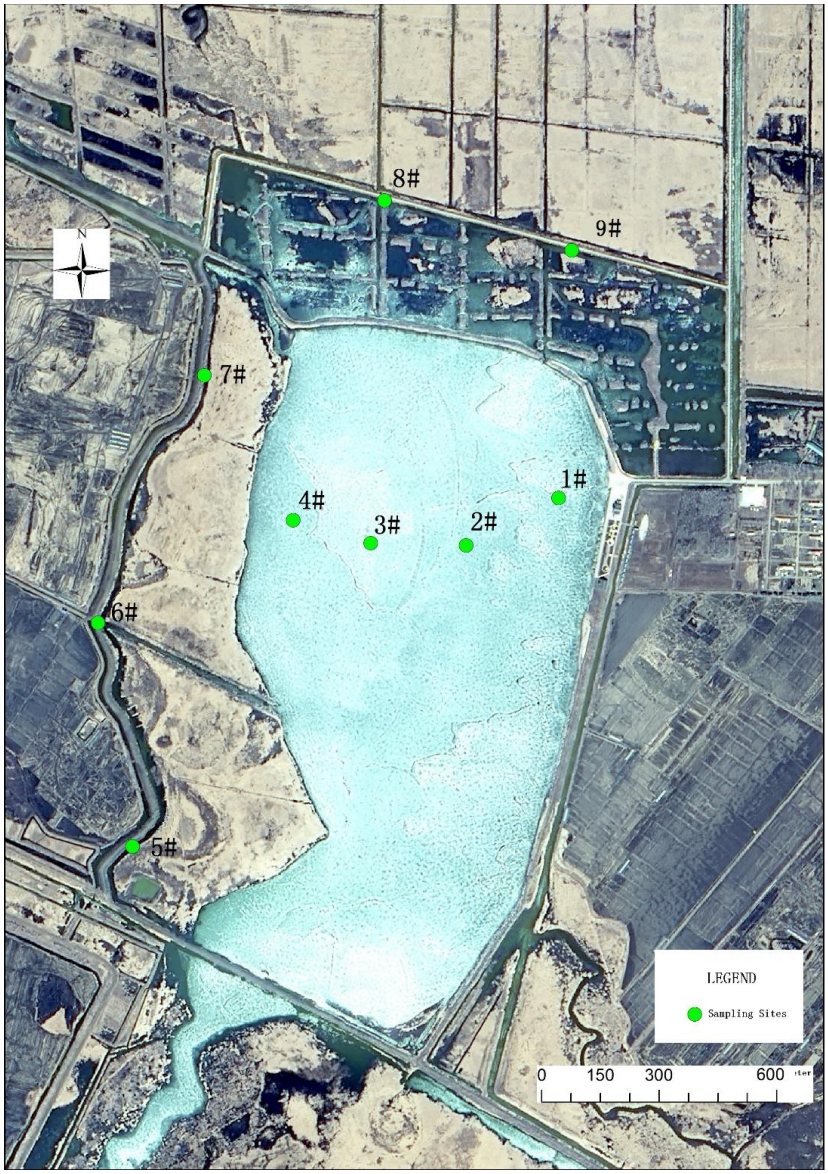

Figure 1. *Sampling sites in Wuxing Lake. 1#–4# are located in lake center (LC), 5#–9# are located in inlet channel (IC)*

Sampling and analysis

Nine representative sampling sites were selected from Wuxing Lake with 4 in lake center (LC, 1#-4#) and 5 in inlet channel (IC, 5#-9#). Samples were collected in summer (June, 2019), autumn (October, 2019) and spring (May, 2020), no sampling was conducted in winter for reason of coverage of ice and snow.

Water temperature (WT), conductivity (EC), dissolved oxygen (DO), turbidity (Tur,) and potential of hydrogen (pH) were recorded in situ by multi-parameter probe (YSI 6600, USA), transparency (SD) was measured using Secchi disk and water depth (WD) by band tape. 500 ml water sample was collected from subsurface water (5–50 cm) at each sampling site for analysis of total phosphorus (TP), total nitrogen (TN) and chemical oxygen demand (COD_{Cr}) and then be measured within 24 h according to methods described by HACH (Yuan et al., 2018). Another 1 L water sample was

http://www.aloki.hu ● ISSN 1589 1623 (Print) ● ISSN 1785 0037 (Online)
DOI: http://dx.doi.org/10.15666/aeer/2001_711725

collected and poured into clean plastic bottle for phytoplankton quantification, and then fixed with 15 ml Lugol's iodine solution. The fixed samples were sedimented for 48 h in dark and then concentrated to 30 mL. Identification and counting of phytoplankton were conducted with Motic biological microscope (BA400T) at 400×magnification according to the freshwater algae of China (Hu and Wei, 2006), phytoplankton biomass was estimated by biovolumes (Long et al., 2020).

Statistical analysis

The dominance index (Y) was calculated in *Equation 1* (Lampitt et al., 1993), Shannon-Wiener index (H') and Pielou's evenness index (J') were calculated as shown in *Equations 2-3* (Shannon and Weaver, 1963; Pielou, 1966).

$$Y = \left(\frac{n_i}{N}\right) * f_i \quad \text{(Eq.1)}$$

$$H' = -\sum_{i=1}^{S} P_i \ln p_i \quad \text{(Eq.2)}$$

$$J' = \frac{H'}{\log_n S} \quad \text{(Eq.3)}$$

where n_i is the abundance of species i, N is the total abundance and f_i is the occurrence frequency of species i in all sampling sites. S is the richness of phytoplankton and P_i is the relative abundance of species i which was calculated by n_i/N. Explanations for three indices were expressed as follow: Y > 0.02 indicates that species i is the dominant specie (Lampitt et al., 1993); *H'* and *J'* were used to evaluate water quality of the lake. For *H'*, the value of which vary range from 0 to 1.0 indicates heavy pollution, the values range from 1.0 to 2.0 indicates moderate pollution, the value range from 2.0 to 3.0 indicates light pollution, and the value range from 3.0 to 4.5 indicates slight pollution (Shanthala et al., 2009). While for *J'*, the values of which range between 0 and 0.3 indicates heavy pollution, the value range between 0.3 and 0.5 indicates moderate pollution, the value range between 0.5 and 0.8 indicates light pollution, and the value range between 0.8 and1.0 indicates clean (Kong, 2000).

Spatial and temporal succession of phytoplankton community (one-way ANOVA with Tukey's HSD post hoc test) and Pearson correlation analysis between abundance of phytoplankton and Environmental Factors were performed using SPSS 22.0. $P < 0.05$ indicated that the difference and correlation were statistically significant. Redundancy analysis (RDA) was used to assess relationship between environmental factors and abundance of dominant species with Canoco 5.0 software for the reason that detrended correspondence analysis (DCA) showed the result of the maximum gradient length less than 3 standard deviation units (1.4 SD). Prior to analysis, abundance of phytoplankton and the environmental factors except pH were normalized using the formula log (1 + x).

Results

Environmental variable

The result of mean values of physicochemical variables and one-way ANOVA are presented in *Table 2*. In this study all ten environmental factors in this study showed

http://www.aloki.hu ● ISSN 1589 1623 (Print) ● ISSN 1785 0037 (Online)
DOI: http://dx.doi.org/10.15666/aeer/2001_711725

significant seasonal difference. WT varied between 7.25 ℃ and 24.51 ℃ with the maximum value in summer and minimum in autumn. WD and EC both increased from spring to autumn, values of WD in autumn (222.78 cm) were significantly higher than that in spring (154.78 cm) ($p < 0.01$), while EC varied significantly among different seasons ($p < 0.01$). SD varied from 49.33 cm to 74.22 cm with the values in spring > autumn > summer. The values of DO and pH ranged from 6.25 to 10.71 and 7.22 to 7.61 mg/L respectively with maximum values both in autumn, values of DO in summer was significantly lower than that in spring and autumn ($p < 0.01$), while pH in autumn was higher than spring and summer ($p < 0.01$). Tur increased significantly from spring to summer ($p < 0.01$) and then reduced rapidly due to high water level caused by rainfall in autumn. COD_{Cr} and nutrients (TN, TP) showed a decreasing trend from spring to autumn with the lowest values 14.37 mg/L, 1.93 mg/L and 0.15 mg/L, respectively. Spatial heterogeneity of some environmental factors existed in all seasons. WD was significant different between LC and IC throughout the year ($p < 0.05$). EC, DO, Tur, COD_{Cr} and TN showed significant difference between LC and IC in spring ($p < 0.05$). In autumn, WD, SD and Tur showed significant spatial difference ($p < 0.05$).

Table 2. *The seasonal variation (spring, summer and autumn) of physicochemical variables (mean ± SE) in Wuxing Lake.*

	Spring	Summer	Autumn	P Value
WT (℃)	11.85 ± 0.06^{b}	24.51 ± 0.28^{a}	7.25 ± 0.29^{c}	0.000
WD (cm)	154.78 ± 11.53^{b}	$176.11 \pm 12.07^{a, b}$	222.78 ± 23.39^{a}	0.024
SD (cm)	74.22 ± 4.25^{a}	39.44 ± 1.63^{c}	49.33 ± 2.06^{b}	0.000
EC (ms/m)	0.061 ± 0.01^{c}	0.065 ± 0.01^{b}	0.071 ± 0.01^{a}	0.000
pH	7.22 ± 0.09^{b}	7.35 ± 0.04^{b}	7.61 ± 0.05^{a}	0.001
DO (mg/L)	10.14 ± 0.19^{a}	6.25 ± 0.19^{b}	10.72 ± 0.63^{a}	0.000
Tur (NTU)	1.44 ± 0.39^{c}	20.28 ± 1.44^{a}	11.04 ± 1.16^{b}	0.000
COD_{Cr} (mg/L)	24.59 ± 0.95^{a}	20.33 ± 0.55^{b}	14.37 ± 0.32^{c}	0.000
TN (mg/L)	3.73 ± 0.18^{a}	2.25 ± 0.15^{b}	1.93 ± 0.14^{c}	0.000
TP (mg/L)	0.46 ± 0.04^{a}	0.27 ± 0.02^{b}	0.15 ± 0.01^{c}	0.000

WT, water temperature; WD, water depth; SD, transparency, EC, conductivity; DO, dissolved oxygen; Tur, turbidity; CODcr, chemical oxygen demand; TN, total nitrogen; TP, total phosphorous
P values were from one-way ANOVA test. The significance level of mean difference is 0.05

Succession of phytoplankton community

A total of 112 species of phytoplankton belonging to 8 phyla and 74 genera were identified during three seasons in Wuxing Lake, including Chlorophyta (47 species), Bacillariophyta (35 species), Cyanophyta (12 species), Euglenophyta (8 species), Chrysophyta (4 species), Cryptophyta (2 species), Xanthophyte (2 species) and Pyrrophyta (2 species). Among these species, Chlorophyta, Bacillariophyta and Cyanophyta were main species of phytoplankton community which account for 42.0%,31.1% and 10.5% of the total species respectively (*Fig. 2a*). Species richness was the highest in spring (83 species), Chlorophyta (38.6%) and Bacillariophyta (34.9%) were main species, a decrease of phytoplankton species number with 70 species was observed in summer, Species number of Chlorophyta increased and became

http://www.aloki.hu ● ISSN 1589 1623 (Print) ● ISSN 1785 0037 (Online)
DOI: http://dx.doi.org/10.15666/aeer/2001_711725

dominant (54.3%); the number of phytoplankton species in autumn remained the same in summer (70 species) while Bacillariophyta (40.0%) and Chlorophyta (31.4%) dominated phytoplankton in autumn (*Fig. 2a, b*).

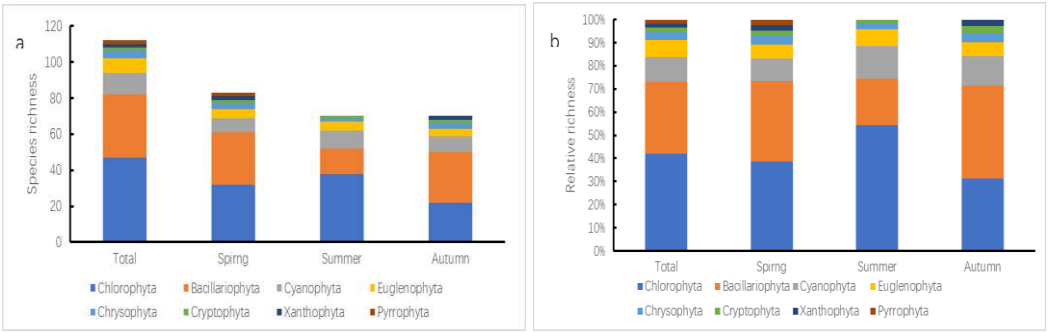

Figure 2. *Phytoplankton species richness (a), relative richness (b) in Wuxing Lake*

Phytoplankton abundance ranged from 1.38×10^6 to 1.27×10^7 cells/L and biomass ranged from 1.04 to 25.47 mg/L with the average 4.64×10^6 cells and 6.13 mg/L respectively in the lake. No statistically significant differences were observed in abundance and biomass among three seasons ($p > 0.05$), while both phytoplankton abundance and biomass showed the same seasonal variation as summer > autumn > spring (*Fig. 3a, b*). Maximum phytoplankton abundance (1.27×10^7 cells/L) and biomass (25.47 mg/L) both occurred at summer 2# while the minimum values of abundance (1.26×10^6 cells/L) and biomass (1.04 mg/L) appeared at 9# in autumn and 6 # in summer respectively. In terms of spatial distribution, the abundance and biomass of phytoplankton showed significant difference between LC and IC in summer ($P < 0.05$). While no significant spatial difference of phytoplankton abundance and biomass were found in spring and autumn.

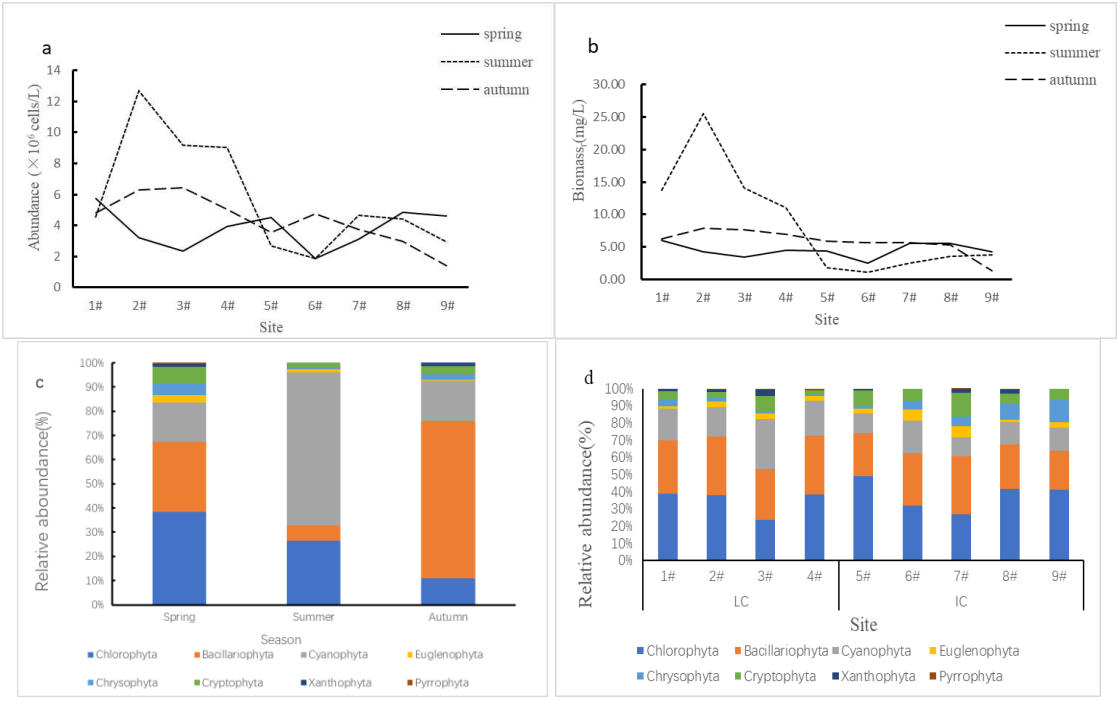

http://www.aloki.hu ● ISSN 1589 1623 (Print) ● ISSN 1785 0037 (Online)
DOI: http://dx.doi.org/10.15666/aeer/2001_711725

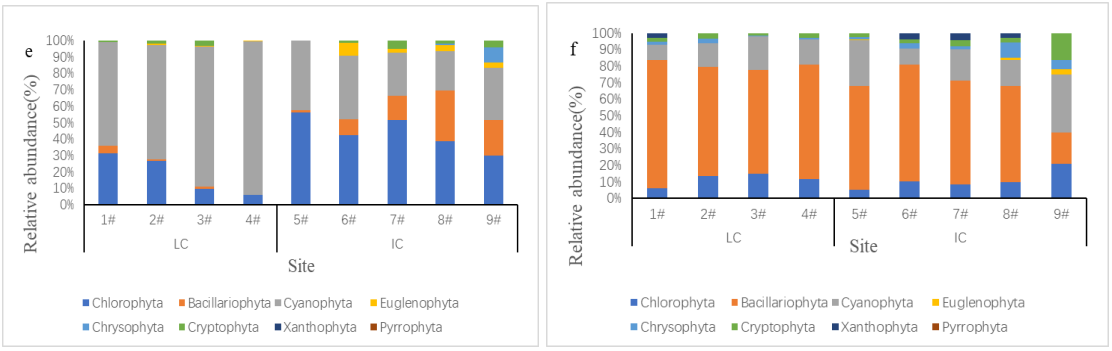

Figure 3. *Temporal and spatial variations of phytoplankton community in Wuxing Lake. (a) abundance of phytoplankton; (b) biomass of phytoplankton;(c) seasonal variation of relative abundance of phytoplankton community; (d-f) spatial variation of relative abundance of phytoplankton community at sampling sites in spring, summer and autumn*

Phytoplankton community Chlorophyta, Bacillariophyta and Cyanophyta are the main groups in the lake (*Fig. 3c*). In spring Chlorophyta and Bacillariophyta shared dominance with relative abundance of 38.32% and 29.00% respectively, meanwhile Cyanophyta also occupied high relative abundance (16.25%). Phytoplankton composition were similar at nine sampling sites (*Fig. 3d*). Relative abundance of Cyanophyta increased significantly and became dominant species (63.43%) in summer (*Fig. 3c*). Spatial, the relative abundance of Cyanophyta reigned supreme in LC with the highest value of 93.22%; while phytoplankton community was dominated by Chlorophyta and Cyanophyta in IC in the lake with 43.74% and 32.62% respectively (*Fig. 3e*). In autumn, Bacillariophyta became dominant species (*Fig. 3c*). The relative abundance of Bacillariophyta varied from 58.30% to 77.81% with a mean value 66.27% except site 9# (19.13%) (*Fig. 3f*).

According to the standard of dominant phytoplankton species ($Y > 0.02$),20 dominant species were selected during three seasons (*Table 3*). The number of dominant species was 15, 8 and 6 in spring, summer and autumn respectively with dominance index varied from 0.022 to 0.38. *Merismopedia minima* was the dominant specie existed in three seasons. The relative abundance of 20 dominant species (*Table 3*) predominant the phytoplankton abundance in spring (74.31%), summer (69.92%) and autumn (69.16%) in the lake, hence were used to analyze the relationship between phytoplankton community and environmental factors.

Table 3. *Dominant species and dominance index (Y) of phytoplankton during three seasons in Wuxing Lake*

Code	Species	Dominance index (Y)		
		Spring	Summer	Autumn
Chlorophyta				
sp1	*Dictyosphaerium pulchellum*	0.099	0.059	
sp2	*Selenastrum minutum*	0.024		
sp3	*Ankistrodesmus falcatus*	0.066		
sp4	*Ankistrodesmus angustus*	0.037	0.024	
sp5	*Scenedesmus quadricauda*	0.022		
sp6	*Chlamydomonas aggregata*	0.031		
sp7	*nephrocytium agardhianum*		0.037	
sp8	*Chlorella pyrenoidosa*		0.026	0.043

http://www.aloki.hu ● ISSN 1589 1623 (Print) ● ISSN 1785 0037 (Online)
DOI: http://dx.doi.org/10.15666/aeer/2001_711725

Cyanophyta				
sp9	*Microcystis incerta*	0.029		
sp10	*Merismopedia minima*	0.120	0.06	0.061
sp11	*Synechocystis willei*		0.064	
sp12	*Anabaena circinalis*		0.380	
sp13	*Aphanizomenon flos-aquae*		0.029	
Bacillariophyta				
sp14	*Nitzschia acicularis*	0.024		
sp15	*Cyclotella meneghiniana*	0.060		0.160
sp16	*Synedra acus*	0.061		
sp17	*Melosira granulata var. angustissima*	0.033		0.330
sp18	*Asterionella formosa*	0.046		0.030
Chrysophyta				
sp19	*Dinobryon bavaricum*	0.035		
Cryptophyta				
sp20	*Cryptomonas erosa*	0.049		0.025

Pearson correlation analysis

Results of Pearson correlation analysis (*Table 4*) showed that abundance of phytoplankton was positively correlated with WD, Tur and negatively correlated with SD. EC, COD_{Cr}, TP, pH and WT were the main factors influencing abundance of Chlorophyta. The abundance of Cyanophyta was very significant correlation with WT, DO ($p < 0.01$) while significantly relevant with SD and Tur ($P < 0.05$) (*Table 4*). In addition, abundance of Bacillariophyta was positive with WD, DO and EC while negative with WT, COD_{Cr}, and TP (*Table 4*).

Table 4. *Relationships between phytoplankton abundance (annual average abundance expressed as abundance, abundance of dominant species including Chlorophyta, Cyanophyta and Bacillariophyta) and environmental variables in Wuxing Lake*

	WT	**WD**	**SD**	**EC**	**pH**	**DO**	**Tur**	**COD_{Cr}**	**TN**	**TP**
Abundance		0.398*	-0.414*				0.417*			
Chlorophyta	0.400*			-.496**	-0.39*			0.437*		0.406*
Cyanophyta	0.539**		-0.445*			-0.497**	0.478*			
Bacillariophyta	-0.72**	0.598**		0.455*		0.689**		-0.595**		-0.418*

Variables without significant correlations are not included. * $p < 0.05$, ** $p < 0.01$

Diversity index of phytoplankton

The spatial and temporal variations of Shannon-Wiener index (*H'*) and Pielou's evenness index (*J'*) were presented in *Figure 4. H'* was higher in spring (3.11) than that in summer (2.30) and autumn (2.25) (*Fig. 4a*). The result Indicated that water quality was slight pollution in spring and light pollution in summer and autumn. Significant decline of *H'* values were observed at 3# (1.34) and 4# (1.05) in summer, indicating the water quality was deteriorated to moderate pollution in LC in summer. Similar variation trend of *J'* was observed with the highest values in spring (0.83) and Lower values in summer (0.69) and autumn (0.67) (*Fig. 4b*). The values of *J'* demonstrated that the water quality was clean in spring and slightly polluted in summer and autumn. The

http://www.aloki.hu ● ISSN 1589 1623 (Print) ● ISSN 1785 0037 (Online)
DOI: http://dx.doi.org/10.15666/aeer/2001_711725

lowest J' values also appeared at 3# (0.43) and 4# (0.33) in summer, indicating the moderate pollution of water quality in LC.

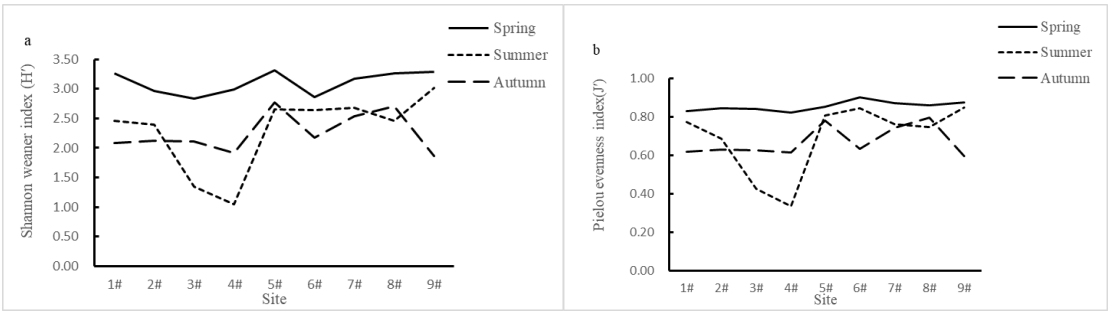

Figure 4. *Spatial and temporal variations of diversity index of phytoplankton: (a) Shannon-Wiener index (H'); (b) Pielou's evenness index (J')*

Relationship between dominant species and environmental factors

RDA ordination diagram of dominant species and environmental variables in Wuxing Lake was shown in *Figure 5*. Environmental variables explained 63.8% of the variations in phytoplankton abundance (*Fig. 5*). The eigenvalues of the first two RDA axes were 0.3322, 0.1997 and accounted for 53.18% of the cumulative variation. The Pseudo-canonical correlations for AX1 and AX2 were 0.9974 and 0.8907 respectively, indicating environmental variables can well explain species composition. SD, WD and TP were most important environmental factors influencing the abundance of dominant species, accounting for 27%, 16.3% and 6.5% respectively.

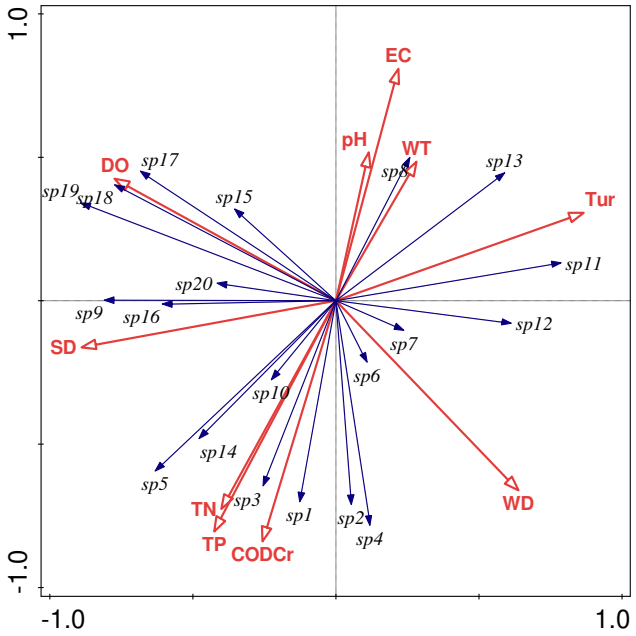

Figure 5. *Redundancy analysis (RDA) ordination diagram of the dominant species (blue lines) and environmental factors (red lines) in Wuxing Lake. The interpretation for codes of dominant phytoplankton species were shown in Table 2*

http://www.aloki.hu ● ISSN 1589 1623 (Print) ● ISSN 1785 0037 (Online)
DOI: http://dx.doi.org/10.15666/aeer/2001_711725

Discussion

Spatial and seasonal variation of phytoplankton community in Wuxing Lake

Seasonal succession of phytoplankton community structure is the main content of studying dynamic change of phytoplankton community (Wei et al., 2020; Cao et al., 2018; Tian et al., 2013). However, seasonal variation of phytoplankton community in tropical area was not obvious, Cyanophyta dominated in most lakes during most seasons (Nankabirwa et al., 2019). Other scholars reported a two seasonal model (dry and rainy season) of phytoplankton succession in tropical aquatic systems while extraordinary high abundance of Cyanophyta during rainy season (Duong et al., 2012). In temperate regions, Bacillariophyta was dominant in spring with low temperature and Cyanophyta and Chlorophyta in summer and autumn (Ma et al., 2019). The main reason for the difference in phytoplankton succession between tropical and temperate regions can be explained by water temperature (Ke et al., 2008). Cyanophyta could better adapt high water temperatures compared to other phytoplankton, resulting in persistent dominance of cyanobacteria throughout the year in lakes and reservoirs in tropical areas (Nankabirwa et al., 2019; Barcante et al., 2020). While large variation of water temperature in temperate areas is beneficial to the growth and reproduction of various species of phytoplankton (Yuan et al., 2018; Zhao et al., 2017).

In our study significant seasonal succession of phytoplankton community structure was observed in Wuxing Lake. In spring phytoplankton community was dominated by Chlorophyta and Bacillariophyta which reflected the environmental characteristics of low WT and high concentration of TP (*Table 2*). During summer with the arrival of rainy season, surface runoff caused by precipitation carried large amount of sediment into the lake increased the Tur of the water, Cyanophyta with strong competitive ability proliferated rapidly and eventually predominated the phytoplankton community and led an outbreak of algae bloom. Large amounts of precipitation during autumn resulted in the highest water level and improved water quality of the lake (*Table 2*), as a result, Bacillariophyta became the dominant species.

Light condition represented by SD and Tur was the main factor influencing the abundance of phytoplankton according to the results of Pearson analysis. In addition, high correlation was observed between abundance of phytoplankton and Chlorophyta by Pearson correlation analysis ($r^2 = 0.847$, $p = 0.000$) indicating that controlling the abundance of Chlorophyta is the key to prevent the occurrence of phytoplankton blooms in Wuxing Lake. Cyanophyta is more tolerant to temperature than other algae and could grow with the optimum temperature between 30 and 35 °C (Yu et al., 2014), water temperature, light availability and nutrient are main factors influencing the competitive ability of Cyanophyta (Sekadende et al., 2005; Dalu and Wasserman, 2018). In this study, abundance of Cyanophyta may be more affected by environmental factors related to light conditions. WD, DO and EC were positive factors while WT, COD_{Cr}, and TP were negative variables of abundance of Bacillariophyta. The environmental characteristic of Wuxing Lake was low WT in spring and high WD, low WT, low nutrient (TN, TP and COD_{Cr}) in autumn, which facilitating the reproduction of Bacillariophyta (*Fig. 3c*).

Abundance of Cyanophyta showed significantly spatial difference ($p < 005$) in summer in this study. Significantly spatial variation ($p < 0.01$) of phytoplankton abundance was reported in the Lake Xingkai basin and the main reason was considered as differences in environmental factors (Yuan et al., 2018). Wuxing Lake

http://www.aloki.hu ● ISSN 1589 1623 (Print) ● ISSN 1785 0037 (Online)
DOI: http://dx.doi.org/10.15666/aeer/2001_711725

is a small shallow lake which water is from precipitation and drainage of the surrounding farmland. Water entering the lake through inlet channel where distributed large number of Gramineae emergent plants, mainly cattails and reeds, however emergent plants were scarce in the lake. As a result, two areas with obvious differences were formed, including lake center (LC) with wide water surface, higher WD, less aquatic plants and inlet channel (IC) characterized by narrow, shallow in addition with large distribution of aquatic vascular plants. One-way ANOVA showed that some environmental factors (WD, WT, SD and Tur) in these two regions had significant spatial differences, which may be the main reason for the spatial variability of phytoplankton abundance.

Driving factors of phytoplankton community in Wuxing Lake

Dominant species of phytoplankton in Wuxing Lake showed obvious seasonal succession. *Merismopedia minima*, *Dictyosphaerium pulchellum*, *Ankistrodesmus falcatus, Cyclotella meneghiniana* and *Synedra acus* were main dominant species in spring with the dominant index (*Y*) 0.12, 0.099, 0.066, 0.060 and 0.061 respectively (*Table 3*). In summer, *Anabaena circinalis* was the most abundant dominant specie with the *Y* value 0.38, *D. pulchellum* (0.059)*, M. minima* (0.060) and *Synechocystis willei* (0.064) were also dominant species with high abundance. In autumn, Bacillariophyta dominant species represented by *Melosira granulata var. angustissima* and *C. meneghiniana* became the most abundant dominant species which *Y* values 0.33 and 0.16. *M. minima* was also the main dominant species with the *Y* value 0.061.

Factors influencing phytoplankton community composition in lakes including WT, DO, ORP, SD, PH, TP, TSS, COD_{Cr} etc. (Ma et al., 2019; Jiang et al., 2014). In this study, phytoplankton community structure was mainly regulated by SD, WD and TP. Tur, DO, COD_{Cr}, TN and EC were also important environment factors influencing the phytoplankton assemblage. RDA result showed that the abundance of Chlorophyta (sp1-sp5) represented by *D. pulchellum* (sp1) and *A. falcatus* (sp3) were positive with TP and COD_{Cr}, while Cyanophyta (sp11-sp13) represented by *A. circinalis* (sp12) and *S. willei* (sp13) were positive with Tur and negative with SD and DO. Contrary, Bacillariophyta represented by *M.* var. *angustissima* (sp17), *C. meneghiniana* (sp15) and *S. acus* (sp16) were positive correlation with DO, SD and EC.

TP is the main factor stimulating the proliferation of phytoplankton (Li et al., 2021; Schindler et al., 2016), while COD_{Cr} and DO represent organic pollution in water (Kutlu et al., 2020). Large amount farmland backwater containing high concentration of nutrients flowed into the lake in spring and leading to the highest value of TP and COD_{Cr}, accelerating the reproduction of Chlorophyta. Meanwhile, high values of SD and DO in spring were also beneficial to the growth of Bacillariophyta. As a result, the abundance of Chlorophyta and Bacillariophyta dominant in spring. Some scholars reported that poor lighting condition suppressed the growth of Bacillariophyta and Chlorophyta, while facilitated the dominance of Cyanophyta (Liu et al., 2021). With the arrival of summer, precipitation carried large amount of sediment into the lake, which deteriorated the light conditions of the water (low SD, DO and high Tur, *Table 2*), which facilitating the growth of cyanobacteria. Li et al. (2019) reported that the abundance of Bacillariophyta was positive with nutritional level and EC, while negative with WT with cold temperate climate in autumn. In this study, appropriate environmental conditions such as DO, SD and EC stimulating the reproduction of Bacillariophyta and became dominant species in autumn.

http://www.aloki.hu ● ISSN 1589 1623 (Print) ● ISSN 1785 0037 (Online)
DOI: http://dx.doi.org/10.15666/aeer/2001_711725

Water quality assessment and management suggestion for Wuxing Lake

Due to the sensitivity and rapid response to environmental changes, phytoplankton community can be used as indicator of aquatic health (Ni et al., 2018). Shannon-Wiener index (*H'*) and Pielou's evenness index (*J'*) based on phytoplankton community were frequently used to estimate the water quality in water body (Zhu et al., 2020). In this study, the results of *H'* and *J'* were consistent, indicating the slight to light pollution state in the lake. However, the obvious low values of *H'* and *J'* at site 3#,4# in summer indicated the risk of deterioration of water. In fact, Cyanophyta blooms already erupted in summer 2019. Wuxing Lake is a typical eutrophic small lake with water quality meeting the national water quality standard of Level Ⅴ(GB3838-2002,2002). Liu et al. (2021) suggested nutrient below the threshold ($TN \leq 1.5$ mg/L; $TP \leq 0.1$ mg/L) to sustain a good ecological status in the lake. Considering the nutritional status and the role of Wuxing Lake in maintaining ecological diversity, appropriate management measures should be taken to control the occurrence of Cyanophyta bloom in summer. Considering that SD and Tur were main factors affecting the abundance of Cyanophyta, measures to improve SD may be effective.

Conclusion

This study focused on the community structure (including species richness, abundance, biomass and dominant species), spatiotemporal change and driving factors of phytoplankton in Wuxing Lake which was a small eutrophic lake in northeast China. Meanwhile, water quality was evaluated. Chlorophyta, Bacillariophyta and Cyanophyta were main dominant species. The average abundance and biomass were 4.64×10^6 cells and 6.13 mg/L respectively with the values in summer > autumn > spring. Seasonal succession of phytoplankton dominant species (expressed by abundance) in the lake was obvious. Chlorophyta and Bacillariophyta were dominant in spring, Cyanophyta predominated the phytoplankton community in summer, while Bacillariophyta was the most abundance species in autumn. Spatial heterogeneity of phytoplankton abundance was observed in summer. 20 dominant species were selected during three seasons with 15 species in spring,8 species in summer and 6 species in autumn. RDA result showed that SD, WD and TP were most important factors influencing the abundance of dominant species. The results of Shannon-Wiener index (*H'*) and Pielou's evenness index (*J'*) indicating the slight to light pollution in the lake. However, in the lake, outbreak of cyanobacteria bloom in summer indicated that the water quality was deteriorating in recent years. In order to control the reproduction of cyanobacteria in Wuxing Lake in summer, measures should be taken to improve SD and reduce TP. Further studies should focus on long-term changes of phytoplankton community structure and relationship between phytoplankton and zooplankton to better understand the driving factors of phytoplankton community.

Acknowledgements. We thank to the leaders and workers from Heilongjiang Naolihe National Nature Reserve Administration for their support and assistance during field sampling work. This study was supported by Provincial joint fund project (020-43220018).

http://www.aloki.hu ● ISSN 1589 1623 (Print) ● ISSN 1785 0037 (Online)
DOI: http://dx.doi.org/10.15666/aeer/2001_711725

REFERENCES

[1] Barcante, B., Nascimento, N. O., Silva, T. F. G., Reis, L. A., Giani, A. (2020): Cyanobacteria dynamics and phytoplankton species richness as a measure of waterbody recovery: response to phosphorus removal treatment in a tropical eutrophic reservoir. – Ecological Indicators 117: 1-11.

[2] Bouraï, L., Logez, M., Laplace, T., Argillier, C. (2020): How do eutrophication and temperature interact to shape the community structures of phytoplankton and fish in lakes? – Water 12: 1-17.

[3] Boyer, J. N., Kelble, C. R., Ortner, P. B., Rudnicku, D. T. (2009): Phytoplankton bloom status: chlorophyll a biomass as an indicator of water quality condition in the southern estuaries of Florida, USA. – Ecological Indicators 9: 56-67.

[4] Cao, J., Hou, Z., Li, Z., Chu, Z., Yang, P., Zheng, B. (2018): Succession of phytoplankton functional groups and their driving factors in a subtropical plateau Lake. – Science of the Total Environment 631-632: 1127-1137.

[5] Dalu, T., Wasserman, R. J. (2018): Cyanobacteria dynamics in a small tropical reservoir: understanding spatio-temporal variability and influence of environmental variables. – Science of the Total Environment 643: 835-841.

[6] Duong, T. T., Le, T. P., Dao, T. S., Pflugmacher, S., Rochelle, E., Hoang, T. K., Vu, N., Ho, C. T., Dang, D. K. (2012): Seasonal variation of cyanobacteria and microcystins in the Nui Coc Reservoir, Northern Vietnam. – Journal of Applied Phycology 25: 1065-1075.

[7] GB3838-2002 (2002): National Standard of the People's Republic of China: Environmental Quality Standards for Surface Water. – Standardization Administration of China, Beijing (in Chinese).

[8] Hu, H. J., Wei, Y. Y. (2006): The Freshwater Algae of China - Systematics, Taxonomy and Ecology. – Science Technology Press, Beijing (in Chinese).

[9] Huisman, J., Codd, G. A., Perl, H. W., Ibelings, B. W., Verspagen, J. M. H., Visser, P. M. (2018): Cyanobacterial blooms. – Nat Rev Microbiol 16: 471-483.

[10] Jiang, Y. J., He, W., Liu, W. X., Qin, N., Yang, H. L., Wang, Q. M., Kong, X. Z., He, Q. S., Yang, C. Y. B., Xu, F. L. (2014): The seasonal and spatial variations of phytoplankton community and their correlation with environmental factors in a large eutrophic Chinese Lake (Lake Chaohu). – Ecological Indicators 40: 58-67.

[11] Ke, Z., Xie, P., Guo, L. (2008): Controlling factors of spring–summer phytoplankton succession in Lake Taihu (Meiliang Bay, China). – Hydrobiologia 607: 41-49.

[12] Kong, F. X. (2000): Environmental Biology. – Higher Education Press, Beijing.

[13] Kutlu, B., Aydin, R., Danabas, D., Serda, O. 2020: Temporal and seasonal variations in phytoplankton community structure in Uzuncayir Dam Lake (Tunceli, Turkey). – Environmental Monitoring and Assessment 192: 105: 1-12.

[14] Lampitt, R. S., Wishner, K. F., Turley, C. M., Angel, M. V. (1993): Marine snow studies in the Northeast Atlantic Ocean: distribution, composition and role as a food source for migrating plankton. – Marine Biology 116: 689-702.

[15] Li, X., Yu, H., Wang, H., Ma, C. X. (2019): Phytoplankton community structure in relation to environmental factors and ecological assessment of water quality in the upper reaches of the Genhe River in the Greater Hinggan Mountains. – Environmental Science and Pollution Research International 26: 17512-17519.

[16] Li, Y. R., Yu, Z. D., Ji, S. P., Meng, J., Kong, Q., Wang, R. Q., Liu, J. (2021): Diverse drivers of phytoplankton dynamics in different phyla across the annual cycle in a freshwater Lake. – Journal of Freshwater Ecology 36: 13-29.

[17] Liu, J. F., Chen, Y. W., Li, M. J., Liu. B. G., Liu. X., Wu, Z. S., Cai, Y. J., Xu, J. Y., Wang, J. J. (2019): Water-level fluctuations are key for phytoplankton taxonomic communities and functional groups in Poyang Lake. – Ecological Indicators 104: 470-478.

http://www.aloki.hu ● ISSN 1589 1623 (Print) ● ISSN 1785 0037 (Online)
DOI: http://dx.doi.org/10.15666/aeer/2001_711725

[18] Liu, X., Chen, L., Zhang, G., Zhang, J., Wu, Y., Ju, H. (2021): Spatiotemporal dynamics of succession and growth limitation of phytoplankton for nutrients and light in a large shallow lake. – Water Research194: 1-13.
[19] Long, S., Zhang, T., Fan, J., Li, C., Xiong, K. (2020): Responses of phytoplankton functional groups to environmental factors in the Pearl River, South China. – Environmental Science and Pollution Research International 27: 42242-42253.
[20] Ma, C. X., Mwagona, P. C., Yu, H. X., Sun, X. W., Liang, L. Q., Mahboob, S. (2019): Spatial and temporal variation of phytoplankton functional groups in extremely alkaline Dali Nur Lake, North China. – Journal of Freshwater Ecology 34: 91-105.
[21] Nankabirwa, A., Wannes, D. C. A., Thijs, V. D. M., Christine, C., Plisner, P. D., Balirwa, J., Verschiuren, D. (2019): Phytoplankton communities in the crater Lakes of western Uganda, and their indicator species in relation to Lake trophic status. – Ecological Indicators 107: 1-15.
[22] Ni, M., Yuan, J. L., Liu, M., Gu, Z. M. (2018): Assessment of water quality and phytoplankton community of Limpenaeus vannamei pond in intertidal zone of Hangzhou Bay. – China Aquaculture Reports 11: 53-58.
[23] Padisák, J., Scheffler, W., Sípos, C., Kasprzak, P., Krienitz, L. (2003): Spatial and temporal pattern of development and decline of the spring diatom populations in Lake Stechlin in 1999.pdf. – Advances in Limnology 58: 135-155.
[24] Pielou, E. C. (1966): The measurement of diversity in different types of biological collections. – Journal of Theoretical Biology 13: 131-144.
[25] Preece, E. P., Hardy, F. J., Moore, B. C., Bryan, M. (2017): A review of microcystin detections in Estuarine and Marine waters: environmental implications and human health risk. – Harmful Algae 61: 31-45.
[26] Sakamoto, S., Lim, W. A., Lu, D., Dai, X., Orlova, T., Iwataki, M. (2021): Harmful algal blooms and associated fisheries damage in East Asia: current status and trends in China, Japan, Korea and Russia. – Harmful Algae 102: 1-14.
[27] Schindler, D. W., Carpenter, S. R., Chapra, S. C., Hecky, R. E., Orihel, D. M. (2016): Reducing Phosphorus to Curb Lake Eutrophication is a Success. – Environmental Science & Technology 50: 8923-8929.
[28] Sekadende, B. C., Lyimo, T. J., Kurmayer, R (2005): Microcystin production by cyanobacteria in the Mwanza Gulf (Lake Victoria, Tanzania). – Hydrobiologia 543: 299-304.
[29] Shannon, C. E., Weaver, W. (1963): The Mathematical Theory of Communication. – University of Illinois Press, Urbana.
[30] Shanthala, M., Hosmanl, S. P., Hosetti, B. B. (2009): Diversity of phytoplanktons in a waste stabilization pond at Shimoga Town, Karnataka State, India. – Environmental Monitoring and Assessment 151: 437-443.
[31] Thiebaut, G., Tixier, G., Guerold, F., Muller, S. (2006): Comparison of different biological indices for the assessment of river quality: application to the upper river Moselle (France). – Hydrobiologia 570: 159-164.
[32] Tian, C., Lu, X., Pei, H., Hu, W., Xie, J. (2013): Seasonal dynamics of phytoplankton and its relationship with the environmental factors in Dongping Lake, China. – Environmental Monitoring and Assessment 185: 2627-2645.
[33] Vincon, L. B., Casenave, C. (2019): Modelling eutrophication in Lake ecosystems: a review. – Science of the Total Environment 651: 2985-3001.
[34] Wang, J., Fu, Z., Qiao, H., Liu, F. (2019): Assessment of eutrophication and water quality in the estuarine area of Lake Wuli, Lake Taihu, China. – Science of the Total Environment 650: 1392-1402.
[35] Wei, J., Wang, M., Chen, C., Wu, H., Llin, L., Li, M. (2020): Seasonal succession of phytoplankton in two temperate artificial Lakes with different water sources. – Environmental Science and Pollution Research International 27: 42324-42334.

http://www.aloki.hu ● ISSN 1589 1623 (Print) ● ISSN 1785 0037 (Online)
DOI: http://dx.doi.org/10.15666/aeer/2001_711725

[36] Xiao, L. J., Wang, T., Hu, R., Han, B. P., Wang, S., Qian, X., Padisak, J. (2011): Succession of phytoplankton functional groups regulated by monsoonal hydrology in a large canyon-shaped reservoir. – Water Research 45: 5099-5109.
[37] Yang, J., Lv, H., Yang, J., Liu, L., Yu, X., Chen, H. (2016): Decline in water level boosts cyanobacteria dominance in subtropical reservoirs. – Science of the Total Environment 557-558: 445-452.
[38] Yu, J., Wang, C., Su, Z. Y., Xiong, P., Liu, J. Q. (2014.): Response of microalgae growth and cell characteristics to various temperatures. – Asian Journal of Chemistry 26: 3366-3370.
[39] Yuan, Y. X., Jiang, M., Liu, X. T., Yu, H. X., Otte, M. L., Ma, C. X., Her, Y. G. (2018): Environmental variables influencing phytoplankton communities in hydrologically connected aquatic habitats in the Lake Xingkai basin. – Ecological Indicators 91: 1-12.
[40] Zhao, W. X., Li, Y. Y., Jiao, Y. J., Zhou, B., Vogt, R. D., Liu, H. L., Ji, M., Ma, Z., Li, A. D., Zhou, B. H., Xu, Y. P. (2017): Spatial and temporal variations in environmental variables in relation to phytoplankton community structure in a eutrophic river-type reservoir. – Water 9: 1-15.
[41] Zhu, H., Liu, X. G., Cheng, S. P. (2020): Phytoplankton community structure and water quality assessment in an ecological restoration area of Baiyangdian Lake, China. – International Journal of Environmental Science and Technology 18: 1529-1536.

http://www.aloki.hu ● ISSN 1589 1623 (Print) ● ISSN 1785 0037 (Online)
DOI: http://dx.doi.org/10.15666/aeer/2001_711725

GRID-SCALE EXPLORATION OF THE RELATIONSHIP BETWEEN ECOLOGICAL HEALTH AND HUMAN PRESSURE IN THE THREE GORGES RESERVOIR REGION

XIAO, Z. L.[1,2,3] – GAO, Y. H.[1*] – YANG, Q. Y.[3]

[1]*Chongqing institute of meteorological sciences, Chongqing 401147, China*

[2]*Chongqing Key Laboratory of GIS Application Research, Chongqing Normal University, Chongqing 401331, China*

[3]*School of Geographical Sciences, Southwest University, Chongqing 400715, China*

[*]*Corresponding author*
e-mail: gaoyanghua@sina.com

(Received 8th Sep 2021; accepted 23rd Nov 2021)

Abstract. Human activity is becoming the key factor influencing ecological health changes and clarifying the nature of that influence could effectively promote regional ecological restoration. Commonly used human-related factors (e.g., social and economic census data) can only be constrained at the administrative division, and they lead to a loss of detailed spatial characteristics. In this study, we applied human activity intensity (HAI), mapped at the grid scale, to represent pressures of human activity on the ecosystem. Taking the Three Gorges Reservoir Region (TGRR) as the study area, the spatial heterogeneity of the influences of human pressure on ecological health was analyzed. The results showed that, in the TGRR from 2000 to 2018, there was an overall improvement of ecological health and a significant spatial reorganization of HAI. The impact of HAI on ecological health had significant spatial heterogeneity. In areas where HAI had decreased, ecological health was prone to improve significantly. In contrast, in areas where HAI had increased, ecological health tended to become worse, and only when the increase of HAI exceeded 0.08 would that tendency be significant. Compared to urban areas, HAI change had even broader impacts on ecological health in remote mountain areas, where a more remarkable restoration of the ecosystem was experienced.
Keywords: *ecosystem health, human activity intensity, spatial heterogeneity, finer scale, GIS*

Introduction

Ecological health and its evaluation have played a critical role in human sustainable development (Sivakumar, 2007; D'Odorico et al., 2013). Studies show that human activity and natural factors could both strongly affect ecological health evolution (Shi et al., 2007; Sun et al., 2012; Ma et al., 2013, 2014). With the human population increasing to 9.1 billion by 2050, followed by accelerating urbanization and increasing challenges of generating enough food, human pressure on ecological health is becoming increasingly important and could generate a decisive influence on ecological health in a shorter amount of time (Halpern et al., 2008; Cao et al., 2014; Feng et al., 2015). This situation is highlighted in the Three Gorges Reservoir Region (TGRR) (Chen et al., 2019).

The world-famous Three Gorges Dam, as the largest hydroelectric project along the Yangtze River (Nilsson et al., 2005), has formed a unique geomorphological region called the Three Gorges Reservoir Region (Shao et al., 2018) that covers a total water and land surface area of 57,900 km^2, comprising 20 county-level divisions of the Chongqing municipality and Hubei province in China. Because of its special geographic

http://www.aloki.hu ● ISSN 1589 1623 (Print) ● ISSN1785 0037 (Online)
DOI: http://dx.doi.org/10.15666/aeer/2001_727741

environment, TGRR is characterized by typical ecological fragility with serious conflicts between the increasing human population and limited land surface. The construction of the hydroelectric project itself and the following strenuous adjustment in TGRR, such as resettlements of environmental migrants and the removal and reconstruction of towns, made the TGRR experience a remarkable spatial reorganization of the human factor in recent decades, suffering from a series of unprecedented ecological problems. Studying the relationship of human pressure and ecological health in TGRR is helpful for local ecological restoration, providing an important reference for the planning of large hydroelectric project constructions in other areas.

Costanza et al. (1992) first defined the concept of ecosystem health, which refers to the ability to keep its structure and recover by itself after disturbances. Myneni et al. (1992) reported that "ecological health is closely linked to the idea of sustainability, which is seen to be a comprehensive, multiscale, dynamic measure of system resilience, organization, and vigor". In recent decades, ecological health evaluation has become a research hotspot, and has been carried out in different areas and ecosystem types (Wu et al., 2018). The pressure–state–response (PSR) framework has been widely adopted to evaluate ecological health, which classifies ecological indicators on the basis of interactions between humans and ecosystems (Neri et al., 2016; Schumacher et al., 2016). The PSR framework performs well on ecological health simulation on the grid scale for studying spatial heterogeneity evolution (Allen et al., 2002), which is critical for detecting detailed spatial characteristics of ecological health evolution. However, with regard to the relationship between ecological health and human activity, the consideration of spatial heterogeneity in existing studies is insufficient (Li and Li, 2014; Jin et al., 2016; Niu et al., 2017). The main reason is that commonly used human-related factors (e.g., social and economic census data) can only be constrained at the administrative division in terms of scale. Therefore, when dealing with the impacts of human pressure on ecological health evolution, previous studies often focused on their statistical relationships by treating administrative divisions as sampling units (Zhao et al., 2016; He et al., 2019); others were usually conducted based on a limited number of the on-site samples which are incomplete and unsystematic (Zhang et al., 2013; Bebianno et al., 2015; Tang et al., 2015; Li et al., 2017). Thus, an in-depth study at finer scale is urgently needed. Particularly for the TGRR, this specific region having a highly discretized ecosystem in complex terrain and experiencing remarkable spatial reorganization due to human factors, the spatial heterogeneity of the relationship between ecological health and human pressure should be studied for the better understanding of the mechanism of human activity on ecological health evolution, and to provide better references for maintaining and recovering ecological health.

Because of the shortcomings of commonly used human-related factors, we applied human activity intensity (HAI) to quantitatively represent human influence on the ecosystem. HAI was proposed by Sanderson et al. (2002), and could be mapped at the grid scale by using four human pressure types (i.e., land use, population density, road distribution, and grazing density) on land on the basis of integrated GIS techniques (Li et al., 2018). Its comprehensiveness and availability on a fine scale made the HAI index an ideal proxy of human pressure on the ecosystem for our study. Therefore, the objective of this study was to calculate the ecological health of the study area by using PSR and map the HAI at the grid scale, then quantitatively analyzed the temporal-spatial change characteristics of ecological health and HAI, and their relationship.

http://www.aloki.hu ● ISSN 1589 1623 (Print) ● ISSN1785 0037 (Online)
DOI: http://dx.doi.org/10.15666/aeer/2001_727741

Materials and Methods

Study Area

The Three Gorges Reservoir Region is a modern geographical concept that refers to the region directly or indirectly influenced by the construction of the Three Gorges Dam, comprising 20 county-level divisions of Chongqing and Hubei province of China, with a total area of 57,900 km². Our study selected the section located in Chongqing province, accounting for 85% of the whole TGRR, as the study area (*Fig. 1*), which stretches along the Yangtze River from Jiangjin to Wushan county in Chongqing. The 20 counties of the study area can be classified into two categories. There are 9 developed counties including Nanan, Jiangbei, Yubei, Yuzhong, Beibei, Shapingba, Jiulongpo, Dadukou and Banan, which cluster together and form a metropolitan region of Chongqing province. The other counties all belong to developing counties, mainly distributed in remote mountainous areas. The study area consists mainly of mountainous and hilly areas representing 74% and 21.7% of the region, respectively, with only 4.3% of the plain areas in the river valley. This region belongs to the transition zone between the northern temperate and subtropical zones, and has typical subtropical monsoon climate characteristics with high temperatures (annual mean temperature is 18.2℃) and large amounts of precipitation (annual mean precipitation is 1200 mm) (Wang and Geng, 2013). The study area has various land-use types, with forestland accounting for the largest proportion (48.9%) of the total area. Agricultural land is the second major land-use type, with a proportion of 14.4%. In 2016, the study area had a total year-end population of 14.8 million, and GDP of RMB 776.6 billion (Ding et al., 2020). In recent years, the importance of the economic and ecological status of TGRR has been gradually recognized, and a favorable situation of its ecological health is becoming the basic guarantee for the sustainable development of the Yangtze economic zone.

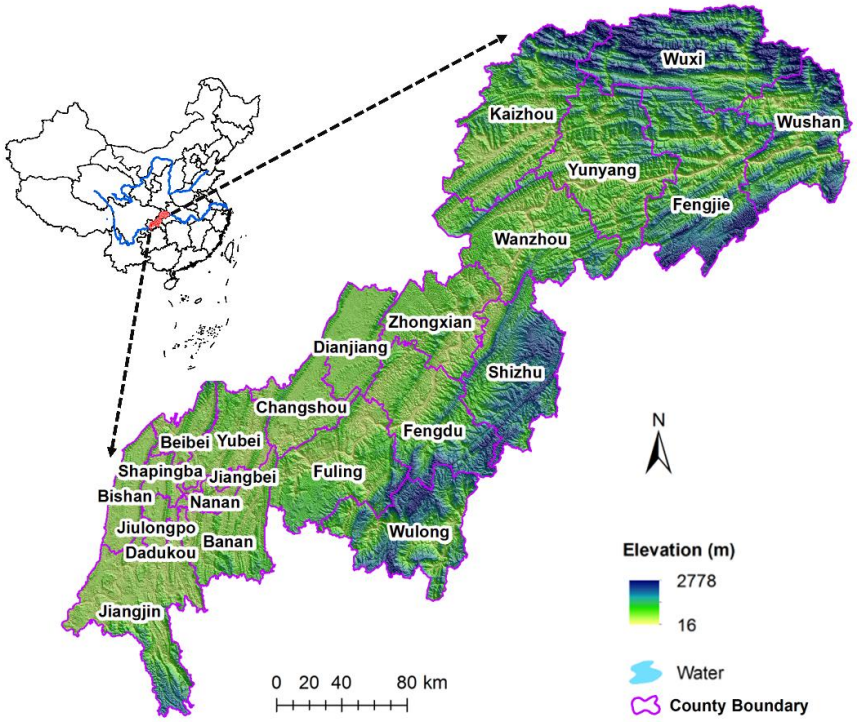

Figure 1. *Study area*

http://www.aloki.hu ● ISSN 1589 1623 (Print) ● ISSN1785 0037 (Online)
DOI: http://dx.doi.org/10.15666/aeer/2001_727741

Data Sources

By using the visual interpretation method, we applied the Landsat Thematic Mapper (TM) and Operational Land Imager (OLI) to produce the land-use dataset for 2000 and 2018, respectively (*Table 1*). All TM/OLI images, and the atmospheric correction before the interpretation, were georeferenced. We used survey results, conducted in 2018 by our study group, to validate the land-use dataset, and found that the overall accuracy of the land-use dataset in 2018 was 93%. We classified land-use types into six groups: farmland, forestland, grassland, water areas, wetland, and urban and rural settlements. Spatialized population data with a spatial resolution of 500 m × 500 m for 2000 and 2018 were provide by the Data Center for Resources and Environmental Sciences, Chinese Academy of Sciences (http://www.resdc.cn). We adopted a MODIS vegetation index (VI) product with spatial resolution of 500 ×500 m and temporal resolution of 16 days obtained from NASA's Earth Observing System to produce the normalized difference vegetation index (NDVI) dataset. First, the maximum value composite (MVC) method was applied to generate the monthly NDVI for 2000 and 2018, respectively. Then, the values of the monthly NDVI from April to November were averaged to obtain the growing-season NDVI (GSN). The GSN is a robust approximation of the vigor of the ecosystem (Tong et al., 2016). Road distribution data for 2000 and 2018 were extracted from the traffic map of Chongqing province, published by the Chongqing Surveying and Mapping Bureau. Grazing density data were extracted on the basis of the land-use dataset according to research of Li et al. (2018).

Table 1. *Description of data*

Name	Type	Scale/Resolution	Sources
TM/OLI images	grid	30 m × 30 m	The Institute of Remote Sensing and Digital Earth, Chinese Academy of Sciences (CAS)
Spatialized population data	grid	500 m × 500 m	The Data Center for Resources and Environmental Sciences, CAS
MODIS vegetation index (VI) product	grid	500 m × 500 m	NASA's Earth Observing System
Road distribution data	shp	1:100,000	Chongqing Surveying and Mapping Bureau
Grazing density data	grid	30 m × 30 m	Extracted based on land-use dataset

Methodology

Ecological Health Evaluation

The PSR model, which was initially proposed by the Organization of Economic Co-Operation and Development (OECD), was applied to evaluate the ecological health of the study area (Walz, 2000). The framework comprises three parts, pressure (P), state (S) and response (R). Each part can be complex when developed into different levels. According to the PSR model associated with our study aims, and data availability on the regional scale, we established a three-level index system for ecological health assessment in the TGRR (*Table 2*). Seven indices, weighted by the analytic hierarchy process (AHP) (Saaty and Vargas, 2001), were applied as the proxy of the pressure, state, and response of the study area ecosystem. Each index was standardized into an interval of (0–1) for comparison analysis. A larger value meant a better ecosystem

http://www.aloki.hu ● ISSN 1589 1623 (Print) ● ISSN1785 0037 (Online)
DOI: http://dx.doi.org/10.15666/aeer/2001_727741

condition. The combination of all standardized indices refers to ecological health (EH), which was calculated by using *Equation (1)*:

$$EH = \sum_{i=1}^{n} W_i * A_i \quad \text{(Eq.1)}$$

where, n is number of indices; W_i, weight of index i; and A_i, value of index i, which is standardized. The larger EH is, the better the ecological health, and vice versa.

Table 2. *Index system for ecological health assessment*

Target Level	Standard Level		Index Level
Ecological health assessment	Pressure (0.3)		Population Density
	State (0.6)	Vigor (0.13)	NDVI
		Organization (0.2)	Landscape diversity (0.1)
			Average patch area (0.1)
		Function (0.2)	Ecological service value
		Resilience (0.07)	Ecological resilience
	Response (0.1)		Landscape fragmentation

The produce of each index is as follows:

Population density: spatial population density data were applied to represent human pressure intensity.

NDVI: It could effectively measure the vigor of the vegetation cover. In our study, the NDVI was obtained from the MODIS vegetation index product by using the maximum value composite (MVC) method, which minimizes effects from cloud contamination.

Landscape diversity and average patch area: The organization index represents the complexity of ecosystem structure, which was characterized by using two landscape ecology indices (landscape diversity and average patch area) in this study. The two landscape ecology indices were produced by using the Fragstats software (Wu, 2000).

Ecological service value: Ecosystem services are benefits that human directly or indirectly gain from an ecosystem, such as water conservation, waste disposal and food production. In this study, the ecological service value was extracted from land use data according to the research of Xie et al. (2003), and Liao et al. (2018) (*Table 3*).

Ecological resilience: Ecological resilience represents the capacity of the ecosystem to withstand disturbances from natural and human activities (e.g., climate change and deforestation). Ecological resilience could be valued by using the ecological resilience index (ERI), which was calculated by using *Equation (2)*:

$$ERI = LD \times \sum_{i=1}^{n} R_i * S_i \quad \text{(Eq.2)}$$

where LD, landscape diversity index; R_i, area ratio of landscape type i to the study area; and S_i, resilience value of landscape type i, which is referred to in the study of Du et al. (2013).

http://www.aloki.hu ● ISSN 1589 1623 (Print) ● ISSN1785 0037 (Online)
DOI: http://dx.doi.org/10.15666/aeer/2001_727741

Table 3. *Ecosystem service value (¥/hm^2) for different land use types derived from Xie et al. (2003), and Liao et al. (2018)*

	Forest	Grass	Water	Farmland	Urban	Other
Gas regulation	3097	707.9	1592.7	442.4	0	0
Climate regulation	2389.1	796.4	15130.9	787.5	407	0
Water conservation	2831.5	707.9	13715.2	530.9	18033.2	26.5
Soil formation	3450.9	1725.5	1513.1	1291.9	8.8	17.7
Waste disposal	1159.2	1159.2	16086.6	1451.2	16086.6	8.8
Bio-diversity	2884.6	964.5	2212.2	628.2	2203.3	300.8
Food production	88.5	265.5	265.5	884.9	88.5	8.8
Raw materials	2300.6	44.2	61.9	88.5	8.8	0
Entertainment	1132.6	35.4	4910.9	8.8	3840.2	8.8
Total	19334	6406.5	55489	6114.3	40676.4	371.4

Landscape fragmentation: It reflects composite information containing both the complexity of the landscape pattern and the intensity of human activity. According to the research of Chen (2007), we adopted landscape fragmentation as the proxy of the response from human activity. The landscape fragmentation index was calculated on the basis of land use data by using *Equation (3)*:

$$L_i = N_i / S_i \quad \text{(Eq.3)}$$

where L_i, landscape fragmentation index of landscape i; N_i, number of patches of landscape i; and S_i, area of landscape i.

Mapping of Human Activity Intensity (HAI)

In the Anthropocene era, humans have dramatically influenced the ecosystem. Mapping human activity intensity (HAI), that is, quantitatively expressing the human pressure on a grid scale, is an important way to promote the study between the humans and ecosystems (Li et al., 2018). In this paper, we mapped TGRR HAI on a 500 × 500 m grid in 2000 and 2018 by tailoring the methodology of Sanderson et al. (2002). By considering the regional, biophysical, and cultural characteristics of the TGRR, we selected land use, population density, road accessibility, and grazing density as geographic input datasets. Then, each input dataset was normalized and assigned relative pressure scores of human activity intensity. Lastly, we summed up the human-activity scores for each of the four datasets to calculate human activity intensity.

Results and Discussion

Variation Characteristics in Ecological Health and HAI between 2000 and 2018

According to our estimates, the averaged grid-value of the ecological health map in 2000 was 0.54, and the corresponding value in 2018 was 0.61, which indicated an overall improvement of ecological health in the Three Gorges Reservoir Region from 2000 to 2018. With regard to the standardized indices referring to ecological health

http://www.aloki.hu ● ISSN 1589 1623 (Print) ● ISSN1785 0037 (Online)
DOI: http://dx.doi.org/10.15666/aeer/2001_727741

(*Fig. 2*), we yielded the averaged grid-value as follows: resilience index (0.40), vegetation vigor (0.60), organization index (0.30), ecosystem service index (0.12), fragmentation index (0.63), and population density index (0.99). The corresponding values in 2018 were 0.47, 0.77, 0.40, 0.16, 0.67, and 0.98, respectively. From 2000 to 2018, except for the population density index, which slightly decreased, the other five standardized indices all increased to some extent. The decrease in the population density index, where a larger value means a better ecosystem condition, could be explained by the increase in population in recent decades in the study area (Shao et al., 2018).

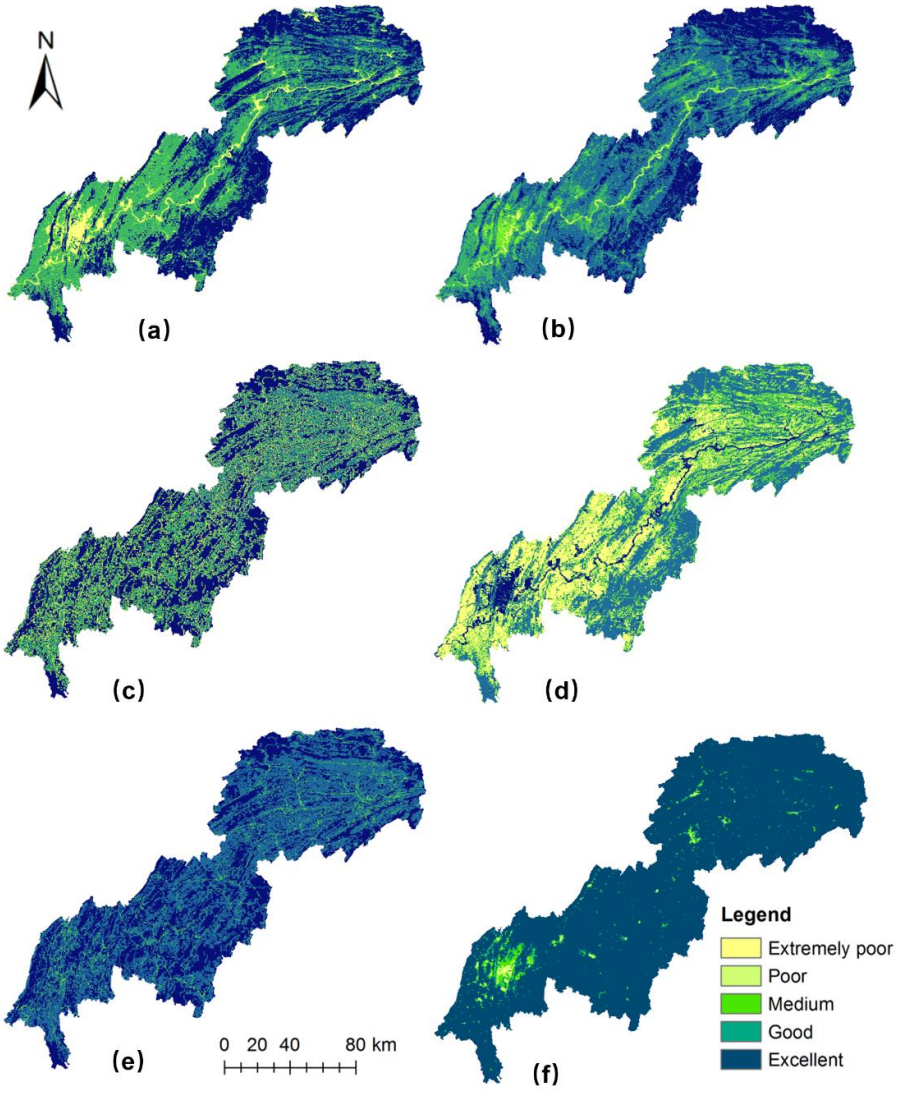

Figure 2. *Different standardized indices describing ecological health for 2018. (**a**) Ecological resilience index; (**b**) NDVI as proxy for vegetation vigor; (**c**) organization index; (**d**) ecosystem services index; (**e**) fragmentation index; (**f**) the population density index*

By using GIS technology, we generated ecological health and HAI changes from 2000 to 2018, respectively (*Fig. 3*), which provided detailed spatial information for better understanding the relationship between ecological health evolution and human activity disturbances. *Figure 3a* shows that, despite an overall improvement, there were

http://www.aloki.hu ● ISSN 1589 1623 (Print) ● ISSN1785 0037 (Online)
DOI: http://dx.doi.org/10.15666/aeer/2001_727741

some areas that experienced deterioration, which accounted for 13.3% of the total study area according to our statistics. The most obvious deterioration occurred in a region in the shape of a circle, located in the southwestern part of the study area (*Fig. 3a*). This region is the metropolitan area of Chongqing province, with high human activity density (*Fig. 3b*), and it has been experiencing a rapid urban expansion process while occupying farmlands (Liu et al., 2018). Therefore, urban expansion might trigger the formation of the deterioration circle of the ecological system.

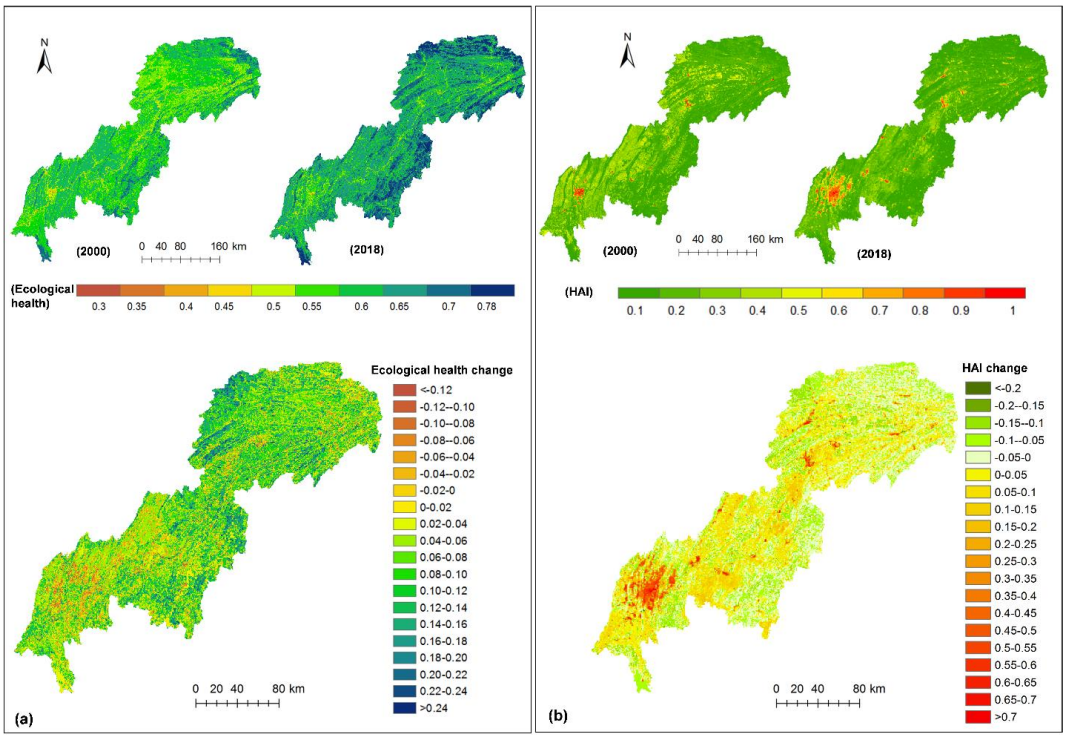

Figure 3. *(**a**) Ecological health of 2000 and 2018, and ecological health changes from 2000 to 2018; (**b**) human activity intensity (HAI) of 2000 and 2018, and HAI changes from 2000 to 2018*

According to *Figure 3b*, we could confirm the significant spatial reorganization of human activity intensity from 2000 to 2018 in the study area. About 77.93% of the total study area experienced an increase in HAI. The most obvious increase occurred in the metropolitan areas, and grids experiencing a decrease in HAI were distributed mainly in remote mountainous areas with high elevation and steep slopes (*Figs. 1 and 3b*). This phenomenon could be closely related to population movements, peasants migrating from villages to cities, which happened in the wide mountainous regions in China (Zhang et al., 2018). In mountainous areas, the outmigrant population directly relieved pressure from human activity on local ecosystems. Conversely, in the city area, ecosystems might suffer more from human disturbance because of immigrant populations. To sum up, in the Three Gorges Reservoir Region, from 2000 to 2018, the temporal and spatial changes of ecological health and human activity intensity were both significant. From the perspective of spatial detail mining, the relationship between ecological health and human pressure could be very complicated.

http://www.aloki.hu ● ISSN 1589 1623 (Print) ● ISSN1785 0037 (Online)
DOI: http://dx.doi.org/10.15666/aeer/2001_727741

Relationships between Human Activity Intensity and the Ecological Health Evolution

In order to quantitatively clarify the relationship between HAI and ecological health, linear regression analysis was used to treat samples extracted from two different scales, respectively. There are 24 counties (administrative region unit) in the study area (*Fig. 4f*). We averaged the grid values for each county in terms of ecological health and HAI and their changes for 2000 and 2018, and then plotted them on a scattered point diagram (*Fig. 4a-c*). We also generated 1930 uniformly distributed sample points in the study area (*Fig. 4f*) in the GIS environment to mine on a finer scale the influence characteristics of HAI changes on ecological health changes. The 1930 sample points were classified into two groups according to whether the HAI change on the points increased or decreased. The scattered point diagrams of the two sample point groups were also produced (*Fig. 4d,e*).

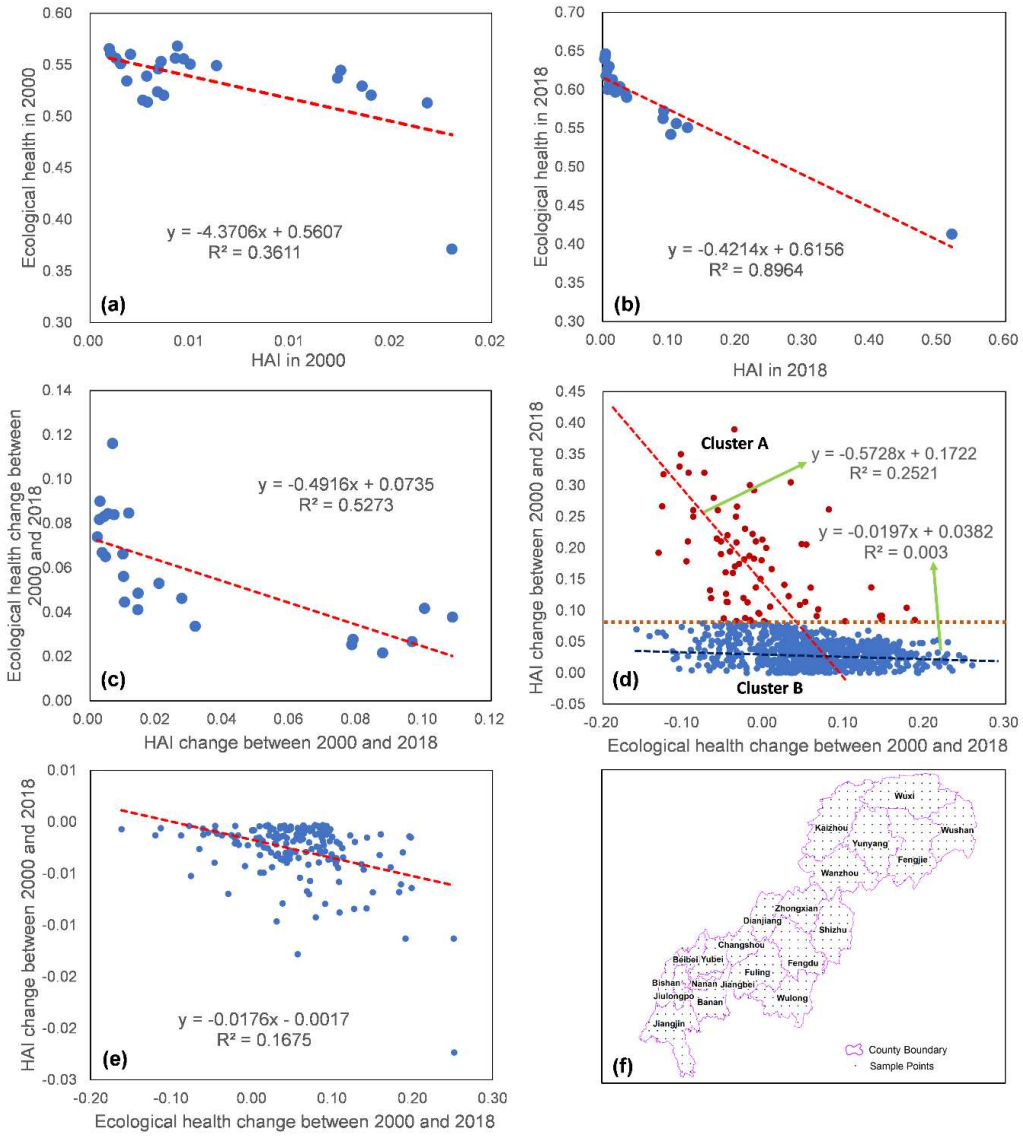

Figure 4. *Relationship between ecological health and human activity intensity on a county scale (**a**) in 2000, (**b**) in 2018, and (**c**) between 2000 and 2018; scattered sample points experiencing HAI (**d**) increase and (**e**) decrease; (**f**) county and sample point distribution*

http://www.aloki.hu ● ISSN 1589 1623 (Print) ● ISSN1785 0037 (Online)
DOI: http://dx.doi.org/10.15666/aeer/2001_727741

According to *Figure 4a,b*, there was a significant negative relationship between HAI and ecological health in both 2000 and 2018. Comparatively, the coefficient of determination (R^2) that we yielded in 2018 (R^2 = 0.89) was larger than that in 2000 (R^2 = 0.36). Therefore, in the Three Gorges Reservoir Region from 2000 to 2018, the impact of human activity pressure on the ecosystem became more serious. It could be further confirmed by the significant negative correlation between HAI and ecological health changes, exhibited in *Figure 4c*. On the finer scale, by classifying the sample points according to increase or decrease of HAI, we safely obtained two laws: in areas where HAI had increased, ecological health was prone to worsening (*Fig. 4d*); in areas where HAI had decreased, ecological health improved (*Fig. 4e*). Notably, if we check the *Figure 4d* carefully, the sample points could be divided into two clusters: cluster A composed of sample points with HAI increase exceeding 0.08, and cluster B composed of the others with relative less HAI increase. The linear regression analysis shows that, only when the increase of HAI is beyond 0.08, its impact on ecological health toward deterioration is significant (e.g., cluster A). When it is below 0.08, there is no remarkable effect (e.g., cluster B). In contrast, in the *Figure 4e*, with the decrease of HAI, the ecological health improved constantly and significantly. Therefore, in different ranges of HAI change, its effects on ecological health could vary greatly.

To sum up, it is explicit that the spatial reorganization of HAI has significantly driven the evolution of ecological health from 2000 to 2018 in the Three Gorges Reservoir Region. Nevertheless, *Figure 4* only revealed the general relationship between HAI and ecological health for the entire study area.

The advantages of the grid-scale spatial data enabled us to put insights into each county of study area. By using the GIS technology, we generated 100 uniformly distributed sample points in each county. The grid-values of ecological health and HAI were extracted to the sample points, and then ecological health change from 2000 to 2018, and the correlation coefficients between ecological heath and HAI for each county were calculated. From *Figure 5*, we found an especial phenomenon: there were a group of counties (Yuzhong, Yubei, Shapingba, Nanan, Jiulongpo, Jiangbei, Dadukou, Beibei and Banan), with relative lower ecological health improvement and irregular fluctuation of correlation coefficients, did not follow the rule illuminated in the *Figure 4*. The rest counties belong to the other group with higher ecological health increase and keep consistent with the rule exhibited for the entire study area. Interestingly, all the counties of first group were collectively located in urban areas with high economy development (developed counties), which accounted for merely 11.25% of the total area of TGRR; the counties in the second group all had backward economic development (developing counties), and mainly distributed in remote mountainous areas. This found might optimize the finding obtained from *Figure 4*. The impacts of human activity intensity on the evolution of ecological health would be more significant in remote mountainous areas than urban areas. Thus, we believe that, making a difference between remote mountains areas and urban areas, should be essential for better understanding the driving mechanism of human activity on ecological health change in the future study in TGRR.

A Special Case in TGRR

When compared to other places reported by previous studies of ecosystem evolution, what happened in TGRR is unique. Many studies reported on ecosystem degradation in ecologically fragile regions, especially in remote mountainous areas with serious

http://www.aloki.hu ● ISSN 1589 1623 (Print) ● ISSN1785 0037 (Online)
DOI: http://dx.doi.org/10.15666/aeer/2001_727741

conflict between increasing human populations and limited natural resources (Han et al., 2020), such as the northeast Tibetan Plateau (Liu et al., 2020), the Eastern Black Sea Region (Bekci, 2021), and the Manica Highlands of southern Africa (Clark et al., 2019). In these places, increasing population pressure and food shortages have forced residents to exploit remaining natural resources with unsustainable activities such as deforestation, overgrazing, and the reclamation of cultivated land, thereby exacerbating ecosystem degradation. Ecosystem degradation conversely worsens food production, and then leads to more exploitation. This is called a vicious cycle of ecosystem degradation.

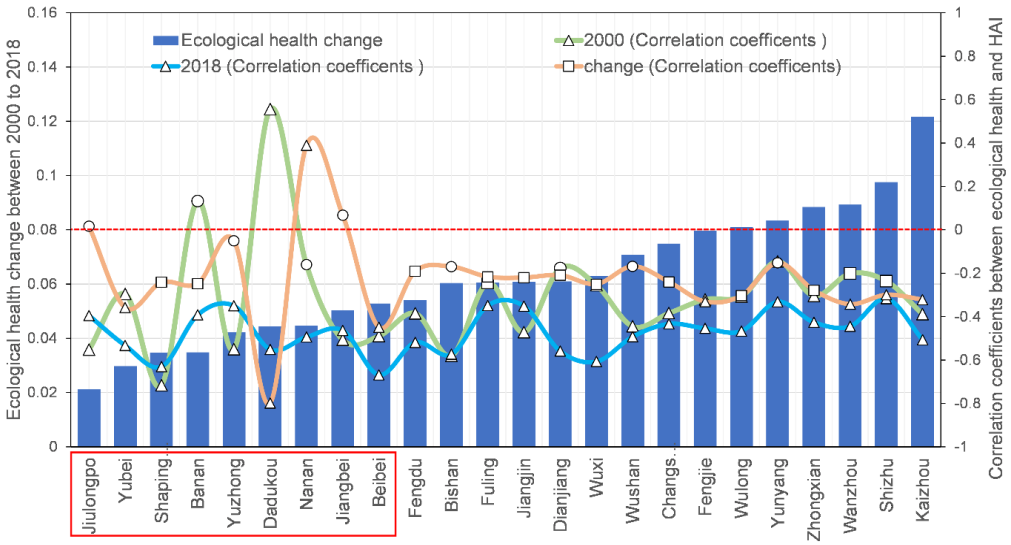

Figure 5. *Ecological health change from 2000 to 2018, and the correlation coefficients between ecological heath and HAI for each county (△: highly significant correlation (P<0.01), □: significant correlation (P<0.05), ○: no significant correlation)*

The Three Gorges Reservoir Region is a typical ecologically fragile region with serious conflict between increasing human populations and limited land surface (Tong et al., 2018). However, according to our study, it jumped out of the vicious cycle of ecosystem degradation, and achieved an obvious improvement of ecological health from 2000 to 2018. Although ecological health was negatively correlated with HAI, the ecological environment of remote mountainous areas widely distributed in the study area had the opportunity to recover because of the spatial reorganization of human activity intensity. Large-scale and long-term population migrants in the Three Gorges Reservoir Region have deeply influenced the spatial reorganization of human activity intensity (Li and Tan, 2018), which might lastly foster the uniqueness of ecological health evolution. At present, study of the relationship between human activity and ecological health continues to deepen (Jaiswal and Pandey, 2021). In the Chuandong region of China, Han et al. (2020) found that the negatively linear relationship between human disturbances and ecosystem service varied across different terrain gradients. In the Three Gorges Reservoir Region, we identified that variation between remote mountains areas and urban areas, which has not been reported by previous studies. It might be another unique characteristic of the study area. Our study quantitatively clarified the relationship between HAI and ecological health on a finer scale, which

http://www.aloki.hu ● ISSN 1589 1623 (Print) ● ISSN1785 0037 (Online)
DOI: http://dx.doi.org/10.15666/aeer/2001_727741

enable us to yield detailed effecting natures of human pressure on ecological health. Using measured migrant population data with questionnaire surveys to explore the internal impact mechanisms of human activity on ecosystem changes will be a research trend in the Three Gorges Reservoir Region.

Conclusion

We established a three-level index system for ecological health assessment in the Three Gorges Reservoir Region by using the PSR model, and calculated the ecological health products of 2000 and 2018, respectively. We found an overall improvement in ecological health from 2000 to 2018. With regard to the standardized indices, except for the population density index, which slightly decreased, the five other standardized indices (resilience, vegetation, organization, ecosystem service, and fragmentation indices) were all increased to some extent. Around the metropolitan area, a deterioration circle of the ecological system exists. From 2000 to 2018, there was significant spatial reorganization of human activity intensity triggered by the migrant population from mountainous areas to cities. Ecological health was negatively correlated to HAI both in 2000 and 2018. From 2000 to 2018, the impact of HAI on ecological health has significant spatial heterogeneity. In areas where HAI had increased, ecological health was prone to becoming worse, and only when the increase of HAI is beyond 0.08, its impact on ecological health toward deterioration is significant; in areas where HAI had decreased, ecological health improved constantly and significantly according to statistical analysis. Compared to urban areas, the effect of HAI change on ecological health is more outstanding in remote mountain areas, where the reduction of HAI promoted the restoration of the ecosystem.

Our study first applied human activity intensity (HAI) to quantitatively represent human pressure on the ecosystem, and attempted to clarify the relationship between HAI and ecological health on a finer scale to overcome the shortcomings of the county scale in the Three Gorges Reservoir Region. Nevertheless, the impact mechanism of specific human activity (e.g., reclaiming farmlands, afforestation, rural laborers moving out to work) on ecological health is still obscure. In the future, employing detailed household survey data that are specifically tailored to the migrant population–human activity–ecosystem relationship would promote a deeper understanding of the related mechanisms.

Acknowledgments. This work was supported by Chongqing Research Program of Basic Research and Frontier Technology (No. cstc2019jcyj-msxmX0515), National Natural Science Foundation of China (No. 42001388, 41771460, 41801063), Project funded by China Postdoctoral Science Foundation (No. 2019M653830XB), Youth Innovation Promotion Association, China (No. 2018417).

Conflicts of Interests. The authors declare no conflict of interests.

REFERENCES

[1] Allen, C. D., Savage, M., Falk, D. A., Suckling, K. F., Swetnam, T. W., Schulke, T., Stacey, P. B., Morgan, P., Hoffman, M., Klingel, J. T. (2002): Ecological restoration of southwestern ponderosa pine ecosystems: a broad perspective. – Ecological Applications 12: 1418-1433.

http://www.aloki.hu ● ISSN 1589 1623 (Print) ● ISSN1785 0037 (Online)
DOI: http://dx.doi.org/10.15666/aeer/2001_727741

[2] Bebianno, M. J., Pereira, C. G., Rey, F., Cravo, A., Duarte, D., D'Errico, G., Regoli, F. (2015): Integrated approach to assess ecosystem health in harbor areas. – Science of the Total Environment 514: 92-107.
[3] Bekci, B. (2021): A case study on the interdependence between the coastal ecosystem and humankind. – Ocean & Coastal Management 210: 105666.
[4] Cao, S. X., Ma, H., Yuan, W. P., Wang, X. (2014): Interaction of ecological and social factors affects vegetation recovery in China. – Biological Conservation 180: 270-277.
[5] Chen, P. (2007): Ecological health assessment at the landscape scale based on RS and GIS, A case study from the New District of a Bay-type city. – Acta Scientiae Circumstantiae 27(10): 1744-1752.
[6] Chen, C. D., Cheng, H., Jia, J. S., Wang, X. Y., Zhao, J. J. (2019): Use it or not: An agro-ecological perspective to flooded riparian land along the Three Gorges Reservoir. – Science of the Total Environment 650: 1062-1072.
[7] Clark, V. R., Vidal, J. D., Grundy, I. M., Fakarayi, T., Childes, S. L., Barker, N. P., Linder, H. P. (2019): Bridging the divide between intuitive social-ecological value and sustainability in the Manica Highlands of southern Africa (Zimbabwe-Mozambique). – Ecosystem Services 39: 100999.
[8] Costanza, R., Norton, B. G., Haskell, B. D. (1992): Ecosystem Health: New Goals for Environmental Management. – Island Press, Washington, DC.
[9] Ding, X. K., Wang, Y. Q., Han, Y. G., Fu, J. (2020): Evaluating of net anthropogenic nitrogen inputs and its influencing factors in the Three Gorges Reservoir Area. – China Environmental Science 1: 206-216.
[10] D'Odorico, P., Bhattachan, A., Davis, K. F., Ravi, S., Runyan, C. W. (2013): Global desertification: drivers and feedbacks. – Advances in Water Resources 51: 326-344.
[11] Du, P. J., Xia, J. S., Du, Q., Luo, Y., Tan, K. (2013): Evaluation of the spatio-temporal pattern of urban ecological security using remote sensing and GIS. – International Journal of Remote Sensing 34: 848-863.
[12] Feng, Q., Ma, H., Jiang, X. M., Wang, X., Cao, S. X. (2015): What has caused desertification in China? – Scientific Reports 5: 15998.
[13] Halpern, B. S., Walbridge, S., Selkoe, K. A., Kappel, C. V., Micheli, F., D'Agrosa, C., Bruno, J. F., Casey, K. S., Ebert, C., Fox, H. E., Fujita, R., Heinemann, D., Lenihan, H. S., Madin, E. M., Perry, M. T., Selig, E. R., Spalding, M., Steneck, R., Watson, R. (2008): A global map of human impact on marine ecosystems. – Science 319: 948-952.
[14] Han, R., Feng, C.-C., Xu, N., Guo, L. (2020): Spatial heterogeneous relationship between ecosystem services and human disturbances: A case study in Chuandong, China. – Science of The Total Environment 721: 137818.
[15] He, J. H., Pan, Z. Z., Liu, D. F., Guo, X. N. (2019): Exploring the regional differences of ecosystem health and its driving factors in China. – Science of the total environment 673: 553-564.
[16] Jaiswal, D., Pandey, J. (2021): Human-driven changes in sediment-water interactions may increase the degradation of ecosystem functioning in the Ganga River. – Journal of Hydrology 598: 126261.
[17] Jin, Y., Yang, W., Sun, T., Yang, Z., Li, M. (2016): Effects of seashore reclamation activities on the health of wetland ecosystems: a case study in the Yellow River Delta, China. – Ocean & Coastal Management 123: 44-52.
[18] Li, Y., Li, D. (2014): Assessment and forecast of Beijing and Shanghai's urban ecosystem health. – Science of the Total Environment 487: 154-163.
[19] Li, B., Li, X., Bouma, T. J., Soissons, L. M., Cozzoli, F., Wang, Q., Zhou, Z., Chen, L. (2017): Analysis of macrobenthic assemblages and ecological health of Yellow River Delta, China, using AMBI & M-AMBI assessment method. – Marine Pollution Bulletin 119(2): 23-32.

http://www.aloki.hu ● ISSN 1589 1623 (Print) ● ISSN1785 0037 (Online)
DOI: http://dx.doi.org/10.15666/aeer/2001_727741

[20] Li, W., Tan, H. M. (2018): Spatial redistribution of populations in mountainous areas and its impact on vegetation change in southwest China: A riverside case study. – Acta Ecologica Sinica 38(24): 8879-8887.
[21] Li, S. C., Zhang, Y. L., Wang, Z., Li, L. (2018): Mapping human influence intensity in the Tibetan Plateau for conservation of ecological service functions. – Ecosystem Services 30: 276-286.
[22] Liao, C. J., Yue, Y. M., Wang, K. L., Fensholt, R., Tong, X. W., Brandt, M. (2018): Ecological restoration enhances ecosystem health in the karst regions of southwest China. – Ecological Indicators 90: 416-425.
[23] Liu, R., Xiao, L. L., Liu, Z., Dai, J. C. (2018): Quantifying the relative impacts of climate and human activities on vegetation changes at the regional scale. – Ecological Indicators 93: 91-99.
[24] Liu, C. L., Li, W. L., Zhu, G. F., Zhou, H. K., Yan, H. P., Xue, P. F. (2020): Land use/land cover changes and their driving factors in the Northeastern Tibetan Plateau based on geographical detectors and google earth engine: a case study in Gannan Prefecture. – Remote Sensing 12(19): 3139.
[25] Liu, Y. Q., Lv, C. H., Fu, B. J. (2021): Terrestrial ecosystem classification and its spatiotemporal changes in China during last 20 years. – Acta Ecologica Sinica 41(10): 3975-3987.
[26] Ma, D., Liu, Z. Y., Liu, S. H., Notaro, M., Rong, X. Y., Chen, G. S., Wang, F. Y. (2013): Short term effects of vegetation changes in the East Asian monsoon on local climate. – Science Bulletin 58(17): 1661-1669. (in Chinese).
[27] Ma, H., Wang, Y. Q., Wang, L., Wang, Y. K. (2014): Coupling relationship between vegetation cover and climate change and rural economic development in rocky desertification area in recent 20 years in China. – Journal of Mountain Science 32(1): 38-45. (in Chinese).
[28] Myneni, R., Asrar, G., Hall, F. (1992): A three-dimensional radiative transfer method for optical remote sensing of vegetated land surfaces. – Remote Sensing of Environment 41: 105-121.
[29] Neri, A. C., Dupin, P., Sánchez, L. E. (2016): A pressure–state–response approach to cumulative impact assessment. – Journal of Cleaner Production 126: 288-298.
[30] Nilsson, C., Reidy, C. A., Dynesius, M., Revenga, C. (2005): Fragmentation and flow regulation of the world's large river systems. – Science 308(5720): 405-408.
[31] Niu, M. X., Wang, J., Xu, B. D. (2017): Assessment of the ecosystem health of the YellowRiver Estuary based on the pressure-state-response model. – Acta Ecologica Sinica 37: 943-952. (in Chinese).
[32] Saaty, T. L., Vargas, L. G. (2001): Models, Methods, Concepts & Applications of the Analytic Hierarchy Process. – Springer, Boston, MA.
[33] Sanderson, E. W., Jaiteh, M., Levy, M. A., Redford, K. H., Wannebo, A. V., Woolmer, G. (2002): The human footprint and the last of the wild. – Bioscience 52: 891-904.
[34] Schumacher, P., Mislimshoeva, B., Brenning, A., Zandler, H., Brandt, M., Samimi, C., Koellner, T. (2016): Do red edge and texture attributes from high-resolution satellite data improve wood volume estimation in a semi-arid mountainous region? – Remote Sensing 8: 540.
[35] Shao, J. A., Dang, Y. F., Wang, W., Zhang, S. C. (2018): Simulation of future land-use scenarios in the Three Gorges Reservoir Region under the effects of multiple factors. – Journal of Geographical Sciences 28(12): 1907-1932.
[36] Shi, Z. G., Yan, X. D., Yin, C. H., Wang, Z. M. (2007): Impact of historical changes in human land use on climate. – Chinese Science Bulletin 52(12): 1436-1444. (in Chinese).
[37] Sivakumar, M. V. K. (2007): Interactions between climate and desertification. – Agricultural and Forest Meteorology 142: 143-155.

http://www.aloki.hu ● ISSN 1589 1623 (Print) ● ISSN1785 0037 (Online)
DOI: http://dx.doi.org/10.15666/aeer/2001_727741

[38] Sun, X. P., Wang, T. M., Ko, X. J., Ge, J. P. (2012): Analysis of long-time sequential normalized vegetation index changes and their driving forces in the Jinghe river basin of the loess plateau. – Chinese Journal of Plant Ecology 36(6): 511-521. (in Chinese).
[39] Tang, D., Zou, X., Liu, X., Liu, P., Zhamangulova, N., Xu, X., Zhao, Y. (2015): Integrated ecosystem health assessment based on eco-exergy theory: a case study of the Jiangsu coastal area. – Ecological Indicators 48: 107-119.
[40] Tong, L., Liu, C., Nie, H. (2016): Assessing future vegetation trends and restoration prospects in the karst regions of southwest China. – Remote Sensing 8: 357.
[41] Tong, X., Brandt, M., Yue, Y., Horion, S., Wang, K., De Keersmaecker, W., Tian, F., Schurgers, G., Xiao, X., Luo, Y. (2018): Increased vegetation growth and carbon stock in China karst via ecological engineering. – Nature Sustainability 1: 44.
[42] Walz, R. (2000): Development of environmental indicator systems: experiences from Germany. – Environmental Management 25: 613-623.
[43] Wang, Y. H., Geng, Y. H. (2013): Effects of soil water losses during different ecological restoration stages of small watersheds in the Three Gorges Reservoir Area. – Journal of Soil and Water Conservation 27(4): 78-82.
[44] Wu, J. G. (2000): Landscape Ecology: Pattern, Process, Scale and Hierarchy. – Higher Education Press, Beijing.
[45] Wu, L., You, W., Ji, Z., Xiao, S., He, D. (2018): Ecosystem health assessment of Dongshan Island based on its ability to provide ecological services that regulate heavy rainfall. – Ecological Indicators 84: 393-403.
[46] Xie, G. D., Lu, C. X., Leng, Y. F., Zheng, D., Li, S. C. (2003): Ecological assets valuation of the Tibetan Plateau. – Natural Resources Journal 18: 189-196.
[47] Zhang, L. L., Liu, J. L., Yang, Z. F., Li, Y., Yang, Y. (2013): Integrated ecosystem health assessment of a macrophyte-dominated lake. – Ecological Modelling 252(1): 141-152.
[48] Zhang, B. L., Gao, J. B., Gao, Y., Cai, W. M., Zhang, F. R. (2018): Land use transition of mountainous rural areas in China. – Acta Geographica Sinica 73(3): 503-517. (in Chinese).
[49] Zhao, H. B., Zheng, H., Miao, C. H. (2016): Spatial-temporal pattern and factor diagnoses of agroecosystem health in major grain producing areas of Northeast China: A case study in Jilin Province. – Chinese Journal of Applied Ecology 27(10): 3290-3298. (in Chinese).

http://www.aloki.hu ● ISSN 1589 1623 (Print) ● ISSN1785 0037 (Online)
DOI: http://dx.doi.org/10.15666/aeer/2001_727741

MULTI-OBJECTIVE OPTIMIZATION OF POTATO VARIETIES AND EFFECTIVE WAYS TO IMPROVE POTATO (*SOLANUM TUBEROSUM* L.) TUBER QUALITY IN THE LOESS PLATEAU OF CHINA

WANG, X. K.* – XIE, K.

College of Life Science, Yan'an University, Yan'an, Shaanxi 716000, PR China

**Corresponding author*
e-mail: wangxiukang@126.com

(Received 10th Sep 2021; accepted 28th Oct 2021)

Abstract. Choosing varieties that are suitable for planting in different areas has become a key scientific issue. We used principal component analysis (PCA) to evaluate and select better varieties with relatively high potato tuber yield and quality in the Loess Plateau of China. We selected fifteen potato varieties that are mainly grown locally for the experiment. The potato variety significantly affected potato tuber yield, dry matter accumulation, starch content, protein content, reducing sugar, total soluble sugar, vitamin C, and browning intensity. The soil nitrate N content in 0-20 cm was 17.8% and 28.6% higher than that in 20-40 cm and 40-60 cm, respectively. Potato tuber yield was significantly correlated with the soil water, soil ammonium N, soil alkali-hydrolyzable N, and soil available phosphorus contents. The starch content of potato tubers was significantly correlated with soil pH value and soil electrical conductivity. The potato variety of Xiapoti had the relatively high potato tuber yield, dry mater accumulation, starch content, total soluble sugar, and protein content. Therefore, Xiapoti is recommended as an optimal potato variety in the Loess Plateau of China.
Keywords: *soil water content, soil nitrate nitrogen, soil organic matter, protein content, total soluble sugar, browning intensity*

Introduction

Potato (*Solanum tuberosum* L.), a food crop in the Solanaceae family, is the fourth largest staple crop after corn, rice and wheat. It can provide more carbohydrates, proteins, minerals and vitamins per unit land area and time than other potential food crops (Hameed et al., 2018). In addition to being edible, potatoes are used industrially for processed foods, alcohol, starch, animal feed and biofuel production. Short crop durations and extensive climate adaptation have contributed to the spread of the potato across different geographical boundaries from its South American origin. Worldwide, there are more than 4,500 varieties of potatoes (e.g., Fovorita, Kexin No. 15, Atlantic…) are grown in more than 100 countries (Seibt et al., 2012). In terms of nutrition, the potato is a complex source of nutrients (vitamins, carotenoids, antioxidant phenols, proteins, magnesium, etc.), as well as a number of antinutrients (mainly glycoalkaloids). Potato tubers contain 77% water, 20% carbohydrates, and less than 3% protein, dietary fiber, minerals, vitamins, and other compounds on average (Camire et al., 2009; Visvanathan et al., 2016; Zaheer and Akhtar, 2016). The global importance of the potato is indisputable, placing it in the fight against food shortages and poverty.

The selection of varieties suitable for planting in different regions has become a key scientific problem. In particular, screening potato varieties with high yield and resistance to disease is more difficult. Hongmei is a new potato variety developed in recent years, which is also a rich source of high value proteins, antioxidants, phenolic compounds, and

http://www.aloki.hu ● ISSN 1589 1623 (Print) ● ISSN1785 0037 (Online)
DOI: http://dx.doi.org/10.15666/aeer/2001_743769

important minerals such as K and Zn (Xu et al., 2018). Choi et al. (2016) comprehensively analyzed the contents of protein amino acids, non-protein amino acids, glucose, fructose, sucrose, phenols and flavonoids in different varieties of potato. The characteristics and genes of different varieties were determined by plant biomass, gene variation, amino acid profile analysis and gene expression analysis to optimize potato varieties (Tiwari et al., 2020). The potato varieties suitable for local cultivation were screened through the effect of single virus and mixed virus infection on the yield of twelve varieties (eight locally bred and four imported) (Mulabisana et al., 2019). Yamdeu Galani et al. (2017) selected the better potato varieties by studying the adaptability evaluation of the contents of vitamin C, total phenol, phenolic acid and antioxidant capacity of different potato varieties to storage temperature. Studies have shown that Saturna and Alegria have higher starch content and lower sucrose content in tubers under limited nitrogen conditions, which makes them excellent breeding candidates (Van Dingenen et al., 2019). However, these studies were limited to the merits of specific potato qualities and subjective evaluations based on data.

As the farmers in some areas have been planting potato varieties for a long time, the potato varieties in this area are deteriorating more and more seriously, thus making the potato yield lower and quality worse. This is closely related to soil physical and chemical properties and soil fertility in different areas. Soil available potassium had a positive effect on potato tuber starch and reducing sugar contents, and a negative effect on soluble protein and browning intensity (Xing et al., 2020; Xing et al., 2022). Potato tuber quality can be improved by increasing the calcium content of tubers (Palta, 2010). Soil nitrogen content is the key nutrient to improve the cv 'Symphonia' growth, yield and tuber quality in the local growing conditions of Punjab province Pakistan on sandy loam soil (Ayyub et al., 2019). Potato tuber yield is closely related to soil organic matter, K and P content in the northeastern United States (Porter et al., 1999). The effects on protein content, total phenols and antioxidant activity of healthy tubers depend on the interaction between environmental factors and genotype in southern Chile (Ávila-Valdés et al., 2020). Low soil moisture content decreased tuber dry weight, sugar and protein content, but increased polyphenols content and antioxidant activity (Elhani et al., 2019).

In the potato growing areas of the Loess Plateau in China, 50.3% of farmers overapply fertilizer, which not only increases the planting cost, but also poses a potential threat to the soil (Wang et al., 2020). Therefore, it is necessary to study the local soil nutrient status in order to identify the most effective fertilization strategy. There are few reports on the correlation between tuber quality and soil nutrients of different potato varieties in the Loess Plateau area. The comprehensive evaluation of tuber yield and quality of different potato varieties on the Loess Plateau and the coupling effect between tuber yield and quality and soil nutrients have important theoretical and practical significance for optimizing field management. The objective of this study was (1) to quantify the coupling relationship between tuber quality of different potato varieties and soil nutrients; (2) to find out an optimal potato variety of yield and quality is relatively high based on principal component analysis (PCA).

http://www.aloki.hu ● ISSN 1589 1623 (Print) ● ISSN1785 0037 (Online)
DOI: http://dx.doi.org/10.15666/aeer/2001_743769

Materials and methods

Site description

The experiment was carried out in the potato test station in Yulin Modern Agricultural Science and Technology Demonstration Park of Shaanxi Province from April to September 2019 and 2020. The experimental site is located at 109°45'30"E, 38°22'37"N, with an altitude of 1100 m. The annual precipitation is concentrated in June, July and August, with an average precipitation of 400 mm, annual evaporation of 1900 mm, annual total sunshine hours of 2900 h, and annual temperature of 8.5℃ on average. According to the USDA soil classification system, the experimental site soil is sandy. The average sand, silt and clay contents in the 0- 60 cm soil profile were measured with a laser particle size analyzer (Dandong Haoyu Technology Co., Ltd), and the values were 80.2%, 14.1% and 5.7%, respectively. Before the experiment, the soil pH value was 8.1; the soil bulk density of 0-60 cm surface layer was 1.38 g cm^{-3}; the soil field capacity was 21.4%; the soil ammonium nitrogen content was 5.8 mg kg^{-1}, soil nitrate nitrogen content was 2.1 mg kg^{-1}, soil available phosphorus content was 6.2 mg kg^{-1}, and soil available potassium content was 67.4 mg kg^{-1}.

Experimental design

The experiment consisted of 15 different potato varieties, which were 1463-115 (T1), Feiurita (T2), Shaza (T3), Yushu 3 (T4), Qingshu 17 (T5), Laokoupi (T6), He 14 (T7), Qingshu 9 (T8), Xingjing 2 (T9), Longshu 13 (T10), Zhongshu 3 (T11), Akeria (T12), Yushu 4 (T13), Xiapoti (T14) and Longshu 7 (T15). According to the local actual production experience, the lower limit of soil moisture was set at different growth stages, and the soil moisture content of 65% soil field capacity (SFC) at seedling stage, tuber formation stage (70% SFC), tuber expansion stage (75% SFC), starch accumulation stage (65% SFC) and maturity stage (65% SFC). Fertilizer application amount (N-P_2O_5-K_2O) according to the local field fertilization standard is 240-120-300 kg ha^{-1}. The plot length is 20 m, the width is 3.6 m, and the plot area is 72 m^2. In this experiment, potatoes were planted by mechanically ridging, the width between ridges was 90 cm, the sowing distance between two potato plants was 25 cm, and the planting density was about 45000 plants ha^{-1}.

Field potato drip irrigation uses ridge drip irrigation. Since the root system of potato is mainly distributed in 0-40 cm, the average soil water content below the surface of the soil is selected as 40 cm. When the soil water content is lower than the lower limit of irrigation, irrigation will be started until the soil water content reaches the field water capacity. The thin-walled maze drip irrigation pipe with diameter of 16 mm was used for irrigation. The spacing between the transmitters was 0.3 meters. Water meters and ball valves are used to control the amount of water in each plot.

The N, P and K fertilizers applied in the experiment were urea, ammonium dihydrogen phosphate and potassium nitrate. The proportion of five times fertilizer application was 0: 2: 5: 3: 0 in the whole growth stage (seedling stage; tuber formation stage; tuber expansion stage; starch accumulation stage; maturity stage). The water-soluble fertilizer was applied to the soil with drip irrigation, and the utilization coefficient of irrigation water was 0.95.

Potatoes were sown on May 8 and harvested on September 28, 2019. During the growth, from phase 39 on the BBCH scale (complete crop cover), the potato plants were treated thrice, in 20- to 30-day intervals, with growth stage.

http://www.aloki.hu ● ISSN 1589 1623 (Print) ● ISSN1785 0037 (Online)
DOI: http://dx.doi.org/10.15666/aeer/2001_743769

Measurements and calculations

Tuber yield and tuber quality

Potato tuber samples were taken from September 26 to September 28 in 2019. At the time of harvest, the fresh tuber weight per plant (g plant^{-1}) were determined by the plants harvested (5 plants) from the central rows of the plots. At the same time. The starch content was measured using iodine colorimetry (Wang et al., 2019). The soluble protein content was determined by coomassie bright blue method (Liu et al., 2017). The vitamin C content was measured by titration (Wang et al., 2019). The reducing sugar content was determined by 3, 5-2 nitrosalicylic acid colorimetric method (Gao et al., 2015).

Soil physical and chemical properties

Soil samples were taken from September 26 to September 28 in 2019. The soil nitrate-N content (N = 5) in the 60 cm profile was measured using a spectrophotometer (UV–VIS 8500, China) with sampling a depth interval of 20 cm (Wang et al., 2018). Soil organic matter content was determined by potassium dichromate volumetric method (external heating method) with five replications and with a sampling depth interval of 0 cm to 60 cm. Soil available phosphorus was determined by molybdenum antimony anti-spectrophotometry method with $NaHCO_3$ extraction. Soil available potassium was determined by flame photometry method with NH_4OAc extraction.

PCA of the potato yield and tuber quality

Principal component analysis (PCA) is a general term for a technique that uses complex basic mathematical principles to convert some variables that may be relevant into a smaller number of variables called principal components. The process for the analysis is as follows:

(1) Select sample parameters.

$$X = \begin{bmatrix} X_{11} & X_{12} & \cdots & X_{1p} \\ X_{21} & X_{22} & \cdots & X_{2p} \\ \vdots & \vdots & & \vdots \\ X_{n1} & X_{n2} & \cdots & X_{np} \end{bmatrix} \quad \text{(Eq.1)}$$

where n is the measured value of the sample number (i.e., the potato yield, tuber quality), and p is the variable number.

(2) Sample parameters are converted to standardized values.

$$x_{ij}^{*} = \frac{x_{ij} - \overline{x}_j}{s_j} \qquad i = 1, 2, ..., n;\ j = 1, 2, ..., p \quad \text{(Eq.2)}$$

where $\overline{x}_j = \frac{1}{n}\sum_{i=1}^{n} x_{ij}$, $s_j^2 = \frac{1}{n-1}\sum_{i=1}^{n}(x_{ij} - \overline{x}_j)^2$, and n is the measured value of the sample number.

http://www.aloki.hu ● ISSN 1589 1623 (Print) ● ISSN1785 0037 (Online)
DOI: http://dx.doi.org/10.15666/aeer/2001_743769

(3) Calculate correlation matrix.

$$R = \begin{bmatrix} r_{11} & r_{12} & \cdots & r_{1p} \\ r_{21} & r_{22} & \cdots & r_{2p} \\ \vdots & \vdots & & \vdots \\ r_{p1} & r_{p2} & \cdots & r_{pp} \end{bmatrix} \quad \text{(Eq.3)}$$

where r_{ij} is the correlation coefficient of the original variable, $r_{ij} = r_{ji}$, and r_{ij} is given by the following equation:

$$r_{ij} = \frac{\sum_{k=1}^{n} (X_{ki} - \overline{X}_i)(X_{kj} - \overline{X}_j)}{\sqrt{\sum_{k=1}^{n} (X_{ki} - \overline{X}_i)^2 \sum_{k=1}^{n} (X_{kj} - \overline{X}_j)^2}} \quad \text{(Eq.4)}$$

(4) The eigenvalues of R and eigenvectors of each sample number are calculated.

$$|\lambda E - R| = 0 \quad \text{(Eq.5)}$$

where λ is the eigenvalue, E is the identity matrix and R is the correlation matrix. Next, these eigenvalues are sized down as $\lambda_1 \geq \lambda_2 \geq \cdots \geq \lambda_p \geq 0$, and the respective eigenvector e_i $(i = 1, 2, \cdots\cdots)$ solved for: $\|e_i\|=1$

where e_{ij} is the j-th component of e_i. $\sum_{j=1}^{p} e_{ij}^2 = 1$

(5) The characteristic values were used to calculate the contribution rate (C_r) and accumulative contribution rate (AC_r).

$$C_r = \frac{\lambda_i}{\sum_{k=1}^{p} \lambda_k} \quad (i = 1,2, \cdots, p) \quad \text{(Eq.6)}$$

$$AC_r = \frac{\sum_{k=1}^{i} \lambda_k}{\sum_{k=1}^{p} \lambda_k} \quad (i = 1,2, \cdots, p) \quad \text{(Eq.7)}$$

(6) The mathematical model is established based on the PCA, as defined in the following equation:

http://www.aloki.hu ● ISSN 1589 1623 (Print) ● ISSN1785 0037 (Online)
DOI: http://dx.doi.org/10.15666/aeer/2001_743769

$$\begin{aligned} Q_1 &= S_{11}X_1 + S_{12}X_2 + \cdots + S_{1p}X_p \\ Q_2 &= S_{21}X_1 + S_{22}X_2 + \cdots + S_{2p}X_p \\ &\cdots\cdots \\ Q_t &= S_{t1}X_1 + S_{t2}X_2 + \cdots + S_{tp}X_p \end{aligned} \quad \text{(Eq.8)}$$

where S_{1i}, S_{2i}, ⋯, S_{ti} ($i = 1, 2, \cdots, t$) are the eigenvectors corresponding to the principal components, and $X_1, X_2, \cdots, X_p$ are the standardized values, the value of which is converted based on the sample parameters.

(7) The evaluation process is determined according to the comprehensive evaluation index (Q).

$$Q = \lambda_1 Q_1 + \lambda_2 Q_2 + \cdots + \lambda_t Q_t \quad \text{(Eq.9)}$$

where $\lambda_1, \lambda_2 \cdots \lambda_t$ are the characteristic values corresponding to the principal components, and $Q_1, Q_2, \cdots, Q_t$ are the evaluation values of the different irrigation and fertilization treatments. The advantages and disadvantages of treatment are positively correlated with the comprehensive evaluation indexes.

Data analysis

Analysis of variance was conducted to evaluate the effect of different potato varieties on tuber yield and quality. Significant differences between the detected parameters were compared by Tukey's HSD test at One-way ANOVA the 95% confidence level ($p < 0.05$). In addition, the effect of different potato varieties on the relationships among all the parameters was calculated using bivariate correlations analysis (Correlation coefficients, Pearson; Test of Significance, Two-tailed). SPSS statistical software 16.0 and Sigma Plot 14.0 were used for statistical analysis and data plotting.

Results

Potato tuber yield and quality

Significant differences in potato tuber yield, dry matter accumulation, starch content, and protein content were observed in different potato varieties (*Fig. 1*). The high potato tuber yield was observed in T2 (1.45 kg plant^{-1}), which was 20% to 71.7% higher than that in other potato varieties (*Fig. 1A*). The average tuber yield of each treatment in order from high to low in the top three was: T2 > T5 > T7 (*Fig. 1A*).

The high dry matter accumulation was observed in T14 (1.24 kg plant^{-1}), which was 1.4%, 11.3%, and 24.4% higher than that in T2, T5, and T7, respectively (*Fig. 1B*). The high starch content was observed in T4 (11.6%), which was 1.6% to 39.9% higher than that in other potato varieties (*Fig. 1C*). The starch content in T4 was 3.9%, 7.2%, and 25.1% higher than that in T2, T5, and T7, respectively (*Fig. 1C*). The high protein content

http://www.aloki.hu ● ISSN 1589 1623 (Print) ● ISSN1785 0037 (Online)
DOI: http://dx.doi.org/10.15666/aeer/2001_743769

was observed in T15, which was 47.7%, 48.1%, and 64% higher than that in T2, T5, and T7, respectively (*Fig. 1D*).

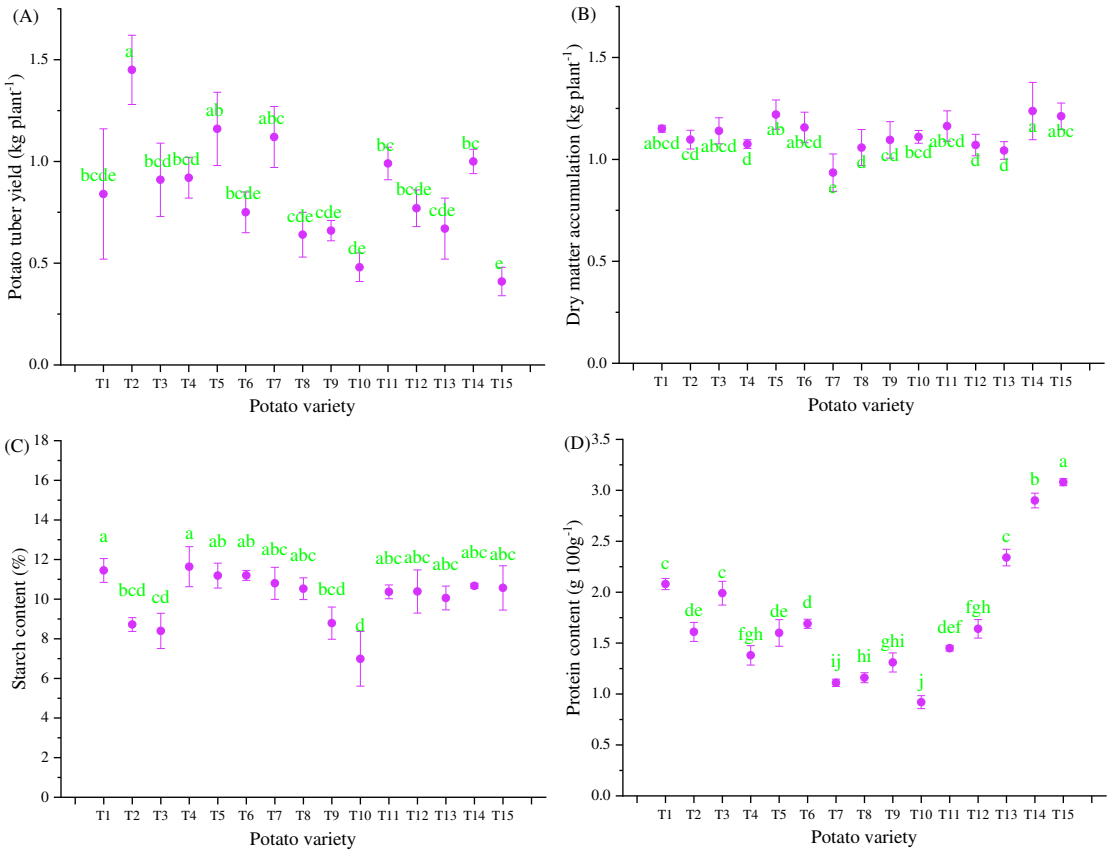

Figure 1. *Effects of different potato varieties on potato tuber yield (A), dry matter accumulation (B), Starch content (C), and protein content (D). Note: T1, 1463-115; T2, Feiurita; T3, Shaza; T4, Yushu 3; T5, Qingshu 17; T6, Laokoupi; T7, He 14; T8, Qingshu 9; T9, Xingjing 2; T10, Longshu 13; T11, Zhongshu 3; T12, Akeria; T13, Yushu 4; T14, Xiapoti; T15, Longshu 7. Different lowercase letters indicate significant difference between treatments by the Tukey HSD test ($p < 0.05$)*

The potato variety significantly affected potato reducing sugar, total soluble sugar, vitamin C, and browning intensity (*Fig. 2*). The high potato reducing sugar was observed in T3, which was 6.8% to 70.5% higher than that in other potato varieties (*Fig. 2A*). The average reducing sugar of each treatment in order from high to low in the top three was: T3 > T13 > T7 (*Fig. 2A*). The high total soluble sugar was observed in T13 (3.4%), which was 20.8% to 63.5% higher than that in other potato varieties (*Fig. 2B*). The average total soluble sugar of each treatment in order from high to low in the top three was: T13 > T1 > T9 (*Fig. 2B*). The high vitamin C was observed in T1, which was 17.3%, 25.3%, and 27.6% higher than that in T2, T5, and T7, respectively (*Fig. 2C*). The high browning intensity was observed in T11, which was 23.8% to 70.1% higher than that in other potato varieties (*Fig. 2D*). The browning intensity in T11 was 61.6% and 25.1% higher than that in T2 and T5, respectively (*Fig. 2D*).

http://www.aloki.hu ● ISSN 1589 1623 (Print) ● ISSN1785 0037 (Online)
DOI: http://dx.doi.org/10.15666/aeer/2001_743769

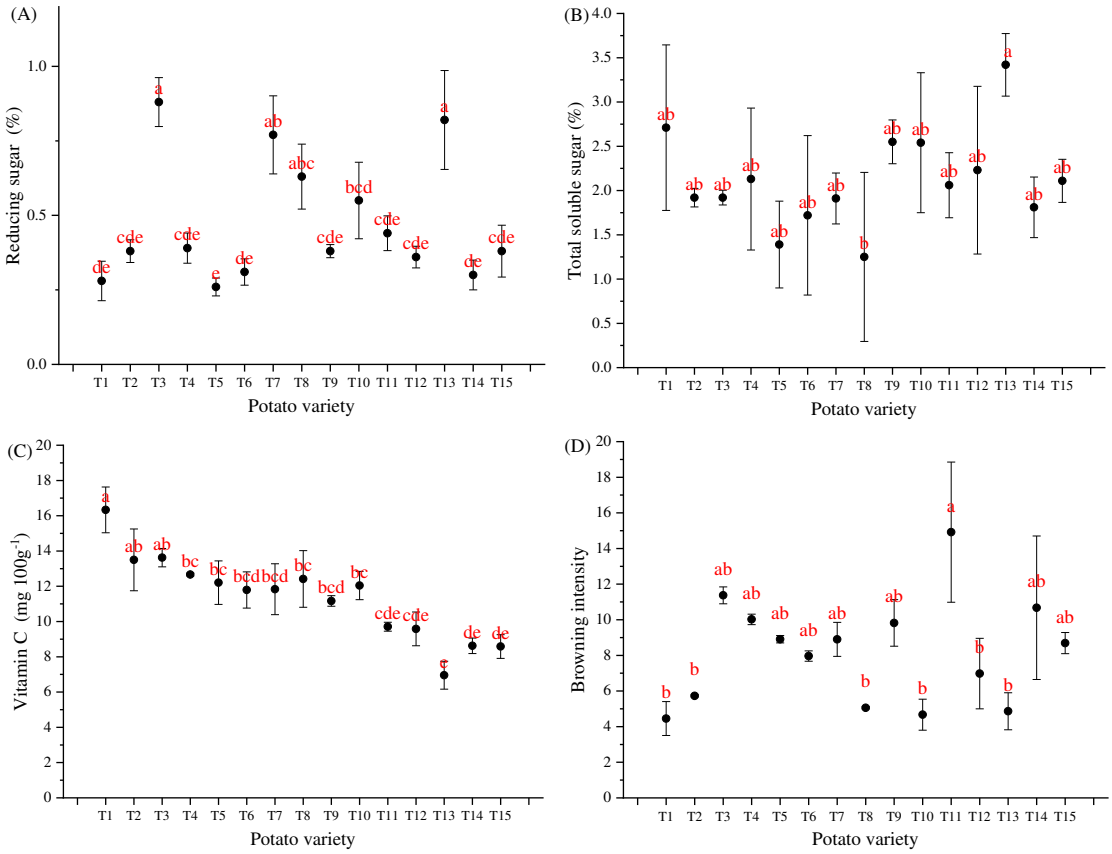

Figure 2. *Effects of different potato varieties on reducing sugar (A), total soluble sugar (B), vitamin C (C), and browning intensity (D). Note: T1, 1463-115; T2, Feiurita; T3, Shaza; T4, Yushu 3; T5, Qingshu 17; T6, Laokoupi; T7, He 14; T8, Qingshu 9; T9, Xingjing 2; T10, Longshu 13; T11, Zhongshu 3; T12, Akeria; T13, Yushu 4; T14, Xiapoti; T15, Longshu 7. Different lowercase letters indicate significant difference between treatments by the Tukey HSD test ($p < 0.05$)*

Soil physical and chemical properties

Significant differences in different soil depths of soil water content, pH, and soil electric conductivity were observed in different potato varieties (*Fig. 3*). On average potato varieties, the soil water content decreased with the increase of soil depth, and the soil water content in 0-20 cm was 30.2% and 35.7% higher than that in 20-40 cm and 40-60 cm, respectively (*Fig. 3A, D, G*). On average soil depth, the high soil water content was observed in T11 (13%), which was 17.3%, 25.3%, and 27.6% higher than that in T2, T5, and T7, respectively (*Fig. 3A, D, G*). On average soil depth, the high pH was observed in T7, which was 1.9% to 8.3% higher than that in other potato varieties (*Fig. 3B, E, H*). The soil pH on average soil depth of each treatment in order from high to low in the top three was: T7 > T14 > T12 (*Fig. 3B, E, H*). On average potato varieties, the soil electric conductivity increased with the increase of soil depth, and the soil electric conductivity in 0-20 cm was 6.5% and 27.5% lower than that in 20-40 cm and 40-60 cm, respectively (*Fig. 3C, F, I*). On average soil depth, the high electric conductivity was observed in T5, which was 8.3% to 44.1% higher than that in other potato varieties (*Fig. 3C, F, I*).

http://www.aloki.hu ● ISSN 1589 1623 (Print) ● ISSN1785 0037 (Online)
DOI: http://dx.doi.org/10.15666/aeer/2001_743769

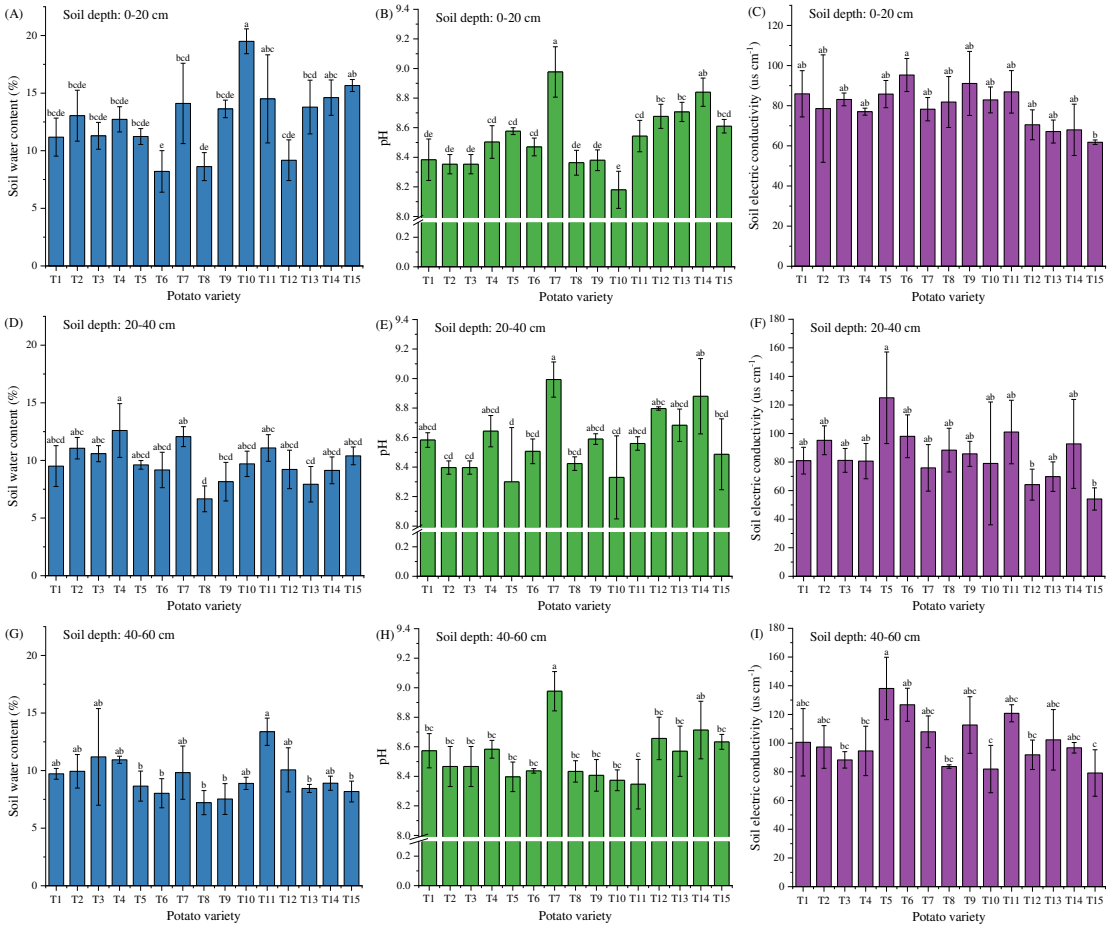

Figure 3. *Effects of different potato varieties on soil water content (A, D, G), pH (B, E, H), and soil electric conductivity (C, F, I) in different soil depths (0-20 cm, A, B, C; 20- 40 cm, D, E, F; 40- 60 cm, G, H, I). Note: T1, 1463-115; T2, Feiurita; T3, Shaza; T4, Yushu 3; T5, Qingshu 17; T6, Laokoupi; T7, He 14; T8, Qingshu 9; T9, Xingjing 2; T10, Longshu 13; T11, Zhongshu 3; T12, Akeria; T13, Yushu 4; T14, Xiapoti; T15, Longshu 7. Different lowercase letters indicate significant difference between treatments by the Tukey HSD test ($p < 0.05$)*

The potato variety significantly affected soil nitrate N, ammonium N and alkali-hydrolyzed N contents (*Fig. 4*). On average potato varieties, the soil nitrate N content decreased with the increase of soil depth, and the soil nitrate N content in 0-20 cm was 17.8% and 28.6% higher than that in 20-40 cm and 40-60 cm, respectively (*Fig. 4A, D, G*). On average soil depth, the high soil nitrate N content was observed in T11, which was 20.4% to 74% higher than that in other potato varieties (*Fig. 4A, D, G*). On average soil depth, the highest soil ammonium N content was observed in T11 (10.2 mg kg^{-1}), which was 21.1%, 32%, and 30.3% higher than that in T2, T5, and T7, respectively (*Fig. 4B, E, H*). On average potato varieties, the soil alkali-hydrolyzed N content decreased with the increase of soil depth, and the soil alkali-hydrolyzed N content in 0-20 cm was 6% and 18.3% higher than that in 20-40 cm and 40-60 cm, respectively (*Fig. 4C, F, I*). On average soil depth, the high soil alkali-hydrolyzed N content was observed in T2, which was 3.5% to 42.3% higher than that in other potato varieties (*Fig. 4C, F, I*).

http://www.aloki.hu ● ISSN 1589 1623 (Print) ● ISSN1785 0037 (Online)
DOI: http://dx.doi.org/10.15666/aeer/2001_743769

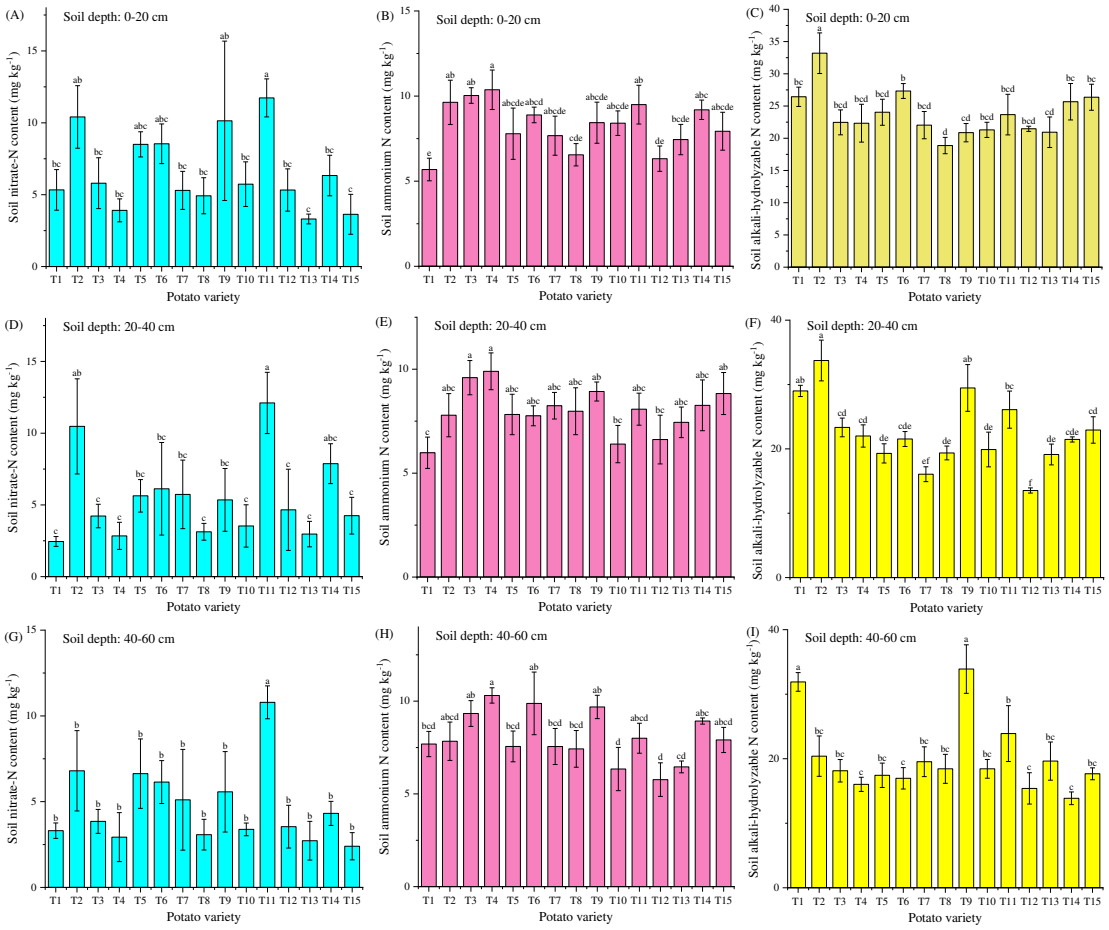

Figure 4. *Effects of different potato varieties on soil nitrate-N content (A, D, G), soil ammonium N content (B, E, H), and soil alkali-hydrolyzable N content (C, F, I) in different soil depths (0-20 cm, A, B, C; 20- 40 cm, D, E, F; 40- 60 cm, G, H, I). Note: T1, 1463-115; T2, Feiurita; T3, Shaza; T4, Yushu 3; T5, Qingshu 17; T6, Laokoupi; T7, He 14; T8, Qingshu 9; T9, Xingjing 2; T10, Longshu 13; T11, Zhongshu 3; T12, Akeria; T13, Yushu 4; T14, Xiapoti; T15, Longshu 7. Different lowercase letters indicate significant difference between treatments by the Tukey HSD test ($p < 0.05$)*

The potato variety significantly affected soil organic matter content, soil available phosphorus content, and soil available potassium content (*Fig. 5*). On average potato varieties, the soil organic matter content decreased with the increase of soil depth, and the soil organic matter content in 0-20 cm was 4.4% and 16.7% higher than that in 20-40 cm and 40-60 cm, respectively (*Fig. 5A, D, G*). On average soil depth, the high soil organic matter content was observed in T11, which was 6.2% to 50.7% higher than that in other potato varieties (*Fig. 5A, D, G*). On average potato varieties, the soil available phosphorus content decreased with the increase of soil depth, and the soil available phosphorus content in 0-20 cm was 25.2% and 28.3% higher than that in 20-40 cm and 40-60 cm, respectively (*Fig. 5B, E, H*). On average soil depth, the high soil available phosphorus content was observed in T12, which was 34%, 33.9%, and 45.2% higher than that in T2, T5, and T7, respectively (*Fig. 5B, E, H*). On average soil depth, the high soil available potassium content was observed in T2, which was 22.4% to 90.7% higher than that in

http://www.aloki.hu ● ISSN 1589 1623 (Print) ● ISSN1785 0037 (Online)
DOI: http://dx.doi.org/10.15666/aeer/2001_743769

other potato varieties, and the soil available potassium content in order from high to low in the top three was: T2 > T14 > T5 (*Fig. 5C, F, I*).

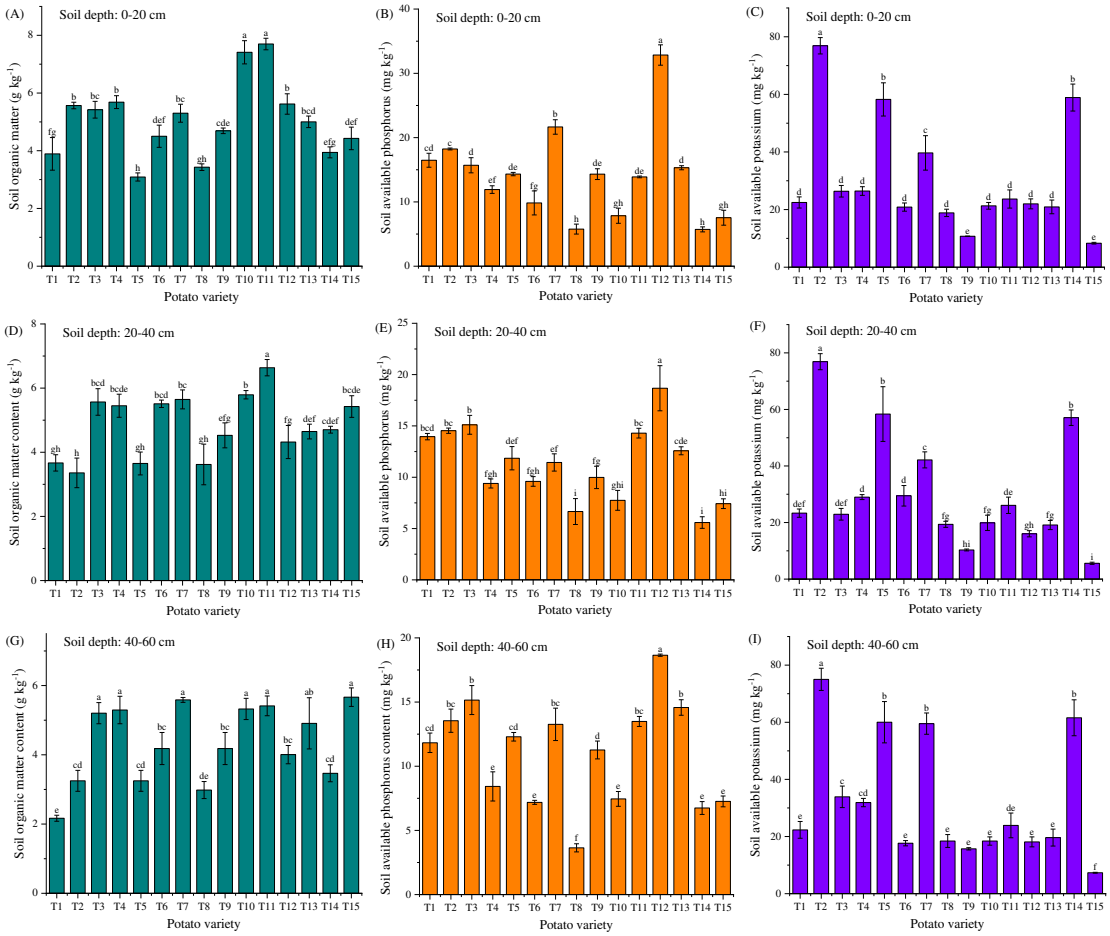

Figure 5. *Effects of different potato varieties on soil organic matter content (A, D, G), soil available phosphorus content (B, E, H), and soil available potassium content (C, F, I) in different soil depths (0-20 cm, A, B, C; 20- 40 cm, D, E, F; 40- 60 cm, G, H, I). Note: T1, 1463-115; T2, Feiurita; T3, Shaza; T4, Yushu 3; T5, Qingshu 17; T6, Laokoupi; T7, He 14; T8, Qingshu 9; T9, Xingjing 2; T10, Longshu 13; T11, Zhongshu 3; T12, Akeria; T13, Yushu 4; T14, Xiapoti; T15, Longshu 7. Different lowercase letters indicate significant difference between treatments by the Tukey HSD test ($p < 0.05$)*

Correlation analysis and principal component analysis

There were very significant ($p<0.01$) correlations between potato tuber yield and soil electric conductivity ($R^2= 0.3062$), soil nitrate-N content ($R^2= 0.3178$), soil available potassium ($R^2= 0.5433$) (*Table 1, Fig. 6*). In addition, the potato tuber yield was significant ($p<0.05$) correlated with the soil water content ($R^2= 0.1181$), soil ammonium N content ($R^2= 0.1024$), soil alkali-hydrolyzable N content ($R^2= 0.093$), and soil available phosphorus ($R^2= 0.1065$) (*Table 1, Fig. 6*). The potato tuber starch content was very significant ($p<0.01$) correlated with the soil pH ($R^2= 0.2107$) and soil electric conductivity ($R^2= 0.1494$) (*Table 1, Fig. 6*).

http://www.aloki.hu ● ISSN 1589 1623 (Print) ● ISSN1785 0037 (Online)
DOI: http://dx.doi.org/10.15666/aeer/2001_743769

Table 1. *The correlation among the potato tuber yield, tuber quality, soil physical and chemical index using the average values (n=3)*

Item	TY	DMA	SC	PC	RS	TSS	VC	BI	SWC	pH	SEC	SNNC	SANC	SHNC	SOM	P	K
TY	1																
DMA	0.19	1															
SC	.380*	.301*	1														
PC	-0.026	.520**	0.286	1													
RS	0.146	-0.171	0.036	-0.066	1												
TSS	0.219	0.209	.315*	0.173	.398**	1											
VC	.453**	0.18	0.206	-0.232	0.116	0.215	1										
BI	0.285	.386**	0.225	0.135	0.085	0.073	-0.068	1									
SWC	.344*	0.213	0.048	0.07	0.271	.376*	0.123	.430**	1								
pH	0.241	-0.157	.459**	0.237	0.186	0.179	-0.222	0.188	0.178	1							
SEC	.553**	.305*	.387**	-0.202	-0.056	0.134	.398**	.318*	0.048	-0.102	1						
SNNC	.564**	.319*	0.103	-0.11	-0.131	0.048	0.115	.483**	.320*	-0.074	.663**	1					
SANC	.320*	0.286	0.218	0.188	0.164	0.08	0.172	.603**	.346*	0.014	.296*	.317*	1				
SHNC	.305*	0.271	0.029	0.161	-0.186	0.255	.452**	0.105	0.186	-0.274	.316*	.476**	0.212	1			
SOM	-0.097	-0.114	-0.195	-0.165	.378*	0.2	-0.203	.416**	.678**	0.075	-0.116	0.186	.311*	-0.158	1		
P	.326*	-0.217	0.022	-0.22	0.132	0.178	0.08	0.032	0.097	0.242	0.029	0.16	-0.262	0.044	0.078	1	
K	.737**	0.107	0.054	0.006	-0.125	-0.172	0.188	0.075	0.175	0.174	.335*	.412**	0.155	0.137	-0.289	0.103	1

Note: TY, potato tuber yield; DMA, dry matter accumulation; SC, Starch content; PC, protein content; RS, reducing sugar; TSS, total soluble sugar; VC, vitamin C; BI, browning intensity; SWC, soil water content; pH, soil pH; SEC, soil electric conductivity; SNNC, soil nitrate-N content; SANC, soil ammonium N content; SHNC, soil alkali-hydrolyzable N content. SOM, soil organic matter; P, soil available phosphorus; K, soil available potassium; **, Correlation is significant at the 0.01 level (2-tailed); *, Correlation is significant at the 0.05 level (2-tailed)

http://www.aloki.hu ● ISSN 1589 1623 (Print) ● ISSN1785 0037 (Online)
DOI: http://dx.doi.org/10.15666/aeer/2001_743769

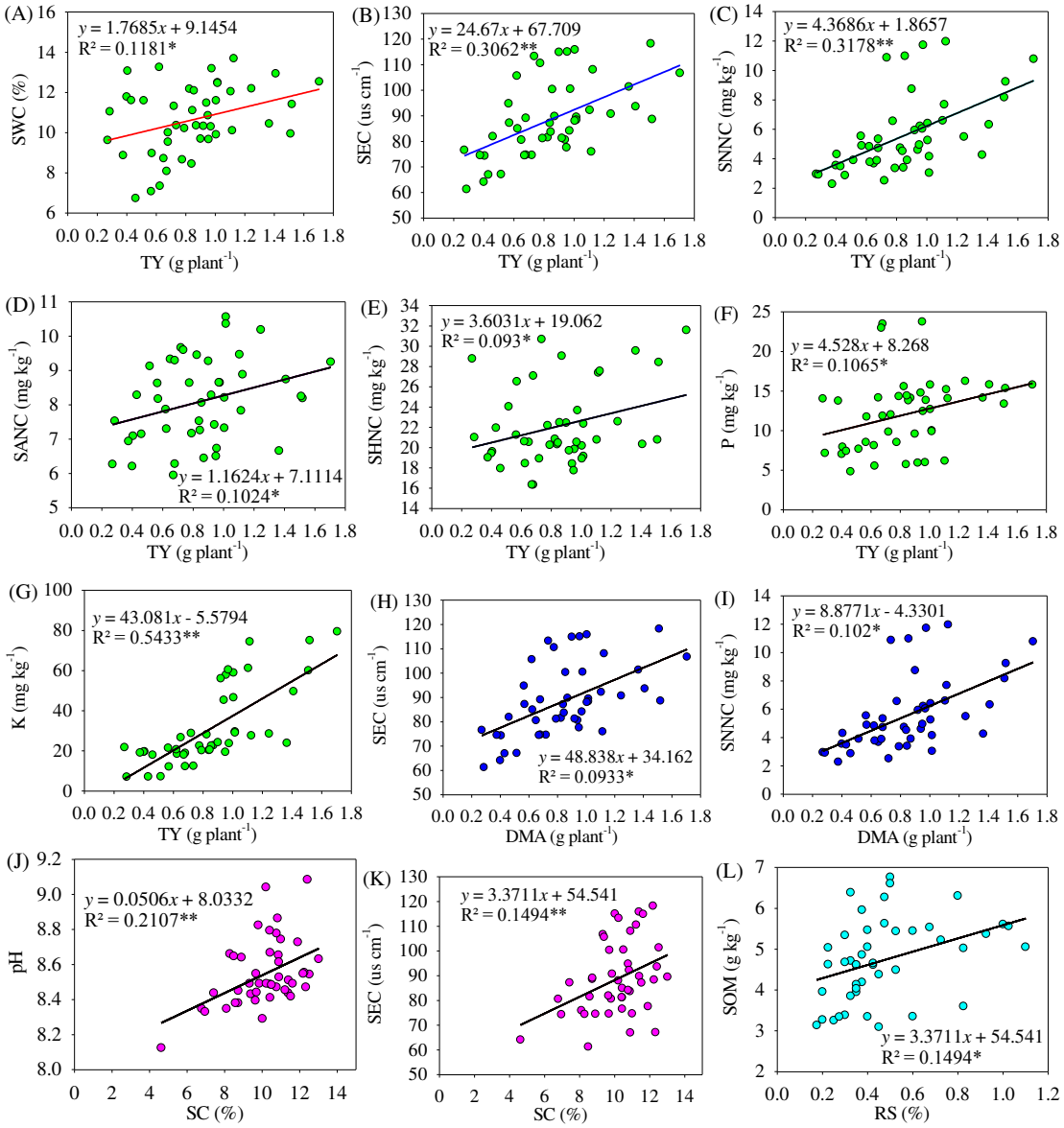

Figure 6. *The linear relationship between soil index and potato tuber quality. Note: TY, potato tuber yield; DMA, dry matter accumulation; SC, Starch content; RS, reducing sugar; SWC, soil water content; pH, soil pH; SEC, soil electric conductivity; SNNC, soil nitrate-N content; SANC, soil ammonium N content; SHNC, soil alkali-hydrolyzable N content; SOM, soil organic matter; P, soil available phosphorus; K, soil available potassium; **, Correlation is significant at the 0.01 level (2-tailed); *, Correlation is significant at the 0.05 level (2-tailed)*

The vitamin C content was very significant ($p<0.01$) correlated with the soil electric conductivity ($R^2= 0.1587$) and soil alkali-hydrolyzable N content ($R^2= 0.2039$) (*Table 1, Fig. 7*). The browning intensity was very significant ($p<0.01$) correlated with the soil water content ($R^2= 0.1846$), soil nitrate-N content ($R^2= 0.2333$), soil ammonium N content ($R^2= 0.3632$), and soil organic matter ($R^2= 0.1729$) (*Table 1, Fig. 7*). There was a significant linear relationship between potato tuber quality (*Supplemental Fig. 1*) and soil physical and chemical properties (*Supplemental Fig. 2*).

http://www.aloki.hu ● ISSN 1589 1623 (Print) ● ISSN1785 0037 (Online)
DOI: http://dx.doi.org/10.15666/aeer/2001_743769

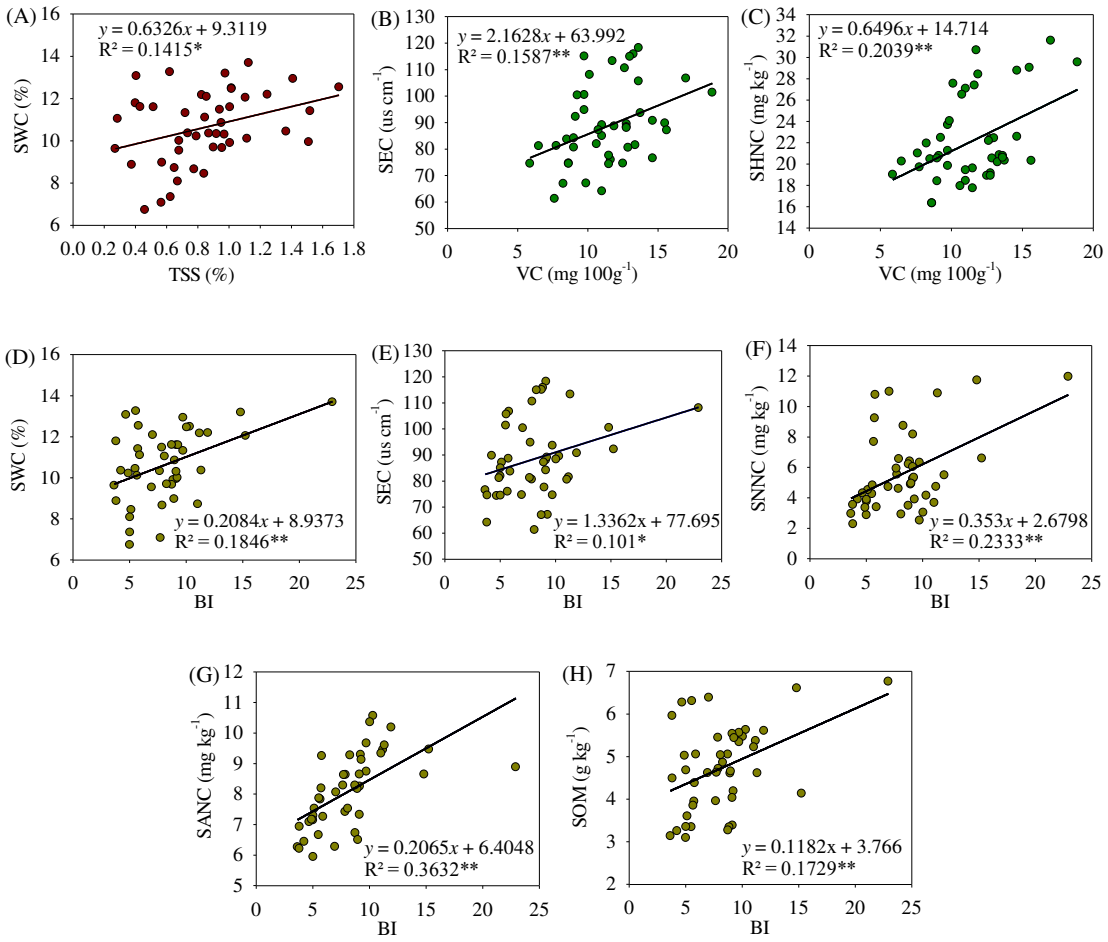

Figure 7. *The linear relationship between soil index and potato tuber quality. Note: TSS, total soluble sugar; VC, vitamin C; BI, browning intensity; SWC, soil water content; SEC, soil electric conductivity; SNNC, soil nitrate-N content; SANC, soil ammonium N content; SHNC, soil alkali-hydrolyzable N content; SOM, soil organic matter; **, Correlation is significant at the 0.01 level (2-tailed); *, Correlation is significant at the 0.05 level (2-tailed)*

Based on all the collected data for the potato tuber yield, dry matter accumulation, Starch content, protein content, reducing sugar, total soluble sugar, vitamin C, and browning intensity (*Supplemental Table S1*), it is theoretically possible to consider the standardized values as variables representing potato tuber quality (*Supplemental Table S2*). A correlation matrix was calculated from the standardized values (*Supplemental Table S3*). Then, the total variance explained by the Cr and the ACr, based on eigenvalues was obtained by PCA (*Supplemental Table S4*). In this analysis, three components were extracted from the matrix of potato tuber quality parameters (*Supplemental Table S5*). Three component scores were also extracted from the matrix of fruit quality parameters (*Supplemental Table S6*). The comprehensive parameter rankings based on the PCA are shown in *Table 2*; T14 was ranked first, followed by T2 and T11, and T10 was clearly last.

http://www.aloki.hu ● ISSN 1589 1623 (Print) ● ISSN1785 0037 (Online)
DOI: http://dx.doi.org/10.15666/aeer/2001_743769

Table 2. *The score and rank of the comprehensive potato tuber yield, dry matter accumulation, Starch content, protein content, reducing sugar, total soluble sugar, vitamin C, and browning intensity in a PCA of the potato varieties*

Treatments	Q1	Q2	Q3	Q	Rank
T1	1.121	-0.759	-1.961	-0.147	10
T2	-0.183	0.793	-1.100	-0.024	8
T3	-0.984	0.602	0.785	-0.022	7
T4	0.040	0.665	-0.242	0.134	6
T5	1.151	1.208	-0.377	0.559	2
T6	0.809	0.186	-0.390	0.217	5
T7	-1.781	1.115	0.140	-0.221	12
T8	-0.581	0.247	-0.841	-0.229	13
T9	-0.399	-0.390	0.047	-0.199	11
T10	-0.993	-1.304	-0.981	-0.735	15
T11	-0.009	1.149	1.479	0.485	3
T12	-0.002	-0.405	-0.048	-0.104	9
T13	-1.031	-2.057	1.070	-0.626	14
T14	1.480	0.203	1.310	0.659	1
T15	1.362	-1.254	1.111	0.250	4

Note: T1, 1463-115; T2, Feiurita; T3, Shaza; T4, Yushu 3; T5, Qingshu 17; T6, Laokoupi; T7, He 14; T8, Qingshu 9; T9, Xingjing 2; T10, Longshu 13; T11, Zhongshu 3; T12, Akeria; T13, Yushu 4; T14, Xiapoti; T15, Longshu 7

Discussion

In sandy soils, potato tuber yields are often limited by water shortages and soil nutrient deficiencies. Therefore, more accurate farmland management technology is an effective way to increase potato yield (Wang et al., 2020). In this study, the potato tuber yield was more correlated to the soil available potassium (R^2= 0.5433) than to the soil water content (R^2= 0.1181). The correlation order of potato tuber yield to soil nutrients was as follows: soil available potassium > soil nitrate N content > soil electric conductivity > soil water content > soil available phosphorus (*Table 1*). Studies have shown that the most important soil nutrient that affects potato yield is available potassium content (Panique et al., 1997; Koch et al., 2020). The critical level of soil exchangeable potassium at 90% relative yield was 105 mg kg^{-1} which can be a reference for potassium recommendation (Li et al., 2015). Fertilization recommendations should consider the balance between the input and output of soil potassium. Fertilizer potassium levels based on potassium removal rates depend on soil potassium levels and targets. In order to maintain the potassium content of the soil, the recommended amount of potassium in the fertilizer should be the same as that removed from the potato plant (Job et al., 2019). Because the soil potassium content in this study area is insufficient and the soil potassium resources are limited, it is suggested that the application amount of potassium fertilizer should be greater than the amount of potassium fertilizer removed to improve the soil potassium capacity. The amount of potassium application can not only meet the needs of crop, but also increase the soil potassium content, so that the soil potassium test value can be increased above the critical value. Therefore, the amount of potassium removed from the potato plant at the target yield can be calculated according to the relationship between the total potassium absorbed

http://www.aloki.hu ● ISSN 1589 1623 (Print) ● ISSN1785 0037 (Online)
DOI: http://dx.doi.org/10.15666/aeer/2001_743769

by the potato plant and the tuber yield. In order to determine the exact application rate, it is necessary to study the target potato tuber yield in this area.

This study showed that there was no significant correlation between soil pH and potato tuber yield. However, Jasim et al. (2020) reported that soil pH was significantly correlated with total potato tuber yield ($R^2 = 0.38$). The reason for this phenomenon may be that the acid soil has a significant effect on potato tuber yield, while the alkaline soil has no significant effect on potato tuber yield. We found for the first time that potato tuber starch content is strongly correlated with soil pH value and soil electrical conductivity. Soil pH value is the key factor affecting phosphorus availability in potato production (Visscher et al., 2020). The average soil C and P concentrations were significantly increased and the soil pH and K values were decreased under the tillage method with average mineral nitrogen fertilizer (Tein et al., 2014). This study showed that the potato tuber starch content increased with the increase of soil pH value. Potato planting has an effect on soil pH, but the change is not enough to cause significant problems with pH between some of the agricultural systems seen after potato planting (Senbayram et al., 2015). The pH value in the organic system was significantly higher than that in the conventional system with average and heavy application of nitrogen fertilizer (Grandy et al., 2002). In this study, the change of soil pH was not a problem, but if this trend continues, the soil in the conventional system may become more alkaline.

This study showed that the potato tuber reducing sugar content was only significantly correlated with the soil organic matter content, and the reducing sugar content was increased with the increase of soil organic matter content. Zhang et al. (2020) reported that nitrogen application had significant effect on the concentration of potato tuber reducing sugar. However, this study shows that there is no significant negative correlation between soil nitrate N content and potato tuber reducing sugar content. This phenomenon indicates that potato varieties have more influence on the content of reducing sugar in tubers than soil fertility. The higher is the reducing sugars content, the darker is the colour of fried potatoes by effect of the Maillard reaction with aminoacids during frying (Illera-Vives et al., 2017). The increase of reducing sugar may be due to the delay of maturation by excessive nitrogen application, which increases the content of dry matter and reducing sugar (Petropoulos et al., 2020). Most potato varieties in this study had more reducing sugars than the recommended level of potato chips (< 0.25%), which meet the recommended range for potato chips and flakes (0.4-0.6% and 0.4-1%, respectively).

The total soluble sugar of potato tuber was positively correlated with soil water content in this study. The potato tuber total soluble sugar was significantly affected by soil temperature and soil water content in a Duric Hapludand soil (Ávila-Valdés et al., 2020). The potato tuber total soluble sugar was significantly accumulated under drought stress, and the tuber total soluble was significantly decreased with the increase of age, with the result that the difference between different treatments was increased by 18.7% (Rudack et al., 2017). In this study, the total soluble sugar content of potato tubers increased with the increase of soil water content, and the increase rate was 0.63. We found for the first time that a significant correlation between potato vitamin C content and soil electrical conductivity. In this study, the vitamin C content of potato tubers increased with the increase of soil electrical conductivity. The internal mechanism of the effect of soil conductivity on the potato tuber vitamin C content needs to be further studied, which will be conducive to the further adjustment of soil conductivity to achieve the goal of improving vitamin C content. The potato tuber vitamin C content was greatly correlated to the soil alkali-hydrolyzable N content. Gao et al. (2015) showed that there was no

http://www.aloki.hu ● ISSN 1589 1623 (Print) ● ISSN1785 0037 (Online)
DOI: http://dx.doi.org/10.15666/aeer/2001_743769

significant difference in the contents of vitamin C, soluble protein and starch in potato tubers under different N fertilization conditions. This is consistent with our research that there was no significant correlation between vitamin C content and soil nitrate N content.

The potato tuber browning intensity was significantly correlated with the contents of soil nitrate-N (R^2= 0.2333), soil ammonium N (R^2= 0.3632), and soil organic matter (R^2= 0.1729) in this study. Browning reaction often occurs during the processing of fresh potato tuber, which leads to the decrease of the quality and nutritional value of processed products (Xing et al., 2020). Several researchers have shown that the relationship between soil nutrient supply and physiological processes has an important effect on potato tuber quality, such as potassium which has the greatest effect on potato tuber quality potato growth and photosynthesis (Naumann et al., 2020). The undesirable Browning of potato is the result of the joint action of potato chemical composition and enzyme activity. The Browning of fresh-cut potato is caused by the activation of enzymes when exposed to oxygen in the process of cutting potato. Phenolic compounds are converted to quinones, which in turn form melanin (Dite Hunjek et al., 2020). The susceptibility of many varieties to Browning has been studied. In several studies, the following varieties have been studied according to the browning sensitivity sequence: Monalisa > Spunta > Speech > Cara > Agria (Cantos et al., 2002) and Marabel > Agata > Agria > Vivaldi > Almera (Cabezas-Serrano et al., 2009). The potato tuber browning intensity in this study was ranked as: T11 (Zhongshu 3) > T3 (Shaza) > T14 (Xiapoti) > T4 (Yushu 3) > T9 (Xingjing 2). Besides potato variety, the enzymes activity could be helpful for browning decrease (Zhou et al., 2019). It can be inferred from the results of this study that the best measure to adjust the browning intensity is to increase the soil nitrate-N, ammonium N and organic matter content.

Principal component analysis (PCA) is an unsupervised multivariate analysis used to transform a set. It converts the observed variables into a new set of unrelated variables and reduces the dimension by designing a new coordinate axis, called the principal component (de Mello et al., 2016). Many researchers suggest that PCA is used for data analysis when selecting the optimal parameter combination in various fields (Jolliffe Ian and Cadima, 2016; Tyanova et al., 2016; Li et al., 2018; Xing et al., 2021). Dersseh et al. (2016) explored that improved varieties, inorganic fertilizers, and strong marketing products are the best combination of potato farming systems in Chencha, Ethiopia by using PCA. Muthoni et al. (2015) used PCA method to select the best genotype and environmental factors suitable for the stability of potato tuber yield and resistance to bacterial wilt in Kenya. The first three principal components contributing about 89.9% in 2017 and 93.1% in 2018 of the variances with eigenvalues of >1.0 were employed to draw the distribution map of factor loading (Wang et al., 2020). Our study shows that the first three principal components contributing about 66.7% of the variances with eigenvalues of >1.0 were employed to draw the distribution map of factor loading.

Our study shows that T14 (Xiapoti) ranks the first through the PCA. The T14 treatment had the relatively high dry mater accumulation, starch content and total soluble sugar. Especially, the T14 treatment has relatively moderate potato tuber yield, protein content in this study. Therefore, T14 treatment is recommended to be as an optimal potato variety in sandy soil areas. This research method further clarifies the objectivity of selecting the optimal potato variety suitable for sandy soil, and explores the importance of field management in regulating potato tuber quality.

http://www.aloki.hu ● ISSN 1589 1623 (Print) ● ISSN1785 0037 (Online)
DOI: http://dx.doi.org/10.15666/aeer/2001_743769

Conclusion

The potato variety significantly affected potato tuber yield and quality. The contents of soil nitrate N, ammonium N and alkali-hydrolyzed N decreased with the increase of soil depth on average potato varieties. The soil nitrate N content in 0-20 cm was 17.8% and 28.6% higher than that in 20-40 cm and 40-60 cm, respectively. The soil available potassium content in order from high to low in the top three was: T2 > T14 > T5. Potato tuber yield was significantly correlated with the contents of soil water, soil ammonium N, soil alkali-hydrolyzable N, and soil available phosphorus. The starch content of potato tuber was significantly correlated with soil pH value and soil electrical conductivity. The content of vitamin C was significantly correlated with soil electrical conductivity and soil alkali-hydrolyzable nitrogen N content. The intensity of browning was significantly correlated with the contents of soil water, ammonium N, alkali-hydrolyzed N and organic matter. The potato variety of Xiapoti (T14) had the relatively high dry mater accumulation, starch content and total soluble sugar. This method elucidates the contribution and impact of these measures and provides a basis for evaluating and selecting better potato varieties. These results are of great significance for improving field crop fertilizer input management in Northwest China and other regions of the world. In the future, we will focus on irrigation and fertilization levels, including more fractional levels, to better estimate the input of Xiapoti.

Acknowledgments. This research was supported by the National Natural Science Foundation of China (51809224) and Graduate Education Innovation Program of Yan'an University (YCX2021076).

REFERENCES

[1] Ávila-Valdés, A., Quinet, M., Lutts, S., Martínez, J. P., Lizana, X. C. (2020): Tuber yield and quality responses of potato to moderate temperature increase during tuber bulking under two water availability scenarios. – Field Crops Research 251: 107786.

[2] Ayyub, C. M., Muhammad, W. H., Faisal, Z., Zainul, A., Shawn, R. W. (2019): Potato tuber yield and quality in response to different nitrogen fertilizer application rates under two split doses in an irrigated sandy loam soil. – Journal of Plant Nutrition 42: 1850-60.

[3] Cabezas-Serrano, A. B., Amodio, M. L., Cornacchia, R., Rinaldi, R., Colelli, G. (2009): Suitability of five different potato cultivars (*Solanum tuberosum* L.) to be processed as fresh-cut products. – Postharvest Biology and Technology 53(3): 138-44.

[4] Camire, M. E., Stan, K., Danielle, J. D. (2009): Potatoes and Human Health. – Critical Reviews in Food Science and Nutrition 49: 823-40.

[5] Cantos, E., Tudela, J. A., Gil, M. I., Espín, J. C. (2002): Phenolic Compounds and Related Enzymes Are Not Rate-Limiting in Browning Development of Fresh-Cut Potatoes. – Journal of Agricultural and Food Chemistry 50: 3015-23.

[6] Choi, S., Nobuyuki, K., Hyun-Jeong, K., Mendel, F. (2016): Analysis of protein amino acids, non-protein amino acids and metabolites, dietary protein, glucose, fructose, sucrose, phenolic, and flavonoid content and antioxidative properties of potato tubers, peels, and cortexes (Pulps). – Journal of Food Composition and Analysis 50: 77-87.

[7] de Mello, C. S., van Dijk, J. P., Voorhuijzen, M., Kok, E. J., Maisonnave Arisi, A. C. (2016): Tuber proteome comparison of five potato varieties by principal component analysis. – Journal of the Science of Food and Agriculture 96: 3928-36.

[8] Dersseh, W. M., Yenenesh, T. G., Rogier, P. O. S., Paul, C. (2016): Struik. The analysis of potato farming systems in Chencha, Ethiopia: input, output and constraints. – American Journal of Potato Research 93: 436-47.

http://www.aloki.hu ● ISSN 1589 1623 (Print) ● ISSN1785 0037 (Online)
DOI: http://dx.doi.org/10.15666/aeer/2001_743769

[9] Dite, H., Draženka, M. R., Mario, Š., Sven, K., Nada, V., Damir, J., Kata, G., Branka, L. (2020): Effect of anti-browning agents and package atmosphere on the quality and sensory of fresh-cut birgit and lady claire potato during storage at different temperatures. – Journal of Food Processing and Preservation 44: 14391.
[10] Elhani, S., Maroua, H., Csákvári, E., Hamim, A., Villányi, V., Douaik, A., Bánfalvi, Zs. (2019): Effects of partial root-zone drying and deficit irrigation on yield, irrigation water-use efficiency and some potato (*Solanum Tuberosum* L.) quality traits under glasshouse conditions. – Agricultural Water Management 224: 105745.
[11] Gao, X., Li, C., Zhang, M., Wang, R., Chen B. (2015): Controlled release urea improved the nitrogen use efficiency, yield and quality of potato (*Solanum Tuberosum* L.) on silt loamy soil. – Field Crops Research 181: 60-68.
[12] Grandy, A. S., Porter, G. A., Erich, M. S. (2002): Organic amendment and rotation crop effects on the recovery of soil organic matter and aggregation in potato cropping systems. – Soil Science Society of America Journal 66(4): 1311-1319.
[13] Hameed, A., Syed, S. Z., Sara, S., Shahid, M. (2018): Applications of New Breeding Technologies for Potato Improvement. – Frontiers in Plant Science 9: 925.
[14] Illera-Vives, M., Labandeira, S. S., Loureiro, L. I., López-Mosquera, M. E. (2017): Agronomic assessment of a compost consisting of seaweed and fish waste as an organic fertilizer for organic potato crops. – Journal of Applied Phycology 29: 1663-71.
[15] Jasim, A., Sharma, L., Zaeen, A. A., Bali, S., Buzza, A., Alyokhin, A. (2020): Potato phosphorus response in soils with high value of phosphorus. – Agriculture 10(7): 264.
[16] Job, A. L. G., Soratto, R. P., Fernandes, A. M., Assuncao, N. S., Fernandes, F. M., Yagi, R. (2019): Potassium fertilization for fresh market potato production in tropical soils. – Agronomy Journal 111: 63351-62.
[17] Jolliffe, I. T., Jorge, C. (2016): Principal Component Analysis: A review and recent developments. – Philosophical Transactions of the Royal Society A: Mathematical, Physical and Engineering Sciences 374: 20150202.
[18] Koch, M., Naumann, M., Pawelzik, E., Gransee, A., Thiel, H. (2020): The importance of nutrient management for potato production Part I: plant nutrition and yield. – Potato Research 63: 97-119.
[19] Li, S., Duan, Y., Guo, T., Zhang, P., He, P., Johnston, A., Shcherbakov, A. (2015): Potassium management in potato production in Northwest Region of China. – Field Crops Research 174: 48-54.
[20] Li, Y., Zhang, J., Wang, Y. (2018): Ft-Mir and Nir spectral data fusion: a synergetic strategy for the geographical traceability of panax notoginseng. – Analytical and Bioanalytical Chemistry 410: 91-103.
[21] Liu, Q., Guo, Q., Akbar, S., Zhi, Y., El Tahchy, A., Mitchell, M., Li, Z., Shrestha, P., Vanhercke, T., Ral, J. P., Liang, G., Wang, M. B., White, R., Larkin, P., Singh, S., Petrie, J. (2017): Genetic enhancement of oil content in potato tuber (*Solanum Tuberosum* L.) through an integrated metabolic engineering strategy. – Plant Biotechnology Journal 15(1): 56-67.
[22] Mulabisana, J., Cloete, M., Laurie, S. M., Mphela, W. M., Maserumule, M. M., Nhlapo, T., Cochrane, N. M., Oelofse, D., Rey, C. E. (2019): Yield evaluation of multiple and co-infections of begomoviruses and potyviruses on sweet potato varieties under field conditions and confirmation of multiple infection by NGS. – Crop Protection 119: 102-12.
[23] Muthoni, J., Hussein, S., Rob, M. (2015): Genotype and environment interaction and stability of potato tuber yield and bacterial wilt resistance in Kenya. – American Journal of Potato Research 92: 367-78.
[24] Naumann, M., Koch, M., Thiel, H., Gransee, A., Pawelzik, E. (2020): The importance of nutrient management for potato production part ii: plant nutrition and tuber quality. – Potato Research 63: 121-37.
[25] Palta, J. P. (2010): Improving potato tuber quality and production by targeted calcium nutrition: the discovery of tuber roots leading to a new concept in potato nutrition. – Potato

http://www.aloki.hu ● ISSN 1589 1623 (Print) ● ISSN1785 0037 (Online)
DOI: http://dx.doi.org/10.15666/aeer/2001_743769

Research 53: 267-75.
[26] Panique, E., Kelling, K. A., Schulte, E. E., Hero, D. E., Stevenson, W. R., James, R. V. (1997): Potassium rate and source effects on potato yield, quality, and disease interaction. – American Potato Journal 74: 379-98.
[27] Petropoulos, S. A., Fernandes, Â., Polyzos, N., Antoniadis, V., Barros, L., Ferreira, C. F. R. I. (2020): The impact of fertilization regime on the crop performance and chemical composition of potato (*Solanum Tuberosum* L.). – Cultivated in Central Greece. Agronomy 10: 474.
[28] Porter, G. A., Bradbury, W. B., Jonathan, A. S., Geraldine, B. O., Jeffrey, C. M. (1999): Soil management and supplemental irrigation effects on potato: i. soil properties, tuber yield, and quality. – Agronomy Journal 91: 416-25.
[29] Rudack, K., Seddig, S., Sprenger, H., Köhl, R. K., Ordon, U. F. (2017): Drought Stress-Induced changes in starch yield and physiological traits in potato. – Journal of Agronomy and Crop Science 203: 494-505.
[30] Seibt, K. M., Wenke, T., Wollrab, C., Junghans, H., Muders, K., Dehmer, K. J., Diekmann, K., Schmidt, T. (2012): Development and Application of Sine-Based Markers for Genotyping of Potato Varieties. – Theoretical and Applied Genetics 125: 185-96.
[31] Senbayram, M., Gransee, A., Wahle, V., Thiel, H. (2015): Role of magnesium fertilisers in agriculture: plant–soil continuum. – Crop and Pasture Science 66(12): 1219-29.
[32] Tein, B., Kauer, K., Eremeev, V., Luik, A., Selge, A., Loit, E. (2014): Farming systems affect potato (*Solanum tuberosum* L.) tuber and soil quality. – Field Crops Research 156: 1-11.
[33] Tiwari, J. K., Sapna, D., Tanuja, B., Nilofer, A., Rajesh, K. S., Rasna, Z., Vijay, K. D., Swarup, K. C. (2020): Precision phenotyping of contrasting potato (Solanum tuberosum L.) varieties in a novel aeroponics system for improving nitrogen use efficiency: in search of key traits and genes. – Journal of Integrative Agriculture 19: 51-61.
[34] Tyanova, S., Temu, T., Sinitcyn, P., Carlson, A., Hein, M. Y., Geiger, T., Mann, M., Cox, J. (2016): The perseus computational platform for comprehensive analysis of (Prote) omics data. – Nature Methods 13: 731-740.
[35] Van Dingenen, J., Hanzalova, K., Salem, M. A. A., Abel, C., Seibert, T., Giavalisco, P., ahl, V. (2019): Limited nitrogen availability has cultivar-dependent effects on potato tuber yield and tuber quality traits. – Food Chemistry 288: 170-77.
[36] Visscher, A. M., Vanek, S., Meza, K., de Goede, R. G. M., Valverde, A. A., Ccanto, R., Olivera, E., Scurrah, M., Fonte, S. J. (2020): Eucalyptus and alder field margins differ in their impact on ecosystem services and biodiversity within cropping fields of the Peruvian Andes. – Agriculture, Ecosystems & Environment 303: 107107.
[37] Visvanathan, R., Chathuni, J., Barana, C. J., Ruvini, L. (2016): Health-Beneficial Properties of Potato and Compounds of Interest. – Journal of the Science of Food and Agriculture 96: 4850-60.
[38] Wang, X., Wang, N., Xing, Y., Yun, J., Zhang, H. (2018): Effects of plastic mulching and basal nitrogen application depth on nitrogen use efficiency and yield in maize. – Frontiers in Plant Science 9: 1446.
[39] Wang, H., Xiukang, W., Lifei, B., Ying, W., Junliang, F., Fucang, Z., Xianghao, H., Minghui, C., Wenhui, H., Lifeng, W., Youzhen, X. (2019): Multi-objective optimization of water and fertilizer management for potato production in sandy areas of northern china based on TOPSIS. – Field Crops Research 240: 55-68.
[40] Wang, X., Fan, J., Xing, Y., Xu, G., Wang, H., Deng, J., Wang, Y., Zhang, F., Li, P., Li, Z. (2019): The effects of mulch and nitrogen fertilizer on the soil environment of crop plants. – Adv. Agron. 153: 121-173.
[41] Wang, X., Guo, T., Wang, Y., Xing, Y., Wang, Y., He, X. (2020): Exploring the optimization of water and fertilizer management practices for potato production in the sandy loam soils of northwest china based on PCA. – Agricultural Water Management 237: 106180.
[42] Xing, Y., Niu, X., Wang, N., Jiang, W., Gao, Y., Wang, X. (2020): The Correlation between

http://www.aloki.hu ● ISSN 1589 1623 (Print) ● ISSN1785 0037 (Online)
DOI: http://dx.doi.org/10.15666/aeer/2001_743769

Soil Nutrient and Potato Quality in Loess Plateau of China Based on Plsr. – Sustainability 12: 1588.

[43] Xing, Y., Li, Z., Wang, Y., Wang, Y., Zhang, T., Mi, F., Wang, X. (2021): Exploring optimization of water and nitrogen fertilizer management for potted maize based on PCA. – Pakistan Journal of Botany 53(6): 2067-2083.

[44] Xing, Y., Zhang, T., Jiang, W., Li, P., Shi, P., Xu, G., Cheng, S., Cheng, Y., Zhang, F., Wang, X. (2022): Effects of irrigation and fertilization on different potato varieties growth, yield and resources use efficiency in the Northwest China. – Agricultural Water Management 261: 107351.

[45] Yamdeu Galani, J. H., Mankad, P. M., Shah, A. K., Patel, N. J., Acharya, R. R., Talati, J. G. (2017): Effect of storage temperature on vitamin C, total phenolics, uplc phenolic acid profile and antioxidant capacity of eleven potatos (*Solanum tuberosum*) varieties. – Horticultural Plant Journal 3(2): 73-89.

[46] Zaheer, K., Akhtar, M. H. (2016): Potato Production, Usage, and Nutrition-a Review. – Critical Reviews in Food Science and Nutrition 56: 711-21.

[47] Zhang, H., Liu, X., Song, B., Nie, B., Wei, Z., Zhao, Z. (2020): Effect of excessive nitrogen on levels of amino acids and sugars, and differential response to post-harvest cold storage in potato (*Solanum Tuberosum* L.) tubers. – Plant Physiology and Biochemistry 157: 38-46.

[48] Zhou, L., Mu, T., Ma, M., Zhang, R., Sun, Q., Xu, Y. (2019): Nutritional evaluation of different cultivars of potatoes (*Solanum Tuberosum* L.) from china by grey relational analysis (gra) and its application in potato steamed bread making. – Journal of Integrative Agriculture 18: 231-45.

http://www.aloki.hu ● ISSN 1589 1623 (Print) ● ISSN1785 0037 (Online)
DOI: http://dx.doi.org/10.15666/aeer/2001_743769

APPENDIX

Supplementary Table S1. *Mean TY (potato tuber yield), DMA (dry matter accumulation), SC (Starch content), PC (protein content), RS (reducing sugar), TSS (total soluble sugar), VC (vitamin C), and BI (browning intensity)*

Item	TY	DMA	SC	PC	RS	TSS	VC	BI
T1	0.84	1.1505	11.45	2.08	0.28	2.71	16.333	4.4547
T2	1.45	1.097	8.72	1.61	0.38	1.92	13.5	5.7287
T3	0.91	1.14	8.4	1.99	0.88	1.92	13.625	11.372
T4	0.92	1.075	11.64	1.38	0.39	2.13	12.667	10.021
T5	1.16	1.22	11.19	1.6	0.26	1.39	12.208	8.9073
T6	0.75	1.1565	11.2	1.69	0.31	1.72	11.792	7.96
T7	1.12	0.935	10.8	1.11	0.77	1.91	11.833	8.8993
T8	0.64	1.058	10.53	1.16	0.63	1.25	12.417	5.058
T9	0.66	1.0955	8.79	1.31	0.38	2.55	11.167	9.82
T10	0.48	1.1105	6.99	0.92	0.55	2.54	12.042	4.6733
T11	0.99	1.1635	10.37	1.45	0.44	2.06	9.7083	14.92
T12	0.77	1.0705	10.39	1.64	0.36	2.23	9.5833	6.98
T13	0.67	1.0435	10.06	2.34	0.82	3.42	6.9583	4.8633
T14	1	1.237	10.67	2.9	0.3	1.81	8.625	10.677
T15	0.41	1.2115	10.57	3.08	0.38	2.11	8.5833	8.69

Supplementary Table S2. *The standardized values of TY (potato tuber yield), DMA (dry matter accumulation), SC (Starch content), PC (protein content), RS (reducing sugar), TSS (total soluble sugar), VC (vitamin C), and BI (browning intensity)*

Item	TY	DMA	SC	PC	RS	TSS	VC	BI
T1	-0.042	0.419	1.014	0.524	-0.951	1.108	2.071	-1.261
T2	2.197	-0.263	-1.064	-0.224	-0.464	-0.354	0.881	-0.832
T3	0.215	0.286	-1.308	0.381	1.970	-0.354	0.934	1.067
T4	0.252	-0.543	1.159	-0.590	-0.415	0.035	0.531	0.612
T5	1.133	1.305	0.816	-0.240	-1.048	-1.336	0.338	0.237
T6	-0.372	0.496	0.824	-0.097	-0.805	-0.725	0.163	-0.081
T7	0.986	-2.328	0.519	-1.019	1.435	-0.373	0.181	0.235
T8	-0.776	-0.760	0.314	-0.940	0.753	-1.595	0.426	-1.058
T9	-0.702	-0.282	-1.011	-0.701	-0.464	0.812	-0.099	0.545
T10	-1.363	-0.091	-2.382	-1.322	0.364	0.794	0.268	-1.187
T11	0.509	0.585	0.192	-0.478	-0.172	-0.095	-0.712	2.261
T12	-0.299	-0.600	0.207	-0.176	-0.562	0.220	-0.764	-0.411
T13	-0.666	-0.945	-0.044	0.938	1.678	2.423	-1.867	-1.123
T14	0.546	1.522	0.420	1.829	-0.854	-0.558	-1.167	0.833
T15	-1.620	1.197	0.344	2.115	-0.464	-0.002	-1.184	0.164

http://www.aloki.hu ● ISSN 1589 1623 (Print) ● ISSN1785 0037 (Online)
DOI: http://dx.doi.org/10.15666/aeer/2001_743769

Supplementary Table S3. *The standardized values of TY (potato tuber yield), DMA (dry matter accumulation), SC (Starch content), PC (protein content), RS (reducing sugar), TSS (total soluble sugar), VC (vitamin C), and BI (browning intensity)*

Items	TY	DMA	SC	PC	RS	TSS	VC	BI
TY	1	-0.055	0.158	-0.146	-0.117	-0.353	0.318	0.243
DMA	-0.055	1	0.094	0.572	-0.591	-0.23	-0.071	0.303
SC	0.158	0.094	1	0.262	-0.372	-0.243	-0.032	0.137
PC	-0.146	0.572	0.262	1	-0.156	0.172	-0.425	0.091
RS	-0.117	-0.591	-0.372	-0.156	1	0.214	-0.111	-0.052
TSS	-0.353	-0.23	-0.243	0.172	0.214	1	-0.249	-0.294
VC	0.318	-0.071	-0.032	-0.425	-0.111	-0.249	1	-0.222
BI	0.243	0.303	0.137	0.091	-0.052	-0.294	-0.222	1

Supplementary Table S4. *Total variance explained of the contribution rate and accumulative of contribution rate with eigenvalues was calculated by principal component analysis*

Component	Initial Eigenvalues			Extraction Sums of Squared Loadings			Rotation Sums of Squared Loadings		
	Total	% of Variance	Cumulative %	Total	% of Variance	Cumulative %	Total	% of Variance	Cumulative %
1	2.273	28.418	28.418	2.273	28.418	28.418	2.081	26.012	26.012
2	1.901	23.762	52.180	1.901	23.762	52.180	1.801	22.513	48.525
3	1.163	14.539	66.719	1.163	14.539	66.719	1.456	18.194	66.719
4	.928	11.600	78.319						
5	.676	8.446	86.765						
6	.546	6.821	93.586						
7	.424	5.295	98.881						
8	.090	1.119	100.000						

Supplementary Table S5. *The three components are extracted matrix by principal component analysis of all parameters*

Items	Component		
	1	2	3
TY	0.219	0.685	0.248
DMA	0.813	-0.221	-0.184
SC	0.549	0.119	-0.066
PC	0.557	-0.648	-0.02
RS	-0.709	-0.126	0.506
TSS	-0.444	-0.63	-0.177
VC	-0.126	0.726	-0.464
BI	0.487	0.098	0.749
TY	0.219	0.685	0.248

Extraction Method: Principal Component Analysis. a. 3 components extracted. Note: TY, potato tuber yield; DMA, dry matter accumulation; SC, Starch content; PC, protein content; RS, reducing sugar; TSS, total soluble sugar; VC, vitamin C; BI, browning intensity

http://www.aloki.hu ● ISSN 1589 1623 (Print) ● ISSN1785 0037 (Online)
DOI: http://dx.doi.org/10.15666/aeer/2001_743769

Supplementary Table S6. *The three component scores are extracted coefficient matrix by principal component analysis of all parameters*

Items	Component		
	1	2	3
TY	-0.052	0.426	0.007
DMA	0.404	-0.048	0.034
SC	0.232	0.108	-0.012
PC	0.277	-0.211	0.235
RS	-0.449	0.031	0.297
TSS	-0.066	-0.408	0
VC	0.057	0.126	-0.537
BI	-0.077	0.396	0.548

Note: TY, potato tuber yield; DMA, dry matter accumulation; SC, Starch content; PC, protein content; RS, reducing sugar; TSS, total soluble sugar; VC, vitamin C; BI, browning intensity

Supplementary Table S7. *The first component scores are calculated by extracted coefficient matrix one by principal component analysis*

Item	TY	DMA	SC	PC	RS	TSS	VC	BI	Sum
T1	0.002	0.169	0.235	0.145	0.427	-0.073	0.118	0.097	1.121
T2	-0.114	-0.106	-0.247	-0.062	0.208	0.023	0.050	0.064	-0.183
T3	-0.011	0.115	-0.303	0.105	-0.885	0.023	0.053	-0.082	-0.984
T4	-0.013	-0.219	0.269	-0.163	0.187	-0.002	0.030	-0.047	0.040
T5	-0.059	0.527	0.189	-0.066	0.471	0.088	0.019	-0.018	1.151
T6	0.019	0.200	0.191	-0.027	0.361	0.048	0.009	0.006	0.809
T7	-0.051	-0.940	0.120	-0.282	-0.644	0.025	0.010	-0.018	-1.781
T8	0.040	-0.307	0.073	-0.260	-0.338	0.105	0.024	0.081	-0.581
T9	0.037	-0.114	-0.235	-0.194	0.208	-0.054	-0.006	-0.042	-0.399
T10	0.071	-0.037	-0.553	-0.366	-0.163	-0.052	0.015	0.091	-0.993
T11	-0.026	0.236	0.045	-0.133	0.077	0.006	-0.041	-0.174	-0.009
T12	0.016	-0.243	0.048	-0.049	0.252	-0.015	-0.044	0.032	-0.002
T13	0.035	-0.382	-0.010	0.260	-0.753	-0.160	-0.106	0.086	-1.031
T14	-0.028	0.615	0.098	0.507	0.383	0.037	-0.067	-0.064	1.480
T15	0.084	0.484	0.080	0.586	0.208	0.000	-0.068	-0.013	1.362

Supplementary Table S8. *The second component scores are calculated by extracted coefficient matrix two by principal component analysis*

Item	TY	DMA	SC	PC	RS	TSS	VC	BI	Sum
T1	-0.018	-0.020	0.110	-0.111	-0.029	-0.452	0.261	-0.499	-0.759
T2	0.936	0.013	-0.115	0.047	-0.014	0.145	0.111	-0.330	0.793
T3	0.092	-0.014	-0.141	-0.080	0.061	0.145	0.118	0.422	0.602
T4	0.107	0.026	0.125	0.124	-0.013	-0.014	0.067	0.242	0.665
T5	0.483	-0.063	0.088	0.051	-0.033	0.545	0.043	0.094	1.208
T6	-0.158	-0.024	0.089	0.020	-0.025	0.296	0.021	-0.032	0.186
T7	0.420	0.112	0.056	0.215	0.044	0.152	0.023	0.093	1.115
T8	-0.330	0.036	0.034	0.198	0.023	0.651	0.054	-0.419	0.247
T9	-0.299	0.014	-0.109	0.148	-0.014	-0.331	-0.012	0.216	-0.390
T10	-0.581	0.004	-0.257	0.279	0.011	-0.324	0.034	-0.470	-1.304
T11	0.217	-0.028	0.021	0.101	-0.005	0.039	-0.090	0.895	1.149
T12	-0.127	0.029	0.022	0.037	-0.017	-0.090	-0.096	-0.163	-0.405
T13	-0.284	0.045	-0.005	-0.198	0.052	-0.989	-0.235	-0.445	-2.057
T14	0.232	-0.073	0.045	-0.386	-0.026	0.228	-0.147	0.330	0.203
T15	-0.690	-0.057	0.037	-0.446	-0.014	0.001	-0.149	0.065	-1.254

http://www.aloki.hu ● ISSN 1589 1623 (Print) ● ISSN1785 0037 (Online)
DOI: http://dx.doi.org/10.15666/aeer/2001_743769

Supplementary Table S9. *The third component scores are calculated by extracted coefficient matrix three by principal component analysis*

Item	TY	DMA	SC	PC	RS	TSS	VC	BI	Sum
T1	-0.018	-0.020	0.110	-0.111	-0.029	-0.452	0.261	-0.499	-0.759
T2	0.936	0.013	-0.115	0.047	-0.014	0.145	0.111	-0.330	0.793
T3	0.092	-0.014	-0.141	-0.080	0.061	0.145	0.118	0.422	0.602
T4	0.107	0.026	0.125	0.124	-0.013	-0.014	0.067	0.242	0.665
T5	0.483	-0.063	0.088	0.051	-0.033	0.545	0.043	0.094	1.208
T6	-0.158	-0.024	0.089	0.020	-0.025	0.296	0.021	-0.032	0.186
T7	0.420	0.112	0.056	0.215	0.044	0.152	0.023	0.093	1.115
T8	-0.330	0.036	0.034	0.198	0.023	0.651	0.054	-0.419	0.247
T9	-0.299	0.014	-0.109	0.148	-0.014	-0.331	-0.012	0.216	-0.390
T10	-0.581	0.004	-0.257	0.279	0.011	-0.324	0.034	-0.470	-1.304
T11	0.217	-0.028	0.021	0.101	-0.005	0.039	-0.090	0.895	1.149
T12	-0.127	0.029	0.022	0.037	-0.017	-0.090	-0.096	-0.163	-0.405
T13	-0.284	0.045	-0.005	-0.198	0.052	-0.989	-0.235	-0.445	-2.057
T14	0.232	-0.073	0.045	-0.386	-0.026	0.228	-0.147	0.330	0.203
T15	-0.690	-0.057	0.037	-0.446	-0.014	0.001	-0.149	0.065	-1.254

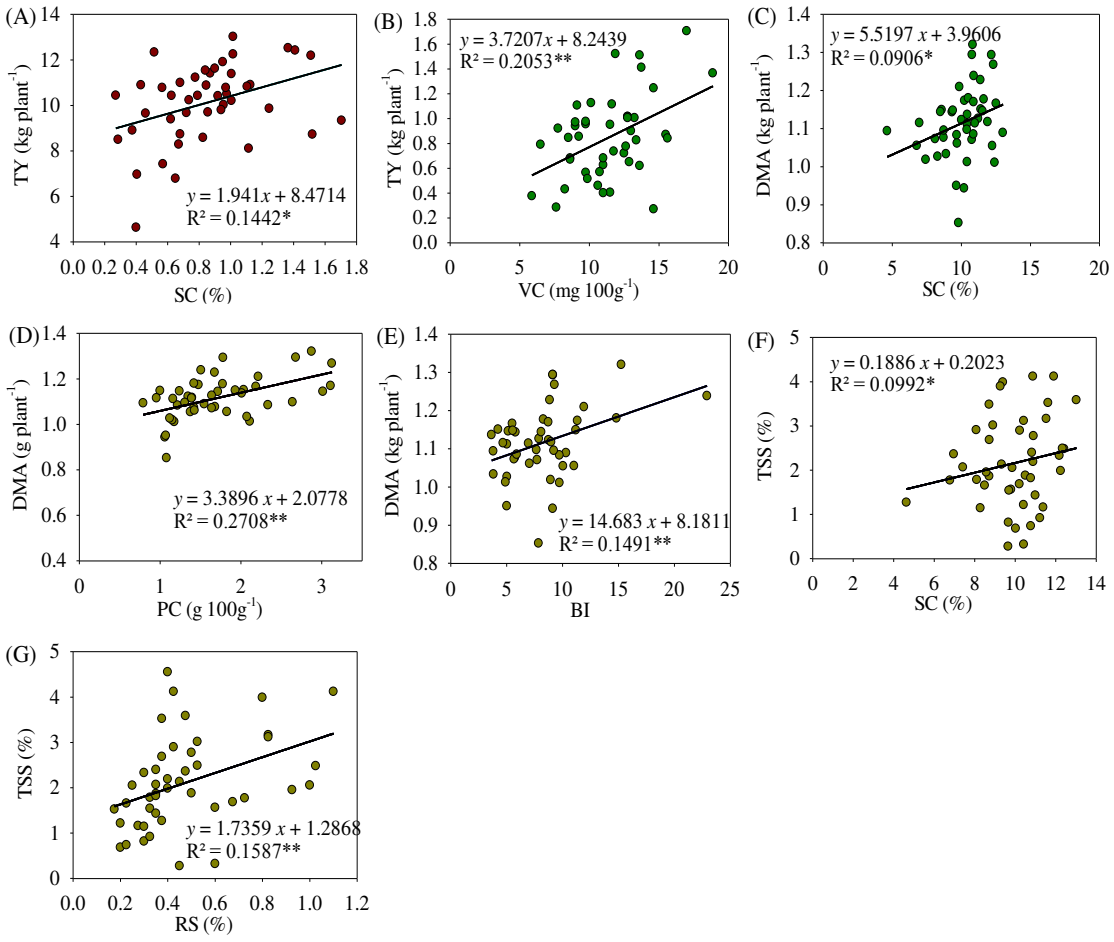

Supplementary Figure S1. *The linear relationship between potato tuber quality. Note: TY, potato tuber yield; DMA, dry matter accumulation; SC, Starch content; PC, protein content; RS, reducing sugar; TSS, total soluble sugar; VC, vitamin C; BI, browning intensity*

http://www.aloki.hu ● ISSN 1589 1623 (Print) ● ISSN1785 0037 (Online)
DOI: http://dx.doi.org/10.15666/aeer/2001_743769

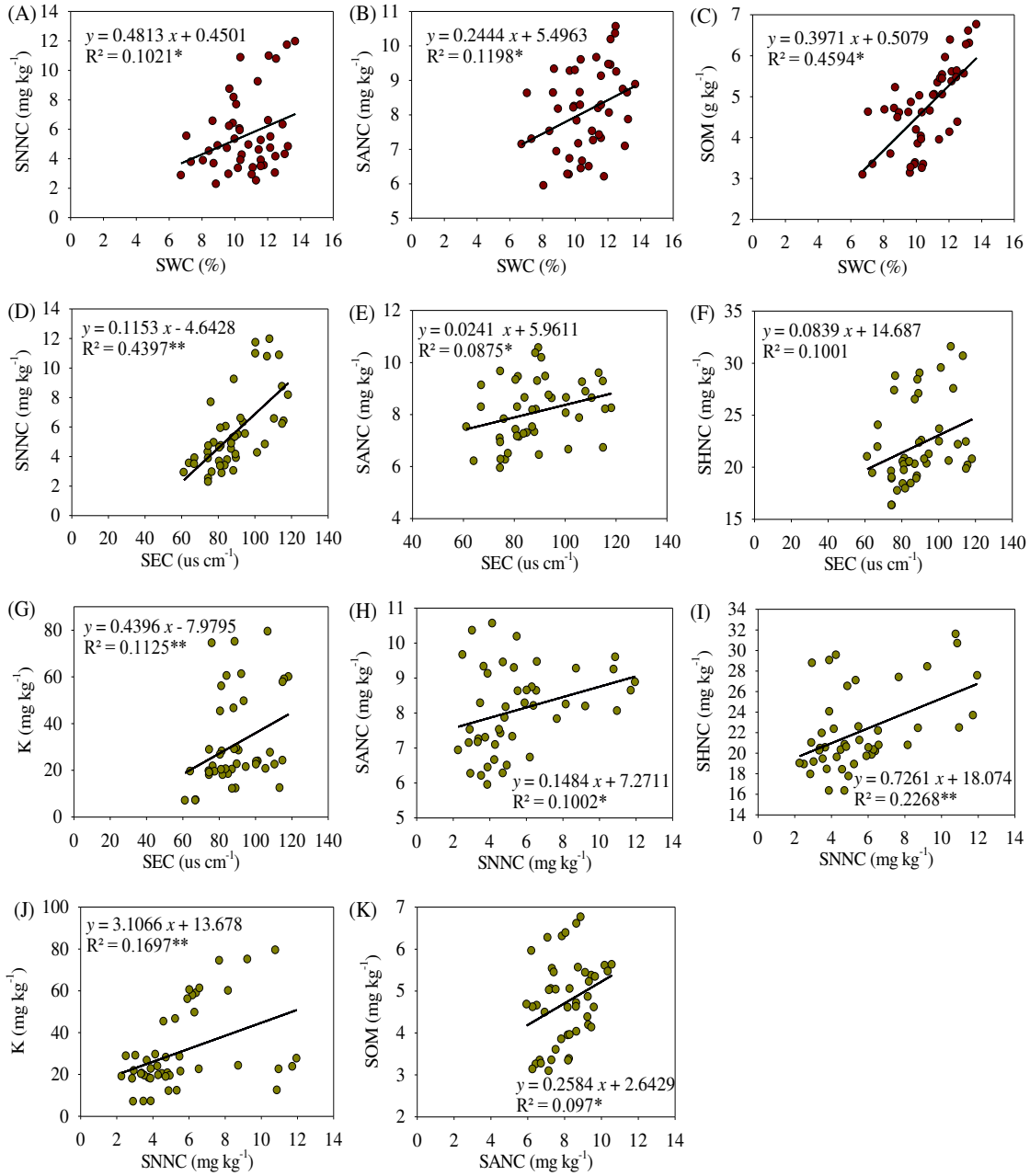

Supplementary Figure S2. *The linear relationship between soil indexes. Note: SWC, soil water content; pH, soil pH; SEC, soil electric conductivity; SNNC, soil nitrate-N content; SANC, soil ammonium N content; SHNC, soil alkali-hydrolyzable N content. SOM, soil organic matter; P, soil available phosphorus; K, soil available potassium*

http://www.aloki.hu ● ISSN 1589 1623 (Print) ● ISSN1785 0037 (Online)
DOI: http://dx.doi.org/10.15666/aeer/2001_743769

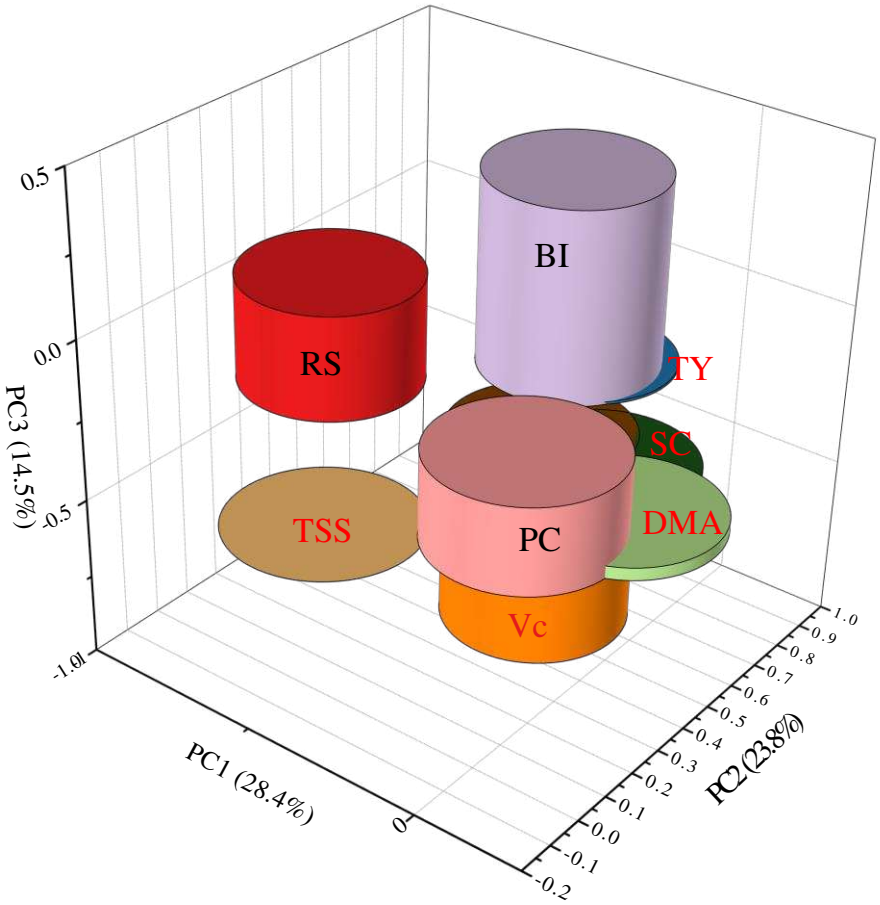

Supplementary Figure S3. *Principal component analysis of potato tuber yield and tuber quality. Note: TY, potato tuber yield; DMA, dry matter accumulation; SC, Starch content; PC, protein content; RS, reducing sugar; TSS, total soluble sugar; VC, vitamin C; BI, browning intensity*

http://www.aloki.hu ● ISSN 1589 1623 (Print) ● ISSN1785 0037 (Online)
DOI: http://dx.doi.org/10.15666/aeer/2001_743769

DROUGHT RESPONSIVE GENE MECHANISMS DURING THE INITIAL GROWTH PHASE IN MAIZE (*ZEA MAYS* L.)

IBRAR, M.[1,2] – MALIK, S. I.[1] – SHAH, M. K. N.[1] – UL HASSAN, F.[3]

[1]*Department of Plant Breeding and Genetics, PMAS Arid Agriculture University, Rawalpindi, Pakistan*

[2]*Agriculture Research Institute, Sariab, Government of Balochistan, Quetta, Pakistan*

[3]*Department of Agronomy, PMAS Arid Agriculture University, Rawalpindi, Pakistan*

**Corresponding author*
e-mail: abrarquetta@gmail.com

(Received 12th Sep 2021; accepted 23rd Nov 2021)

Abstract. Climate change, global warming and increasing drought are critical issues for the world and particularly for developing countries. Drought severely affects maize and causes heavy yield losses. Improving maize genetically against drought stress is an integral strategy to overcome this problem. Identifying drought responsive genes and their expression profiling is helpful for this purpose. Drought-responsive genes from phylogenetically related crops were hunted for the maize genome. Candidate maize genes with unknown functions were analyzed. Out of 9 selected candidate genes, two genes *GSNOR* and *CDPK7* were found differentially regulating under drought stress. They displayed down regulation in roots, whereas, in leaves both genes were up-regulated under drought conditions. Apparently, under stress conditions signaling of Ca^{+2} and NO initiated in roots, then moved to stem and leaves shifting its load to aerial plant parts to overcome water deficit conditions. Results suggest that *GSNOR* and *CDPK7* have potential to enhance maize plants' ability to resist water deficit conditions. *GSNOR* and *CDPK7* enable maize plants to encounter drought stress through nitrosylation and phosphorylation of their target proteins. Thus, they modify downstream gene expression, protein functions and activity. Identified genes may prove useful in improving maize plants to face drought stress conditions.
Keywords: *drought responsive genes, phosphorylation, gene expression profiling, S-nitrosoglutathione reductase (GSNOR), calcium dependent protein kinases (CDPK7)*

Introduction

The developing countries of South East Asia face the challenge of water scarcity (Greve et al., 2018). Unfortunately, Pakistan also confronted by agricultural and domestic water shortage. Pakistan is one of the countries which are facing water scarcity and the situation is expected to get worse in the forthcoming years (Khoso et al., 2015). Scarcity of water inflicts a quite significant and heavy economic loss to the agricultural crops and climatic changes taking place globally are predicted to make the problem worse (Battisti and Naylor, 2009; Marris, 2008). Drought and salinity are the two factors that cause about 50% reduction in yields of main crops throughout the world (Majeed and Muhammad, 2019). The drought problem is quite ubiquitous, alarming and it may have a catastrophic effect on economy of a country relying on agriculture produce (Ali et al., 2017).

In case of maize, water deficient conditions influence the crop physiology thus inflicting heavy production losses. Due to water deficiency at initial reproductive growth stages, defoliation takes place in maize crop which ultimately reduces the grain yield (Jaleel et al., 2009; Monneveux et al., 2006). Water deficiency has negative impacts during anthesis, pollination, anthesis-silking stage and formation of the grains in corn (Aslam et al., 2013). An unfortunate fact found by the plant breeders was that

http://www.aloki.hu ● ISSN 1589 1623 (Print) ● ISSN 1785 0037 (Online)
DOI: http://dx.doi.org/10.15666/aeer/2001_771784

tolerance against drought in maize is quite complex feature, thus it becomes difficult for them to make a selection, screening and breeding for the suitable features (Luo et al., 2019). One of the possible solutions to cope with drought conditions is development of drought tolerant cultivars (Nuccio et al., 2015). However, lack of sufficient genetic resources available in maize is the reason for slow progress towards development of drought tolerant cultivars (Mugo et al., 2005). Several studies have employed the forward genetic approaches like proteome analysis, quantitative real-time PCR and field evaluation for identifying differential expression of candidate genes under drought stress in maize (Wang et al., 2019). A large number of genes are conserved across the plant species which have similar structure and function. These conserved genes are searched in other phylogenetically related plant species (Alexandrov et al., 2009). Identification of genes which are responsive against water deficit conditions can be a useful tool to understand biological systems adapted by the plants against drought stress (Langridge and Reynolds, 2015). Several molecular markers have been developed and genes identified on the basis of differential expression of candidate genes and these findings are being applied to maize improvement programmes focused on drought tolerance (Mao et al., 2015). Identification of genes which are responsive against water deficit conditions can be a useful tool to understand biological systems adapted by the plants against drought stress (Langridge and Reynolds, 2015).

Several genes are reported to play their role under drought stress conditions. For instance, Liang et al. (2011) stated that *RAB18* showed its response against water deficit conditions in the presence of ABA as stimulus via ABA-dependent pathway. SNF1-related protein kinase 2 proteins (*SnRKs*) play major function in phosphorylation process of AREB1 through ABA dependent pathway (Yoshida et al., 2010). Similarly, *NRGA1* from Arabidopsis acts as pyruvate carrier for mitochondria and it negatively controls guard cell signaling, induced by ABA (Li et al., 2014). When *nrga* loss-of-function mutants were tested, plants showed high sensitivity in the presence of ABA in perspective of stomatal movements, demonstrated an intensified tolerance against drought stress. In contrast to this, over-expressing lines for *NRGA1* depicted contrasting stomatal responses, decreased tolerance against drought and activation for anion channels. Another gene *AtCIPK1* depicted its key importance in stress induced pathways. *AtCIPK1* combine both ABA-dependent as well as ABA-independent features for signaling against abiotic stresses (D'Angelo et al., 2006). It was found that *AtCIPK23* initiates channel for potassium ions, controls transpiration process in leaves and absorption of potassium ions in Arabidopsis while interacting along with *CBL9* and *CBL1* (Cheong et al., 2007). Another stress responsive gene *CIPK* found in *Pisum sativum* showed up-regulation in coordination with *CBL* and gave relative response against biotic and abiotic stresses, SA and calcium (Mahajan et al., 2006). For various environmental signaling, calcium ions play a central part as secondary messenger intracellularly. Calcineurin B-like proteins, as well as their targeted proteins depicted mediatory role in signaling network against various environmental stresses faced by the plants (Chen et al., 2011). Nakashima et al. (2007) implied that a drought responsive gene in rice *NAC6* showed its expression in biotic and abiotic stress conditions. If *OsNAC6* is used in combination with stress inducible promoters, this technique can be beneficial in molecular breeding against stress tolerance. Transgenic tomato plants were developed by inserting yeast *TPS1* gene. These transgenic plants showed enhanced chlorophyll as well as starch contents and as a result their tolerance against drought, oxidative stress and salt stress was increased (Cortina and Culianez-Macia, 2005).

http://www.aloki.hu ● ISSN 1589 1623 (Print) ● ISSN 1785 0037 (Online)
DOI: http://dx.doi.org/10.15666/aeer/2001_771784

GSNOR plays pivotal role under various stresses. The gene plays vital part in maintaining homeostatic balance of nitric oxide and thus regulating the process of nitrosylation. S-nitrosoglutathione reductase (GSNOR), catabolizes and splits GSNO into oxidized glutathione (GSSG) and ammonia. As a result, *GSNOR* regulates and maintains GSNO levels in various biotic as well as abiotic stresses (Leterrier et al., 2011). Moreover, GSNO is able to perform transnitrosylation, during which NO functional group is shifted from S-nitroshthiol to any cysteine thiol group of a particular target protein. GSNO is studied for S-nitrosylation of various proteins as GSNO is associated with responses of plants which are exposed to various types of stresses (Chaki et al., 2009).

Nitrosylation and phosphorylation are analogous in cellular biology, as both change the expression of their target genes and alter protein activity as well as function. As GSNOR regulates the process of nitrosylation, similarly CDPKs perform phosphorylation reactions. Both *GSNOR* and *CDPKs* regulate the process of nitrosylation and phosphorylation respectively, thus affecting downstream events taking place in the cytosol, for the purpose of drought management. Several biochemical reactions in plants are closely linked with phosphorylation of proteins (Luo et al., 2018). Calcium ions play a significant role in transmitting messages for several signal transduction routes among such signal transduction pathways (Asano et al., 2012). In response to a particular environmental stimulus (e.g., abiotic stress) concentration of Ca^{2+} is enhanced temporarily and this elevation is identified by many Ca^{2+} sensors or Ca-binding proteins (Rudd and Franklin-Tong, 2001). The elevation of Ca^{2+} introduces modified protein phosphorylation as well as changes in the gene expression patterns as downstream effects (Tuteja and Mahajan, 2007).

Identification and characterization of drought responsive genes is one important step in this direction. The main objective of this study was to identify novel drought responsive genes in maize and conducting their expression profiling. As we know genes are conserved among all species, therefore it was hypothesized that drought responsive genes, reported in crops which are phylogenetically related to maize, would be present in maize genome as well. Therefore, such genes were hunted in maize genome and their gene expression profiling was carried out under drought stress conditions. The main objective of this research was to identify drought responsive genes in maize genome and to perform their expression profiling.

Materials and methods

Plant materials and growth conditions

The research was carried out in PMAS Arid Agriculture University Rawalpindi, Pakistan. The seedlings of maize genotype Soan-3 were grown in glasshouse (32 ± 4 °C) to examine their drought tolerance at early development stage. Soan-3 cultivar was taken as Reference Genome. The selected genotype was grown in potting media with the composition of sand, soil and farm yard manure (FYM) at 1:2:1 ratio, respectively. Size of all pots was 250 ml.

Drought stress treatment

The maize seedlings were grown in pots and watered regularly up to 14 days. Two-weeks old maize seedlings were maintained under similar growth conditions and subjected

http://www.aloki.hu ● ISSN 1589 1623 (Print) ● ISSN 1785 0037 (Online)
DOI: http://dx.doi.org/10.15666/aeer/2001_771784

to drought stress by withholding water for two days. After withholding water for two days i.e., for 48 h, then the time points for six drought stress treatments were counted. The drought stress treatments were given at 0 h, 6 h, 12 h, 24 h, 30 h and finally 10 h after providing recovery irrigation. These six time points of collecting samples were based on observations of gradual increase in symptoms of drought stress on maize seedlings. BBCH growth stage of the maize seedlings was V3. After two weeks of seed germination, it was V3 stage when drought stress treatments were given and samples were collected. Four plants represented one treatment of drought stress for each time course.

Selection of drought responsive genes

The drought responsive genes were searched in crops which are phylogenetically related to maize. Then their orthologues were searched in maize genome with an assumption that their homologous sequences may be present in maize genome as well. Maize genome sequence databases (Mittal et al., 2017) and available online tools were used (Jiao et al., 2017). The decision of selecting identical sequences was taken on protein homology as proteins are functional entities rather than nucleotides. Thus, several amino acids' sequences were used through Basic Local Alignment Search Tool (BLAST) (Pearson, 2013). Among all the searched genes only those were chosen as our candidate genes which depicted more than 70% homology of amino acid sequences and their role against drought stress was not reported in maize (*Table 1*). As a result of this search, nine genes were shortlisted with their orthologues present in maize genome.

Table 1. *Short-listed genes chosen for the expression profiling*

S. No.	Gene name	Plant	References	Best hit in maize genome	Protein		
					Coverage	Seq. ID	C.W score
1	*RAB18*	Arabidopsis	Muller et al., 2012	GRMZM5G83647_T05	93	85	83.5
2	*SnRK2*	Arabidopsis	Zheng et al., 2010	GRMZM2G155593_T01	84	86	80.9
3	*GSNOR*	Arabidopsis	Kwon et al., 2012	GRMZM5G824600_T03	99	90.4	89.4
4	*BADH15*	Sorghum	Wood et al., 1996	GRMZM2G135470_T01	100	81	82.4
5	*AtCBL1*	Arabidopsis	Kudla et al., 1999	GRMZM2G107575_T01	100	77	77
6	*OsCDPK7*	Rice	Saijo et al., 2000	GRMZM2G314396_T01	100	89	89.6
7	*OsNAC6*	Rice	Nakashima et al., 2007	GRMZM2G014653_T01	81.5	80	83
8	*AtNRGA1*	Arabidopsis	Li et al., 2014	GRMZM2G003642_T01	90	77.5	70
9	*OsTPS1*	Rice	Li et al., 2011	GRMZM2G068943_T01	94	84	88

Total RNA isolation

Collected leaves samples were immediately frozen in liquid nitrogen (LN_2). To extract RNA TRIzol method was used (Sambrook and Russel, 2001). After extraction it was resolved on TAE agarose gel of 1.2% concentration at 60 V for 45 min. Then it was stained with Ethidium bromide and observed under UV light. It depicted a good quality of RNA with two distinct bands of *28S* and *18S* ribosomal RNA. The purity and concentration of RNA was calculated by mass spectrophotometry. Later, RNA samples were equilibrated by adding nucleases free water accordingly.

Synthesis of 1st strand of cDNA

The mRNA preps were used for the synthesis of first strand of cDNA by using cDNA synthesis kit. To verify successful synthesis of cDNA, PCR was performed using primers

http://www.aloki.hu ● ISSN 1589 1623 (Print) ● ISSN 1785 0037 (Online)
DOI: http://dx.doi.org/10.15666/aeer/2001_771784

of *ZmActin,* followed by gel electrophoresis. Moreover, the uniformity of bands for all the six drought stress treatments confirmed the synthesis of cDNA with equal concentration.

Primer designing

Primers were designed using available online tools justbio.com and primer3 (*Table 2*). Only exon regions of sequences were used to design primers. Every primer pair was specifically designed so that it should uniquely amplify the conserved region of the gene under investigation.

Table 2. *Detail of the primers designed for the putative short-listed drought responsive genes*

S. No.	Gene name	Sequence	L	GC%	Tm	PS	References
1	RAB18-F	GATTCCTCCTCCTCCTCGTC	20	60	60	453	Ayarpadikannan et al., 2014
2	RAB18-R	AGCAAATTCAATCCCCTCCT	20	45	58		
3	SnRK2-F	CTGATTTGTGGCGTCAGCTA	20	50	56	721	Kulik et al., 2011
4	SnRK2-R	GGACTTGCTTCACCTGCTTC	20	55	58		
5	GSNOR-F	AAGTTTTGCAAGAGCGGAAA	20	40	52	309	Xu et al., 2013
6	GSNOR-R	TTCCAATGCACTCAAAGCTG	20	45	54		
7	BADH15-F	TAGGCCTACCACCAGGTGTC	20	60	60	635	Wood et al., 1996
8	BADH15-R	TGCAAGTTCCACAGCTTCAC	20	50	56		
9	AtCBL1-F-	GGCCTGATCAACAAGGAAGA	20	50	56	226	Kudla et al., 1999
10	AtCBL1-R	CAATAAACCCTGTGCCATCC	20	50	56		
11	OsCDPK7-F	CAAGAACGTCGTCGCTATCA	20	50	56	428	Wang et al., 2008
12	OsCDPK7--R	AAAATGGAGGCACACCACTC	20	50	56		
13	OsNAC6-F	TGGTGATGCACTACCTCTGC	20	55	58	391	Nakashima et al., 2007
14	OsNAC6-R	ACCCAGTCATCCAACCTGAG	20	55	58		
15	AtNRGA-F	CATGCACTGGACTCATTTGG	20	50	56	168	Li et al., 2014
16	AtNRGA-R	CTTCCAGTTGTGAAGCAGCA	20	50	56		
17	OsTPS1-F	TGTGAGGATGAGCGCACTAC	20	55	58	416	Kim et al., 2005
18	OsTPS1-R	ATTGCAGCACCCTTGGTAAC	20	50	56		

PCR for gene expression profiling

PCR was performed using primer pairs specific for each candidate gene. PCR conditions were optimized. Initial denaturation temperature was 94 °C while the annealing temperatures were kept a few degrees lesser than the melting temperature (T_m) of primers. Extension was performed at 72 °C for 30 s. The final extension was performed at 72 °C. The reaction products were separated by gel electrophoresis at 70 V for 45 min.

Tissue specific gene expression

For Tissue-Specific gene expression similar procedure was repeated. Same size of pots i.e., 250 ml was used, water was withheld for two days i.e., 48 h and then six drought stress treatments were given as 0 h, 6 h, 12 h, 24 h, 30 h and then 10 h after recovery irrigation. In this experiment, samples of stem and roots were collected from maize seedlings to investigate the gene expression in roots and stem other than leaves. Procedure of RNA isolation from samples, RNA equilibration, cDNA synthesis, primer designing and PCR was repeated for gene expression profiling in stem and roots. For quantifying the intensity of expressed genes, image J software was used.

http://www.aloki.hu ● ISSN 1589 1623 (Print) ● ISSN 1785 0037 (Online)
DOI: http://dx.doi.org/10.15666/aeer/2001_771784

Results

Gene expression profiling

In genes expression study, two genes namely *GSNOR* of Arabidopsis (*FDH1*) with its maize orthologue GRMZM5G824600 and *CDPK7* from rice with its maize orthologue GRMZM2G314396 were identified. However, seven genes *RAB18, SnRK2, BADH15, AtCBL1, OsNAC6, AtNRGA1, OsTPS1* could not show their expression.

GRMZM5G824600 – A maize orthologue for GSNOR

The maize orthologue GRMZM5G824600 found as a result of BLAST on Maize GDB with its source gene *AtGSNOR* from *Arabidopsis thaliana*, expressed during the gene expression profiling. The gene showed a steady up regulation with increasing levels of drought stress (*Fig. 1a*). When two weeks old maize seedlings were subjected to water deficit conditions, *AtGSNOR* gene started showing its presence. At 0 h, which was a control experiment, expression of the gene was at its minimum level and could be hardly detected. At 6 h the gene expression was observed easily. The drought stress was at its peak with successive increase of drought stress duration at 12 h, 24 h and finally at 30 h. The gene showed a gradual increase with highest intensity at 30 h. However, this gene showed a reverse trend in its expression intensity after 10 h of recovery irrigation.

PCR for GRMZM2G314396 – A maize orthologue for OsCDPK7

The gene selected from rice Os*CDPK7* expressed itself as the maize orthologue, GRMZM2G314396 and showed its presence in maize genome. The gene displayed a certain expression pattern during the step wise exposure of the maize seedlings to drought stress conditions. The expression profiling provided evidence that it is functioning as drought responsive gene by showing up regulation from 0 h till 12 h of drought stress in maize genome. However, after 12 h of drought stress it showed a gradient of down regulation (*Fig. 2a*).

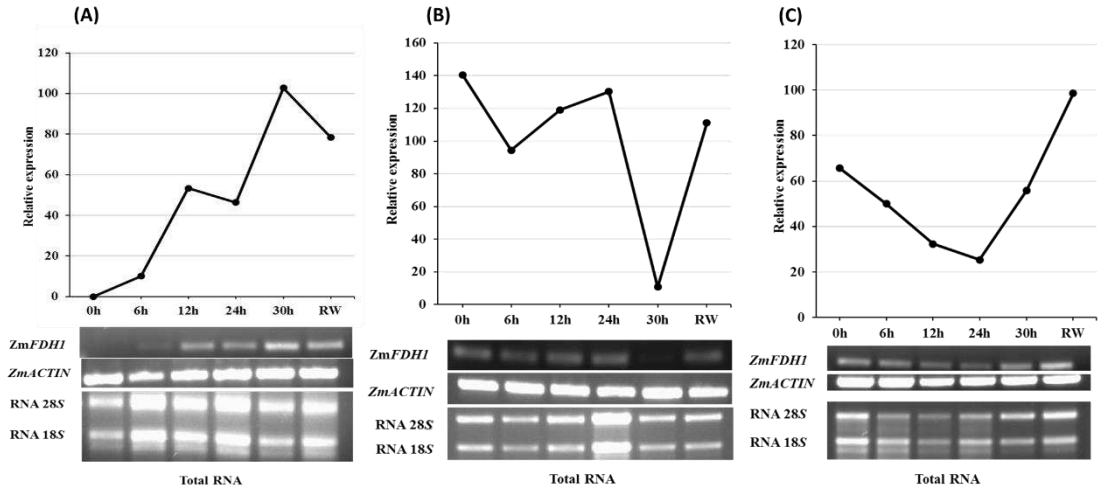

Figure 1. *Expression pattern of GSNOR with size 309 bp upon exposure to drought stress. ZmActin is maize Actin gene loading control. Total RNA obtained shows ribosomal RNA bands of 28S and 18S. The line graphs depict the gene expression pattern. (A) Gene expression profiling in leaves showing upregulation followed by down regulation at recovery irrigation. (B) Expression profiling obtained in roots. (C) Gene expression pattern in stem*

http://www.aloki.hu ● ISSN 1589 1623 (Print) ● ISSN 1785 0037 (Online)
DOI: http://dx.doi.org/10.15666/aeer/2001_771784

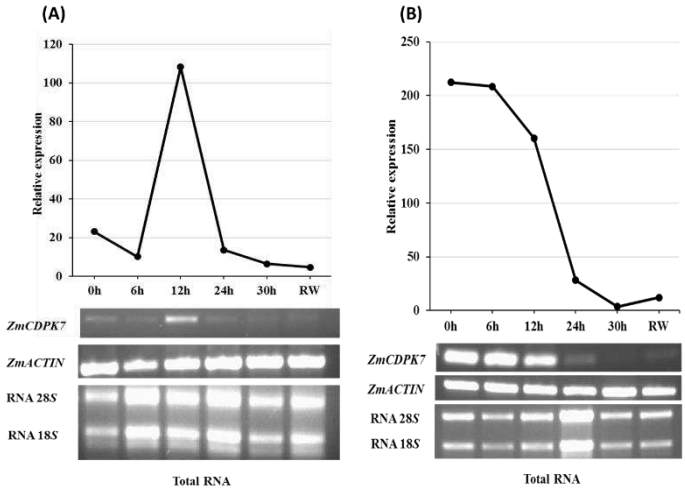

Figure 2. *Expression profiling of CDPK7 with size 428 bp at various levels of drought stress. ZmActin is used as loading control. Total RNA obtained shows ribosomal RNA bands of 28S and 18S. The line graphs display the gene expression patterns. (A) Gene expression profiling in leaves showing upregulation of the gene till 12 h followed by down regulation. (B) Expression profiling obtained in roots displaying an explicit pattern of down regulation*

GSNOR expression in tissues (roots and stem)

In addition to leaves, gene expression was analyzed in roots and stem. On performing PCR for finding gene expression pattern of GSNOR in roots, it was observed that GSNOR displayed an overall declining pattern. Especially at 30 h of drought stress, expression of the gene was at its minimum level (*Fig. 1b*). The expression pattern in stem showed that the gene displayed a general trend of down regulation in first five treatments of drought stress, i.e., starting from 0 h till 30 h of exposure to water deficit conditions. GSNOR gene depicted an overall declining trend while on providing recovery irrigation it showed a sign of rejuvenation (*Fig. 1c*).

CDPK7 expression in tissues (roots and stem)

In roots an obvious down regulated pattern for *CDPK7* was observed (*Fig. 2b*). Initially its expression was found higher at 0 h and then it displayed a steady decline with subsequent increased levels of stress while at 30 h the gene expression almost vanished. However, after 10 h of recovery irrigation when *CDPK7* expression was checked it showed a sign of little reappearance. While expression of *CDPK7* could not be detected in stem.

Discussion

GSNOR/FDH1 gene is induced by ABA and therefore it is included among the genes which follow ABA dependent pathway (Wang et al., 2015). ABA plays a very important role under abiotic conditions and more specifically under water deficit situations (Roychoudhury et al., 2013). Upon exposure to drought conditions, the expression of a drought responsive gene induced by ABA is quite logical. ABA accumulation in leaves makes the guard cells flaccid and results in closure of the stomata thus preventing loss of water through transpiration (Yamaguchi-Shinozaki and

http://www.aloki.hu ● ISSN 1589 1623 (Print) ● ISSN 1785 0037 (Online)
DOI: http://dx.doi.org/10.15666/aeer/2001_771784

Shinozaki, 2006). Accumulation of ABA initiates Nitric Oxide (NO) signaling. When plants are exposed to various environmental stresses, NO plays its role as secondary messenger in transduction of signals against these stresses (Gill et al., 2013). Along with NO, the part played by S-nitrosoglutathione (GSNO) is equally important. GSNO is greatly important because it acts as internal reservoir for NO in cells and by possessing lesser molecular weight as compared to other biological molecules it acts as a carrier of NO (Leitner et al., 2009). Thus, GSNO performs S-nitrosylation of its target proteins and modify their functions. GSNO is associated with responses of plants against stress conditions (Chaki et al., 2009). The gene *GSNOR* catalyzes GSNO and modulates its level thus maintaining homeostatic environment in plants (Staab et al., 2008). *GSNOR* mutants showed thermotolerance defects, resistance to programmed cell death and diminished fertility (Chen et al., 2009). Such kinds of pleiotropic effects provide sufficient evidence that *GSNOR* participates not only in maintaining homeostatic environment, but it also takes part in responses against biotic as well as abiotic stress conditions (Xu et al., 2013). While considering the role of *GSNOR,* it is worthy to mention that it scavenges reactive oxygen species by controlling enzymes involved in anti-oxidation activity (Cheng et al., 2018).

In our experiment *GSNOR/FDH1* depicted a steady up regulation in leaves thus proving its role under conditions of drought stress (*Fig. 1a*). Upon comparing the results displayed in *Figure 1a, b* and *c*, it can be concluded that *GSNOR* gene was initially being expressed in roots. On gradual exposure of maize seedlings to drought stress, gene expression shifted from roots and stem towards leaves in order to modulate the consequences of consistently increasing drought stress. *GSNOR* is expressed constitutively in all tissues (Shi et al., 2014). In addition, as nitric oxide plays its role in root elongation and handling osmotic stress condition through accumulation of osmolytes, therefore its presence and expression in roots is understandable and can be justified (Leitner et al., 2009). GSNO, which is the substrate of the enzyme GSNOR, is the carrier and donor of NO (Malik et al., 2011). GSNO has lesser molecular weight as compared to other biological molecules (Corpas et al., 2013), therefore it is trans located through phloem to upper parts of the plant (Espunya et al., 2012) and while passing through stem, it eventually reaches to the leaves for donating NO. Analyzing the expression of *GSNOR* in leaves and roots shows that in case of roots the gene expression is minimum at 30 h while in contrast to this, in leaves its expression is at its peak. These results clearly indicate that due to the translocation of the substrate GSNO, the need for enzyme GSNOR gradually increased in leaves instead of roots and thus its expression displayed a gradual shift between tissues. The expression pattern in roots is almost opposite to the gene expression profile in leaves (*Fig. 1a, b, c*). Thus, it can be concluded that *GSNOR* shifted its expression from roots and stem towards leaves upon step wise exposure of the maize seedlings to drought conditions. The expression of *GSNOR* is closely associated with GSNO which is the substrate of the enzyme GSNOR. We can say that the activity of GSNOR enzyme is correlated with its substrate GSNO. When and where the GSNO concentration gets higher and seems to disrupt the homeostatic balance in cytosol, the GSNOR enzyme turns active and starts decomposing its substrate, hence the expression of *GSNOR* intensifies. The literature illustrates the significance of GSNO as carrier and donor of nitric oxide. Malik et al. (2011) reported that GSNO is trans located through phloem and it acts as a carrier of nitric oxide, trans locating it to the distant targets. It is necessary for signaling through mechanism of oxidation reduction reactions. It can be deduced that when concentration

http://www.aloki.hu ● ISSN 1589 1623 (Print) ● ISSN 1785 0037 (Online)
DOI: http://dx.doi.org/10.15666/aeer/2001_771784

of GSNO was higher in a certain tissue the need for its catabolism into GSSG and GSH was also greater. Upon excessive accumulation of GSNO, the NADH-dependent enzyme S-nitrosoglutathione reductase (GSNOR) catabolizes and splits GSNO into oxidized glutathione (GSSG) and ammonia. As a result, *GSNOR* regulates and maintains the GSNO levels under biotic and abiotic stress conditions (Xu et al., 2013).

Due to abiotic stress conditions and more specifically under water deficit conditions, ABA concentration increases (Zhu, 2002). The rise in ABA enhances the levels of Ca^{2+} in cytosol (Kohler and Blatt, 2002). Whatever information are encoded in various stimuli, this information introduces an enhanced level of Ca^{2+} in cytosol and thus it determines the nature of response. This increase in calcium ions concentration is termed as calcium signatures (Evans et al., 2001). The elevation of Ca^{2+} ions is detected by a group of calcium sensors known as calcium responders for instance kinases which transmit the message downstream to their concerned targets (Reddy and Reddy, 2004). Similarly, Harmon et al. (2000) reported that calcium dependent protein kinases (CDPKs), sense, decode and ultimately translate the elevation of Ca^{2+} concentration into increased activity of proteins kinases and consecutive downstream signaling. When kinases e.g., CDPKs gets active they bring downstream events of phosphorylation of their target proteins and as a result enable the plant to cope against drought stress conditions. Phosphorylation of proteins is a reversible reaction which plays a significant role in stress signaling in eukaryotes. It is considered that protein phosphorylation regulates several basic cellular incidences (Xu et al., 2009). Plentiful evidences disclosed that several biochemical reactions in plants are closely linked with phosphorylation of proteins (Shen et al., 2004). On induction of *CDPKs* the phosphorylation cascade is triggered and stress responsive genes or the transcription factors are targeted (Mahajan and Tuteja, 2005). Upon exposure of plants to various types of abiotic and biotic stresses for example drought, disease and saline environment, Ca^{2+} concentration is enhanced rapidly in cytoplasm of the cells (Hashimoto and Kudla, 2011). Thus various Ca^{2+} sensor proteins, sense and translate these Ca^{2+} signals into respective responses in the cells. The spatiotemporal changes in Ca^{2+} are regulated by sensor proteins (DeFalco et al., 2010). Kinases are an example of such kind of proteins. At first Ca^{2+} increase in cytosol. As a result, Ca^{2+} attach to elongation hand of calcium dependent protein kinase and as it is also obvious from its name that its functionality depends on attaching Ca^{2+} to its EF motif, hence upon activating, calcium dependent protein kinase starts performing phosphorylation of its target proteins.

Examining the expression pattern of *CDPK7* in leaves (*Fig. 2a*), indicates that the gene upregulated up to 12 h but later on it displayed down regulation in successive treatments of drought stress. We can interpret from this obtained pattern that till 12 h of drought stress, the expression of the gene synthesized sufficient concentration of its product i.e., calcium dependent protein kinase. Therefore, in successive drought stress treatments of 24 h and 30 h, the gene *CDPK7* did not need to be expressed with same intensity and thus it got down regulated. The expression pattern depicted in *Figure 2a* and *b* suggests that *CDPK7* is involved in signaling mechanism. The signaling initiated in roots and then it gradually moved towards leaves. A comparison of *CDPK7* expression between roots and leaves shows that in roots the gene is displaying a steady declining trend (*Fig. 2b*) while in leaves the gene up regulates up to 12 h followed be down regulation (*Fig. 2a*). This comparison indicates that *CDPK7* initiated signaling from roots which gradually switched towards the aerial parts i.e., leaves. The higher expression of *CDPK7* in roots, at control conditions (i.e., 0 h) suggests its involvement

http://www.aloki.hu ● ISSN 1589 1623 (Print) ● ISSN 1785 0037 (Online)
DOI: http://dx.doi.org/10.15666/aeer/2001_771784

in root development and elongation of root hair cells (Ivashuta et al., 2005). With subsequent increased level of dehydration stress the expression apparently moved towards leaves. It can be deduced that the activity of kinases is required during stress conditions as they perform phosphorylation of their target proteins (Mahajan and Tuteja, 2005) and thus altering proteins activity, functioning and at times their cellular location. The overall net impact of this phosphorylation appears in the form of better survival of the plants which encounters osmotic stress conditions.

Conclusions

Drought is one of the major problems for agriculture in present as well as in near future. Developing drought tolerant varieties should be the integral part of a comprehensive plan to face this challenge. Therefore, identifying novel drought responsive genes and investigating their expression pattern was thought necessary and provided a motivation to conduct this research. Two genes namely *GSNOR* and *CDPK7* were identified and their expression pattern was analyzed. It was deduced that these identified genes regulate certain important biochemical as well as physiological phenomena thus enabling maize plants to encounter drought stress. In future, a comprehensive screening program of various maize genotypes for drought tolerance is recommended through using gene expression profiling of drought responsive genes such as *GSNOR* and *CDPK7*. Altogether it is recommended to exploit the identified genes for developing drought resilience in maize crop through selection, hybridization and gene transformation.

Acknowledgements. This work is a part of PhD study. The author highly acknowledges Agriculture Department, Government of Balochistan for providing study leave and Department of Plant Breeding and Genetics, PMAS Arid Agriculture University Rawalpindi for facilitating this research work. The financial assistance to complete this research activity was granted by "Prime Minister's Fee Reimbursement Scheme for Less Developed Areas".

REFERENCES

[1] Alexandrov, N. N., Brover, V. V., Freidin, S., Troukhan, M. E., Tatarinova, T. V., Zhang, H., Swaller, T. J., Lu, Y., Bouck, J., Flavell, R. B., Feldmann, K. A. (2009): Insights into corn genes derived from large-scale cDNA sequencing. – Plant Molecular Biology 69(1-2): 179.

[2] Ali, S., Liu, Y., Ishaq, M., Shah, T., Ilyas, A., Din, I. U. (2017): Climate change and its impact on the yield of major food crops: evidence from Pakistan. – Foods 6(6): 39.

[3] Asano, T., Hayashi, N., Kikuchi, S., Ohsugi, R. (2012): CDPK-mediated abiotic stress signaling. – Plant Signaling and Behavior 7(7): 817-821.

[4] Aslam, M., Maqbool, M. A., Zaman, Q. U., Latif, M., Ahmad, R. (2013): Responses of Mungbean genotypes to drought stress at early growth stages. – International Journal of Basic and Applied Sciences 13(5): 22-27.

[5] Ayarpadikannan, S., Chung, E., Kim, K., So, H. A., Schraufnagle, K. R., Lee, J. H. (2014): RsERF1 derived from wild radish (*Raphanus sativus*) confers salt stress tolerance in Arabidopsis. – Acta Physiologiae Plantarum 36(4): 993-1008.

[6] Battisti, D. S., Naylor, R. L. (2009): Historical warnings of future food insecurity with unprecedented seasonal heat. – Science 323(5911): 240-244.

http://www.aloki.hu ● ISSN 1589 1623 (Print) ● ISSN 1785 0037 (Online)
DOI: http://dx.doi.org/10.15666/aeer/2001_771784

[7] Chaki, M., Valderrama, R., Fernández-Ocaña, A. M., Carreras, A., López-Jaramillo, J., Luque, F., Sanchez-Calvo, B. (2009): Protein targets of tyrosine nitration in sunflower (*Helianthus annuus* L.) hypocotyls. – Journal of Experimental Botany 60(15): 4221-4234.
[8] Chen, R., Sun, S., Wang, C., Li, Y., Liang, Y., An, F. (2009): The Arabidopsis *paraquat resistant2* gene encodes an S-nitrosoglutathione reductase that is a key regulator of cell death. – Cell Research 19: 1377-1387.
[9] Chen, X., Gu, Z., Xin, D., Hao, L., Liu, C., Huang, J., Ma, B., Zhang, H. (2011): Identification and characterization of putative CIPK genes in maize. – Journal of Genetics and Genomics 38(2): 77-87.
[10] Cheng, T., Shi, J., Dong, Y., Ma, Y., Peng, Y., Hu, X., Chen, J. (2018): Hydrogen sulfide enhances poplar tolerance to high-temperature stress by increasing S-nitrosoglutathione reductase (GSNOR) activity and reducing reactive oxygen/nitrogen damage. – Plant Growth Regulation 4: 1-13.
[11] Cheong, Y. H., Pandey, G. K., Grant, J. J., Batistic, O., Li, L., Kim, B. G., Lee, S., Kudla, J., Luan, S. (2007): Two calcineurin B-like calcium sensors, interacting with protein kinase CIPK23, regulate leaf transpiration and root potassium uptake in Arabidopsis. – The Plant Journal 52(2): 223-239.
[12] Corpas, F. J., Alché, J. d. D., Barroso, J. B. (2013): Current overview of S-nitrosoglutathione (GSNO) in higher plants. – Frontiers in Plant Science 4: 126.
[13] Cortina, C., Culiáñez-Macia, F. A. (2005): Tomato abiotic stress enhanced tolerance by trehalose biosynthesis. – Plant Science 169(1): 75-82.
[14] D'Angelo, C., Weinl, S., Batistic, O., Pandey, G. K., Cheong, Y. H., Schültke, S., Albrecht, V., Ehlert, B., Schulz, B., Harter, K., Luan, S., Bock, R., Kudla, J. (2006): Alternative complex formation of the Ca2 + regulated protein kinase CIPK1 controls abscisic acid-dependent and independent stress responses in Arabidopsis. – The Plant Journal 48(6): 857-872.
[15] DeFalco, T. A., Bender, K. W., Snedden, W. A. (2010): Breaking the code: Ca^{2+} sensors in plant signalling. – Biochemical Journal 425(1): 27-40.
[16] Espunya, M. C., De Michele, R., Gómez-Cadenas, A., Martínez, M. C. (2012): S-Nitrosoglutathione is a component of wound-and salicylic acid-induced systemic responses in Arabidopsis thaliana. – Journal of Experimental Botany 63(8): 3219-3227.
[17] Evans, N. H., McAinsh, M. R., Hetherington, A. M. (2001): Calcium oscillations in higher plants. – Current Opinion in Plant Biology 4(5): 415-420.
[18] Gill, S. S., Hasanuzzaman, M., Nahar, K., Macovei, A., Tuteja, N. (2013): Importance of nitric oxide in cadmium stress tolerance in crop plants. – Plant Physiology and Biochemistry 63: 254-261.
[19] Greve, P., Kahil, T., Mochizuki, J., Schinko, T., Satoh, Y., Burek, P., G. Fischer, G., Tramberend, S., Burtscher, R., Langan, S., Wada, S. (2018): Global assessment of water challenges under uncertainty in water scarcity projections. – Nature Sustainability 1(9): 486-494.
[20] Harmon, A. C., Gribskov, M., Harper, J. F. (2000): CDPKs–a kinase for every Ca^{2+} signal? – Trends in Plant Science 5(4): 154-159.
[21] Hashimoto, K., Kudla, J. (2011): Calcium decoding mechanisms in plants. – Biochimie 93(12): 2054-2059.
[22] Ivashuta, S., Liu, J., Liu, J., Lohar, D. P., Haridas, S., Bucciarelli, B., Gantt, J. S. (2005): RNA interference identifies a calcium-dependent protein kinase involved in Medicago truncatula root development. – The Plant Cell 17(11): 2911-2921.
[23] Jaleel, C. A., Manivannan, P., Wahid, A., Farooq, M., Al-Juburi, H. J., Somasundaram, R., Panneerselvam, R. (2009): Drought stress in plants: a review on morphological characteristics and pigments composition. – International Journal of Agricultural Biology 11(1): 100-105.
[24] Jiao, J., Peluso, P., Shi, J., Liang, T., Stitzer, M. C., Wang, B., Campbell, M. S., Stein, J. C., Wei, X., Chin, C., Guill, K., Regulski, M., Kumari, S., Olson, A., Gent, J., Schneider,

http://www.aloki.hu ● ISSN 1589 1623 (Print) ● ISSN 1785 0037 (Online)
DOI: http://dx.doi.org/10.15666/aeer/2001_771784

K. L., Wolfgruber, T. K. May, M. R., Springer, N. M., Antoniou, E., McCombie, W. R., Presting, G. G., McMullen, M., Ross-Ibarra, J., Dawe, R. K., Hastie, A., Rank, D. R., Ware, D. (2017): Improved maize reference genome with single-molecule technologies. – Nature 546(7659): 524-527.

[25] Khoso, S., Wagan, F. H., Tunio, A. H., Ansari, A. A. (2015): An overview on emerging water scarcity in Pakistan, its causes, impacts and remedial measures. – Journal of Applied Engineering Science 13(1): 35-44.

[26] Kim, S. J., Jeong, D. H., An, G., Kim, S. R. (2005): Characterization of a drought-responsive gene, OsTPS1, identified by the T-DNA gene-trap system in rice. – Journal of Plant Biology 48(4): 371-379.

[27] Kohler, B., Blatt, M. R. (2002): Protein phosphorylation activates the guard cell Ca^{2+} channel and is a prerequisite for gating by abscisic acid. – The Plant Journal 32(2): 185-194.

[28] Kudla, J., Xu, Q., Harter, K., Gruissem, W., Luan, S. (1999): Genes for calcineurin B-like proteins in Arabidopsis are differentially regulated by stress signals. – Proceedings of the National Academy of Sciences 96(8): 4718-4723.

[29] Kulik, A., Wawer, I., Krzywińska, E., Bucholc, M., Dobrowolska, G. (2011): SnRK2 protein kinases-key regulators of plant response to abiotic stresses. – Omics: A Journal of Integrative Biology 15(12): 859-872.

[30] Kwon, E., Feechan, A., Yun, B. W., Hwang, B. H., Pallas, J. A., Kang, J. G., Loake, G. J. (2012): AtGSNOR1 function is required for multiple developmental programs in Arabidopsis. – Planta 236(3): 887-900.

[31] Langridge, P., Reynolds, M. P. (2015): Genomic tools to assist breeding for drought tolerance. – Current Opinion in Biotechnology 32: 130-135.

[32] Leitner, M., Vandelle, E., Gaupels, F., Bellin, D., Delledonne, M. (2009): NO signals in the haze: nitric oxide signalling in plant defence. – Current Opinion in Plant Biology 12(4): 451-458.

[33] Leterrier, M., Chaki, M., Airaki, M., Valderrama, R., Palma, J. M., Barroso, J. B., Corpas, F. J. (2011): Function of S-nitrosoglutathione reductase (GSNOR) in plant development and under biotic/abiotic stress. – Plant Signaling and Behavior 6(6): 789-793.

[34] Li, H. W., Zang, B. S., Deng, X. W., Wang, X. P. (2011): Overexpression of the trehalose-6-phosphate synthase gene OsTPS1 enhances abiotic stress tolerance in rice. – Planta 234(5): 1007-1018.

[35] Li, C. L., Wang, M., Ma, X. Y., Zhang, W. (2014): NRGA1, a putative mitochondrial pyruvate carrier, mediates ABA regulation of guard cell ion channels and drought stress responses in Arabidopsis. – Molecular Plant 7(10): 1508-1521.

[36] Liang, Y., Zhang, F., Wang, J., Joshi, T., Wang, Y., Xu, D. (2011): Prediction of drought-resistant genes in Arabidopsis thaliana using SVM-RFE. – Plos One 6(7): 21750.

[37] Luo, F., Deng, X., Liu, Y., Yan, Y. (2018): Identification of phosphorylation proteins in response to water deficit during wheat flag and grain development. – Botanical Studies 59(1): 28.

[38] Luo, L., Xia, H., Lu, B. R. (2019): Crop breeding for drought resistance. – Frontiers in Plant Science 10: 314.

[39] Mahajan, S., Sopory, S. K., Tuteja, N. (2006): Cloning and characterization of CBL-CIPK signalling components from a legume (*Pisum sativum*). – The FEBS Journal 273(5): 907-925.

[40] Mahajan, S., Tuteja, N. (2005): Cold, salinity and drought stresses: an overview. – Biochemistry and Biophysiology 444: 139-158.

[41] Majeed, A., Muhammad, Z. (2019): Salinity: a major agricultural problem-causes, impacts on crop productivity and management strategies. – Plant Abiotic Stress Tolerance 3: 83-99.

http://www.aloki.hu ● ISSN 1589 1623 (Print) ● ISSN 1785 0037 (Online)
DOI: http://dx.doi.org/10.15666/aeer/2001_771784

[42] Malik, S. I., Hussain, A., Yun, B. W., Spoel, S. H., Loake, G. J. (2011): GSNOR-mediated de-nitrosylation in the plant defence response. – Plant Science 181(5): 540-544.
[43] Mao, H., Wang, H., Liu, S., Li, Z., Yang, X., Yan, J., Jiansheng Li, J., Tran, L. P., Qin, F. (2015): A transposable element in a NAC gene is associated with drought tolerance in maize seedlings. – Nature Communications 6(1): 1-13.
[44] Marris, E. (2008): Water: more crop per drop. – Nature 452: 273-277.
[45] Mittal, S., Mallikarjuna, M. G., Rao, A. R., Jain, P. A., Dash, P. K., Thirunavukkarasu, N. (2017): Comparative analysis of CDPK family in maize, arabidopsis, rice and sorghum revealed potential targets for drought tolerance improvement. – Frontiers in Chemistry 5: 115.
[46] Monneveux, P., Sanchez, C., Beck, D., Edmeades, G. (2006): Drought tolerance improvement in tropical maize source populations. – Crop Science 46(1): 180-191.
[47] Mugo, S., De Groote, H., Bergvinson, D., Mulaa, M., Songa, J., Gichuki, S. (2005): Developing Bt maize for resource-poor farmers - recent advances in the IRMA project. – African Journal of Biotechnology 4(13): 19-30.
[48] Nakashima, K., Tran, L. S. P., Van Nguyen, D., Fujita, M., Maruyama, K., Todaka, D., Ito, Y., Hayashi, N., Shinozaki, K., Yamaguchi-Shinozaki, K. (2007): Functional analysis of a NAC-type transcription factor OsNAC6 involved in abiotic and biotic stress-responsive gene expression in rice. – The Plant Journal 51(4): 617-630.
[49] Nuccio, M. L., Wu, J., Mowers, R., Zhou, H. P., Meghji, M., Primavesi, L. F., Paul, M. J., Chen, X., Gao, Y., Haque, E., Basu, S. S., Lagrimini, L. M. (2015): Expression of trehalose-6-phosphate phosphatase in maize ears improves yield in well-watered and drought conditions. – Nature Biotechnology 33(8): 862-869.
[50] Pearson, W. R. (2013): An introduction to sequence similarity "homology" searching. – Current Protocols in Bioinformatics 42(1): 1-3.
[51] Reddy, V. S., Reddy, A. S. (2004): Proteomics of calcium-signaling components in plants. – Phytochemistry 65(12): 1745-1776.
[52] Roychoudhury, A., Paul, S., Basu, S. (2013): Cross-talk between abscisic acid-dependent and abscisic acid-independent pathways during abiotic stress. – Plant Cell Reports 32(7): 985-1006.
[53] Rudd, J. J., Franklin-Tong, V. E. (2001): Unravelling response-specificity in Ca^{2+} signalling pathways in plant cells. – New Phytologist 151(1): 7-33.
[54] Saijo, Y., Hata, S., Kyozuka, J., Shimamoto, K., Izui, K. (2000): Over-expression of a single Ca2+-dependent protein kinase confers both cold and salt/drought tolerance on rice plants. – The Plant Journal 23(3): 319-327.
[55] Sambrook, J., Russel, D. W. (2001): Gel Retardation Assays for DNA Binding Proteins. Molecular Cloning: A Laboratory Manual. – Cold Spring Harbor Laboratory, Cold Spring, NY, pp. 13-17.
[56] Shen, Y. Y., Duan, C. Q., Liang, X. E., Zhang, D. P. (2004): Membrane-associated protein kinase activities in the developing mesocarp of grape berry. – Journal of Plant Physiology 161(1): 15-23.
[57] Shi, H., Ye, T., Zhu, J. K., Chan, Z. (2014): Constitutive production of nitric oxide leads to enhanced drought stress resistance and extensive transcriptional reprogramming in Arabidopsis. – Journal of Experimental Botany 65(15): 4119-4131.
[58] Staab, C. A., Alander, J., Brandt, M., Lengqvist, J., Morgenstern, R., Grafstrom, R. C., Hoog, J. O. (2008): Reduction of S-nitrosoglutathione by alcohol dehydrogenase 3 is facilitated by substrate alcohols via direct cofactor recycling and leads to GSH-controlled formation of glutathione transferase inhibitors. – Biochemical Journal 413(3): 493-504.
[59] Tuteja, N., Mahajan, S. (2007): Calcium signaling network in plants: an overview. – Plant Signaling and Behavior 2(2): 79-85.
[60] Wang, C. R., Yang, A. F., Yue, G. D., Gao, Q., Yin, H. Y., Zhang, J. R. (2008): Enhanced expression of phospholipase C1 (ZmPLC1) improves drought tolerance in transgenic maize. – Planta 227(5): 1127-1140.

http://www.aloki.hu ● ISSN 1589 1623 (Print) ● ISSN 1785 0037 (Online)
DOI: http://dx.doi.org/10.15666/aeer/2001_771784

[61] Wang, P., Du. Y., Hou, Y., Zhao, Y., Hsu, C., Yuan, F., Zhu, X., Tao, W., Song, C., Zhu, J. (2015): Nitric oxide negatively regulates abscisic acid signaling in guard cells by S-nitrosylation of OST1. – Proceedings of the National Academy Sciences of USA 112(2): 613-618.

[62] Wang, X., Zenda, T., Liu, S., Liu, G., Jin, H., Dai, L., Dong, A., Yang, Y., Duan, H. (2019): Comparative proteomics and physiological analyses reveal important maize filling-kernel drought-responsive genes and metabolic pathways. – International Journal of Molecular Sciences 20(15): 3743.

[63] Wood, A. J., Saneoka, H., Rhodes, D., Joly, R. J., Goldsbrough, P. B. (1996): Betaine aldehyde dehydrogenase in sorghum (molecular cloning and expression of two related genes). – Plant Physiology 110(4): 1301-1308.

[64] Xu, S., Ding, H., Su, F., Zhang, A., Jiang, M. (2009): Involvement of protein phosphorylation in water stress-induced antioxidant defense in maize leaves. – Journal of Integrative Plant Biology 51(7): 654-662.

[65] Xu, S., Guerra, D., Lee, U., Vierling, E. (2013): S-nitrosoglutathione reductases are low-copy number, cysteine-rich proteins in plants that control multiple developmental and defense responses in Arabidopsis. – Frontiers in Plant Science 4: 430.

[66] Yamaguchi-Shinozaki, K., Shinozaki, K. (2006): Transcriptional regulatory networks in cellular responses and tolerance to dehydration and cold stresses. – Annual Review Plant Biology 57: 781-803.

[67] Yoshida, T., Fujita, Y., Sayama, H., Kidokoro, S., Maruyama, K., Mizoi, J., Shinozaki, K., Yamaguchi-Shinozaki, K. (2010): AREB1, AREB2, and ABF3 are master transcription factors that cooperatively regulate ABRE-dependent ABA signaling involved in drought stress tolerance and require ABA for full activation. – The Plant Journal 61(4): 672-685.

[68] Zheng, Z., Xu, X., Crosley, R. A., Greenwalt, S. A., Sun, Y., Blakeslee, B., Wang, L., Ni, W., Sopko, S. M., Yao, C., Yau, K., Burton, S., Zhuang, M., McCaskill, D. G., Gachotte, D., Thompson, M., Greene, T. W. (2010): The protein kinase SnRK2. 6 mediates the regulation of sucrose metabolism and plant growth in Arabidopsis. – Plant Physiology 153(1): 99-113.

[69] Zhu, J. K. (2002): Salt and drought stress signal transduction in plants. – Annual Review Plant Biology 53: 247-273.

http://www.aloki.hu ● ISSN 1589 1623 (Print) ● ISSN 1785 0037 (Online)
DOI: http://dx.doi.org/10.15666/aeer/2001_771784

EFFECT OF DIFFERENT PROPORTIONAL MIXTURES OF CORN STRAW AND PEAT ON HUMUS COMPOSITION AND HUMIC ACID STRUCTURE OF BLACK SOILS

LI, S. Y.[1,2] – CHEN, X. W.[2] – DOU. S.[1*] – ZHANG, Y. F.[1] – MA, R.[1] – ZHANG, B. Y.[1] – HAN, L.[1] – NI, L.[1]

[1]*College of Resource and Environment, Jilin Agricultural University, Changchun 130118, China*

[2]*Key Laboratory of Mollisols Agroecology, Northeast Institute of Geography and Agroecology, Chinese Academy of Sciences, Changchun 130102, China*

**Corresponding author*
e-mail: dousen1959@126.com

(Received 13th Sep 2021; accepted 23rd Nov 2021)

Abstract. In order to mitigate the degradation of black soil organic matter, this paper designed a field microplot experiment with different proportional mixtures of corn straw and peat with an equal carbon amount. Treatments included (i) no organic materials applied (CK), (ii) Application of peat (P), (iii) Peat and corn straw are 2:1(2/3P), (iv) Peat and corn straw are 1:2(1/3P) and (v) Application of corn straw (0P). The humus composition and humic acid (HA) structural characteristics of black soil were studied using elemental analysis, Fourier transform infrared (FTIR) spectroscopy, fluorescence spectrum and thermogravimetric analysis. The results demonstrated that water-soluble substances carbon (WSS-C) content increased with the increase of straw application amount, SOC, humification rate (PQ) and carbon content of other humus fractions increased with the increase of peat application amount. In addition, the higher peat applied, the stronger the aromatic nature of HA structure, the more stable and complex the structure of HA, the higher corn straw applied, the stronger the aliphatic nature of HA structure, and the simpler the structure of HA. With the consideration of the humus composition and HA structural characteristics of black soil, the appropriate ratio of the application of corn straw and peat deemed 2:1.
Keywords: *organic materials, soil organic matter, humic acid structure, elemental analysis, fluorescence spectrum*

Introduction

Humic substances (HS) is an important portion of soil organic matter, which represents the key function of soil fertility. The major fractions of HS are humic acids (HA), fulvic acids (FA), and humin (Hm). Humic acid (HA) is an active substance in HS. Its structure and properties directly affect soil fertility (Dou et al., 2020). In northeast China, the black soils are the main grain-producing area in China. Recently, in the cultivated soils, the soil organic carbon content (SOC) decreased and the deterioration of HA due to the successive production and the unsustainable use of organic matter resources (Xu et al., 2010; Zhao et al., 2018a; Gu et al., 2018). Using organic material instead of inorganic fertilizer is one of the most effective methods of improvement (Luan et al., 2019; Wang et al., 2019). Several studies have shown that the application of organic materials could significantly improve the content of humus and the structure of HA in soil (Dou and Jiang, 1988). And improving soil HA structure can improve soil fertility and soil C stock (Amoah-Antwi et al., 2020).

Corn straw and peat are two representative organic materials. However, the two organic materials have different effects on the soil due to their own characteristics. Corn

http://www.aloki.hu ● ISSN 1589 1623 (Print) ● ISSN 1785 0037 (Online)
DOI: http://dx.doi.org/10.15666/aeer/2001_785799

straw is a rich organic material, rich in cellulose, hemicellulose, lignin and other polymers (Chen et al., 2019; Huang et al., 2018). Studies have shown that returning corn straw to the field can improve crop yield and SOC content (Xu et al., 2019), reduce the oxidation degree of HA and improve the humification degree of HA (Gao et al., 2019), increase the carbon component of soil HS. The aliphatic, hydroxyl, methoxy and carboxyl compounds in HA molecules are increased, which simplifies the molecular structure of HA (Ndzelu et al., 2020).

Peat is a precious natural resource (Zaccone et al., 2018), It is a highly humic organic material formed by the long-term accumulation of plant residue that cannot be wholly decomposed under anaerobic conditions (Rydin et al., 2013). The formed HS has a higher degree of condensation, aromatization and more complex molecular structure, which has excellent potential to enhance soil organic matter (SOM) (Zheng et al., 2019). Studies have shown that the application of peat can be used for nutrient retention to maintain and improve soil fertility (Zhang et al., 2017), increase the carbon composition of soil HS and enhance the degree of humification and the aromaticity of HA (Wu et al., 2020).

Current researches suggest that both corn straw and peat can increase soil humus component and improve HA structure. At present, there are many researches about improving soil quality and fertility by corn straw and peat, but there are few researches on soil HA structure. Therefore, this paper designs the corn straw and peat different mixing proportion in field microplot experiment, the objectives were to (ⅰ) Compare the effect of applied corn straw and peat on soil improvement (ii) evaluate changes in HA structural characteristics under different mixing ratios of two organic materials applied (ⅲ) comprehensive considering the change of soil humus composition and HA structure, find the optimum mix proportion of corn strow and peat for black soil fertilizing. In order to provide a scientific basis for organic material mixed fertilization black soil.

Materials and methods

Study site

The test site is located in the teaching and research base of Jilin Agricultural University in Jilin Province China (N43°48′43.57″, E125°23′38.50″). It is a temperate continental humid climate with an annual precipitation of 600-700 mm, a frost-free period of 140-150 days and an annual freezing period of 5 months. The soil type is black soil, belonging to Argiudolls according to the American soil classification system. The basic chemical soil properties are presented in *Table 1* (Zhang et al., 2020). All the specification of treatments' plots is 1 m × 1 m, surrounded by bricks, with 1.5-m intervals between the treatments' plots. The experimental corn straw was collected from the teaching and research base of Jilin Agricultural University in September 2019, and the peat was collected from the cultivated land of peat soil in Da qiao Town, Dun hua City in October 2019. The two kinds of organic materials are air-dried and smash into 2-3-cm pieces before the application, and their initial basic elemental composition is shown in *Table 2*.

Experimental design

The experiment was designed in a plot experiment in May 15th, 2020. The organic materials were applied at equal carbon mass and C/N ratio. The carbon amount was

http://www.aloki.hu ● ISSN 1589 1623 (Print) ● ISSN 1785 0037 (Online)
DOI: http://dx.doi.org/10.15666/aeer/2001_785799

calculated according to the total carbon amount of corn straw returned to the field (10000 kg/hm^2) and C/N was 20/1. Five treatments were designed as follows: (ⅰ) CK (untreated control), (ⅱ) P (1.19 kg of peat and 12.73 g of urea), (ⅲ) 2/3P (793.7 g of peat + 333.3 g of corn straw + 10.26 g of urea), (ⅳ) 1/3P (396.9 g of peat + 666.6 g of corn straw + 7.81 g of urea), and (ⅴ) CS (1 kg of corn straw + 5.37 g of urea). The specific operation is taking out 20 cm of soil within the treatment and put it on the plastic film, and then mix it with organic matter evenly and return it. Each treatment plot was set with four planting points and two corn seeds were sown per point and 2 weeks after emergence one of the poor growing corn was uprooted in each point. Each treatment was repeated 3 times. The experiment was harvested in September 20th, 2020.

Table 1. *Basic soil chemical soil properties*

Soil type	Organic matter (g/kg)	pH	Total nutrient (g/kg)			Available nutrient (mg/kg)		
			N	P	K	N	P	K
Argiudolls	17.22	6.89	1.74	0.41	11.48	86.74	33.76	121.98

The total nutrient is total nitrogen, total phosphorus, and total potassium. Available N is nitrogen extracted by NaOH; Available P is phosphorus extracted by activated charcoal, and available K is potassium extracted by Ammonium acetate

Table 2. *Initial basic elemental composition of the organic materials in study*

Organic materials	Element content (g.kg^{-1})				C/N (mol)	O/C (mol)	H/C (mol)
	C	N	H	O			
Peat	403.45	18.58	49.55	528.41	25.33	0.87	1.47
Corn straw	480.34	25.53	58.76	435.36	21.95	0.60	1.47

C, N, H and O represent the content of carbon, nitrogen, hydrogen and oxygen elements in organic materials; C/N, O/C and H/C represent the mole ratios of elements

Soil sampling and analysis

Five soil samples (0-20 cm) were taken from different places of each plot, and then mixed to form a representative sample. The soil samples were air-dried, then pass through a 2-mm sieve for chemical analysis.

Soil organic carbon

SOC was directly determined by the potassium dichromate external heating method (Dou, 2010). Briefly, 0.2 g of pass through 60 mesh soil weighed into a 50-mL volumetric flask was treated with 10 mL of 0.4 N $K_2Cr_2O_7$-H_2SO_4 solution and covered with a curved funnel. The soil-solution mixture was heated at 180 °C until the first drop appeared from the funnel. The heating was maintained for another 5 min. After cooling to room temperature, it was titrated with 0.2 N $FeSO_4$ after drop two drops of o-phenanthroline indicator.

Sequential extraction of soil humus fractions carbon

Water-soluble substance (WSS), water floating substances (WFS), and humic substances (HS) were sequentially extracted following the modified method as

http://www.aloki.hu ● ISSN 1589 1623 (Print) ● ISSN 1785 0037 (Online)
DOI: http://dx.doi.org/10.15666/aeer/2001_785799

described by (Dou, 2010). Briefly, 5 g of air-dried soil sample was sequentially extracted with 30 mL of distilled water to extract WSS. After filtrate of WSS, the water floating substance was dried and calculated. The C content of WSS was measured by using a TOC analyzer (Shimadzu TOC-Vcph, Japan). Thereafter, the remaining part of sample was treated with 30 mL of a mixture solution of 0.1 M of NaOH + $Na_4P_2O_7$ under continuous shaking at 70 ℃ for 1 h to extract HS. After acidification with 1 M of H_2SO_4, the coagulated fraction represents humic acids (HA), while the supernatant represents fulvic acids (FA). The HA part was dissolved with warming 0.05 M NaOH and transferred into 50 ml volumetric flask. As well, FA was completed by 0.05 N H_2SO_4 into 50 ml volumetric flask. The residual fraction represents the humin (HM). The C content of HA, FA, and HM was determined by dichromate method. Humification rate (PQ) was computed as *Equation 1*.

$$PQ = HA - C/(HA - C + FA - C) \quad \text{(Eq.1)}$$

Isolation and purification of humic acid

The HA was extracted and purified using the International Humic Substances Society method (IHSS) (Kuwatsuka et al., 1992). Briefly, 50 g of air-dried soil sample was extracted with 0.1 m NaOH for HS extraction. This step was repeated three times. HS solution was acidified with 1M HCl to precipitate HA. After high-speed centrifugation of acidified suspension, electro-dialyzed, rotary evaporation and freeze-drying, solid pure HA was obtained.

Structural composition of HA

An elemental analyser (Vario-EL-III Hanau, Germany) was used to assess C, H, N and O contents of solid HA.

Fourier transform infrared (FTIR) spectra was obtained using 1.5–2 mg of solid HA sample mixed with potassium bromide (KBr). The obtained pellet was analyzed with FTIR (Spectrum Two PerkinElmer, USA), covering a frequency range of 4000–400 cm^{-1}, under 4 cm^{-1} wave number resolution, 16 scans and pure KBr spectra as a background.

Fluorescence spectra of the soil HA was obtained using Perkin Elmer FL-6500 fluorescence spectrophotometers. Two mg of the solid HA sample was dissolved by 0.05 mol/L NaHCO3 and constant volume to 50 ml for measuring. Fluorescence spectra in the form of excitation/emission matrices (EEM) were recorded over the emission wavelength range of 250–750 nm and excitation wavelength range of 250–650 nm. Em and Ex slits were fixed at 10 nm. Scanning speed was 2400 nm/min. The voltage of PMT was 550 mV.

Thermogravimetric (TG) and Derivative Thermogravimetric (DTG) analysis of solid HA samples were performed using STA 2500 Regulus thermogravimetric analyzer (Netzsch, German). About 4–6 mg of solid HA sample was heated to 750 ℃ at a constant heating rate of 15 ℃/min.

Data analysis

Data processing was performed using Microsoft Excel and statistical analyses were performed using SPSS software (IBM Statistics 20.0). One-way analysis of variance with the least significant difference (LSD) test was applied to test the significance of

http://www.aloki.hu ● ISSN 1589 1623 (Print) ● ISSN 1785 0037 (Online)
DOI: http://dx.doi.org/10.15666/aeer/2001_785799

difference at $p < 0.05$ among treatments. Spectra and graphs were compiled using the Origin 2018 software. TG and DTA charts were analyzed using TA Universal Analysis software.

Results

Effects of different treatments on SOC content and humus composition

After six months of field microplot experiment, the contents of SOC and WFS-C increased in the order of: CK < 0P < 1/3P < 2/3P ≤ P (*Table 3*). Compared to CK, the SOC in P, 2/3P, 1/3P and 0P treatments increased by 52.2%, 46.4%, 34.8% and 17.4%, respectively. And no significant difference between 2/3p and P treatment. The 0P treatment possessed significantly greater WSS-C than other treatments following the order of: CK < P < 2/3P < 1/3P < 0P (*Table 3*). Furthermore, the difference between treatments was significant.

Similar to SOC, the contents of HA-C, FA-C and HM-C increased in the order of: CK < 0P < 1/3P < 2/3P < P (*Table 3*). The P treatment possessed significantly greater HA-C than other treatments. No significant difference was observed in FA-C content between P and 2/3P, and a significant difference was observed in HM-C content between the 0P treatment and other treatments. Compared with CK (54.18%) treatment, P (62.80%), 2/3P (61.23%), 1/3P (58.81%) and 0P (56.51%) treatments all increased PQ significantly (*Table 3*).

Table 3. *Effects of different proportional mixtures of corn straw and peat on SOC content and humus carbon content*

Treatment	(g.kg^{-1})						PQ (%)
	SOC	WFS-C	WSS-C	HA-C	FA-C	HM-C	
P	15.23 ± 0.160a	0.901 ± 0.035a	0.239 ± 0.003d	3.35 ± 0.009a	1.99 ± 0.021a	8.75 ± 0.122a	62.80 ± 0.003a
2/3P	14.66 ± 0.291a	0.810 ± 0.023b	0.258 ± 0.005c	3.06 ± 0.032b	1.94 ± 0.039a	8.60 ± 0.226a	61.23 ± 0.004b
1/3P	13.50 ± 0.126b	0.728 ± 0.062c	0.269 ± 0.003b	2.56 ± 0.035c	1.79 ± 0.030b	8.15 ± 0.113a	58.81 ± 0.007c
0P	11.75 ± 0.534c	0.602 ± 0.013d	0.283 ± 0.005a	2.26 ± 0.037d	1.74 ± 0.040bc	6.87 ± 0.543b	56.51 ± 0.003d
CK	10.01 ± 0.425d	0.502 ± 0.020e	0.206 ± 0.002e	2.00 ± 0.015e	1.69 ± 0.017c	5.62 ± 0.415c	54.18 ± 0.004e

P, all peat; 2/3P, peat and corn straw are 2:1; 1/3P, peat and corn straw are 1:2; 0P, all corn straw; CK, no organic materials applied; SOC, soil organic carbon; WFS-C, water floating substance carbon; WSS-C, water soluble substances carbon; HA-C, humic acid carbon; FA-C, fulvic acid carbon; HM-C, humin carbon; PQ, humification rate calculated as HA-C/(HA-C + FA-C). The values represent the means ± standard error (SE), Means that do not share the same letter superscript within a column are significantly different ($p < 0.05$)

Elemental composition of HA

Table 4 shows the elemental composition of soil HA across all treatments, the contents of C and N in all treatments in the order of CK < 0P < 1/3P < 2/3P < P, and the difference between P and 2/3P treatments was not significant. Compared with CK treatment, the content of H in HA under 0P, 1/3P, 2/3P and P treatments increased by 2.8%, 2.4%, 1.9% and 1.3%, respectively, while the content of O decreased by 1.3%, 2.3%, 2.9% and 3.2%, respectively (*Table 4*). The H/C ratio across all treatments followed this order: 2/3P < P < CK < 1/3P < 0P, while the O/C ratio followed the order of: CK < 0P < 1/3P < 2/3P = P (*Table 4*).

http://www.aloki.hu ● ISSN 1589 1623 (Print) ● ISSN 1785 0037 (Online)
DOI: http://dx.doi.org/10.15666/aeer/2001_785799

Table 4. *Effects of different proportional mixtures of corn straw and peat on the elemental composition of soil humic acid*

Treatment	Element content (g.kg^{-1})				Ratio (mol)	
	C	N	H	O	O/C	H/C
P	534.1±1.72a	25.71±0.30a	47.22±0.17b	393.0±1.39d	0.552±0.004c	1.061±0.006b
2/3P	532.7±1.33a	25.70±0.21a	47.50±0.43ab	394.1±1.87cd	0.555±0.004c	1.070±0.007b
1/3P	529.8±0.98b	25.58±0.18ab	47.73±0.27ab	396.9±1.00c	0.562±0.002c	1.081±0.007b
0P	525.0±1.09c	25.24±0.05b	47.95±0.12a	400.8±1.18b	0.572±0.003b	1.094±0.003a
CK	522.7±1.44d	24.68±0.15c	46.61±0.39c	406.0±1.90a	0.583±0.004a	1.070±0.006b

P, all peat; 2/3P, peat and corn straw are 2:1; 1/3P, peat and corn straw are 1:2; 0P, all corn straw; CK, no organic materials applied. Mean elemental values ± SE that do not share the same letter superscript within a column are significantly different ($P < 0.05$)

FTIR spectra of HA

The FTIR spectrum of soil HA for different treatments is shown in *Figure 1*. All treatments exhibited similar peak characteristics, differing only in their absorption intensities (*Table 5*). The P treatment showed higher absorption intensity at 1620 cm^{-1} peak, and the 0P treatment showed more abundant peaks at 2920 cm^{-1} and 2850 cm^{-1} (*Table 5*). Compared with CK, the ratio of I2920/I1720 was significantly increased in all treatments, following the order of: CK < 0P < 1/3P < 2/3P < P. Besides, the ratio of I2920/I1620 was decreased in P and 2/3P treatments, while 1/3P and 0P treatments were opposite (*Table 5*).

Table 5. *Effect of different proportional mixtures of corn straw and peat on the relative intensity of the main absorption peaks from Fourier transform infrared spectra of soil humic acid*

Treatment	Relative intensity (%)				Ratio	
	2920 cm^{-1}	2850 cm^{-1}	1720 cm^{-1}	1620 cm^{-1}	I_{2920}/I_{1720}	I_{2920}/I_{1620}
P	2.80±0.21c	0.88±0.03c	6.18±0.08d	13.18±0.28a	0.597±0.046a	0.279±0.013d
2/3P	3.07±0.12bc	1.00±0.09b	6.91±0.20c	12.83±0.33a	0.589±0.031ab	0.317±0.018c
1/3P	3.38±0.22ab	1.06±0.04b	7.92±0.10b	10.57±0.51b	0.561±0.035abc	0.420±0.015b
0P	3.52±0.24a	1.15±0.04a	8.83±0.09a	10.02±0.21b	0.529±0.028bc	0.466±0.026a
CK	2.15±0.09d	0.81±0.02c	5.78±0.30e	9.11±0.03c	0.513±0.027c	0.325±0.009c

P, all peat; 2/3P, peat and corn straw are 2:1; 1/3P, peat and corn straw are 1:2; 0P, all corn straw; CK, no organic materials applied. I2920/I1720, absorption intensity ratio of 2920 cm^{-1} and 1720 cm^{-1} calculated as (2920 + 2850)/1720; I2920/I1620, absorption intensity ratio of 2920 cm^{-1} and 1620 cm^{-1} calculated as (2920 + 2850)/1620. Values are means ± SE and means that share the same letter superscript within a column of a given depth are not significantly different ($P < 0.05$)

Fluorescence spectra of HA

The fluorescence spectra of HA revealed three fluorophores (peaks A, B and C) across all treatments (*Fig. 2*). Peak A (400-490/475-575 nm), peak B (310-400/475-560 nm) and peak C (260-310/460-550 nm) were all approximately situated in fluorescent regions belonged to HA component. Indicated that three organic substances in HA could emit fluorescence. The difference is the fluorescence intensity of the peak.

http://www.aloki.hu ● ISSN 1589 1623 (Print) ● ISSN 1785 0037 (Online)
DOI: http://dx.doi.org/10.15666/aeer/2001_785799

Compared with CK, the fluorescence intensity of peak A, peak B and peak C under P and 2/3P treatment was decreased, while that under 1/3P and 0P treatment were increased (*Fig. 2*).

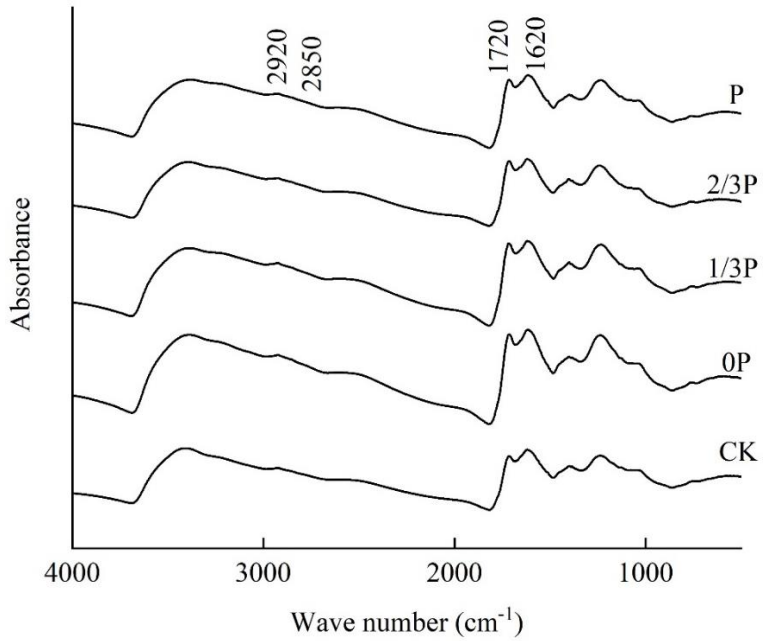

Figure 1. *Fourier transform infrared spectrum of soil humic acid under different proportional mixtures of corn straw and peat*

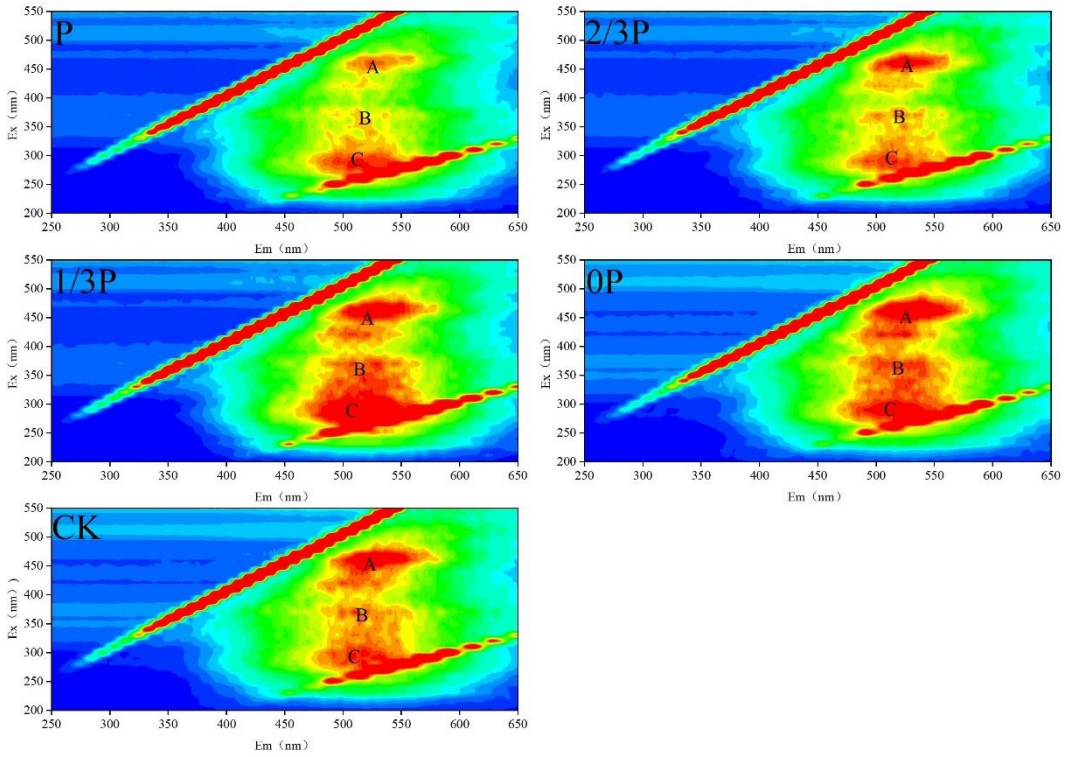

Figure 2. *The excitation/emission matrices fluorescence spectra of soil humic acid under different proportional mixtures of corn straw and peat*

http://www.aloki.hu ● ISSN 1589 1623 (Print) ● ISSN 1785 0037 (Online)
DOI: http://dx.doi.org/10.15666/aeer/2001_785799

Thermal analysis of HA

The DTA and TG curves of soil HA under all treatments are shown in *Figures 3* and *4*. During the pyrolysis process. HA samples showed heat release and weight loss at moderate temperature (302.35 ℃ ~ 322.86 ℃) and high temperature (490.08 ℃ ~ 521.34 ℃). Compared with CK, the medium and high temperature under 2/3P and P treatment increased, while that under 1/3P and 0P treatment decreased (*Fig. 3*). Moreover, heat release and weight loss were increased in all treatments at moderate and high temperatures (*Table 6*). The heat release and weight loss were highest under the 0P treatment at moderate temperature, following CK < P < 2/3P < 1/3P < 0P. The P treatment was highest at high temperature, following CK < 0P < 1/3P < 2/3P < P (*Table 6*).

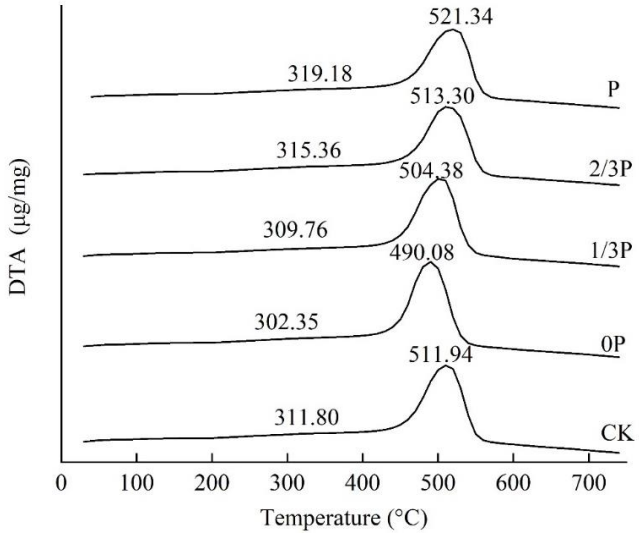

Figure 3. *The thermogravimetric analysis (DTA) curve of soil humic acid under different proportional mixtures of corn straw and peat*

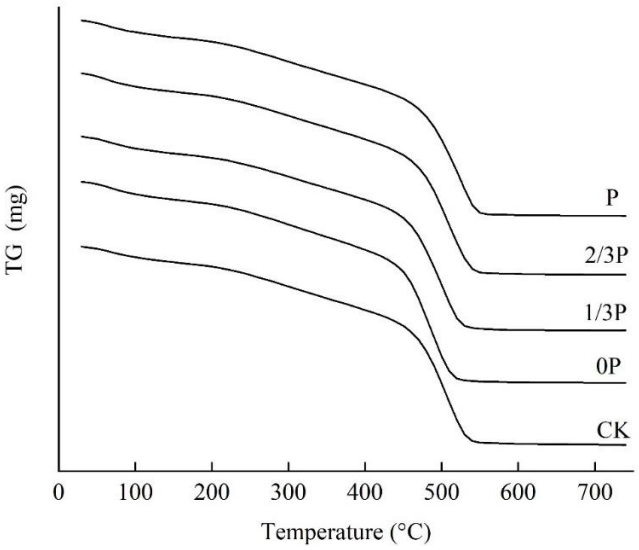

Figure 4. *The thermogravimetric (TG) curve of soil humic acid under different proportional mixtures of corn straw and peat*

http://www.aloki.hu ● ISSN 1589 1623 (Print) ● ISSN 1785 0037 (Online)
DOI: http://dx.doi.org/10.15666/aeer/2001_785799

Table 6. *Effects of different proportional mixtures of corn straw and peat on heat release and weight loss of soil humic acid*

Treatment	Exothermic heat (kJ g^{-1})		Exothermic heat ratio of moderate and high temperature	Mass loss (mg g^{-1})		Ratio of high and moderate mass loss
	Moderate temperature	High temperature		Moderate temperature	High temperature	
P	0.056 ± 0.004a	9.83 ± 0.46a	177.1 ± 5.8a	138.5 ± 4.0cd	687.4 ± 6.6a	4.97 ± 0.18a
2/3P	0.060 ± 0.003ab	9.46 ± 0.11ab	159.0 ± 8.8b	144.1 ± 4.1bc	677.3 ± 6.2a	4.70 ± 0.09b
1/3P	0.064 ± 0.002bc	8.90 ± 0.34bc	138.4 ± 6.6c	151.4 ± 2.7b	657.1 ± 6.4b	4.34 ± 0.05c
0P	0.069 ± 0.002c	8.29 ± 0.29cd	120.3 ± 4.9d	162.8 ± 7.1a	633.2 ± 4.9c	3.89 ± 0.15d
CK	0.049 ± 0.002d	7.71 ± 0.44d	158.7 ± 6.0b	131.3 ± 1.7d	615.7 ± 4.2d	4.69 ± 0.05b

P, all peat; 2/3P, peat and corn straw are 2:1; 1/3P, peat and corn straw are 1:2; 0P, all corn straw; CK, no organic materials applied. Values are means ± SE and means that share the same letter superscript within a column of a given depth are not significantly different ($P < 0.05$)

Discussion

Effect of different proportional mixtures of corn straw and peat on soil SOC and humus composition

Multiple studies have shown that organic materials or green fertilizers can significantly improve the SOC and humus contents in the soil (Wu et al., 2021; Zhang et al., 2019b; Yu et al., 2020). This is the same as the research results of this paper, compared with CK, the SOC, carbon content of humus fractions and PQ of P, 2/3P, 1/3p and 0P were significantly increased (*Table 3*). Corn straw and peat are C-rich substance and contains specific quantities of humus fractions (Han et al., 2020a; Rydin et al., 2013). Therefore, their application increased the SOC and carbon content of soil humus fractions. Compared with CK, except WSS-C, the increase of SOC and carbon content of other humus fractions are in the order of 0P < 1/3P < 2/3P < P. This is broadly consistent with the results of other researchers (Zhao et al., 2018b; Zhang et al., 2020). The result is related to the nature of organic materials (Tamura et al., 2017). Compared with corn straw, the degree of humification is greater, and the content of unstable organic carbon in peat is relatively less (Xu et al., 2020). Therefore, the content of WSS-C was increased with the increase of corn straw application amount, while the C of peat was more easily transformed into the soil after being applied to the soil. Moreover, peat can increase the diversity of soil microorganisms (Xiang et al., 2020; Cong et al., 2020), and is more conducive to increase SOC content. (Xu et al., 2017) believes that the way to transform organic materials into soil humus is to transform to HM first, followed by HA and FA fractions. Compared with peat, corn straw decomposition is slower (Tang et al., 2020), so SOC, HM-C, HA-C, FA-C and PQ were increased with the increase of peat application amount.

Effect of different proportional mixtures of corn straw and peat on HA structural characteristics

The application of organic materials can change the structure of HA in soil, but the change of HA structure depends on the nature of materials, soil properties and soil microorganisms (El-Naggar et al., 2018; Han et al., 2020b; Brunetti et al., 2007). The proportion of unsaturated lipids and lignin-derived compounds in soil with high SOC content was higher. On the other hand, a lower SOC level was associated with a higher proportion of saturated lipids (Jimenez-Gonzalez et al., 2020). The results of this paper showed that the aromaticity of HA was increased with the increase of peat application

http://www.aloki.hu ● ISSN 1589 1623 (Print) ● ISSN 1785 0037 (Online)
DOI: http://dx.doi.org/10.15666/aeer/2001_785799

amount, the aliphaticity and the length of aliphatic chain hydrocarbon of HA were increased with the increase of corn straw application amount. Compared with CK, the H/C ratio (*Table 4*), I_{2920}/I_{1620} ratio (*Table 5*) and peak fluorescence intensity (*Fig. 2*) of P and 2/3P treatments were reduced, the 0P and 1/3P treatments are the opposite, specifically, following the order of: P < 2/3P < CK < 1/3P < 0P. And the P treatment showed higher absorption intensity at the aromatic peak and the 0P treatment showed more abundant aliphatic peaks (*Fig. 1*). The H/C ratio represents the molecular complexity of HA, while the O/C ratio represent the oxidation degree of HA (Xiaoli et al., 2008; Zhang et al., 2015). The values of I2920/I1720 and I2920/I1620 were used to indicate the oxidation degree and aromaticity of HA structure (Gao et al., 2018; Pospisilova et al., 2020). Peak fluorescence intensity can indicate the aromaticity and the content of aliphatic compounds of HA in fluorescence spectra (Chen et al., 2003; Liu et al., 2020b; Hu et al., 2019). This is because the highly aromatic soil humic acid structure is mainly derived from black carbon, while the carboxy-rich aliphatic structure is mainly derived from natural organic matter (DiDonato et al., 2016; Haumaier and Zech, 1995). Moreover, the leading functional group in HA is the carboxylic acid formed by the bonding of alicyclic and aromatic molecules, both of them are derived from the oxidation of lignin in organic materials (DiDonato and Hatcher, 2017). In addition, both peat and corn straw can reduce the oxidation degree of HA, and the degree of decrease increased with the increase of peat application, because compared with CK, the O/C ratio of all treatments is reduced (*Table 4*), while the I_{2920}/I_{1720} ratio is increased (*Table 5*), manifested explicitly as P < 2/3P < 1/3P < 0P < CK.

In the thermal stability analysis, the pyrolysis of HA is dominated by aliphatic and aromatic compounds (Guo et al., 2020a). Heat release at medium temperature is the decomposition decarboxylation of the acidic group, carbohydrate and fatty acid in the sample structure (Schulten and Leinweber, 1996). A high temperature is the destruction of aromatic structure and the cleavage of the C-C bond's cleavage (Francioso et al., 2005). Compared with CK, the peak temperature of the medium and high temperature under 2/3P and P treatments increased, while that under 1/3P and 0P treatments decreased (*Fig. 3*). Indicated that the application of peat could enhance the thermal stability of the HA structure and make the structure of HA more complex and stable. In contrast, corn straw was on the contrary, this is related to the content of aromatic C (Kim et al., 2020). P treatment had the highest ratio of heat release and weight loss at high temperature (CK < 0P < 1/3P < 2/3P < P), and 0P treatment had the highest ratio at medium temperature (CK < P < 2/3P < 1/3P < 0P) (*Table 6*). Indicates that the application of peat is more conducive to increasing the aromatic compounds in the HA structure, while the application of straw makes the aliphatic compounds in the HA structure more abundant. This result also confirms the results of elemental analysis (*Table 4*) and infrared spectroscopy (*Table 5*).

The optimum ratio of straw and peat to fertilize black soil

Multiple studies have shown that soil organic matter's quantity, quality, and stability are essential indexes of soil fertility, which should be comprehensively considered when fertilizing soil (Bi et al., 2020; Guo et al., 2020b; Simansky et al., 2019). In the research results of this paper, compared with CK, SOC, WFS-C, HM-C, HA-C, and FA-C contents in P and 2/3P treatments increased more, and WSS-C contents increased less, the 0P and 1/3P treatments are the opposite. Simultaneously, the HA structure of the soil showed a stronger aromaticity and stability under the treatment of P and 2/3P, But

http://www.aloki.hu ● ISSN 1589 1623 (Print) ● ISSN 1785 0037 (Online)
DOI: http://dx.doi.org/10.15666/aeer/2001_785799

the humic acid with high aromaticity has strong complexing ability and can increase the content of some heavy metals in the soil (Fan et al., 2020; Zhang et al., 2019a). Moreover, WSS-C is the most active carbon in the soil, and its content and structure are near related to the soil microbial community and mineralization of SOC (Liu et al., 2020a; Ma et al., 2019). Although WSS-C content under 0P treatment increased the most, its SOC and carbon content of other humus fractions increased less, and the stability of HA structure decreased and showing strong aliphaticity. Humic acids with more aliphatic and decomposable structure showed greater fungistatic activities, and thus reduced the ecological risk of crop infection by phytopathogenic fungi (Wu et al., 2019). Careful consideration, SOC and carbon content of each fraction of humus under 1/3P treatment increased significantly, and HA structure stability, aromaticity, and aliphatic ratio were appropriate, which was more suitable for black soil fertilization.

Conclusion

(ⅰ) Applied different proportional mixtures of corn straw and peat, all ratios can increase SOC and the carbon content of each humus fractions of black soil. WSS-C content is increased with the increase of corn straw application amount; SOC, PQ and carbon content of other humus fractions are increased with the increase of peat application amount.

(ⅱ) Applied different proportional mixtures of corn straw and peat, the more the proportion of peat, the stronger the aromatic nature of HA structure, the more stable and complex the structure of HA, and the more the proportion of corn straw, the stronger the aliphatic nature of HA structure, and the simpler the structure of HA.

(ⅲ) Comprehensive consideration of the changes of humus composition, and HA structural characteristics of black soil, the 2:1 ratio of corn straw and peat was appropriate. Under this ratio, SOC and WSS-C contents increased by 34.8% and 30.6%, respectively, and the HA structural aromaticity and aliphatic proportional were appropriate.

Acknowledgements. The study was supported by the National Natural Science Foundation of China (42077022) and the Key Research and Development Program of Jilin Province (20200402098NC). The authors are very grateful to anonymous reviewers and responsible editors of this journal for valuable comments and suggestions to improve this manuscript.

REFERENCES

[1] Amoah-Antwi, C., Kwiatkowska-Malina, J., Thornton, S. F., Fenton, O., Malina, G., Szara, E. (2020): Restoration of soil quality using biochar and brown coal waste: a review. – Science of the Total Environment 722.

[2] Bi, Y. C., Cai, S. Y., Wang, Y., Zhao, X., Wang, S. Q., Xing, G. X., Zhu, Z. L. (2020): Structural and microbial evidence for different soil carbon sequestration after four-year successive biochar application in two different paddy soils. – Chemosphere 254.

[3] Brunetti, G., Plaza, C., Clapp, C. E., Senesi, N. (2007): Compositional and functional features of humic acids from organic amendments and amended soils in Minnesota, USA. – Soil Biology & Biochemistry 39: 1355-1365.

http://www.aloki.hu ● ISSN 1589 1623 (Print) ● ISSN 1785 0037 (Online)
DOI: http://dx.doi.org/10.15666/aeer/2001_785799

[4] Chen, W., Westerhoff, P., Leenheer, J. A., Booksh, K. (2003): Fluorescence excitation−emission matrix regional integration to quantify spectra for dissolved organic matter. – Environmental Science & Technology 37: 5701-5710.
[5] Chen, Y. X., Dong, L., Miao, J. X., Wang, J., Zhu, C. S., Xu, Y. Y., Chen, G. Y., Liu, J. (2019): Hydrothermal liquefaction of corn straw with mixed catalysts for the production of bio-oil and aromatic compounds. – Bioresource Technology 294.
[6] Cong, P., Wang, J., Li, Y. Y., Liu, N., Dong, J. X., Pang, H. C., Zhang, L., Gao, Z. J. (2020): Changes in soil organic carbon and microbial community under varying straw incorporation strategies. – Soil & Tillage Research 204.
[7] Didonato, N., Hatcher, P. G. (2017): Alicyclic carboxylic acids in soil humic acid as detected with ultrahigh resolution mass spectrometry and multi-dimensional NMR. – Organic Geochemistry 112: 33-46.
[8] Didonato, N., Chen, H. M., Waggoner, D., Hatcher, P. G. (2016): Potential origin and formation for molecular components of humic acids in soils. – Geochimica et Cosmochimica Acta 178: 210-222.
[9] Dou, S. (2010): Soil Organic Matter. – Science Press, Beijing.
[10] Dou, S., Jiang, Y. (1988): Effect of application of organic materials on the properties of humic substances in organo-mineral complexes of soils — Ⅱ Effect of organic materials on the humus composition and optical characteristics of humic acids in organo-mineral complexes. – Acta Pedologica Sinica 252-261.
[11] Dou, S., Shan, J., Song, X. Y., Cao, R., Wu, M., Li, C. L., Guan, S. (2020): Are humic substances soil microbial residues or unique synthesized compounds? A perspective on their distinctiveness. – Pedosphere 30: 159-167.
[12] El-Naggar, A., Lee, S. S., Awad, Y. M., Yang, X., Ryu, C., Rizwan, M., Rinklebe, J., Tsang, D. C. W., Ok, Y. S. (2018): Influence of soil properties and feedstocks on biochar potential for carbon mineralization and improvement of infertile soils. – Geoderma 332: 100-108.
[13] Fan, Q. Y., Sun, J. X., Quan, G. X., Yan, J. L., Gao, J. H., Zou, X. Q., Cui, L. Q. (2020): Insights into the effects of long-term biochar loading on water-soluble organic matter in soil: implications for the vertical co-migration of heavy metals. – Environment International 136.
[14] Francioso, O., Montecchio, D., Gioacchini, P., Ciavatta, C. (2005): Thermal analysis (TG-DTA) and isotopic characterization ((13)C-(15)N) of humic acids from different origins. – Applied Geochemistry 20: 537-544.
[15] Gao, S. J., Gao, J. S., Cao, W. D., Zou, C. Q., Huang, J., Bai, J. S., Dou, F. G. (2018): Effects of long-term green manure application on the content and structure of dissolved organic matter in red paddy soil. – Journal of Integrative Agriculture 17: 1852-1860.
[16] Gao, J. F., Dou, S., Wang, Z. G. (2019): Structural analysis of humic acid in soil at different corn straw returning modes through fluorescence spectroscopy and infrared spectroscopy. – International Journal of Analytical Chemistry. https://doi.org/10.1155/2019/1086324.
[17] Gu, Z. J., Xie, Y., Gao, Y., Ren, X. Y., Cheng, C. C., Wang, S. C. (2018): Quantitative assessment of soil productivity and predicted impacts of water erosion in the black soil region of northeastern China. – Science of the Total Environment 637: 706-716.
[18] Guo, F., Qin, S., Xu, L., Bai, Y. C., Xing, B. S. (2020a): Thermal degradation features of soil humic acid sub-fractions in pyrolytic treatment and their relation to molecular signatures. – Science of the Total Environment 749.
[19] Guo, X. X., Liu, H. T., Zhang, J. (2020b): The role of biochar in organic waste composting and soil improvement: a review. – Waste Management 102: 884-899.
[20] Han, Y., Ma, W., Zhou, B., Salah, A., Geng, M., Cao, C., Zhan, M., Zhao, M. (2020a): Straw return increases crop grain yields and K-use efficiency under a maize-rice cropping system. – The Crop Journal. https://doi.org/10.1016/j.cj.2020.04.003.

http://www.aloki.hu ● ISSN 1589 1623 (Print) ● ISSN 1785 0037 (Online)
DOI: http://dx.doi.org/10.15666/aeer/2001_785799

[21] Han, Y., Yao, S. H., Jiang, H., Ge, X. L., Zhang, Y. L., Mao, J. D., Dou, S., Zhang, B. (2020b): Effects of mixing maize straw with soil and placement depths on decomposition rates and products at two cold sites in the mollisol region of China. – Soil & Tillage Research 197.
[22] Haumaier, L., Zech, W. (1995): Black carbon—possible source of highly aromatic components of soil humic acids. – Organic Geochemistry 23: 191-196.
[23] Hu, J., Wu, J. G., Sharaf, A., Sun, J. M., Qu, X. J. (2019): Effects of organic wastes on structural characterizations of fulvic acid in semiarid soil under plastic mulched drip irrigation. – Chemosphere 234: 830-836.
[24] Huang, D. D., Chen, X. W., Cao, G. J., Liang, A. Z., Jia, S. X., Liu, S. X. (2018): Effects of long-term conservation tillage on soil nitrogen content and organic nitrogen components in a Chinese mollisol. – Applied Ecology and Environmental Research 16: 5517-5528.
[25] Jimenez-Gonzalez, M. A., Almendros, G., Waggoner, D. C., Alvarez, A. M., Hatcher, P. G. (2020): Assessment of the molecular composition of humic acid as an indicator of soil carbon levels by ultra-high-resolution mass spectrometric analysis. – Organic Geochemistry 143.
[26] Kim, H. B., Kim, J. G., Kim, T., Alessi, D. S., Baek, K. (2020): Mobility of arsenic in soil amended with biochar derived from biomass with different lignin contents: Relationships between lignin content and dissolved organic matter leaching. – Chemical Engineering Journal 393.
[27] Kuwatsuka, S., Watanabe, A., Itoh, K., Arai, S. (1992): Comparison of two methods of preparation of humic and fulvic acids, IHSS method and NAGOYA method. – Soil Science and Plant Nutrition 38: 23-30.
[28] Liu, F., Wang, D., Zhang, B., Huang, J. (2020a): Concentration and biodegradability of dissolved organic carbon derived from soils: a global perspective. – Science of The Total Environment. DOI:10.1016/j.scitotenv.2020.142378.
[29] Liu, S., Benedetti, M. F., Han, W., Korshin, G. V. (2020b): Comparison of the properties of standard soil and aquatic fulvic and humic acids based on the data of differential absorbance and fluorescence spectroscopy. – Chemosphere 261: 128189.
[30] Luan, H. A., Gao, W., Huang, S. W., Tang, J. W., Li, M. Y., Zhang, H. Z., Chen, X. P. (2019): Partial substitution of chemical fertilizer with organic amendments affects soil organic carbon composition and stability in a greenhouse vegetable production system. – Soil & Tillage Research 191: 185-196.
[31] Ma, C., Chen, X., Zhang, J. Z., Zhu, Y. P., Kalkhajeh, Y. K., Chai, R. S., Ye, X. X., Gao, H. J., Chu, W. Y., Mao, J. D., Thompson, M. L. (2019): Linking chemical structure of dissolved organic carbon and microbial community composition with submergence-induced soil organic carbon mineralization. – Science of the Total Environment 692: 930-939.
[32] Ndzelu, B. S., Dou, S., Zhang, X. W. (2020): Changes in soil humus composition and humic acid structural characteristics under different corn straw returning modes. – Soil Research 58: 452-460.
[33] Pospisilova, L., Horakova, E., Fisera, M., Jerzykiewicz, M., Mensik, L. (2020): Effect of selected organic materials on soil humic acids chemical properties. – Environmental Research 187.
[34] Rydin, H., Jeglum, J. K., Bennett, K. D. (2013): The Biology of Peatlands. 2nd Ed. – Oxford university Press, Oxford.
[35] Schulten, H.-R., Leinweber, P. (1996): Characterization of humic and soil particles by analytical pyrolysis and computer modeling. – Journal of Analytical and Applied Pyrolysis 38: 1-53.
[36] Simansky, V., Juriga, M., Jonczak, J., Uzarowicz, L., Stepien, W. (2019): How relationships between soil organic matter parameters and soil structure characteristics are affected by the long-term fertilization of a sandy soil. – Geoderma 342: 75-84.

http://www.aloki.hu ● ISSN 1589 1623 (Print) ● ISSN 1785 0037 (Online)
DOI: http://dx.doi.org/10.15666/aeer/2001_785799

[37] Tamura, M., Suseela, V., Simpson, M., Powell, B., Tharayil, N. (2017): Plant litter chemistry alters the content and composition of organic carbon associated with soil mineral and aggregate fractions in invaded ecosystems. – Global Change Biology 23: 4002-4018.
[38] Tang, Y., Luo, L., Carswell, A., Misselbrook, T., Shen, J., Han, J. (2020): Changes in soil organic carbon status and microbial community structure following biogas slurry application in a wheat-rice rotation. – Science of The Total Environment 143786.
[39] Wang, H. X., Xu, J. L., Liu, X. J., Zhang, D., Li, L. W., Li, W., Sheng, L. X. (2019): Effects of long-term application of organic fertilizer on improving organic matter content and retarding acidity in red soil from China. – Soil & Tillage Research 195.
[40] Wu, D., Dou, S., Ma, R., Xie, S., Zhang, B. (2020): Effects of corn stover and wood peat on soil improvement. – Journal of Jilin Agricultural University 1-7.
[41] Wu, L. P., Zhang, S. R., Ma, R. H., Chen, M. M., Wei, W. L., Ding, X. D. (2021): Carbon sequestration under different organic amendments in saline-alkaline soils. – Catena 196.
[42] Wu, M., Wei, S. P., Liu, J., Liu, M., Jiang, C. Y., Li, Z. P. (2019): Long-term mineral fertilization in paddy soil alters the chemical structures and decreases the fungistatic activities of humic acids. – European Journal of Soil Science 70: 776-785.
[43] Xiang, X. J., Liu, J., Zhang, J., Li, D. M., Xu, C. X., Kuzyakov, Y. (2020): Divergence in fungal abundance and community structure between soils under long-term mineral and organic fertilization. – Soil & Tillage Research 196.
[44] Xiaoli, C., Shimaoka, T. Y., Qiang, G., Youcai, Z. (2008): Characterization of humic and fulvic acids extracted from landfill by elemental composition, C-13 CP/MAS NMR and TMAH-Py-GC/MS. – Waste Management 28: 896-903.
[45] Xu, X. Z., Xu, Y., Chen, S. C., Xu, S. G., Zhang, H. W. (2010): Soil loss and conservation in the black soil region of Northeast China: a retrospective study. – Environmental Science & Policy 13: 793-800.
[46] Xu, J. S., Zhao, B. Z., Chu, W. Y., Mao, J. D., Zhang, J. B. (2017): Chemical nature of humic substances in two typical Chinese soils (upland vs paddy soil): a comparative advanced solid state NMR study. – Science of the Total Environment 576: 444-452.
[47] Xu, J., Han, H. F., Ning, T. Y., Li, Z. J., Lal, R. (2019): Long-term effects of tillage and straw management on soil organic carbon, crop yield, and yield stability in a wheat-maize system. – Field Crops Research 233: 33-40.
[48] Xu, X. R., Schaeffer, S., Sun, Z. H., Zhang, J. M., An, T. T., Wang, J. K. (2020): Carbon stabilization in aggregate fractions responds to straw input levels under varied soil fertility levels. – Soil & Tillage Research 199.
[49] Yu, Q. G., Hu, X., Ma, J. W., Ye, J., Sun, W. C., Wang, Q., Lin, H. (2020): Effects of long-term organic material applications on soil carbon and nitrogen fractions in paddy fields. – Soil & Tillage Research 196.
[50] Zaccone, C., Plaza, C., Ciavatta, C., Miano, T. M., Shotyk, W. (2018): Advances in the determination of humification degree in peat since Achard (1786): Applications in geochemical and paleoenvironmental studies. – Earth-Science Reviews 185: 163-178.
[51] Zhang, J., Lv, B. Y., Xing, M. Y., Yang, J. (2015): Tracking the composition and transformation of humic and fulvic acids during vermicomposting of sewage sludge by elemental analysis and fluorescence excitation-emission matrix. – Waste Management 39: 111-118.
[52] Zhang, X., Zhao, Y., Zhu, L. J., Cui, H. Y., Jia, L. M., Xie, X. Y., Li, J. M., Wei, Z. M. (2017): Assessing the use of composts from multiple sources based on the characteristics of carbon mineralization in soil. – Waste Management 70: 30-36.
[53] Zhang, J., Yin, H. L., Wang, H., Xu, L., Samuel, B., Chang, J. J., Liu, F., Chen, H. H. (2019a): Molecular structure-reactivity correlations of humic acid and humin fractions from a typical black soil for hexavalent chromium reduction. – Science of the Total Environment 651: 2975-2984.

http://www.aloki.hu ● ISSN 1589 1623 (Print) ● ISSN 1785 0037 (Online)
DOI: http://dx.doi.org/10.15666/aeer/2001_785799

[54] Zhang, J. J., Wei, Y. X., Liu, J. Z., Yuan, J. C., Liang, Y., Ren, J., Cai, H. G. (2019b): Effects of maize straw and its biochar application on organic and humic carbon in water-stable aggregates of a Mollisol in Northeast China: a five-year field experiment. – Soil & Tillage Research 190: 1-9.
[55] Zhang, X. W., Dou, S., Ndzelu, B. S., Guan, X. W., Zhang, B. Y., Bai, Y. (2020): Effects of different corn straw amendments on humus composition and structural characteristics of humic acid in black soil. – Communications in Soil Science and Plant Analysis 51: 107-117.
[56] Zhao, P. Z., Li, S., Wang, E. H., Chen, X. W., Deng, J. F., Zhao, Y. S. (2018a): Tillage erosion and its effect on spatial variations of soil organic carbon in the black soil region of China. – Soil & Tillage Research 178: 72-81.
[57] Zhao, S. X., Ta, N., Li, Z. H., Yang, Y., Zhang, X., Liu, D., Zhang, A., Wang, X. D. (2018b): Varying pyrolysis temperature impacts application effects of biochar on soil labile organic carbon and humic fractions. – Applied Soil Ecology 123: 484-493.
[58] Zheng, Y., Zhang, J., Tan, J., Zang, C., Yu, Z. (2019): Chemical composition and structure of humus relative to sources. – Acta Pedologica Sinica 56: 386-397.

http://www.aloki.hu ● ISSN 1589 1623 (Print) ● ISSN 1785 0037 (Online)
DOI: http://dx.doi.org/10.15666/aeer/2001_785799

BIOMASS MATERIAL AMENDMENT MAINTAINED THE STRUCTURE OF UNDERGROUND CULTURAL RELICS BY DECREASING THE VARIATION OF SOIL WATER CONTENT

MU, B. G.[1*] – ZHANG, Y.[1] – YU, Y. J.[2,3] – PETROPOULOS, E.[3]

[1]*School of Civil Engineering, Southeast University, 211189 Nanjing, China*

[2]*Nanjing University of Information and Technology, Nanjing 210044, China*

[3]*School of Engineering, Newcastle University, Newcastle upon Tyne, NE1 7RU, UK*

**Corresponding author*
e-mail: mubaogang@seu.edu.cn; phone: +86-25-5209-1223; fax: +86-25-5209-1223

(Received 15th Sep 2021; accepted 23rd Nov 2021)

Abstract. Consistency of soil water content in the case of underground cultural brick relics is critical for the preservation of their structure and existence. However, natural topographical activity and illegal digging often damage water permeability and retention capacity of the soil layer covering the underground brick relics. To maintain the stabilization of underground brick relics' structure, a 2% biomass amendment was applied to the soil layer near a centuries-old relic at east China. The results showed that biomass amendment technology improved the soil water permeability and retention capacity by maintaining soil water content in a certain range. The analogous calculation showed that the biomass amendment technology improved the change range of the internal friction angle along the precipitation intensity from 24.81°-31.14°in the control to 25.03°-31.28° under biomass treatment. Soil cohesion in biomass treatment was kept in a smaller range than that of control treatment. Biomass treatment held a lower range for the horizontal and vertical pressure originating from surrounding soil caused by heavy short-time rainfall compared to the control. This study demonstrated that biomass amendment can improve the performance of soil shearing strength through the better regulation of soil hydraulic characteristics.
Keywords: architectural heritage, ancient mausoleum, historic preservation, water permeability, loading effect

Introduction

Ancient nobles and emperors often arranged grand and magnificent underground architectures for their mausoleums or tombs. Today, archaeological excavation founds a large number of these high-grade underground architectures, which have been buried for hundreds or even thousands of years (Fu et al., 2020; Ying et al., 2015). When most architectures were buried at a certain depth at ancient ages, soil layers with different thicknesses were positioned on top to protect the underground arched structure, including walls and vault (*Fig. 1A*). This kind of soil layer is usually not positioned at a flat level, but as a mound piled above the ground on top of the tomb. In ancient China, for such emperors and generals' mausoleums, the mound is often large in scale to highlight the imperial identity and power (Shi et al., 2020). For such structures, the soil layers were stacked on the top of the mausoleums, shaping a trapezoid with a large surface on the bottom of the structure. The shape of the top soil layer was always square before Eastern Han Dynasty approximately two thousand years ago. This square shaped soil layer was reformed into a flat-round shape since Eastern Han Dynasty (*Fig. 1B, C*) (Xiong, 2014). Then it had become the most widely used and most common form of soil sealing in the history of Chinese tombs. However, both of these two shapes of soil

http://www.aloki.hu ● ISSN 1589 1623 (Print) ● ISSN 1785 0037 (Online)
DOI: http://dx.doi.org/10.15666/aeer/2001_801814

sealing layer upon the underground cultural relics were at the risk of erosion by plurosion effect after hundreds or thousands of years.

Figure 1. *The typical views of mausoleums in Nanjing. (A), vertical section view of the two mausoleums of Southern Tang Dynasty; (B), Aerial view of Shunling mausoleum; (C), Aerial view of Hanjing mausoleums*

The protection of underground cultural relics is an important step to inherit the excellent human traditional culture, but our understanding of the underground relic environment related to heritage conservation is still limited (Chen et al., 2007). To protect the underground mausoleum, the soil sealing layer is one of the most important objects to prevent the underground structure from flooding or structural failure from the presence and pressure of groundwater respectively (Liu et al., 2019b). This layer acts as a balancing element to ensure the stability and sturdiness of the mausoleum's 'cap'. At the same time, it prevents ground water ingress due to its low porosity. The consistency of water content ensured the effectiveness of protective effect in the sealing soil layer (Zhang et al., 2001). This soil watertight property can be kept in a short time, but changes in hydrogeological permeability and topography in hundreds or thousands of years often lead to deterioration of the water-tightness and further structural failure (Cao et al., 2021; Guo and Huang, 2002). Changes in water content may lead to a radical change in the bulk density of the overlying soil (Kemper and Rosenau, 1984). After water ingress and saturation, the additional water increased the bulk structure density resulting in structure deformation and plausible failure. The soil water displacement from the structure to the nearby ground formations will cause the reduction in density and buoyancy effect to underground architecture, which resulted in the deformation or failure to the underground architecture. These adverse effects were found not only on the top structure of the mausoleum but also on the stability of the murals and carvings inside the tomb (Zhang et al., 2001). Additionally, an increase in soil water content generally affects the mechanical properties of the soil overlying layer itself (Oades, 1984). Specifically, numerous studies

http://www.aloki.hu ● ISSN 1589 1623 (Print) ● ISSN 1785 0037 (Online)
DOI: http://dx.doi.org/10.15666/aeer/2001_801814

confirmed that changes in the water content of unsaturated soils could result in the unbalance of shear strength index, which will cause potential systemic risks, such as instability of retaining walls and landslides (Cokca et al., 2004; Fredlund et al., 1995; Liu et al., 2019c). The amendment of high polymer materials to soil sealing layer are often used to prevent seepage water caused by rainfall and groundwater movement (Ma and Zhu, 2016). However, polymer anti-seepage materials cannot change the water absorption and drainage capacity of the soil layer. In addition, polymer materials will disturb the metabolic activity of the aboveground plants. Consequently, the changes in ecosystem on the top of ancient architecture will affect the landscape as well as the overall aesthetics of such scenic spots. It has been demonstrated that soil organic matter can effectively maintain water content, as well as it is beneficial to the growth of plants as it promotes fertility (Liu et al., 2019a; Oades, 1984). Therefore, the amendment of organic biomass to modify the properties of upper soil layer can be beneficial for the structural stability of such underground cultural relics.

In this study, organic biomass was amended to the upper soil layer to estimate its effect on the change of soil water content and subsequent possible influences on mechanical properties of underground relic structures. The experiment was performed in a green space near an ancient emperor's mausoleum with centuries of history in Nanjing City, China (Li et al., 2016). This typical underground architecture is at the risk of rainfall and weathering after a long history of crustal movement or illegal tomb trespassing. The findings from this study will be beneficial for the development of strategies to improve the state of such underground structures in the meet of the new generations of architecture and archaeology.

Materials and methods

Experimental site

The experimental site was set in a green park nearby the two mausoleums of the Southern Tang Dynasty situated in Nanjing City (31°76-32°87′N, 117°50-118°90′E), Jiangsu Province, China. The two mausoleums of Southern Tang Dynasty, Qinling Mausoleum and Shunling Mausoleum, were built between 937 AD and 975 AD according to archaeological studies (Yuan et al., 2016). The surface structures for the two mausoleums have been destroyed, leaving behind only the two mounds. The dilapidated mound of Qinling Mausoleum is about five meters high and 30 meters in diameter. The Shunling Mausoleum, built against a mountain slope, has a mound smaller than that of Qinling Mausoleum. Remnant earth banks in the south and southwest of Shunling Mausoleum were probably the boundaries of the original mausoleum garden. The terrace inside was probably the foundation of the mausoleum hall. In the reclaiming land on the terrace, tenants had unearthed several bricks, three plinths, broken tiles, and white porcelain items. Annual precipitation of the study site varies between 979 and 1113 mm. The recent temperature fluctuates from -2.6 ℃ to 40 ℃ with an average value of 17 ℃ (average of 2019 as reference). Relative humidity fluctuated between 15.8% and 100% (http://data.cma.cn/en).

Field improvement experiment

To assess the role of the carbon-rich biomass amendment on the underground structure, two 4 m^2 (2 m × 2 m) fields were selected in the studied site on April 18, 2019.

http://www.aloki.hu ● ISSN 1589 1623 (Print) ● ISSN 1785 0037 (Online)
DOI: http://dx.doi.org/10.15666/aeer/2001_801814

In Nanjing, the largest short-term rainfall generally occurs during summer, so a three-month field study was performed during this period in the two selected fields. We expect that this period will be representative to cover the worst-case scenario in terms of the water saturation level in soils. Both fields were dug down to 1.0 m using a small excavator. In one of the two fields, the soil was excavated and mixed with biomass material at a ratio of 1:50 in weight by weight according to the previous studies of biomass amendment (Ding et al., 2014; Zhang et al., 2020). Another field was set as the unamended control treatment, the soil in this field was dug out, mixed well but without biomass amendment. The biomass matter was naturally air-dried manure without composting. Before mixing with soil, the biomass was ground to debris and sieved through a 2 mm sieve. Then the mixed soil with biomass material was filled back into the plot. In both plots, three EC-5 soil moisture sensors (Decagon Devices, Pullman, WA, USA) were buried at a depth of 60 cm to monitor soil water content in real-time (*Fig. 2*). The EC-5 soil moisture sensors used were connected to an EM50 data acquisition unit. The data acquisition frequency was set at once every 3 h. Consequently, each EC-5 sensor could collect 8 soil moisture data per day. After 3 months, the EC-5 sensors and EM50 data collector were taken out (August 8, 2019). The real-time monitoring data of the soil moisture content after approximately 3 months (from April 18 to August 8) were analyzed with ECH2O utility software (v3.2.0) (Decagon Device Inc., USA). The rainfall data were recorded by HOBO meteorological station (HOBO RX3003, US) located at the two mausoleums of the Southern Tang Dynasty.

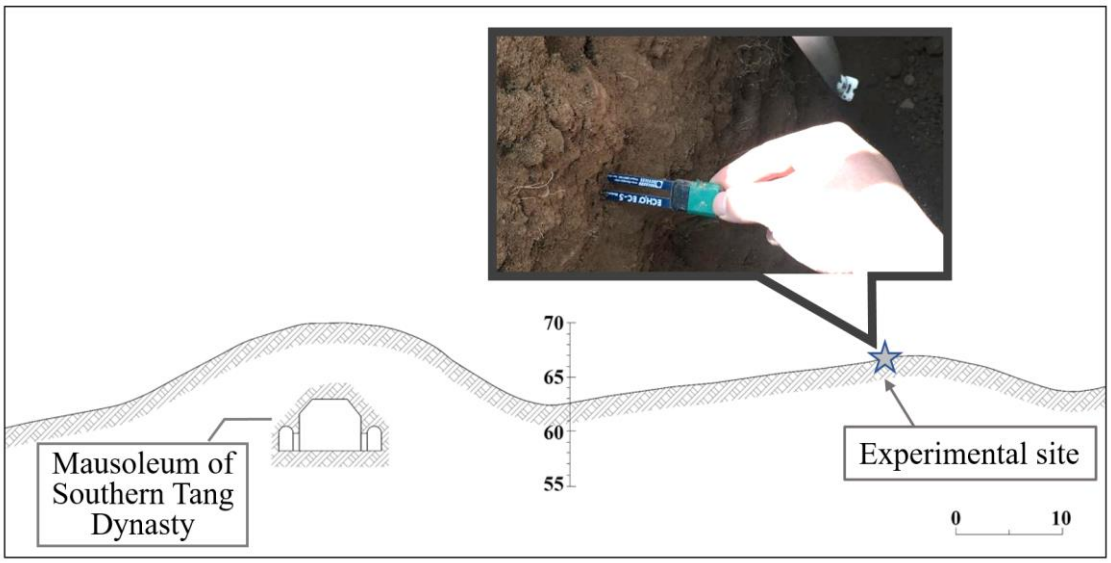

Figure 2. *The experimental site near the mausoleum of Southern Tang Dynasty*

Estimation of the relationship between soil water content and shearing strength

A laboratory experiment was performed to determine the relationship between soil water content and shearing strength. Soil samples were collected at the green park in our experiment field. Before use, the soils were air-dried, homogenized, and screened through a 2 mm sieve. Gravel, roots, and other impurities were carefully removed. Based on the actual water content during the field experiment, 6 levels of soil water content (from 0.09 to 0.44 m^3/m^3 at intervals of 0.07 m^3/m^3) were set for the test. A

http://www.aloki.hu ● ISSN 1589 1623 (Print) ● ISSN 1785 0037 (Online)
DOI: http://dx.doi.org/10.15666/aeer/2001_801814

certain amount of deionized water was sprayed into the soils to meet the calculated water demand. Then the mixed soil sample was sealed with plastic wrap and kept in a dry container for 24 h to complete soakage. Triaxial compression tests were undertaken with an automatic triaxial compression system (STSZ-9, Zhejiang Tugong Instrument Co., Ltd., China). The shear velocity was 0.80 mm min^{-1}, and four confining pressures, i.e. 100, 200, 300, and 400 kPa, were applied to determine shearing strength. The shear strength parameters, the cohesion (c) and internal friction angle (φ), were calculated in accordance with Standards for Soil Test Methods (GB/T50123-1999). According to the laboratory experiment, the relationship between soil water content and shearing strength was listed as following equations (*Eq. 1* and *2*) (*Fig. 3*).

$$\varphi = 20.559w^{-0.207} \quad \text{(Eq.1)}$$

where φ is the internal frictional angle, and w is the soil water content.

$$c = -807.87w^2 + 449.5w + 7.4117 \quad \text{(Eq.2)}$$

where c is cohesion, and w is soil water content.

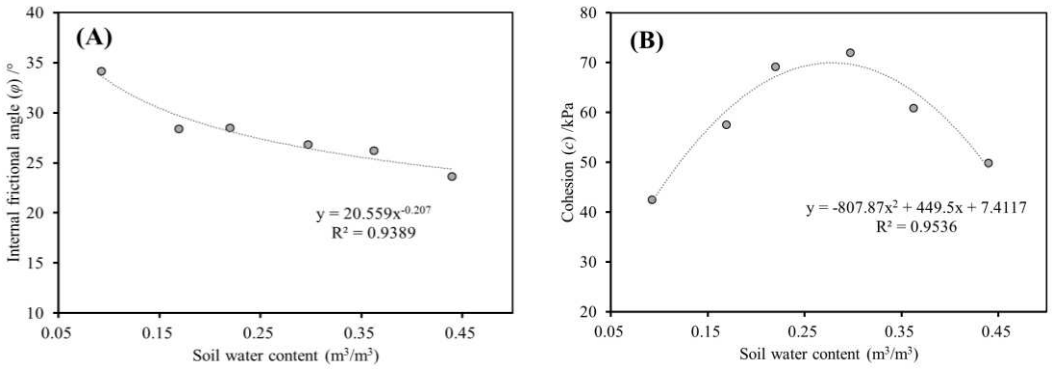

Figure 3. *Relationship between soil water content and shearing strength parameters (A, internal frictional angle; B, cohesion)*

Data analysis

Statistical analysis was implemented using the IBM Statistical Product and Service Solutions (SPSS) Statistics for Windows (Version 16.0). The data were expressed as means of measurements with standard deviation (SD); different letters indicate significant differences among different treatments. Analysis of variance (ANOVA) was performed to determine the significance of the biomass amendment, followed by Tukey's HSD test. Differences of $p < 0.05$ were considered significant.

Results

Effects of biomass amendment on soil water content

The soil water content for both the unamended control and biomass treatment changed consistently during rainfall periods (*Fig. 4*). It can be observed that during the

http://www.aloki.hu ● ISSN 1589 1623 (Print) ● ISSN 1785 0037 (Online)
DOI: http://dx.doi.org/10.15666/aeer/2001_801814

first three days, from April 18 to April 20, no difference appeared in the water content, likely due to insufficient compaction after the mechanical filling of the excavation. This period can be considered as the adaptation period for soils. After the adaption period, the soil water content will have its peaks after heavy rainfall and then gradually decrease, corresponding to the process of the soil storing and draining water. It can be generally said that the higher the rainfall intensity, the higher value of the soil water content. These results confirm that the buried soil moisture sensor can accurately and real-time record the dynamic changes of the soil moisture, which in other words supports that is a credible data acquisition basis for the study of the water status in underground soil.

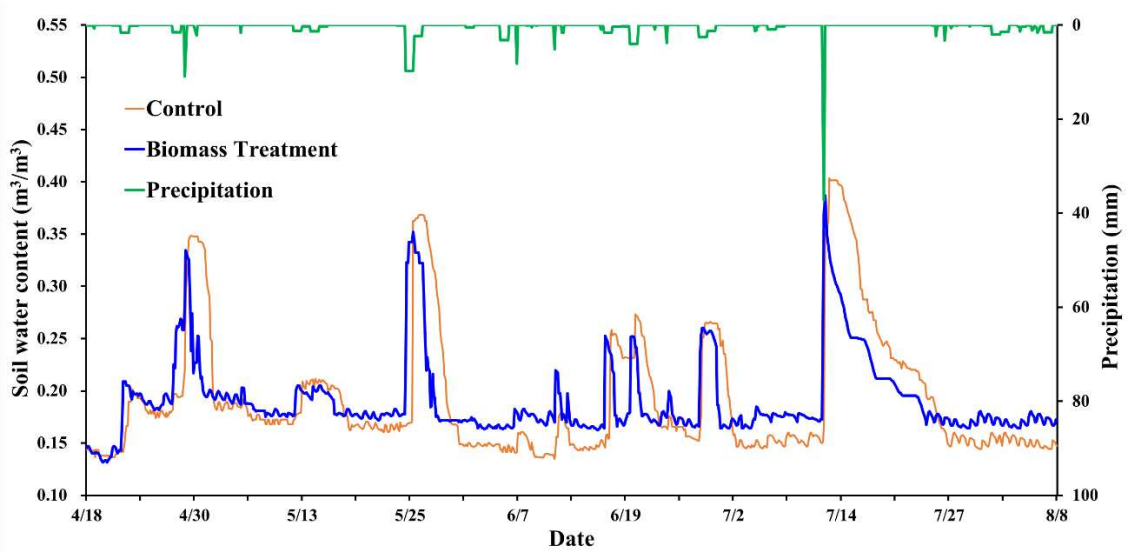

Figure 4. *Soil water content and rainfall in the experimental area from 18th Apr to 8th Aug 2019*

To assess the influence of consistent rainfall type and short-time heavy rainfall type on soil water content, two typical rainy periods were selected for further analysis (*Fig. 5*). One period was a rainfall process consistent from April 28 to April 30, and the total rainfall in these three days was 33.56 mm (*Fig. 5A*). The other period was a short-time heavy rainfall occurred on July 12, when the rainfall reached 57.62 mm within 9 h (*Fig. 5B*). The slow rainfall process in April, which was distributed within 3 days, made the maximum and minimum values of soil water content as 0.349 $m^3 \cdot m^{-3}$ and 0.168 $m^3 \cdot m^{-3}$ respectively in the control treatment (*Fig. 5A*). While in biomass treatment, the peak and valley value of water content showed as 0.330 $m^3 \cdot m^{-3}$ and 0.175 $m^3 \cdot m^{-3}$ during the three days of rainfall in late April (*Fig. 5A*). During the short-term heavy rainfall period, the minimum and maximum values of soil moisture content in the control treatment were 0.401 and 0.144 respectively, while the minimum and maximum values of soil moisture under biomass treatment were 0.387 and 0.164 respectively.

In both consistent rain processes and short-time heavy rain processes, the maximum value of soil water content in biomass treatment was lower than the control treatment. This phenomenon of the maximum water content value indicated that biomass treatment could benefit the drainage capacity when the environmental water increased either in a consistent slow rain type or a short-time heavy rain type. The minimum value of soil

http://www.aloki.hu ● ISSN 1589 1623 (Print) ● ISSN 1785 0037 (Online)
DOI: http://dx.doi.org/10.15666/aeer/2001_801814

water content in the two observed rain periods showed a lower value in biomass treatment than that of control. Furthermore, the consistent rainfall made soil water content in biomass treatment maintained at the range of 0.283~0.334 only for 12 h, while it made soil water content in control treatment maintained at the range of 0.313~0.348 for 96 h (*Fig. 5*). During the short-time heavy rainfall period, the soil water content in biomass treatment decreased rapidly after reaching the peak value and decreased to the minimum value on the 11th day after the end of this short-time heavy rainfall. However, in the control treatment, soil moisture did not decrease significantly after reaching the peak value, but lasted about 48 h in the range of 0.313 ~ 0.401 $m^3 \cdot m^{-3}$, and reached the minimum value 13 days after the end of short-time heavy rainfall (*Fig. 5B*). This phenomenon indicates that the addition of biomass changes the water permeability of the soil.

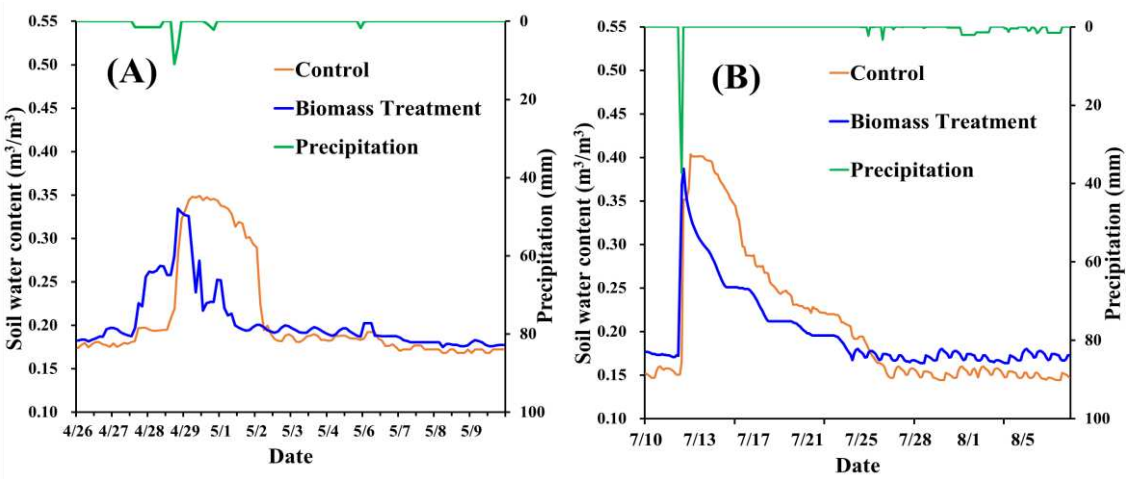

Figure 5. *The changes of soil water content under two typical rainfall periods (A, period from April 26 to May 10; B, period from July 10 to August 8)*

Effects of biomass amendment on soil shear strength

To assess the effect of soil water content on the underground relics, an analogous calculation was performed based on the structure data from the Shunling mausoleum, one of the tombs of Southern Tang Dynasty at Nanjing (*Fig. 6*). The bottom of the tomb is 8 m deep, the side wall is 2 m high, and the width of the tomb is 5 m. The back of the wall is upright and smooth, the roof is an arch structure. The ground surface is approximated by a horizontal plane (*Fig. 6*). To assess the response of soil shear strength from the biomass amended treatment, soil density (ρ), internal frictional angle (φ), and cohesion (c) were calculated according to the fitting equation. Since the first three days, from April 18 to April 20, were a period with no differentiation (soil adaptation), all the shear strength parameters were calculated from the data obtained from April 21 to August 8. The minimum, maximum value, and variance of the data during this period were listed in *Table 1*. It can be observed that the maximum value of these three parameters in the biomass amended treatment was lower than that of the control treatment, while the minimum value was higher than that of the control. The control treatment had a higher variance than that of the biomass amended one, indicating a more divergent data set.

http://www.aloki.hu ● ISSN 1589 1623 (Print) ● ISSN 1785 0037 (Online)
DOI: http://dx.doi.org/10.15666/aeer/2001_801814

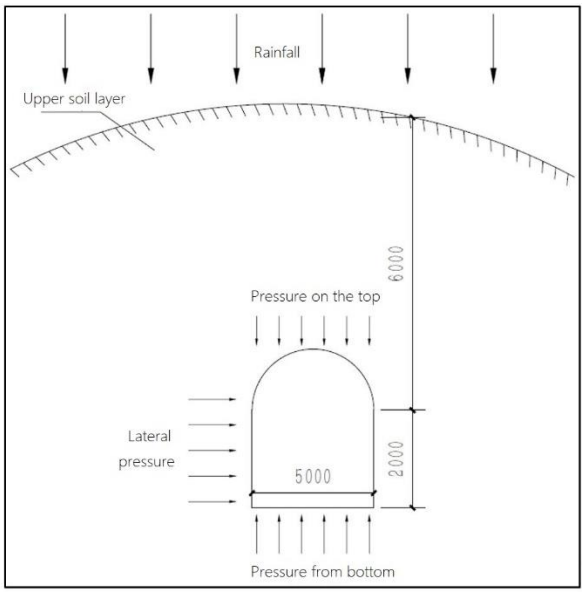

Figure 6. *Schematic diagram of force in the Shunling mausoleum*

Table 1. *The soil shear strength parameters in control and biomass treatments*

	Soil density (ρ)	**Internal frictional angle (φ)**	**Cohesion (c)**
$Control_{max}$	17.54	31.14	69.94
$Control_{min}$	16.51	24.81	53.25
$Control_{var}$	0.05	2.45	22.39
$Biomass_{max}$	17.47	31.28	69.94
$Biomass_{min}$	16.50	25.03	52.61
$Biomass_{var}$	0.02	1.02	11.09

$Control_{max}$, the maximum value parameter in Control treatment; $Biomass_{max}$, the maximum value parameter in Biomass treatment. $Control_{min}$, the minimum value parameter in Control treatment; $Biomass_{min}$, the maximum value parameter in Biomass treatment. $Control_{var}$, the variance value parameter in Control treatment; $Biomass_{var}$, the variance value parameter in Biomass treatment

Effects of biomass amendment on horizontal and vertical force on the underground relics

The changes in horizontal and vertical pressures caused by biomass amendment were assessed by analogy calculation in Shunling mausoleum. Since the burial time of the underground relics has been hundreds of thousands of years, static pressure was considered in this case. The short-time heavy rainfall period, from July 10 to August 8, was used for the estimation of the maximum expected horizontal and vertical pressure on the underground relics. The horizontal pressure on the lateral wall of the underground relics, in this case, was calculated at the depth of 6.00 m, 6.50 m, 7.00 m, 7.50 m, and 8.00 m (*Table 2*). It was found that the maximum and minimum value of the horizontal pressure on the retaining wall at different depths was very similar between the control and the biomass amended trials. However, the variance of the horizontal pressure at each depth was lower in biomass amended treatment compared to the control (*Table 2*).

http://www.aloki.hu ● ISSN 1589 1623 (Print) ● ISSN 1785 0037 (Online)
DOI: http://dx.doi.org/10.15666/aeer/2001_801814

Table 2. *The horizontal pressure on retaining wall of different depth in control and biomass treatments*

	Horizontal pressure on retaining wall of different depth /kPa				
	6.0 m below	**6.5 m below**	**7.0 m below**	**7.5 m below**	**8.0 m below**
$Control_{max}$	209.35	226.79	244.24	261.68	279.13
$Control_{min}$	5.81×10^{-3}	6.29×10^{-3}	6.78×10^{-3}	7.26×10^{-3}	7.74×10^{-3}
$Control_{var}$	4517.6	5301.9	6148.9	7058.7	8031.3
$Biomass_{max}$	207.13	224.39	241.66	258.92	276.18
$Biomass_{min}$	5.81×10^{-3}	6.29×10^{-3}	6.78×10^{-3}	7.26×10^{-3}	7.74×10^{-3}
$Biomass_{var}$	4543.6	5332.7	6184.3	7099.3	8077.4

$Control_{max}$, the maximum value parameter in Control treatment; $Biomass_{max}$, the maximum value parameter in Biomass treatment. $Control_{min}$, the minimum value parameter in Control treatment; $Biomass_{min}$, the maximum value parameter in Biomass treatment. $Control_{var}$, the variance value parameter in Control treatment; $Biomass_{var}$, the variance value parameter in Biomass treatment

To assess the resultant vertical pressure on the underground relics resulting from biomass amendment, the pressure on the top of chamber, the pressure from the bottom of chamber, and the buoyant pressure to chamber taken into consideration based on analogy calculations (*Fig. 7*). The vertical pressures in this case were calculated based on the data from April 21 to August 8. The maximum pressure on the top of the tomb from the biomass amended trial was estimated 0.56 kPa lower than that of control, while the minimum pressure on top of the tomb was 0.93 kPa higher in biomass treatment than that of the control treatment (*Fig. 7A*). A similar phenomenon was observed in the pressure from the bottom and buoyancy to the chamber. It was found that 0.90 kPa decrease of the maximum pressure from the bottom because of biomass treatment, while 1.49 kPa increase of the minimum pressure from the bottom due to biomass treatment (*Fig. 7B*). Biomass made the buoyant pressure of chamber 0.34 kPa decrease and 0.56 kPa increase compared to control treatment (*Fig. 7C*). The variance of all the three vertical pressures was less than two-fifth times lower in biomass treatment than that of control treatment.

Discussion

The hydraulic behavior of the soil layer on top of the underground relics plays a vital role in the stability of the engineered structure and subsequently in the conservation of the heritage. In this study, biomass amendment to soil was trialed to assess its effect on the soil hydraulic curve and the parameters of soil strength and structure for the purpose of protecting underground culture relics.

The impact of biomass amendment on soil water content

The biomass amendment was extensively used to improve soil structure in numerous studies mainly due to its direct effect of the increase in soil organic matter (Buss et al., 2016; Dessureault-Rompré et al., 2020; García-Orenes et al., 2005; Liu et al., 2016). In this study, the in situ experiment showed that the biomass amended soil can decelerate the loss of water avoiding large fluctuations in the soil water content when rainfall is relatively slow and of light intensity; while when short-term heavy rainfall, the biomass

http://www.aloki.hu ● ISSN 1589 1623 (Print) ● ISSN 1785 0037 (Online)
DOI: http://dx.doi.org/10.15666/aeer/2001_801814

treatment can seep water quickly to avoid water accumulation. The increased organic matter due to biomass amendment improves soil physical properties (Haynes and Naidu, 1998; Oades, 1984). The humus produced by the decomposition of organic matter can increase soil adhesion and promote the formation of aggregates (Kholodov et al., 2019). The soil organic matter is pliable, flocculent and porous, and the cohesive pressure is not as strong as that of soil (typically clay particles); clay particles are easy to form scattered aggregates after being coated with organic matter, which renders the soil also pliable and no longer forms hard lumps (Kemper et al., 1987). This subsequently can improve soil structure, and alter soil permeability, water storage, and aeration.

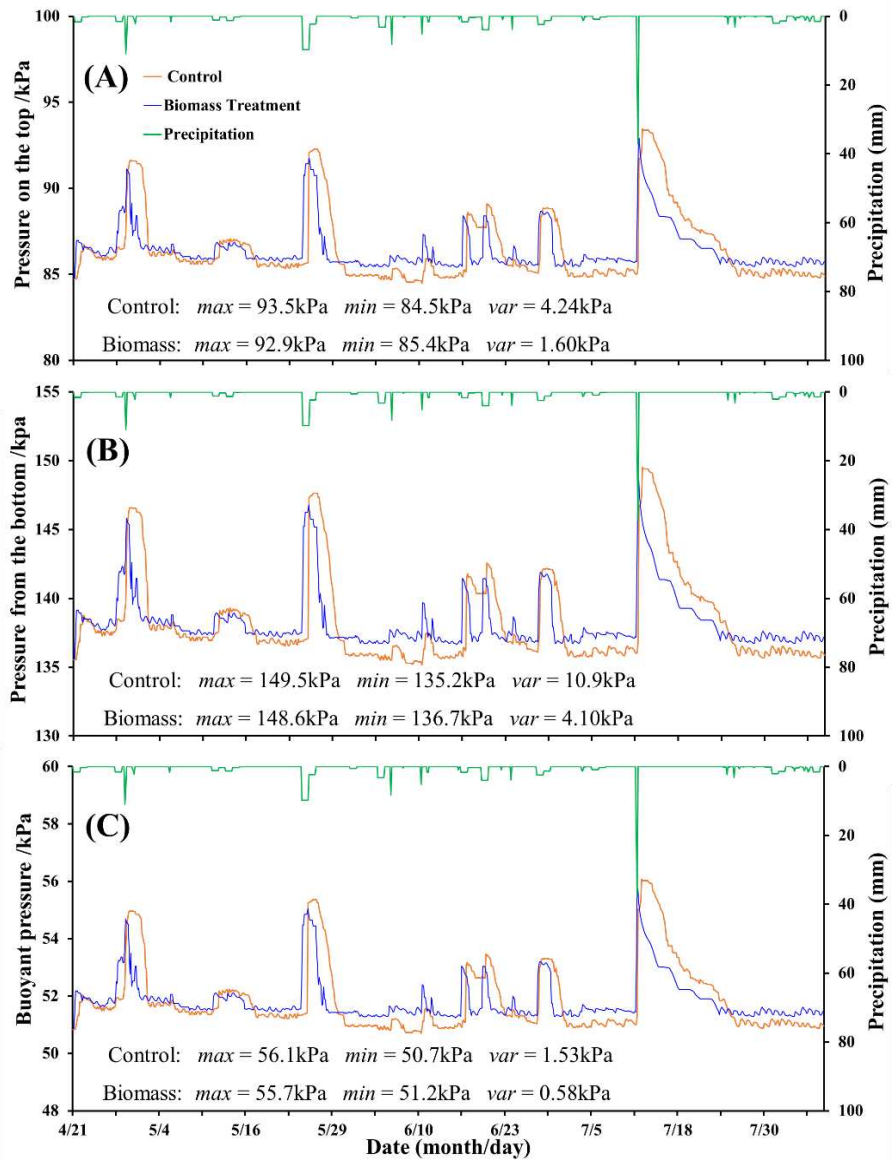

Figure 7. *Vertical force on the underground relics in control and biomass treatments. (A), the pressure on the top of chamber; (B), the pressure from the bottom of chamber; (C), the buoyancy to chamber*

The biomass amendment can alter the soil's chemical properties and promote the growth of above-ground vegetation (plants) (Gebhardt et al., 2017; Quaye et al., 2011).

http://www.aloki.hu ● ISSN 1589 1623 (Print) ● ISSN 1785 0037 (Online)
DOI: http://dx.doi.org/10.15666/aeer/2001_801814

Organic matter contains nitrogen, phosphorus, sulfur, calcium, magnesium, and other trace elements, which will directly change the proportion of nutrient elements in the soil. Soil organic matter can enhance the ability to decompose soil mineral components (Torn et al., 1997). The increased nutrients will promote the growth of aboveground plants. Humic acids in organic matter can enhance plant respiration and nutrient absorption, vitamins (Tremblay et al., 2002). Some hormones in organic matter can promote plant growth and development. Humic acids in biomass matter have been proved to be a kind of physiologically active substance (Al-Taey, 2018), which can accelerate seed germination, enhance root activity and promote crop growth. The growth of plants on the soil base up the underground relics is beneficial for maintaining soil water content. Therefore, in summary, biomass material not only has the function of water retention and storage, but also has the function of drainage, which can maintain the stability of the water content of the soil within a certain range protecting the underground relic overburden.

The impact of biomass amendment on soil engineering strength

For underground relic buildings, the solid structure will not dramatically change in a local range, but the change of water content will relatively affect the shearing strength parameters of the underground soil layer (Zhang et al., 2001). In this study, the analogy calculation showed that an increase in water content will lead to an increase in the soil bulk density, which in turn will increase the lateral earth pressure on the walls of the underground cultural relics. Moreover, within a certain range, the deeper depth could lead to higher underground pressure and subsequently greater risk on the structure of underground heritage. The water storage and water retention effect of biomass materials could keep the soil moisture content at a relatively high level, which consequently increases the weight of the overlying soil layer and reduce the influence of buoyancy on the small deformation of the tomb structure. When soil water content increases, the liquid index increases, and the mechanical strength of soil decreases, the stability of soil will then get affected (Kemper and Rosenau, 1984). The gravity of soil increases with the increase of water content. Generally, for cohesive soil, the gravity can increase by 1/7 ~ 1/315 after soil saturation (Chao et al., 2018). The weight of the collapsed body increases with the increase of gravity, which accelerates the collapse of the soil cave vault. When the water content increases, it expands, when it is dry, it shrinks, and then vertical cracks appear, the soil gets deteriorated, and its mechanical strength decreases (Liu et al., 2019b; Ringelberg et al., 2014). These changes of building materials are conducive to the infiltration of rainwater and surface water, then it will accelerate the potential erosion and make the vault of the soil cave collapse more easily. Soil moisture has a floating effect on soil (Li et al., 2021). The buoyancy is directly proportional to the volume of soil water content. When the water content decreases, the buoyancy decreases, and the soil mass changes from effective gravity to natural gravity. Combined with other factors, it may lead to the instability of the soil at the top of the soil cave, resulting in collapse. Therefore, the biomass amendment to the soil base could maintain the stability of the arch voucher of the underground heritage.

Conclusion

In this study, the amendment of biomass can improve the stability of the soil layer on top of ancient underground cultural relics. The presence of biomass assists in the

http://www.aloki.hu ● ISSN 1589 1623 (Print) ● ISSN 1785 0037 (Online)
DOI: http://dx.doi.org/10.15666/aeer/2001_801814

regulation of the water content and subsequently maintain the protective effect of this overlying soil layer against deterioration and structural failure. The amendment of biomass material to soils not only has the ability to securely retain and store water but also to promote accelerated drainage. For the soil shear strength, an increase of water content due to biomass amendment increases the soil bulk density, which in turn increases the lateral earth pressure on the walls of underground cultural relics. Biomass amendment reduces the possibility for structure buoyancy and increased the stability of the arch voucher. Further study should be conducted with other types of soils and the associated calculation equations should be modified according to the soil types.

Acknowledgments. The study was supported by the National Key R&D Program of China (No. 2019YFC1520700), and Guangxi Key Science and Technology Innovation Base on Karst Dynamics (No. KDL&Guangxi 202008).

REFERENCES

[1] Al-Taey, D. K. (2018): The role of GA and organic matter to reduce the salinity effect on growth and leaves contents of elements and antioxidant in pepper. – Plant Archive 18(1): 479-488.

[2] Buss, W., Graham, M. C., Shepherd, J. G., Mašek, O. (2016): Suitability of marginal biomass-derived biochars for soil amendment. – Science of the Total Environment 547: 314-322.

[3] Cao, J., Mai, B., Chen, H., Li, Y., Wang, J. (2021): Geotechnical investigation for the groundwater damage analysis of the Shahe ancient bridge site in Xi'an, China. – Research Square. DOI: 10.21203/rs.3.rs-141276/v1.

[4] Chao, N. C., Jhe-Wei, L., Weicheng, L. (2018): Gravity effect on consolidation in poroelastic soils under saturated and unsaturated conditions. – Journal of Hydrology 566: 99-108.

[5] Chen, Z., Zhang, P., Li, J. (2007): Development and utilization of underground space for the protection of relics in the Yang Emperor Mausoleum of the Han Dynasty. – Frontiers of Architecture & Civil Engineering in China. 1(2): 229-233.

[6] Cokca, E., Erol, O., Armangil, F. (2004): Effects of compaction moisture content on the shear strength of an unsaturated clay. – Geotechnical & Geological Engineering 22(2): 285-297.

[7] Dessureault-Rompré, J., Libbrecht, C., Caron, J. (2020): Biomass crops as a soil amendment in cultivated histosols: can we reach carbon equilibrium? – Soil Science Society of America Journal 84(2): 597-608.

[8] Ding, X., Yuan, Y., Liang, Y., Li, L., Han, X. (2014): Impact of long-term application of manure, crop residue, and mineral fertilizer on organic carbon pools and crop yields in a mollisol. – Journal of Soils & Sediments 14(5): 854-859.

[9] Fredlund, D. G., Xing, A., Fredlund, M., Barbour, S. L. (1995): The relationship of the unsaturated soil shear strength to the soil-water characteristic curve. – Canadian Geotechnical Journal 32(3): 440-448.

[10] Fu, Y., Chen, Z., Zhou, S., Wei, S. (2020): Comparative study of the materials and lacquering techniques of the lacquer objects from Warring States Period China. – Journal of Archaeological Science 144: 105060.

[11] García-Orenes, F., Guerrero, C., Mataix-Solera, J., Navarro-Pedreño, J., Gómez, I., Mataix-Beneyto, J. (2005): Factors controlling the aggregate stability and bulk density in two different degraded soils amended with biosolids. – Soil and Tillage Research 82(1): 65-76.

http://www.aloki.hu ● ISSN 1589 1623 (Print) ● ISSN 1785 0037 (Online)
DOI: http://dx.doi.org/10.15666/aeer/2001_801814

[12] Gebhardt, M., Fehmi, J. S., Rasmussen, C., Gallery, R. E. (2017): Soil amendments alter plant biomass and soil microbial activity in a semi-desert grassland. – Plant and soil 419(1): 53-70.
[13] Guo, H., Huang, H. (2002): Damage problems in the protection of cultural relics. – Sciences of Conservation and Archaeology 14(1): 56-62.
[14] Haynes, R. J., Naidu, R. (1998): Influence of lime, fertilizer and manure applications on soil organic matter content and soil physical conditions: a review. – Nutrient Cycling in Agroecosystems 51(2): 123-137.
[15] Kemper, W., Rosenau, R. (1984): Soil cohesion as affected by time and water content. – Soil Science Society of America Journal 48(5): 1001-1006.
[16] Kemper, W., Rosenau, R., Dexter, A. (1987): Cohesion development in disrupted soils as affected by clay and organic matter content and temperature. – Soil Science Society of America Journal 51(4): 860-867.
[17] Kholodov, V., Yaroslavtseva, N., Farkhodov, Y. R., Belobrov, V., Yudin, S., Aydiev, A. Y., Lazarev, V., Frid, A. (2019): Changes in the ratio of aggregate fractions in humus horizons of chernozems in response to the type of their use. – Eurasian Soil Science 52(2): 162-170.
[18] Li, X., Yin, X., Wang, Y. (2016): Diversity and ecology of vascular plants established on the extant world-longest ancient city wall of Nanjing, China. – Urban Forestry & Urban Greening 18: 41-52.
[19] Li, J., Zhu, G., Wang, J., Zeng, P. (2021): Application of active anti-floating in underground structure based on automatic drainage system. – IOP Conference Series: Earth and Environmental Science 636(1): 012034.
[20] Liu, S., Zhang, Y., Zong, Y., Hu, Z., Wu, S., Zhou, J., Jin, Y., Zou, J. (2016): Response of soil carbon dioxide fluxes, soil organic carbon and microbial biomass carbon to biochar amendment: a meta-analysis. – GCB Bioenergy 8(2): 392-406.
[21] Liu, Y., Miao, H., Chang, X., Wu, G. (2019a): Higher species diversity improves soil water infiltration capacity by increasing soil organic matter content in semiarid grasslands. – Land Degradation & Development. 30(13): 1599-1606.
[22] Liu, Y., He, L., Jiang, Y., Sun, M., Chen, E., Lee, F.-H. (2019b): Effect of in situ water content variation on the spatial variation of strength of deep cement-mixed clay. – Geotechnique 69(5): 391-405.
[23] Liu, Z., Liu, J., Li, X., Fang, J. (2019c): Experimental study on the volume and strength change of an unsaturated silty clay upon freezing. – Cold Regions Science and Technology 157: 1-12.
[24] Ma, Q. W., Zhu, M. M. (2016): Discussion on a new technique for controlling the seepage damage to an ancient tomb. – Electronic Journal of Geotechnical Engineering 21: 5319-5328.
[25] Oades, J. M. (1984): Soil organic matter and structural stability: mechanisms and implications for management. – Plant and Soil 76(1): 319-337.
[26] Quaye, A. K., Volk, T. A., Hafner, S., Leopold, D. J., Schirmer, C. (2011): Impacts of paper sludge and manure on soil and biomass production of willow. – Biomass and Bioenergy 35(7): 2796-2806.
[27] Ringelberg, D., Cole, D., Foley, K., Ruidaz-Santiago, C., Reynolds, C. (2014): Compressive strength of soils amended with a bacterial succinoglycan: effects of soluble salts and organic matter. – Canadian Geotechnical Journal 51(7): 747-757.
[28] Shi, Z., Yu, T., Shi, M. (2020): Investigate the layout and age of a large-scale mausoleum in Hangzhou, China using combined geophysical technologies and archaeological documents. – Archaeological Prospection. 27(4): 301-313.
[29] Torn, M. S., Trumbore, S. E., Chadwick, O. A., Vitousek, P. M., Hendricks, D. M. (1997): Mineral control of soil organic carbon storage and turnover. – Nature 389(6647): 170-173.

http://www.aloki.hu ● ISSN 1589 1623 (Print) ● ISSN 1785 0037 (Online)
DOI: http://dx.doi.org/10.15666/aeer/2001_801814

[30] Tremblay, H., Duchesne, J., Locat, J., Leroueil, S. (2002): Influence of the nature of organic compounds on fine soil stabilization with cement. – Canadian Geotechnical Journal 39(3): 535-546.
[31] Xiong, Z. (2014): The Hepu Han tombs and the maritime Silk Road of the Han Dynasty. – Antiquity 88(342): 1229-1243.
[32] Ying, Q., Li, H., Yang, X., Huang, H., Xie, Y. (2015): Experimental dissolution of lead from bronze vessels and the lead content of human bones from Western Zhou dynasty tombs in Hengshui, Shanxi, China. – Journal of Archaeological Science 64: 22-29.
[33] Yuan, F., Gao, J., Wu, J. (2016): Nanjing - an ancient city rising in transitional China. – Cities 50: 82-92.
[34] Zhang, B., Zhao, Q., Horn, R., Baumgartl, T. (2001): Shear strength of surface soil as affected by soil bulk density and soil water content. – Soil and Tillage Research 59(3-4): 97-106.
[35] Zhang, J., Huang, M., Petropoulos, E., Song, L., He, S. (2020): Animal manure functions as soil amendment for urban green space in the Loess Plateau. – Applied Ecology and Environmental Research 18(3): 3861-3872.

http://www.aloki.hu ● ISSN 1589 1623 (Print) ● ISSN 1785 0037 (Online)
DOI: http://dx.doi.org/10.15666/aeer/2001_801814

OPTIMIZING APPLICATION RATE OF WINERY SOLID WASTE COMPOST FOR IMPROVING THE PERFORMANCE OF MAIZE (*ZEA MAYS* L.) GROWN ON LUVISOL AND CAMBISOL

MASOWA, M. M.[1*] – KUTU, F. R.[2] – BABALOLA, O. O.[1] – MULIDZI, A. R.[3]

[1]*Food Security and Safety Niche Area Research Group, Faculty of Natural and Agricultural Sciences, North-West University, Private Bag X2046, Mmabatho 2745, South Africa*
(e-mail: masowmm@gmail.com; olubukola.babalola@nwu.ac.za
phone: +27-18-389-2568)

[2]*School of Agricultural Sciences, University of Mpumalanga, Private Bag X11283, Mbombela 1200, South Africa*
(e-mail: funso.kutu@ump.ac.za; phone: +27-13-002-0218)

[3]*Agricultural Research Council - Infruitec/Nietvoorbij, Private Bag X5026, Stellenbosch 7599, South Africa*
(e-mail: mulidzir@arc.agric.za; phone: +27-21-809-3070)

[*]*Corresponding author*
e-mail: masowmm@gmail.com; phone: +27-18-389-2568

(Received 17th Sep 2021; accepted 23rd Nov 2021)

Abstract. The use of winery solid waste compost (WSW) on croplands represents an important strategy for WSW management. However, the full benefits of the use of this compost as an organic fertilizer can be derived with accurate recommendations. Hence, a 4×7×2 factorial experiment was conducted under tunnel-house conditions to determine the optimum rates of the WSW compost using quadratic and linear-plus-plateau models. The trial comprised of four WSW compost types applied at various rates (0, 5, 10, 20, and 40 t/ha) on two soils (Luvisol and Cambisol). Generally, stem girth, plant height, leaf number per plant, dry matter yield (DMY), and relative agronomic effectiveness (RAE) increased with higher compost rates. The Principal Component Analysis showed that there is a high correlation between the 20 t/ha rate of WSW compost and DMY. The models had comparable R^2 values. Optimum rates predicted across the two soils by the linear-plus-plateau model ranged from 11.78 to 26.03 t/ha but from 28.16 to 39.53 t/ha with the quadratic model. Higher compost rate predicted by the quadratic model than the linear-plus plateau model resulted in a marginal increase in DMY with few exceptions. Consequently, the linear-plus-plateau model may be a preferred model when predicting the optimum WSW compost rate for maize. The results showed that the WSW compost at a rate of 20 t/ha can be recommended for maize.
Keywords: *dry matter yield, linear-plus-plateau model, maize, organic fertilizer rate, quadratic model*

Introduction

The declining soil fertility and productivity are part of the major problems contributing to food and nutrition insecurities in South Africa and other sub-Saharan African (SSA) countries. Nearly 40% of soils in these countries contain low nutrient capital reserves, less than 10% weatherable minerals, and 25% suffer from aluminium toxicity while 18% have a high leaching potential (Tully et al., 2015). For instance, a reported estimated net annual soil nutrients loss of 7629900 metric tons in SSA and 110900 metric tons in South Africa were reported during 1993-1995 (Henao and Baanante, 1999). Hence, nutrient depletion and organic matter decline in soils in these countries have been attributed to continuous cultivation, inappropriate farming methods, and farmers' poor management practices that include none to low or sub-optimal fertilizer uses (Onduru et al., 2008; Kutu, 2012).

http://www.aloki.hu ● ISSN 1589 1623 (Print) ● ISSN 1785 0037 (Online)
DOI: http://dx.doi.org/10.15666/aeer/2001_815828

Amelioration of soil nutrients depletion is swiftly achieved with the application of inorganic fertilizers. However, limited access and high costs of inorganic fertilizers are some of the major constraints restricting the reliance on their use by smallholder farmers in SSA (Onduru et al., 2008; Kihara et al., 2016). The integrated use of chemical and organic sources such as manures and composts is widely recognized as a way of sustainably increasing crop productivity (Baghdadi et al., 2018). This strategy improves soil organic matter, soil structure, water-holding capacity, nutrient cycling and cation exchange capacity, and the soil's biological activity (Mahmood et al., 2017). Compost application on soil may also help in disease and pest control (Erhart and Hartl, 2010).

Wine production often results in the generation of huge amounts of by-products mainly consisting of organic wastes, wastewater, greenhouse gas emissions, and inorganic residues (Teixeira et al., 2014). The organic wastes produced during winemaking include grape pomace (seeds, pulp and skins, grape stems, and grape leaves) while the inorganic waste components include diatomaceous earth, bentonite clay, and perlite (Teixeira et al., 2014). The resulting composting products of these wastes have been reported to possess great potential for use as nutrients and organic matter sources (García-Martínez, 2009; Masowa et al., 2018). Several studies have indicated the positive effects of the application of composted winery and distillery waste on various crops (García-Martínez, 2009; Masowa et al., 2016, 2021; Raquel et al., 2018). However, the determination of optimum application rates of WSW compost for judicious use on croplands has not gained much attention in previous studies. The application of adequate amounts of nutrients is a key aspect for improving crop production and optimizing yield (Alonso et al., 2016) since optimal nutrients uptake only takes place when nutrients are adequately provided in balanced quantities to satisfy plants' needs (Sala et al., 2015).

Mathematical models have been used to describe the response of crops to fertilization (Bullock and Bullock, 1994; Mahd, 2008). However, the ability of a model to account for the gap between applied nutrient and plant nutrient demand, and to accurately predict the optimum nutrient required is often affected by factors such as temperature, rainfall (timing, intensity and amount), and several other interconnected variables (Morris et al., 2018) including farmers' management practices. Cerrato and Blackmer (1990) reported that the selection of one model over the others deserves more attention than it has received in the past particularly when making decisions concerning amounts of fertilizer required for profitable crop production. Xia and Yan (2011) reported that the quadratic model as opposed to the exponential and square root models best describes crop yield response to fertilizer rates and gives the optimal fertilizer rates considering environmental and economic effects. Similarly, an earlier study by Bélanger et al. (2000) also revealed that the quadratic model was more appropriate than the exponential and square root model for describing yield and predicting the optimum fertilizer rates in potato. Nevertheless, a report by Marvi (2008) suggests that the quadratic model tends to overestimate crop response if the maximum point on the curve is used as the best fertilization rate. Results of earlier work by Cerratto and Blackmer (1990) suggest that the linear-plateau model tends to overestimate the maize (*Zea mays* L.) yield in the response curve close to the optimum level of N. Several authors have reported that both linear-plus-plateau and quadratic models tend to perform better in cases of yield stagnation (Hafner, 2003; Brisson et al., 2010; Finger, 2010; Michel and Makowski, 2013). Considering the above-mentioned information, this study was initiated to (i) compare the performance of two mathematical models (quadratic and linear-plus-plateau) and (ii) determine the optimum application rate of the WSW compost and their effects on growth and yield of maize.

http://www.aloki.hu ● ISSN 1589 1623 (Print) ● ISSN 1785 0037 (Online)
DOI: http://dx.doi.org/10.15666/aeer/2001_815828

Materials and methods

Description of the study site

A pot experiment was conducted in 2017 (from November to December) under a tunnel-house for 7 weeks at the North-West University Experimental Farm (25°48' S, 25°38' E), Mafikeng, South Africa. The maximum temperature of 28°C in the tunnel-house during the day was maintained using thermostatically activated fans and a wet wall cooling system.

Description of WSW compost production processes and compost analysis

The aerobic-thermophilic production process of WSW compost types and their physico-chemical properties have been presented in an earlier study (Masowa et al., 2018). Briefly, the WSW compost types produced comprised inoculated compost with an initial heap height (hereafter referred to as pile size) of 1 m (INC1), inoculated compost with pile size of 1.5 m (INC1.5), uninoculated compost with pile size of 1 m (UNC1), and uninoculated compost with pile size of 1.5 m (UNC1.5). The compost piles were prepared by mixing the filter materials and waste plant materials at a ratio of 40:60 on a percent volume basis. The effective microorganisms (EM) inoculant was used for microbial inoculation. The pH(KCl) values of the composts ranged from 9.68 to 9.76 while the electrical conductivity varied between 9.03 and 10.23 dS/m. The measured total contents of N, P, K, and Na in composts ranged from 1.23 to 1.80%, 4.87 to 6.04 g/kg, 2.10 to 2.56%, and 5.03 to 6.20 g/kg, respectively.

Experimental design, treatments and procedure

The pot experiment (*Figure 1*) comprised of a 4×7×2 factorial experiment fitted in a completely randomized design with the treatment factors comprising of four WSW compost types, each applied at seven rates (0, 5, 10, 20, 40, 80, and 100 t/ha dry weight) in two different soils. Each treatment combination was replicated four times. Surface soils (0-15 cm) were collected from the cropland of the North-West University Experimental Farm located in Mafikeng (25°48' S, 25°38' E) and from the farmer's field in Ventersdorp (26.2774°S, 26.7614°E) both located in the North-West Province of South Africa. The soil from Mafikeng is classified as Ferric Luvisol while the soil from Ventersdorp soil is classified as Ferralic Cambisol (World Reference Base for Soil Resources, 2015). For the purposes of this paper, the soils from Mafikeng and Ventersdorp will hereafter be referred to as Luvisol and Cambisol, respectively. A surface soil sample was collected for the determination of physical and chemical properties prior to the commencement of the trial. The results showed that Luvisol had 5.1% clay (hydrometer method), 0.42% organic C (Walkley-Black method), pH (H_2O) of 6.77, 6.95 mg/kg total mineral-N (0.5 M K_2SO_4), 80 mg/kg P (Bray-1), 235 mg/kg exchangeable K, 10 mg/kg exchangeable Na, 555 mg/kg Ca and 293 mg/kg Mg (1 N NH_4OAc). A sample of Cambisol test values of 6.3% clay, 1.13% organic C, 6.06 pH (H_2O), 19.35 mg/kg total mineral-N, 75 mg/kg Bray-1 P, 168 mg/kg exchangeable K, exchangeable Na content of 5 mg/kg, and exchangeable Ca and Mg contents of 648 and 228 mg/kg, respectively (Non-Affiliated Soil Analyses Work Committee, 1990).

The air-dried soils were passed through a 6 mm sieve to remove stones and plant roots. Following this, the plastic pots (30 cm diameter) were filled with 12 kg of soil. Each compost type was mixed with the soil based on the calculated weight of soil used per pot and an assumption of the weight of soil (2 million kg) per hectare furrow slice (Masowa

http://www.aloki.hu ● ISSN 1589 1623 (Print) ● ISSN 1785 0037 (Online)
DOI: http://dx.doi.org/10.15666/aeer/2001_815828

et al., 2016). The holes at the bottom of each pot were blocked using cotton wool in order to prevent soil losses. Pots were watered with municipal water, thereafter allowed to equilibrate for 5 hours prior to sowing three seeds of maize (cv. WE6206B) in each pot. Maize seedlings in each pot were thinned down to two seedlings after one week of seedling emergence. The pots received uniform irrigation throughout the period of plant growth. The trial was terminated at 7 weeks after planting by harvesting plant shoots. The seedlings in pots treated with composts at 80 and 100 t/ha died after showing signs of salt stress one week after emergence. Consequently, soil samples were collected from each pot and analyzed for exchangeable soil-Na content. The soil test results revealed that the application of WSW compost at 80 and 100 t/ha significantly increased the exchangeable soil-Na content by up to 175%, which may be the reason for the death of the seedlings (data not shown).

Figure 1. *An experimental layout in completely randomized design for the pot experiment of maize cultivation*

Data collection

The morphological and chlorophyll content data were collected prior to harvesting of shoots. Chlorophyll content was measured around the mid-point of a healthy and longest leaf using a portable CCM-200 *plus* chlorophyll content meter (Opti-Sciences Inc, USA). The morphological data collected include the number of functional leaves per plant, plant height, and stem diameter. The functional leaves per plant were counted manually. Plant height was measured using a measuring tape from the soil surface up to the tip of the highest leaf (Ayub et al., 2012). The stem diameter was measured 10 cm from the soil surface using a Vernier caliper and thereafter converted to girth using the *Equation 1* (Ukonze et al., 2016):

$$\text{Stem girth} = \text{stem diameter} \times \pi\ (pi) \qquad \text{(Eq.1)}$$

Maize shoots harvested from the soil surface using a sharp knife were washed with deionized water, then oven-dried at 70°C to constant weight for dry matter yield (DMY) determination. The computation of the relative agronomic effectiveness (RAE) followed the equation adapted from Law-Ogbomo et al. (2012):

$$\text{RAE}\ (\%) = (\text{DMY}_T - \text{DMY}_C)/(\text{DMY}_C) \qquad \text{(Eq.2)}$$

where: DMY_T = maize dry matter yield from compost treated pots, DMY_C = maize dry matter yield from control pots.

http://www.aloki.hu ● ISSN 1589 1623 (Print) ● ISSN 1785 0037 (Online)
DOI: http://dx.doi.org/10.15666/aeer/2001_815828

Data analysis

Data on plant growth, chlorophyll content and DMY were subjected to analysis of variance (ANOVA) using the statistical analysis system (SAS) software 9.4. The significant differences among treatment means were detected by the Duncan Multiple Range test at $p<0.05$. The analysis of the correlations between maize growth parameters and dry matter yield was done using the IBM SPSS Statistics software (Version 23). Principal component analysis (PCA) (XLSTAT 2021 statistical software) was aimed at revealing the relation among the examined compost rates and maize growth parameters as well as DMY. The communalities values of the variables were calculated using the IBM SPSS Statistics software (Version 23). Bartlett's test of sphericity was done at 5% level of significance (Jordaan et al., 2015).

Linear-plus-plateau and quadratic polynomial models were fitted to the DMY data using the NLIN and PROC REG procedures of SAS software 10.0, respectively, to determine the optimum application rate and DMY (Cerrato and Blackmer, 1990; Moswatsi et al., 2013). The quadratic polynomial model is defined by equation 3 below:

$$Y = a + bX + cX^2 \quad \text{(Eq.3)}$$

where: Y = dry matter yield (g/pot); X = application rate (t/ha); a (intercept); b (linear coefficient); and c (quadratic coefficient) (Moswatsi et al., 2013).

The linear-plus-plateau is defined by equation 4 below:

$$Y = a + bX \quad \text{(Eq.4)}$$

If X is less than C

$$Y = P \quad \text{(Eq.5)}$$

if X is greater and equal to C
where: Y = dry matter yield (g/pot); X = application rate (t/ha); a (intercept); b (linear coefficient); b (linear coefficient), C (critical rate of fertilization, which occurs at the intersection of the linear response and the plateau lines), and P (plateau yield) are constants obtained by fitting the model to the data (Cerrato and Blackmer, 1990).

Results

Growth attributes, leaf chlorophyll content, DMY and RAE

The ANOVA showed that variation of WSW composts with microbial inoculation and pile size did not induce significant effects on maize growth attributes, leaf chlorophyll content, DMY and RAE. The measured plant growth attributes and DMY were significantly influenced by the soil type, compost type and application rate while chlorophyll content and RAE were influenced by the compost type and application rate (*Table 1*). Plants grown on Luvisol had a higher mean number of functional leaves per plant but had thicker stems, taller stalks and higher DMY when grown on Cambisol. The different composts significantly improved the number of functional leaves per plant, chlorophyll content, stem girth, plant height and DMY relative to the control. In general,

http://www.aloki.hu ● ISSN 1589 1623 (Print) ● ISSN 1785 0037 (Online)
DOI: http://dx.doi.org/10.15666/aeer/2001_815828

chlorophyll content, mean number of functional leaves per plant, plant height, DMY and RAE increased with increasing compost rates.

Table 1. *Effects of soil type, compost type and compost application rate on maize growth attributes, dry matter yield (DMY) and relative agronomic effectiveness (RAE)*

Treatments	Number of functional leaves per plant	Leaf chlorophyll content (CCI)	Stem girth (mm)	Plant height (cm)	DMY (g/pot)	RAE (%)
Soil type						
Luvisol	11.63^{a}	5.22^{a}	58^{b}	117^{b}	71^{b}	97^{a}
Cambisol	10.00^{b}	5.90^{a}	64^{a}	135^{a}	104^{a}	58^{b}
p-value	<0.001	0.069	<0.001	<0.001	<0.001	<0.001
Compost type						
INC1	10.92^{a}	5.73^{a}	62^{a}	128^{a}	92^{a}	82^{a}
UNC1	10.96^{a}	5.48^{a}	61^{a}	128^{a}	91^{a}	81^{a}
INC1.5	11.04^{a}	5.81^{a}	61^{a}	127^{a}	88^{a}	74^{a}
UNC1.5	10.87^{a}	5.08^{a}	61^{a}	126^{a}	88^{a}	73^{a}
Control	8.68^{b}	3.5^{b}	53^{b}	104^{b}	53^{b}	-
p-value	<0.001	<0.001	<0.001	<0.001	<0.001	0.462
Compost rate (t/ha)						
0	8.68^{e}	3.50^{c}	53^{c}	104^{d}	53^{d}	-
5	9.82^{d}	4.02^{c}	60^{b}	119^{c}	75^{c}	44^{c}
10	10.45^{c}	4.22^{c}	60^{b}	121^{c}	82^{b}	62^{b}
20	11.5^{b}	5.53^{b}	63^{a}	131^{b}	99^{a}	98^{a}
40	12.03^{a}	8.33^{a}	64^{a}	140^{a}	103^{a}	106^{a}
p-value	<0.001	<0.001	<0.001	<0.001	<0.001	<0.001

Means with the same letter(s) within a column and treatment are not significantly different at the 5% probability level

The interaction effect of soil type and application rate significantly influenced the number of functional leaves per plant (*Figure 2A*) and DMY (*Figure 2B*). The highest value of the mean number of functional leaves per plant was recorded from 40 t/ha rate (12.88) under the Cambisol, while the lowest value was obtained from the untreated control (7.75) under the Luvisol. The DMY given by the 20 and 40 t/ha rates in each soil type were statistically at par and higher than that given by the remaining rates.

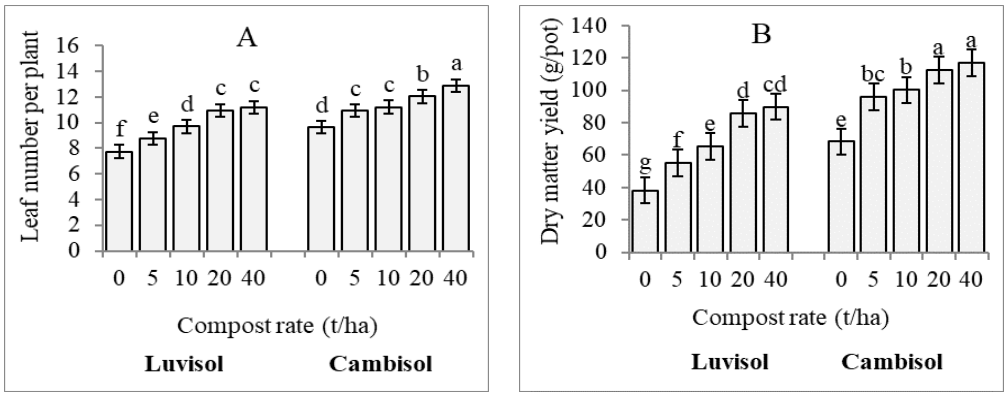

Figure 2. *Interaction effect of soil type and compost rate on the (A) leaf number per plant ($p < 0.001$) and (B) dry matter yield ($p = 0.011$). Means with the same letter(s) are not significantly different. Bars indicate the standard error of the treatment mean*

http://www.aloki.hu ● ISSN 1589 1623 (Print) ● ISSN 1785 0037 (Online)
DOI: http://dx.doi.org/10.15666/aeer/2001_815828

Significant interaction effect of soil type, compost type and compost rate on the number of functional leaves per plant and RAE was observed (*Table 2*). The mean number of functional leaves per plant ranged from 7.75 (untreated control) to 11.62 (INC1 at 40 t/ha) under the Luvisol, and from 9.62 (untreated control) to 13 (UNC1 and INC1.5 applied at 40 t/ha) under the Cambisol. In most cases, the 20 and 40 t/ha rates gave significantly higher mean number of functional leaves per plant than the 5 and 10 t/ha rates. However, the 20 and 40 t/ha rates were statistically at par in their effects on the number of functional leaves per plant. Except for INC1 at 5 t/ha under the Luvisol, the remaining treatments gave significantly higher values of the mean number of functional leaves per plant in comparison with the control of each soil type. The RAE values ranged from 34% with INC1 (5 t/ha) to 165% with UNC1 (40 t/ha) under the Luvisol, and from 34% with UNC1.5 (5 t/ha) to 80% with INC1.5 (40 t/ha) under the Cambisol. The RAE values obtained from the 20 t/ha rate were significantly higher than those recorded at 5 and 10 t/ha under Luvisol. Similar results were recorded from the 40 t/ha rate except under the INC1 treatment in which the 10 t/ha rate was statistically at par with it under the Luvisol. An increase in the application rate of each compost type from 20 to 40 t/ha within each soil type did not result in a significant difference in the RAE value.

Table 2. *Interaction effect of soil type, compost type and compost rate on the number of functional leaves per plant and relative agronomic effectiveness*

Treatments	Application rate (t/ha)	Number of functional leaves per plant		Relative agronomic effectiveness (%)	
		Luvisol	Cambisol	Luvisol	Cambisol
INC1	5	8.00^{hi}	11.00^{de}	34^{f}	50^{ef}
	10	9.87^{f}	11.00^{de}	81^{de}	53^{ef}
	20	11.12^{de}	12.00^{bc}	142^{abc}	67^{ef}
	40	11.62^{cd}	12.75^{ab}	153^{ab}	74^{def}
UNC1	5	8.62^{gh}	11.00^{de}	51^{ef}	43^{ef}
	10	9.75^{f}	11.37^{cde}	72^{def}	52^{ef}
	20	10.75^{e}	12.00^{bc}	127^{abc}	67^{ef}
	40	11.25^{cde}	13.00^{a}	165^{a}	68^{ef}
INC1.5	5	9.25^{fg}	10.75^{e}	56^{ef}	40^{ef}
	10	9.62^{f}	11.25^{cde}	70^{def}	42^{ef}
	20	11.00^{de}	12.50^{ab}	124^{bc}	67^{ef}
	40	11.00^{de}	13.00^{a}	111^{cd}	80^{ed}
UNC1.5	5	9.12^{fg}	10.87^{de}	46^{ef}	34^{f}
	10	9.50^{f}	11.25^{cde}	78^{de}	46^{ef}
	20	11.00^{de}	11.62^{cd}	119^{bc}	69^{ef}
	40	10.87^{de}	12.75^{ab}	122^{bc}	71^{def}
Control	0	7.75^{i}	9.62^{f}	-	-
p-value		0.032		<0.001	
CV (%)		4.55		32.75	

Means with the same letter(s) for each variable are not significantly different at the 5% probability level; CV = coefficient of variance

PCA and correlations among the growth parameters and DMY

The correlations among the maize growth parameters, chlorophyll content and DMY were highly significant ($p<0.01$; *Table 3*). The results of the PCA show that all the variables that were included in the factor analysis had Kaiser-Meyer-Olkin values ranging from 0.793 to 0.863, and were above the acceptable value of 0.500. The communalities

http://www.aloki.hu ● ISSN 1589 1623 (Print) ● ISSN 1785 0037 (Online)
DOI: http://dx.doi.org/10.15666/aeer/2001_815828

values of the variables ranged from 0.785 to 0.978, and were higher than the acceptable value of 0.300. Bartlett's test of sphericity was also significant ($p<0.0001$). Given these overall indicators, factor analysis was suitable to increase the interpretability of agronomic data and for selecting a suitable compost rate for improving maize dry matter yield. The PC1 accounted for 90.95%, whilst the PC2 accounted for 6.24% of the variation (*Figure 3*). The agronomic parameters were loaded on the PC1. The 20 t/ha rate loaded the number of functional leaves per plant, stem girth and DMY, while the 40 t/ha loaded plant height and leaf chlorophyll content.

Table 3. *Correlation between maize growth parameters, leaf chlorophyll content, and dry matter yield in Luvisol and Cambisol*

Parameters	Leaf number per plant	Leaf chlorophyll content	Stem girth	Plant height	Dry matter yield
	Luvisol				
Leaf number per plant	1				
Leaf chlorophyll content	0.630**	1			
Stem girth	0.639**	0.467**	1		
Plant height	0.907**	0.742**	0.649**	1	
Dry matter yield	0.937**	0.706**	0.630**	0.942**	1
	Cambisol				
Leaf number per plant	1				
Leaf chlorophyll content	0.899**	1			
Stem girth	0.839**	0.720**	1		
Plant height	0.941**	0.911**	0.865**	1	
Dry matter yield	0.890**	0.746**	0.924**	0.911**	1

**Correlation was significant at the 0.01 level

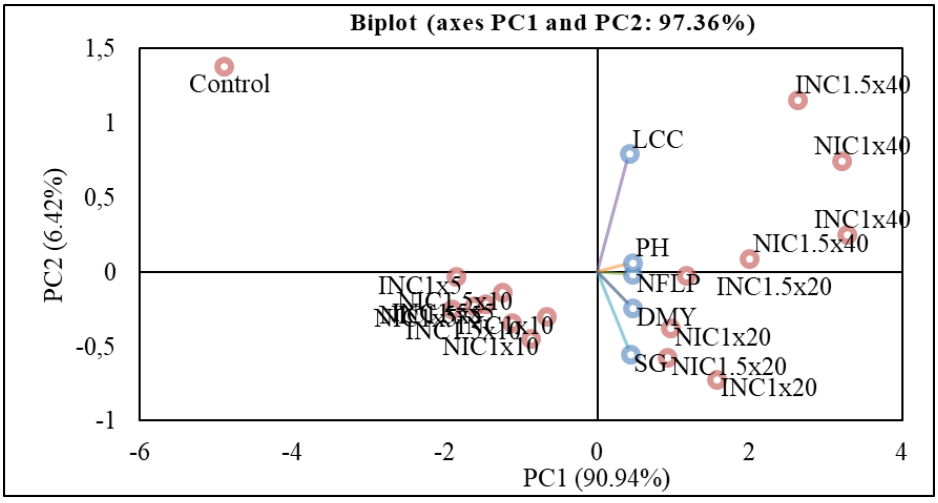

Figure 3. *Principal component biplot showing the variations between the number of functional leaves per plant (NFLP), leaf chlorophyll content (LCC), stem girth (SG), plant height (PH), dry matter yield (DMY) in response to compost type and compost rate across the soil type. (INC1x5, INC1x10, INC1x20 and INC1x40 denote INC1 applied at 5, 10, 20 and 40 t/ha, respectively; UNC1x5, UNC1x10, UNC1x20 and UNC1x40 denote UNC1 applied at 5, 10, 20 and 40 t/ha, respectively)*

http://www.aloki.hu ● ISSN 1589 1623 (Print) ● ISSN 1785 0037 (Online)
DOI: http://dx.doi.org/10.15666/aeer/2001_815828

Optimum compost application rate and dry matter yield

The quadratic model predicted higher optimum rates for each compost type as compared to the linear-plus-plateau model but with DMY that was nearly similar to those predicted by the linear-plus-plateau model (*Table 4*). The optimum rates predicted by the linear-plus-plateau model ranged from 11.78 to 26.03 t/ha while the predicted rates by the quadratic model ranged from 28.16 to 39.53 t/ha. In general, greater R^2 values were obtained from the relationship between predicted optimum application rate and dry matter yield under Luvisol compared to the Cambisol. Nevertheless, both models gave significant R^2 values that were either equal or nearly equal for each compost type.

Table 4. *Predicted compost application rates and dry matter yield*

Treatments	Linear-plus-plateau model			Quadratic model		
	Application rate (t/ha)	Dry matter yield (g/pot)	R^2	Application rate (t/ha)	Dry matter yield (g/pot)	R^2
Luvisol						
INC1	21.34	95.41	0.93***	32.96	98.69	0.93***
UNC1	26.03	99.74	0.92***	39.53	99.69	0.92***
INC1.5	16.24	81.96	0.78***	28.35	87.60	0.79***
UNC1.5	20.06	84.53	0.79***	30.78	88.87	0.80***
Cambisol						
INC1	11.78	115.00	0.64**	29.29	122.69	0.62*
UNC1	12.00	112.97	0.76***	28.16	120.81	0.74***
INC1.5	23.18	120.63	0.71***	33.52	121.90	0.74***
UNC1.5	14.23	114.69	0.83***	29.96	121.07	0.83***

***significant at p<0.0001; **significant at p=0.0002; *significant at p=0.0003

Discussion

The positive results on the number of functional leaves per plant, stem girth, plant height, chlorophyll content, and DMY following application of WSW compost soil can be attributed to the soil ameliorative effects of compost. Compost or organic wastes improve the soil structure, water retention, cation exchange capacity, and air content of the soil, microbiological activity (Demir and Gülser, 2015), and increase plant nutrients, particularly N, P (Tambone et al., 2007) and K (Kabil et al., 2015). The ability of WSW compost to release plant-available N and K in the soil had been reported through a laboratory incubation experiment (Kutu and Masowa, 2018). Hence, the general increase in the measured growth parameters following an increase in the compost rate may be attributed to the increased plant availability N from the WSW compost. Masowa et al. (2016) reported a similar finding on the maize growth parameters and DMY. The observation that the various compost types and application rates exerted similar effects on maize growth parameters and DMY across both soil types suggests that EM inoculation and pile size may not necessarily exert influence on the agronomic potential of WSW compost. This may be attributed to the non-significant effects exerted by EM inoculation and pile size on the quality parameters of WSW compost as reported by Masowa et al. (2018).

http://www.aloki.hu ● ISSN 1589 1623 (Print) ● ISSN 1785 0037 (Online)
DOI: http://dx.doi.org/10.15666/aeer/2001_815828

It is evident that the higher available N in the Cambisol resulted in higher stem girth, plant height, and DMY than in the Luvisol across the compost types and application rates. However, the higher available N in Cambisol did not translate to a higher number of functional leaves per plant and chlorophyll content in the Luvisol. The general and significant increase in the measured growth parameters, chlorophyll content, and DMY given by 20 and 40 t/ha rates as compared to the 5 and 10 t/ha rates may be attributed to the increase in the availability of soil nutrients under these rates. Adejumo et al. (2010) also reported the highest maize plant height, DMY, leaf area, and grain yield at a higher dose (40 t/ha) of municipal solid waste compost. The recorded significant and positive correlation of DMY with the measured growth parameters affirms the DMY as one of the key indicators of plant growth (Laekemariam and Gidago, 2013). Carpici and Celik (2010) reported a positive and significant correlation between maize dry forage yield and plant height. Kumar and Singh (2004) similarly reported a significant and positive correlation of maize dry forage yield per plant with plant height, number of leaves per plant, and stem diameter.

Except for the UNC1 in Luvisol, quantitatively higher optimum compost rates predicted in both soils by the quadratic model were only associated with marginal yield increases compared to yield predicted by the linear-plus-plateau model. The use of the quadratic model has been reported to lead to overestimation of fertilizer recommendations derived from crop responses to fertilizer (Bullock and Bullock, 1994; Hochmuth et al., 2011) particularly when the maximum point on the curve is taken as the best fertilization rate (Mahd, 2008). However, both models gave R^2 values that were either equal or nearly equal for both composts. Hence, the use of R^2 statistics to select the best model for predicting the optimum rate and DMY may constitute a limitation in this study. This finding also confirms that fitting the same dataset in both models can give comparable R^2 values, but different optimal application rates of fertilizer, which is in agreement with an earlier report by Xia and Yan (2011). This further affirms the non-reliability of the R^2 value as an absolute indicator for predicting the optimum fertilizer rate since it varies with the chosen model (Bachmaier and Gandorfer, 2012). The more than 90% for the R^2 values in the Luvisol suggests that the models described the data quite well under INC1 and UNC1 treatments. The recorded high R^2 values in Luvisol than Cambisol indicate that the predicted rates and DMY may be highly influenced by the soil type. Nevertheless, the use of the predicted optimum DMY may be an option for selecting the best model. Therefore, the linear-plus-plateau model is preferable to the quadratic model for predicting optimum WSW compost rate for maize dry matter production. The range of 11.78 to 39.53 t/ha for the predicted optimum rates in both soils was within the range of those used in practice which ranges from 10 to 40 t/ha (fresh weight) (Elherradi et al., 2005). The current predicted optimum rates of the WSW compost types contradict the earlier optimum rate of 87 t/ha predicted by Masowa et al. (2016) for maize grown in sandy soil under greenhouse conditions suggesting that the optimum rates for these composts are not only site-specific but also dependent on soil types and characteristics. Alivelu et al. (2006) recommended the site-specific or season-specific knowledge of crop nutrient requirements and nutrient supply from the soil in order to achieve maximum yields. The 20 t/ha rate gave the DMY and RAE values that were comparable to those obtained from the 40 t/ha rate and it is within the range of the optimum rates predicted by the linear-plus-plateau model. Consequently, the 20 t/ha rate may be a better WSW compost rate when growing maize for dry matter yield. The PCA also indicated that there is a high correlation between the 20 t/ha rate of WSW compost and DMY.

http://www.aloki.hu ● ISSN 1589 1623 (Print) ● ISSN 1785 0037 (Online)
DOI: http://dx.doi.org/10.15666/aeer/2001_815828

Conclusion

The application of compost improved growth and DMY of maize. The measured growth parameters and DMY increased with increasing compost rates. The differences in WSW compost associated with pile size and EM inoculation do not influence the compost agronomic effectiveness because the compost types exerted similar effects on the measured growth parameters. The quadratic model predicted quantitatively higher optimum rates associated with marginally higher DMYs compared with the DMYs predicted by the linear-plus-plateau model. Thus, the linear-plus-plateau model is preferable to the quadratic model for predicting optimum rates of WSW compost for maize dry matter production. The 20 t/ha compost application rate is recommended for optimum DMY of maize. However, follow-up field experiments across several sites with different climate and soils are highly recommended to validate the predicted rates.

Acknowledgements. Authors acknowledge the financial assistance provided by the North-West University, National Research Foundation of South Africa [Grant UID: 108605], and Agricultural Research Council of South Africa.

REFERENCES

[1] Adejumo, S. A., Togun, A. O., Adediran, J. A., Ogundiran, M. B. (2010): Effects of compost application on remediation and the growth of maize planted on lead contaminated soil. – Proc. 19th World Congress of Soil Science, Soil Solutions for a Changing World, Brisbane, Australia, pp. 99-102.

[2] Alivelu, K., Rao, A. S., Sanjay, S., Singh, K. N., Raju, N. S., Madhuri, P. (2006): Prediction of optimal nitrogen application rate of rice based on soil test values. – European Journal of Agronomy 25: 71-73.

[3] Alonso, G. M. M., Díaz, A. P., Espinosa, R. R., González, C. B., Núñez, R. V., Nualles, M. V. (2016): Comparison of two models of response to nitrogen doses in corn and coffee. – Cultivos Tropicales 37: 155-164.

[4] Ayub, M., Nadeem, M. A., Naeem, M., Tahir, M., Tariq, M., Ahmad, W. (2012): Effect of different levels of P and K on growth, forage yield and quality of cluster bean (*Cyamopsis tetragonolobus* L.). – Journal of Animal and Plant Sciences 22: 479-483.

[5] Bachmaier, M., Gandorfer, M. (2012): Estimating uncertainty of economically optimum N fertilizer rates. – International Journal of Agronomy 2012: 1-10.

[6] Baghdadi, A., Halim, R. A., Ghasemzadeh, A., Ramlan, M. F., Sakimin, S. Z. (2018): Impact of organic and inorganic fertilizers on the yield and quality of silage corn intercropped with soybean. – PeerJ 6: e5280. DOI 10.7717/peerj.5280.

[7] Bélanger, G., Walsh, J. R., Richards, J. E., Milburn, P. H., Ziada, N. (2000): Comparison of three statistical methods describing potato yield response to nitrogen fertilizer. – Agronomy Journal 92: 902-908.

[8] Brisson, N. P., Gate, P., Gouache, D., Charmet, G., Oury, F-X., Huard, F. (2010): Why are wheat yields stagnating in Europe? A comprehensive data analysis for France. – Field Crops Research 119: 201-212.

[9] Bullock, D. G., Bullock, D. S. (1994): Quadratic and quadratic-plus-plateau models for predicting optimal nitrogen rate of corn: a comparison. – Agronomy Journal 86: 191-195.

[10] Carpici, E. B., Celik, N. (2010): Determining possible relationships between yield and yield-related components in forage maize (*Zea mays* L.) using correlation and path analyses. – Notulae Botanicae Horti Agrobotanici Cluj-Napoca 38: 280-285.

[11] Cerrato, M. E., Blackmer, A. M. (1990): Comparison of models for describing; corn yield response to nitrogen fertilizer. – Agronomy Journal 82: 138-143.

http://www.aloki.hu ● ISSN 1589 1623 (Print) ● ISSN 1785 0037 (Online)
DOI: http://dx.doi.org/10.15666/aeer/2001_815828

[12] Demir, Z., Gülser, C. (2015): Effects of rice husk compost application on soil quality parameters in tunnel house conditions. – Eurasian Journal of Soil Science 4: 185-190.
[13] Elherradi, E., Soudi, B., Chiang, C., Elkacemi, K. (2005): Evaluation of nitrogen fertilizing value of composted household solid waste under tunnel house conditions. – Agronomy for Sustainable Development 25: 169-175.
[14] Erhart, E., Hartl, W. (2010): Compost use in organic farming. – In: Lichtfouse, E. (ed.) Genetic engineering, biofertilisation, soil quality and organic farming. Sustainable agriculture reviews, Springer, Dordrecht.
[15] Finger, R. (2010): Evidence of slowing yield growth? The example of Swiss cereal yields. – Food Policy 35: 175-18.
[16] García-Martínez, S., Grau, A., Agulló, E., Bustamante, M. A., Paredes, C., Moral, R., Ruiz, J. J. (2009): Use of composts derived from winery wastes in tomato crop. – Communications in Soil Science and Plant Analysis 40: 445-452.
[17] Hafner, S. (2003): Trends in maize, rice, and wheat yields for 188 nations over the past 40 years: a prevalence of linear growth. – Agriculture, Ecosystems & Environment 97: 275-283.
[18] Henao, J., Baanante, C. (1999): Estimating rates of nutrient depletion in soils of agricultural lands of Africa. – Muscle Shoals, Alabama, International Fertilizer Development Center, USA.
[19] Hochmuth, G., Hanlon, E., Overman, A. (2011): Fertilizer experimentation, data analyses, and interpretation for developing fertilization recommendations: examples with vegetable crop research. – University of Florida, IFAS Extension.
[20] Jordaan, H., Bahta, Y. T., Sabastain, G. (2015): Management practices that affect technical efficiency and coping strategies of smallholder maize irrigation farmer in Zimbabwe. – 20th International Farm Management Congress, Laval University, Québec City, Québec, Canada. Vol.1 - Peer Review July 2015 - ISBN 978-92-990062-3-8 - www.ifmaonline.org - Congress Proceedings. pp. 171-179.
[21] Kabil, E. M., Faize, M., Makroum, K., Assobhei, O., Rafrafi, M., Loizidou, M., Aajjane, A. (2015): Effect of compost made with sludge and organic residues on soil and sugar beet crop in Morocco. – Journal of Agronomy 14: 264-271.
[22] Kihara, J., Nziguheba, G., Zingore, S., Coulibaly, A., Esilaba, A., Kabambe, V., Njoroge, S., Palm, C., Huising, J. (2016): Understanding variability in crop response to fertilizer and amendments in sub-Saharan Africa. – Agriculture, Ecosystems & Environment 229: 1-12.
[23] Kumar, S. S., Singh, U. P. (2004): Genetic variability, character association and path analysis of yield and its component traits in forage maize (*Zea mays* L.). – Range Management and Agroforestry 25: 149-153.
[24] Kutu, F. R. (2012): Effect of conservation agriculture management practices on maize productivity and selected soil quality indices under South Africa dryland conditions. – African Journal of Agricultural Research 7: 3839-3846.
[25] Kutu, F. R., Masowa, M. M. (2018): Nitrogen and potassium mineralization from winery solid waste compost in sandy and sandy loam soils. – Archives of Agronomy and Soil Science 64: 1094-1105.
[26] Laekemariam, F., Gidago, G. (2013): Growth and yield response of maize (*Zea mays* L.) to variable rates of compost and inorganic fertilizer integration in Wolaita, Southern Ethiopia. – American Journal of Plant Nutrition and Fertilization Technology 3: 43-52.
[27] Law-Ogbomo, K. E., Osaigbovo, A. U., Ekwueme, I. (2012): Agronomic efficacy of compost manure and NPK fertilizer on some soil chemical properties and maize production in an ultisol environment. – Journal of Applied and Natural Science 4: 172-177.
[28] Mahd, S. P. M. (2008): A comparison of three mathematical models of response to applied nitrogen using spinach. – American-Eurasian Journal of Agricultural & Environmental Sciences 4: 611-616.

http://www.aloki.hu ● ISSN 1589 1623 (Print) ● ISSN 1785 0037 (Online)
DOI: http://dx.doi.org/10.15666/aeer/2001_815828

[29] Mahmood, F., Khan, I., Ashraf, U., Shahzad, T., Hussain, S., Shahid, M., Abid, M., Ullah S. (2017): Effects of organic and inorganic manures on maize and their residual impact on soil physico-chemical properties. – Journal of Soil Science and Plant Nutrition 17: 22-32.
[30] Marvi, S. P. (2008): A comparison of three mathematical models of response to applied nitrogen using lettuce. – World Journal of Agricultural Sciences 4: 699-703.
[31] Masowa, M. M., Kutu, F. R., Shange, P. L., Mulidzi, R., Vanassche, F. M. G. (2016): The effect of winery solid waste compost application on maize growth, biomass yield, and nutrient content under tunnel house conditions. – Archives of Agronomy and Soil Science 62: 1082-1094.
[32] Masowa, M. M., Kutu, F. R., Babalola, O. O., Mulidzi, A. R. (2018): Physico-chemical properties and phyto-toxicity assessment of co-composted winery solid waste with and without effective microorganism inoculation. – Research on Crops 19: 549-559.
[33] Masowa, M. M., Kutu, F. R., Babalola, O. O., Mulidzi, A. R., Dlamini, P. E. (2021): Effects of complementary and sole applications of inorganic fertilizers and winery solid waste compost on maize yield and soil health indices. – Emirates Journal of Food and Agriculture 33: 565-574.
[34] Michel, L., Makowski, D. (2013): Comparison of statistical models for analyzing wheat yield time series. – PloSOne 8: e78615. DOI: org/10.1371/journal.pone.0078615.
[35] Morris, T. F., Murrell, T. S., Beegle, D. B., Camberato, J. J., Ferguson, R. B., Grove, J., Ketterings, Q., Kyveryga, P. M., Laboski, C. A. M. (2018): Strengths and limitations of nitrogen rate recommendations for corn and opportunities for improvement. – Agronomy Journal 110: 1-37.
[36] Moswatsi, M. S., Kutu, F. R., Mafeo, T. P. (2013): Response of cowpea to variable rates and methods of zinc application under different field conditions. – African Crop Science Conference Proceedings 11: 757-762.
[37] Non-Affiliated Soil Analyses Work Committee (1990): Handbook of standard soil testing methods for advisory purposes. – Soil Science Society of South Africa, Pretoria.
[38] Onduru, D. D., Snijders, P., Muchena, F. N., Wouters, B., De Jager, A., Gachimbi, L., Gachini, G. N. (2008): Manure and soil fertility management in sub-humid and semi-arid farming systems of Sub-Saharan Africa: experiences from Kenya. – International Journal of Agricultural Research 3: 166-187.
[39] Raquel, V., Castellanos, M. T., Cartagena, M. C., Ribas, F., Arce, A., Cabello, M. J., Requejo, M. I. (2018): Winery distillery waste compost effect on the performance of melon crop under field conditions. – Scientia Agricola 75: 494-503.
[40] Sala, F., Boldea, M., Rawashdeh, H., Nemet, I. (2015): Mathematical model for determining the optimal doses of mineral fertilizers for wheat crops. – Pakistan Journal of Agricultural Sciences 52: 609-617.
[41] Tambone, F., Genevini, P., Adani, F. (2007): The effects of short-term compost application on soil chemical properties and on nutritional status of maize plant. – Compost Science and Utilization 15: 176-183.
[42] Teixeira, A., Baenas, N., Dominguez-Perles, R., Barros, A., Rosa, E., Moreno, D. A., Garcia-Viguera, C. (2014): Natural bioactive compounds from winery by-products as health promoters: a review. – International Journal of Molecular Sciences 15: 15638-15678.
[43] Tully, K., Sullivan, C., Weil, R., Sanchez, P. (2015): The state of soil degradation in sub-Saharan Africa: baselines, trajectories, and solutions. – Sustainability 7: 6523-6552.
[44] Ukonze, J. A., Okor, V. O., Ndubuaku, U. M. (2016): Comparative analysis of three different spacing on the performance and yield of late maize cultivation in Etche local government area of Rivers State, Nigeria. – African Journal of Agricultural Research 11: 1187-1193.
[45] World Reference Base for Soil Resources (2015): World reference base for soil resources 2014, international soil classification system for naming soils and creating legends for soil

http://www.aloki.hu ● ISSN 1589 1623 (Print) ● ISSN 1785 0037 (Online)
DOI: http://dx.doi.org/10.15666/aeer/2001_815828

maps. – World Soil Resources Reports 106. Food and Agriculture Organization of the United Nations, Rome.

[46] Xia, Y., Yan, X. (2011): Comparison of statistical models for predicting cost effective nitrogen rate at rice-wheat cropping systems. – Soil Science and Plant Nutrition 57: 320-330.

http://www.aloki.hu ● ISSN 1589 1623 (Print) ● ISSN 1785 0037 (Online)
DOI: http://dx.doi.org/10.15666/aeer/2001_815828

INFLUENCES OF THE 28-YEAR APPLICATION OF FERTILIZER AND MANURE ON SOIL ORGANIC CARBON FRACTIONS IN A MAIZE-WHEAT ROTATION FIELD IN SOUTHERN CHINA

ZHANG, L. M.[1,2] – LOU, Y. L.[3*] – XU, M. G.[4] – WANG, X. L.[5]

[1]Research Center of Karst Ecological Environment, The Key laboratory of Plant Resource Conservation and Germplasm Innovation in Mountainous Region (Ministry of Education)/Collaborative Innovation Center for Mountain Ecology & Agro-Bioengineering, College of Life Sciences/Institute of Agro-Bioengineering, Guizhou University, Guiyang 550025, Guizhou Province, China
(e-mail: zhanglimin563406@163.com)

[2]Institute of Guizhou Mountain Resources, Guizhou Academy of Sciences, Guiyang 550001, Guizhou Province, China

[3]Institute of Environment and Sustainable Development in Agriculture, Chinese Academy of Agricultural Sciences, 100081 Beijing, China

[4]Institute of Agricultural Resources and Regional Planning, Chinese Academy of Agricultural Sciences, 100081 Beijing, China
(e-mail: mgxu@caas.ac.cn)

[5]College of Agriculture, Guizhou University, Guiyang 550025, Guizhou Province, China
(e-mail: ls.wangxl@gzu.edu.cn)

**Corresponding author*
e-mail: louyilai@caas.cn

(Received 26th Sep 2021; accepted 23rd Nov 2021)

Abstract. Soil organic carbon (SOC) is an important indicator of soil quality and crop production. In order to optimize management practices and balance agronomic and environmental interests, we conducted physicochemical fractionation to determine the effect of different fertilization treatments on a maize-wheat field in southern China. The fertilization treatments include unfertilized control (CK), nitrogen fertilizer alone (N), balanced fertilizer (NPK) and application of fertilizer plus manure (NPKM). SOC in CK was 6.5 g kg^{-1} lower than that in the NPKM treatment and 1.4 g kg^{-1} higher than that in the N treatment. The proportions of C fractions to SOC in unprotected pool, physically protected pool and stably protected pool (chemically protected pool plus biochemically protected pool) were 22.2~43.9%, 4.8~6.9%, and 49.4~71.6%, respectively. Soil organic carbon was mainly contained in the unprotected C pool. In addition, the biochemically protected C showed changing saturation levels in different fertilization treatments. Therefore, the application of fertilizer plus manure might be the best option in order to improve soil TOC and C fractions in the maize-wheat cropping system.
Keywords: different carbon fraction, long-term fertilization, physicochemical fractionation, climate change, southern China

Introduction

Soil organic carbon (SOC) plays a key role in nutrient supply, improvement of soil physical properties, and erosion control (Stevenson, 1994; Di et al., 2018). SOC is also the source and sink of atmospheric CO_2 and it is important for global carbon (C) cycling (Lou et al., 2011; Sun et al., 2021). Therefore, a satisfactory level of SOC is crucial for

http://www.aloki.hu ● ISSN 1589 1623 (Print) ● ISSN 1785 0037 (Online)
DOI: http://dx.doi.org/10.15666/aeer/2001_829840

ensuring food security and mitigating climate warming. SOC is a heterogeneous and dynamic substance that varies in C and N contents, molecular structure, decomposition rate, and turnover time (Oades, 1988). Soil total organic carbon (TOC) is not able to respond rapidly to soil changes in terrestrial ecosystems, such as fertilization, tillage, and land use. Thus, it is important to classify TOC into different carbon pools according to their decomposition rates or controlling factors, such as water-soluble organic C (Xu et al., 2011), microbial biomass C (Wu et al., 2005), and $KMnO_4$-oxidizable C (Blair et al., 1995). These C fractions are more sensitive to the changes in soil management practices than soil TOC. TOC was classified into free particulate organic C, intra-microaggregate particulate organic C, and mineral- associated organic C though the stabilization of SOC by Six et al. (2000, 2002). Based on the physical fractionation method by Six et al. (2000, 2002), Stewart et al. (2008, 2009) proposed a physicochemical fractionation procedure and the associated conceptual SOC model and separated the TOC into various conceptual fraction pools according to different protection mechanisms: unprotected C pool, physically protected C pool, chemically protected C pool, and biochemically protected C pool. These C pools provide the basis for understanding the effect of SOC with different management measures.

Numerous studied reported that mineral fertilizers and manure application could increase TOC and C fractions in farmland ecosystems (Tong et al., 2014; Tripathi et al., 2014; Ding et al., 2014; Javaid et al., 2021), but Stewart et al. (2008) and Six et al. (2002) found that silt- or clay-sized C fractions did not respond to manure and might reach C saturation level. However, unbalanced or balanced fertilization showed no consistent effects on SOC and C fractions. Some studies showed that mineral fertilizer (N, NK, NP, and NPK) alone could significantly increase SOC and C fractions (Li et al., 2010; Sun et al., 2013). These results were not consistent with those of another long-term experiment in the Loess Plateau of China by Wu et al. (2004), who reported that the N fertilizer alone led to lower concentrations of TOC and LFC than the control treatment (CK). Zhang et al. (2009) also demonstrated that only applying N fertilizer might not sequester C in the red soil of China. The differences among these study results were mainly ascribed to climate factors, topography, soil types, organic fertilizer addition rates, and the initial SOC level.

There are about 56.9 Mha of red soil, which accounts for 6.5% of the total arable land in China (Xu et al., 2006; Zhang et al., 2009). Double cropping winter wheat (*Triticum aestivium* L.) and summer maize (*Zea mays* L.) are the uppermost grains in this agricultural region. The different C fractions of long-term fertilizers will affect directly the grain yield and productivity in red soil. The effects of manure or mineral fertilizer on carbon concentration was seldom reported. The physicochemical fractionation procedure of SOC was not used to study SOC fractions in red soil. Therefore, the study aims to explore the influences of 28-year fertilization treatments in this wheat-maize rotation system on TOC concentration and C fractions of unprotected C pool, physically protected C pool, chemically protected C pool, and biochemically protected C pool.

Materials and methods

Site descriptions

The long-term fertilization experiment was carried out at Qiyang Red soil experimental station in Hunan Province of China (26°45′N, 111°52′E). The

http://www.aloki.hu ● ISSN 1589 1623 (Print) ● ISSN 1785 0037 (Online)
DOI: http://dx.doi.org/10.15666/aeer/2001_829840

meteorological parameters in the site are provided as follows: subtropical humid monsoon, average annual sunshine of about 1623 h, mean annual precipitation of 1431 mm, mean annual temperature of 18 °C, and effective accumulated temperature of about 5600 °C (Zhang et al., 2009).

The experimental site was constructed in 1990 and the red soil was developed from Quaternary red clay (11.63% sand,18.44% silt,74.18% clay) and classified as Ferralic Cambisol (FAO, 1988). The soil physical and chemical parameters of topsoil (0~20 cm) in the initial year (1990) were provided as follows: total organic carbon (TOC) of 8.58 g kg^{-1}, total N of 1.07 g kg^{-1}, total P of 0.45 g kg^{-1}, total K of 13.28 g kg^{-1}, available N of 79.00 mg kg^{-1}, available P of 10.80 mg kg^{-1}, available K of 122.00 mg kg^{-1}, bulk density of 1.10 g cm^{-3}, and pH 5.70 (soil/water 1:1). The field has been continuously cultivated for 28 years under the wheat-maize rotation mode (Tong et al., 2014).

Experimental design and crop management

Four fertilization treatments were chosen from eleven treatments of this experiment in the study (*Table 1*). These treatments include unfertilized control (CK), nitrogen fertilizer alone (N), balanced fertilizer (NPK) and application of fertilizer plus manure (NPKM). Annual application designs of inorganic N, P and K fertilizers and pig manure in various fertilization treatments are shown in *Table 1* Mineral inorganic nitrogen, phosphorus and potassium fertilizers were respectively urea, calcium superphosphate, and potassium chloride and pure pig manure was applied. This study just considered about the nitrogen content equaled between the treatment with manure and without manure. The ratio of organic to inorganic nitrogen was 7:3. The carbon and nitrogen concentrations in pig manure were 413.2 g kg^{-1} and 1.67 g kg^{-1} (dry base), respectively. Mineral fertilization was applied before sowing each crop (30% of mineral N, P and K were applied for the wheat crop and 70% for the maize crop). However, aboveground biomass was removed from the fields in the plots of all fertilization treatments.

Each treatment was replicated three times in a randomized block design. The area of each plot was 196 m^2 (20 m × 9.8 m). In each year, winter wheat (*Triticum aestivium* L.) hybrid 'Xiangmai 11' was sown in strips on November 10, and harvested in early May of the next year. Summer maize (*Zea mays* L.) hybrid 'Yedan 13' was sown in holes between two wheat strips in early April and harvested in July of the same year (Tong et al., 2014). No irrigation was applied in both crops, but herbicides and pesticides were applied during the crop growth periods as required. Grains and straws were air-dried, threshed, oven-dried at 60 °C to a uniform moisture level, and then weighed separately after harvesting.

Table 1. *Annual application of inorganic N, P and K fertilizers and pig manure (dry weight) under various fertilization treatments*

Treatments	Wheat				Maize			
	Inorganic N (kg ha^{-1})	Inorganic P (kg ha^{-1})	Inorganic K (kg ha^{-1})	Pig manure (Mg ha^{-1})	Inorganic N (kg ha^{-1})	Inorganic P (kg ha^{-1})	Inorganic K (kg ha^{-1})	Pig manure (Mg ha^{-1})
CK	0	0	0	0	0	0	0	0
N	90	0	0	0	210	0	0	0
NPK	90	16	31	0	210	37	73	0
NPKM	27	16	31	3.9	63	37	73	9.4

[a]Inorganic N fertilizer is urea; P is Calcium superphosphate; K is KCl
[b]In dry weight

http://www.aloki.hu ● ISSN 1589 1623 (Print) ● ISSN 1785 0037 (Online)
DOI: http://dx.doi.org/10.15666/aeer/2001_829840

Soil sampling

Three composite soil samples for each plot was prepared by mixing five soil cores (inner diameter: 5 cm; height: 20 cm) collected randomly from the surface soil (0~20 cm) after harvesting summer maize in 2017. Six samples were collected for each treatment. Samples were packaged to maintain the uncompacted state at constant temperature and then brought to the laboratory. Large rocks, obvious litters, and roots were removed after samples were air-dried and then carefully broken by hands and passed through an 8-mm sieve, a 2 mm sieve and a 0.15 mm sieve. Soil sample passing through a 2 mm sieve was subjected to fractionation and soil sample passing through a 0.15 mm sieve was used to measure total organic carbon. All samples of each treatment were stored at room temperature for further analysis.

Soil fractionation and C analyses

Three fractionation steps of soil organic carbon were detailed and given by Stewart et al. (2008, 2009). These steps included wet sieving-isolation of microaggregates, density flotation, and acid hydrolysis (*Fig. 1*). In the first step, > 250 μm coarse particulate organic matter (cPOM), 53~250 μm microaggregate C fractions, and < 53 μm silt- and clay-sized C fractions (d-silt and d-clay) were obtained. Soil sample (20 g) was placed on a 250 μm sieve and carefully shaken with 30 glass beads on the top of the microaggregate isolator containing water filling two thirds of the volume of the isolator. After 20 min, the fraction with the size > 250 μm and the fraction with the size between 250 μm and 53 μm fractions were collected in an aluminium specimen box. The fraction with the size < 53 μm and water was centrifuged (127×*g* for 7 min, 1730×*g* for 15 min) in a bucket to separate the easily dispersed silt- and clay-sized C fractions. All fractions were dried at 60 °C, weighed, and stored.

The second step involved further density flotation and dispersion of microaggregate fraction obtained in the first step. This step generated fine particulate organic matter (fPOM), physically protected C fractions (iPOM) with the size > 53 μm, and microaggregate-derived silt- and clay-sized C fractions (μ-silt and μ-clay) with the size < 53 μm. Firstly, 50 mL of 1.70 g cm^{-3} sodium iodide solution was used to initiate density flotation. Then, these samples were centrifuged at 1250×*g* for 20 min at room temperature, filtered with the filter paper of 0.45 μm, and then washed with deionized water for five times to remove sodium iodide. The components on the 0.45 μm filter paper were fine fraction and this filtrate was collected for reuse. Meanwhile, the heavy fraction left in centrifuge tube was washed five times with deionized water, and then 60 mL of 5 g L^{-1} sodium hexametaphosphate was added, shaken for 18 h with 12 glass beads in oscillator, and passed through a 53 μm sieve to separate the physically protected C fractions and silt- and clay-sized C fractions. The further separation step of silt- and clay-sized C was the same with that in the first step.

The third step involved acid hydrolysis of the silt- and clay-sized C fractions (d-silt and d-clay; μ-silt and μ-clay). In the acid hydrolysis step, 6 mol L^{-1} HCl was added in the sample, which was immersed in water bath at 95 °C for 16 h. After refluxing, the sample was filtered and washed with deionized water. All residues were collected in an aluminium specimen box, dried at 60 °C, and weighed. Acid hydrolysis fractions included H-dsilt, H-dclay, H-μsilt, and H-μdsilt. Non- hydrolysis fractions including NH-dsilt, NH-dclay, NH-μsilt, and NH-μdsilt were obtained by subtracting carbon concentration of acid hydrolysis fractions from total carbon concentration. Carbon

http://www.aloki.hu ● ISSN 1589 1623 (Print) ● ISSN 1785 0037 (Online)
DOI: http://dx.doi.org/10.15666/aeer/2001_829840

concentrations in all fractions were measured with an EA 3000 elemental analyzer (Italy) (From Shanghai Wolong Instrument Co., Ltd).

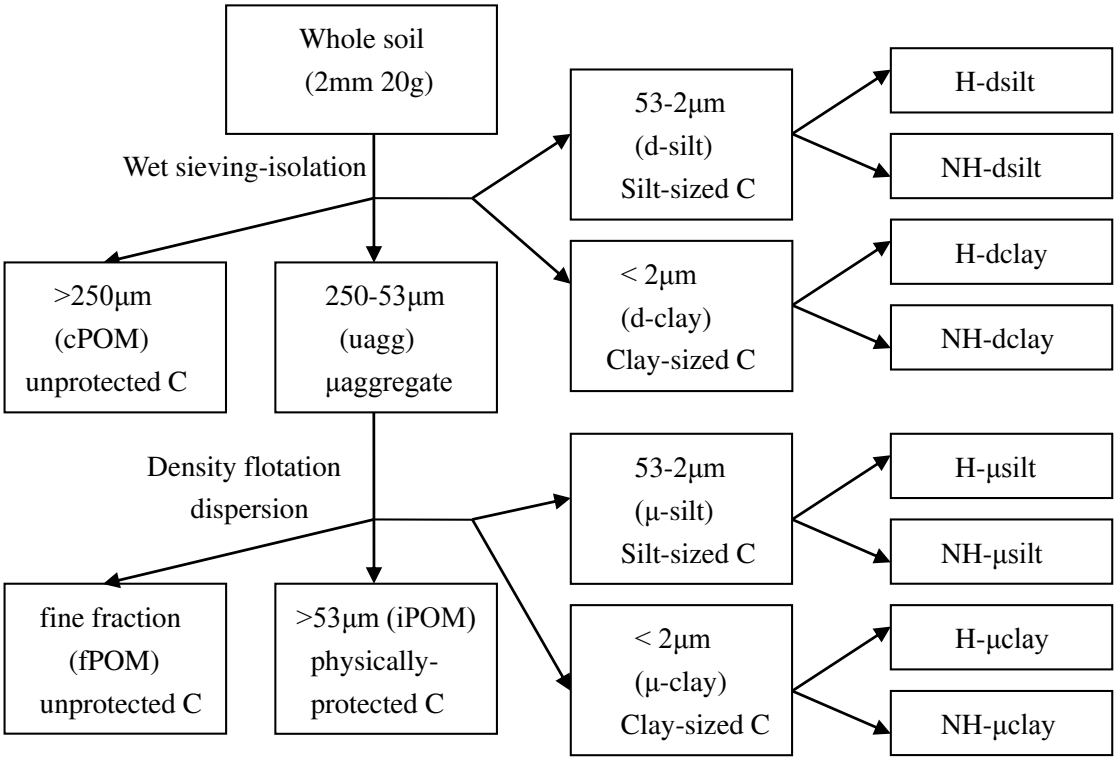

Figure 1. *Fractionation procedure of soil organic carbon for different C pools. cPOM and fPOM indicate unprotected C; iPOM indicate physically protected C; H-dsilt, H-dclay, H-μsilt, and H-μclay (hydrolysable silt & clay) indicate chemically protected C; NH-dsilt, NH-dclay, NH-μsilt, and NH-μclay (non-hydrolysable silt & clay) indicate biochemically protected C*

Data analysis

Annual grain yield and annual carbon input were calculated with the data from 1990 to 2017. All data were analyzed by SPSS Statistics 17.0. Analysis of variance (ANOVA) was performed with a LSD test to analyze the significant difference among different treatments ($P < 0.05$) was considered to be statistically significant.

Results

Soil TOC

Figure 2 shows soil TOC concentrations in different fertilizations treatments. Soil TOC concentrations in different treatments in the 28-year wheat-maize rotation period were decreased according to the following order: NPKM > NPK > CK > N. Obviously, TOC concentration in the soil in the NPKM treatment showed the greatest increase of 13.9 g kg^{-1} and was 4.5 g kg^{-1}, 7.9 g kg^{-1}, and 6.5 g kg^{-1} higher than TOC in the soil in the treatments of NPK, N, and CK. However, TOC concentration in the soil in the N treatment was the lowest (6.0 g kg^{-1}) and 1.4 g kg^{-1} lower than that in the CK treatment.

http://www.aloki.hu ● ISSN 1589 1623 (Print) ● ISSN 1785 0037 (Online)
DOI: http://dx.doi.org/10.15666/aeer/2001_829840

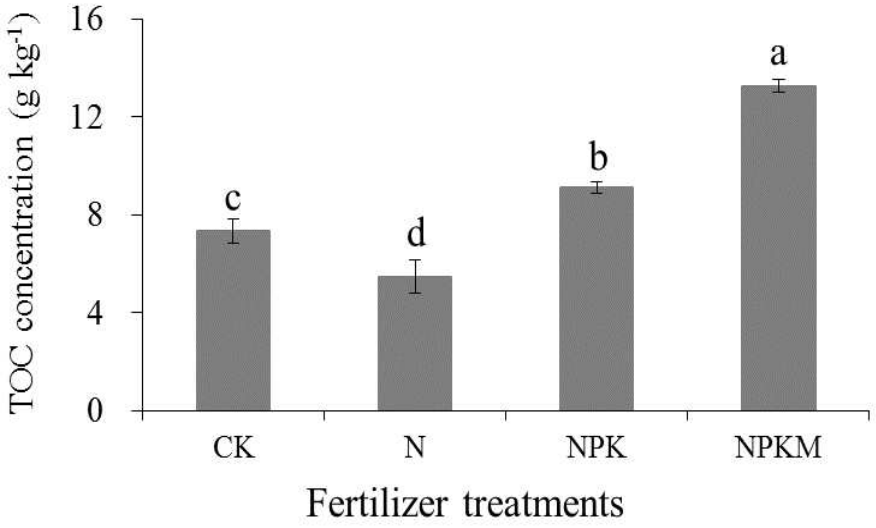

Figure 2. *Effects of long-term fertilization on content of soil total organic carbon (TOC). Bars represent mean + standard error. Different lowercase letters indicate significant differences among all treatments ($P < 0.05$)*

Soil C fractions

As expected, the application of fertilizer plus manure (NPKM) resulted in significant increases in various carbon fractions except NH-clay (*Table 2*). In the unprotected C pool, NPKM treatment had the highest C concentration in cPOM fraction, which was 1 time, 4 times, and 2 times than that in NPK, N and CK treatments. However, fPOM fraction showed the lowest C concentration in all C fractions. Soil C concentrations in different treatments was decreased according to the following order: NPKM > NPK > N = CK in iPOM of physically protected C pool. Soil C concentration in chemically protected C pool in NPKM treatment was 1.25 g kg^{-1} higher than that in CK treatment. In biochemically protected C pool, all treatments assumed different effects on C concentration. In biochemically protected C pool, C concentration in NPKM treatment was 0.68 g kg^{-1} higher than that in the CK treatment and C concentration in N treatment was 0.62 g kg^{-1} lower than that in the CK treatment. Furthermore, stable fractions showed the highest C concentration in all fractions after long-term fertilization treatments.

Soil C fractions in TOC

In all treatments, the proportion of stable C fractions (chemically protected plus biochemically protected) to TOC was the highest (*Fig. 3*). The proportions of various C fractions to TOC were decreased according to the following order: stable C fractions (49.4~71.6%) > unprotected C fractions (22.2~43.9%) > physically protected C fractions (4.8~6.9%). Compared with CK, NPKM treatment significantly improved the proportions of unprotected and physically protected C fractions, but decreased the proportion of stable C fractions. In the NPK treatment, only physically protected C fractions was increased significantly. Meanwhile, N treatment reduced unprotected C fractions and significantly increased chemically protected C fractions. However, the proportion of stable C fractions in the NPKM treatment was the lowest and the highest in the N treatment.

http://www.aloki.hu ● ISSN 1589 1623 (Print) ● ISSN 1785 0037 (Online)
DOI: http://dx.doi.org/10.15666/aeer/2001_829840

Table 2. *Soil organic carbon fractions of different carbon pools under long-term fertilization treatments (g kg^{-1} soil)*[&]

Treatments	SOC fractions							
	Unprotected		Physically protected	Chemically protected		Biochemically protected		Stable fractions
	cPOM	fPOM	iPOM[#]	H-silt	H-clay	NH-silt	NH-clay	Total[$]
CK	2.08c	0.27b	0.35c	1.76b	0.65b	1.65b	0.56a	4.63bc
N	1.03d	0.18b	0.34c	1.42b	0.90ab	1.21c	0.37b	3.92c
NPK	2.69b	0.29ab	0.63b	2.17ab	0.79b	1.90b	0.64a	5.49b
NPKM	5.39a	0.43a	0.88a	2.57a	1.09a	2.29a	0.61a	6.55a

[#]cPOM indicate coarse unprotected particulate organic matter (> 250 μm); fPOM indicate fine unprotected POM (lighter than 1.70 g cm^3, 53-250 μm); iPOM indicate physically protected POM (heavier than 1.70 g cm^3, > 53 μm); H-silt indicate hydrolysable silt-sized fraction (acid soluble, 53-2 μm); H-clay indicate hydrolysable clay-sized fraction (acid soluble, < 2 μm); NH-silt indicate non-hydrolysable silt-sized fraction (acid resistant, 53-2 μm); NH-clay indicate non-hydrolysable clay-sized fraction (acid resistant, < 2 μm)
[&]Different lowercase letters indicate significant differences among all treatments ($P < 0.05$)
[$]The sum of H-silt, H-clay, NH-silt and NH-clay

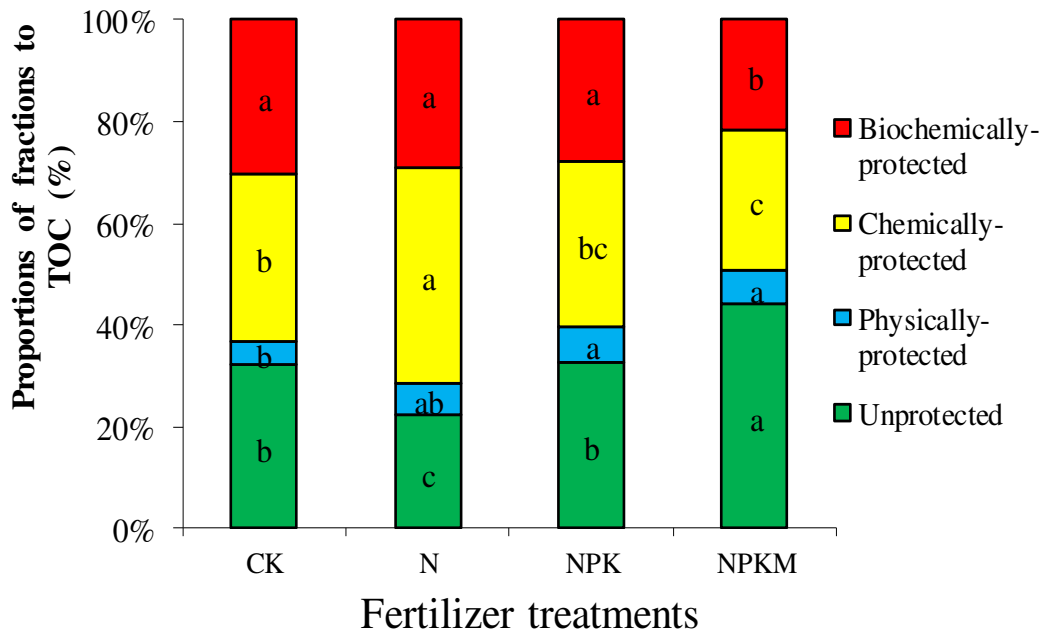

Figure 3. *Effects of long-term fertilization on the proportions of soil fractions carbon to total organic carbon. Different lowercase letters indicate significant differences among all treatments ($P < 0.05$)*

Discussion

The application of chemical fertilizer and manure increased significantly soil organic carbon concentration (Bhattacharyya et al., 2010; Liang et al., 2014; Di et al., 2018; Che et al., 2021). In our studies, soil TOC was improved by 88% after the long-term application of mineral fertilizer and manure compared with CK treatment (*Fig. 2*). Long-term applications of animal manure generally increased TOC in two ways.

http://www.aloki.hu ● ISSN 1589 1623 (Print) ● ISSN 1785 0037 (Online)
DOI: http://dx.doi.org/10.15666/aeer/2001_829840

Organic matters contained in applied manure increased TOC and the increased organic matters of crop residues due to the higher crop yields after the application of manure correspondingly increased TOC (Batande et al., 2020). In the plot, mean annual grain yield of wheat and maize in NPKM treatment was the highest (6883 kg ha^{-1} yr^{-1}), thus leading to a tremendous carbon input (6.29 t ha^{-1} yr^{-1}) compared with other treatments (*Table 3*). The more the carbon input was, the greater the C-saturated degree in TOC of soil was (Six et al., 2002; Stewart et al., 2008; Huo et al., 2018). The effects of fertilizer and manure application on TOC have been realized and utilized for nearly 4000 years in China, Japan, and Korea (Dormaar et al., 1988).

Table 3. *Effects of long-term different fertilization treatments to grain yield and carbon input*

Treatments	Wheat	Maize	Total	Carbon input		Total
	Annual grain yield			Crop	Manure	
	kg ha^{-1} yr^{-1}			t ha^{-1} yr^{-1}		
CK	362	286	648c	0.24	0.00	0.24c
N	303	545	848c	0.25	0.00	0.25c
NPK	1060	2876	3937b	0.83	0.00	0.83b
NPKM	1772	5111	6883a	1.50	4.79	6.29a

Annual grain yield is dry weight. Different lowercase letters indicate significant differences among all treatments ($P < 0.05$)

However, the TOC in the N treatment was the lowest (6.0 g kg^{-1}), which was even lower than that in the CK treatment (7.4 g kg^{-1}). No significant difference in carbon input was observed between the N treatment and CK treatment, but the lowest pH (3.77) occurred in 2017 after successive N fertilizer application (*Table 3, Fig. 4*). Soil acidification would lead to soil hardening and the decline in soil fertility and may not sequester C (Zhang et al., 2009). Only N fertilizer may enhance the decomposition of TOC in the soil due to the high temperature and abundant rainfall. The observation was not consistent with the previous reports (Campbell et al., 1991). Wu et al. (2004) found that N fertilizer stimulated microbial activities and enhanced TOC decomposition and that the MB-C in N fertilizer treatment was 17~110% higher than in the control. The higher MB-C suggested the higher activities of microorganisms and the more intensive decomposition activities of soil organic carbon (Ci et al., 2015; Li et al., 2017).

Effects of fertilization on soil C fractions Kandeler et al. (1999) in Germany and Gerzabek et al. (2001) in central Sweden demonstrated that organic manure could increase in SOC concentration in particle-sized fractions. In this study, NPKM treatment increased significantly each C fraction, especially cPOM of unprotected pool, which was 2.6 times of that in the CK treatment. Sleutel et al. (2006) also proved that fertilizer and manure application promoted the C fractions in the unprotected pool. In our experiments, the proportions of C fractions to TOC in unprotected pool, physically protected pool, and stably protected pool (chemically protected pool plus biochemically protected pool) were respectively 22.2~43.9%, 4.8~6.9%, and 49.4~71.6% (*Fig. 3*). Stewart et al. (2009) stated that the C fractions of the unprotected pool (cPOM + fPOM) accounted for 9~46% of TOC. Köbl and Kögel-Knabner (2004) reported that the C fractions of the physically protected pool (iPOM) accounted for 5.0~9.8% of TOC in silty clay loam soils. Tong et al. (2014) found that the C fractions of stable C pool

http://www.aloki.hu ● ISSN 1589 1623 (Print) ● ISSN 1785 0037 (Online)
DOI: http://dx.doi.org/10.15666/aeer/2001_829840

accounted for 45.2~76.6% of TOC under different fertilization treatments in red soil in southern China. The results were consistent with previous results (Stewart et al., 2012; Ding et al., 2014).

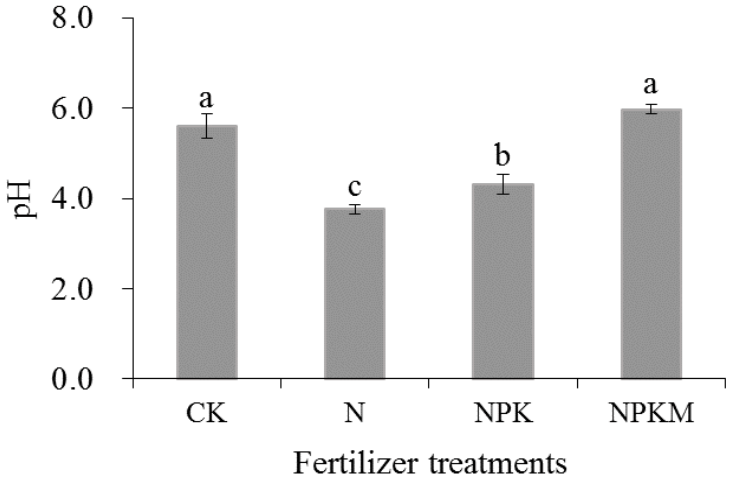

Figure 4. *Effects of long-term fertilizer to soil pH. Bars represent mean + standard error. Different lowercase letters indicate significant differences among all treatments ($P < 0.05$)*

The biochemically protected C pool is acquiring protection through condensation and complexation reactions or the inherent complex biochemical nature of the material (Lu et al., 2021). Biochemically protected C consisting of the non-hydrolyzable silt and clay particles are old stabilized organic carbon, which is hypothesized to be unaffected by management or interacted with charcoal or other materials. Biochemically protected C would be expected to reach a saturation level. In this study, the proportion of biochemically protected C fractions to stable C fractions showed no significant change among different fertilization treatments except N treatment. This phenomenon indicated that biochemically protected C fractions might reach a saturation level. The result was consistent with previous reports (Six et al., 2002; Stewart et al., 2008; Wang et al., 2021). The different result of the N treatment might be ascribed to the low pH (3.77) and the high concentration of HCL (6 mol L^{-1}), which stimulated the degree of acid hydrolysis. It is necessary to adopt more powerful analytical tools, such as polymerase chain reaction (PCR) technique and ^{13}C NMR spectroscopy to explore the phenomenon of biochemically protected C fractions in the N treatment.

Conclusions

Continuous application of fertilizer plus manure in 28 years significantly increased soil TOC and C fractions, but the application of N fertilizer alone showed the inconsistent result with CK treatment in the wheat-maize rotation system in the red soil in southern China. Soil organic carbon was mainly contained in the unprotected C pool, indicating that the unprotected C pool was the more sensitive indicator than soil TOC or other C fractions. In addition, biochemically protected C showed the tendency of a saturation level in different fertilization treatments. It is necessary to adopt the polymerase chain reaction (PCR) technique or ^{13}C NMR spectroscopy to further explore the effects of fertilizer and manure application on soil carbon fractions.

http://www.aloki.hu ● ISSN 1589 1623 (Print) ● ISSN 1785 0037 (Online)
DOI: http://dx.doi.org/10.15666/aeer/2001_829840

Acknowledgments. Funding was provided by the Project of National Key Research and Development Program of China (grant number 2016YFC0502604); and the Construction Program of Biology First-class Discipline in Guizhou (GNYL[2017]009).

Author contributions. L. Z. analyzed the data and wrote the manuscript. L. Z. and X. W. performed the experiments. M. X. provided helpful suggestions in design of the project. Y. L. conceived and designed the project. All authors read and approved the final manuscript.

Conflict of interests. The authors declare no conflict of interests.

REFERENCES

[1] Batande, S. N., Dou, S., Zhang, X. W. (2020): Corn straw return can increase labile soil organic carbon fractions and improve water-stable aggregates in Haplic Cambisol. – Journal of Arid Land 12: 1018-1030.

[2] Bhattacharyya, R., Ved Prakash Kundu, S., Srivastva, A. K., Gupta, H. S. (2010): Long term effects of fertilization on carbon and nitrogen sequestration and aggregate associated carbon and nitrogen in the Indian sub-Himalayas. – Nutrient Cycling Agroecosyst 86: 1-16.

[3] Blair, G. J., Lefroy, R. D., Lise, L. (1995): Soil carbon fractions based on their degree of oxidation, and the development of a carbon management index for agricultural systems. – Australia Journal Agricultural Research 46: 1459-1466.

[4] Campbell, C. A., Biederbeck, V. O., Zentner, R. P., LaFond, G. P. (1991): Effect of crop rotations and cultural practices on soil organic matter, microbial biomass and respiration in a thin Black Chernozem. – Canada Journal Soil Science 71: 363-376.

[5] Che, Q. J., Li, M., Zhang, Z. S. (2021): Effects of biochar application on soil organic carbon in degraded saline-sodic wetlands of Songnen Plain, Northeast China. – Chinese Geographical Science 31: 877-887.

[6] Ci, E., Mahdi, M. A., Wang, L., Ding, C. H., Xie, D. T. (2015): Soil organic carbon mineralization as affected by cyclical temperature fluctuations in a karst region of southwestern China. – Pedosphere 25: 512-523.

[7] Di, J. Y., Xu, M. G., Zhang, W. J., Tong, X. G., He, X. H., Gao, H. J., Liu, H., Wang, B. R. (2018): Combinations of soil properties, carbon inputs and climate control the saturation deficit dynamics of stable soil carbon over 17-year fertilization. – Scientific Reports 8: 1-10.

[8] Ding, X., Yuan, Y., Liang, Y., Li, L., Han, X. (2014): Impact of long-term application of manure, crop residue, and mineral fertilizer on organic carbon pools and crop yields in a Mollisol. – Journal of Soils and Sediments 14: 854-859.

[9] Dormaar, J. F., Lindwall, C. W., Kozub, G. C. (1988): Effectiveness of manure and commercial fertilizer in restoring productivity of an artificially eroded Dark Brown Chernozemic soil under dryland conditions. – Canada Journal Soil Science 68: 669-679.

[10] Gerzabek, M. H., Haberhaue,r G., Kirchman, H. (2001): Soil organic matter pools and carbon-13 natural abundances in article-size fractions of a long-term agricultural field experiment receiving organic amendments. – Soil Science Social American Journal 65: 352-358.

[11] Huo, L. L., Zou, Y. C., Yu, X. G., Zhang, Z. S., Wang, X. H. (2018): Effect of Wetland reclamation on soil organic carbon stability in peat mire soil around Xingkai Lake in Northeast China. – Chinese Geographical Science 28: 325-336.

[12] Javaid, M. D., Lotfollah A. L. (2021): Changes in soil organic carbon, nitrogen and sulphur along a slope gradient in apple orchard soils of Kashmir Himalaya. – Journal of Mountain Science 18: 2377-2387.

[13] Kandeler, E., Stemmer, M., Klimanek, E. M. (1999): Response of soil microbial biomass, urease and xylanase within particle size fractions to long-term soil management. – Soil Biological Biochem 31: 261-273.

http://www.aloki.hu ● ISSN 1589 1623 (Print) ● ISSN 1785 0037 (Online)
DOI: http://dx.doi.org/10.15666/aeer/2001_829840

[14] Köbl, A., Kögel-Knabner, I. (2004): Content and composition of free and occluded particulate organic matter in a differently textured arable Cambisol as revealed by solid-state ^{13}C NMR spectroscopy. – Journal Plant Nutrient Soil Science 167: 45-53.
[15] Li, Z., Liu, M., Wu, X., Han, F., Zhang, T. (2010): Effects of long-term chemical fertilization and organic amendments on dynamics of soil organic C and total N in paddy soil derived from barren land in subtropical China. – Soil Tillage Research 106: 268-274.
[16] Li, D. J., Xiao, K. C., He, T. G. (2017): Impacts of vegetation restoration strategies on soil organic carbon and nitrogen dynamics in a karst area, southwest China. – Ecological Engineering 101: 247-254.
[17] Liang, Q., Chen, H., Gong, Y., Yang, H., Fan, M., Kuzyakov, Y. (2014): Effects of 15 years of manure and mineral fertilizers on enzyme activities in particle-size fractions in a North China Plain soil. – European Journal of Soil Biology 60: 112-119.
[18] Lou, Y. Y., Wang, J., Liang, W. (2011): Impacts of 22-year organic and inorganic N managements on soil organic C fractions in a maize field, northeast China. – Catena 87: 386-390.
[19] Lu, X. L., Li, S. S., Liu, J. H., Duan, Y. X., Yue, H., Kang, J. H., Wu, H. L. (2021): Distribution of soil water-stable aggregates and organic carbon content affected by tillage systems: a meta-analysis. – Journal of Drainage and Irrigation Machinery Engineering 39: 1051-1055.
[20] Oades, J. M. (1988): The retention of organic matter in soils. – Biogeochemistry 5: 35-70.
[21] Six, J., Elliot, E. T., Paustian, K. (2000): Soil macroaggregate turnover and microaggregate formation: a mechanism for C sequestration under no-tillage agriculture. – Soil Biology & Biochemistry 32: 2099-2103.
[22] Six, J., Conant, R. T., Paul, E. A., Paustian, K. (2002): Stabilization mechanisms of soil organic matter: implications for C-saturation of soils. – Plant and Soil 241: 155-176.
[23] Sleutel, S., De Neve, Németh, T., Tóth, T., Hofman, G. (2006): Effect of manure and fertilizer application on the distribution of organic carbon in different soil fractions in long-term field experiments. – European Journal of Agronomy 25: 280-288.
[24] Stevenson, F. J. (1994): Humus Chemistry: Genesis, Composition, Reaction. – Wiley, New York, pp. 1-24.
[25] Stewart, C. E., Plante, A. F., Paustian, K., Conant, R. T., Six, J. (2008): Soil carbon saturation: linking concept and measurable carbon pools. – Soil Science Society of American Journal 72: 379-392.
[26] Stewart, C. E., Paustian, K., Conant, R. T., Plante, A. F., Six, J. (2009): Soil carbon saturation: Implications for measurable carbon pool dynamics in long-term incubations. – Soil Biology and Biochemistry 41: 357-366.
[27] Sun, Y., Huang, S., Yu, X., Zhang, W. (2013): Stability and saturation of soil organic carbon in rice fields: evidence from a long-term fertilization experiment in subtropical China. – Journal Soils Sediments 13: 1327-1334.
[28] Sun, Z. X., Bai, H. Q., Ye, H. C., Zhou, Z. Q., Huang, W. J. (2021): Three-dimensional modelling of soil organic carbon density and carbon sequestration potential estimation in a dryland farming region of China. – Journal of Geographical Sciences 31: 1453-1468.
[29] Tong, X. G., Xu, M. G., Wang, X., Bhattacharyya, R., Zhang, W. J., Cong, R. (2014): Long-term fertilization effects on organic carbon fractions in a red soil of China. – Catena 113: 251-259.
[30] Tripathi, R., Nayak, A. K., Bhattacharyya, P., Shukla, A. K., Shahid, M., Raja, R., Panda, B. B., Mohanty, S., Kumar, A., Thilagam, V. K. (2014): Soil aggregation and distribution of carbon and nitrogen in different fractions after 41 years long-term fertilizer experiment in tropical rice-rice system. – Geoderma 213: 280-286.
[31] Wang, R. J., Song, J. S., Feng, Y. T., Zhou, J. X., Xie, J. Y., Asif, K., Che, Z. X., Zhang, S. L., Yang, X. Y. (2021): Changes in soil organic carbon pools following long-term fertilization under a rain-fed cropping system in the Loess Plateau, China. – Journal of Integrative Agriculture 20: 2512-2525.

http://www.aloki.hu ● ISSN 1589 1623 (Print) ● ISSN 1785 0037 (Online)
DOI: http://dx.doi.org/10.15666/aeer/2001_829840

[32] Wu, T. Y., Schoenau, J. J., Li, F. M., Qian, P. Y., Malhi, S. S., Shi, Y. C., Xue, F. L. (2004): Influence of cultivation and fertilization on total organic carbon and carbon fractions in soils from the Loess Plateau of China. – Soil Tillage Research 77: 59-68.
[33] Wu, T. Y., Schoenau, J. J., Li, F. M., Qian, P. Y., Malhi, S. S., Shi, Y. C. (2005): Influence of fertilization and organic amendments on organic-carbon fractions in Heilu soil on the loess plateau of China. – Journal Plant Nutrient Soil Science 168: 100-107.
[34] Xu, M. G., Liang, G. Q., Zhang, F. D. (2006): Evolution of Soil Fertility in China. – Agricultural Science and Technology Press of China, Beijing, pp. 88-90 (in Chinese).
[35] Xu, M. G., Lou, Y. Y., Sun, X., Wang, W. M., Baniyamuddin, K. Z. (2011): Soil organic carbon active fractions as early indicators for total carbon change under straw incorporation. –Biology and Fertility of Soils 47: 745-752.
[36] Zhang, H. M., Wang, B. R., Xu, M. G., Fan, T. L. (2009): Crop yield and soil responses to long-term fertilization on a red soil in southern China. – Pedosphere 19: 199-207.

http://www.aloki.hu ● ISSN 1589 1623 (Print) ● ISSN 1785 0037 (Online)
DOI: http://dx.doi.org/10.15666/aeer/2001_829840

EFFECTS OF GYPSUM COMBINED WITH DIFFERENT AMOUNTS OF BIOCHEMICAL HUMIC ACID ON SOIL IMPROVEMENT AND COTTON (*GOSSYPIUM HIRSUTUM* L.) YIELD ON SALINE-ALKALI LAND

SHAN, Y. Y.[1] – LI, G.[1] – BAI, Y. G.[3] – LIU, H. B.[2,3*] – ZHANG, J. H.[1] – WEI, K.[1] – WANG, Q. J.[1] – CAO, L.[4]

[1]*State Key Laboratory of Eco-hydraulics in Northwest Arid Region of China, Xi'an University of Technology, Xi'an 710048, China*

[2]*College of Hydraulic and Civil Engineering of Xinjiang Agricultural University, Urumqi 830052, China*

[3]*Xinjiang Institute of Water Resources and Hydropower Research, Urumqi 830049, China*

[4]*Shaanxi Fengxi Xincheng Investment Development Co., Ltd, Xi'an 710048, China*

[*]*Corresponding author*
e-mail: 82914024@qq.com

(Received 28th Sep 2021; accepted 23rd Nov 2021)

Abstract. This study was conducted to investigate the effects of gypsum combined with different amounts of biochemical humic acid (BHA) on the improvement of saline-alkali soil and cotton (*Gossypium hirsutum* L.) yield under film-mulched drip irrigation in Shaya County, Aksu Prefecture, Xinjiang, China. Using the micro zone test method, taking the single application of gypsum as the control (CK, gypsum 15 t·ha^{-1}), 3 ratios of BHA were applied: A (gypsum 15 t·ha^{-1} + BHA 0.35 t·ha^{-1}), B (gypsum 15 t·ha^{-1} + BHA 0.75 t·ha^{-1}) and C (gypsum 15 t·ha^{-1} + BHA 1.50 t·ha^{-1}). The results showed that the combined application of gypsum and BHA significantly reduced soil pH and electric conductibility, while increased soil porosity. Compared to the control, the large aggregates (>0.25mm) in 0-10 cm and 10-20 cm soil layers of the three treatments increased by 10.00%, 20.33%, 33.68% and 7.39%, 20.61% and 25.00%, respectively. Besides, the content of Na^+ in topsoil decreased significantly, while the content of Mg^{2+} increased obviously. In addition, the cotton yield increased by 5.86%, 12.50% and 18.13%, respectively compared with the control. Considering the yield investment ratio of agricultural production and the comprehensive effect of soil improvement, the combined application mode of gypsum 15 t·ha^{-1}+ biochemical humic acid 1.50 t·ha^{-1} had the best result among all three treatments.
Keywords: *humic acid, saline-alkali soil, soil structure, soil cation, cotton*

Introduction

Due to the long-term unreasonable development and utilization of land and the unique geographical conditions of Xinjiang, China, the problem of soil salinization is becoming more and more serious (Heng et al., 2018; Liang et al., 2021). The area of saline-alkali wasteland in Xinjiang is 2.81×10^7 ha, accounting for about one-third of the total area of saline-alkali land in China (Yan et al., 2021; Zhou et al., 2021). Salinization has completely restricted the agricultural development and sustainable development of Xinjiang. Finding ways to eliminate the harm of salt and alkali to the greatest extent through comprehensive improvement measures is essential to ensure food security and sustainable agricultural development in Xinjiang, China.

http://www.aloki.hu ● ISSN 1589 1623 (Print) ● ISSN 1785 0037 (Online)
DOI: http://dx.doi.org/10.15666/aeer/2001_841854

Gypsum has been proven to be an effective measure to improve saline-alkali soil (Wang et al., 2017a; Zhang et al., 2020). Wang et al. (2021) showed that the pH value, alkalinity, and total salt content of alkali soil decreased by 17.20%, 42.63% and 46.43%, respectively three years after the application of gypsum. Mao et al. (2014) pointed out that the percentage of soil exchangeable sodium decreased significantly when gypsum was applied. Furthermore, the application of gypsum could promote the growth of rice seedlings and improve the survival rate of *Lycium barbarum* seedlings (Zhao et al., 2018; Liu et al., 2020). However, since gypsum itself is salt, the effect of improper application will be counterproductive. Sakai et al. (2004) found that excessive application of gypsum or poor management could cause soil salt accumulation and increase the total salt content of soil. Zhao et al. (2019) indicated that the application amount of gypsum was not as much as possible through indoor soil column tests. Therefore, by improving the application mode of gypsum, strengthening its improvement effect on saline-alkali soil and optimizing the application structure, so as to achieve the purpose of scientifically using coal-fired desulfurization waste to improve saline alkali soil. Zhao et al. (2020) found that the 1:1 combination of gypsum and humic acid reduced the soil pH, significantly increased the content of available potassium, and increased the corn yield by 40%. Nan et al. (2016) took the saline-alkali land in the northern coastal area of Jiangsu Province as the experimental area, and found that the effect of improving saline alkali with 3.2 $t \cdot ha^{-1}$ gypsum combined with 1.5 $t \cdot ha^{-1}$ humic acid was the best, and the yield increasing effect of rape was obvious. Xia et al. (2019) pointed out that under the combined action of gypsum and humic acid, soil bulk density significantly decreased, and the emergence rate and yield of silage corn significantly increased.

This paper studied the effects of combined application of gypsum and different amounts of biochemical humic acid (BHA) on the physical and chemical properties of saline-alkali soil and cotton (*Gossypium hirsutum* L.) yield, and looked for the best ratio of gypsum and BHA, so as to reduce the required amount of gypsum and improve its saline-alkali soil improvement effect, so as to provide a reference for scientific and rational utilization of gypsum, and technical support and theoretical basis for the large-scale popularization of using it to improve saline-alkali land in arid and semi-arid regions.

Materials and methods

Overview of test area

The experiment was conducted in Shaya County (41°25'N, 84°47'E) in Aksu Prefecture, Xinjiang, China. This region is located in the south of the middle section of Tianshan Mountain, the north edge of Taklimakan Desert and the middle reaches of Tarim River, with an altitude of 946-1050 m. Moreover, the region is far from the sea, the East, South and West are surrounded by deserts, and the ecological environment is relatively fragile. In addition, the region is a typical continental warm temperate arid climate, with annual precipitation of 57.44 mm, evaporation of 2756 mm, average temperature of 11.32 ℃, annual sunshine number of 2965 h, wind speed of 2.54 $m \cdot s^{-1}$, and frost-free period of 148 days (Liang et al., 2021). Before the experiment, the physical and chemical properties of the initial soil were determined. The soil in the study area (0-40 cm) was sandy loam (63.32% sand, 34.23% silt, 2.45% clay) saturated water content was 0.396 $cm^3 \cdot cm^{-3}$, wilting water content was 0.048 $cm^3 \cdot cm^{-3}$, field water capacity was 0.203 $cm^3 \cdot cm^{-3}$ (Zhou et al., 2021).

http://www.aloki.hu ● ISSN 1589 1623 (Print) ● ISSN 1785 0037 (Online)
DOI: http://dx.doi.org/10.15666/aeer/2001_841854

Experimental design

The micro zone test was carried out in the study area from April 22 to 28, 2019. A single factor completely randomized block design was adopted. Each treatment was set for 3 repetitions, and the area of each cell was 5 m × 6 m (30 m^2). A total of 4 treatments were set as follows:

(1) CK (single application of gypsum 15 $t \cdot ha^{-1}$),
(2) A (gypsum 15 $t \cdot ha^{-1}$ + BHA 0.35 $t \cdot ha^{-1}$),
(3) B (gypsum 15 $t \cdot ha^{-1}$ + BHA 0.75 $t \cdot ha^{-1}$),
(4) C (gypsum 15 $t \cdot ha^{-1}$ + BHA 1.50$t \cdot ha^{-1}$).

Biochemical humic acid (BHA) is produced by Beijing Aojia Ecological Agriculture Co., Ltd. After gypsum and BHA were evenly spread in each community, the harrow was carried out with a disc harrow, and the harrow depth was 0-20 cm. The cotton was cultivated by drip irrigation under film, and the cultivation mode was 1 film, 2 tubes and 6 rows. The field management level in the later stage of treatment was the same. Conventional irrigation was adopted in the whole growth period of cotton, and the irrigation amount was consistent with the actual production. The irrigation quota of cotton growth period was 5700 $m^3 \cdot ha^{-1}$, the irrigation period was 7-10 days, and the total irrigation time was 9 times. The soil conditions of the test site before the test were shown in *Table 1*.

Table 1. *The condition of soil in the study area*

pH	Electric conductibility ($dS \cdot m^{-1}$)	Bulk density ($g \cdot kg^{-3}$)	Alkalinity (%)	Available phosphorus ($mg \cdot kg^{-1}$)	Tatal phosphorus ($g \cdot kg^{-1}$)	Alkali-hydrolyzed nitrogen ($mg \cdot kg^{-1}$)	Organic matter ($g \cdot kg^{-1}$)
8.9	1.87	1.63	10.8	11.23	0.35	38.49	9.35

Investigate items and methods

On September 20, 2019, the soil in the harvested cotton field was sampled. Three sections (60 cm) were randomly excavated in each plot, and soil samples of 0-10, 10-20, 20-40 and 40-60 cm were collected, respectively. The soil samples of the same soil layer at the three sample points were evenly mixed, and the collected soil was brought back to the laboratory for natural air drying and pass through 1 mm sieve. The 0-10, 10-20, 20-40 and 40-60 cm soil samples of the test field were collected in plastic boxes, respectively. The soil samples were brought back to the laboratory and dried at room temperature. After the samples reached the plastic limit (about 20% water content), they would be sieved through 8 mm sieve for aggregate analysis.

The composition and distribution of soil aggregates were determined by dry sieving method. During air drying, the soil samples was gently broken into small soil blocks with a diameter of about 1 cm^3 along with the natural structure of the soil. The plant roots and stones in soil samples were removed. The soil samples (100 g, three replicates) were passed through a set of screen groups with a diameter of 30 cm. The pore sizes of the sieve were 8, 5, 2, 1, 0.25 mm and 0.053 mm, respectively. There was a cover above the screen group and a bottom below the screen group. The screening time shall be controlled as 10 min. after screening, the weight of soil sample on the sieve of each aperture was

http://www.aloki.hu ● ISSN 1589 1623 (Print) ● ISSN 1785 0037 (Online)
DOI: http://dx.doi.org/10.15666/aeer/2001_841854

measured. The soil pH value was measured by BPH 252 pH meter (soil water ratio 1:2.5, HACH, USA). The soil electric conductivity was determined by DDSJ-308A electric conductivity meter (soil water ratio 1:5, Shanghai Yifen Scientific Instrument Co., Ltd, China). The contents of K^+, Ca^{2+}, Na^+, Mg^{2+} in soil samples were determined by ICP (plasma emission spectrometry, SPECK, Germany).

On September 15, 2019, the cotton yield under each treatment in the experimental plot of the study area was measured. 3 sample points were taken from each community. 11 lines were taken from each sample point to measure the line spacing and calculate the average line spacing. 21 plants in one row were randomly selected from each sample point to measure the plant spacing and calculate the average plant spacing. 3 rows were randomly selected from each sample point, 10 plants in each row, a total of 30 plants, and the number of bolls was investigated. 100 bolls were collected randomly at each sample point to weigh them after drying and calculate the average single boll weight. Cotton yield was calculated by the average line spacing, plant spacing, number of bolls per plant and average single boll weight.

Composition of gypsum

The gypsum used in the test was provided by the Huadian Xinjiang Power Generation Co., Ltd. The main component of gypsum is $CaSO_4 \cdot 2H_2O$, with a content of 74.76%, and water content 38.23%, pH value 7.36, electric conductivity 2.84 $dS \cdot m^{-1}$, total salt content 16 $g \cdot kg^{-1}$, K content 5.39 $g \cdot kg^{-1}$, Na content 12.35 $g \cdot kg^{-1}$, Ca content 226.71 $g \cdot kg^{-1}$, Mg content 4.16 $g \cdot kg^{-1}$.

Data processing and analysis

Data processing were carried out with Microsoft Excel 2019. The analysis of variance was performed by SPSS 22.0 statistical software. One way ANOVA and LSD were used to test the significance of multiple comparison differences (α=0.05). Fu et al. (2019) proposed the calculation method of soil porosity(P):

$$P = 1 - \gamma_d / 2.65 \quad \text{(Eq.1)}$$

where, γ_d is soil bulk density ($g \cdot kg^{-3}$).

Results

Effects of gypsum combined with different amounts of BHA on soil porosity

Gypsum combined with different amounts of BHA treatment significantly increased soil porosity as a whole (*Fig. 1*). With the increase of the proportion of gypsum combined with BHA, the soil porosity showed an increasing trend (C > B> A). The soil porosity of 0-10 cm soil layer increased by 16.00%, 23.61% and 35.03%, respectively compared with single application of gypsum. The soil porosity in 10-20 cm soil layer increased by 14.05%, 4.45% and 1.26%, respectively compared with single application of gypsum. The soil porosity in 20-40 cm soil layer increased by 7.63%, 7.66% and 2.55%, respectively, compared with single application of gypsum. There was no significant difference in soil porosity among treatments A, B and C in 40-60 cm soil layer (p> 0.05).

http://www.aloki.hu ● ISSN 1589 1623 (Print) ● ISSN 1785 0037 (Online)
DOI: http://dx.doi.org/10.15666/aeer/2001_841854

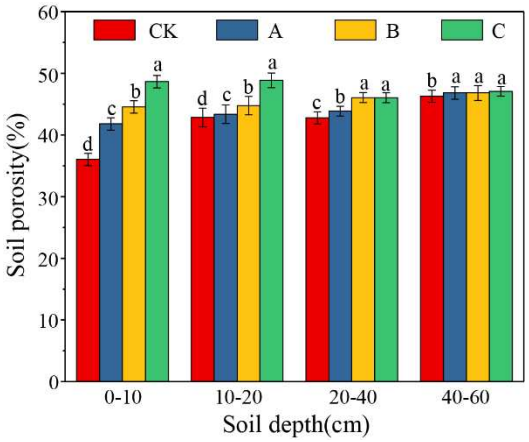

Figure 1. *Influence of gypsum combined with different amount of BHA on soil porosity. CK represents single application of gypsum 15 t·ha^{-1}, A represents gypsum 15 t·ha^{-1} + BHA 0.35 t·ha^{-1}, B represents gypsum 15 t·ha^{-1} + BHA 0.75 t·ha^{-1}, and C represents gypsum 15 t·ha^{-1} + BHA 1.50t·ha^{-1}. The error lines represent the standard variance, and different lowercase letters represent significant differences among treatments in the same soil layer ($p < 0.05$)*

The effect of gypsum combined with different amounts of BHA on soil aggregate

Gypsum combined with different amounts of BHA increased the proportion of large aggregates (> 0.25 mm) in plough layer (0-10 cm and 10-20 cm) soil and 20-40 cm soil layer, and decreased the proportion of small aggregates (0.053-0.25 mm) and micro aggregates (< 0.053 mm) (*Table 2*). Gypsum combined with BHA had the most significant effect on the increase of the proportion of aggregates > 0.25 mm in the cultivated soil, and the increase effect showed a weakening trend with the increase of soil depth ($p < 0.05$). The proportion of large aggregates in 0-10 cm and 10-20 cm soil layers increased by 10.00%, 20.33%, 33.68% and 7.39%, 20.61% and 25.00%, respectively, compared with single application of gypsum. In 0-40 cm soil layer, the proportion of large aggregates was C > B > A, and there was significant difference among treatments ($p < 0.05$). There was no significant difference in the proportion of large aggregates among treatments A, B and C in 40-60 cm soil layer ($p > 0.05$).

The effect of gypsum combined with different amounts of BHA on soil pH

The treatment of gypsum combined with different amounts of BHA significantly reduced the pH value of soil than that of single application of gypsum (*Fig. 2*). In 0-10 cm soil layer, with the increase of the amount of BHA, the soil pH value decreased first and then increased. Treatment B was the lowest, significantly lower than other treatments, and there was no significant difference between treatment A and C ($p > 0.05$). In 10-20 cm soil layer, with the increase of the proportion of BHA, the soil pH value showed a downward trend. There was no significant difference between treatment B ($p > 0.05$), treatment A and treatment C, and treatment A was significantly greater than treatment C ($p < 0.05$). In 20-40 cm soil layer, treatment A was significantly higher than treatment B and C ($p < 0.05$), and there was no significant difference between treatment B and C ($p > 0.05$). In 40-60 cm soil layer, with the increase of the proportion of BHA, the soil pH value showed a downward trend. There was no significant difference between treatment A and treatment B ($p > 0.05$), but they were significantly higher than treatment C ($p < 0.05$).

http://www.aloki.hu ● ISSN 1589 1623 (Print) ● ISSN 1785 0037 (Online)
DOI: http://dx.doi.org/10.15666/aeer/2001_841854

Table 2. *Effects of gypsum combined with different amount of BHA on soil aggregates*

Soil depth (cm)	Treatment	Soil aggregates in different size (%)		
		>0.25mm	0.053-0.25mm	<0.053mm
0-10	CK	57.89d	33.10a	9.01a
	A	63.68c	29.23b	7.09b
	B	69.66b	26.60c	3.74c
	C	77.39a	20.00d	2.61d
10-20	CK	66.81d	25.17a	8.02a
	A	71.75c	21.17b	7.08b
	B	80.58b	16.27c	3.15c
	C	83.51a	12.68d	3.81c
20-40	CK	47.97d	37.48c	14.55a
	A	50.66c	39.42b	9.92b
	B	52.69b	40.59a	6.72c
	C	53.80a	41.64a	4.56d
40-60	CK	20.65a	63.03a	16.32c
	A	19.43a	60.33b	20.24b
	B	20.05a	59.70b	20.25b
	C	19.24a	57.78c	22.98a

CK represents single application of gypsum 15 t·ha^{-1}, A represents gypsum 15 t·ha^{-1} + BHA 0.35 t·ha^{-1}, B represents gypsum 15 t·ha^{-1} + BHA 0.75 t·ha^{-1}, and C represents gypsum 15 t·ha^{-1} + BHA 1.50t·ha^{-1}. The different lowercase letters represent significant differences among treatments in the same soil layer ($p< 0.05$)

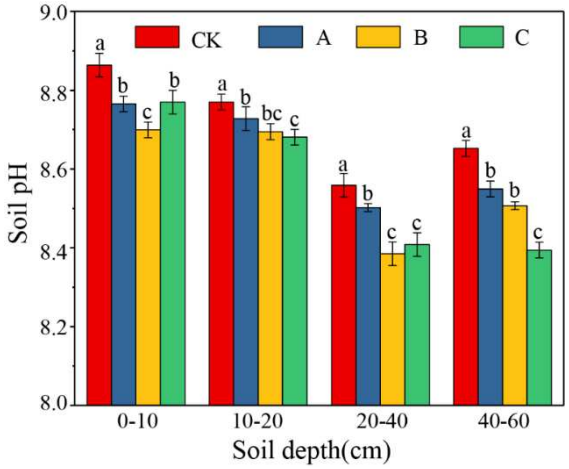

Figure 2. *Influence of gypsum combined with different amount of BHA on soil pH. CK represents single application of gypsum 15 t·ha^{-1}, A represents gypsum 15 t·ha^{-1} + BHA 0.35 t·ha^{-1}, B represents gypsum 15 t·ha^{-1} + BHA 0.75 t·ha^{-1}, and C represents gypsum 15 t·ha^{-1} + BHA 1.50t·ha^{-1}. The error lines represent the standard variance, and different lowercase letters represent significant differences among treatments in the same soil layer ($p< 0.05$)*

The effect of effect of gypsum combined with different amounts of BHA on soil alkalinity

In 0-10 cm soil layer, there was no significant difference between treatment A and gypsum treatment, but it was significantly higher than treatment B and C, and treatment C was significantly lower than other treatments (*Fig. 3*). In 10-20 cm soil layer, treatment A was significantly higher than that of single application of gypsum and treatment B and

http://www.aloki.hu ● ISSN 1589 1623 (Print) ● ISSN 1785 0037 (Online)
DOI: http://dx.doi.org/10.15666/aeer/2001_841854

C (p< 0.05), the difference between each treatment was significant (p< 0.05), and treatment C was the lowest. In 20-40 cm soil layer, the treatment of gypsum combined with BHA was significantly lower than that of single application of gypsum (p< 0.05), and with the increase of the proportion of BHA, the soil alkalinity showed a downward trend. There was no significant difference between treatment B (p> 0.05), treatment A and treatment C, and treatment A was significantly greater than that of treatment C (p< 0.05). There was no significant difference among treatments in 40-60 cm soil layer (p> 0.05).

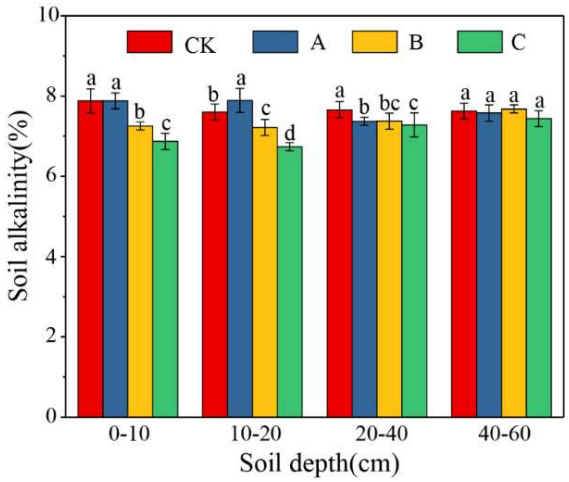

Figure 3. *Influence of gypsum combined with different amount of BHA on soil alkalinity. CK represents single application of gypsum 15 t·ha^{-1}, A represents gypsum 15 t·ha^{-1} + BHA 0.35 t·ha^{-1}, B represents gypsum 15 t·ha^{-1} + BHA 0.75 t·ha^{-1}, and C represents gypsum 15 t·ha^{-1} + BHA 1.50t·ha^{-1}. The error lines represent the standard variance, and different lowercase letters represent significant differences among treatments in the same soil layer (p< 0.05)*

The effect of gypsum combined with different amounts of BHA on soil electric conductibility

Gypsum combined with BHA treatments significantly reduced the electric conductivity of 0-10 cm, 10-20 cm and 20-40 cm soil layers (*Fig. 4*). In 0-10 cm soil layer, there were significant differences among treatments (p< 0.05). With the increase of the application amount of BHA, the soil electric conductivity showed a decreasing trend. Treatment A, B and C decreased by 51.25%, 66.80% and 70.00%, respectively, compared with the treatment of single application of gypsum. In 10-20 cm soil layer, with the increase of BHA application rate, the soil electric conductivity showed a decreasing trend, and there was no significant difference between treatment B and treatment C (p> 0.05). In 20-40 cm soil layer, with the increase of the amount of BHA, there was no significant difference between CK and treatment A and B (p> 0.05), while treatment A was significantly higher than treatment B and C (p< 0.05), and there was no significant difference between treatment B and C (p> 0.05). In the soil layer of 40-60 cm, with the increase of the application amount of BHA, the soil electric conductivity decreased first and then increased. There was no significant difference between CK and treatment A and B (p> 0.05), while there was significant difference between treatment A, B and C (p< 0.05), and treatment C was the highest.

http://www.aloki.hu ● ISSN 1589 1623 (Print) ● ISSN 1785 0037 (Online)
DOI: http://dx.doi.org/10.15666/aeer/2001_841854

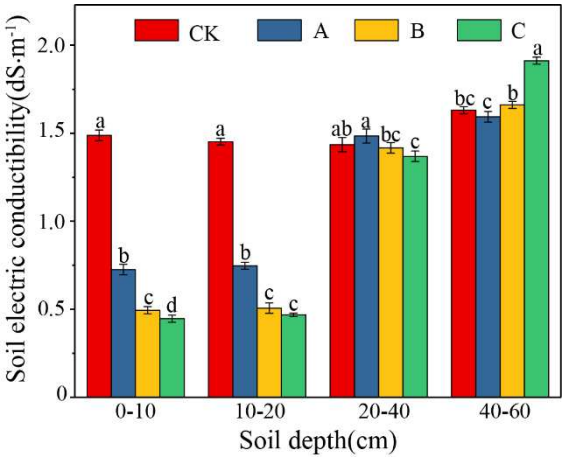

Figure 4. *Influence of gypsum combined with different amount of BHA on soil electric conductibility. CK represents single application of gypsum 15 t·ha^{-1}, A represents gypsum 15 t·ha^{-1} + BHA 0.35 t·ha^{-1}, B represents gypsum 15 t·ha^{-1} + BHA 0.75 t·ha^{-1}, and C represents gypsum 15 t·ha^{-1} + BHA 1.50t·ha^{-1}. The error lines represent the standard variance, and different lowercase letters represent significant differences among treatments in the same soil layer ($p < 0.05$)*

The effect of gypsum combined with different amounts of BHA on soil cation

In 0-10 cm and 20-40 cm soil layers, the K^+ content of gypsum combined with BHA treatment was significantly lower than that of gypsum treatment alone, and the C treatment was the lowest (*Fig. 5a*). Each treatment decreased by 12.35%, 12.47%, 26.18% and 33.45%, 30.99% and 38.50%, respectively, compared with the control. In 10-20 cm soil layer, the K^+ content of each treatment was significantly higher than that of gypsum treatment alone ($p < 0.05$). Treatment A was the highest, with an increase of 48.31%, and treatment C was significantly lower than that of treatment a but significantly higher than that of treatment B ($p < 0.05$). In 40-60 cm soil layer, the K^+ content of each treatment increased significantly, but the increase was small ($p < 0.05$). In the soil layer of 0-10 cm, the Ca^{2+} content of treatment A was significantly higher than that of treatment with single application of gypsum ($p < 0.05$), increased by 3.88%, treatment B was significantly lower than that of treatment A and treatment with single application of gypsum ($p < 0.05$), and the Ca^{2+} content was 6.61% lower than that of treatment with single application of gypsum (*Fig. 5b*). There was no significant difference between treatment C and treatment with single application of gypsum, but it was significantly higher than that of treatment B ($p < 0.05$). In the soil layer of 20-40 cm, the Ca^{2+} content of treatment A, B and C was significantly higher than that of single application of gypsum ($p < 0.05$). There was no significant difference between treatment A and B, but it was significantly lower than that of treatment C. In 40-60 cm soil layer, there was no significant difference among gypsum treatment, A and C treatment, but they were significantly lower than B treatment ($p > 0.05$, *Fig. 5c*). B treatment increased by 45.51% compared with gypsum treatment. In the soil layers of 0-10, 10-20 cm and 20-40 cm, the Na^+ content of gypsum combined with BHA treatment was significantly lower than that of single application of gypsum ($p < 0.05$). With the increase of the application amount of BHA, the Na^+ content showed a downward trend. There was no significant difference between treatments B and C in 0-10 cm soil layer ($p > 0.05$), but it was significantly lower than that of treatment A ($p < 0.05$). There were significant differences between treatments

http://www.aloki.hu ● ISSN 1589 1623 (Print) ● ISSN 1785 0037 (Online)
DOI: http://dx.doi.org/10.15666/aeer/2001_841854

in 10-20 cm and 20-40 cm soil layer ($p< 0.05$). In 40-60 cm soil layer, there was no significant difference between treatment A and gypsum treatment alone ($p> 0.05$). With the increase of the amount of BHA, the Na^+ content showed an increasing trend. There were significant differences among soil Mg^{2+} treatments in 0-10 and 10-20 cm soil layer ($p< 0.05$), and it showed an increasing trend with the increase of the amount of BHA (*Fig. 5d*). The content of Mg^{2+} in 20-40 cm soil layer was significantly higher than that in gypsum treatment alone ($p< 0.05$), and the increase range was B > A > C. The change of soil Mg^{2+} content in 40-60 cm soil layer changed slightly ($p> 0.05$).

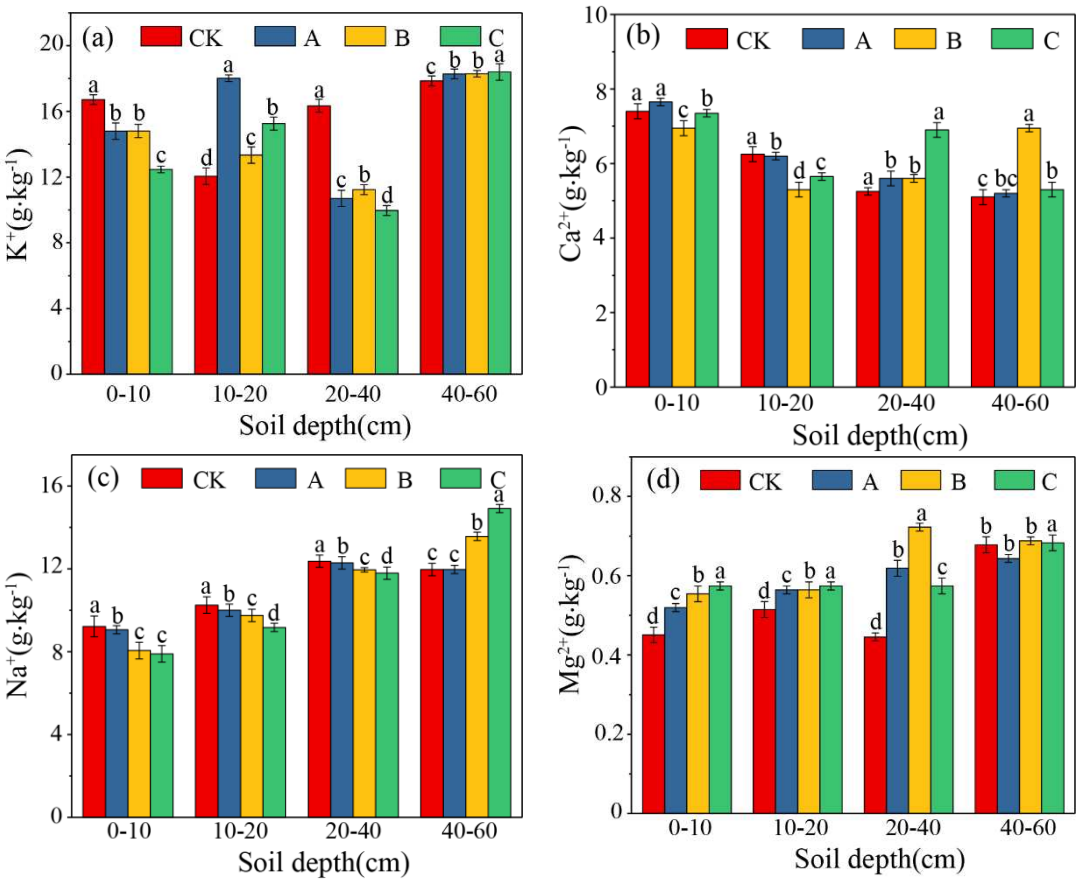

Figure 5. *Influence of gypsum combined with different amount of BHA on soil cation. CK represents single application of gypsum 15 t·ha^{-1}, A represents gypsum 15 t·ha^{-1} + BHA 0.35 t·ha^{-1}, B represents gypsum 15 t·ha^{-1} + BHA 0.75 t·ha^{-1}, and C represents gypsum 15 t·ha^{-1} + BHA 1.50t·ha^{-1}. The error lines represent the standard variance, and different lowercase letters represent significant differences among treatments in the same soil layer ($p< 0.05$)*

The effect of gypsum combined with different amounts of BHA on cotton yield

The difference of cotton yield under each treatment was analyzed (*Fig. 6*). Treatment A, B and C obviously increased the cotton yield. The difference of cotton yield between treatment C was significantly higher than that of other treatments ($p< 0.05$). The combined application of gypsum and BHA was better than that of alone ($p< 0.05$). The cotton yield of treatment A, B and C improved by 5.86%,12.50% and 18.13%, respectively, compared with the treatment of single application of gypsum.

http://www.aloki.hu ● ISSN 1589 1623 (Print) ● ISSN 1785 0037 (Online)
DOI: http://dx.doi.org/10.15666/aeer/2001_841854

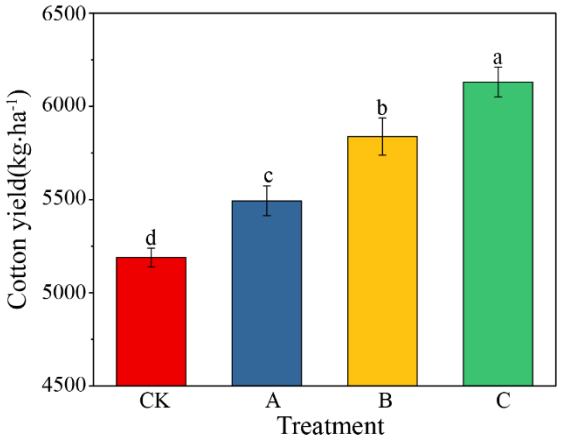

Figure 6. *Influence of different amount of BHA combined with gypsum on cotton yield. CK represents single application of gypsum 15 t·ha^{-1}, A represents gypsum 15 t·ha^{-1} + BHA 0.35 t·ha^{-1}, B represents gypsum 15 t·ha^{-1} + BHA 0.75 t·ha^{-1}, and C represents gypsum 15 t·ha^{-1} + BHA 1.50t·ha^{-1}. The error lines represent the standard variance, and different lowercase letters represent significant differences among treatments in the same soil layer ($p < 0.05$)*

Discussion

The combination of gypsum and different amount of BHA can improve soil physicochemical properties

Our results showed that the combined application of gypsum and different amounts of biochemical humic acid (BHA) increased the percentage of large aggregates and decreased the percentage of small and micro aggregates in the topsoil soil (0-40 cm, *Table 2*). The increase order of large aggregates was C (gypsum 15 t·ha^{-1} + BHA 1.50 t·ha^{-1}) >B (gypsum 15 t·ha^{-1} + BHA 0.75 t·ha^{-1}) > A (gypsum 15 t·ha^{-1} + BHA 0.35 t·ha^{-1}). The effect of combined application of gypsum and BHA on soil porosity (*Fig. 1*) and aggregates (*Table 2*) was significantly higher than that of single application of gypsum ($p < 0.05$). Different combined application schemes significantly improve the content of large aggregates (> 0.25 mm) in soil ($p < 0.05$). Chen et al. (2020) reported that with the increase of gypsum application, the content of soil water stable aggregates increased significantly. It is concluded that Ca^{2+} produced by gypsum directly participates in the formation of soil organic-inorganic complex, which is an important mechanism for the improvement of alkaline soil aggregate structure (Knevitz et al., 2021). With the increase of the amount of gypsum and BHA, the soil porosity showed an increasing trend, and the soil porosity increased significantly under the maximum amount of gypsum and BHA (*Fig. 1*). Han et al. (2016) also found that the mixed modifier of gypsum and humic acid increased the total soil porosity by 0.16%-10.52% compared with the basic soil. Our results showed that the total soil porosity increased with the increase of modifier application, showing a significant positive correlation (*Fig. 1*). In this study, the pH (*Fig. 2*), alkalinity (*Fig. 3*) and electric conductivity (*Fig. 4*) of topsoil soil decreased significantly after the combined application of gypsum and BHA ($p < 0.05$), which is consistent with the conclusion that the application of modifier in soil significantly reduced the pH value and alkalinity of soil found by Koralegedara et al. (2017) and Li et al. (2012). The reason is that Na^{+} in soil colloid is replaced by Ca^{2+} in gypsum, which reduces the salt and alkali content in soil and leaches it in combination with irrigation to achieve the

http://www.aloki.hu ● ISSN 1589 1623 (Print) ● ISSN 1785 0037 (Online)
DOI: http://dx.doi.org/10.15666/aeer/2001_841854

purpose of soil improvement (Watts and Dick, 2014; Mao et al., 2015). Our results showed that after the combined application of gypsum and BHA, the soil electric conductivity of 0-40 cm soil layer decreased and that of 40-60 cm soil layer increased (*Fig. 4*). This may be due to the increase of porosity, water permeability and air permeability of soil surface layer caused by the application of gypsum and BHA (Armando et al., 2021). With irrigation and leaching, salt moves underwater and accumulates in the lower layer (40-60 cm), it leads to the increase of soil electric conductivity. The decrease of Na^+ content in 0-20 cm soil layer was the largest (*Fig. 5b*), because Ca^{2+} provided by gypsum replaces Na^+ adsorbed on soil colloid. The decrease of Ca^{2+} content (*Fig. 5c*) may be due to the replacement reaction between Ca^{2+} and Na^+, resulting in the precipitation reaction between Ca^{2+} and HCO_3^- and CO_3^{2-} in the soil, which reduces the content of soil Ca^{2+} (Zhu et al., 2020). The content of Mg^{2+} in soil increased (*Fig. 5d*), which was mainly related to the chemical exchange of Na^+ and Mg^{2+} (Cera et al., 2021).

The combination of gypsum and different amount of BHA increase the cotton yield

Numerous investigations suggest shows that gypsum has fine particles and low water content, which can be directly applied to saline-alkali soil to accelerate desalination, improve soil structure and increase soil permeability (Aydemir and Najjar, 2005; Yu et al., 2014; Koralegedara et al., 2019; Liu et al., 2021; Zhang et al., 2021). In addition, gypsum contains a large number of trace and nutrient elements, which can also promote plant growth and improve the emergence rate and yield of crops in saline alkali land (Wang et al., 2017b; Zhao et al., 2018; Cao et al., 2019). In this study, with the increase of the amount of gypsum combined with BHA, the cotton yield showed an increasing trend, reaching the maximum when gypsum 15 $t{\cdot}ha^{-1}$ and BHA 1.50$t{\cdot}ha^{-1}$ was applied (*Fig. 6*). The effect of gypsum combined with BHA on cotton yield was better than that of single application ($p< 0.05$). At the same time, Ali et al. (2018) showed that the combined application of humic acid provided sufficient nutrients for soil and crops, improved the disease resistance of crops, and increased the yield of cabbage and maize. Wong et al. (2009) found that the application of gypsum modifier in saline-alkali land could significantly improve the emergence rate and fresh grass yield of alfalfa. On the one hand, the application of gypsum and BHA participate in the formation of soil aggregate structure, improves soil aggregate structure (Kim et al., 2017), and adjusts soil pH. On the other hand, the application of gypsum increases S, Ca, Si and other elements beneficial to plant growth, improves plant resistance to harsh environment, improves nutrient deficiency, which is beneficial to crop growth (Mailapalli and Thompson, 2011).

In summary, the combined application mode of gypsum 15 $t{\cdot}ha^{-1}$ and BHA 1.50 $t{\cdot}ha^{-1}$ is more suitable for agricultural production. The combined application of gypsum and BHA can solve the problem of industrial waste treatment and optimize the utilization of resources.

Conclusions

1) Gypsum combined with different amounts of biochemical humic acid (BHA) had an obvious effect on the increase of soil porosity and the number of large aggregates.

2) After applying gypsum and BHA, the pH value, alkalinity and electric conductivity of topsoil soil decreased, and the combined application effect was better than that of single application of gypsum.

http://www.aloki.hu ● ISSN 1589 1623 (Print) ● ISSN 1785 0037 (Online)
DOI: http://dx.doi.org/10.15666/aeer/2001_841854

However, as an industrial waste, gypsum contains a certain amount of heavy metals. Whether long-term application will cause some environmental problems has not been studied clearly. Therefore, how to further improve cotton yield on the basis of improving saline-alkali land without causing environmental pollution is a problem that we will continue to pay attention to and study in the future.

Acknowledgements. This work was supported by the Major Special Science and Technology Project of Xinjiang Province (2020A01002-1).

REFERENCES

[1] Ali, S., Jan, A., Manzoor, Sohail, A., Khan, A., Khan, M. I., Inamullah, Zhang, J., Daur, I. (2018): Soil amendments strategies to improve water-use efficiency and productivity of maize under different irrigation conditions. – Agricultural Water Management 210: 88-95.

[2] Armando, V., Dazzi, C., Delgado, A., Barros, H., Scalenghe, R., Sim, U. (2021): Relief and calcium from gypsum as key factors for net inorganic carbon accumulation in soils of a semiarid Mediterranean environment. – Geoderma 398: 115115.

[3] Aydemir, S., Najjar, N. F. (2005): Application of two amendments (gypsum and langbeinite) to reclaim sodic soil using sodic irrigation water. – Australian Journal of Soil Research 43: 547-553.

[4] Cao, Y., Gao, Y., Li, J., Tian, Y. (2019): Straw composts, gypsum and their mixtures enhance tomato yields under continuous saline water irrigation. – Agricultural Water Management 223: 105721.

[5] Cera, A., Montserrat-Martí, G., Pedro, J., Drenovsky, R. E., Palacio, S. (2021): Gypsum-exclusive plants accumulate more leaf S than non-exclusive species both in and off gypsum. – Environmental and Experimental Botany 182: 104294.

[6] Chen, X. D., Yaa, O. K., Wu, J. (2020): Effects of different organic materials application on soil physicochemical properties in a primary saline-alkali soil. – Eurasian Soil Science 53: 798-808.

[7] Fu, Y., Tian, Z., Amoozegar, A., Heitman, J. (2019): Measuring dynamic changes of soil porosity during compaction. – Soil and Tillage Research 193: 114-121.

[8] Han, Y. S., Tokunaga, T. K., Salve, R., Chon, C. M. (2016): Environmental feasibility of soil amendment with flue gas desulfurization gypsum (FGDG) for terrestrial carbon sequestration. – Environmental Earth Sciences 75: 1-9.

[9] Heng, T., Liao, R., Wang, Z., Wu, W., Li, W., Zhang, J. (2018): Effects of combined drip irrigation and sub-surface pipe drainage on water and salt transport of saline-alkali soil in Xinjiang, China. – Journal of Arid Land 10: 932-945.

[10] Kim, Y., Choo, B., Cho, J. (2017): Effect of gypsum and rice straw compost application on improvements of soil quality during desalination of reclaimed coastal tideland soils: Ten years of long-term experiments. – Catena 156: 131-138.

[11] Knevitz, R., Basso, D., Laerson, G., Mallmann, K. (2021): Limestone and gypsum reapplication in an oxisol under no-tillage promotes low soybean and corn yield increase under tropical conditions. – Soil and Tillage Research 214: 105165.

[12] Koralegedara, N. H., Al-Abed, S. R., Rodrigo, S. K., Karna, R. R., Scheckel, K. G., Dionysiou, D. D. (2017): Alterations of lead speciation by sulfate from addition of flue gas desulfurization gypsum (FGDG) in two contaminated soils. – Science of The Total Environment 575: 1522-1529.

[13] Koralegedara, N. H., Pinto, P. X., Dionysiou, D. D., Al-Abed, S. R. (2019): Recent advances in flue gas desulfurization gypsum processes and applications - A review. – Journal of environmental management 251: 109572.

http://www.aloki.hu ● ISSN 1589 1623 (Print) ● ISSN 1785 0037 (Online)
DOI: http://dx.doi.org/10.15666/aeer/2001_841854

[14] Li, M., Jiang, L., Sun, Z., Wang, J., Rui, Y., Zhong, L., Wang, Y., Kardol, P. (2012): Effects of flue gas desulfurization gypsum by-products on microbial biomass and community structure in alkaline-saline soils. – Journal of Soils and Sediments 12: 1040-1053.
[15] Liang, J., Li, Y., Si, B., Wang, Y., Chen, X., Wang, X., Chen, H., Wang, H., Zhang, F., Bai, Y., Biswas, A. (2021): Optimizing biochar application to improve soil physical and hydraulic properties in saline-alkali soils. – Science of the Total Environment 771: 144802.
[16] Liu, M., Wang, C., Liu, X., Lu, Y., Wang, Y. (2020): Saline-alkali soil applied with vermicompost and humic acid fertilizer improved macroaggregate microstructure to enhance salt leaching and inhibit nitrogen losses. – Applied Soil Ecology 156: 103705.
[17] Liu, S., Liu, W., Jiao, F., Qin, W., Yang, C. (2021): Production and resource utilization of flue gas desulfurized gypsum in China - A review. – Environmental Pollution 288: 117799.
[18] Mailapalli, D. R., Thompson, A. M. (2011): Polyacrylamide coated MilorganiteTM and gypsum for controlling sediment and phosphorus loads. – Agricultural Water Management 101: 27-34.
[19] Mao, G., Xu, X., Chen, Q., Yue, Z., Zhu, L. (2014). Flue gas desulfurization gypsum by-products alters cytosolic Ca^{2+} distribution and Ca^{2+}-ATPase activity in leaf cells of oil sunflower in alkaline soil. – Journal of Plant Interactions 9: 152-158.
[20] Mao, Y., Li, X., Dick, W. A., Chen, L. (2015): Remediation of saline–sodic soil with flue gas desulfurization gypsum in a reclaimed tidal flat of southeast China. – Journal of Environmental Sciences 45: 224-232.
[21] Nan, J., Chen, X., Wang, X., Lashari, M. S., Wang, Y., Guo, Z., Du, Z. (2016): Effects of applying flue gas desulfurization gypsum and humic acid on soil physicochemical properties and rapeseed yield of a saline-sodic cropland in the eastern coastal area of China. – Journal of Soils and Sediments 16: 38-50.
[22] Sakai, Y., Matsumoto, S., Sadakata, M. (2004): Alkali soil reclamation with flue gas desulfurization gypsum in China and assessment of metal content in corn grains. – Soil and Sediment Contamination 13: 65-80.
[23] Wang, Q., Men, L., Gao, L., Tian, Y. (2017a): Effect of grafting and gypsum application on cucumber (*Cucumis sativus* L.) growth under saline water irrigation. – Agricultural Water Management 188: 79-90.
[24] Wang, S. J., Chen, Q., Li, Y., Zhuo, Y. Q., Xu, L. Z. (2017b): Research on saline-alkali soil amelioration with FGD gypsum. – Resources, Conservation and Recycling 121: 82-92.
[25] Wang, X., Wang, J., Wang, J. P. (2021): Seasonality of soil respiration under gypsum and straw amendments in an arid saline-alkali soil. – Journal of Environmental Management 277: 111494.
[26] Watts, D. B., Dick, W. A. (2014): Sustainable uses of FGD gypsum in agricultural systems: introduction. – Journal of Environmental Quality 43: 246-252.
[27] Wong, V. N. L., Dalal, R. C., Greene, R. S. B. (2009): Carbon dynamics of sodic and saline soils following gypsum and organic material additions: A laboratory incubation. – Applied Soil Ecology 41: 29-40.
[28] Xia, J., Ren, J., Zhang, S., Wang, Y., Fang, Y. (2019): Forest and grass composite patterns improve the soil quality in the coastal saline-alkali land of the Yellow River Delta, China. – Geoderma 349: 25-35.
[29] Yan, F., Zhang, F., Fan, J., Hou, X., Bai, W., Liu, X., Wang, Y., Pan, X. (2021): Optimization of irrigation and nitrogen fertilization increases ash salt accumulation and ions absorption of drip-fertigated sugar beet in saline-alkali soils. – Field Crops Research 271: 108247.
[30] Yu, H., Yang, P., Lin, H., Ren, S., He, X. (2014): Effects of sodic soil reclamation using flue gas desulphurization gypsum on soil pore characteristics, bulk density, and saturated hydraulic conductivity. – Soil Science Society of America Journal 78: 1201-1213.

http://www.aloki.hu ● ISSN 1589 1623 (Print) ● ISSN 1785 0037 (Online)
DOI: http://dx.doi.org/10.15666/aeer/2001_841854

[31] Zhang, Y., Yang, J., Yao, R., Wang, X., Xie, W. (2020): Short-term effects of biochar and gypsum on soil hydraulic properties and sodicity in a saline-alkali soil. – Pedosphere 30: 694-702.
[32] Zhang, W., Zhang, W., Wang, S., Liu, J., Li, Y., Zhuo, Y., Xu, L., Zhao, Y. (2021): Band application of flue gas desulfurization gypsum improves sodic soil amelioration. – Journal of Environmental Management 298: 113535.
[33] Zhao, Y., Wang, S., Li, Y., Liu, J., Zhuo, Y., Zhang, W., Wang, J., Xu, L. (2018): Long-term performance of flue gas desulfurization gypsum in a large-scale application in a saline-alkali wasteland in northwest China. – Agriculture, Ecosystems and Environment 261: 115-124.
[34] Zhao, Y., Wang, S., Li, Y., Zhuo, Y., Liu, J. (2019): Effects of straw layer and flue gas desulfurization gypsum treatments on soil salinity and sodicity in relation to sunflower yield. – Geoderma 352: 13-21.
[35] Zhao, Y., Li, Y., Wang, S., Wang, J., Xu, L. (2020): Combined application of a straw layer and flue gas desulphurization gypsum to reduce soil salinity and alkalinity. – Pedosphere 30: 226-235.
[36] Zhou, B., Yang, L., Chen, X., Ye, S., Peng, Y., Liang, C. (2021): Effect of magnetic water irrigation on the improvement of salinized soil and cotton growth in Xinjiang. – Agricultural Water Management 248: 106784.
[37] Zhu, H., Yang, J., Yao, R., Wang, X., Xie, W., Zhu, W., Liu, X., Cao, Y., Tao, J. (2020): Interactive effects of soil amendments (biochar and gypsum) and salinity on ammonia volatilization in coastal saline soil. – Catena 190: 104527.

http://www.aloki.hu ● ISSN 1589 1623 (Print) ● ISSN 1785 0037 (Online)
DOI: http://dx.doi.org/10.15666/aeer/2001_841854

ASSESSMENT OF GENETIC VARIATION IN WILD MYRTLE (*MYRTUS COMMUNIS* L.) GENOTYPES GROWING AROUND THE MEDITERRANEAN REGION OF TURKEY

TÜZÜN-KIS, B. – İKTEN, H.*

Department of Agricultural Biotechnology, Faculty of Agriculture, Akdeniz University, Antalya, Turkey

**Corresponding author*
e-mail: haticeikten@akdeniz.edu.tr

(Received 28th Sep 2021; accepted 22nd Dec 2021)

Abstract. Myrtle (*Myrtus communis*) grows naturally on the Mediterranean coast and the Aegean region of Turkey and is used as medicine, food and ornamental plant. Availability of genetic resources with genetic diversity constitutes an important material for researching genes that may be needed in future breeding studies. The goal of this study was to analyze the genetic diversity of the myrtle genotypes in order to develop further cultivation, regeneration or breeding strategies. Nine traits (length, width, weight and color of the fruit, number of seeds, weight of seeds, pulp weight, length, and width of the leaf) were evaluated. PCR amplification was performed using Simple Sequence Repeats (SSR) and Inter- Primer Binding (iPBS) primers. The variation was found between genotypes in terms of the morphological characters considered. Using molecular analyses, the genetic diversity among the genotypes was determined based on the 64 SSR and 80 polymorphic iPBS bands. The genetic variation obtained by morphological and molecular analyses shows that these genotypes may be useful for future breeding and cultivation practices and can be considered as valuable genetic resources. It has also been shown that some of the iPBS primers were highly polymorphic and can be used in phylogenetic analyzes and mapping studies of myrtle.
Keywords: *genetic relationship, genetic resources, iPBS, SSR, diversity*

Introduction

Myrtle (*Myrtus communis* L.) is a diploid (2n = 2x = 22), medicinal and aromatic plant and grows wildly on the rocky slopes, *Pinus brutia* forests and coastal regions of the Mediterranean Basin (Özkan and Güray, 2009). These plants can reach up to 5 m in height and grow at altitudes ranging from 50–500 m above sea level. It is an evergreen shrub with ovate lanceolate leaves, white flowers and is very aromatic because of the high oil content of its leaves (Agrimonti et al., 2006). The fruits have two different color (*Fig. 1*), a dark blue and a white (yellowish-white) form (Traveset et al., 2001; Messaoud et al., 2011; Serçe et al., 2010). Dark blue fruits contain higher polyphenolic content and antioxidant activity than white fruits and they are rich in α-pinene, linalool and α-terpineol whereas white fruits were rich in myrtenyl acetate and unsaturated fatty acids like linoleic and oleic acids (Messaoud et al., 2011) and myrtle pigmented berries are a good anthocyanin source. The myrtle has value as ornamental and aromatic plant and shows hypoglycemic, antimicrobial, antihemorrhagic properties (Özek et al., 2000; Sepici et al., 2004). The aromatic leaves contain essential oil which are used in the pharmaceutical, cosmetic, food industries (Mulas, et al., 1998; Messaoud et al., 2005) and for liquor production. Nineteen compounds, concerning mostly to polyphenol compounds and a new class of hydrolysable tannins were identified in these berries (mostly in seeds) for the first time by D'Urso et al. (2017). Composition of essential oils found quite variable with a number of compounds ranging from 31 to 78 depending on

http://www.aloki.hu ● ISSN 1589 1623 (Print) ● ISSN 1785 0037 (Online)
DOI: http://dx.doi.org/10.15666/aeer/2001_855873

cultivar (Usai et al., 2020). There is an increasing interest to myrtle for medicinal uses and food industries. The increasing demand is causing uncontrolled collection of leaves and berries from the wild plants. To protect the genetic resources and control of reduction of myrtle populations, a domestication program and a conservation program was carried out starting in 1995 in Sardinia island (Mulas and Cani, 1999) and evaluation of the selected genotypes and breeding programs within the scope of this program continues (Medda and Mulas, 2021). The same scenario is also true for Turkey. Uncontrolled harvesting of leaves, and fruits, cutting branches for ornamental usage, decoration at traditional wedding ceremonies (Özkan and Güray, 2009) and increased construction activity cause the reduction of diversity of genotypes. Genetic diversity is a major benchmark in the choice of genetic resources and wild genotypes are important particularly for tolerance to biotic and abiotic stresses. Well-characterized genetic resources play an important role in guiding breeding studies, since breeders are usually looking for plant material containing desirable agricultural traits (e.g. disease resistance, or fruit traits). Management of genetic resources by morphological and molecular characterization, evaluation and conservation is necessary to maximize the benefits of genetic resources. Analysis of genetic diversity in germplasm collections can provide reliable classification of genotypes and help to understand the capacity of the gene pool for specific breeding purposes. Therefore, morphological, and molecular characterization of germplasm is an essential tool and ideally molecular characterization should be carried out by a suitable a marker system that is polymorphic and can reveal genetic variations. A limited number of studies have been conducted on morphological characterization of myrtle (Ciccarelli et al., 2008; Serçe et al., 2010; Messaoud and Boussaid, 2011).

Figure 1. *Myrtus communis samples collected from: (A) Mersin, Erdemli-Kumkuyu, white fruited morphs, (B) Muğla, Marmaris-Armutalan, dark blue fruited morphs*

Studies at the molecular level for the identification, characterization and relatedness analysis of *Myrtus communis* (myrtle; Myrtaceae) have been performed using molecular markers, such as AFLP (Bruna et al., 2005; Agrimonti et al., 2006; Bruna et al., 2007; Albaladejo et al., 2009; Melito et al., 2014, 2016, 2017; Messaoud et al., 2011), RAPD (Messaoud et al., 2007), ISSR (Melito et al., 2013; Sımsek et al., 2019), SRAP

http://www.aloki.hu ● ISSN 1589 1623 (Print) ● ISSN 1785 0037 (Online)
DOI: http://dx.doi.org/10.15666/aeer/2001_855873

(Ghafouri and Rahimmalek, 2018) and SSR (Albaladejo et al., 2010; Nora et al., 2014; Corona et al., 2017; Mele et al., 2019).

The goal of this study was to analyse the genetic diversity of the naturally grown myrtle genotypes around the Mediterranean Region of Turkey based on morphological and molecular characterization in order to develop further cultivation, regeneration or breeding strategies. Molecular characterization was performed by using iPBS Kalendar et al. (2010) and previously described SSR primers by Albaladejo et al. (2010).

SSR markers have some advantages over other marker systems that include high potential for automation, co-dominant inheritance, distribution throughout the genome, high levels of polymorphism and repeatability. Small amount of DNA is sufficient for amplification of SSR markers (Park et al., 2009) and have been successfully used to examine genetic diversity, fingerprinting and genotyping in different plant species (Abdurakhmonov, 2016).

The inter-primer binding site (iPBS) amplification technique utilizes the conserved parts of - primer binding site (PBS) sequences that are universally found almost all long terminal repeats (LTR) retrotransposon and used for determining the variations caused by retrotransposon movements or recombinations (Kalendar and Schulman, 2014). The LTR transposon elements contain a conserved region for binding of tRNA that act as a primer in the conversion of the retrotransposon RNA to DNA before enters its new position in the genome. iPBS markers (Kalendar et al., 2010; Kalendar and Schulman, 2014) have been used to investigate the genetic relationship among the genotypes of apricot (*Prunus armeniaca* L.) (Baránek et al., 2012) and apple (*Malus pumila* Mill.) (Kuras et al., 2013), guava (*Psidium guajava* L.) (Mehmood et al., 2015), grapevine (*Vitis vinifera* L. ssp. sativa D.C.) (Milovanov et al., 2019), Laurel (*Laurus nobilis* L.) (Karık et al., 2019), wild Cicer species (Andeden et al., 2013), pea (Pisum sativum) (Baloch, 2015), Motherwort (*Leonurus cardiaca* L.) (Borna et al., 2016). To our knowledge, no prior studies have examined iPBS markers in *Myrtus communis.*

Genetically diverse germplasm resources constitute an important material for researching genotypes that may carry the desired characters. Identification and protection of *Myrtus communis* genotypes which are widely grown naturally in the Mediterranean and Aegean coasts of Turkey, are important in terms of providing material for future breeding studies and preserving genetic diversity.

Material and methods

Plant material

The 48 myrtle genotypes were used as study material (*Table 1*). The leaves and fruit samples were collected from 20 different locations (included 8 provinces) covering an area of ~1200 km along the Mediterranean coastline and Aegean region of Turkey in the period of fruit ripening (October to January) in 2017 and 2018 from either very ancient myrtle trees or young shrubs (*Fig. 2*). The map in *Figure 3* and *Table 1* shows the sampling locations.

Morphological analysis

On each genotype nine morphological traits (length, width, weight and color of the fruit, number of seeds, weight of seeds, pulp weight, length and width of the leaf) were evaluated. The samples were examined morphologically using the method described by

http://www.aloki.hu ● ISSN 1589 1623 (Print) ● ISSN 1785 0037 (Online)
DOI: http://dx.doi.org/10.15666/aeer/2001_855873

Melito et al. (2016) and Uzun et al. (2016). The fruits were harvested and measured in full ripening stage and a sample of 50 fruits and leaves was taken from each genotype from all sides of the shrubs. The leaves were stored at – 70 °C for further molecular analysis. All analyses of morphological characteristic were performed using analysis of variance (ANOVA) in SPSS 20.0 software package (IBM, 2020). Normality test performed, and the data showed normal distribution. Variance analysis (one-way ANOVA-Duncan) was used to determine variations among the genotypes based on measured properties. Pearson's correlation analysis was performed to find correlation between the morphological characteristics and altitude.

Figure 2. *(a) The 'Old myrtle' shrub (Antalya, Bahtılı), (b) myrtle shrub (Antalya-Göynük)*

Figure 3. *The sampling areas in the Mediterranean Region of Turkey*

http://www.aloki.hu ● ISSN 1589 1623 (Print) ● ISSN 1785 0037 (Online)
DOI: http://dx.doi.org/10.15666/aeer/2001_855873

Table 1. *List of the studied genotypes, their identification codes, fruit color, location, geographical coordinates of the collection sites*

Genotype code	Fruit color	Introduced genotype location	Longitude	Latitude	Altitude (m)
Hty1B	Dark blue	Hatay, Samandağı, Fidanlı	E36°01'28.54"	N36°09'04.75"	141
Ant3B	Dark blue	Antalya, Kumluca, Belen	E30°23'34.80"	N36°22'28.66"	505
Ant4W	White	Antalya, Kumluca, Belen	E30°23'34.80"	N36°22'28.66"	505
Ant5W	White	Antalya, Kumluca, Belen	E30°23'34.80"	N36°22'28.66"	505
Ant6W	White	Antalya, Kumluca, Belen	E30°23'34.80"	N36°22'28.66"	505
Ant7B	Dark blue	Antalya, Alanya, Okurcalar	E31°41'51.00"	N36°39'00.00"	23
Ant8W	White	Antalya, Alanya, Okurcalar	E31°41'51.00"	N36°39'00.00"	23
Ant9B	Dark blue	Antalya, Göynük Kanyon	E30°32'02.75"	N36°40'57.40"	64
Ant10B	Dark blue	Antalya Göynük Kanyon	E30°32'02.75"	N36°40'57.40"	64
Ant11W	White	Antalya, Kemer, Arslanbucak	E30°33'35.14"	N36°36'10.05"	122
Ant12W	White	Antalya, Kemer, Kuzdere	E30°31'53.71"	N36°34'59.51"	45
Ant13W	White	Antalya, Kemer, Kuzdere	E30°31'53.71"	N36°34'59.51"	45
Ant14B	Dark blue	Antalya, Kemer, Çamyuva	E30°34'00.00"	N36°34'00.00"	9
Ant15B	Dark blue	Antalya, Kemer, Çamyuva	E30°34'00.00"	N36°34'00.00"	9
Ant16B	Dark blue	Antalya, Kemer, Tekirova	E30°31'35.01"	N36°30'06.93"	14
Ant17W	White	Antalya, Kemer, Tekirova	E30°31'35.01"	N36°30'06.93"	14
Isp18W	White	Isparta, Çobanpınar	E30°48'24.23"	N37°23'03.06"	339
Ant19B	Dark blue	Antalya, Alanya, Dereköy	E32°02'01.54"	N36°39'31.24"	659
Ant20W	White	Antalya, Manavgat, Hatipler	E31°24'38.94"	N36°48'40.10"	42
Ant21W	White	Antalya, Finike, Sahilkent	E30°12'17.06"	N36°20'15.72"	21
Ant22B	Dark blue	Antalya, Akdeniz Univ.	E30°39'07.97"	N36°53'31.48"	27
Ant23B	Dark blue	Antalya, Akdeniz Univ.	E30°39'07.97"	N36°53'31.48"	27
Izm24W	White	İzmir, Değirmen Dere	E27°08'58.03"	N27°37'37.83"	20
Izm25B	Dark blue	İzmir, Değirmen Dere	E27°08'58.03"	N27°37'37.83"	20
Izm26W	White	İzmir, Değirmen Dere	E27°08'58.03"	N27°37'37.83"	20
Mgl27W	White	Muğla, Datça	E27°41'09.04"	N36°43'34.38"	10
Mgl28B	Dark blue	Muğla, Datça	E27°41'09.04"	N36°43'34.38"	10
Mgl29W	White	Muğla, Marmaris, Armutalan	E28°14'15.13"	N36°51'23.64"	37
Mgl30B	Dark blue	Muğla, Marmaris, Armutalan	E28°14'15.13"	N36°51'23.64"	37
Izm31B	Dark blue	İzmir, Menemen, Yamanlar	E27°13'38.47"	N38°32'44.90"	946
Ayd32B	Dark blue	Aydın	E28°29'11.03"	N37°48'42.13"	1358
Ant33B	Dark blue	Antalya, Bahtılı	E30°34'27.71"	N36°53'16.82"	38
Ant34W	White	Antalya, Serik, Şatırlı	E30°34'27.71"	N36°53'16.82"	15
Ant35W	White	Antalya, Konyaaltı	E30°42'47.96"	N36°53'48.81"	56
Ant36W	White	Antalya, Geyikbayırı	E30°27'53.86"	N36°52'31.58"	614
Ant37B	Dark blue	Antalya, Gökçam	E30°32'46.99"	N36°53'41.11"	66
Ant38B	Dark blue	Antalya, Gökçam	E30°32'46.99"	N36°53'41.11"	66
Ant44B	Dark blue	Antalya, Gökçam	E30°32'46.99"	N36°53'41.11"	66
Mrs48W	White	Mersin, Erdemli, Kumkuyu	E34°12'00.00"	N36°32'00.00"	183
Mrs49W	White	Mersin, Erdemli, Kumkuyu	E34°12'00.00"	N36°32'00.00"	183
Mrs50B	Dark blue	Mersin, Erdemli, Ayaş	E34°11'00.00"	N36°29'00.00"	0
Ant51B	Dark blue	Antalya, Döşemealtı	E30°36'04.35"	N37°01'22.89"	302
Ant52B	Dark blue	Antalya, Döşemealtı	E30°36'04.35"	N37°01'22.89"	302
Ant53W	White	Antalya, Döşemealtı	E30°36'04.35"	N36°55'16.06"	302
Hty55B	Dark blue	Hatay, Erzin, Kuzuyuk	E36°16'12.10"	N37°01'22.89"	469
Hty56W	White	Hatay, Erzin, Kuzuyuk	E36°16'12.10"	N36°55'16.06"	469
Ant57B	Dark blue	Antalya, Alanya, Okurcalar	E31°41'51.00"	N36°39'00.00"	23
Mgl59W	White	Muğla, Fethiye	E29°07'34.85"	N36°39'33.29"	25

Molecular analysis

DNA extraction

Genomic DNA was extracted from leaf tissues of 48 genotypes using a modified cetyltrimethylammonium bromide (CTAB) method (Doyle and Doyle, 1990). The leaves (200 mg) were cut into small pieces with a help of scalpel and grind to a fine

http://www.aloki.hu ● ISSN 1589 1623 (Print) ● ISSN 1785 0037 (Online)
DOI: http://dx.doi.org/10.15666/aeer/2001_855873

paste in a 600 µl CTAB buffer (2% CTAB, EDTA 20 mM, Tris-Cl 100 mM, NaCl 1.4 M, 0.2% Mercaptoethanol) using mortar and pestle. The CTAB/plant extract mixture transferred to the Eppendorf tube and incubated 1 h at 65 °C. After two times Chloroform: Isoamyl alcohol (24:1) treatment and 15 min centrifugation was performed at 13,000 × g, then upper aqueous phase was transferred to clean tube and 500 µl isopropanol alcohol added. Following the centrifugation for 15 min, the upper phase was discarded. The pellet was washed with 70% ethanol two times and leave to dry (approximately 15 min) at the room temperature. The quality of DNA was checked by 1% agarose gel electrophoresis with ethidium bromide staining.

DNA amplification with SSR

PCR amplification was performed using 12 SSR primer pairs developed by Albaladejo et al. (2010) (*Table 4*). PCR reactions were performed in a 15-µl volume containing 20-30 ng genomic DNA, 0.2 mM dNTPs, 1.5 mM MgCl2, 0.5 µM each primer, and 1 U Taq DNA polymerase (Thermo). An adaptor sequences (GGAAACAGCTATGACCAT) were ligated to at its 5' end of the reverse primers and fluorescently labeled with either IRDye 700 or IRDye 800 fluorescent dyes according to the protocol by Schuelke (2000).

Amplifications were conducted using a program with an initial denaturation step at 95 °C for 3 min. followed by 35 cycles at 94 °C for 45 s, 50–65 °C for 30 s and 72 °C for1 min with a final cycle of 72 °C for 5 min. A 1.5- to 2-µl aliquot of PCR product (depending on the performance of amplification of each primer pair) was mixed with10 µl of loading dye including 98% formamide, 10 mM EDTA, 0.25% bromophenol blue, 0.25% xylenecyanol and denatured at 95 °C for 4 min. and placed in ice until loaded. PCR products were separated on a 25 cm 6% polyacrylamide gel (0.25 mm thick) containing acrylamide: bis-acrylamide (19:1), 8 M urea, and TBE 1X using a 32-well square comb. The separated bands were visualized in a Li-Cor -IR2 4200 Genetic Analyzer (Li-Cor Biosciences).

DNA amplification with iPBS

Twelve iPBS primers were selected from the study of Kalender et al. (2010) (*Table 5*). DNA amplification was carried out by using a modified protocol of Kalendar et al. (2010). PCR was performed in a volume of 15 µL containing10 mM Tris–HCl (pH 9.0), 50 mM KCl, 1.5 mM MgCl2, 0.2 mM of each dNTP, 10 pmol of each primer, 50 ng genomic DNA, and 1U Taq DNA polymerase (Thermo) using the following temperature profile: 95 °C for 3 min, 35 cycles of denaturation at 94 °C for 30 s, annealing at 50–60 °C (the annealing temperature varied depending on the primer used) for 45 s and 72 °C for 1 min, and an extension step at 72 °C for 5 min. PCR was performed two times for some primers to confirm band pattern consistency. Products were separated by gel electrophoresis in 2% (w/v) agarose gels and visualized by staining ethidium bromide under UV light.

Data analysis

The allelic data matrix of "1" or "0" was used to calculate the genetic analysis by using NTSYS (Numeracal Taxonomy Multivariate Analysis System, NTSYS-pc version 2.1 Exeter Software, Setauket, N.Y. USA (Rohlf, 1993). A genetic similarity matrix was constructed with in the SIMGEND module and similarity matrices were utilized to

http://www.aloki.hu ● ISSN 1589 1623 (Print) ● ISSN 1785 0037 (Online)
DOI: http://dx.doi.org/10.15666/aeer/2001_855873

construct the UPGMA (unweighted pair group method with arithmetic average) dendrograms. Principal component analysis (PCA) was performed to show the differences among the genotypes. Eigen values were calculated using the EIGEN module and based on the variance–covariance matrix. Two dimensional plots calculated between each two pairs of the 48 myrtle genotypes. The polymorphism information content (PIC) of SSR and iPBS markers was calculated as the mean of the PIC of each allele using the formula of Roldan-Ruiz et al. (2000) (*Eq. 1*).

$$PICi = 2fi(1 - fi) \quad \text{(Eq.1)}$$

where "PICi" is the polymorphism information content of allele "I" and "fi" is the frequency of occurrence of allele "I" (fragment present) in the 48 individuals.

Results and discussion

Morphological analysis

Morphological characterization of genetic resources provides the most important guiding information for identification, classification, and conservation of the genetic resources. Knowledge of morphological characters is the first step in the parental selection in the breeding programs. In this study the important morphological traits of the myrtle genotypes were determined in their natural ecosystems. Fifty fruits and leaves from each genotype were evaluated in terms of morphological characters and results are shown in *Table 2*.

The fruit weight, fruit length and fruit width ranged 0.05 to 1.18, 6.44 mm to 15.69 mm and 4.16 to 12.72 mm respectively. Results showed that the highest values for six out of the eight morphological characters (fruit weight, length, width, number of seed per fruit, seed weight, pulp weight) were recorded in genotype Ant8W. The lowest value for fruit weight, width, seed weight and pulp weight were measured in genotype Ant17W (*Table 2*). In the previous studies Melito et al. (2016) reported the fruit weight from 0.25 g to 0.34 g, fruit length 7.18 mm to 9.03 mm and fruit width 5.74 to 8.22 in Sicily. Uzun et al. (2016) measured highest values for fruit weight 1.33 g, fruit length 15.33 mm and fruit width 13.27 mm in the myrtle genotypes with white fruit color in coastal conditions of Antalya, Turkey. The highest and lowest values for fruit weight, length and width were recorded as 0.26 to 2.01, 7.52 to 16.73 mm and 5.52 to 14.74 mm respectively by Yıldırım et al. (2013) in the study carried out in Adana and Mersin province of Turkey. In the current study the number of seed for per fruit, seed weight and pulp weight are ranged 2.2-22.4, 0.02-0.21 g and 0.03-0.93 g respectively. Melito et al. (2016) reported a narrower range than we find between the highest and lowest values of the seed number for per fruit (10.34-18.43), seed weight (0.04 g-0.05 g) and pulp weight (0.20 g - 0.29 g). In the present work the seed weight ranged 0.02- 0.21 in genotypes with white berries and 0.02-0.13 in genotypes with black berries. The number of seeds ranged 2.2- 22.4 in genotypes with white berries and 2.2 – 10.8 in genotypes with black berries. Measurements varied between 13.95 (Ant22) and 32.85 mm (Ant13W) for leaf length, 5.5 (Ant23B) and 15.3 mm (Ant35W) for leaf width. The studied genotypes showed variation for all morphological traits evaluated. There were statistically significant differences ($p < 0.01$) among the genotypes for all fruit and leaf traits measured (*Table 3*). Samples were collected from different altitudes from 0 to 1358 m. According to the

http://www.aloki.hu ● ISSN 1589 1623 (Print) ● ISSN 1785 0037 (Online)
DOI: http://dx.doi.org/10.15666/aeer/2001_855873

results of the correlation analysis, there were negative and significant ($p < 0.01$) correlations between altitude and fruit length (r = -,088**), fruit weight (r = -,078**) and pulp weight (-,082**). Medda et al. (2021) found no effect of altitude on leaf total phenols, whereas a negative correlation was reported on berries total phenols and tannins concentrations.

Table 2. *Means of fruit and leaf characteristics for wild myrtle genotypes (mean ± SE)*

Genotype code	Fruit length (mm)	Fruit width (mm)	Fruit weight (g)	Number of seed per fruit	Seed weight (g)	Pulp weight (g)	Leaf length (mm)	Leaf width (mm)
Hty1B	8.55 ± 0.16	6.81 ± 0.17	0.19 ± 0.01	6.06 ± 0.43	0.06 ± 0.00	0.12 ± 0.009	23.40 ± 0.64	9.59 ± 0.38
Ant3B	9.05 ± 0.10	6.52 ± 0.09	0.19 ± 0.00	4.12 ± 0.22	0.05 ± 0.00	0.14 ± 0.004	25.44 ± 0.83	8.16 ± 0.34
Ant4W	14.8 ± 0.16	10.89 ± 0.13	0.83 ± 0.02	19.87 ± 1.18	0.17 ± 0.01	0.66 ± 0.02	32.06 ± 1.25	14.3 ± 0.57
Ant5W	9.17 ± 0.10	6.53 ± 0.09	0.20 ± 0.00	4.68 ± 0.33	0.05 ± 0.00	0.14 ± 0.005	26.01 ± 1.1	8.75 ± 0.35
Ant6W	9.3 ± 0.13	8.30 ± 0.11	0.32 ± 0.01	6.75 ± 0.50	0.09 ± 0.00	0.23 ± 0.008	19.79 ± 0.80	9.37 ± 0.29
Ant7B	13.56 ± 0.14	8.99 ± 0.12	0.55 ± 0.02	5 ± 0.30	0.09 ± 0.00	0.45 ± 0.01	24.35 ± 0.73	9.51 ± 0.26
Ant8W	15.69 ± 0.26	12.72 ± 0.20	1.18 ± 0.04	22.4 ± 1.19	0.21 ± 0.01	0.93 ± 0.04	28.35 ± 1.04	12.94 ± 0.40
Ant9B	9.36 ± 0.11	6.53 ± 0.09	0.20 ± 0.00	8.48 ± 0.32	0.08 ± 0.00	0.12 ± 0.006	27.20 ± 0.92	9.39 ± 0.33
Ant10B	9.28 ± 0.19	4.99 ± 0.12	0.12 ± 0.00	6.48 ± 0.37	0.04 ± 0.00	0.08 ± 0.006	23.39 ± 1.29	9.37 ± 0.51
Ant11W	14.28 ± 0.20	10.15 ± 0.12	0.66 ± 0.02	11.08 ± 0.73	0.10 ± 0.00	0.55 ± 0.01	21.17 ± 0.89	8.64 ± 0.38
Ant12W	8.16 ± 0.15	5.91 ± 0.11	0.13 ± 0.00	7.42 ± 0.50	0.05 ± 0.00	0.08 ± 0.005	25.44 ± 0.98	11.37 ± 0.39
Ant13W	8.54 ± 0.22	6.13 ± 0.23	0.16 ± 0.01	4.7 ± 0.35	0.04 ± 0.00	0.12 ± 0.007	32.85 ± 0.70	12.92 ± 0.29
Ant14B	10.65 ± 0.22	7.98 ± 0.18	0.32 ± 0.01	5.52 ± 0.40	0.08 ± 0.00	0.24 ± 0.01	25.75 ± 0.82	10.72 ± 0.42
Ant15B*							22.87 ± 1.03	8.54 ± 0.40
Ant16B*							23.45 ± 0.79	8.95 ± 0.47
Ant17W	6.67 ± 0.11	4.16 ± 0.11	0.05 ± 0.00	2.66 ± 0.26	0.02 ± 0.00	0.03 ± 0.003	22.91 ± 0.77	8.47 ± 0.43
Isp18W	13.62 ± 0.26	10.75 ± 0.18	0.77 ± 0.03	12.46 ± 1.15	0.15 ± 0.01	0.61 ± 0.02	23.60 ± 0.70	9.26 ± 0.28
Ant19B	11.07 ± 0.15	7.73 ± 0.15	0.33 ± 0.01	8.08 ± 0.86	0.09 ± 0.00	0.23 ± 0.009	25.33 ± 0.58	8.55 ± 0.21
Ant20W	13.67 ± 0.26	9.95 ± 0.17	0.62 ± 0.03	14.12 ± 1.50	0.13 ± 0.01	0.49 ± 0.02	27.65 ± 0.75	12.74 ± 0.31
Ant21W	12.8 ± 0.16	10.10 ± 0.14	0.65 ± 0.02	8.86 ± 0.50	0.10 ± 0.00	0.55 ± 0.02	24.56 ± 0.74	10.95 ± 0.27
Ant22B*							13.95 ± 0.33	6.19 ± 0.14
Ant23B	9.09 ± 0.12	6.99 ± 0.06	0.18 ± 0.00	5.44 ± 0.31	0.07 ± 0.00	0.11 ± 0.004	18.41 ± 0.33	5.50 ± 0.10
Izm24W	8.86 ± 0.07	6.26 ± 0.06	0.17 ± 0.00	5.14 ± 0.23	0.06 ± 0.00	0.11 ± 0.004	23.44 ± 0.94	8.87 ± 0.27
Izm25B	7.84 ± 0.15	5.29 ± 0.11	0.10 ± 0.00	4.76 ± 0.29	0.06 ± 0.00	0.04 ± 0.003	26.99 ± 1.07	9.67 ± 0.34
Izm26W	8.58 ± 0.2	6.38 ± 0.21	0.21 ± 0.01	6.06 ± 0.45	0.07 ± 0.00	0.13 ± 0.01	29.79 ± 0.94	11.01 ± 0.38
Mgl27W	10.47 ± 0.18	8.17 ± 0.13	0.36 ± 0.01	13.28 ± 0.72	0.12 ± 0.00	0.23 ± 0.01	16.89 ± 0.82	7.75 ± 0.35
Mgl28B	11.81 ± 0.07	8.11 ± 0.15	0.35 ± 0.01	10.8 ± 0.67	0.13 ± 0.00	0.22 ± 0.009	20.88 ± 0.87	6.73 ± 0.17
Mgl29W	10.69 ± 0.17	8.33 ± 0.15	0.41 ± 0.01	9.46 ± 0.63	0.11 ± 0.00	0.29 ± 0.01	32.10 ± 0.72	12.35 ± 0.37
Mgl30B	11.68 ± 0.15	9.13 ± 0.13	0.51 ± 0.01	7.64 ± 0.56	0.07 ± 0.00	0.44 ± 0.01	28.21 ± 1.04	11.89 ± 0.42
Izm31B	7.82 ± 0.12	6.42 ± 0.14	0.15 ± 0.00	3.4 ± 0.26	0.04 ± 0.00	0.11 ± 0.007	22.27 ± 0.60	8.08 ± 0.17
Ayd32B	10.71 ± 0.18	8.16 ± 0.15	0.30 ± 0.01	9.51 ± 0.64	0.10 ± 0.00	0.20 ± 0.01	27.88 ± 0.76	11.23 ± 0.22
Ant33B	9.5 ± 0.26	6.26 ± 0.14	0.20 ± 0.01	4.84 ± 0.29	0.05 ± 0.00	0.15 ± 0.01	26.24 ± 0.35	10.57 ± 0.18
Ant34W	13.26 ± 0.29	10.28 ± 0.22	0.68 ± 0.03	11.68 ± 0.76	0.15 ± 0.00	0.53 ± 0.03	28.79 ± 0.81	12.74 ± 0.28
Ant35W	11.03 ± 0.24	9.89 ± 0.17	0.53 ± 0.03	15.24 ± 1.11	0.17 ± 0.01	0.36 ± 0.01	32.03 ± 0.65	15.30 ± 0.33
Ant36W	12.08 ± 0.22	9.59 ± 0.16	0.54 ± 0.02	7.71 ± 0.90	0.08 ± 0.001	0.46 ± 0.02	25.93 ± 0.6	11.25 ± 0.30
Ant37B	7.59 ± 0.19	5.72 ± 0.14	0.13 ± 0.00	2.26 ± 0.21	0.03 ± 0.002	0.10 ± 0.007	27.45 ± 0.65	11.77 ± 0.30
Ant38B	6.44 ± 0.19	4.77 ± 0.15	0.09 ± 0.00	2.22 ± 0.13	0.02 ± 0.001	0.06 ± 0.007	24.04 ± 0.69	9.08 ± 0.33
Ant44B	7.58 ± 0.14	6.85 ± 0.17	0.21 ± 0.01	3.25 ± 0.21	0.06 ± 0.004	0.14 ± 0.01	17.54 ± 0.30	6.94 ± 0.16
Mrs48W	12.46 ± 0.16	10.54 ± 0.12	0.67 ± 0.02	15.3 ± 1.03	0.19 ± 0.01	0.47 ± 0.02	24.25 ± 1.09	10.57 ± 0.42
Mrs49W	9.35 ± 0.16	8.31 ± 0.18	0.35 ± 0.02	2.26 ± 0.14	0.03 ± 0.003	0.32 ± 0.02	20.79 ± 0.71	7.45 ± 0.27
Mrs50B	11.73 ± 0.16	6.90 ± 0.10	0.22 ± 0.00	6.58 ± 0.55	0.07 ± 0.005	0.14 ± 0.005	23.41 ± 0.84	9.29 ± 0.28
Ant51B	8.54 ± 0.17	7.52 ± 0.25	0.28 ± 0.01	5.12 ± 0.47	0.05 ± 0.002	0.23 ± 0.01	22.46 ± 0.75	9.77 ± 0.37
Ant52B	11.33 ± 0.11	7.18 ± 0.08	0.29 ± 0.00	5.3 ± 0.37	0.07 ± 0.004	0.21 ± 0.005	28.57 ± 0.83	9.87 ± 0.22
Ant53W	8.18 ± 0.22	6.72 ± 0.25	0.19 ± 0.01	12 ± 1.34	0.10 ± 0.009	0.09 ± 0.01	22.15 ± 0.62	9.71 ± 0.31
Hty55B	9.53 ± 0.12	7.34 ± 0.11	0.24 ± 0.00	8.14 ± 0.40	0.09 ± 0.003	0.14 ± 0.008	22.29 ± 0.53	9.90 ± 0.27
Hty56W	11.41 ± 0.29	8.52 ± 0.28	0.43 ± 0.03	9.13 ± 0.90	0.10 ± 0.01	0.33 ± 0.02	28.84 ± 0.77	13.71 ± 0.31
Ant57B	12.5 ± 0.27	6.11 ± 0.16	0.16 ± 0.01	7.04 ± 0.60	0.07 ± 0.005	0.08 ± 0.006	32.06 ± 1.19	7.87 ± 0.34
Mgl59W	13.41 ± 0.45	11.22 ± 0.39	0.81 ± 0.06	14.45 ± 2.04	0.12 ± 0.01	0.69 ± 0.05	27.39 ± 0.77	13.38 ± 0.41

*Sufficient number of fruits could not be collected for Ant15B, Ant16B and Ant22B

http://www.aloki.hu ● ISSN 1589 1623 (Print) ● ISSN 1785 0037 (Online)
DOI: http://dx.doi.org/10.15666/aeer/2001_855873

Table 3. *ANOVA of morphological characteristics*

	Sum of squares	df	Mean square	F	Sig.
Fruit length	7269.623	44	165.219	137.175	.000
Fruit weight	84.074	44	1.911	147.834	.000
Number of Seed	28091.839	44	638.451	44.178	.000
Seed weight	2.932	44	,067	47.557	.000
Pulp weight	59.594	44	1.354	152.736	.000
Leaf length	39853.370	47	847.944	25.153	.000
Leaf width	46946.082	47	998.853	1.562	.009

The mean differences are significant 0.01 level

Molecular analysis

Molecular analysis was done separately with two marker system as well as in combination of SSR and iPBS data sets.

Simple sequence repeats (SSR)

Eleven out of the 12 markers designed for *Myrtus communis* (Albaladejo et al., 2010) were polymorphic in 48 wild myrtle genotypes and produced a total of 64 alleles. The number of fragments varied from one to nine with an average 5.3 per SSR primer pair (*Table 4*). In line with previous studies of Corona et al. (2017) and Mele et al. (2019) five SSR primer pairs, namely *Myrcom2, Myrcom4, Myrcom7, Myrcom8, Myrcom11*, were highly polymorphic, each producing 7-9 alleles. Three primers *Myrcom5, Myrcom6, Myrcom9* were moderately polymorphic, each producing 4 to 5 alleles. The remaining four SSR primer pairs, *Myrcom1, Myrcom3, Myrcom10, Myrcom12*, were less polymorphic by producing two to three alleles each (*Table 3*). The findings for *Myrcom1* and *Myrcom12* primers of current study are in accordance with findings of Corona et al. (2017) with 2 alleles for each primer and a similar band pattern was obtained by Albaladejo et al. (2010) for the Myrcom1, Myrcom5, Myrcom7 primer pairs. The PIC values of SSR primers ranged from 0.45 (Myrcom1, Myrcom6) to 0.99 (Myrcom8) with an average of 0.70 (*Table 4*). Similarity index ranged from 0.31 to 1.00 based on the similarity matrix (data not shown). A phylogenetic tree obtained based on the similarity matrix for SSR markers shown in *Figure 4*. The genetic distance coefficients ranged from 0.63 to 0.97 with an average of 0.82. Based on phylogenetic analysis, the 48 genotypes were clearly clustered into two major clades (A and B) at the 0.63 similarity coefficient level. Clades A divided two groups (A1 and A2) at the similarity index of 0.65. Seven different genotypes collected from Antalya province are clustered together in cluster A1. Similar pattern was observed in accession from İzmir and Aydın (both located on the Aegan region) that grouped together in cluster A.2. The cluster A2. 1 contained 18 accessions 13 of which have white fruit color. Seven genotypes clustered in A2.1. clade namely Ant4W, Ant8W, Ant11W, Ant20W, Ant34W, Mrs48W, Hty56W found genetically similar by SSR markers. B1.2.2 included 13 genotypes with both black and white berries and collected from different regions.

Inter-primer binding site (iPBS)

Initially 30 primers were screened with bulk DNA, which was prepared by taking equal amounts of DNA samples from each genotype and 12 polymorphic primers were

http://www.aloki.hu ● ISSN 1589 1623 (Print) ● ISSN 1785 0037 (Online)
DOI: http://dx.doi.org/10.15666/aeer/2001_855873

selected for further investigations (*Table 5*). The iPBS analysis was performed on 48 genotypes revealing 135 total and 80 polymorphic bands with a mean of 11.25 total bands for each tested primer. Maximum 14 fragments were generated with primers 2378 and 2394, minimum 8 fragments were generated with 2078 and 2221. A total of 80 polymorphic bands were obtained with a mean of 6.66 bands for each primer and 2378 was the most polymorphic one with 13 bands, while primer 2221 produced only two polymorphic bands. The sizes of reproducible and scorable bands ranged from175 bp to 2000 bp. Percentage of polymorphism ranged from 25.0% (2221) to 92.8% (2378), with an average polymorphism of 57.26% across all the genotypes. Similarity index ranged from 0.44 to 1.00 based on the similarity matrix (data not shown). The PIC observed for 2078 marker was the highest thus, this marker could be more efficient in genotypic differentiation of myrtle genotypes. A dendrogram based on UPGMA analysis with iPBS data is shown in *Figure 5*. The 47 genotypes were grouped into one cluster (B) at the 0.58 similarity coefficient level whereas one genotype (Ant19) separated from the population (A) showing less similarity coefficient (0.58) with other genotypes studied. Genotypes within clade B are further grouped into two subclusters, B1 and B2 at the 0.63 similarity coefficient level. Clade B2 comprised 4 genotypes and clade B1 comprised 43 genotypes and separated into two sub-group. Six genotypes with white fruit color, collected from different geographical locations namely: Ant4W, Ant21W, Ant35W, Mrs48W, Hty56W, Mgl59W found genetically similar and located in the subcluster B1.1. The genotypes Ant11W, Isp18W, Ant20W, Ant34W placed in the cluster B1.1 also found genetically similar with iPBS markers (*Fig. 5*). Ant4W, Mrs48W, Hty56W and Ant11W, Ant20W genotypes were found genetically similar by both SSR and iPBS markers.

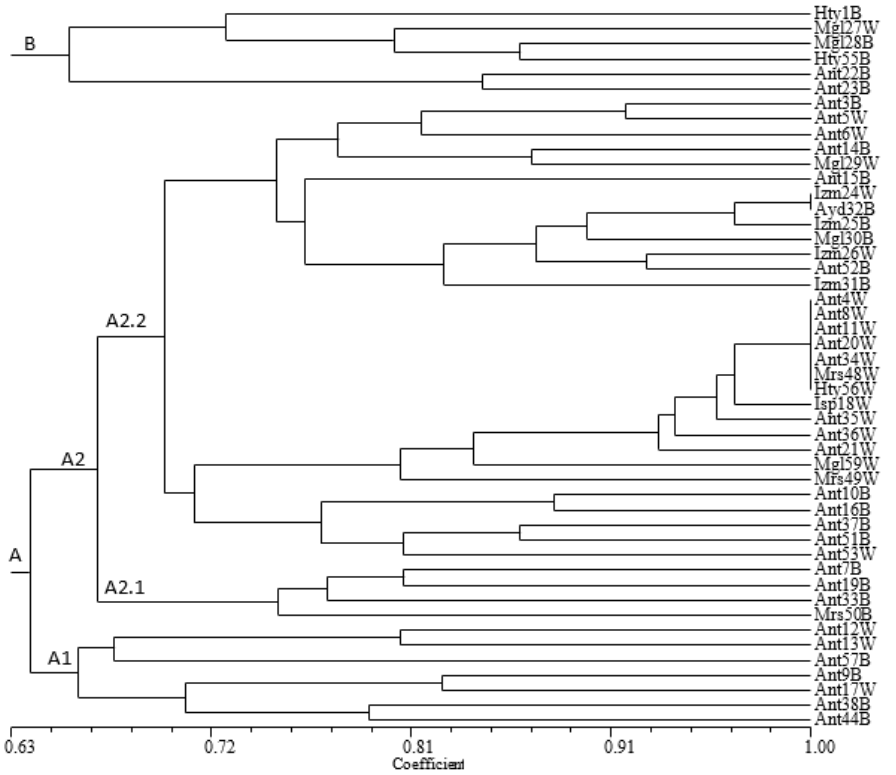

Figure 4. *Dendrogram for 48 Myrtus communis accessions derived from a UPGMA cluster analysis based on 12 SSR markers*

http://www.aloki.hu ● ISSN 1589 1623 (Print) ● ISSN 1785 0037 (Online)
DOI: http://dx.doi.org/10.15666/aeer/2001_855873

Table 4. *List of SSR primers and sequence, number of bands and polymorphic bans, allele size range (bp) and polymorphic information content value generated by each primer*

Primer	Primer sequences 5'-3'	NTA	NPA	PPA	Size (bp)	PIC
Myrcom1	F: CGTGATGCACACTGAACTGA R: AACCCCTTTTGCCAACATTT	3	3	100	225-230	0.45
Myrcom2	F: ATAGCTCTTACCCGCCATTG R: GTGCATGGTCCTCGATAGGT	9	9	100	213-240	0.88
Myrcom3	F: GGCAGCTACCAGTCATACCC R: TTTGCAGCATTTCAAAGTGG	2	2	100	183-187	0.77
Myrcom4	F: CAACCACATCCACCCATAGA R: CCACAGTCAAGAGGGAGAGC	8	7	100	162-187	0.52
Myrcom5	F: TGAGAGATCAGCAACCAAAAAG R: CATGAATGGCAACGATGAAA	5	5	100	253-269	0.75
Myrcom6	F: AAATGAAAAAGCTAAAAGTTAAAC R: AACAGGAAGAGCAAGCCAAG	4	4	100	179-181	0.45
Myrcom7	F: AGACATGCTCAAACTTGTATGC R: AATGTATCCCAACATGTCAGA	9	9	100	177-213	0.87
Myrcom8	F: TGCTCGGTCATTAATTGGTGT R: TCAAAACCGTCTCCATGAAA	9	9	100	230-270	0.99
Myrcom9	F: GAAAGTTGCACTGTTTATTTCCAA R: TCTTCCTTCCAATCCTCATCA	4	4	100	181-187	0.67
Myrcom10	F: TTAAGTGCCTTTGGCATTTGT R: AGAGGACCTCGCGATAGACA	1	-	100	166	
Myrcom11	F: GCAAATAAAAAGCGAGTTAAATGA R: CCACACTTTTAAGAATTTGTGGTC	8	8	100	230-250	0.97
Myrcom12	F: CCCTCCATTTTTCCCTTCTC R: AGCCGAAGCTCCAAGAAAC	3	3	100	140-146	0.49

NTA: number of total allele, NPA: number of polymorphic allele, PPA: percentage of polymorphic allele, PIC: polymorphic information content

Table 5. *List of iPBS primers and sequence, number of bands and polymorphic bands, band size range (bp) and polymorphic information content value generated by each primer*

Primer	Primer sequences 5'-3'	NTB	NPB	PPB	Size (bp)	PIC
2078	GCGGAGTCGCCA	8	5	62.5	250-1300	0.63
2079	AGGTGGGCGCCA	11	3	27.2	250-1500	0.13
2080	CAGACGGCGCCA	12	6	50	300-1500	0.46
2081	GCAACGGCGCCA	12	8	66.6	350-1450	0.51
2095	GCTCGGATACCA	9	5	55.5	245-1750	0.31
2221	ACCTAGCTCACGATGCCA	8	2	25	245-1500	0.38
2270	ACCTGGCGTGCCA	12	8	66.6	245-1750	0.36
2277	GGCGATGATACCA	12	10	83.3	250-1500	0.31
2376	TAGATGGCACCA	12	6	50	250-1650	0.22
2378	GGTCCTCATCCA	14	13	92.8	175-2000	0.25
2383	GCATGGCCTCCA	11	4	36.3	295-1500	0.49
2394	GAGCCTAGGCCA	14	10	71.4	250-1500	0.40

NTB: number of total bands, NPB: number of polymorphic bands, PPB: percentage of polymorphic band, PIC: polymorphic information content

http://www.aloki.hu ● ISSN 1589 1623 (Print) ● ISSN 1785 0037 (Online)
DOI: http://dx.doi.org/10.15666/aeer/2001_855873

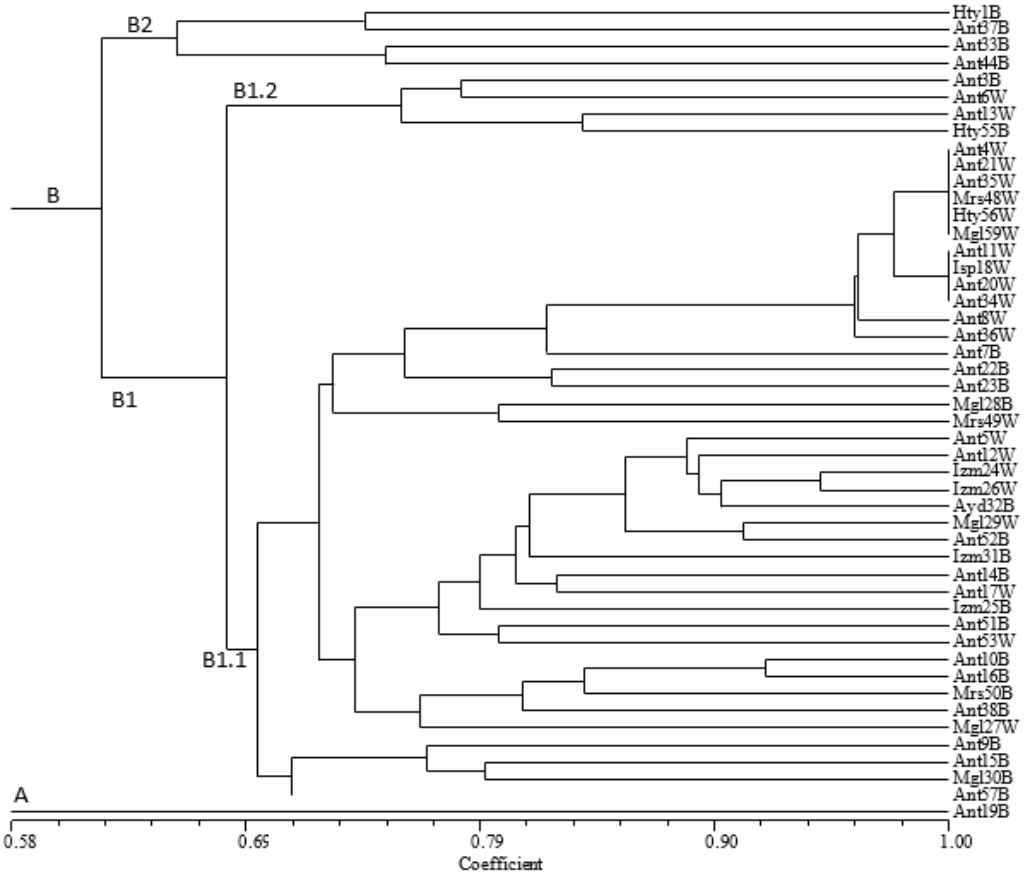

Figure 5. *Dendrogram for 48 Myrtus communis accessions derived from a UPGMA cluster analysis based on 12 iPBS markers*

Evaluation of combined data of SSR and iPBS results with morphological findings

Similarity coefficient ranged from 0.64 to 1.00 in the dendrogram based on UPGMA analysis performed with combined data of SSR and iPBS primers and the population divided to two main group (A and B) at the similarity value of 0.64. Clade B comprised 8 genotypes, all with black fruit, and 7 of these genotypes were collected from Antalya province except Hty1B. Clade A divided into sub-clusters and sub-cluster A2 comprised 39 genotypes. Only one genotype (Ant 57) placed in sub-cluster A1 and appeared to be distinct from all others based on the combined SSR and iPBS based data sets (*Fig. 6*). The genotypes Ant4W, Mrs48W, Hty56W and Ant11W, Ant20W, Ant34W were found genetically very close (similarity index 1.00) with SSR and iPBS markers and placed together in the same clade with Ant 21W, Ant 36W and Mugl59W, Ant8W, Ant35W and Isp18W at the 0.92-0.98 similarity index value (*Fig. 6*). All these 12 genotypes have berries with white color and larger fruits (ranged from 0.43 g to 1.18 g with average fruit weight 0.65) than the other genotypes which have an average fruit weight of 0.23 g. The average number of seeds per fruit and seed weight of these 12 genotypes 13.41 and 0.13 g respectively, the remaining genotypes have an average 6.77 seed per fruit and 0.07 g seed weight. These genotypes with white and larger berries may be semi-cultivated and selected genotypes and probably genetically very similar or identical. Our results demonstrated that the genotypes are found to be genetically indistinguishable usually consisted of berries with white color. Uzun et al. (2016) also mentioned a selected

http://www.aloki.hu ● ISSN 1589 1623 (Print) ● ISSN 1785 0037 (Online)
DOI: http://dx.doi.org/10.15666/aeer/2001_855873

genotype (Hambeles) usually grown at the edges of the land with white fruit color and average 1.06 g fruit weight. In the current study fruit weight of the genotypes with white berries ranged from 0.06 to 1.28 g with average 0.48 g and genotypes with black berries ranged from 0.20 to 0.60 with average 0.25 g respectively. Messaoud et al. (2005) and Messaoud and Boussaid (2011) reported that the white fruits are smaller and showed high number of seeds per fruit than the dark blue fruit. The genetic relationship within the population of white berries and within the population with black berries were also analyzed with combined data of iPBS and SSR markers. The similarity co-efficient of genotypes with white berries and black berries ranged 0.69 to 1.00 and 0.61-0.90 respectively (*Figs. 7a* and *8a*). As seen in dendrograms the genotypes with black berries have higher genetic diversity than white ones. This result ties well with previous studies wherein similar results reported with dark blue morph population in Tunisia (Messaoud et al., 2011). In the current study the genotypes with white berries show less diversity than genotypes with black berries. At a similarity index value of 0.69 the genotypes with white berries were divided into two major clusters and first clade 6 genotypes. The second clade includes 17 genotypes and 11 of those were genetically most related and form a subgroup at the similarity index value of 0.96 (*Fig. 7a*). The 2D plot generated from the PCA of the combined iPBS and SSR data (*Figs. 7b* and *8b*) supported the clustering pattern of the UPGMA dendrogram. As with the scatter plot of the principal component analysis, overlapping in grouping was observed in accessions with white berries (*Fig. 7b*) and genotypes with black berries are dispersed (*Fig. 8b*).

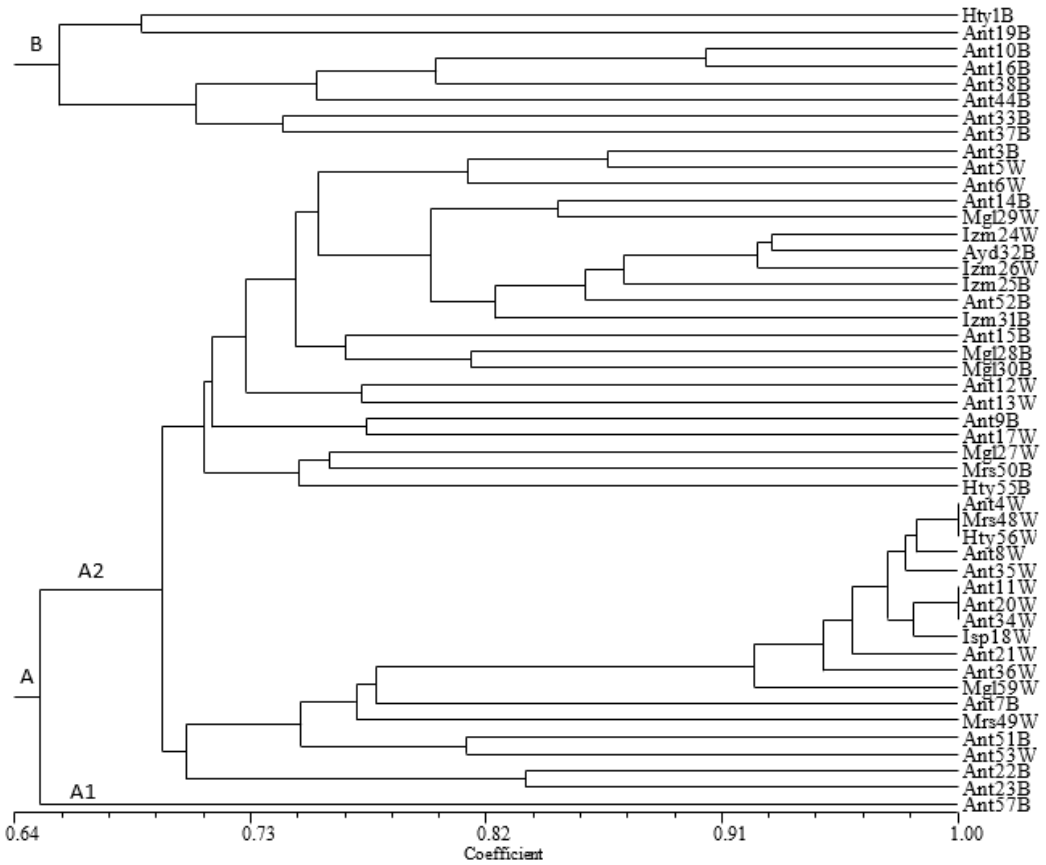

Figure 6. *Dendrogram for 48 Myrtus communis accessions derived from a UPGMA cluster analysis based on combined data of iPBS-SSR markers*

http://www.aloki.hu ● ISSN 1589 1623 (Print) ● ISSN 1785 0037 (Online)
DOI: http://dx.doi.org/10.15666/aeer/2001_855873

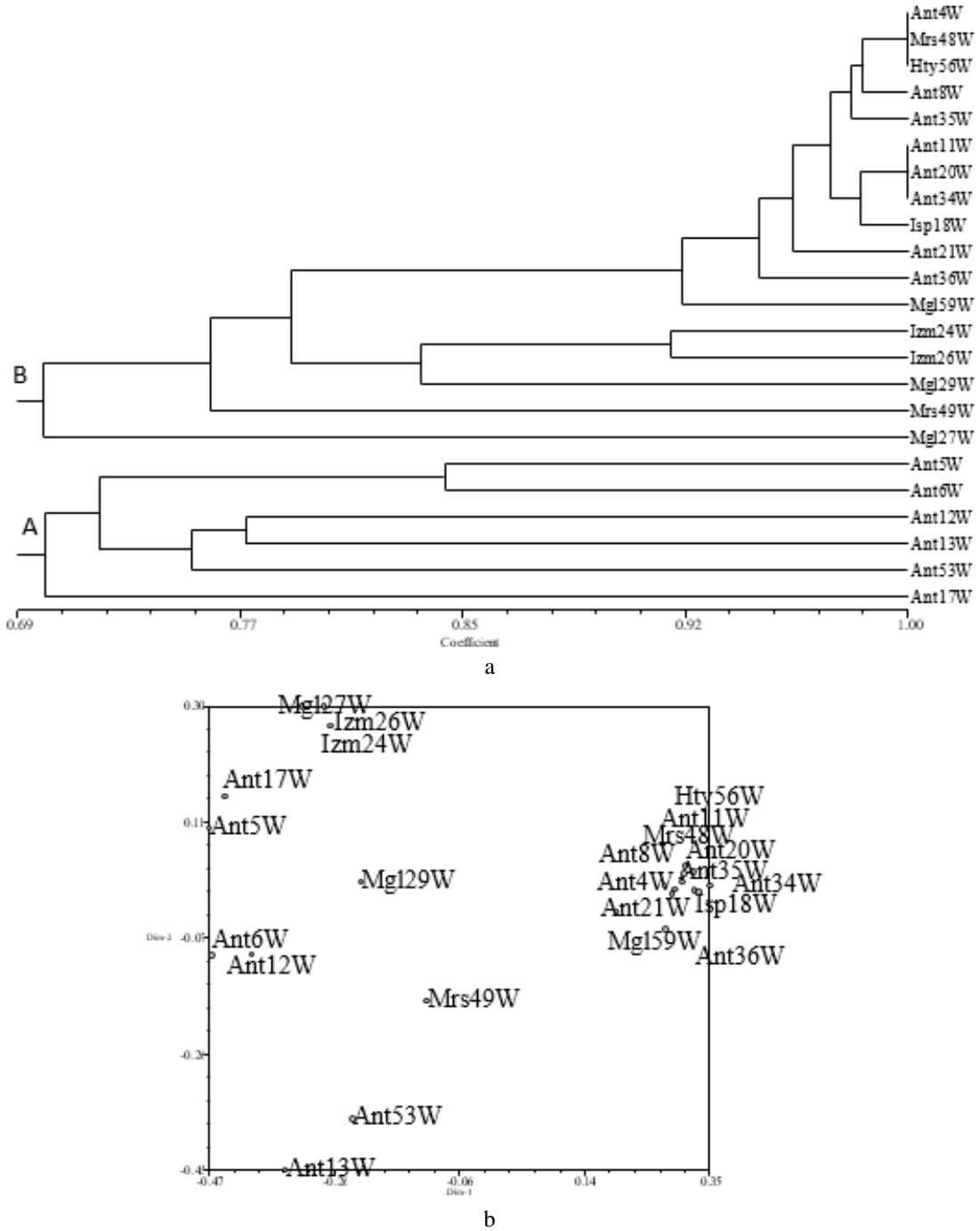

Figure 7. *(a) Dendrogram for 23 Myrtus communis accessions with white fruits derived from a UPGMA cluster analysis based on combined data of iPBS-SSR markers. (b) Two-dimensional plot of principal components (PC) 1 and 2 based on combined data of iPBS-SSR markers*

Both marker techniques (iPBS and SSR) proved to be effective in discriminating the 48 genotypes. To our knowledge, iPBS primers for *Myrtus communis* were used for the first time in this study and according to the results obtained ıPBS primers can be used in phylogenetic analyzes and mapping studies of myrtle.

http://www.aloki.hu ● ISSN 1589 1623 (Print) ● ISSN 1785 0037 (Online)
DOI: http://dx.doi.org/10.15666/aeer/2001_855873

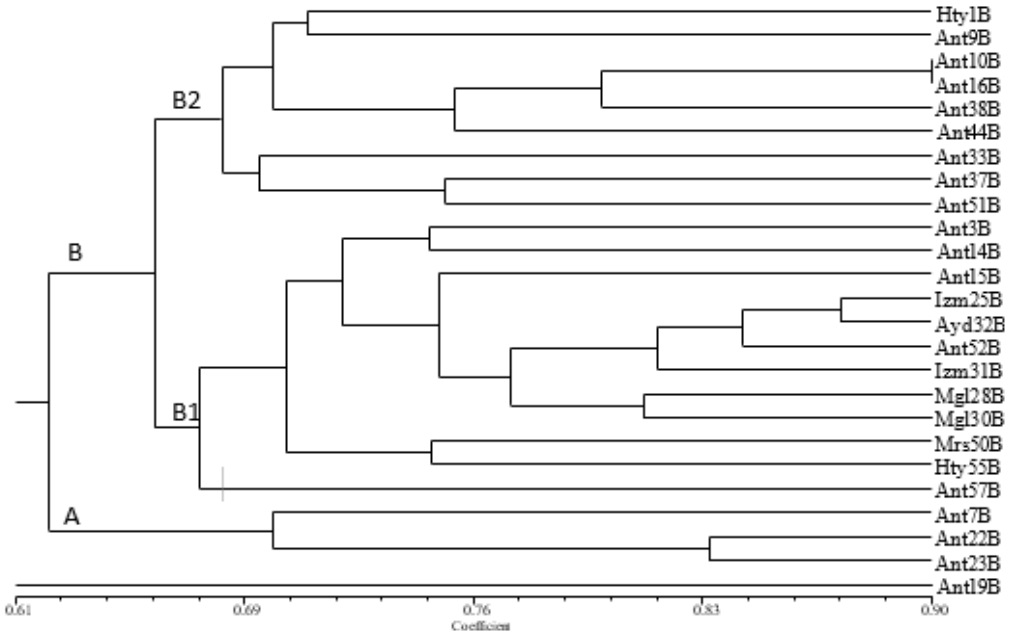

a

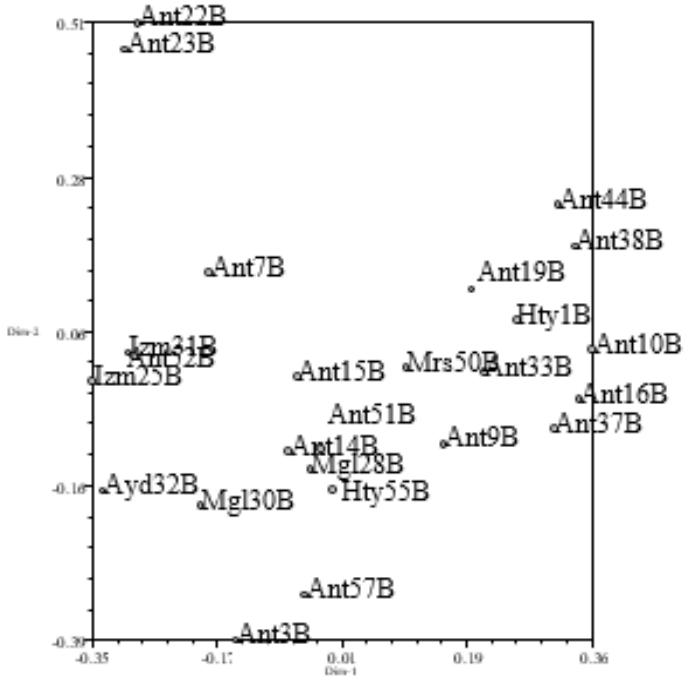

b

Figure 8. *(a) Dendrogram for 25 Myrtus communis accessions with dark blue berries derived from a UPGMA cluster analysis based on combined data of iPBS-SSR markers. (b) Two dimensional plot of principal components (PC) 1 and 2 based on combined data of iPBS-SSR markers*

Conclusion

Genetic diversity is fundamental for germplasm collections. Natural floras in the Mediterranean Sea Coastal of Turkey have a significant amount of myrtle (*Myrtus communis*) genotypes. Using genetic resources available, new cultivars can be improved

http://www.aloki.hu ● ISSN 1589 1623 (Print) ● ISSN 1785 0037 (Online)
DOI: http://dx.doi.org/10.15666/aeer/2001_855873

by gathering of plants from natural flora, selection of superior species that have characteristics desired for further cultivation and breeding practices.

Characterization and evaluation of myrtle is an imperative step for germplasm conservation and utilization in the breeding programs. Moreover, characterization of available germplasm is very crucial to identify desired traits or genes. The genetic variation obtained by morphological and molecular analyzes between genotypes shows that these genotypes can be useful for future breeding and cultivation practices and can be considered as valuable genetic resources that need to be protected. These results are valuable for further reproduction and conservation programs for *Myrtus communis.* Additional studies to understand the genetic characteristics of the genotypes regarding the genes associated with important traits are required.

Acknowledgements. The authors would like to thank the Akdeniz University Scientific Research Projects Coordination Unit, Turkey for financial support. (Project No: FYL-2018-4201).

REFERENCES

[1] Abdurakhmonov, I. Y. (2016): Introduction to Microsatellites: Basics, Trends and Highlights. – Intech Open, London. DOI: 10.5772/66446. http://dx.doi.org/10.5772/66446.

[2] Agrimonti, C., Bianchi, R., Bianchi, A., Ballero, M., Poli, F., Marmiroli. N. (2006): Understanding biological conservation strategies: a molecular-genetic approach to the case of myrtle (Myrtuscommunis L.) in two Italian regions: Sardinia and Calabria. – Conservation Genetics 8: 385-396.

[3] Albaladejo, R. G., Carrillo, L. F., Aparicio, A., Fernández-Manjarrés, J. F., González-Varo, J. P. (2009): Population genetic structure in Myrtus communis L. - in a chronically fragmented landscape in the Mediterranean: can gene flow counteract habitat perturbation? – Plant Biology 11(3): 442-453.

[4] Albaladejo, R. G., Sebastiani, F., Gonzalez-Martinez, S. C., Gonzalez-Varo, J., Vendramin, G. G., Aparicio, A. (2010): Isolation of microsatellite markers for the common Mediterranean shrub Myrtus communıs (Myrtaceae). – Am J Bot 97(5): e23-5. DOI: 10.3732/ajb.1000060.

[5] Andeden, E. E., Baloch, F. S., Derya, M., Kilian, B., Özkan, H. (2013): iPBS-Retrotransposons-based genetic diversity and relationship among wild annual Cicer species. – J. Plant Biochem. Biotechnol. 22: 453-466 https://doi.org/10.1007/s13562-012-0175-5.

[6] Baloch, F. S., Alsaleh, A., de Miera, L. E. S., Hatipoglu, R., Çiftçi, V., Karakoy, T., Yildiz, M., Ozkan, H. (2015): DNA based iPBS-retrotransposon markers for investigating the population structure of pea (Pisum sativum) germplasm from Turkey. – Biochemical Systematics and Ecology 61: 244-252.

[7] Baránek, M., Meszáros, M., Sochorová, J. Čechová, J., Raddová, J. (2012): Utility of retrotransposon-derived marker systems for differentiation of presumed clones of the apricot cultivar Velkopavlovická. – Sci Hortic-Amsterdam 143: 1-6.

[8] Borna, F., Luo, S., Ahmad, N. M., Nazeri, V., Shokrpour, M., Trethowan, R. (2016): Genetic diversity in populations of the medicinal plant Leonurus cadiaca L. Revealed by inter-primer binding site (iPBS) markers. – Genetic Resources and Crop Evolution 64: 479-492.

[9] Bruna, S., Mercuri, A., Cervelli, C., Braglia, L., De Benedetti, L., Schiva. T. (2005): Genetic characterization of Myrtus communis L. wild genotypes using AFLP markers. Acta Horticulturae 683: 431-436.

http://www.aloki.hu ● ISSN 1589 1623 (Print) ● ISSN 1785 0037 (Online)
DOI: http://dx.doi.org/10.15666/aeer/2001_855873

[10] Bruna, S., Portis, E., Cervelli, C., De Benetti, L., Schiva, T., Mercuri, A. (2007): AFLP-based genetic relationships in the Mediterranean myrtle (Myrtus communis L.). – Scientia Horticulturae 113: 370-375.
[11] Ciccarelli, D., Garbari, F. and Pagni, A. M. (2008): The flower of Myrtus communis (Myrtaceae): Secretory structures, unicellular papillae, and their ecological role. – Flora 203: 85-93.
[12] Corona, L., Mele, C., Chessa, I., Mulas, M. (2017): Analysis of Sardinian myrtle (Myrtus communis L.) germplasm selections by SSR markers. – Acta Hortic. 1172: 165-170. DOI: 10.17660/ActaHortic.2017.1172.32.
[13] Doyle, J. J., Doyle, J. L. (1990): Isolation of plant DNA from fresh tissue. – Focus 12: 13-15.
[14] D'Urso, G., Sarais, G., Lai, C., Pizza, C., Montoro, P. (2017): LC-MS based metabolomics study of different parts of myrtle berry from Sardinia (Italy). – J Berry Res. 7(3): 217-29.
[15] Ghafouri, F., Rahimmalek, M. (2018): Genetic structure and variation in different Iranian myrtle (Myrtus communis L.) populations based on morphological, phytochemical and molecular markers. – Industrial Crops & Products 123: 489-499.
[16] Kalendar, R., Schulman, A. H. (2014): Transposon-based tagging: IRAP, REMAP, and iPBS. – Methods Mol. Biol 1115: 233-255.
[17] Kalendar, R., Antonlus, K., Smykal, P., Schulman, A. (2010): iPBS: a universal method for DNA fingerprinting and retrotransposon isolation. – Theor Appl Genet 1211: 1419-1430.
[18] Karık, Ü., Nadeem, M. A., Habyarimana, E., Ercisli, S., Yildiz, M., Yılmaz, A., Yang, S. H., Chung, G., Baloch, F. S. (2019): Exploring the genetic diversity and population structure of Turkish laurel germplasm by the iPBS-retrotransposon marker system. – Agronomy 9(10): 647. https://doi.org/10.3390/agronomy9100647.
[19] Kuras, A., Antonius, K., Kalendar, R., Kruczynska, D., Korbin, M. (2013): Application of five DNA marker techniques to distinguish between five apple (Malus × domestica Borkh.) cultivars and their sports. – J Hortic Sci Biotechnol 88(6): 790-794. https://doi. org/10.1080/14620 316.2013.11513 040.
[20] Medda, S., Mulas, M. (2021): Fruit quality characters of myrtle (Myrtus communis l.) selections: review of a domestication process. – Sustainability 13(16): 8785. https://doi.org/10.3390/su13168785.
[21] Medda, S., Fadda, A., Dessena, L., Mulas, M. (2021): Quantification of total phenols, tannins, anthocyanins content in Myrtus communis L. and antioxidant activity evaluation in function of plant development stages and altitude of origin site. – Agronomy 11(6): 1-19.
[22] Mehmood, A., Luo, S., Ahmad, N. M., Dong, C., Mahmood, T., Sajjad, Y., Jaskani, M. J., Sharp. P. (2015): Molecular variability and phylogenetic relationships of guava (Psidium guajava L.) cultivars using inter-primer binding site (iPBS) and microsatellite (SSR) markers. – Genet. Resour. Crop. Ev. 63(8): 1345-1361. https://doi. org/10.1007/s1072 2-015-0322-7.
[23] Mele, C., Corona, L., Melito, S., Raggi, L., Mulas, M. (2019): The genetic diversity of selections and wild populations of myrtle revealed by molecular geographic contexts. – Industrial Crops & Products 132: 168-176.
[24] Melito, S., Chessa, I., Erre, P., Podani, J., Malus. M. (2013): The genetic diversity of Sardinian myrtle (Myrtus communis L.) populations. – Electronic Journal of Biotechnology 16(6).
[25] Melito, S., Fadda, A., Rapposelli, E., Mulas, M. (2014): Genetic diversity and population structure of Sardinian myrtle (Mytrus communis L.) selections as obtained by AFLP markers. – Hort Science 49: 531-537.
[26] Melito, S., La Bella, S., Martinelli, F., Cammalleri, I., Tuttolomondo, T., Leto, C., Fadda, A., Molinu, M. G., Mulas. M. (2016): Morphological, chemical, and genetic diversity of

http://www.aloki.hu ● ISSN 1589 1623 (Print) ● ISSN 1785 0037 (Online)
DOI: http://dx.doi.org/10.15666/aeer/2001_855873

wild myrtle (Myrtus communis L.) populations in Sicily. – Turkish Journal of Agriculture and Forestry 40(2): 249-261.

[27] Melito, S., Dessena, L., Sale, L., Mulas, M. (2017): Genetic diversity and population structure of wild Sardinian myrtle (Myrtus communis L.) genotypes from different microclimatic areas. – Australian Journal of Crop Science 11(11): 1488-1496.

[28] Messaoud, C., Boussaid. M. (2011): *Myrtus communis* berry color morphs: a comparative analysis of essential oils, fatty acids, phenolic compounds and antioxidant activities. – Chemistry & Biodiversity 8(2): 300-310.

[29] Messaoud, C., Zaouali, Y., Ben Salah, A., Koudja, M. L., Baussaid, M. (2005): *Myrtus communis* in Tunisia: variability of the essential oil composition in natural populations. – Flavourand Fragrance Journal 20: 577-582.

[30] Messaoud, C., Afıf, M., Boulila, A., Rejeb, M., Boussaıd. M. (2007): Genetic variation of Tunisian *Myrtus communis L. (Myrtaceae)* populations assessed by isozymes and RAPDs. – Annals of Forest Science 64: 845-853.

[31] Messaoud, C., Bejaoui, A., Boussaid. M. (2011): Fruitcolor, cheminal and genetic diversity and structure of *Myrtus communis* L. var. Italica Mill. morphpopulations. – Biochemical Systematics and Ecology 39: 570-580.

[32] Milovanov, A., Zvyagin, A., Daniyarov, A., Kalendar, R., Troshin, L. (2019): Genetic analysis of the grapevine genotypes of the Russian Vitis ampelographic collection using iPBS markers. – Genetica 147: 91-101.

[33] Mulas, M., Cani, M. R. (1999): Germplasm evaluation of spontaneous myrtle (*Myrtus communis*) for cultivar selection and crop development. – Journal of Herbs, Spices and Medicinal Plants 6: 3: 31-49.

[34] Mulas, M., Cani, M. R., Brigaglia. N. (1998): Characters useful to cultivation in spontaneous populations of *Myrtus communis* L. – Acta Horticulturae 457: 271-278.

[35] Nora, S., Albaladejo, R. G., Aparicio, A. (2014): Genetic variation and structure in the Mediterranean shrubs Myrtus communis and Pistacia lentiscus indifferent landscape contexts. –PlantBiology 17: 311-319.

[36] Özek, T., Demirci, B., Baser, K. H. C. (2000): Chemical composition of Turkish myrtle oil. – J Essent Oil Res. 12: 541-544.

[37] Özkan, A. M. G. Güray, Ç. G. (2009): A Mediterranean: *Myrtus Communis* L. (Myrtle). – In: Morel, J. P. Mercuri, A. M. (eds.) Plants and Culture: Seed of the Cultural Heritage of Europe. Edipuglia, Bari, pp.158-168.

[38] Park, Y. J., Lee, J. K., Kim, N. S. (2009): Simple sequence repeat polymorphisms (SSRPs) for evaluation of molecular diversity and germplasm classification of minor crops. – Molecules 14: 4546-4569. DOI: 10.3390/molecules14114546.

[39] Rohlf, F. J. (1993): NTSYS-pc. Version 1.X0. – Exeter Software, Setauket, NY.

[40] Roldan-Ruiz, I., Dendauw, J., Van Bockstaele, E., Depicker, A., De Loose. M. (2000): AFLP markers reveal high polymorphic rates in ryegrasses (*Lolium* spp.). – Mol Breed. 6: 125-134. DOI: 10.1023/A:1009680614564.

[41] Schuelke, M. (2000): An economic method for the fluorescent labeling of PCR fragments. – Nature Biotechnology 18: 233 – 234.

[42] Sepici, A., Gurbuz, I., Cevik, C., Yesilada. E. (2004): Hypoglycaemic effects of myrtle oil in normal and alloxan-diabetic rabbits. – J Ethnopharmacol 93(2-3): 311-318.

[43] Serçe, S., Ekbiç, E., Suda, J., Gündüz, K., Kiyga. Y. (2010): Karyological features of wild and cultivated forms of myrtle. – Genetic and Molecular Research 9(1): 429-433.

[44] Sımsek, O., Donmez, D., Sarıdas, M. A., Paydas-Kargı, S., Aka-Kacar, Y. (2019): Genetic relationship and polymorphism of Turkish myrtles (*Myrtus communis* L.) as revealed by inter simple sequence repeat (ISSR). – Applied Ecology and Environmental Research 18(1): 1141-1149.

[45] Traveset, A., Núrıa, R., Mas, R. E. (2001): Ecology of fruit-colour polymorphism in *Myrtus communis* and differential effects of birds and mammals on seed germination and seedling growth. – Journal of Ecology 89: 749-76.

http://www.aloki.hu ● ISSN 1589 1623 (Print) ● ISSN 1785 0037 (Online)
DOI: http://dx.doi.org/10.15666/aeer/2001_855873

[46] Usai, M., Marchetti, M., Culeddu, N., Mulas, M. (2020): Chemotaxonomic evaluation by volatolomics analysis of fifty-two genotypes of *Myrtus communis* L. – Plants. 9(10): 1-20.
[47] Uzun, H. İ., Aksoy, U., Gözlekçi, Ş., Bayır Yeğin, A., Selçuk, N. (2016): Studies on the yield and quality characteristics of myrtle (Myrtus communis L.) grown in two different ecologies. – Derim 33(2): 159-174 (in Turkish).
[48] Yıldırım, H., Kargı, S., Karabıyık. Ş. (2013): Research on naturally grown myrtle (Myrtus communis L.) plants at Adana and Mersin ecological conditions. – Alatatarım 12(1): 1-9 (in Turkish).

http://www.aloki.hu ● ISSN 1589 1623 (Print) ● ISSN 1785 0037 (Online)
DOI: http://dx.doi.org/10.15666/aeer/2001_855873

TRACE ELEMENT BIOACCUMULATION IN THE EDIBLE MILK SNAIL (*OTALA LACTEA)* AND CABRILLA (*OTALA PUNCTATA)* IN MARRAKECH, MOROCCO

SEBBAN, H.[1*] – AIT BELCAID, H.[1] – EL ALAOUI EL FELS, A.[2] – BOURIQI, A.[1] – PINEAU, A.[3] – SEDKI, A.[1]

[1]*Department of Biology, Faculty of Science Semlalia, Cadi Ayyad University, Marrakech, Morocco*

[2]*Department of Biology, Faculty of Science and Techniques, Cadi Ayyad University, Marrakech, Morocco*

[3]*Department of Clinical Pharmacology, University Hospital of Nantes, Nantes, France*

**Corresponding author*
e-mail: hajarsebban@gmail.com

(Received 13th Oct 2021; accepted 22nd Dec 2021)

Abstract. Morocco is the first land snail exporter in the world and the majority of snail production consists of individuals collected from nature. These gastropods are known to accumulate high levels of trace metals in their tissues hence the main objective of this study. We aimed firstly to investigate the bioaccumulation efficiency of Pb, Cd, Zn, Cu and Ca in *Otala spp.* snails, the most commonly widespread and the most consumed species in the Marrakech region, and then evaluate the potential risk on human health. Soil, foot, viscera and shell of adult snails were picked from six sampling stations in Al Haouz plain and analysed by ICP-MS. Results showed that the investigated snails accumulated all the examined elements with significant variations among the different tissues. The Principal Component and Bioaccumulation Factor analyses demonstrated that *Otala spp.* are macroconcentrators for Cd and microconcentrators for Pb. Furthermore, their shell accumulated more Ca, foot accumulated more Cu and viscera accumulated more Zn, Cd and Pb. In addition, the detected concentrations of toxic metals (Pb and Cd) were higher than the maximum admissible limits according to the European regulation except for Pb in the reference station. In conclusion, *Otala spp.* snails in our region can be used as bioindicators of trace element bioavailability and their consumption must be limited to avoid any possible intoxications.
Keywords: *terrestrial invertebrates, bioindicators, metallic pollution, ICP-MS, health risk assessment*

Introduction

During the last few decades, the environment and its compartments have been severely degraded due to the increasing anthropogenic activities. Most of these activities, especially industrial and agricultural ones, are responsible for the most trace element contaminations occurring in soil, air, water and organisms. Thus, the non-degradable state and the detrimental effect of these trace elements on the physiological functions of living organisms (Luczynska et al., 2018; Parolini et al., 2021) are becoming a big concern around the world.

To detect the deposition, accumulation and distribution of metallic pollution, direct measurements with physical and chemical methods can be used but require high expenditure and expertise, take more time and can release additional waste to the environment. In this context, Biomonitoring becomes an alternative to provide real and momentary information about the biological changes deriving from environmental exposure to chemicals. In fact, a biomonitor is an organism giving information on the

http://www.aloki.hu ● ISSN 1589 1623 (Print) ● ISSN 1785 0037 (Online)
DOI: http://dx.doi.org/10.15666/aeer/2001_875892

quality of its habitat; it is usually characterized by its sedentary lifestyle, wide distribution and ease of identification and collection (Parmar et al., 2016; Jahan and Strezov, 2019). Furthermore, several studies worldwide have shown the success of this approach to evaluate soil quality with the aid of soil invertebrates (Minodora, 2017; Chrzan, 2017) such as land snails (De Roma, 2017), isopods (Ghemari et al., 2017) and earthworms (Wang et al., 2018), air quality with plant leaves, pollen and barks (Ejidike and Onianwa, 2015; Shahid et al., 2016; Orcid and Orcid, 2019) and water quality with algae and aquatic mollusks (Pankova et al., 2015; Manev et al., 2020).

In the soil, trace elements are absorbed by microorganisms or assimilated by root systems (Munees, 2019; Caracciolo and Terenzi, 2021). It is for this reason that the use of sentinel terrestrial organisms to monitor the soil quality is very practical, due to their distribution, easy sampling, tolerance to stress and their ability to accumulate various pollutants (Anim et al., 2011; Mohammadein et al., 2013). Land snails are among the best bioindicators of terrestrial pollution because of their direct contact with several elements of their biotope (Gomot De Vaufleury and Pihan, 2000; Shotuyo et al., 2016; Ugbaja et al., 2020). These macro-invertebrates are ideally located at the interface between soil, plants and air; they eat soil and vegetation, and breathe through a big pneumostoma which can transport some particles to the pallial cavity. Moreover, the important place occupied by these gastropods in the food chain of terrestrial ecosystems may threaten organisms at higher trophic levels, such as humans and some snail predators.

For a long time, land snails, commonly named “Bebouch” or “Ghlala” have been a traditional dish in Moroccan cuisine and still highly appreciated by local consumers and tourists. They are considered a valuable source of nutrients, rich in proteins of high biological value and low in saturated fat. They are also rich in certain minerals and trace elements such as Calcium, Magnesium, Phosphorus, Iron, Copper and vitamins (B6, B12 and C) (Gomot, 1998). Furthermore, Morocco remains the top snail exporter in the world (15.7% of world exports) followed by Romania (7.42%), Turkey (5.94%), France (5.93%) and Indonesia (5.71%) (Indexbox, 2019). The majority of the Moroccan production comes from snails gathered in the wild which develop naturally without any human intervention. These snails are found in abundance in limestone areas, in forests, gardens, fields and other localities that may be contaminated (pesticides, molluscicides, fertilizers, wastewater…). In these environments, snails can assimilate contaminants through ingestion, respiratory or skin tract and can sometimes become invalid for consumption.

The aim of this study is to document and evaluate some trace element contents (Pb, Cd, Zn, Cu and Ca) in soils, foot, viscera and shell of *Otala lactea* and *Otala punctata* snails, the most consumed snails in the Marrakech region and the most exported species in the international market. The purpose is firstly to assess the potential of these land snails as biomonitors of terrestrial environment quality of five farms with agricultural activities, then to evaluate their safety as a food resource based on the levels of accumulated toxic elements (Pb and Cd) especially in foot, the most edible part of snails.

Materials and methods

All experiments were ethically conducted in conformity to principles and guidelines of animal welfare in scientific research (APA, 2018).

http://www.aloki.hu ● ISSN 1589 1623 (Print) ● ISSN 1785 0037 (Online)
DOI: http://dx.doi.org/10.15666/aeer/2001_875892

Study area description

The study was carried out in six regions in Al Haouz plain (Marrakech, Morocco). Al Haouz plain is located in the Tensift basin, on the Northern slope of the High Atlas. It covers an area of approximately 6000 km² with the city of Marrakech as the capital. The sampling locations belong to Four Provinces, namely Marrakech Province, Al Haouz Province, Rehamna Province and El-Kelaa des Sraghnas Province (*Fig. 1*).

The sampling technique was similar to that of the commercial snail collectors who respect specific collecting places and times. Generally, snails are collected from private farms or from public fields known for their limestone-rich soil and high humidity such as cool mountain areas and steamy forests. Furthermore, it is necessary to collect only adult snails obligatorily out of rest periods (only during spring and autumn in our region).

Following the same process, our soil and *Otala spp*. snail samples were collected in April 2019 from six different sampling stations (*Table 1*). Loudaya, Ourika and Laâtamna stations are big farms with commercial production. Contrariwise, Tahannaout and Sâada stations are small farms with personal production. El Argoub station is an open area without any agricultural production and was considered as a reference site during this study.

The choice of the study areas was based on the investigation of the High Commission for Planning of Morocco (HCP) showing that there is an intensive use of fertilizers and pesticides in the Marrakech region contributing directly to soil contamination. This region uses nearly 120,000 tons of fertilizers annually, i.e. 16% of the national consumption of these products. Otherwise, the excessive use of these elements also causes pollution of water resources (between 30% and 39% of groundwater resources are of poor quality) (HCP, 2018).

Loudaya, Ourika and Laâtamna stations are more exposed to these possible contamination sources due to the intensive agricultural activities intended for the large market.

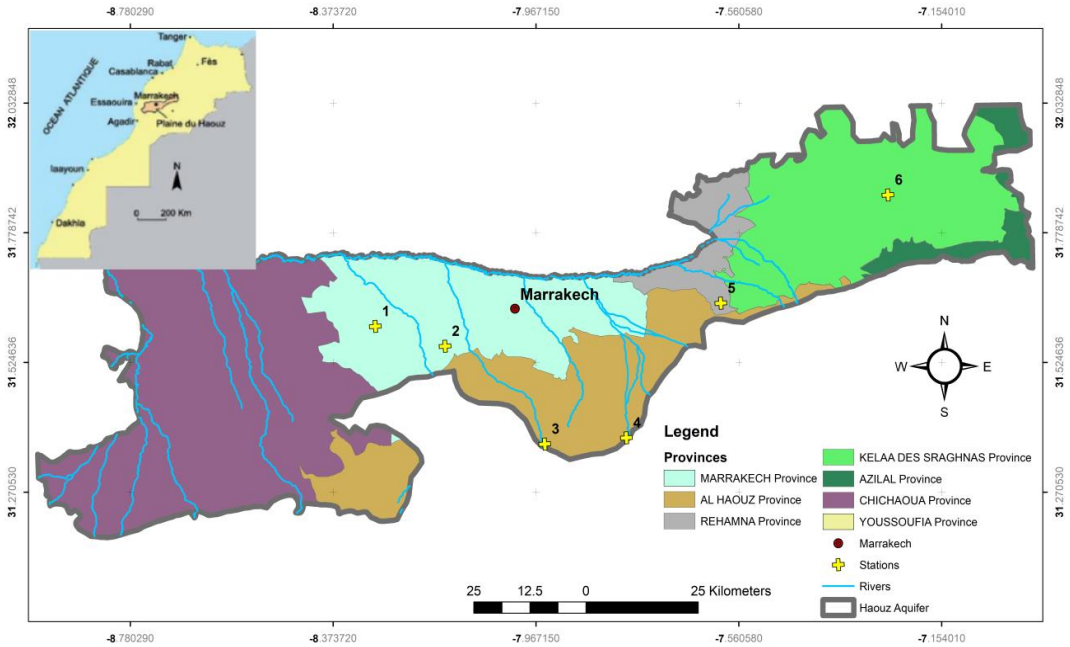

Figure 1. *Map showing the geographical distribution of soil and snail sampling stations*

http://www.aloki.hu ● ISSN 1589 1623 (Print) ● ISSN 1785 0037 (Online)
DOI: http://dx.doi.org/10.15666/aeer/2001_875892

Snail sampling

A minimum of 30 - 40 adult snail specimens were collected at each sampling site in order to obtain enough biomass for different identification and chemical analyses. The choice of plots was random and depended in particular on the presence of a sufficient number of individuals. Subsequently, all the collected individuals were subjected to a descriptive study measuring the following parameters: shell height and shell width with a digital vernier caliper (Selecta 5900603) and snail weight with precision analytical balance (Radwag AS 220.R2) (*Table 1*).

Table 1. *Soil and snail sampling stations and snails description*

Station code	Station	Geographic coordinates	Altitude	Snail wet weight (g)	Shell height (mm)	Shell width (mm)
S1	Loudaya	31°35'34.8" N, 8°17'15.1" W	403 m	4.8 ± 0.2	15.4 ± 0.6	29.6 ± 1.0
S2	Sâada	31°33'15.3" N, 8°08'52.1" W	451 m	4.7 ± 0.1	13.8 ± 0.3	26.4 ± 0.4
S3	Tahannaout	31°21'44.9" N, 7°56'52.6" W	896 m	6.7 ± 0.3	16.9 ± 0.5	30.7 ± 0.5
S4	Ourika	31°22'28.7" N, 7°47'04.3" W	855 m	5.3 ± 0.3	16.3 ± 0.7	30.1 ± 1.6
S5	El Argoub	31°38'18.7" N, 7°35'42.4" W	593 m	6.4 ± 0.4	15.5 ± 0.5	30.0 ± 0.6
S6	Laâtamna	31°51'02.1" N, 7°15'36.3" W	615 m	5.6 ± 0.3	17.7 ± 0.8	29.4 ± 0.7

Snail species

Otala spp. snails are chosen for this investigation because they are the most widespread and the most common edible species in Marrakech and regions. They are also relatively abundant and well spatially distributed over the study areas. In addition, the trace element contents and the accumulative potential of these species have never been studied. There are two popular species that have been used as food since ancient times, namely *Otala lactea* and *Otala punctata* (Müller, 1774). They are very similar morphologically and sometimes require a dissection for a correct identification.

Otala lactea (Helicidae family) is a land snail generally native to the Mediterranean. It is characterized by a solid shell with a whitish, yellow or brown color (influences by habitat) with 4 to 5 darker bands. Likewise, *Otala punctata* (Helicidae family) is native to the Iberian Peninsula, southern France and the Maghreb region of North Africa. (Herbert, 2010). The shell of this species is patterned of dark and light, brownish, spiral bands overlain with numerous tiny white spots. *O. lactea* is distinguished from *O. punctata* by the color of the aperture and peristome, which is very dark or black in the first and light brown or whitish in the second. *Otala lactea* occurs sympatrically with *Otala punctata* and both species exhibit similar life cycle patterns. (Robinson et al., 1998).

Snails and soil preparation

Soil preparation

For each selected station, three soil samples were collected randomly from 0-5 cm of sediments with a hand grab sampler. Then, they are homogenized, kept in zip-locked plastic bags, labeled and transported to the laboratory for further treatments and analyses. Once in the laboratory, they are air-dried for 7-10 days at ambient temperature, sieved by a 2 mm sieve and weighed for the next analysis step.

http://www.aloki.hu ● ISSN 1589 1623 (Print) ● ISSN 1785 0037 (Online)
DOI: http://dx.doi.org/10.15666/aeer/2001_875892

Snail dissection and tissue preparation

Collected snails were transported to the laboratory in coolers, then, purged by starvation for 48 h to remove unabsorbed food and feces from their digestive tract. Afterwards, they are washed three times with deionized water to remove impurities and to avoid possible interference between the metals present in the ingested food and the real amounts of metals accumulated in the snail tissues.

As already mentioned, this study focused on *O. lactea* and *O. punctata* species. For this reason, the individuals are firstly sorted based on their morphology, and then a group of 5 individuals per location was a subject of a reproductive system dissection, the most important indicator for classifying snails, to confirm the preliminary selection. Results of this dissection are presented in *Figure 2*.

The other groups of selected snails were sacrificed by freezing at -20 °C. The next step was to remove the whole soft tissue from the shell and separate the viscera from the foot. Afterwards, shells, feet and viscera were oven-dried separately at 60 °C until they reached a constant dry weight, then grinded to a powder by using a mortar made of steel guaranteed "without Trace Metallic Elements".

The control snail rearing

The snails used for the control sample were obtained by snail rearing in standard conditions in an aboveground system at the laboratory. For that, adult *Otala spp.* snails, already gathered and identified, were placed in a refrigerator at 6-7 °C for 3 months, to trigger the hibernation process and promote the chances of mating after awakening. They are then put in a regulated room with a photoperiod of 18 h of light per day, a temperature of 22 °C and a relative humidity of about 85%.

In those conditions, individuals mating, nest digging and eggs lying take about 30 days. After the eggs hatch, the baby snails are transferred to plastic boxes and fed, for a period ranging from 3 to 4 months, with a composed food containing a source of calcium, proteins and energy. Adult individuals went through the same preparation steps already mentioned for the other samples.

Chemical preparation

Soil analysis

Soil samples were chemically analyzed for detection of trace elements (Pb, Cd, Zn, Cu, Ca) using the digestion technique by aqua regia (HNO_3 + HCl). This digestion consisted of soaking 250 mg of each soil sample in 3 mL of ultrapure Nitric acid 65% for 2 h, and then adding 6 mL of Chloric acid 34%. The digestion of all samples was carried out in pressure vessels using a microwave (Multiwave GO) according to the following program:

- 10 min at 80 °C
- 15 min at 80 °C
- 5 min at 150 °C
- and finally 35 min 150 °C.

After the end of this process, the samples were cooled, centrifuged for 10 min and filtered. Afterwards, 1 mL of each digested sample was diluted to 10 mL with ultrapure water and stored at 4 °C prior to analysis.

http://www.aloki.hu ● ISSN 1589 1623 (Print) ● ISSN 1785 0037 (Online)
DOI: http://dx.doi.org/10.15666/aeer/2001_875892

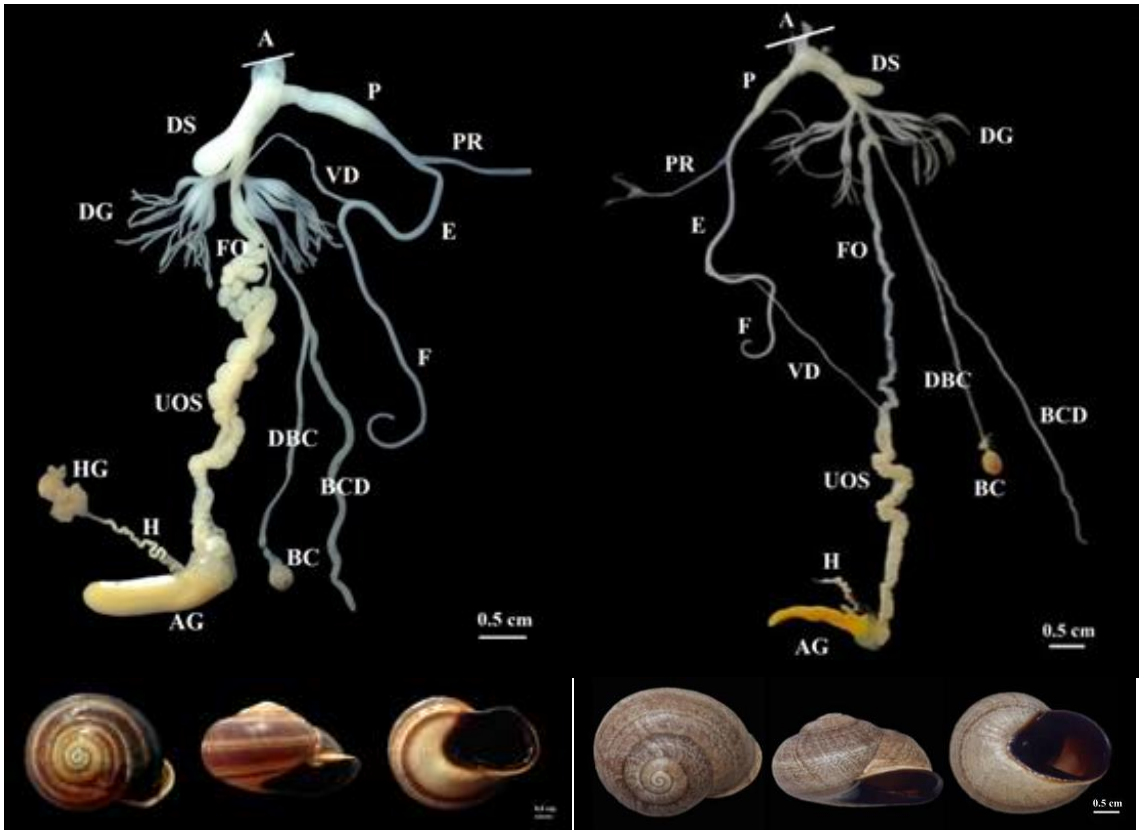

Figure 2. *Shell and reproductive system dissection of Otala punctata (A) and Otala lactea (B) snails. Legend: A: atrium; AG: albumen gland; BC: bursa copulatrix; BCD: diverticulum of the bursa copulatrix; DBC: duct of the bursa copulatrix; DG: digitiform glands; DS: dart sac; E: epiphallus; F: flagellum; FO: free oviduct; H: hermaphroditic duct; HG: Hermaphroditic glandula; P: penis; PR: penial retractor muscle; UOS: uterine ovispermiduct; VD: vas deferens*

Snail analysis

At the same time of soil, snail analysis was carried out as follows: 100 mg of each sample of shells, feet and viscera was digested separately in 1 mL of Nitric acid 65% for 24 h. Subsequently, the mineralization process was completed on a hot plate at 80 °C for 1 h. One hour of digestion was sufficient to completely digest the samples without leaving any traces or debris. Then, 1 mL of each concentrate was diluted with 1 mL of ultrapure water. The dilution factor was chosen based on the results of preliminary assays.

Trace elements concentrations (Pb, Cd, Zn, Cu) in soil, shells, feet and viscera samples were determined by inductively coupled plasma mass spectrometry (ICP-MS (Perkin Elmer)). Two standard reference materials were used to validate the method, NIST 1643 and NIST 1640 for snail samples and NIST 1643 with MESS-2 for soil samples.

Afterwards, Calcium contents were measured by a Flame Photometer (Sherwood 360). The stock solution of feet, viscera and soil was diluted 100-fold; the stock solution of shells was diluted 1000-fold. These dilutions were necessary in order to obtain more credible results.

http://www.aloki.hu ● ISSN 1589 1623 (Print) ● ISSN 1785 0037 (Online)
DOI: http://dx.doi.org/10.15666/aeer/2001_875892

Statistical analysis

Mean and standard deviation (SD) were calculated for all variables. The soil mean values and snail mean values were compared by unpaired student's t-test for statistically significant differences. Differences were considered significant when $p \leq 0.05$. In order to estimate the proportion in which metal occurs in the snail tissues and in associated soil, the bioaccumulation factor (BAF) was calculated according to the formula: Concentration of the element in snail tissue / Concentration of the same element in soil. Then, to evaluate the metals' concentrations in the different snails' parts (Foot, viscera and shell), Principal Components Analysis (PCA) was used. All the statistical analyses were performed using R-studio.

Results

Trace element concentrations in soils of sampling locations

Levels of investigated elements (Pb, Cd, Zn, Cu and Ca (µg/g, dry weight)) in soils of the different studied stations are presented in *Figure 3*. The results showed Cd presented the lowest concentrations, followed by Pb, Cu, Zn then Ca.

The collected data showed also that the studied elements were ranged between 0.16-0.38, 13.73-22.89, 33.57-61.06, 104.77-155.33, and 1406.25-27000 µg/g for Cd, Pb, Cu, Zn and Ca respectively. Furthermore, the reference station registered the lowest levels of toxic elements (Pb and Cd) while Loudaya station registered the highest concentration of these metals.

In comparison with the reference station, it has been observed that there was a statistically significant difference ($p \leq 0.05$) between the reference station and all the sampling stations for Cd and Ca concentrations in soil. However, the difference in Pb concentrations was statistically significant only between the reference station and Loudaya, Tahannaout and Ourika. The Zn concentrations in the soil of El Argoub were significantly lower than those in Loudaya, Tahannaout and Ourika soils. Furthermore, there was no significant difference in Cu concentrations between the reference station and Ourika ($p = 0{,}170$).

Trace element concentrations in Otala spp. snails

The levels of the examined elements Pb, Cd, Zn, Cu, and Ca (µg/g, dry weight) in different parts of *Otala spp*. snails collected from the six sampling stations are given in *Table 2*. In fact, all the studied trace elements were detected in our sampled snails.

The obtained results from the analysis of these snail samples were firstly compared for the whole snail body (soft tissue and shell) in different sampling stations. It was found that at each locality the concentrations fluctuate in the following order: Pb < Cd < Zn < Cu < Ca. The results also revealed that the recorded average of non-essential element concentrations vary between 1.41 µg/g and 6.63 µg/g for Pb and between 8.33 µg/g and 15.48 µg/g for Cd and that Cd is more concentrated than Pb. On the other hand, the recorded essential element concentrations are within 233.28 µg/g and 363.67 µg/g, 280.23 µg/g and 572.06 µg/g and $388.08.10^3$ and 442.10^3 µg/g µg/g for Zinc, Copper and Calcium respectively.

The comparison between the control animals and all the other samples shows that the Pb, Cd and Cu contents in control snails were significantly lower than those of the examined ones (including the reference station). Zn contents were significantly different

http://www.aloki.hu ● ISSN 1589 1623 (Print) ● ISSN 1785 0037 (Online)
DOI: http://dx.doi.org/10.15666/aeer/2001_875892

for only Tahannaout and Ourika stations. In contrast, there was no significant difference in Ca concentrations ($p > 0.05$).

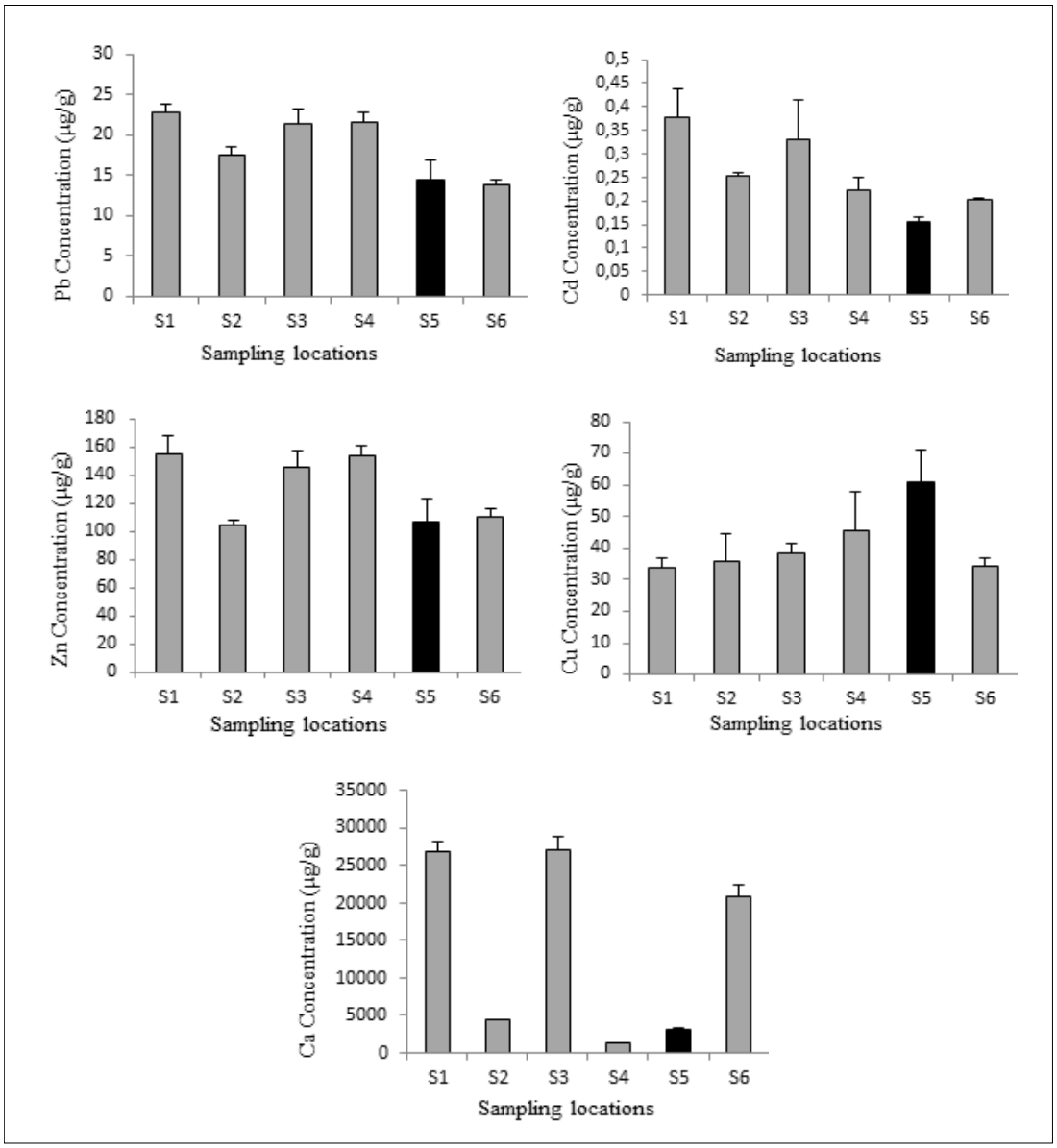

Figure 3. *Concentrations (Mean ± SD) of Lead (Pb), Cadmium (Cd), Zinc (Zn), Copper (Cu) and Calcium (Ca) in soils of the six sampling stations in Al Haouz plain. (S5: Reference station). Maximum permissible limits suggested by the WHO (100 µg/g for Pb, 3 µg/g for Cd, 300 µg/g for Zn and 100 µg/g for Cu) (Focus et al., 2021)*

Trace element concentration in Otala spp. tissues

The contents of Pb, Cd, Zn, Cu and Ca were evaluated in the feet, viscera and shells of *Otala spp*. snails collected from the six sampling stations using Principal Components Analysis (PCA) (*Fig. 4*). The first (69.3%) and second principle (21.2%) components (PC) together explained 90.45% of the total variation. Dimension 1 (*Fig. 4A, B, D*) opposes snail parts such as S3-F, S4-F and S6-V (on the right of the

http://www.aloki.hu ● ISSN 1589 1623 (Print) ● ISSN 1785 0037 (Online)
DOI: http://dx.doi.org/10.15666/aeer/2001_875892

graph, characterized by a strongly positive coordinate on the axis) to snail parts such as S6-Sh, S3-Sh, S5- Sh, S4-Sh, S2-Sh and S1-Sh (on the left of the graph, characterized by a strongly negative coordinate on the axis).

Table 2. *Trace element concentrations (µg/g, dry weight) in different Otala spp. snail tissues from the six sampling stations (S1-S6) and the control snails (C). F: foot, V: viscera, Sh: shell*

Station	Sample	Pb	Cd	Zn	Cu	Fe	Ca
S1	F	0.63 ± 0.06	1.70 ± 0.11	74.36 ± 7.85	190.83 ± 7.90	69.23 ± 6.93	1750.00 ± 250.00
	V	5.96 ± 0.34	7.30 ± 0.60	178.11 ± 6.90	87.92 ± 2.66	246.73 ± 16.03	8437.50 ± 937.50
	Sh	0.05 ± 0.00	0.03 ± 0.00	0.12 ± 0.01	1.47 ± 0.04	490.37 ± 12.91	431818.18 ± 26515.15
S2	F	0.59 ± 0.02	2.04 ± 0.68	123.91 ± 6.54	233.60 ± 12.33	107.71 ± 5.30	1250.00 ± 433.01
	V	1.98 ± 0.11	7.42 ± 1.02	142.12 ± 16.39	131.59 ± 12.05	164.01 ± 12.14	2750.00 ± 0.00
	Sh	0.04 ± 0.01	0.21 ± 0.00	0.06 ± 0.00	5.16 ± 0.24	489.24 ± 10.27	420454.55 ± 0.00
S3	F	0.42 ± 0.04	2.69 ± 0.38	121.00 ± 7.08	359.97 ± 24.23	175.47 ± 4.85	3000.00 ± 0.00
	V	0.97 ± 0.02	12.74 ± 1.94	186.47 ± 13.78	192.90 ± 15.16	182.36 ± 12.30	3000.00 ± 250.00
	Sh	0.03 ± 0.01	0.05 ± 0.01	0.25 ± 0.04	3.35 ± 0.05	496.00 ± 21.87	409090.91 ± 10021.79
S4	F	0.57 ± 0.03	2.17 ± 0.09	118.16 ± 17.22	285.02 ± 18.86	152.90 ± 15.58	2750.00 ± 250.00
	V	2.08 ± 0.31	6.32 ± 1.08	245.41 ± 11.02	186.15 ± 6.62	234.13 ± 29.58	2750.00 ± 250.00
	Sh	0.03 ± 0.00	0.05 ± 0.00	0.10 ± 0.00	1.87 ± 0.52	497.68 ± 13.55	382575.76 ± 15151.52
S5	F	0.47 ± 0.02	1.39 ± 0.06	72.56 ± 9.47	389.74 ± 14.23	100.09 ± 16.43	5937.50 ± 826.80
	V	2.10 ± 0.23	6.95 ± 2.43	160.64 ± 21.31	181.89 ± 11.33	169.46 ± 20.21	3000.00 ± 250.00
	Sh	0.02 ± 0.00	0.00 ± 0.00	0.08 ± 0.01	0.43 ± 0.04	471.55 ± 18.24	416666.67 ± 29584.28
S6	F	0.84 ± 0.08	3.12 ± 0.88	144.21 ± 21.83	256.12 ± 28.44	230.09 ± 17.16	4375.00 ± 312.50
	V	2.18 ± 0.32	8.44 ± 1.26	167.10 ± 14.45	225.55 ± 24.65	192.92 ± 8.83	3000.00 ± 0.00
	Sh	0.05 ± 0.00	0.15 ± 0.02	0.15 ± 0.04	5.61 ± 0.86	470.82 ± 16.04	401515.15 ± 24838.78
Control	F	0.11 ± 0.01	0.15 ± 0.04	41.99 ± 5.87	79.91 ± 6.99	578.20 ± 14.81	22666.67 ± 1222.02
	V	0.16 ± 0.04	0.21 ± 0.07	200.73 ± 11.62	122.30 ± 17.08	144.81 ± 9.87	17500.00 ± 0.00
	Sh	0.03 ± 0.01	0.00 ± 0.00	0.91 ± 0.23	2.02 ± 0.66	486.05 ± 9.44	378787.88 ± 13121.60

The classification carried out on individuals reveals 3 classes:

Class 1 is made up of individuals such as S1-Sh, S2-Sh, S3-Sh, S4-Sh, S5-Sh and S6-Sh. This group is characterized by:

- High values for the variable Ca
- Low values for the variables Zn, Cu, Cd and Pb (from the most extreme to the least extreme)

Class 2 is made up of individuals such as S3-F, S4-F and S5-F. This group is characterized by:

- High values for the Cu variable
- Low values for the variable Ca

Class 3 is made up of individuals such as S1-V, S3-V, S4-V and S6-V. This group is characterized by:

- High values for the variables Cd, Zn and Pb (from the most extreme to the least extreme)
- Low values for the variable Ca

The distribution according to sampling stations (*Fig. 4C*) showed that they had no apparent impact on metals' concentrations.

http://www.aloki.hu ● ISSN 1589 1623 (Print) ● ISSN 1785 0037 (Online)
DOI: http://dx.doi.org/10.15666/aeer/2001_875892

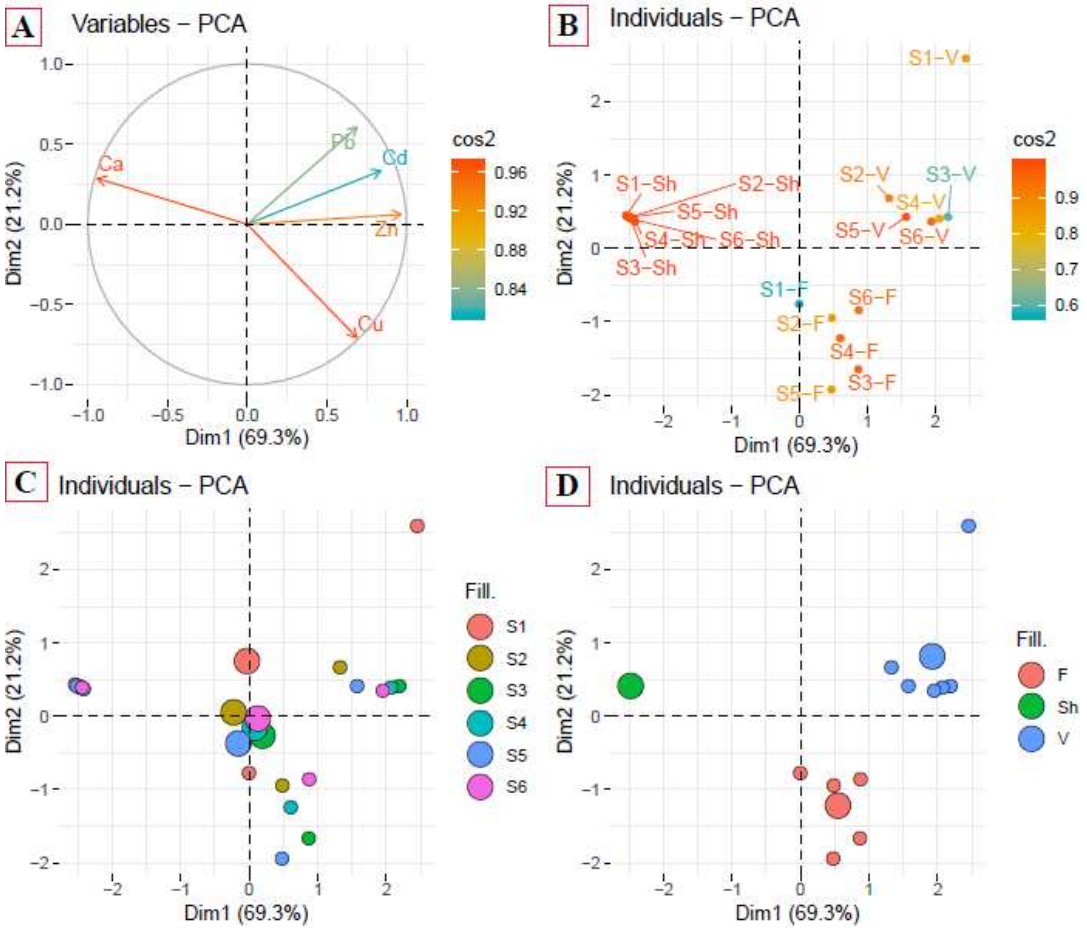

Figure 4. *PCA analysis of trace element concentrations in Otala spp. snail tissues (A: Metal distribution, B and D: tissue distribution, C: station distribution)*

Bioaccumulation factor

In order to compare and to assess the metal levels in snail tissues and in associated soil, the Bioaccumulation Factor was calculated (*Fig. 5*) (Adediran et al., 2003). This can be represented in *Equation 1:*

$$BAF = \frac{Concentration\ of\ the\ element\ in\ tissue}{Concentration\ of\ the\ same\ element\ in\ soil} \quad \text{(Eq.1)}$$

We considered that the element bioaccumulation is low when BAF < 1, medium when 1 < BAF < 5 and high when BAF > 5.

The calculated BAF_F, BAF_V and BAF_{Sh} values were very low for Pb in the six sampling stations with an average ranging between 0.019-0.061, 0.04-0.26 and 0.001-0.003 respectively. The BAF values below 1 indicate that Pb do not bioaccumulate in snail tissues.

Cd showed high bioaccumulation factor values for foot and viscera and low values for shell. These values ranged between 4.49-15.44 for foot, 19.26-44.35 for viscera and 0.014-0.84 for shell.

Otherwise, BAF values of the three essential elements Zn, Cu and Ca show variable results depending on the snail part as well as the sampling station. Generally, shells

http://www.aloki.hu ● ISSN 1589 1623 (Print) ● ISSN 1785 0037 (Online)
DOI: http://dx.doi.org/10.15666/aeer/2001_875892

registered the lower values for Zn and Cu ($BAF_{sh} < 1$) but the highest for Ca ($15.15 < BAF_{sh} < 272.05$).

Foot part demonstrated better efficiency in accumulating Cu with a BAF_{Cu} up to 9.34 while viscera presented a high BAF_{Cu} only in Tahannaout and Laâtamna ($BAF_{Cu} = 5$ and $BAF_{Cu} = 6.6$).

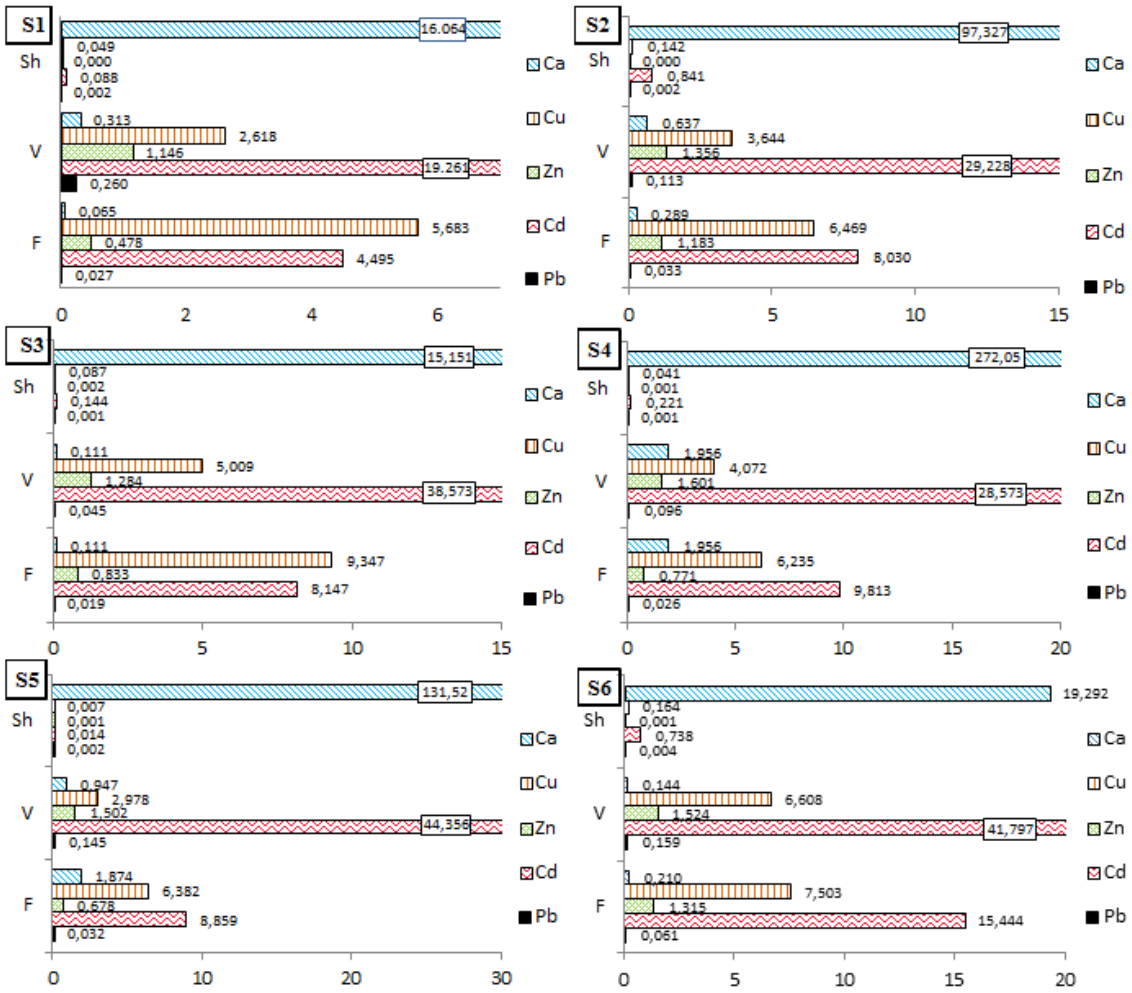

Figure 5. *Bioaccumulation factors (BAF) of Pb, Cd, Zn, Cu and Ca in different parts of Otala spp. snails compared to soil of the six sampling stations*

Discussion

Our study was carried out in five farms with agricultural activities, while the reference station was an open area without any agricultural activity. Farmers use fertilizers and pesticides to improve their production and control crop pests and weeds. However, these products may contain trace elements and their random usage can modify the characteristics of soil and even promote the bioavailability of some trace elements. Hence, because of the lack of control and awareness on the correct use of these products, they can turn from beneficial elements into a source of pollution for the abiotic compartments as well as for terrestrial organisms including snails.

Otala spp. snails are the most commonly widespread and the most consumed species in Marrakech. Besides being a popular local dish, large amounts of these species,

http://www.aloki.hu ● ISSN 1589 1623 (Print) ● ISSN 1785 0037 (Online)
DOI: http://dx.doi.org/10.15666/aeer/2001_875892

generally coming from unregulated collecting in the wild and farms, are intended for international consumption and exported from Morocco annually. Despite their national and international popularity, the quality of *O. lactea* and *O. punctata* snails, the trace element contents and the accumulation efficiency have never been studied before. The objective of this study is to fill this gap and to raise public awareness about food quality, especially for snail meat consumers, and then to push authorities to regularize the collection of these gastropods in order to avoid any human health risks and to protect a lot of endangered snail species.

The first results of this study showed significant differences between the analyzed soil samples that were possibly caused by anthropogenic activities especially for Cu which is a principal constituent of fertilizers. That is a rational reason since we are investigating in lands with agricultural activities. Otherwise, all the terrestrial metal concentrations of this study were below the maximum permissible limits suggested by the World Health Organization (100 µg/g for Pb, 3 µg/g for Cd, 300 µg/g for Zn and 100 µg/g for Cu) (Focus et al., 2021). They are also lower than those of Notten et al. (2005) and Madejón et al. (2013) but higher than those of Khalil (2013) except for Cd.

Moreover, the measurement of metallic element concentrations in land snails has been widely used to monitor the environmental levels of these elements in soils, specifically thanks to their ability of accumulation in high concentrations (Madejón et al., 2013; De Roma, 2017). It has been revealed in this study that all the studied trace elements were detected in the sampled snails. This result confirms the ability of terrestrial snails, including *Otala spp.*, to assimilate and accumulate trace elements as reported by several previous investigations (Fritsch et al., 2011; Magdalena et al., 2013; Larba and Soltani, 2014; Esposito et al., 2016).

Compared to other researches, *Otala spp*. snails in this study accumulated more levels of Pb, Cd, Zn and Cu than *Theba pisana* land snail (Madejón et al., 2013) and *Lanistes carinatus* freshwater snail. (Abdel Gawad, 2018). However, high values up to 33 µg/g for Cd, up to 313 µg/g for Pb and up to 2422 µg/g for Zn have been recorded in *Cantareus aspersus* garden snail (Pauget et al., 2015).

These elements accumulate by ingestion, as snails not only feed on plants which in turn may contain concentrations of trace elements, but they also ingest significant amounts of soil. On the other hand, the respiratory or dermal tract may also be a significant source of accumulation. Firstly, because land snails have a vascularized lung with a big pneumostome and a skin covered with mucus which can promote several interactions with their biotope. Therefore, snails can sometimes concentrate high levels and become biological and chemical contaminant vectors, especially in the case of snail predators (Wijnhoven et al., 2007; Scaffardi and Giordana, 2007).

The levels of accumulated Cd were higher than those of Pb. Concordant and similar results were observed in experiments on other land snails which found that they are macroconcentrators for Cd and microconcentrators for Pb. These elements are known to be accumulated in organs with high metabolic activity such us hepatopancreas and digestive gland (Manzl et al., 2004; Nica et al., 2014; Mleiki et al., 2016; Baroudi et al., 2020).

Studying trace element levels in *Otala spp.* snail tissues seems necessary to understand the bioaccumulation and the transfer process from the soil to the higher trophic levels of the food chain, especially those of snails' predators and humans. By doing this, we can get an idea about the levels of bioaccumulated trace elements and then to evaluate the risk of these cumulative metals on the other organisms' health.

http://www.aloki.hu ● ISSN 1589 1623 (Print) ● ISSN 1785 0037 (Online)
DOI: http://dx.doi.org/10.15666/aeer/2001_875892

In short, the PCA analysis revealed that the levels of most metallic trace elements were higher in the viscera than the foot, while shell accumulates only low concentrations. On the other hand, it was noteworthy that shells accumulate higher levels of Calcium than the other snail parts. Large amounts of Calcium are generally used by snails and other shelled animals to form their shells hence its elevated values in these findings (Ebenso, 2003). These results corroborate with several studies on snails (Deng et al., 2008; Bao et al., 2018).

It has been noticed also that Cu contents were higher in the foot part. In fact, this is an obvious result since Copper is an essential constituent of the oxygen-carrying protein, haemocyanin. (Otitoloju et al., 2009). Viscera accumulate more Cd, Zn and Pb than the other parts. Earlier studies have shown that the detoxification process of bioavailable non-essential elements and essential elements, assumed in excess, occurs in digestive gland and their bioaccumulation is due to the compartmentalization in intercellular granules or vesicles in the digestive gland or other tissues (Regoli et al., 2006; Boshoff et al., 2013).

These concentrations are usually influenced by diverse parameters such as snail age, physico-chemical soil properties, soil and air moisture, vegetation and concentrations of metals in soil. They can be very variable even in snails collected from the same area (Bargagli, 1998). Other studies confirm these findings and demonstrate that the metal concentration and soil characteristics explain 40-67% of the accumulation of metals in snails. Furthermore, pH, Cation-exchange capacity (CEC) and oxides (Fe and Al) modulate the bioavailability of Cd, Pb and Zn for snails (Pauget, 2012).

Pb accumulated in invertebrates is considered as a non-essential element (Rainbow, 2007; Lanno et al., 2019; Kumar et al., 2020). Unlike Pb, Cd, which has no important role for biological needs of the organism body (Kubier et al., 2019), showed high bioaccumulation factor values for foot and viscera and low values for shell. Similar results have been obtained by other authors in *Helix vladika* and *Helix secernenda* of Montenegro ($BAF_{Pb} < 1$ and $1.2 < BAF_{Cd} < 25.2$) (Vukašinovic-Pešic et al., 2020) while Mohammadein et al. (2013) found that both BAF_{Pb} and BAF_{Cd} are below 1 in tissues of *Eobania vermiculata* of Taif city. As found by other studies, our findings confirm that *Otala lactea* and *Otala punctata* snails are macrconcentrators for Cd, especially in their flesh, because they concentrate higher levels than their environment.

Generally, shells accumulated the lower levels for Zn and Cu but the highest for Ca. Feet demonstrated better efficiency in accumulating Cu. Dallinger and Wiesser (1984) showed that there was no preference for any organ in the distribution of Cu in *Helix pomatia* snails. In addition, earlier studies corroborates that gastropods usually showed much higher concentrations of Zn in their soft tissues than in their shells (De Wolf et al., 2001).

All these findings validate the hypothesis that *O. lactea* and *O. punctata,* like the most previously investigated species, are promising trace element bioindicators especially for Cd, Cu, Ca and Zn.

On the other hand, the toxic element contents in the edible part (foot) ranged between 0.42 and 0.84 µg/g for Pb and between 1.39 and 3.12 µg/g for Cd. We can observe that Pb contents are below the permissible levels (1.5 µg/g (dry weight)) established by the national and EU regulations (EU commission regulation No 1881/2006 of 19 December, 2006) in all the sampling stations. Contrariwise, Cd contents are above the allowable limits in mollusk meat (1.0 µg/g (dry weight)). This can threaten the safety of snail meat consumers especially in the long term, hence the exigency to establish and impose collection regulations in lands without any suspected metallic contaminations.

http://www.aloki.hu ● ISSN 1589 1623 (Print) ● ISSN 1785 0037 (Online)
DOI: http://dx.doi.org/10.15666/aeer/2001_875892

Conclusion

The edible *Otala lactea* and *Otala punctata* snails of Marrakech can be used as sentinel species to evaluate terrestrial pollution by trace metals. The results of this investigation showed large variability in concentrations of studied trace elements depending on the snail tissues and metal bioavailability. These snail species also have the quality of macroconcentration for Cd and microconcentration for Pb with levels that reached 15.48 μg/g (Cd) and 6.63 μg/g (Pb). Ca appears to be the most accumulated element in the shell (382.58*103 μg/g < Ca < 431.09*103 μg/g) while Cu is the most accumulated in the foot (190.83 μg/g < Cu < 389.74 μg/g). Viscera had a tendency to accumulate more toxic metals (0.97 μg/g < Pb < 5.96 μg/g and 6.32 < Cd < 12.74 μg/g) and Zn (142.1 μg/g < Zn < 245.41 μg/g) than the other parts. The detected concentrations may pose a potential health risk to consumers as well as to snail predators hence the necessity of continuous monitoring of the snail products intended for consumption. Moreover, organic farming must also be encouraged to preserve these endangered species and improve the quality of the product marketed nationally and internationally. In conclusion, the dataset confirmed that Otala spp. snails represent a potential candidate to monitor soil contamination in terrestrial ecosystems. However, no information exists in the literature concerning their limitations as ecological indicators, their usage in atmospheric monitoring, and the toxic effects of trace elements for these snails. For that several studies and further analysis must be conducted in the future to answer all the previous questions.

Acknowledgements. We would greatly thank Yannick François for the rendered help during the sample analysis and Fatima Zahra Guennoun for the species identification.

REFERENCES

[1] Abdel Gawad, S. (2018): Concentrations of heavy metals in water, sediment and mollusk gastropod, Lanistes carinatus from Lake Manzala, Egypt. – The Egyptian Journal of Aquatic Research 44(2): 77-82.

[2] Adediran, J. A., De Baets, N., Mnkeni, P. N. S., Kienkens, L., Muyima, N. Y. O., Thys, A. (2003): Organic waste materials for soil fertility improvement in the border region of the eastern cape. South Africa. – Biol. Agric. Hortic. 20: 283-300.

[3] American Psychological Association (APA). (2018): Guidelines for Ethical Conduct in the Care and Use of Nonhuman Animals in Research. – Committee on Animal Research and Ethics (CARE), Washington, DC.

[4] Anim, A. K., Ackah, M., Fianko, J. R., Kpattah, L., Osei, J., SerforArmah, Y., Gyamfi, E. T. (2011): Trace elements composition of Achatina achatina samples from the Madina Market in Accra, Ghana. – Research Journal of Environmental and Earth Sciences 3: 564-570.

[5] Bao, S., Huang, J., Liu, X., Tang, W., Fang, T. (2018): Tissue distribution of Ag and oxidative stress responses in the freshwater snail *Bellamya aeruginosa* exposed to sediment-associated Ag nanoparticles. Sci Total Environ. 644: 736-746.

[6] Bargagli, R. (1998): Trace Elements in Terrestrial Plants: An Ecophysiological Approach to Biomonitoring and Biorecovery. – Springer-Verlag, Berlin.

[7] Baroudi, F., Al Alam, J., Fajloun, Z., Millet, M. (2020): Snail as sentinel organism for monitoring the environmental pollution; a review. – Ecological Indicators 113: 106240.

[8] Boshoff, M., Jordaens, K., Backeljau, T., Lettens, S., Tack, F., Vandecasteele, B., De Jonge, M., Bervoets, L. (2013): Organ- and species-specific accumulation of metals in

http://www.aloki.hu ● ISSN 1589 1623 (Print) ● ISSN 1785 0037 (Online)
DOI: http://dx.doi.org/10.15666/aeer/2001_875892

two land snail species (Gastropoda, Pulmonata). – Science of The Total Environment 449: 470-481.

[9] Caracciolo, A. B., Terenzi, V. (2021): Rhizosphere microbial communities and heavy metals. – Microorganisms 9(7): 1462.

[10] Chrzan, A. (2017): The impact of heavy metals on the soil fauna of selected habitats in Niepołomice forest. – Polish J. Soil Sci. 2: 291-300.

[11] Dallinger, R., Wieser, W. (1984): Patterns of accumulation, distribution and liberation of Zn, Cu, Cd, and Pb in different organs of the land snail Helix pomatia L. Comp. Biochem. – Phys. C 79: 117-124.

[12] De Roma, A., Neola, B., Serpe, F. P., Sansone, D., Picazio, G., Cerino, P. M. (2017): Land snails (Helix aspersa) as Bioindicators of Trace Element Contamination in Campania (Italy). – OALib 4(2): 1-12.

[13] De Wolf, H., Ulomi, S. A., Backeljau, T., Pratap, H. B., Blust, R. (2001): Heavy metal levels in the sediments of four Dar es Salaam mangroves accumulation in, and effect on the morphology of the periwinkle, Littoraria scabra (Mollusca: Gastropoda). – Environment International 26: 243-249.

[14] Deng, P. Y., Shu, W. S., Lan, C. Y., Liu, W. (2008): Metal contamination in the sediment, pondweed, and snails of a stream receiving effluent from a lead/zinc mine in southern China. – Bull Environ Contam Toxicol. 81: 69-74.

[15] Ebenso, I. E. (2003): Dietary calcium supplement for edible tropical land snails *Archachatina marginata* in Niger Delta, Nigeria. – Livestock Research for Rural Development 15: 1-5.

[16] Ejidike, I. P., Onianwa, P. C. (2015): Assessment of trace metals concentration in tree barks as indicator of atmospheric pollution within Ibadan City, South-West, Nigeria. – J. Anal. Methods Chem. 243601.

[17] Esposito, M., Serpe, F. P., Neola, B., Sansone, D., Fiorito, F., Cerino, P. (2016): Use of Snails (Helix aspersa) as Sentinels to Evaluate Environmental Contamination by Polycyclic Aromatic Hydrocarbons and Trace Element. – 70th Convegno SISVET ts Conference, Palermo, Italy.

[18] Focus, E., Rwiza, M. J., Mohammed, N. K., Banzi, F. P. (2021): Health risk assessment of trace elements in soil for people living and working in a mining area. – Journal of Environmental and Public Health. DOI: 10.1155/2021/9976048.

[19] Fritsch, C., Cœurdassier, M., Gimbert, F., Crini, N., Scheifler, R., de Vaufleury, A. (2011): Investigations of responses to metal pollution in land snail populations (Cantareus aspersus and Cepaea nemoralis) from a smelter-impacted area. – Ecotoxicology 20: 739-59.

[20] Ghemari, C., Waterlot, C., Ayari, A., Leclercq, J., Douay, F., Nasri-Ammar, K. (2017): Assessment of heavy metals in soil and terrestrial isopod Porcellio laevis in Tunsian industrialized areas. – Environ Earth 76: 623.

[21] Gomot De Vaufeury, A., Pihan, F. (2000): Growing snails used as sentinels to evaluate terrestrial environment contamination by trace elements. – Chemosphere 40: 275-284.

[22] Gomot, A. (1998): Biochemical composition of Helix snails: influence of genetic and physiopathological factors. – Journal of Mollusca. Studies 64: 173-181.

[23] Herbert, D. G. (2010): The Introduced Terrestrial Mollusca of South Africa. – SANBI Biodiversity Series 15. South African National Biodiversity Institute, Pretoria.

[24] High Commission for Planning, Regional Planning Directorate for the Marrakech - Safi Region (2018): Regional Monograph. – Marrakech, Safi Region.

[25] Indexbox (2019): World - Snails (Except Sea Snails) - Market Analysis, Forecast, Size, Trends and Insights. – Indexbox.

[26] Jahan, S., Strezov, V. (2019): Assessment of trace elements pollution in the sea ports of New South Wales (NSW), Australia using oysters as bioindicators. – Sci Rep. 9: 1416.

http://www.aloki.hu ● ISSN 1589 1623 (Print) ● ISSN 1785 0037 (Online)
DOI: http://dx.doi.org/10.15666/aeer/2001_875892

[27] Khalil, A. M. (2013): The effects of soil heavy metals pollution and seasonal variations on gametogenesis and energy reserves of the land snail *Eobania vermiculata*. – J Biol Earth Sci. 3(2): 206-213.
[28] Kubier, A., Wilkin, R. T., Pichler, T. (2019): Cadmium in soils and groundwater: a review. – Applied Geochemistry 108: 104388.
[29] Kumar, A., Cabral-Pinto, M. M. S., Chaturvedi, A. K., Shabnam, A. A., Subrahmanyam, G., Mondal, R., Gupta, D. K., Malyan, S. K., Kumar, S., Khan, A. S., Yadav, K. K. (2020): Lead toxicity: health hazards, influence on food chain, and sustainable remediation approaches. – International Journal of Environmental Research and Public Health 17(7): 2179.
[30] Lanno, R. P., Oorts, K., Smolders, E., Albanese, K., Chowdhurye, M. J. (2019): Effects of soil properties on the toxicity and bioaccumulation of lead in soil invertebrates. – Environmental Toxicology and Chemistry 38: 1486-1494.
[31] Larba, R., Soltani, N. (2014): Use of the land snail Helix aspersa for monitoring heavy metal soil contamination in Northeast Algeria. – Environmental Monitoring and Assessment 186: 4987-4995.
[32] Luczynska, J., Paszczyk, B., Luczynski, M. J. (2018): Fish as a bioindicator of heavy metals pollution in aquatic ecosystem of Pluszne Lake, Poland, and risk assessment for consumer's health. – Ecotoxicol Environ Saf. 153: 60-67.
[33] Madejón, P., Arrébola, J., Madejón, E., Burgos, P., López-Garrido, R., Cárcaba, A., Cabrera, F., Murillo, J. M. (2013): The snail *Theba pisana* as an indicator of soil contamination by trace elements: potential exposure for animals and humans. – J. Sci. Food Agric. 93: 2259-2266.
[34] Magdalena, B., Kurt, J., Thierry, B., Suzanna, L., Filip, T., Bart, V., Maarten, D. J., Lieven, B. (2013): Organ- and species-specific accumulation of metals in two land snail species (Gastropoda, Pulmonata). – Science of the Total Environment 449: 470-481.
[35] Manev, I., Kirov, V., Neshovska, H. (2020): Heavy metals accumulation in black sea ecosystems: seawater, sediment, algae, benthic organisms. – Tradition And Modernity in Veterinary Medicine 5: 88-99.
[36] Manzl, C., Krumschnabel, G., Schwarzbaum, P. J., Dallinger, R. (2004): Acute toxicity of cadmium and copper in hepatopancreas cells from the Roman snail (Helix pomatia). – Comparative Biochemistry and Physiology Part C: Toxicology & Pharmacology 138: 45-52.
[37] Minodora, M. (2017): Soil invertebrates - a useful tool in biomonitoring of heavy metal pollution. A Review. – Studia Universitatis "Vasile Goldiş", Seria Ştiinţele Vieţii 27(4): 247-258.
[38] Mleiki, A., Irizar, A., Zaldibar, B., El Menif, N. T., Marigómez, I. (2016): Bioaccumulation and tissue distribution of Pb and Cd and growth effects in the green garden snail, Cantareus apertus (Born, 1778), after dietary exposure to the metals alone and in combination. – Sci Tot Environ. 547: 148-156.
[39] Mohammadein, A., El-Shenawy, N. S., Al-Fahmie, Z. H. H. (2013): Bioaccumulation and histopathological changes of the digestive gland of the land snail Eobania vermiculata (Mollusca: Gastropoda), as biomarkers of terrestrial heavy metal pollution in Taif city. – Ital. J. Zool. 80: 345-357.
[40] Müller, O. F. (1774): Vermium terrestrium et fluviatilium, seu animalium infusorium, Helminthicorum, et testaceorum, non marinorum, succincta historia. V 2: I-XXXVI, 1-214. – Heineck et Faber, Havnia et Lipsia.
[41] Munees, A. (2019): Remediation of metalliferous soils through the heavy metal resistant plant growth promoting bacteria: paradigms and prospects. – Arabian Journal of Chemistry 12(7): 1365-1377.
[42] Nica, D. V., Bordean, D-M., Hărmănescu, M., Buram, G. I. (2014): Interactions among heavy metals (Cu, Cd, Zn, Pb) and metallic macroelements (K, Ca, Na, Mg) in Roman snail (Helix pomatia) soft tissues. – Acta Metallomica - MEEMB 11: 65-71.

http://www.aloki.hu ● ISSN 1589 1623 (Print) ● ISSN 1785 0037 (Online)
DOI: http://dx.doi.org/10.15666/aeer/2001_875892

[43] Notten, M., Oosthoek, A., Rozema, J., Aerts, R. (2005): Heavy metal concentrations in a soil–plant–snail food chain along a terrestrial soil pollution gradient. – Environ. Pollut. 138: 178-190.
[44] Orcid, O. K., Orcid, O. S. (2019): Heavy metals in the dandelion and apple tree pollen from the different terrestrial ecosystems of the Carpathian region. – Acta Sci. Pol. Zootechnica 18(3): 15-20.
[45] Otitoloju, A. A., Ajikobi, D. O., Egonmwan, R. I. (2009): Histopathology and bioaccumulation of heavy metals (Cu & Pb) in the giant land snail, Archachatina marginata (Swainson). – The Open Environmental Pollution and Toxicology Journal 1: 79-88.
[46] Pankova, E. S., Kamnev, A. N., Golubeva, E. I. (2015): Features of the distribution of heavy metals in brown algae Cystoseira barbata. – International Popular Science Journal Europe-Asia. Earth Sciences 5: 25-28.
[47] Parmar, T., Rawtani, D., Agrawal, Y. (2016): Bioindicators: the natural indicator of environmental pollution. – Frontiers in Life Science 9: 1-9.
[48] Parolini, M., Sturini, M., Maraschi, F., Profumo, A., Costanzo, A., Caprioli, M., Rubolini, D., Ambrosini, R., Canova, L. (2021): Trace elements fingerprint of feathers differs between breeding and non-breeding areas in an Afro-Palearctic migratory bird, the barn swallow (Hirundo rustica). – Environ Sci Pollut Res Int. 28(13): 15828-15837.
[49] Pauget, B. (2012): Determination of the soil parameters that influence the metal bioavailability and accumulation for the snails (Cantareus aspersus). – Thesis Université de Franche-comté U.F.R. des sciences et techniques Laboratoire Chrono-Environnement (UMR CNRS/UFC 6249, Usc INRA).
[50] Pauget, B., Faure, O., Conord, C., Crini, N., De Vaufleury, A. (2015): In situ assessment of phyto and zooavailability of trace elements: a complementary approach to chemical extraction procedures. – Sci Total Environ 521-522: 400-410.
[51] Rainbow, P. S. (2007): Trace metal bioaccumulation: model, metabolic availability and toxicity. – Environment International 33(4): 576-82.
[52] Regoli, F., Gorbi, S., Fattorini, D., Tedesco, S., Notti, A., Machella, N., Bocchetti, R., Benedetti, M., Piva, F. (2006): Use of the land snail Helix aspersa as sentinel organism for monitoring ecotoxicologic effects of urban pollution: an integrated approach. – Environ. Health Perspect. 114: 63-69.
[53] Robinson, D. G., Redmond, L., Hennessey, R. (1998): Importation and interstate movement of live, edible land snails: Cantareus apertus (Born), Cryptomphalus aspersus (Müller), Eobania vermiculata (Müller), Helix pomatia Linné, and Otala lactea (Müller) (Pulmonata: Helicidae). – Qualitative Pest Risk Assessment. USDA APHIS PPQ Scientific Services, Riverdale, MD.
[54] Scaffardi, E., Ru, G., Giordana, G. (2007): Accumulo di metalli pesanti in chiocciole della specie Helix pomatia L. (Pulmonata, Helicidae) destinate al consumo umano. – Il Chirone 1: 8-11.
[55] Shahid, M., Dumat, C., Khalid, S., Schreck, E., Xiong, T., Niazi, N. K. (2016): Foliar heavy metal uptake, toxicity and detoxification in plants: a comparison of foliar and root metal uptake. – Journal of Hazardous Materials, Elsevier 325: 36-58.
[56] Shotuyo, A. L., Bambgose, O., Oduntan, O. O., et al. (2016): Levels of some heavy metals in African Giant Land Snail (Archachatina marginata) in major markets in Abeokuta, South West Nigeria. – International Journal of Molecular Ecology and Conservation 6(1): 1-6.
[57] Ugbaja, R. N., Enilolobo, M. A., James, A. S., Akinhanmi, T. F., Akamo, A. J., Babayemi, D. O., Ademuyiwa, O. (2020): Bioaccumulation of heavy metals, lipid profiles, and antioxidant status of snails (Achatina achatina) around cement factory vicinities. – Toxicol. Ind. Health 36(11): 863-875.
[58] Vukašinovic-Pešic, V., Pilarczyk, B., Miller, T., Rajkowskamysliwiec, R., Podlasinska, J., Tomza-Marciniak, A., Blagojevic, N., Trubljanin, N., Zawal, A., Pešic, V. (2020):

http://www.aloki.hu ● ISSN 1589 1623 (Print) ● ISSN 1785 0037 (Online)
DOI: http://dx.doi.org/10.15666/aeer/2001_875892

Toxic elements and mineral content of different tissues of endemic edible snails (Helix vladika and H. secernenda) of Montenegro. – Foods 9: 731.

[59] Wang, K., Qiao, Y., Zhang, H., Yue, S., Li, H., Ji, X., Liu, L. (2018): Bioaccumulation of heavy metals in earthworms from field contaminated soil in a subtropical area of China. – Ecotoxicology and Environmental Safety 148: 876-883.

[60] Wijnhoven, S., Leuven, R., van der Velde, G., Jungheim, G., Koelemij, E., de Vries, F., Eijsackers, H., Smits, A. (2007): Heavy-metal concentrations in small mammals from a diffusely polluted floodplain: importance of species- and location specific characteristics. – Archives of Environmental Contamination and Toxicology 52: 603-613.

http://www.aloki.hu ● ISSN 1589 1623 (Print) ● ISSN 1785 0037 (Online)
DOI: http://dx.doi.org/10.15666/aeer/2001_875892

COMBINED EFFECTS OF STRAW RETURNING AND NITROGEN FERTILIZER APPLICATION ON CROP YIELD AND NITROGEN UTILIZATION IN THE CHERNOZEM OF NORTHEAST CHINA

GAO, H. J.[1] – CHEN, X. W.[2*] – LIANG, A. Z.[2] – PENG, C.[1*] – ZHU, P.[1] – ZHANG, X. Z.[1]

[1]*Institute of Agricultural Resource and Environment, Jilin Academy of Agricultural Sciences, Changchun 130033, China*

[2]*Key Laboratory of Mollisols Agroecology, Northeast Institute of Geography and Agroecology, Chinese Academy of Sciences, Changchun 130102, China*

[*]*Corresponding authors*
e-mail: chenxuewen@iga.ac.cn (Chen, X. W.); pengchang2005@163.com (Peng, C.)

(Received 13th Oct 2021; accepted 22nd Dec 2021)

Abstract. Balancing the relationship between straw returning and fertilizer, especially nitrogen fertilizer application is vital for achieving the goal of reducing fertilization and improving soil fertility. To better understand their combined effects on crop yield and nitrogen utilization, a study was conducted to explore the effects of straw returning and nitrogen fertilizer application on crop yield and nitrogen utilization. In contrast to straw return, nitrogen fertilizer application had a more significant effect on the crop yield. Straw ploughing led to significantly higher crop yield under the nitrogen fertilizer application rates of 0, 90, 150 kg/ha compared to straw mulching ($P < 0.05$). No significant differences for > 150 kg/ha concerning their effects on crop yield were observed between straw ploughing and mulching. The optimal residual return amount was 9000 kg/ha and straw return was not decisive to crop yield under the same nitrogen fertilizer application rate. Straw ploughing better promoted nitrogen uptake, utilization, harvest and retention than straw mulching and no residue addition when combined with nitrogen fertilizer application. These findings demonstrate that straw ploughing and 150 kg/ha nitrogen fertilizer application rate is a better combination for implementing stable production and enhancing nitrogen utilization synchronously in the chernozem of Northeast China.
Keywords: *straw ploughing, straw mulching, residual return amount, corn nitrogen uptake, soil total nitrogen*

Introduction

Soil nitrogen is an essential nutrient for plant growth and development in an ecosystem meanwhile an important element that restricts crop yield (Osterholz et al., 2018). Proper application of nitrogen fertilizer is an effective means to increase crop yield (Tenelli et al., 2021). However, in order to achieve high yields, people over apply nitrogen fertilizer that exceeds the requirements of plants (Li et al., 2021). Excessive application of nitrogen fertilizer not only resulted in serious waste of nitrogen fertilizer, but also reduced utilization rate and significantly increased apparent loss (Ahmed et al., 2017). At the same time, it led to a series of environmental problems (water pollution, soil acidification, greenhouse effect, etc.) (Huang et al., 2018; Asibi et al., 2019; Rahman et al., 2021). Therefore, reduced fertilization is the development trend of future farmland management and crop production.

Nonetheless, significant reduction in the application of nitrogen fertilizer will affect crop growth (Ruffatti et al., 2019). Hence, on the basis of proper fertilization, reasonable utilization of the soil's own capacity to provide fertilizer and the adoption of a reasonable way to cultivate fertilizer are the main ways to improve the utilization rate of nitrogen

http://www.aloki.hu ● ISSN 1589 1623 (Print) ● ISSN1785 0037 (Online)
DOI: http://dx.doi.org/10.15666/aeer/2001_893903

fertilizer, reduce environmental pollution, and improve crop yield and quality (Dimkpa et al., 2020). Straw returning is an effective measure to cultivate fertilizer and it can increase soil organic matter content and nutrient recycling efficiency, balance crop nutrients, and significantly change the relationship between source and reservoir in crop (Wang et al., 2018). C/N ratio in crop straw is relatively high which often causes soil nitrogen fixation after straw returning to the field (Farooq et al., 2019). In such a condition, this will reduce soil nitrogen supply capacity and affect crop growth and thus it is necessary to apply nitrogen fertilizer to ensure the nitrogen supply after straw returning to the field (Weih et al., 2018). On the other hand, straw returning alone cannot meet the nutrient demand of crops and cannot achieve high yield whereas nitrogen fertilizer application could increase crop yield by increasing effective panicle number, grain number per panicle and grain weight (Guan et al., 2020). Therefore, combined application of straw returning and nitrogen fertilizer may increase crop yield more effectively, and it is also considered as an effective tillage management practice (Mabagala et al., 2020). However, the combined effects of straw returning and nitrogen fertilizer application on crop yield is as yet largely unknown.

On the other hand, the relationship between straw returning and nitrogen fertilizer utilization rate is still controversial. Some studies have pointed out that straw returning would reduce the nitrogen fertilizer utilization rate, there also exists opposite views (Dimkpa et al., 2020; Janke et al., 2020). Moreover, straw returning also affects nitrogen uptake and crop yield (Ma et al., 2021). The main reason for this is whether or not straw returning affect nitrogen utilization and crop yield alone. Thus we hypothesized that combined application of straw returning and nitrogen fertilizer application rates when there is a specific combination between them could stabilize crop yield and improve nitrogen utilization simultaneously. Furthermore, since chernozem is not as common as mollisol in Northeast China, and little information was available on the influence of straw returning and nitrogen fertilizer application on crop yield and nitrogen utilization in chernozem, more data in the comparison are required for the soil protection work in Northeast China.

Consequently, the objectives of this study were to (1) compare the effects of straw returning and nitrogen fertilizer application on crop yield and (2) analyze the effects of straw returning and nitrogen fertilizer application on nitrogen utilization. The present study may provide technical reference for the rational application of nitrogen fertilizer and the increment of corn yield under straw returning in dryland agricultural production conditions.

Materials and methods

Field site and treatments

The studied area was established in 2011 at the Experimental Station (44°56′N, 125°18′E) of Jilin Academy of Agricultural Sciences, in Nong'an County, Jilin Province, Northeast China. It has a mid-temperate continental monsoon climate with the mean annual temperature of 4.7 °C. The mean annual precipitation was 507.7 mm. The soil type studied in the present study was typical chernozem with a high pH value (pH > 7) and a high calcium carbonate ($CaCO_3$) content according to FAO (1998). Prior to the establishment of the current experiment, detailed soil chemical properties in 0-20 cm depth were as follows: 22.3 g/kg of soil organic matter, 1.537 g/kg of soil total nitrogen, 0.565 g/kg of soil total phosphorus, 22.7 g/kg of soil total potassium, 128.2 mg/kg of soil

http://www.aloki.hu ● ISSN 1589 1623 (Print) ● ISSN1785 0037 (Online)
DOI: http://dx.doi.org/10.15666/aeer/2001_893903

alkali-hydrolyzable nitrogen, 12.9 mg/kg of soil rapid available phosphorus, 132.5 mg/kg of soil rapid available potassium, 7.75 of soil pH.

Experimental design

The current experiment included two parts: (1) The objective for the first part was to compare the effects of different straw returning methods and different nitrogen fertilizer application rates. Under the same residual return amount (9000 kg/ha) to the field, six nitrogen fertilizer application rates level of 0 (N0), 90 (N6), 150 (N10), 210 (N14), 270 (N18), 330 (N22) kg/ha combined with 2 straw returning methods (straw ploughing and straw mulching). 9000 kg/ha was the residual return amount for local farmers (Zhao et al., 2019). Different residual return amount (0, 4500, 9000, 13500 kg/ha) and different straw returning methods (straw ploughing, straw mulching and no residue addition) under the same fertilizer application rate (210 kg/ha) was also involved in this part; (2) The objective for the second part was to compare the effects of straw returning and nitrogen fertilizer application on nitrogen utilization. Three straw returning methods (straw ploughing, straw mulching and no residue addition) under the same fertilizer application rate (210 kg/ha) was included in this part.

All the above treatments were arranged in a randomized complete block design with three replicates. Each treatment plot was 80 m^2. Phosphorus and potash fertilizers were applied as starter fertilizer at rates of 105 kg P/ha and 105 kg K/ha. For straw ploughing, after corn harvest, the straw was artificially scattered in each treatment plot according to the different application amount of corn straw, and then the straw was crushed by a straw grinder (the length was less than 6 cm), and the straw was returned to the field with a depth of about 16 cm by a high-horsepower agricultural machine to deep spiral, so that the straw was fully and evenly mixed with the soil, and finally the straw was heavily compressed. For straw mulching, after corn harvest, the straw crusher was used to crush the straw (the length was below 10 cm), and the no-tillage planter was used to complete the sowing, fertilization and repression operation at one time. Single column vibration local deep loosening operation was used once a year, and the depth of deep loosening was about 30 cm. Corn cultivar planted in the experimental plot was Pioneer Corn 335 planted at a density of 60, 000 plants/ha. One third of the nitrogen applied to corn was applied as starter fertilizer before spring sowing, the remaining 2/3 nitrogen fertilizer was topdressing at jointing stage. Nutrient content in corn straw was 42.6% C, 0.8% N, 0.32% P_2O_5, 0.75% K_2O, respectively. Corn was sown on or about April 28 and harvested on or about September 27 each year, plant spacing and row spacing were 65 cm and 18 cm, respectively, and field management measures were consistent in each treatment period.

Sampling and analysis

Three representative plants were taken in each plot at the mature stage of corn in 2016, which were divided into four parts: stem, leaf (bract), grain and shaft. The plants were de-enzyme at 105℃ for 30 min, dried at 80℃ to constant weight, and weighed as dry matter weight. Then all the samples were smashed and sifted 0.05 mm, and H_2SO_4-H_2O_2 digestion. The nitrogen content of plant samples was determined by Kjeldahl method. At the same time, composite soil samples were collected down to a depth of 20 cm from each plot using a manual soil probe and then used Elemental Analyzer to determine soil total nitrogen.

http://www.aloki.hu ● ISSN 1589 1623 (Print) ● ISSN1785 0037 (Online)
DOI: http://dx.doi.org/10.15666/aeer/2001_893903

Nitrogen partial factor productivity and nitrogen harvest index determination

Nitrogen partial factor productivity (kg/kg) was calculated by formula (1) (Sawyer et al., 2017):

$$\text{Nitrogen partial factor productivity} = \frac{Grain\ yield}{\text{Fertilizer nitrogen input}} \quad \text{(Eq.1)}$$

Nitrogen harvest index (%) calculation was according to formula (2) (Chen et al., 2011):

$$\text{Nitrogen harvest index} = \frac{Nitrogen\ uptake\ by\ grains}{Nitrogen\ uptake\ by\ plants} \times 100\% \quad \text{(Eq.2)}$$

Statistical analysis

The SPSS 13.0 software (SPSS Inc., Chicago, USA) was used for all of the statistical analyses. Multifactor interactions among the straw returning method, residual return amount and nitrogen fertilizer application rates on crop yield were used for an *F*-test analysis at a statistical significance of the 5% level. Treatment main effects on crop yield under the combination of straw returning and nitrogen fertilizer application, and under the same fertilizer application rate were tested using one-way analysis of variance (ANOVA). Treatment main effects on corn nitrogen uptake, nitrogen partial factor productivity, nitrogen harvest index and soil total nitrogen applied the above same statistical analysis method. Treatment means were compared using the least significant difference (LSD) at $P < 0.05$. Analysis of variance was used to test for differences in resulting crop yield for straw returning method and nitrogen fertilizer application. A probability value of 0.05 was used to delineate significant treatment effects.

Results

Effects of straw returning and nitrogen fertilizer application on crop yield

A multifactor interaction analysis was conducted to better understanding the effect of straw returning method (SRM), residual return amount (RRA) and nitrogen fertilizer application rates (NFAR) on crop yield (*Table 1*). According to the significant p-value for analysis of variance *F*-test, SRM and RRA did not have significant effect on crop yield (*Table 1*). NFAR and SRM×NFAR significantly affected crop yield (*Table 1*).

Table 1. *Significant p-value for analysis of variance F-test for crop yield as affected by straw returning method (SRM), residual return amount (RRA) and nitrogen fertilizer application rates (NFAR)*

	SRM	**RRA**	**NFAR**	**SRM×RRA**	**SRM×NFAR**	**RRA×NFAR**	**SRM×RRA×NFAR**
Crop yield	0.089	0.747	0.000**	0.995	0.000**	0.986	1

**Significant at 1% level

Straw ploughing led to significantly increment of crop yield under N0, N10 compared to straw mulching by 37.47% and 6.21%, respectively ($P < 0.05$), N6 treatment was not significant (*Fig. 1*). However, no significant differences were observed for nitrogen

http://www.aloki.hu ● ISSN 1589 1623 (Print) ● ISSN1785 0037 (Online)
DOI: http://dx.doi.org/10.15666/aeer/2001_893903

fertilizer application rates > 150 kg/ha (N14, N18, N22) between straw ploughing and straw mulching (*Fig. 1*).

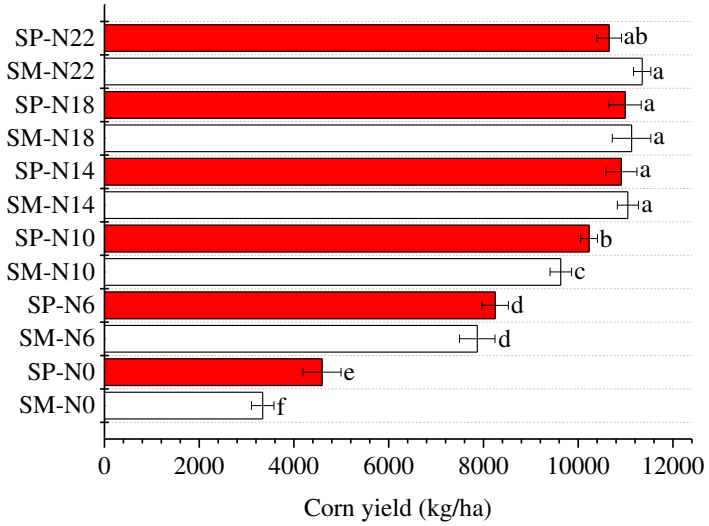

Figure 1. *Effects of different straw returning method and nitrogen fertilizer application rates on corn yield. SP: straw ploughing; SM: straw mulching; N0, N6, N10, N14, N18, N22 represents the nitrogen fertilizer application rates level of 0, 90, 150, 210, 270, 330 kg/ha, respectively*

Under the same fertilizer application rate (210 kg/ha), corn yield at no residue addition treatment was significantly lower than that at the residual return amount of 9000 kg/ha (*Fig. 2*). There were no significant differences for crop yield among different residual return amount of 0, 4500 and 13500 kg/ha treatment (*Fig. 2*). No residue addition, straw mulching and straw ploughing had no significant ($P > 0.05$) effect on crop yield under the same fertilizer application rate (*Fig. 2*).

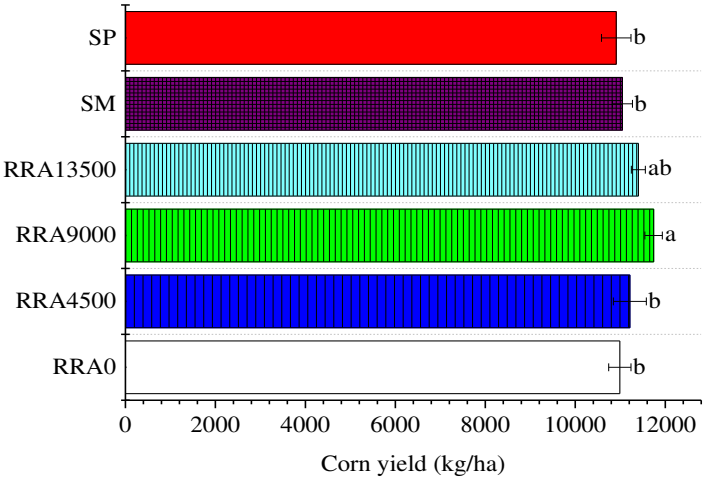

Figure 2. *Effects of different residual return amount and straw returning method on corn yield under the same fertilizer application rate (210 kg/ha). SP: straw ploughing; SM: straw mulching; RRA0, RRA4500, RRA9000, RRA13500 represents the residual return amount of 0, 4500, 9000, 13500 kg/ha, respectively*

http://www.aloki.hu ● ISSN 1589 1623 (Print) ● ISSN1785 0037 (Online)
DOI: http://dx.doi.org/10.15666/aeer/2001_893903

Change in crop yield by straw returning method and nitrogen fertilizer application rates was significantly affected by the nitrogen fertilizer application rates of 0-90 and 0-150 kg/ha, but it was not affected by 0-210, 0-270 and 0-330 kg/ha (*Table 2*).

Table 2. *Analysis of Variance for straw returning method and nitrogen fertilizer application effects on crop yield*

Different range of nitrogen fertilizer application rates (kg/ha)		Sum of Squares	df	Mean Square	F	Sig.
0-90	Between Groups (Replicate)	1141448.167	1	1141448.167	53.991	0.002
	Within Groups (Error)	84565.333	4	21141.333		
	Total	1226013.5	5			
0-150	Between Groups (Replicate)	639613.5	1	639613.5	6.717	0.044
	Within Groups (Error)	380920	4	95230		
	Total	1020533.5	5			
0-210	Between Groups (Replicate)	2891204.167	1	2891204.167	8.442	0.061
	Within Groups (Error)	1369880.667	4	342470.167		
	Total	4261084.834	5			
0-270	Between Groups (Replicate)	2888428.167	1	2888428.167	15.48	0.067
	Within Groups (Error)	746386.667	4	186596.667		
	Total	3634814.834	5			
0-330	Between Groups (Replicate)	5709601.5	1	5709601.5	18.708	0.072
	Within Groups (Error)	1220798	4	305199.5		
	Total	6930399.5	5			

Effects of straw returning and nitrogen fertilizer application on nitrogen utilization

Under the same nitrogen fertilizer application rate (210 kg/ha), straw returning method affected corn nitrogen uptake significantly (*Table 3*). Both straw mulching and straw ploughing had significantly ($P < 0.05$) greater corn nitrogen uptake than no residue addition treatment (*Table 3*). A similar trend was also found for the soil total nitrogen (*Table 3*). Though straw ploughing resulted in similar corn nitrogen uptake and soil total nitrogen values with straw mulching, the former was 1.33% and 4.43% higher than the latter, respectively (*Table 3*). Nitrogen harvest index in straw ploughing was significantly higher than in no residue addition and straw mulching treatments ($P < 0.05$) (*Table 3*). Nitrogen partial factor productivity among the residual return methods was not significantly different ($P > 0.05$) (*Table 3*).

Table 3. *Mean values (standard errors in parentheses) of corn nitrogen uptake, nitrogen partial factor productivity, nitrogen harvest index and soil total nitrogen for different treatments*

Treatment	Corn nitrogen uptake (kg/ha)	Nitrogen partial factor productivity (kg/kg)	Nitrogen harvest index (%)	Soil total nitrogen (g/kg)
No residue addition	206.57 (3.30) b	52.34 (0.68) a	66.86 (0.54) b	1.49 (0.01) b
Straw mulching	218.43 (2.42) a	52.61 (0.61) a	65.44 (0.41) b	1.58 (0.02) a
Straw ploughing	221.33 (1.27) a	51.97 (0.91) a	69.72 (0.52) a	1.65 (0.03) a

Different lowercase letters in a column means significant difference between treatments at $P < 0.05$

http://www.aloki.hu ● ISSN 1589 1623 (Print) ● ISSN1785 0037 (Online)
DOI: http://dx.doi.org/10.15666/aeer/2001_893903

Discussion

Effects of straw returning and nitrogen fertilizer application on crop yield

According to the multifactor interaction analysis, neither the straw returning method nor the residual return amount affected crop yield. However, nitrogen fertilizer application rates have a significant impact on crop yield. This implies there exists a long-term cumulative process about the effects of combined straw returning and nitrogen application on crop yield and this effect does not appear immediately. The reason for this situation was that soil nitrogen supply capacity would be reduced in the early stage of straw returning and this was not conducive to early crop growth (Nasielski and Deen, 2019), thus in that case nitrogen fertilizer should be applied in conjunction to regulate soil nitrogen content for crop growth (Harindintwali et al., 2021). What this paper showed was the fifth year result of the experiment, another reason may be due to the lower decay rate of residue. For residual return amount, lower amount did not manifest beneficial effects on crop yield (Li et al., 2018) whereas higher amount changed carbon and nitrogen transformation in soil ecosystem and further nitrogen supply capacity (Qin et al., 2021). So when residual return amount reached a certain critical value, it would affect crop growth. Similar result was obtained by Yin et al. (2018) who found corn yield was not affected by straw returning under different nitrogen fertilizer application rates. Significant effect was observed in the influence of the SRM×NFAR interaction on crop yield. It was mainly attributed to the important role of nitrogen fertilizer application. Straw ploughing resulted in higher crop yield under N0, N6, N10 relative to straw mulching. The possible explanation was nitrogen fertilizer application took more important effect on crop yield under the combination of straw returning and nitrogen fertilizer application. On the other hand, it can be seen that the combination of nitrogen fertilizer application and straw ploughing is more beneficial to crop growth than straw mulching. No significant effect on crop yield were observed between straw ploughing and straw mulching under the nitrogen fertilizer application rates > 150 kg/ha (N14, N18, N22). This means there exists a threshold value of nitrogen fertilizer application rates to affect crop growth. It was consistent with those reported by Sadeghi et al. (2018) who found when the nitrogen application rate increased to a certain extent, the increment in crop yield would be less pronounced, and it may even show a downward trend. No residue addition treatment resulted in significantly lower corn yield than that at the residual return amount of 9000 kg/ha under the same fertilizer application rate (210 kg/ha). It indicated that no residual returning certainly do no good to crop growth. Furthermore, different residual return amount of 0, 4500 and 13500 kg/ha treatment had no significant ($P > 0.05$) effect on crop yield. These results suggest that 9000 kg/ha should be the optimum residual return amount considering 210 kg/ha is the amount of nitrogen fertilizer applied by local farmers (Yu et al., 2021). It also confirms the critical value of residual return amount as discussed before. There were no significant differences for crop yield among no residue addition, straw mulching and straw ploughing under the same fertilizer application rate. This result means straw returning method is not decisive to crop yield under the same fertilizer application rate. In other words, either straw ploughing or straw mulching is a good way to avoid straw burning-caused environmental problems compared with no residue addition. The result that change in crop yield by residual return method and nitrogen fertilizer application rates was significantly affected by the nitrogen fertilizer application rates of 0-90 and 0-150 kg/ha rather than 0-210, 0-270 and 0-330 kg/ha verifies the above threshold value of nitrogen fertilizer application rates on crop growth. This illustrated that

http://www.aloki.hu ● ISSN 1589 1623 (Print) ● ISSN1785 0037 (Online)
DOI: http://dx.doi.org/10.15666/aeer/2001_893903

150 kg/ha was the optimum amount of nitrogen fertilizer application rates on crop yield in this study.

Effects of straw returning and nitrogen fertilizer application on nitrogen utilization

In order to facilitate comparison, this study compared the effects of straw returning and nitrogen fertilizer application on nitrogen utilization under the same fertilizer application rate (210 kg/ha). Both straw mulching and straw ploughing led to significantly greater corn nitrogen uptake compared to no residue addition treatment ($P < 0.05$). This was mainly related to the fact that nitrogen of returned straw was released during the decomposition process and increasing the soil nitrogen supply (Nafi et al., 2019). It was agreed upon by previous research (Fang et al., 2018) whereas contrasted with the study of Chen et al. (2014). The underlying reason for this was different crop cultivation systems, different field management methods and different temperature and climate would all affect the results of straw returning and nitrogen fertilizer application on corn nitrogen uptake. Interestingly, the corn nitrogen uptake in either straw mulching or straw ploughing was greater than the nitrogen fertilizer application rate. Since crop absorption is the main way of soil nitrogen expenditure, this also explains the promotion effect of straw returning on corn nitrogen uptake. Straw returning method resulted in significantly different values of soil total nitrogen ($P < 0.05$). In contrast to no residue addition, both straw mulching and straw ploughing had a significantly greater soil total nitrogen. This was in accordance with the results obtained by Xue et al. (2015) who found straw ploughing and straw mulching increased soil total nitrogen significantly on the topsoil. Dong et al. (2018) further pointed out that straw ploughing increased soil total nitrogen than no residue addition treatment. It was owing to the fact that residual itself as an organic fertilizer could improve total nitrogen fixation when mixed with topsoil. This result indicated that either residue added on the soil surface or residue incorporated into soil was more favorable for nitrogen retention than no residue addition on soil under the same fertilizer application rate. The reason why straw ploughing resulted in similar corn nitrogen uptake and soil total nitrogen values with straw mulching whereas the former was a little higher than the latter was different position of straw in soil and different contact degree with soil affecting the decomposition rate and soil nitrogen supply. Nitrogen harvest index reflects the sensitivity of grain to nitrogen and indicates the efficiency of nitrogen transfer to grain (Banger et al., 2019). In current study, nitrogen harvest index in straw ploughing was significantly higher than no residue addition and straw mulching treatment. It indicated that straw ploughing could better promote the transfer of nitrogen absorbed by the plant to the grain. There are many parameters to characterize the use efficiency of nitrogen fertilizer, but nitrogen partial factor productivity is commonly used in the international agricultural community (Cordero et al., 2019). Because it does not need blank area yield and nutrient absorption measurement, and it is simple and clear for farmers to master (Obade, 2019). Generally speaking, nitrogen partial factor productivity decreases with the increment of nitrogen fertilizer applied rates and straw returning can increase the nitrogen partial factor productivity (Hamoud et al., 2019). It was worth noting that straw returning methods did not significantly affect nitrogen partial factor productivity in the present study. This means that nitrogen partial factor productivity is related with the threshold value of nitrogen fertilizer application rates. When the critical value is reached, nitrogen partial factor productivity does not change much. Combined with the previous analysis, here it confirms 150 kg/ha was the optimum amount of nitrogen fertilizer application rates on

http://www.aloki.hu ● ISSN 1589 1623 (Print) ● ISSN1785 0037 (Online)
DOI: http://dx.doi.org/10.15666/aeer/2001_893903

crop yield again in this study. Synthesize the above discussion, straw ploughing is more beneficial to nitrogen uptake, utilization, harvest and retention than straw mulching and no residue addition treatment when combined with nitrogen fertilizer application. Therefore, it is better to use the combination of straw ploughing and 150 kg/ha nitrogen fertilizer application rates when taking into account both reduced fertilization and improved soil fertility in the chernozem of Northeast China.

Conclusion

In the present study, we investigated the effects of strawing return and nitrogen fertilizer application on crop yield and nitrogen utilization. Our results revealed that nitrogen fertilizer application rather than straw returning method was dominate factor affecting crop yield when using the combination of straw returning and nitrogen fertilizer application. Straw ploughing had a significantly higher crop yield under the nitrogen fertilizer application rates of 0, 90, 150 kg/ha contrasted with straw mulching. No significant differences were found for nitrogen fertilizer application rates > 150 kg/ha on crop yield between straw ploughing and straw mulching. Under the same fertilizer application rate, the optimum residual return amount was 9000 kg/ha and straw returning method was not decisive to crop yield. Among different straw returning method, straw ploughing is more favorable to nitrogen uptake, utilization, harvest and retention than straw mulching and no residue addition treatment when combined with nitrogen fertilizer application. Consequently, straw ploughing and 150 kg/ha nitrogen fertilizer application rates would be a better option when considering crop yield stabilization and nitrogen utilization improvement simultaneously in the chernozem of Northeast China. Future studies are needed on how to apply and extend this combination management practice to the agricultural field.

Acknowledgements. This research was funded by the Key Research and Development Project of Jilin Province (20200402103NC), Major Science and Technology Project of Jilin Province (20200503004SF), Innovation Leadership and Team Program in Sciences and Technologies for Young and Middle-aged Scientists of Jilin Province (20200301022RQ).

REFERENCES

[1] Ahmed, M., Rauf, M., Mukhtar, Z., Saeed, N. A. (2017): Excessive use of nitrogenous fertilizers: an unawareness causing serious threats to environment and human health. – Environmental Science and Pollution Research 24(35): 26983-26987.

[2] Asibi, A. E., Chai, Q., Coulter, J. A. (2019): Mechanisms of nitrogen use in maize. – Agronomy-Basel 9(12): 775.

[3] Banger, K., Nafziger, E. D., Wang, J. M., Pittelkow, C. M. (2019): Modeling inorganic soil nitrogen status in maize agroecosystems. – Soil Science Society of America Journal 83(5): 1564-1574.

[4] Chen, C. C., Han, G. Q., He, H. Q., Westcott, M. (2011): Yield, protein, and remobilization of water soluble carbohydrate and nitrogen of three spring wheat cultivars as influenced by nitrogen input. – Agronomy Journal 103(3): 786-795.

[5] Chen, B. Q., Liu, E. K., Tian, Q. Z., Yan, C. R., Zhang, Y. Q. (2014): Soil nitrogen dynamics and crop residues. A review. – Agronomy for Sustainable Development 34(2): 429-442.

http://www.aloki.hu ● ISSN 1589 1623 (Print) ● ISSN1785 0037 (Online)
DOI: http://dx.doi.org/10.15666/aeer/2001_893903

[6] Cordero, E., Longchamps, L., Khosla, R., Sacco, D. (2019): Spatial management strategies for nitrogen in maize production based on soil and crop data. – Science of the Total Environment 697: 133854.
[7] Dimkpa, C. O., Fugice, J., Singh, U., Lewis, T. D. (2020): Development of fertilizers for enhanced nitrogen use efficiency - Trends and perspectives. – Science of The Total Environment 731: 139113.
[8] Dong, Q. G., Yang, Y. C., Yu, K., Feng, H. (2018): Effects of straw mulching and plastic film mulching on improving soil organic carbon and nitrogen fractions, crop yield and water use efficiency in the Loess Plateau, China. – Agricultural Water Management 201: 133-143.
[9] Fang, Y. Y., Nazaries, L., Singh, B. K., Singh, B. P. (2018): Microbial mechanisms of carbon priming effects revealed during the interaction of crop residue and nutrient inputs in contrasting soils. – Global Change Biology 24(7): 2775-2790.
[10] FAO. (1998): World reference base for soil resources. – Food and Agriculture Organization of the United Nations, Rome.
[11] Farooq, N., Iqbal, M., Farooq, M., Zahir, Z. A. (2019): Interactive effects of synthetic fertilizer and organic residue inputs on soil fertility and wheat crop under various moisture regimes. – International Journal of Agriculture and Biology 21(1): 244-250.
[12] Guan, X. K., Wei, L., Turner, N. C., Ma, S. C., Yang, M. D., Wang, T. C. (2020): Improved straw management practices promote in situ straw decomposition and nutrient release, and increase crop production. – Journal of Cleaner Production 250: 119514.
[13] Hamoud, Y. A., Shaghaleh, H., Sheteiwy, M., Guo, X. P., Elshaikh, N. A., Khan, N. U., Oumarou, A., Rahim, S. F. (2019): Impact of alternative wetting and soil drying and soil clay content on the morphological and physiological traits of rice roots and their relationships to yield and nutrient use-efficiency. – Agricultural Water Management 223: 105706.
[14] Harindintwali, J. D., Zhou, J. L., Muhoza, B., Wang, F., Herzberger, A., Yu, X. B. (2021): Integrated eco-strategies towards sustainable carbon and nitrogen cycling in agriculture. – Journal of Environmental management 293: 112856.
[15] Huang, D. D., Chen, X. W., Cao, G. J., Liang, A. Z., Jia, S. X., Liu, S. X. (2018): Effects of long-term conservation tillage on soil nitrogen content and organic nitrogen components in a Chinese Mollisol. – Applied Ecology and Environmental Research 16(5): 5517-5528.
[16] Janke, C. K., Moody, P., Bell, M. J. (2020): Three-dimensional dynamics of nitrogen from banded enhanced efficiency fertilizers. – Nutrient Cycling in Agroecosystems 118(3): 227-247.
[17] Li, H., Dai, M. W., Dai, S. L., Dong, X. J. (2018): Current status and environment impact of direct straw return in China's cropland - A review. – Ecotoxicology and Environmental Safety 159: 293-300.
[18] Li, G. H., Cheng, G. G., Lu, W. P., Lu, D. L. (2021): Differences of yield and nitrogen use efficiency under different applications of slow release fertilizer in spring maize. – Journal of Integrative Agriculture 20(2): 554-564.
[19] Ma, Q., Jiang, C. M., Li, S. L., Yu, W. T. (2021): Maize yield and nitrogen-use characteristics were promoted as consistently improved soil fertility: 6-year straw incorporation in Northeast China. – Plant Soil and Environment 67(7): 383-389.
[20] Mabagala, F. S., Geng, Y. H., Cao, G. J., Wang, L. C., Wang, M., Zhang, M. L. (2020): Effect of silicon on crop yield, and nitrogen use efficiency applied under straw return treatments. – Applied Ecology and Environmental Research 18(4): 5577-5590.
[21] Nafi, E., Webber, H., Danso, I., Naab, J. B., Frei, M., Gaiser, T. (2019): Soil tillage, residue management and site interactions affecting nitrogen use efficiency in maize and cotton in the Sudan Savanna of Africa. – Field Crops Research 244: 107629.
[22] Nasielski, J., Deen, B. (2019): Nitrogen applications made close to silking: Implications for yield formation in maize. – Field Crops Research 243: 107621.

http://www.aloki.hu ● ISSN 1589 1623 (Print) ● ISSN1785 0037 (Online)
DOI: http://dx.doi.org/10.15666/aeer/2001_893903

[23] Obade, V. D. (2019): Integrating management information with soil quality dynamics to monitor agricultural productivity. – Science of the Total Environment 651: 2036-2043.
[24] Osterholz, W. R., Liebman, M., Castellano, M. J. (2018): Can soil nitrogen dynamics explain the yield benefit of crop diversification? – Field Crops Research 219: 33-42.
[25] Qin, X. L., Huang, T. T., Lu, C., Dang, P. F., Zhang, M. M., Guan, X. K., Wen, P. F., Wang, T. C., Chen, Y. L., Siddique, K. H. M. (2021): Benefits and limitations of straw mulching and incorporation on maize yield, water use efficiency, and nitrogen use efficiency. – Agricultural Water Management 256: 107128.
[26] Rahman, M. H., Haque, K. M. S., Khan, M. Z. H. (2021): A review on application of controlled released fertilizers influencing the sustainable agricultural production: A Cleaner production process. – Environmental Technology & Innovation 23: 101697.
[27] Ruffatti, M. D., Roth, R. T., Lacey, C. G., Armstrong, S. D. (2019): Impacts of nitrogen application timing and cover crop inclusion on subsurface drainage water quality. – Agricultural Water Management 211: 81-88.
[28] Sadeghi, S. M., Noorhosseini, S. A., Damalas, C. A. (2018): Environmental sustainability of corn (*Zea mays* L.) production on the basis of nitrogen fertilizer application: The case of Lahijan, Iran. – Renewable & Sustainable Energy Reviews 95: 48-55.
[29] Sawyer, J. E., Woli, K. P., Barker, D. W., Pantoja, J. L. (2017): Stover Removal Impact on Corn Plant Biomass, Nitrogen, and Use Efficiency. – Agronomy Journal 109(3): 802-810.
[30] Tenelli, S., Otto, R., Bordonal, R. O., Carvalho, J. L. N. (2021): How do nitrogen fertilization and cover crop influence soil C-N stocks and subsequent yields of sugarcane? – Soil & Tillage Research 211: 104999.
[31] Wang, M., Pendall, E., Fang, C. M., Li, B., Nie, M. (2018): A global perspective on agroecosystem nitrogen cycles after returning crop residue. – Agriculture Ecosystems & Environment 266: 49-54.
[32] Weih, M., Hamner, K., Pourazari, F. (2018): Analyzing plant nutrient uptake and utilization efficiencies: comparison between crops and approaches. – Plant and Soil 430(1-2): 7-21.
[33] Xue, J. F., Pu, C., Liu, S. L., Chen, Z. D., Chen, F., Xiao, X. P., Lal, R., Zhang, H. L. (2015): Effects of tillage systems on soil organic carbon and total nitrogen in a double paddy cropping system in Southern China. – Soil & Tillage Research 153: 161-168.
[34] Yin, H. J., Zhao, W. Q., Li, T., Cheng, X. Y., Liu, Q. (2018): Balancing straw returning and chemical fertilizers in China: Role of straw nutrient resources. – Renewable & Sustainable Energy Reviews 81: 2695-2702.
[35] Yu, Y., Qian, C. R., Gu, W. R., Li, C. F. (2021): Responses of root characteristic parameters and plant dry matter accumulation, distribution and transportation to nitrogen levels for spring maize in Northeast China. – Agriculture-Basel 11(4): 308.
[36] Zhao, J. L., Lu, Y., Tian, H. L., Jia, H. L., Guo, M. Z. (2019): Effects of straw returning and residue cleaner on the soil moisture content, soil temperature, and maize emergence rate in China's three major maize producing areas. – Sustainability 11(20): 5796.

http://www.aloki.hu ● ISSN 1589 1623 (Print) ● ISSN1785 0037 (Online)
DOI: http://dx.doi.org/10.15666/aeer/2001_893903

FUNCTIONAL ROLE OF MOSS BIOCRUST IN DISTURBED SEMIARID SHRUBLANDS OF NORTH-EASTERN PATAGONIA, ARGENTINA

KRÖPFL, A. I.[1*] – DISTEL, R. A.[2] – †CECCHI, G. A.[3] – VILLASUSO, N. M.[1]

[1]*Centro Universitario Regional Zona Atlántica (CURZA), Universidad Nacional del Comahue, 8500 Viedma, Argentina*

[2]*Departamento de Agronomía, Universidad Nacional del Sur, and Centro de Recursos Naturales Renovables de la Zona Semiárida, Consejo Nacional de Investigaciones Científicas y Técnicas de la República Argentina, 8000 Bahía Blanca, Argentina*

[3]*Estación Experimental Agropecuaria Valle Inferior, Convenio Instituto Nacional de Tecnología Agropecuaria (INTA)-Provincia de Río Negro, 8500 Viedma, Argentina*

[*]*Corresponding author*
e-mail: akropfl@yahoo.com.ar; phone: +54-9-2920-60-0921

(Received 16th Oct 2021; accepted 22nd Dec 2021)

Abstract. Biocrusts are key biotic components of arid and semi-arid ecosystems worldwide. In the semi-arid ecosystems of north-eastern Patagonia, the moss biocrust is present both beneath shrubs and in intershrub spaces. In this study we ran a series of field and greenhouse trials aimed at quantifying the moss biocrust cover at sites that differed in grazing and/or shrub mechanical (chaining) disturbance and evaluating its seed entrapping capacity, and its effect on the superficial water balance and grass seedling growth. Grazing or the combined effect of grazing and chaining impacted negatively on the moss biocrust cover. The presence of moss biocrust facilitated seed entrapment and increased the seed density of perennial grasses in the soil seed bank, improved the superficial water balance, and enhanced grass seedling growth. In conclusion, in the semi-arid shrublands in north-eastern Patagonia, the moss biocrust appeared vulnerable to grazing and shrub mechanical disturbance, and it showed functional roles that may facilitate seedling establishment for perennial grasses.
Keywords: *grazing disturbance, shrub mechanical disturbance, seed entrapment, water balance, perennial grasses establishment*

Introduction

Biocrusts are key biotic components of arid and semi-arid ecosystems worldwide, due to their important role in primary ecological processes (Maestre et al., 2011; Weber et al., 2016). They are composed of varying proportions of cyanobacteria, algae, microfungi, lichens, and mosses, constituting communities that colonize the soil surface (Belnap and Lange, 2003). Although it was widely accepted that biocrust succession follows a general pattern starting with cyanobacteria and algae and concluding with bryophytes at the later stages, recent studies have proposed that mosses can develop in the early stages of succession under favorable and stable soil conditions (Belnap et al., 2016; Condon and Pike, 2018).

The positive influence of biocrusts on soil surface hydrological processes in semiarid ecosystems has been documented by many authors (e.g., Belnap, 2006; Daryanto et al., 2013; Chamizo et al., 2016; Faist et al., 2017). Soil biocrusts generally increase water infiltration, soil water retention, and decrease evaporative losses, resulting in reduced runoff erosion and an increase in water available for plants. In addition, soil biocrusts

http://www.aloki.hu ● ISSN 1589 1623 (Print) ● ISSN1785 0037 (Online)
DOI: http://dx.doi.org/10.15666/aeer/2001_905917

can increase the superficial soil temperature in the cool season (Xiao et al., 2013). Altogether, the hydric and thermal improvements in the microenvironment determine that biocrusts can represent safe sites for seedling establishment. Moreover, when seeds are secondarily moved by wind, the seed entrapment capacity of biocrusts may contribute to the development of the soil seed bank (Bertiller and Ares, 2011).

On the other hand, soil biocrusts are highly vulnerable to both natural and anthropogenic disturbances (Zaady et al., 2016). Among the latter, domestic livestock grazing is recognized as the most widespread stress factor in grasslands. For instance, in the Monte Desert of Argentina, Gómez et al. (2012) found that grazing negatively impacted on the moss biocrust, which only developed under protection from vascular plants. Similarly, mechanical woody plant control in shrublands can have a negative effect on soil biocrusts, particularly when causing a marked superficial soil disturbance like root ploughing (Daryanto et al., 2013). However, other mechanical treatments for shrub control, such as chaining that produces moderate superficial soil scarification (Stevens and Monsen, 2004), may have less adverse effects on the soil biocrusts. Chaining involves the use of a heavy ship anchor chain towed between two tractors, and represents a common large-scale mechanical disturbance used for shrub control in rangelands (Stephens et al., 2016).

In undisturbed or low-disturbed areas of shrublands in north-eastern Patagonia, Argentina, the moss biocrust is often present both beneath and between shrubs. Contrarily, the moss biocrust proved to be impoverished in areas disturbed by heavy grazing alone or in combination with mechanical shrub control, the latter being a common practice in the region (Kröpfl et al., 2007). However, this observation is just qualitative, since quantitative controlled studies on soil biocrusts are still scarce in Argentina (Navas Romero et al., 2020). In this study we sought to address the extent of the impact of grazing and/or shrub mechanical disturbance by chaining on the moss biocrust cover, and the role of the moss biocrust on seedling recruitment of perennial grasses. Based on the available knowledge we hypothesized (1) that the moss biocrust cover is lowest when chained or unchained conditions are disturbed by heavy grazing, and highest in chained ungrazed conditions, and (2) that the moss biocrust facilitates seedling recruitment of perennial grasses. Therefore, the objectives of our study were (1) to quantify the moss biocrust cover at sites differing in livestock grazing and/or chaining, and (2) to evaluate the moss biocrust seed retention capacity and assess its effect on the superficial water balance and grass seedling growth.

Materials and methods

Study area

The study was carried out in 2003, at a site near Viedma, Río Negro province, Argentina. The overall characteristics of the climate, soil and vegetation have been described by Godagnone and Bran (2009). The climate of the area is temperate, semiarid. The long-term average annual precipitation is 395 mm (CV=35%). Precipitation peaks in autumn and spring, whereas in winter it rains frequently but in small amounts. The mean annual potential evapotranspiration is 800 mm. Soils are sandy to loamy sands, and taxonomically defined as Typic Torripsaments.

The study area is located in the south-eastern Monte Phytogeographical Province (Cabrera, 1976). The physiognomy of the vegetation is a shrubby steppe, with an overstory dominated by the multi-stemmed evergreen shrub *Larrea divaricata* Cav. and

http://www.aloki.hu ● ISSN 1589 1623 (Print) ● ISSN1785 0037 (Online)
DOI: http://dx.doi.org/10.15666/aeer/2001_905917

isolated specimens or clumps of *Geoffroea decorticans* (Gillies ex Hook. and Arn.) Burkart. The understory is a predominantly cool-season grassland dominated by *Nassella tenuis* (Phil.) Barkworth and *Piptochaetium napostaense* (Speg.*)* Hack and accompanied by other perennial grasses, such as *Poa ligularis* Nees ex Steud. var. ligularis, and *Pappostipa speciosa* (Trin. and Rupr.) Romaschenko var. *speciosa*. Perennial grasses start growing at the beginning of autumn and set seed at the end of spring, whereas seeds germinate primarily in the autumn. Annual grasses and forbs are represented mainly by *Hordeum murinum* L. subsp. *leporinum* (Link.) Arcang., *Bromus hordaceus* L., *Schismus barbatus* (L.) Thell*,* and *Erodium cicutarium* (L.) L'Hér. ex Aiton. The soil biocrust is dominated by two moss species, which were identified as *Syntrichia princeps* (De Not.) Mitt and *Ceratodon purpureus* (Hedw.) (Prof. Dr. Celina Matteri, Museo Argentino de Ciencias Naturales "Bernardino Rivadavia", Buenos Aires, Argentina, 2000).

Trials

We ran a series of field and greenhouse trials. The field trials were conducted in a 300-ha paddock (40º55'04" S and 63º07'27" W) with a long history (over 30 years) of heavy continuous grazing by cattle (stocking rate ~0.1 cows ha^{-1}). The paddock had strips of intact vegetation (*Figure 1*) alongside strips where the aboveground biomass of shrubs had been mechanically disturbed by chaining 3 years earlier (*Figure 2*). At the beginning of the study, the shrubs in the chained strips had resprouted from basal buds to a height of less than a meter. In a chained strip there was also a 9-ha grazing exclosure, which was constructed immediately after chaining (*Figure 2*).

Figure 1. *Unchained site*

Figure 2. *Chained site: at the left side, grazed; at the right side, the ungrazed exclosure*

Climatic data of the year are shown in the *Appendix Table 1*.

Moss biocrust cover

To evaluate the moss biocrust cover under grazed-chained and grazed-unchained conditions, quadrats (225 cm^2, n=26) were placed at 4 m intervals along two randomly located line transects (60 m each) in both the grazed-chained and grazed-unchained areas. The moss biocrust cover was estimated within the mentioned quadrats in autumn. Immediately before the estimation, the plots were wetted to improve the visibility of the

http://www.aloki.hu ● ISSN 1589 1623 (Print) ● ISSN1785 0037 (Online)
DOI: http://dx.doi.org/10.15666/aeer/2001_905917

moss biocrust (Rosentreter and Eldridge, 2002). A similar procedure was followed to quantify the moss biocrust cover under chained-grazed and chained-ungrazed (exclosure) conditions. In this case, quadrats (225 cm^2, n=42) were placed at 4 m intervals along two randomly located line transects (90 m each) in both the chained-ungrazed and adjacent chained-grazed areas. In order to enrich the interpretation of the results, we also placed quadrats (225 cm^2, n=42) inside the exclosure at 4 m intervals along two randomly located line transects (90 m each), to measure both the moss biocrust cover and the grass cover. Each sample was categorized according to whether it was in a mound (beneath shrubs) or flat (intershrub spaces) microsite, and whether it was exposed to the sun or under the shade of grasses.

Moss biocrust seed trap

To test whether the moss biocrust acts as a seed trap, we buried 30 paired circular plots at random (plastic rings of 23,55 cm of perimeter) inside the exclosure, in autumn, either with or without moss biocrust, and manually removed all the propagules (seeded fruit with sharp tips and twisted hydro-active awns) of *N. tenuis* in each plot. This task was possible as the awns remain temporarily attached to the propagule and extend above the soil surface. Then we laid down 20 intact propagules of *N. tenuis* on the surface of each plot and recounted them three weeks later. Additionally, we counted the number of seeds of *N. tenuis* in the soil bank in the presence or absence of moss biocrust, before seed germination in the autumn. We randomly extracted 30 paired soil samples (7.5 cm diameter, 3.5 cm deep), either with or without moss biocrust, along a 100 m transect in the exclosure. From each sample we sorted out moss biocrust, litter and seeds of *N. tenuis* by sieving and manual separation. Then, we determined the dry weight of the moss biocrust and litter and counted the number of seeds collected.

We also tested whether the moss biocrust contributes positively to seed retention under greenhouse conditions. Aluminium trays (n=20) were filled with superficial soil cores (21 cm long x 15 cm wide x 4.5 cm deep) collected from the exclosure in spring, either with or without moss biocrust. Once the trays were on the greenhouse benches all intact seeds of *N. tenuis* were manually removed from each tray. Immediately afterwards, 10 intact seeds of *N. tenuis* were laid down on the surface of each tray, and their permanence was recorded two weeks later. It is worth mentioning that the greenhouse had natural ventilation; therefore, the seeds could be potentially moved by air currents inside it. This test was repeated twice. Greenhouse had no temperature or humidity control, but the trials only lasted some weeks during the spring or the fall.

Moss biocrust and grass seedling growth and survival

To assess the influence of the moss biocrust on seedling growth of perennial grasses, we randomly selected 30 paired plots (225 cm^2) inside the exclosure, either with or without moss biocrust, and marked all the seedlings of the dominant perennial grass *N. tenuis*. Then, we counted the number of tillers and the number of leaves per seedling five times between June and May of the following year. We also recorded the number of new seedlings of *N. tenuis* emerging in the plots during the autumn (March-April-May).

To determine the influence of the moss biocrust on perennial grass seedling survival, in spring we filled pots (n=20) with soil cores (7.5 cm diameter, 14.5 cm deep) collected from the exclosure, either with or without moss biocrust. Once in the greenhouse, all pots were irrigated to promote germination of the seeds originally present in the soil, and all emerging seedlings were removed. Then, the pots were left untreated until

http://www.aloki.hu ● ISSN 1589 1623 (Print) ● ISSN1785 0037 (Online)
DOI: http://dx.doi.org/10.15666/aeer/2001_905917

autumn when we sowed 10 intact seeds of *N. tenuis* in each one. Afterwards, the pots were watered to maintain field water capacity until germination occurred and then they were thinned to one seedling per pot. The irrigation was discontinued and seedling survival time (days to death) was recorded. We also measured the leaf length, and calculated the leaf relative growth rate of the *N. tenuis* seedlings for three weeks.

Moss biocrust and water balance

To evaluate the effect of the moss biocrust on the water storage capacity and water evaporation, we extracted undisturbed soil cores from the exclosure in spring, either with or without moss biocrust, and filled pots (n=10) of 10 cm in diameter and 5 cm in depth. Once in the greenhouse, all pots were watered to saturation and weighed prior to allowing them to drain the excess water for 24 hours. Thereafter, irrigation was discontinued, and all pots were weighed daily until reaching a constant weight. The daily loss of water was calculated by difference in weight.

Statistical analyses

Data were analysed through One-Way ANOVAs and t tests for comparisons between sites or treatments, except for seedling survival that was analysed through the nonparametric Log-Rank test. When necessary, data were transformed to fulfil ANOVA assumptions. We also performed simple linear regression analysis to determine the relationship between the variables of interest. Differences between means were considered significant at $p<0.05$. All analyses were made using the statistical package InfoStat P (Di Rienzo et al., 2017).

Results

Moss biocrust cover

Moss biocrust cover was higher ($p=0.0008$) in the grazed unchained condition (38.2±5.4%, mean±1SE) than in the grazed chained condition (25.8±5.4%) (*Appendix Table 2*), whereas it was higher ($p<0.0001$) in the chained ungrazed condition (46.2±6.5%) than in the chained grazed condition (29.5±4.6%) (*Appendix Table 3*).

In flat intershrub microsites of the chained ungrazed condition (exclosure), the moss biocrust cover was higher ($p=0.01$) in shady (53.1±6.2%) than in sunny conditions (28.3±4.1%), and it did not correlate with grass cover in either sunny ($p=0.13$) or shady ($p=0.15$) conditions (*Fig. 3a*). Similarly, in the mound microsites beneath shrubs, moss biocrusts cover was higher ($p=0.05$) in shady conditions (39.2±5.4%) than in sunny conditions (18.1±9.8%) and it did not correlate with grass cover in either sunny ($p=0.66$) or shady ($p=0.97$) conditions.

In flat intershrub microsites of the chained grazed condition, moss biocrust cover was higher ($p=0.025$) in shady conditions (34.6±6.3%) than in sunny conditions (19.4±3.1%), and it correlated linearly and positively ($p<0.01$) with grass cover in sunny conditions only (*Fig. 3b*). Similarly, in mound microsites beneath shrubs, the moss biocrust cover was higher ($p=0.013$) in shady conditions (42.4±4.7%) than in sunny conditions (21.2±4.0%), although there was no correlation with grass cover in either sunny or shady conditions.

http://www.aloki.hu ● ISSN 1589 1623 (Print) ● ISSN1785 0037 (Online)
DOI: http://dx.doi.org/10.15666/aeer/2001_905917

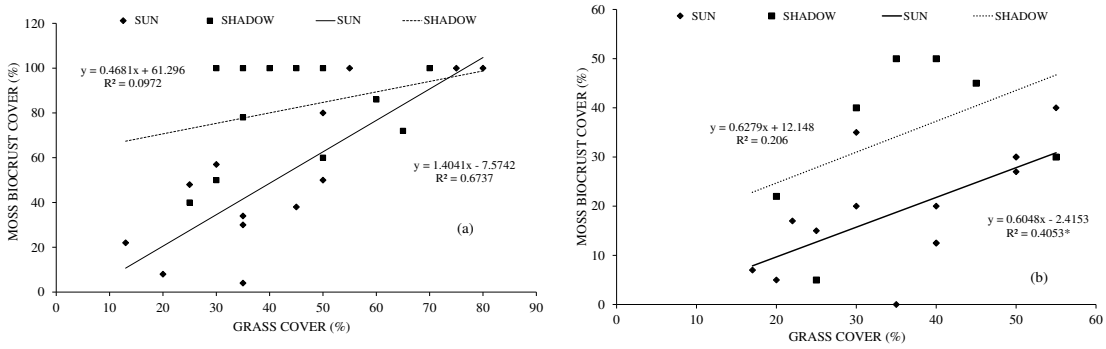

Figure 3. *Relationship between moss biocrusts and grass cover in intershrub spaces of either (a) ungrazed (*** p<0.001) or (b) grazed conditions (* p<0.05), located in either sunny or shady places*

Moss biocrust seed retention

In the experimental plots located in the chained grazing exclosure, the number of seeds of *N. tenuis* retained after three weeks was more than three times higher (p<0.001) with moss biocrust (13.9±1.25) than without it (3.7±0.46). Consequently, the number of seeds of *N. tenuis* in the soil seed bank was higher (p<0.001) with moss biocrust (5.9±0.68) than without it (1.5±0.23). Similarly, under greenhouse conditions the number of *N. tenuis* seeds retained in the experimental trays was higher (p<0.001) in that presence rather than in the absence of moss biocrust (6.0±0.30 *vs*. 1.9±0.29, and 3.7±0.37 vs. 1.9±0.23, for the first and the second test, respectively). The seed quantity correlated positively with the biomass of litter in the plots without moss biocrust, and with the biomass of litter plus crust in the plots with moss biocrust (*Fig. 4*).

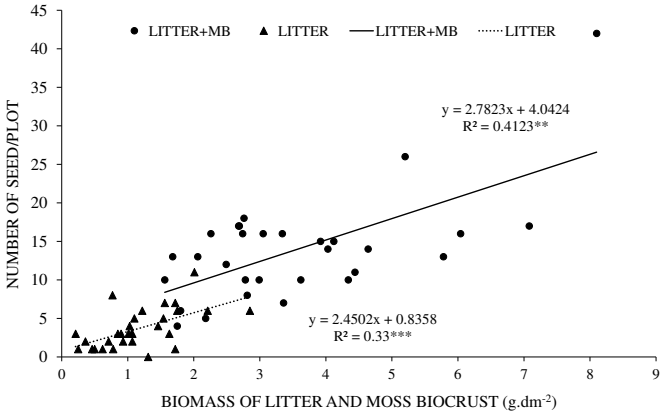

Figure 4. *Relationship between the number of seeds per plot (156 cm^3) in the soil seed bank and the biomass of either litter plus moss biocrusts (LITTER+MB) or litter alone, for microsites with and without moss biocrusts (MB), respectively. ** p<0.01*

Moss biocrust and grass seedling growth and survival

There were no significant differences in tiller (2.1±0.22 *vs.* 2.1±0.23, p=0,919) and leaf numbers (6.8±0.68 *vs*. 7.1±0.74, p=0.752) of the *N. tenuis* seedlings between plots, with and without moss biocrust, in the chained grazing exclosure throughout the

http://www.aloki.hu ● ISSN 1589 1623 (Print) ● ISSN1785 0037 (Online)
DOI: http://dx.doi.org/10.15666/aeer/2001_905917

observation period. Neither was there any difference (p=0.589) in the number of *N. tenuis* seedlings emerging in autumn between plots either with (1.3±0.21) or without (1.2±0.22) moss biocrust.

Under greenhouse conditions, both the total green leaf length (*Fig. 5*) and relative leaf growth rate (*Fig. 6*) of *N. tenuis* seedlings were higher (p=0.004 and p<0.001, respectively) in the plots with moss biocrust than in the plots without. On the other hand, seedling survival time did not differ (p=0.400) between plots either with (19.4±1.4 days) or without (18.9±1.7 days) moss biocrust.

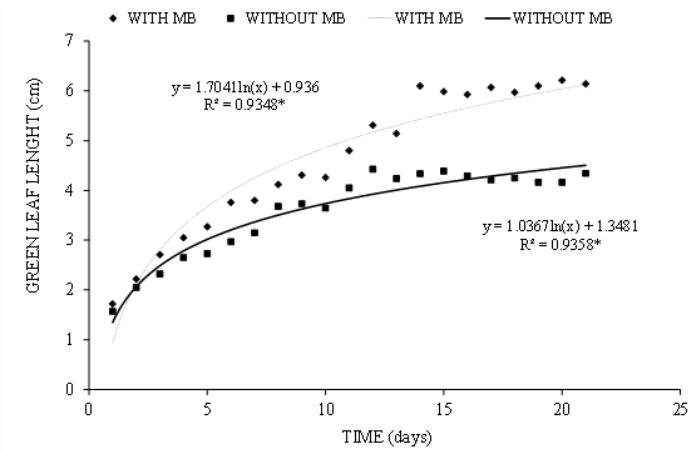

Figure 5. *Total green leaf length of Nassella tenuis seedlings grown in pots with moss biocrusts ("with MB") or without moss biocrusts ("without MB"). The slopes of the regression lines differ significantly (*p<0.05)*

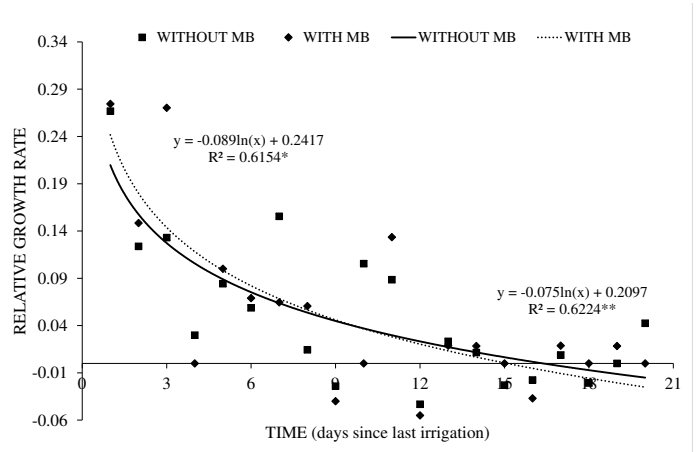

Figure 6. *Leaf relative growth rate of Nassella tenuis seedlings grown in pots either with moss biocrusts ("with MB") or without moss biocrusts ("without MB") since the interruption of irrigation. * p<0.05, ** p<0.01*

Moss biocrust and water balance

Water storage capacity (cm^3 water per cm^3 soil) was higher (p=0.002) in the soil with moss biocrust (0.39±0.1) than in the soil without (0.33±0.1), whereas the initial water evaporation rate was slower (p<0.001) with moss biocrust than without (*Fig. 7*).

http://www.aloki.hu ● ISSN 1589 1623 (Print) ● ISSN1785 0037 (Online)
DOI: http://dx.doi.org/10.15666/aeer/2001_905917

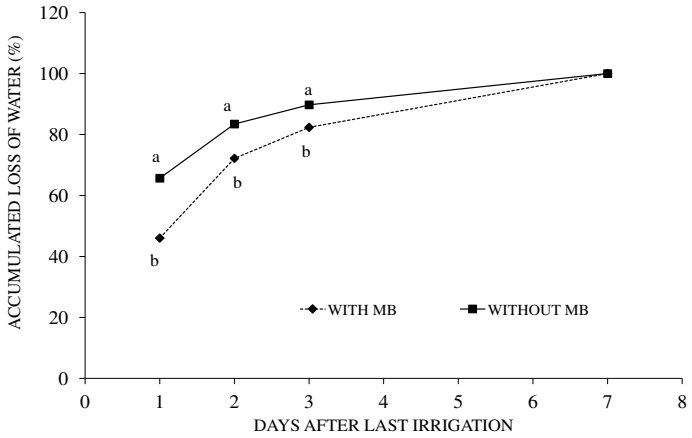

Figure 7. *Accumulated weight loss of pots either with moss biocrusts ("with MB") or without moss biocrusts ("without MB"), expressed as a percentage of the water storage capacity. At each time interval, means with different letters are significantly different ($p<0.05$)*

Discussion

Overall, our results showed that the moss biocrusts that predominate in the semiarid shrublands in north-eastern Patagonia, Argentina, on one hand are sensitive to heavy grazing, or a combination of heavy grazing and shrub mechanical control, and on the other hand they play functional roles that may facilitate the seedling recruitment of perennial grasses. Similar conclusions have been reached for diverse biocrusts in other arid and semiarid regions around the world (e.g., Zaady et al., 2016; Zhang et al., 2016; Condon and Pike, 2018).

The relatively higher negative impact on the moss biocrust of chaining in combination with livestock grazing, compared with the impact of the latter disturbance only, may be explained mainly by a more spatially homogeneous trampling and grass utilization by livestock due to shrub disturbance. The moss biocrust was sensitive to ungulate trampling, as found by other authors (e.g. Muscha and Hild, 2006; Concostrina-Zubiri et al., 2014), but also to sun exposure, as mosses increased with increasing grass cover. This last result agrees with the finding of Garcia et al. (2015) that biocrusts in dry environments develop preferentially when associated with vascular plants, as lower irradiation reduces dessication, and Gómez et al. (2012) recorded a greater cover of mosses beneath shrubs, particularly in the Monte.

When we compared the grazed *vs.* ungrazed areas that had been mechanically disturbed three years earlier, we observed a similar moss biocrust cover under the canopy of shrubs resprouting after chaining (mound microtopographic positions), in which shade and protection against grazing activity (defoliation, trampling) may facilitate moss biocrust growth. Shrubs protect mosses from trampling, and their litter and shade improve the soil moisture (Bowker et al., 2006). Contrarily, in the inter-shrub spaces (flat microtopographic positions), where trampling and defoliation concentrate, the moss biocrust cover was higher in the absence of grazing. In the ungrazed condition, undisturbed grasses may moderate the physical environment (radiation, temperature, humidity) at ground level facilitating growth of moss biocrust (Maestre, 2003; Concostrina-Zubiri et al., 2014; Tabeni et al., 2014), which may explain the positive correlation observed in this study between moss biocrust cover and grass cover in the

http://www.aloki.hu ● ISSN 1589 1623 (Print) ● ISSN1785 0037 (Online)
DOI: http://dx.doi.org/10.15666/aeer/2001_905917

inter-shrub spaces exposed to the sun. Moreover, the fact that the highest moss biocrust cover under the experimental conditions was observed in the chained ungrazed condition suggests that the moss species in the study area are early successional species, since they developed fast after exclusion of the mechanical disturbance and livestock. These results agree with those of Read et al. (2011), who found that mosses, rather than cyanobacteria, are the most important colonizers in southeast Australia following livestock exclusion. Unfortunately, no information exists on the dynamics of moss biocrust communities in north-eastern Patagonia region.

In agreement with findings in other arid and semiarid ecosystems (Bliss and Gold, 1999; Bertiller and Ares, 2011; Belnap and Weber, 2013), our results showed that the moss biocrust in the study area has the capacity to trap seeds of perennial grasses, enhancing their density in the soil seed bank. Moreover, we observed that moss biocrust plus litter was a better substrate for seed capture and retention, compared to litter alone. The seeds of dominant perennial grasses in the study area, like those of the other Stipeae, have a hydro-active awn that enables them to bury themselves into the ground during wet conditions. But, in order for a seed to be buried in a particular place, it must first be retained on the soil surface until the required conditions (rain) happen. This requirement is particularly critical in inter-shrub spaces, where recruitment of perennial grasses is most necessary in degraded rangelands. Strong winds are of common occurrence in the study area, and in the inter-shrub spaces with bare ground most of the seeds are blown away and entrapped under the shrub canopies, leading to the distribution of vegetation in shrub islands interspersed in a matrix of bare ground or low-herbaceous cover soil (Aguiar and Sala, 1999; Odorico et al., 2012; Qu et al., 2018).

Our results from greenhouse trials showed that moss biocrust can improve the water balance in the superficial soil layer, due to a greater storage capacity and lower evaporation rate. In agreement, *N. tenuis* seedlings grown in pots during a desiccation event grew better with moss biocrust than without it. It has been found that mosses can significantly increase superficial soil water availability (Xiao and Hu, 2017; Sun et al., 2021), as well as seedling survivorship, height, biomass, root growth, and tissue water and micronutrient content (Thiet et al., 2014; Peter et al., 2016). Under field conditions, however, we did not observe any positive effects of moss biocrust on *N. tenuis* seedlings tiller and leaf number throughout a year. This result was in agreement with the lack of the effect of moss biocrust on the survival of *N. tenuis* seedlings under field conditions reported by Peter et al. (2016). The discrepancies between results from controlled and field conditions most probably reflect differences in the environmental conditions in general, and hydrological processes in particular, since they vary according to the scale considered (Gómez et al., 2012; Concostrina-Zubiri et al., 2014; Tabeni et al., 2014).

Conclusions

In the semi-arid shrublands in north-eastern Patagonia, the moss biocrust appears to be vulnerable to livestock grazing or the combination of grazing and shrub mechanical disturbance. It showed functional roles that may facilitate the seedling establishment of perennial grasses in inter-shrub spaces, where recruitment is most needed in degraded shrublands. In addition, other functional aspects of these biocrusts related to its facilitating role should be studied, such as nitrogen fixation, since this is the second

http://www.aloki.hu ● ISSN 1589 1623 (Print) ● ISSN1785 0037 (Online)
DOI: http://dx.doi.org/10.15666/aeer/2001_905917

limiting factor for plant growth. Although studies carried out in other semi-arid systems have shown the importance of crusts in this function, there are no data in this regard in the Monte region.

Our results suggest the need to consider moss biocrust in management planning, to preserve its important roles in the ecosystem function. Future studies should focus on determining the time required to recover the coverage of these crusts after a disturbance has occurred, in terms of planning the rests needed to achieve it, as well as continue analysing the other benefits that they can bring to the system.

Acknowledgements. This study was financially supported by the Universidad Nacional del Comahue, Argentina. Funds provided by the Universidad Nacional del Sur and the Consejo Nacional de Investigaciones Científicas y Técnicas de la República Argentina (CONICET) to RAD are also acknowledged.

Conflict of interests statement. Authors have no conflict of interests to declare.

REFERENCES

[1] Aguiar, M., Sala, O. (1999): Patch structure, dynamics and implications for the functioning of arid ecosystems. – Trends in Ecology & Evolution 14: 273-277. Retrieved from http://www.ncbi.nlm.nih.gov/pubmed/10370263.

[2] Belnap, J., Lange, O. L. (eds.) (2003): Biological soil crusts: structure, function, and management. – Ecological Studies 150. Springer-Verlag Berlin, Heidelberg. https://doi.org/10.1007/978-3-642-56475-8.

[3] Belnap, J. (2006): The potential roles of biological soil crusts in dryland hydrologic cycles. – Hydrological Processes 20: 3159-3178. https://doi.org/10.1002/hyp.6325.

[4] Belnap, J., Weber, B. (2013): Biological soil crusts as an integral component of desert environments. – Ecological Processes 2: 11. https://doi.org/10.1186/2192-1709-2-11.

[5] Belnap, J., Weber, B., Büdel, B. (2016): Biological Soil Crusts as an Organizing Principle in Drylands. – In: Weber, B., Büdel, B., Belnap, J. (eds.) Biological Soil Crusts: An Organizing Principle in Drylands. Ecological Studies (Analysis and Synthesis) 226: 3-13. Springer, Cham. https://doi.org/10.1007/978-3-319-30214-0_1.

[6] Bertiller, M. B., Ares, J. O. (2011): Does sheep selectivity along grazing paths negatively affect biological crusts and soil seed banks in arid shrublands? A case study in the Patagonian Monte, Argentina. – Journal of Environmental Management 92: 2091-2096. https://doi.org/10.1016/J.JENVMAN.2011.03.027.

[7] Bliss, L. C., Gold, W. G. (1999): Vascular plant reproduction, establishment, and growth and the effects of cryptogamic crusts within a polar desert ecosystem, Devon Island, N.W.T., Canada. – Canadian Journal of Botany 77: 623-636. https://doi.org/10.1139/b99-031.

[8] Bowker, M. A., Belnap, J., Miller, M. E. (2006): Spatial modeling of biological soil crusts to support rangeland assessment and monitoring. – Rangeland Ecology and Management 59: 519-529. https://doi.org/10.2111/05-179R1.1.

[9] Cabrera, A. L. (1976): Regiones fitogeográficas Argentinas. – BUENOS AIRES: ACME. Retrieved from: https://www.google.com.ar/search?q=regiones+fitogeograficas+de+argentina+cabrera&sa=X&ved=0ahUKEwiB8NGz38fdAhUIOZAKHQjPDNkQ1QIIiQEoAA.

[10] Chamizo, S., Cantón, Y., Rodríguez-Caballero, E., Domingo, F. (2016): Biocrusts positively affect the soil water balance in semiarid ecosystems. – Ecohydrology 9: 1208-1221. https://doi.org/10.1002/eco.1719.

http://www.aloki.hu ● ISSN 1589 1623 (Print) ● ISSN1785 0037 (Online)
DOI: http://dx.doi.org/10.15666/aeer/2001_905917

[11] Concostrina-Zubiri, L., Huber-Sannwald, E., Martínez, I., Flores Flores, J. L., Reyes-Agüero, J. A., Escudero, A., Belnap, J. (2014): Biological soil crusts across disturbance-recovery scenarios: Effect of grazing regime on community dynamics. – Ecological Applications 24: 1863-1877. https://doi.org/10.1890/13-1416.1.

[12] Condon, L. A., Pyke, D. A. (2018): Fire and grazing influence site resistance to Bromus tectorum through their effects on shrub, bunchgrass and biocrust communities in the Great Basin (USA). – Ecosystems 21: 1416-1431. https://doi.org/10.1007/s10021-018-0230-8.

[13] Daryanto, S., Eldridge, D. J., Throop, H. L. (2013): Managing semi-arid woodlands for carbon storage: Grazing and shrub effects on above- and belowground carbon. – Agriculture, Ecosystems and Environment 169: 1–11. https://doi.org/10.1016/j.agee.2013.02.001.

[14] Di Rienzo, J. A., Casanoves, F., Balzarini, M. G., Gonzalez, L., Tablada, M., Robledo, C. W. (2017): InfoStat versión 2017. – Grupo InfoStat, FCA, Universidad Nacional de Córdoba, Argentina. URL http://www.infostat.com.ar.

[15] Faist, A. M., Herrick, J. E., Belnap, J., Zee, J. W. V., Barger, N. N. (2017): Biological soil crust and disturbance controls on surface hydrology in a semi-arid ecosystem. – Ecosphere 8: 3. https://doi.org/10.1002/ecs2.1691.

[16] Garcia, V., Aranibar, J., Pietrasiak, N. (2015): Multiscale effects on biological soil crusts cover and spatial distribution in the Monte Desert. – Acta Oecologica 69: 35-45. https://doi.org/10.1016/j.actao.2015.08.005.

[17] Godagnone, R., Bran, D. E. (eds.) (2009): Inventario integrado de los recursos naturales de la Provincia de Río Negro. – 1st ed. Buenos Aires: Ediciones INTA. Retrieved from https://inta.gob.ar/sites/default/files/script-img-inventario_integrado_de_los_recursos_naturales_de.jpg.

[18] Gómez, D. A., Aranibar, J. N., Tabeni, S., Villagra, P. E., Garibotti, I. A., Atencio, A. (2012): Biological soil crust recovery after long-term grazing exclusion in the Monte Desert (Argentina). Changes in coverage, spatial distribution, and soil nitrogen. – Acta Oecologica 38: 33-40. https://doi.org/10.1016/j.actao.2011.09.001.

[19] Kröpfl, A. I., Deregibus, V. A., Cecchi, G. A. (2007): Disturbios en una estepa arbustiva del Monte: cambios en la vegetación. – Ecologia Austral 17: 257-268.

[20] Maestre, F. (2003): Variaciones en el patrón espacial a pequeña escala de los componentes de la costra biológica en un ecosistema mediterráneo semiárido. – Revista Chilena De Historia Natural 76: 35-46. https://doi.org/10.4067/S0716-078X2003000100004.

[21] Maestre, F. T., Bowker, M. A., Cantón, Y., Castillo-Monroy, A. P., Cortina, J., Escolar, C., Escudero, A., Lázaro, R., Martínez, I. (2011): Ecology and functional roles of biological soil crusts in semi-arid ecosystems of Spain. – Journal of Arid Environments 75: 1282-1291. https://doi.org/10.1016/j.jaridenv.2010.12.008.

[22] Muscha, J. M., Hild, A. L. (2006): Biological soil crusts in grazed and ungrazed Wyoming sagebrush steppe. – Journal of Arid Environments 67: 195-207. https://doi.org/10.1016/j.jaridenv.2006.02.010.

[23] Navas Romero, A. L., Herrera Moratta, M. A., Vento, B., Rodriguez, R. A., Martínez Carretero, E. E. (2020): Variations in the coverage of biological soil crusts along an aridity gradient in the central-west Argentina. – Acta Oecologica 109. https://doi.org/10.1016/j.jaridenv.2020.104099.

[24] Odorico, P. D., Okin, G. S., Bestelmeyer, B. T. (2012): A synthetic review of feedbacks and drivers of shrub encroachment in arid grasslands. – Ecohydrology 5: 520-530. https://doi.org/10.1002/eco.259.

[25] Peter, G., Leder, C. V., Funk, F. A. (2016): Effects of biological soil crust and water availability on seedlings of three perennial Patagonian species. – Journal of Arid Environments 125: 122-126. https://doi.org/10.1016/j.jaridenv.2015.10.015.

http://www.aloki.hu ● ISSN 1589 1623 (Print) ● ISSN1785 0037 (Online)
DOI: http://dx.doi.org/10.15666/aeer/2001_905917

[26] Qu, L., Wang, Z., Huang, Y., Zhang, Y., Song, C., Ma, K. (2018): Effects of plant coverage on shrub fertile islands in the Upper Minjiang River Valley. – Science China Life Sciences 61: 340-347. https://doi.org/10.1007/s11427-017-9144-9.

[27] Read, C., Duncan, D., Vesk, P., Elith, J. (2011): Surprisingly fast recovery of biological soil crusts following livestock removal in southern Australia. – Journal of Vegetation Science 22: 905-916. https://doi.org/10.1111/j.1654-1103.2011.01296.x.

[28] Rosentreter, R., Eldridge, D. J. (2002): Monitoring Biodiversity and Ecosystem Function: Grasslands, Deserts, and Steppe. – Monitoring Lichens 7: 223-237. https://doi.org/10.1007/978-94-010-0423-7_15.

[29] Stephens, G. J., Johnston, D. B., Jonas, J. L., Paschke, M. W. (2016): Understory Responses to Mechanical Treatment of Pinyon-Juniper in Northwestern Colorado. – Rangeland Ecology & Management 69: 351-359. https://www.sciencedirect.com/science/article/pii/S1550742416300318ste.

[30] Stevens, R., Monsen, S. B. (2004): Mechanical Plant Control. – In: Restoring Western Ranges and Wildlands - Chapter 9, pp. 65-88. USDA Forest Service Gen. Tech. Rep. RMRS-GTR-136-1.

[31] Sun, F., Xiao, B., Li, S., Kidron, G. J. (2021): Towards moss biocrust effects on surface soil water holding capacity: Soil water retention curve analysis and modeling. – Geoderma 399: 115120. https://doi.org/10.1016/j.geoderma.2021.114930.

[32] Tabeni, S., Garibotti, I. A., Pissolito, C., Aranibar, J. N. (2014): Grazing effects on biological soil crusts and their interactionwith shrubs and grasses in an arid rangeland. – Journal of Vegetation Science 25: 1417-1425. https://doi.org/10.1111/jvs.12204.

[33] Thiet, R. K., Doshas, A., Smith, S. M. (2014): Effects of biocrusts and lichen-moss mats on plant productivity in a US sand dune ecosystem. – Plant Soil 377: 235-244. https://doi.org/DOI: 10.1007/s11104-013-2002-8.

[34] Weber, B., Belnap, J., Büdel, B. (2016): Synthesis on Biological Soil Crust Research. – In: Weber, B., Büdel, B., Belnap, J. (eds.) Biological Soil Crusts: An Organizing Principle in Drylands. Ecological Studies (Analysis and Synthesis) 226: 527-534. Cham: Springer Switzerland. https://doi.org/10.1007/978-3-319-30214-0_25.

[35] Xiao, B., Wang, H., Fan, J., Fischer, T., Veste, M. (2013): Biological soil crusts decrease soil temperature in summer and increase soil temperature in winter in semiarid environment. – Ecological Engineering 58: 52-56. https://doi.org/10.1016/j.ecoleng.2013.06.009,

[36] Xiao, B., Hu, K. (2017): Moss-dominated biocrusts decrease soil moisture and result in the degradation of artificially planted shrubs under semiarid climate. – Geoderma 291: 47-54. https://doi.org/10.1016/j.geoderma.2017.01.009https://doi.org/10.1016/j.ecoleng.2013.06.009.

[37] Zaady, E., Eldridge, D. J., Bowker, M. A. (2016): Effects of local-scale disturbance on biocrusts. – In: Weber, B., Büdel, B., Belnap, J. (eds.) Biological Soil Crusts: An Organizing Principle in Drylands. Ecological Studies (Analysis and Synthesis) 226: 429-449. Cham: Springer Switzerland. https://doi.org/10.1007/978-3-319-30214-0_21.

[38] Zhang, Y., Aradottir, A. L., Serpe, M., Boeken, B. (2016): Interactions of biological soil crusts with vascular plants. – In: Weber, B., Büdel, B., Belnap, J. (eds.) Biological Soil Crusts: An Organizing Principle in Drylands. Ecological Studies (Analysis and Synthesis) 226: 385-406. Cham: Springer Switzerland. https://doi.org/10.1007/978-3-319-30214-0_19.

http://www.aloki.hu ● ISSN 1589 1623 (Print) ● ISSN1785 0037 (Online)
DOI: http://dx.doi.org/10.15666/aeer/2001_905917

APPENDIX

Table 1. *Mean temperatures (°C) and monthly precipitations (mm) of the study site along the year. Last column shows the average anual temperature, and the total rainfall of the year*

Month	**J**	**F**	**M**	**A**	**M**	**J**	**J**	**A**	**S**	**O**	**N**	**D**	
Temperature (°C)	21.3	20.7	19.3	13.2	10.1	8.5	6.4	8.0	11.3	15.2	17.0	18.4	**14.1**
Precipitations (mm)	4.6	93.8	34.2	27.6	36.2	24.6	39.4	10.8	8.2	34.2	28.2	11.2.	**353**

Table 2. *Moss biocrust cover in plots of grazed condition in the unchained and chained sites*

Source	***Sum of Squares***	***Df***	***Mean Square***	***F-Ratio***	***P-Value***
Between groups	6739.69	1	6739.69	12.81	0.0008
Within groups	26299.5	50	525.991		
Total (Corr.)	33039.2	51			

Table 3. *Moss biocrust cover in plots of grazed or ungrazed condition in the chained site*

Source	***Sum of Squares***	***Df***	***Mean Square***	***F-Ratio***	***P-Value***
Between groups	79716.2	1	79716.2	742.61	0.0000
Within groups	6226.03	58	107.345		
Total (Corr.)	85942.2	59			

http://www.aloki.hu ● ISSN 1589 1623 (Print) ● ISSN1785 0037 (Online)
DOI: http://dx.doi.org/10.15666/aeer/2001_905917